UNIVERSITY OF NIŠ
FACULTY OF MECHANICAL ENGINEERING IN NIŠ

THE FIFTH INTERNATIONAL CONFERENCE
"MECHANICAL ENGINEERING IN XXI CENTURY"

- MASING 2020 -

PROCEEDINGS

Niš, December 09-10, 2020

ORGANIZERS

UNIVERSITY OF NIŠ
FACULTY OF MECHANICAL ENGINEERING IN NIŠ

with support of:
Ministry of Education, Science and Technological Development

Chairman of the International conference

Prof. Dr Nenad T. PAVLOVIĆ, Dean
Faculty of Mechanical Engineering in Niš

SCIENTIFIC COMMITTEE

Prof. **Nenad T. Pavlović**, chairman, University of Niš, Faculty of Mechanical Engineering, Serbia
Prof. **Ljiljana Radović**, University of Niš, Faculty of Mechanical Engineering, Serbia
Prof. **Dragoljub Đorđević**, University of Niš, Faculty of Mechanical Engineering, Serbia
Prof. **Peđa Milosavljević**, University of Niš, Faculty of Mechanical Engineering, Serbia
Prof. **Boban Anđelković**, University of Niš, Faculty of Mechanical Engineering, Serbia
Prof. **Vlastimir Nikolić**, University of Niš, Faculty of Mechanical Engineering, Serbia
Prof. **Mića Vukić**, University of Niš, Faculty of Mechanical Engineering, Serbia
Prof. **Miodrag Manić**, University of Niš, Faculty of Mechanical Engineering, Serbia
Prof. **Predrag Rajković**, University of Niš, Faculty of Mechanical Engineering, Serbia
Prof. **Goran Janevski**, University of Niš, Faculty of Mechanical Engineering, Serbia
Prof. **Dejan Mitrović**, University of Niš, Faculty of Mechanical Engineering, Serbia
Prof. **Goran Petrović**, University of Niš, Faculty of Mechanical Engineering, Serbia
Prof. **Dragan B. Jovanović**, University of Niš, Faculty of Mechanical Engineering, Serbia
Prof. **Živan Spasić**, University of Niš, Faculty of Mechanical Engineering, Serbia
Prof. Dr.-Ing. habil. **Manfred Zehn**, Technical University of Berlin, Faculty of Mechanical Engineering and Transport Systems, Germany
Prof. **Rosen Mitrev**, Technical University of Sofia, Faculty of Mechanical Engineering, Bulgaria
Prof. **Alpar Lošonc**, University of Novi Sad, Faculty of Technical Sciences, Serbia
Prof. **Miran Komac**, University of Ljubljana, Faculty of Social Sciences, Slovenia
Prof. **Matthew P. Cartmell**, University of Strathclyde, Department of Mechanical & Aerospace Engineering, UK
Prof. Dr.-Ing. habil. **Reinhold Kienzler**, University of Bremen, Bremen Institute for Mechanical Engineering, Germany
Prof. **Marjan Leber**, University of Maribor, Faculty of Mechanical Engineering, Slovenia
Prof. **Sanjin Troha**, University of Rijeka, Faculty of Technical Sciences, Croatia
Prof. **Miloš Nedeljković**, University of Belgrade, Faculty of Mechanical Engineering, Serbia
Prof. **Uroš Karadžić**, University of Montenegro, Faculty of Mechanical Engineering, Montenegro
Prof. **Ivan Samardžić**, University of Osijek, Faculty of Mechanical Engineering in Slavonski Brod, Croatia
Prof. **Janez Kramberger**, University of Maribor, Faculty of Mechanical Engineering, Slovenia
Prof. Dr.-Ing. habil **Lena Zentner**, Ilmenau University of Technology, Faculty of Mechanical Engineering, Germany
Dr **Nataša Markovska**, Macedonian Academy of Science and Arts, North Macedonia
Prof. **Cristian Barz**, PhD, Technical University of Cluj Napoca, North University of Baia Mare, Romania
Prof. **Milica Rančić**, Mälardalen University, Division of Applied Mathematics, School of Education, Culture and Communication, Sweden
Prof. **Tibor K. Pogány**, PhD, Dr habil, Óbuda University, Institute of Applied Mathematics
Budapest, Hungary
Prof. **Radivoje Mitrović**, University of Belgrade, Faculty of Mechanical Engineering, Serbia
Prof. **Dobrica Milanović**, University of Kragujevac, Faculty of Engineering Sciences, Serbia
Prof. **Mile Savković**, University of Kragujevac, Faculty for Mechanical and Civil Engineering in Kraljevo, Serbia
Prof. **Rade Doroslovački**, University of Novi Sad, Faculty for Technical Sciences, Serbia

Prof. **Darko Knežević**, University of Banja Luka , Faculty of Mechanical Engineering, B&H
Prof. **Milija Krajišnik**, University of East Sarajevo, Faculty of Mechanical Engineering, B&H
Prof. **Nebojša Arsić**, University of Priština, Faculty of Technical Sciences in Kosovska Mitrovica, Serbia
Dr.-Ing. **Dragan Marinković**, Technical University of Berlin, Faculty of Mechanical Engineering and Transport Systems, Germany
Dr.-Ing. **Danijela Ristić-Durrant**, University of Bremen, Institute of Automation, Germany
Prof. **Dragan Djurdjanović**, The University of Texas at Austin, Walker Department of Mechanical Engineering, USA

Organizing Committee

dr **Predrag Janković**, President, University of Niš, Faculty of Mechanical Engineering, Serbia
dr **Mirjana Laković Paunović**
dr **Danijel Marković**
dr **Jelena Dinić**
dr **Miloš Kocić**
dr **Goran Vučković**
dr **Miloš Tasić**
dr **Miloš Madić**
dr **Emina Petrović**
Milica Milunović
Nikola Despenić
Milena Rajić
Nataša Zdravković
Vesna Grozdanović
Dušanka Nikolić, technical secretary

Publication:
Proceedings of The Fifth International Conference – MASING 2020

Edition:
"MECHANICAL ENGINEERING IN XXI CENTURY"
ISSN 2738-103X

Publisher:
Faculty of Mechanical Engineering in Niš
Prof. Dr Nenad T. Pavlović, Dean

Editor:
Prof. Dr Predrag Janković

Number of copies:
120

Printing:
Grafika Galeb, Niš

CIP- Каталогизација у публикацији
Народна библиотека Србије

ISBN 978-86-6055-139-1

All the publications in this Proceedings are subject to authorship, with the authors of the papers carrying the entire responsibility for originality and content

GENERAL SPONSOR

Serbian Government

Ministry of Education, Science and Technological Development

PREFACE

Six decades of tradition, high standards in the education of generations of students, modernly equipped classrooms, professional teaching and associate staff, their references and recognizability, position the Faculty of Mechanical Engineering, University of Niš, as the leader in the field of engineering sciences and technological sciences, not only on the territory of the Republic of Serbia but also in the wider region of the Western Balkans.

The Proceedings of the 5th International Conference **MECHANICAL ENGINEERING IN XXI CENTURY** appear in the year when the Faculty of Mechanical Engineering, University of Niš, celebrates its the sixtieth anniversary. The Department of Mechanical Engineering of the Faculty of Engineering in Niš was founded on May 18, 1960, and it developed into the Faculty of Mechanical Engineering of the University of Niš in 1971. The Faculty of Mechanical Engineering grew intensely, thus becoming one of the most renowned scientific and educational institutions in the country.

The mission of the Faculty is to organize and conduct academic study programs and to develop and perform scientific and professional work in the field of engineering sciences and technology. Its vision is to be recognizable in the European and global academic environment in the areas of mechanical engineering and engineering management.

More than 90 teachers and associates, around 40 members of non-teaching staff, as well as numerous teachers and associates from other faculties and the industry, are working hard every day to accomplish the mission and vision of the Faculty.

The Faculty of Mechanical Engineering, University of Niš, is accredited in compliance with the Law on Higher Education within the scientific and educational field of engineering sciences and technology. It conducts the academic studies of the first degree – undergraduate studies, the second degree – master academic studies, and the third degree – doctoral studies, within the scientific area of mechanical engineering and engineering management.

The Faculty of Mechanical Engineering is a scientific research institution, in addition to being an educational one. There are 11 international scientific research projects within the framework of HORIZON 2020, ERASMUS, CEEPUS and DAAD programs. The participation of teachers and associates from the Faculty in these projects is of utmost importance for their educational and research work and their further career.

The 5th International Conference **MECHANICAL ENGINEERING IN XXI CENTURY** represents a forum for the presentation of latest results, basic and developmental research and application within the topics of:

- Energetics, energy efficiency and process engineering,
- Mechanical design, development and engineering
- Mechatronics and control
- Production and information technologies
- Traffic engineering, transport, and logistics
- Theoretical and applied mechanics and mathematics
- Challenges of the engineering profession in modern industry and
- Engineering management.

The MASING 2020 Conference has attracted just over 200 participants from 14 countries, with over 80 papers. The papers present the research results within the scientific work financially supported by the Ministry of Education, Science and Technological Development of the Republic of Serbia, as well as the research results within international projects.

The main goal of the Conference is to bring together researchers from scientific and industrial institutions so that they can present and communicate their newest results, create personal contacts, promote research within the area of mechanical engineering, and stimulate the exchange of results and ideas within the fields encompassed by the Conference.

As Dean of the Faculty of Mechanical Engineering in Niš, I am honored to greet all participants of the Conference and wish them very successful work..

Dean of the Faculty of Mechanical Engineering,
University of Niš

Prof. dr Nenad T. Pavlović

Niš, December 2020

Table of Contents

PLENARY SESSION

Zoran MILJKOVIĆ, Milica PETROVIĆ
A Survey of Swarm Intelligence-based Optimization Algorithms for Tuning of Cascade Control Systems: Concepts, Models and Applications 3

Srđan BOŠNJAK, Nebojša GNJATOVIĆ
Bucket Wheel Excavators: Balancing and Dynamic Response of the Slewing Superstructure 9

Rado MAKSIMOVIC
Access to Measuring and Balancing of Enterprise's Key Performance Indicators 27

Alpar LOŠONC
Engineering Ethics in the Pandemic 37

ENERGETICS, ENERGY EFFICIENCY AND PROCESS ENGINEERING

Saša PAVLOVIĆ, Velimir STEFANOVIĆ, Evangelos BELLOS, Christos TZIVANIDIS
Solar Thermal Collector Efficiency Map: A New Evaluation Tool 43

Anna LIMANSKAYA, Goran VUČKOVIĆ, Mića VUKIĆ, Mirko STOJILJKOVIĆ
Determination of the Equivalent Thermal Conductivity of an Inhomogeneous Building Block of Complex Geometry . 47

Ljubov SOKOLOVA, Saša PAVLOVIĆ, Tamara TIHOMIROVA, Predrag ZIVKOVIC, Velimir STEFANOVIC, Anna LIMANSKAYA, Selishev ALEKSEI
Application of Solar Energy in Serbia and Russia 51

Jelena MALENOVIĆ-NIKOLIĆ, Dejan KRSTIĆ
Engineering Management in Dealing with Emergencies in the Energy Industry 57

Marko MANČIĆ, Dragoljub ŽIVKOVIĆ, Mirjana LAKOVIĆ, Milena MANČIĆ, Milan ĐORĐEVIĆ
A Model for Coupling Polygeneration System Superstructure Model to Building Load Models in Trnsys 61

Milica JOVČEVSKI, Miloš JOVANOVIĆ, Mirjana LAKOVIĆ, Marjan JOVČEVSKI
Justification of Using Turbulators Stripes in Biomass Heating Stoves 65

Dragoljub ŽIVKOVIĆ, Milena RAJIĆ, Marko MANČIĆ
Thermal Stresses of Hot Water Boiler Structure During the Process of Start-up 71

Mirko M. STOJILJKOVIĆ, Goran D. VUČKOVIĆ, Marko G. IGNJATOVIĆ
Classification of Building Renovation Measures with Ensembles of Decision Trees 77

Ana MOMČILOVIĆ, Gordana STEFANOVIĆ, Biljana MILUTINOVIĆ, Dragiša SAVIĆ
Assessment of Possible Organic Waste Inclusion and Implementation in Closed Loop System 81

Emir NOVALIĆ, Jelena JANEVSKI, Predrag ŽIVKOVIĆ, Mića VUKIĆ, Dejan MITROVIĆ
Finned Radiator Thermal Characteristics Calculation 87

Miloš KOCIĆ, Živojin STAMENKOVIĆ, Jelena PETROVIĆ and Milica NIKODIJEVIĆ
MHD Flow and Heat Transfer of Two Immiscible Micropolar Fluids 93

Jelena PETROVIĆ, Miloš KOCIĆ, Milica NIKODIJEVIĆ, Jasmina BOGDANOVIĆ-JOVANOVIĆ
Nanofluid Flow and Heat Transfer Between Horizontal Plates in Porous Media 97

Jasmina BOGDANOVIĆ JOVANOVIĆ, Živojin STAMENKOVIĆ, Veljko BEGOVIĆ
Operating and Acoustic Characteristics of Low-Pressure Centrifugal Fans with Backward Curved Blades 103

Filip STOJKOVSKI, Zoran MARKOV, Valentino STOJKOVSKI
CFD Study of Radial Guide Vane Cascade with Convex and Concave Blade Sets for Variable Speed Francis turbines 109

Marija LAZAREVIKJ
An Approach to Determine the Origin of Forces Acting on a Blade in a Cascade 115

Valentino STOJKOVSKI, Zoran MARKOV, Filip STOJKOVSKI
Dilemmas for Choice an Installed Discharge at the Run-off River SHPP - Energy or Economic Approach 119

Živan SPASIĆ, Veljko BEGOVIĆ, Miloš JOVANOVIĆ, Saša MILANOVIĆ
Numerical Research into the Influence of Impeller Reduction on Centrifugal Pump Performance 123

MECHANICAL DESIGN, DEVELOPMENT AND ENGINEERING

Tanasije JOJIĆ, Jovan VLADIĆ, Radomir ĐOKIĆ
Zipline Design Issues and Analysis of the Influencing Parameters on Passenger's Velocity 129

Marko MLADENOVIĆ, Natalija TOMIĆ, Boban ANĐELKOVIĆ, Miloš MILOŠEVIĆ
Current State of Fused Deposition Modelling 3D Printer Systems 133

Natalija B. TOMIĆ, Marko V. MLADENOVIĆ, Boban R. ANĐELKOVIĆ, Aleksandar G. STANKOVIĆ, Milan Z. GROZDANOVIĆ
Selection of Fused Deposition Modeling 3D Printer using Multi-Criteria Decision-Making Method 139

Sulaiman E. Al-basaqr, Amir Alsammarraie, Abed Fares Ali
Investigating Fatigue Life of E-glass fiber/Novolac/epoxy (DGEBA) hybrid Composites 145

Goran PAVLOVIĆ, Mile SAVKOVIĆ, Nebojša ZDRAVKOVIĆ and Goran MARKOVIĆ
Optimal Design for the Welded Girder of the Crane Runway Beam 151

Miodrag ARSIĆ, Srđan BOŠNJAK, Vencislav GRABULOV, Mladen MLADENOVIĆ, Zoran SAVIĆ
Sanation of the Synchronous Valve Casing of Hydroelectric Generating Set on Hydro Power Plant Pirot 157

Dušan ĆIRIĆ, Jelena MIHAJLOVIĆ and Miroslav MIJAJLOVIĆ
Transient Finite Element Analysis (FEA) in Material Selection Process: Introduction 161

Dušan STAMENKOVIĆ, Milan BANIĆ, Milan NIKOLIĆ, Aleksandar MILTENOVIĆ, Uroš STANKOVIĆ
Experimental Estimation of Footwear Slip Resistance 167

Sanjin TROHA, Jelena STEFANOVIĆ-MARINOVIĆ, Željko VRCAN
Basic Kinematic Characterstics of Two-Speed Planetary Gear Trains with Brakes on Single Shafts 171

Mića ĐURĐEV, Eleonora DESNICA, Jasmina PEKEZ, Vladimir ŠINIK
Optimization of the Speed Reducer Design Problem using Nature-inspired Algorithms 175

Aleksandar PETROVIĆ, Milan BANIĆ, Gavrilo ADAMOVIĆ
Comparison of Interpolation and Approximation Curves and Their Application in Computer Graphics 179

Dejan MARIĆ, Mijat SAMARDŽIĆ, Tihomir MARSENIĆ, Tomislav ŠOLIĆ, Josip PAVIĆ, Ivan SAMARDŽIĆ, Božo DESPOTOVIĆ
On-line Monitoring of MAG-CMT Welding Process 183

Marko PERIĆ, Aleksandar MILTENOVIĆ, Dušan STAMENKOVIĆ, Milica BARAĆ
Surface Roughness of Parts Made by FDM 3D Printing 187

Aleksija ĐURIĆ, Dragan MILČIĆ, Damjan KLOBČAR
Joining Lightweight Components by Resistance Element Welding – REW 191

MECHATRONICS AND CONTROL

Stevan STANKOVSKI, Dragan KUKOLJ, Gordana OSTOJIĆ, Igor BARANOVSKI, Sandra NEMET
Trends in Artificial Intelligence for Automated Industrial Systems 197

Lara LABAN, Mitra VESOVIĆ
Classification of COVID-CT Images Utilizing Four Types of Deep Convolutional Neural Networks 201

Mitra VESOVIĆ, Radiša JOVANOVIĆ, Vladmir ZARIĆ
Modelling and Speed Control in a Series Direct Current (DC) Machines Using Feedback Linearization Approach 207

Vladimir ZARIĆ, Radiša JOVANOVIĆ, Lara LABAN
Identification of a Coupled-Tank Plant and Takagi-Sugeno Model Optimization Using a Whale Optimizer 213

Dušan STOJILJKOVIĆ, Nenad T. PAVLOVIĆ
Influence of Flexure Hinges Design on Guiding Accuracy of Roberts-Чебышев Compliant Mechanism 217

Andrija MILOJEVIĆ, Kenn OLDHAM
Design of a New Micro-robotic Appendages Comprised of Active Thin-film Piezoelectric Material 221

Andrija MILOJEVIĆ, Kyrre GLETTE
Design Optimization of Terrestrial-Walking Soft Robots 225

Sava RAMANOVIĆ, Nenad PAVLOVIĆ, Miloš STOJKOVIĆ, Žarko ĆOJBAŠIĆ
Smart Mitkovic External Fixation System for Bones 229

PRODUCTION AND INFORMATION TECHNOLOGIES

David POTOČNIK, Lucijano BERUS, Mirko FICKO
Overview of grain size determination in metallography 235

Milos MILOVANCEVIC, Dragan MILČIĆ Dalibor PETKOVIĆ
ANFIS prediction of mean surface roughness and material removal rate in plasma arc cutting 241

Dragan RODIĆ, Marin GOSTIMIROVIĆ, Milenko SEKULIĆ and Anđelko ALEKSIĆ
Application of fuzzy logic for modeling and predicting the electrical discharge machining accuracy 247

Pawan KUMAR
Empirical model to predict surface roughness for drilling GFRP 251

Milan TRIFUNOVIĆ, Predrag JANKOVIĆ, Nikola VITKOVIĆ
Optimization of Cutting Parameters for Minimizing Part Production Costs in Multi-Pass Rough Turning of EN-GJL-250 Grey Cast Iron 255

Miloš MADIĆ, Marko VELIČKOVIĆ, Nikola JOVANOVIĆ, Dimitrije PETROVIĆ
Optimization of Variable Costs Considering Process Constraints in CO_2 Laser Cutting of P265GH Steel 259

Saša RANĐELOVIĆ, Mladomir MILUTINOVIĆ, Vladislav BLAGOJEVIĆ, Dejan MOVRIN
The future of Manufacturing Processes with Support I4.0 263

Vladislav BLAGOJEVIĆ, Saša RANĐELOVIĆ, and Saša MILANOVIĆ
The Expert System for Investigation of Hydraulic and Pneumatic Combinatory Automata - CAR-ex 267

Marko SIMONOVIĆ, Bogdan NEDIĆ, Milan SIMONOVIĆ, Dragan LAZAREVIĆ
Comparison of optical measuring systems and CMM for smaller parts 273

Mileta JANJIĆ, Ramiz KURBEGOVIĆ, Milan VUKCEVIĆ
Engineering Economic Analysis of Abrasive Water Jet Machining Quantitative Characteristics 279

Dušan PETKOVIĆ, Miloš MADIĆ, Goran RADENKOVIĆ
Decision Support System for Biomaterial Selection 283

Milica BARAĆ, Nikola VITKOVIĆ, Miodrag MANIĆ, Marko PERIĆ
A Review of Cutting Fluids in Manufacturing Engineering and Environmental Impact 287

Rajko TURUDIJA, Miodrag MANIĆ, Miloš STOJKOVIĆ
Overview of Software for Simulation and Verification of G-code for CNC machine 291

TRAFFIC ENGINEERING, TRANSPORT AND LOGISTIC

Ivan GRUJIĆ, Nadica STOJANOVIĆ, Jovan DORIĆ
The Design of Unconventional Piston Mechanism for 3.0 L IC Engine 299

Nadica STOJANOVIĆ, Ivan GRUJIĆ, Jasna GLIŠOVIĆ, Danijela MILORADOVIĆ, Jovan DORIĆ
Influence of Rear Spoiler Inclination on Aerodynamics and Stability of Car 303

Nikola PETROVIĆ, Vesna JOVANOVIĆ, Jovan PAVLOVIĆ, Jelena MIHAJLOVIĆ
Determining the Impacts of Passenger Transport Modes on Air Pollution in the European Union 307

Tanja ŽIVOJINOVIĆ, Nataša BOJKOVIĆ, Marijana PETROVIĆ, Nikola PETROVIĆ
Mobility as a Service: Key Topics and Challenges 311

Nikola SIMIĆ, Miladin STEFANOVIĆ, Aleksandar STANKOVIĆ, Goran PETROVIĆ
Smart Technology Application in Spare Parts Management Processes in Company FRITECH 317

THEORETICAL AND APPLIED MECHANICS AND MATHEMATICS

Julijana SIMONOVIĆ
Mathematical Model of Bone Cells Adaptation on External Signals 324

Hedrih (Stevanović) R. Katica
Running with nonlinear sciences – nonlinear mechanics and nonlinear dynamics 327

Hedrih (Stevanović) R. Katica
Methodology of vibro-impact dynamics research on new theory of rolling body collisions 333

Ivan PETKOVIĆ, Đorđe HERCEG
Computer Visualization of Popovski-like Methods for Solving Nonlinear Equations 337

Predrag RAJKOVIĆ, Slađana MARINKOVIĆ, Miomir STANKOVIĆ
Functions Defined by Infinite Products and the Corresponding Equations 343

Dragana DIMITRIJEVIĆ JOVANOVIĆ, Ljiljana RADOVIĆ
Parametric Modelling in Architecture 347

Ljiljana RADOVIĆ, Predrag RAJKOVIĆ
Linearity of multiline path 353

Dragan B. Jovanović
Reconstruction of Strain Energy Surfaces at The Crack Tip Vicinity 357

CHALLENGES OF THE ENGINEERING PROFESSION IN MODERN INDUSTRY

Dušan MOJIĆ, Branka MATIJEVIĆ
ICT Study Programs in Higher Education in Serbia: Analysis of Main Trends 363

Vesna STANKOVIĆ PEJNOVIĆ
Instrumentalization of Knowledge in Neoliberalism 367

Ivana ILIĆ-KRSTIĆ, Vesna MILTOJEVIĆ
Engineers, Ethics and Professionalism 371

Alpar LOŠONC, Andrea IVANIŠEVIĆ
Bounded Rationality and Engineering Ethics 375

Gordana V. STOJIĆ
The World of Machines and Engineers in Kurt Vonnegut's Negative Utopia 379

Miloš TASIĆ, Jelena DINIĆ, Dragoljub B. ĐORĐEVIĆ
Engineers' Perception of the Importance of English in Their Professional and Academic Careers 383

Mahouton Norbert Hounkonnou, Melanija MITROVIĆ
Mathematics for human flourishing In the time of COVID-19 and post COVID-19 387

ENGINEERING MANAGEMENT

Biljana PETKOVIĆ, Dalibor PETKOVIĆ, Ivan RADOJKOVIĆ, Miloš MILOVANČEVIĆ
Determination of the optimal parameters of the wastewater systems based on the largest economic profit 393

Dragan PAVLOVIĆ, Peđa MILOSAVLJEVIĆ, Srđan MLADENOVIĆ
Synergy between Industry 4.0 and Lean Methodology 399

Ivana MARINOVIC MATOVIC, Andjela LAZAREVIC
Covid-19 Crisis Management in Manufacturing Industry Organizations in the Republic of Serbia 403

Andjela LAZAREVIC, Ivana MARINOVIC MATOVIC, Srdjan MLADENOVIC
The Role and Importance of Standards for the Quality of Services in Educational Institutions in the Field of Mechanical Engineering 407

Ivan RADOJKOVIĆ, Branislav RANĐELOVIĆ
A New Risk Management Model for Auto insurance in Serbia 411

Dragan TEMELJKOVSKI, Marko PAVLOVIC, Stojanče NUSEV, Dragana TEMELJKOVSKI NOVAKOVIĆ
Reengineering of Aluminium Melting and Casting Plants in Aluminum Processing Factory 415

Zorana KOSTIĆ
Economic Challenges and Integration Engineering: The Smart Cities Context 421

Milena RAJIĆ, Pedja MILOSAVLJEVIĆ, Rado MAKSIMOVIĆ, Dragan PAVLOVIĆ
Energy Management Model for Sustainable Production Process – A Case Study 425

Miroslav FERENČAK, Dušan DOBROMIROV, Mladen RADIŠIĆ
Personal Income and Aversion to a Sure Loss – Are Money-Makers willing to Risk More to Evade Certain Loss? .. 429

PLENARY SESSION

THE 5th INTERNATIONAL CONFERENCE
MECHANICAL ENGINEERING IN XXI CENTURY

December 9-10, 2020
Faculty of Mechanical Engineering in Niš, Serbia

A Survey of Swarm Intelligence-based Optimization Algorithms for Tuning of Cascade Control Systems: Concepts, Models and Applications

Zoran MILJKOVIĆ, Milica PETROVIĆ
University of Belgrade, Faculty of Mechanical Engineering, Department of Production Engineering, 11120 Belgrade
zmiljkovic@mas.bg.ac.rs, mmpetrovic@mas.bg.ac.rs

***Abstract*—Nowadays, cascade control is still one of the most used control strategies in the manufacturing and process industries. The new requirements of precision and robustness of position and trajectory tracking in control systems for manufacturing components at micro-scale, influenced by hard nonlinearities such as friction and backlash, have motivated the effort toward the development of algorithms for optimal tuning of control parameters. This paper presents a literature review of the algorithms and methods used to solve this problem. Swarm intelligence inspired optimization algorithms, namely particle swarm optimization algorithm (PSO) and grey wolf optimization algorithm (GWO), are applied for tuning of P-PI cascade controllers of CNC machine tool servo system in the presence of friction and backlash. The objective of the optimization is to minimize the maximum position error during the reversal of the axes. A comparative analysis of proposed algorithms with a standard industry-based fine tune (FT) method is also provided. Simulation study as well as real-world experiments carried out on a CNC machine tool controller show a remarkable improvement in the performance of the cascade control system using the proposed swarm intelligence-based strategy.**

***Keywords*—swarm intelligence, particle swarm optimization, grey wolf optimizer, cascade control systems**

I. Introduction

Cascade control systems are one of the most used control structures not only in process industries but also in manufacturing industries, particularly in the field of computer numerical control. Comparing to conventional single-loop feedback control systems, cascade control systems have the ability to correct or eliminate disturbances before they influence the controlled variable of interest and overcome the drawbacks when such disturbances related to the manipulated variable occur. A typical configuration of the cascade control system is based on two controllers within two nested loops, inner and outer loop. The controller in the inner loop is the primary (also called master) and the controller in the outer loop is secondary (aka slave). According to [1], the principal benefits of implementing such a control scheme are in the following two aspects (i) fast dynamic of the inner loop which can eliminate input disturbances, and (ii) improvement of the system response speed. On the other hand, their simple structure and easy way of implementation make them widely adopted in the industrial processes, especially in the process control industry and manufacturing industry.

Design and tuning of cascade control parameters are the most significant issues in this field. Therefore, many methods and approaches have been proposed to tune the parameters of controllers and achieve better control performance. One of the possible approaches that can be found in the state-of-the-art literature is based on the classical auto-tuning method. The authors in [2] proposed an on-line pattern recognition approach to acquire the parameters and expert system based on fuzzy logic inference to tune cascade control parameters of PID controllers online. The authors in [3] designed a cascade control system with the ability to tune one optimal parameter of PID controllers. Furthermore, an automatic tuning methodology was proposed in [4] in order to take into consideration high load disturbance rejection performance. Achieved simulation results lead towards conclusions that the proposed open–loop procedure allows advantages in terms of simultaneous tuning of the PID controllers as well as in the determination of a command signal.

On the other side, many approaches based on a single relay feedback test were reported in the relevant literature. The methodology for tuning parameters of the cascade control system was presented in [1], where two cases were analyzed (i) when process models are available and (ii) when process models are not available. According to the aforementioned methodology, the authors developed an auto-tuning method that uses relay feedback. As a result, phases of identification and tuning of the parameters are decoupled without the need for an extensive trial- and -error efforts for modeling and tuning. Furthermore, the authors in [5] proposed an auto-tuning procedure based on a single relay experiment. This procedure allows parameters for both loops to be identified simultaneously. The automatic tuning method based on a single relay experiment was proposed in [6]. The experimental results demonstrated the effectiveness of the tuning method when it is implemented in the domain of process control.

In other more contemporary works, algorithms are suggested for the direct design of cascade controllers driven by input-output data with a focus based on Virtual Feedback Tuning (VRFT). In this way, the experimental

data serve to adjust the internal and external loops [7]. The automatic method that simultaneously tunes both PID controllers of the cascade control system was developed [8]. The method is based on a single closed-loop step test, while process information is represented by using the B-spline series. Optimization in the frequency domain with restrictions on maximum sensitivity, the limit of multiplicative uncertainty, and sensitivity to measurement noise is shown in [9]. However, these works are applied to systems with slow dynamics and with requirements of precision and quality in the dynamic response that are not very demanding. A large variety of control techniques such as predictive control and sliding control have been reported in the literature [10], [11], and fuzzy and neuro-fuzzy control techniques have been reported in [12], [13].

According to the presented literature review, optimal tuning of cascade control systems' parameters becomes a cumbersome task in the presence of hard nonlinearities (friction, backslash, stiction). In the last two decades, nature-inspired swarm intelligence metaheuristic algorithms have been used as very efficient techniques for obtaining the optimal solutions of high-dimensional, nonlinear, and complex optimization problems [14]. The popularity of those algorithms is due to several main reasons [15]: simplicity in concept, flexibility to adapt to different problems, gradient-free mechanism, and ability to avoid local optima. Therefore, some of the metaheuristic methods were applied in the tuning of the controllers for cascade control systems. A multi-objective GA for optimal tuning of a networked linear controller applied to control a high-performance drilling process was proposed in [16]. The tool's working life and the material removal rate are criteria to be maximized. Furthermore, investigations in this field have been continued and authors in [13] implemented a hybrid approach based on an adaptive neuro-fuzzy inference system for modeling and control of the cutting force during the high-performance drilling process. An evolutionary algorithm called differential evolution (DE) was applied in [17] to tune the parameters of the adaptive cascade controller. Although the DE algorithm demonstrated effectiveness in trajectory tracking control of the hydraulic actuator, practical implementation of the proposed controller was not presented in the paper. In literature [18], a novel swarm intelligence-based Whale Optimization Algorithm (WOA) is applied for optimal design and tuning parameters of fuzzy control systems.

The particle swarm optimization (PSO) algorithm is a population-based method originally proposed in [19]. It has been proven to be a powerful tool for solving global engineering optimization problems. Compared to other algorithms, the advantages of the PSO algorithm lie in its easy programming and implementation, fast convergence speed, and effective performance [20], [21], [22]. These advantages motivated us to introduce the PSO algorithm to optimize the parameters of servosystem influenced by hard nonlinearities such as friction and backlash. Another motivation comes from a literature survey of current state-of-the-art methods. Although the authors in [23] presented a cascade control system where the inner and outer loop of the controllers are tuned by the PSO algorithm, to the best of authors' knowledge, none of the literature sources in the field has carried out the influence of the hard nonlinearities (friction and backslash) on cascade controllers.

On the other side, a grey wolf optimizer (GWO) is a novel population-based method proposed in [15]. According to [24], the main advantages of this method are (i) simple and free from computational burden, (ii) flexible to apply for different problems without any special modification of its structure (iii) better capability to avoid local optima in comparison to the conventional optimization algorithm, (iv) easy to transform into the programming language and implement.

Therefore, in this paper, PSO and GWO algorithms are applied to identify optimal parameters of servosystem influenced by hard nonlinearities such as friction and backlash, as well as to provide near-optimal solutions of P/PI cascade controllers' parameters. The main objective is to minimize the maximum position error while maintaining accuracy and without significantly increasing the control effort. The performance of the proposed PSO and GWO algorithms are experimentally verified and compared with the standard industry approach called Fine Tune (FT).

The structure of the paper is organized as follows. The literature overview of the cascade controllers and approaches used to model and optimize those systems are presented in introductory Section 1. Section 2 introduces a problem formulation with the mechanical modeling of the proposed system. Section 3 gives a description of the PSO algorithm, while Section 4 presents the GWO algorithm applied for tuning of P/PI controller parameters. The experimental results are given in Section 5. The concluding remarks of the paper are summarized in Section 6.

II. Problem formulation

The drive system of the CNC machine tool analyzed in this paper is based on two masses (motor and load) linked with the both elastic and dumping connection. The motor coupled to load (Fig. 1) is represented as a two-mass oscillator, where the first mass represents the moment of inertia of the drive and the second mass refers to the moment of inertia of the load side. The elastic and dumping components are modeled by spring and dumper, respectively. The parameters of this mechanical model are as follows:

- K is the torsion spring constant;
- B is the inner damping coefficient of the shaft;
- J_M is the motor moment of inertia;
- J_L is the load moment of inertia;
- M_M is the motor torque;
- M_L is the load torque disturbance;
- M_S is the transmitted shaft torque.

In the model used in this paper, the motor angular velocity (ω_M), and load angular velocity (ω_L), as well as the transmitted shaft torque (M_S), are used as state variables.

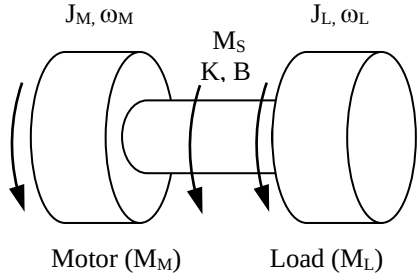

Fig. 1. Model of the two-mass system

After a series of transformations, the transfer function of motor angular velocity (ω_M) to the motor torque (M_M) is given by equation (1):

$$H_{\omega_M/M_M}(s) = \frac{1}{J_M s} \cdot \frac{s^2 + 2D_1\omega_{01}s + \omega_{01}^2}{s^2 + 2D_2\omega_{02}s + \omega_{02}^2} \quad (1)$$

where characteristic angular frequencies ω_{01} and ω_{02} are introduced as (2) and (3):

$$\omega_{01} = \sqrt{K / J_L}, \quad (2)$$

$$\omega_{02} = \omega_{01}\sqrt{1 + (J_L / J_M)}, \quad (3)$$

and damping coefficients D_1 and D_2 are given by (4) and (5):

$$D_1 = \frac{B}{2\omega_{01}J_L}, \quad (4)$$

$$D_2 = D_1\sqrt{1 + \frac{J_L}{J_M}} = \frac{B(J_M + J_L)}{2J_M J_L \omega_{02}}. \quad (5)$$

Furthermore, the transfer function between angular velocity of the load (ω_L) and angular velocity of the motor (ω_M) is presented by equation (6):

$$H_{\omega_L/\omega_M}(s) = \frac{2D_1\omega_{01}s + \omega_{01}^2}{s^2 + 2D_1\omega_{01}s + \omega_{01}^2} \quad (6)$$

A. Friction

Friction is a phenomenon that has a strong influence on the performance and behavior of both mechanical and electromechanical systems. Since the effect of friction can lead to significant error of CNC machine tools positioning system, good representation and prediction of friction force are important for control of such kind of electromechanical systems. Therefore, in order to compensate the error caused by the friction force, the combined Coulomb-viscous model of friction force F is adopted (equation 7):

$$F = F_C \operatorname{sgn}(v) + F_V v \quad (7)$$

where F is the friction force, v is the relative velocity between two surfaces in contact, F_C is the Coulomb friction level, and component F_V represents a small viscous friction.

B. Backlash

Besides friction, the backlash is another common nonlinear factor that affects the behavior of the CNC machine tools positioning systems. In order to model this nonlinearity, the classic dead zone model is utilized in this paper. The exponential model for leads-crew backlash compensation is performed according to the following equation (8):

$$R_P = PP_2\, \mathrm{e}^{-t/PP_3} \quad (8)$$

where PP_2 and PP_3 are backlash peak amplitude and backlash peak time period, respectively.

In order to model the phenomenon of hysteresis nonlinearity in the actuator, parameter f_H which represents the amplitude of the hysteresis is adopted in the proposed control system.

C. Fitness function

According to the aforementioned analysis, a target function for optimization is represented by the following six parameters, equation (9):

$$K = \left[K_p^{pos}\ K_p^{vel}\ K_i^{vel}\ PP_2\ PP_3\ f_H \right] \quad (9)$$

where K_p^{pos} represents the proportional gain of the position controller in the outer loop, K_i^{vel} and K_p^{vel} represent the proportional and integral gain of the speed controller in the inner loop, PP_2 and PP_3 are the backlash peak amplitude and the backlash peak time compensators, respectively, and f_H is the parameter that compensates the friction hysteresis.

The main objective of this research is to minimize the maximum position error E_{pk} (equation 10) which is caused by changing the direction of the axis or by changing the trajectory of the movement. E_{pk} is directly influenced by hard nonlinearities of the mechanical systems such as friction and backlash and its minimization is of high importance for the improvement of the product quality.

$$K = \left[K_p^{pos}\ K_p^{vel}\ K_i^{vel}\ PP_2\ PP_3\ f_H \right]_{OPT} = \arg\min\left(\max(E_{pk})\right) \quad (10)$$

III. Particle Swarm Optimization Algorithm

Particle swarm optimization (PSO) algorithm, originally proposed in [19], is a population-based optimization method inspired by the movement and intelligence of the organisms in a swarm (e.g., a flock of birds, or school of fish). In order to search for food, each member of the swarm determines its velocity based on their personal experience as well as information gained through interaction with other members of the swarm.

Traditional PSO algorithm is initialized with a population of randomly generated candidate solutions known as particles. Each particle flies through the multidimensional search space of the optimization problem with a specific velocity searching for the optimal solution; its position represents a potential solution of the problem and its velocity is dynamically adjusted according to its own flying experience and according to the neighbouring flying experience. Particle position and particle velocity are updated iteratively by using equation (11) and equation (12):

$$V_{id}^{t+1} = W \cdot V_{id}^t + C_1 \cdot rand() \cdot (P_{Id}^t - X_{id}^t) + C_2 \cdot Rand() \cdot (P_{gd}^t - X_{id}^t) \quad (11)$$

$$X_{id}^{t+1} = X_{id}^t + V_{id}^{t+1} \quad (12)$$

$$W = W_{max} - \frac{W_{max} - W_{min}}{iter_{max}} \cdot iter \quad (13)$$

where:

- t is the generation number;
- represents the velocity of the particle i in generation t,
- represents the velocity of the particle i in generation t+1;
- represents the position of the particle i in generation t;
- represent the positions of the particle i in generation t+1;
- is the local best solution ("pbest") of each particle;
- is the global best solution ("gbest") of the swarm;
- W is inertia weight set as in equation (13);
- C_1 and C_2 are positive acceleration constants;
- rand() and Rand() are two random numbers in the range [0,1].

The pseudocode of PSO algorithm implemented to optimize fitness function given by equation (10) is described in Table I [25]:

TABLE I. PSEUDO CODE OF PSO ALGORITHM

Initialize the parameters of PSO algorithm (swarm size, maximum number of generation, inertia weights, W_{max} and W_{min}, acceleration constants, C_1 and C_2);

Initialize a swarm of particles with random positions and velocities (equations 14 and 15);

Evaluate each particle's fitness function by using (equation 10);

Initialize the global ("gbest") and the local best position ("pbest");

Repeat

generation = generation + 1;

generate next swarm by updating the velocities and positions of the particles;

evaluate swarm;

compute each particle's fitness function (equation 10);

find new global ("gbest") and the local best position ("pbest");

update "gbest" of the swarm and "pbest" of each particle;

Until the maximum of generation is not met

Output: the optimal parameters

$\left[K_{\mathrm{p}}^{\mathrm{pos}}\ K_{\mathrm{p}}^{\mathrm{vel}}\ K_{i}^{\mathrm{vel}}\ PP_2\ PP_3\ f_{\mathrm{H}}\right]_{\mathrm{OPT}}$

IV. GREY WOLF OPTIMIZATION ALGORITHM

Grey Wolf Optimization (GWO) algorithm, initially proposed in [15], belongs to a class of novel swarm-based meta-heuristics inspired by the social leadership and hunting technique of grey wolves in nature. According to the GWO algorithm, the grey wolves are classified into four levels of social hierarchy: alpha (α), beta (β), delta (δ), and omega (ω). The alphas are the leaders of the group responsible for the hunting process and making decisions. The betas belong to the second level of the hierarchy and they assist the alphas in making decisions, while deltas belong to the third level and dominate the wolves of the last level omega. The omegas are the lowest ranking grey wolves on the pyramid of social hierarchy.

GWO algorithm is based on the aforementioned social behavior of the grey wolves. The optimization (hunting) process is initialized with randomly generated candidate solutions (grey wolves) in a multi-dimensional search space. This phase of searching for prey is also known as exploration. The best fitness solution is defined as alpha (α), the second and third best solutions are beta (β) and delta (δ), and the rest of the solutions are assumed to be omega (ω). In order to catch the prey, the α, β, and δ grey wolves firstly encircle the victim. During the optimization (hunting) process, they estimate the victim position and update their positions randomly around the victim according to the mathematical model given by the following equations (14) and (15):

$$D = \left|\vec{C} \cdot \vec{X}_p(\mathrm{t}) - \vec{X}(\mathrm{t})\right| \tag{14}$$

$$\vec{X}(\mathrm{t}+1) = \vec{X}_p(\mathrm{t}) - \vec{\mathrm{A}} \cdot \vec{\mathrm{D}} \tag{15}$$

where t represents iteration, $\vec{X}_p$ is the position vector of the prey, $\vec{X}$ is the position vector of a grey wolf, $\vec{A}$ and $\vec{C}$ are coefficient vectors calculated by (16), (17):

$$\vec{A} = 2\vec{a} \cdot \vec{r}_1 - \vec{a} \tag{16}$$

$$\vec{C} = 2 \cdot \vec{r}_2 \tag{17}$$

The components of vector $\vec{a}$ linearly decrease from 2 to 0, and r_1 and r_2 are random vectors in [0,1].

Furthermore, hunting behavior of the grey wolves can be mathematically modeled by equations (18), (19) and (20):

$$D_\alpha = \left|\vec{C}_1 \cdot \vec{X}_\alpha - \vec{X}\right| \tag{18}$$

$$D_\beta = \left|\vec{C}_1 \cdot \vec{X}_\beta - \vec{X}\right| \tag{19}$$

$$D_\delta = \left|\vec{C}_1 \cdot \vec{X}_\delta - \vec{X}\right| \tag{20}$$

The positions of α, β, and δ grey wolves (the first free best solutions) are updated according to the following formulas (21), (22), (23) and (24):

$$\vec{X}_1 = \vec{X}_\alpha - \vec{A}_1(\vec{\mathrm{D}}_\alpha) \tag{21}$$

$$\vec{X}_2 = \vec{X}_\beta - \vec{A}_2(\vec{\mathrm{D}}_\beta) \tag{22}$$

$$\vec{X}_3 = \vec{X}_\delta - \vec{A}_3(\vec{\mathrm{D}}_\delta) \tag{23}$$

$$\vec{X}(\mathrm{t}+1) = \frac{\vec{X}_1 + \vec{X}_2 + \vec{X}_3}{3} \tag{24}$$

Finally, the hunting process is finished by attaching the prey (exploitation phase). The pseudocode of the GWO algorithm is presented in Table II:

TABLE II. PSEUDO CODE OF GWO ALGORITHM

Initialize the parameters of GWO algorithm (population size, maximum number of iterations, position vector X, and vectors A, a, C);

Initialize a population of grey wolves (equations 14 and 15);

Evaluate each grey wolf's fitness function by using (equation 10);

Identify three best wolves (the best search agent - X_α, the second best search agent - X_β, the third best search agent - X_δ) according to their fitness functions;

Repeat

generate next population by updating each agent position (21-23);

update a, A, C by using (16) and (17);

compute each agent's fitness function (equation 10);

update X_α, X_β, X_δ;

Until the maximum of generation is not met

Output: the optimal parameters

$$\left[K_p^{pos}\ K_p^{vel}\ K_i^{vel}\ PP_2\ PP_3\ f_H\right]_{OPT}$$

V. EXPERIMENTAL RESULTS

In order to validate the proposed optimization methodology, experimental simulations are performed in Matlab software package. The parameters of the PSO algorithm are set as follows: the size of population is 20, the maximum number of generations is 100, the inertia weight W is set starting with 1.1 and is linearly decreased to 0.1. Acceleration constants C_1 and C_2 are set to 2.0. The parameters for the GWO algorithm are set as follows: the size of population is 20, the maximum number of iterations is 100, the parameter *a* linearly decreased from 2 to 0, and r_1 and r_2 are random vectors in [0,1]. The simulation results of the PSO and GWO algorithm are compared with the results achieved by one of the standard industry approaches used to manually tune CNC machine tools - Fine Tune (FT) method. After the performing optimization process, the achieved optimal values of the six parameters, $\left[K_p^{pos}\ K_p^{vel}\ K_i^{vel}\ PP_2\ PP_3\ f_H\right]$, are presented in Table III.

TABLE III. CONTROL PARAMETERS

Control parameters	Optimization method		
	Fine Tune method	***PSO algorithm***	***Grey Wolf Optimizer***
K_p^{pos}	66.6667	74.5	75
K_p^{vel}	0.2865	0.4983	0.2632
K_i^{vel}	0.0080	0.002401	0.0012
PP_2	0.7184	0.0902	0.4368
PP_3	0.0080	7.6635e-05	0.04393
f_H	0.1288	0.00596	0.00231

Fig. 2 shows experimental comparisons of the FT method, PSO, and GWO approach for three merit functions, maximum position error (maxE), the accuracy (ITAE), and the control effort (IAU), respectively. As might be seen from Fig. 2, the GWO algorithm achieves a significant improvement in minimization of maximum error (66.4%) comparing with the FT method. The second-best result is achieved by the PSO algorithm with an improvement of (62.5%) comparing to the FT method. However, even though the position error achieved using swarm intelligence-based optimization algorithms is less, results reported in Fig. 2 show that the accuracy (ITAE) of the FT method was better in relation to the other two methods with less the control effort (IAU) required to follow the desired trajectory.

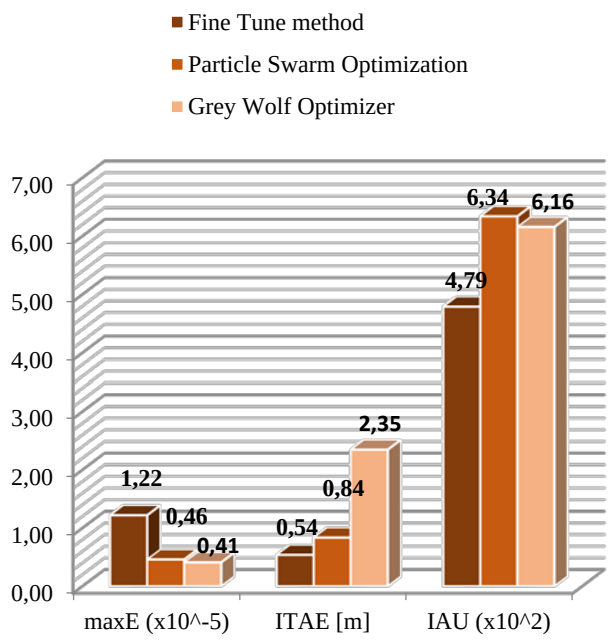

Fig. 2. Simulation results

VI. CONCLUSIONS

This paper presents two biologically inspired swarm intelligence-based optimization algorithms, namely particle swarm optimization algorithm (PSO) and grey wolf optimization (GWO) algorithm, implemented to optimally adjust parameters of the P-PI cascade controllers for CNC machine tool positioning system. Both the algorithms are proposed in order to simultaneously tune a proportional position controller in the external loop and a proportional-integral speed controller in the internal loop of the proposed cascade control system in the presence of nonlinearities. The minimization of the maximum position error directly influenced by nonlinearities such as friction and backlash is the main optimization objective of this work. The proposed optimization procedure results in a set of six optimal parameters of the servosystem: the proportional gain of the outer loop, the proportional and integral gain of the inner loop, the backlash peak amplitude, the backlash peak time, and the friction hysteresis parameter. The proposed PSO and GWO algorithms are implemented in Matlab software environment and experimental results are compared with ones obtained by applying the industry-driven methods named Fine Tune (FT) method. The achieved experimental results show a very important improvement in the tuning and behavior of the control system by minimization of the peak of the trajectory error. The advantage of the GWO over the FT method through the improvement of the maximum peak error is 66.4%, while the improvement of the PSO algorithm is 62.5%. Although the achieved position error (maxE) using swarm intelligence based optimization algorithms is less, better results in terms of accuracy (ITAE) are obtained using the

Fine Tune method. One of the future research directions could be oriented towards the implementation of multi-objective swarm intelligence-based optimization algorithms for the optimal design of cascade control systems.

ACKNOWLEDGMENT

This work has been financially supported by the Ministry of Education, Science and Technological Development of the Serbian Government, through the project "Integrated research in macro, micro, and nano mechanical engineering – Deep learning of intelligent manufacturing systems in production engineering", under the contract number 451-03-68/2020-14/200105, and by the Science Fund of the Republic of Serbia, Grant No. 6523109, AI - MISSION4.0, 2020-2022.

REFERENCES

[1] H. P. Huang, I. L. Chien, Y. C. Lee, and G. Bin Wang, "A simple method for tuning cascade control systems," *Chem. Eng. Commun.*, vol. 165, no. 1, pp. 89–121, 1998, doi: 10.1080/00986449808912371.

[2] M. X. Li, P. M. Bruijn, and H. B. Verbruggen, "Tuning cascade PID controllers using fuzzy logic," *Math. Comput. Simul.*, vol. 37, no. 2–3, pp. 143–151, 1994, doi: 10.1016/0378-4754(94)00003-4.

[3] F. S. Wang, W. S. Juang, and C. T. Chan, "Optimal tuning of PID controllers for single and cascade control loops," *Chem. Eng. Commun.*, vol. 132, no. 1, pp. 15–34, 1995.

[4] A. Visioli and A. Piazzi, "An automatic tuning method for cascade control systems," *Proc. IEEE Int. Conf. Control Appl.*, vol. 2, pp. 2968–2973, 2006, doi: 10.1109/CACSD-CCA-ISIC.2006.4777110.

[5] S. Song, W. Cai, and Y. G. Wang, "Auto-tuning of cascade control systems," *ISA Trans.*, vol. 42, no. 1, pp. 63–72, 2003, doi: 10.1016/s0019-0578(07)60114-1.

[6] A. Leva and F. Donida, "Autotuning in cascaded systems based on a single relay experiment," *J. Process Control*, vol. 19, no. 5, pp. 896–905, 2009, doi: 10.1016/j.jprocont.2008.11.013.

[7] S. Formentin, A. Cologni, D. Belloli, F. Previdi, and S. M. Savaresi, *Fast tuning of cascade control systems*, vol. 44, no. 1 PART 1. IFAC, 2011.

[8] J. C. Jeng and M. W. Lee, "Simultaneous automatic tuning of cascade control systems from closed-loop step response data," *J. Process Control*, vol. 22, no. 6, pp. 1020–1033, 2012, doi: 10.1016/j.jprocont.2012.04.010.

[9] A. I. Ribić and M. R. Mataušek, "An analysis, design and tuning of Cascade Control Systems in the presence of constraints in actuator and process outputs," *J. Process Control*, vol. 24, no. 12, pp. 7–17, 2014, doi: 10.1016/j.jprocont.2014.09.014.

[10] P. J. Serkies and K. Szabat, "Application of the MPC to the position control of the two-mass drive system," *IEEE Trans. Ind. Electron.*, vol. 60, no. 9, pp. 3679–3688, 2013, doi: 10.1109/TIE.2012.2208435.

[11] K. Szabat, T. Orowska-Kowalska, and P. Serkies, "Robust Control of the Two-mass Drive System Using Model Predictive Control," *Robust Control. Theory Appl.*, 2011, doi: 10.5772/15730.

[12] R. E. Haber, J. R. Alique, A. Alique, and R. H. Haber, "Controlling a complex electromechanical process on the basis of a neurofuzzy approach," *Futur. Gener. Comput. Syst.*, vol. 21, no. 7, pp. 1083–1095, 2005, doi: 10.1016/j.future.2004.03.008.

[13] A. G. Martin and R. E. H. Guerra, "Internal model control based on a neurofuzzy system for network applications. a case study on the high-performance drilling process," *IEEE Trans. Autom. Sci. Eng.*, vol. 6, no. 2, pp. 367–372, 2009, doi: 10.1109/TASE.2008.2006686.

[14] M. Petrović and Z. Miljković, "Grey Wolf Optimization Algorithm for Single Mobile Robot Scheduling," *Proc. 4th Int. Conf. Electr. Electron. Comput. Eng. IcETRAN*, p. ROI1.2.1-6, 2017.

[15] S. Mirjalili, S. M. Mirjalili, and A. Lewis, "Grey Wolf Optimizer," *Adv. Eng. Softw.*, vol. 69, pp. 46–61, 2014, doi: 10.1016/j.advengsoft.2013.12.007.

[16] D. Martin, R. del Toro, R. Haber, and J. Dorronsoro, "Optimal tuning of a networked linear controller using a multi-objective genetic algorithm and its application to one complex electromechanical process," *Int. J. Innov. Comput. Inf. Control*, vol. 5, no. 10(B), pp. 3405–3414, 2009.

[17] L. D. S. Coelho and M. A. B. Cunha, "Adaptive cascade control of a hydraulic actuator with an adaptive dead-zone compensation and optimization based on evolutionary algorithms," *Expert Syst. Appl.*, vol. 38, no. 10, pp. 12262–12269, 2011, doi: 10.1016/j.eswa.2011.04.004.

[18] R. C. David, R. E. Precup, S. Preitl, E. M. Petriu, A. I. Szedlak-Stinean, and R. C. Roman, "Design of low-cost fuzzy controllers with reduced parametric sensitivity based on whale optimization algorithm," *28th Mediterr. Conf. Control Autom. (MED). IEEE*, pp. 440–445, 2020, doi: 10.1109/FUZZ48607.2020.9177536.

[19] J. Kennedy and R. Eberhart, "Particle swarm optimization," *Proc. IEEE Int. Conf. Neural Netw.*, pp. 1942–1948, 1995, doi: 10.1007/978-3-642-37846-1_3.

[20] M. Petrović, N. Vuković, M. Mitić, and Z. Miljković, "Integration of process planning and scheduling using chaotic particle swarm optimization algorithm," *Expert Syst. Appl.*, vol. 64, 2016, doi: 10.1016/j.eswa.2016.08.019.

[21] M. Petrović, M. Mitić, N. Vuković, and Z. Miljković, "Chaotic particle swarm optimization algorithm for flexible process planning," *Int. J. Adv. Manuf. Technol.*, vol. 85, no. 9–12, 2016, doi: 10.1007/s00170-015-7991-4.

[22] Z. Miljković and M. Petrović, "Application of modified multi-objective particle swarm optimisation algorithm for flexible process planning problem," *Int. J. Comput. Integr. Manuf.*, 2016, doi: 10.1080/0951192X.2016.1145804.

[23] A. L. Sangeetha, N. Bharathi, A. B. Ganesh, and T. K. Radhakrishnan, "Particle swarm optimization tuned cascade control system in an Internet of Things (IoT) environment," *Measurement*, vol. 117, pp. 80–89, 2018, doi: 10.1016/j.measurement.2017.12.014.

[24] B. Nayak, A. Mohapatra, and K. B. Mohanty, "Parameter estimation of single diode PV module based on GWO algorithm," *Renew. Energy Focus*, vol. 30, no. 00, pp. 1–12, 2019, doi: 10.1016/j.ref.2019.04.003.

[25] M. Petrovic, A. Villalonga, Z. Miljkovic, F. Castano, S. Strzelczak, and R. Haber, "Optimal tuning of cascade controllers for feed drive systems using particle swarm optimization," *IEEE Int. Conf. Ind. Informatics*, pp. 325–330, 2019, doi: 10.1109/INDIN41052.2019.8972132.

THE 5th INTERNATIONAL CONFERENCE
MECHANICAL ENGINEERING IN XXI CENTURY

December 9-10, 2020
Faculty of Mechanical Engineering in Niš, Serbia

Bucket Wheel Excavators: Balancing and Dynamic Response of the Slewing Superstructure

Srđan BOŠNJAK, Nebojša GNJATOVIĆ

First Author affiliation: University of Belgrade-Faculty of Mechanical Engineering, Kraljice Marije 16, Belgrade, Serbia
Second Author affiliation: University of Belgrade-Faculty of Mechanical Engineering, Kraljice Marije 16, Belgrade, Serbia
sbosnjak@mas.bg.ac.rs; ngnjatovic@mas.bg.ac.rs

***Abstract*—A slewing superstructure (SS) represents a key functional subsystem of bucket wheel excavators (BWEs). Identification of its basic parameters of static stability (BPSS: weight and position of the center of gravity) is of equally crucial significance in design of a BWE and in its exploitation. The BPSS dominantly determine the static stability of a BWE SS and, coupled with stiffness, its dynamic response. This paper presents the results of research on the impact of the difference between the experimentally and analytically determined SS BPSS on the: (1) intensities of forces in the ropes of the bucket wheel boom hoisting mechanism; (2) maximum loads of the SS radiaxial slew bearing balls; (3) dynamic response of the SS. The presented research represents the initial stage in forming of the integral methodology for the assessment of impact of the mentioned differences on the key indicators which determine the lifespan and integrity, as well as reliability and safety of the SS of BWEs and related surface mining and material handling machines.**

***Keywords*—Bucket Wheel Excavator, Slewing Superstructure, Weighing, Balancing, Dynamic Response**

I. INTRODUCTION

Thermal power plants hold the biggest share of the energy production in Serbia. According to [1], [2] roughly 70% of electricity produced in Serbia comes from lignite. In Europe, only Germany and Turkey hold bigger reserves of lignite than Serbia, meaning that lignite will remain the primary energetic potential of Serbia for the foreseeable future [1], [3]. Serbian lignite reserves are large enough to support the projected energy consumption until the end of the 21st century [3].

The backbone of lignite production lies in the surface mining systems (SMSs), which are regarded as one of the most significant achievements in the field of mining in the 20th century [4], [5]. The heart of any such system is a bucket wheel excavator (BWE), which dominantly determines its performance, first and foremost reflected on its capacity.

BWEs, the biggest self-propelled machines in existence [6], are exploited in harsh working conditions (24/7) [7], in which they are exposed to the loads of a pronounced dynamic and stochastic character [8]–[11]. Downtimes in their operation adversely affect the coal production and consequently lead to very high direct and/or indirect expenses [5], [12], [13].

A slewing superstructure (SS) represents a vital functional subsystem of a BWE. Due to its large size and mass, changeable geometric configuration and complex loading conditions, a SS has a dominant impact on the static stability of the machine. Furthermore, relatively small stiffness of the SS substructures combined with, from the dynamic behavior standpoint, unfavorable distribution of relatively large masses, makes it sensitive to the action of periodic excitation caused by the resistance to excavation.

Static stability of the SS is determined by its so called 'basic parameters of static stability' (BPSS) [14]: the weight and position of the center of gravity (CoG). Furthermore, balancing of the SS affects the: (a) integrity and lifespan of the large scale radiaxial slew bearing (RSB) [20], [21] and the vital elements of the structure of, for example, the bucket wheel boom (BWB) stays [23]; (b) dynamic characteristics and response [24]–[32]. For this reason, the SS weight and CoG position are, immediately upon the first erection, determined experimentally by the so called 'weighing' [15]–[19]. Assessing the impact of the unavoidable difference between the experimentally and analytically determined BPSS represents a serious engineering challenge because this problem is, in authors' opinion, unacceptably marginalized in the referent literature and technical regulations. Only the paper [33] presents a method for forming the analytical model for the proof of static stability of the SS, based on the difference between the experimentally and analytically determined BPSS. It is for this reason that the basic analysis of the impact of said difference on the definitive counterweight (CW) mass, loading of the RSB and the dynamic response of the SS is presented in this paper, on the example of the BWE SchRs 1600, Fig. 1. A spatial reduced dynamic model of the SS, developed in [34] based on the procedure presented in [35] and [36], is used in papers [37] and [38] for the analysis of the impact of mass of the CW and mass of the adhered material on the response of the SS. Using a planar dynamic model formed on the basis of procedures presented in [35] and [36], the paper [39] analyzes the impact of mass of the bucket wheel with drive on the

dynamic response of the SS. However, the research presented in papers [37]–[39] were not focused on the explicit analysis of the impact of change in the position of the SS CoG, inevitably caused by the variation in the masses of the CW, the adhered material and the bucket wheel with drive. Therefore, the research presented in this paper present the initial stage in the development of an integral methodology for the assessment of the impact of the difference between the experimentally and analytically determined BPSS on the key indicators which determine the integrity and lifespan, and the reliability and safety of the SSs of BWEs and related surface mining and material handling machines.

Fig. 1 BWE SchRs 1600 in the open pit mine "Tamnava West Field"- Serbia (total mass 2420 t)

II. Balancing of the Slewing Superstructure

Changeability of the position of the SS CoG is the consequence of change in the BWB inclination angle. In the case of BWE SchRs 1600, this angle varies between α_{BWB}==–19.52° (BWB in low position) and α_{BWB}=14.1° (BWB in high position). Identification of BPSS of the designed slewing superstructure of the BWE SchRs 1600, Figs. 2 and 3, as well as mass of the CW for balancing of its deadweight, Fig. 4, was achieved using an analytical model based on the 3D model created from the technical documentation [40] provided by the manufacturer (Krupp), Table I. Such analytical model (model 1: M1) represents the designed image of the slewing superstructure i.e. it's so called 'a priori' model [33].

According to [41], the mass of the CW needed for balancing of the superstructure deadweight in horizontal position (H) of the BWB ($x_{CoG,H,M1}$=0) is $m_{CW,0,H,F}$=177.5 t. For this reason, the first weighing (W1) of the SS was performed with CW mass of $m_{CW,W1}$=177.017 t, Table II [42]. The BPSS of the SS model M1 for the CW mass $m_{CW,W1}$ are presented in Table III.

The averaged mass of the SS established from the results of W1 was determined from the expression

$$m_{SS,0,M1,W1,A} = \frac{\sum_p G_{SS,W1,p}}{3g} - m_{CW,W1} =$$

$$= \frac{11499.2 + 11501.1 + 11494.4}{3 \times 9.81} - 177.017 = 995.246 \text{ t}, \quad (1)$$

where p is the indicator of the BWB measuring position: L, H, Hi, Table II. The difference between the experimentally determined and the designed mass of the SS, model M1, Table I, is

$$m_{cor} = m_{SS,0,M1,W1,A} - m_{SS,0,M1} =$$
$$= 995.246 - 978.266 = 16.98 \text{ t} \quad (2)$$

is in the paper [14] labeled as corrective mass. The procedure for determining the coordinates of its center of mass relative to the local coordinate system of the BWB is presented in [14], while the Table IV showcases the values of said coordinates relative to the coordinate system *Oxyz*, Fig. 2. By introducing the corrective mass into the SS model M1 a real image (present state) of the SS i.e. a so called 'a posteriori' model [33], M2, was formed, Tables V and VI. Impacts of the corrective mass on the SS CoG abscissas' values and the intensities of the BWB hoisting mechanism ropes are presented in Figs. 5 and 6. Upon the correction of the CW mass (Δm_{CW}=54.96 t added [43], [44]), a control weighing was conducted (W2), Fig 7, in which the BWB was in the low position, at the angle α_{BWB}=–11.4° [44]. Therefore, the excavator was deployed with the CW mass of

$$m_{CW,E} = m_{CW,W2} = m_{CW,W1} + \Delta m_{CW} =$$

$$= 177.017 + 54.96 = 231.977 \text{ t.}$$

in place of the designed CW mass of $m_{CW,D,P}$=197 t [45], or, $m_{CW,D,F}$=221 t according to [41]. The impacts of the CW mass in the domain of its variation from $m_{CW,D,P}$=197 t to $m_{CW,E}$=231.977 t on the total masses of the SS models M1 and M2 as well as the calculated CoG abscissas are given in Figs. 8 and 9, respectively.

After determining the definitive mass of the CW, the next step in the examination of the SS balancing is to analyze the position of the point where the vertical component of the principal load vector intersects the referent plane of the RSB (point A), under the effects of the main operating loads: the SS deadweight ($E=m_{SS}g$), the weight of the transported material (F_1) and the incrustation (V_1) on the BWB conveyor (the so called 'conveyor 1'), the weight of the incrustation on the BW (V_0), the tangential (U) and the lateral (S) component of cutting force. The intensities of the non-permanently acting loads (F_1, V_1, V_0, U_F, U_L, S_F and S_L), listed in Table VII, are determined in accordance to the standard [46]. For the assessment of the position of the point A on the BW side, the horizontal position of the BWB is representative, while the high position of the BWB is referent for assessing the said position on the side of the CW. The coordinates of the principal vector and the principal moment of the SS load, referent for determining the position of the point A, are calculated with the expressions

$$Z = \sum_i Z_i,$$

$$M_x = \sum_i (Z_i y_i - Y_i z_i),$$

$$M_y = \sum_i (X_i z_i - Z_i x_i),$$

where i=E, F_1, V_0, V_1, U_F and S_F for the BW side i.e. i=E,U_L and S_L for the CW side. Coordinates of the point A are determined with the expressions

$$x_A = -\frac{M_y}{Z},$$

$$y_A = \frac{M_x}{Z}.$$

Based on the eccentricity of the vertical coordinate of the principal vector (e_Z) to the center of mass of the RSB,

$$e_Z = \sqrt{x_A^2 + y_A^2},$$

its relative eccentricity is determined

$$e_r = \frac{e_Z}{D_{RSB}},$$

Fig. 10, where D_{RSB}=11 m is the race diameter of the RSB. Having in mind the fact that the relative eccentricity was determined for the set of loads acting during normal operation of the machine (in relation to the load case H1.1 [46] only the impact of the inclination was omitted), it is necessary to determine if the vertical component of the principal vector is acting within the core of the supporting contour cross section (a circle with the radius of e=0.25D_{RSB}), i.e. to meet the condition

$$e_r < 0.25, \tag{3}$$

which ensures that the load is distributed across all the balls of the RSB. The maximum load of a RSB ball is determined according to the expression [15]

$$F_{B,max} = \frac{|Z|}{n_B}(1 + 4e_r),$$

Fig. 11, where n_B=141 is the total number of balls in the considered RSB.

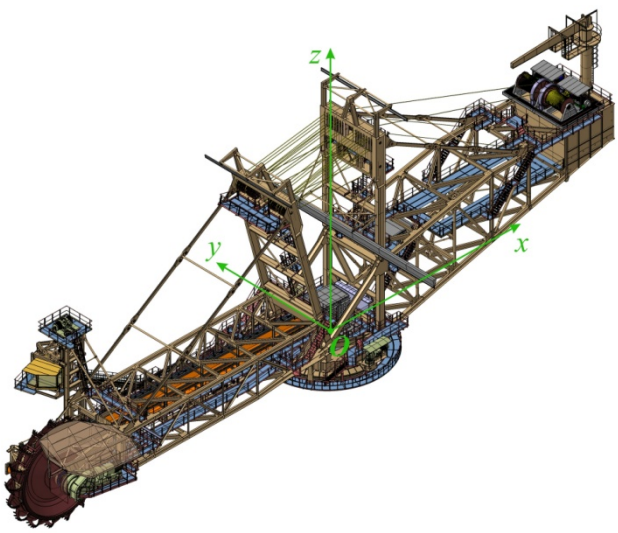

Fig. 2 Slewing superstructure of the BWE SchRs 1600 (total mass without counterweight: $m_{SS,0,M1}$=978.266 t; *Oxyz*-coordinate system related to the center of the RSB)

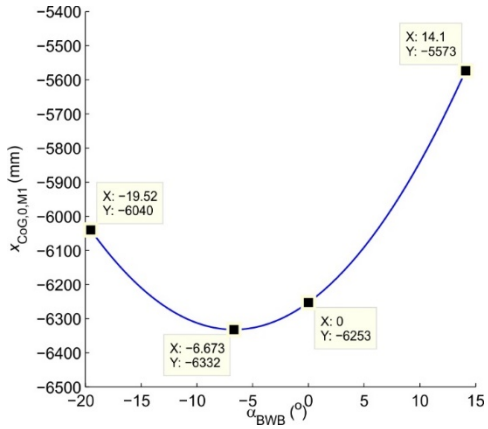

Fig. 3 Abscissa (x_{CoG}) of the SS model M1 CoG (without CW)

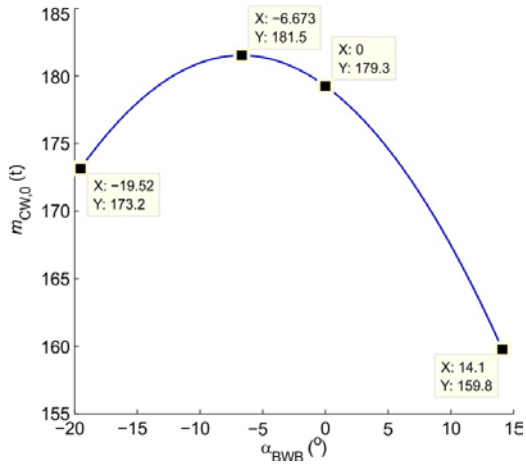

Fig. 4 Mass of the CW ($m_{CW,0}$) for balancing the SS model M1 deadweight

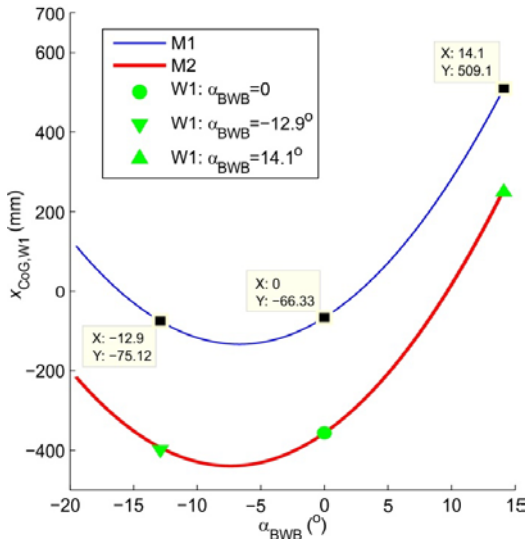

Fig. 5 Calculation CoG abscissas of the SS models M1 and M2 (with CW mass $m_{CW,W1}$=177.017 t) vs. experimentally determined CoG abscissa (W1)

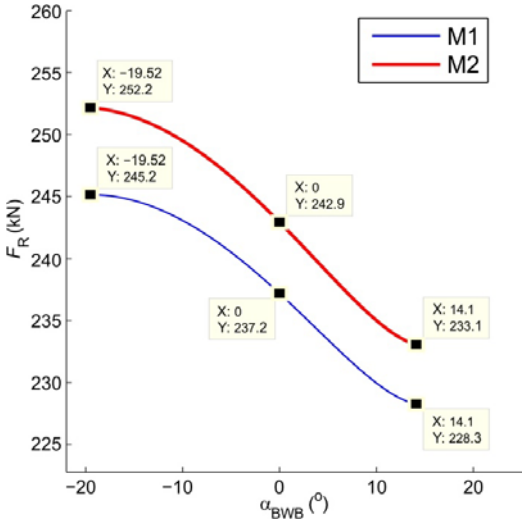

Fig. 6 Winch rope forces caused by the deadweight: M1 vs. M2

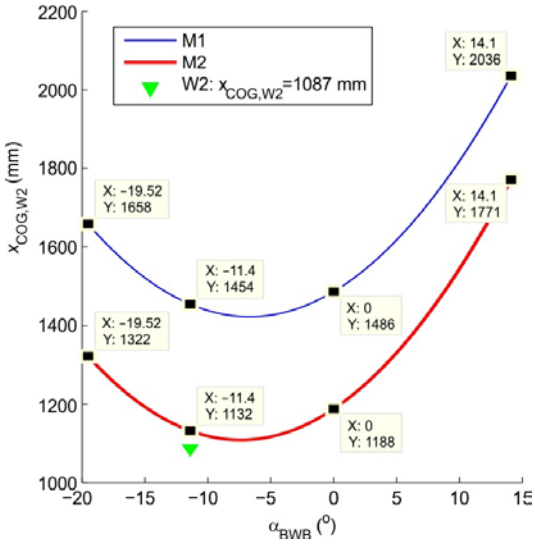

Fig. 7 Calculation CoG abscissas of the SS models M1 and M2 (with CW mass $m_{CW,W2}$=231.977 t) vs. experimentally determined CoG abscissa (W2)

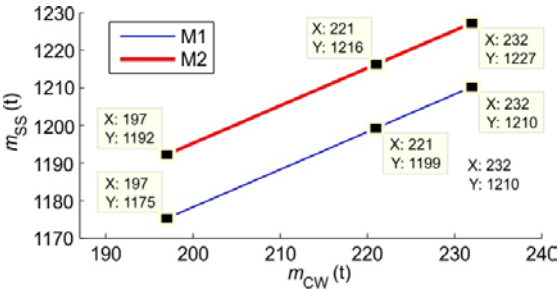

Fig. 8 Impact of the CW mass on the SS models M1 and M2 total mass

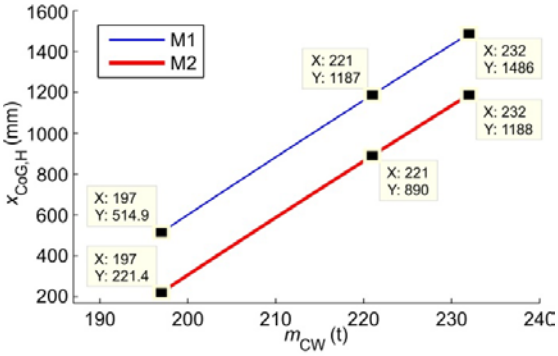

(a)

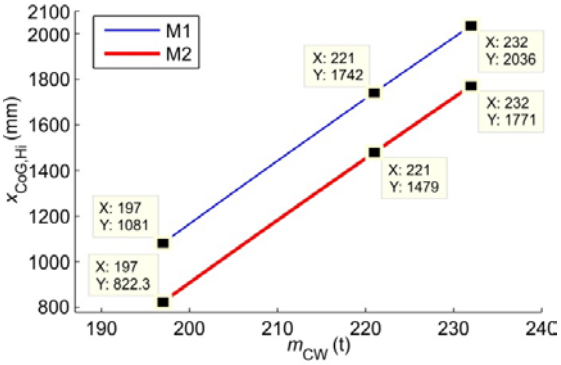

(b)

Fig. 9 Impact of the CW mass on calculation CoG abscissas of the SS models M1 and M2 for BWB position H (a) and Hi (b)

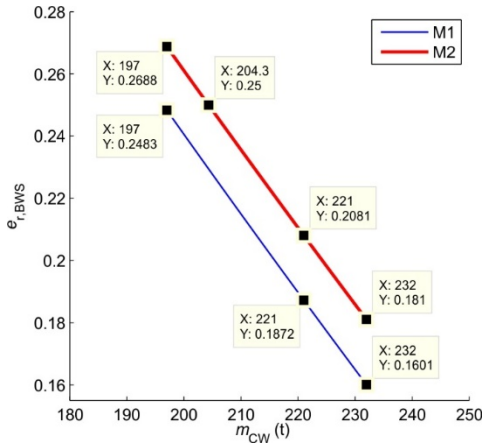

(a)

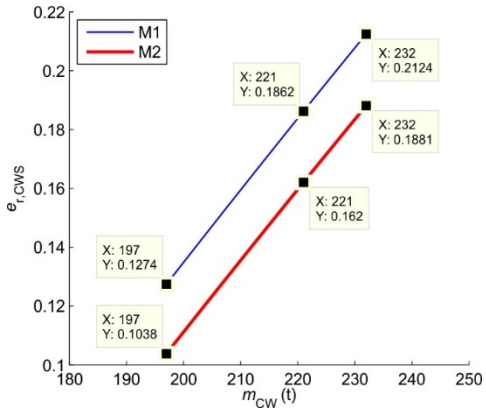

(b)

Fig. 10 Impact of the CW mass on the relative RSB vertical load eccentricity on the BW side (a) and CW side (b)

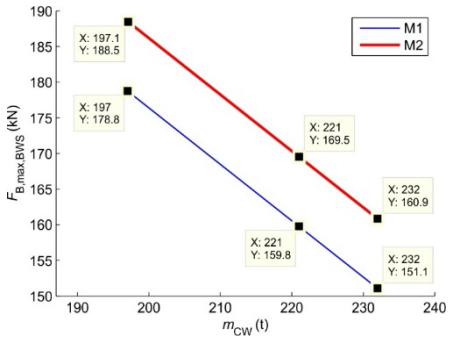

(a)

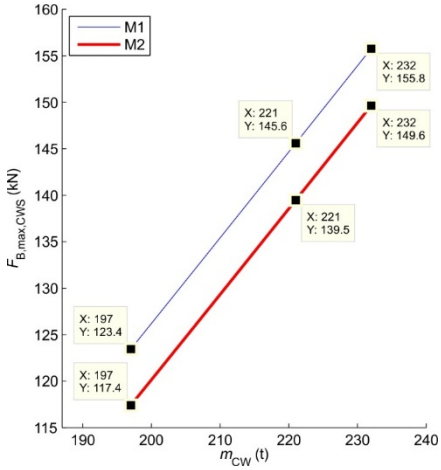

(b)

Fig. 11 Impact of the CW mass on the RSB balls' maximum load

TABLE I BPSS OF THE SS MODEL M1 (WITHOUT COUNTERWEIGHT)

Nomenclature	Notation	Value
Mass	$m_{SS,0,M1}$	978.266 t
CoG abscissa	$x_{CoG,0,M1}$	–6253 mm (α_{BWB}=0)
		–5573 mm (α_{BWB}=14.1°)
		–6040 mm (α_{BWB}=–19.52°)
CoG ordinate	$y_{CoG,0,M1}$	–154 mm

TABLE II RESULTS OF THE FIRST SS WEIGHING (W1)

BWB measuring position	Weight* (kN)	CoG position (mm)	
	$G_{SS,W1}$	$x_{CoG,W1}$	$y_{CoG,W1}$
Low (L): α_{BWB}=–12.9°	11499.2	–398	–121
Horizontal (H): α_{BWB}=0	11501.1	–356	–125
High (Hi): α_{BWB}=14.1	11499.4	249	–118

*counterweight mass: $m_{CW,W1}$=177.017 t

TABLE III CALCULATED BPSS OF THE SS MODEL M1 FROM W1

BWB measuring position	Mass* (t)	CoG position (mm)	
	$m_{SS,W1,M1}$	$x_{CoG,W1,M1}$	$y_{CoG,W1,M1}$
Low (L): α_{BWB}=–12.9°	1155.283	–75	–130
Horizontal (H): α_{BWB}=0		–66	
High (Hi): α_{BWB}=14.1		509	

*counterweight mass: $m_{CW,W1}$=177.017 t

TABLE IV POSITION OF THE CORRECTIVE MASS CENTER (CMC)

BWB measuring position	CMC coordinates (mm)		
	x_{CMC}	y_{CMC}	z_{CMC}
Low (L): α_{BWB}=–12.9°	–22001	475	6511
Horizontal (H): α_{BWB}=0	–20090		14068
High (Hi): α_{BWB}=14.1	–17070		17704

TABLE V BPSS OF THE SS MODEL M2 (WITHOUT COUNTERWEIGHT)

Nomenclature	Notation	Value
Mass	$m_{SS,0,M2}$	995.246 t
CoG abscissa	$x_{CoG,0,M2}$	–6489 mm (α_{BWB}=0)
		–5769 mm (α_{BWB}=14.1°)
		–6323 mm (α_{BWB}=–19.52°)
CoG ordinate	$y_{CoG,0,M2}$	–143 mm

TABLE VI CALCULATION BPSS OF THE SS MODEL M2 FROM W1

BWB measuring position	Mass* (t)	CoG position (mm)	
	$m_{SS,W1,M2}$	$x_{CoG,W1,M2}$	$y_{CoG,W1,M2}$
Low (L): α_{BWB}=–12.9°	1172.263	–393	–121
Horizontal (H): α_{BWB}=0		–356	
High (Hi): α_{BWB}=14.1		–255	

*counterweight mass: $m_{CW,W1}$=177.017 t

TABLE VII INTENSITIES AND POSITIONS OF THE LOADS

Load	Intensity (kN)	Position of points of application		
		x (m)	y (m)	z (m)
BWB position: H				
F_1	376.1	–22.078	0.85	4.475
V_1	37.6	–22.078	0.85	4.475
V_0	196.6	–40.166	–0.76	3.675
U_F	505.1	–46.291	–0.12	4.035
S_F	204.4	–46.291	–0.12	4.035
BWB position: Hi				
U_L	505.1	–38.985	–0.12	6.74
S_L	235.5	–38.985	–0.12	6.74

III. DYNAMIC RESPONSE OF THE SLEWING SUPERSTRUCTURE

The analysis of the influence of the CW mass on the modal characteristics and the dynamic response of the SS was conducted using reduced spatial dynamic models M1 ('a priori' model) and M2 ('a posteriori' model) of the SS, developed according to the procedure presented in detail in [34], Fig. 12. Dynamic models formed in this manner enable the analysis of the BWE SS dynamic behavior in the conditions of continuous variation of both the constructional parameters and the parameters of excitation. BWB inclination angle, as proven in [47], does not have a significant impact on the modal characteristics of the analyzed SS of the BWE SchRs 1600, which is the consequence of a relatively small length and extension of the ropes of the BWB hoisting mechanism, thus the horizontal position of the BWB was adopted as referent for further analysis.

Under the assumption that the excavating angle is equal to $\psi_E=\pi/2$ and having in mind the fact that the appearance of parametric oscillations has not been observed during the exploitation of the excavator [37], identification of the external loads caused by the resistance to excavation was performed according to the procedures presented in [48], [49]. Available moment of excavation was determined according to the equation,

$$M_{E,av} = \frac{\eta_{BWD} P_{BWD} - P_h}{\omega_{BW}}, \tag{4}$$

where η_{BWD}=0.9 is the efficiency of the BW drivetrain, P_{BWD}=1150 kW is BW drive power and P_h is the power used to lift the material in the BW obtained from the expression:

$$P_h = Q_{th}\rho_o g h_Q. \quad (5)$$

In the expression (5), Q_{th}=6600 m^3/h represents the theoretical capacity of the machine, ρ_o=1700 kg/m^3 is the mass density of the overburden (loose), g=9.81 m/s^2 is the gravity constant, while $h_Q=D_{BW}/2=12.25/2=6.125$ m is the material lifting height [15]. Angular frequency of the BW is calculated using the equation,

$$\omega_{BW} = \frac{n_D 2\pi}{n_B}, \quad (6)$$

where n_D=69.4 min^{-1} is the frequency of bucket discharge, while n_B=17 represents the number of buckets.

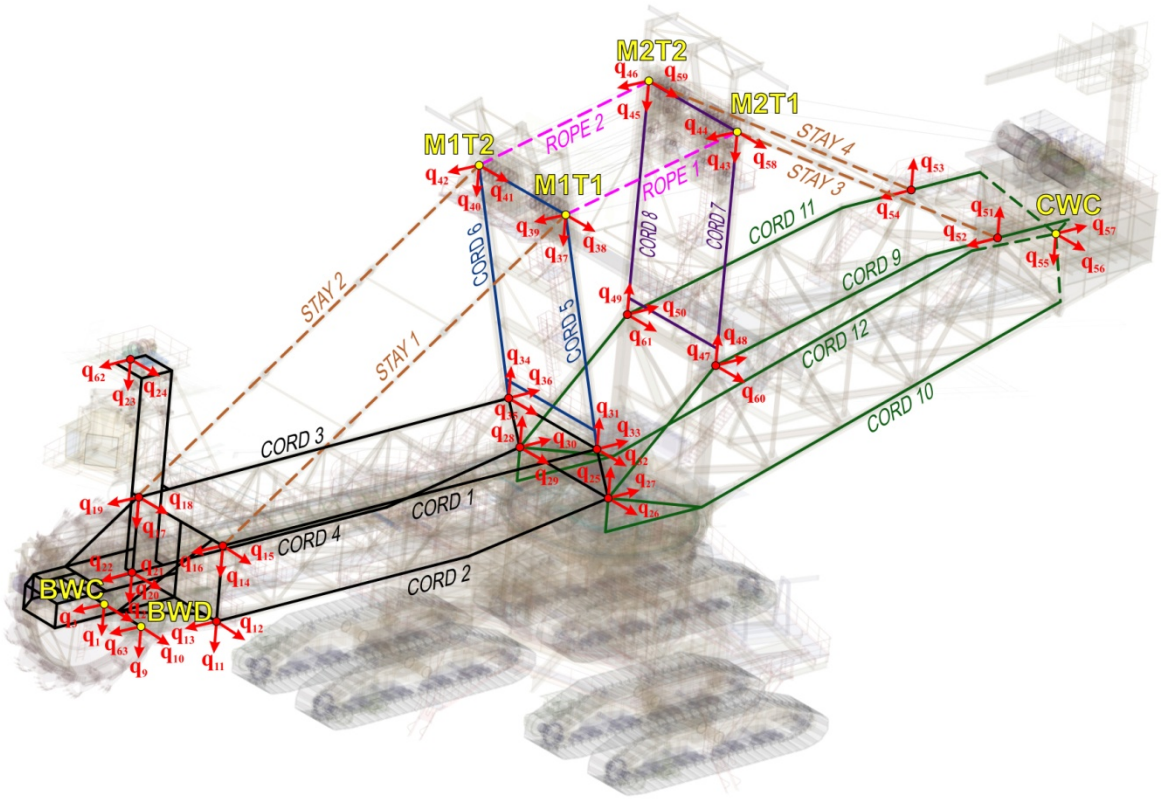

Fig. 12 Spatial reduced dynamic model of the BWE SchRs 1600 superstructure (extracted from Fig. 2 in [47])

If the maximum moment of excavation ($M_{E,max}$), occurring when the maximum number of buckets are engaged in the cut ($n_{B,E,max}=n_{B,E,min}+1$), is calculated according to the expression,

$$M_{E,max} = \frac{D_{BW}}{2} k_F s_0 b_0 \sum_{i=0}^{n_{B,E,min}} \sin(\psi_E - i\theta_B) = M_{E,av}, \quad (7)$$

then the expression (7) yields to

$$k_F s_0 b_0 = \frac{2M_{E,av}}{D_{BW} \sum_{i=0}^{n_{B,E,min}} \sin(\psi_E - i\theta_B)}, \quad (8)$$

allowing the calculation of the minimum moment of excavation ($M_{E,min}$) occurring when the minimum number of buckets are engaged in the cut ($n_{B,E,min}$=int(ψ_E/θ_B)):

$$M_{E,min} = \frac{M_{E,av}}{\sum_{i=0}^{n_{B,E,min}} \sin(\psi_E - i\theta_B)} \sum_{i=1}^{n_{B,E,min}} \sin(\psi_E - i\theta_B), \quad (9)$$

where $\theta_B=2\pi/n_B$ is the angular step of the buckets. The obtained external loads, caused by the resistance to excavation, were approximated with trigonometric polynomials with n=5 harmonics, using the Fourier coefficients, as indicated in [37]. The trigonometric polynomial of the excavation moment ($M_{E,F}$(t)), Fig. 13, was formed according to the equation,

$$M_{E,F}(t) = \frac{M_{E,max} + M_{E,min}}{2} + \sum_{n=1}^{5} \frac{M_{E,min} - M_{E,max}}{n\pi} \sin(n\Omega t), \quad (10)$$

where $\Omega=2\pi n_D$ is the fundamental angular frequency of excitation.

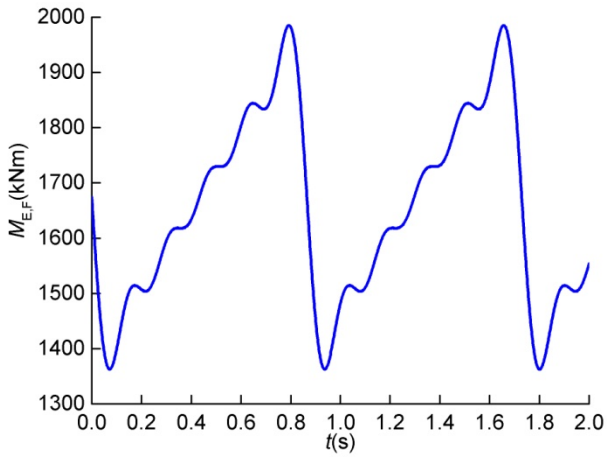

Fig. 13 Moment of excavation $M_{E,F}$(t)

The forced responses of the dynamic models M1 and M2 were determined by applying the Lagrange's second order equations, under the assumption that the structural damping may be considered negligible in the out-of-resonance region, while also having in mind the fact that

free vibration responses are quickly attenuated in operation.

Under the previous assumptions, the system of differential equations of motion yields to [37]

$$\mathbf{M}(m_{\mathrm{CW}})\cdot\ddot{\mathbf{q}}(m_{\mathrm{CW}},t)+\mathbf{K}\cdot\mathbf{q}(m_{\mathrm{CW}},t)= \\ =\mathbf{Q}_{\Omega}^{0}+\sum_{n=1}^{5}\mathbf{Q}_{\Omega}^{n}\sin(n\Omega t). \tag{11}$$

It is important to note that the mass matrix of the system $\mathbf{M}(m_{\mathrm{CW}})$ is dependent on the CW mass, ranging from $m_{\mathrm{CW,D,P}}$=197 t to $m_{\mathrm{CW,E}}$=231.977 t ≈232 t, which makes the generalized displacements,

$$\mathbf{q}(m_{\mathrm{CW}},t)=\mathbf{A_0}+\sum_{n=1}^{5}\mathbf{A_n}(m_{\mathrm{CW}})\sin(n\Omega t), \tag{12}$$

and accelerations of the system referent points,

$$\mathbf{a}(m_{\mathrm{CW}},t)=-\sum_{n=1}^{5}n^2\Omega^2\mathbf{A_n}(m_{\mathrm{CW}})\sin(n\Omega t), \tag{13}$$

dependent on the CW mass in addition to time.

The spectrum of natural frequencies of the model was adopted in a way that accounts for the first five frequencies of excitation [37], while the transformation from M1 to M2 model was realized with the inclusion of the corrective mass (m_{cor}) as a lumped mass with coordinates enclosed in Table IV.

Modal characteristics of both analyzed models (M1 and M2) in the conditions of continuous CW mass variation are presented in Fig. 14, while the values of first 13 natural frequencies obtained for the initial and ultimate values of parameter range are enclosed in Table VIII.

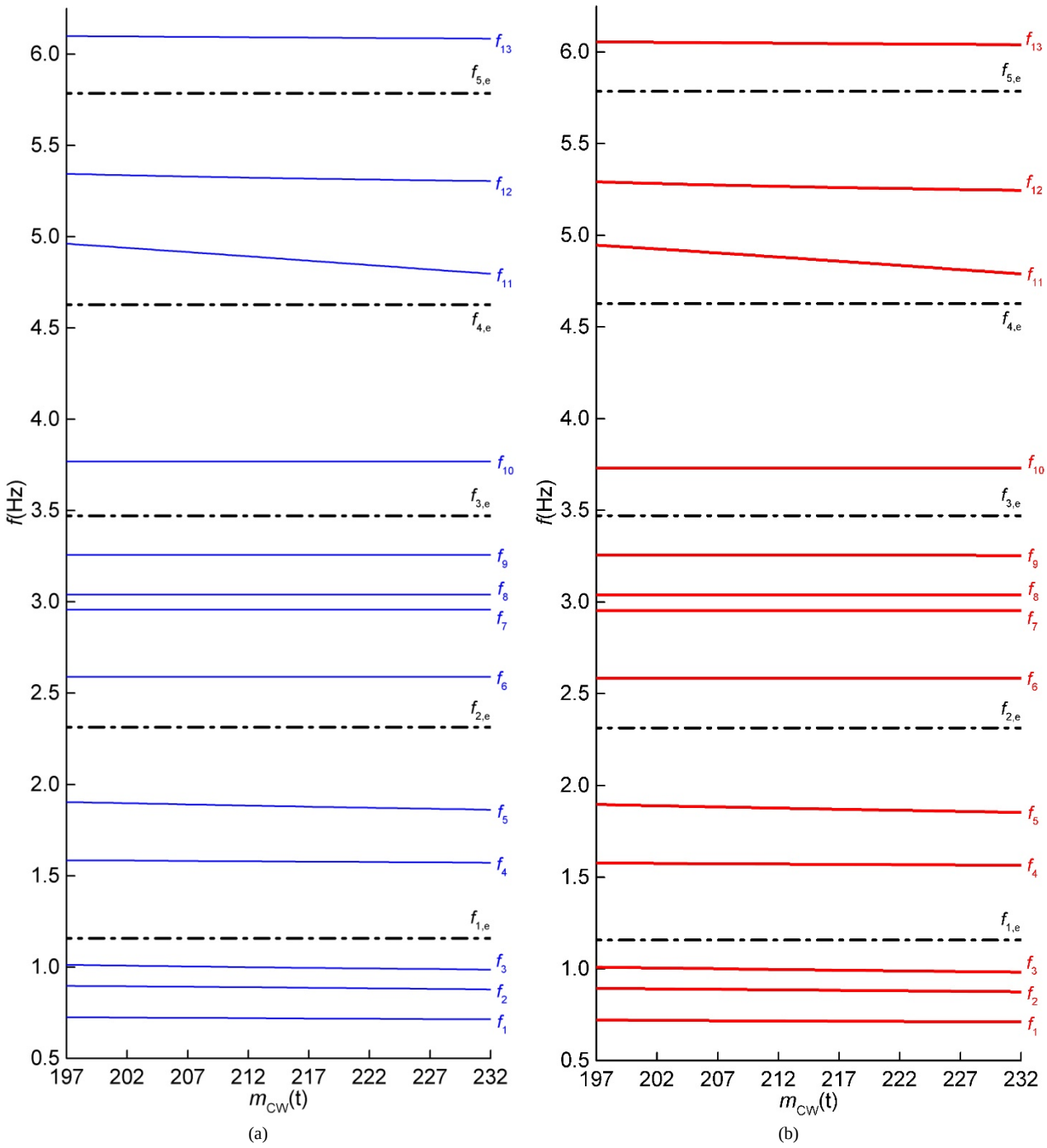

Fig. 14 Dependence of natural frequencies on the CW mass: (a) model M1; (b) model M2 (free vibration frequencies of M1 - blue continuous lines;

free vibration frequencies of M2 - red continuous lines; forced vibration frequencies - black dash-dot lines)

TABLE VIII INFLUENCE OF THE CW MASS ON THE SPECTRUM OF NATURAL FREQUENCIES – MODELS M1 & M2

Model	m_{CW}	Natural frequency (Hz)												
		f_1	f_2	f_3	f_4	f_5	f_6	f_7	f_8	f_9	f_{10}	f_{11}	f_{12}	f_{13}
M1	$m_{CW,D,P}$	0.725	0.897	1.012	1.585	1.904	2.589	2.957	3.039	3.257	3.768	4.961	5.344	6.098
	$m_{CW,E}$	0.714	0.877	0.986	1.571	1.861	2.589	2.957	3.039	3.257	3.768	4.797	5.304	6.084
M2	$m_{CW,D,P}$	0.721	0.893	1.01	1.577	1.897	2.586	2.954	3.039	3.255	3.730	4.946	5.291	6.055
	$m_{CW,E}$	0.711	0.875	0.983	1.565	1.853	2.586	2.954	3.039	3.254	3.730	4.789	5.245	6.039

Analysis of the dynamic response was conducted by monitoring the generalized vertical and lateral displacements and accelerations of the referent points of the system which are most sensitive to the variation of the constructional parameters [7], [32], [39], [47]. Maximum generalized displacements of: (a) bucket wheel center – BWC; (b) bucket wheel drive gearbox center of gravity – BWD; (c) tips of the mast 1 – M1T1 and M1T2; (d) tips of the mast 2 – M2T1 and M2T2; (e) counterweight center of gravity – CWC, Fig. 12, are presented in Figs. 15-26, while the maximum vertical and lateral accelerations of these referent points are enclosed in Figs. 27-38.

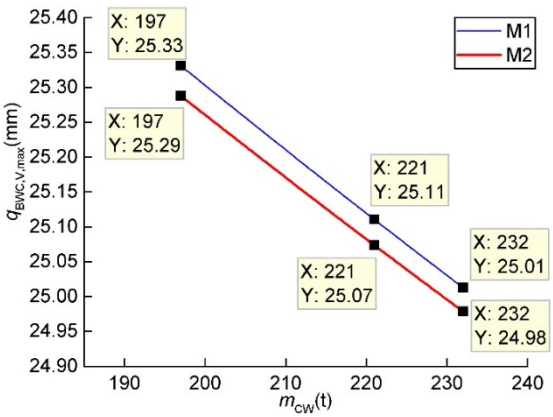

Fig. 15 Maximum vertical displacements of the BWC

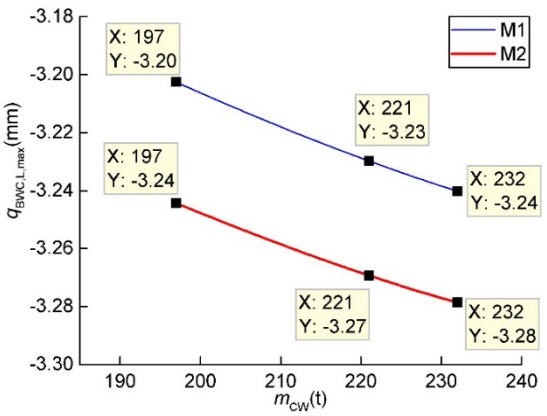

Fig. 16 Maximum lateral displacements of the BWC

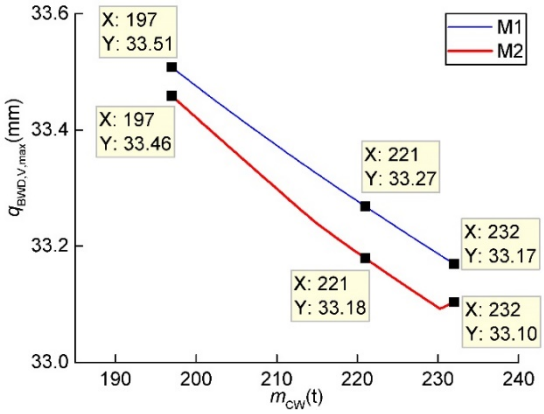

Fig. 17 Maximum vertical displacements of the BWD

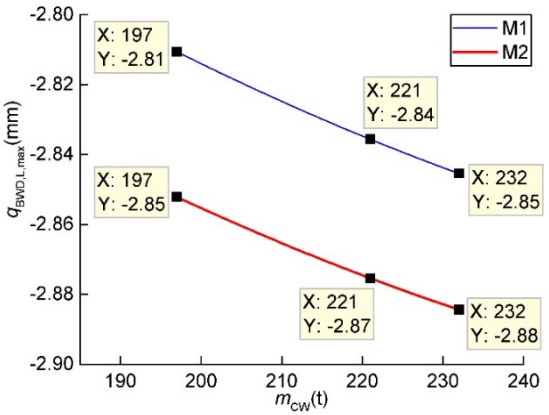

Fig. 18 Maximum lateral displacements of the BWD

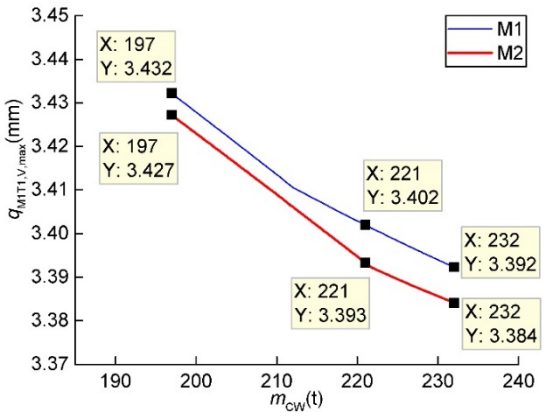

Fig. 19 Maximum vertical displacements of the M1T1

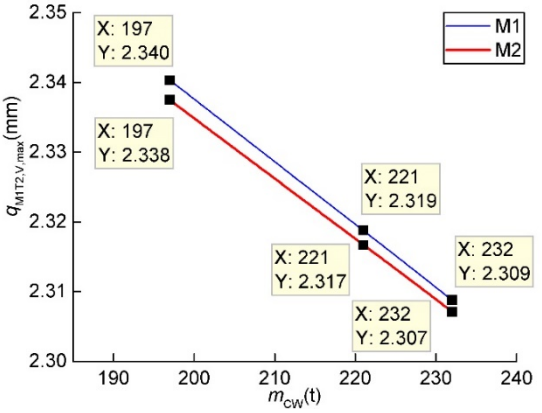

Fig. 20 Maximum vertical displacements of the M1T2

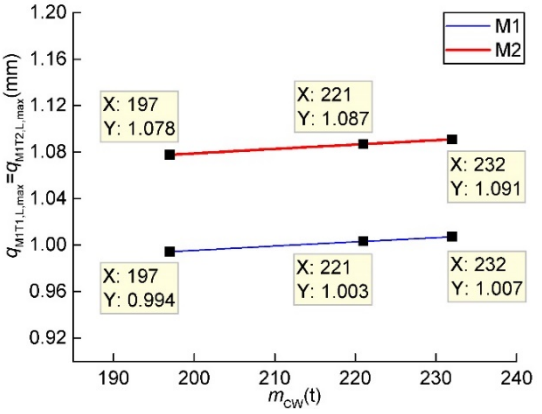

Fig. 21 Maximum lateral displacements of the M1T1 and M1T2

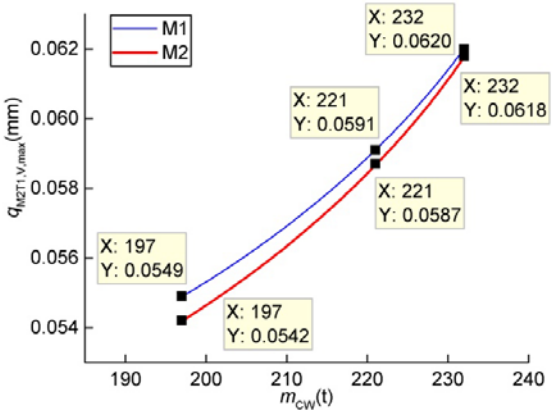

Fig. 22 Maximum vertical displacements of the M2T1

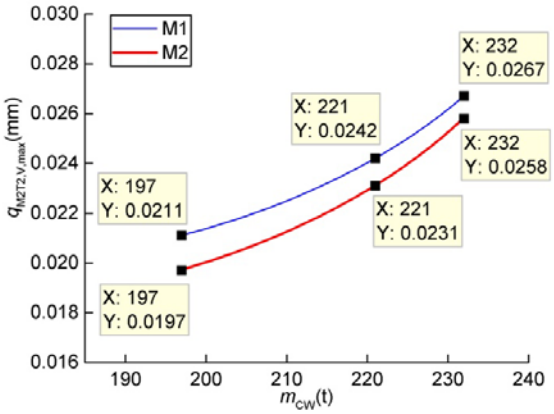

Fig. 23 Maximum vertical displacements of the M2T2

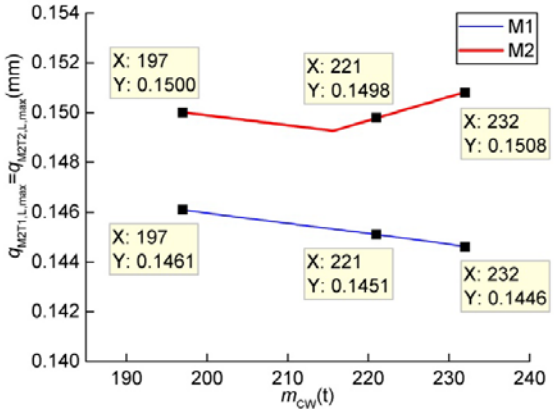

Fig. 24 Maximum lateral displacements of the M2T1 and M2T2

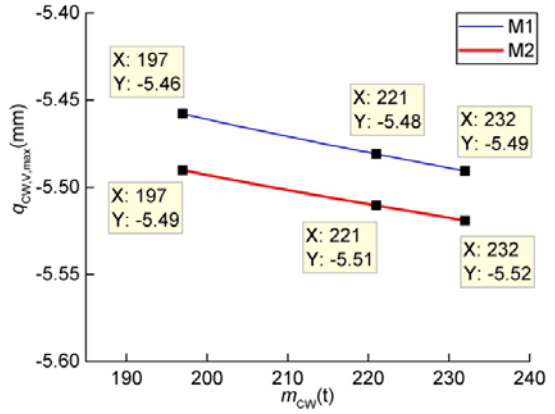

Fig. 25 Maximum vertical displacements of the CWC

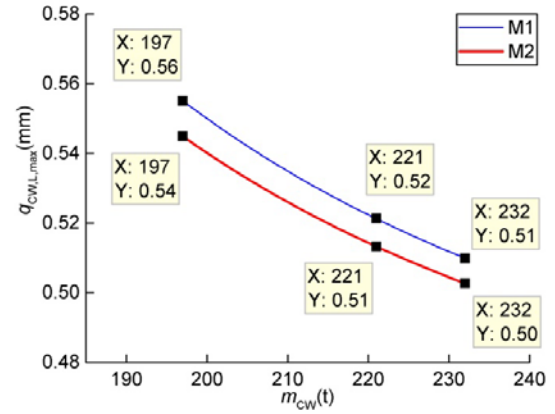

Fig. 26 Maximum lateral displacements of the CWC

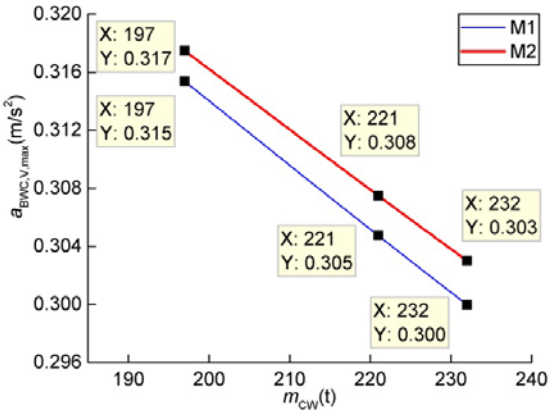

Fig. 27 Maximum vertical accelerations of the BWC

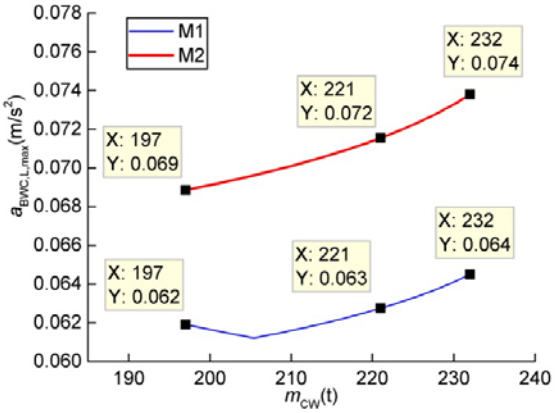

Fig. 28 Maximum lateral accelerations of the BWC

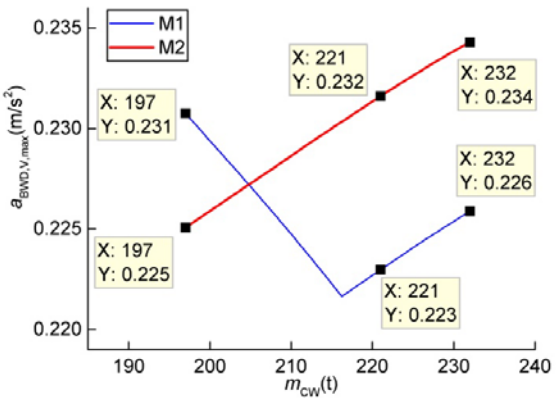

Fig. 29 Maximum vertical accelerations of the BWD

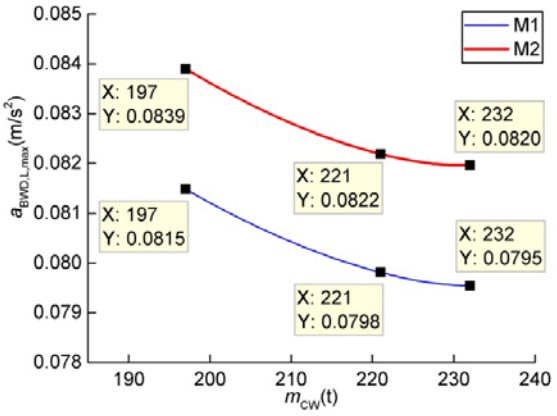

Fig. 30 Maximum lateral accelerations of the BWD

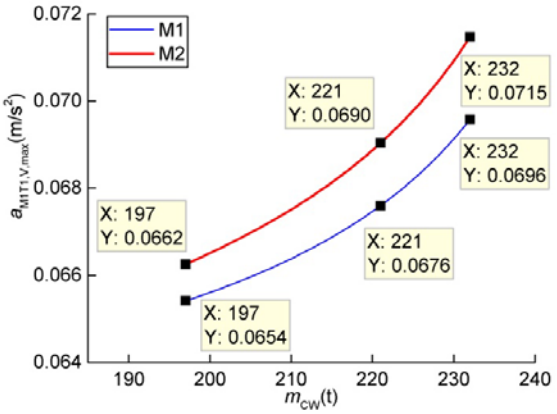

Fig. 31 Maximum vertical accelerations of the M1T1

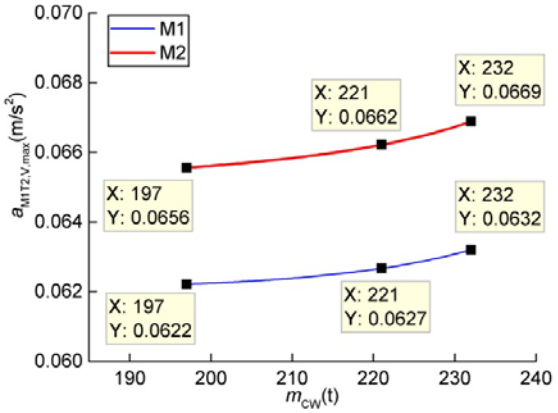

Fig. 32 Maximum vertical accelerations of the M1T2

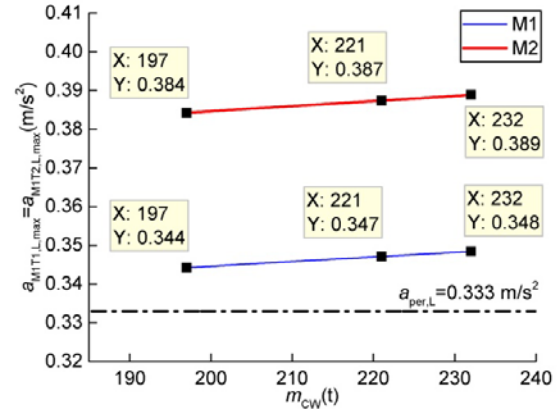

Fig. 33 Maximum lateral accelerations of the M1T1 and M1T2

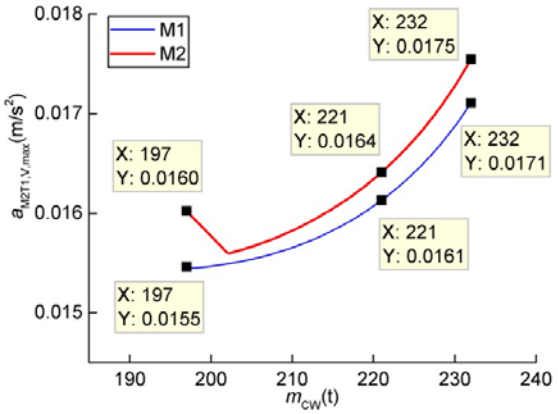

Fig. 34 Maximum vertical accelerations of the M2T1

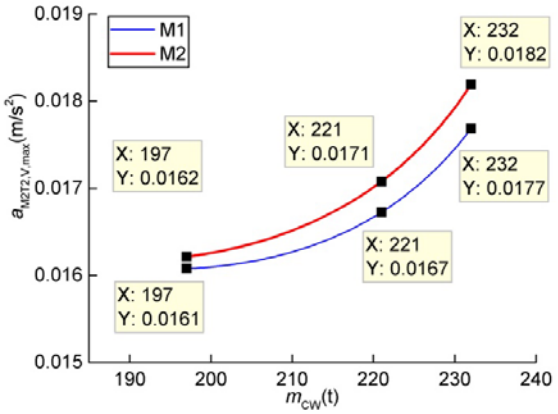

Fig. 35 Maximum vertical accelerations of the M2T2

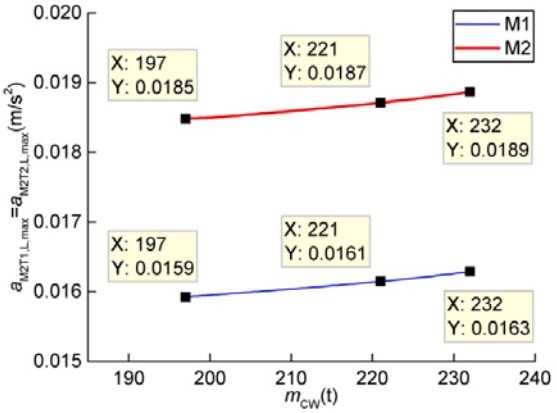

Fig. 36 Maximum lateral accelerations of the M2T1 and M2T2

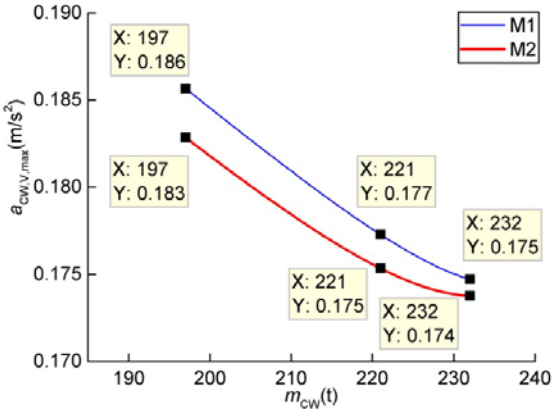

Fig. 37 Maximum vertical accelerations of the CWC

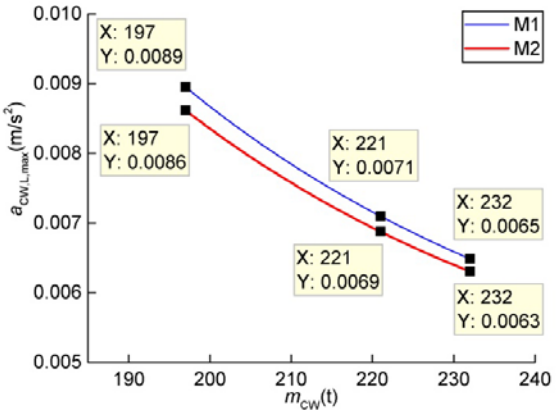

Fig. 38 Maximum lateral accelerations of the CWC

IV. Discussion

By harmonizing the mass of the 'a priori' model of the SS (model M1), Table I, and the mass of the SS, equation (1), determined by the results of the weighing W1, Table II, an 'a posteriori' model (model M2) of the SS has been formed. Its mass, Table V, is equal to the experimentally (W1) determined mass of the SS. Based on the values of the abscissas of the corrective mass, Table IV, it is concluded that excess mass of the model M2, in relation to the model M1, exists on the BWB.

Based on the comparative analysis of the results of the weighing W1, Table II, and the results obtained using the models M1 and M2, Tables III and V, the following conclusions are drawn: (1) the CoG abscissas of the model M1 deviate considerably from the experimentally determined SS CoG abscissas, Fig. 5, Table IX: the lowest absolute value of deviation occurs at the high position of the BWB and equals to 260 mm, and the highest, which is 323 mm, occurs at the low position of the BWB; (2) the CoG abscissas of the model M2 are in good accordance with the experimentally determined SS CoG abscissas, Table IX: the lowest absolute value of deviation occurs at the horizontal BWB position and, with the adopted level of precision equals to 0, and the highest, which is 6 mm, occurs at the high position of the BWB; (3) ordinate deviations are within acceptable ranges for both models, whereby said deviations are considerably lower in the case of model M2, Table IX. In control weighing W2 (CW mass $m_{CW,E}$=231.977 t) the deviations of CoG abscissas of the models M1 and M2 from the experimentally determined SS CoG abscissa, Fig. 7, equal to 367 mm and 45 mm, respectively. The increase of the considered deviations from the deviations in weighing W1 is dominantly the consequence of the presence of foreign bodies (≈1.24 t) and snow accumulation [44].

TABLE IX CoG Position: W1 vs. Models M1 and M2

BWB measuring position	Deviation (mm)			
	Δx_{CoG}*		Δy_{CoG}**	
	M1	M2	M1	M2
Low (L): α_{BWB}=–12.9°	–323	–5	9	0
Horizontal (H): α_{BWB}=0	–290	0	5	–4
High (Hi): α_{BWB}=14.1	–260	–6	12	3

The differences of the CoG abscissas of the models M1 and M2 are positive and monotonously declining over the entire domain of change of the BWB inclination angle, Fig. 39. Additionally, it is observed that the considered differences of abscissas rise as the mass of the counterweight increases, which is explained by the lower sensitivity of the BPSS of the M2 to the impact of the CW mass.

The corrective mass, i.e. the difference of the SS mass determined based on the results of weighing W1, equation (1), and its designed mass, Table I, equals to m_{cor}=16.98 t, equation (2), which represents

$$\Delta m_{SS,per} = 100\frac{m_{cor}}{m_{SS,0,M1}} = 100\frac{16.98}{978.266} = 1.7\%$$

of the designed mass of the SS. According to [15, page 233] "If the weighing results differ by more than a certain amount, in general 5% of the theoretical values calculated for stability, the calculation must be checked and the weighing procedure repeated. The ballast must then be adjusted according to the weighing results so that the position of the COG in the plane of the jacking points corresponds to the desired theoretical values.". Therefore, the provided quote, as well as the standard [50], imply that, having in mind the deviation of the designed and the SS mass determined by weighing is considerably lower than 5%, the correction of the ballast is not necessary. However, the results of the first weighing, conducted with the ballast mass of $m_{CW,W1}$=177.017 t, which is close to the mass of the ballast necessary for balancing of the SS deadweight: $m_{CW,0,H,F}$=177.5 t [41] i.e. $m_{CW,0,H,M1}$=179.263 t, Fig. 4, point to the significant impact of the corrective mass, which is the consequence of relatively high absolute values of its CoG abscissas, Table IV. For this reason it

was necessary to perform a correction to the designed ballast $m_{CW,D,F}$=221 t [41] (ballast CoG abscissa: x_{CW}=34.123 m) by adding

$$\Delta_1 m_{CW} = -\frac{m_{cor} x_{CMC,H}}{x_{CW}} = -\frac{16.98 \times (-20.09)}{34.123} = 9.997 \text{ t.}$$

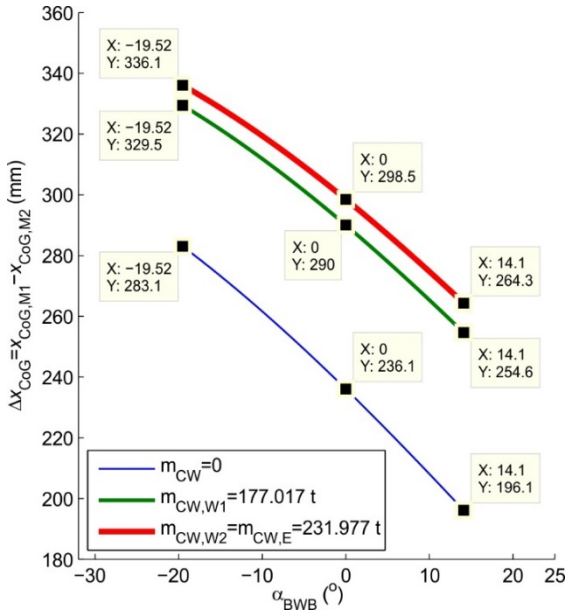

Fig. 39 Impact of the BWB angle on the difference of the SS models CoG abscissas

The higher mass of the BWB in the model M2 causes the increase in the intensity of forces in the ropes of the BWB hoisting mechanism, Fig. 6. The percent increment of the intensities of these forces, Fig. 40, monotonously decreases from 2.9% in the low position of the BWB, to 2.1% in its high position.

The differences of the CoG abscissas of the M1 and M2 SS models, for both referent positions of the BW, monotonously slowly rise as the mass of the CW increases, Fig. 41, which is the consequence of the mentioned lower sensitivity of the M2 BPSS to the influence of the CW mass. Additionally, it is observed that the mentioned differences are somewhat higher in the horizontal BWB position, which is explained by the higher impact of the corrective mass because of the greater distance of its center of mass from the RSB axis of rotation (*Oz*). The maximum values of abscissa differences $\Delta x_{CoG,H,max}$=299 mm and $\Delta x_{CoG,Hi,max}$=265 mm, Fig. 41, occur for the CW mass of $m_{CW,E}$=231.977 t with which the excavator was deployed. With this CW mass, the CoG abscissas of the designed SS (model M1) are $x_{CoG,H,M1}$=1486 mm and $x_{CoG,Hi,M1}$=2036 mm, Fig. 9, which means that the CoG abscissa of the deployed-state SS (M2) is lower by

$$100\frac{\Delta x_{CoG,H,max}}{x_{CoG,H,M1}} = 100\frac{299}{1486} = 20.1\%$$

in the horizontal position of the BWB, and

$$100\frac{\Delta x_{CoG,Hi,max}}{x_{CoG,Hi,M1}} = 100\frac{265}{2036} = 13.0\%$$

in the high BWB position.

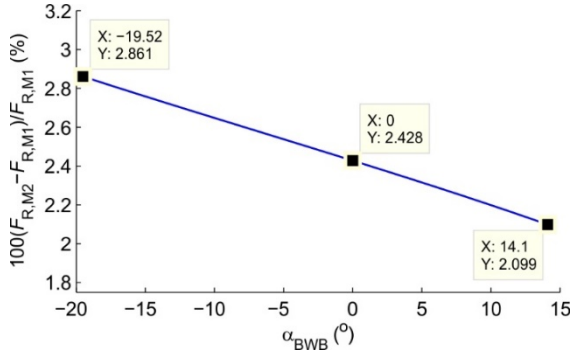

Fig. 40 Percentage difference of the winch rope forces

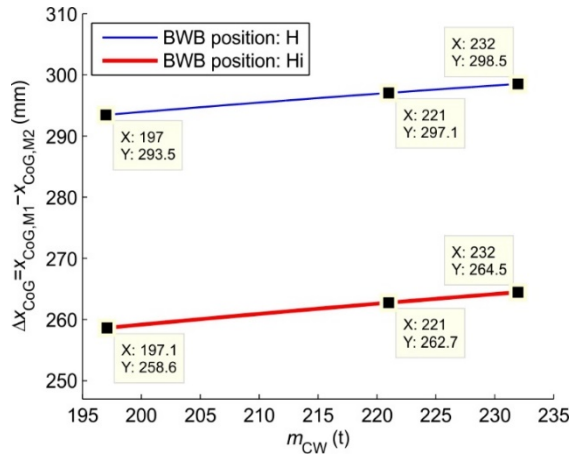

Fig. 41 Impact of the CW mass on the difference of the SS models CoG abscissas

A change in the CW mass significantly impacts the relative eccentricity of the vertical coordinate of the principal vector of loads on the RSB caused by main operating loads, Fig. 10. In the horizontal position of the BWB (BW side), the relative eccentricity monotonously decreases as the CW mass increases, Fig. 10(a), while in the high position of the BWB it is of a monotonously rising character, Fig. 10(b). Relative eccentricity of the load on the BW side in the model M2 does not satisfy the condition defined by the equation (3) for CW masses m_{CW}≤204.3 t. Fig. 10(a). In every other case, the relative eccentricities of the loads are lower than 0.25 for both SS models. It is observed, Fig. 10(a), that the relative eccentricity of loads on the BW side are higher in case of the model M2, while on the CW side it is higher in the model M1, Fig. 10(b). If the values of the relative eccentricities of loads for the model M1 are adopted as the basis for comparison, the percentage differences, Fig. 42, are of a monotonously rising character. At the CW mass $m_{CW,E}$=231.977 t, the relative eccentricity of the vertical load in the model M2 is 13.1% higher on the BW side and 11.5% lower on the CW side, Fig. 42. This means that the conditions for static stability of the SS of the model M2 are less favorable on the BW side and more favorable on the side of the CW.

A change in the mass of the SS and the relative eccentricity of the RSB load leads, naturally, to the change in the RSB ball maximum load, Fig. 11. The character of its dependence on the CW mass is the same as the character of dependence on the relative RSB vertical load eccentricity, Figs. 10 and 11. The same applies to the character of dependence of the percentage differences of the RSB ball maximum loads, Fig. 43. For

the CW mass of $m_{CW,E}$=231.977 t the maximum RSB ball load in the model M2 is 6.5% higher on the BW side and 3.9% lower on the CW side, Fig. 43.

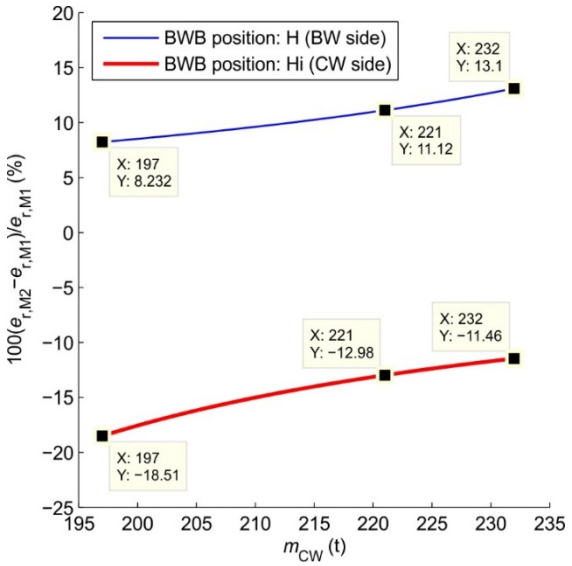

Fig. 42 Percentage difference of the relative eccentricity of the vertical RSB load

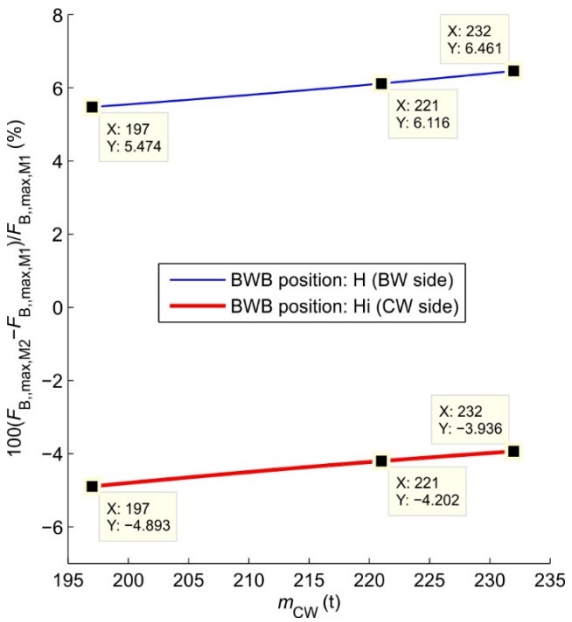

Fig. 43 Percentage difference of the RSB ball maximum load

The increase of both M1 and M2 models' masses has led, as expected, to the decrease in the values of their natural frequencies, Fig. 14 and Table VIII. The eleventh natural frequency of both models is the most affected by the increase of the CW mass, Table X. The second, third and fifth natural frequencies are declining by more than 2% in both of the analyzed models. The fundamental natural frequency of the model M1 is 1.5% lower when m_{CW}=$m_{CW,E}$ compared to the state of the model with m_{CW}=$m_{CW,D,P}$. For the same conditions, the fundamental, natural frequency of the model M2 is 1.4% lower, Table X. The decreases in the fourth, twelfth and thirteenth natural frequencies are lower than 1%, while the sixth through tenth natural frequencies are practically unaffected by the change in the CW mass for both of the analyzed models.

The transition from the 'a priori' image of the SS (model M1 with the mass of the CW $m_{CW,E}$) to the state in which the excavator was put in exploitation (model M2 with the CW mass $m_{CW,E}$) does not have any significant impact on the values of the natural frequencies, Table XI. The tenth and twelfth natural frequencies are 1.1% and 1.0% lower for the 'a posteriori' model, while all of the other analyzed natural frequencies are dropping by less than 1%, Table XI.

In the complete domain of CW mass change there is no appearance of resonances for neither of the analyzed models.

Maximum vertical displacements of the referent points which are influenced by the change in the CW mass the most are those of the tips of the mast 2 for both of the analyzed models, Table XII. Nevertheless, these displacements are an order of magnitude lower than the remainder of the analyzed displacements, Figs. 22 and 23, and are, for this reason, of no significance in further analysis. Maximum generalized vertical displacements of the referent points of the SS are influenced by the change of the CW mass in the domain from 0.5% to 1.3% for both of the analyzed models, drawing a conclusion that, from the engineering standpoint, this influence can be considered negligible, Table XII. Similar conclusions may be drawn when analyzing the influence of transition from the 'a priori' to the 'a posteriori' state of the SS where maximum vertical displacements of the BWD and M1T1 are 0.2% lower, followed by 0.1% lower displacements of the BWC and M1T2, Table XIII. Only the maximum vertical displacement of the CWC is higher, by 0.5%.

Maximum generalized lateral displacement most affected by the change of the CW mass is the displacement of the CWC, Fig. 26, which is 8.9% and 7.4% lower, respectively, at the end compared to the start of the analyzed interval of parameter change for models M1 and M2, Table XIV. The model M1 is slightly more affected by the change in the CW mass, Table XIV, although, from the engineering standpoint, this impact on the lateral displacements of other referent points can be considered negligible. On the other hand, the transition from the 'a priori' to the 'a posteriori' state of the SS has an impact on the lateral displacements of the referent points which may not be neglected steaming from the fact that M1T1 and M1T2 displacements are 8.3% higher, followed by 4.3%, 1.2% and 1.1% higher displacements of the tips of masts 2, BWC and BWD, Table XV. The maximum lateral displacement of the CWC is 2.0% lower.

Lateral displacements, Figs. 21 and 24, and accelerations, Figs. 33 and 36, of the tips of the mast 1 and the mast 2 are equal since these structures are symmetrical, symmetrically supported and symmetrically loaded constructions in the lateral direction.

All of the obtained maximum vertical accelerations of the SS referent points, for both of the analyzed models, are lower than permitted values prescribed by the code [46], Table XVI. Since the maximum obtained vertical accelerations of the tips of the masts 1 and 2, Figs. 31, 32, 34 and 35, are more than five times lower than the permitted values, Table XVI, these accelerations will not be discussed during further analysis. The reason behind the obtainment of the results of such low values lies in high axial stiffness of the cords of the analyzed masts (cords 5-8 in Fig. 12). Maximum vertical accelerations of

the CWC are the most affected by the variation of the CW mass. Vertical accelerations of this referent point are declining by 5.9% for model M1 and 6.5% for model M2, Fig. 37 and Table XVII. Maximum vertical accelerations of the BWC decline by 4.8% and 4.4%, with the increase of the CW mass for the models M1 and M2, respectively, Fig. 27 and Table XVII. This trend is also present in the maximum vertical accelerations of the BWD for the model M1 where a 2.2% decrease is observed, while these accelerations increase by 4% in case of the model M2. The character of the diagram of maximum vertical accelerations of the BWD for the model M1, Fig. 29, is the consequence of the fourth order resonant state, the influence of which was analyzed in [37].

Disregarding the percentage differences of the values of maximum vertical accelerations of the tips of the masts 1 and 2 for the already enclosed reasons, the transition from the 'a priori' to the 'a posteriori' state of the SS has the biggest effect on the vertical accelerations of the BWD, reflected in the increase of 3.5%, Table XVIII. The increase of values is also observed when analyzing the maximum vertical accelerations of the BWC (1.0%). Said transition has a slight positive influence only on the maximum vertical accelerations of the CWC, which decline by 0.6%, Table XVIII.

Having in mind the fact that the maximum lateral accelerations of the tips of the mast 2 (M2T1 and M2T2) and the CWC are by an order of magnitude lower than their permitted values, Table XVI, over the entire domain of the parameter change for both of the analyzed models it is conclusive that they are of no interest for further analysis, Figs. 36 and 38. With the increase in the CW mass, the values of the maximum lateral accelerations of the BWC increase by 3.2% and 7.2% for the models M1 and M2, respectively, Fig. 28, Table XIX. On the other hand, maximum lateral accelerations of the BWD decline by 2.5% (M1) and 2.3% (M2), Table XIX. The increase in the values of maximum lateral accelerations of the tips of the mast 1 with the increase of the CW mass is practically negligible (≤1.3%) for both of the analyzed models, Table XIX. However, unlike the maximum lateral accelerations of the BWC and the BWD, which are lower than the permitted value on the complete interval of the parameter change for both of the analyzed models, the values of the maximum lateral accelerations of the tips of the mast 1 are slightly higher (3.3% at the beginning and 4.5% at the end of the analyzed interval of change) than the permitted value for the model M1, Fig. 33 and Table XVI. Negative dynamic effects are even more pronounced when said accelerations are analyzed for model M2, for which the values are higher by 15.3% and 16.8% for $m_{\mathrm{CW,D,P}}$ and $m_{\mathrm{CW,E}}$, than the permitted value prescribed by [46], respectively.

For the previously stated reasons, the influence of the transition from the 'a priori' to the 'a posteriori' state of the SS on the maximum lateral accelerations of the tips of the mast 2 and the CWC was not analyzed. Said transition has a significant impact on the values of maximum lateral accelerations of the BWC (increase of 15.6%) and the tips of the mast 1 (increase of 11.8%), while the BWD is slightly less affected (increase of 3.1%), Table XX. Finally, the values of maximum lateral accelerations of the tips of the mast 1 are only 4.5% higher than the permitted value when the 'a priori' state of the SS is analyzed, compared to 16.8% higher values obtained for the state of the SS that was put in exploitation.

TABLE X PERCENTAGE DECREASE OF M1 AND M2 NATURAL FREQUENCIES CAUSED BY CW MASS INCREASE

Model	**Percentage difference**	**Natural frequency (*i*=1,2...13)**												
		f_1	f_2	f_3	f_4	f_5	f_6	f_7	f_8	f_9	f_{10}	f_{11}	f_{12}	f_{13}
M1	$\frac{f_i^{m_{\mathrm{CW,E}}} - f_i^{m_{\mathrm{CW,D,P}}}}{f_i^{m_{\mathrm{CW,D,P}}}} \times 100$	-1.5	-2.2	-2.6	-0.9	-2.3	0.0	0.0	0.0	0.0	0.0	-3.3	-0.7	-0.2
M2		-1.4	-2.0	-2.7	-0.8	-2.3	0.0	0.0	0.0	0.0	0.0	-3.2	-0.9	-0.3

TABLE XI TRANSITION FROM THE 'A PRIORI' TO THE 'A POSTERIORI' STATE OF THE SS - IMPACT ON THE SPECTRUM OF NATURAL FREQUENCIES

Percentage difference	**Natural frequency (*i*=1,2...13)**												
	f_1	f_2	f_3	f_4	f_5	f_6	f_7	f_8	f_9	f_{10}	f_{11}	f_{12}	f_{13}
$\frac{f_i^{\mathrm{M2}(m_{\mathrm{CW,E}})} - f_i^{\mathrm{M1}(m_{\mathrm{CW,E}})}}{f_i^{\mathrm{M1}(m_{\mathrm{CW,E}})}} \times 100$	-0.4	-0.2	-0.3	-0.4	-0.4	-0.1	-0.1	0.0	-0.1	-1.0	-0.2	-1.1	-0.7

TABLE XII DEVIATION OF MAXIMUM GENERALIZED VERTICAL DISPLACEMENTS CAUSED BY CW MASS INCREASE

Model	**Percentage difference**	**Referent point (*RP*)**						
		BWC	BWD	M1T1	M1T2	M2T1	M2T2	CWC
M1	$\frac{q_{RP,\mathrm{V,max}}^{m_{\mathrm{CW,E}}} - q_{RP,\mathrm{V,max}}^{m_{\mathrm{CW,D,P}}}}{q_{RP,\mathrm{V,max}}^{m_{\mathrm{CW,D,P}}}} \times 100$	-1.3	-1.0	-1.2	-1.3	12.9	26.5	0.5
M2		-1.2	-1.1	-1.3	-1.3	14.0	31.0	0.5

TABLE XIII TRANSITION FROM THE 'A PRIORI' TO THE 'A POSTERIORI' STATE OF THE SS - IMPACT ON THE MAXIMUM VERTICAL DISPLACEMENTS

Percentage difference	**Referent point (*RP*)**						
	BWC	BWD	M1T1	M1T2	M2T1	M2T2	CWC
$\frac{q_{RP,\mathrm{V,max}}^{\mathrm{M2}(m_{\mathrm{CW,E}})} - q_{RP,\mathrm{V,max}}^{\mathrm{M1}(m_{\mathrm{CW,E}})}}{q_{RP,\mathrm{V,max}}^{\mathrm{M1}(m_{\mathrm{CW,E}})}} \times 100$	-0.1	-0.2	-0.2	-0.1	-0.3	-3.4	0.5

TABLE XIV DEVIATION OF MAXIMUM GENERALIZED LATERAL DISPLACEMENTS CAUSED BY CW MASS INCREASE

Model	Percentage difference	Referent point (*RP*)				
		BWC	BWD	M1T1; M1T2	M2T1; M2T2	CWC
M1	$\frac{q_{RP,\mathrm{L,max}}^{m_{\mathrm{CW,E}}} - q_{RP,\mathrm{L,max}}^{m_{\mathrm{CW,D,P}}}}{q_{RP,\mathrm{L,max}}^{m_{\mathrm{CW,D,P}}}} \times 100$	1.3	1.4	1.3	-1.0	-8.9
M2		1.2	1.1	1.2	0.5	-7.4

TABLE XV TRANSITION FROM THE 'A PRIORI' TO THE 'A POSTERIORI' STATE OF THE SS - IMPACT ON THE MAXIMUM LATERAL DISPLACEMENTS

Percentage difference	Referent point (*RP*)				
	BWC	BWD	M1T1; M1T2	M2T1; M2T2	CWC
$\frac{q_{RP,\mathrm{L,max}}^{\mathrm{M2}(m_{\mathrm{CW,E}})} - q_{RP,\mathrm{L,max}}^{\mathrm{M1}(m_{\mathrm{CW,E}})}}{q_{RP,\mathrm{L,max}}^{\mathrm{M1}(m_{\mathrm{CW,E}})}} \times 100$	1.2	1.1	8.3	4.3	-2.0

TABLE XVI PERMITTED ACCELERATION VALUES ACCORDING TO THE STANDARD [46]

Permitted acceleration (m/s^2)	Referent point (*RP*)	
	BWC; BWD	M1T1; M1T2; M2T1; M2T2; CWC
Vertical direction	1	0.4
Lateral direction	0.167	0.333

TABLE XVII DEVIATION OF MAXIMUM GENERALIZED VERTICAL ACCELERATIONS CAUSED BY CW MASS INCREASE

Model	Percentage difference	Referent point (*RP*)						
		BWC	BWD	M1T1	M1T2	M2T1	M2T2	CWC
M1	$\frac{a_{RP,\mathrm{V,max}}^{m_{\mathrm{CW,E}}} - a_{RP,\mathrm{V,max}}^{m_{\mathrm{CW,D,P}}}}{a_{RP,\mathrm{V,max}}^{m_{\mathrm{CW,D,P}}}} \times 100$	-4.8	-2.2	6.4	1.6	10.3	9.9	-5.9
M2		-4.4	4.0	8.0	2.0	9.4	12.3	-6.5

TABLE XVIII TRANSITION FROM THE 'A PRIORI' TO THE 'A POSTERIORI' STATE OF THE SS - IMPACT ON THE MAXIMUM VERTICAL ACCELERATIONS

Percentage difference	Referent point (*RP*)						
	BWC	BWD	M1T1	M1T2	M2T1	M2T2	CWC
$\frac{a_{RP,\mathrm{V,max}}^{\mathrm{M2}(m_{\mathrm{CW,E}})} - a_{RP,\mathrm{V,max}}^{\mathrm{M1}(m_{\mathrm{CW,E}})}}{a_{RP,\mathrm{V,max}}^{\mathrm{M1}(m_{\mathrm{CW,E}})}} \times 100$	1.0	3.5	2.7	5.9	2.3	2.8	-0.6

TABLE XIX DEVIATION OF MAXIMUM GENERALIZED LATERAL ACCELERATIONS CAUSED BY CW MASS INCREASE

Model	Percentage difference	Referent point (*RP*)				
		BWC	BWD	M1T1; M1T2	M2T1; M2T2	CWC
M1	$\frac{a_{RP,\mathrm{L,max}}^{m_{\mathrm{CW,E}}} - a_{RP,\mathrm{L,max}}^{m_{\mathrm{CW,D,P}}}}{a_{RP,\mathrm{L,max}}^{m_{\mathrm{CW,D,P}}}} \times 100$	3.2	-2.5	1.2	2.5	-27.0
M2		7.2	-2.3	1.3	2.2	-26.7

TABLE XX TRANSITION FROM THE 'A PRIORI' TO THE 'A POSTERIORI' STATE OF THE SS - IMPACT ON THE MAXIMUM LATERAL ACCELERATIONS

Percentage difference	Referent point (*RP*)				
	BWC	BWD	M1T1; M1T2	M2T1; M2T2	CWC
$\frac{a_{RP,\mathrm{L,max}}^{\mathrm{M2}(m_{\mathrm{CW,E}})} - a_{RP,\mathrm{L,max}}^{\mathrm{M1}(m_{\mathrm{CW,E}})}}{a_{RP,\mathrm{L,max}}^{\mathrm{M1}(m_{\mathrm{CW,E}})}} \times 100$	15.6	3.1	11.8	16.0	-3.1

V. CONCLUSIONS

Balancing of the BWE SS represents the final stage of the excavator's production. Conducted upon the conclusion of the first erection and before the excavator undergoes the proof of capacity and the test run, the outcome of this procedure significantly affects the exploitation behavior and the lifespan of the vital elements of the machine.

The basis for the balancing of the SS lies in the results of the experimental determination of its weight and CoG position. In the referent literature [15] and technical regulations [50] it is stated that the adjustment of the ballast is to be conducted if the obtained weight of the SS is more than 5% higher than the analytically determined weight. Based on the results of the research presented in this paper it is concluded that a noticeably smaller difference (1.7%) between the experimentally and

analytically determined SS weights has a significant impact on the position of its CoG. Results of the weighing conducted with the analytically determined mass of the CW needed for the balancing of the SS deadweight have shown that the CoG abscissas of the realized SS are considerably lower than designed (‘a priori’ model of the SS): by 323 mm for the BWB in low measuring position, 290 mm for BWB in horizontal position and 260 mm for BWB in high position. Because of this, an ‘a posteriori’ model of the SS was developed based on the experimental results, whose mass matches the experimentally determined SS mass. Validation of this model, which simultaneously yields good approximations of the abscissa (maximum absolute deviation of 6 mm) and the ordinate (maximum absolute deviation of 4 mm), was performed on the basis of the results of two weighings. Results of the calculation indicate the following facts:

- over the entire domain of the BWB inclination angle, with the CW mass of m_{CW}=0, the CoG abscissas of the SS 'a posteriori' model are significantly lower (the biggest difference occurs in the high BWB position and equals 283 mm);
- over the entire domain of the BWB inclination angle, the difference of the CoG abscissas of the ‘a priori’ and ‘a posteriori’ models of the SS rises with the increase in the CW mass;
- the biggest percentage increment in the intensity of the forces in the ropes of the BWB hoisting mechanism in the 'a posteriori' model of the SS, caused by the increased deadweight of the SS (excess mass compared to the 'a priori' model exists on the BWB substructure), equals 2.9% and occurs in the its low position;

Based on the comparative analysis of the results obtained from the 'a priori' and 'a posteriori' models of the SS, with the CW mass of $m_{CW,E}$=231.977 t, with which the excavator was deployed, the following has been concluded:

- the CoG abscissa of the 'a posteriori' SS model in the horizontal BWB position, which is relevant for the proof of stability on the BW side, is 20.1% lower, meaning that in that case the results of the static stability calculations for the 'a priori' model are not on the side of safety;
- the CoG abscissa of the 'a posteriori' SS model in the high BWB position, which is relevant for the proof of stability on the CW side, is 13.0% lower, meaning that in that case the results of the static stability calculations for the 'a priori' model are on the side of safety;
- the relative eccentricity of the vertical load on the RSB caused by the main operating loads in the 'a posteriori' SS model are 13.1% higher on the BW side and 11.5% lower on the CW side;
- the maximum RSB ball load in the 'a posteriori' SS model is 6.5% higher on the BW side and 3.9% lower on the CW side;
- the transition from the ‘a priori’ image of the SS to the state in which the excavator was put in exploitation does not have any significant impact on the values of the natural frequencies. The tenth and the twelfth natural frequencies are 1.1% and 1.0% lower, respectively, for the ‘a posteriori’ model, while all the other analyzed natural frequencies are dropping by less than 1%;
- similar conclusions may be drawn when analyzing the influence of the said transition on the maximum vertical displacements of the system referent points, where the highest deviation of the maximum vertical displacement is observed for the CWC (a rise of 0.5%);
- on the other hand, the influence of the transition from the ‘a priori’ to the ‘a posteriori’ state of the SS has an impact on the lateral displacements of the referent points which cannot be neglected, stemming from the fact that the displacements of the M1T1 and M1T2 are 8.3% higher, followed by 4.3%, 1.2% and 1.1% higher displacements of the tips of the mast 2, BWC and BWD. The maximum lateral displacement of the CWC is 2.0% lower;
- the transition from the ‘a priori’ to the ‘a posteriori’ state of the SS has the most significant effect on the vertical accelerations of the BWD, reflected on the increase by 3.5%;
- said transition has a significant negative impact on the values of maximum lateral accelerations of the BWC (increase of 15.6%) and the tips of the mast 1 (increase of 11.8%), while the BWD is slightly less affected (increase of 3.1%);
- finally, the values of maximum lateral accelerations of the tips of the mast 1 are 4.5% higher than the permitted value when the ‘a priori’ state of the SS is analyzed. Negative dynamic effects are even more pronounced for the state of the SS put in exploitation, where 16.8% higher values of the analyzed maximum accelerations are obtained.

Based on the presented, it is concluded that, upon the experimental determination of the mass and the CoG position of the SS, even in case of deviations lower than 5% to that of the designed state, it is necessary to analyze the levels of impact of the determined differences on the: (1) static stability; (2) intensities of forces in the ropes of the BWB hoisting mechanism; (3) maximum RSB ball loads; (4) dynamic response of the SS. Finally, having in mind the variety of design conceptions, dimensions and masses of the SSs in BWEs, the results of the presented research on the level of impact of the unharmonized designed and realized states cannot be generalized, but point to the necessity to form a consistent methodology for harmonizing the calculation models with the realized states of BWE SSs. In addition to BWEs, such a methodology could successfully be applied to bucket wheel reclaimers and spreaders.

ACKNOWLEDGMENT

This work is a contribution to the Ministry of Education, Science and Technological Development of Serbia funded project "Integrated research in the fields of macro, micro and nano mechanical engineering" (Contract number: 451-03-68/2020-14/200105).

The authors would like to express their gratitude to the ITO Foundation and The Joint Japan-Serbia Center for the Promotion of Science and Technology for providing the resources to conduct simulations.

REFERENCES

[1] Coal industry across Europe, 7th ed. Brussels: EURACOAL AISBL - European Association for Coal and Lignite, 2020.

[2] Production of electricity. Belgrade: Electric Power Industry of Serbia (EPS), http://www.eps.rs/eng/Poslovanje-EE.

[3] Energy sector development strategy of the Republic of Serbia for the period by 2025 with projections by 2030. Belgrade: Ministry of Mining and Energy, 2016.

[4] H. Hartman and J. Mutmansky, Introductory mining engineering, 2nd ed. Hoboken, New Jersey: John Wiley & Sons, 2002.

[5] M. Pantelić, S. Bošnjak, M. Misita, N. Gnjatović, and A. Stefanović, "Service FMECA of a bucket wheel excavator", Eng. Fail Anal., Vol. 108, article number104289, 2020.

[6] B. Schlecht, Investigation and optimization of the dynamic behavior of bucket wheel drives (Final report of the research project 16575 BR funded by the Federal Ministry for Economic Affairs and Energy of Germany). Dresden: Technische Universität IMM, 2014.

[7] E. Rusiński, J. Czmochowski, P. Moczko and D. Pietrusiak, Surface Mining Machines - Problems of Maintenance and Modernization. Cham: Springer International Publishing AG, 2017.

[8] S. Bošnjak, Z. Petković, N. Zrnić and S. Petrić, "Mathematical modeling of dynamic processes of bucket wheel excavators", in Proceedings of the 5th MATHMOD. Vienna: ARGESIM–Verlag, 2006, pp. 4.1-4.10.

[9] S. Bošnjak, N. Zrnić and Z. Petković, "Bucket wheel excavators and trenchers–computer added calculation of loads caused by resistance to excavation", in Machine Design, S. Kuzmanović, Ed. Novi Sad: University of Novi Sad, 2008, pp. 121-128.

[10] S. Bošnjak, Z. Petković, N. Zrnić, G. Simić, and A. Simonović, "Cracks, repair and reconstruction of bucket wheel excavator slewing platform", Eng. Fail Anal., Vol. 16, Issue 5, pp. 1631-1642, 2009.

[11] S. Bošnjak, N. Zrnić, V. Gašić, Z. Petković and A. Simonović, "External load variability of multibucket machines for mechanization", Adv. Mater. Res., Vol. 422, pp. 678-683, 2012.

[12] S. Bošnjak, M. Arsić, N. Zrnić, M. Rakin and M. Pantelić, "Bucket wheel excavator: Integrity assessment of the bucket wheel boom tie-rod welded joint", Eng. Fail. Anal., Vol 18, Issue 1, pp. 212-222, 2011.

[13] S. Bošnjak, M. Arsić, S. Savićević, G. Milojević and D. Arsić, "Fracture analysis of the pulley of a bucket wheel boom hoist system", Eksploat. Niezawodn., Vol 18, No. 2, pp. 155-163, 2016.

[14] S. Bošnjak, N. Gnjatović, S. Savićević, M. Pantelić and I. Milenović, "Basic parameters of the static stability, loads and strengthof the vital parts of a bucket wheel excavator's slewing superstructure", J. Zhejiang. Univ.-Sc. A, Vol. 17, Issue 5, pp. 353-365, 2016.

[15] W. Durst and W. Vogt, Bucket Wheel Excavator. Clausthal-Zellerfeld: Trans Tech Publications, 1988.

[16] D. Dudek, "Experimentelle Ermittlung der Stabilitat von Maschinen auf Schienenfahrwerken", Fördern und Heben, Vol. 40, No. 8, pp. 546-548, 1990.

[17] P. Maslak, G. Przybylek and T. Smolnicki, "Comparison of selected methods for the determination of the center of gravity in surface mining machines", in Materials Today: Proceedings, Vol. 4, No. 5 (part 1), pp. 5877-5882, 2017.

[18] N. Nan, I. Kovacs, I. and F. Popescu, "Balance control by weighting and tensiometric measurements of bucket wheel excavators", in WSEAS Transactions on Systems and Control, Vol. 3, No. 11, pp. 927-938, 2008.

[19] T. Smolnicki and M. Stańco, "Determination of Centre of Gravity of Machines with the Rail Undercarriage", Sol. St. Phen., Vol. 165, pp. 359-364, 2010.

[20] T. Smolnicki, M. Stańco and D. Pietrusiak, "Distribution of loads in the large size bearing – problems of identification", Teh. Vjesn., Vol. 20, No. 5, pp. 831-836, 2013.

[21] T. Smolnicki, G. Pękalski, J. Jakubik and P. Harnatkiewicz, "Investigation into wear mechanisms of the bearing raceway used in bucket wheel excavators", Arch. Civ. Mech. Eng., Vol. 17, Issue 1, pp. 1-8, 2017.

[22] P. Jovančić, D. Ignjatović, M. Tanasijević and T. Maneski, "Load-bearing steel structure diagnostics on bucket wheel excavator, for the purpose of failure prevention", Eng. Fail. Anal., Vol. 18, Issue 4, pp. 1203-1211, 2011.

[23] S. Bošnjak, N. Zrnić, D. Momčilović, N. Gnjatović and I. Milenović, "Tie-rods of the Bucket Wheel Excavator Slewing Superstructure: A Study of the Eye Plate Stress State", Eng. Struct., Vol. 207, article number 110233, 2020.

[24] E. Rusiński, S. Dragan, P. Moczko and D. Pietrusiak, "Implementation of experimental method of determining modal characteristics of surface mining machinery in the modernization of the excavating unit", Arch. Civ. Mech. Eng., Vol.12, Issue 4, pp. 471-476, 2012.

[25] D. Pietrusiak, P. Moczko and E. Rusiński, "Recent achievements in investigations of dynamics of surface mining heavy machines", in Proceedings of the 24th World Mining Congress. Rio de Janeiro: IBRAM, 2016, pp. 295-308.

[26] D. Pietrusiak, "Evaluation of large-scale load-carrying structures of machines with the application of the dynamic effects factor", Eksploat. Niezawodn., Vol. 19, No. 4, pp. 542-551, 2017.

[27] D. Pietrusiak, P. Moczko and E. Rusiński, "World's largest movable mining machine vibration testing - numerical and experimental approach", in Proceedings of International Conference on Noise and Vibration Engineering (ISMA2016) and International Conference on Uncertainty in Structural Dynamics (USD2016). Leuven: Katholieke Universitet Leuven,2016, pp. 2287–2299.

[28] P. Moczko and D. Pietrusiak, "Experimental–numerical method for assessing the condition of opencast mining and material handling equipment", Aust. J. Struct. Eng., vol. 20, issue 4, pp. 248-258, 2019.

[29] P. Moczko, D. Pietrusiak and E. Rusiński, "Material handling and mining equipment - International standards, recommendations for design and testing", FME Trans., Vol. 46, No. 3, pp. 291-298, 2018.

[30] P. Jovančić, D. Ignjatović, T. Maneski, D. Novaković and Č. Slavković, "Diagnostic procedure of bucket wheel and boom computer modeling – A case study: Revitalization bucket wheel and drive of BWE SRs 2000", in Proceedings of the 14th International Scientific Conference: Computer Aided Engineering. CAE 2018, Lecture Notes in Mechanical Engineering, E. Rusiński and D. Pietrusiak, Eds. Cham: Springer, pp. 310-318, 2019.

[31] A. Brkić, T. Maneski, D. Ignjatović, P. Jovančić and V. Spasojević Brkić, "Diagnostics of bucket wheel excavator discharge boom dynamic performance and its

reconstruction", Eksploat. Niezawodn., Vol. 16, No. 2, pp. 188-197, 2014.

[32] J. Gottvald, "The calculation and measurement of the natural frequencies of the bucket wheel excavator SchRs 1320/4x30", Transport, Vol. 25, No. 3, pp. 269-277, 2010.

[33] S. Bošnjak, N. Gnjatović and I. Milenović, "From 'a priori' to 'a posteriori' static stability of the slewing superstructure of a bucket wheel excavator", Eksploat. Niezawodn.,
Vol. 20, No. 2, pp. 190-206, 2018.

[34] N. Gnjatović, S. Bošnjak and N. Zrnić, "Spatial Reduced Dynamic Model of a Bucket Wheel Excavator with Two Masts", in Proceedings of the 14th International Scientific Conference: Computer Aided Engineering. CAE 2018, Lecture Notes in Mechanical Engineering, E. Rusiński and D. Pietrusiak, Eds. Cham: Springer, pp. 215-235, 2019.

[35] S. Bošnjak, D. Oguamanam and N. Zrnić, "On the dynamic modeling of bucket wheel excavators", FME Trans.,
Vol. 34, No. 4, pp. 221-226, 2006.

[36] S. Bošnjak and N. Gnjatović, "The influence of geometric configuration on response of the bucket wheel excavator superstructure", FME Trans., Vol. 44, No. 3, pp. 313-323, 2016.

[37] N. Gnjatović, S. Bošnjak and A. Stefanović, "The dependency of the dynamic response of a two mast bucket wheel excavator superstructure on the counterweight mass and the degree of Fourier approximation of the digging resistance", Arch. Min. Sci., Vol. 63, No. 2, pp. 491-509, 2018.

[38] N. Gnjatović, S. Bošnjak and I. Milenović, "The influence of incrustation and chute blockage on the dynamic behaviour of a bucket wheel excavator slewing superstructure", J. Theor. Appl. Mech., Vol. 58, No. 3, pp. 573-584, 2020.

[39] S. Bošnjak, D. Oguamanam and N. Zrnić, "The influence of constructive parameters on response of bucket wheel excavator superstructure in the out-of-resonance region", Arch. Civ. Mech. Eng., Vol. 15, Issue 4, pp. 977-985, 2015.

[40] S. Bošnjak, N. Gnjatović, Z. Petković, I. Milenović and A. Stefanović, "Determination of the static stability parameters of the superstructure of the bucket wheel excavator SchRs 1600 deployed in the open pit mine Tamnava West Field", comissioned by the Mining Basin "Kolubara", Belgrade: University of Belgrade-Faculty of Mechanical Engineering, 2015.

[41] BWE SchRs 1600: Final stability calculation-Rev 1. ThyssenKrupp Fördertechnik, 2009.

[42] BWE SchRs 1600: Weighing report No. 01/10. Vreoci: Kolubara-Metal, 2010.

[43] BWE SchRs 1600: Weighing. ThyssenKrupp Fördertechnik, 2010.

[44] BWE SchRs 1600: Weighing report No. 02/10. Vreoci: Kolubara-Metal, 2010.

[45] BWE SchRs 1600: Preliminary stability calculation-Rev 1. ThyssenKrupp Fördertechnik, 2007.

[46] DIN 22261-2: Excavators, spreaders and auxiliary equipment in opencast lignite mines – Part 2: Calculation principles. Berlin: Deutsches Institut für Normung, 2016.

[47] N. Gnjatović, S. Bošnjak, I. Milenović and A. Stefanović, "Bucket wheel excavators: Dynamic response as a criterion for validation of the total number of buckets", Eng. Struct., Article in Press, 2020.

[48] Rasper L. The Bucket Wheel Excavator Development Design Application. Clausthal-Zellerfeld: Trans Tech Publications; 1973.

[49] Volkov DP, Cherkasov VA. Dynamics and strength of multi-bucket excavators and stackers (in Russian). Moscow: Mašinostroenie; 1969.

[50] AS4324.1: Mobile equipment for continuous handling of bulk materials Part 1 - General requirements for the design of steel structures. Sydney: Standards Australia, 1995.

THE 5th INTERNATIONAL CONFERENCE
MECHANICAL ENGINEERING IN XXI CENTURY

December 9-10, 2020
Faculty of Mechanical Engineering in Niš, Serbia

Access to Measuring and Balancing of Enterprise's Key Performance Indicators

Rado MAKSIMOVIC

University of Novi Sad, Faculty of Technical Sciences
rado@uns.ac.rs

***Abstract*— Measuring performances business processes nowadays, has become routine practice in enterprises that have adopted quality management system according to ISO 9001 standard requests, since that is one of key requests of that standard. On the other hand, in a recent scientific literature the term "Key Performance Indicators (KPIs)" is introduced, primarily as a tool for enterprise's market performance analysis. However, reviewing the mentioned literature as well as insight in practical use in the enterprises have shown that measuring and analyzing enterprise's performances doesn't have systematic approach, and that there is a large number of different models in use. Rarely, one can find business field where Key Performance Indicators model has been brought to the level of standardization. This paper is about establishing comprehensive, systematic model of enterprise's performances identification and their measuring methods through appropriate key indicators, according to the existing models, a step forward was made in terms of suggesting the way of reaching satisfying level of performances balance, by putting them into Balanced Scorecard. The method of constant monitoring over the performances is implied (over their indicators), as well as the case study.**

***Keywords*— Enterprise, Performance, Key Performance Indicators, Balanced Scorecard, Monitoring**

I. Introduction

Today, enterprise performance indicators are defined as Key Performance Indicators (KPIs) and represent measures that reflect the company's performance based on quantified objectives.

KPIs are used in intelligent business to assess the real situation in the company and determine the basic directions of management in the future. In addition to numerical, they include "difficult to measure" quantities such as the benefits of marketing, development and other functions or parameters that measure the characteristics of employees - innovation, charisma, commitment, helpfulness, satisfaction...

The original application of KPIs is in determining an organization's strategy and measuring progress in achieving goals (for example, when using appropriate management techniques such as the *Balanced Scorecard*).

The essential application of KPIs is reflected in the establishment of criteria for their own supervision over the characteristics - performance of the company. However, in the case when, in a certain field of activity, these indicators are brought to the level of standardization, then they determine the market position - rating and basis for comparison with competing companies.

II. Performance Indicators - A brief review of the literature

The January 2004 edition of Industry Week [1, 2] includes two articles on manufacturing that include "Key performance indicators". Both articles deal with the measurement and rank measures of manufacturing industrial areas, whereby standardized measures (KPIs) and comparison criteria in the form of 3 categories have been established:

- Low performance, the company is in the "last 25%",
- Average performance as a "mediocre position", and
- High performance, the company is in the "top 25%".

Performance data and specific criteria for assessing the degree of goodness of the company are given in Tables I - VI and are recommended as an opportunity to establish "good practice in production" to assess their own results and compare with leaders in the field.

TABLE I Supply Chain Planning

Key Performance Indicators	Bottom 25%	Median	Top 25%
Cash-to-cash cycle time (days)	90	56	30
Total inventory turn rate	3.2	6.0	10.0
Production schedule attainment	77%	90%	97%
Cost of Quality - percent of annual revenues	3.1%	0.7%	0.1%

TABLE III New Product Development

Key Performance Indicators	Bottom 25%	Median	Top 25%
Percent of sales pf previous year products	10%	15%	25%
Time to market (days)	258	150	60
Products launched on budget	50%	75%	90%
Products launched on time	30%	60%	86%
Percent R&D cost for new products	3%	25%	50%

TABLE IIIII PROCUREMENT

Key Performance Indicators	Bottom 25%	Median	Top 25%
Supplier lead time (days)	28	14	7
On-time delivery	80%	90%	95%
Purchases from certified vendors (% of total spend)	40%	75%	90%
Direct materials sourced outside the country	2%	10%	25%

TABLE IVV CUSTOMER ORDER MANAGEMENT

Key Performance Indicators	Bottom 25%	Median	Top 25%
Percent of total sales orders without intervention	0.0%	15.0%	30.0%
Total annual sales orders delivered on time	85.0%	93.0%	97.5%
Percent of annual sales orders not fulfilled on tim	5.0%	2.0%	0.0%
Customer retention rate over the past three years	80.0%	90.0%	95.8%

TABLE V LOGISTICS

Key Performance Indicators	Bottom 25%	Median	Top 25%
Customer order-to-delivery time (days)	14	7	3
Supplier delivery dock-to-stock cycle time (hours)	12	4	2
Customer order pick-to-ship cycle time (hours)	10	4	2
Order fill rate	90.3%	97.7%	99.0%
Total logistics costs as a percentage of sales	10%	4.3%	2.0%

TABLE VI MANUFACTURING

Key Performance Indicators	Median	Top 25%
Average wage for production employees ($/hour)	$13.00	$15.50
Annual sales per employee	$ 150,000	$ 220,000
Raw material turns (COGS/Average raw material)	11.6	22.0
Work-in-Progress turns (COGS/Average value WIP)	16.0	38.2
Finished Goods Turns (COGS/ Average Value Finished Goods)	12.0	25.0
Total Inventory Turns (COGS/ Av. Value of Total Inventory)	8.0	13.0
Asset Turn Ratio (COGS/Average Assets)	2.5	4.0
Return on Invested Capital	13.5	25.0

The previous tables indicate the effort made to establish comparison and ranking criteria, but also the absence of a systematic approach in establishing generally applicable benchmarking rules.

As evidence of insufficient systematicity in considering key performance through standardized indicators - KPIs, Figures 1-4 show original examples of reports in the production and distribution of oil and gas [3], and Figures 5-7 in the field of education [4].

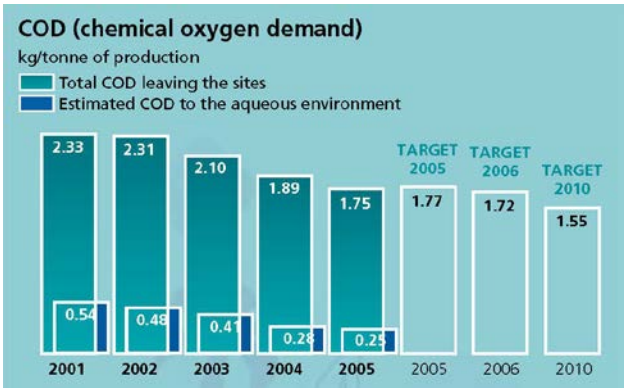

Fig. 1 KPI: COD (chemical oxigen demend)

Fig. 2 KPI: Water

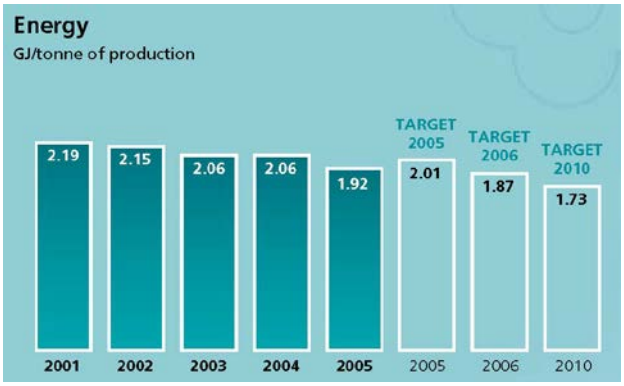

Fig. 3 KPI: Energy

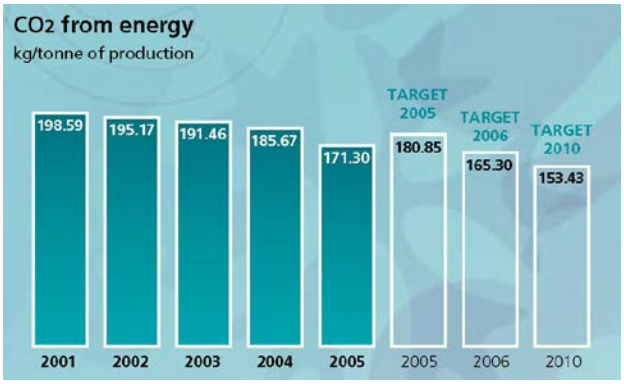

Fig. 4 KPI: CO2 from energy

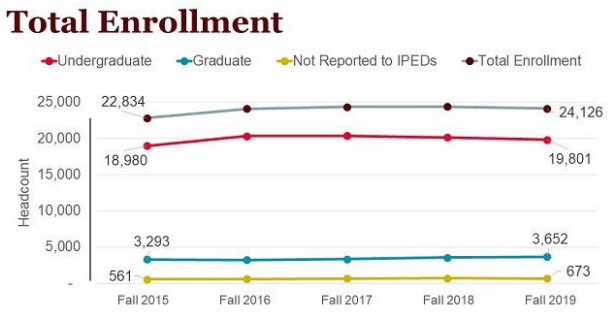

Fig. 5 KPI: Total Enrollment

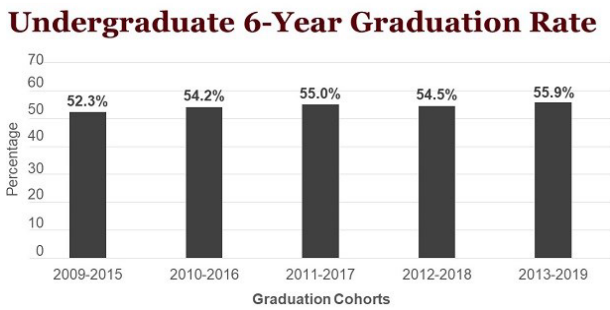

Fig. 6 KPI: Undergraduate 6-Year Graduation Rate

Fig. 7 KPI: Degrees and Certificates Awarded

Table 9 contains the "pioneering" proposal of the KPI for technical faculties in Serbia, created as a result of research on the student and teacher population [5].

The practice of establishing a system for monitoring the parameters that reflect the quality of business operations of the company is widely accepted. The main motive of the company for the establishment of such a system is the need for management structures to have and timely use data on all relevant characteristics (parameters) of individual processes and systems - the company as a whole in decision making. The term can be understood in a timely manner in terms of the need for management action online, ie in real time, but also in terms of making decisions whose effect is long-term, such as decisions on strategy selection, work program changes, investment and other similar decisions.

TABLE VIII KEY PERFORMANCE INDICATORS U OBRAZOVNOJ DELATNOSTI (PREDLOG KPI ZA TEHNIČKE FAKULTETE U SRBIJI)

No	Common indicators			
	KPI Code	Indicator name	Rank S	Rank N
1	C07	Laboratory capacities	1	1
2	C23	Availability of information on the Website	2	19
3	F03	Networking with foreign faculties	14	2
4	C17	Professional practice	3	12
5	C19	Organization of teaching	4	3
6	E01	Scope of cooperation with the economy	4	23
7	C11	Computer equipment capacities	5	8
8	D01	The volume of investment in scientific research	11	6
9	C20	Interpersonal relations	7	13
10	E02	Joint research projects with the economy	21	7
11	C18	Student research work	24	9
12	C13	Classroom capacity and equipment	12	18
13	C16	Availability of teaching staff	10	20
14	F01	Possibility of student exchange with foreign faculties	25	10
15	C22	Capacity of student services	13	15
16	C12	Library capacity	15	24
17	F02	Joint study programs with foreign faculties	18	16

No	Students				Teachers			
	KPI Code	Indicator name	Rank S	Rank N	KPI Code	Indicator name	Rank N	Rank S
1	F10	Employment in international companies	6	30	F06	International projects with foreign faculties	5	29
2	G10	Employment in regional companies	8	35	F09	Scientific papers in international journals	11	56
3	C05	The amount of funds for teaching	9	28	F04	Foreign students' interest in enrollment	14	32
4	G09	Professional practice in regional companies	16	39	F07	Visiting professors from abroad	17	31
5	E03	Trainings and courses for companies	17	31	G07	Interest in enrollment	21	30
6	C06	Possibility to use the Internet	19	26	C21	Scope of student exchange	22	28
7	C02	Possibility of employment	20	54	C09	Teaching group size	23	45
8	E04	Teacher's experience in economics	22	33	F05	Earnings from international research projects	25	54

The process of establishing a system for monitoring the parameters of the quality of business operations of the company runs separately and almost independently in different areas of activity. Despite the obvious contribution to managerial practice, it can be stated that this approach is characterized by:

- isolated comparisons of the quality of the company's business with itself in different periods, based on their own, most often subjective criteria,

- elaboration of branch criteria for a certain area of activity for the purpose of comparison with oneself in time and comparison with the average in the region, country and with the leader, based on criteria that are important for that activity,
- elaboration of systemic, general criteria for determining the competitive ability of a company.

One of the contributions is the adoption of generally valid international standards in the field of quality - ISO 9000 series standards. These standards require organizations of all types to establish and implement their own approaches to measuring and continuously improving process performance. Unfortunately, attention is focused on the quality of individual processes, ie on measures of the quality of parts of the system, and not the whole.

Theoretical basis is insufficient - there are no models for monitoring the parameters of business quality of the company which would establish a standardized System for providing Key Performance Indicators (KPIs).

The Key Performance Indicators (KPIs) system should, with its continuity of application and up-to-dateness of data, improve the approach to enterprise management, replacing the approach in which occasional "campaigns" of data collection, processing and analysis using appropriate methods and techniques provide the basis for decision making.

III. BALANCED SCORECARD - A BRIEF REVIEW OF THE LITERATURE

The lack of integrativeness of the process model of measuring the performance of the company as well as its limitation to predominantly measurable process parameters has caused saturation - a relatively limited range in improving the business characteristics of the company.

In the era of industrialization, companies created value by using physically tangible assets (land, buildings, equipment and supplies), that is, by transforming it into products. Research shows that today the book value of tangible assets is at the level of 10-15% of the market value of the company.

Today, the value of physically intangible resources is growing significantly and intangible assets are becoming the main source of competitive advantage. The most valuable intangible assets relate to consumer relations, employee skills and their knowledge and organizational culture focused on innovation, problem solving and general business improvement [6].

The decline in the relative importance of tangible assets has led to a decline in the importance of technical and financial measures of company quality and business success. The synthesized technical and financial indicators do not include intangible assets, and do not have the role of targeting profitable areas.

The system, which complements conventional technical and financial reporting and appropriate benchmarks as drivers of future performance, was created under the name Balanced Scorecard (BSC) [7]. The results of successful global companies show that the Balanced Scorecard approach is a framework that allows the strategy to be operational - to become a day-to-day business and an ongoing process in the enterprise.

Performance measures, according to the Balanced Scorecard concept, are derived from the company's vision and strategy. Target performance and their criteria are defined from four perspectives (Fig. 8):

1. Financial perspective,
2. Customer perspective,
3. Perspective of internal processes and
4. Learning and development perspective.

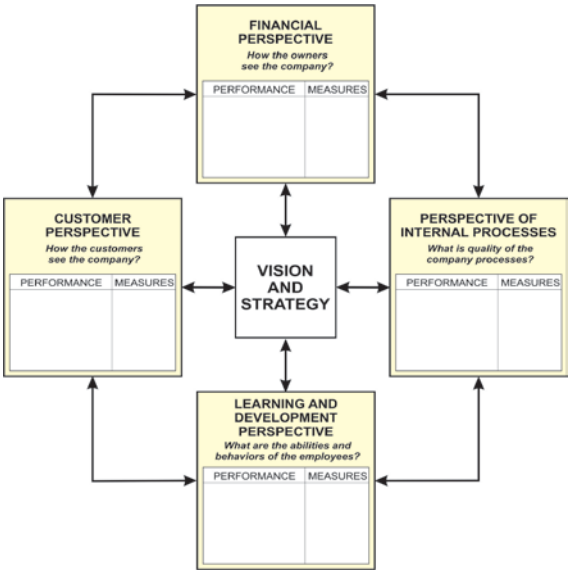

Fig. 8 Perspectives of the Balanced Scorecard concept

The Balanced Scorecard concept, viewed as a tool to ensure the necessary and sufficient performance of the company, contains, as shown in Figure 6, the following basic elements:

a) BASIS, which comes down to strategic planning for the future of the company, determined by their mission. The mission and basic values that the company's employees believe in are information that describes the projected position of the company in the future - the vision.

Vision is the basis for formulating a company's strategy. Clearly set target performance and their benchmarks (via BSC) are the basis for identifying strategic initiatives and decisions that translate into business plans. In this way, the translation of the mission into concrete, projected outcomes is ensured: satisfied owners and consumers, effective processes, trained and motivated employees. The process is shown in Fig. 9.

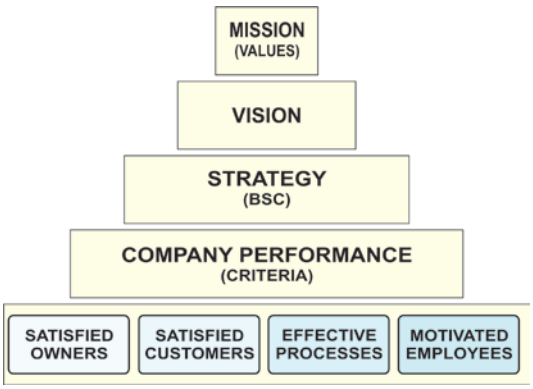

Fig. 9 The basis of the Balanced Scorecard concept

b) PERSPECTIVES, which should provide the management structure (company management) with data and information on the following elements:

b.1) FINANCIAL PERSPECTIVE

Creating value for owners is an outcome that any business strategy should achieve. A comprehensive, long-term indicator of success, such as Economic Value Added - EVA, is usually chosen. This is followed by cash return on investments, various variations of discounted cash flow, etc. However, regardless of the measure of financial success, companies increase their economic value through two approaches: revenue growth and increased productivity, which opens a very wide space for choosing the right financial parameters - performance and measures - criteria for success.

***Note**: It is necessary to emphasize, however, that the "financial perspective" of business can be viewed more broadly, not only from the point of view of business owners, especially when the BSC approach is used in the analysis of business of special types - public, state and similar. Then, other indicators of success can be included in this perspective - oriented to knowledge about the general benefit of the company for the wider environment - society. In that sense, the perspective marked as "financial", in the analysis of the quality of the company's performance, is extended to a set of general business indicators (success) of the company for which Top Management is in charge.*

b.2) CUSTOMER PERSPECTIVE

It consists in evaluating the relationship between companies and customers/users of products and services, which is a first-class task of marketing and commercial functions.

Success indicators in these areas are reflected in the quality of market-related elements of the strategy in general terms - market participation and feedback related to orientations in terms of quality and volume of exchange, development of work programs and/or entry into new markets, as well as operational relations - measured by the current volume and value of exchange and, in particular, the satisfaction of customers (users, consumers) of products and services.

"Customer perspective" is built into many approaches that deal with the problem of company success - marketing mix, leadership, "differentiation", cost leadership and others, and is certainly in the first place in the process model of measuring company performance.

In that sense, the "customer perspective", in the analysis of the quality of the company's performance, refers to the set of business (success) indicators for which the functions of marketing and commercial business are in charge.

***Note**: It is necessary to note, however, that the "consumer perspective", although one of the most important sets of information about the company, in the concept of BSC unjustifiably stands out from the other side of the market relationship - and that is the supplier market. It must be borne in mind that the enterprise-environment relationship is integral and that relations with suppliers of materials and services must be placed on the same level of importance as relations with customers / users / consumers.*

B.3) PERSPECTIVE OF INTERNAL PROCESSES

This perspective, in the original form of the BSC concept, is defined in a simplified way - as a common way of controlling the parameters of individual processes, primarily referring to operational processes. In some, less economically based interpretations, this perspective extends to notions of the type:

- Innovation processes (invention, product development, speed of delivery to the market),
- Consumer management processes (solution development, customer service, customer relationship management, advisory services),
- Operational processes (supply chain management, production efficiency, cost reduction, quality improvement, reduction of production cycle time, better capacity management),
- Processes related to the regulatory environment (health, safety, ecology and society).

***Note**: It is obvious that many "interpreters" of the BSC concept intend to "bypass the problem" of the quality of internal processes in the company instead of solving it!!! It is clear that the aforementioned set of enterprise quality parameters cannot be interpreted as dependent and less significant, and especially not as a non-systemically determined structure of "process characteristics" which is beyond the basic idea of "balance of parameters and indicators" of an enterprise. Therefore, the parameters of individual processes - far more broadly defined in the process approach to measuring the performance of the company, are the basis for integration into the general model of this type.*

b.4) LEARNING AND DEVELOPMENT PERSPECTIVE

Theoretically the least processed, and therefore especially challenging area of the BSC concept is the stated perspective. This perspective, in the original sense, defines the following three categories of intangible assets that are necessary for the implementation of the company's strategy:

- Strategic competencies: skills and knowledge - the ability of employees to support strategy,
- Strategic technologies: information system, databases - necessary to support the strategy,
- Organizational climate: cultural changes that will provide motivation and authority to employees to implement the strategy.

***Note**: Considerations regarding the perspective of the quality of the company's internal processes have indicated the unsystematic interpretation of the original BSC concept. Strategic technologies, information system, databases and support technologies are additionally and completely unjustifiably included in the perspective of "learning and development". It is necessary, in order to create a real innovative climate in the company, to isolate these concepts of a technical nature from the approach to knowledge management and the parameters of organizational and cultural behavior of employees in the company.*

c) APPLICATION OF BSC MODEL

Practical implementation of Balanced Scorecard concept, suggests the need to adjust to the nature and characteristics of the case (the area of business, size of company etc.), as shown in Fig. 10.

In the practical implementation of the application of Balanced Scorecard concept is necessary to identify key performance indicators for companies in all four areas of observation, with clearly outlined need that measures of these areas of observation are standardized to a level that ensures the needs of company - without "burdening" with the concepts of financial, technical or nonfinancial.

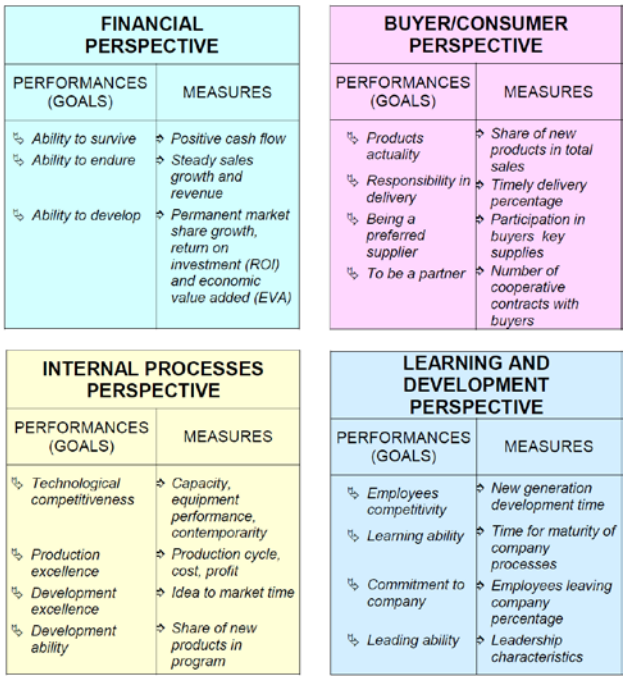

Fig. 10 Development of the Balanced Scorecard concept - adapted [7]

IV. PROCESS MODEL OF ENTERPRISE'S PERFORMANCE MEASUREMENT

The quality management system, according to the requirements of international standards in the field of quality - ISO 9000, is based on a process approach in management, which requires:

- identification of all processes that have an impact on the quality of products and business as a whole,
- determining the necessary documented information for the functioning of the process,
- determining the objectives of the process and the limits of tolerances,
- determining the necessary resources for the functioning of the process - documentation, human and infrastructural,
- defining process performance - as a basis for monitoring the functioning of the process and
- defining measured values (criteria) - the limit of permissible deviations as a basis for evaluating the quality of the process.

The process analysis methodology is based on the definition that a process is a set of interrelated activities that convert input elements into outputs using appropriate resources (Fig. 11).

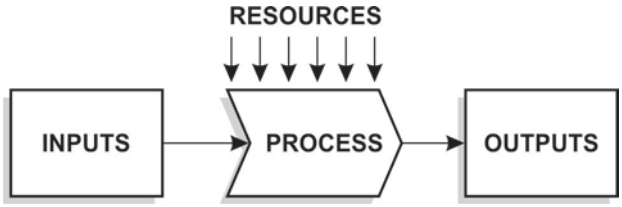

Fig. 11 Basic process definition

Different techniques can be used for a detailed analysis of process performance. A suitable tool is the "process map" which contains basic information about the process necessary for later detailed elaboration of the rules of process implementation according to the ISO 9001 standard.

V. CASE STUDY - APPLICATION OF KEY PERFORMANCE MODEL IN AN INDUSTRIAL COMPANY

Model for the measurement of key performance indicators is applied on the real example of a complex industrial company with different areas of activity for a period of one year [8].

Structure of the identified processes in the analysed complex industrial company is shown in Table IX.

TABLE IX PROCESSES IN A GIVEN COMPLEX COMPANY

Process of Planning and analysis
Process of Human Resource Management
Process of business legal regulation
Process of quality insurance
Process of marketing
Process of sales
Process of supply
Process of finance and accounting
Process of developing products and services
Process of applying IT
Process of production of bauxite
Process of production of non-metals
Process of production of construction materials
Process of machine production
Process of processing of agricultural products
Process of freight traffic
Process of long-distance traffic
Process of passenger traffic
Process of construction services
Process of catering services
Process of storing
Process of maintenance
Process of managing measuring equipment
Process of employees safety
Process of securing buildings and property

A. *Process model of performance measurement*

In this Case Study is applied the highly accepted in the literature, *technique - „mapping process“*. In this sense, the *map of key performances of process* was used for conducting the process analysis, checking developed model for measuring of the key performance indicators of the company, in this case, for all internal process. In continuation presented are developed map of the key

performances for the supply process selected as an example, shown at Figure 12. For selected process in the company the following key performance indicators of the processes were defined:

- *IQN* - Index of quality of supply;
- *IZP* - Index of submission of requests for offer;
- *IPO* - Index of submission of supplier's offer;
- *IZN* - Index of supply delays.

QUALITY PROCESS CHARACTERISTICS 330 - SUPPLY

Index of quality of supply

$$IQN = 101 - \frac{\sum_{i=1}^{3} F_{ti} \times n_i}{N}$$

where:

IQN – an index of quality of products purchased in this period;

F_{ti} – factor of the input supply products in relation to their quality;

n_i – number of deliveries to the same factor of significance for a fixed quality;

N – total number of incoming product deliveries in the period;

F_{ti}	Delivery quality
1	For deliveries done without or with minor deficiencies
50	For deliveries done with significant deficiencies
100	For rejected deliveries

Index of submission of requests for offer

$$IZP_n = 100 - \frac{\sum_{i=1}^{n} DZP_i - DZN_i}{N} \times 10[\%]$$

where:

IZP_n – an index for offer request submitted;

DZP_i – date for offer request for supplier, observed in certain period;

DZN_i – date of procurement request that correspond to DZP_i;

N – total amount offer requests observed in certain period;

Index of submission of supplier's offer

$$IPO_n = 100 - \frac{\sum_{i=1}^{n} DP_i - DZP_i}{N} \times 10[\%]$$

where:

IPO_n – an index for providing offer;

DP_i – date of supplier's offer observed in certain period;

DZP_i – offer request date that correspond to DP_i;

N – total amount of offers observed in certain period;

Index of supply delays

$$IZN_n = 100 - \frac{UVI_n^1}{N} \times 100[\%]$$

where:

IZN_n – an index for delayed procurements;

UVI_i^1 – the number of delayed deliveries in certain period;

DZP_i – date of offer request that correspond to DP_i;

N – total amount of deliveries in the observed period;

Data sources

Index of quality of supply	Index of submission of requests for offer	Index of submission of supplier's offer	Index of supply delays
F_{ti}, n_i, N: Supply realization record	DZP_i, DZN_i, N: Supply realization record	DP_i, DZP_i, N: Supply realization record	UVI_i^1, N: Supply realization record

PROCESS GOALS MEASURING RESULTS 330 - SUPPLY

Process characteristics					
IQN	IZP_n	IPO_n	IZN_n		
68	52	75	68	Process characteristics values	
≤ 100	≤ 100	≤ 100	≤ 100	10	Process characteristics rating scale
≤ 90	≤ 90	≤ 90	≤ 90	9	
≤ 80	≤ 80	**≤ 80**	≤ 80	8	
≤ 70	≤ 70	≤ 70	**≤ 70**	7	
≤ 60	**≤ 60**	≤ 60	≤ 60	6	
≤ 50	≤ 50	≤ 50	≤ 50	5	
≤ 40	≤ 40	≤ 40	≤ 40	4	
≤ 30	≤ 30	≤ 30	≤ 30	3	
≤ 20	≤ 20	≤ 20	≤ 20	2	
≤ 10	≤ 10	≤ 10	≤ 10	1	
7	6	8	7	Grade O	
3	2	2	3	Ponder P	
21	12	16	21	Points = OxP	
Total points				70	
30	20	20	30	100% max goal value	
Goal accomplishment percentage				70%	

Fig. 12 Map of key performance of supply process

Information system provides an overview of the process KPI´s in a defined time period (month, quarter, year), including the possibility of obtaining review of the process, organizational units, employee and business partner. The system limit the reviewing of information in accordance with the authorization of a system user, through the personalization of content.

The user accesses the system, the system performs its identification, records user's activity, and then takes the appropriate data from the business processes records based on them calculates KPI´s for the corresponding processes. Finally, the system displays the process performance to the user.

In figures 13-18 are shown the obtained key performance indicators of supply and selling processes for observed company, the sample in year 2014 [9].

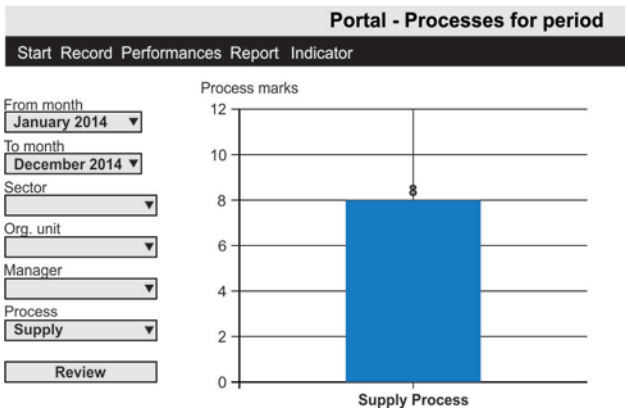

Fig. 13 Valuation of the supply process for the year 2014

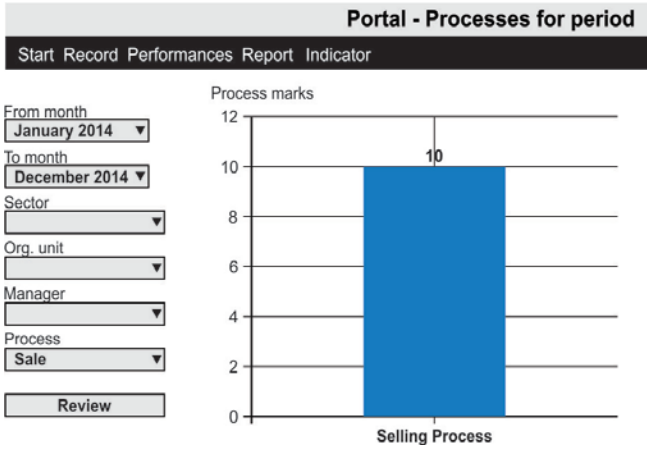

Fig. 14 Valuation of the selling process for the year 2014

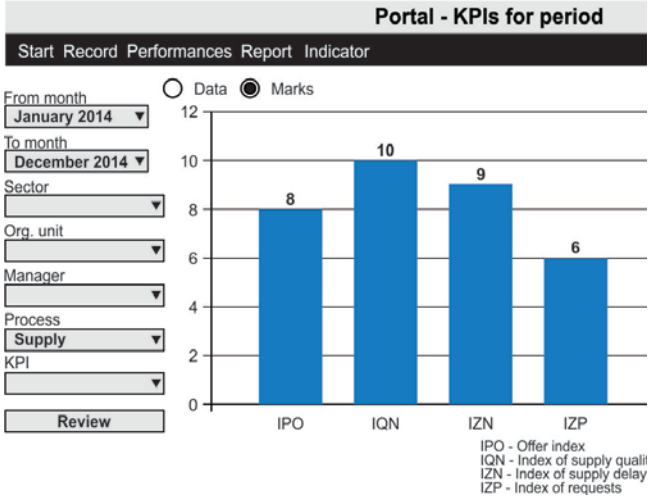

Fig. 15 Data of KPI´s supply process for the year 2014

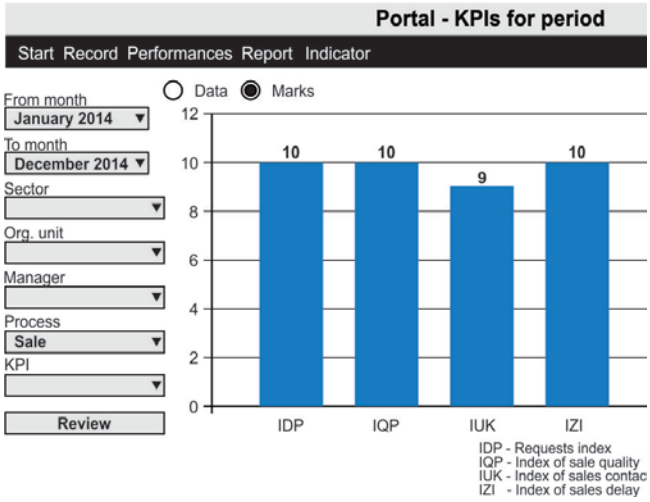

Fig. 16 Data of KPI´s selling process for the year 2014

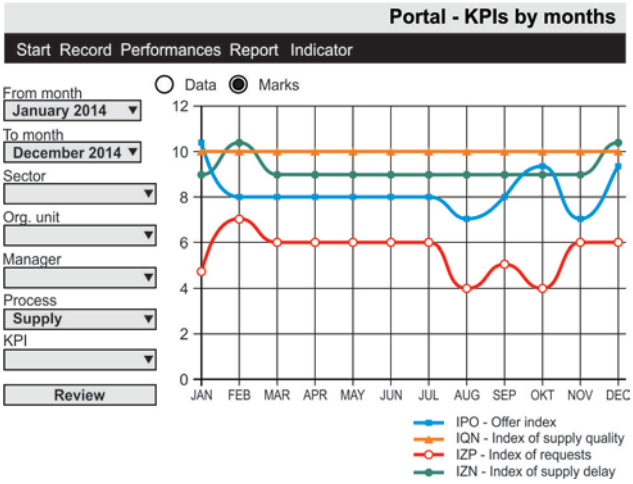

Fig. 17 Valuation of the supply process for period Jan. - Dec. 2014

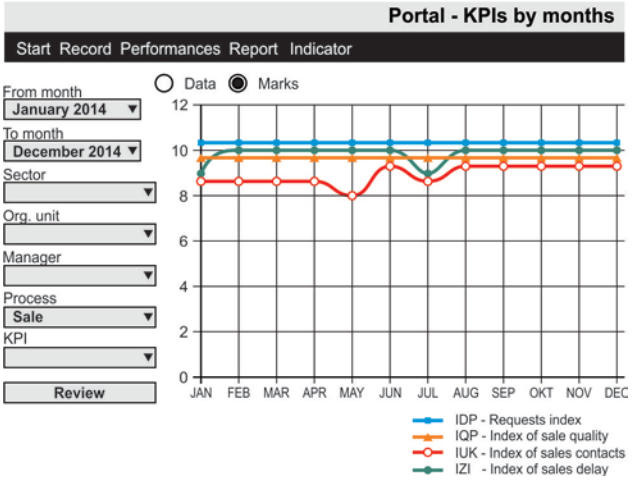

Fig. 18 Valuation of the selling process for period Jan. - Dec. 2014

Analyses of the presented results of measuring the supply and selling processes goals in the sample industrial company indicate the state of performances of individual processes, and they are used as input for the process of reviewing the company effectiveness by the management, which secures information for improving the performances of the company as a whole. Practically, the analysis of measurement the process goals allows the identification of *"critical points"* in each process based on lower of key performance indicators of the process, and then it allows comparing to the planned and the performance of competing companies, so as to thereby identify areas for process improvement. Analysis of the results provides possibility to establish the root causes of existing or potential problems, and thus represents a source for initiating corrective and preventive measures.

Availability of information indicating the status of the process directly or indirectly, as already noted, is the requirement for taking action to improve process performance.

B. Balance Scorecard in a real industrial enterprise

In this industrial company a system of managing performance and goals is established, i.e. a system for making, measuring and control of achieving the goals.

Access to concretization of key performances of the process in case of joint-stock company (Fig. 19) [8], is based on experiences in the application of process approach according to ISO 9000 standards.

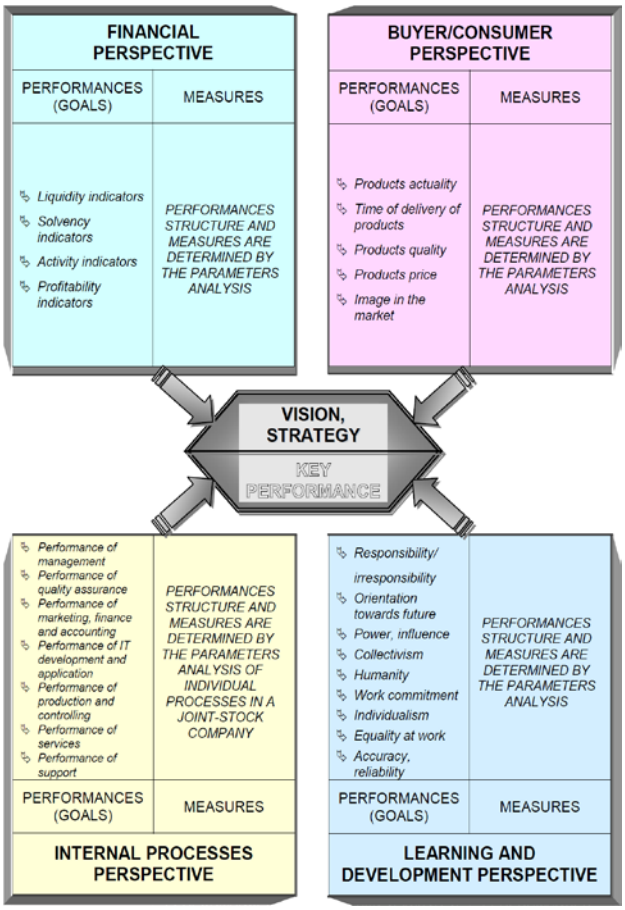

Fig. 19 The balanced scorecard concept adapted to the joint-stock company

C. *A new view at the "learning and development perspective"*

There are different interpretations of the "learning and development perspective" in the application of the BSC approach to balanced monitoring of key indicators of enterprise quality: from simple considerations related to the number and structure of employees in the company and the related problem of "degree of utilization - burden" of employees, to the analysis of data and information related to innovation, intellectual capital and other, significant indicators, which are indicators of the quality of "internal processes" in the company.

Given the marked inconsistency in literature sources and in practical applications, the approach was accepted that "learning and development perspectives" essentially signify the quality of a company's human resources.

In this sense, the defined performance of the company seen from the "perspective of learning and development" shown in Figure 14, harmonized with the eleven-year research of the so-called. cultural dimensions carried out within the world-renowned "GLOBE PROJECT" [10, 11], and based on previous research by G. Hofstede, given in [12].

The basic hypothesis set in the mentioned research is that the organizational culture in the company is connected with a group of special and in a special way measurable parameters. Prostije rečeno, želi se dokazati da u različitim kulturama ne važe jednaki standardi u načinu vođenja i upravljanja nego da na ljude veliki uticaj ima kultura sredine u kojoj žive.

For the sake of comparability of results, a research method was adopted with an elaborated "tool" for research, which included determining the characteristics that "measure" the cultural dimensions and organizational behaviors of employees in the company. This tool includes nine so-called "cultural dimensions" of employees, shown in the table X.

TABLE X NINE "CULTURAL DIMENSIONS" OF EMPLOYEES

1. Power distance	**4.** Collectivism (institutional)	**7.** Gender egalitarianism
2. Uncertainty avoidance	**5.** Collectivism (in group)	**8.** Future orientation
3. Humane orientation	**6.** Assertiveness	**9.** Performance orientation

The first thing to notice is that the tool for measuring the characteristics of organizational culture has been expanded in relation to some earlier research (for example Geert Hofstede's 4 cultural dimensions), and that is because it was necessary to investigate the overall organizational culture, ie the behavior of all employees. Secondly, it can be seen that all 9 mentioned measures are descriptive - qualitative, ie non-numerical, and that was a special problem for the research procedure. A special problem is the interpretation of the mentioned terms due to the possibility of comparing the obtained results.

In order to establish an "independent tool for measuring" the dimensions of organizational behavior, a unique scale was introduced (Fig. 20) which translates the different responses related to each individual dimension into numerical data. This scale includes the translation of descriptive performance into numerical - from 1 to 7, but each number of this scale is assigned an interpretation of the respondent's answer, and this interpretation represents the degree of explicit acceptance of a particular answer - from ***1*** - *Greatly Non-Assertive* (not) to ***7*** - *Greatly Assertive* (yes). In between are the answers: ***2*** - *Somewhat Non-Assertive*, ***3*** - *Sightly Non-Assertive*, ***4*** - *Neither Assertive nor Non-Assertive*, ***5*** - *Sightly Assertive*, ***6*** - *Somewhat Assertive*.

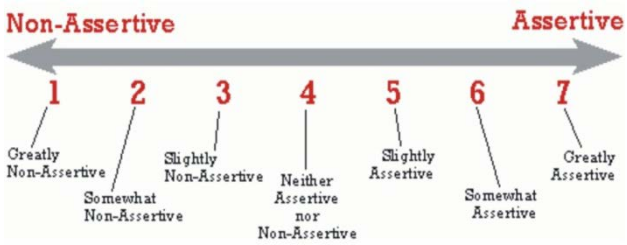

Fig. 20 Scale for translating quality employee performance into numerical expression

The described new view on the “learning and development perspective” was applied to the same company observed in the case study in this chapter. In the research, all employees in the company were surveyed, 650 of them.

A summary of all dimensions of organizational behavior for the observed company is shown in Fig. 21.

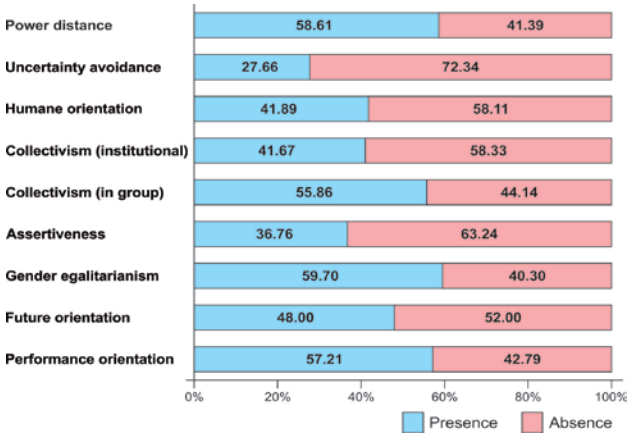

Fig. 21 Summary overview of the organizational behavior dimension in the observed company

VI. Conclusions

The survey, whose results are presented in this paper, represents a concrete contribution to the application of management methods intended for measuring the business success of complex industrial enterprise.

An important component of the developed model, which measures the success of the business by reaching the strategic goals, are the quality characteristics of processes and key performance indicators of process, which are again base for an industrial company to learn and implement changes according to the experience from the past.

Starting from the findings that have been reached in this study, it is possible to draw conclusions that point to such a solution which should ensure a way of settling problems that occur in the system of establishing and managing key performance indicators used to measure, monitor and manage business performance in the industrial company, in other words, determining the actual level of interdependence between the achieved quality of individual processes and indicators of effectiveness of the entire business enterprise. Achieving the integrity of certain perspectives or areas of the model of key performance of the industrial enterprise processes makes it possible to get insight into the important indicators of actual business results of enterprise, and determine which business processes should be improved and how to impact on their future design.

Also, research in the framework of this study have shown that it is possible to establish a standardized system of criteria - parameters (performance) of the process, which in required and sufficient measure reflect the process effectiveness and the overall success of the industrial enterprise. A general model of key process performance is developed as a suitable tool for measuring and analysis of key performance indicators of work processes in industrial enterprise.

Automating the collection and processing of necessary data and information in the company provides more accurate, more complete and more up to date information related to the manner of keeping records on the processes implementation, especially when these records are governed by appropriate procedures.

Thus, performance measurement process focuses to the short period of time, it enables analysis on time and efficient way to resolve inconsistencies with the goals of process improvement, products / services and overall company results.

Applied solutions presented in this paper directly link IT resources with business goals of the organization, helping the organization to build connections with customers and suppliers, and internal links of organizational units, allowing more accurate, more complete and more accurate information, crucial for making quality decisions, and at the same time supporting key business processes through the increased availability of information which significantly influence increasing the total effectiveness of the company.

References

[1] Drickmamer, D., TIES THAT BIND: IndustryWeekValue Chain Study revelas manufacturers' struggle to add value from product development to delivery, Industry Week, January 2004, p. 49.

[2] Drickmamer, D., TICK TOCK IW/MPI Census of Manufacturers shows challenges, reality and, yes, even optimism, Industry Week, January 2004, p. 20.

[3] 2005 Unilever Environmental and Social Report, Unilever US, Inc, USA, 2005.

[4] Missouri Department of Higher Education (MDHE), https://mis.missouristate.edu/KeyPerformanceIndicators/ (19. 10. 2020)

[5] Tasic, N., Delic, M., Maksimovic, R., Lalic, B., Cukusic, M., Selecting Key Performance Indicators in Universities – Academic perspective, Proceedings of XVII International Scientific Conference on Industrial Systems (IS'17), Novi Sad, Serbia, October 4–6, 2017, pp. 518-521.

[6] Kaličanin, Đ.: Balanced Scorecard i strategijski fokusirana organizacija - okvir za uspešnu operacionalizaciju strategije i njenu implementaciju u informatičkoj eri, Economic Annals No 158, pp. 169-187, July 2003 - September 2003.

[7] Kaplan, R. S., Norton, D. P.P.: The Balanced Scorecard - Measures that Drive performance, Harvard Business Review - HBR January-February 1992, 71-80, 1999.

[8] Djuric, Z., M., Maksimovic, R., Measuring and Analysis of the Key Performance Indicators in an Industrial Enterprise Applying Information System, Proceedings of BALCOR 2013, Belgrade & Zlatibor, 7-11 September, 2013, pp. 69-78.

[9] Tasic N., Djuric Z., Malesevic D., Maksimovic R., Radakovic N.: Automation of Process Performance Management in a Company, Technical Gazette, 2018, Vol. 25, No 2, pp. 565-572.

[10] Cornelius, N. G. G: Leadership Style Variations Across Cultures, GroveWel Global Leadership Solutions LCC, Pensylvania, USA, 2007.

[11] Cornelius, N. G. G: Worldwide Differences in Business Values and Practices, GroveWel Global Leadership Solutions LCC, Pensylvania, USA, 2007.

[12] Hofstede, G.: Cultures and Organisations: Software of the Mind, McGraw Hil, London, 1991

THE 5th INTERNATIONAL CONFERENCE
MECHANICAL ENGINEERING IN XXI CENTURY

December 9-10, 2020
Faculty of Mechanical Engineering in Niš, Serbia

Engineering Ethics in the Pandemic

Alpar LOŠONC

Faculty of Technical Sciences, University of Novi Sad, Trg Dositeja Obradovića 6, 21000 Novi Sad, Serbia
alpar@uns.ac.rs

***Abstract*— How to treat the exceptional importance of engineering ethics that is reflected in multiple forms of certain engagement? This paper is divided into three parts. The first part focuses on the explanation of why ethical reflection has penetrated deeply into engineering. The second part focuses on the analysis of certain moments during the pandemic, that is, the problematization of coevolution of technology, society, and nature. In the third, the final part, the focus is on three serious ethical dilemmas facing engineering ethics.**

***Keywords*— Engineering Ethics, Pandemic, Ethical dilemmas, Coevolutionary Crisis.**

I. The Inevitability of the Connection Between Engineering and Ethical Reflection: Why?

The engineering ethics is unequivocally in expansion in terms of covering certain topics (for example, Martin & Schinzinger [1]). Furthermore, its presence in various discourses is evident.

This process can be considered an organic part of the growing general sensitization towards ethical issues. It would be sufficient for us only to look at the way ethical reflection penetrated different domains that had not been opened earlier towards the same mode of reflection. In the past, such reflections were described as too "philosophical", "foreign" concerning the domain in question, which externally wanted to impose normative reflexivity to engineers for example. Today, ethics, as a "compulsory subject", has been introduced in the university curriculum, at various conferences, and educational programs containing appropriate articulations of non-routine moral conflicts. Various representative associations of engineers find it necessary to codify certain rules or make comments on sensitive moral issues.

This is why self-understanding of engineering is impossible today without ethical reflexivity. Engineers are also affected by numerous issues, namely "imperative of responsibility" [2].

Naturally, we can approach engineering in different ways. There are very clear and robust "engineer's influences" in the world. Ethics complicates this impact by weighing the seemingly rhetoric question [3]: how many "benefits" or disadvantages are derived from engineering? How "harmful" by-products are?

In doing so, we could analyze engineering in terms of "problem-solving", "learning and teaching design", or "expert knowledge" [4]. We can thematize engineering based on the application of "model thinking" which distinguishes between "scientific" and "engineering reasoning", whereby the first trend focuses on the scope of necessity, and engineering reasoning aims at articulation of contextual contingencies (which gives it greater "complexity" than science) [5]. However, regardless of the differences in approach to the engineering sphere, ethics remains an inevitable horizon for engineering. Ethics offers elements for orientation in the world by providing conditions for adequate assessment of our actions, intentions, results. Engineering needs both orientation and elements for evaluation (for example, for whistleblowing [6]). The more complex the world in which engineering is positioned, the need for evaluation and orientation is more growing.

At the same time, engineering is not just a part of the recent affirmation of ethical reflection; it is an immanent-constitutive element of the existing processes of ethical problems. To be more precise, the increased significance of engineering in the modern world and the diversity of its presence necessarily place engineering in the position in which ethical problems are accumulated. "Design of technological systems", "framing" of technological features, "processing of data", application of knowledge, "loop between knowledge and information", that is, everything that necessarily belongs to engineering actually represents the relationship between engineering and ethics.

The ethicization of engineering is set in the context of the contours, which we use to describe the processes of de-differentiation.1 If we take a look at today's different descriptions that are relevant to our topic, then we can identify the processes in which we notice a certain convergence between technological systems, nature, and social relations. Just a simple analysis of the correlation between the leading terms can lead to a conclusion that the same terms, mutatis mutandis, can be recognized in the mentioned domains.

I will mention just a few examples without being too exhaustive. This way, the term "indeterminatedness" is a term that has comprehensive aspects, emphasizing the possibility of seizing regularity in the world and marking the positioning of engineering: the former imagination of scientific epistemology, which involves firm determinations by the developed method, has disappeared. The result of this is the emphasized importance of "risk

[1] De-differentiation is used in different disciplines (for example, there is „cell dedifferentiation". Here, we use it in the mentioned context.

perception", the well-known "risk society", but also engineering, which is constantly involved in posing and assessing various risks with appropriate ethical consequences. This is when the necessity of a new form of ethics arises, after the "end of certainty" ([7], [8]). In fact, we would not be wrong to claim that it is this loss of certainty that significantly generates ethical reflexivity for engineering.

Furthermore, "complexity" is a term that satisfies the specified criterion; it can be found in all mentioned domains. "Complexity" was initially a framework that offered the possibility of adopting any kind of orientation, including engineering orientation as well. It reports on "structured" interaction and structurally-biased "interactive varieties" of elements within the system based on "growing diversity of interactions between human beings and between people and their technology" ([9], [10]). Some interpreters even extend the term complexity to the concept of "globality" and discuss "global complexity" or "the globality as complexity" ([11], [12]). However, a series of additional terms is linked to complexity: "emergence", "irreversibility", "contingent openness", "path dependence", "non-linear interaction", "cybernetic architectures", that is, a full register of terms that mark ethical reflexivity today. "Huge increase in the number of components within products" ([12], p. 48) is undoubtedly an engineering moment that expresses the logic of complexity, but, at the same time, it is not just an engineering phenomenon.

Therefore, it can be concluded that "complexity" represents a meta-framework for engineering: namely, it treats complexity as a subject, that is, as a material of its performance. This way, "complexity engineering" [13] has been introduced. In other words: "*complexity" is both the element of design for engineering and the element for ethical evaluations, that is, the element which cannot be ignored by any ethical orientation*.

The conclusion here is that the "coevolution" of nature and society has been the topic in ecology for a long time (especially in ecological engineering). *Engineering ethics has been in a triad of co-evolutionary processes between technological systems, social relations, and nature*.

II. Pandemic: co-evolutionary and sequential crisis

Diagnoses of social, environmental, political, and economic consequences of the pandemic are harsh, although they differ in the assessment of the extent of the seriousness of the corresponding consequences. The debates additionally focus on the question as to whether the caused changes are irreversible or not, and whether they allow *restitution in integrum* or not. The debate cannot be won for now, because there are too many uncertain factors that prevent us from drawing conclusions.

Every crisis occurs temporally from both retrospective and prospective aspects. If irreversibility is analyzed from a prospective aspect because the future consequences are assessed, then positioning the pandemic crisis backward shows the retrospective logic. Therefore, the pandemic can be categorized into certain crisis processes that had already existed; it shows the condensation of earlier tendencies. This way, we can interpret, for example, the comprehensive diagnosis of UNCTAD [14]; crisis processes revealed by the pandemic represent a certain sequence in a series of different crises. This does not mean that the pandemic does not introduce certain novelties in the perception of crisis, but it means that it is related to the already existing sequential crises which use the logic of cumulative causality or "self-enforcing" mechanisms to develop potential crises. This way, the aforementioned report of UNCTAD also draws attention to the crises of equalities/inequalities, growth/degrowth, employment/unemployment that have marked the last decades. Those are past tendencies and the pandemic is only reinforcing them. In other words, the pandemic is the part of broader processes and it can only be understood if analyzed from a broader perspective.

Naturally, the genealogy of the pandemic itself causes engineering ethics. We know there are certain competitive debates about the origin of the pandemic, but even though we have not analyzed various narratives in detail, we can accept the following logic: pandemics usually have multi-causal determinations and, as it is presented in research ([15], [16]), they are involved in natural processes, penetration in basic mechanisms of nature by creating an impact on the change in metabolism between a man and nature. It is particularly related to global pandemics that make up the whole: Covid 19 certainly represents this type of pandemic. The *present pandemic is a paradigmatic example of a co-evolutionary crisis when different tendencies are manifested at the same time*.

Therefore, according to the logic mentioned above, engineering ethics is today in the *"co-evolutionary" crisis* in technological systems, nature, and society. We would diminish the value if we were to leave out any elements of the specified triad. Penetration into nature must depend on certain modes of engineering, for example, the design of bioengineering, on the projection of involvement in nature that influenced the outbreak of the pandemic [17]. At the same time, we must not forget the original position of engineering in the configuration of social relations [18]; technological designs have never been in a "vacuum" but they have been anchored in socially profiled contexts to which engineering ethics must show sensitivity. The co-evolutionary crisis requires a multi-perspective approach to engineering ethics; it would have to analyze all three elements of the triad if it was to meet the requirements directed to it.

III. Ethical dilemmas in the time of the pandemic and engineering ethics

Understandably, the problems of the co-evolutionary crisis determine both the direction and principles of engineering ethics. However, there is a certain pattern that must be followed during the pandemic: it is *public* health or *public* "safety". In other words, a parameter that engineering ethics must also accept is the *public* sphere that needs to be reconceptualized. The top issue is the reconfiguration of togetherness in today's conditions of high economic and technical connection and, as we have already said above, in the constellation of "global complexity". Namely, following the socio-economic tendencies of the last decades, there has been the privatization of health-sustaining practice. This is, of

course, a problem in itself and a source of multiple dilemmas. The same problem applies to the phenomenon of the pandemic: the crucial moment of the pandemic is the organization of public health because it is obvious that privatization-processes do not provide adequate answers to the problems of the crisis (some countries even tried to involve private health organizations, but there were just a few cases).

Now, I would like to list three crucial ethical dilemmas that engineering ethics should not be indifferent to. In doing so, we should take into account that the roles, motivational mechanisms, goals, strategic and instrumental forms of engineer rationality are conditioned by institutional positions. Namely, engineers are situated in institutionally different contexts: there are significant differences between performance and position of "corporate manager-engineer" and singular "engineer-entrepreneur", for example. That is, we can assume that engineers have different approaches to managing pandemic.

However, what is important here is that management of pandemic represents primarily an intensive "risk-government", a constant interpretation of intensification of accumulated risks that pose threat to public health. *Engineers have an impact on the "perception of risk" that has been a focus of attention today for many professionals interested in management*. We can say that pandemic is a situation in which "risk-perception" is of significant importance but there are always question that cannot be covered by the same management.[2]

Furthermore, pandemic *exacerbates the problem of the percentage of human labor in technological dynamics*. Automation, semi-automation, robotics, and other technological systems diminish the importance of humans with problematic consequences regarding the employment. Certain discussions do complicate this simple assessment but the tendency is clear. Recent research warns us that many companies have taken advantage of the current pandemic in terms of affirming the capital-intensive technology to the detriment of workers [20]. The fact that there is an ethical dilemma for engineers can be seen for example in the following: "Amazon engineer quits after he "snapped" when the company fired workers who called for coronavirus protections" [21].

Finally, the transition towards a post-Covid state creates numerous dilemmas: competition for finding a vaccine against Covid-19 is full of ethical conflicts. The problem can in short be understood as *penetration of engineering in the integrity of human beings.* "Engineering" of human nature, which has been promised by those commanding the breakthrough of technology in genetic structure, expansion of biotechnology, and managing biotechnology, creates numerous ethically problematic situations. Engineering ethics is only at the beginning of assessing the complex and uncertain relationship between benefits and harms.

IV. Conclusion

Engineering ethics is expanding because the influence of engineering on the world is extending and the number of indirect consequences of engineering is increasing. Engineering ethics is situated in coevolution between natural determinations, societal tendencies, and technological designs. The pandemic is an expression of the co-evolutionary crisis. It is sequential because it condenses earlier crisis processes. It can be said that engineering ethics during the pandemic is confronted with all elements of the triad that frame the co-evolutionary crisis in the present epoch.

[2] For "risk perception" and "heuristics of fear" (Jonas), see [19].

References

[1] M. W. Martin, R. Schinzinger, "Ethics in Engineering". New York: McGraw-Hill, 1996.

[2] H. Jonas, "Responsibility Today: The Ethics of an Endangered Future," Social Research, vol. 43, no. 1, pp. 77-97, 1976.

[3] P. Dias, "The disciplines of engineering and history: some common ground," Sci. Eng. Ethics, vol. 20, iss. 2, pp. 539–549, 2014.

[4] H. Simon, "What We Know About Learning," Journal of Engineering Education, pp. 343-348, October 1988.

[5] P. Dias, "Philosophy for Engineering Practice, Context, Ethics, Models, Failure". Berlin: Springer, 2019, p. 4.

[6] N. Sakellariou, R. Milleron (ed.) "Ethics, Politics, and Whistleblowing in Engineering", Taylor & Francis Group, LLC, 2019.

[7] Z. Baumann, "Alone Again, Ethics After Certainty," London: Demos, 1994.

[8] I. Prigogine, "The End of Certainty". New York: The Free Press, 1997.

[9] G. M. Hodgson, "Capitalism, Complexity, and Inequality," J. Econ Issues, vol. XXXVII, no. 2, p. 473, June 2003.

[10] M. Waldrop, "Complexity". London: Penguin, 1994.

[11] N. Thrift, "The Place of Complexity," Theory, Culture & Society, vol. 16, iss. 3, pp. 31–70, 1999.

[12] J. Urry, "Global Complexity". Cambridge: Polity, 2003.

[13] R. Frei, G. Di Marzo Serugendo, "The future of complexity engineering," Cent. Eur. J. Eng., vol. 2, iss. 2, pp. 164-188, 2012. DOI: 10.2478/s13531-011-0071-0

[14] United Nations Conference on Trade and Development, "Trade and development report 2020. From global pandemic to prosperity for all: Avoiding Another Lost Decade," Report by the secretariat of the United Nations Conference on Trade and Development. Geneva: United Nations, 2020.

[15] R. G. Wallace, L. Bergmann, R. Kock, M. Gilbert, L. Hogerwerf, R. Wallace, M. Holmberg, "The Dawn of Structural One Health: A New Science Tracking Disease Emergence Along Circuits of Capital," Soc. Sci. Med., vol. 129, pp. 68–77, 2015.

[16] J. Pépin, "The Origins of AIDS Cambridge University Press, Cambridge," Cambridge, UK: Cambridge University Press, 2011.

[17] Johns Hopkins University of Medicine. COVID-19 Dashboard by the Center for Systems Science and Engineering (CSSE) at johns Hopkins University (JHU). Available online: https://coronavirus.jhu.edu/map.html/, accessed on 28 April 2020.

[18] R. Lawlor (ed.), "Engineering in Society," London: Royal Academy of Engineering, 2020.

[19] L. Cori, F. Bianchi, E. Cadum, and C. Anthonj, "Risk Perception and COVID-19," Int. J. Environ. Res. Public Health 2020, vol. 17, 3114; doi:10.3390/ijerph17093114

[20] M. Roberts, “Ending the pandemic slump – a return to Keynes?” – Michael Roberts Blog, https://thenextrecession.wordpress.com/2020/09/28/ending-the-pandemic-slump-a-return-to-keynes/, accessed, 10/6/2020.

[21] nbc.com/2020/05/04/amazon-engineer-resigns-over-companys-treatment-of-workers.html, accessed, 10/14/2020.

Energetics, energy efficiency and process engineering

THE 5th INTERNATIONAL CONFERENCE
MECHANICAL ENGINEERING IN XXI CENTURY

December 9-10, 2020
Faculty of Mechanical Engineering in Niš, Serbia

Solar Thermal Collector Efficiency Map: A New Evaluation Tool

Saša PAVLOVIĆ[a], Velimir STEFANOVIĆ[a], Evangelos BELLOS[b], Christos TZIVANIDIS[b]

[a]University of Niš Faculty of Mechanical Engineering, Niš, Republic of Serbia,
[b]National Technical University of Athens, School of Mechanical Engineering, Athens, Greece,
sasa.pavlovic@masfak.ni.ac.rs, veljas@masfak.ni.ac.rs, lmirrjana@masfak.ni.ac.rs,
ctzivan@central.ntua.gr, bellose@central.ntua.gr

***Abstract*— Abstract This work presents the new concept of the solar collector efficiency map which is a two-dimensional depiction of the solar collector performance, with thermal efficiency in the horizontal axis and exergetic efficiency on the vertical axis. More specifically, this depiction includes results for various mass flow rates and inlet temperature levels in order to give the collector performance in different operating scenarios. The goal of this depiction is to present with a simple and direct way the optimum operating area of the collectorin order for the system designers to select the proper application for using every solar technology. In the present work, the commercial parabolic trough solar collector Eurotrough is investigated, as an example, with a validated thermal model developed in EES in steady-state conditions. The optimum operating conditions were found for inlet temperatures between 450 K and 650 K, while the mass flow rate has to be over 1 kg/s, according to the developed efficiency map. This map can be used in order to determine quickly both thermal end exergyefficiency and to know in which cases the collector has to be used for thermal or electricity applications.**

***Keywords*—Efficiency map, thermal efficiency, exergetic efficiency, evaluation tool, parabolic trough collector**

I. Introduction

Solar energy is one of the best candidates among renewable energy sources. Solar thermal collectors are the devices that capture the incident solar irradiation and convert it into useful heat atvarious temperature levels. The suitable evaluation of these devices, which are usually characterized as heat exchangers, is vital for the broader adoption of this technology.

In the literature, there are numerous studies and regulations for the thermal evaluation of solar collectors which arewell-established by some decades before. Rojas et al. [1] described with details the methodology for evaluating the thermal performance of a solar collector. Moreover, the following standards are usually used: ASHRAE 93 [2], ISO 9806-1 [3] and EN12975-2 [4]. On the other hand, the exergetic evaluation of solar thermal collectors gains more and more attentionin the last years because this procedure aids in the optimization of the solar collector by minimizing the irreversibilities. This has been stated by Sciubba and Wall [5] with a deep study, as well as there are numerous studies in the literature with theexergetic evaluation of solar collectors, such asFarahat et al. [6] who examined and optimized a flat plate collector with exergetic analysis. Padillia et al. [7] examined a solar parabolic troughcollector (PTC) exergetically in various operating conditions. More specifically, they examined various inlet temperature levels, various mass flow rates and wind velocities in order to determine the optimum operating conditions forthe examined PTC. Recently, Kalogirou et al. [8] stated the importance of exergetic analysis in the solar thermal collector by giving an extended review.

However, there are not literature studies thatexamine the thermal and exergetic performance of solar thermal collectors simultaneously. The objective of this work is to present a methodology for evaluating thermal and exergetic efficiency at the same time. The efficiency map of the solar collector isintroduced as a depiction of the operation of the solar collector in all the possible operating conditions.

II. Material and Methods

First of all, it is essential to define the basic parameters of the present study which are associated with the efficiency indexes. The thermal efficiency (ηth) of the collector is defined as the ratio of the useful heat (Qu) to the available solar irradiation (Qs):

$$\eta_{th} = \frac{Q_u}{Q_s} \tag{1}$$

The exergetic efficiency (η_{ex}) can be written as the ratio of the useful exergy (E_u) to the available exergy of the solar irradiation (E_s).

$$\eta_{ex} = \frac{E_u}{E_s} \tag{2}$$

The useful exergy in a solar heating process(E_u) with liquid working fluid is written as. [9].

$$E_u = m \cdot c_p \cdot \left(T_{out} - T_{in}\right) - m \cdot c_p \cdot \ln\left[\frac{T_{out}}{T_{in}}\right] \tag{3}$$

The exergy flow of the undiluted solar irradiation (Es) is calculated by the Petela formula [10] which is the most accepted model:

$$E_s = Q_s \cdot \left(1 - \frac{4}{3} \cdot \frac{T_{am}}{T_{sun}} + \frac{1}{3} \cdot \left[\frac{T_{am}}{T_{sun}}\right]^4\right) \qquad (4)$$

The sun temperature (Tsun) can be taken equal to 5770 K, which is a representative value for the outer layer of the sun.

In this study, the module of a commercial parabolic trough collector (Eurotrough [11]) is examined for operation with Therminol VP-1[12] which is depicted in Figure 1. The developed thermal model is presented briefly in figure 2 and this model has been also used and validated in other literature studies [9, 13]. All the inputs, the outputs and the used equations are given in figure 2. The simulation tool is EES (Engineering Equation Solver) by F-Chart [14].

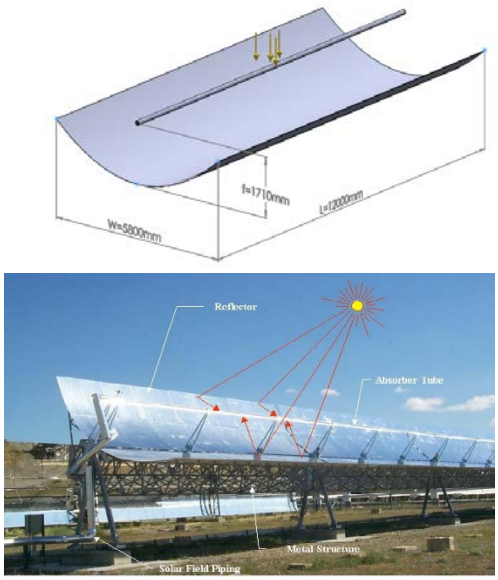

Fig. 1a and 1b - The examined module of Eurotrough PTC (CAD and real experimental setup model)[11]

In the developed model, different combinations of mass flow rates and inlettemperature levels are inserted in order to take as output the thermal and the exergetic efficiency for every case. The results firstly are evaluated with the usual techniques in figures with the usual parameter ([Tin-Tam]/Gb) in the horizontal axis. The next step is the creation of the efficiency map by using the thermal efficiency in the horizontal axis and the exergeticefficiency in the vertical axis. Also, the operation points of the same inlet temperature level are depicted in this figure. It is essential to state that the inlet temperature is ranged from 300 K to 650 K in order for the collector to operate in the allowed temperature levels. The ambient temperature is selected at 300 K, the solar beam irradiation is 800 W/m2, the solar angle is zero and the wind velocity is about 1 m/s in order to have a heat transfer coefficient between cover and ambient at 10 W/m2K. Lastly, it is important to be stated that the solar beam irradiation has been selected to be vertical to the collector aperture and the analysis was performed in steady-state conditions.

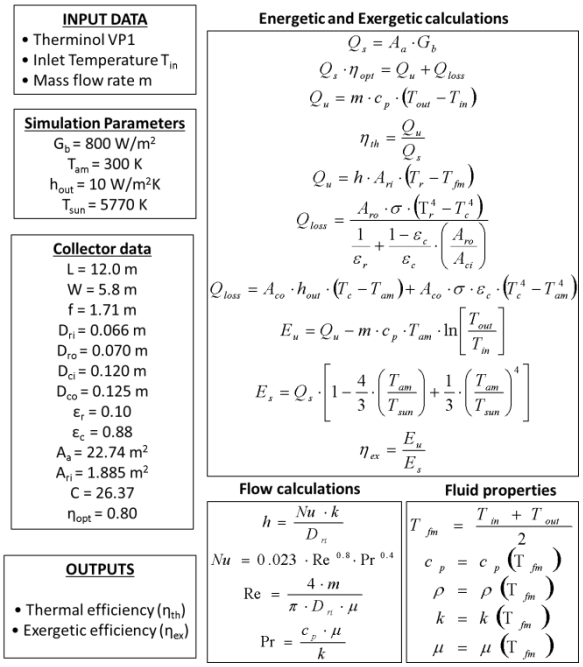

Fig. 2 - The basic mathematical equations of the present modeling and the input data

III. Results and Discussion

In this section, the results are presented in figures 3 to 5. Figure 3 shows the thermal efficiency of the solar collector and figure 4 the exergetic efficiency for the examined cases. It is obvious that a higher mass flow rate leads to higher thermal efficiency and higher inlet temperature level to lower thermal efficiency. On the other hand, greater inlet temperature leads to higher exergetic efficiency. In low temperatures, the optimum mass flow rate is the lowestexamined, while in higher temperature levels the highest examined mass flow rate is optimum.

Figure 5 is the efficiency map of the examined solar collector. This depiction is innovative and indicates the thermal and exergetic efficiency of the solar collector for all the examined cases. This depiction is similar to the “compressor map” and illustrates by a brief way the collector performance. Especially for concentrating collectors, which usually are used in power production applications or polygeneration systems, the exergetic evaluation is vital for designing sustainable systems. Observing this efficiency map, the designer can select the optimum operating area by taking into account both energetic/thermal and exergetic performance. For the present case in figure 4, the optimum area seems to be from 450 K to 550 K and for mass flow rates over 1 kg/s. Moreover, it could be said that this depiction is able to show how the increase in the exergetic efficiency is conjugated with a penalty in the thermal efficiency.So, by determining the optimum operating area of the examined collector, the system designer is able to know the applications that the examined collector has to be used.

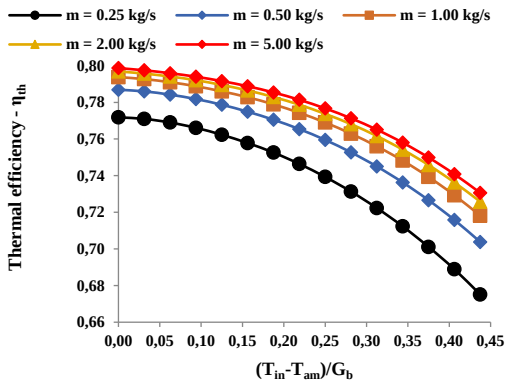

Fig.3 - Thermal efficiency of the examined solar collector

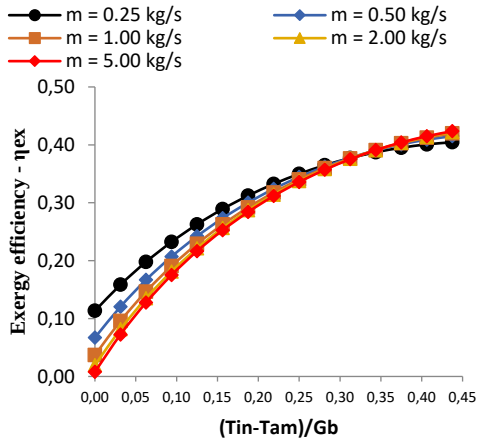

Fig.4 - Exergetic efficiency of the examined solar collector

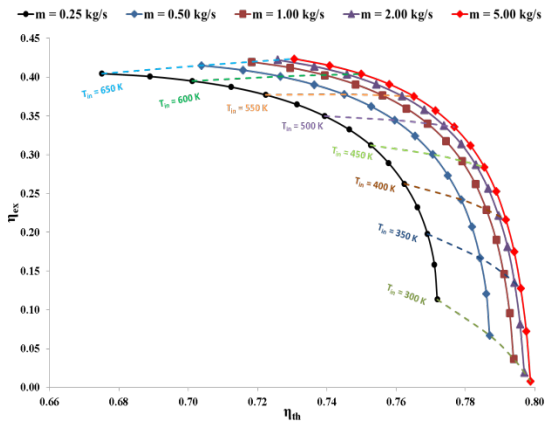

Fig.5The efficiency map of the examined solar collector

IV. Conclusion

In this paper, a new way of evaluating the efficiency of solar thermal collectors was presented. The solar collector efficiency map is this tool and it is a two-dimensional depiction of the thermal and exergetic efficiency of solar collectors. This chart aids the designer to determine quickly the optimum region and to decide the application that this collector can be used. More specifically, the cases with thermal efficiency correspond to designs for heating production (e.g. industrial heating) and the cases with high exergy efficiency correspond to applications of electricity production (e.g. Organic Rankine Cycle). For the examined solar collector (Eurotrough), the optimum operating area is estimated to be for inlet temperatures between 450 K and 550 K,whilethe mass flow rate has to be greater than 1 kg/s. In the future, the efficiency map can be extended for different values of the solar beam irradiation and the incident solar angle. Also, efficiency maps can be developed for other collector types like solar dish collectors.

Acknowledgment

This research was financially supported by the Ministry ofEducation, Science and Technological Development ofthe Republic of Serbia.

Nomenclature

A	Area, m^2
C	Concentration ratio, -
c_p	Specific heat capacity under constant pressure, J/kgK
D	Diameter, m
E	Exergy flow, W
f	Focal length, m
G_b	Solar beam radiation, W/m^2
h	Convection coefficient, W/m^2K
h_{out}	Convection coefficient between cover and ambient, W/m^2K
k	Thermal conductivity, W/mK
L	Tube length, m
m	Mass flow rate, kg/s
Nu	Mean Nusselt number, -
Pr	Prandtl number, -
Q	Heat flux, W
Re	Reynolds number, -
T	Temperature, K
W	Width, m

Greek symbols

α	Absorbance, -
ε	Emittance, -
η	Efficiency, -
μ	Dynamic viscosity, Pa s
ρ	Density, kg/m^3
σ	Stefan–Boltzmann constant [= $5.67 \cdot 10^{-8}$ W/m^2K^4]

Subscripts and superscripts

a	aperture
am	ambient
c	cover
ci	inner cover
co	outer cover
ex	exergetic
fm	mean fluid
in	inlet
loss	thermal losses
opt	optical
out	outlet
r	receiver
ri	inner receiver
ro	outer receiver
s	solar
sun	sun
th	thermal

u useful

ABBREVIATIONS

EES Engineer Equation Solver
PTC Parabolic trough collector

REFERENCES

[1] Rojas, D., Beermann, J., Klein, S.A., Reindl, D.T., Thermal performance testing of flat-plate collectors, Solar Energy 2008;82:746-757

[2] ANSI/ASHRAE Standard 93-2003, 2003. Methods of Testing to Determine Thermal Performance of Solar Collectors, ISSN: 1041-2336, ASHRAE, Inc., 1791 Tullie Circle, Ne, Atlanta, GA30329

[3] [3] ISO Standard 9806-1:1994(E), 1994. Test Methods for Solar Collectors – Part 1: Thermal Performance of Glazed Liquid Heating Collectors Including Pressure Drop, ISO, Case Postale 56, CH-1211 Geneve 20, Switzerland.

[4] [4] European Standard EN12975-2:2001. 2001. Thermal Solar Systems and Components – Solar Collectors – Part 2: Test Methods, CEN, Rue de Stasart, 36, B-1050, Brussels.

[5] [5] Sciubba E, Wall G. A brief commented history of exergy from the beginnings to 2004. Int J Thermodyn 2007;10(1):1–26.

[6] [6] Farahat, S., Sarhaddi, F., Ajam H., Exergetic optimization of flat plate solar collectors, Renewable Energy 2009;34:1169–1174

[7] [7] Padilla, R.V., Fontalvo, A., Demirkaya, G., Martinez, A., Quiroga, A.G., Exergy analysis of parabolic trough solar receiver, Applied Thermal Engineering 2014;67(1-2):579-586

[8] [8] Kalogirou, S.A., Karellas, S., Braimakis, K., Stanciu, C., Badescu, V., Exergy analysis of solar thermal collectors and processes, Progress in Energy and Combustion Science 2016;56: 106–137

[9] [9] Bellos, E., Tzivanidis, C., Antonopoulos, K.A., A detailed working fluid investigation for solar parabolic trough collectors, Applied Thermal Engineering 2017;114(A):374-386

[10] [10] Petela, R., Exergy of undiluted thermal radiation, Solar Energy 2003;74:469–488

[11] [11] EuroTrough: Development of a Low Cost European Parabolic Trough Collector - EuroTrough. Final Report, Research funded in part by The European Commission in the framework of the Non-Nuclear Energy Programme JOULE III. Contract JOR3-CT98-0231;2001.

[12] [12] http://www.therminol.com/pages/bulletins/therminol_VP1.pdf

[13] [13] Bellos, E., Tzivanidis, C., Antonopoulos, K.A., Daniil, I., The use of gas working fluids in parabolic trough collectors – An energetic and exergetic analysis, Applied Thermal Engineering 2016;109(A):1-14

[14] [14] F-Chart Software, Engineering Equation Solver (EES); 2015. (http://www. fchart.com/ees).

THE 5th INTERNATIONAL CONFERENCE
MECHANICAL ENGINEERING IN XXI CENTURY

December 9-10, 2020
Faculty of Mechanical Engineering in Niš, Serbia

Determination of the Equivalent Thermal Conductivity of an Inhomogeneous Building Block of Complex Geometry

Anna LIMANSKAYA, Goran VUČKOVIĆ, Mića VUKIĆ, Mirko STOJILJKOVIĆ

First Author affiliation: University of Niš, Faculty of Mechanical Engineering in Niš, Aleksandra Medvedeva 14, 18000 Niš, Serbia

Second Author affiliation: University of Niš, Faculty of Mechanical Engineering in Niš, Aleksandra Medvedeva 14, 18000 Niš, Serbia

Third Author affiliation: University of Niš, Faculty of Mechanical Engineering in Niš, Aleksandra Medvedeva 14, 18000 Niš, Serbia

Fourth Author affiliation: University of Niš, Faculty of Mechanical Engineering in Niš, Aleksandra Medvedeva 14, 18000 Niš, Serbia

limanskayaanna@mail.ru, goran.vuckovic@masfak.ni.ac.rs
mica.vukic@masfak.ni.ac.rs, mirko.stojiljkovic@masfak.ni.ac.rs

***Abstract*— Energy efficiency of buildings has worldwide importance. Construction standards imply use of increased building insulation thickness, resulting in thicker walls and increased occupation of usable space. Typical energy efficient masonry brick tends to lower specific density and has vertical empty holes which should trap air during proper construction. The last generation masonry brick available at the general market is a clay brick with vertical holes filled with insulation material. In this paper we considered inhomogeneous building block with complex geometry. We used the Hot Disk Thermal Constants Analyser to get thermal conductivity of clay and mineral wool of which the block consists. We derived the equivalent thermal conductivity 0.1297 W/mK for this block.**

***Keywords*— the thermal conductivity, energy efficiency of buildings, inhomogeneous building block**

I. Introduction and Background

Energy efficiency of buildings has worldwide importance. Energy efficiency is typically improved by increased building insulation thickness, resulting in thicker walls and reduced building usable space, and labour costs for each layer. Typical construction solutions involve construction of individual layers (masonry, concrete, insulation, mortar etc.). With the tendency to construct thinner walls, for better utilization of available space for construction, typical construction market solutions reduce construction element density to improve insulation characteristics, reducing building mass and heat storage capacity in walls [1]. Disposition of the construction mass with higher heat capacity along the cross section of the building envelope has significant impact on heat storage in wall mass, that helps retain thermal comfort conditions in the periods without actual energy use [2].

Natural brick walls always create a healthy indoor environment. The clay building blocks are environmentally friendly, sustainable, durable and do not lose value over time [3].

In the article [4] presents the results of experimental research carried out in two real-scale detached energy efficient single-family buildings designed to be almost identical with exempt to the construction of their external and internal walls; lightweight skeletal versus traditional masonry construction. As the results of this study show, the use of cellular concrete walls instead of lightweight timber frame walls can be very effective in reducing the maximum and average daily temperatures in buildings during hot summers in temperate climate countries. The cooling effect of the thermal mass of the building remained stable during the heat wave and was relatively independent of the duration and distribution of the hottest days. The use of high thermal mass in studied buildings reduced the demand for cooling energy by 67-75% depending on assumed temperature threshold.

In the paper [5] considers effects of varying amount and location of thermal mass on dynamic heat-transfer characteristics of insulated building walls with same nominal resistance (Rn-value) are investigated numerically under steady periodic conditions using climatic data of Riyadh. Results show that for a given thermal mass, a wall with outside insulation gives better overall thermal performance compared to a wall with inside insulation. Early cooling and heating transmission loads decrease with increasing Lmas and reach asymptotically constant values. Peak cooling and heating transmission loads and decrement factor decrease with increasing Lmas, while the time lag increases with increasing Lmas. It is recommended that building walls should contain as a minimum critical amount of thermal

mass that correspond to energy savings potential in the range $90\% \le \Delta \le 97\%$ and that the insulation layer should be placed on the outside for applications with continuously operating AC.

The paper [6] reviews the new approaches of building materials (such as Aluminum, Brick, Ceramic, Cement, Concrete, Glass, Marble, Plaster, and Granite) for thermal transport and other properties associated with them and discusses and classifies the nonthermal and thermal properties of building materials. At the end, this review points out several important clues in future issues.

In the study [7], two types of a detached residential house with two floors and four bedrooms in Sydney were analysed using a building energy simulation program. Several scenarios were built based on various parameters, such as Passive Solar and Energy Efficiency Design Strategies (PSEEDS) and different external walls and floor systems, to determine their influence on the total energy required to achieve thermal comfort in the house. This study shows that increasing the thermal mass (building materials with higher R values) through utilizing different walls and flooring system, by replacing fibro house with brick veneer house and applying the PSEEDS, total energy requirement could be reduced by up to 58%. Thus incorporating PSEEDS and higher thermal mass in the construction of residential buildings can yield significant savings in energy costs over the considered lifetime of 50 years period. Energy consumptions obtained through simulation were verified with the real data and found to be within the tolerance limit of 16%.

The aim of the study [8] is to point out which are the relevant parameters for the thermal inertia of insulated blocks. A finite-volume method is used to solve the two-dimensional equation of conduction heat transfer, using a triangular-pulse temperature excitation to analyse the heat flux response. The effects of both the type of clay and the insulating filler are investigated and discussed at length. The results obtained show that the wall front mass is not the basic independent variable, since clay and insulating filler thermal diffusivities are more important controlling parameters.

In this paper we considered an inhomogeneous building block with complex geometry. We used the Hot Disk Thermal Constants Analyser (TPS 500) and the Transient Plane Source (TPS) method to get thermal conductivity of clay and mineral wool of which the block consists. For verification of our results we compared thermal conductivity values that we get in our experiment with the theoretical values. Then we derived the equivalent thermal conductivity of the inhomogeneous building block with complex geometry $\lambda_{ekv} = 0.1297 W/(m \cdot K)$.

II. Formulation of the Problem and Methodology

The considered block is a prism shape with dimensions $L \times \delta \times H$ $0.375 \times 0.250 \times 0.249$ m (Fig. 1). The block is symmetrical along all three axes, so that its center of gravity is in the center of the volume. In building constructions, the block is placed so that the fillings with the isolation are vertical, and the wall thickness corresponds to the width of the block.

Dimensions of inhomogeneous building block with complex geometry (Fig. 1) are:

$$\delta = 0.25m,$$
$$\delta_1 = 0.016m,$$
$$L = 0.375m,$$
$$l_1 = 0.015m,$$
$$H = 0.249m.$$

Other dimensions we can derive from block geometry:

$$\delta_2 = \frac{\delta - (n+1)\delta_1}{n} = 0.0308m,$$

$$l_2 = \frac{L - (m+1)l_1}{m} = 0.105m.$$

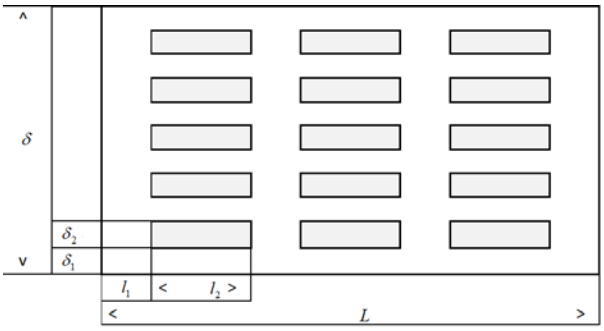

Fig.1. The inhomogeneous building block

In the building block we have $m = 3$ columns and $n = 5$ rows of vertical holes filled with insulation material. The rest of the block is a solid clay structure. The ratio of clay to insulation is 0.933. We denotes number of holes filled with insulation material as $k = 5$.

The heat flows throe the whole block is [9]:

$$\Phi = qLH = (m+1)q_1 l_1 H + m q_2 l_2 H \qquad (1)$$

We can also derive the specific heat flow as [9]:

$$q = \frac{\lambda_{ekv}}{\delta}(T_U - T_S) = \frac{T_U - T_S}{\frac{\delta}{\lambda_{ekv}}} \qquad (2)$$

The specific heat flow of the part made of clay we can get as:

$$q_1 = \frac{\lambda_1}{\delta}(T_U - T_S) = \frac{T_U - T_S}{\frac{\delta}{\lambda_1}} \qquad (3)$$

The specific heat flow of the part with holes with insulation material we derive as:

$$q_2 == \frac{T_U - T_S}{(n+1)\frac{\delta_1}{\lambda_1} + (n-k)\frac{\delta_2}{\lambda_1} + k\frac{\delta_2}{\lambda_2}} \qquad (4)$$

Putting (2)-(4) into (1) we get the equivalent thermal conductivity of the inhomogeneous building block:

$$\lambda_{eqv} = \lambda_1 \left[(m+1)\frac{l_1}{L} + \right. \qquad (5)$$

$$+m\frac{l_2}{L}\frac{\lambda_2}{(n+1)\frac{\delta_1}{\delta}\lambda_2+(n-k)\frac{\delta_2}{\delta}\lambda_2+k\frac{\delta_2}{\delta}\lambda_1}\Bigg]$$

We need to derive the thermal conductivity of of clay and mineral wool to get the equivalent thermal conductivity of the block.

III. Description of the experiment

We used the Hot Disk Thermal Constants Analyser (TPS 500) and the Transient Plane Source (TPS) method (Fig. 2) to get thermal conductivity of clay and mineral wool of which the block consists.

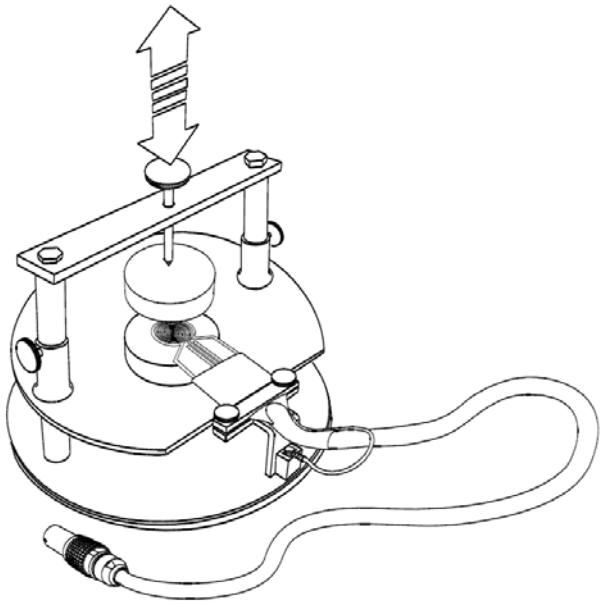

Fig. 2. The room temperature sample holder of the Hot Disk Thermal Constants Analyser [10]

The Transient Plane Source (TPS) method is today arguably the most precise and convenient technique for studying thermal transport properties. It is an absolute technique, yielding information on thermal conductivity, thermal diffusivity as well as specific heat per unit volume of the material under study, in accordance with ISO 22007-2. The TPS method is based on the use of a transiently heated plane sensor and is in its most common adaptation referred to as the Hot Disk Thermal Constants Analyser. [10]

The Hot Disk sensors are designed to be placed between the plane surfaces of two sample pieces of the material under investigation (Fig. 3). The basic assumption of the theory for this experimental technique is that the sensor is located in an infinite material.

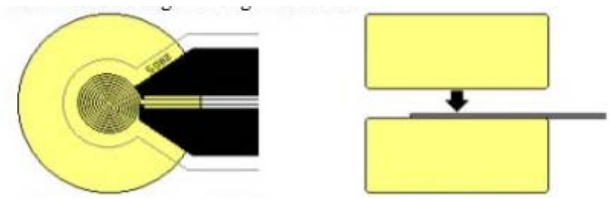

Fig. 3. Detail of the sensor position between sample pieces [10]

The sample pieces should be clamped firmly around the sensors to avoid any possible air gap between the two sample pieces and the sensor.

The samples were round with a diameter of 0.02 m and a thickness of 0.06 m. Two samples were made for each material (Fig. 4). The sample temperature was the same as a temperature in the room and equalled $16°C$. The encapsulated Ni-spiral sensor was then sandwiched between two samples. This Hot Disk sensor acts both as a heat source for increasing the temperature of the sample and as a "resistance thermometer" for recording the time-dependent temperature increase. During a pre-set time, 200 resistance recordings were taken and from these the relation between temperature and time was established [10].

Fig. 4. The samples of mineral wool (left) and clay (right)

During the experiment we measured the difference between the temperature of the sample and the temperature in the room. Then we got the dependence of temperature increase on time for each sample.

IV. Results and discussion

Based on the conducted experimental measurements, it took the clay 50% more time to reach the max temperature than the rock wool, with the temperature increase of the mineral wool being higher (11.0 K compared to the clay 6.0 K).

Then we used the original measuring equipment software to calculate the thermal conductivity of considering materials. For verification of our results we compared thermal conductivity values that we get in our experiment with the theoretical values (Table 1).

TABLE I Comparing theoretical and experimental thermal conductivity of different materials

	Theoretical thermal conductivity, W/(mK)	Experimental thermal conductivity, W/(mK)
Mineral wool	0.034-0.039 [11]	0.03557
Clay	0.47-0.58 [11]	0.5199

The values of thermal conductivity of materials in the table 1 are rather good. The experimental results for both materials were within theoretical limits. So, we can use experimental thermal conductivity of the insulation material and the clay to get the equivalent thermal conductivity of the inhomogeneous building block.

We derived the thermal conductivity of the clay:

$$\lambda_1 = 0.5199W/(m\cdot K),$$

and the mineral wool:

$$\lambda_2 = 0.03557W/(m\cdot K).$$

Putting this values and geometrical parameters of the block in (5) we get the equivalent thermal conductivity of

the inhomogeneous building block with complex geometry:
$\lambda_{ekv} = 0.1297 W/(m \cdot K)$.

V. Conclusions

We derived the equivalent thermal conductivity of the inhomogeneous building block 0.129 W/mK.

To improve the thermal properties of the block we suppose to change its geometry to take away "heat flow bridges". It will decrease the heat flow through the wall and provide good enough thermal resistance.

We also supposed to fill some holes in the inner side of the block by clay instead insulation material. So we will increase mass of a material with good heat capacity properties on the indoor side of the building thermal envelope and therefore increase the heat capacity (i.e. energy storage in the building mass), that helps retain thermal comfort conditions in the periods without actual energy use.

Nomenclature

H - height of the block, m
k - number of holes filled with insulation material
l_1 - length between holes, m
l_2 - length of the hole, m
L - length of the block, m
m - number of columns of vertical empty holes
n - number of rows of vertical empty holes
q - equivalent specific heat flow of the block, W/m^2
q_1 - specific heat flow of the part made of clay, W/m^2
q_2 - specific heat flow of the part with holes, W/m^2
T_S - temperature outside, K
T_U - temperature in a room, K

Greek Symbol:

δ - width of the block, m
δ_1 - width between holes, m
δ_2 - width of the hole, m
Φ - heat flow, W
λ_{ekv} - equivalent thermal conductivity of block, W/(mK)
λ_1 - thermal conductivity of the clay, W/(mK)
λ_2 - thermal conductivity of the mineral wool, W/(mK)

Acknowledgment

The authors would like to acknowledge Professor P. Zivković and Ph.D. Student L. Sokolova for their help with experimental decision of thermal conductivity.

This research was financially supported by the Ministry of Education, Science and Technological Development of the Republic of Serbia and partially conducted within the project "Research and development of new generation machine systems in the function of the technological development of Serbia".

References

[1] M. Ljubenović, M. Ignjatović, J. Janevski, B. Stojanović, “The impact of the wall structure on its dynamic characteristics“, SIMTERM2017 Conference, Proceedings, 2017, pp. 87-94

[2] V. Bogdanović, “Building physics - Thermal protection of buildings“, (in Serbian): Faculty of civil engineering and architecture in Niš, Niš, 2018

[3] https://www.wienerberger.com/en/brands-and-products/wall.html

[4] T. Kuczynski, A. Staszczuk, “Experimental study of the influence of thermal mass on thermal comfort and cooling energy demand in residential buildings”, Energy, vol. 195, March 2020, 116984

[5] Sami A. Al-Sanea, M.F. Zedan, S.N. Al-Hussain, “Effect of thermal mass on performance of insulated building walls and the concept of energy savings potential,” Applied Energy, vol. 89, Issue 1, January 2012, pp. 430-442

[6] Z. Pezeshki, A. Soleimani, A. Darabi, S.M. Mazinani, “Thermal transport in: Building materials”, Construction and Building Materials, vol. 181, 2018, pp. 238–252

[7] Haider Albayyaa, Dharmappa Hagare, Swapan Saha, “Energy conservation in residential buildings by incorporating Passive Solar and Energy Efficiency Design Strategies and higher thermal mass”, Energy & Buildings, vol. 182, 2019, pp. 205–213

[8] Cianfrini, M.; De Lieto Vollaro, R.; Habib, E. “Dynamic Thermal Features of Insulated Blocks: Actual Behavior and Myths”, Energies 2017, vol. 10, 1807.

[9] G. Ilić, M. Vukić, N. Radojković, P. Živković, I. Stojanović, “Thermodynamics II - Basics of heat and mass transfer“, (in Serbian): Faculty of Mechanical Engineering in, Niš , 2014

[10] Hot Disk Thermal Constants Analyser Instruction Manual Revision date 2014-03-27

[11] Rulebook of Energy efficiency in buildings (in Serbian), Official Gazette, No. 061/2011.

THE 5th INTERNATIONAL CONFERENCE
MECHANICAL ENGINEERING IN XXI CENTURY

December 9-10, 2020
Faculty of Mechanical Engineering in Niš, Serbia

Application of Solar Energy in Serbia and Russia

Ljubov SOKOLOVA[a], Saša PAVLOVIC[b], Tamara TIHOMIROVA[b], Predrag ZIVKOVIC[a], Velimir STEFANOVIC[a], Anna LIMANSKAYA[a], Selishev ALEKSEI[b]

[a]*University of Niš Faculty of Mechanical Engineering, Niš, Republic of Serbia*
[b]*Belgorod State Technological University named V.G. Shukhov, Power Engineering Institute, Belgorod, Russia,*
sokolova106.8@mail.ru, sasa.pavlovic@masfak.ni.ac.rs, tixo-mir@list.ru, pzivkovic@masfak.ni.ac.rs, veljas@masfak.ni.ac.rs, limanskayaanna@mail.ru, selishevaleksei2@gmail.com

***Abstract*— The global problem in the form of climate change is becoming more and more pronounced. As a result, most countries around the world are facing serious energy shortages, and forecasts indicate that such a situation will be similar in the near future. High consumption and population growth in the world will force the inhabitants of a large number of countries to face the problem of critical reduction of stocks of domestic fossil energy sources. The current energy dependence of most countries on oil and its derivatives requires significant economic expenditures and in the future suggests negative effects on national economies, as well as on the international security situation. Fossil fuel supplies are rapidly depleting, and within a decade or two, most countries will be forced to use renewable energy sources to meet their energy needs.Given the great relevance of the application of renewable energy sources around the world, this work aims to present the most commonly used, in terms of potential and opportunities, use in the field of solar energy in European countries: southeaster Serbia and eastern Russia. The main attention will be paid to solar concentration collectors, which are the most common and whose use from the technical-technological aspect has reached the highest level.In addition, economic indicators in terms of investment and exploitation profitability will be presented.**

***Keywords*—renewable energy sources, solar collector, potential, possibility of exploitation, technological point, economic indicators, investment conditions**

I. SOLAR ENERGY

Solar energy is directly or indirectly the source of almost all energy on Earth.[1]. Renewable sources are in the long run a valuable alternative. Many areas in the world abound in free solar energy while in some other areas wind and other types of renewable sources of energy impose themselves as a logical choice.Having in mind that fossil fuels on Earth are limited and that their usage ensues the emission of CO2 that exerts negative influence on the environment, more and more renewable sources of energy are being used worldwide with the Sun as a primary source of energy By means of the adequate equipment the energy of the sun irradiation can be converted into thermal and electrical energy. The critical energy situation forces the mankind to reconsider thoroughly all possibilities given by renewable energy sources, and our present knowledge and technology.[2]

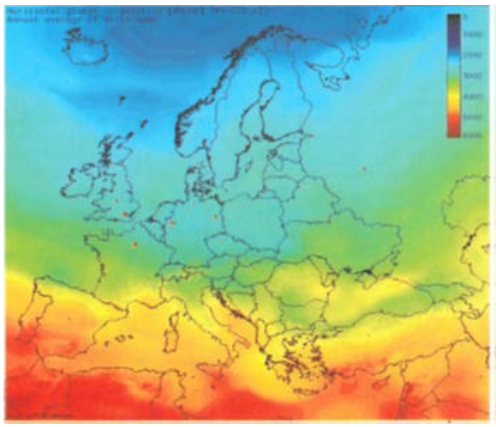

Fig. 1. Annual average of daily energy of global solar irradiation on horizontal plane in Europe [Wh/m^2], PV-GIS v2

A. *Solar energy potential in Serbia*

Serbia is located between 41°46'40" and 46°11'25" of the north latitude and 18°06' and 23°01' east longitude. Serbia belongs to the continental climate regions that can be divided into the continental climate in the Panonic lowlands, moderate-continental climate in lower parts of the mountain region and the mountain climate on high mountains. [2]North part of Serbia comprises a vast Panonic area which is wide open and exposed to the climate influences coming from the north and the east. The Panonic lowlands show continental climate that encompasses Vojvodina and its edge until 800 m of height. Winters are long and harsh and autumns and springs are mild and short Results of long term meteorological measurements have shown that natural potentials of climatic recourses of Serbia are very good. In Serbia the energy potential of the sun irradiation and potential of biomass is around 30% higher than in the Middle Europe (average annual sun irradiation energy in Europe is 1096 kWh/m2 year, and in Serbia is around 1400 kWh/m2 year). Mean values for January are in the range from 1,1 kWh/m2 in the north of the country, to 1,7

kWh/m2 in the south. Such spatial distribution is caused by the influence of daily cloudiness, which is most pronounced in the mountainous regions. Average daily global solar irradiation on horizontal plane in July, in Serbia is shown in Fig. 2. Annual average of daily energy of global solar irradiation on horizontal plane in Serbia is shown in Fig. 3.

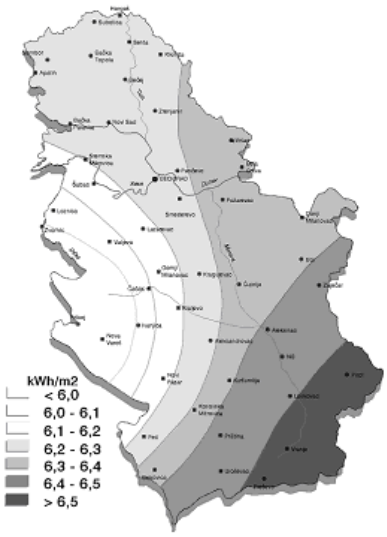

Fig. 2. Average daily global solar irradiation on horizontal plane in Ju1 in Serbia

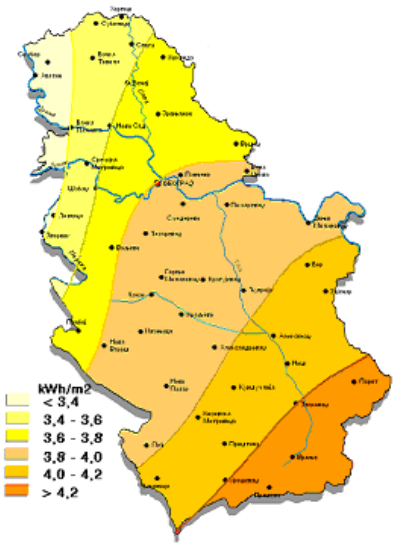

Fig. 3. Annual average of daily energy of global solar irradiation on horizontal plane in Serbia

B. *Geography and features of the use of solar collectors in Russia.*

The rise in energy prices in Russia is forcing interest in cheap energy sources. Solar energy is the most readily available. The energy of solar radiation falling on the Earth 10,000 times exceeds the amount of energy generated by mankind.[3]

Problems arise in the technology of energy collection and in connection with the uneven supply of energy to solar plants. Therefore, solar collectors and solar panels are used either in conjunction with energy storage or as a means of additional feeding for the main power plant.

Fig. 4. Solar energy input

Areas of maximum solar radiation intensity. More than 5 kWh comes per 1 square meter. solar energy per day. Along the southern border of Russia from Baikal to Vladivostok, in the Yakutsk region, in the south of the Republic of Tyva and the Republic of Buryatia, oddly enough, beyond the Arctic Circle in the eastern part of Severnaya Zemlya.

Solar energy supply from 4 to 4.5 kWh per 1 sq. meter per day. Krasnodar Territory, North Caucasus, Rostov Region, southern part of the Volga region, southern regions of Novosibirsk and Irkutsk regions, Buryatia, Tyva, Khakassia, Primorsky and Khabarovsk Territories, Amur Region, Sakhalin Island, vast territories from Krasnoyarsk Territory to Magadan, Severnaya Zemlya, north east of the Yamalo-Nenets Autonomous Okrug.

From 2.5 to 3 kWh per sq. meter per day - along the western arc - Nizhny Novgorod, Moscow, St. Petersburg, Salekhard, the eastern part of Chukotka and Kamchatka.

From 3 to 4 kWh per 1 sq. meter per day - the rest of the country.

The energy flow is most intense in May, June and July. During this period, in central Russia, 1 sq. meter of surface accounts for 5 kWh per day. The lowest intensity is in December - January, when 1 sq. meter of surface accounts for 0.7 kWh per day.

II. SOLAR TECHNOLOGY

By means of the adequate equipment the energy of the sun irradiation can be converted into thermal and electrical energy. The critical energy situation forces the mankind to reconsider thoroughly all possibilities given by renewable energy sources, and our present knowledge and technology. Depending on the degree of the heating of the working fluid we can differ between the low-temperature ($T<100^oC$), middle-temperature ($100^oC<T<400^oC$) and high-temperature conversion ($400^oC<T<4000^oC$). For low-temperature solar energy conversion one uses flat collectors with water and air, for middle-temperature conversion one uses vacuum colletors and collectors with concentrators, and for high-temperature one uses solar furnaces and CSP plants Pavlović [4] and Fernández-García et al. [5]. Middle and high-temperature systems are applicable for refrigeration systems, industrial processes and polygenerations systems.

A. *Solar technology, types of solar concentrating collectors*

Solar dish systems convert the thermal energy of solar radiation to mechanical energy and then to electrical

energy similar to the way that convectional power plants convert thermal energy from combustion of a fossil fuel to electricity. [6]-[7].

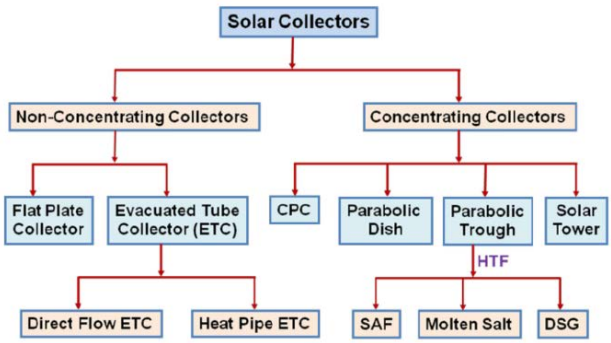

Fig.5. STypes of solar collectors. CPC-compound parabolic concentrator; SAF-Synthetic aromatic fluid; DSG-Direct steam generation; HTF-Heat transfer fluid

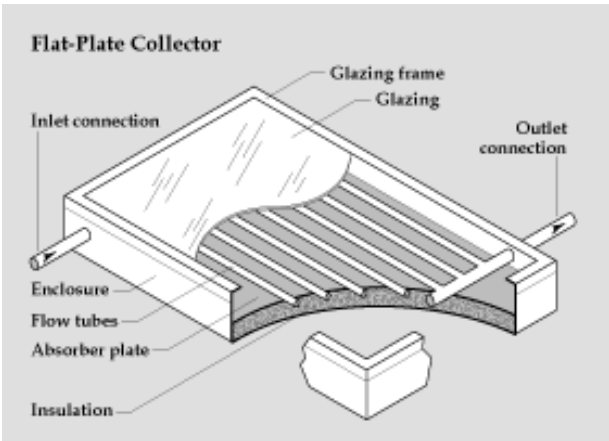

Fig. 6. A diagram of a flat plate solar collector

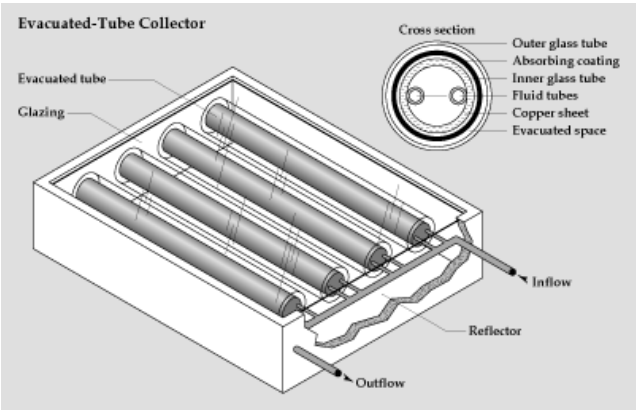

Fig. 7. A diagram of an evacuated tube solar collector.

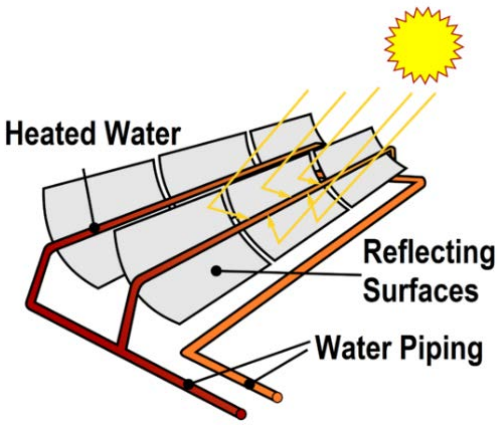

Fig. 8. A diagram of a line focus solar collector

Fig. 9. A point focus solar collector

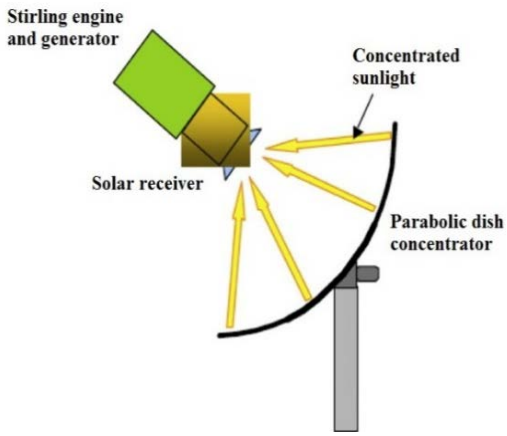

Fig. 10 Solar dish Stirling system

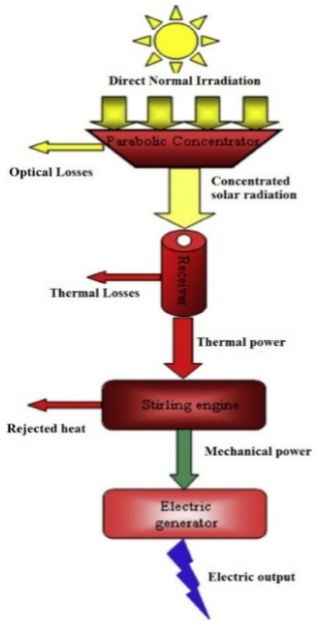

Fig.11. Solar dish Stirling System energetic chain

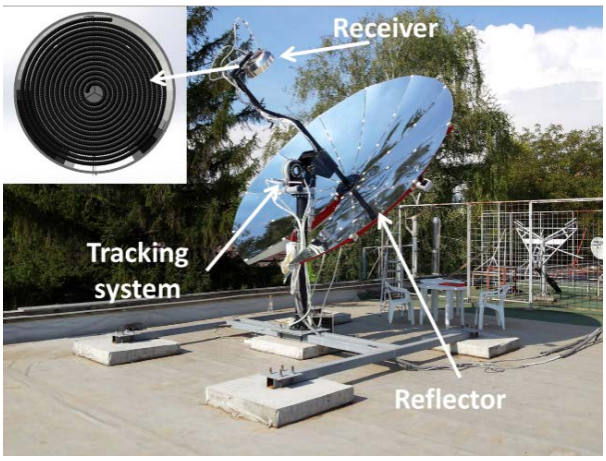

Fig.12. The examined solar dish prototype collector-Faculty of Mechanical Engineering-Thermal Engineering Department [8].

The examined collector is a concentrating collector with dish reflector. The collector is shown in Figure 12 where the main parts are indicated. The solar dish reflector consists of 11 curvilinear trapezoidal reflective petals constructed by PMMA (Polymethyl methacrylate) with a silvered mirror layer. The 12th part of the reflector is missing because of the existence of a bracket which supports the system. The stainless-steel absorber is a corrugated spiral tube which is located inside an aluminum housing. [8].

The collector has been created from low-cost materials inorder to reduce the total investment cost, while sufficient performance is maintained. The total cost of the system was about 7000 €. The tracking system cost about 2000 €, reflectors approximately 2000 € and the other parts about 3000 €. Apart from the low cost, this collector also has a lightweight construction and is easier to install than other similar systems.

Table 1 includes the main data for the collector characteristics. Geometrical characteristics as well as thermal and optical properties are given. The final reflectance was estimated to be about 80%. This value was selected due to dust and some stains on the mirrors. The absorber tube is not selective and for this reason its emittance is high. However, its low cost is an advantage of this selection.

TABLE IBASIC PARAMETERS OF THE EXAMINED COLLECTOR

	Parameter	Value
1	Concentration ratio	28.26
2	Concentrator diameter	3.80 m
3	Paraboloid rim angle	45.6 º
4	Focal distance	2.26 m
5	Collector aperture	10.29 m^2
6	Spiral length	9.5 m
7	Spiral outer mean diameter	12.2 mm
8	Spiral inner maximum diameter	11.7 mm
9	Spiral inner mean diameter	10.5 mm
10	Spiral inner minimum diameter	9.3 mm
11	Absorber emittance	0.9
12	Absorber absorbance	0.9
13	Mirror reflectance	0.6
14	Distance between absorber and reflector base	2100 mm

A regression model is developed in order to approximate the thermal efficiency (ηth) and it is given in equation 1. This model has an R2 equal to 99.97%

$$\eta_{th} = 0.68199 - 0.19456 \cdot \frac{T_{in}-T_{am}}{G_b} - 0.00056 \cdot \frac{(T_{in}-T_{am})^2}{G_b} \quad (1)$$

Solar-driven polygeneration systems are promising technologies for covering many energy demands with a renewable and sustainable way. The examined trigeneration system is depicted in figure 13. Solar dish collectors are used in order to produce the useful heat which is stored in a storage tank. Four solar dishes with a total collecting area of about 40 m^2 are used in this work. The storage tank feeds and ORC and the utilized working fluid in the solar loop and the tank system is Therminol VP-1. This thermal oil is able to operate up to 400ºC with a safety under a pressure level of 15 bar . The costs of the electricity, heating and cooling are selected at 0.20 €/kWh, 0.10 €/kWh and 0.067 €/kWh respectively.

The most used commonly solar collector types are flat collectors followed by parabolic and vacuum tubular collectors. However, in terms of occupied area, parabolic collectors are superior to flat and vacuum ones.

The largest manufacturers of flat solar collectors are Chinese companies - Sunrain (annual turnover of more than 600 million US dollars), BTE Solar, FiveStar and others.

The list of leading companies among manufacturers of solar collectors in 2017 also includes the Austrian company Greenonetec and the German BoschThermotechnik.

III. EVALUATION OF THE ECONOMIC EFFICIENCY OF SOLAR COLLECTORS

This document is created and editted in Microsoft Word 2007 and saved as Word 97-2003 Document version. The economic efficiency of industrial solar

collectors, as well as other devices for converting solar energy, primarily depends on the level of solar insolation, which determines their performance.[9]. Other significant factors are the initial cost of the collector itself, installation and maintenance costs and the length of the solar collector's life cycle. All these factors, as well as the discount factor, are taken into account in the "levelized cost of energy" (LCOE) indicator, which is the most common in the comparative assessment of the economic efficiency of various energy technologies and reflects the average unit cost of energy produced using a given generating device for the entire period of equipment operation.The calculation of the reduced cost of energy is carried out according to the formula:

$$LCOE = \frac{I_0 + \sum_{t=1}^{T} A_t \cdot (1+r)^{-t}}{\sum_{t=1}^{T} SE \cdot (1+r)^{-t}}, \quad (2)$$

where I_0 - is the unit cost of equipment, taking into account the installation (EUR / sq.m.);

A_t- the cost of equipment maintenance in the year t (for solar collectors it is assumed equal to 0.25-0.5% of I_0, depending on the type of collector);

SE- is the amount of energy produced in the year t;

T-is the duration of the operating period of the generating equipment (years);

R- is the discount factor reflecting the change in the value of money over time (for settlements in euros, as a rule, it is assumed to be 3%).

According to IEA SHC Task49 / IV SHIP experts, the LCOE for large-scale solar collectors used for domestic hot water supply ranges from 2-euro cents (in 2016 prices) per kWh of heat energy in India to 14-euro cents in Austria. Denmark, Canada, and France. Considering that the cost of an installed industrial solar collector, similar in quality and performance, is approximately equal to the cost of a collector used for hot water supply (from 200 to 1160 euros / sq.m), and the temperature of water heating in them is comparable to the temperature required to provide heat low-temperature industrial processes, and based on the data on the performance of solar collectors depending on the level of solar radiation given in the source for 62 capitals of the world, it is possible to estimate the expected LCOE for industrial collectors in Russia.For this, according to the source [9], we construct a paired linear regression model describing the relationship between the level of solar insolation (X) and the performance of an average large-scale solar collector with a horizontal panel for hot water supply (Y). Using the least common squares method implemented in the STATISTICA 10.1 application package, we obtain the following dependence:

$$Y = 0{,}389 \cdot X + 41{,}719 \quad (3)$$

The calculated value of Fisher's F-statistic for the constructed model is 814.42, the level of statistical significance of the regression coefficient is $p<0.001$, the level of statistical significance of the free term is $p = 0.054$, $R^2 = 0.972$. The standard error of the regression coefficient is 0.014.

Given the high statistical quality of the constructed model (3), it can be used to predict the expected performance of a solar collector anywhere in the world

The assessment of the cost of thermal energy produced by solar collectors is higher than when using traditional hydrocarbon technologies, however, with the rise in the cost of hydrocarbon sources or the introduction of taxes on greenhouse gas emissions (which is currently being discussed in the world expert community as a necessary measure to implement the goals of the Paris Agreement on climate), the commercial attractiveness of new technologies can significantly increase in the Republic of Serbia and in those regions of Russia where the average annual level of solar insolation is relatively high, and the need to provide energy for low-temperature industrial processes is quite high. In addition, the economic feasibility of using solar collectors increases significantly if it is impossible to connect to centralized heating networks, as well as in case of seasonal workload of enterprises.

IV. Conclusion

The paper is focused on basic functional principles of solar collectors. Development of solar energy technologies and their continuous use are evident in developed countries of Europe and world. Serbia has favourable climatic conditions for the construction of Concentrating Solar Power plants. Annual average of daily energy of global solar irradiation on the horizontal plane in Serbia is less than 3,4 kWh/m2 in the north and more than 4,2 kWh/m2 in the south part of Serbia. contribute to a greater extent to the construction and use of CSP power plants in Serbia. According to the predicted estimates, the present value of the energy produced by industrial solar collectors in the southern regions of Russia may amount to 3.8-6.6 roubles/ kWh(0,05-0,086 €/kWh). Despite the fact that the forecast estimates are higher than current tariffs, the economic feasibility of using solar collectors in industry increases significantly if it is not possible to connect to centralized heating networks, as well as in the case of seasonal workload of enterprises. Solar power presents a technology that have been applied more than twenty years for electricity generation and heat production. Serbia and Russian have favourable climatic conditions for the construction of Concentrating Solar Power plants.

Acknowledgements

This research was financially supported by the Ministry ofEducation, Science and Technological Development ofthe Republic of Serbia.

References

[1] T. Pavlović, Z. Pavlović, L. Kostić, L. Pantić, R. Stojiljković, "Obnovljiviizvorienergije, Vodić zapraktičnuprimenu,"Niš, 2008.

[2] S. Pavlovic, and V. Stefanović, (2013),"Systems with concentrating solar radiation," 2. 931-988. 10.4018/978-1-4666-4450-2.ch031

[3] https://andi-grupp.ru/informatsiya/stati/solnechnye-kolektory-v-rossii/

[4] T. Pavlović, B. Čabrić, 2007, "Physics and techniques of solar energy", Građevinska knjiga, Belgrade, (in Serbian).

[5] A. Fernández-García, E. Zarza, L. Valenzuela, M. Pérez, 2010, Parabolic-trough solar collectors and their applications, Renewable and Sustainable Energy Reviews, 14, , pp. 1695-1721.

[6] https://www.researchgate.net/figure/Types-of-solar-collectors_fig1_277327602

[7] https://energyeducation.ca/encyclopedia/Solar_collector

[8] S. Pavlovic, "Research into the optimal parameters of solar parabolic dish concentrating thermal collectors from the aspect of application in polygeneration systems,"PhD Thesis, March, 2017 Year. pp. 280, Faculty of Mechanical Engineering in Nis, University of Nis.

[9] S. Ratner, "Solar collectors in the industry: analysis of foreign experience of application and economic assessment of prospects of introduction of regional power system," Novocherkassk. Russia,Drukerovskij vestnik,August2019, pp. 132-148

THE 5th INTERNATIONAL CONFERENCE
MECHANICAL ENGINEERING IN XXI CENTURY

December 9-10, 2020
Faculty of Mechanical Engineering in Niš, Serbia

Engineering Management in Dealing with Emergencies in the Energy Industry

Jelena MALENOVIĆ-NIKOLIĆ[1], Dejan KRSTIĆ[1]

[1] Faculty of Occupational Safety, University of Niš, Čarnojevića 10a, Niš, Serbia
malenovicfznr@gmail.com, dekikrs@ gmail.com,

***Abstract*— Engineering management is very important when dealing with emergencies. It is necessary to organize activities that rely on the available machinery to help preserve material and human resources. The energy industry cannot function properly during emergencies due to the seriousness of potential consequences. Events such as cracking dams due to heavy precipitation, collapsing wind turbine towers, fires in solar power plants, or corrosions in geothermal power plants warrant a more improved development of energy management in the use of renewables. There are also serious issues with the use of fossil fuels, particularly the use of coal, gas, oil, and oil shales, which require complex mining machinery. Engineering management in the energy industry is also crucial for a timely emergency response.**

***Keywords*— energy, failures, energy sources, emergencies, engineering**

I. Introduction

Whether they are natural or anthropogenic, emergencies in the energy industry affect the proper supply and distribution of electricity. An even bigger issue is the damage to human health and destruction of energy facilities. It is possible to take corrective safety measures, with more or less success, but the outcome of a risk event depends on the organization of engineering management procedures.

Proper organization of the management system in the energy industry, based on the cooperation within the engineering team, can prevent potential failures and mitigate any effects due to emergencies. Involvement of engineers of various profiles is meant to provide different perspectives when analyzing any situation so as to identify problems in a timely manner.

Within the management system, the team of experts needs to plan its responsibilities in advance. Another and no less important task is to use a functioning management system to ensure a rational situational analysis and to adapt the response plan accordingly. Specific activities in the field, with minimal harmful effects, should be performed only by engineers who are adequately trained in management aspects.

Successful resolution of unforeseen issues caused by natural disasters or fires greatly depends on engineers' team work and actions in accordance with emergency response plans.

However, acting according to the response plans in an emergency without the ad hoc reasoning of engineers can sometimes make the situation worse. The management system has to provide an option to improve the response plans directly in the field using methods of multi-criteria analysis. The aforementioned reasons suggest the necessity of hiring exceptional teams of engineers for work in the energy industry, which has a high expectancy of activities with increased risk.

II. Emergencies in the Energy Industry

Emergencies can seriously disturb the energy stability of the affected area as well as the supply and distribution of electricity in the entire country.

Disruptions in the regular operation of thermal power plants due to emergencies can threaten the safety and health of workers who are involved in the emergency response.

This paper analyzes emergencies in terms of how they affect the energy industry, in order to highlight the importance of implementing energy risk management in the mitigation of the effects.

Emergencies are analyzed for the purpose of emphasizing the issues that await teams of engineers. The analysis of risk events will then prepare the engineers to face the serious tasks and unpredictable situations ahead of them. In terms of energy system stability and potential negative effects, emergency management in the energy industry is one of the primary tasks of the management system.

Energy sector management based on increased use of renewables can contribute to sustainable energy development, but only if the legislation on environmental quality preservation is implemented fully and consistently. The use of renewables requires proper preventive measures. Emergencies also tend to occur when solar energy is utilized, e.g. fires due to the use of photovoltaic technology and damage to conductors.

Solar power plants can catch fire due to improper positioning of the mirrors. Fires are usually caused by errors in the focusing of solar energy, whereby energy is concentrated in the wrong part of the tower outside the boiler space, damaging the electrical cables.

Fig. 1 Fire at a solar power plant

The fire destroys the steam boilers and fire suppression is sometimes required at the heights of over 100 m (Fig. 1).

Operational management of a geothermal power plant is a serious task, because the use of thermal mineral water often leads to corrosion.

Fig. 2 Geothermal power plant

Corrosion (Fig. 2) can cause the shutdown of a geothermal power plant after only several years of operation, which makes it impossible to cover the initial investment costs.

Fires can also be caused by wind turbine failures, resulting in the burning and melting of the blades (Fig. 3).

Fig. 3 Wind turbine on fire [1]

Wind turbines containing gear wheels have been known to catch fire due to failures caused by broken gear wheels or uncontrolled increase of rotation speed due to worn bearings.

III. Serbian energy industry

The energy industry in Serbia, as well as in other countries, is continuously exposed to higher risk of an emergency, whether natural or anthropogenic. The higher risk of emergencies in the energy industry and the possibility of serious consequences requires a timely implementation of preventive and corrective measures.

The heavy flooding of the Serbian town of Obrenovac in 2014 jeopardized the distribution of electric power, which was handled by means of reduced consumption and electricity import. A bigger problem was the damaged equipment in the open-pit mine of the thermal power plant. The flooded open-pit mine is shown in Figure 4, revealing parts of the excavator above the water, which completely filled the pit.

Fig. 4 Flooded “Kolubara” open-pit mine [1]

Emergencies due to cracks in ash pond embankments require considerable mitigation efforts, whereby the work is performed in very unsafe conditions. Workers are at risk of falling into the ash pond (Fig. 5) and all the people in the vicinity are threatened by potential ash dispersion.

Fig. 5 Ash pond [1]

A characteristic energy industry emergency can occur due to snow deposits. The ice forming on power lines and pylons can halt the electric power supply, with snowbound access roads preventing any emergency interventions (Fig.6).

Fig. 6 Damaged electric power grid on Tresibaba mountain [1]

Adverse weather conditions make it difficult to perform any work to restore the electric power grid and replace the damaged power lines.

Emergencies can also occur due to oil spills or fires at oil drilling rigs during exploration or extraction.

Fig. 7 Fire at an oil rig in Kostolac [1]

For instance, a large fire broke out at an oil drill near the town of Kostolac (Fig. 7), injuring two workers. A spark ignited the gas that abundantly formed above the crude oil being extracted.

IV. Emergency management

The presented emergencies that occurred in Serbia or abroad are intended to demonstrate what the various teams of engineers in the energy sector had to deal with, often with the support of firefighting units.

It is also necessary to consider the problems that field workers encounter, because the work they perform is also a part of the management system. Engineers should serve as support in the field but also to participate in the design of emergency plans and programs. The analysis of the problems facing the workers in charge of repairing electric power grid failures and restoring the energy distribution system is a serious task of engineering management. Work performance entails conditions that threaten workers, e.g. working at heights or live-line working, which is why engineers always have to consider the workers who perform high-risk jobs.

To ensure prompt emergency response, engineering management in the energy industry needs to include preliminary planning, risk analysis, definition of preventive measures, implementation of a crisis management system, and the evaluation of all the preceding phases.

Table I shows the phases of engineering management in the energy industry with regard to activities pertaining to emergencies.

TABLE I Engineering management phases

Phase	**Engineering management**
	Emergency management in the energy industry
Phase 1 Prevention	- Studying of emergencies in energy facilities (thermal power plants, mines, hydropower plants, SHP plants, solar power plants, photovoltaic roof panels, wind turbines, electric power grids) - Designation of high-risk locations - Planning of monitoring system design
Phase 2 Anticipation	- Monitoring of the situation at energy facilities - Prediction of potential risk events and preparation of preventive measures - Dissemination of information about the observed inadequacies or reported failures
Phase 1 Response	- Emergency response activities in energy facilities using corrective safety measures
Phase 1 Recovery	- Mitigation of material damage and removal of damaged pieces of the energy facility - Rehabilitation of human resources and restoration of material resources - Creation of a field report and input of all relevant details into the database for emergencies in the energy industry

Fire is a significant risk that may lead to an emergency in the energy sector. In addition to fires, events such as floods, landslides, and erosion processes also have to be monitored on a regular basis to predict and prepare for a potential emergency.

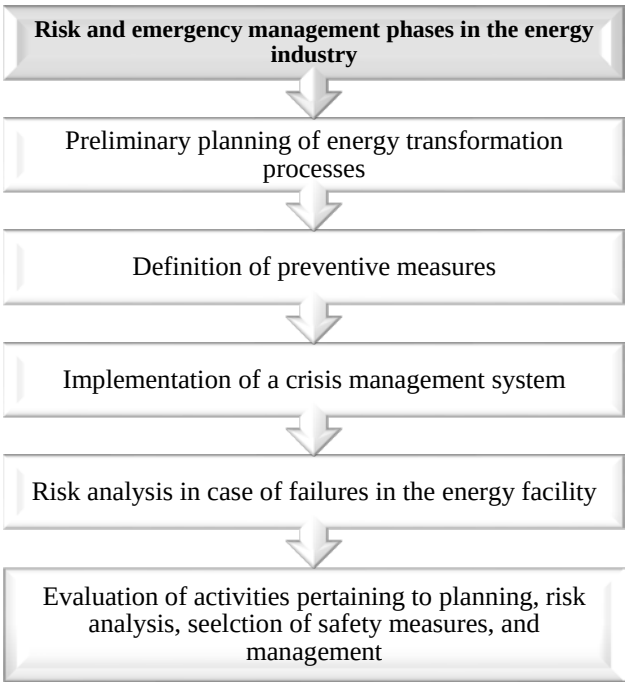

Fig. 8 Risk and emergency management phases

The goal of implementing preventive measures and training and hiring professional personnel within engineering management is to reduce the risk of large-scale failures during the exploitation of energy-generating products, energy transformation processes, and distribution of electricity.

Fires in energy facilities pose a great threat as they can spread rapidly and uncontrollably, engulfing vast areas. Therefore, fire prevention is a crucial aspect of engineering management.

A dedicated team of engineers should monitor the status of equipment and devices on a regular basis to ensure that any potential inadequacies can be promptly addressed. The key factor in fire prevention is to prevent the conditions that would allow the fire to spread rapidly over a short period.

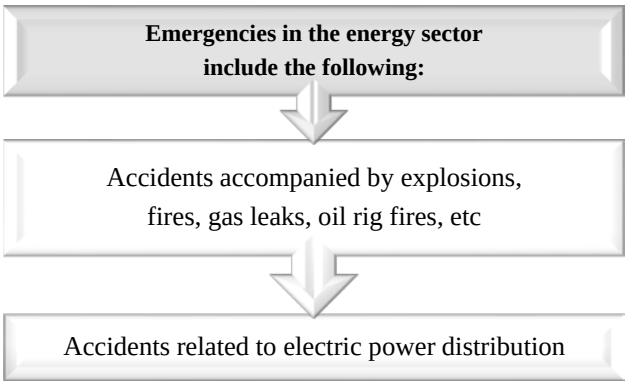

Fig. 9 Emergencies in the energy sector

Emergencies can also occur as a consequence of human negligence or error during job performance. Therefore, it is crucial to implement the prescribed procedures for each particular job in the energy sector.

Accidents on machinery, devices, and installations, which lead to fires and explosions, as well as failures of electric power facilities, should be key points of interest in engineering management.

V. Conclusion

Preventive action against natural and other disasters and emergencies within engineering management is a part of prevention procedures against the occurrence of technological accidents and disasters. A designated team of engineers must be capable of completing the set tasks in order to predict any emergency and promptly determine the course of action for emergency response.

Emergency procedures are prescribed by the legislation and statutes of the Republic of Serbia. According to the Serbian Law on Emergencies, the purpose of engineering management is to devise an emergency management system for the entire energy industry sector. Implementation of preventive and operational measures as a part of emergency response depends on the preparedness and training for preventive action of everyone involved in dealing with emergencies.

References

[1] J. Farley, “Clean coal technologies for power generation, Proceedings of the Institution of Civil Engineers”, Energy 160, Paper 300003, 2007, pp. 15–20.

[2] A. Esser, “Evaluation of primary energy factor calcula-tion options for electricity”, Final report, Karlsruhe: Fraunhofer-Institut fur System-und Innovations for schung(ISI), 2020 https://ec.europa. eu/energy/sites/ener /files/ docu-ments/final_report_pef_eed.pdf (2016.

[3] Chronology of an Unprecedented Accident at Kolubara Mining Basin, Elektroprivreda Srbije, kWh, Maj-Jun, 2014, no. 484, year XL.

[4] J. T. Clarke, McLeskey, The constrained design space of double-flash geothermalpower plants, Geothermics, vol. 51, 2014, pp. 31-37.

[5] S. Tka, “Hydro power plants, an overview of the current types and technology”, Journal of Civil Engineering 13(s1), 2018, pp. 115-126.

[6] H. Ganjehsarabi, A. Gungor, I. Dincer, “Exergetic performance analysis of Dora IIgeothermal power plant in Turkey”, Energy, vol. 46, no. 1, 2012, pp. 101-108.

[7] Z. Shengjun, W. Huaixin, G. Tao, “Performance comparison and parametric optimizationof subcritical Organic Rankine Cycle (ORC) and transcritical power cycle system for low-temperature geothermal power generation”, Applied Energy, vol. 88, no. 8, 2011, pp. 2740-2754

THE 5th INTERNATIONAL CONFERENCE
MECHANICAL ENGINEERING IN XXI CENTURY

December 9-10, 2020
Faculty of Mechanical Engineering in Niš, Serbia

A model for coupling polygeneration system superstructure model to building load models in Trnsys

Marko MANČIĆ, Dragoljub ŽIVKOVIĆ, Mirjana LAKOVIĆ, Milena MANČIĆ, Milan ĐORĐEVIĆ

First Author affiliation: Department of Energy and process engineering, University of Niš, Faculty of Mechanical Engineering, Aleksandra Medvedeva 14, Niš, Serbia
Second Author affiliation: Department of Energy and process engineering, University of Niš, Faculty of Mechanical Engineering, Aleksandra Medvedeva 14, Niš, Serbia
Third Author affiliation: Department of Energy and process engineering, University of Niš, Faculty of Mechanical Engineering, Aleksandra Medvedeva 14, Niš, Serbia
Fourth Author affiliation: Department of Energy processes and safety, University of Niš, Faculty of occupational safety, Čarnojevića 10a, Niš, Serbia
Fifht Author affiliation: Department of Mehcanical Engineering, University of Pristina, Faculty of Technical Sciences in Kosovska Mitrovica, Kosovska Mitrovica, Serbia

***Abstract*— A polygeneration system is an integrated energy system capable of providing multiple energy outputs to meet local demands. The system can consist of many polygeeration modules, including renewable energy modules and convention-al modules for transformation of available energy sources to meet the heating, cooling and electricity demands. The problems for operation of such system are related not only to following of heating and cooling loads, but also on integration criteria and engagement priority of each of the modules of the polygeneration system. In this paper, a model used for control of heat supply of a superstructure of a polygeneration system for heating and cooling supply of the consumer is presented. The model operates according to the set-point temperatures of the consumer, heat and cold storage. The presented model is based on application with TRNSYS software simulation environment.**

***Keywords*— Polygeneration, renewable energy, energy supply control, Trnsys**

I. Introduction

A polygeneration system can be defined as a system for combined production of two or more energy utilities by using a single integrated process [1] [2]. The high level of integration of a polygeneration system affects the complexity of the system itself, improves overall system efficiency – thermodynamic, environmental and economic [3]. Polygeneration systems transform available primary energy sources to meet the local final energy demands [4]. Configuration of a polygeneration system should be de-fined to best meet the local energy demands taking advantage of available integrated energy transformation technology. A polygeneration system may consist of both conventional and renewable energy technologies, and as such may be considered a hybirid energy system. Polygeneration systems may be considered more complex than the conventional systems, with high dependency between locally produced utilities. Design and planning of polygeneration systems is a challenging optimization problem, which includes thermodynamic, environmental and eco-nomic system efficiency [2]. Optimization of polygeneration systems focuses either on system operation parameters and strategy or on system configuration [1-9]. In this paper, a method for determination of the optimal configuration and capacity of polygeneration system is presented.

Applicable polygeneration modules, form a system super-structure of the optimization problem [7] [8]. The superstructure formation of the problem of optimisation of configuration of polygeneration systems can used with Mixed Integer Linear Programming [7] [8], but the results are limited to optimization of system configuration. In this paper, superstructure is integrated for the technically feasible system and subsystem configurations, which relate to technically feasible system and/or subsystem module combinations. In this paper, in addition to the convention-al heating and cooling technologies, and cogeneration technologies, integration of the polygeneraiton system superstructure included technologies for utilization of renewable energy sources (RES). The nominal capacity of the polygeneration system is defined by the sum of the nominal heating, cooling and electricity production capacities of the modules constituting the polygeneration system, limited to the design load capacities.

In order to investigate proper behaviour of such highly integrated systems, and mutual interaction between polygeneration modules, it is important to define the control and utilization criteria, which is performed using TRNSYS soft-ware, as presented in this paper. This approach is applied for the case study of a public indoor swimming pool building, and its energy demands, but can be considered general and applicable to other polygeneration simulation problems as well. Trnsys simulation coupled to GenOpt optimisation was used to pinpoint the optimal configuration and capacity of a polygeneration system for a livestock farm [2]. The analysed superstructure model, formed for an optimization problem is presented in fig 1. The superstructure is defined based on the data acquisition about the location, it's energy

demands and local resources, identification of locally applicable energy sources in addition to the conventional sources, determination of design loads, integration of the superstructure of the polygeneration system. With the defined superstructure consisting of applicable technically feasible polygeneration modules, energy demand, supply and the superstructure of the polygeneration system are modelled and simulated using TRNSYS software [9] .

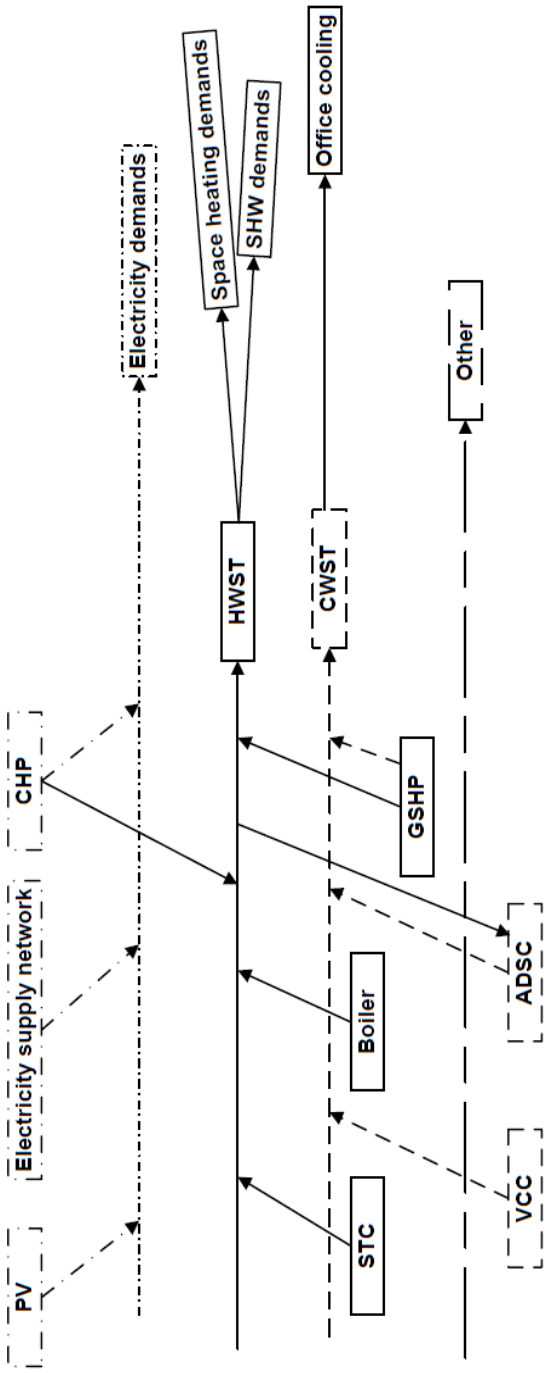

Fig. 1. Analysed polygeneration superstructure model

The simulation energy demand and supply model results are compared to the measured data, acquired through measurements on the real object to validate the model. Applicable polygeneration modules, form a system superstructure of the optimization problem [11] [12]. The superstructure formation of the problem of optimisation of configuration of polygeneration systems can used with Mixed Integer Linear Programming [11] [12], but the results are limited to optimization of system configuration. In this paper, superstructure is integrated for the technically feasible system and subsystem configurations, which relate to technically feasible system and/or subsystem module combinations. In addition to the conventional heating and cooling technologies, and cogeneration technologies, integration of the polygeneraiton system superstructure included technologies for utilization of renewable energy sources (RES). The nominal capacity of the polygeneration system is defined by the sum of the nominal heating, cooling and electricity production capacities of the modules constituting the polygeneration system, limited to the design load capacities.

II. Energy supply control model

The control functions and thus the behaviour and interaction of the presented superstructure of a polygeneration system are defined in TRNSYS software [16], on two levels. Level one defines the output of the polygeneration system active superstructure configuration, for meeting the energy demands of the analysed demand side model, with heating and cooling loads as a priority. Electricity production of the polygonation system is not controlled. Instead, it is assumed that the produced electricity during the operation of the system, which is guided to meet the heating and cooling demands of the model as a priority, can be transferred to the grid at each of the simulation timesteps, or utilized on-site. The same rule could be applied to the other polygonation system outputs, such as material outputs in a scenario analysis which considers material products of the polygeneraiton system. The second level of the control considered is the level of the superstructure which is designed to set the priority of activation and utilization (i.e. engaging) the polygeneration modules constituting the analysed polygeneration system superstructure.

For the first level of control model, Type 23 model from the Trnsys library [9] is used to define the exact three-way mixing valve control value for the heating and cooling regime. The three-way mixing valve can be considered the main valve, which regulates the output temperature and mass flow rate of the fluid at the output after the heat storage of the model of the polygeneration system superstructure. Similar approach is used to define the desired output capacity values of the superstructure for each time step. The heating and cooling hysteresis, and thus the ON/OFF control functions for both heating and cooling regimes are defined using the Type 2 controller model [9]. Outputs of these components are used to define the exact control signals by creating a subroutine for performing calculations of the exact control signal numerical values at each simulation timestep, based on the numerical results of the TYPE 2 and TYPE 23 model outputs [9]. The free cooling mode, which bypasses the engagement of cooling modules of the superstructure, thus saving energy, can be calculated using Trnsys syntaxis as [9]:

CS_FCH=FCH*gt(Text,Tbound)*lt(Text, TreturnPrev-DT)) (1)

Where Text is the external temperature, T bound is the boundary temperature for free cooling model, TreturnPrev is the value of the return temperature from the previous timestep, DT is the temperature difference, and the rest of the values are obtained as outputs from the Trnsys component model outputs.

Similar, the heating and cooling control signals are given as:

HeatCS=
(lt(Text,Tub),HeatingHYST)!min(lt(Text,Tub)+HeatingHYST,CSmax)
(2)

CoolCS=lt(FCM,CSmax)*lt(HeatingCS,CSmax)*min(CSmax,gt(Text,Tub)+CoolingHYST)
(3)

Where, Tub is the boundary indoor temperature for engaging the superstructure system for heating/cooling, CSmax is the upper boundary of the control signal equal, FCH is the free cooling mode control signal and the rest of the equation variable values take the numerical value of the out-puts of the control types for each simulation timestep as mentioned above. The explained control Trnsys model is presented in fig. 2.

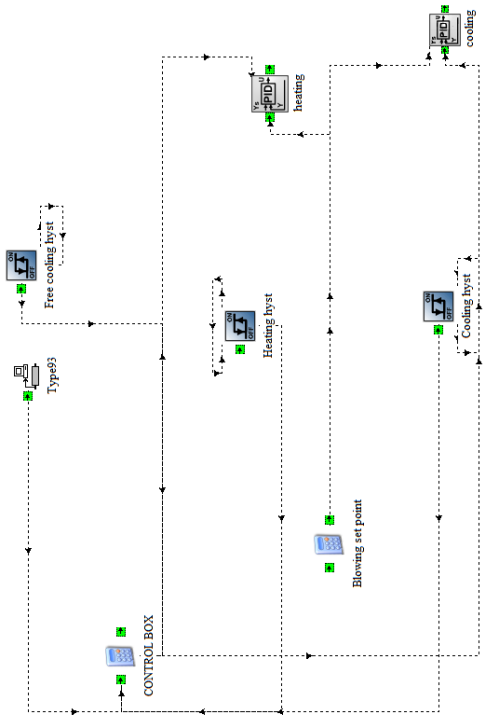

Fig. 2. Trnsys control model

The presented control model is in interaction with the rest of the model, both demand side and superstructure model.

The interaction model is given in fig 3. The model present-ed in fig 3 illustrates the Trnsys model, with focus on the utilized control models components, as mentioned above. The model transports polygeneration superstructure heating and cooling ouputs via the modelled heat exchanger network to the demand side model. The demand side model is defined using the Type 56 multizone building model.

Signal with respect to the current change in heating demands is significantly lower than the maximum value, with similar behaviour of the mixing valve control signals. However, since the model is created with the idea of optimal sizing of the superstructure model, this also reveals important information about the polygeneration system heating capacity: The analysed heating capacity of the super-structure is significantly higher for the analysed loads. As a consequence, the calculated blowing set point temperatures for the air ventilation heating system can also be considered relatively low.

The obtained control functions represent the control signal values obtained during simulation, as well as obtained temperatures at the monitored points in the model. For the analysed period, the free cooling mode is not engaged, since the presented results are valid for the heating period. The figure represents the values of the three way mix valve control signal and heating control signal, as well as desired outlet temperature. It can be observed, that for the analysed scenario, with the analysed heating capacity of the superstructure polygeneraiton system model, the heating control

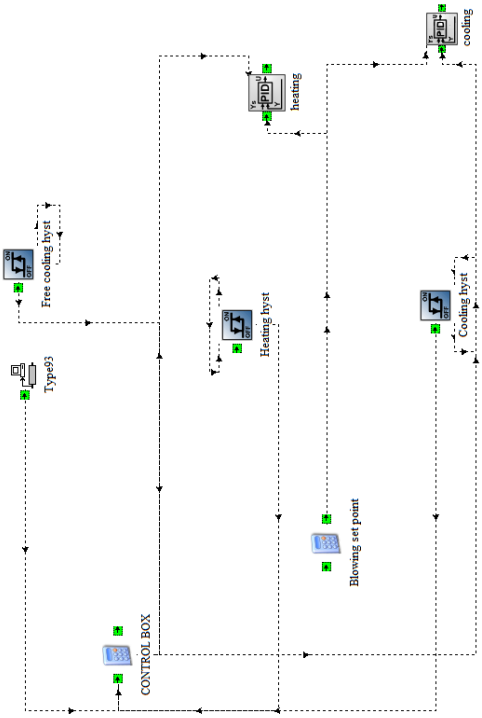

Fig. 3. Trnsys heating and cooling loop model

On the other hand side, it can be considered that the model has performed well and fulfilled its basic task, which is to adopt the output values of the polygeneration system superstructure with the change of the heating loads. Similar behavior could be observed with the cooling regime. It should be noted, that the intention of this paper is to present a functioning simple control model, which is designed to adopt the output capacity of the polygeneraiton model superstructure at the first level of the control, and not to present the best match of the capacity of the polygeneration system superstructure model and the analysed load profile.

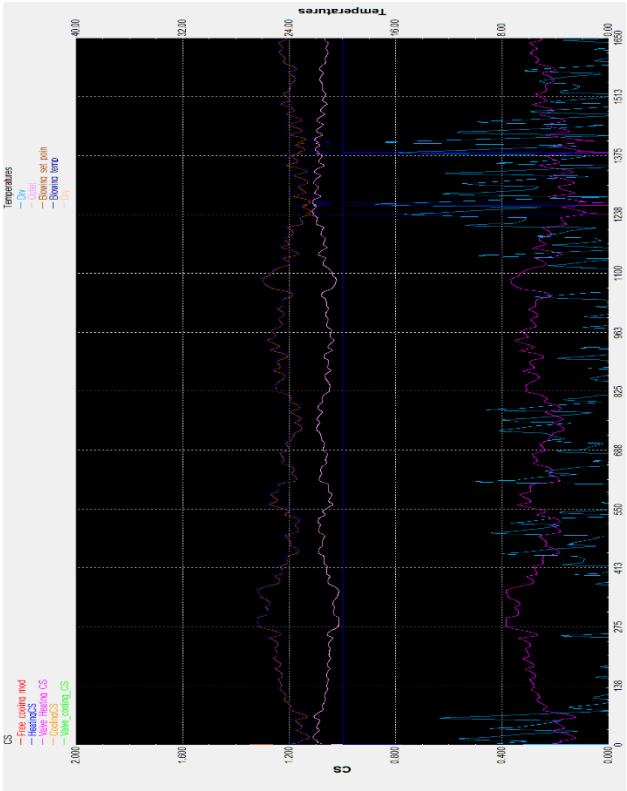

Fig 4. Control signals obtained using the presented model for the simulation time from 0 to 1650h

III. Conclusions (use style MASING Heading 1)

In this paper, a simple TRNSYS control model used for the first level of control, i.e. coupling of the superstructure of the polygeneraiton system to the heating and cooling loads is presented. The illustration of the model in TRNSYS interface is given in the paper, as well as the equations for in TRNSYS sintax applied to define the control signals for heating, cooling and the mixing three way valve, after the polygeneration system, which control temperature and flow rates of the working medium towards the load, based on the calculated load value at each time step. The model takes advantage of the available control model Types in Trnsys, from the component model library, but extends the functionality and adopts the model by using the presented mathematical control signal equations, energy demands and local resources, identification of locally applicable energy sources in addition to the conventional sources, determination of design loads, integration of the superstructure of the polygeneration system. With the defined superstructure consisting of applicable technically feasible polygeneration modules, energy demand, supply and the superstructure of the polygeneration system are modelled and simulated using TRNSYS software [9] . The simulation energy demand and supply model results should be compared to the measured data, acquired through measurements on the real object to validate the model, preferably with similar control systems available on the real object. In order to investigate proper behavior of such highly integrated systems, and mutual interaction between polygeneration modules, it is important to define the control and utilization criteria, which is performed using TRNSYS software, as presented in this paper. This approach is applied for the case study buildingand its energy demands, and can be considered general and applicable to other polygeneration simulation problems as well. Trnsys simulation coupled to GenOpt optimisation was used to pinpoint the optimal configuration and capacity of a polygeneration system for a livestock farm [2]. The analysed superstructure model, formed for an optimization problem, which represents variable supply system configuration, with variable output supply temperatures. Hence, it is imorotant to account for these changes in order to provide similar quality of the energy supply for the end user, in terms of heating and cooling.

Acknowledgment

This research was financially supported by the Ministry of Education, Science and Technological Development of the Republic of Serbia.

References

[1] Lahdelma R., Rong A., Role of polygeneration in sustainable energy system development challenges and opportunities from optimization viewpoints. 2016, Renewable and Sustainable Energy Reviews 53, pp. 363–372.

[2] Mančić M., Živković D., Đorđević M., Rajić M., Optimization of a polygeneration system for energy demands of a livestock farm.. 5, 2016, THERMAL SCIENCE, Vol. 20, pp. 1285-1300.

[3] Sudipta De, Kuntal J., Sustainable polygeneration design and assessment through combined thermodynamic, economic and environmental analysis. 2015, Energy 91, p. 540e555.

[4] Khan, Er. U. and Martin, A.R., Optimization of hybrid renewable energy polygeneration system with membrane distillation for rural households in Bangladesh. 2015, Energy 93, pp. 1116–1127.

[5] Mančić M., Živković D., Milosavljević P., Todorović M., Mathematical modelling and simulation of the thermal performance of a solar heated indoor swimming pool. 3, 2014, THERMAL SCIENCE, Vol. 18, pp. 999-1010.

[6] Meteonorm. Global Meteorological Database Handbook version 7, The meteorological Reference for Solar Energy Applications, Building Desing, Heating & Cooling Systems, Education Renewable Energy System Design, Agriculture and Forestry, Environmental Research. s.l. : Meteonorm, 2015.

[7] Liu P., Gerogiorgis D., Pistokopoulos E., Modeling and optimization of polygeneration energy systems. s.l. : Catalysis Today, Volume 127, 1–4, 2007.

[8] Liu P., Pistokopoulos E., Li Z., A multi-objective optimization approach to polygeneration energy systems design. s.l. : Process Systems Engineering, Vol 56, 5, pp 1218-1234, 2009, Vol 56, 5, pp 1218-1234.

[9] Klein S.A., Beckman W.A., Mitchell J.W., Duffie J.A., Duffie N.A., Freeman T.L., Mitchell J.C., Braun, B.L. Evans, J.P. Kummer, R.E. Urban, A. Fiksel, J.W. Thornton, N.J. Blair P.M. Williams, D.E. Bradley J.E., McDowell T.P., Kummert M., Arias D.A.. TRNSYS 17, a Transient System Simulation program. Wisconsin-Madison : Solar Energy Laboratory, University of Wisconsin-Madison, 2014.

THE 5th INTERNATIONAL CONFERENCE
MECHANICAL ENGINEERING IN XXI CENTURY

December 9-10, 2020
Faculty of Mechanical Engineering in Niš, Serbia

Justification of Using Turbulators Stripes in Biomass Heating Stoves

Milica JOVČEVSKI[1], Miloš JOVANOVIĆ[1], Mirjana LAKOVIĆ[1], Marjan JOVČEVSKI[2]

[1] Faculty of Mechanical Engineering, University of Niš, Serbia,
[2] University "Ss. Cyril and Methodius", Faculty of Mechanical Engineering Skopje, North Macedonia.
milica.jovic@masfak.ni.ac.rs, jmilos@masfak.ni.ac.rs, lmirjana@masfak.ni.ac.rs, makos@gmail.com

***Abstract*—In this paper, a mathematical model is examined for heat transfer at heat exchangers. The target is to obtain higher efficiency of a pellet stove, and from that, the heat transfer is the crucial parameters for their efficient operation. The stove which is analysed is operating on wooden mass pellets. Heated gasses flow through the pipes of the heat exchanger. The observed stove has 6 vertical gas pipes in the exchanger. Heat convection is achieved from the gasses to the internal pipe walls, observing the physical mechanism for the heat transfer coefficient in a turbulent boundary layer, where flow shear stress occurs as part from provoked increased turbulence i.e. Reynolds analogy, where the assumption being made is that the mechanisms of heat and momentum transfer are similar. With application of turbulator stripes in the pipes of the heat exchangers, internal heat transfer area increases, the shear stresses of the flow near the pipe walls is increased which leads to increased heat transfer efficiency and overall efficiency of the stove.**

***Keywords*— Heat transfer, Pellet stove, Convection, Turbulator stripes, Reynolds analogy, Efficiency**

I. Introduction

Heat exchangers present an important part of operation for many systems. Over the past quarter century, the importance of heat exchangers has increased in terms of energy conversion and energy efficiency. Much more attention is paid to heat exchangers for environmental protection, such as thermal, air and water pollution, and waste heat recovery. They can be considered as key equipment in the chemical process industry. A heat exchanger is a finite volume device used to transfer heat between a solid surface and a fluid or between two or more fluids. These two fluids are separated by a solid wall to prevent mixing and also to prevent direct contact between them.

Heat exchangers are used in various processes such as conversion, utilization and recovery of thermal energy in various industrial and commercial processes. The most common examples include:

- Steam production and condensation in power plants and cogeneration plants.
- Heating and cooling in heat treatment of chemical, pharmaceutical products.
- Heating fluids in the production industry
- Recovery of waste heat, etc.

Pellet stoves are heat exchangers that burn compressed fuel and create a heat source for residential or industrial buildings. By constantly feeding fuel from a pellet storage tank, the stove produces a constant flame that requires little physical adjustment. Today's central heating systems operate with wood pellets since renewable energy can reach an efficiency factor of over 90%[1].

Pellet stoves are relatively new devices and are constantly being developed to reduce the daily activities of users towards them, but also to improve performance and utilization levels. Various types of stoves can be seen on the market that use pellets as an energy source.

Increasing the heat exchanger performance can lead to a more economical heat exchanger design that can help save energy, material, time and resources associated with the heat exchange process.

The need to increase the thermal performance as well as the energy efficiency of heat exchangers in order to save costs leads to the development and use of many techniques to improve heat transfer. The main idea for improving heat transfer refers to the Optimization of Thermo-technical Performances [2].

II. Techniques for Improving Heat Transfer

Techniques for improving heat transfer in a heat exchanger are classified into three different categories [3]:

- Passive techniques
- Active techniques
- Complex techniques.

Passive techniques generally use surface or geometric modifications of the flow channel by inserting additional devices (turbulators). These additional devices promote higher heat transfer coefficients by distorting or altering the fluid flowconditionand the flow from laminar to turbulent, which also leads to an increase in pressure drop. Increasing heat transfer with these techniques can be achieved by using:

- Treated surfaces: This technique involves using cavities or recesses to change the surface of the area of heat transfer that can be continuous or uninterrupted.
- Rough surfaces: These surface modifications especially create a disturbance in the viscous layer. These techniques are applied primarily in conducting one-way heat transfer.
- Turbulent flow devices: They produce turbulent flow or secondary circulation of axial flow in a channel. Spiral tape, and

various forms of elements that are used for change of tangential to axial direction are common examples of turbulent flow devices.

Active techniques are more complex from the point of view of use and design, because the method requires external input of electricity to cause the desired modification of the flow and improve the degree of heat transfer. It has limited application due to the need for external power in many practical versions. Compared to passive techniques, these techniques do not show much application potential because it is difficult to provide external energy.

Complex techniques for improving heat transfer are those techniques that are a combination of two or more of the above techniques in order to improve the performance of a heat exchanger.

III. Turbulent flow devices (turbulators)

Turbulators cause rotational flow or secondary fluid flow. Various devices can be used to induce this effect, which includes the insertion of strips, arrangements to change the flow through the pipes, and modifications to the geometry of the channels. Dimensions, ribs, spirally twisted strips are examples of modification of their geometry. Turbulator inserts include tapered parts, spiral strips, or inserts such as nuts and wire coils [4].

There are several types of turbolators. Here are 4 types of turbolators:

- Angular
- Coiled rod
- Twisted tape
- Process

On the Figure 1 it can be seen this models of turbulators [5].

For concrete model of pellet stove twisted tape turbulators were used.

The twisted tape turbulator is formed in a spiral shape and is usually used in heat exchangers which are composed of pipe walls, and fluid flows through the pipes. This form of turbulators in heat exchangers increase heat transfer coefficients with relatively low heat reduction. They are known to be one of the latest turbulent flow devices used in conducting one-way heat transfer. Due to the design and practicality of their application, they are widely used in thermal devices to generate turbulent fluid flow. Due to this, the size of the heat exchanger can be reduced, and the same performance can be obtained, which would have a favorable effect on its cost. Spiral strips are also suitable for their application in heat exchangers because they allow easy installation and disassembly and thus simple reading and maintenance of the heat exchanger.

Pellet stove is for residential heating. It is capacity of 18kW. In this stove is inserted 6 twisted tape turbulators.

The reason for installing the turbulators is to get a higher degree of efficiency of the stove itself.

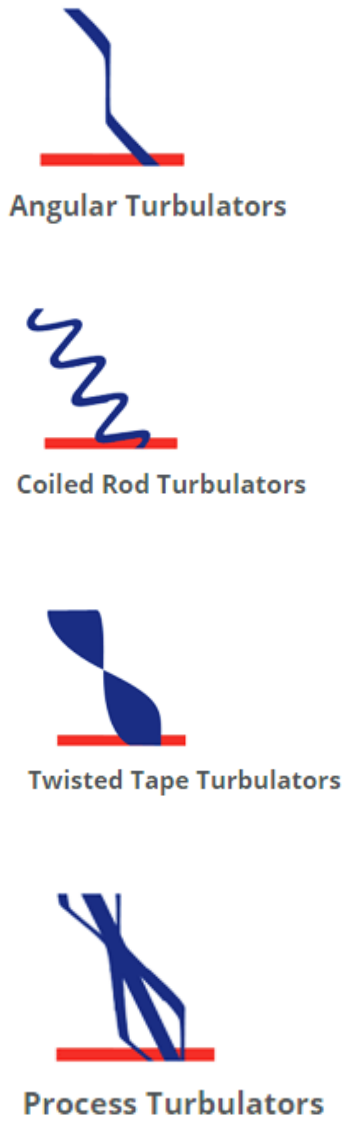

Fig. 1. Types of turbulators

As the exhaust gases in pellet stoves are high, the task of the turbulator is to enable a larger contact area, the transition of flow from laminar to turbulent flow and thus reduce the temperature of the exhaust gases and increase the efficiency of the boiler.

The turbulators are self-made in order to serve for the further experimental part and to confirm the results of mathematical model presented in this paper.

IV. Modeling the working process, energy exchange and heat transmission mechanisms in pellet stove

This chapter describes the mechanism of heat transfer in the boilers, as well as the mathematical models of the process of work and energy exchange, in order to obtain the dominant parameters that define the efficiency of the boiler, which are later determined through experimental measurements. A schematic representation of the operation and connection of the boiler is given in Fig.2.

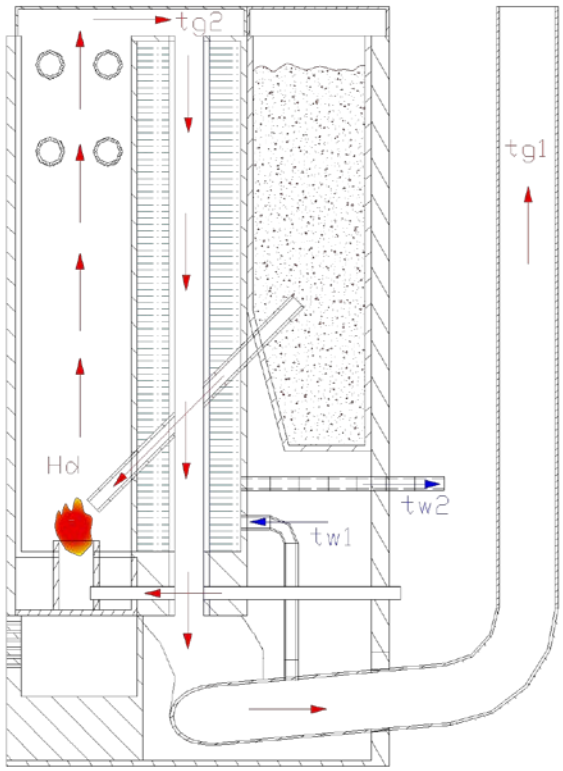

Fig.2 Hot water boiler operating scheme

From thermodynamics known mechanisms of heat transfer are the conductive, convective and inductive mechanisms. First, it is necessary to determine which heat transfer mechanisms directly participate in the operation of the boiler itself. Due to the fact of forced ventilation through the boiler there is a forced convective heat transfer. Forced convection takes place in the fireplace of pellet boiler where combustion process occurs (the combustion process is not part of the analysis of this paper). Then the combustion gases with increased temperature from the combustion process are transported to the heat exchanger where they transfer the heat through the wall of the pipe to the space filled with water. At the end from there the gases with reduced temperature are removed through the chimney. According to this, local convection-conduction-convection can be derived as a mechanism of heat transfer in the heat exchanger - pipes. Schematic representation of the temperature distribution of these boilers is given in Fig.3.

From the temperature distribution scheme of the boilers, the following relations can be derived:When pellets burn in the boiler fire place, the temperature t_lis released where the gases with that temperature are transported to the inlet of the pipes of the heat exchanger, so that the inlet temperature to the pipes of the heat exchanger can be adopted with sufficient accuracy as the temperature in the fireplace. Hence, the gases with that temperature t_g2≈t_l flow through the pipes of the heat exchanger and transfer some of the heat to the water tank from the heat exchanger. Here occurs the complex mechanism of heat transfer, convection - the gases transfer heat to the inner wall of the tubes of the exchanger, then conduction - the heat of the inner wall is transferred to the outer wall of the tubes, and convection - the heat of the outer wall of the tubes is transferred to the working medium in the tank. The thermal energy of the gases transmitted to the working medium through the pipes of the exchanger has a reduced thermal potential expressed through the temperature t_g1 and thus the gases are taken out through the chimney.

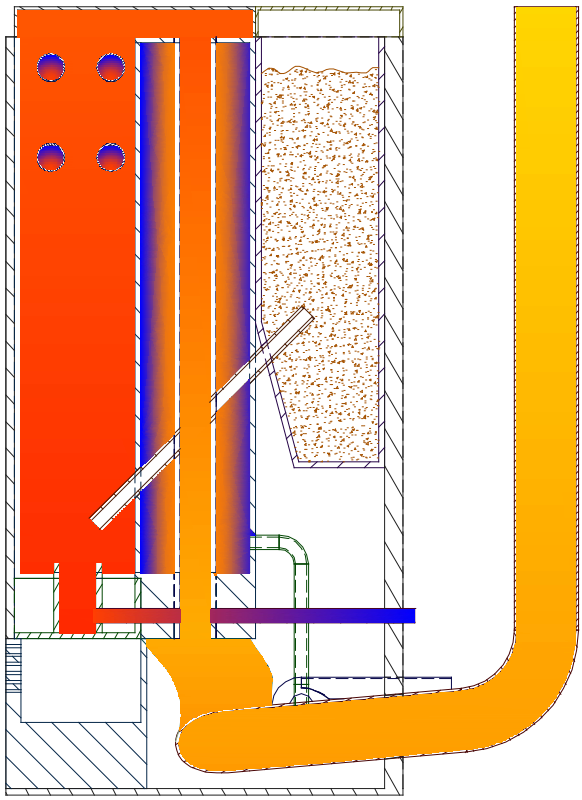

Fig.3. Temperature distribution in a hot water boiler

A schematic representation of the heat exchanger is given in Fig.4 where the temperature distribution in the whole boiler is presented. The segment where the energy exchange takes place between the gases and the working medium is elaborated at this point. It can be concluded that heat transfer takes place in three steps, i.e. convection, conduction and convection [6].

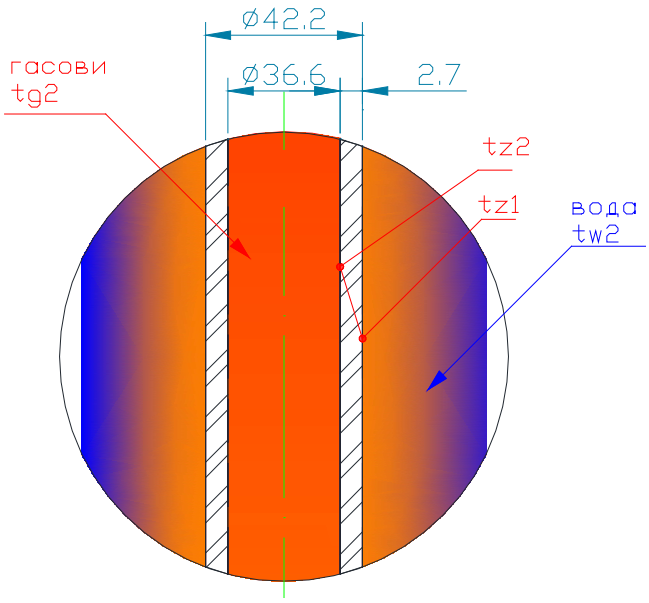

Fig.4. Heat transfer in the heat exchanger

For such a case when the fluids are separated from each other by a single-layer cylindrical wall, the heat fluxes in the stationary state can be written as[7]:

Flux 1 – Gas towards the inner wall - Convection

$$\phi_1 = A_1\alpha_1(t_{g2} - t_{z2}) \quad (1)$$

Where:

$A_1 = D_1\pi Z$ - the surface of the inner shell of the pipe [m^2],

α_1- the convective coefficient of heat transfer from the gases to the inner wall [W/m^{2}K],

t_{g2}- the temperature of the gases in the pipe [K] and

t_{z2}- the temperature of the inner wall of the pipe [K].

Flux 2 - External wall of the pipe towards the working medium – Convection

$$\phi_2 = A_2\alpha_2(t_{z1} - t_{w2}) \quad (2)$$

$A_2 = D_2\pi Z$- the surface of the outer shell of the pipe [m^2],

α_2- the convective coefficient of heat transfer from the outer wall of the tube to the working medium [W/m^{2}K],

t_{z1}- the temperature of outer wall [K],

t_{w2}- the temperature of water in the heat exchanger tank [K].

Flux 3 - Inner to outer wall - Conduction

In differential form:

$$\phi_3 = -\lambda \cdot 2r\pi \cdot \left(\frac{dt}{dr}\right) \quad (3)$$

That is, in absolute form:

$$\phi_3 = \frac{t_{z2} - t_{z1}}{\frac{1}{2\pi\lambda} \cdot \ln\frac{D_2}{D_1}} \quad (4)$$

$\frac{D_2}{D_1}$ the ratio of the outer and inner diameters of the tube [mm],

λ- the coefficient of thermal conductivity [W/m^{2}K]

$t_{z2} - t_{z1}$- is the difference between the temperatures of the inner and outer tube walls [K].

By equalizing these expressions for heat (fluxes), we get the total heat transfer coefficient of 1 [m] longitudinal cylindrical wall:

$$k_c = \frac{1}{\frac{1}{D_1\pi\alpha_1} + \frac{1}{2\pi\lambda}\ln\frac{D_2}{D_1} + \frac{1}{D_2\pi\alpha_2}} \quad (5)$$

The total heat flux:

$$\phi = k_c(t_{g2} - t_{w2}) \quad (6)$$

V. Description of flux 1 - gas convection through the inner wall of the pipe

Due to further analyses that go in the direction of increasing the rate of heat transfer from the gases to the wall of the pipe, heat transfer through flux 1 is elaborated in order to see the dominant physical parameters that affect the increase of heat transfer.

This is defined by the phenomenon of forced convection in turbulent currents taking into account the Reynolds analogy.It studies the behaviour of the boundary layer of the fluid. It makes use of similarity, between the mechanism of fluid momentum transfer to the wall and the transfer of heat by convection [8].

Reynolds analogy is based on the existence of a similarity between forced convection and friction losses from the flow in the tubes, and thus to predict the amount of heat transfer through high surface resistance on the pipe. If we take into account the flow along the wall, there are shear stresses in the flow that can be simply written as:

$$\tau_\nu = \mu\left(\frac{dU}{dy}\right) = \rho\nu\left(\frac{dU}{dy}\right) \quad (7)$$

where the shear stress caused by the flow in the layer is defined by the dynamic viscosity of the fluid and the change of velocity along the height of the layers. If the shear stress at the wall is expressed in terms of the dynamic head of the fluid, it follows:

$$\tau_\nu = f \cdot \frac{\rho\overline{v^2}}{2} \quad (8)$$

and for fully turbulent developed flow, the shear stress at the wall can be expressed as:

$$f = \frac{0.0791}{Re^{1/4}} \quad (9)$$

which is called *Friction law of Blasius*, which can be used for Reynolds number range up to $2 \cdot 10^5$[8].

The weighted mean velocity v_m for the turbulent velocity profile can be calculated by using the *Prandtl's power law of the wall*:

$$\int_0^r \rho \cdot v_r \cdot \left(\frac{y}{r}\right)^{\frac{1}{7}} \cdot 2\pi(r-y)dy = \rho \cdot r^2\pi \cdot v_m \quad (10)$$

So far, it has not been possible to produce a complete analytical solution for heat transfer by forced convection when the flow is turbulent. The Reynolds analogy suggests that there is a similarity between the forced convective heat transfer and fluid friction. Analogously to this, the heat flow by molecular conduction in this zone can be written as:

$$q_\alpha = -\rho c_p \alpha\left(\frac{dt}{dy}\right) \quad (11)$$

where the heat transfer in the layer directly depends on the density, the specific heat coefficient, the heat transfer

coefficient and the change in temperature along the height of the layer.

A similarity is apparent between these two equations, ie a direct connection of the shape of the flow with the heat transfer. When equalizing the equations for the same gradient in the height of the flow layer (in our case the radius of the tube) it is obtained that the tangential stress in the flow layer increases as the change of the velocity in the direction of the radius increases [8]:

$$\tau_v = \mu\left(\frac{dU}{dr}\right) \tag{12}$$

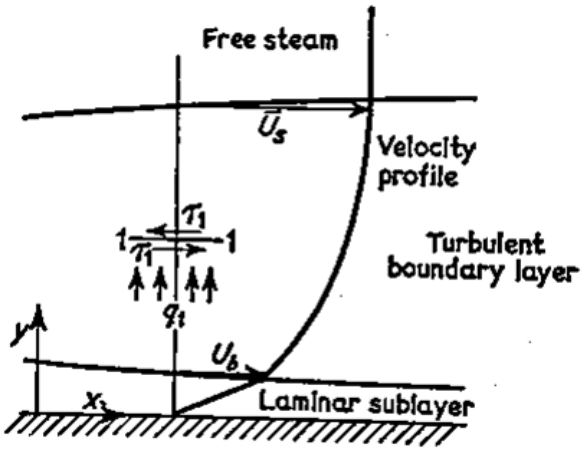

Fig 5. Similarity between heat flow and shear stress in fluid boundary layer [8]

Since the assumption is that there is a relation between the heat flow and the shear stress, the final relations for the analogy can be written as:

$$\frac{q_\alpha}{\tau_v c_p} = \frac{\theta_m}{v_m} \tag{13}$$

Whereθ_m is the average temperature difference at the observed section between the inlet/outlet fluid temperature and the wall temperature. The shear force at the wall is represented through the pressure difference at a portion of area observed:

$$F_{\tau_v} = \Delta p \cdot A \tag{14}$$

This conclusion clarifies the possibility of using the so-called turbulators in the tubes of the heat exchanger, in order to increase the shear stresses from the flow of the tube wall, i.e. the pressure drop increases.

In the figure 6 is presented the fluid flow with and without turbulators.

Pressure losses are minor without turbulator stripes:

$$\Delta p_n = p_0 - p_1 < \Delta p_t = p_{0t} - p_{1t} \tag{15}$$

Since this is valid, the shear force on the wall increases:

$$F_{\tau_{vn}} = \Delta p_n \cdot A < F_{\tau_{vt}} = \Delta p_t \cdot A \tag{16}$$

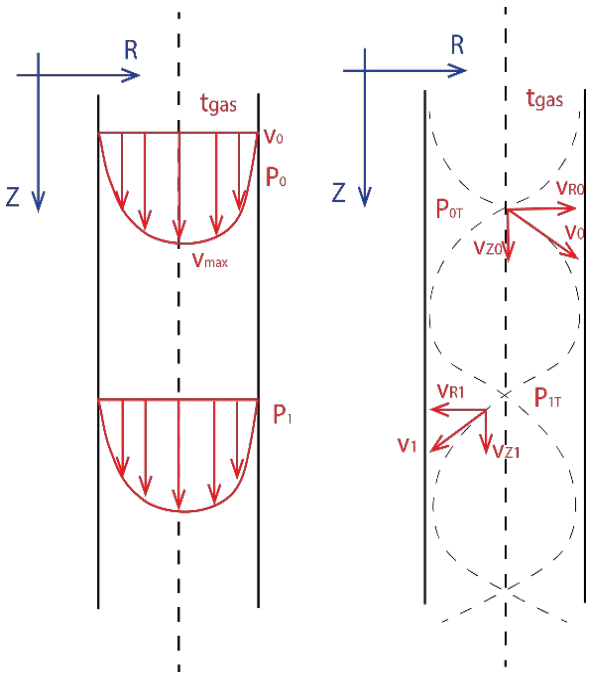

Fig 6. Flow without and with turbulators

In the case of a completely laminar flow, with Re<2300, the generation of a swirl motion determines the presence of a turbulence. The flow corresponding to this particular flow field is defined as pseudo-laminar. Because of the complexity of the flow and temperature field it is necessary to use advanced numerical tools for the study of the problem.

VI. Conclusions

Heat exchangers have multiple applications. Their design is complex and requires an accurate analysis to estimate the thermal power and pressure losses. Their design also requires an estimate of the performances in the long term and an accurate economic analysis.

Turbulators used inside tubes of pellet stove to improve the turbulent convective heat transfer coefficient in the gas side, since the heat transfer coefficient on the outside is very high. The overall objective in this application is to improve the boiler efficiency, although other factors such as: pressure drop, changes in the water side heat transfer coefficient, fouling, and manufacturing cost are also important.

Heat transfer enhancement is mainly due to flow blockage, eventual flow separations and secondary flows. The blockage increases the pressur drop along with increase in flow velocity. The secondary flow creates swirl and the resulting mixing of fluid improves the temperature gradient, which ultimately leads to a highheat transfer coefficient.

It is observed that use of twisted tape as insert is a good technique to improve thermal performance.

References

[1] M. Jovčevski, M. Jovčevski, F. Stojkovski, M. Laković, “Performance Analysis of a Pellet Stove with Turbulator Installments”, 19th Conference on Thermal Science and Engineering of Serbia,Sokobanja, pp.253-259, 2019

[2] K. Kiran , Asalammaraja, Manoj, C. Umesh, “A Review on Effect of Various Types of Tube Inserts on Performance Parameters of Heat Exchanger”, International Journal of Research in Advent Technology, Vol.2, No.3, June 2014, E-ISSN: 2321-9637

[3] D. Shriwas, J. Saini, “Heat Transfer Enhancement Technique in Heat Exchanger: An Overview”, 2018 IJRTI ,Volume 3, Issue 9 | ISSN: 2456-3315

[4] Quality Certification Scheme, ENplus Handbook For countries not managed by any national licenser/supporter, Part 3: Pellet Quality, Brussels: European Pellet Council (EPC), 2015.

[5] https://www.fuelefficiencyllc.com/]

[6] HRN EN 303-5: Heating boilers - Part 5: Heating boilers for solid fuels, manually and automatically stoked, nominal heat output of up to 500 kW - Terminology, requirements, testing and marking

[7] Laković, S., Thermal plants, (In Serbian), Faculty of Mechanical Engineering, Nis, Serbia, 1975

[8] G.F.C. Rogers &Y. R. Mayhew – Engineering Thermodynamics – Work and Heat Transfer (3rd edition, Longman, 1980).

THE 5th INTERNATIONAL CONFERENCE
MECHANICAL ENGINEERING IN XXI CENTURY

December 9-10, 2020
Faculty of Mechanical Engineering in Niš, Serbia

Thermal Stresses of Hot Water Boiler Structure During the Process of Start-up

Dragoljub ŽIVKOVIĆ, Milena RAJIĆ, Marko MANČIĆ

Faculty of Mechanical Engineering, University of Niš, Niš, RS
dzivkovic50@gmail.com, milena.rajic@masfak.ni.ac.rs, milan.banic@masfak.ni.ac.rs, markomancic@yahoo.com

***Abstract*—The maneuvering characteristics and safe operation conditions of hot water boilers are limited by thermal stresses of their structure. The greatest thermal stresses occur in non-stationary operating modes such as starting-up, changing operating mode or sudden shutdown due to protection system when permitted parameters are exceeded. Under these conditions uneven heating or cooling of the boiler element occurs, resulting in formation of large temperature gradients causing high thermal stresses. The paper presents the results of numerical and experimental analysis of the hot water boiler "Minel-Kotlogradnja", capacity 8.7 MW, during the process of starting-up. The aim of the paper was to determine the state of thermal stress of the hot water boiler structure during the process of starting-up and identifying the most important influencing parameters.**

***Keywords*—Hot Water Boiler, Start up, Thermal stresses, Transient Regime, Finite Element Method**

I. INTRODUCTION

The operational experiences of boiler plants indicate the failures occurrence that represents a consequence of breakdowns in certain parts of the boiler elements. These failures are usually caused by corrosion process, as well as inadequate handling of the plant, but also by the occurrence of material fatigue of those boiler elements that are exposed to high pressures and temperatures [1].

Transient operational modes, are considered as non-stationary, have not only the load change, but also the stress state change of the structure. This is especially evident when there is sudden load change, change of operational modes, start of the boiler or sudden abrupt stoppage due to accidents or necessary interventions. In such cases, the large temperature gradients exist in the boiler elements, which cause the appearance of thermal stresses that are dominant and much higher than the stresses caused by high pressures of the working fluid [2-4]. These transient regimes are specifically analysed in this paper.

One of the potentially critical transient operational modes is considered to be the process of starting-up the boiler, when there are high thermal stresses in the boiler elements. Thermal stresses represent a consequence of the resulting temperature differences in the boiler structure, due to the high temperature gradients of the combustion products during the process of starting-up the boiler and low temperatures of the structure itself. Thermal stresses are especially high in boiler elements with a large wall thickness [5-7]. The thermal stresses of the tube plate of the first reversing chamber are considered to be of the great importance, where the major failures had been occurring [8-16] and where the largest temperatures differences appear.

This paper presents the numerical and experimental results of hot water boiler in the regime of starting-up. Thermal stresses of boiler's structure are especially analysed in critical moment of time during the starting up.

II. DYNAMIC PROBLEM OF THERMOELASTICITY

Problem of starting up the boiler presents the complex dynamic problem of thermoelasticity of its structure. When setting up a mathematical model for thermoelasticity problems, it is necessary to define the constitutive equations of thermoelasticity [17]:

$$\{\varepsilon\} = [D]^{-1}\{\sigma\} + \{\alpha\}\Delta T \tag{1}$$

$$S = \{\alpha\}^T\{\sigma\} + \frac{\rho C_p}{T_0}\Delta T \tag{2}$$

Where: $\{\varepsilon\}$ - total strain tensor (Cauchy strain tensor); $[D]^{-1}$ - elasticity matrix; $\{\sigma\}$ - tensor determined by Hooke's law for an ideal elastic body as $\{\sigma\} = [D]\{\varepsilon^{el}\}$; $\{\varepsilon^{el}\}$ - elastic strain tensor; $\{\alpha\}$ - tensor of the coefficient of the linear thermal expansion; $\Delta T = T - T_{ref}$ where T - temperature for which the value of relative deformation is required and T_{ref} - reference temperature at which the relative deformation in all directions is equal to 0; S – entropy, where $Q = T_0 S$ and T_0 - absolute reference temperature.

Using the total strain tensor $\{\varepsilon\} = \left[\varepsilon_x \varepsilon_y \varepsilon_z \varepsilon_{xy} \varepsilon_{yz} \varepsilon_{xz}\right]^T$ and temperature change ΔT as independently variables and replacing entropy S with the amount of heat Q according to the second law of thermodynamics for return processes in the eq.(2) is obtained:

$$\{\sigma\} = [D]\{\varepsilon\} - \{\beta\}\Delta T \tag{3}$$

$$Q = T_0\{\beta\}^T\{\varepsilon\} + \rho C_v \Delta T \tag{4}$$

Where: $\{\beta\}$ - thermoelastic coefficient vector $\{\beta\} = [D]\cdot\{\alpha\}$; C_v - specific heat capacity at constant deformation or volume $C_v = C_p - \frac{T_0}{\rho}\{\alpha\}^T \cdot \{\beta\}$.

Substituting Q from eq.(4) into the equation of conservation of thermal energy according to the first law of thermodynamics, where it refers to the differential control volume given in eq. (5) it is obtain eq.(6):

$$\rho c\left(\frac{\partial T}{\partial t}+\{v\}^T\{L\}T\right)+\{L\}^T\{q\}=\ddot{q} \tag{5}$$

$$\frac{\partial Q}{\partial t}=T_0\{\beta\}^T\frac{\partial\{\varepsilon\}}{\partial t}+\rho C_v\frac{\partial(\Delta T)}{\partial t}-[K]\nabla^2 T \tag{6}$$

Where: $\{L\}$ - vector operator; $\{v\}$ - heat transfer velocity vector; $\{q\}$ - heat flux vector; $\ddot{q}$ - rate of thermal energy generation per unit volume; $[K]$ - thermal conductivity matrix.

In static and transient thermoelasticity analyses, the instantaneous total stress energy of an element (for FEA-finite element analysis) is calculated as:

$$U_t=\frac{1}{2}\int_V\{\sigma\}^T\{\varepsilon\}\,dV \tag{7}$$

The most general case of the thermoelasticity equations, expressed in vector form representing the coupled dynamic thermoelasticity problem [17-19], is given as:

$$\mu\nabla^2[u]+(\lambda+\mu)graddiv[u]-(3\lambda+2\mu)\alpha_t grad\theta+[F]-\rho[\ddot{u}]=0 \tag{8}$$

$$\nabla^2\theta-\frac{1}{a}\dot{\theta}+\frac{W}{\lambda_0}-\frac{(3\lambda+2\mu)\alpha_t T_0}{\lambda_0}div[\dot{u}]=0 \tag{9}$$

Where the coupling of the equations is achieved by the fourth term of the eq.(9). In eq.(8) and eq.(9) are given: $\{u\}$- displacement vector; μ and λ - Lame constants given as $\lambda=\frac{\nu E}{(1+\nu)(1-2\nu)}$ and $\mu=\frac{E}{2(1+\nu)}$; α_t - coefficient of linear thermal expansion.

The coupled quasi-stationary thermoelasticity problem is obtained with a slow thermal process, when the acceleration of displacement can be neglected ($[\ddot{u}]=0$)and in the absence of volume forces ($[F]=0$), then the equations (8) and (9) are reduced to:

$$\mu\nabla^2[u]+(\lambda+\mu)graddiv[u]-(3\lambda+2\mu)\alpha_t grad\theta=0 \tag{10}$$

$$\nabla^2\theta-\frac{1}{a}(1+\varepsilon_s)\dot{\theta}+\frac{W}{\lambda_0}=0 \tag{11}$$

Where ε_s represents the coupled coefficient of temperature field and displacement field and is defined according to [17] as $\varepsilon_s=\frac{(3\lambda+2\mu)^2\alpha_t^2 T_0}{(\lambda+2\mu)c_\varepsilon}$.

The uncoupled quasi-stationary problem of thermoelasticity is obtained by neglecting the coupling and acceleration of displacement:

$$\mu\nabla^2[u]+(\lambda+\mu)graddiv[u]-(3\lambda+2\mu)\alpha_t grad\theta=0 \tag{12}$$

$$\nabla^2\theta-\frac{1}{a}\dot{\theta}+\frac{W}{\lambda_0}=0 \tag{13}$$

The stationary thermoelasticity problem is obtained when there is no change in size over time. The basic equations are further simplified and take the form:

$$\mu\nabla\text{^}2\,[u]+(\lambda+\mu)graddiv[u]-(3\lambda+2\mu)\,\alpha_t\,grad\theta=0 \tag{14}$$

$$\nabla^2\theta+\frac{W}{\lambda_0}=0 \tag{15}$$

With these relations given in the previous steps, the stiffness matrix is obtained which is used for numerical analysis.

III. Experimental analysis

In order to examine the influence of the regime of the starting up the hot water boiler on its structure, temperature measurements were performed. The experimental measurement procedure included obtaining the temperatures of the boiler walls. Due to the lack of adequate literature data on the temperature value of the boiler construction, as well as on the change of temperature field over time, the obtained data are of exceptional importance. The data were used to form a numerical model for the analysis of boiler start up.

The aim of the experiment was to determine the temperatures of the tube plates of the first and second reversing chambers, at defined points and at certain boiler loads. In this way, knowing the temperature field of the structure, the analysis of thermal stresses that are presented would be more accurate and reliable comparing the real data.

The experimental method of temperature measurement was performed by using temperature probes. The measurement procedure required the determination of exact locations for the installation of measuring probes. The measurement is planned to be on the tube plates on the gas side, where unobstructed access is enabled as well as installation of probes. There were adopted 6 measuring points, with 4 on the tube plate of the first reversing chamber and 2 on the tube plate of the second reversing chamber. As the temperature of the flue gases at the nominal operating mode of the boiler is around 1200 °C at the outlet of the fire tube, a mantle probe, 3.5 m long, was adopted. On the same tube plate of the second draft, 2 measuring points were selected at defined places located in the zone of flue gases that leave the third draft, go in the shielded reversing chamber from the back and go to the chimney. The flue gas temperature to which the thermocouples would be exposed in this zone is around 230 °C. There are 2 more measuring points on the tube plate of the second reversing chamber, in the zone of flue gases that leave the second and enter the third draft, the temperature of the gases in this zone is around 450 °C (Fig.1). The aim of this experiment was to determine the change in temperature at certain points of the tube plate during the starting up the boiler, i.e. in the range of 0% to 100% load change.

Fig. 1 Installation of temperature probes

All output signals were connected to the computer and the system made it possible to monitor the change in temperature in real time, in different load conditions, during the operation of the hot water boiler.

The temperature of the structure was monitored and recorded in different operating modes of the boiler. According to the boiler load, with the experimental results, temperature gradients were monitored, which lead to thermal stresses.

The obtained measured temperature values were used to define the boundary conditions and more closely determine the numerical model. In this way, a more precise temperature field of the structure was used and the numerical model approached the exact thermal state of the real structure. The measured values were also used for the validation of the numerical model, not only in the nominal mode of operation, but also in the mode of starting up the boiler.

IV. Numerical analysis

Stress-strain analysis of the hot water boiler structure was performed using FEM in ANSYS program package, while a CAD model was created using SOLIDWORKS software package according to technical documentation of the boiler manufacturer [9,20]. Since the geometric model is symmetrical in relation to the plane that passes through its longitudinal axis and is normal to the plane of the substrate, considering the assumed heat load symmetry, half of the geometric model is neglected – the right side of the symmetry plane. The influence of the neglected part of the model is defined by the limitation of the number of degrees of movement freedom of nodes in the symmetry plane applied by a software package symmetry relation. The geometric model analysis results have determined that some elements of the model have a function of connecting the hot water boiler to the water supply network. These elements are also excluded from the analysis since they have no significant effect on the stress-strain state of the model. In addition to these elements, the boiler connection elements that have safety features are also neglected. The geometric model was transformed into the discretized FEM with the application of advanced meshing tool capable of creating adaptive discrete model. The discretized model consisted of 1661038 nodes, forming 310620 finite elements. The discretized model is presented in Fig.2. In the analysis, the materials that are used (which correspond to the real state of boiler construction) have the characteristics given in [9,21,22].

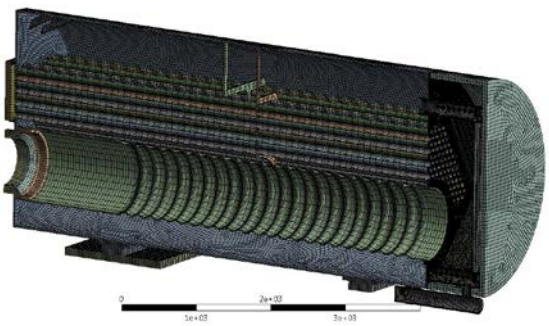

Fig. 2 Discretized structure of hot water boiler

By analyzing the structural load of the boiler, it can be determined that boiler loads are: loads resulting from the weight of the boiler elements themselves, loads resulting from the thermal expansion on higher temperatures and boiler operating loads (that is changed during the observed time period).

Numerical analysis model is analysed in the time domain. The presented model is considered to be of great importance while it is based on the variable operating mode from 0% to 100% of the load in a given time. In the case of the real hot water boiler, based on the experimental results, there is load reduced after 100*s* when the boiler starts. In numerical model, this period of reducing load is not considered. The numerical model is defined so that the load is not reduced as on a real boiler, but that the boiler load increases linearly, as is the case up to 100*s*. The aim of this analysis is to see what would happen to the structure if there were no changes in the character of the temperature rise curve of the structure, i.e. if the safety protection on the boiler did not work.

The analysis included the heat load that changes over time. The predicted heat load to which the boiler structure is exposed, which originates from the combustion of fuel in the fire tube is set from 0 to 100*s* based on the data obtained experimentally by measurements on a hot water boiler. An increase in boiler load up to 120*s* by extrapolating the curve was then considered to analyse the case without changing the character of the structure temperature curve (Fig. 3).

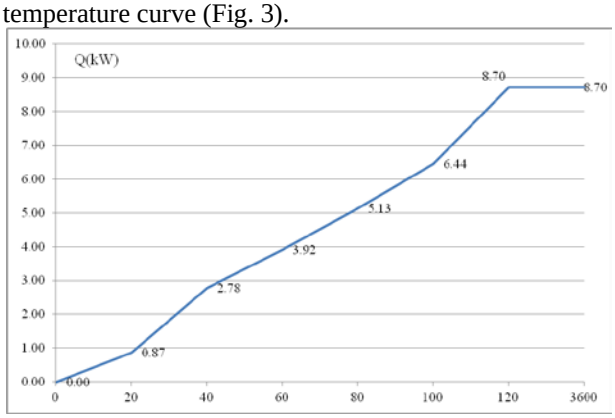

Fig. 3 Heat load change of fire tube Q as a function of time t (s)

The change of the boiler temperature in time period was simulated by applying thermal analysis in the transient mode during 3600*s*, i.e. one hour from the starting up the boiler, i.e. from the starting the heating of the boiler elements.

It is noticed that a relatively short period of time is needed until the approximately stationary state is obtained, in which the temperature field of the boiler does not change over time. The results show that after an hour, steady state is established. The temperature fields of the boiler structure, observed at time period 50*s*, 100*s* and an hour, are shown in Fig. 4, 5 and 6. The changes in the temperature field of individual parts of the structure, such as the tube plate of the first reversing chamber are shown in Fig. 7, 8 and 9.

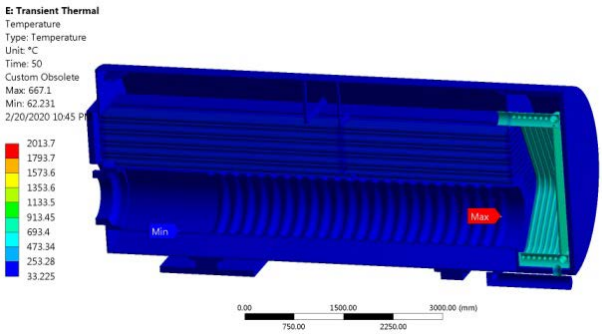

Fig. 4 Temperature distribution of boiler elements after 50s from the moment of starting up the boiler

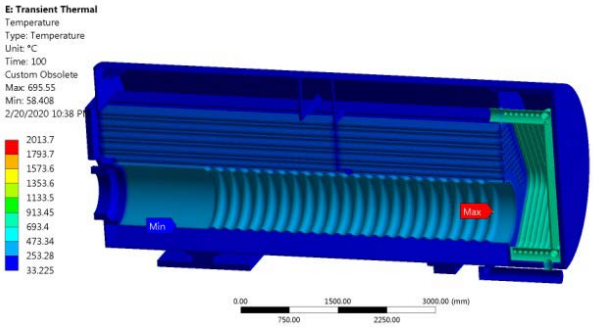

Fig. 5 Temperature distribution of boiler elements after 100s from the moment of starting up the boiler

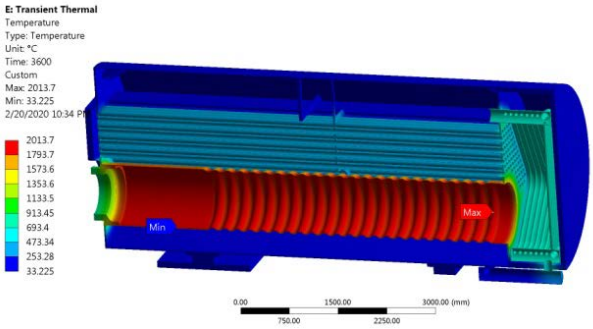

Fig. 6 Temperature distribution of boiler elements after 3600s from the moment of starting up the boiler

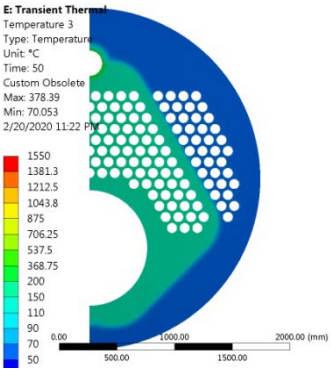

Fig. 7 Temperature distribution of the tube plate of the first reversing chamber after 50s from the moment of starting up the boiler

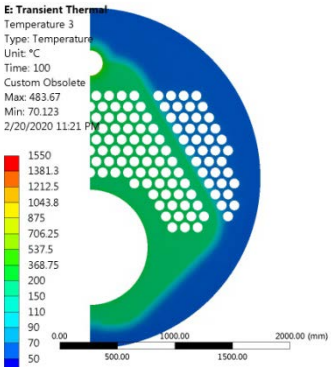

Fig. 8 Temperature distribution of the tube plate of the first reversing chamber after 100s from the moment of starting up the boiler

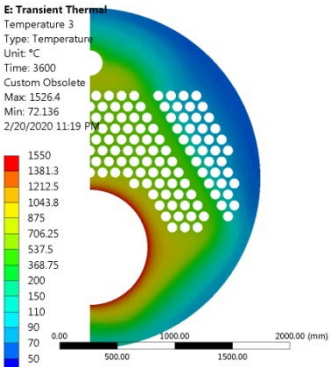

Fig. 9 Temperature distribution of the tube plate of the first reversing chamber after 3600s from the moment of starting up the boiler

The presented results of the change of the temperature field of the boiler structure (Fig. 5 and 8) are compared with the measured values on the real object. Based on the measured temperature values by the experimental procedure, the numerical model can be verified. This was the reason to install thermocouples on the pipe plates. By verifying the temperature field on these elements, the resulting temperature field of the structure can be adopted with certainty. In the previous chapter, 6 measuring points on the boiler were defined, where the values of the construction temperature are experimentally determined. The locations of these measuring points were also identified on the numerical model, in order to compare the values. The comparative values of the temperatures on the pipe plate of the first turning chamber are shown in the Table 1.

TABLE I COMPARATIVE ANALYSIS OF TEMPERATURES OBTAINED BY EXPERIMENTAL AND NUMERICAL ANALYSIS

No	Position	Experimental value [°C]	Numerical analysis [°C]
1	Tube plate 1 – t1	805.5	595.7
2	Tube plate 1 – t2	727	577.9
3	Tube plate 2 – t1	133.6	133.6
4	Tube plate 2 – t2	136.6	133.4
5	Tube plate 1 – t3	83.1	96.1
6	Tube plate 1 – t4	80.7	94.4

The results indicate a significant match between the measured values of temperatures and the values obtained numerically. Especially of the measuring points on the tube plate of the second reversing chamber and on the tube plate of the first turning chamber, but towards the outer circle (third flue). A relative difference of 26%

refers to the measured temperatures of the tube plate of the first reversing chamber, closer to the fire tube. The measured temperature values, which are higher than those obtained by numerical analysis, can be explained by the high sensitivity of the probes and the positioning of the probe tips. Also, in this part, the measurement was difficult due to the high flue gas flow rates.

Comparative analysis of the results also allows verifying the numerical model. It is very important to emphasize that in the process of starting-up the boiler, the accumulation of thermal energy is done first in the walls of the structure, and only later, when stable operation is achieved, the water is heated.

V. Results and Discussion

In order to analyse the stress state of the hot water boiler structure, the critical moment was chosen to present the results. At the considered moment, i.e. at time t = 100*s* from the beginning of boiler start up, the stress-strain state of the structure was analysed. As the temperature differences between the construction and the heating medium are large at this moment, it is expected that the stresses are the highest. Fig. 10 and 11 show the state of stress and strain (respectively) at a given moment of time.

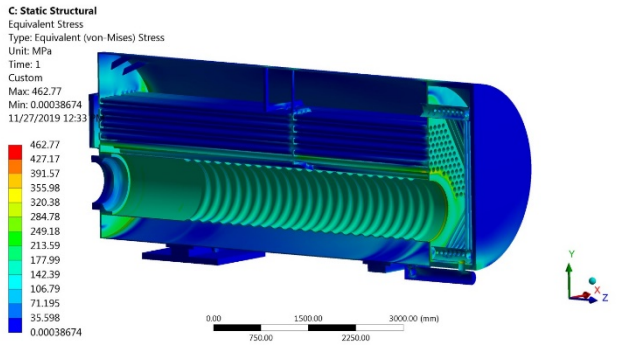

Fig. 10 Equivalent stresses of hot water boiler structural elements at 100s from the moment of starting up the boiler

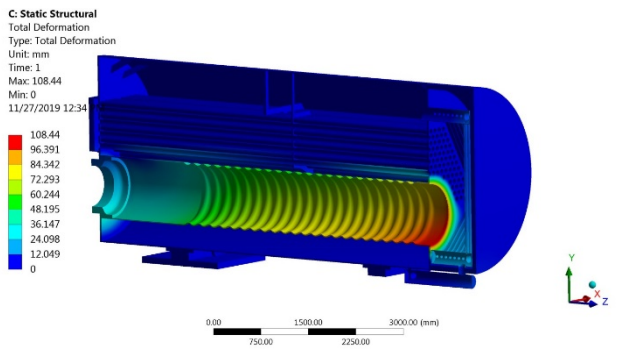

Fig. 11 Total deformation of hot water boiler structure at 100s from the moment of starting up the boiler

As can be seen from the Fig.12, the maximum stress values are about 410 MPa, while the tensile strength of the material itself (P265GH according to DIN EN 10028-2 [9,15,16]) of which the pipe wall is made Rm = 410-530 N/mm2, and yield strength Rp = 255 N/mm2. At high temperatures of the tube wall, the yield strength is even significantly lower. The maximum stress values are exactly on the tube plate, in the zone of the first line flue gas pipes of the second draft (Fig.10). This also indicates that these are the critical values. The stresses state in the tube plate is shown in Fig. 12 where these critical stresses can be observed. Under these conditions, the results of direct deformation in the axis normal to the tube plate are given in Fig. 13. The installed protection system, which reduces the heat load at that time t = 100*s*, leads to a reduction of the stress state from the critical obtained values. Without exposing the boiler construction to elevated stress, the boiler operation is then safe and secure.

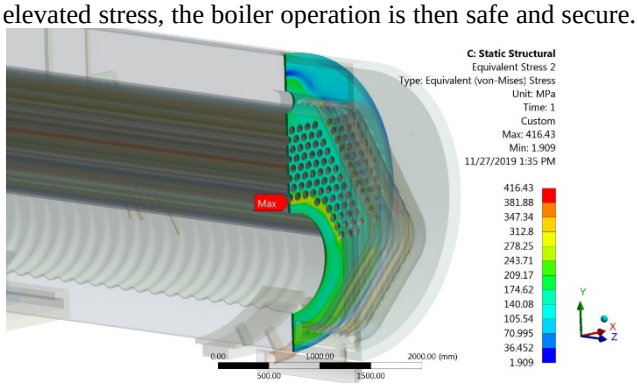

Fig. 12 Equivalent stresses of tube plate of the first reversing chamber at 100s from the moment of starting up the boiler

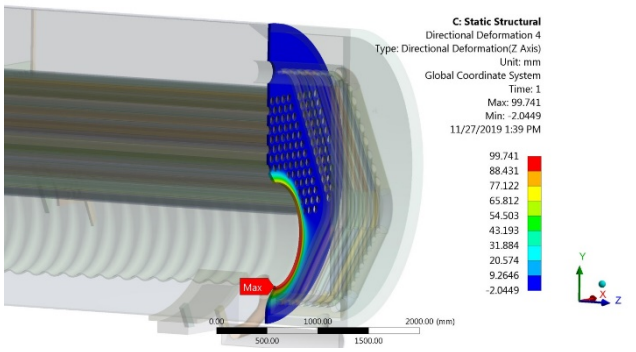

Fig. 13 Total deformation (directional Z Axis) of the tube plate of the first reversing chamber at 100s from the moment of starting up the boiler

VI. Conclusions

The performed analysis showed that the tube plate of the first reversing chamber, the boiler element with the thickest wall, is exposed to the highest thermal stresses. This part of the boiler is exposed to temperatures $t > 500$ °C, which means it is exposed to yield stress. In this condition, continuous accumulation of plastic deformations occurs at a rate that depends on the level of stress, temperature and material characteristics. Intermittent cycles of drying, operation in stationary mode and cooling process, which are difficult to describe analytically, affect the fields of residual deformations and stresses before the considered n-th cycle of boiler operation. In strain-stress analysis in function of constructive parameters and load history of an element, the zero initial state of the previous stress is usually taken. However, it should be taken into account that such initial conditions lead to higher calculated values of the allowed rate of drying.

Experimental research of hot water boilers shows that the heating of the tube plate during the process of starting-up the can be presented as an approximate quasi-static temperature change. Under these conditions, the temperature field in the tube plate is quasi-stationary, i.e. only its level changes until the character of the change remains the same.

At the beginning of the process of boiler start-up, when temperature of the tube plate is the lowest, maximal

temperature differences occur. Due to the high temperature differences, the equivalent stresses are also the highest. Having that in mind, it can be concluded that the stresses are highest at the lowest temperatures of the tube plate, when the creep strain rate has the highest values. This means that the material is the strongest at the highest load.

ACKNOWLEDGMENT

This research was financially supported by the Ministry of Education, Science and Technological Development of the Republic of Serbia.

REFERENCES

[1] M. Todorović, D. Živković, M. Mančić, "Breakdowns of hot water boilers", Proceedings of the17th International Symposium on Thermal Science and Engineering of Serbia SIMTERM 2015, Sokobanja, Serbia, pp. 761-769, 2015.

[2] L. Cwynar, Pusk parowych kotlow, Moskva, Energoizdat, p.312, 1981.

[3] J. Taler, P. Dzierwa, D. Taler, P. Harchut, "Optimization of the boiler start-up taking into account thermal stresses", *Energy*, 2015, 92 (1), pp.160-170.

[4] F. Alobaid, K. Karner, J. Belz, B. Epple, H.G. Kim, "Numerical and experimental study of a heat recovery steam generator during start-up procedure", *Energy*, 2014, 64, pp.1057-1070. doi:10.1016/j.energy.2013.11.007.

[5] P. Dzierwa, D. Taler D, J. Taler, M. Trojan, "Optimum Heating of Thick Wall Pressure Components of Steam Boilers", Proceedings of the ASME 2014 Power Conference POWER2014, July 28-31, 2014, Baltimore, Maryland, USA, American Society of Mechanical Engineers, Power Division (Publication) POWER, 2014.

[6] B Gaćeša, V. Milošević-Mitić, T. Maneski, D. Kozak, J. Sertić, "Numerical and experimental strength analysis of fire-tube boiler construction", *Tehnički vjesnik* 2011, 18 (2), pp. 237-242.

[7] P. Duda, D. Rzasa , "Numerical method for determining the allowable medium temperature during the heating operation of a thick-walled boiler element in a supercritical steam power plant", Int. J. Energy Res. 2012, 36, pp. 703-709.

[8] D. Živković, D. Milčić, M. Banić, P. Milosavljević, "Thermomechanical Finite Element Analysis of Hot Water Boiler Structure", Thermal Science 2012, 16 (Suppl. 2), pp. 443 – 456.

[9] M. Rajić, M. Banić, D. Živković, M. Tomić, M. Mančić, "Construction Optimization of Hot Water Fire-Tube Boiler Using Thermomechanical Finite Element Analysis", Thermal Science 2018, 22 (Suppl. 5), S1511-S1523.

[10] H. Zuogang, Z. Zhikang, "Analysis about the Boiler Structure and Tube Plate Strength", *Journal of Anshan Institute of Iron and Steel Tehnology* 1999, 02.

[11] Šijački Žeravčić V, Bakić G, Đukić M, Anđelić B, Analysis of test results of hot-water boiler as a basic for its integrity assessment, *Structural Integrity and Life* 2007, 7 (2), pp.133-140

[12] [53] Caligiuri R, Foulds J, Sire R, Andrew S, Thermal Constraint Consideration in Design of a Heat Recovery Boiler, *Engineering Failure Analysis* 2006, 13(8), pp.1388-1396.

[13] [54] Arsić M, Aleksić V, Hut N, Analysis of state and integrity assessment of boilers – Structural performance diagnostics, *Structural Integrity and Life* 2005, 5 (1), pp. 3-17.

[14] [55] Milošević-Mitić V, Gaćeša B, Kozak D, Maneski T, Sertić J, Modeling of boiler membrane wall using finite element of reduced orthotropic plate, *Strojarstvo* 2012, 54 (1).

[15] [56] Kurai J, Burzić Z, Garić N, Zrilić M, Aleksić B, Initial stress state of boiler tubes for structural integrity assessment, *Structural Integrity and Life* 2007, 7(3), pp. 187-194.

[16] [57] Sarma G B, Pawel S J, Singh P M, Modelling of Recovery Boiler Tube Wall Panels to Investigate the Effect of Attachment Welds on Stress-Assisted Corrosion, Corrosion 2006, San Diego CA, NACE International, March 2006.

[17] J.F. Nye, Physical Properties of Crystals: Their Representation by Tensors and Matrices, Clarendon Press, Oxford, 1957.

[18] S. Damjanović, "Thermal stresses of the steam turbine rotor during stationary and non-stationary modes of operation", Master's thesis, University of Belgrade, Faculty of Mechanical Engineering, Belgrade, 1995.

[19] D. Živković, M. Rajić, M. Banić, M. Mančić, B. Popobić, "The Analysis of Thermo-Mechanical State of Steam Turbine Rotor in Non-Stationary Modes of Operation", Proceedings of the 4th International Conference Mechanical Engineering in XXI Century, Faculty of Mechanical Engineering, 2018, Niš, Serbia, pp. 33-36.

[20] Technical Documentation of Hot Water Boiler "Minel kotlogradnja – TE110V", (in Serbia), Minel kotlogradnja, Belgrade, 1992.

[21] ThyssenKrupp Materials International, Seamless Carbon Steel Pipe for High-Temperature Service, www.s-k-h.com

[22] Lucefin Group, Tehnical Card – P235GH, 2011, www.lucefin.com

THE 5th INTERNATIONAL CONFERENCE
MECHANICAL ENGINEERING IN XXI CENTURY

December 9-10, 2020
Faculty of Mechanical Engineering in Niš, Serbia

Classification of Building Renovation Measures with Ensembles of Decision Trees

Mirko STOJILJKOVIĆ, Goran VUČKOVIĆ, Marko IGNJATOVIĆ

University of Niš, Faculty of Mechanical Engineering in Niš, Aleksandra Medvedeva 14, 18000 Niš — Crveni Krst, Serbia

mirko.stojiljkovic@masfak.ni.ac.rs, goran.vuckovic@masfak.ni.ac.rs, marko.ignjatovic@masfak.ni.ac.rs

***Abstract*— Economic indicators of building renovation measures are often crucial in the process of decision-making related to buildings energy savings. The global cost is one of the widely used indicators for evaluating and comparing the measures. To perform an analysis with the appropriate precision, adequate models are necessary. The models based on physical phenomena are historically dominant, but recently data-driven surrogate models that use machine learning techniques started to gain the attention of the researchers in the buildings sector. This paper uses four classification methods to predict whether the global cost of a set of building renovation measures is above or below the predefined threshold. The results indicate that high prediction performance — with the F1 score, recall, and precision between 0.98 and 1 — can be achieved, except in the cases of very small training sets.**

***Keywords*— classification, global cost, machine learning, residential buildings, retrofit**

I. Introduction

Energy saving and greenhouse gases emission reduction measures in buildings are strongly related to the cost savings potential. Not only that cost-saving opportunities motivate the realization of energy efficiency measures, but also define energy policy targets [1, 2]. Economic performance of buildings renovation measures is expressed with the indicators such as simple and dynamic payback periods, net present value, internal rate of return, global cost (GC), etc. GC is defined in Ref. [3] as a discounted quantity that accounts the investment, replacement, disposal, operation and maintenance, residual value, etc.

There is a wide range of models used to assess quantities related to buildings energy supply and demand. They vary in complexity and accuracy, but also in approach applied. According to Foucquier et al. [4], they can be:

- White-box models that are based on the knowledge on physical phenomena; they can vary in the level of details and be overly complex in some cases.
- Black-box models that use the existing data and apply machine learning methods to predict the outputs or extract conclusions; they strongly depend on the volume and quality of data.
- Hybrid models that combine the previous two and exploit the advantages of both.

Among data-driven and machine-learning-based models, supervised regression techniques dominate. They can be applied to predict heating/cooling/electricity demand, occupancy, user behavior, thermal comfort parameters, etc. [5–9]. In addition, they can be combined with metaheuristic optimization of energy retrofit measures [10–13] and for short-term prediction and data-driven control applications [14, 15]. Classification methods are used to learn human interactions [16], control systems rules [17], etc. Unsupervised learning, especially cluster analysis is suitable to be used for preprocessing [18, 19].

This paper extends research presented in Refs. [20, 21]. It analyzes the predictive performance of the surrogate models that estimate economic attractiveness of a set of building energy retrofit measures. Unlike most of the models from the literature, this approach directly predicts whether GC is below a given threshold (project is attractive) or not. Like Ref. [21], this paper operates with potentially imbalanced datasets and small training sets aiming at obtaining the results with satisfactory precision as quickly as possible. It examines the performance of decision trees (DT) and three ensemble methods based on DT: (1) random forest (RF), (2) adaptive boosting (AB), and (3) gradient boosting (GB).

II. Problem Formulation

The problem described above is defined and solved as a binary classification problem having in mind the possibility of having an imbalanced dataset, need for quick training, validation, and testing procedures, as well as the possibility of working with very small training sets.

The case study analyses an existing five-story building with the floor are of 755 m² located in Niš, Serbia. The building is connected to the district heating network and is not insulated.

The input variables are related to the retrofit options:

- Thermal conduction resistance of the insulation of exterior walls, in [m²K/W],
- Thermal conduction resistance of the insulation of interior walls, in [m²K/W],
- Thermal conduction resistance of the insulation of floor, in [m²K/W],
- Thermal conduction resistance of the insulation of ceiling or roof, in [m²K/W],

- Thermal transmittance (*U*-value) of the windows, in [W/(m²K)],
- Total solar energy transmittance of the windows,
- Category of the fenestration frames.

The output of the model is equal to 1 if GC is below the predefined threshold (financially attractive) and 0 otherwise. In this case, the threshold is equal to GC for the do-nothing scenario.

This case study examines three scenarios that differ in the discount rate and prices development rates. Scenario 1 has moderate values of the rates. Scenario 2 has the values that correspond to larger GC and thus has more solutions with the output of 1. Scenario 3 has the rates that yield less attractive GC values.

References [20, 21] provide more information about the building, scenarios, inputs, and classification problem.

III. Methodology

The binary classification problem is solved with four machine learning methods, DT and three ensemble methods based on DT: RF, AB, and GB. DT-based methods are applied because they are faster to train compared to neural networks and support vector machines, which are dominant in this field. In addition, they have fewer hyperparameters to tune, which also improves required time and computational resources. They also require little or no data preparation, work well with categorical variables, ensembles are resistant to overfitting to a certain extent, out-of-bag data can be used, feature importance is calculated, etc. These methods, especially RF and GB are widely used in other fields.

Having in mind that the datasets might be imbalanced, the classification accuracy is not used to quantify classification performance. Instead, this paper uses precision p, recall r, and F_1 score:

$$r = \frac{n_{\mathrm{TP}}}{n_{\mathrm{TP}} + n_{\mathrm{FN}}}; \quad p = \frac{n_{\mathrm{TP}}}{n_{\mathrm{TP}} + n_{\mathrm{FP}}}; \quad F_1 = \frac{2rp}{r + p}$$

where n_{TP} is the number of true positive items, n_{FN} is the number of false negatives, and n_{FP} is the number of false positives. It should be noted that the choice of the adequate quantity depends on the case.

The dataset used is obtained by evaluating all measures in the exhaustive search manner. A small, randomly chosen part of the dataset is used for training. The remaining observations are used for testing.

IV. Results and Discussion

The total number of observations, i.e. possible combinations of retrofit measures is 217,800. Scenario 1 has a balanced dataset because almost 62% belong to the positive class (below the threshold) and about 38% to the negative. In scenario 2, over 98% of observations are positive, while in scenario 3, almost 91% are negative. Thus, these two scenarios have imbalanced data.

Figures 1–4 illustrate the values of the quantities that measure the classification performance. For the training set portions larger than 0.01, i.e. the cases where the number of observations used for training is at least 1% of the total number of observations, almost all values for RF and GB are above 98%. DT and AB have slightly lower precision. All values are above 90% and rarely drop below 95%, which indicates good prediction performance. Scenario 2 has higher precision compared to other scenarios, due to many positive observations.

Very small training sets remain problematic. They have lower prediction performance that sometimes decreases when the training set size increases. This might be due to a small number of the observations that belong to the minority class, and their high variation from case to case because of random selection. It is questionable what is the best way to ensure that such small random training sets contain enough minority class observations to obtain better performance.

Validation procedure, e.g. the *k*-fold cross-validation combined with hyperparameters tunning might provide better insights into mentioned problems. Using out-of-bag data could be considered.

Reference [21] suggests that the size of the dataset also has important role.

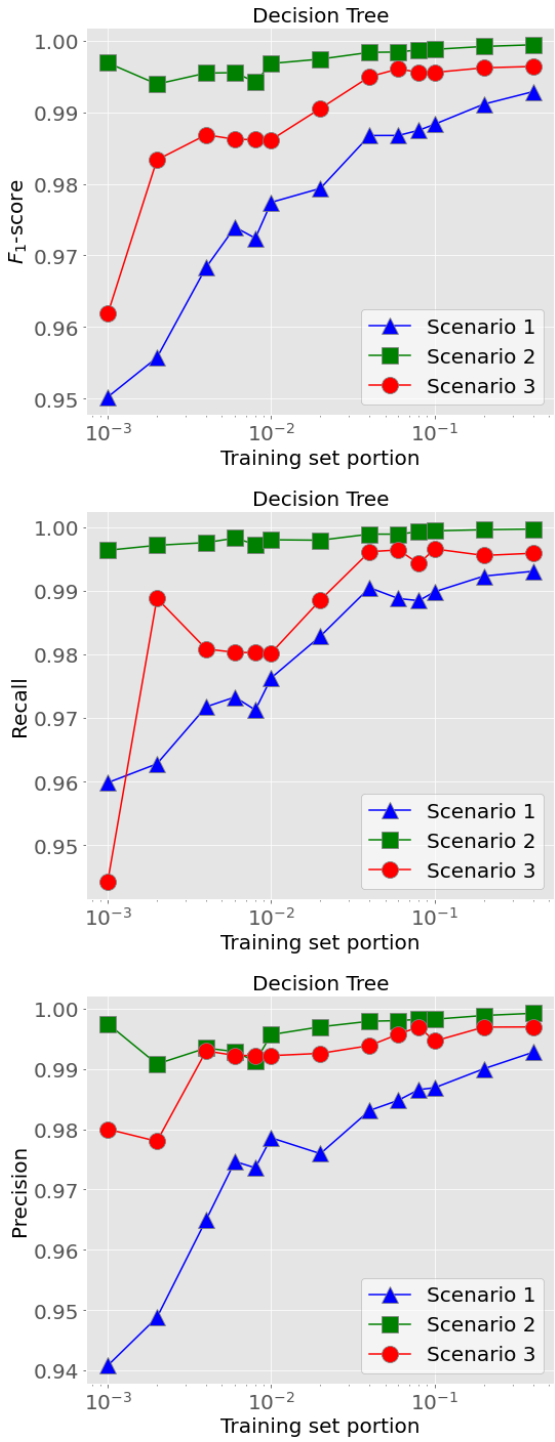

Fig. 1. Classification performance obtained with decision trees

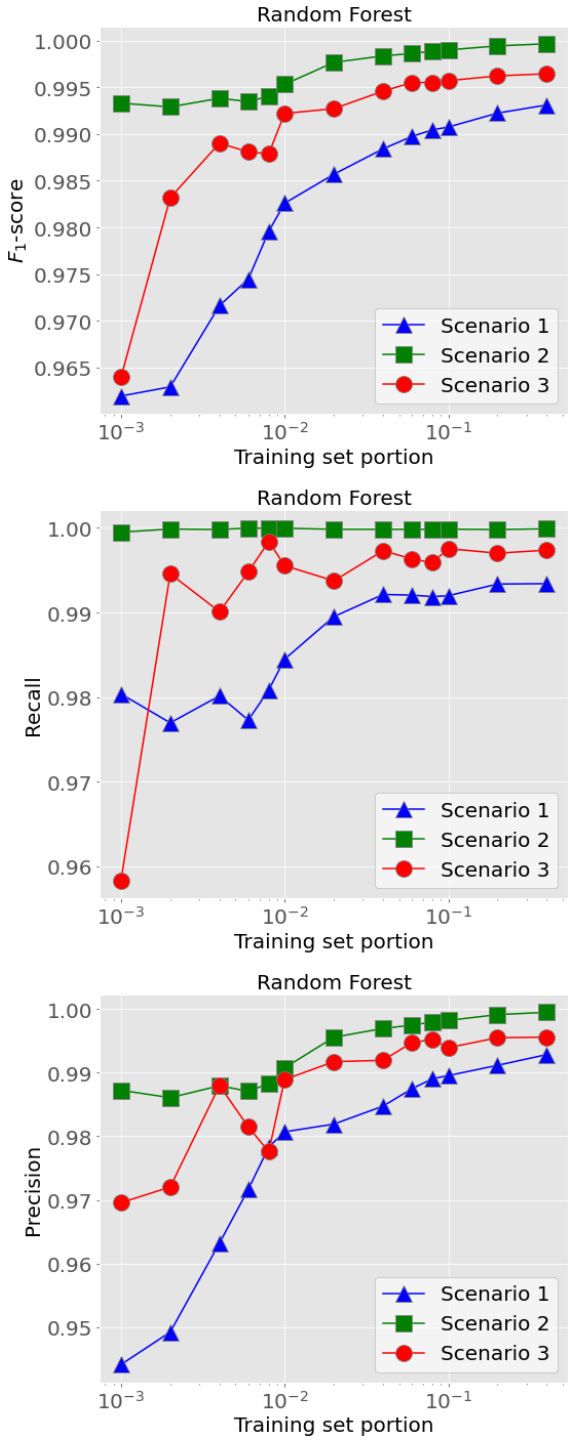

Fig. 2. Classification performance obtained with random forest

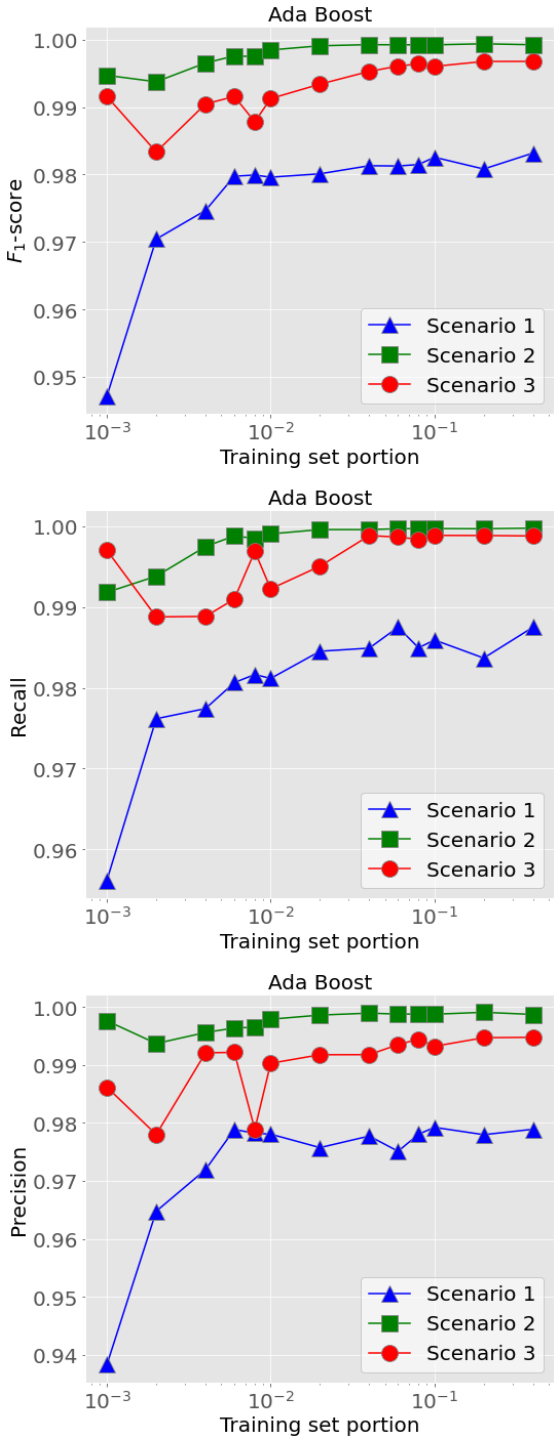

Fig. 3. Classification performance obtained with adaptive boosting

V. Conclusion

This paper evaluates the classification performance of the surrogate models that predict whether the global cost value is below a predefined threshold or not, given the inputs that describe energy retrofit measures for buildings like heat transfer resistance and properties of fenestration.

Random forest and gradient boosting yield the precision above 98% for the datasets with 217,800 observations, some of which are heavily imbalanced, and the training sets that have at least 1% of observations. Decision trees and adaptive boost have similar, but generally slightly lower precision.

Decision-tree-based ensembles are precise, powerful, and fast to train and adjust the hyperparameters. This paper illustrates one option for their application.

The cases with very small training sets are problematic in terms of performance and learning stability. This probably happens because the number of randomly items that belong to the minority class varies considerably from case to case. Thus, additional work in needed to ensure large enough minority class to obtain better performance.

Acknowledgment

This research was financially supported by the Ministry of Education, Science and Technological Development of the Republic of Serbia and partially conducted within the project “Research and development of new generation machine systems in the function of the technological development of Serbia”.

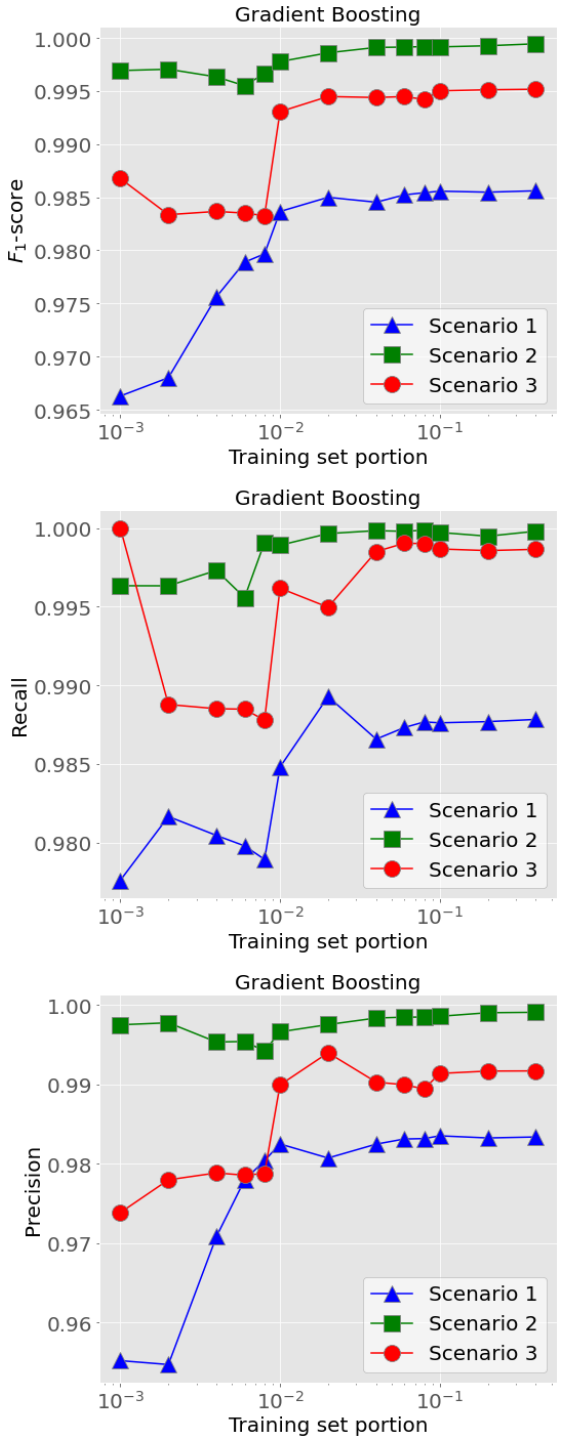

Fig. 4. Classification performance obtained with gradient boosting

References

[1] ****, Directive (EU) 2018/844 of the European Parliament and of the Council, Official Journal of the European Union L 156 (2018), pp. 75–91.

[2] ****, Commission recommendation (EU) 2016/1318 Official Journal of the European Union L 208 (2016), pp. 46–57.

[3] ****, SRPS EN 15459-1:2017 Energy performance of buildings - Economic evaluation procedure for energy systems in buildings - Part 1: Calculation procedures, Module M1-14, Institute for Standardization of Serbia, 2017.

[4] Foucquier A. et al., State of the art in building modelling and energy performances prediction: A review, Renewable and Sustainable Energy Reviews 23 (2013), pp. 272–288.

[5] Mosavi A. et al., State of the Art of Machine Learning Models in Energy Systems, a Systematic Review, Energies 12 (2019), 7, 1301.

[6] Zeng A. et al., Prediction of building electricity usage using Gaussian Process Regression, Journal of Building Engineering 28 (2020), 101054.

[7] Seyedzadeh S. et al., Tuning machine learning models for prediction of building energy loads, Sustainable Cities and Society 47 (2019) 101484.

[8] Seyedzadeh S. et al., Data driven model improved by multi-objective optimisation for prediction of building energy loads, Automation in Construction 116 (2020), 103188.

[9] Dai X. et al., A review of studies applying machine learning models to predict occupancy and window opening behaviours in smart buildings, Energy & Buildings 223 (2020), 110159.

[10] Gan V. J. L. et al., Simulation optimisation towards energy efficient green buildings: Current status and future trends, Journal of Cleaner Production 254 (2020), 120012.

[11] Asadi E. et al., Multi-objective optimization for building retrofit: A model using genetic algorithm and artificial neural network and an application, Energy and Buildings 81 (2014), pp. 444–456.

[12] Sharif S. A., Hammad A., Developing surrogate ANN for selecting near-optimal building energy renovation methods considering energy consumption, LCC and LCA, Journal of Building Engineering 25 (2019), 100790.

[13] Chen X., Yang H., A multi-stage optimization of passively designed high-rise residential buildings in multiple building operation scenarios, Applied Energy 206 (2017), pp. 541–557.

[14] Smarra F., Data-driven model predictive control using random forests for building energy optimization and climate control, Applied Energy 226 (2018), pp. 1252–1272.

[15] Wang J. et al., Data-driven model predictive control for building climate control: Three case studies on different buildings, Building and Environment 160 (2019), 106204.

[16] Ghahramani A. et al., Learning occupants' workplace interactions from wearable and stationary ambient sensing systems, Applied Energy 230 (2018), pp. 42–51.

[17] Domahidi A. et al., Learning decision rules for energy efficient building control, Journal of Process Control 24 (2014), pp. 763–772.

[18] Ding Y. et al., Effect of input variables on cooling load prediction accuracy of an office building, Applied Thermal Engineering 128 (2018), pp. 225–234.

[19] Westermann P. et al., Unsupervised learning of energy signatures to identify the heating system an building type using smart meter data, Applied Energy 264 (2020), 114715.

[20] Stojiljković M. M. et al., Cost-optimal energy retrofit for Serbian residential buildings connected to district heating systems, Thermal Science 23 (2019), Suppl. 5, pp. 1707–1717.

[21] Stojiljković M. M. et al., Classification of retrofit measures for residential buildings according to the global cost, Thermal Science 2020 OnLine-First, https://doi.org/10.2298/TSCI200825306S.

THE 5th INTERNATIONAL CONFERENCE
MECHANICAL ENGINEERING IN XXI CENTURY

December 9-10, 2020
Faculty of Mechanical Engineering in Niš, Serbia

Assessment of Possible Organic Waste Inclusion and Implementation in Closed Loop System

Ana MOMČILOVIĆ[1], Gordana STEFANOVIĆ[1], Biljana MILUTINOVIĆ[2] and Dragiša SAVIĆ[3]

[1] Faculty of Mechanical Engineering, University of Niš, A. Medvedeva 14, Niš, Serbia
[2] College of Applied Technical Sciences Niš, A. Medvedeva 20, Niš, Serbia,
[3] Faculty of Technology, University of Niš, Bul. Oslobodjenja 124, Leskovac, Serbia,
momcilovic.ana.92@gmail.com, gordana.stefanovic@masfak.ni.ac.rs, pedja.rajk@gmail.com,
bimilutinovic@gmail.com, savic@junis.ni.ac.rs

***Abstract*—Organic waste, due to its characteristics, represents a challenging type of waste for implementation in the flows of circular economy, economic model based on closed loop system. The main idea of the paper is assessment of the inclusion possibility of different types of organic waste generated in the area of one city in the flows of the circular economy. For this purpose, a mathematical model was developed and applied. Based on the mathematical model, the optimum mixing ratio of the several organic waste fractions, which will be subjected to the anaerobic digestion treatment and composting, is determined. Developed scenarios are based on the organic waste types and quantities available in considered area. In each of the scenarios, process products, in the form of biogas and compost, are introduced into the flows of the circular economy. Based on the inputs and outputs in developed scenarios, the efficiency of the circular economy for each scenario is determined.**

***Keywords*—Circular Economy, Evaluation, Anaerobic Digestion, Composting, Modelling**

I. Introduction

In response to growing problems caused by the decline in material and energy resources, ways to find new sources of resources have been sought. The possibility of using waste as a source of energy and materials was recognized as one of the solutions. In this sense, the concept of circular economy (CE), within the role of waste changes, from the final stages of the product life cycle to the source of raw materials and energy, is used to close the circle in the movement of matter. Therefore, the concept of "cradle to grave" changed in the concept of "cradle to cradle" [1].

In the last few decades, since the concept of circular economy has become an alternative to the then existing concept of linear economy, it has found application in various forms in most economic and industrial sectors [2]. The circular economy requires careful management of material flows, which are of two types: as biological nutrients—materials designed to re-enter the biosphere safely and rebuild natural capital, and technical nutrients, designed to circulate at high quality without entering the biosphere [1]. Aware of the fact that by applying this concept contribute to the sustainable development, conservation of resources and environmental protection, companies and society increasingly apply the principles of circular economy at all levels: it operates at the micro level (products, companies, consumers), meso level (eco-industrial parks) and macro level (city, region, nation and beyond) [3].

After the introduction and application of the concept of circular economy, the question of monitoring and measuring the success of the implementation of this concept aroused. Until recently, there is not recognized one way of measuring the effectiveness of transition from „linear“ to „circular“ economy [4]. Nowadays, there are large variety of measurement approaches that aim to assess the progress. The different assessment methodologies cover different and varied aspects of circular economy transition and are seemingly unrelated to each other [5]. Therefore, various indicators, methodologies and models for measuring the successful implementation of the circular economy concept have been developed and applied. Circularity metrics are useful for empirically assessing the effects of a circular economy in terms of profitability, job creation, and environmental impacts [6].

In Swiss waste management system the recycling rates, an indicator for the circulating behaviour of materials, was recognised and used as measure for the degree of circularity of an economy [7]. In China two indicators sets were designed for both macro level and industrial park level analyses and monitoring, with 22 indicators and 12 indicators respectively. A detailed set of calculations and explanations were also provided. These calculations and explanations are used to facilitate more detailed methodological processes for managing circular economy situations [8]. Some authors [9] proposed CE indicators, based on eco-innovation factors, and existing data set. They recommended using of five group indicators for measuring regional CE–eco-innovation: three of proposed indicator groups are associated directly with innovations, taking into account the principles of CE: CE–eco-innovation inputs, CE–eco-innovation activities and CE–eco-innovation outputs, and other two groups of indicators are effects of the CE–eco-innovation introduction: resource efficiency outcomes and socio-

economic outcomes. Also, other authors [10] believe, considering that the CE paradigm usually involves five main phases: the material input, the design, the production, the consumption, and, finally, the end-of-life resource management, which provides inputs for the first phase in a closed loop logic, that in the proposed framework, the processes, whose performances must be measured through index methods to evaluate how circular is the overall system in analysis. Further, a set of indicators linking circular economy principles, circular business model and the pillars of sustainability was developed based in the hypothetic-deductive approach, following a number of iterations (cycles) and testing the theory in the empirical world [11]. Researches can be found in the literature, that used mathematical approach for defining the circular economy as a function of a metric, departing from a well-defined material flow and value system, i.e. a metric that is derived from maximizing the value to society of materials used in the production of commodities that provide services to consumers [12].

A particular issue is the measurement of the application of the circular economy concept to organic waste management, since it has a significant share in the total composition of municipal waste. There is small number of researches that results in the development of indicators or models for measuring the success of circular economy applications for organic waste management [13]. In order to evaluate bio waste valorisation in a future circular economy, valorisation efficiency (output product/kg OW) and potential revenue by valorising the OW into different products (€/t OW) was analysed [14]. To study the circularity of nutrients within a system that handles the organic waste (OW) generated in the Spanish region of Cantabria indicator was applied. A superstructure was developed to determine the optimal configuration of the system. It is composed of alternative unit processes for the management of OW and the application of the recovered products as soil amendment to grow corn. A multiobjective mixed integer linear programming problem was formulated under two policy scenarios with different source separation rates. The problem was optimized according to six objective functions: the circularity indicators of carbon, nitrogen, and phosphorus, which are maximized, and their associated environmental impacts to be minimized (global warming, marine eutrophication, and freshwater eutrophication) [15].

The aim of this paper is to present a model for the efficiency of utilization of organic waste in terms of circular economy. Three indicators have been developed within the model: the degree of incorporation of organic matter into the closed loop, the circularity of matter, and the circularity of energy. Eight scenarios were developed in which four different fractions of organic waste (organic fraction of solid municipal waste garden waste, brewers' grains, and dairy waste) were treated by composting and anaerobic digestion.

II. Materials and methods

Circular economy is the closure of a loop in which various processes are involved, with the idea of avoiding any leakage of matter (waste) or energy or the introduction of new resources to meet the needs in the closed loop. The paths to achieving this goal may differ. Of course, avoiding any leakage is idealistic at the moment, but in principle, aspiration is completely realistic. In order to make a good choice of the loop closing method, a lot of analysis should be done and the problems of all the elements involved in the considered loop. Certainly, one of the criteria is the degree of system elements involved, that is, whether and how much their leakage is from the system. The smaller the percentage of this leakage, the more efficient the system can be. Another criterion that can be taken to evaluate the efficiency of a circular economy is to consider how well the chosen principle of circulating matter in the loop can produce a profit that will satisfy all needs in the loop. Also, such a choice must entail consideration of any problems that may in some way have an adverse impact on the environment, which will be discussed in a future paper.

Do not add any kind of pagination anywhere in the paper. Do not number text headers.

A. *Mathematical model*

For the purpose of evaluating the efficiency of the circular economy of a closed system (company, city, region), a mathematical model has been developed that includes the analysis of the inclusion of individual elements of the system and the material-energy analysis of the closed loop. The system under consideration is the territory of a city where different types of organic waste have been generated. The elements of the system are generators of organic waste, i.e. organic raw materials: the organic part of municipal waste (OFMSW), garden waste (GW) and organic waste generated by processes in industry (DW and BG). The processes under consideration for the treatment of organic raw materials are composting and anaerobic digestion. It is considered that the composting process and anaerobic digestion take place at the same location. The composting treatment considered by this model is outdoor composting without additional energy requirements, while the anaerobic digestion process using thermophilic anaerobic digestion at 60ºC in a continuous anaerobic digester with a process duration 14 days. Biogas and compost are obtained as the product of AD, while the compost is obtained as product of composting process. The resulting biogas is used to meet the energy needs of maintaining the organic raw material treatment system as well as the overall energy transportation needs. As biogas produced from OW contains 69% methane and based on the fact that the lower heating value (H_d) of biogas with 95% methane is H_d = 37.78 MJ/m^3 [16], the calculated H_d of biogas with 69% methane is 26 MJ/m^3. Calculation of energy required for process AD includes the energy required to heat the digester relative to the outside design temperature for the observed city (summer 25^{0}C and winter -5^{0}C) and the energy required to heat the substrate at the inlet of the digester, as well as the energy required for mixing within the digester . When considering the system, all transport elements are included. The model involves the collection and transportation of organic waste from households and green waste to the processing site. The calculation also took into account the transport of compost to the point of application, or to the green areas from which the garden waste was collected. The

data on diesel fuel consumption for transport of waste carried out by already established routes was obtained from the PUC which deals with the collection and transportation of waste in a given territory [17]. According to EN 590: 2009 the lower heating value of diesel fuel is 43.1 MJ/kg [18], while the diesel fuel density is 0.832 kg/l. Comparing the lower heating value of diesel fuel 35.85 MJ/l and the lower heating value of biogas 26 MJ/m^3, it can be calculated that 1.37 m^3 of biogas can replace 1 l of diesel fuel. For transport of 1 ton of waste from public green areas to a biogas plant, it requires 7.14 litres of diesel fuel, respectively, 9.78 m^3 of biogas. Based on the previously mentioned ratio of diesel and biogas and diesel consumed for waste transport in the area the amount of diesel fuel and energy required for OW transport was calculated. For compost transport, an approximation was taken to represent the average energy consumption for transporting one tonne of waste in a given territory. The amount of compost generated is 0.4085 t of compost / tonnes of recovered organic waste [19]. For the model development for optimization of co-substrate mixing ratio, the simplex method of multicriteria optimization was used. Carbon (C) content, nitrogen (N) content, (M) moisture content and C/N ratio were used as input parameters when the model was developed. The main problem, while developing this model, was keeping in mind multiple conflicting objectives that should be considered simultaneously. The method of global criterion is applied, where the distance between a desirable reference point in the objective space and the feasible objective region is minimized [20,21].

In the developed model, the problem was reduced to tree functions of n variables (1), (2) and (3):

$$(x) = \sum_{i=1}^{n} C_i x_i \tag{1}$$

$$\boldsymbol{N(x)} = \sum_{\boldsymbol{i=1}}^{\boldsymbol{n}} \boldsymbol{N_i x_i} \tag{2}$$

$$\boldsymbol{M(x)} = \sum_{\boldsymbol{i=1}}^{\boldsymbol{n}} \boldsymbol{M_i x_i} \tag{3}$$

where C is carbon content in specific co-substrate (in %), N is nitrogen content in specific co-substrate (in %), M is moisture content in specific co-substrate (in %) is co-substrate combination, n is the number of organic waste fractions.

The constraints are $x_1 + x_2 + \ldots + x_n = 1$ and $x_i \geq 0, \quad \forall i$.

For unhindered activity of methanogenic bacteria in AD process, a necessary condition is the favourable C/N ratio in digesting matter. A favourable C/N ratio ranges from 20 to 25 where would be ideal because methanogenic bacteria consume about 30 times more carbon than nitrogen [22], while the most favourable C/N ratio ranges from 25 to 30 when it comes to composting process [22]. The additional condition $\boldsymbol{a} \leq \frac{\boldsymbol{C(x)}}{\boldsymbol{N(x)}} \leq \boldsymbol{b}$ can be written in the form, wherefrom two constraints could be recognized in (4) and (5):

$$0 \leq C(x) - a\,N(x) \tag{4}$$

$$0 \leq b\,N(x) - C(x) \tag{5}$$

where b is the upper limit of C/N ratio used as a constraint in the developed mathematical model, and a is the lower limit of C/N ratio with a condition for $b>a$.

Using constraints mentioned above (4) and (5), the feasible region can be defined.

The main problem is a multi-criteria optimization presented in (6):

$$\left\{ \begin{array}{ll} \max C(x), & \min N(x) \\ x \in D & x \in D \end{array} \right\}. \tag{6}$$

To solve the multi-criteria problem, the global criterion should be considered:

$$G(x) = \left(\frac{C^* - C(x)}{C^*} \right)^2 + \left(\frac{N^* - N(x)}{N^*} \right)^2. \tag{7}$$

By solving the multi-criteria problem presented by the equation 7 using the simplex method, the Pareto optimum point is obtained, that is, the optimal co-substrate mixing ratio for the AD process and composting.

The mathematical model was developed to evaluate the circularity of matter and energy through a closed loop. The mathematical model is used to observe the degree of involvement of organic matter in the closed loop of circular economy, the leakage of matter and energy from the closed loop, then the degree of circularity of matter and the degree of circularity of energy.

The degree of incorporation of organic matter into the closed loop of a circular economy is the ratio of the amount of organic matter involved in the flows of CE and the organic matter that is available and can be calculated on the basis of equation (8).

$$\boldsymbol{D_{im}} = \frac{\boldsymbol{m_i}}{\boldsymbol{m_a}} \tag{8}$$

Where are $\boldsymbol{D_{im}}$ is the degree of incorporation of organic matter into the closed loop of a circular economy, $\boldsymbol{m_i}$ is matter involved and $\boldsymbol{m_a}$ is matter available.

Closed-loop leakage is defined as the surplus amount of organic matter in the closed-loop, that is not used for meeting the requirements of the loop.

Closed-loop energy leakage is defined as the surplus of energy in the closed-loop, that is not used for meeting the requirements of the loop.

Degree of circularity of matter is defined as the ratio of the amount of matter that has been treated and used to meet the needs and the total matter that circulates in a closed loop and can be calculated on the basis of equation (9).

$$C_m = \frac{m_{adc} + m_u}{m_t} * 100\% = \frac{m_{adc} + m_u}{m_{adc} + m_u + m_l} * 100\% \quad (9)$$

Where are C_m is the degree of the matter circularity, m_{adc} is matter treated with AD or composting process, m_u is matter used to meet the requirements of the closed loop, m_l – matter leakage, while m_t is total amount of the matter in the closed loop.

The degree of energy circularity is defined as the ratio of energy used to meet energy needs within a loop and the total amount of energy generated in a closed loop.

$$C_e = \frac{E_r}{E_g} * 100\% \quad (10)$$

Where are C_e is the degree of energy circularity, E_r is energy requirements of the closed loop (energy requirements for treatment and transport), and E_g is energy gains in the closed loop (energy gains from biogas).

III. Preliminary research

The basic idea when considering the possibility of incorporating different substrates into the circuits of a circular economy is to include, as far as possible, all the resulting organic fraction of solid municipal waste (OFMSW) and GW, while other substrates will be generated in the food industry (dairy waste and brewers grains), be involved as far as is processual, economically and organizationally justified. Anaerobic digestion with aerobic stabilization and composting are considered as methods for treatment of organic waste, while available quantities of substrates are considered as parameters for the inclusion of certain substrates in CE, the optimal mixing ratio of these raw materials based on the C/N ratio, using AD as the optimum ratio 20-25, and for composting 25-30. and moisture content between 60-70%. On the basis of the input raw materials available in the territory of Nis (Table 1), possible scenarios of organic waste management are formed in the territory of Nis (Table 2). Material and energy balances and, as well as possible loop leaks, are used as parameters for evaluating each of the proposed scenarios. The substrates to be considered are generated in the area of the city of Nis.

TABLE I Main characteristics of available feedstock [15, 17, 22]

Type of feedstock	Generated amount [t/year]	Moisture [%]	C to N ratio
OFMSW	9,011	70	15.45
GW	8,855	60	30
DW	132	92	13
BG	9,191	66	15

Based on the data presented in Table 1, different organic waste management scenarios have been developed.

B. Developed scenarios

Substrates that will be treated by the AD process and composting are an organic part of municipal waste and garden waste, while other raw materials will be from industries such as milk processing or beer production. The treatment of organic waste would include raw materials generated at the optimum distance from the treatment site. Biogas obtained by treatment of organic raw materials is used to meet the energy needs of the plant and transport, while excess biogas is recognized as energy leakage from the loop. The compost generated by the composting process or the AD process with subsequent stabilization is used to cover the soil requirements for the nutrients from which the green waste was collected. The excess of the resulting compost is recognized as a matter leakage from the loop. Based on inputs and final products in the developed scenarios, the sustainability of each developed scenario is determined. For the purposes of this research, 8 scenarios were developed, two base BS1-BS2 and six S1-S6 (Table 2), some of which include AD treatment or composting of different optimal substrate mixtures, while in the latter scenario, all substrates (composting and AD) are treated. Table 2 shows the types of substrates to be treated in each scenario, their specific mixing ratio obtained on the basis of set criteria, the selected treatment of organic raw materials, the annual amount of substrates covered by the scenario, the C/N ratio and the moisture content of the optimal mixture.

Baseline scenario 1 (BS1) involves the composting of 13,417 t of organic waste: a partial amount of organic solid municipal waste (4,562 t) and the total amount of garden waste (8,855 t) in ratio 34%:66%.

Baseline Scenario 2 (BS2) involves anaerobic digestion of 17,866 t of organic waste: the total amount of organic fraction of solid municipal waste (9,011 t) and garden waste (8,855 t) in ratio 50.4%:49.56%.

Scenario1 (S1) involves the composting of 13,022 t of the organic waste: the partial amount of organic fraction of solid municipal waste (2,475 t) the total amount of garden waste (8,855 t) and the partial amount of brewer's grains (1,692.86 t) in ratio 19%:68%:13%.

Scenario 2 (S2) involves anaerobic digestion of 27,057 t of organic waste: the total amount of organic fraction of solid municipal waste (9,011 t), the total amount of garden waste (8,855 t) and the total amount of dairy waste (132 t) in ratio 33.3%:32.7%:33.9%.

Scenario 3 (S3) involves anaerobic digestion of 17,998 t of organic waste: the total amount of organic fraction of solid municipal waste (9,011 t), the total amount of garden waste (8,855 t) and the total amount of dairy waste (132 t) in ratio 50%:49.2%:0.8%.

Scenario 4 (S4) involves anaerobic digestion of total amount of 27,189 t of organic waste: the total amount of organic fraction of solid municipal waste (9,011 t), the total amount of garden waste (8,855 t), the total amount of brewers grains (9,191 t), and the total amount of dairy waste (132 t) in ratio 33.14%:32.56%:33.8%:0.4%.

Scenario 5 (S5) involves composting of 12,471 t of organic waste: the partial amount of organic fraction of

solid municipal waste (1,745.54 t), the total amount of garden waste (8,855 t), the partial amount of brewer's grains (99.76 t), and the total amount of dairy waste (132 t) in ratio 14%:71%:14.2%:0.8%.

Scenario 6 (S6) involves composting and anaerobic digestion of total amount of 27,189 t of organic waste: amount of 12,471 t of mixture of all fraction of organic waste (14%:71%:14.2%:0.8%) is composting, and rest mixture of organic fraction of solid municipal waste and brewers grains (14,718 t in total) is treated in anaerobic digestion (51%:48.1%).

TABLE III SCENARIOS MAIN FEATURES

	Feedstock [t/year]	**Organic waste**	**Optimal mixing ratio**	**C/N**	**Moisture [%]**
BS1	13,417	OFMSW+ GW	0.34:0.66	25.0	63.40
BS2	17,866	OFMSW+ GW	0.504:0.4956	22.6	65.02
S1	13,022	OFMSW+ GW+ BG	0.19:0.68:0.13	25.2	62.68
S2	27,057	OFMSW+ GW+ BG	0.333:0.327:0.339	20.0	65.27
S3	17,998	OFMSW+ GW+ DW	0.50:0.492:0.008	22.5	65.22
S4	27,189	OFMSW+GW+ BG+ DW	0.3314:0325 6:0.338:0.004	20.0	65.38
S5	12,471	OFMSW+ GW+ BG+ DW	0.14:0.71:0.142:0.008	25.6	62.58
S6	AD:14,718 C: 12,471	OFMSW+GW+ BG+ DW	AD:0.51:0:0.481:0 C:0.14:0.71:0.142:0.008	AD: 15 C:25	AD:67.4 C: 62.58

In all developed scenarios, the resulting biogas is used to meet the energy needs of transporting organic raw materials and compost, the energy needs existing for the treatment of organic raw materials. The amount of compost used for nutrient recovery is 3723 tonnes/year for 3,030,526 m^2 of public green space [17, 19].

IV. RESULTS AND DISCUSSION

Table 3 shows the material and energy balance of the developed scenarios, the degree of involvement of organic matter in the flows of the circular economy, as well as the material and energy leaks from the loop and the degree of circularity of matter and energy for each scenario Negative values of energy leaks are recognized as necessary energy demand that is needed for closing the loop. Observing the energy and material balance of the developed scenarios, it can be seen that the scenarios in which the raw materials are treated by the anaerobic digestion process (BS2, S3, S3, S4) have the degree of incorporation of organic matter in circular economy flows, 100%, while the scenarios in which the raw materials are treated by composting (BS1, S1, S5) have a much lower degree of incorporation of organic matter in circular economy flows 45,86-75.09%.

When it comes to incorporation of matter into CE streams, the highest amount of treated substrate is achieved in scenarios S4 and S6 when 27189 tonnes of organic matter are successfully treated annually by the AD process or by a combination of AD process and composting, that is, the total amount of organic matter taken up in the consideration.

In the case of leakage of matter from the system, after meeting the soil requirements for nutrients from which garden waste is collected, leaks occur in all scenarios, while the smallest leaks occur in scenarios BS1, S1, S5 where organic substrate is treated with composting, i.e. highest circularity of matter in closed loop (over 90%). Energy gains in the form of biogas occur in scenarios BS2, S3, S3, S4 and S6, with the highest energy gains occurring in scenario S4, where a large energy leak also causes a large leakage of energy from a given loop.

TABLE IIIII MATERIAL AND ENERGY BALANCE AND INDICATORS OF EFFICIENCY OF CIRCULAR ECONOMY APPLICATION FOR DEVELOPED SCENARIOS

	Leakage of matter [t/t OW]	**Leakage of energy [MJ/t OW]**	**Degree of incorporation of organic matter [%]**	**Matter circularity [%]**	**Energy circularity [%]**
BS1	0.2045	-245.52	75.09	90.70	n.a.
BS2	0.2045	1069.57	100.00	85.79	75.24
S1	0.2045	-245.52	48.12	91.29	n.a.
S2	0.2045	1069.57	100.00	80.76	75.27
S3	0.2045	1069.57	100.00	85.31	75.25
S4	0.2045	1069.57	100.00	80.72	75.25
S5	0.2045	-245.52	45.86	91.71	n.a.
S6	0.2045	2453.24	100.00	80.72	79.87

In scenario S6, where a certain amount of raw material is composted and the rest is treated by the AD process, the leakage of the highest energy leakage occurs compared to other scenarios due to the lower energy requirement for waste treatment and transportation. In some scenarios (BS1, S1, S5) there is an energy deficit, i.e. for successful closing of the loop it is necessary to bring a certain amount of energy to the system. Regarding the circularity of the energy in the loop, which is considered in the case of scenarios in which the organic feedstock is treated by the AD process, it can be seen that it ranges from 75 to 80%, or that there are leaks between 20-25%. Obviously, within the system limits of the proposed model, it should be possible to include excess energy in energy flows, which could be done by including industrial systems where part of the energy needs of production would be covered by the generated surplus energy.

V. CONCLUSIONS

In this paper, a mathematical model is developed that aims to estimate the circularity of matter and energy in the closed loop of circular economy in the flow of organic matter at the selected location through the material and energy balance of the system. Eight scenarios were formed to look at the CE efficiency problem and, on this occasion, cases of treatment of four different organics materials were considered: (OFMSW, GW, BG, DW) composting and anaerobic digestion at optimal conditions (C to N ratio and moisture). The energy generated from biogas is used to meet the energy needs of organic matter treatment plants, the transport of organic matter and the resulting compost. The resulting

compost is used to recover nutrients from the soil from which the garden waste was collected. Based on the material and energy balance, three different indicators have been developed: the degree of incorporation of organic waste into the closed loop, the circularity of matter and the circularity of energy.

Degree of incorporation of organic matter in circular economy flows in scenarios where AD treatment is always 100%, while this indicator for composting is much smaller and ranges from 45 to 75%. When it comes to circularity of matter, much greater circularity is achieved in scenarios where composting treatment is performed and ranges from 90.7 to 91.7%, while in cases where AD is used it is smaller and ranges from 80.7 to 85.72%.

Energy circularity can only be observed in scenarios where the AD process is applied, and ranges about 75%. The energy circularity increases in the scenario when the organic matter is treated with a combination of anaerobic digestion and composting average of almost 80% and then the highest. When it is necessary to perform the highest degree of matter involvement and in order to satisfy energy needs, it is best to include the anaerobic digestion process, the highest circularity of matter is achieved by using composting. Scenario S6 in which organic matter is treated with a combination of both processes has the best values of these three indicators.

Given that there is a surplus of energy in all scenarios, further research will consider ways to involve industry as an energy recipient. Further development of the mathematical model will include environmental impact on the closed-loop applications of CE.

REFERENCES

[1] McDonough W., Braungart M., Cradle to Cradle: Remaking the Way We Make Things. North Point Press, New York; 2002.

[2] Winans K., Kendall A., Deng H., The history and current applications of the circular economy concept. Renew Sust Energ Rev 2017; 68:825–833.

[3] Saidani M., Yannou B., Leroy Y., Cluzel F., Kendall A., A taxonomy of circular economy indicators. J Clean Prod 2019; 207:542-559.

[4] Ellen MacArthur Foundation and Granta Design. An approach to measuring circularity-Methodology. Cowes, UK: Ellen Mac Arthur Foundation; 2015.

[5] Parchomenko A., Nelen D., Gillabel J., Rechberger H., Measuring the circular economy - A Multiple Correspondence Analysis of 63 metrics. J Clean Prod 2019; 210:200-216-

[6] Linder M., Sarasini S., van Loon P., A Metric for Quantifying Product-Level Circularity. J Ind Ecol 2017;21(3):545-558.

[7] Haupt M., Vadenbo C., Hellweg S., Do We Have the Right Performance Indicators for the Circular Economy? Insight into the Swiss Waste Management System. J Ind Ecol 2017;21(3):615-627.

[8] Geng Y., Fu J., Sarkis J., Xue B., Towards a national circular economy indicator system in China: an evaluation and critical analysis. J Clean Prod 2012; 23:216-224.

[9] Smol M., Kulczycka J., Avdiushchenko A., Circular economy indicators in relation to eco-innovation in European regions. Clean Techn Environ Policy 2017; 19:669–678.

[10] Elia V., Gnoni M.G., Tornese F., Measuring circular economy strategies through index methods: A critical analysis. J Clean Prod 2017; 142:2741-2751.

[11] Rossi E., Bertassini A.C., dos Santos Ferreira C., do Amaral W.A.N., Ometto A.R., Circular economy indicators for organizations considering sustainability and business models: Plastic, textile and electro-electronic cases. J Clean Prod 2020; 247:119-137.

[12] García-Barragán J.F., Eyckmans J., Rousseau S., Defining and Measuring the Circular Economy: A Mathematical Approach. Ecol Econ 2019; 157:369-372.

[13] Bertolucci Paes L.A., Stolte Bezerra B., Mattos Deus R., Jugend D., Gomes Battistelle R.A., Organic solid waste management in a circular economy perspective – A systematic review and SWOT analysis. J Clean Prod 2019; 239:118086.

[14] Vea E.B., Romeo D., Thomsen M., Biowaste valorisation in a future circular bioeconomy. Procedia CIRP 2018; 69:591–596.

[15] Cobo S., Dominguez-Ramos A., Irabien A., Trade-Offs between Nutrient Circularity and Environmental Impacts in the Management of Organic Waste. Environ Sci Technol 2018; 52:10923−10933.

[16] D. Murphy, E. McKeogh, G. Kiely, Technical/economic/environmental analysis of biogas utilization, Appl Energ 2004;77:407–427

[17] PUC “Medijana”. Official web site – Avaliable at: <http://www.jkpmediana.rs/> [accessed 20.12.2016].

[18] Europen Commettee for Standardization. EN 590:2009. Automotive fuels - Diesel - Requirements and test methods, Brussels, 2009.

[19] Wynd, F. L. Feed the Soil. Sci Mon 1952;74(4):223-229.

[20] Zelany, M. A concept of compromise solutions and the method of the displaced ideal. Computers & Operations Research 1974, 1(3-4), 479-496.

[21] Yu, P. L. A class of solutions for group decision problems. Management Science 1973, 19(8), 936-946.

[22] Tanimu M, Mohd Ghazi T, Harun M, Idris A. Effects of feedstock carbon to nitrogen ratio and organic loading on foaming potential in mesophilic food waste anaerobic digestion. Applied Microbiology and Biotechnology 2015 ;(10):4509.

THE 5th INTERNATIONAL CONFERENCE
MECHANICAL ENGINEERING IN XXI CENTURY

December 9-10, 2020
Faculty of Mechanical Engineering in Niš, Serbia

Finned Radiator Thermal Characteristics Calculation

Emir NOVALIĆ, Jelena JANEVSKI, Predrag ŽIVKOVIĆ, Mića VUKIĆ, Dejan MITROVIĆ

Faculty of Mechanical Engineering, University in Niš, Serbia
novalicemir19@gmail.com; emir.novalic@nova-dpi.rs

***Abstract*— Water that is not well treated and maintained, despite all the benefits, may have devastating effect to the radiator body. Chemically untreated water can have a high PH value. Data collected while maintaining radiators in use has shown that with the increased PH value of water, corrosion occurs on the inner side of aluminium radiators. In addition to water quality treatment, one of the practical solutions is the addition of a steel pipe insert in the interior of the aluminium heater. Addition of the pipe insert increases the material thickness, and thus the overall heat conduction resistance. Increasing the heat conduction resistance affects the change in the heat transfer intensity of the radiator. The subject of this paper is research of the influence of a steel pipe insert on the heat transfer intensity of a finned aluminium heater. The method for stationary heat conduction through fines was used for analytical calculation.**

***Keywords* — energy management, energy performance indicator, food industry, energy flow analysis**

I. Introduction

In practical use, it has been shown that corrosion occurs in aluminium radiators (radiators) on the water side with increased PH value of water. How harmful corrosion is for thermal power plants is shown by the data available from the Institute for Power Research in the USA (EPRI). The annual damage from corrosion of thermal power plants in USA amounts to 3.5 billion dollars, of which about 600 million dollars is from corrosion of turbine plants [9].

Generally, it can be concluded that corrosion as an irreversible process of metal destruction:

- shortens the life of equipment,
- makes its maintenance more expensive,
- reduces the production capacities of corroded and related equipment,
- causes downtime and accidents,
- affects the reduction of plant reliability, which ultimately affects the reduction of plant availability and capacity [9].

Therefore, one of the solutions introduced by radiator manufacturer Aklimat, in addition to chemical treatment and improvement of water quality in plants, is the steel pipe insert addition in the water space of the radiator, so that water does not get into direct contact with the aluminium body.

II. Energy Equation in General Form for Heat Transfer by Convection and Radiation from the Finned Surface

Energy equation in general form for heat transfer by convection and radiation from the finned surface is

$$\frac{d^2T}{dx^2}+\left(\frac{1}{f(x)}\cdot\frac{df(x)}{dx}\right)\cdot\frac{dT}{dx}-\left(\frac{1}{f(x)}\cdot\frac{\alpha}{\lambda}\cdot\frac{dU(x)}{dx}\right)\cdot\left(T-T_f\right)-\left(\frac{1}{f(x)}\cdot\frac{\varepsilon\cdot\sigma}{\lambda}\cdot\frac{dU(x)}{dx}\right)\left(T^4-T_f^{\,4}\right)=0 \quad (1)$$

where are

- T - temperature of the fin at a distance x;
- T_f - ambient temperature;
- f(x) - cross-sectional area of the considered fin at the distance from the base of the fin x;
- U(x) - the outer surface of the fin from the base to a given cross section, which is also a function of x;
- λ - heat conduction coefficient of the fin material;
- α - heat transfer coefficient from the outer surface of the fin to surrounding fluid;
- ε - integral (average) blackness or emissivity degree;
- σ - Stefan-Boltzmann constant.

This differential equation describes the change of temperature along the length of the fin influenced by convection and radiation [4].

For the given conditions, f(x)=f=const. and U(x)=U·x, one can obtain

$$\frac{d^2T}{dx^2}-\frac{U\cdot\alpha}{f\cdot\lambda}\cdot\left(T-T_f\right)-\frac{U\cdot\varepsilon\cdot\sigma}{f\cdot\lambda}\left(T^4-T_f^{\,4}\right)=0 \quad (2)$$

where are

- U - the fin perimeter;
- f - is the cross-sectional area of the fin.

The boundary conditions that are required to obtain the temperature distribution along the fin are

$$T\big|_{x=0}=T_b \quad (3)$$

$$-\lambda\cdot f(L)\cdot\frac{dT}{dx}\Big|_{x=L}=\alpha_L\cdot f(L)\cdot\left(T_L-T_f\right)+\varepsilon\cdot\sigma\cdot f(L)\cdot\left(T_L^4-T_f^{\,4}\right) \quad (4)$$

where are

- T_b – temperature of the fin base;
- L – the fin length.

Heat transferred from the entire fin can be determined as follows

$$q_{tot} = \int_{F_r} \begin{bmatrix} \alpha \cdot \left(T(x) - T_f\right) + \\ + \varepsilon \cdot \sigma \cdot \left(T(x)^4 - T_f^{\,4}\right) \end{bmatrix} \cdot dU(x) \qquad (5)$$

where the ratio U(x)=U·x is valid, and

- F_r - total area of the fin with the tip;
- q_{tot} - the total amount of heat transferred for a given condition.

This calculation is very complex for practical engineering calculations, and therefore a simpler methodology for calculating heat transfer from a finned surface has been developed in this paper.

III. CALCULATION OF THERMAL CHARACTERISTICS OF A FINNED RADIATOR

The calculation of thermal characteristics of the aluminium radiator as a heating body with a steel pipe insert with a wall thickness of 2 mm, which is inserted into the water space of the radiator (Fig. 1) will be presented in this paper.

Fig. 1 - Section of aluminium radiator with steel pipe insert by Aklimat manufacturer (Bimetal type)

According to the manufacturer Aklimat, the radiator cell has the following characteristics

- the water temperature at the inlet and outlet of the radiator is 90/70°C, respectively;
- the temperature of the room in which the radiator is located is 20°C;
- the thermal output of the radiator cell is $\dot{Q}$ =115 W;
- the height of the radiator cell is L=350 mm;
- the total exchange area of the radiator cell is A_{uk}=0,33 m^2;
- the thickness of the finned surfaces is 1 mm;
- inner diameter of the radiator cell water side is D=20 mm; D_1=20-4=16 mm;
- outer diameter of the radiator cell D_2=23 mm.

Due to the simplification of solving the problem and the complexity of the original radiator cell geometry, a finned longitudinal cylinder with the same exchange surface, the same fin thickness, the same diameter on the water side, as well as the cylinder wall thickness will be used for calculation. It is an approximated version of the given radiator cell (Fig. 1) with simplified geometry (Figs. 2 and 3).

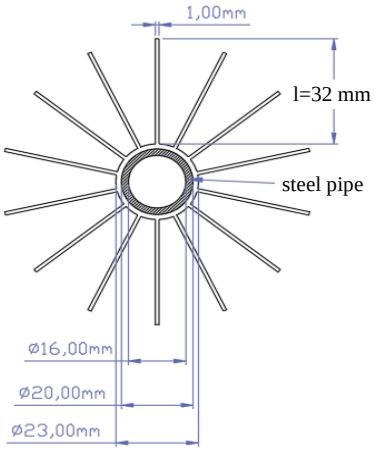

Fig. 2 - Cross section of an aluminium heating element with a steel pipe insert

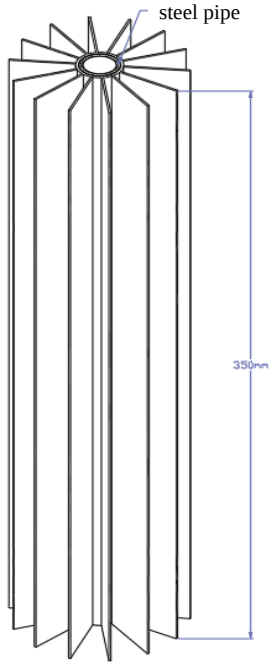

Fig. 3 - 3D geometry of the heating element with pipe insert

IV. CALCULATION OF A HEATING ELEMENT WITH A PIPE INSERT THERMAL CHARACTERISTICS

- Determination of thermo-physical properties of fluids

Due to the steel pipe insert, the flowing area on the water side is reduced and it is assumed that there will be an increase in the flow velocity of the water, which brings a change to the heat transfer coefficient. This will be determined by the following calculation steps.

In order to define the heat transfer coefficient on the inner side of the exchanger, the velocity of water in the radiator cell as well as the thermo-physical properties of water in the radiator and the air that surrounds it must be determined.

Therefore, the thermo-physical properties of the fluid are determined by appropriate thermodynamic tables.

Thermo-physical properties of water [6] are

$\Delta T_w = \frac{90+70}{2} = 80\ ^\circ C$ - mean temperature of water flowing through the radiator cell;

$\vartheta = 1{,}0285 \cdot 10^{-3}\ m^3/kg$ - specific volume of water;

$c_w = 4{,}197\ kJ/kgK$ - specific heat capacity of water;

$\mu = 354 \cdot 10^{-6}\ Ns/m^2$ - dynamic viscosity of water;

$\lambda = 670 \cdot 10^{-3}\ W/mK$ - water heat conduction coefficient;

$Pr = 2{,}2$ - Prandtl number for water at 80 °C;

$\beta = 638{,}3 \cdot 10^{-6}\ 1/K$ - water expansion coefficient.

- Determination of water flow rate and Reynolds number

Mass flow of water through the radiator cell is

$$\dot{Q} = \dot{m} \cdot c_w \cdot \Delta T$$

$$115 = \dot{m} \cdot 4197 \cdot (90-70)$$

$$\dot{m} = 1{,}37 \cdot 10^{-3} kg/s$$

Water flow rate through the radiator cell

$$\omega = \frac{\dot{m} \cdot 4}{\rho \cdot \pi \cdot D_1^2} = \frac{1{,}37x10^{-3} \cdot 4}{972{,}3 \cdot \pi \cdot 0{,}016^2} = 0{,}007 \frac{m}{s}$$

Reynolds number

$$\omega = \frac{\dot{m} \cdot 4}{\rho \cdot \pi \cdot D_1^2} = \frac{1{,}37x10^{-3} \cdot 4}{972{,}3 \cdot \pi \cdot 0{,}016^2} = 0{,}007 \frac{m}{s}$$

$$Re = \frac{\omega \cdot D_1}{\nu} = \frac{\omega \cdot D_1 \cdot \rho}{\mu} = \frac{0{,}007 \cdot 0{,}016 \cdot 972{,}3}{354x10^{-6}} = 308$$

Based on the obtained Reynolds number, a laminar flow inside the radiator cell is determined.

- Determination of Nusselt number and convection coefficient on the water side

Nusselt number for the case of a laminar internal flow [7] is

$$Nu = 1{,}86 \cdot \left(\frac{Re \cdot Pr}{\frac{L}{D_1}} \right)^{\frac{1}{3}} \cdot \left(\frac{\mu}{\mu_s} \right)^{0{,}14}$$

assumed that $0{,}6 \le Pr \le 5$ and $0{,}0044 \le \frac{\mu}{\mu_s} \le 9{,}75$

Based on the previous equation we get

$$Pr = 2{,}2 \quad \text{and} \quad \frac{\mu}{\mu_s} \approx 1$$

$$Nu = 1{,}86 \cdot \left(\frac{308 \cdot 2{,}2}{\frac{350}{16}} \right)^{\frac{1}{3}} \cdot (1)^{0{,}14} = 5{,}84$$

Therefore, the convection coefficient on the water side is determined as

$$\alpha_1 = \frac{Nu \cdot \lambda}{D_1} = \frac{5{,}84 \cdot 0{,}670}{0{,}016} = 245 \frac{W}{m^2 K}$$

- Determination the heat transfer coefficient as well as the temperature on the outer surface of the cylinder and the base of the radiator cell fins

Conduction coefficients for steel and aluminium were chosen as

$\lambda_č = 60\ W/mK$ - conduction coefficient for steel;

$\lambda_{Al} = 180\ W/mK$ - conduction coefficient for aluminium;

Therefore, the heat transfer resistance coefficient can be determined as

$$R_{uk} = \frac{1}{D_1 \cdot \pi \cdot \alpha_1} + \frac{1}{2 \cdot \pi \cdot \lambda_č} \cdot \ln \frac{D_2}{D_1} + \frac{1}{2 \cdot \pi \cdot \lambda_{Al}} \cdot \ln \frac{D_3}{D_2}$$

$$R_{uk} = \frac{1}{0{,}016 \cdot \pi \cdot 245} + \frac{1}{2 \cdot \pi \cdot 60} \cdot \ln \frac{20}{16} + \frac{1}{2 \cdot \pi \cdot 180} \cdot \ln \frac{23}{20}$$

$$R_{uk} = 0{,}082\ mK/W$$

The inversion of this coefficient gives the heat transfer coefficient

$$k_{uk} = \frac{1}{R_{uk}} = \frac{1}{0{,}082} = 12{,}2\ W/mK$$

The temperature of the outer surface of the radiator cell and the base of the fins is

$$\dot{Q} = k_{uk} \cdot L \cdot (\Delta T_w - T_b)$$

$$T_b = \Delta T_w - \frac{\dot{Q}}{k_{uk} \cdot L} = 80 - \frac{115}{12{,}189 \cdot 0{,}35} = 53\ ^\circ C$$

- Determination of thermo-physical properties of fluids on the air side

To determine the Nusselt number as well as the heat transfer coefficient on the air side, the thermo-physical properties of the air should be determined.

Thermo-physical properties of air are taken from thermodynamic tables for air temperatures of 53°C - the temperature of the air that is in contact with the outer surface of the radiator and 36,5 °C - the mean

temperature of the air flowing over the outer surface of the radiator

$\Delta T_v = \frac{53+20}{2} = 36{,}5\ ^\circ C$ - mean temperature of air;

$\rho = 1{,}1403\ kg/m^3$ - density of air;

$c_p = 1{,}007\ kJ/kgK$ - specific heat capacity of air;

$\mu = 189{,}8 \cdot 10^{-7}\ Ns/m^2$ - dynamic viscosity of air;

$\lambda = 26{,}82 \cdot 10^{-3}\ W/mK$ - air heat conduction coefficient;

$Pr = 0{,}713$ - Prandtl number for air 36,5 °C;

$Pr_z = 0{,}71$ - Prandtl number for air at 53 °C;

$\beta = 3{,}23 \cdot 10^{-3}\ 1/K$ - air expansion coefficient.

- Determination of convection coefficient on the air side of the radiator cell

The Nusselt number for free convection will be determined by using the following formula according to the literature [8]

$$Nu = \varepsilon_R \cdot A \cdot (Gr \cdot Pr)^m \cdot \left(\frac{Pr}{Pr_z}\right)^n$$

The constants in the previous equation are adopted for the following conditions

- laminar flow

$$10^3 < Gr \cdot Pr < 10^9 \Rightarrow A = 0{,}75;\ m = 0{,}25;\ n = 0{,}25$$

- turbulent flow

$$Gr \cdot Pr > 10^9 \ \Rightarrow\ A = 0{,}15;\ m = 0{,}33;\ n = 0{,}25$$

- flow regime stabilized

$$\frac{L}{D_2} > 50 \ \Rightarrow\ \varepsilon_R = 1$$

- flow regime not stabilized

$$\frac{L}{D_2} < 50 \ \Rightarrow\ \varepsilon_R > 1$$

The expression for the Grashoff number is

$$Gr = \frac{\beta \cdot g \cdot L^3}{\nu^2} \cdot \Delta T = \frac{\beta \cdot g \cdot L^3}{\left(\frac{\mu}{\rho}\right)^2} \cdot \Delta T$$

it follows

$$Gr = \frac{3{,}23 \cdot 10^{-3} \cdot 9{,}81 \cdot 0{,}35^3}{\left(\frac{189{,}8 \cdot 10^{-7}}{1{,}1403}\right)^2} \cdot (53-20) = 1{,}6182 \cdot 10^8$$

$$Gr \cdot Pr = 1{,}6182 \cdot 10^8 \cdot 0{,}713 = 1{,}1538 \cdot 10^8$$

$$\frac{L}{D_1} = \frac{350}{16} = 21{,}875 < 50 \ \Rightarrow\ \varepsilon_R = 1{,}12$$

The value of the Nusselt number is as follows

$$Nu = \varepsilon_R \cdot A \cdot (Gr \cdot Pr)^m \cdot \left(\frac{Pr}{Pr_z}\right)^n$$

$$Nu = 1{,}12 \cdot 0{,}75 \cdot \left(1{,}1538 \cdot 10^8\right)^{0{,}25} \left(\frac{0{,}713}{0{,}710}\right)^{0{,}25} = 87$$

According to previous results, the heat transfer coefficient is

$$\alpha_2 = \frac{Nu \cdot \lambda}{L} = \frac{87 \cdot 0{,}02682}{0{,}35} = 6{,}7\ W/m^2K$$

- Determining the height and number of fins of the radiator cell

The total exchange area of the radiator cell is A_{uk}=0,33 m^2. The total fin perimeter is

$$U_{uk} = \frac{A_{uk}}{L} = \frac{0{,}33}{0{,}35} = 0{,}943\ m$$

$$U_{uk} = (\pi \cdot D_2 - n_{reb} \cdot 2 \cdot \delta) + n_{reb} \cdot (2l + 2 \cdot \delta)$$

Number of fins

$$U_{uk} = (\pi \cdot D_2 - n_{reb} \cdot 2 \cdot \delta) + n_{reb} \cdot (2 \cdot l + 2 \cdot \delta)$$

$$n_{reb} = \frac{U_{uk} - \pi \cdot D_2}{2 \cdot l} = \frac{0{,}943 - \pi \cdot 0{,}023}{2 \cdot 0{,}032}$$

$$n_{reb} = 13{,}6$$

where are

$l = 32\ mm$ - fin height;

$2 \cdot \delta = 1\ mm$ - fin thickness;

$n_{reb} = 14$ - adopted number of fins;

The new exchange area

$$A_{uk} = U_{uk} \cdot L = (\pi \cdot D_2 + n_{reb} \cdot 2 \cdot l) \cdot L$$

$$A_{uk} = (\pi \cdot 0{,}023 + 14 \cdot 2 \cdot 0{,}032) \cdot 0{,}35 = 0{,}339\ m^2$$

- Determination of the total heat flux transferred from the surface of the radiator cell

Linear heat flux exchanged from the surface of the fin to the air by convection [3] is

$$\Phi^{(1)} = 2 \cdot \lambda_{Al} \cdot m \cdot \delta \cdot (T_b - T_f) \cdot \tanh(m \cdot l)\ \left[\frac{W}{m}\right]$$

$$m=\sqrt{\frac{\alpha_2}{\lambda_{Al}\cdot\delta}}=\sqrt{\frac{6,7}{180\cdot 0,0005}}=8,63$$

$$m\cdot l=8,63\cdot 0,032=0,276$$

$$T_b-T_f=53-20=33\ ^oC$$

Heat exchanged by convection per meter of the fin

$$\Phi^{(1)}=2\cdot 180\cdot 8,63\cdot 0,0005\cdot 33\cdot \tanh(0,276\cdot\frac{180}{\pi})$$

$$\Phi^{(1)}=13,8\ W/m$$

Heat exchanged by convection per meter of all fins

$$\Phi_r^{(1)}=\Phi^{(1)}\cdot n_{reb}=13,8\cdot 14=193,2\ W/m$$

Heat transfer by convection from the fins

$$\dot{Q}_r=\Phi_r^{(1)}\cdot L=193,2\cdot 0,35=67,6\ W$$

Unfinned cylinder exchange surface on the air side

$$A_z=(\pi\cdot D_2-n_{reb}\cdot 2\cdot\delta)\cdot l\left[\frac{m^2}{m}\right]$$

$$A_z=(\pi\cdot 0,023-14\cdot 0,001)\cdot 1=0,0582\ m^2/m$$

Heat exchanged by convection per meter of the outer unfinned cylinder surface

$$\Phi_z^{(1)}=\alpha_2\cdot A_z\cdot(T_b-T_f)\left[\frac{W}{m}\right]$$

$$\Phi_z^{(1)}=6,7\cdot 0,0582\cdot 33=12,9\ W/m$$

Heat exchanged by convection from the outer unfinned cylinder surface

$$\dot{Q}_z=\Phi_z^{(1)}\cdot L\ [W]$$

$$\dot{Q}_z=12,9\cdot 0,35=4,5\ W$$

Total heat exchanged by convection from the outer surface of the radiator cell

$$\dot{Q}_{conv}=\dot{Q}_r+\dot{Q}_z=67,6+4,5=72,1\ W$$

Heat exchanged by radiation per square meter

$$\dot{q}_{rad}=\alpha_{rad}\cdot(T_b-T_f)\left[\frac{W}{m^2}\right]$$

$$\dot{q}_{rad}=\varepsilon_{al}\cdot C_c\cdot\left[\left(\frac{T_b}{100}\right)^4-\left(\frac{T_f}{100}\right)^4\right]\left[\frac{W}{m^2}\right]$$

where are

$\varepsilon_{Al}=0,5$ - emission factor of aluminium radiator surface painted white [11];

$C_c=5,67\ \frac{W}{m^2K^4}$ - radiation constant of an absolute black body.

$$\dot{q}_{rad}=0,5\cdot 5,67\cdot\left[\left(\frac{326}{100}\right)^4-\left(\frac{293}{100}\right)^4\right]=111,3\ W/m^2$$

Heat exchanged by radiation from the surface of the radiator cell

$$\dot{Q}_{rad}=\dot{q}_{rad}\cdot A_{uk}=111,3\cdot 0,339=37,7\ W$$

Total heat exchanged from the surface of a given radiator cell

$$\dot{Q}_{tot}=\dot{Q}_{conv}+\dot{Q}_{rad}=72,1+37,7=109,8\ W$$

For the same geometry of a finned radiator cell without a steel pipe insert, the total heat exchanged from the finned surface by convection and radiation is calculated at the value of 113,2W. Thus, addition of a steel pipe insert slightly reduces heat dissipation from the radiator surface.

V. CONCLUSION

On the water side of the radiator cell, by adding a steel pipe insert, the flow surface was reduced, which resulted in an increase in the fluid flow rate. Increasing the flow rate of water through the interior of the radiator also increased the value of the Reynolds number, and eventually increased the heat transfer coefficient. By adding a new layer of material, it increased the total resistance to heat conduction. All this eventually caused a decrease in the total heating capacity of the radiator cell by 3% (Table 1).

Finally, it could be concluded that the solution of adding a steel insert is technically acceptable, which gives additional corrosion protection to the radiator. Corrosion negatively affects the radiator capacity, so its reduction extends the service life and mechanical resistance of the radiator.

TABLE 1. CALCULATION RESULTS

		without steel pipe insert	**with** steel pipe insert	change %
D_1	mm	20	16	-25
α_1	W/m^2K	196	245	+25
α_2	W/m^2K	6,9	6,7	-2,9
$\dot{Q}_{conv}$	W	75,2	72,1	-4,1
$\dot{Q}_{rad}$	W	38,0	37,7	-0,8
$\dot{Q}_{tot}$	W	113,2	109,8	-3,0

ACKNOWLEDGMENT

This paper is a part of the master work under tittle "Research of the influence of a steel pipe insert on the heat transfer intensity in a finned aluminium heater", which was presented on 30.10.2020 at the Faculty of Mechanical Engineering in Niš. The mentor of the master work is prof. dr Mića Vukić, to whom I thank for the effort and useful advices which improved the quality of the named master work.

REFERENCES

[1] Boris Labudović, Zdravko Paić, Robert Vuk: Priručnik za grijanje, Energetika marketing, ISBN 953-6759-25-X, Zagreb, 2005.

[2] Reknagel, Šprenger, Šramek, Čeperković: Grejanje i klimatizacija uključujući toplu vodu i tehniku hlađenja, INTERKLIMA-GRAFIKA, Vrnjačka Banja, ISBN 86-82685-13-2, Vrnjačka Banja, 2004.

[3] Gradimir S. Ilić, Mića V. Vukić, Nenad V. Radojković, Predrag M. Živković, Ivan H. Stojanović: Termodinamika II - osnove prostiranja toplote i materije, Mašinski fakultet Univerziteta u Nišu, Unigraf X-Copy, ISBN 978-86-6055-056-1 (COBISS.SR-ID209242892), Niš, 2014.

[4] M. HATAMI, D.D. GANJI: Optimization of configurations to enhance heat transfer from a longitudinal fin exposed to natural convection and radiation, Esfarayen University of Technology, Department of Mechanical Engineering, Esfarayen, North Khorasan, Iran, Department of Mechanical Engineering, Babol University of Technology, Babol, Iran, P.O.Box 484, Proceedings of ISER 10th International Conference, Kuala Lumpur, Malaysia, 8th November 2015, ISBN 978-93-85832-34-5.

[5] Allan D. Kraus, Abdul Aziz, James Welty: Extended Surface Heat Transfer, John Wiley & Sons, 2002, ISBN 0471436631, 9780471436638

[6] http://www.mhtl.uwaterloo.ca/old/onlinetools/airprop/airprop.html

[7] Theodore L. Bergman, Frank P. Incropera, David P. DeWitt, Adrienne S. Lavine: Fundamentals of Heat and Mass Transfer, John Wiley & Sons, 2011, ISBN 0470501979, 9780470501979.

[8] B. Đorđević, V. Valent, S. Šerbanović: Termodinamika sa termotehnikom, Tehnološko-metalurški fakultet Univerziteta u Beogradu, Zavod za grafičku tehniku Tehnološko-metalurškog fakulteta, ISBN 086-7401-130-6 (ID81224972), Beograd, 2000.

[9] M. V. Tomić, G. Tadić, M. G. Pavlović, Lj. J. Pavlović: Uzroci korozije u termoenergetskim postrojenjima i načini prevencije, Originalni naučni rad UDC:620.193.194:624.311.
3.22=861, ZAŠTITA MATERIJALA 50 (2009) broj 1.

[10] Ljubinka V. Rajković: Korozijski procesi u termoenergetskim postrojenjima usled neadekvatnog kvaliteta vode, Tehnološko-metalurški fakultet Univerziteta u Beogradu, Karnegijeva 4, Beograd, 2007.

[11] https://www.engineeringtoolbox.com/emissivity-coefficients-d_447.html

[12] Henk Kaarle Versteeg, Weeratunge Malalasekera: An Introduction to Computational Fluid Dynamics: The finite volume method, Pearson Education Limited, 2007, ISBN 0131274988, 9780131274983.

THE 5th INTERNATIONAL CONFERENCE
MECHANICAL ENGINEERING IN XXI CENTURY

December 9-10, 2020
Faculty of Mechanical Engineering in Niš, Serbia

MHD Flow and Heat Transfer of Two Immiscible Micropolar Fluids

Miloš KOCIĆ[a], Živojin STAMENKOVIĆ[a], Jelena PETROVIĆ[a] and Milica NIKODIJEVIĆ[b]

[a]Faculty of Mechanical Engineering, University of Niš, A. Medvedeva 14, 18000 Niš, Serbia
[b]Faculty of Occupational Safety Univerity of Niš, Čarnojevića 10a, 18000 Niš, Serbia
milos.kocic@masfak.ni.ac.rs, zivojin.stamenkovic@masfak.ni.ac.rs, jelena.nikodijevic.petrovic@masfak.ni.ac.rs, milica.nikodijevic@znrfak.ni.ac.rs

***Abstract*—The steady flow and heat transfer of two incompressible electrically conducting micropolar fluids, between two infinite parallel plates, is investigated in this paper. The upper and lower plates have been kept at the two constant different temperatures and the plates are electrically insulated. Applied magnetic field is perpendicular to the flow and considered problem is in induction-less approximation. The general equations that describe the discussed problem under the adopted assumptions are reduced to ordinary differential equations and three closed-form solutions are obtained. The velocity, micro-rotation and temperature fields in function of Hartmann number, Reynolds number, the coupling parameter and the spin-gradient viscosity parameter are graphically shown and discussed.**

***Keywords*—micropolar fluid, two fluids, heat transfer, MHD flow, micro-rotation**

I. Introduction (use style MASING Heading 1)

The requirements of modern technology have stimulated the interest in fluid flow studies, which involve the interaction of several phenomena. One of these phenomena is certainly flow of electrically conducting micropolar fluid in the presence of a magnetic field. The theory of thermo-micropolar fluids has been developed by Eringen [1], taking into account the effect of micro-elements of fluids on both the kinematics and conduction of heat. The concept of micropolar fluid is introduced in an attempt to explain the behavior of a certain fluid containing polymeric additives and naturally occurring fluids such as the phenomenon of the flow of colloidal fluids, real fluid with suspensions, liquid crystals and animal blood, etc...

Eringen [1] initiated the concept of micropolar fluids to characterize the suspensions of neutrally buoyant rigid particles in a viscous fluid. The micropolar fluids exhibit micro-rotational and micro-inertial effects and support body couple and couple stresses. It may be noted that micropolar fluids take care of the microrotation of fluid particles by means of an independent kinematic vector called microrotation vector.

The research interest in the MHD flows of micropolar fluids has increased substantially over the past decades due to the occurrence of these fluids in industrial and magneto-biological processes. These flows take into account the effect arising from the local structure and micro-motions of the fluid elements. A comprehensive review of the subject and applications of micropolar fluid mechanics was given by Chamkha et al. [2] and Bachok et al. [3].

The MHD heat transfer of micropolar fluid can be divided in two parts. One contains problems in which the heating is an incidental byproduct of electromagnetic fields as in MHD generators etc, and the second consists of problems in which the primary use of electromagnetic fields is to control the heat transfer. Heat transfer in micropolar fluid flow in the presence of magnetic field has gained considerable attention in recent years because of its various applications in contemporary technology. These applications include liquid crystals [4], blood flow in lungs or in arteries [5], flow and thermal control of polymeric processing [6]...

Basic ideas and techniques for both steady and unsteady flow problems of Newtonian and non-Newtonian fluids are given by Ellahi [7]. The basic equations governing the flow of couple stress fluids are non-linear in nature and even of higher order than the Navier Stokes equations. Different numerical, perturbation techniques and a reasonable simplification are commonly used for obtaining solutions of these equations [8].

There are many problems in the fields of hydrology and reservoir mechanics in which systems involving two or more immiscible fluids of different densities/viscosities flowing in same pipe or channel or through porous media are encountered. Lohrasbi and Sahai [9] studied two-phase MHD flow and heat transfer in parallel plate channel with the fluid in one phase being conducting. Due the importance of the two fluid flow models, in our previous paper [10] was investigated flow and heat transfer of two immiscible fluids in the presence of uniform inclined magnetic field. Blood flow in arteries has been studied by many researchers considering the flow of blood as a multi phase flow [11].

Keeping in view the wide area of practical importance of micropolar fluid flow and heat transfer as mentioned above, the objective of the present study is to investigate the MHD flow and heat transfer characteristics of a two electrically conducting incompressible micropolar fluids in a parallel plate channel.

II. PHYSICAL AND MATHEMATICAL MODEL

The problem of laminar MHD flow and heat transfer of two incompressible electrically conducting micropolar fluids between parallel plates is considered. MHD channel flow analysis is usually performed assuming the fluid constant electrical conductivity and treating the problem as a one-dimensional one. The physical model shown in Figure 1, consists of two infinite parallel plates extending in the *x* and *z*-direction. Fully developed flow takes place between parallel plates that are at a distance *2h*. Electrically conductive fluids flows through the channel due to the constant pressure gradient. A uniform magnetic field of the strength *B* is applied in the *y* direction. The upper and lower plate have been kept at the two constant temperatures Tw_1 and Tw_2 respectively. The fluid velocity vector **v** and magnetic field induction vector **B** are:

$$\mathbf{v}=u\vec{i}, \tag{1}$$

$$\mathbf{B}=B\vec{j}. \tag{2}$$

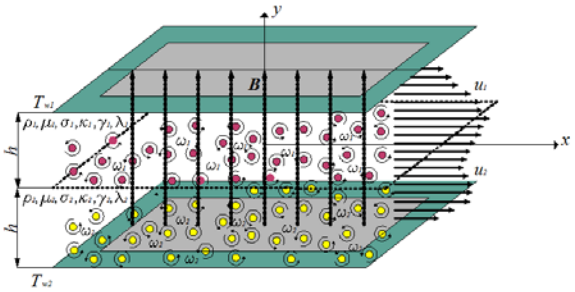

Fig. 1 Physical model and coordinate system

Described laminar MHD flow and heat transfer is mathematically presented with following nondimensional equations:

$$(1+K_i)\frac{d^2u_i}{dy^2}+K_i\frac{d\omega_i}{dy}-Ha_i^2u_i+Re_iG=0, \tag{3}$$

$$\Gamma_i\frac{d^2\omega_i}{dy^2}-K_i\frac{du_i}{dy}-2K_i\omega_i=0, \tag{4}$$

$$\frac{d^2\theta_i}{dy^2}+(1+K_i)\Pr_i Ec_i\left(\frac{du_i}{dy}\right)^2+Ec_i\Pr_i Ha_i^2u_i^2=0. \tag{5}$$

The boundary dimensionless conditions for previous equations are:

$$\begin{aligned}
&u_1=0,\ \omega_1=0,\ \theta_1=1 \quad \text{for} \quad y=1,\\
&u_2=0,\ \omega_2=0,\ \theta_2=0 \quad \text{for} \quad y=-1,\\
&u_1=u_2,\ \omega_1=\omega_2,\ \theta_1=\theta_2 \quad \text{for} \quad y=0,\\
&(1+K_1)\frac{du_1}{dy}+K_1\omega_1=h^*\mu^*(1+K_2)\frac{du_2}{dy}+h^*\mu^*K_2\omega_2\\
&\text{for} \quad y=0,\\
&\frac{d\theta_1}{dy}=h^*k^*\frac{d\theta_2}{dy} \quad \text{for} \quad y=0,\\
&\frac{d\omega_1}{dy}=h^{*2}\lambda^*\frac{d\omega_2}{dy} \quad \text{for} \quad y=0.
\end{aligned} \tag{6}$$

The no slip conditions and isothermal conditions, together with continuity of temperature and heat flux, as well as the equality of stresses and constant cell rotational velocity at the interface, are the boundary conditions for the observed problem.

The following transformations have been used to transform equations to nondimensional form:

$$\begin{aligned}
&y_i=\frac{y^*}{h_i},x_i=\frac{x^*}{h_i},u_i=\frac{u_i^*}{U_0},G=-\frac{dp}{dx}=const,\\
&p=\frac{p^*}{\rho_iU_0^2},K_i=\frac{\lambda_i}{\mu_i},\Gamma_i=\frac{\gamma_i}{\mu_ih_i^2},Ha_i=Bh_i\sqrt{\frac{\sigma_i}{\mu_i}},\\
&\Pr_i=\frac{\mu_ic_{pi}}{k_i},\mathrm{Re}_i=\frac{h_iU_0\rho_i}{\mu_i},Ec_i=\frac{U^2}{c_{pi}(T_{w1}-T_{w2})},
\end{aligned} \tag{7}$$

where:

$$h^*=\frac{h_1}{h_2},\mu^*=\frac{\mu_2}{\mu_1},k^*=\frac{k_2}{k_1},\lambda^*=\frac{\lambda_2}{\lambda_1}. \tag{8}$$

After basic mathematical transformations from equations (3) and (4) the equation for velocity is:

$$u_i^{iv}-a_iu_i''+b_iu_i-d_i=0 \tag{9}$$

where a_i, b_i, d_i are constants.

The solution of equation (9) has three possible cases and there are three corresponding solutions for temperature and micro rotation, but due to restriction of the number of pages, just the solution for the velocity are given.

$$\begin{aligned}
u_i=&C_{1i}\exp(\delta_{1i}y)+C_{2i}\exp(\delta_{2i}y)+\\
&+C_{3i}\exp(\delta_{3i}y)+C_{4i}\exp(\delta_{4i}y)+\frac{d_i}{b_i}.
\end{aligned} \tag{10}$$

$$\begin{aligned}
u_i=&(C_{5i}+C_{6i}y)\exp(\xi_{1i}y)+\\
&+(C_{7i}+C_{8i}y)\exp(\xi_{2i}y)+\frac{d_i}{b_i}.
\end{aligned} \tag{11}$$

$$\begin{aligned}
u_i=&\left[C_{9i}\cos(\beta_{1i}y)+C_{10i}\sin(\beta_{1i}y)\right]\exp(\alpha_{1i}y)+\\
&+\left[C_{11i}\cos(\beta_{1i}y)+C_{12i}\sin(\beta_{1i}y)\right]\exp(-\alpha_{1i}y)+\\
&+\frac{d_i}{b_i}.
\end{aligned} \tag{12}$$

III. RESULTS AND DISCUSION

The results obtained in previous section, now are used to graphical show influence of Hartmann number *Ha*, Reynolds number *Re*, together with coupling *K* and spin gradient viscosity parameter *Γ* on velocity, microrotation and temperature field.

The ratio of nondimensional parameters of two micropolar fluids, are given in the next form:

$$\Gamma=\frac{\Gamma_1}{\Gamma_2};\ K=\frac{K_1}{K_2},\ Ha=\frac{Ha_1}{Ha_2};\ \mathrm{Re}=\frac{\mathrm{Re}_1}{\mathrm{Re}_2}. \tag{13}$$

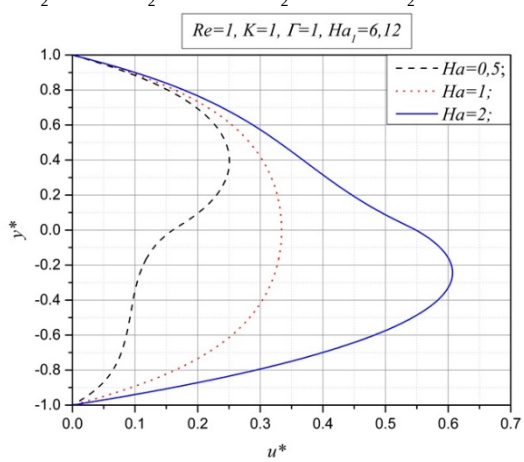

Fig. 2 Velocity profiles for different values of the Hartmann number

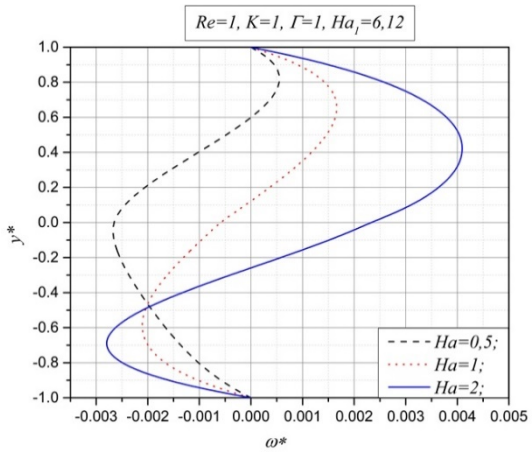

Fig. 3 Micro-rotation in function of the Hartmann number

The effect of Hartmann number on the velocity and micro rotation is shown in Figures 2 and 3.

It can be seen from those figures that the velocity, as it is expected, decreases for large values of *Ha*. As the value of Hartman number for second fluid increase, the velocity in lower part of the channel decrease. This happens because of the imposing of a magnetic field normal to the flow direction, which creates a Lorentz force opposite to the flow direction. Similarly the microrotation decreases with the increase of Hartman number i.e. the magnetic field reduces the expected behaviour of micropolar fluids and even have tendency to change direction of microrotation.

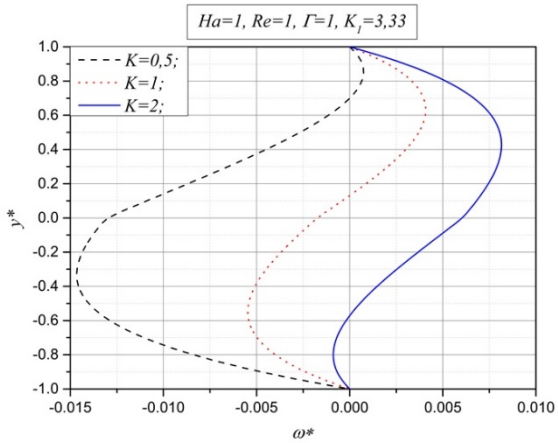

Fig. 4 Micro-rotation for different values of the coupling parameter

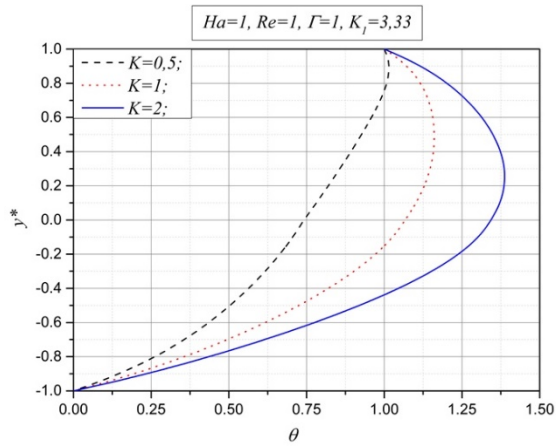

Fig. 5 Temperature as a function of the coupling parameter

The microrotation component ω increases in absolute value near the lower plate with increasing K_2, showing a tendency to change rotation near boundaries, which is shown on Figure 4.

Increasing of the coupling parameter K_2 causes a decrease of dimensionless temperature over the entire height of the channel, which is shown on Figure 5. Increase of the coupling parameter reduces the amount of energy transformed in the fluid.

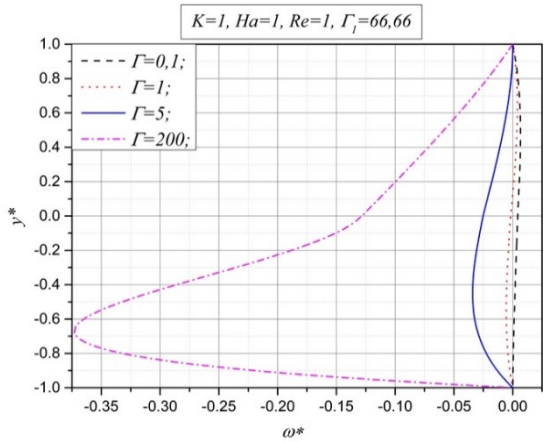

Fig. 6 Micro-rotation for different values of the spin-gradient viscosity parameter

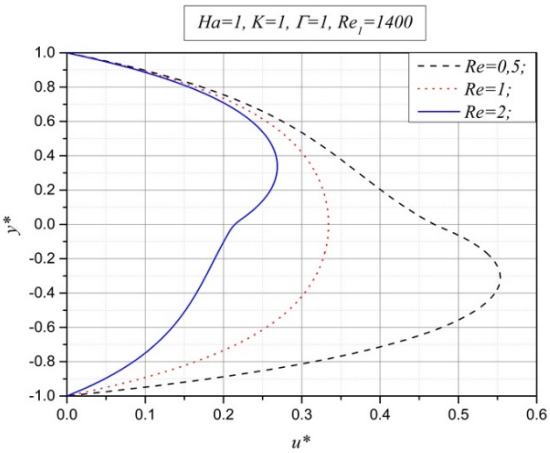

Fig. 7 Velocity profiles for different values of the Reynolds number

Micro-rotation in function of the spin-gradient viscosity parameter is shown in the Figure 6. From the lower part of the channel it can be noted that increasing of the spin-gradient viscosity parameter causes a decrease in absolute values of micro-rotation, while the changes of micro-rotation in the upper part of the channel are negligible and they are consequences of changes which happens in lower part.

Increasing of Reynolds number (Re_2) in lower part of the channel is leading to increase of velocity, which is expected as the ratio of inertial and viscous forces are becoming larger, and that is shown on Figure 7.

IV. CONCLUSION

In this paper, the steady flow and heat transfer of two incompressible electrically conducting micropolar fluids through a parallel plate channel is investigated. Applied magnetic field is perpendicular to the flow, while the Reynolds magnetic number is significantly lower than one. The general equations that describe the discussed problem under the adopted

assumptions are reduced to ordinary differential equations and closed-form solutions are obtained. Effects of Hartmann number, Reynolds number, the coupling parameter and the spin-gradient viscosity parameter on the heat and mass transfer have been analysed.

ACKNOWLEDGMENTS

This research was financially supported by the Ministry of Education, Science and Technological Development ofthe Republic of Serbia.

REFERENCES

[1] Erigen, A. C., *"Theory of micropolar fluids"*, J. Math. Mech. Vol. 16, pp. 1-18, 1966.

[2] Chamkha, A., et al., *"Unsteady MHD natural convection from a heated vertical porous plate in a micropolar fluid with Joule heating, chemical reaction and radiaton effects"*, Meccanica, Vol. 46, pp. 399-411, 2011

[3] Bachok, N., et al., *"Flow and heat transfer over an unsteady stretching sheet in a micropolar fluid"*, Meccanica, Vol. 46, pp. 935-942, 2011

[4] Sengupta, A., et al., *"Liquid Crystal Microfluidics for Tunable Flow Shaping"*, Phys. Rev. Lett. Vol. 110, 2013

[5] Mekheimer, Kh. S., El Kot, M. A., *"The micropolar fluid model for blood flow through a tapered artery with a stenosis"*, Acta Mechanica Sinica, Vol. 24, pp. 637-644, 2008

[6] Toshivo, T., et al., *"Magnetizing force modelled and numerically solved for natural convection of air in a cubic enclosure: effect of the direction of the magnetic field"*, International Journal of Heat and Mass Transfer, Vol. 45, pp. 267–277, 2002

[7] Ellahi, R., *"Steady and Unsteady Flow Problems for Newtonian and Non-Newtonian Fluids: Basics, Concepts, Methods"*, VDM Verlag, Germany, 2009

[8] Nor Azizah Yacob, et al., *"Hydromagnetic flow and heat transfer adjacent to a stretching vertical sheet in a micropolar fluid"*, Thermal Science, Vol. 17, pp. 525- 532, 2013

[9] J. Lohrasbi and V. Sahai, *"Magnetohydrodynamic heat transfer in two-phase flow between parallel plates"*, Applied Scientific Research, Vol. 45, pp. 53–66, 1988

[10] D. Nikodijević, Ž. Stamenković, D. Milenković, B. Blagojević and J. Nikodijević, *"Flow and heat transfer of two immiscible fluids in the presence of uniform inclined magnetic field"*, Hindawi Publishing Corporation, Mahtematical problem in engineering, Vol. 2011, 2011

[11] J. C. Umavathi, J. Prathap Kumar, A. J. Chamkha, *"Flow and heat transfer of a micropolar fluid sandwiched between viscous fluid layers"*, Canadian Journal of Physics, Vol. 86, pp. 08-022, 2008

THE 5th INTERNATIONAL CONFERENCE
MECHANICAL ENGINEERING IN XXI CENTURY

December 9-10, 2020
Faculty of Mechanical Engineering in Niš, Serbia

Nanofluid Flow and Heat Transfer Between Horizontal Plates in Porous Media

Jelena Petrović[1], Miloš Kocić[1], Milica Nikodijević[2], Jasmina Bogdanović-Jovanović[1]

[1] *Department of Hydroenergetics, Faculty of Mechanical Engineering Univerity of Niš, Aleksandra Medvedeva 14, 18000 Niš, Serbia*

[2] *Chair of preventive engineering, Faculty of Occupational Safety Univerity of Niš, Čarnojevića 10a, 18000 Niš, Serbia*

jelena.nikodijevic.petrovic@masfak.ni.ac.rs, zivojin.stamenkovic@masfak.ni.ac.rs
milos.kocic@masfak.ni.ac.rs, milica.nikodijevic@znrfak.ni.ac.rs, jasmina.bogdanovic.jovanovic@masfak.ni.ac.rs

Abstract - In this paper, we have presented an analytical solution to the problem of MHD flow and heat transfer of nanofluid between horizontal plates in porous medium. Nanofluid is homogeneous, incompressible and electrically conducting. Horizontal plates are fixed and kept at different constant temperatures. Applied magnetic field is perpendicular to the plates while electric field is perpendicular to the vertical plane of the channel. Discussed problem is in induction-less approximation. The influence of important non-dimensional parameters on velocity and temperature fields are graphically illustrated and analysed in detail.

***Keywords*— MHD flow, heat transfer, porous media, nanofluid**

I. Introduction

Fow and heat transfer of an electrically-conductive fluid in channels with a magnetic and an electric field have a wide application in magnetohydrodynamics, specifically with regard to pumps, generators, accelerators, flowmeters, nuclear reactors, geothermal systems, etc. The common goal regarding all these problems is to improve heat transfer. A good way to improve heat transfer is to use porous media with a metal matrix, magnetic field, electric field and from 1995, with Choi [1] publication, nanofluids.

These fluids contain solid particles (nanoparticles) with a typical length of 1-50 *nm*. There is increasing research of heat and mass transfer of nanofluids MHD flow in porous media. According to Das et al. [2], several hundred research teams throughout the world studied nanofluids in 2007, and there are so many more today. The majority of those studies are accessible to the scientific and professional community.

Wang and Mujumdar [3] reviewed the studies of convection flows and heat transfer of nanofluids and suggested some options for further research. Gorla and Chamka [4] investigated the natural convective boundary layer flow over a horizontal plate in a porous medium saturated with a nanofluid. Khalili et al. [5] numerically analyzed the unsteady MHD flow and heat transfer of a nanofluid over a sheet stretching/shrinking near the stagnation point. Das et al. [6] investigated a fully developed mixed convective flow of nanofluids in a vertical channel with an applied homogeneous transverse magnetic field and an induced magnetic field. Aaiza et al. [7] investigated the energy transfer in unsteady mixed convection MHD flow of a nanofluid in a channel filled with a saturated porous medium. The channel walls were vertical, at different temperatures, and influenced by a perpendicular homogeneous magnetic field. Akbar et al. [8] numerically analysed the heat and mass transfer of unsteady MHD flow of a nanofluid through a porous horizontal channel filled with a porous medium. Sharma and Manjeet [9] examined the MHD nanofluid flow and heat convection in a horizontal channel between two parallel plates through a porous medium. Kasaeian et al. [10] reviewed the cases of using nanofluids and porous media to improve heat transfer in thermal systems with different structures, flow regimes, and boundary conditions. Petrović et al. [11] studied the MHD flow and heat transfer of two immiscible fluids in a porous saturated medium between horizontal plates at different temperatures. The external magnetic field was homogeneous and inclined in relation to the flow direction and the electric field was homogeneous and perpendicular to the vertical longitudinal plane of the channel. Eldabe et al. [12] studied the peristaltic transport of Carreau nanofluid with heat and mass transfer through a porous medium inside an asymmetric channel. They considered the Hall effect, Joule heating, viscous dissipation, and the applied homogeneous magnetic field. Swarnalathamma [13] investigated the heat and mass transfer of MHD nanofluid flow over an isothermal sphere with thermal slip effects and the applied radial magnetic field. Umavathi and Sheremet [14] numerically analyzed the heat and mass transfer of a coupled stress nanofluid sandwiched between two viscous fluids. Singh and Srinivasa [15] investigated the influence of the magnetic field, variable viscosities and thermal conductivity on the flow of nanofluids over a flat plate. Khan and Alqahtani [16] investigated the MHD flow and heat transfer of a nanofluid in a vertical channel with porous walls at constant but different temperatures and through a porous medium. Raju and Ojjela [17] conducted a comparative study of the flow and heat transfer of viscous and Jeffrey nanofluids between two parallel plates with periodical injection/suction and with convective boundary conditions,

placed inside a porous medium and influenced by an induced magnetic field, Brownian motion, and thermophoresis. Umavathi and Sheremet [18] analysed the mixed convection in a vertical channel whose left and right thirds are filled with a porous medium. A nanofluids flowed through the left and right thirds, while a viscous fluid flowed through the middle third of the channel.

In the available literature there is not enough research on the simultaneous influence of externally applied magnetic and electric fields on the heat and mass transfer of nanofluids in porous medium. Bearing in mind the previous statement this paper analytically examines the MHD flow and heat transfer of nanofluids in a horizontal channel between two parallel walls. The channel walls are at constant and different temperatures and medium inside the channel is porous. The applied magnetic field is perpendicular to the channel walls and the applied electric field is perpendicular to the vertical plane of the channel. The pressure drop along the channel is constant.

II. Mathematical Model

This paper examines the flow and heat transfer of nanofluids in a horizontal channel whose walls are two infinite impermeable parallel plates at a distance h from one another, whereby the top plate is at constant temperature T_{w1}, and the bottom one at constant temperature T_{w2} ($T_{w1} > T_{w2}$). The medium in the channel is porous and its permeability is constant K_0. The applied external magnetic field is homogeneous and perpendicular to the channel walls, with intensity B, and the applied external electric field is homogeneous and perpendicular to the vertical plane of the channel, with intensity E. It is assumed that the MHD flow is steady and fully developed and that the nanofluid properties are constant. It is also assumed that the flow occurs by means of a constant pressure gradient $P = -\partial p / \partial x$ and due to the combined effect of the electric and magnetic fields.

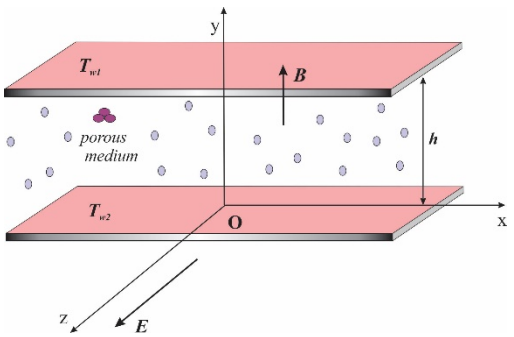

Fig.1 Physical model

With these assumptions and the chosen Cartesian coordinate system (figure 1) following equations of motion and energy (Umavathi et al. [19], Petrović et al. [20]) are:

$$P + \mu_{nf}\frac{d^2u}{dy^2} - \frac{\mu_{nf}}{K_0}u - B\sigma_{nf}\left(E + Bu\right) = 0 \qquad (1)$$

$$k_{nf}\frac{d^2T}{dy^2} + \mu_{nf}\left(\frac{du}{dy}\right)^2 + \frac{\mu_{nf}}{K_0}u^2 + \sigma_{nf}\left(E + Bu\right)^2 = 0 \qquad (2)$$

respectively, and the boundary conditions are:

$$u(0) = 0,\ u(h) = 0, \quad T(0) = T_{w2}, \quad T(h) = T_{w1}. \qquad (3)$$

In previous equations and boundary conditions the following labels were used: u, T – fluid velocity and fluid temperatures, respectively, x, y are longitudinal and transverse coordinate, $\mu_{nf}, \sigma_{nf}, k_{nf}$ are dynamic viscosity, electrical conductivity and thermal conductivity and they are given by following expressions (Akbar et al. [16]):

$$\mu_{nf} = \mu_f / \varphi_1, k_{nf} = \varphi_2 k_f, \sigma_{nf} = \varphi_3 \sigma_f. \qquad (4)$$

where:

$$\varphi_1 = (1-\phi)^{2.5},$$

$$\varphi_2 = [2k_f - 2\phi(k_f - k_s) + k_s][2k_f + \phi(k_f - k_s) + k_s]^{-1},$$

$$\varphi_3 = 1 + 3\phi(\frac{\sigma_s}{\sigma_f} - 1)[\frac{\sigma_s}{\sigma_f} + 2 - \phi(\frac{\sigma_s}{\sigma_f} - 1)]^{-1} \qquad (5)$$

where: ϕ – volume fraction of nanoparticles, μ, k, σ – viscosity, thermal conductivity and electrical conductivity, while the subscripts f and s refer to the base fluid and the nanoparticles, respectively.

Equations (1) and (2) and conditions (3) constitute the mathematical model of the presented problem. In order to obtain dimensionless mathematical model the following dimensionless quantities are introduced:

$$y^* = \frac{y}{h},\ u_i^* = \frac{u}{U},\ \theta = \frac{T - T_{w2}}{T_{w1} - T_{w2}},\ (U = \frac{Ph^2}{\mu_f}) \qquad (6)$$

and equation (1) is now transformed into following form:

$$\frac{d^2u}{dy^2} - \omega^2 u = A \qquad (7)$$

where labels are:

$$\omega^2 = \Lambda + aHa^2, \quad A = aKHa^2 - \varphi_1, \quad a = \varphi_1\varphi_3,$$

$$\Lambda = \frac{h^2}{K_0}, \quad K = \frac{E}{BU}, \quad Ha = Bh\sqrt{\frac{\sigma_f}{\mu_f}}. \qquad (8)$$

'Star' symbol for dimensionless quantity is omitted for simplicity of notation but dimensionless quantities are implied. Equation (2) is now transformed into the following dimensionless equation:

$$\frac{d^2\theta}{dy^2} + Br\left[b\left(\frac{du}{dy}\right)^2 + b\Lambda u^2 + cHa^2\left(K + u\right)^2\right] = 0 \qquad (9)$$

where:

$$b = \frac{1}{\varphi_1\varphi_2}, \quad c = \frac{\varphi_3}{\varphi_2},$$

$Br = \Pr Ec$ Brinkman number,

$\Pr = \dfrac{\mu_1 c_{p1}}{k_1}$ – Prandtl number,

$Ec = \dfrac{U_0^2}{c_{p1}\left(T_{w1} - T_{w2}\right)}$ – Eckert number

c_{pf} – specific heat capacity at constant pressure. (10)

Boundary conditions in dimensionless form are:

$$u(0) = 0, \quad u(1) = 0, \quad \theta(0) = 0, \quad \theta(1) = 1. \qquad (11)$$

Equations (7), and (9) and conditions (11) constitute the mathematical model of the presented problem in its dimensionless form.

III. Solution

For further research of this problem, the equations (7) and (9) with boundaries (11) need to be solved. The solution of the equation (7) representing the distribution of the dimensionless velocity of the nanofluid in the channel is given by the equation:

$$u(y) = C_1 \exp(\omega y) + C_2 \exp(-\omega y) + D \tag{12}$$

where $D = -A/\omega^2$ and constants of integration C_1 and C_2 are determinated from boundary conditions (11):

$$C_1 = D\frac{\exp(-\omega)-1}{\exp(\omega)-\exp(-\omega)},$$

$$C_2 = D\frac{1-\exp(\omega)}{\exp(\omega)-\exp(-\omega)}. \tag{13}$$

The solution of the equation (9) representing the distribution of the dimensionless temperature of the nanofluid in the channel is given by the equation:

$$\theta(y) = -Br[R_4 \exp(2\omega y) + R_5 \exp(-2\omega y) + R_7 \exp(\omega y) + R_8 \exp(-\omega y) + R_2 y^2 + C_3 y + C_4] \tag{14}$$

where:

$$R_1 = b\Lambda + cHa^2$$

$$R_2 = \frac{1}{2}[R_1(D^2 + 2C_1C_2) - 2b\omega^2 C_1 C_2 + cKHa^2(2D+K)]$$

$$R_3 = \frac{1}{4\omega^2}(b\omega^2 + R_1),\quad R_4 = R_3 C_1^2,\quad R_5 = R_3 C_2^2,$$

$$R_6 = \frac{2}{\omega^2}(DR_1 + cKHa^2),\ R_7 = R_6 C_1,\ R_8 = R_6 C_2. \tag{15}$$

where constants of integration are:

$$C_3 = R_4[1-\exp(2\omega)] + R_5[1-\exp(-2\omega)] + R_7[1-\exp(\omega)] + R_8[1-\exp(-\omega)] - \frac{1}{Br} - R_2,$$

$$C_4 = -(R_4 + R_5 + R_7 + R_8). \tag{16}$$

IV. Results analysis

In this part of the paper, due to the limited length, only a part of the obtained results are given. Therefore results are given for the case when channel is operating in pump mode. Pressure gradient in flow direction is constant $-\partial p/\partial x = const$ while as additional label appears $-B\sigma_{nf}(-E) = BE\sigma_{nf}$ which changes the velocity field in the channel.

These facts lead to the value of the external electric load factor being negative. The results are given for the case when base fluid is water and nanoparticles are of cooper, alumina or titanium oxide. Water-copper nanofluid was used to analyze the influence of the applied magnetic field, the permeability of porous medium, the external electric field and the volume fraction of nanoparticles on the flow and heat transfer. The physical properties of water and nanoparticles given in the table 1 were used (Das et. al. [21]).

Figure 2 shows the distribution of dimensionless velocity of water-copper nanofluids for different values of the Hartmann number for $\Lambda = 5, K = -0.75$ and $\phi = 0.2$. It is shown that for these parameter values with increasing Hartmann number ie. with the amplification of the externaly applied magnetic field, the velocity of the nanofluid in the chanel increases. This figure also shows that increase of Hartmann number flattens velocity curve and increases the tangential stresses on the channel walls.

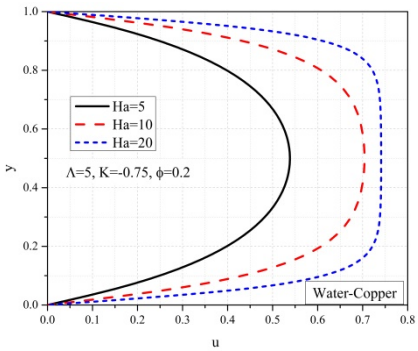

Fig.2 Velocity distribution for different values of Ha

Table 1 Physical properties

Physical properties	Water (H_2O)	Copper (Cu)	Aluminum oxide (Al_2O_3)	Titanium dioxide (T_iO_2)
$\rho(kg/m^3)$	997.1	8933	3970	4250
$c_p(J/(kgK))$	4179	385	765	686.2
$K(W/(Km))$	0.613	401	40	8.9538
$\sigma(S/m)$	$5.5\cdot10^{-6}$	$59.6\cdot10^{6}$	$35\cdot10^{6}$	$2.6\cdot10^{6}$
$\mu(Pas)$	0.01	-	-	-

Figure 3 shows dimensionless temperature distribution of nanofluids in the channel for the same values as in previous figure. Higher values of the Hartmann number correspond to higher value of dimensionless temperature. The reason for the increase in nanofluid temperature in the channel is Joule heat increase. Same figure shows that the heat from the upper wall of the channel is transported to the nanofluid for all the values of the Hartmann number given here.

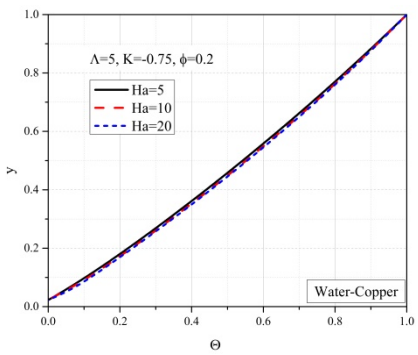

Fig.3 Temperature distribution for different values of Ha

The dimensionless velocity for different values of the porosity factor (reciprocal value of the Darcy number) are given in Figure 4. From this figure it is noticed that the increase of porosity factor ie reducing the permeability of the porous medium in the channel causes a decrease in the velocity of the nanofluid and flattening its profile

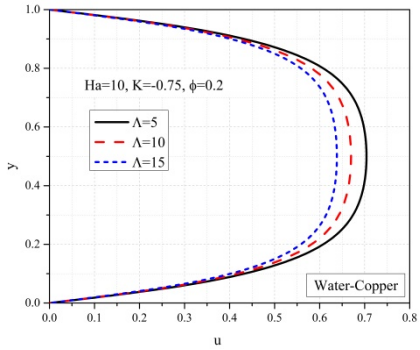

Fig.4 Velocity distribution for different values of Λ

Figure 5 shows the distribution of dimensionless temperature of nanofluid in the channel for different values of porosity factor. It can be seen that an increase of porosity factor leads to an increase in the temperature of the nanofluids in the channel and to a decrease in the amount of heat transported from upper wall of the channel to the nanofluid.

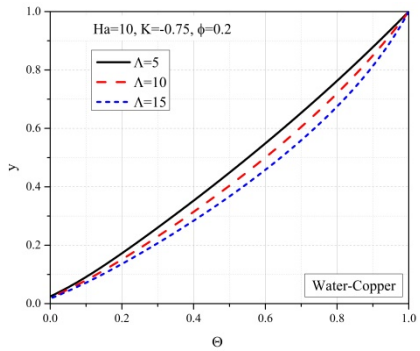

Fig.5 Temperature distribution for different values of Λ

The distribution of the dimensionless velocity of water-copper nanofluids for different values of the volume fraction of copper nanoparticles is shown in Figure 6. The values of the used parameters are given in the same picture. It is noticed that the velocity is the highest when there are no nanoparticles ie. when pure water flows through a channel with porous medium. With an increase in the volume fraction of copper nanoparticles the velocity of nanofluids in the channel decreases, velocity profile flattens and tangential stresses on the channel walls decrease.

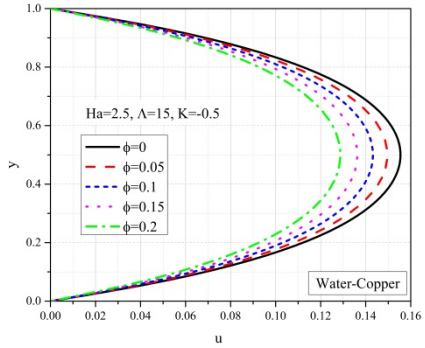

Fig.6 Velocity distribution for different values of ϕ

This velocity decrease is caused with decrease in the nanofluids flow through the channel. This influence is similar to the influence of the permeability of the porous medium. An increase in volume fraction of particles leads to an increase in the concentration of nanoparticles in this fluid which does not allow the base fluid to flow freely.

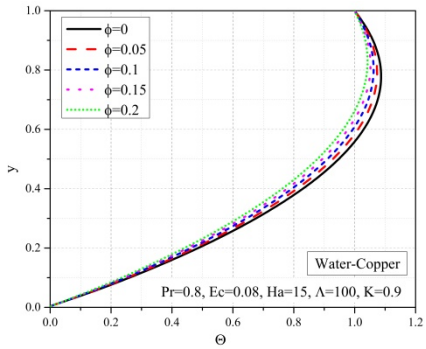

Fig.7 Temperature distribution for different values of ϕ

Figure 7 shows the dimensionless temperature distrubution for different values of the copper nanoparticles volume. In this case the channel operates in generator mode. It can be seen that an increase in ϕ leads to a decrease in the dimensionless temperature in the channel. In the upper part of the channel the temperature of nanofluid is higher than the temperature of the lower wall of the channel. For all values of ϕ the heat is transported from the nanofluid to the upper wall.

Figures 8 and 9 show the velocity and temperature distributions, respectively, for different nanofluids. Water-copper, water-alumina and water-titanium dioxide nanofluids are considered here.

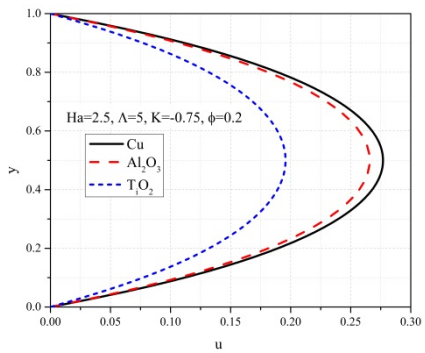

Fig.8 Velocity distribution for different nanofluids

Figure 8 shows that the velocity is highest when water-copper nanofluid flows in the channel, followed by water-alumina and finally water-titanium dioxide. In this order, the tangential stresses on the channel walls also decrease.

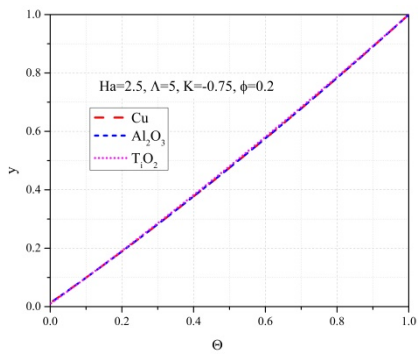

Fig.9 Temperature distribution for different nanofluids

Figure 9 shows that the temperatures for these nanofluids differ very little and that heat transport is mainly due to conduction.

Figures 10 and 11 show velocity and temperature distributions, respectively, for different values of electric load factor.

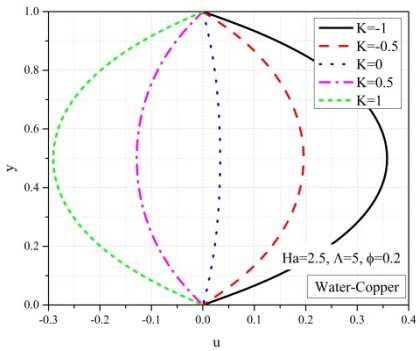

Fig.10 Velocity distribution for different load factor

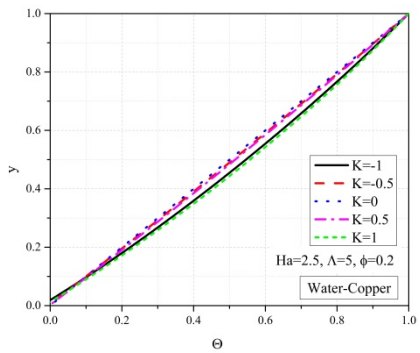

Fig.11 Temperature distribution for different load factor

The sign of this factor can change if the direction of the external electric field, the direction of the external magnetic field or the operation mode of the channel in the system is changed.

From figure 10 it is concluded that a change in the sign of the load factor leads to a change in the direction of the nanofluid velocity in the channel. It is also concluded that higher absolute values of this factor correspond to higher velocities, higher flows in the channel and higher tangential stresses on the channel walls. For smaller absolute values of load factor the velocity profiles are flatter.

From figure 11 it can be seen that in the case when there is no external electric field the heat transfer in the channel is mainly by conduction. It can also be seen that for the same absolute values of the load factor the temperature profiles almost coincide. For all the values of load factor given in the figure 11, the heat transport is from the upper wall to the nanofluid.

V. Conclusion

This paper investigates the flow and heat transfer of nanofluids in a channel with porous medium. Channel walls are horizontal plates on constant and different temperatures. The channel is under the influence of an external homogeneous magnetic field and an external homogeneous electric field perpendicular to the vertical longitudinal plane of the channel. Solutions for dimensionless velocity and dimensionless temperature of nanofluid were obtained analytically. For easier analysis, the solutions are also presented graphically. Based on the obtained results, conclusions were drawn, the main ones being the following:

-Increasing the Hartmann number increase the velocity and temperature of the nanofluids in the porous medium channel.

-An increase of porosity factor ie. a decrease of permeability of the medium decreases the velocity but increases the temperature of the nanofluid.

- Increasing the volume fraction of nanoparticles reduces the velocity and temperature of nanofluids in the horizontal channel with porous medium.

-The use of different nanoparticles can affect the velocity and temperature of nanofluid

- By changing the value of the external electric load factor, the velocity of the nanofluid changes, and for the same absolute values of this factor, the temperature distributions are the same.

ACKNOWLEDGMENT

This was financially supported by the Ministry of Education, Science and Technological Development of the Republic of Serbia (Project No. TR 35016).

References

[1] S. U. S. Choi (1995), Enhancing thermal conductivity of fluids with nanoparticles, Developments and Applications of Non-Newtonian Flows, MD vol. 231 and FED vol. 66. ASME, pp. 95-105

[2] S. K. Das, S. U. S. Choi, W. Yu, T. Pradeep (2007), Nanofluids: Science and Technology, Wiley-interscience, A John Wiley and Sons, INC Publication

[3] Xiang-Qi Wang, Arun S. Mujumdar (2007), Heat transfer characteristics of nanofluids: a review, International Journal of Thermal Sciences 46, pp. 1-19

[4] Rama Subba Reddy Gorla, Ali Chamka (2011), Natural Convective Boundary Layer Flow over a Horizontal Plate Embedded in a Porous Medium Saturated with a Nanofluid, Journal of Modern Physics, 2, pp. 62-71

[5] Sadegh Khalili, Saeed Dinarvand, Reza Hosseini, Hassein Tamim and Ioan Pop (2014), Unsteady MHD flow and heat transfer near stagnation point over a stretching/shrinking sheet in porous medium filled with a

nanofluid, Chin. Phys. B, Vol. 23, No. 4, 048203 doi: 10.1088/1674-1056/23/4/048203

[6] S. Das, R. N. Jana, O.D. Makinde (2015), Mixed convective magnetohydrodynamic flow in a vertical channel filled with nanofluids, Engineering Science and Technology, an International Journal doi: 10.1016/j.jestch.2014.12.009

[7] Gul Aaiza, Ilyas Khan and Sharidan Shafie (2015), Energy transfer in Mixed Convection MHD Flow of Nanofluid Containing Different Shapes of Nanoparticles in a Channel Filled with Saturated Porous Medium, Nanoscale Research Letters, 10:490 doi: 10.1186/s11671-015-1144-4

[8] Muhammad Zubair Akbar, Muhammad Ashrof, Muhammad Farooq Iqbal and Kashif Ali (2016), Heat and mass transfer analysis of unsteady MHD nanofluid flow through a channel with moving porous walls and medium, AIP Advances 6, 045222

[9] M. K. Sharma and Manjeet (2017), Nanofluid Flow and Heat Convection in a Channel Filled with Porous Medium, Journal of International Academy of Physical Sciences, Vol. 21, No. 2, pp. 167-188

[10] Alibakhsh Kasaeian, Reza Daneshazarian, Omid Mahian, Lioma Kolsi, Ali J. Chamkha, Somchai Wongwises, Ioan Pop (2017), Nanofluid flow and heat transfer in porous media: A review of the latest developments, International Journal of Heat and Mass Transfer 107, pp. 778-791

[11] Jelena Petrović, Živojin Stamenković, Miloš Kocić, Milica Nikodijević and Jasmina Bogdanović-Jovanović MHD Mixed Convection Flow Through Porous Medium in a Inclined Channel“ 19 th International Conference on Thermal Science and Engineering of Serbia, Sokobanja, Serbia, October 22-25, 2019 ISBN 978-6055-124-7, pp. 526-534

[12] Nabel T. M. Eldabe, Osama M. Abo-Seida, Adel A. S. Abo-Seliem, A. A. El-Shekhipy, Nada Hegazy (2017), Peristaltic Transport of Magnetohydrodynamic Carreau Nanofluid with Heat and Mass Transfer inside Asymmetric Channel, American Journal of Computational Mathematics, 7, pp. 1-20

[13] B. V. Swarnalathamma (2018), Heat and Mass transfer on MHD flow of Nanofluid with thermal slip effects, International Journal of Applied Engineering Research, Volume 13, No. 18, pp. 13705-13726

[14] J. C. Umavathi, Mikhail Sheremet (2019), Flow and heat transfer of couple stress nanofluid sandwiched between viscous fluids, International Journal of Numerical Methods for Heat and Fluid Flow, 29(11), pp. 4262-4276

[15] Jitendra Kumar Singh and Srinivasa C.T. (2019), Effect of Variable Fluid Properties on Magnetohydrodinamic Flow of Nanofluid Past a Flat Plate, Journal of Nanofluids 8(3): 520-525 doi:10.1166/jon.2019.1608

[16] Ilyas Khan and Aisha M. Alqahtani (2019), MHD Nanofluids in a Permeable Channel with Porosity, Symmetry, 11, 378 doi:10.3390/sym11030378

[17] Adigoppula Raju, Odelu Ojjela (2019), Effects of the induced magnetic field, thermophoresis and Brownian motion on mixed convective Jeffrey nanofluid flow through a porous channel, Engineering Reports. WILEY, e212053, doi: 10.1002/eng2.12053

[18] Jawali C. Umavathi, Mikhail A. Sheremet (2020), Heat transfer of viscous fluid in a vertical channel sandwiched between nanofluid porous zones, Journal of Thermal Analysis and Calorimetry doi: 10.1007/s10973-020-09664-1

[19] J. C. Umavathi, Ali J. Chamkha, Abdul Mateen and J. Prathap Kumar (2008), Unsteady magnetohydrodynamic two fluid flow and heat transfer in a horizontal channel, Heat and Technology, Vol. 26, No.2, pp. 121-133

[20] J. Petrović, Ž. Stamenković, M. Kocić, M. Nikodijević (2016), Porous medium magnetohydrodynamic flow and heat transfer of two immiscible fluids, Thermal Science, Vol. 20, Suppl. 5, pp. S1405-S1417

[21] S. Das, A. S. Banu, R. N. Jana, O. D. Makinde (2015), Entropy analysis on MHD pseudo-plastic nanofluid flow through a vertical porous channel with convective heating, Alexandia Engineering Journal doi: 10.1016/j.aej.2015.05.003

THE 5th INTERNATIONAL CONFERENCE
MECHANICAL ENGINEERING IN XXI CENTURY

December 9-10, 2020
Faculty of Mechanical Engineering in Niš, Serbia

Operating and Acoustic Characteristics of Low-Pressure Centrifugal Fans with Backward Curved Blades

Jasmina BOGDANOVIĆ JOVANOVIĆ, Živojin STAMENKOVIĆ,Veljko BEGOVIĆ

Department of Hydroenergetics, Faculty of Mechanical Engineering, Aleksandra Medvedeva 14
jasmina.bogdanovic.jovanovic@masfak.ni.ac.rs, zikas@masfak.ni.ac.rs, petrovic@masfak.ni.ac.rs, veljko.begovic@masfak.ni.ac.rs

***Abstract*— Optimal fan operation ensures the optimum energy efficiency of the fan and, hopefully, the best acoustic characteristics of the fan. The enormous use of fans today, for various purposes, requires great energy resources, which is why the fan should operate at maximum efficiency. On the other hand, the noise characteristics of fans are just as important, and they are often a limiting factor for their application. Therefore, the prediction of fan noise in the operating regime is very important. With the development of numerical simulations, it is possible to determine its operating parameters and to perform analysis of the obtained results, in order to optimize its geometrical parameters. Many different centrifugal fans with backward-curved blades, which have the same dimensions of impeller and spiral casing, but different blade angles, were numerically simulated and analysed. The results of aerodynamic and acoustic characteristics of fans are presented in the paper.**

***Keywords*— centrifugal fans, numerical simulations, operating and acoustic characteristics**

I. Introduction

Low-pressure centrifugal fans are classified according to the value of the total pressure of the fan, which is lower than 1kPa (Δp_t<1 kPa). In the low-pressure fans, the air density increases less than 0,7%, in mid-pressure fans less than 2%, which practically allows the air to be considered incompressible [1]. Operating characteristics of centrifugal fans are the functional dependence of fan operating parameters on the fan volume flow rate. They depend on the centrifugal fan geometrical parameters, in the first instance on the shape of the impeller blades. There are some published results of experimental and numerical investigations, dealing with the influence of impeller geometry on centrifugal fan operating parameters, mostly with radial and radial curved blades [2,3], making some conclusions about the extent to which certain performance characteristics are affected by the geometrical parameters of the fan and the blade number [3]. Numerical and experimental investigation on the influence of impeller geometry on the unsteady flow in forward-curved centrifugal fans is conducted by Younsi et al [4]. Some researches offer algorithms and methodology for optimal designing od centrifugal fans [5, 6] The effect of some geometrical parameters, such as inlet blade angle or blade number, on operating parameters of centrifugal fans is investigated numerically [7, 8]. Further on, some experimental and numerical investigations of the effects of guide vanes on the acoustic characteristics of the centrifugal fan ware conducted [9], showing the possibility of reducing the fan noise using the stationary diffuser vane. Results of many experimental investigations of centrifugal fans have been given in various literatures. For example, Solomahova [10,11] presented results of centrifugal fan testing and their performance recalculation for different centrifugal fans of the same type. The acoustic characteristics of some of the centrifugal fans tested were also presented in the appropriate diagrams. However, there are fewer investigations regarding the influence of impeller geometry on the acoustic characteristics of centrifugal fans.

With the development of numerical methods and CFD techniques, and using available CFD software, it is possible to obtain aerodynamic and acoustic parameters of centrifugal fans. The fan operation is always accompanied by noise; therefore, the acoustic characteristics of the fan are also very important for the application of the fan in practice. Some researchers have been concerned with determining fan noise numerically, using the unsteady Large-Eddy simulations and acoustic analogy [12,13]. But this type of approach requires considerable computing resources and is harder to put into practice when designing multiple fans and determining their operating modes. Considering the practical application and rapid determination of the fan operating parameters, certainly, a much more acceptable approach is the stationary RANS numerical simulations [14,15]. With the development of a tool for determining acoustic performances (fan noise calculator), Ansys 19.0 has provided the basis for quickly predicting the acoustic performance of a fan.

In this study, the aerodynamic and acoustic characteristics of backward curved centrifugal fans with different blade angles were numerically investigated, using Ansys CFX 19.0. The possibility to determine acoustic parameters by calculating the Praudman's sound power level was used, first to compare these results with experimental results and then to apply this methodology to different fan geometry designs. The objective of the article is to determine how the performance and acoustic

characteristics of a centrifugal fan change with the change of the impeller blade geometry, particularly the blade angles (inlet blade angle β_1 and outlet blade angle β_2).

II. Aerodynamic and Acoustic Characteristics of Centrifugal Fans

A. Determination of fan operating parameters

Operating parameters of a fan are: volume flow rate, the total and static pressure of the fan, fan efficiency and fan power. The operating characteristics of the fan (operating curves), are functional dependence of fan pressure, efficiency and power on volume flow rate, and are given in a form of graphic curves.

The volume flow rate of the fan is the value of the flow rate on the inlet cross-section of the fan ($Q=Q_I$).

The total pressure of the fan is defined as the difference between the total pressure values in the outlet (II) and the inlet (I) cross-section of the fan:

$$\Delta p_t = p_{t.II} - p_{t.I} = p_s - p_d. \quad (1)$$

The dynamic pressure of the fan is the dynamic pressure on the fan outlet:

$$p_d = p_{d.II} = 0.5 \cdot \rho_{II} \cdot c_{II}^2, \quad (2)$$

where c_{II} and ρ_{II} are the values of flow velocity and air density on the outlet cross-section, respectively.

For low-pressure and mid-pressure fans, when (Δp_t<3 kPa, the air density can be considered a constant value, with an error of less than 2% [1].

The power of the fan (N) is the value obtained by the motor, when the fan is directly connected to the motor. The effective fan power (N_{ef}) is obtained using the equation:

$$N_{ef} = Q \cdot \Delta p_t \quad (3)$$

The overall fan efficiency is the ratio of N_{ef} and N:

$$\eta = \frac{N_{ef}}{N} = \frac{Q \cdot \Delta p_t}{N} \quad (4)$$

and static efficiency can be determined by the formula:

$$\eta = \frac{Q \cdot p_s}{N} \quad (5)$$

Dimensionless flow coefficient (φ) and pressure coefficient (ψ) of the fan can be also calculated:

$$\varphi = \frac{4Q}{D^2 \pi u} \text{ and } \psi = \frac{2\Delta p_t}{\rho u^2}, \quad (6)$$

where: D – fan diameter and u - circumference velocity.

B. Determination of acoustic parameters

The intensity of sound waves (I_s) is the power of sound waves per unit area, which is normal to their propagation ($I_s=N_s/A$). The human ear registers the intensity of sound waves from $I_{s.0}=10^{-12}$ W/m2 (on the threshold of audibility) to 10 W/m^2 (at the limit of pain). Both sound intensity and sound power change according to the logarithmic law.

The sound pressure level (L_p) can be calculated:

$$L_I = L_p = 10\log(p_s/p_{s.0}) = 20log(p_s) + 94 \ [dB] \quad (7)$$

where p_s is the sound pressure and c_s is the sound velocity:

$$p_s = \sqrt{\rho \cdot c_s \cdot I_s} \quad (8)$$

The values of the sound pressure level are between 0 dB (on the threshold of audibility) to 130 dB (at the limit of pain).

The definition of the sound power level (L_w [dB]) is given using the power of the sound waves ($N_s=I_s \cdot A$, where the unit area A is the surface normal to the direction of sound waves):

$$L_w = 10\log(N_s/N_{s.0}) = 20log(N_s) + 120 \ [dB] \quad (9)$$

An acoustic characteristic of the fan is determined by measuring the functional dependence of the total sound power level and the flow rate of the fan ($L_W(Q)$).

Using the similarity laws, the aerodynamic noise of the fan can be mathematically expressed as a function of the fan diameter and the circumference velocity of the fan runner [9,10]:

$$L_w = \bar{L}_w^* + 20\log(D) + 60\log(u/10) \quad (10)$$

where $\bar{L}_w^*$ is the sound power level of the geometrically similar fan with D=1 m and u=10 m/s, and K_a – parameter of the similarity criterion:

$$\bar{L}_w^* = 10\log(K_a \rho / c_s^3) + 180. \quad (11)$$

Sound power level can be obtained using the total pressure of the fan and volume flow rate values:

$$\bar{L}_w^* = \tilde{L}_w^* + 10\log(Q) + 25log(\Delta p_t/10) \quad (11)$$

where $\tilde{L}_w^*$ is the sound power level of the geometrically similar fan operating with Q=1 m^3/s and Δp_t=10 Pa:

$$\tilde{L}_w^* = 10\log\left(\frac{K_a}{\varphi\psi^{2.5}}\right) + 10\log\left(\frac{7.2}{\rho^{1.5} c_s^3}\right) + 145 \quad (13)$$

C. Influence of the impeller blade shape on fan performance

Aerodynamic and acoustic characteristics of centrifugal fans depend on the geometrical parameters of a fan and the geometry of the flow domain. Centrifugal fans can be designed with different blade shapes (Fig.1).

Fig. 1. Backward inclined, backward, forward curved and radial blades

The shape of the impeller blades affects the shape of the fan operating curves, as it is shown in Fig.2.

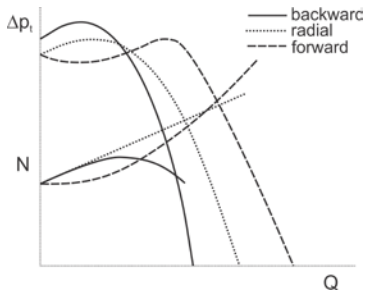

Fig. 2. Fan operating curves for forward, backward and radial blades

There have been many attempts to give more specific conclusions about the effects of centrifugal impeller shape and the number of blades on operating and acoustic parameters. A smaller number of blades generate a

nonhomogeneous flow in the centrifugal fans. The reduction of the number of blades generates strong aerodynamic interactions between the volute tongue on the stationary casing and rotating blades, which contribute to accentuating the tonal noise at the blade passing frequency (BPF) and gives the highest sound power level [4].

III. Numerical simulation of the backward curved centrifugal fan

The investigated centrifugal fan with backward-curved impeller blades (β_2<90º), with 6 curved, circular-arches, non-profiled blades, where the inlet blade angle is β_1=8º and the outlet blade angle is β_2=38º (fan C4-57 [9, 10]).

The centrifugal fan geometry and its dimensionless operating curves are shown in Fig.3.

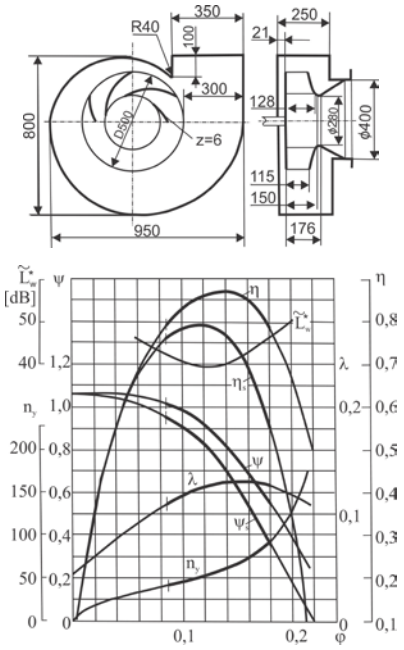

Fig. 3. Centrifugal fan geometry and its operating curves (n=1200 min^{-1})

The optimal operating point, when the maximum efficiency is η=0.87, is defined by the flow coefficient φ=0.14 and the pressure coefficient ψ=0.8.

Centrifugal fan with backward-curved blades obtains the best efficiency, compared to other types of fans with non-profiled blades (up to 85%).

D. Numerical mesh

The numerical mesh consists of two domains (the fan impeller and the spiral casing), both discretised using ICEM CFD software. The mesh is unstructured, made of 1736675 nodes and 5775022 elements (mostly tetrahedral 3877531, wedges 1896065 and pyramids 1426). The fan impeller discretization mesh is made of more than 4 million elements, to obtain the good quality mesh in the blade area (Fig.4).

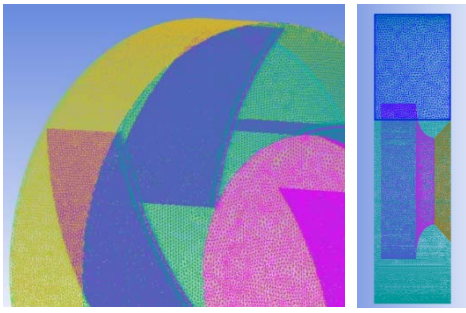

Fig. 4. Discretization mesh of the fan impeller and the spiral casing

The mesh refinement was done in the near-wall region, around the blades, where the maximal value of y^+=31.7, while the average value of y^+<6. The spiral casing wall has the average value of y^+=13.6.

For numerical interpolation was used a high-resolution scheme. The turbulent model is standard k-ε. The convergence criteria were that the root mean square values of the equation residuals are 10^{-4}.

E. Grid independence test

The reliability of the discretization mesh has to be proven by testing several meshes composed of the same types of elements, but with a different number of elements (~$3.5\cdot10^6$, $5.8\cdot10^6$ and $6.5\cdot10^6$ elements). In this case, 3 meshes, composed of predominantly tetrahedral elements and with prismatic elements over the flow surfaces, were considered. Numerical simulations were conducted for volume flow rate Q=0.864 m^3/s when the total pressure of the fan has a value Δp_t=468 Pa, for rotational speed of the fan n=1200 min^{-1}. The results of the greed independence test are given in Table 1.

TABLE I Grid independence test

	Number of elements	Δp_t [Pa]	Relative error [%]	p_s [Pa]	Relative error [%]
1.	~$3.5\cdot10^6$	483	3.25	427	4.31
2.	~$5.8\cdot10^6$	472	0.89	414	1.13
3.	~$6.5\cdot10^6$	468	0.04	409	0.05

According to results in Table 1 and considering the time required for numerical simulations, for the further analysis, the second mesh was used (consists of $5.8\cdot10^6$ elements).

F. Validation of numerical model

The numerical model validation was performed by comparing the numerical results with results obtained by centrifugal fan testing. Therefore, the fan performance curves of total and static fan pressure were compared in several operating points.

The results of numerical model validation are shown in Fig.5, showing that the pressure difference in the area of optimal fan operation is less than 1%, while the maximum deviation of the results in the observed operating regimes is up to 7%.

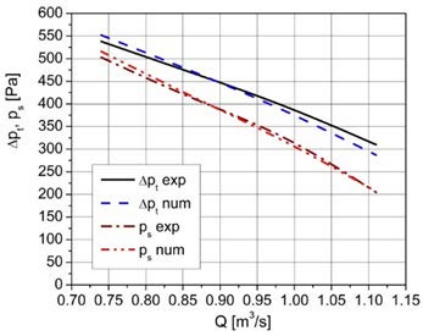

Fig. 5. Centrifugal fan pressure curves (Δp_t and p_s)

G. *Obtaining the acoustic characteristics of fans*

The fan noise may be more or less bearable. In some cases, the noise level may limit the fan application or may even have an eliminatory character when selecting a fan.

According to the cause of the occurrence, fan noise may be mechanical and aerodynamic [1].

Mechanical noise is most often caused by the following causes: impeller imbalance, bearing oscillations, housing jitter, coupling mismatch, etc. It can be lowered by relatively simple design measures using the different types of bearings, rubber washers or rubber dampers, etc.

The aerodynamic noise of the fan is caused by the pres-sure pulsations that occur while the air is passing through the fan domain. There are several reasons for the generation of aerodynamic noise in fans [1]: 1) Vortex shedding noise, caused by pressure pulsations resulting from the vortex formation and its detachment from the solid surfaces; 2) Boundary layers noise caused by pressure pulsations in the turbulent boundary layers along the solid surfaces; 3) Unsteady flow noise, caused by periodic pressure pulsations due to finite number of blades and unsteady flow in the impeller blades, and due to the vortex traces created by the elements in front of the impeller; 4) Turbulent flow noise, caused by pressure pulsations due to the transverse transfer of the vortex from the vortex traces behind the blades; 5) Unstable fan operation noise, caused by pressure pulsations occurring in unstable regimes.

Aerodynamic noise primarily depends on the constructive solution of the fan, and the only way to influence the acoustic characteristics of a fan is during the design process. Experience and the empirical data take an important role in the fan designing process. With the development of numerical models, the problem of fan noise can also be considered numerically.

Numerical treatment of the fan noise issue is based on Proudman's formula, semi empirical correlations and acoustic analogy. The Proudman noise source model [16] calculates and predicts acoustic power per unit volume and determines the noise of turbulent flow. This model is incorporated in ANSYS 19 and is very handy for quickly determining the value of turbulent turbine noise.

The Proudman magnitude can be calculated:

$$AP = \alpha\rho_0 \frac{v^3}{l}\frac{v^5}{a_o^2} \tag{14}$$

where: v – the turbulent velocity, l – the length scales, α_o – the speed of sound, and α – the model constant.

For estimation of the overall noise level of the fan, The Broadband noise model was used in Ansys CFX 19.0. The Broadband noise model is derived from Proudman's formula for sound power level, which enables prediction of overall sound power on the entire flow domain. In further analysis of centrifugal fans, numerical results of sound power level are compared with the experimental values (Fig.6).

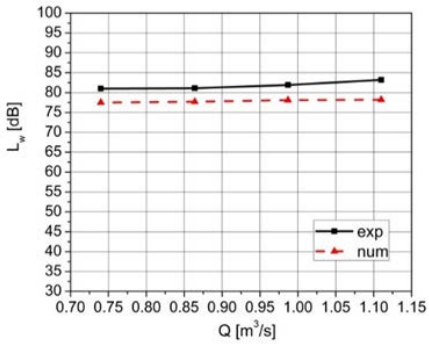

Fig. 6. Sound power level of the fan – numerical and experimental results

Numerically obtained values of overall sound power level are less than experimental values, varying up to 8% (for the smaller volume flow rate in the area of high fan efficiency), while the mean deviation of the values, in the area of high fan efficiency is around 5%.

IV. Centrifugal fans with different blade angles – numerical results

Changing the outlet and inlet blade angles leads to a change in the flow domain of the fan and its performance. Many different centrifugal fans, with different blade angles, but the same geometrical parameters of the impeller diameters and the same spiral casing, were investigated numerically. Their aerodynamic and acoustic operating characteristics were compared and analysed.

H. *Operating characteristics of centrifugal fans with different outlet blade angles*

There are cases with the same inlet blade angles (β_1=7° and 18°) and different outlet blade angles are investigated (Fig.7).

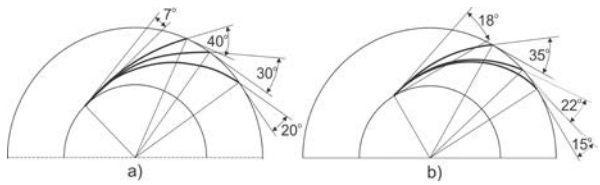

Fig. 7. Geometry of the centrifugal fan blades: a) β_1=7°, b) β_1=18°

Every numerical model tested in this research, have the unstructured mesh consisting of $5.5\cdot10^6$ to $7.2\cdot10^6$ elements, which can be considered as very fine numerical grids. Discretization methodology and all numerical settings were performed as previously described, allowing good convergence of the numerical process. The numerical results of total pressure and hydraulic efficiency of fans with the same blade inlet angle and different outlet angles (given in Fig.7), are shown in Fig.8.

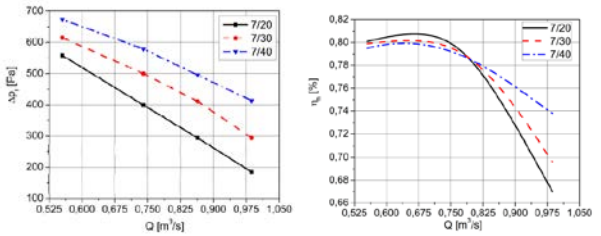

a)

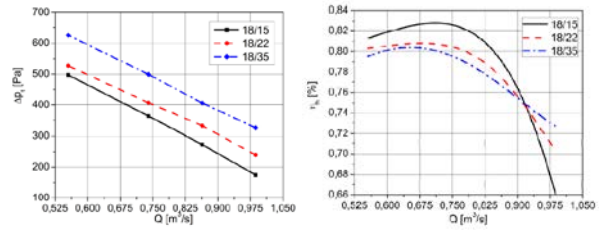

b)

Fig. 8. Total fan pressure and hydraulic efficiency for: a) β_1=7°, b) β_1=18°, and different outlet angle β_2

With increasing the outlet blade angle, the total pressure of the fan also increases. For the cases when the inlet angle β_1=7°, changing the outlet blade angle from 20 to 40° causes a change in the total pressure of the fan from 13.3 to 52.4%.

For the case of fan with inlet blade angle β_1=18°, the outlet blade angle also changes by a total of 20° (from 15 to 35°). Then, changing the total fan pressure goes from 28.5% to 55%, from smaller to larger flows respectively.

I. Operating characteristics of fans with different inlet and outlet blade angles

In addition to the previously given fans with the same inlet but different outlet angles, the two cases of fans with slightly different inlet and outlet blade angles are also studied.

One case study is when the outlet blade angles are greater than 30° (33÷40°), while in the other case study the outlet blade angles are 20÷25°. The numerical results of the total pressure curves and hydraulic efficiency of fans are shown in Fig.9.

In Fig. 9.a is a noticeable variation of inlet and outlet blade angles from 7 to 18o, while outlet blade angles are up to 40°. The maximum difference of the total pressure values varies up to 26,7%. Total pressure curves of fans with very different inlet blade angles, but similar outlet blade angles (20, 22 and 25°), are shown in Fig. 9.b. The resulting total pressure curves have a steeper drop for smaller values of inlet blade angles. The bigger difference in inlet blade angle leads to the great difference in fan total pressure values. For example, fans with inlet blade angles 7° and 30° and the same outlet blade angles 20°, have the total pressure difference up to 20%.

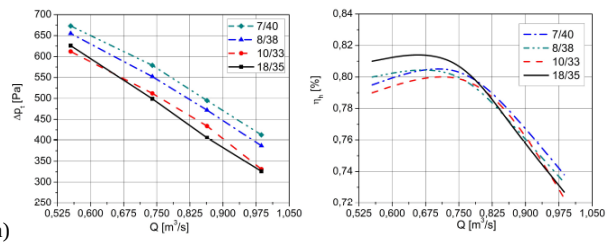

a)

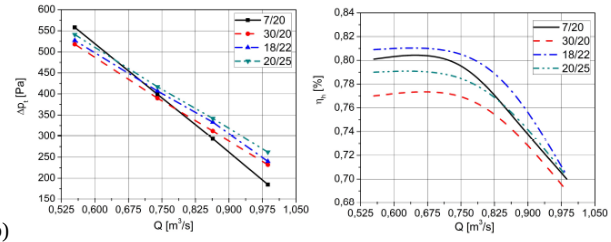

b)

Fig. 9. Total pressure of the fan and hydraulic efficiency, for different angles β_1 and β_2.

V. Acoustic characteristics of centrifugal fans with different blade angles

The acoustic characteristics (sound power level, L_w) of numerically tested fans, whose pressure curves were given in the previous section, were also numerically obtained.

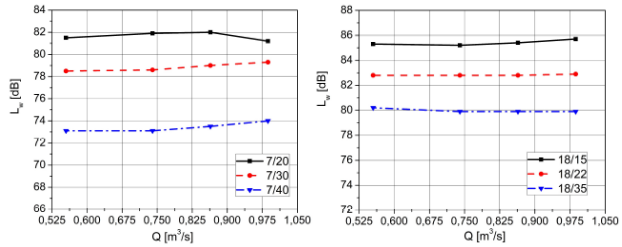

Fig. 10. Sound power level of fans with slightly different β_1 and β_2.

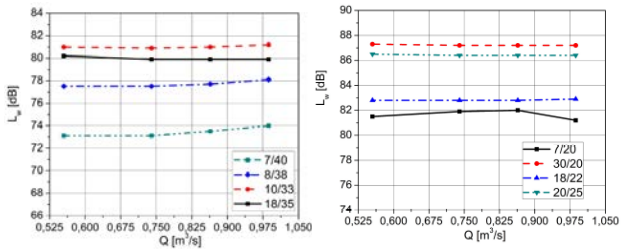

Fig. 11. Sound power level of fans given in Fig. 9 (a and b).

The acoustic characteristics (LW(Q)) of two fan cases, with inlet blade angles 7° and 18° and different outlet blade angles (presented in part 4.1 on Fig.8), are shown in Fig.10. The acoustics characteristics of the cases presented in part 4.2 (Fig.9), are shown in Fig.11. In both cases is shown that around the optimal fan regimes, with increasing the outlet blade angle, sound power level of fan decreases.

Ansys CFX Post 19.0 provides the good visualization of the noise, calculated by using Proudman's formula. Broadband noise isosurfaces at 95% of Proudman Sound Power are given in Fig.12, where the sound power level is set to min 50 dB.

Fig. 12. Broandband noise isosurface at 95% of Proudman Sound Power for two different fan blades (8/38 and 18/35).

VI. CONCLUSIONS

Numerical simulations of fluid flow in centrifugal fans provide a relatively fast and satisfactory assessment of its aerodynamic and acoustic characteristics. The validation of numerical results for the first centrifugal fan investigated as a numerical model (β_1=8° and β_2=38°), was within 7% of relative error for the total fan pressure values. The numerically determined acoustic characteristics of the fan (LW) are satisfactory, whereby the relative error is higher at smaller flow rates.

When testing centrifugal fans with the same inlet blade angle and different outlet blade angles, it's obtained, as expected, that with increasing the outlet blade angle, the total pressure of the fan increases. On the other hand, increasing the outlet blade angle leads to decreasing the values of sound power level. With increasing the inlet blade angle the sound power level of fan also tends to increase. As both angles change, the slope of the pressure curve changes, giving a more complex effect on the operating and acoustic characteristics of the fan.

ACKNOWLEDGMENT

This research was financially supported by the Ministry of Education, Science and Technological Development ofthe Republic of Serbia.

REFERENCES

[1] B. Bogdanovic, D. Milenkovic, J. Bogdanovic-Jovanovic, "Fans – Operating characteristics and exploitation", (in Serbian University of Nis, Faculty of Mechanical Engineering, 2006.

[2] L. Xiaomin, D. Qun, X. Guang, "Performance Improvement of Centrifugal Fan by using CFD", Engineering Applications of Computational Fluid Mechanics, 2 (2), pp. 130–140, 2008.

[3] O. P. Singh, R. Khilwani, T. Sreenivasulu, M. Kannan, "Parametric Study of Centrifugal Fan Performace: Experiments and Numerical Simulation", International Journal of Advances in Engineering & Technology, Vol. 1, Issue 2, pp. 33-50, 2011.

[4] M. Younsi, F. Bakir, S. Kouidri, R. Rey, "Influence of Impeller Geometry on the Unsteady Flow in a Centrifugal Fan: Numerical and Experimental Analyses", International Journal of Rotating Machinery, Vol. 2007, Article ID 34901, 10 pages, 2007.

[5] C.H. Huang, M.H. Hung, "An optimal design algorithm for centrifugal fans: Theoretical and experimental studies", Journal of Mechanical Science and Technology, 27(3), pp. 761-773, 2012.

[6] T. Selvaraj, P. Hariharasakthisudhan, S. Pandiaraj, K. Sathickbasha, A. B. Mohamed Aslam Noorani, "Optimizing the Design Parameters of Radial Tip Centrifugal Blower for Dust Test Chamber Application Through Numerical and Statistical Analysis", FME Transactions, Vol. 48, pp. 236-245, 2020.

[7] C. N. Jayapragasan, K. Janardhan Reddy, "Design Optimization and Experimental study on the Blower for Fluffs Collection System", Journal of Engineering Science and Technology, 12 (5), pp. 1318 – 1336, 2017.

[8] F. N. Meng, L. W. Wang, G. Z. Xie, F. Zhao, D. H. Zhang, W.L. Du, "Effects of Blade Inlet Angle on Flow Field of Centrifugal Fan", International Conference on Mechanical Engineering and Control Automation, ISBN: 978-1-60595-449-3, 2017.

[9] K. Paramasivam, S. Rajoo, A. Romagnoli, "Reduction of Tonal Noise in Centrifugal Fan using Guide Vanes", Proc. EuroNoise 2015, pp. 2279-2284, 2015, ISSN 226-5147.

[10] T. S. Solomahova, "Centrifugal fans", Masinostroenie, Moscow, 1975.

[11] T. S. Solomahova, K. V. Chebisheva, "Centrifugal fans", Masinostroenie, Moscow, 1980.

[12] Q. Liu, D. Qi, H. Tang, "Computation of aerodynamic noise of centrifugal fan using large eddy simulation approach", acoustic analogy and vortex sound theory, Proc. IMechE 2007, Vol. 221 Part C: J. Mechanical Engineering Science, pp.1321-1332, 2007.

[13] E. Sorguven, Y. Dogan, F. Bayraktar, Y. Sanliturk, "Noise Prediction via Large Eddy Simulation: Application to radial fans", Noise Control Eng. J. 57 (3), pp. 169-178, 2009.

[14] Q. Liu, D. Qi, Y. Mao, "Numerical calculation of centrifugal fan noise", Proc. IMechE, Vol. 220 Part C, pp. 1167-1177, 2006.

[15] V. R. Naik, V. B. Magdum, "Design and Development of Blower Impeller by Reverse Engineering for Noise Reduction using CFD", International Journal of Applied Engineering Research, ISSN 0973-4562 13(11), pp. 9982-9987, 2018.

[16] I. Proudman, "The Generation of Noise by Isotropic Turbulence", Proc. Roy. Soc. London, A214, 119, 1952.

THE 5th INTERNATIONAL CONFERENCE
MECHANICAL ENGINEERING IN XXI CENTURY

December 9-10, 2020
Faculty of Mechanical Engineering in Niš, Serbia

CFD Study of Radial Guide Vane Cascade with Convex and Concave Blade Sets for Variable Speed Francis turbines

Filip Stojkovski[1], Zoran Markov[2], Valentino Stojkovski[2]

Ss. Cyril and Methodius, University in Skopje
Faculty of Mechanical Engineering, Skopje
filip_stojkovski@outlook.com, zoran.markov@mf.edu.mk, valentino.stojkovski@mf.edu.mk

***Abstract*— The water flow conditions in front of the turbine runner, i.e. the turbine vaneless space is created from the guide vanes, which represents a radial (annular) cascade consisted of blades. It is characterized with their hydrofoil shape, their chord spacing and flow inlet and outlet angles, so an axisymmetric irrotational vortex flow condition in front of the runner is created. For variable speed operating conditions of the turbine, the flow parameters in front of the runner changes significantly. Investigations show that uniform shape of the guide vanes is insufficient for flow supply to the runner when variable speed operation is considered. A CFD analysis is carried out for a developed radial cascade in this paper. The blades have an asymmetric shape, positioned to the stream in a convex and concave manner, so to obtain shock free flow conditions in front of the cascade and in front of the runner. Furthermore, the aim is to determine the flow conditions in the cascade, the flow created in the vaneless space and how they influence on the turbine performance when variable speed operation is considered.**

***Keywords*— Guide vanes, Francis turbine, Variable speed, CFD**

I. Introduction

The design theory of hydraulic turbomachines, so far is developed for one operating point and constant synchronous rotational speed. In this case, the flow parameters are more or less known and predictable, especially in the pre-runner space, which is of main research interest in this paper. Development of radial guide vane cascades for runner feeding is based on simplified mathematical models, where the general design can be easily achieved.

For variable operating speed turbines, the flow parameters at first can be derived with the similarity laws, where the head, flow rate and rotational speed changes for given turbine configuration. That is why, variable speed operation is expected to give more performance benefit at variable head operated turbines. In our case, the change of head is avoided, assuming that quasi-stationary conditions occur in the operation, i.e. the levels of the top reservoir and the tail water in the hydropower plant do not change in a relatively short period of time. As this conditions are adopted, the variable speed operation no longer can be predicted with the standard similarity laws, so other phenomena occur in the pre-runner space.

Radial blade cascades have been studied throughout the years mostly by simplifying the radial geometry and converting them into straight blade rows i.e. straight cascades, for simplified analysis. The lack of the straight cascade rows is that the accelerating phenomenon which the fluid has in the radial cascade caused by the change of the radius is not observed. This effect is present only in radial cascades and occurs in the spaces where the blades in the cascade do not interfere each other, i.e. out of the inner blade channel at the inlet and at the outlet.

In this paper, 3 design models are considered within a previously determined design space for a guide vanes, to test different inlet conditions in the cascade, and how they influence on the feeding and performance of a variable speed operated Francis turbine.

II. Development of radial cascade blade rows

The guide vanes of Francis hydraulic turbines are represented with radial blade cascades, where some flow conditions at the inlet and especially at the outlet of the cascade shall be met. The outlet flow conditions are strictly guided from the turbine runner operation i.e. the head, design flow rate and rotational speed. These conditions give velocities relations and ratios which give the angles needed to feed the runner.

Simplified start to develop the needed flow angles is from the Euler turbine equation, where in the pre-runner space, assuming the best efficiency operating zone, the equation stands:

$$gH_n \cdot \eta = u_1 c_{1u} - u_2 \cancel{c_{2u}} \qquad (1)$$

As the outflow parameters of the runner are considered as zero (non-swirling outflow), the maximal efficiency is obtained. With simple perturbations, the inflow angle of the runner can be written as [4]:

$$tg\alpha_1 = \frac{n}{60} \cdot \frac{Q}{B_{r1} \cdot g \cdot H_n} \; ; \; \alpha_1 \approx \alpha_o \qquad (2)$$

where B_{r1} is the runner inlet height, α_1 is the angle of the absolute velocity vector needed to feed the runner at certain rotational speed n, certain net head H_n at certain

flow rate Q. The angle α_o is the flow output angle of the cascade which needs to develop at its outlet, and slightly differs from the absolute velocity angle due to the "free vortex" effect in the vaneless space. The radial cascade outflow conditions are guided from the total velocity and its components in the radial (flow rate) and tangential (circulation) manner [2]. The free vortex law which preserves in the vaneless space is transferred from the runner inlet to the guide vanes outlet, respecting the change of the radial distance as:

$$v_{ou} = c_{1u} \cdot \frac{R_{r1}}{R_{gvo}} \tag{3}$$

The radial velocity component is directly influenced from the turbine flow rate at certain radial distance, with respected cascade height B_{gv} as:

$$v_{or} = \frac{Q}{2R_{gvo}\pi B_{gv}} \tag{4}$$

The vector sum of these two components gives the total outlet velocity of the cascade:

$$\overrightarrow{v_o} = \overrightarrow{v_{or}} + \overrightarrow{v_{ou}} \tag{5}$$

which has an inclination angle at the cascade outlet:

$$tg\alpha_o = \frac{v_{or}}{v_{ou}} \tag{6}$$

A correlation can be done between the total velocity and its radial component which are directly influenced from the flow rate as:

$$\frac{v_o}{v_{ro}} = \frac{2R_{gvo}\pi}{Z_{bl} \cdot a_o} \tag{7}$$

where a_o is the needed opening (shortest perpendicular distance) between two guide vanes in the cascade, and Z_{bl} is the number of blades in the cascade. For given turbine operating conditions i.e. design head, flow rate and rotational speed, the following velocities and geometry parameters of the cascade are obtained.

Reaction type stationary blade cascade suitable for reaction turbines are designed to provide the needed outflow angle α_o to the turbine runner, at opening distance a_o between the blades. The inflow conditions of the cascade are strongly dependent from the turbine spiral and stay vanes outflow conditions. The spiral and the stay vanes in this analysis are neglected, for the purposes of development different cascade inflow conditions, to obtain convex and concave blade rows. The purpose of this analysis comes out from the theory of turbomachinery, the theoretical analysis of infinite blade rows [7]:

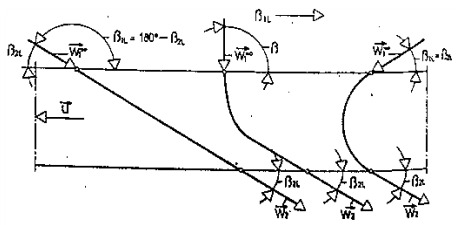

Fig.1. Cascade for variable inflow and constant outflow conditions

The idea to test this is to determine how the change of inflow streamline influence the overall performance of the cascade and the turbine, keeping the outflow angle constant, which is needed for the runner for creating shock-free entrance [2], and changing the inflow angle from 90 [deg] as straight inflow to the cascade and 35 [deg] as given from the spiral and stay vanes, i.e. the first two configurations presented in fig.1. Additional configuration between these two is analysed. All blade sets are designed for shock-free inflow conditions [2].

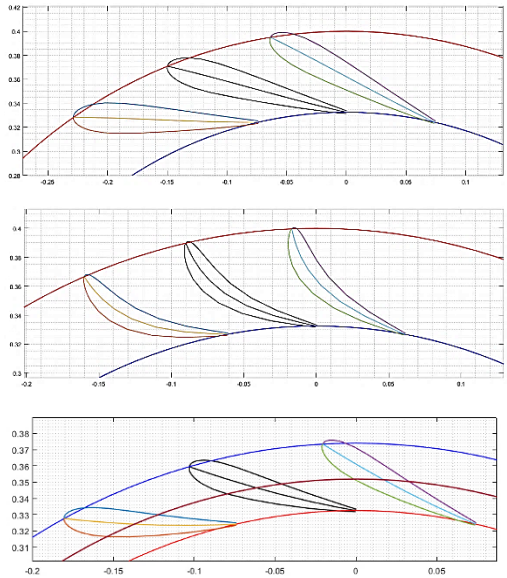

Fig.2. Developed cascades (from top to down – model 1, 2 and 3)

The developing of the models is based on geometry parameters previously developed in a MATLAB code. The code solves the geometry relations between the calculated velocities based on the equations in this paper, where the crucial geometry/flow parameters are the streamlines angles at the cascade inlet and outlet. The blades camber-line and thickness distribution is based on experience data and manually developed mathematical relations [9].

All models have the same outflow conditions specified, i.e. $a_o \approx const.$ and $\alpha_o = const.$ The cascades density is different (length/pitch ratio), i.e. Model 1 is the cascade with convex blades with $L/t = 1.96$ and Model 2 is the cascade with concave blades with $L/t = 1.64$ respecitvely. The third Model has slightly concave blades for inflow conditions as Model 1, with density of $L/t = 1.35$. The designs are obtained according to the turbine design point, which parameters are given in table 1.

TABLE I TURBINE DESIGN POINT (BEP)

Net head	Hn [m]	11,4
Design flow rate	Qd [m3/s]	0,22
Design rotational speed	nd [rpm]	333,33
Runner inlet diameter	Dr1 [m]	0,62
Runner outlet diameter	Dr2 [m]	0,349
Guide vanes height	Bgv [m]	0,06
Guide vanes outflow circumference diameter	Dgvo [m]	0,665
Speed Factor (IEC60193)	ned [-]	0,183
Discharge factor (IEC60193)	Qed [-]	0,171

III. CFD ANALYSIS

The developed models were tested via CFD calculations, to predict their performance in the best efficiency operating zone and around it, by changing the rotational speed of the runner in the range of ±20%.

The geometry of the guide vanes was created in Matlab, and developed in Ansys Workbench. The CFD simulations were executed in Ansys Fluent. The numerical domain is reduced, consisted only from the guide vanes, the runner and the draft tube cone. The mesh for the blade rows (guide vanes and runner) was created in TurboGrid, and assembled in ICEM CFD. It is consisted of 1.25 – 1.35 million cells, all hexahedral elements, with respecting boundary layers on the walls.

The simulations are guided as steady, for constant head, as mentioned previously in the paper. The boundary condition at the inlet is set as total pressure inlet, respecting the cylindrical coordinate system for developing inflow angles into the guide vane cascade, especially for model 1 and 3 where the inflow angle is 35 [deg]. For model 2, the total pressure is set be normal at the boundary, as the blades are designed for those inflow conditions. Static pressure outlet was set on the outlet section of the draft tube cone, with intensity of the atmospheric pressure with averaging the pressure throughout the outlet section, to enable flexibility in the solution and better convergence, as backflows are expected because the domain is reduced. The runner domain is set as rotating frame along with its wall surfaces (blades, hub, shroud and nose). The non-conformal meshes between the guide vanes, runner and the draft tube are connected with interfaces, which are suitable for future transient simulations (sliding mesh). The turbulence model used in the simulations is k-ε realizable, with standard wall functions, as recommended from Fluent when rotating frames are present in the model. The solution methods are set as default – SIMPLE algorithm with Spatial Discretisation of the Pressure as Second Order. Other good method for this type of models is the usage of the COUPLED solver algorithm with enabled pseudo-transient module, which is a form of implicit under-relaxation for steady-state cases, also recommended when rotating frame is present in the model. The solutions converged with great success reaching a residuals to 10^{-6}. The results from the simulations are presented in the following figures and charts. The results presented are normalized upon the input design data from table 1. All the results are presented in relative manner, because no physical measured data is available in this moment to validate the numerical results.

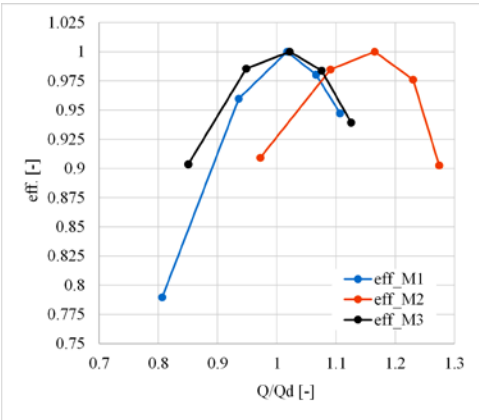

Fig. 3 Relative turbine efficiency plotted against relative flow rate

Fig.3 shows the turbine characteristics, where Model 2 with perpendicular inflow conditions shifts the characteristic for increased flow rates for 17%, because smaller head losses in the cascade. Model 1 and Model 3 for same inflow conditions share almost the same flow rate at the peak efficiency, behave similar for increased flow rates, but for decreased flow rates, model 3 expands the operating zone of the turbine, resulting in increased efficiency.

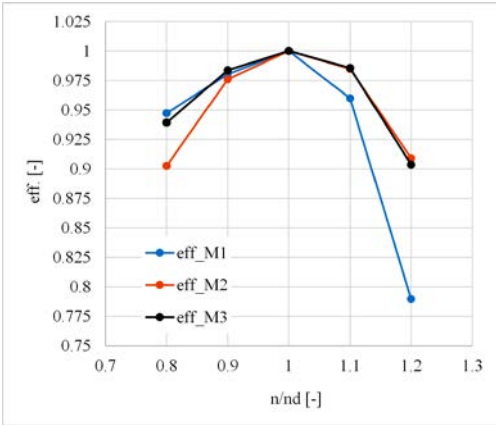

Fig. 4 Relative turbine efficiency plotted against rotational speed

Fig. 4 shows the turbine characteristics against the rotational speed of the runner, where Model 2 compared to model 1, shows better performance at increased rotational speed, and vice versa. Model 3 shows best efficiency coverage around the optimal zone. This indicates that somewhere between Model 1 and 2, in that design space, optimal solution can be found for the guide vanes.

The difference between the characteristics is observed throughout the velocity profile formed at the guide vanes outlet circumference (guide vanes pitch t_{gv}) for different rotational speeds.

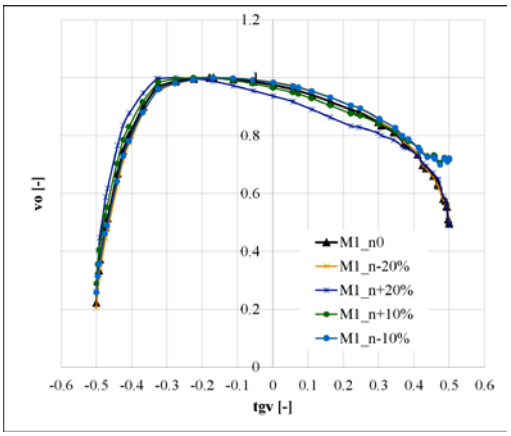

Fig. 5 Velocity profile distribution for Model 1

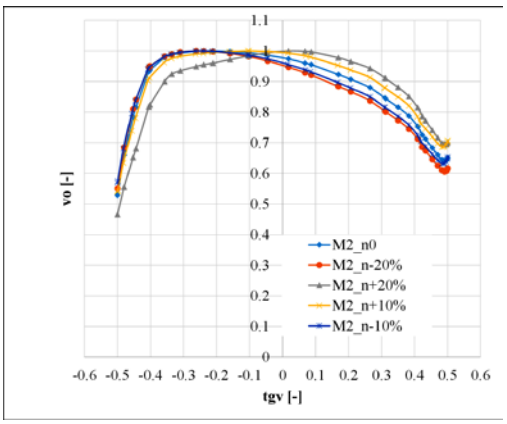

Fig. 6 Velocity profile distribution for Model 2

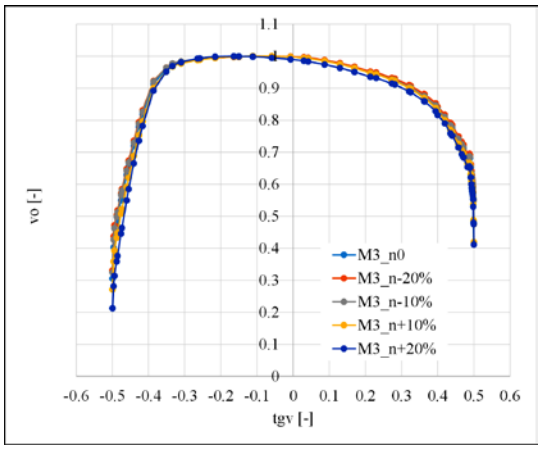

Fig. 7 Velocity profile distribution for Model 3

Fig.5 shows velocity profile for Model 1 for different operating speeds of the turbine. For increased rotational speed +20%, the velocity profile deforms and leans the distribution more to the second blade. Model 2 on the other hand, form deformed velocity profile, as rotational speed is increased to +20%, the profile straightens, which shows how the efficiency is less deviant on fig.2. Fig.7 shows the velocity profiles for Model 3 where insignificant variance is obtained for different rotational speeds, i.e. the profile maintains it shape and uniformity. Because of that, Model 3 remains more stable turbine characteristics around the best efficiency zone.

Pressure distribution is presented along the blades for nominal rotational speed of the runner, where it is shown how the different inflow conditions and overlap of the blades changes the distribution, and how it changes the location of the resultant force on the blade.

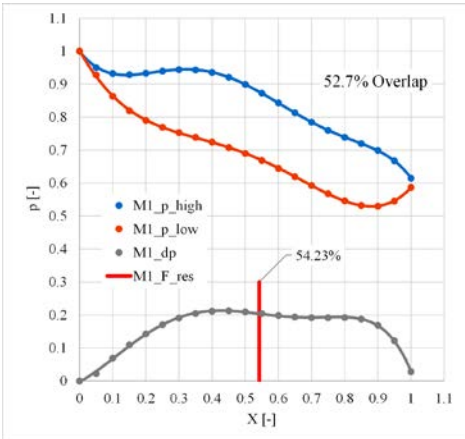

Fig.8 Pressure distribution on 1 blade and resultant force location for Model 1

Fig.8 shows that on the suction side of the blade behaves as pressure side for these inflow conditions (blue line), the pressure starts to drop after 40% of the blade length portion which shows that the fluid enters between the blades. Despite the blades overlap at 52.7%, this shows that the cascade bends the pressure and influence the flow cca. 12.7% earlier. The resultant force is calculated according to the pressure difference on both blade sides. The area under the force curve is calculated with trapezoidal rule of integration, and its centre is found with the *Steiner's* theorem, to find the location of the resultant force. It shows that the force is obtained at 54.23% of the blade length, or 1.53% backwards from the neighbour blade leading edge.

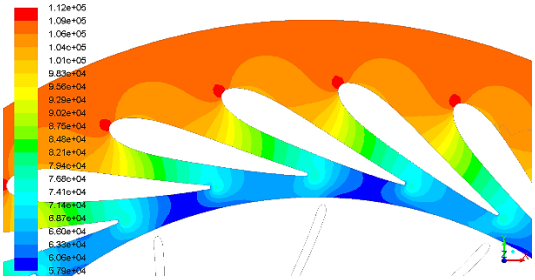

Fig.8.a. Static pressure contours for Model 1

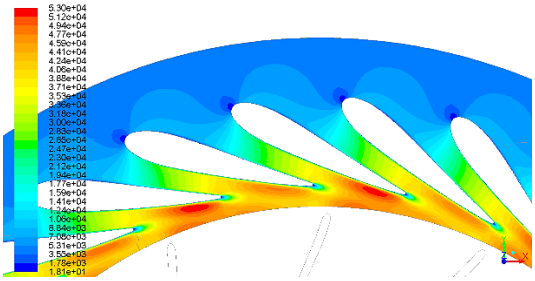

Fig.8.b. Dynamic pressure contours for Model 1

Fig.8.b. show the dynamic pressure contours localized in the guide vanes domain, where on every second blade on the lower side, near the trailing edge, a raise of the dynamic pressure occurs as results of the interference with the runner blades.

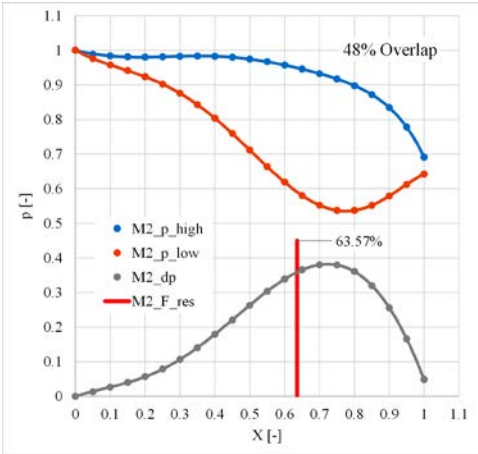

Fig.9. Pressure distribution on 1 blade and resultant force location for Model 2

Fig.9 shows the pressure distribution or model 2, where the inflow conditions are normal to the blades. The pressure starts to drop after 45% of the portion of blade length on the pressure side (blue line) which shows that compared to model 1, the cascade bends the pressure almost at same portion as the overlap. The resultant force is located at 63.57% of the blade length, exactly at the zone where the trailing edge of the neighbouring blade transverse up to the pressurised side of the blade.

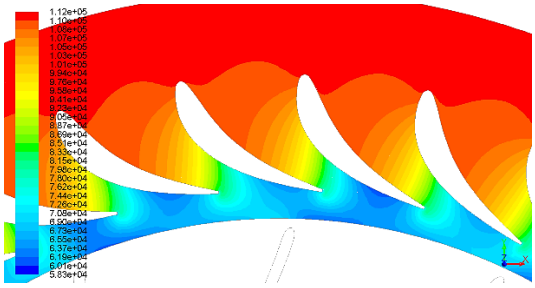

Fig.9.a. Static pressure contours for Model 2

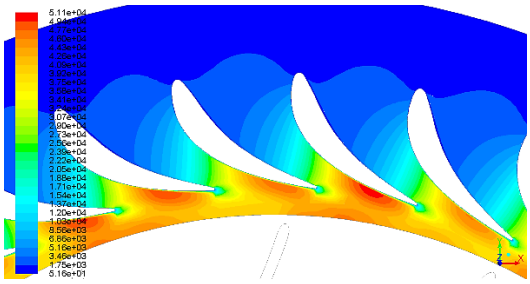

Fig.9.b. Dynamic pressure contours for Model 2

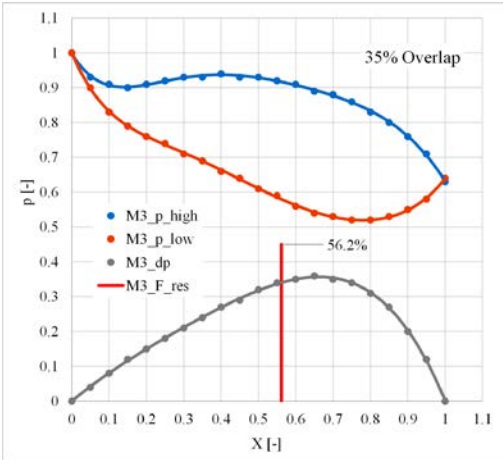

Fig.10. Pressure distribution on 1 blade and resultant force location for Model 3

Fig.10 shows the static pressure distribution of model 3, concave blade with inflow conditions as model 1. The blades geometrically overlap at 35%, i.e. at 65% starting from the leading edge, observed from the length portion. The pressure starts dropping after 50% of the length, which shows that the cascade bends the pressure almost 15% before the start of the inner blade channel. The resultant force on the blade is found at 56.2% of the length portion, i.e. 8.8% after the neighbour blade leading edge.

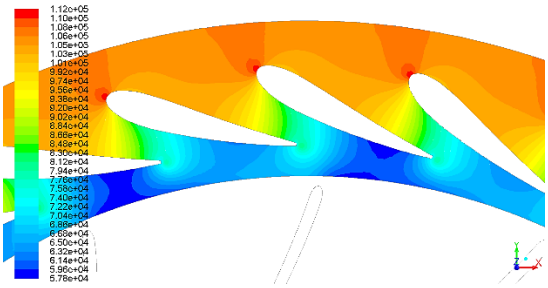

Fig.10.a. Static pressure contours for Model 3

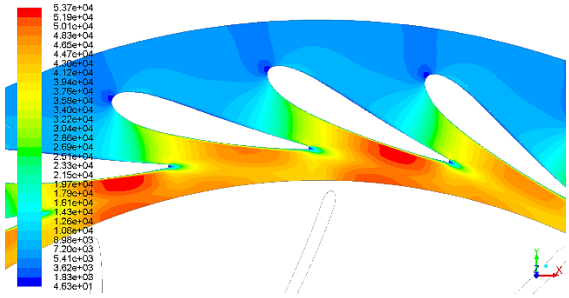

Fig.10.b. Dynamic pressure contours for Model 3

Fig.10.b. shows the dynamic pressure contours, where as other models also, every second blade at the trailing edge has a raise of the dynamic pressure, where this effect can be minimized by increasing the outlet circumference diameter of the cascade, i.e. expanding the blades outwards the runner. By that, wakes behind the blades will be reduced and the feeding will be more axisymmetric towards the runner.

The results obtained for the pressure distributions and location of the force on the blades has to be analysed with other configurations of cascade, i.e. different cascades densities, overlaps and location of maximal thickness and leading edge radius, to obtain clearer picture about the behaviour and the interference between two blades in the cascade, related with the location of the resultant force, so the pivot point of the blades can be estimated easily.

IV. Conclusions

In this paper, an analysis is carried out for different setups of radial guide vane cascades, developed for certain turbine input (design) parameters. The idea was to test the cascade behavior for different inflow conditions i.e. radial inflow condition normal to the cascade blades, which resulted into a concave blade sets, swirling inflow condition which resulted into a convex blade sets and swirling inflow condition at other inlet circumference which resulted into a concave blade sets. The generated configurations were tested via CFD simulations.

The analysis was carried out in a way of determining the turbine characteristics in the best efficiency operating zone, and to variate the rotational speed ±20% of the nominal, to see which model of cascade performs well at off-design conditions. The results are presented in a relative manner, so to obtain a better understanding of the physicality which the parameters give. Further laboratory tests are planned where the CFD models later will be validated.

The convex blade set of model 1 gave more precise prediction of the best efficiency zone, and less efficiency deviations reduced rotational speed of the turbine. The reason for that comes from the analysis of the velocity profiles at the cascade outlet circumference, where the velocity profile was more uniform for decreased rotational speeds.

The concave blade set of model 2 shifted the turbine characteristic curve for increased flow rates about 17% of the design point, because it has smaller head losses. On the other hand, it resulted with less efficiency deviations for increased rotational speeds, where the outlet velocity profile was more uniform.

The concave blade set for swirling inflow conditions of model 3 gave most precise prediction of the best efficiency

zone, and less efficiency deviations both for reduced and increased rotational speed of the turbine. Observing the velocity profile at the outlet circumference, the profile uniformity remained almost constant for all operating speeds.

According these results, it can be concluded that the future development of radial guide vane cascades for variable speed operated turbines shall be in a manner of obtaining uniform velocity profile at cascade outlet for all operating conditions. Comparison between the models shows that an “optimal” solutions can be found between these two limit positions (model 1 and 2).

Cavitation resistance of the cascade shall be examined in further cascade development, which is highly relatable with the developed fluid velocities at the cascade outlet, eventual flow separation between the blades and the geometry of the blades. The analyzed cascades in this paper are all cavitation resistant, because the geometry is modified for all of them to be with shock-free (zero incidence) inflow conditions.

Also, other results were carried out from the analysis, in a way of determining the pressure distributions on the blades in the cascades, to obtain the influence of two blades in a row and the location of the resultant force. The results are promising, but not enough, for generalizing the location of the resultant force according to the inflow conditions and blade geometrical overlap, so to obtain some relations between the force and the overlap, so in the future, a criteria can be carried out for determining the pivot point (axis of rotation) of the blades easily.

This research is part of future Ph.D. thesis, which will take this analysis as basis for development of “optimal” radial cascade for variable speed operated turbine. The idea for further development of the cascade lies in the variation of flow rate with the rotational speed. As the rotational speed decreases, the flow rate increases, which leads to the usage of convex blade sets. As the rotational speed increases, the flow rate decreases, which leads to the usage of concave blade sets. A combination of all these sections is planned to be generated, as “profiled” blade from convex to concave, which will be selected upon a criteria between the sections to see which section combination gives the same pressure/flow characteristic curve. The idea is to observe the influence on the total turbine characteristics and how it behaves at off-design rotation of the turbine, to expand the operating region.

REFERENCES

[1] Farell C. et. all – Hydromechanics of variable speed turbines (Minnesota, 1983)

[2] Krivchenko G. I. – Hydraulic Machines – Turbines and Pumps (Moscow, 1986)

[3] Gerov V. – Vodni turbini (Sofia, 1973)

[4] Barlit V. V. – Gidravlichesky turbini (Kiev, 1977)

[5] Lewis R. I. – Vortex element methods for fluid dynamic analysis of engineering systems (Cambridge University Press, 1991)

[6] Miroslav Benišek – Hidraulične turbine (Mašinski fakultet Beograd, 1998)

[7] Milun B. & Svetislav S. – Osnove Turbomašina (Naučna knjiga Beograd, 1990)

[8] IEC 60193 – Hydraulic turbines, storage pumps and pump-turbines – Model acceptance tests

[9] Filip Stojkovski, Zoran Markov, Zvonimir Kostikj – Design of radial blade cascades using parametrization and correlation of geometry and flow parameters (5th International Scientific Conference COMETa 2020)

THE 5th INTERNATIONAL CONFERENCE
MECHANICAL ENGINEERING IN XXI CENTURY

December 9-10, 2020
Faculty of Mechanical Engineering in Niš, Serbia

An Approach to Determine the Origin of Forces Acting on a Blade in a Cascade

Marija LAZAREVIKJ

"Ss. Cyril and Methodius" University, Faculty of Mechanical Engineering-Skopje, Skopje, North Macedonia, marija.lazarevikj@mf.edu.mk

***Abstract*— The flow characteristics and performance of a cascade depend on the mutual geometrical position of the blades. For the purpose of determining the origin of the forces acting on a blade in a cascade, the effect of the geometrical parameters that describe the cascade is analysed. Three different types of cascades are considered. Firstly, linear cascade consisting of equally spaced blades which are parallel to each other, defining a full overlap of inter-blade region is observed. The flow domain of the second cascade has a semi overlap of inter-blade region which is obtained with vertical displacement of each neighbouring blade. The third one is obtained by adding rotation of each blade for the value of pitch angle, with aim to present the specific fluid flow conditions in radial cascade. A new approach for analysing the origin of forces on blade in a cascade is suggested. The fluid flow domain between two consecutive blades in the cascade is divided into three characteristic zones: free flow inflow, inter-blade region and free flow outflow. CFD numerical modelling and simulations of two-dimensional steady and incompressible flow through the selected cascades are performed. Conclusions are drawn related to the influence of the zones on pressure distribution around blade and origin of forces in a cascade**

***Keywords*— blade cascade, forces, CFD, blade profiles, parameters**

I. INTRODUCTION

When an isolated aerofoil blade is set in a fluid flow field, there are lift and drag forces acting on it. The forces origin from the pressure distribution along the profile and aerofoil blade shape. In case of presence of neighbouring parallel blades forming a blade cascade, then the neighbouring blade has influence on the pressure distribution along the profile, that means the distribution of elementary forces (lift and drag) is changed. The intensity of influence of the neighbouring blade depends on the relative geometrical disposition, which defines the shape of the fluid flow domain and the inter acting zone which are recognized by the fluid flow domain and geometrical (solid) relative boundary conditions. Besides the geometrical disposition of the blades and the obtained fluid flow domain, the blade angle of attack influences the pressure distribution along the blade profile.

The relative disposition of the blades in a cascade can be defined as:

- linear cascade - where the blades are parallel to each other (the axis going through the center of gravity is a straight line)
- semi linear cascade – where the blades are parallel to each other by displacement for a certain step in parallel direction (the axis going through the center of gravity is a straight inclined line)
- radial disposition of cascade- where the blades are displaced in parallel direction and each blade additionally has its own rotation around the center of gravity (the axis going through the center of gravity is a straight inclined line rotated around the center of gravity).

The relative disposition of the blades in a cascade is defining different recognized zones for fluid flow. There are: inflow zone which is "inlet free flow" in the intake area of cascade, controlled or "boundary limited zone" defined with the shape of the solid boundary by body of the blade and outlet zone with "outflow free flow" condition. Each of these zones has an influence on the fluid flow regimes and respectively on the pressure distribution along the blade surface.

The flow conditions and influence of each of this zone on pressure distribution along the profile is numerically tested by 2D CFD model. The aim of this work is to present the recognized zones specific flow conditions and phenomena which has an influence in the flow domain in the blade cascade.

II. NUMERICAL SETUP

A subject of analysis in this paper is a segment of a cascade consisted of five blades, set in an air flow field. Two-dimensional steady flow of air over the blades in is numerically simulated in order to analyze the pressure distribution along the central blade upper and lower surface. For that purpose, the central blade is positioned so that a shock-free entrance is provided. Boundary conditions that are used are mass flow inlet and pressure outlet – the air enters the channel with mass flow rate of 1.2 kg/s and it is released at atmospheric pressure. k-ε turbulence model is used. The mesh is tetrahedral having approximately 75260 cells, depending on the type of cascade (Fig. 1).

Three different scenarios are examined to evaluate the influence of the zones on the pressure distribution on a blade in a cascade. The linear cascade consists of blades which are parallel to each other and equally placed, as shown on Fig. 2. The blades in a semi linear cascade are parallel to each other and the previous/following blade in

relation to the observed one, is displaced for a certain step in parallel direction, as shown in Fig. 3. In addition, in a radial cascade (Fig. 4), each blade has its own rotation around the center of gravity.

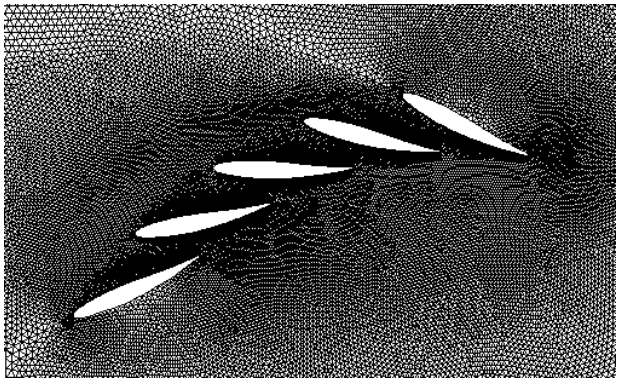

Fig. 1. Numerical grid

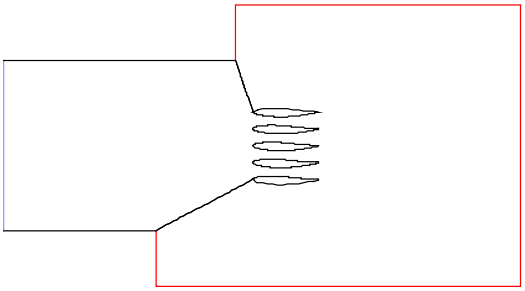

Fig. 2. Numerical model for linear cascade

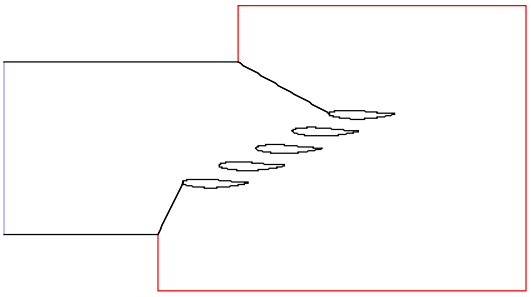

Fig. 3. Numerical model for semi-linear cascade

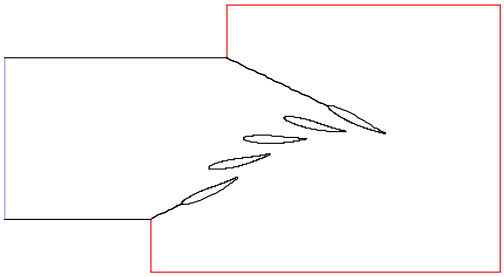

Fig. 4. Numerical model for radial cascade

III. RESULTS FROM NUMERICAL SIMULATIONS

The static pressure distribution is obtained for each scenario.

Fig. 5 shows the pressure distribution on the pressure and suction surface of the centrally placed blade in the linear cascade.

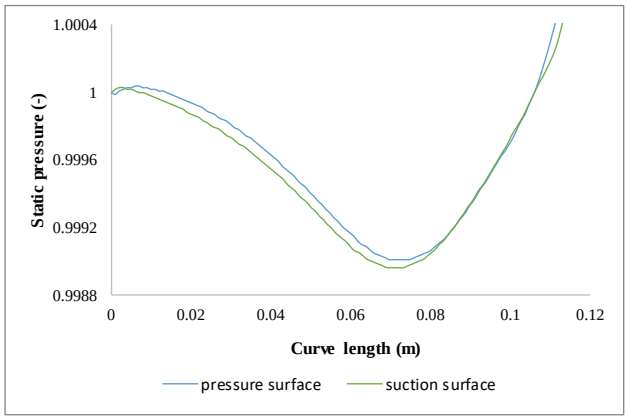

Fig. 5. Pressure distribution along blade surface in a linear cascade

Fig. 6 shows the flow field in the case of a linear cascade.

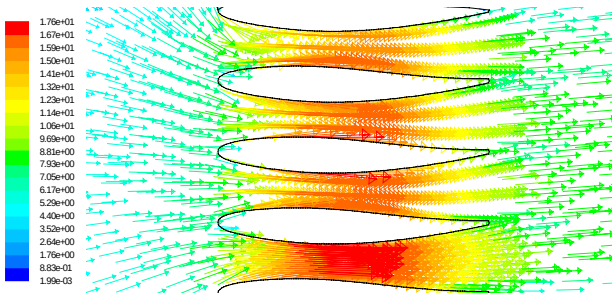

Fig. 6. Vectors of velocity in case of a linear cascade

The pressure profiles on both blade surfaces are following the same trend: the pressure slightly decreases as the flow accelerates and then it sharply increases with the flow deceleration. The flow acceleration and deceleration which directly affect the pressure distribution are a consequence of the geometry of the flow domain defined by the disposition of the neighboring blades.

The pressure distribution on the pressure and suction surface of the centrally placed blade in the semi-linear cascade is given in Fig. 7.

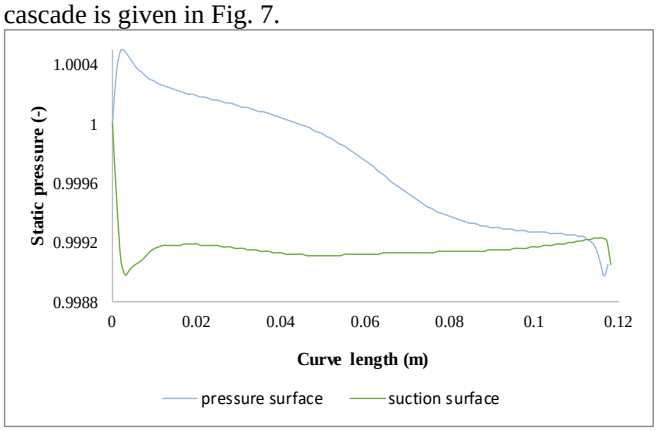

Fig. 7. Pressure distribution along blade surface in a semi-linear cascade

Fig. 8 shows the flow field in the case of a semi-linear cascade.

The pressure gradually decreases on the blade pressure side due to the free flow entrance, whereas it hardly changes on the suction side which is imposed by the form of the inter-blade channel.

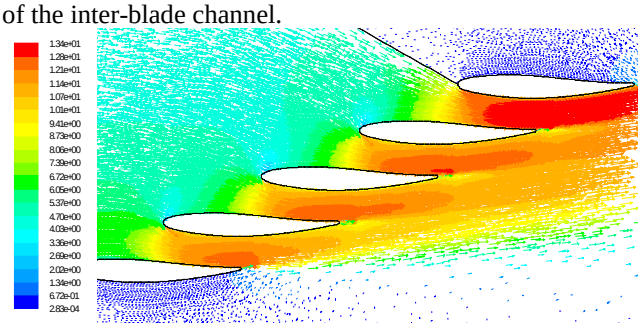

Fig. 8. Vectors of velocity in case of a semi- linear cascade

Pressure distribution along the central blade in the radial cascade scenario is given in Fig. 9.

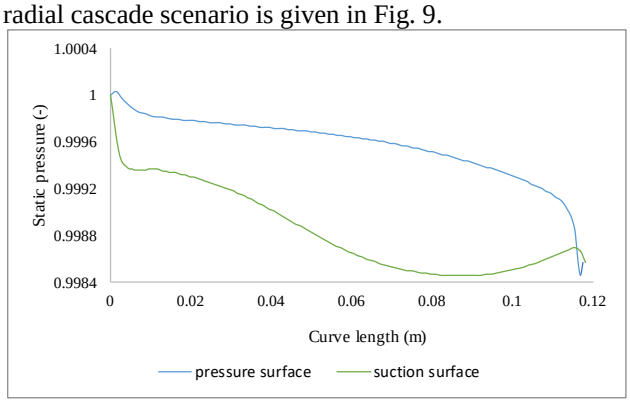

Fig. 9. Pressure distribution along blade surface in a radial cascade

Fig. 10 shows the flow field in the case of a radial cascade.

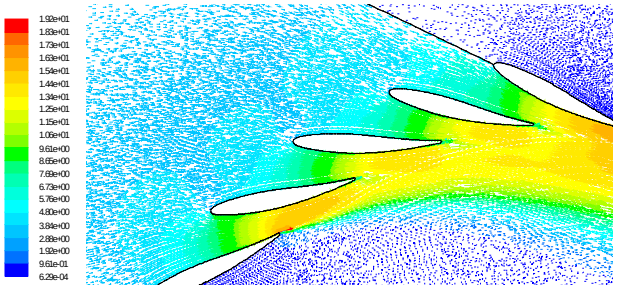

Fig. 10. Vectors of velocity in case of a radial cascade

Pressure decrement along the blade pressure side is determined by the free inflow zone and inter-blade zone. Pressure gradually decreases on the blade pressure side as a result of effect of radius reduction. On the suction side, pressure decreases till the beginning of the free outflow jet when there is no influence from the channel so pressure starts to increase. It can be seen that the flow between the blades is accelerating due to shape of the domain formed. However, the presence of the other zones additionally influences the pressure profile of the blade.

IV. DISCUSSION

The three analysed types of cascades define different fluid flow zones: inlet free flow zone in the cascade intake area, boundary limited zone defined by the shape of the inter-blade region, and outlet free flow. These zones depend on the relative disposition of the blades and affect the fluid flow, and consequently the blade pressure distribution.

The relative disposition of the blades defines the type of the cascade. In the case of a linear cascade (Fig. 11), only the boundary limited zone is present. As a result, the pressure distribution is dependent only on the inter-blade domain shape. While the channel is convergent, flow is accelerating and the pressure decreases. Afterwards, the pressure slightly increases because of the channel being expanded.

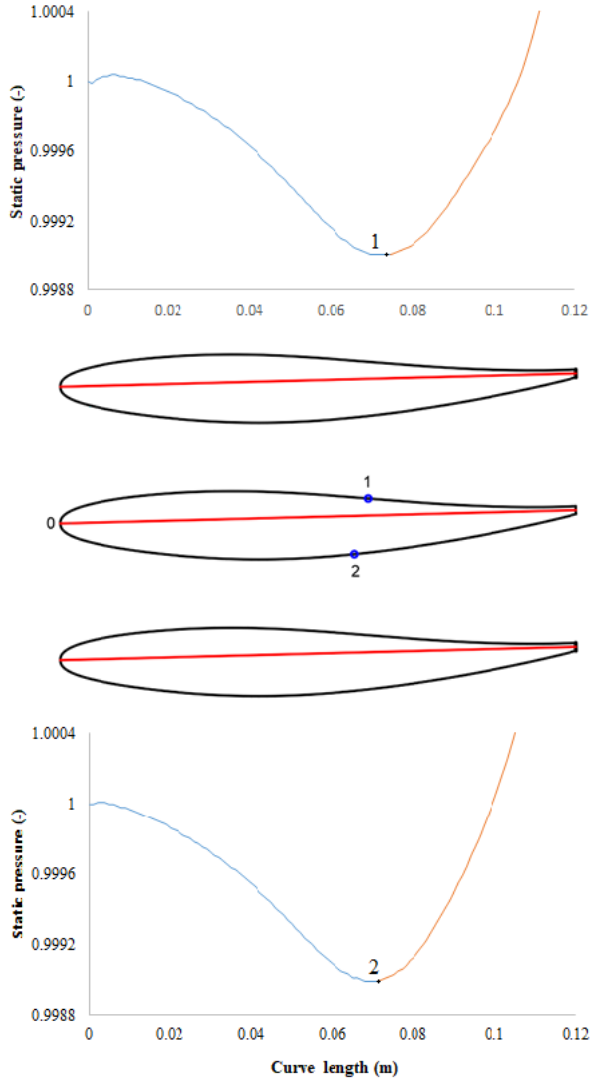

Fig. 11. Detecting boundary limited zone based on blade pressure profile in case of a linear cascade

When analysing the semi-linear cascade, it is concluded that all three zones are present (Fig. 12).

The pressure on the blade pressure surface gradually decreases in the free inlet zone (curve 1-4).

The solid boundary limited zone influences the pressure distribution on both pressure and suction surface: the pressure insignificantly decreases on the suction and pressure surface due to the geometry of the defined zone.

The outlet zone (curve 9-11) affects the blade suction surface. In this zone, the flow is firstly still under the influence of the inter-blade region and the pressure on the suction surface hardly changes (curve 9-10). Then the pressure starts to insignificantly decrease (curve 10-11) on the ending part of the suction surface where the inter-blade zone has no effect.

The presence of the three zones is detected in the case of a radial cascade (Fig. 13).

The inlet flow is accompanied by a pressure decrement on the pressure surface (curve 1-4) because of the effect of radius reduction as a property of a radial cascade.

The solid boundary limited zone determines the pressure decrement on the pressure surface (curve 4-5) as a result of the flow acceleration because of the channel shape.

The suction surface of the blade is affected by the boundary limited zone. The pressure is abruptly decreasing starting from the leading edge since the fluid velocity increases due to the zone shape (curve 11-9).

The pressure profile on the remaining part of the suction surface (curve 9-6) is influenced by the outlet zone. It can be noticed that this zone is divided into two sub-zones: the first one under the influence of the controlled zone where the trend of pressure decrement continues (curve 9-8), and the second one (curve 8-7) defined by the free jet because of which the pressure starts increasing.

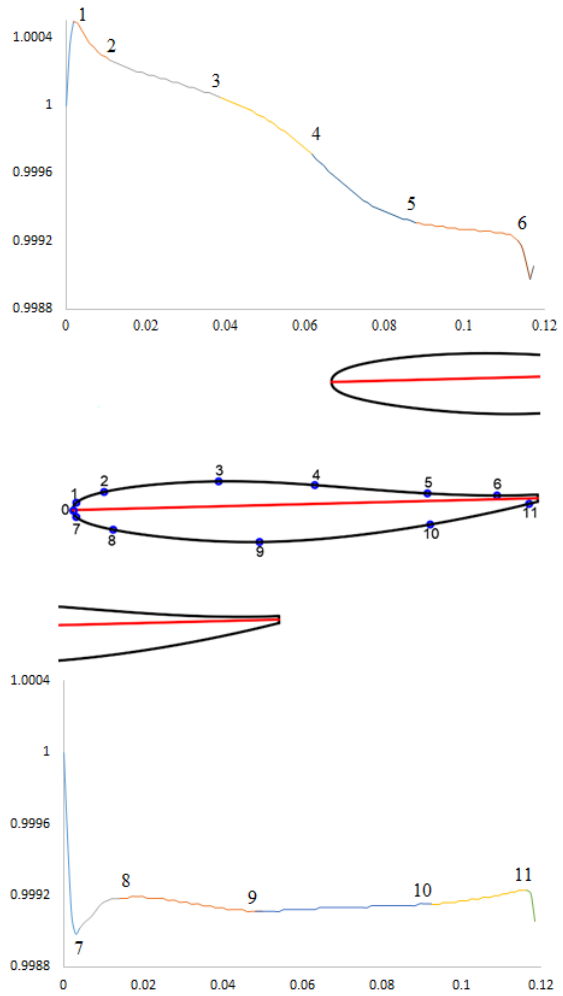

Fig. 12. Detecting zones based on blade pressure profile in case of a semi-linear cascade

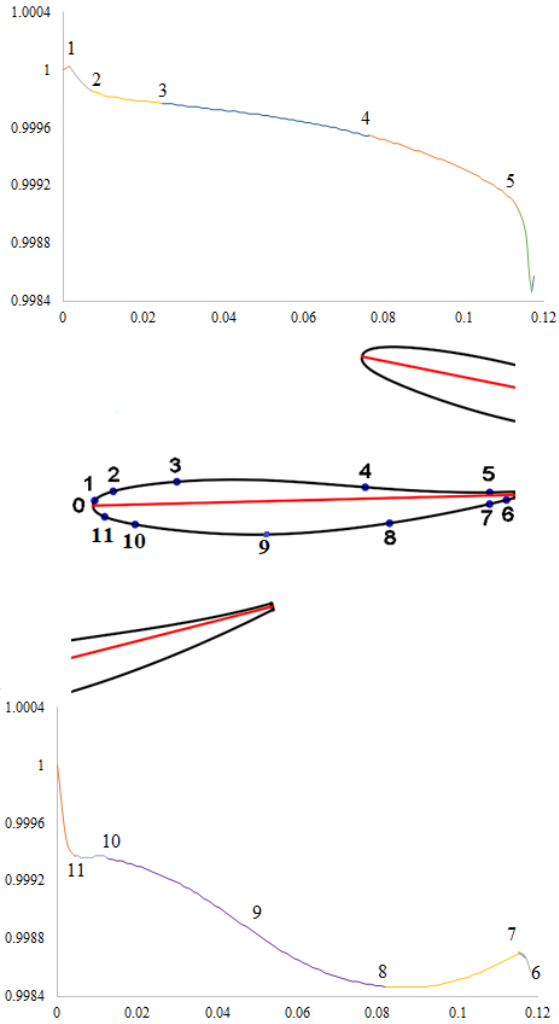

Fig. 13. Detecting zones based on blade pressure profile in case of a radial cascade

V. CONCLUSIONS

The relative disposition of the blades in a cascade defines different recognized zones for fluid flow that influence the pressure distribution along the blade surface. Pressure profile of a blade in a linear, semi-linear and radial cascade, respectively, is numerically obtained in order to evaluate the influence of each zone. The detection of the zones and their relation to the blade pressure profile is established as an approach to determine the origin of forces acting on a blade in a cascade.

REFERENCES

[1] L. Dixon, C. A. Hall, "Fluid Mechanics and Thermodynamics of Turbomachinery", Elsevier, 2010

[2] M. Lazarevikj, V. Stojkovski, A. Noshpal, Numerical investigation of structural behavior of a symmetrical airfoil, Proceedings of SimTerm 2019

[3] M. Lazarevikj, V. Aleksoski, V. Iliev, "Numerical and experimental investigation of airfoil performance in a wind tunnel", American Journal of Engineering Research vol. 9, pp. 119-24, April 2020

[4] F. Stern, M. Muste D. Houser, Wilson M., Ghosh S., Measurement of pressure distribution and forces acting on an airfoil, 57:020 Mechanics of Fluids and Transfer Processes, University of Iowa, 2004

THE 5th INTERNATIONAL CONFERENCE
MECHANICAL ENGINEERING IN XXI CENTURY

December 9-10, 2020
Faculty of Mechanical Engineering in Niš, Serbia

Dilemmas for Choice an Installed Discharge at the Run-off River SHPP - Energy or Economic Approach

Valentino STOJKOVSKI, Zoran MARKOV, Filip STOJKOVSKI

"Ss. Cyril and Methodius" University, Faculty of Mechanical Engineering, Skopje, Republic of North Macedonia
valentino.stojkovskij@mf.edu.mk, zoran.markov@mf.edu.mk, filip_stojkovski@outlook.com

***Abstract*— In run-off river small hydropower plants (SHPP), the selection of installed discharge is very sensitive and depended on the designer's performances for basic parameter. The energy definition approach of the installed discharge is directly depends on the character of the flow duration curve and the choice of turbine equipment, presented by the production of electricity and the revenues received from the sale of electricity. If economic parameterization of the system is introduced through direct investments and costs for construction and maintenance, and represented through the index NPV, B/C, IRR, etc., then the definition of the installed discharge in the run-off river SHPP is different from the technically (energy) defined installed discharge. Software has been developed that through variation of the installed discharge, obtains the dependence of the variability of energy production, revenues (through a feed-in model for the produced electricity price), economic index parameters. The calculation model is developed on the basis of a matrix calculation of hydrological data for average monthly flows per years of a continuous series of hydrological years. The following technical parameters can be varied: type of turbine, number of units and diameter of penstock. On the base of maximal values per each parameter, different discharge is proposed as a result. Some comments and suggestions regarding turbine design to obtain installed discharge are given in this work.**

***Keywords*— SHPP, installed discharge, energy production, economy index**

I. INTRODUCTION

The installed discharge is the key parameter in the design of a run-of river SHPP and has influence on selection of turbine, energy production and investment costs. If take into consideration that the turbine has a technical minimum discharge Qmin, which is percent of the maximal flow of turbine Qmax, depended of the type of turbine (for Pelton turbine is app. 10% of Qmax and for Francis turbine is app 40% of Qmax), then with installed discharge in the same time is defined and minimal discharge which can be used for energy production.

The main source for energy production comes from the flow duration curve (FDC). The shape of the FDC curve has a significant influence on the selection of the turbine type and number of units. In the case of mountain river, the shape of FDC has a characteristic with wet season in a short period through the year (approximately 3 months during snow melting) and the rest is relatively dry season of the year. The quantity of the water in the wet season is 55-60% of the yearly quantity of water.

The criteria for obtaining the installed discharge at run-of river SHPP are not clearly defined. There are two approach for make decision: criteria of energy production or criteria to obtain best economic indexes. Criteria of energy production is a result of the possibilities to transform the natural source (water and geological position) of a particular location to energy in the most efficient way possible. Criteria to obtain best economic indexes introduce a new perception in the SHPP construction, where market prices for realization of project, market prices for sale of electricity and model of investment are changeable and different for each country, but they significantly influence the decision making.

The main goal of this work is to present the effects and differences between these two criteria. The results are produced from the analysis done for twelve different location for potential SHPP development.

II. CALCULATION MODEL

Calculation model is designed to define technical and economical parameters of the project design on the base of variable installed discharge. Results of technical calculation define hydraulic characteristic of the water supply system, diameter of penstock, hydraulic losses, net head, choosing a type of turbine with exploitation characteristic and installed turbine power. On the base of hydrology data for average monthly discharges per years of a continuous series of hydrological years given in matrix form, the energy production is calculated. This model of calculation is implemented for the energy production because the revenue received from the sale of electricity is done on feed-in model, which means that the income is nased on the monthly energy production. The results of the calculations show that energy production and revenue can be analysed through average monthly parameters for each month or through average yearly parameters per each year.

The results of the technical dimensions of the hydraulic structure are the bases for estimation of the basic investment costs for built the SHPP (civil works), penstock and hydro mechanical, hydro-technical and electro-technical equipment.

In economic model of calculation are included additional costs which covered preparing of design

documentation, obligatory taxes by law, expropriation of land, preparatory works and organization of terrain, administrative organization of construction, supervising etc. The basic costs and additional cost represent the total investment cost of SHPP.

The investment model is changeable and considers two periods, period for construction and period of operation. The percentage of bank loan and bank condition can be adjusted according to the customer needs. The results of financial calculation are represented with indexes B/C, NPV, IRR and YPChF. Cash flow diagram is generated on base of constant revenue and on the base of revenue obtained for each year calculated on the base of matrix model of calculation.

The calculation model contain part for sensitive analyses of the investment taking in account:

- intensity of FDC, means the intensity of river discharge is not proper, in variance ±20%
- increased investment up to +20%
- decreased energy production up to -20%

III. DIFFERENT SCENARIO FOR EVALUATION OF LOCATION

The potential for energy production of some location was numerically tested with different scenarios:

- Installed one turbine aggregate
- Installed two turbine aggregates with different maximal discharge (small and large aggregate)

where a various installed discharge is given as a variable site condition.

The installed discharge is defined on base of energetic parameters:

- maximal average energy production per year (EE-srg)
- maximal average energy production per month (EE-srm)

and economic parameters:

- maximal value for indexes B/C and NPV.

IV. RESULTS OF CALCULATIONS

The results of calculation are presented on diagrams where are given:

- the energy production depending on installed discharge
- the economical indexes depending on installed discharge.

The installed discharge is obtained on base of diagram presentation of results when is reach value for maximal energy production or economical indexes.

This method is used for twelve different location for construction of SHPP. The applied method for obtaining the installed discharge is presented through the results of one location.

A. *Determination of installed discharge on base of energetic parameters*

Fig.1 shows results for average energy production per year with installed one turbine unit (PT-2M-1AG) and with two turbine units (PT-MG-30%) depending on installed discharge. The choice of two turbine units which has different maximal turbine discharge, read with possibility of using a small discharge for energy production and obtain a better results for energy production.

The results for average energy production per month with installed one turbine unit (PT-2M-1AG) depending on installed discharge are shown on fig.2. The results are for wet period (April, May, June) and the dry month of July. The obtained installed discharge is done on the base of maximal energy production in wet period (forced discharge).

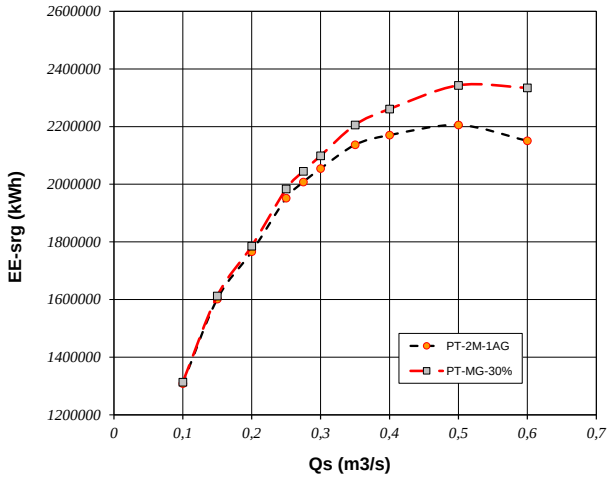

Fig. 1 Average energy production per year depending on installed discharge

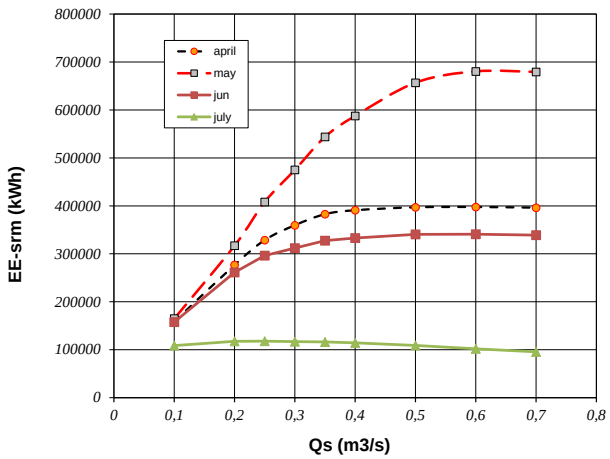

Fig. 2 Average energy production per month depending on installed discharge

In case of average yearly energy production (EE-srg) the installed discharge is 0,5 m^3/s, but on base of average monthly energy production (EE-srm) the installed discharge is 0,6 m^3/s, or the differences for installed discharge is 20%.

B. *Determination of installed discharge on base of economic parameters*

On fig.3 and fig.4 are shown results for indexes B/C and NPV with installed one turbine unit (PT-2M-1AG) and with two turbine unit (PT-MG-30%) depending on installed discharge.

The choice of one turbine units obtain a better results for economical indexes. This results are opposite than conclusion done on base of results for energy production.

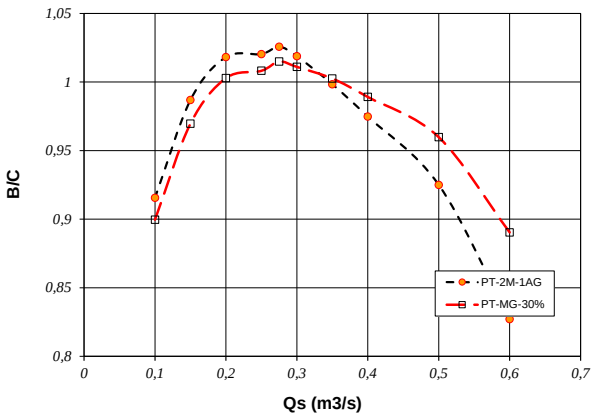

Fig. 3 Economic index B/C depending on installed discharge

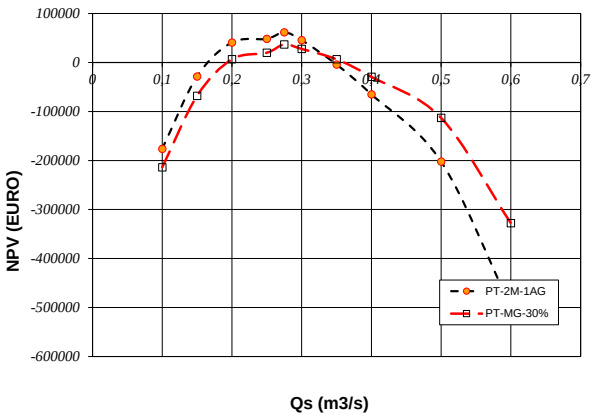

Fig. 4 Economic index NPV depending on installed discharge

Fig.5 shows results for average annual revenue (Cp-srg) with installed one turbine unit (PT-2M-1AG) and with two turbine unit (PT-MG-30%) depending on installed discharge.

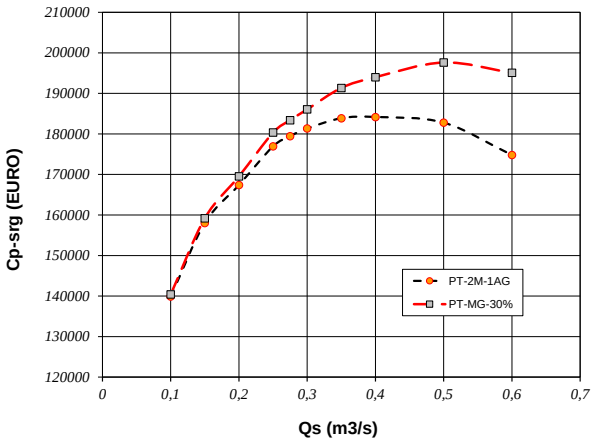

Fig. 5 Average annual revenue (Cp-srg) depending on installed discharge

V. Differences of chosen criteria

The installed discharge (Qmax), obtained for each location on base of criteria:

- average annual energy production (Qmax-EE-srg),
- average monthly energy production (Qmax-EE-srm),
- economy indexes (Qmax-EE-b/c)

are given on fig.6. The maximal installed discharge is biggest for criteria of average monthly energy production, and opposite is for criteria of economy index.

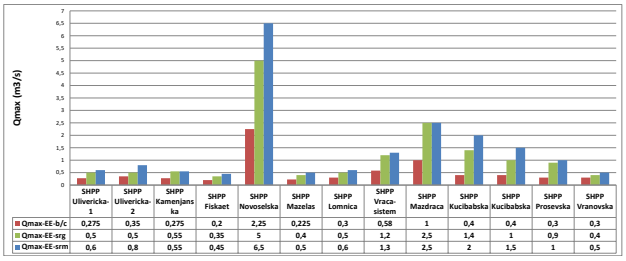

	SHPP Ulivericka-1	SHPP Ulivericka-2	SHPP Kamenjanska	SHPP Fiskaet	SHPP Novoselska	SHPP Mazelas	SHPP Lomnica	SHPP Vraca-sistem	SHPP Mazdraca	SHPP Kucibabska	SHPP Kucibabska	SHPP Prosevska	SHPP Vranovska
Qmax-EE-b/c	0,275	0,35	0,275	0,2	2,25	0,225	0,3	0,58	1	0,4	0,4	0,3	0,3
Qmax-EE-srg	0,5	0,5	0,55	0,35	5	0,4	0,5	1,2	2,5	1,4	1	0,9	0,4
Qmax-EE-srm	0,6	0,8	0,55	0,45	6,5	0,5	0,6	1,3	2,5	2	1,5	1	0,5

Fig. 6 Maximal discharge obtained on base of average annual production (Qmax-EE-srg), average monthly production (Qmax-EE-srm), economi indexes (Qmax-EE-b/c)

The calculated value for average annual energy production for involved criteria for determination installed discharge are given on fig.7. The result shows that minimal energy production is obtain with criteria economy index, but for the additional two criteria are obtained different differences about energy production, where influence depending on specificity of location.

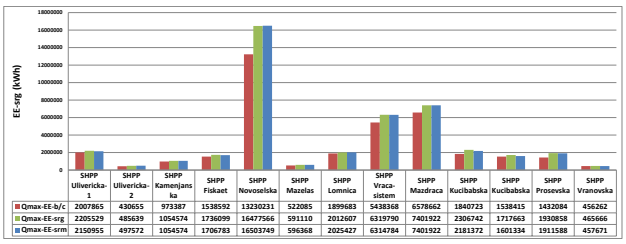

	SHPP Ulivericka-1	SHPP Ulivericka-2	SHPP Kamenjanska	SHPP Fiskaet	SHPP Novoselska	SHPP Mazelas	SHPP Lomnica	SHPP Vraca-sistem	SHPP Mazdraca	SHPP Kucibabska	SHPP Kucibabska	SHPP Prosevska	SHPP Vranovska
Qmax-EE-b/c	2007865	430655	973387	1538592	13230231	522085	1899683	5438368	6578662	1840723	1538415	1432084	456262
Qmax-EE-srg	2205529	485639	1054574	1736099	16477566	591110	2012607	6319790	7401922	2306742	1717663	1930858	465666
Qmax-EE-srm	2150955	497572	1054574	1706783	16503749	596368	2025427	6314784	7401922	2183372	1601334	1911588	457671

Fig. 7 Differences in annual energy production depending on installed maximal discharge

The economy index B/C have trend of lowering with increasing the installed discharge. The results of calculations are shown on fig.8.

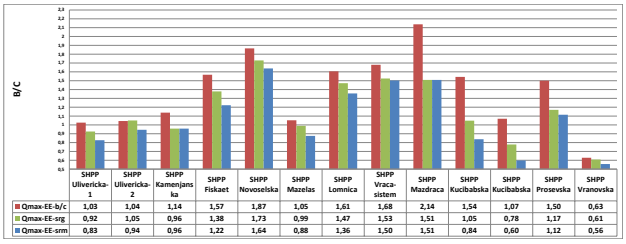

	SHPP Ulivericka-1	SHPP Ulivericka-2	SHPP Kamenjanska	SHPP Fiskaet	SHPP Novoselska	SHPP Mazelas	SHPP Lomnica	SHPP Vraca-sistem	SHPP Mazdraca	SHPP Kucibabska	SHPP Kucibabska	SHPP Prosevska	SHPP Vranovska
Qmax-EE-b/c	1,03	1,04	1,14	1,57	1,87	1,05	1,61	1,68	2,14	1,54	1,07	1,50	0,63
Qmax-EE-srg	0,92	1,05	0,96	1,38	1,73	0,99	1,47	1,53	1,51	1,05	0,78	1,17	0,61
Qmax-EE-srm	0,83	0,94	0,96	1,22	1,64	0,88	1,36	1,50	1,51	0,84	0,60	1,12	0,56

Fig. 8 Differences of economic index B/C depending on installed maximal discharge

The economy index NPV in depend of installed discharge have trend of lowering with increasing the installed discharge. The results of calculations are shown on fig.9. For some locations by increasing the installed discharge are obtained negative value for NPV, that mean the feasibility of that location is debatable.

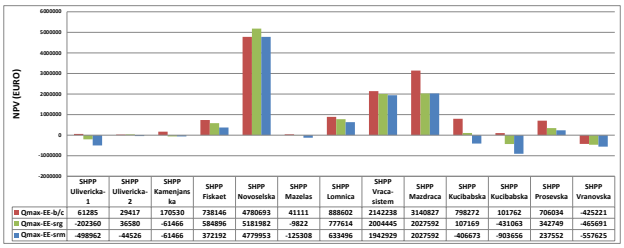

	SHPP Ulivericka-1	SHPP Ulivericka-2	SHPP Kamenjanska	SHPP Fiskaet	SHPP Novoselska	SHPP Mazelas	SHPP Lomnica	SHPP Vraca-sistem	SHPP Mazdraca	SHPP Kucibabska	SHPP Kucibabska	SHPP Prosevska	SHPP Vranovska
Qmax-EE-b/c	61285	29417	170530	738146	4780693	41111	888602	2142238	3140827	798272	101762	706034	-425221
Qmax-EE-srg	-202360	36580	-61466	584896	5181982	-9822	777614	2004445	2027592	107169	-431063	342749	-465691
Qmax-EE-srm	-498962	-44526	-61466	372192	4779953	-125308	633496	1942929	2027592	-406673	-903656	237552	-557625

Fig. 9 Differences of economic index NPV depending on installed maximal discharge

As a general conclusion about differences of results for each test parameter obtained on base of different criteria for prediction of installed discharge can be written that increasing of installed discharge does not mean that is better from view of energy production, because each location has an own specificity which shall be recognized and implemented in calculation and making the decision.

VI. Effect of chosen criteria

Comparing the results for energy production on base of criteria for obtaining installed discharge, as a relative value refer to obtained results on base of economic criteria, can be concluded that criteria on base of average annual energy production has more effective influence. The results of relative values are shown on fig.10.

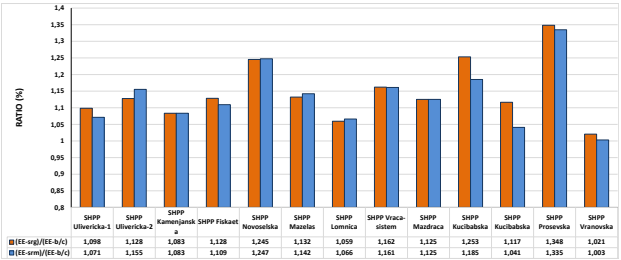

Fig. 10 Effect of criteria on energy production

Effect for chosen installed discharge on base of criteria of average annual energy production has an increased energy production different for each location, but overall can be expected to be app 17%.

Comparing the results for revenue on base of criteria for obtaining installed discharge, as a relative value refer to obtained results on base of economic criteria, can be concluded that criteria on base of average annual energy production has more effective influence. The results of relative values are shown on fig.11.

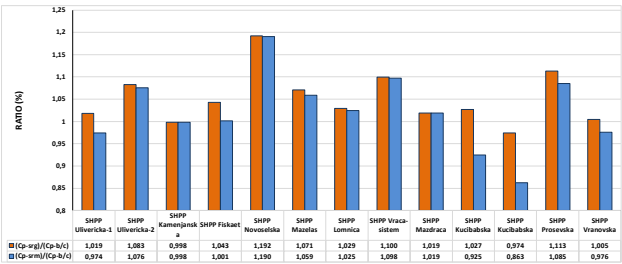

Fig. 11 Effect of criteria on revenue

Effect for chosen installed discharge on base of criteria of average annual energy production has an increased revenue different for each location, but overall can be expected to be app 8-9%.

VII. Conclusions

The presented results for various site characteristic, flow duration curve, choosing of type of turbine and number of units, economic calculations are coming from the created software appropriate for this analyses.

The involving a criteria for defining a installed discharge**,** shows a dilemma for the strategy to develop a some location for construction of an run-of river SHPP. There are two concept for make decision about installed discharge: energy and/or economic.

From point of view to use the natural sources for energy production, leads to implement the criteria on average annual energy production for defining of installed discharge, but in the same moment to be feasible. The economic analysis shows that for some cases this model is not appropriate because the economy indexes are not feasible. In such cases the economy model for defining installed discharge will be more appropriate. The model for selection of the criterion for selection of the installed flow is not ambiguous i.e. it depends on the specifics of the location for SHPP development

References

[1] F.Stojkovski, Z.Kostic, V.Stojkovski, *Assessment Feasibility of Construction a Small Hydropower Plant*, SIMTERM-2015, 17th International Symposium on Thermal Science and Engineering of Serbia, October 20-23,2015

[2] Liucci L., Valigi D., Casadei S. (2014), *A new application of Flow Duration Curve (FDC) in designing run-of-river power plants*, Water Resources Management, 28(3), 881-895

[3] V.Stojkovski, Z.Kostic, A.Nospal: *Transient analisys into the water supply system of hydropower plants with short penstock*, MEDJUNARODNO SAVETOVANJE: ENERGETIKA 2011, Zlatibor 22.03 - 25.03.2011.

[4] Uhunmwangho R, Okedu EK. *Small Hydropower for Sustainable Development*. Pac J Sci Technol 2009; 10(2):535-543.

[5] V.Stojkovski, Z.Kostic: *Prediction the energy production from small hydro power plants*, Proceedings, XXXI Medjunarodno savetovanje ENERGETIKA 2015, Zlatibor, R.Srbija, 24.03-27.03.2015, Vol.1-2, pp117-121

[6] V.Stojkovski, A.Nospal, *Transient fluid flow into paralel pipelines constructed of pipes with different materials*, XXXI *savetovanju* ENERGETIKA 2015, *Zlatibor*, 24.03.- 27.03.2015, Proceeding, No 1-2, pp.305-310

[7] V.Stojkovski, F.Stojkovski, *Influence of water supply system on efficiency at run-of-river small hydro power plant*, International Conference & Workshop REMOO-2016, 18–20 May 2016, Budva, Montenegro

[8] V.Stojkovski, D.Korunoski, *Moving average aproach for prediction an energy production from run-of rivr power plant*, Proceedings, XXXII Medjunarodno saverovanje ENERGETIKA 2016, Zlatibor, R.Srbija, 22.03-25.03.2016, Vol.3-4, pp. 67-73

[9] Anagnostopoulos JS, Papantonis DE, *Optimal sizing of a run-of-river small hydropower plant*, Energ Convers Manage (2007), doi:10.1016/j.enconman. 2007.04.016

[10] E.Bekiri, V.Stojkovski, S.Ilievski, *The hidden energy potencial at the system HPP Vrben*, Proceedings, XXXV Medjunarodno saverovanje ENERGETIKA 2020, Zlatibor, R.Srbija, 24.03-27.03.2020

THE 5th INTERNATIONAL CONFERENCE
MECHANICAL ENGINEERING IN XXI CENTURY

December 9-10, 2020
Faculty of Mechanical Engineering in Niš, Serbia

Numerical Research into the Influence of Impeller Reduction on Centrifugal Pump Performance

Živan SPASIĆ, Veljko BEGOVIĆ, Miloš JOVANOVIĆ, Saša MILANOVIĆ

Department of Hydroenergetics, Faculty of Mechanical Engineering, Aleksandra Medvedeva 14
zivan.spasic@masfak.ni.ac.rs, veljko.begovic@masfak.ni.ac.rs, milos.jovanovic@masfak.ni.ac.rs, sasa.milanovic@masfak.ni.ac.rs

***Abstract*— Manufacturers of centrifugal pumps often predict the possibility of reducing the impeller of a pump. In this way, the pump performance can be quickly and simply adapted to the needs of the customer. The maximum reduction of the impeller depends on the pump type and usually varies from 5% to 20%. The characteristics of a pump with a reduced external diameter of the impeller can only experimentally be determined accurately. Similarity theory or some other related methods given in the literature are often used to approximate performance characteristics of pumps with reduced impellers. There is no complete geometric similarity between a pump and a pump with a reduced impeller, so the theory of similarity cannot be fully applied. Thus the changes in the performance of a pump with a reduced impeller are researched numerically. The aim of this paper is to validate the numerical simulation method for determining the performance of pumps with a reduced impeller. By mastering the numerical method of determining these characteristics, it is possible to reliably numerically predict the performance of pumps with other types of impeller reduction, without expensive and lengthy experiments.**

***Keywords*— Centrifugal Pump, Impeller, Reduction, Performance, Numerical Simulations**

I. Introduction

To expand the operating range of centrifugal pumps, the impeller reduction method is often used. The reduction method implies reducing the diameter of the impeller by trimming. This way of adjusting the pump operation depends on the pump type. By reducing the diameter of the impeller, pump manufacturers can quickly and easily adapt the pump performance to the customer's needs. The extent to which the impeller will be reduced depends on the type of the pump and can be from 5% to 20%. For minor changes in the impeller diameter, the efficiency is only reduced by a few %-points. [1,2].

Single-stage centrifugal pumps behind the impeller can have a volute case or diffuser, and are called volute or diffuser pumps. In the case of diffuser pumps, the characteristic may become unstable if impeller trimming is excessive. The limit must be determined experimentally. In the absence of tests, it is recommended not to trim by more than 5% [1]. For volute centrifugal pumps, a reduction of 10 to 20% is recommended [1,3].

There are 2 major trimming methods, as shown in Fig. 1, straight trimming (a) and oblique trimming (b) [1,4].

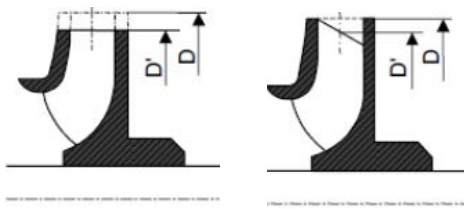

a) straight trimming b) oblique trimming

Fig. 1 Trimming methods for impeller reduction

Straight trimming is a ″traditional trimming method″, it cuts the impeller diameter uniformly along the circumferential direction at the outlet of the impeller. Oblique trimming is used in high-speed pumps where the front disc is short.

The ratio of the diameter of the reduced and the full impeller diameter is denoted as

$$d_2^* = \frac{D_2^{'}}{D_2} \tag{1}$$

The performance of a pump with a reduced outside diameter of the impeller can only experimentally be accurately determined. Similarity theory or some other approximate method is often used for approximate determination of the performance of a reduced pump impeller [5]. There is no complete geometric similarity between a pump with a trimmed impeller and an impeller with a full diameter, so similarity theory cannot be fully applied. One of the modern ways of predicting the performance of pumps with a reduced impeller is the application of numerical simulation methods using the available CFD software [6,7].

Computational Fluid Dynamics (CFD) represents a common practice to design and optimize hydraulic pumps, since it can improve pump design, whilst reducing development cost, widely replacing experimental tests, and accelerating the time to the market. CFD and three-dimensional numerical simulation have been widely applied in hydrodynamics because they can predict the performance of centrifugal pumps [8,9]. A three-dimensional Reynolds averaged Navier-Stokes equation was used in order to analyse incompressible turbulent flow inside the impeller. The governing equation was

discretised using a finite volume method, and a high-resolution scheme that has more than a second degree of accuracy was used to solve the convection-diffusion equations [10,11]. The method of numerical simulation, based on the ANSYS CFX software program, is a volume method of analysis. The calculation accuracy is determined by the mesh type. Although the structured mesh is difficult and time-consuming to generate, the quality and number of the structured mesh are easy to modify [12]. Choosing an adequate mesh can significantly save the time required for numerical simulation.

In this study, characteristics of a centrifugal pump with a different outlet diameter were numerically researched, using Ansys CFX 19.0.

II. Model pump for numerical simulation

The model for numerical simulation was chosen as the spiral centrifugal pump, type SCP100-200 manufacturer ″Jastrebac″ Niš with the following parameters: specific speed n_q = 31.2, flow rate Q = 43 l/s, head H = 51 m, rotational speed n = 2900 min^{-1}, and other geometric parameters are given in Table I. The meridian section of the pump with the basic geometric parameters is given in Fig. 2. The performance of the pump is known, the manufacturer has given it in its performance data sheets. The curves H-Q and η-Q are shown with dashed lines in Fig. 5 and Fig. 6 for the full and the trimmed diameter of the impeller for the nominal pump speed n = 2900 min^{-1}.

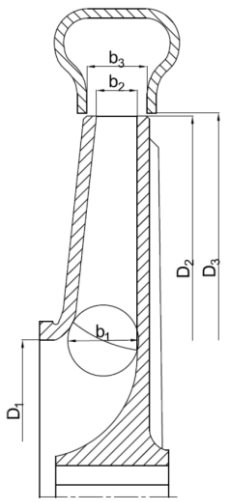

Fig. 2 Meridian section of the pump with basic geometry

Fig. 2 schematically shows the meridian section of the centrifugal pump, with the impeller and the volute.

TABLE I Specifications of the pump model

Blades number, z	7
Impeller inlet diameter, D_1	120 mm
Impeller outlet diameter, D_2	209 mm
Impeller outlet width, b_2	22 mm
Blade outlet angle, β_{2L}	22^0
Blade outlet thickness, δ_2	4 mm
Base volute diameter, D_3	212 mm
Volute inlet width, b_3	32 mm

Two reductions of the diameter of the impeller were performed, first to 180 mm, and second to 160 mm. The straight trimming method was applied. The performance of the pump with the reduced impeller is also known and presented in Fig. 5 and Fig. 6 with dashed lines.

III. Numerical simulation of the centrifugal pump

The 3D geometry of the impeller was generated using ANSYS BladeGEN ver. 19. The computational domains for the numerical analysis were produced using the generated 3D geometry shown in Fig. 3.

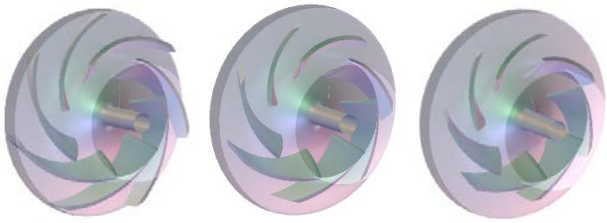

Fig. 3 3D geometries of the impeller

A. Numerical mesh

The impeller and the volute of centrifugal pumps include a space distortion structure, so the unstructured grid is more suitable for its fluid domain; this significantly reduces the duration of the numerical simulation. For the computational domain, an unstructured grid system was generated using ANSYS TurboGrid ver. 19. A grid dependency test of the impeller was conducted to select reliable grids for the performance evaluation. The grid dependency test of the impeller used the head and efficiency results at different numbers of grid nodes [13].

The meshes of flow passages of centrifugal pump with the impeller and volute casing were shown in Fig 3.

Fig. 4 The mesh of flow domain for impeller and volute

The grids number depending on the outlet diameter D_2 is shown in Table II.

TABLE II Grids number of the mesh

D_2	209 mm	180 mm	160 mm
Grids number	1 639 156	1 176 822	917 280

The 3D geometry of the volute was generated using SolidWorks 2017, while the grid was generated in ANSYS Mesh and contains 1 124 846 elements, shown in Fig 4.

B. *Turbulence model*

The choice of the turbulence model is crucial when using CFD codes and the choice of the turbulent model itself largely depends on the complexity of the process. The turbulence model describes the distribution of the Reynolds stresses in the flow domain. Based on the experience from previous research, the standard k-ε model was chosen as an optimal model considering the quality of obtained results and computing power [14].

C. *Boundary conditions*

The following boundary conditions were used for numerical analysis: the reference pressure was set to 1 bar, a flow rate was assigned to the inlet, and a pressure condition of 0 bar was given to the outlet so that the outlet would have an atmospheric pressure state. The number of revolutions of the rotor was set to 2900 rpm, and water was used as the working fluid. At the interface of the impeller and the volute, the stage average condition was applied.

D. *Validation of the numerical model*

The numerical model validation was performed by comparing the numerical results with the results obtained by centrifugal pump testing by the manufacturer (Fig. 5 and Fig. 6

E. *Performance of the pump with reduced impellers – numerical results*

Changing the output diameter of the impeller affects the change in the flow in the numerical domain of the pump and the change in its performance [3,4].

The pump performance results obtained by numerical simulation are shown in Fig. 5 and Fig. 6. Fig. 5 shows the curve for the head H(Q) of the pump with the outer diameter of the impeller D_2=209 mm (black line), D_2 = 180 mm (red line) and D_2=160 mm (blue line). The dashed lines show the curves given by the manufacturer in performance sheets.

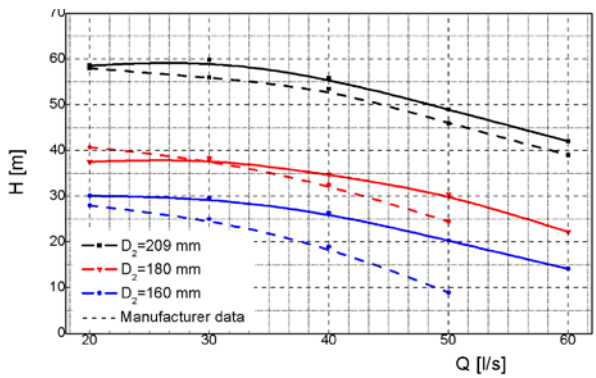

Fig. 5 H-Q curve for different outer diameter D_2

Fig. 5 shows the curve for the efficiency η(Q) of the pump with the impeller outer diameter D_2=209 mm (black line), D_2=180 mm (red line) and D_2 =160 mm (blue line).

Numerical simulations give higher efficiency, because they in fact yield the hydraulic efficiency of the pump.

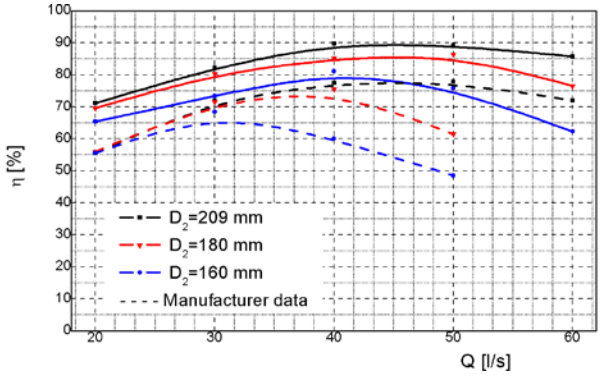

Fig. 6 η-Q curve for different outer diameter D_2

Table II shows the pump parameters for the optimal operating point (BEP) for different diameters of the impeller outlet, as well as the exponents that define the change in flow and head with the change in the diameter of the outlet, denoted by m_K, m_H [15].

TABLE III PARAMETER OF THE PUMP IN BEP

D_2 (mm)	Q (l/s)	H (mm)	η (%)	d*	m_Q	m_H	Δη (%)
209	49	50	89	1	-	-	-
180	43	34	86	0.86	0.87	2.58	3
160	39	27	79	0.77	0.85	2.31	10

The values of the exponents m_Q, and m_H that define the change in flow and head with the change in the outer diameter of the impeller D_2 are obtained within the expected limits [3,15].

F. *Analysis of results*

Figures 5 and 6 show the pump performance, head and efficiency curves, obtained by numerical simulations, and the performance given by the pump manufacturer (shown by dashed lines) for a reduced and full diameter of the impeller.

Numerical simulations (Fig. 5) yielde higher values of head (about 8%) in the entire flow range for the outer diameter D_2=209 mm. Numerical simulations for D_2=180 mm, for lower flow values, yielded lower head values, and for higher flow values yielded higher head values (about 10%), while the values for flow rate of 30 l/s match. The largest deviations of the experimental curves and CFD are for the outer diameter D_2=160 mm (blue line), where the increasing flow increases this difference, and in BEP this difference is about 20%.

These differences indicate that an analysis of the CFD model and curve provided by the manufacturer should be performed.

The values of the efficiency obtained by numerical simulations are higher than the values obtained experimentally by the pump manufacturer (Fig.6). Numerical simulations yield mainly values of hydraulic efficiency. Numerical simulations of the best efficiency point (BEP) have shifted to the right, towards higher flows, with the increasing reduction of the impeller.

Ansys CFX Post 19.0 provides a good visualization of pump flow. The pressure and velocity distribution as well as the complete streamlines in the pump can be observed. It can be seen that the velocity changes with the change in the outer diameter of the impeller (Fig. 7)

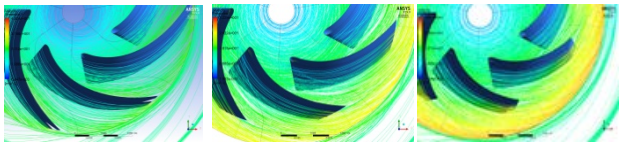

a) D_2=209 mm b) D_2=180 mm c) D_2=160 mm

Fig. 7 Velocity distribution in the pump for different output diameter D_2

IV. Conclusions

Numerical simulations of fluid flow in a centrifugal pump can quickly and fairly reliably predict the performance of the pump after the reduction of the impeller, or for how much to reduce the diameter of the impeller to obtain the appropriate performance of the pump. This would avoid quite expensive and complicated experiments. Of course, it is first necessary to validate the numerical model, so as not to get erroneous results. The paper (Fig. 5) shows that the curves of head, before and after the reduction of the impeller, coincide well with the experimental curves given by the manufacturer near BEP. The values of the efficiency obtained by numerical simulations deviate more than values obtained experimentally by the pump manufacturer, because numerical simulations do not take into account all the existing losses that occur in the pump.

Due to the deviations that occur between the results of numerical simulations and experimental results, the authors doubt the reliability of the manufacturer data, because manufacturers often provide in their catalogs commercial characteristics that frequently deviate from the real ones [15,16]. For the validation of a numerical model, it is best to perform experimental tests on a given model, which the authors plan to perform.

Acknowledgment

This research was financially supported by the Ministry of Education, Science and Technological Development of the Republic of Serbia.

References

[1] J. F. Gülich, Centrifugal Pumps, Springer Berlin Heidelberg New York, Springer-Verlag Berlin Heidelberg, 2008.

[2] S. Chantasiriwan, “Estimation of Power Consumption by Centrifugal Pump with Reduced Impeller Size”, Thammasat International Journal of Science and Technology, vol. 18, No. 1, 2013, pp.10-21.

[3] P. M. Patil, S. B. Gawas, P. P. Pawaskar, R. G. Todkar, “Effect of Geometrical Changes of Impeller on Centrifugal Pump Performance”, International Research Journal of Engineering and Technology (IRJET), vol. 02 Issue 02, 2015, pp.220-224.

[4] C. Somchart, “Estimation of Power Consumption by Centrifugal Pump with Reduced Impeller Size”, Thammasat International Journal of Science and Technology, vol.18, No.1. ,2013, pp. 10-21.

[5] P. Zhou, J. Tang, J. Mou, B. Zhu, Effect of impeller trimming on performance, WORLD PUMPS, Elsevier, pp.38-41, 2016.

[6] K. Joon-Hyung, L. Him-Chan, K. Jin-Hyuk, K.Sung, Y. Joon-Yong, C. Young-Seok, “Design techniques to improve the performance of a centrifugal pump using CFD”, Journal of Mechanical Science and Technology, vol. 29, no 1, 2015, p. 215-225.

[7] J. Pei, W. Wang, S. Yuan, “Multi-point optimization on meridional shape of a centrifugal pump impeller for performance improvement”, Journal of Mechanical Science and Technology, vol. 30, no. 11, 2016, p. 4949-4960.

[8] M. Lorusso, T. Capurso, M. Torresi, B. Fortunato, F. Fornarelli, S.M. Camporeale, R. Monteriso, “Efficient CFD evaluation of the NPSH for centrifugal pumps,” Energy Procedia, vol. 126, p. 778-785, 2017.

[9] D. Wu, S. Yang, B. Xu, Q. Liu, P. Wu, L. Wang, “Investigation of CFD Calculation Method of a Centrifugal Pump with Unshrouded Impeller,” Chinese Journal of Mechanical Engineering, Vol 27, pp. 376-383, 2014.

[10] M. Asuaje, F. Bakir, S. Kouidri, F. Kenyery, R Rey, Numerical Modelization of the Flow in Centrifugal Pump: Volute Influence in Velocity and Pressure Fields. International Journal of Rotating Machinery, no. 3, p. 244-255., 2005.

[11] S. Kim, S. Choi, Y. Lee, Y. Yoon, “Design Optimization of Centrifugal Pump Impellers in a Fixed Meridional Geometry using DOE”, International Journal of Fluid Machinery and Systems, Vol. 2, pp 172-178, 2009.

[12] J. Pei, W. Wang, S. Yuan, “Multi-point optimization on meridional shape of a centrifugal pump impeller for performance improvement”, Journal of Mechanical Science and Technology, vol. 30, pp. 4949-4960, 2016.

[13] V. Begović, Ž. Spasić, S. Milanović, “Analysis and determination of the performance of centrifugal pump using numerical simulations”, DEMI 2019, 14th International Conference on Accomplishments in Electrical and Mechanical Engineering and Information Technology, ISBN 978-99938-39-85-9, pp 335-340, 2019.

[14] S. Keawni, M. Chamaoot, S. Wongwises, “Predicting performance of radial flow type impeller of centrifugal pump using CFD,” Journal of Mechanical Science and Technology, vol. 23, pp 1620–1627, 2009.

[15] Ž. Spasić, M. Jovanović, J. Bogdanović-Jovanović, V. Begović, M. Kocić, “Effects of the impeller reduction on a centrifugal pump performance”, DEMI 2019, 14th International Conference on Accomplishments in Electrical and Mechanical Engineering and Information Technology, Banja Luka, ISBN 978-99938-39-85-9, pp 365-372, 2019.

[16] L. Wen-Guang, “Experiments on impeller trim of a commercial centrifugal oil pump”, The 6th International Conference on Hydraulic Machinery and Hydrodynamics Timisoara, Romania, October 21 - 22, 2004., pp. 217-222.

Mechanical design, development and engineering

THE 5th INTERNATIONAL CONFERENCE
MECHANICAL ENGINEERING IN XXI CENTURY

December 9-10, 2020
Faculty of Mechanical Engineering in Niš, Serbia

Zipline Design Issues and Analysis of the Influencing Parameters on Passenger's Velocity

Tanasije JOJIĆ, Jovan VLADIĆ, Radomir ĐOKIĆ

First Author affiliation: Faculty of Technical Sciences, Trg Dositeja Obradovića 6, Novi Sad, Serbia
Second Author affiliation: Faculty of Technical Sciences, Trg Dositeja Obradovića 6, Novi Sad, Serbia
Third Author affiliation: Faculty of Technical Sciences, Trg Dositeja Obradovića 6, Novi Sad, Serbia
tanasijejojic@uns.ac.rs, vladic@uns.ac.rs, djokic@uns.ac.rs

***Abstract*— This paper explains the issues of zipline designing and provides an analysis of the influencing parameters, relevant model forming, and the procedure for determining kinematic quantities of a passenger traveling along a zipline. The theoretical background consists of two parts, i.e. the first one, which includes static analysis based on catenary theory, and the second, which takes into account inertial forces, movement resistance, air resistance, wind effect, the position of a passenger during lowering, anchoring type, tightening force, etc, on the base of which it is possible to determine all necessary kinematic quantities which are essential for defining the so-called "driving characteristic" of zipline. The analysis are made by computer simulations where the size of significant parameters can be varied. Analysis results are given through diagrams that show a passenger's position, velocity, or acceleration in relation to time or a traveled distance for different lowering positions of the passenger.**

***Keywords*—zipline, anchoring type, air resistance, lowering position, computational model**

I. Introduction

The term "zipline" represents a system of tightened steel rope by which the person is carried by high speed travelling trolley. The trolley and person are moving under the influence of their own weight. The main aim is causing increased excitement, so-called adrenaline sport. They expanded over the past two decades, with construction in various locations such as hilly areas, parks, lakes, bridges, the city cores, etc.

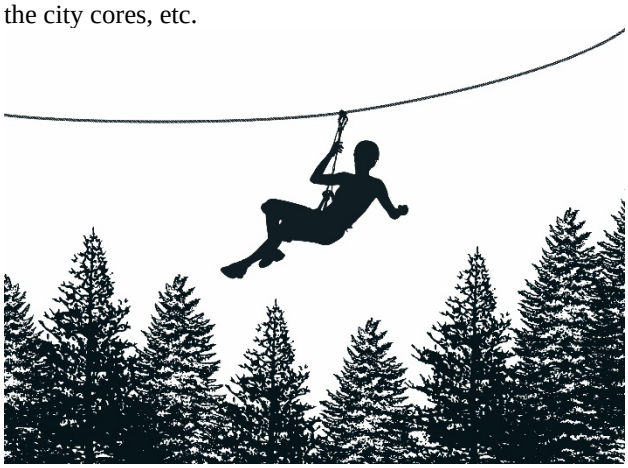

Fig. 1 An example of zipline

The most important kinematic parameters are maximum velocity and range. In accordance to the inclination angle (β), ziplines are classified into two groups - small inclination ziplines and large inclination ziplines (so-called ultimative ziplines). For small inclination ziplines, where the inclination angles are lower than 5°, there is mostly a problem with arriving to the lower station, especially in cases of unfavorable wind direction or changes of the area exposed to the air flow (body position, spreading of hands, etc) during movement. For large inclination angles, arrival to the lower station is practically certain, hence they are called ultimative. On the other side, they often have another problem – to high velocities at the entry of lower station which can be significant problem for safe stopping of the person.

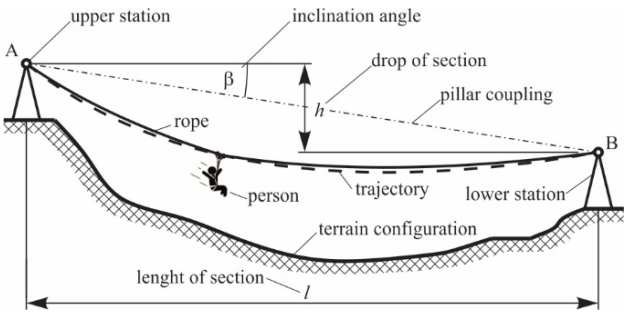

Fig. 2 A schematic representation of zipline with main notions

Furthermore, parameter due to which zipline is considered as an adrenaline sport is not velocity, but acceleration.

II. Fundamentals for first part of analysis

As the theoretical background is detailed described in previous papers such as [1]-[6], only a brief overview will be given here.

The line which represents an elastic flexible thread freely suspended between two supports located on the horizontal (l) and vertical (h) distance and loaded with its own weight (q) is called catenary.

Based on Fig. 3 and after certain mathematical transformations, a catenary equation can be written as:

$$y = C \cdot \mathrm{ch}\left(\frac{x}{C}\right) \tag{1}$$

where the catenary parameter (C) function of tension rope force (H) and the own weight of rope:

$$C = \frac{H}{q} \tag{2}$$

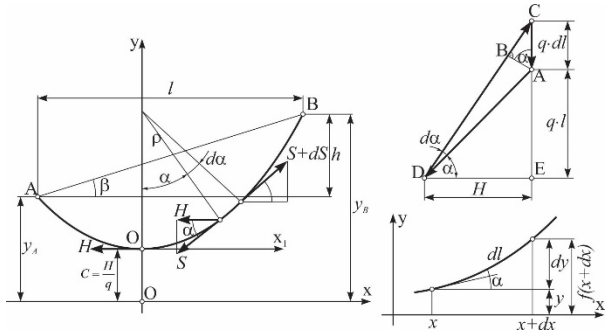

Fig. 3 Parameters of catenary

Catenary theory provides accurate solutions, but the usage of hyperbolic functions is relatively complicated for engineering practice, so the catenary is replaced by the appropriate parabola. This approximation leads to errors in the size of the deflections which amounts 2 ÷ 3%. Accuracy can be increased by introducing a correction coefficient (k). Fig. 4 shows some possibilities for replacing catenary with parabola.

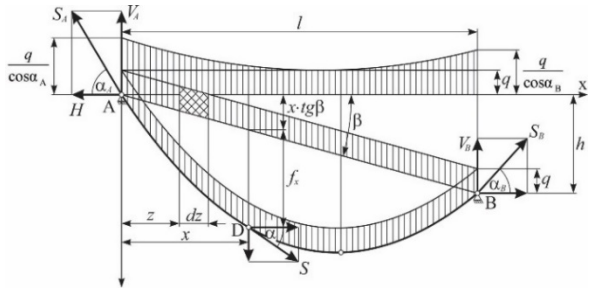

Fig. 4 Parameters of the parabola

Equation of parabola can be written as:

$$y = \frac{q \cdot x \cdot (l - x)}{2 \cdot H \cdot \cos\beta} \cdot k + x \cdot tg\beta \tag{3}$$

where the correction coefficient is calculated as:

$$k = 1 + \frac{\cos^2\beta}{p} \cdot \left[\frac{1}{p} \cdot \left(x^2 - l \cdot x + \frac{l^2}{2} \right) - 2 \cdot (l - 2x) \cdot tg\beta \right] \tag{4}$$

and the parameter of the parabola (p) as:

$$p = \frac{H}{q} \cdot \cos\beta \tag{5}$$

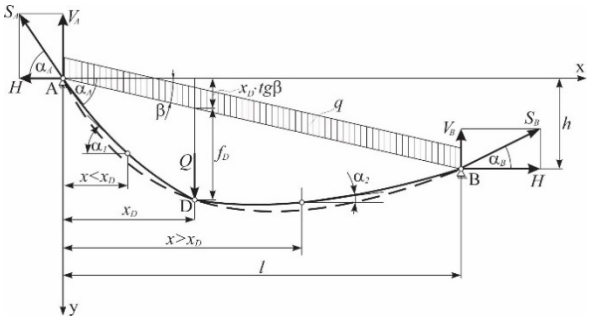

Fig. 5 Model of rope loaded with own weight and concentrated load

Fig. 5 shows a case of a rope, whose supports are at different heights, and which is loaded not only with its own weight but with a concentrated load too. The equation of the trajectory of a person which is lowering can then be represented as:

$$y = x \cdot \mathrm{tg}\beta + f_x \tag{6}$$

where the deflection at a distance x_D at which the load is acting is represented as:

$$f_D = \frac{x_D}{l \cdot H} \cdot \left[Q \cdot (l - x_D) + \frac{q \cdot (l - x_D)}{\cos\beta} \cdot \frac{l}{2} \right] \tag{7}$$

III. Fundamentals for the second part of analysis

The relevant computational model will be formed by neglecting small quantities of high order. The so-called static trajectory of movement is determined by expressions (6) and (7). Person connected with trolley forms a mathematical pendulum, but if the length of the connecting belts is small, the effect of the swing can be neglected as well as the influence of the centrifugal force due to the large radius of the trajectory curvature.

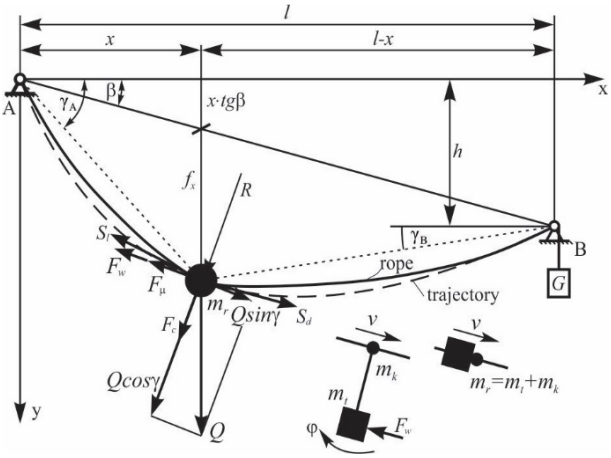

Fig. 6 Computational model of zipline

According to that, the computational model of the zipline, which is shown in Fig. 6, can be represented as the movement of a concentrated mass along the trajectory determined for static conditions. The air resistance and rolling resistance are acting on the concentrated mass while moving in the direction which is always opposite to the direction of movement.

$$F_w = c_w \cdot A \cdot \frac{\rho \cdot (v \pm v_v)^n}{2} \tag{8}$$

According to equation (8), the value of air resistance depends on:

- drag coefficient (c_w),
- area exposed to the air-flow (A),
- air density (ρ),
- relative velocity between the object and airflow (wind), and
- dimensionless coefficient (n), which has value of 2 for velocities between 1 m/s and 300 m/s [7].

As the air density changes relatively little for some standard conditions, and the velocity is more often expressed in km/h than in m/s, the equation (8) can be written in the form:

$$F_w = 0,0473 \cdot c_w \cdot A \cdot v^2 \quad (9)$$

whereby the specific air density is taken as ρ=1,225 kg/m^3, medium air humidity as w=60 %, and medium air temperature as t=15^0 C. If temperature or atmospheric pressure vary from ordinary, air density can be calculated as:

$$\rho = 1,25 \cdot \frac{B}{1,015} \cdot \frac{293}{T} \quad (10)$$

where the pressure (B) is expressed in bar, and the temperature (T) in kelvin.

Fig. 7 shows various lowering positions which have an impact on area exposed to air and drag coefficient.

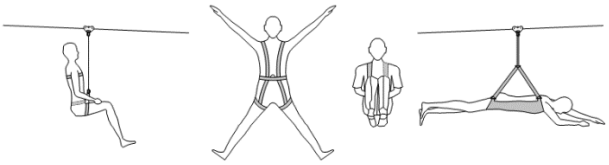

Fig. 7 Various lowering positions

Recommendations for determination of drag coefficient and areas exposed to airflow for various lowering positions are detailed explained in [1], [5] and [8]-[10].

Unlike every other wheel that is rolling along a deformable surface which has a resistance component due to the friction in wheel bearings and due to deformation of contact surfaces, the wheel that is rolling along the rope and has an additional resistance component due to rope stiffness. Unlike a perfectly flexible rope, the real rope will not take the position of the tangents behind and in front of the wheel, which can be seen as a “wrinkling” of rope in front of the wheel.

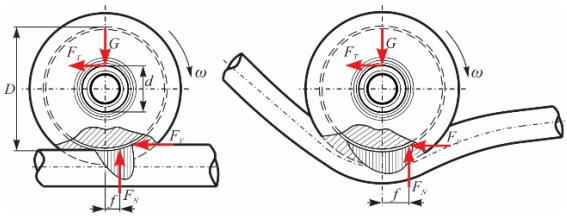

Fig. 8 Zipline wheel model

IV. Results of Analysis

The analysis results which are given below are for the case of a hypothetical zipline of horizontal distance between stations of 1,5 km between which a rope of own weight of 1 kg/m is stretched.

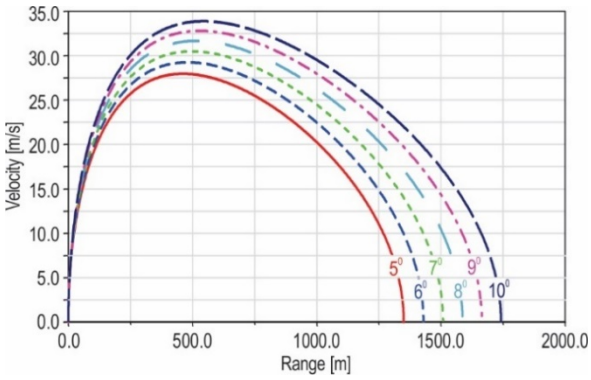

Fig. 9 Diagram of velocity for different inclination angle

Diagram shown in Fig. 9 shows velocity as function of travelled distance for various inclination angles, for tensile rope force of 50 kN and person weighting 50 kg which is lowering in sitting position. It is considered that area exposed to air flow of person lowering in sitting position has value of 0,3 m^2, and drag coefficient of 0,6.

Another factor that has a huge influence on the kinematic parameter is the tensile rope force. Diagram shown in Fig. 10 shows range of person weighing 50 kg as function of traveling time for tensile rope force of 20 kN, 40 kN and 60 kN for inclination angle of 7^0 and sitting lowering position.

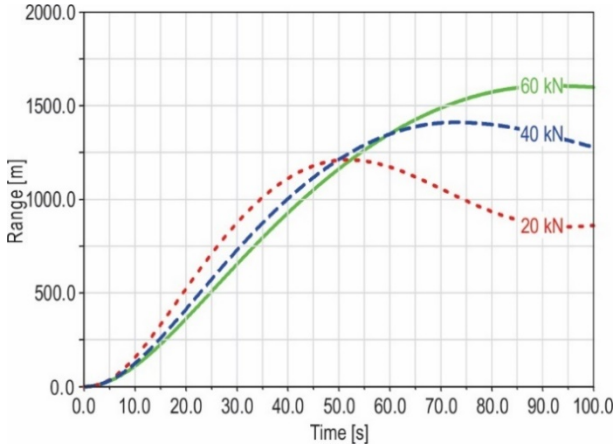

Fig. 10 Diagram of range for different tensile rope force

Diagram shown in Fig. 11 shows velocity for three different masses which can be expected. Under maximal mass of 180 kg is considered lowering of two persons on same trolley.

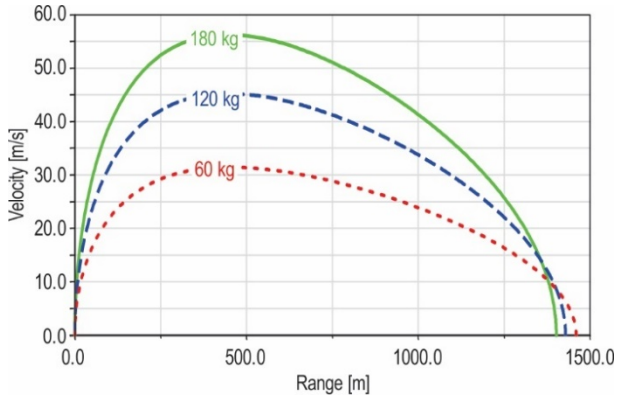

Fig. 11 Diagram of velocity for different values of person’s mass

As the sitting, half-sitting and lying lowering positions are most commonly used, the diagram shown in Fig. 12 shows velocity as the function of range for those three positions.

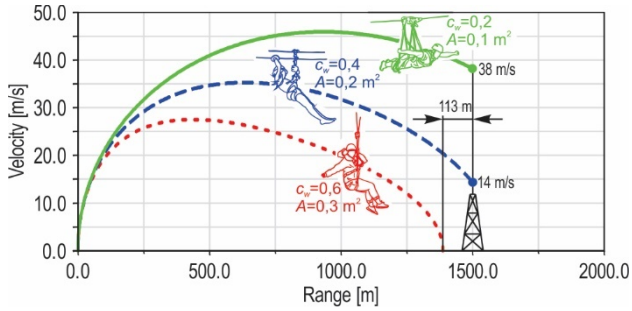

Fig. 12 Diagram of velocity for different lowering positions

V. Conclusions

The most significant parameter is, as mentioned above, the inclination angle. However, since the positions of the stations are mostly already determined, the designers of zipline cannot affect them.

The person's mass has a relatively huge impact on kinematic characteristics, but the designers cannot affect that either. However, if necessary, there is a possibility to attach additional weights to the trolley.

Based on the diagram shown in Fig. 11, it can be concluded that heavier passengers achieve higher velocities, but shorter ranges.

The parameter that has a relatively large impact on range, and which can be easily influenced, is the tensile rope force. In addition to the values of tensile rope force, a slightly smaller influence on driving characteristics has the anchoring type which is detailed discussed in [2].

A parameter that has a relatively large impact on driving characteristics, and which can also be easily influenced is the person's lowering position. Different lowering positions have different surfaces exposed to airflow, but also to different drag coefficients.

References

[1] J. Vladić, R. Đokić, T Jojić, "Theoretical analysis and determination of zipline movement parameters", Tehnika, vol. 68, No. 3, pp. 405-412, 2019.

[2] T. Jojić, J. Vladić, R Đokić, "Anchorage type and tension rope force impact on zipline's kinematic characteristics", Machine Design, vol. 11, No. 4, pp. 149-154, 2019.

[3] J. Vladić, "The Parametric of Equation of a Catenary Line and Theoretical Foundations for Static Analysis a Ropeway", Proceedings of XV European Conference of Material Handling Teaching Professors, pp. 170-178, Novi Sad, Serbia, 2004.

[4] E. Czitary, "Seilschwebebahnen", Springer-Verlag, Wien, 1962.

[5] R. Đokić, J. Vladić, T. Jojić, "Zipline computational model forming and impact of influential sizes", Proceedings of TIL 2019, pp. 71-74, Niš, Serbia, 2019.

[6] T. Jojić, J. Vladić, and R. Đokić, "Specific machines and devices with horizontal rope as carrying element – zipline", Proceedings of the Faculty of Technical Sciences, vol. 33, No. 1, pp. 13-16, 2018.

[7] A. Janković, Car dynamic, Faculty of Mechanical Engineering, Kragujevac, 2008.

[8] J. Vladić, R. Đokić, and T. Jojić, "Elaborats I, II and III - Analysis of the zipline system in Vrdnik", Faculty of Technical Sciences, Novi Sad, 2017.

[9] J. Vladić, T Jojić, R. Đokić, A. Gajić, "Theoretical backgrounds for zipline analysis", Proceedings of MHCL 2019, pp. 147-150, Vienna, Austria, 2019.

[10] H. K. Mun, S. Abdulkareem, A. Mahdi, "Calculation of Aerodynamic Drag of Human Being in Various Positions", Proceedings of EURECA 2013, pp. 99-100, Subang Jaya, Selangor Darul Ehsan, Malaysia, 2013.

THE 5th INTERNATIONAL CONFERENCE
MECHANICAL ENGINEERING IN XXI CENTURY

December 9-10, 2020
Faculty of Mechanical Engineering in Niš, Serbia

Current State of Fused Deposition Modelling 3D Printer Systems

Marko V. MLADENOVIĆ, Natalija B. TOMIĆ, Boban R. ANĐELKOVIĆ, Miloš S. MILOŠEVIĆ

Marko V. Mladenović: Faculty of Mechanical Engineering, University of Niš;
Research and development, Harder Digital Sova, Niš, 18000
Natalija B. Tomić: Faculty of Mechanical Engineering, University of Niš
Boban R. Anđelković: Faculty of Mechanical Engineering, University of Niš
Miloš S. Milošević: Faculty of Mechanical Engineering, University of Niš
mladenovic.marko@hotmail.com, natalija.tomic@masfak.ni.ac.rs, boban.andjelkovic@masfak.ni.ac.rs, milos.milosevic@masfak.ni.ac.rs

***Abstract*— Since their appearance in 1992. Fused Deposition Modelling (FDM) 3D printers have shown the potential to become one of the most economical additive manufacturing techniques. Fused Deposition Modelling (FDM) started to rapidly develop by the expiration of the FDM patent and the subsequent worldwide development of low cost FDM machines by a huge number of small companies. Today, there is a large range of these machines in development and on the market with different printing mechanics. The purpose of this paper is to present different types of FDM machines based on their kinematics as well as pros and cons of different design types of FDM machines and their elements. This paper also present different advanced features designed to suit specific purpose, solve specific problems or improve on other designs.**

***Keywords*— Additive Manufacturing, Fused Deposition Modelling, 3D Printing Mechanisms**

I. Introduction

In 1986, Charles Hull patented his innovation, a process known as Stereolithography (SLA) in the field of additive technologies [1]. The publication of the patent was followed by the development of the field of additive manufacturing known as 3D printing [2].

The additive manufacturing (AM) is constantly growing thanks to its innovative design capacities [3]. The market for this technology is, according to forecasts for 2017, around 5 billion US dollars [4]. Currently, additive manufacturing is becoming a mean of producing end products [5]. Additive manufacturing is widely used in different areas of industry and science such as: engineering for custom products, functional models, pre-surgical models, conceptual models, aircraft, dental prostheses, medical implants and automotive products [6]. However, it is considered that the greatest progress has been made in the use of additive manufacturing in the construction industry [7].

Three-dimensional printing (3D printing) is an Additive manufacturing technique for creating a wide range of structures and complex geometries. Those components are made from three-dimensional (3D) model data which offers design and material freedom. It can be anything, from toys to human bone implant [8]. 3D printing has made it possible to reduce the cost of investing in rapid prototyping and production and the time required for development [9]. According to Keaveney et al [9], current developments in the 3D printing industry have revolutionized the way people view the manufacturing process. The rapid development of 3D printers and the availability of increasingly low-cost components that make it up have led to the cost of 3D printers becoming affordable to almost everyone. The prototyping and manufacturing stages become closer not only to innovators but also to everyone else.

Various 3D printing technologies have been developed. The most striking division of these technologies is based on the aggregate state of the base material they use for printing. The principle of forming a component with additive technologies that use liquid base material differs essentially from those that use base material in solid state. Even with additive technologies that use a solid base material, there is a difference between those that use powder and those that use continuous filament material. There is also a significant difference in additive technologies based on the material used for printing. The most used materials are plastic and metal, but there are also printers for ceramics [2, 10], biomaterials [11-13], cement [14, 15], food [16], etc.

Giberti et al [3], have formed a table with some 3D printing technologies and the years associated with their invention, as well as their inventors companies. This in presented on Table I.

TABLE I Technologies for 3D printing [3]

Company	Foundation year	3D printing technology
3D Systems, USA	1986	SLA, SLS
Stratasys, USA	1992	FDM, Polyjet
ExOne	2005	Binder jetting

El-Sayegh et al [17], in their research paper give a schematic representation of existing additive manufacturing techniques. This schematic representation is presented on Figure 1.

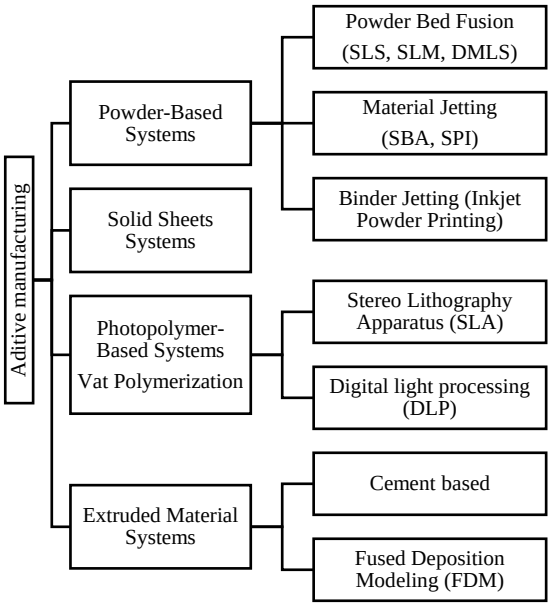

Fig. 1 Additive manufacturing techniques [17]

Typically, AM process use Computer Aided Design (CAD) model to fabricate 3D component. Although there are different technologies, the basic principle of component formation is the same, it adds material layer by layer, in contrast to most traditional manufacturing methods that subtract material. 3D printing technologies rely on computer numerical control (CNC) systems for precise and accurate processing.

II. Fused Deposition Modelling (FDM)

The FDM process use solid plastic (continuous filament) as a material for building components. This plastic is supplied to the nozzle by a flow-control motor. In the nozzle, the plastic is heated to a semi-liquid state. It is then distributed in a controlled manner on the platform or the previous layer on a layer-by-layer technique.

The essential property for this method is the thermoplasticity of the polymer filament [2]. It allows the filaments to fuse together during printing and then to solidify at room temperature.

Although, functional components can be made by the FDM process, the stepped structure on the surface is noticeable (anisotropy in the vertical, z-direction) [16]. Poor surface quality that requires post finishing is actually the biggest disadvantage of this printing method [6]. Although this disadvantage, FDM process is the most commonly used additive manufacturing technique. This can be explained by the low cost and availability of FDM process printers on the market. The price for those printers is very reasonable [18] and most households can afford it. In addition to low cost and availability, another important advantage of these printers is that they significantly reduce product development and production time and cost [19]. Also, the availability of software that is mostly open source is noticeable [20]. The possibility of high-speed printing, ie the production of components and simplicity of the process can also be mentioned as an advantage of the FDM process.

The materials most commonly used for the FDM process are [21]: Acrylonitrile Butadiene Styrene (ABS), Poly Carbonate (PC), Polylactic Acid (PLA), Polyethylene Terephthalate (PET), Thermoplastic Polyurethane (TPU), Nylon, etc. The material used for printing greatly affects the quality of the printed component [21, 22]. However, Wittbrodt and Pearce [22] proved that the colour of the same type of plastic affects the quality and technical properties of the printed component.

The printing process parameters have the most significant influence on the quality of the printed part. Their influence on mechanical characteristics such as: part build orientation, layer thickness, raster angle, part raster width and raster to raster gap, is expressed [23]. Printing process parameters adjustment is an area that is currently in development not only by scientists, but also from printer users.

Another important influence on the quality of the 3D printed part comes from the mechanism used by the printer. The moving parts of the FDM printer are the platform and the nozzle or just one of them.

The cost of a 3D printed component with FDM process depends on the type of plastic, the type of filling (plastic consumption) and the time required to make the part, ie the printing speed. Usually it is determinated by automated calculators that take input from user for all important parameters, and then give price for specific 3Dmodel and parameters to user [24].

III. FDM printer mechanisms

Since the advent of the FDM printer, many different mechanisms of this printing method have emerged. All of these mechanisms can generally be divided into five groups [25]:

- Cartesian,
- Delta,
- SCARA,
- Polar,
- Robotic arm.

A. *Cartesian printers*

The first FDM printers used a Cartesian mechanism. Therefore, it is obvious that this group of mechanisms is the most developed, most represented on the market and has the most variations. Cartesian printers, as their name suggests, use the Cartesian coordinate system, their movement is in the X, Y and Z directions. The Cartesian printer mechanisms can be divided into five subgroups based on the way they move:

- the platform moves horizontally along one axis (X or Y), extruder moves vertically (Z) and along other horizontal axis, (Fig. 3.a)
- the platform moves vertically (Z), the extruder moves along two axes (X and Y), (Fig. 3.b)
- the platform moves vertically (Z) and along one of the horizontal axes (X or Y), the extruder moves along other horizontal axis, (Fig. 3.c)
- the platform does not move, the extruder moves in all tree axes, (Fig. 3.d)
- the platform moves horizontally (X and Y), the extruder moves vertically (Z). (Fig. 3.e)

Figure 2.a presents typical appearance of the Cartesian printer mechanism. Figure 3 presents the Cartesian printer mechanisms subgroups.

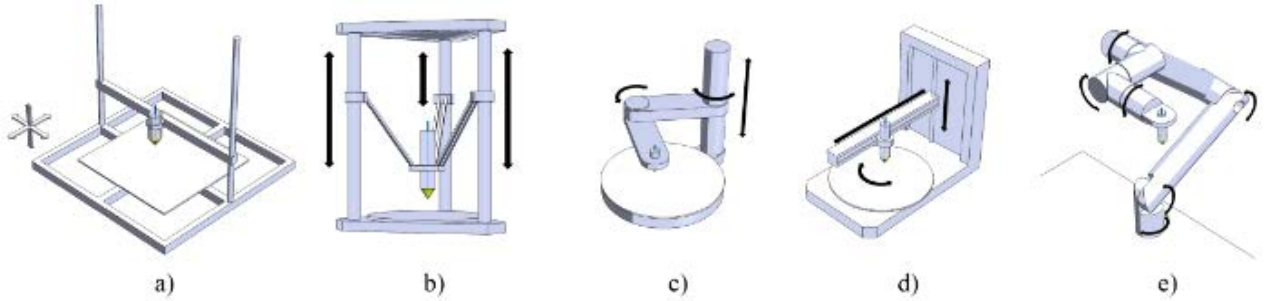

Fig. 2 FDM 3D printer mechanisms: a) Cartesian, b) Delta, c) SCARA, d) Polar and e) Robotic Arm

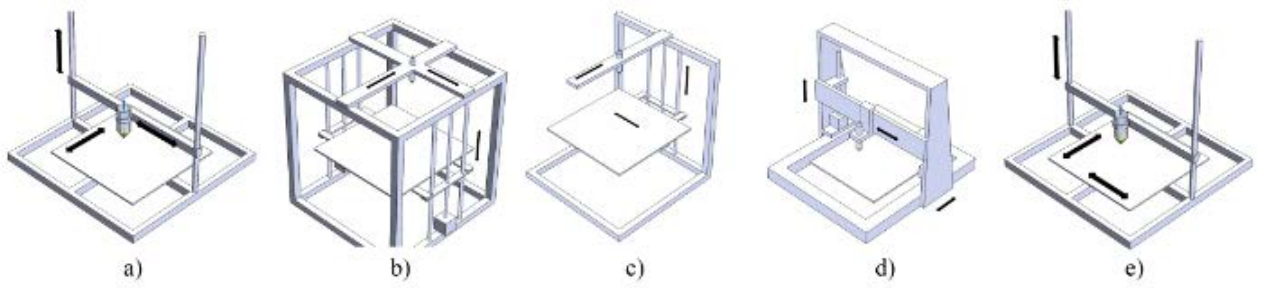

Fig. 3 Cartesian printer mechanisms: a) Mechanism 1, b) Mechanism 2, c) Mechanism 3, d) Mechanism 4 and e) Mechanism 5

B. Delta printers

First Delta 3D printer was a custom-made product by unknown inventor. Since it was open-source, and everybody could see it, many companies and users have seen its potential. Soon after, first delta 3D printer was appearing on market [20]. Delta printers are the second most developed and most represented printers on the market [25].

The way axes are arranged differ Delta printers from Cartesian printers. Delta printers have three vertical axes [26], and because of that, these printers have usually triangular frame. All three axis are mounted so that the stroke is in the vertical direction. Nozzle is placed on carriage. The carriage is mounted on the axis movement and forms one side of a link of parallel arms that connect the carriage to the effector. The platform is usually fixed. Movement of axis affects movement of carriage; axis moves up and down and carriage moves along with it [26].

Schmitt et al [27], in their comparative study proved that a Delta printer gives better surface quality and prints longer than a Cartesian printer for the same parameter settings. Also, a larger deviation in dimensions compared to the CAD model was noticed with the component printed on a Delta printer [27].

Figure 2.b presents typical appearance of the Delta printer mechanism.

C. SCARA printers

The SCARA is actually an abbreviation of “Selective Compliance Assembly Robot Arm” [28]. It was developed in Japan in 1981. by Sankyo Seiki [28]. The SCARA system is widely used in industry but has only recently begun to be used as a 3D printing mechanism. There are not many of these printers on the market and they cannot be found at a low cost like Delta and Cartesian printers. The price for the cheapest Delta and Cartesian printers is approximately 170 US dollars [29], and the cheapest SCARA printer is 1995 US dollars [30].

The SCARA mechanism use Cartesian coordinate system. The mechanism is based on joined arm which moves in two dimensions (X and Y). The movement of platform or the arm provides third dimension in vertical (Z) direction.

Figure 2.c presents typical appearance of the SCARA printer mechanism.

D. Polar printers

The Polar 3D printers, like SCARA printers, are still in the early stages and are not yet as reliable as both Cartesian and Delta printers [31]. These printers are not much represented in the market [18].

The Polar printers use polar coordinate system. The nozzle is moving on horizontal and vertical direction and the platform is rotational [31]. In addition to its rotating motion, the circular print bed can also move forward and backward. The frame is L-shaped, with the filament spool feeding the extruder from the back similar to most 3D printers with a Cartesian mechanism. Another difference between Cartesian and Polar 3D printer is that Polar printers takes up less space, and they are better for making rotational components.

Figure 2.d presents typical appearance of the Polar printer mechanism.

E. Robotic Arm printer

Robotic Arm are widely used in industry and this is their most significant application. There are very few of these mechanisms in the field of 3D printing industry and their cost is around 5 000 US dollars [32].

The Robotic Arms are used for printing in, mainly, 6 dimensions. The platform is stationery and end of arm with nozzle moves. The Robotic Arms are mainly used for large-scale 3D printing [33] because all movements are performed by the arm.

Figure 2.e presents typical appearance of the Robotic Arm printer mechanism.

IV. Current state of FDM system elements

During development of FDM many different concepts have been tested. The most popular and most efficient ones are in use today and are still developed.

A. Extruder mechanism

Efficient and precise extruder mechanism is one of most important part of FDM system.

The basic extruder mechanism consists of a heating part, nozzle and extruder motor. Due to the need to obtain a better surface quality, stability of process or to achieve specific goals or print difficult to print materials, this system may also contain other accessories such as a fan that helps cool the printed plastic to allow us to print faster, filament runout detection to allow repayable printing of large objects.

The heating part serves to heat the filament of the base material to a semi-liquid state. The height of the temperature is completely controllable and is adjusted before the start of printing depending on the material to be printed. The temperature can also be adjusted during printing.

The nozzle is the mechanical part of the 3D printer that extrudes the filament. There are three major characteristics integral to a nozzle's design: its size, material, and inner diameter [20]. The size of the nozzle means its physical mass and length. Standard values with M6x1 thread are used and the most common length is 12mm to 13mm [18]. The various materials are used for the production of nozzles, such as: Brass, Stainless Steel, Hardened Steel, etc. Each material has its own characteristics and affects the quality of printing. The most commonly used material is brass and it is also low- cost [20]. This material is not of great quality and such nozzles can be easily damaged. The inner diameter of the nozzle affects the amount of plastic extruded per second. This property is also known as flow. It determines the maximum extrusion speed.

Larger nozzles have inner diameter larger than 0.4 mm. These nozzles reduce the time required for printing. They are recommended for use when the base material has abrasive properties [20].

Smaller nozzles have inner diameter less than 0.4 mm. Such nozzles are used when high accuracy of dimensions and quality of the printed part is required.

Many variations of extruder mechanisms have been developed and tested with various success. There are mechanisms with two or more nozzles. Current development of those mechanisms goes in couple directions depending on applications.

There are mechanisms, as stated by Pascale and Simion [34], that focuses on combining multiple materials in single printed part for obtaining different mechanical and aesthetic properties. Improvements in multi-material extruders, allows to manufacture unique parts difficult or even impossible to produce by conventional methods. Focus of these improvements is on combining multiple materials in single printed part for obtaining different mechanical and aesthetic properties. In the current state of development, multi material printing is possible due extensive work of many researchers, advancing this branch to solve specific problems emerging from their fields of research.

On the other way, there are advances in designing nozzles for only one material whose characteristics are specific. Requirements for different material properties led to development of specialised extruders for producing parts out of materials difficult to print because they usually require higher temperature, have abrasive properties or have some other specific property, that make them inadequate for standard extruder systems. For example, Heidari-Rarani et al [35], successfully developed a special extruder system for placing carbon fibers inside printed part.

Additive manufacturing is known for less waste of material during manufacturing process but it is still generated. As 3D printing community gets bigger, more and more waste is generated as part of process or some product malfunction. To solve these problems, especially for FDM process some clever ways of recycling are development. Great recycling capabilities of parts produced by FDM 3D printing, are getting improved by developing extruders that can use waste filament and failed prints to produce new parts directly in house, which can greatly reduce costs and help us save nature at the same time. This is presented by Valkenaers et al [36].

Development of FDM extruder systems searches for more precise solutions capable for responding to all growing demand for micro systems and mechanics. The hybrid solutions are one way to go as it was presented by Zhang et al [37]. In search for more precise extruder even hybrid solutions that can produce high resolution 3D models are being developed for micro systems. Those systems combine standard FDM with electro-hydrodynamic technics to fabricate micro structures for bioengineering applications.

B. 3D printer bed surface

Extruding system as system that directly influence characteristics and capabilities of FDM printer is just one part of large picture that incorporates FDM process. Second important part is base surface to be printed upon, commonly known as a bed. In order for the printing to be successful, the bed surface is heated to a certain temperature before printing. The temperature depends on the type of plastic used for printing and serves to keep the base of the printed part on the surface until printing is complete. This temperature is controllable and can be changed during printing.

Different materials have different requirements for bed surface. Some require glass surface, heated surface or surface based on other materials and with different coating and temperature requirements. These mostly composite build surface and coatings are developed continuously with different researches focused to achieve best performances for specific materials or general use. One of such research is presented by Messimer et al [38].

C. Basic materials

Although it is noted that Additive manufacturing is used in almost every existing branch of science and industry, the FDM process is most often used for printing plastic components [39].

Main problem of 3D printing in general is limited availability of materials that can be used. This is major problem that is constantly occupying researchers all around the world. Major advancements have been made in this branch not only to allow usage of already existing materials, but also to introduce new materials specifically

developed for FDM 3D printing. Those new materials followed by other necessary changes push evolution of 3D printing from day to day.

Further development of composite materials demanded new researches in field of Additive technologies. One such research was done by Heidari-Rarani et al [35]. Introduction of fiber reinforced material, and ways to place continuous fiber true part in desired orientation leads to possibility of producing strong durable parts with different properties depending on need, greatly expanding possibilities of usage of 3D printed parts as final product of high quality. At the same time, some necessary changes have been made to accommodate, well established technical materials. This is presented by Berretta et al [40].

Extensive search for new and improved materials is taking place not just in additive manufacturing but in industry as whole. As process that can be highly controllable, and allow us to combine different materials into one part different methods for fiber reinforcements have been developed and in use today.

D. Other

Improvements of different subsystems of FDM 3D printers have led to greater capabilities from aspect of materials, precision and environment control. Anisotropic properties of 3D printed parts led to implementation of 6DOF motion capable FDM machines, as presented by Alsharhan et al [41]. This implementation could be further improved if combined with special extruder systems for placing carbon fibers inside printed part.

Improvements in mechanical aspect of FDM is followed closely by improvements of control software. Different advanced algorithms for generating optimal manufacturing process control code are developed from day to day. Advances of control algorithms and electronics allow 4, 5 or 6 DOF machines to be possible and greatly improve control of mechanical properties, by advanced control of filament deposition path.

As industry 4.0 is currently future manufacturing standard it is being implemented through internet of things into FDM process today. As it is presented by Mayandi et al [42].

V. Results (Discussion)

From early days of additive manufacturing by fused deposition different kinematic models were used, tested and improved. Limitations of current state of technology are dictating ways of development of those machines, and are evolving from day to day. Early limitation for development of high speed and precision machines was introduced mostly by control units available at the time. Development of low-cost and fast control units, allowed usage of more complex kinematics calculations, and development of fast low inertia designs. Even farther development of control electronics, and maturing of control software allowed different advanced functions to be introduced to today 3D printer machines.

Many different designs are in wide use today resulting in fast development and improvements upon different aspects of FDM process and machines.

All mentioned improvements greatly extend capabilities of FDM. With introduction of more than 3 axes those capabilities improve even further. Introduction of multi axes 3D printers is important for industry because it allows us to produce mechanically optimised products, with desired properties, as well as eliminating need for supports thus reducing filament waste and post processing time.

New software, now days even supported by artificial intelligence, make producing of new parts easier and safer every day. Automated printing preparation and monitoring solutions are already available. Great effort is invested currently by community, companies and independent researchers in development and implementation of remote monitoring and control. That will allow many peoples to monitor long printing process while completing other things freely.

Possibility for improvements of FDM process still exist, but maybe require thinking out of box to find out and implement. Hybrid systems of FDM with electro-hydrodynamic for fabricating micro structures for bioengineering applications are direct example of that.

VI. Conclusion

This paper presents current state of FDM thru presenting state of development and usage of different FDM 3D printing mechanisms, new views on ways to improve current 3D printing process and introduce new materials. Thru paper there are presented some of major pros and cons of printer mechanisms. This paper also presents some of most advanced work that has been done in field of FDM 3D printing.

3D printing has great potential for integration in to industry 4.0, as well in to reducing costs of prototyping and even manufacturing. The main issue of 3D printing technology is surface quality of final product, but this field is being developed constantly, and improvements are constant. All of those and many other researches and improvements that are being developed constantly, are the proof that FDM 3D Printing is technology of the future.

Acknowledgment

This research was financially supported by the Ministry of Education, Science and Technological Development of the Republic of Serbia.

References

[1] http://www.google.com/patents/US4575330#v=onepage&q&f=false (accessed on 22.10.2020.).

[2] T. D. Ngo, A. Kashani, G. Imbalzano, K. T.Q. Nguyen, D. Hui, “Additive manufacturing (3D printing): A review of materials, methods, applications and challenges”, Composites part B: Engineering, vol.143, 2018, pp. 172-196.

[3] H. Giberti, E. Fiore1 and L. Sbaglia,” Kinematic synthesis of a new 3D printing solution”, MATEC Web of Conferences 45, 2016.

[4] B. N. Turner, R. Strong and S. A. Gold, “A review of melt extrusion additive manufacturing processes: I. Process design and modeling”, Rapid Prototyping Journal, Vol. 20, 2014, pp. 192 – 204.

[5] A. R. Avdeev, A. A. Shvets and I. S. Torubarov, “Investigation of Kinematics of 3D Printer Print Head Moving Systems”, Proceedings of the 5th International Conference on Industrial Engineering (ICIE 2019), Springer, vol.1, 2019, pp. 461-471.

[6] O. A. Mohamed, S. H. Masood and J. L. Bhowmik, “Optimization of fused deposition modeling process

parameters: a review of current research and future prospects", Adv. Manuf, vol. 3, 2015, pp. 42-53.

[7] P. Wu, J. Wang and X. Wang, "A critical review of the use of 3-D printing in the construction industry", Automation in Construction, vol. 68, 2016, pp. 21-31.

[8] K. Husain, M. Rashid, N. Vitković, J. Mitić, J. Milovanović and M. Stojković, "GEOMETRICAL MODELS OF MANDIBLE FRACTURE AND PLATE IMPLANT", Facta Universitatis, Series: Mechanical Engineering, vol. 16, 2018, pp. 369-379.

[9] S. Keaveney, P. Connolly and E. D. O'Cearbhaill, "Kinematic error modeling and error compensation of desktop 3D printer", Nanotechnology and Precision Engineering, vol.1, 2018, pp. 180-186.

[10] N. Travitzky, A. Bonet, B. Dermeik, T. Fey, I. Filbert-Demut, L. Schlier, T. Schlordt and P. Greil, "Additive Manufacturing of Ceramic-Based Materials". Advanced Engineering Materials. vol. 16, 2014, pp. 729-54.

[11] X. Cui, K. Breitenkamp, M. Finn, M. Lotz and D.D. D'Lima, "Direct human cartilage repair using three-dimensional bioprinting technology", Tissue Engineering Part A, vol. 18, 2012, pp. 1304-1312.

[12] N. Cubo, M. Garcia, J.F. del Cañizo, D. Velasco and J.L. Jorcano,"3D bioprinting of functional human skin: production and in vivo analysis", Biofabrication, vol. 9, 2016.

[13] V.H. Mouser, R. Levato, L.J. Bonassar, D.D. D'lima, D.A. Grande, T.J. Klein, D.B. Saris, M. Zenobi-Wong, D. Gawlitta and J. Malda, "Three-dimensional bioprinting and its potential in the field of articular cartilage regeneration", Cartilage, vol. 8, 2017, pp. 327-40.

[14] A. Perrot, D. Rangeard and A. Pierre, "Structural built-up of cement-based materials used for 3D printing extrusion techniques", Materials and Structures, vol. 49, 2015, pp. 1213-1220.

[15] G. J. Gibbons, R. Williams, P. Purnell and E. Farahi, "3D printing of cement composites", Advances in Applied Ceramics, vol. 109, 2010, 287-290.

[16] A. Pandian, C. Belavek, "A review of trends and challenges in 3D printing", Proceeding of the American Society for Engineering Education ASEE, 2016.

[17] S. El-Sayegh, L. Romdhane and S. Manjikian, "A critical review of 3D printing in construction: benefts, challenges, and risks", Archives of Civil and Mechanical Engineering, 2020, pp. 20-34.

[18] http://amazon.com (accessed on 28.10.2020.)

[19] P. Wu, J. Wang and X. Wang, "A critical review of the use of 3-D printing in the construction industry", Automation in Construction, vol. 68, 2016, pp. 21-31.

[20] https://all3dp.com (accessed on 28.10.2020.)

[21] https://www.3dhubs.com (accessed on 31.10.2020.)

[22] B. Wittbrodt and J. M. Pearce, "The Effects of PLA Color on Material Properties of 3-D Printed Components", Additive manufacturing, vol. 8, 2015, pp. 110-116.

[23] A. K. Sood, R.K. Ohdar and S.S. Mahapatra, "Parametric appraisal of mechanical property of fused deposition modelling processed parts", Materials and Design, vol. 31, 2010, pp. 287-295.

[24] https://www.3dprintplant.rs (accessed on 22.11.2020.).

[25] https://top3dshop.com (accessed on 27.10.2020.)

[26] C. Bell, "3D Printing with Delta Printers", Springer Science + Business Media New York, 2015.

[27] B. M. Schmitt, C. F. Zirbes, C. Bonin, D. Lohmann, D. C. Lencina and A. C. S. Netto, "A Comparative Study of Cartesian and Delta 3D Printers on Producing PLA Parts", Materials Research, vol. 20, 2017, pp. 883-886.

[28] http://www.sankyo-seiki.co.jp (accessed on 27.10.2020.)

[29] https://www.3dnatives.com (accessed on 28.10.2020.)

[30] https://www.3ders.org (accessed on 28.10.2020.)

[31] https://3dinsider.com (accessed on 28.10.2020.)

[32] https://www.mybotshop.de (accessed on 28.10.2020.)

[33] X. Zhang, M. Li, J. H. Lim, Y. Weng, Y. W. D. Tay, H. Pham and Q. C. Pham, "Large-scale 3D printing by a team of mobile robots", Automation in Construction, vol. 95, 2018, pp. 98-106.

[34] D Pascale and I. Simion, "Multi-Material 3D Printer Extruder Concept", Journal of Industrial Design and Engineering Graphics, vol. 13, 2018, pp. 25-28.

[35] M. Heidari-Rarani, M. Rafee-Afarani and A.M. Zahedi, "Mechanical characterization of FDM 3D printing of continuous carbon fiber reinforced PLA composites", Composites Part B, vol. 175, 2019, Article 107147.

[36] H. Valkenaers, F. Vogeler, E. Ferraris, A. Voet and J-P Kruth, "A novel approach to additive manufacturing: screw extrusion 3D-printing", 10th International Conference on Multi-Material Micro Manufacture, 2013, San Sebastian, Spain.

[37] B. Zhang, B. Seong, VD. Nguyen and D. Byun, "3D printing of high-resolution PLA-based structures by hybrid electrohydrodynamic and fused deposition modeling techniques", Journal of Micromechanics and Microengineering, vol. 26, 2016, IOP publishing.

[38] S. L. Messimer, A. E. Patterson, N. Muna, A. P. Deshpande and T. R. Pereira, "Characterization and Processing Behavior of Heated Aluminum-Polycarbonate Composite Build Plates for the FDM Additive Manufacturing Process", Journal of Manufacturing and Materials Processing, vol. 2, 2018, article 12.

[39] https://www.treatstock.com (accessed on 22.11.2020.)

[40] S. Berretta, R. Davies, Y.T. Shyng, Y. Wang, O. Ghita, "Fused Deposition Modelling of high temperature polymers: Exploring CNT PEEK composites", Polymer Testing, vol. 63, 2017, pp. 251-262.

[41] A. T. Alsharhan, T Centea and S. K. Gupta, "ENHANCING MECHANICAL PROPERTIES OF THIN-WALLED STRUCTURES USING NON-PLANAR EXTRUSION BASED ADDITIVE MANUFACTURING", Proceedings of the ASME 2017 12th International Manufacturing Science and Engineering Conference MSEC2017, 2017, Los Angeles, CA, USA.

[42] K. Mayandi, P.S. Ramalingam, S. K. Ganapathy, N. Srivathsan and M. Vasanth, "An Interpretation on Automated 3D Printer Controlled Using Internet of Things (IoT)", International Journal of Control and Automation, vol. 13, 2020, pp. 942 – 951.

THE 5th INTERNATIONAL CONFERENCE
MECHANICAL ENGINEERING IN XXI CENTURY

December 9-10, 2020
Faculty of Mechanical Engineering in Niš, Serbia

Selection of Fused Deposition Modeling 3D Printer using Multi-Criteria Decision-Making Method

Natalija B. TOMIĆ, Marko V. MLADENOVIĆ, Boban R. ANĐELKOVIĆ, Aleksandar G. STANKOVIĆ, Milan Z. GROZDANOVIĆ

Natalija B. Tomić: Faculty of Mechanical Engineering, University of Niš
Marko V. Mladenović: Faculty of Mechanical Engineering, University of Niš;
Research and development, Harder Digital Sova, Niš, 18000
Boban R. Anđelković: Faculty of Mechanical Engineering, University of Niš
Aleksandar G. Stanković: Faculty of Mechanical Engineering, University of Niš
Milan Z. Grozdanović: Faculty of Mechanical Engineering, University of Niš
natalija.tomic@masfak.ni.ac.rs, mladenovic.marko@hotmail.com, boban.andjelkovic@masfak.ni.ac.rs, aleksandar.stankovic@masfak.ni.ac.rs, milan.grozdanovic@masfak.ni.ac.rs

***Abstract*— With the increasing development of the industry, additive technologies have found application in various fields around the world. Creating unique items has never been easier, even at home. Such a rapid development of additive technologies is due to the expiration of the fused deposition modeling (FDM) patent and the development of cheap electronic components needed to control these devices. Such rapid development has brought to the market a large number of devices of different manufacturers, formats and constructions. The existence of a large number of different devices requires the new user to know the advantages and disadvantages of different constructions, kinematics and generally different types of FDM machines. The paper deals with multi-criteria decision-making (MCDM) of FDM printers, where their main criteria will be their economic and technical characteristics. The aim of this paper is to find the most optimal 3D printer according to the selected criteria.**

***Keywords*— Fused Deposition Modeling (FDM), Multi-criteria Decision-making (MCDM), Additive Technologies**

I. INTRODUCTION

The construction industry, as one of the largest industries in the world, has annual revenues of nearly 10 trillion USD; that is about 6% of global GDP [1].

Research on innovation in the construction industry has been conducted in previous decades [2]. The results confirmed that the construction industry is one of the industries with the least innovation [2, 3]. Wu et al [4] believe that this may change due to the introduction of additive technologies in this industry.

Additive technologies, which are also known as 3D printing, bring innovations not only in the construction industry but also in various branches of industry and science. Its application in the mechanical industry and in medicine is noticeable [5].

Since it was introduced in 1986 by Charles Hull [6] additive technologies has been in development [7]. There are several essentially different ways of additive technologies depending on the material they use. El-Sayegh et al [8], give a schematic representation of existing additive manufacturing techniques, this is presented on Figure 1. There is a difference between additive technologies that uses plastic as a material and that uses metals, or other construction material, as a material. Also, various variations of these subgroups have been developed. Bogue [9] defined 3D printing as ”An automated, additive manufacturing process for producing 3D solid objects from a digital (i.e. CAD) model”. In other words, “In a 3D printing process the 3D CAD model will be slicing into series of 2D layers, which will later be deposited by the printer to construct the model”, according to Wo et al [4]. This paper deals only with the mechanisms that appear in FDM printing process.

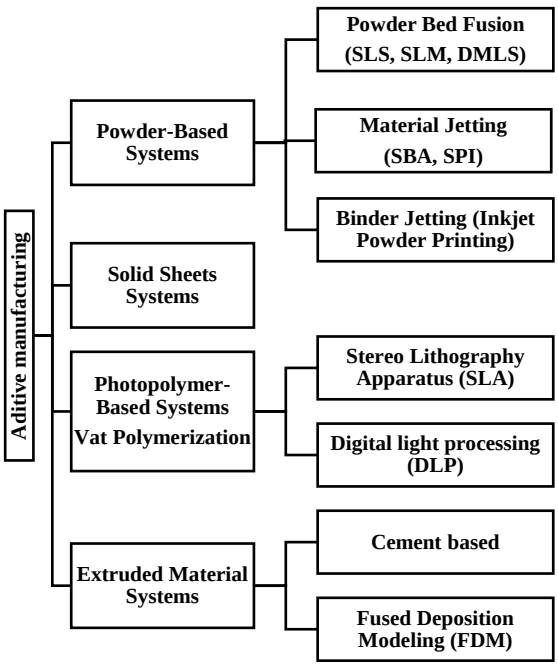

Fig. 1 Additive manufacturing techniques [8]

II. Fused Deposition Modeling (FDM)

Fusion Deposition Modeling (FDM) is one of the most commonly used additive manufacturing technique that has significantly reduced product development time and costs [10]. 3D printers that use the FDM can be found on the market at very reasonable prices. More and more households are able to afford it. The problem is finding a printer with good features at a reasonable price. The printed components with FDM technique, generally, have poor quality and require further post finishing [11]. The quality of a FDM printed component can be observed through several quality criteria:

- Mechanical characteristics,
- Geometric characteristics,
- Surface quality,
- Material properties.

The mechanical characteristics of printed component depends of: part build orientation, layer thickness, raster angle, part raster width, raster to raster gap [12]. This characteristic are defined and can be improved with printing process parameters adjustment [12].

A wide range of materials are available for FDM process, such as acrylonitrile butadiene styrene (ABS), polycarbonate (PC), polylactic acid (PLA), etc. [11] Material properties of printed component directly depends of material which is used for printing [13].

The geometric characteristic and surface quality in addition to the shape of the printed component and external influences, depend on the mechanism used by the printer. Therefore, in this paper, the alternatives for optimization will be the different printing mechanisms that can be found on the market.

FDM printing process was developed in early 1990s by Stratasys Inc. USA [11]. In the FDM process, the starting material is solid plastic. The continuous filament of plastic is heated in the nozzle until it reaches a semi-liquid state. Then this semi-liquid plastic is selectively deposited through a nozzle on the platform or on top of previously printed layers so that traces of the part cross sectional geometry produce 3D part. The part is printing directly from a CAD model in a layer by layer manner.

Figure 2 presents basics of FDM printing process.

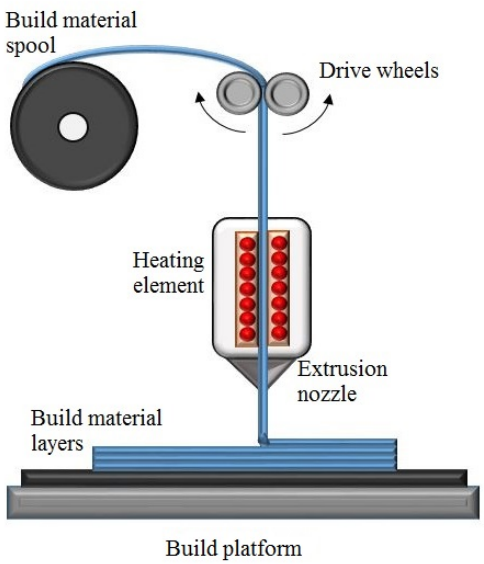

Fig. 2 Principle of FDM process

III. Optimization problem

The moving parts in FDM process are the platform and the extruder or only one of them. Movements are usually made in the X, Y and Z direction. There are different mechanisms for platform and extruder movement in FDM processes. The FDM process mechanisms that appear on the market can be divided into 5 groups [14]:

- Cartesian,
- Delta,
- SCARA,
- Polar,
- Robotic arm.

There are five different subgroups of Cartesian mechanisms:

- the platform moves horizontally along one axis(X or Y), extruder moves vertically (Z) and along other horizontal axis,
- the platform moves vertically (Z), the extruder moves along two axes (X and Y),
- the platform moves vertically (Z) and along one of the horizontal axes (X or Y), the extruder moves along other horizontal axis,
- the platform does not move, the extruder moves in all tree axes,
- the platform moves horizontally (X and Y), the extruder moves vertically (Z).

The Delta printers differ from Cartesian printers in the way the axes are arranged (all three are vertical) and the frame is usually triangular. Each axis is mounted so that the stroke is in the vertical direction. The carriage, on which the nozzle is placed, is mounted on the axis movement and forms one side of a link of parallel arms that connect the carriage to the effector. As the axis moves up and down, the carriage moves along with it [15]. The platform is usually fixed.

The SCARA design is used in the world of industrial robots. It is based on an almost humanoid jointed arm which works in two dimensions (X and Y). The third dimension (Z) is achieved by raising or lowering the whole construction, the platform or the arm.

The Polar printers have a rotating circular print bed or build platform and use a polar coordinate system (instead of a Cartesian coordinate system). The nozzle is attached to an extended arm parallel to the build platform, and moves up and down.

Unlike the other groups mentioned, robotic arms are used for printing in, mainly, 6 dimensions. The nozzle is located at the end of the arm and the platform is stationary.

All these groups of printers are constantly being developed and improved by both manufacturers and users. The groups are roughly defined, there are many subgroups for most of them. The most different variants exist with Cartesian printers, which are also the most common on the market. It should be noted that the average values of the most represented printers on the market were taken as representatives of the groups. With many different variants of mechanisms comes many different criteria. It was decided that the criteria be chosen to define the printing mechanisms themselves. When determining the purchase of a specific printer, it would be desirable to do the optimization within the group itself, and to adopt criteria that take into account the manufacturers.

The criteria that will be used for optimization are:

- Printer cost,

- Maintenance,
- The impact of the quality of printer parts on print quality,
- The impact of printer electronics quality on print quality,
- Ease of use,
- Support,
- Maximum resolution,
- Advanced path optimization.

The prices of each of the groups of printers were taken from the average value from the Amazon site [16]. For Cartesian and Delta printers, the latest recommendations for choosing a printer to determine the average price have also been taken into account [17, 18]. The unit for price criteria is the US dollar. The unit for maximum resolution criterion is mm.

The values of alternatives by criterion for other criteria are not expressed in a particular unit but are formed by a scoring system based on user experience. For the criteria of impact the quality of printing, points were awarded so that 1 represents low, 2 represents medium, 3 represents high and 4 represent the highest. The criterion of Ease of use is presented through three levels: easy (3), medium (2) and difficult (1). The criterion of Support is presented through three levels: large (3), limited (2) and extremely limited (1). For the Advanced path optimization criterion, it was observed to what extent the mechanisms allow the addition of the fourth axis, orienting printing nozzle and support full 6D.

Table I presents the alternative mechanisms that will be used for optimization (and their designations). Table II presents the criteria on the basis of which the best alternative will be decided (and their designations) and values of significance or weighting coefficients for each criterion. The values of the weighting coefficients were obtained on the basis of the survey. The survey was completed by 100 respondents. Since the essence of optimization is to find a printer mechanism that would suit the average citizen, it was not taken into account whether the respondent owns a 3D printer, but the condition was to have basic knowledge related to additive technologies.

TABLE I ALTERNATIVES FOR OPTIMIZATION

Alternatives	Printer mechanism
Alternative 1 (A1)	Cartesian
Alternative 2 (A2)	Delta
Alternative 3 (A3)	SCARA
Alternative 4 (A4)	Polar
Alternative 5 (A5)	Robotic Arm

TABLE II OPTIMIZATION CRITERIA

Criteria		Weight coefficient
Criterion 1 (C1)	Printer cost	100
Criterion 2 (C2)	Maintenance	16
Criterion 3 (C3)	The impact of the quality of printer parts on print quality	37
Criterion 4 (C4)	The impact of printer electronics quality on print quality	29
Criterion 5 (C5)	Ease of use	24
Criterion 6 (C6)	Support	5
Criterion 7 (C7)	Maximum resolution	54
Criterion 8 (C8)	Advanced path optimization	7

IV. ANALYTIC HIERARCHY PROCESS (AHP)

Analytic hierarchy process (AHP) was presented in 1980 by Saaty T. L. [19]. The AHP method is one of the most widely used optimization methods, although it is mainly used as an auxiliary method for determining the values of weight coefficients [20]. Its fuzzy variant (fuzzy AHP) is also widely used [21]. The AHP is a Multi-criteria Decision-making (MCDM) method based on the principle that the decision-making experience and knowledge of people is as important as the data they use [22]. This influence of the subjective attitude is pronounced in determining the weight of the criteria [19].

A typical example of the decision matrix for AHP has hierarchical data structure and is represented by the equation (1) [19],

$$\begin{array}{cccccc} Criterion & C_1 & C_2 & \dots & C_n \\ Weight\ coefficient & w_1 & w_2 & \dots & w_n \\ \hline Alternative & & & & \\ A_1 & a_{11} & a_{12} & \dots & a_{1n} \\ A_2 & a_{21} & a_{22} & \dots & a_{2n} \\ \dots & \dots & \dots & & \dots \\ A_m & a_{m1} & a_{m2} & \dots & a_{mn} \end{array} \tag{1}$$

where:

- m presents the number of alternative,
- n presents the number of criteria,
- a_{ij} presents the value of i-th alternatives for the j-th criterion,
- w_j presents weight coefficient of the j-th criterion,
- C_j presents the j-th criterion,
- A_i presents the i-th alternative.

The values of the weight coefficients are determined on the basis of the pairwise comparison matrix represented by the equation (2) [19],

$$V = \begin{bmatrix} \frac{v_1}{v_1} & \frac{v_1}{v_2} & \dots & \frac{v_1}{v_n} \\ \frac{v_2}{v_1} & \frac{v_2}{v_2} & \dots & \frac{v_2}{v_n} \\ \dots & \dots & & \dots \\ \frac{v_n}{v_1} & \frac{v_n}{v_2} & \dots & \frac{v_n}{v_n} \end{bmatrix} \tag{2}$$

where $\frac{v_k}{v_l}$ presents how much is the v_k criterion important then the v_l criterion.

The vector of weight coefficients w is eigenvector of matrix V. The procedure for determining the vector w is presented by equation (3) [19],

$$Vw = \lambda w \leftrightarrow \begin{bmatrix} \frac{v_1}{v_1} & \frac{v_1}{v_2} & \dots & \frac{v_1}{v_n} \\ \frac{v_2}{v_1} & \frac{v_2}{v_2} & \dots & \frac{v_2}{v_n} \\ \dots & \dots & & \dots \\ \frac{v_n}{v_1} & \frac{v_n}{v_2} & \dots & \frac{v_n}{v_n} \end{bmatrix} \begin{bmatrix} w_1 \\ w_2 \\ \dots \\ w_n \end{bmatrix} = \lambda \begin{bmatrix} w_1 \\ w_2 \\ \dots \\ w_n \end{bmatrix} \tag{3}$$

The pairwise comparison matrix for alternatives are formed for all criteria separately. The pairwise matrix for j-th criterion is presented by equation (4) [19],

$$X_j = \begin{bmatrix} \frac{a_{1,j}}{a_{1,j}} & \dots & \frac{a_{1,j}}{a_{m,j}} \\ \vdots & \ddots & \vdots \\ \frac{a_{m,j}}{a_{1,j}} & \dots & \frac{a_{m,j}}{a_{m,j}} \end{bmatrix} \tag{4}$$

Vectors x_j is eigenvector of matrix X_j. This x_j further form a decision matrix X based on the following equation (5) [19],

$$X = [x_1 \quad x_2 \quad \dots \quad x_n] \tag{5}$$

The product of the decision matrix X and the weight coefficient vector w gives the vector the quality of each alternative and the alternative with the highest value is the best alternative [19]. This is presented on equation (6) [19],

$$[x_1 \quad x_2 \quad \dots \quad x_n] \begin{bmatrix} w_1 \\ w_2 \\ \dots \\ w_n \end{bmatrix} = \begin{bmatrix} r_1 \\ r_2 \\ \dots \\ r_n \end{bmatrix} \tag{6}$$

where r_k is the rank value for k-th alternative.

The AHP decision matrix for a defined optimization problem is presented on Table III.

TABLE III AHP MATRIX

	C1	C2	C3	C4	C5	C6	C7	C8
	100	16	37	29	24	5	54	7
A1	380	1	4	1	3	3	0.05	25
A2	848	2	3	3	3	3	0.05	25
A3	1995	3	3	3	2	2	0.1	25
A4	800	1	3	2	2	2	0.1	25
A5	5500	4	2	4	1	1	0.1	100

The AHP optimization method recognizes the maximum value of alternatives by the criterion as the most desirable. Since the criteria C1, C2, C3, C4 and C7 are undesirable (the minimum value is required as the most desirable), for the values of alternatives by the criterion, reciprocal values will be taken ($\frac{1}{a_{ij}}$) [23]. The decision matrix with modified values is presented on Table IV.

TABLE IV AHP MODIFIED MATRIX

	C1	C2	C3	C4	C5	C6	C7	C8
	100	16	37	29	24	5	54	7
A1	0.0026	1	0.25	1	3	3	20	25
A2	0.0012	0.5	0.3333	0.3333	3	3	20	25
A3	0.0005	0.3333	0.3333	0.3333	2	2	10	25
A4	0.0013	1	0.3333	0.5	2	2	10	25
A5	0.0002	0.25	0.5	0.25	1	1	10	100

V. RESULTS AND DISCUSSION

The values of the weight coefficients are determined on the basis of the equations (2, 3). The equation (7) presents values for vector of weight coefficient (W).

$$W = \begin{bmatrix} 0.37 \\ 0.06 \\ 0.14 \\ 0.11 \\ 0.09 \\ 0.02 \\ 0.20 \\ 0.03 \end{bmatrix} \tag{7}$$

The pairwise comparation matrices for all criterions and their eigenvectors are determined on the basis of the equations (3, 4). This matrices are presented on following equations:

$$AC1 = \begin{bmatrix} 1.00 & 2.17 & 5.20 & 2.00 & 13.00 \\ 0.46 & 1.00 & 2.40 & 0.92 & 6.00 \\ 0.19 & 0.42 & 1.00 & 0.38 & 2.50 \\ 0.50 & 1.08 & 2.60 & 1.00 & 6.50 \\ 0.08 & 0.17 & 0.40 & 0.15 & 1.00 \end{bmatrix} \tag{8}$$

$$AC2 = \begin{bmatrix} 1.00 & 2.00 & 3.00 & 1.00 & 4.00 \\ 0.50 & 1.00 & 1.50 & 0.50 & 2.00 \\ 0.33 & 0.67 & 1.00 & 0.33 & 1.33 \\ 1.00 & 2.00 & 3.00 & 1.00 & 4.00 \\ 0.25 & 0.50 & 0.75 & 0.25 & 1.00 \end{bmatrix} \tag{9}$$

$$AC3 = \begin{bmatrix} 1.00 & 0.75 & 0.75 & 0.75 & 0.50 \\ 1.33 & 1.00 & 1.00 & 1.00 & 0.67 \\ 1.33 & 1.00 & 1.00 & 1.00 & 0.67 \\ 1.33 & 1.00 & 1.00 & 1.00 & 0.67 \\ 2.00 & 1.50 & 1.50 & 1.50 & 1.00 \end{bmatrix} \tag{10}$$

$$AC4 = \begin{bmatrix} 1.00 & 3.00 & 3.00 & 2.00 & 4.00 \\ 0.33 & 1.00 & 1.00 & 0.67 & 1.33 \\ 0.33 & 1.00 & 1.00 & 0.67 & 1.33 \\ 0.50 & 1.50 & 1.50 & 1.00 & 2.00 \\ 0.25 & 0.75 & 0.75 & 0.50 & 1.00 \end{bmatrix} \tag{11}$$

$$AC5 = \begin{bmatrix} 1.00 & 1.00 & 1.50 & 1.50 & 3.00 \\ 1.00 & 1.00 & 1.50 & 1.50 & 3.00 \\ 0.67 & 0.67 & 1.00 & 1.00 & 2.00 \\ 0.67 & 0.67 & 1.00 & 1.00 & 2.00 \\ 0.33 & 0.33 & 0.50 & 0.50 & 1.00 \end{bmatrix} \tag{12}$$

$$AC6 = \begin{bmatrix} 1.00 & 1.00 & 1.50 & 1.50 & 3.00 \\ 1.00 & 1.00 & 1.50 & 1.50 & 3.00 \\ 0.67 & 0.67 & 1.00 & 1.00 & 2.00 \\ 0.67 & 0.67 & 1.00 & 1.00 & 2.00 \\ 0.33 & 0.33 & 0.50 & 0.50 & 1.00 \end{bmatrix} \tag{13}$$

$$AC7 = \begin{bmatrix} 1.00 & 1.00 & 2.00 & 2.00 & 2.00 \\ 1.00 & 1.00 & 2.00 & 2.00 & 2.00 \\ 0.50 & 0.50 & 1.00 & 1.00 & 1.00 \\ 0.50 & 0.50 & 1.00 & 1.00 & 1.00 \\ 0.50 & 0.50 & 1.00 & 1.00 & 1.00 \end{bmatrix} \tag{14}$$

$$AC8 = \begin{bmatrix} 1.00 & 1.00 & 1.00 & 1.00 & 0.25 \\ 1.00 & 1.00 & 1.00 & 1.00 & 0.25 \\ 1.00 & 1.00 & 1.00 & 1.00 & 0.25 \\ 1.00 & 1.00 & 1.00 & 1.00 & 0.25 \\ 4.00 & 4.00 & 4.00 & 4.00 & 1.00 \end{bmatrix} \tag{15}$$

where:

- *AC1* represents the pairwise comparation matrix for criterion C1 (8),
- *AC2* represents the pairwise comparation matrix for criterion C2 (9),
- *AC3* represents the pairwise comparation matrix for criterion C3 (10),
- *AC4* represents the pairwise comparation matrix for criterion C4 (11),
- *AC5* represents the pairwise comparation matrix for criterion C5 (12),
- *AC6* represents the pairwise comparation matrix for criterion C6 (13),
- *AC7* represents the pairwise comparation matrix for criterion C7 (14)
- *AC8* represents the pairwise comparation matrix for criterion C8 (15).

The decision matrix (X) is formed on the equation (5), and it is presented on equation (16).

$$X = \begin{bmatrix} 0.45 & 0.32 & 0.14 & 0.41 & 0.27 & 0.27 & 0.29 & 0.12 \\ 0.21 & 0.16 & 0.19 & 0.14 & 0.27 & 0.27 & 0.29 & 0.12 \\ 0.09 & 0.11 & 0.19 & 0.14 & 0.18 & 0.18 & 0.14 & 0.12 \\ 0.22 & 0.32 & 0.19 & 0.21 & 0.18 & 0.18 & 0.14 & 0.12 \\ 0.03 & 0.08 & 0.29 & 0.10 & 0.09 & 0.09 & 0.14 & 0.50 \end{bmatrix} \tag{16}$$

Results is presented on equation (17).

$$X \cdot W = \begin{bmatrix} 0.34 \\ 0.21 \\ 0.13 \\ 0.20 \\ 0.12 \end{bmatrix} \rightarrow \begin{matrix} A1 \\ A2 \\ A3 \\ A4 \\ A5 \end{matrix} \begin{bmatrix} 1 \\ 2 \\ 4 \\ 3 \\ 5 \end{bmatrix} \quad (17)$$

The results can also be presented graphically for better visibility. Figure 3 presents the optimization results.

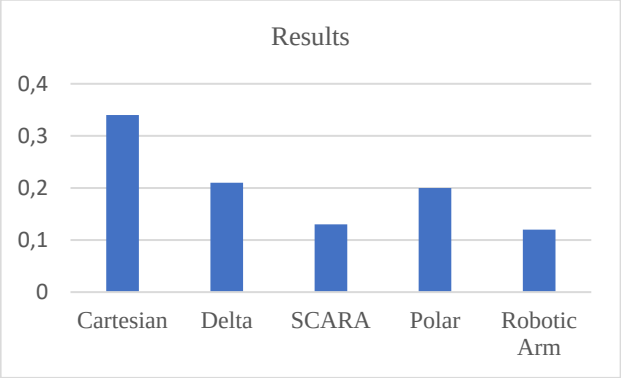

Fig. 3 Results

The optimization results give Cartesian as the printers with the best mechanism for households. Cartesian printers are also generally the best-selling on the market. This can be explained by their price, which is lower than price for other printer mechanisms. And based on the conducted survey, it can be concluded that price is the most important criterion for the average citizen. Cartesian printers are also the most developed, most represented and have the most variants of mechanisms. After Cartesian printers, the printers with the most variations are Delta and Polar printers. These printers can also be found at low prices and take second and third place based on optimization. The other two groups of mechanisms are widely known in mechanical engineering and robotics, but they have been used relatively recently as 3D printers. There are not many of them and their prices are generally high. But their development is being worked on extensively around the world, so there will probably be more of them on the market soon.

VI. Conclusion

Much of the research in the field of improving the quality of a printed component is focused on adjusting the printing parameters which most improve its quality. With the increasing of use and development of 3D printers, new ways to improve quality are being discovered. The influence of moving parts in 3D printers and their way of moving has a negligible influence on the quality of the printed component itself. Research on the impact of the printing mechanism on the printed component is conducted mainly by printer users and companies engaged in the production and development of 3D printers.

The aim of the paper was to determine the best printing mechanism for the household. The alternatives or groups of the mechanisms used for 3D printers are generally roughly formed in this paper. Optimization can certainly be done within the groups of mechanisms. That are most pronounced in Cartesian printers. Optimization within the group of printing mechanisms itself brings a greater variety of criteria. The criteria would be both narrower and related to a specific problem, which is an excellent basis for further research.

Acknowledgments

This research was financially supported by the Ministry of Education, Science and Technological Development of the Republic of Serbia.

References

[1] P. Gerbert, S. Castagnino, C. Rothballer, A. Renz and R. Filitz, “The transformative power of building information modeling”, Boston Consulting Group. 2016.

[2]] C. Harty, “Implementing innovation in construction: contexts, relative boundedness and actor-network theory”, Constr. Manag. Econ. vol. 26 (10), 2008, pp. 1029–1041.

[3] J. Tidd, J. Bessant and K. Pavitt, “Managing Innovation Integrating Technological, Market and Organizational Change”, John Wiley and Sons, Chichester, 1997.

[4] P. Wu, J. Wang and X. Wang, “A critical review of the use of 3-D printing in the construction industry”, Automation in Construction, vol. 68, 2016, pp. 21-31.

[5] M. Stojković, J. Milovanović, N. Vitković, M. Trajanović, N. Grujović, V. Milivojević, S. Milisavljević and S. Mrvić, “Reverse modeling and solid free-form fabrication of sternum implant”, Australas Phys Eng Sci Med, vol. 33, 2010, pp. 243-250.

[6] http://www.google.com/patents/US4575330#v=onepage&q&f=false (accessed on 22.10.2020.)

[7] A. Pandian and C. Belavek, “A review of recent trends and challenges in 3D printing”, Proceedings of the 2016 ASEE North Central Section Conference, American Society for Engineering Education, 2016.

[8] S. El-Sayegh, L. Romdhane and S. Manjikian, “A critical review of 3D printing in construction: benefts, challenges, and risks”, Archives of Civil and Mechanical Engineering, 2020, pp. 20-34.

[9] R. Bogue, “3D printing: the dawn of a new era in manufacturing”, Assem. Autom. vol. 33, 2013, pp. 307–311.

[10] J. S. Chohan, R. Singh, K. S. Boparai, R. Penna and F. Fraternali, “Dimensional Accuracy Analysis of Coupled Fused Deposition Modeling and Vapour Smoothing Operations for Biomedical Applications”, Composites Part B, 2017.

[11] O. A. Mohamed, S. H. Masood and J. L. Bhowmik, “Optimization of fused deposition modeling process parameters: a review of current research and future prospects”, Adv. Manuf, vol. 3, 2015, pp. 42-53.

[12] A. K. Sood, R.K. Ohdar and S.S. Mahapatra, “Parametric appraisal of mechanical property of fused deposition modelling processed parts”, Materials and Design, vol. 31, 2010, pp. 287-295.

[13] B. Wittbrodt and J. M. Pearce, “The Effects of PLA Color on Material Properties of 3-D Printed Components”, Additive manufacturing, vol. 8, 2015, pp. 110-116.

[14] https://top3dshop.com (accessed on 27.10.2020.)

[15] C. Bell, “3D Printing with Delta Printers”, Springer Science + Business Media New York, 2015.

[16] http://amazon.com (accessed on 28.10.2020.)

[17] https://www.3dnatives.com (accessed on 28.10.2020.)

[18] https://all3dp.com (accessed on 28.10.2020.)

[19] T. L. Saaty, "The Analityc Hierarchy Process", New York, USA: McGraw-Hill International, 1980.

[20] L.G. Vargas, "An overwiev of the Analytic Hierarchy Process and its applications", European Journal of Operational Research, vol. 48, 1990, pp. 2-8.

[21] A. Singh, R. K. Ghadai, K. Kalita, P. Chatterjee, D. Pamučar, “EDM Process Parameter Optimization for Efficient Machining of Inconel-718”, Facta Universitatis, Series: Mechanical Engineering, vol. 18, 2020, pp. 473-437.

[22] D. Pamučar, F. Ecer,”Prioritizing the Weights of the Evaluation Criteria under Fuzziness: The Fuzzy full Consistency Method – Fucom-F”, Facta Universitatis, Series: Mechanical Engineering, vol. 18, 2020, pp. 419-490.

[23] T.L. Saaty, M. Ozdemir, “Negative Priorities in the Analytic Hierarchy Process”, Mathematical and Computer Modelling, vol. 37, 2003, pp. 1063—1075.

THE 5th INTERNATIONAL CONFERENCE
MECHANICAL ENGINEERING IN XXI CENTURY

December 9-10, 2020
Faculty of Mechanical Engineering in Niš, Serbia

Investigating Fatigue Life of E-glass Fiber/Novolac/Epoxy (DGEBA) Hybrid Composites

Sulaiman Al-basaqr, Amir Alsammarraie, Abed Fares Ali

University of Tikrit/ Engineering College/ Mechanical Engineering Dep. Tikrit, Iraq
sulaimaninad63@tu.edu.iq,amircraft@tu.edu.iq, abdfaris@tu.edu.iq

***Abstract*— The fatigue considers the type of the failure types for the geometric parts because it suffers from dynamic and fluctuating stress as in the aircraft, the ships, the bridges, and other geometric parts. The fatigue of composite materials is not fully understood which is perfectly different from metal fatigue. In the present study the prepared hybrid composite materials specimen reinforcement E-Glass fiber for 10%,20%, and 30% volume fraction that have two preparation of matrix (80% EP, 60% NO) and (40% EP, 20% NO). has been applied to fatigue loading in-plane bending with R = ±1 and S-N. curves are plotted. the laboratory tests and the results show decreasing in the number of fatigue cycles even failure when the applied load on the specimens increases. The fracture will be brittle because there are adding Novolac materials to obtain hard hybrid composites specimens.**

***Keywords*— Epoxy, glass fiber, Novolac, Fatigue, stress**

I. Introduction

Composite materials are inhomogeneous materials made from two or more materials with relevantly different physical or chemical properties that, E- Glass/ epoxy polymer composites find widespread applications because of their several advantages like high wear resistance, good strength-to-weight ratio, and low cost. They find huge applications in the construction of automotive and aviation body structures, in which they are inevitably subjected to sudden impacts during their construction, maintenance, and functioning. Admittedly that glass fiber reinforced polymer (GFRP) composites should, in principle, be fatigue resistance provided that fibers carry the major part of the load and are not so extensible as to permit large elastic deformations of the matrix.

Influence concentricity of Short carbon fiber on mechanical properties of SCF reinforced polypropylene composites was studied, results showed that an increase of SCF could progress the mechanical properties [1].

Fatigue behavior of epoxy material has been studied by breaking the glass fiber volumes of 30% and 40%, when the external loads on the specimen are increased for both volume fractions 30% and 40%, the number of fatigue cycles to failure of composite materials decreases [2]. Fiber composites and compares it with glass fiber-reinforced polymer (GFRP) and carbon fiber-reinforced polymer (CFRP) used separately was investigated, the performance was evaluated that the CFRP composite has better properties than the GFRP in tensile and flexural [3].

Glass fiber-reinforced polymeric (GFRP) composites were most commonly used in the production of composite materials. The matrix included organic, polyester, thermostable, vinylester, phenolic, and epoxy resins. Polyester resins are classified into bisphenols and ortho or isophthalic [4]. The effect of a change in the ratio of reinforcement by fibers on the thermal conductivity of the polymeric composites consists of an epoxy resin conbextra (EP-10) reinforced by an S-type woven glass fiber (0º-45º), The results showed that the thermal conductivity of the epoxy-type epoxy resin has improved due to the ability of the fibers to conduct heat[5]. On the other hand, experimentally and analytically, has been investigated the effect of the various orientations (0/90; 30/60; 45/90) of E-Glass/epoxy composite plates using ABAQU, it has been revealed that the effective resistance of cross-ply plates is more when compared with angle ply plates[6]. the mechanical properties of (GFRP) element produced by the Brazilian industry to group it for structural applications were determined, results gave conclude that the GFRP element resolve displays structural distribution compatible to E17 class mechanical requirement [7].

Fatigue life predictions associated with the S-N curve have been largely based on empiricism or unfounded theories, or both, due to the complexity involving multiple variables such as fatigue life, applied stress, number of loading cycles, and stress ratio. It's found that S-n curve constant fatigue life diagrams for a carbon/epoxy plates in different fiber directions are identified through the whole range of stress ratio, The experimental results are presented that the S-n constant fatigue life diagram plotted in the plane of alternating and mean stresses head for to shrink and drop to the left of the alternating stress axis more significantly as the off-axis angle of a specimen increases[8]. theory for mathematical validity framework of fatigue damage connected with the S-N curve and to derive a damage function capable of predicting the fatigue life was studied, Comparisons between experimental results from two stress level range loading and theoretical fatigue life predictions are made and a close, covenant between them was found[9]. A nonlinear typical for fatigue damage accumulation under variable amplitude loading is investigated, A single value for the parameter has been set to give filling arrangement with experimental data for four randomly selected sheets of steel, indicating a general tendency[10]. This investigation aimed to study

the fatigue life behaviour of a hybrid composite epoxy/Novolac reinforced by glass fibre

II. Materials and Pieces of Equipment Used

A. *The material:*

The materials used in this paper are commercial, obtained from the (SIKA GROUP Building Trust): Diglycidyle ether of bisphenol-A (DGEBA) Epoxy Resin fig 1c, Curing Agent (Hardener) of Epoxy Resin Diethylenetriamine (DETA), Novolac Resin fig 1d, Curing Agent (Hardener) of Novolac Resin hexamethylenetetramine (Hexamine), E-Glass Fibers, Gel-coat to prevent pasted material on the inner mold surface, Ethanol to cleanig.. because the E-glass fiber is much cheaper and safely less brittle is used in this work, fig.1b. table 1 shows the mechanical properties of the material used in this paper.

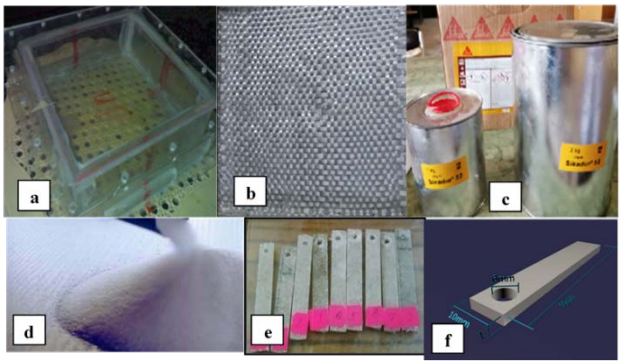

Fig. 1, a) mold of the test specimen, b)E-Glass Fibers, c) Epoxy Resin, d) Novolac Resin, e) types of test specimen f)geometry test specimen.

Because the E-glass fiber is much cheaper and safely less brittle is used in this work, fig.3b. table 1 shows the mechanical properties of the material used in this paper.

Table 1. Mechanical properties materials.

	Viscosity [Cps]	Density [mg/m3]	Tensile strength [MPa]	Tensile modulus	Poisons ratio	Melting point [^{0}c]
epoxy resins	600-1000	1.1-1.4	60-80	3.8-3.0	0.35	-35
novolac resin	[-]	2.235	82	2.5-3.3	0.36	[-]
E-glass fibers	[-]	2.60	3450	72.4	0.22	[-]

B. *Alternating bending fatigue machine*

Alternating bending fatigue machine HSM0 was used to test all the specimens that made by Hi-Tech company. This machine is shown in fig.2. The purpose of this machine is to apply alternating or fluctuating bending **(R±)** to a cantilevered strip of material to determine fatigue life performance. Produced whereby a cantilever could be deflected to impose varying bending stress in the cantilever fig.3. The frequency of the reciprocating force is around 24Hz

To calculating the Maximum Length of specimen while test of fatigue by using the following formula;

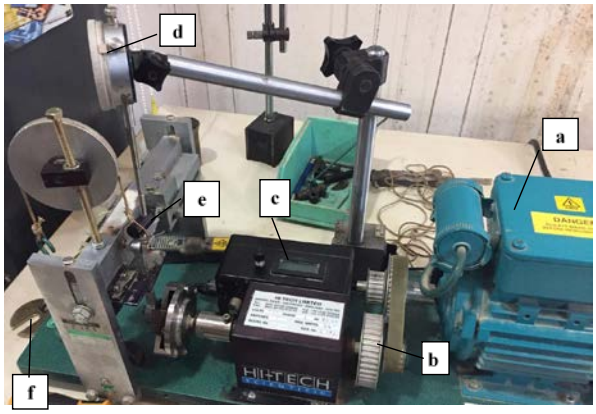

Fig.2 Alternating bending fatigue machine, a) motor, b)gears, c) Cycle counter d) dial gauge,e) test specimen, f) load

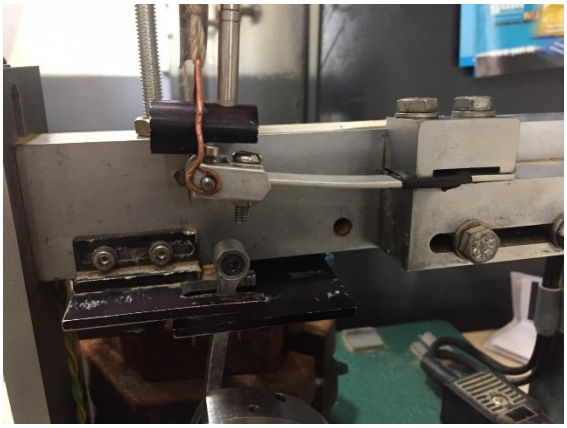

Fig. 3. cantilever type load and deflection

$$\ell = L - h = L - \frac{A^2}{L}, A = 0.758 \cdot \delta \quad (1)$$

Calculating the stress of specimen for fatigue test by using the following formula:

$$\sigma = \frac{6 \cdot F \cdot \ell}{b \cdot t^2} \quad (2)$$

Where is, **A**=$\pi^2\delta^2/16 \approx 0.785\,\delta$ is curvature approximate factor[mm], **L** is a specimen length before applied loads (60 mm), ***l*** is the length of the specimen after applied of load [mm], **σ** is normal stress [Mpa], **F** is a normal load [N], ***b*** is the width of a specimen, [mm], ***t*** is the thickness of specimen, [mm], ***δ*** is free to end deflection, [mm].

III. EXPERIMENTAL

The mold shown in Fig 1a was manufactured and configured to place the composite material and fiberglass and then took it after hardening. Three percentage of glass fiber (10%,20%, and 30%) type E, Fig 1b, was performed. woven roving method to arrange the glass fiber inside the matrix, the epoxy resin used was diglycidyle ether of bisphenol-A (DGEBA) Epoxy Resin with Curing Agent (Hardener)(60%and 80%) Fig 1c and Novolac (40%and 20%) Fig 1d.

The required quantity of the epoxy resin and Novolac were all individually weighed and mixed and a stoichiometric amount of curing agent. Resin with Curing Agent (Hardener) (50%, 20%) respectively, then distributing the matrix by the brush on the mold-covered with gel coat was used to avoid adhesion with mold, then putting. woven roving E-Glass fiber on the matrix. Finally, we put the matrix again on the E-Glass fiber surface and rolling or distribution by roller to cover it very well and

place in furnace or oven(20-40°C) to drying the ethanol then put a suitable load on the matrix and leave it for (24) hours to harden well, A load of 5 kg is placed in the space provided on the mold, to force the bubbles to leave the component, After 24 hours, Slate is separated from the mold. After cleaning Slate by Aston, the test specimens are cut with dimensions 10 mm wide, 60 mm length, with a drill, make a hole with a diameter of 6 mm fig 1f. 20 specimens were manufactured for each weight ratio of fig 1e. The experiment was set up with parameters with more levels because the effects of the fatigue life parameters were complex and non-linear, based on the defined fatigue age parameters and levels, and after the tests were performed, a design matrix was established, Table 2.

TABLE 2. EXPERIMENTAL AND PREDICTED VALUES OF FATIGUE LIFE RESULTS

Exp. trial	Composite		Adding of fibre in the compositeE-GF [wt%]	Load [N]	Max.Length while test *l* [mm]	Stress σ=6*p*l/(b*t^2) [Mpa]	Fatigue cycle [n]
	EP [wt%]	NOV [wt%]					
1	80	20	10	10	44.97127	29.98084787	7900864
2	80	20	10	10.5	44.93246	31.45271977	5776890
3	80	20	10	12	44.88509	35.90806976	3899076
4	80	20	10	15	44.77477	44.77477091	1898876
5	80	20	10	18	44.46055	53.35265789	688790
6	80	20	20	10	44.97127	29.98084787	5677645
7	80	20	20	10.5	44.95391	31.46773504	3900876
8	80	20	20	12	44.92646	35.94116465	2677543
9	80	20	20	15	44.8058	44.80579737	955654
10	80	20	20	18	44.6679	53.60148241	507651
11	80	20	30	10	44.99681	29.99787199	3556787
12	80	20	30	10.5	44.98723	31.49106234	1788656
13	80	20	30	12	44.95863	35.96690511	1009897
14	80	20	30	15	44.9202	44.92019944	700431
15	80	20	30	18	44.76392	53.71670164	487639
16	60	40	10	10	44.95391	29.96927147	9576125
17	60	40	10	10.5	44.9382	31.45674171	7467436
18	60	40	10	12	44.8773	35.90183893	5887621
19	60	40	10	15	44.74145	44.7414462	3597683
20	60	40	10	18	44.44382	53.33258646	1600981
21	60	40	20	10	44.98455	29.98970041	7245439
22	60	40	20	10.5	44.98161	31.48712977	5854345
23	60	40	20	12	44.9202	35.93615956	2756398
24	60	40	20	15	44.79571	44.79571058	1539825
25	60	40	20	18	44.64134	53.56961326	852196
26	60	40	30	10	44.99374	29.99582909	5032879
27	60	40	30	10.5	44.98455	31.48918543	3593426
28	60	40	30	12	44.94369	35.95495418	1800546
29	60	40	30	15	44.8999	44.89989818	599435
30	60	40	30	18	44.74145	53.68973544	354329

IV. RESULTS AND DISCUSSION

A. *Fatigue properties*

The results of S-N curves for all types are plotted in fig. (4 and 5). The constant amplitude fatigue data are summarized in S-N diagrams based upon power laws. The formats of regression trends are typical for fatigue data presentation, [11]. The power-law regression equation is:

$$\sigma = a \cdot N^{b} \tag{3}$$

Where: **σ**: stress Mpa, **N**: is the number of cycles at failure (cycle), **a**: is related to the static bending strength, the constants **b** is related to the fatigue degradation.

The fatigue-life diagram is often used to explain the fatigue failures in tensile fatigue of composites [12]

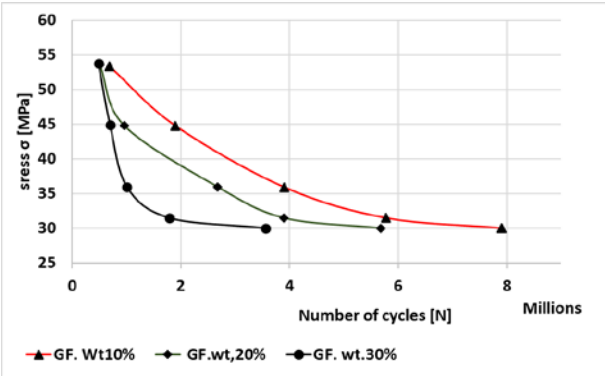

Fig 4. S-Nf curves for Epoxy wt. 80% and Novolac wt. 20% composite content and different GF reinforced.

The results in figures (4) showed that the number of cycle to failure content GF 10% of composite material 80% EP and NOV 20% is greater than the value of the GF 20% and 30% of same epoxy and novolac content, this may be because composite content of more fiberglass is led to increasing hardness and decreases elasticity[13]. which leads to cracks and separation between the glass fibers and composite material, and failure occurs early, i.e. with fewer cycles. This corresponds to clarification for the decrease in the number of cycles with the increase in the GF content to the figure (5)

Increased content NOV. was his influence in fatigue life, where it led to an increase in the number of cycles to failure i.e. an increase of fatigue life composite as shown in figure (5). As compared to content specimen EP 80%, NOV. 20% and GF 10% under load 10 N the number of cycles to failure was 7900864 cycle however for similar under load and GF content but EP 60%, NOV. 40% composite content the number of cycles to failure was

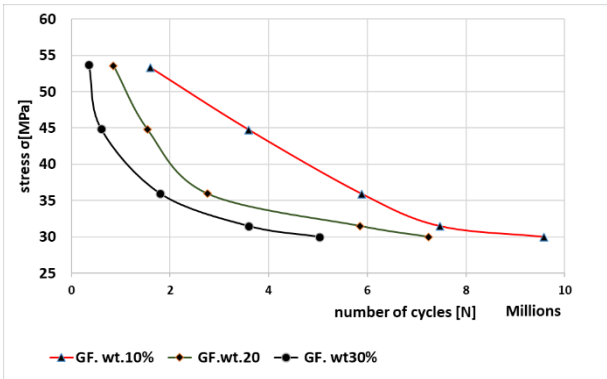

Fig 5. S-Nf curves for Epoxy wt 60% and Novolac wt.40% composite content and different GF reinforced

9576125 cycle increase its amount 1675261 cycle as shown in figure (6), while content specimen EP 80%, NOV. 20% and GF 10% under load 18 N the number of cycles to failure was 688790 cycle however for similar under load and GF content but EP 60%, NOV. 40% composite content the number of cycles to failure was 1600981 cycle increase its amount 912191 cycle, Obviously, with increased loads, decreases the number of cycle to failure i.e. drop fatigue life.

Figure 7 shows an image of the basic samples for the glass fiber content of 10%, 20% and 30%, showing where the failure (breakage) occurred when reaching the fatigue limit.

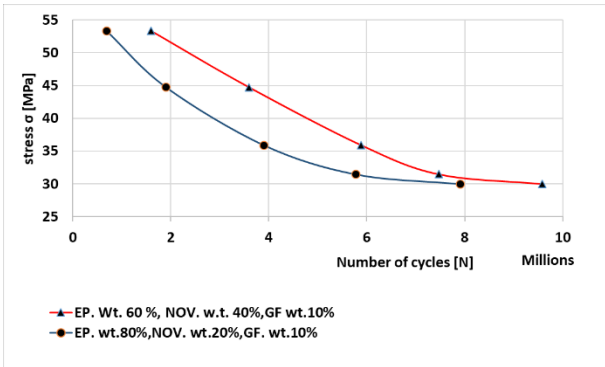

Fig 6. S-Nf curves for different composite content and GF reinforced

Fig 7. images of a sample of the content of glass fiber, 10%, 20% and 30% when reaching the fatigue limit.

B. *Deflection specimen*

Cantilever specimen supported at one end and carrying a load at the other end make a deflection along with specimen, The upper half of the thickness of such a specimen is subjected to tensile stress, tending to elongate the specimen, the lower half to compressive stress, tending to put down specimen for R(-) And vice versa occurs when R (+). This is how the test device works alternating bending fatigue machine. Considering that the specimen component is homogeneous, Therefore, it will be the biggest deflections in the free end of the specimen, which were measured each specimen for the test. For high accuracy deflection was measured by a dial gauge as shown in fig. 2d.

Increased deflections of test specimens due to increased loads lead to strain in the upper and lower surface of the test specimens, and this causes failure and breaking of the test specimens early, i.e. a decrease in the number of cycles, Figure (8) shows this. The number of cycles to failure was at deflection 1.5 mm (load 10 N) decreasing from 7900864 cycles to failure, to 688790 cycles to failure at deflection 5.1 mm for the same composite content (EP. Wt. 80%, NOV. wt. 40%, GF wt. 10%).

Increasing the percentage of GF reinforced leads to the growth of composite hardness, which plays a role in an increased strain test specimen deflection, as the amount of test specimen deflection decreases to 0.5 mm at the same load (10 N) of composite content EP. Wt. 80%, NOV. wt. 40% but GF is wt. 30% and the number of cycles to failure

is 3556787, and the cycle to failure is 487639 when GF is 30% and test specimens deflection is 4.3 mm (load 18 N) as shown in fig (8).

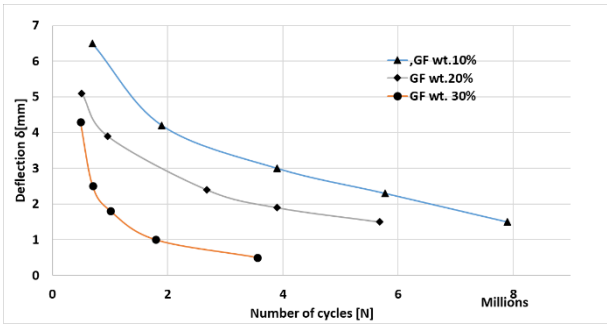

Fig.8. Relationship between deflection and fatigue life for Epoxy wt 80% and Novolac wt.20% composite content and different GF reinforced

Increased NOV content percentage due to composite elastic growth as shown in fig (9). Where fatigue life and test specimens deflection bigger comparison with test specimens in fig (8), for the same content GF WT. 10%, amount test specimens deflection is 1.9 mm and the number of cycles to failure is 9576125 i.e An increase in its amount 0.4 mm and 1675261cycles respectively.

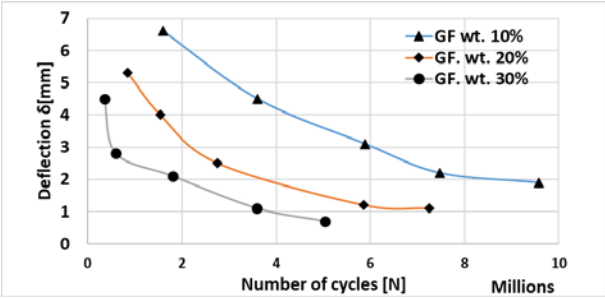

Fig 9. Relationship between deflection and fatigue life for Epoxy wt 60% and Novolac wt.40% composite content and different GF reinforced

The fig. 10 represents a comparison of the amount of deflection and number cycles to failure (fatigue life) reinforced composite material (EP. wt. 80%, and NOV. wt 20%) and reinforced composite material (EP. wt. 60%, NOV. wt40%) both composite with reinforced GF 10%.

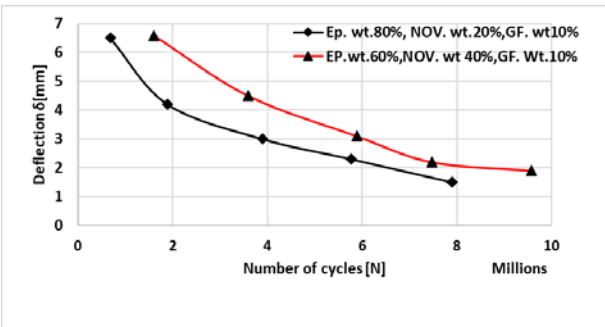

Fig 10 comparison of the amount of deflection and number cycles

A decrease in the number of cycles to failure is observed with a decrease in the amount of test specimens deflection, but an increase in the NOV. content causes an increase in the number of cycles to failure with an increase in the test specimens deflection.

V. Conclusion

In this study, an Alternating bending fatigue machine was used to test the specimens made of a matrix the epoxy resin (60%and 80%), Novolac (40%and 20%), and reinforced with glass fibers(10%,20%, and 30%). The number of fatigue cycles to failure for the composite materials decreases when the applied load on the specimen is increased for all types.

The results showed that the number of cycles to failure decreases to increase GF content, and the number of cycles to failure increases to increase NOV. content.

Increased deflections of test specimens due to increased loads leads to strain in the upper and lower surface of the test specimens, and this causes failure and breaking of the test specimens early. growth of composite hardness to increasing the percentage of GF reinforced leads to increase strain test specimens deflection, as the amount of deflection of specimens. NOV. content increases specimen elasticity to increases test specimen deflection for the same loads, this leads to an increased number of cycles to failure (fatigue life.

Reference

[1] Chuanbao Wang and Sanjiu Ying," Thermal, Tensile and Dynamic Mechanical Properties of ShortCarbon Fibre Reinforced Polypropylene Composites", School of Chemical Engineering, 2012.

[2] Mohammed Hussein, "Study the Effect of Immersion in Gasoline and Kerosene on Fatigue Behavior for Epoxy Composites Reinforcement with Glass Fiber", The Fifth Scientific Conference of University of Wasit, 2011.

[3] C.Elanchezhian, B.Vijaya Ramnath, J.Hemalatha, "Mechanical behavior of glass and carbon fiber-reinforced composites at varying strain rates and temperatures", 3rd International Conference on Materials Processing and Characterisation (ICMPC), 2014.

[4] Lopez FA, Martin MA, Alguacil FJ, et al.," Thermolysis of fiberglass polyester composite and utilization of the glass fiber residue to obtain a glass-ceramic material", J Anal Appl Pyrolysis, 93: 104–112., 2012.

[5] Mohammed H. Al-Maamori, Ali I. Al-Mosawi, " Effect of the percentage of fibers reinforcement on thermal and mechanical properties for polymeric ", The Iraqi Journal For Mechanical and material Engineering, Special Issue, 2015.

[6] Gayatri Vineela. M, Gayathri Tadepalli, A. Krishnaiah, " Impact behavior of Fibre Reinforced composites with a change in Fibre Orientation", International Journal of Current Engineering and Technology, 4106, P-ISSN 2347 – 5161, 2016.

[7] Alexandre Landesmann, Carlos Alexandre Seruti, Eduardo de Miranda Batista," Mechanical Properties of Glass Fiber Reinforced Polymers Members for Structural Applications", Materials Research, ISSN 1516-1439, DOI: http://dx.doi.org/10.1590/1516-1439.044615, 2015.

[8] Kawai, M.; Itoh, N. A," failure-mode based on isomorphic constant life diagram for a unidirectional carbon/epoxy laminate under off-axis fatigue loading at room temperature", J. Compos. Mater, 571–592, 2014.

[9] Eskandari, H.; Kim, H.S. A, " Theory for mathematical framework and fatigue damage function for the S-N plane. In Fatigue and Fracture Test Planning, Test Data Acquisitions, and Analysis; ASTM STP1598; Wei, Z., Nikbin, K., McKeighan, P.C., Harlow, D.G., Eds.; ASTM",

International: West Conshohocken, PA, USA", pp. 299–336, 2017.

[10] Rege, K.; Pavlou, D.G. A, " A one-parameter nonlinear fatigue damage accumulation model", International Journal of Fatigue, Volume 98,234-246, 2017.

[11] Groover, M. P., “Fundamentals of Modern Manufacturing”, 2nd Edition. John Wiley & Sons Inc, 2002.

[12] Rita R., and BOSE N. R., " Behavior of E-glass fiber reinforced vinylester resin composites under fatigue Condition", Bull. Mater. Sci., Vol. 24, 2001.

[13] Ahmed Sahi Mahdi Najah Rustum Mohsin, "Water absorption and fatigue life of an Epoxy composite reinforced by glass fiber", IOP Conf. Series: Materials Science and Engineering 454 (2018), DOI:10.1088/1757-899X/454/1/012007.

THE 5th INTERNATIONAL CONFERENCE
MECHANICAL ENGINEERING IN XXI CENTURY

December 9-10, 2020
Faculty of Mechanical Engineering in Niš, Serbia

Optimal Design for the Welded Girder of the Crane Runway Beam

Goran PAVLOVIĆ[1], Mile SAVKOVIĆ[2], Nebojša ZDRAVKOVIĆ[2] and Goran MARKOVIĆ[2]

[1] University of Niš, Faculty of Electronic Engineering, Serbia
[2] University of Kragujevac, Faculty of Mechanical and Civil Engineering in Kraljevo, Serbia
goran.pavlovic@elfak.ni.ac.rs, savkovic.m@mfkv.kg.ac.rs, zdravkovic.n@mfkv.kg.ac.rs, markovic.g@mfkv.kg.ac.rs

***Abstract*— In this research, multicriteria analysis and optimization of the steel girder of the crane runway were performed. Application of the welded I girder with vertical stiffeners was observed, in comparison with the standard rolled I profile which is most often using for these types of steel structures. The goal was primarily to show savings in the material in applying this design approach. For this reason, the minimization of the mass of the welded girder is set as the objective function. The strength criterion for characteristic points of the girder, local and global stability, the strength criterion for welded joints, as well as the stiffness of the girder, are set as optimization criteria. The optimization procedure was carried out using the Cyclical Parthenogenesis Algorithm (CPA), on the example of one segment of the crane runway track, for one single-beam bridge crane that is in exploitation. In this way, significant savings in the material were achieved, which justifies the presented method of analysis in the design of these types of structures.**

***Keywords*— Buckling, Crane runway, Optimization, Cyclical parthenogenesis algorithm, Welded beam**

I. Introduction

The crane runway beam is a very responsible type of structure and various influences must consider in its design. As the structure of the bridge crane with all its equipment moves along it, due to the failure of this structure, the consequences can be incalculable. For these reasons, it is necessary to particularly pay attention to the selection of the appropriate type of crane runway beam.

When designing these types of structures, to obtain the optimal cross-section of the girder, the welded I-profile is using, as an alternative for the standard types of these profiles.

For the above reasons and importance, analysis, and optimization of these types of structures is the subject of numerous studies. In the paper [1], the type of crane runway beam was analyzed, which web of the I-girder has a sinusoidal shape. The application of FEM in ABAQUS software shows the advantage of these girders in comparison to standard types of I-profiles. The analysis of the crane runway beam failure, which occurred due to fatigue, was performed in the paper [2]. The older procedure of the standard applied for the design of girders is not appropriate for fatigue, whereby the application of Eurocodes was proposed, which better takes into account the load spectrum.

The use of Eurocodes in the analysis of these types of structures is increasing ([2]-[5]). The application of Eurocodes for different types of structures, as well as in crane runway beam structures, was presented in [3]. The analysis of the application of Eurocodes in comparison to national standards for I-girders was presented in papers [4] and [5]. In the paper [6], multicriteria optimization of the welded I-girder of the double-beam bridge crane was performed using GRG2 code and EA code in EXCEL software, taking into account the global stability of the girder. Global stability is of great importance in the analysis of girders with I cross-section ([6]-[10]).

In [7], a multicriteria optimization of the welded I-girder of the single-beam bridge crane was performed, showing the achieved savings in material, in comparison to standard profiles, as well as the justification of this procedure. In researches [8] and [9], the types of girders composed of I and U profiles according to the AISC standard were analyzed, and in [9] experimental tests were performed. In the paper [10], the analysis of the I-profile for the monorail was observed, where the influence of the position of the supports on the global stability of the girder was observed.

Based on the importance of these types of structures, the shown research results, as well as the philosophy of optimal design, this research aims to develop a model for optimizing geometric parameters of the welded I-girder of the crane runway beam, to obtain the smallest possible mass of this type of girder. One metaheuristic method was used for the optimization process, and material savings will be shown, in comparison to existing solutions designed from standard I-profiles.

II. The optimization problem

In this research, the optimization of the crane runway beam is observed, whereby the welded I-profile with vertical stiffeners placed at distance $a=2\cdot h$ was analyzed (Fig. 1). The girder is subject to pressure forces from the wheels of the end carriage of the bridge crane.

The cross-section of the girder shows all required geometric parameters (Fig. 2).

This research aims to minimize the mass of the welded girder of the crane runway beam, where all the necessary conditions must be satisfied.

Design variables are the values that should be defined during the optimization procedure. Each design variable is defined by its upper and lower boundaries.

This research treats five geometric variables:

$$\left[x_1\ x_2\ x_3\ x_4\ x_5\right]=\left[b\ h\ d\ s\ a_s\right] \tag{1}$$

where:

b - the flange width (Fig. 2)

h - the web height (Fig. 2)

d - the flange thickness (Fig. 2)

s - the web thickness (Fig. 2)

a_s - the weld thickness (Fig. 2)

The objective function and constraints are presented in the next chapters.

The input parameters for optimization process are:

$$\left(F_W,\ L,\ L_t,\ \psi,\ \rho_m,\ R_e,\ E,\ \nu,\ K_f,\ t,\ b_s,\ h_s\right) \tag{2}$$

where:

F_W - the vertical load of the end carriage wheel (Fig. 1)

L - the span of the crane runway beam (Fig. 1)

L_t - end carriage wheelbase (Fig. 1)

$\psi = 1,25$ - the dynamic coefficient

$\rho_m = 7850\,kg/m^3$ - the density of material of the girder

R_e - the minimum yield stress of the girder material

$E = 21000\,kN/cm^2$ - the elastic modulus of the girder material

$\nu = 0,3$ - Poisson's ratio of the plate

$K_f = 1/750$ - the coefficient who depends on the purpose of the working conditions of the crane

$t = 5\,mm$ - the stiffener thickness (adopted value in this research)

b_s - the rail width

h_s - the rail height

In this research optimization was performed using the Cyclical Parthenogenesis Algorithm (CPA) in MATLAB software. This population-based metaheuristic algorithm is inspired by reproduction and social behavior of aphids, which can reproduce with and without mating, [11]. A detailed description of this method as well as the MATLAB code are shown in [11] and [12].

III. The objective function

The mass of the crane runway beam consists of both the plates of the I-profile and the plates of vertical stiffeners (Fig.1 and Fig. 2). The mass is increased by 5% due to welded joints, (3).

The objective function is defined as follows:

$$M = 1,05\cdot\rho_m\cdot\left(A_p\cdot L + 2\cdot n_v\cdot A_v\cdot t\right) \tag{3}$$

$$A_p = 2\cdot b\cdot d + h\cdot s \tag{4}$$

$$A_v = h\cdot b_v \tag{5}$$

$$b_v = \frac{b-s}{2} \tag{6}$$

where:

A_p - the cross-sectional area of the welded I-profile (Fig. 2)

b_v - the stiffener width (Fig. 2)

A_v - the area of vertical stiffener (Fig. 2)

n_v - the number of vertical stiffeners (Fig. 1)

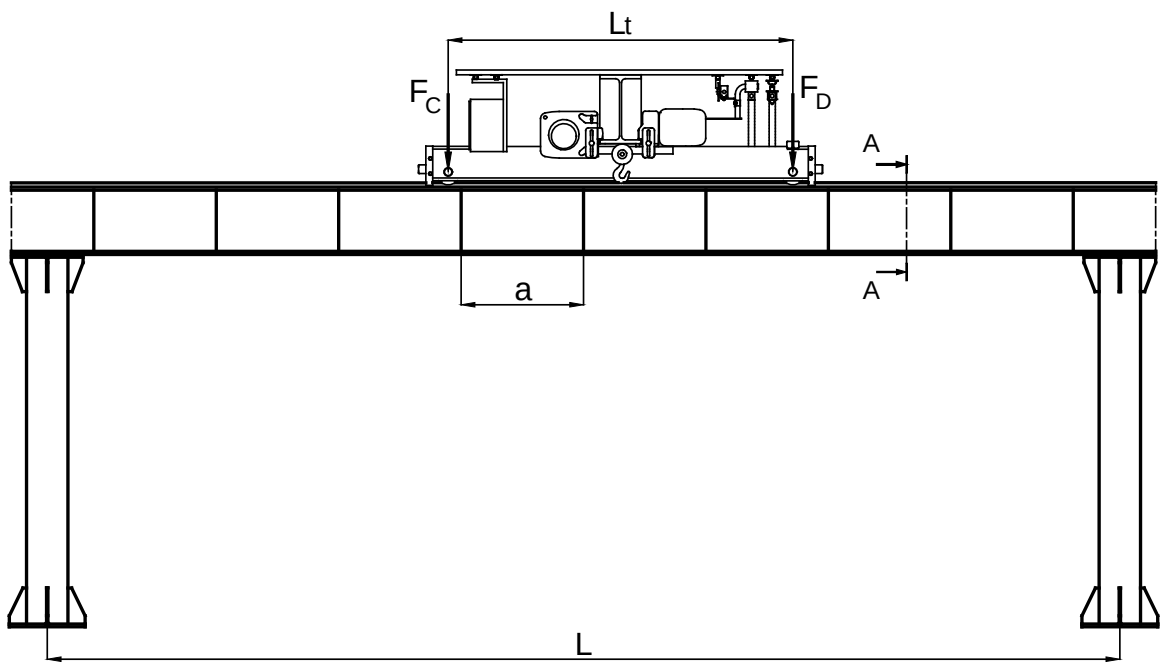

Fig. 1 Disposition of the crane runway beam with the bridge crane

All static parameters necessary for calculations (next chapter) in this optimization problem are (Fig. 1):

$$F_C = F_D = \psi\cdot F_W \tag{7}$$

$$R = F_C + F_D \tag{8}$$

$$q = \frac{M}{L} \cdot g \tag{9}$$

$$M_V = \frac{R}{4 \cdot L} \cdot \left(L - \frac{L_t}{2} \right)^2 + \frac{q \cdot L^2}{8} \tag{10}$$

$$F_T = \frac{R}{2 \cdot L} \cdot \left(L - \frac{L_t}{2} \right) + \frac{q \cdot L}{2} \tag{11}$$

where:

F_C, F_D - forces acting upon girder beneath the end carriage wheels

R - resulting force in the vertical plane

q - specific weight per unit of length of the welded girder

F_T - maximum shear force

M_V - maximum bending moment

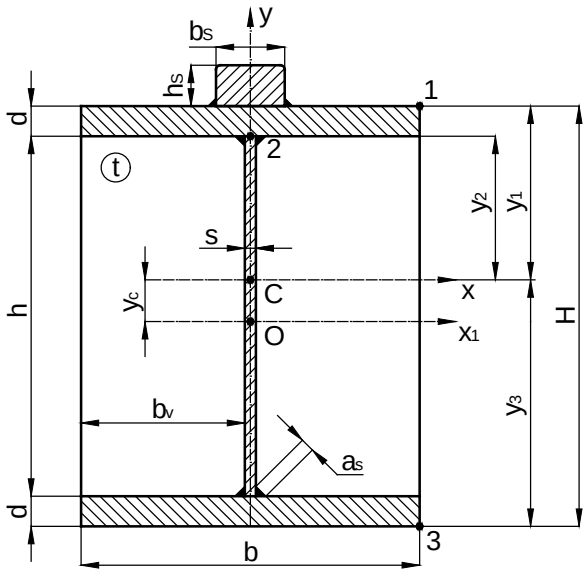

Fig. 2 Cross-section of the crane runway beam (A-A)

The geometric properties in the specific points of I-profile are (Fig. 2):

$$H = h + 2 \cdot d \tag{12}$$

$$A_s = b_s \cdot h_s \tag{13}$$

$$y_c = \frac{A_s \cdot (h + 2 \cdot d + h_s)}{2 \cdot \left(A_p + A_s \right)} \tag{14}$$

$$I_{x1} = \frac{1}{12} \cdot \left(s \cdot h^3 + 2 \cdot b \cdot d^3 + b_s \cdot h_s^{\,3} \right) + \\ + \frac{1}{2} \cdot b \cdot d \cdot \left(h + d \right)^2 + A_s \cdot \left(\frac{h + 2 \cdot d + h_s}{2} \right)^2 \tag{15}$$

$$I_x = I_{x1} + y_c^{\,2} \cdot \left(A_p + A_s \right) \tag{16}$$

$$I_{xb} = \frac{1}{12} \cdot \left(s \cdot h^3 + 2 \cdot b \cdot d^3 \right) + \frac{1}{2} \cdot b \cdot d \cdot \left(h + d \right)^2 \tag{17}$$

$$I_{yb} = \frac{1}{12} \cdot \left(s^3 \cdot h + 2 \cdot b^3 \cdot d \right) \tag{18}$$

$$y_1 = \frac{h}{2} + d - y_c \tag{19}$$

$$y_b = \frac{h}{2} + d \tag{20}$$

$$y_2 = \frac{h}{2} - y_c \tag{21}$$

$$y_3 = \frac{h}{2} + d + y_c \tag{22}$$

$$W_{x1} = \frac{I_x}{y_1} \tag{23}$$

$$W_{xb} = \frac{I_{xb}}{y_b} \tag{24}$$

$$W_{x2} = \frac{I_x}{y_2} \tag{25}$$

$$W_{x3} = \frac{I_x}{y_3} \tag{26}$$

$$S_{x2} = b \cdot d \cdot \left(\frac{h + d}{2} - y_c \right) + A_s \cdot \frac{h + 2 \cdot d + h_s}{2} \tag{27}$$

$$S_{x2b} = b \cdot d \cdot \frac{h + d}{2} \tag{28}$$

IV. Constraint functions

A. *The criterion of stresses*

The stress check is conducted at the specific points of the I-profile of the welded girder (Fig. 2). The value of stress σ must be less than the value of permissible stress σ_d.

The total stress at point 1 is:

$$\sigma_1 = \frac{M_V}{W_{x1}} \le \sigma_d \tag{29}$$

$$\sigma_d = \frac{R_e}{\nu_1} \tag{30}$$

where:

$\nu_1 = 1{,}5$ - the factored load coefficient for load case 1, [13]

The components of normal stresses σ_2 and σ_y at point 2 are:

$$\sigma_2 = \frac{M_V}{W_{x2}} \le \sigma_d \tag{31}$$

$$\sigma_y = \frac{F_C}{s \cdot z_1} \le \sigma_d \tag{32}$$

$$y_\alpha = \frac{b \cdot d^2 + A_s \cdot (h_s + 2 \cdot d)}{2 \cdot \left(b \cdot d + A_s \right)} \tag{33}$$

$$I_\alpha = \frac{b \cdot d^3}{12} + b \cdot d \cdot \left(y_\alpha - \frac{d}{2} \right)^2 + \\ + \frac{b_s \cdot h_s^3}{12} + A_s \cdot \left(\frac{h_s}{2} + d - y_\alpha \right)^2 \quad (34)$$

$$z_1 = 3,25 \cdot \sqrt[3]{\frac{I_\alpha}{s}} \quad (35)$$

The tangential stress at point 2 is:

$$\tau_2 = \frac{F_T \cdot S_{x2}}{I_x \cdot s} \le \tau_d = \frac{\sigma_d}{\sqrt{3}} \quad (36)$$

Finally, the total stress at point 2 is:

$$\sigma_{2,u} = \sqrt{\sigma_2^{\,2} + \sigma_y^2 - \sigma_2 \cdot \sigma_y + 3 \cdot \tau_2^{\,2}} \le \sigma_d \quad (37)$$

The total stress at point 3 is:

$$\sigma_3 = \frac{M_V}{W_{x3}} \le \sigma_d \quad (38)$$

B. The criterion of local stability of the flange plate of I-profile

For this criterion, the condition from equation (39) must be fulfilled, according to [14]:

$$\sigma_p = \nu_1 \cdot \sigma_1 \le \sigma_{p,d} = \chi_p \cdot R_e \cdot c_p \quad (39)$$

$$\psi_p = 1, \ \alpha_p = \frac{a}{h} \ge 1, \ k_\sigma = 0,43 \quad (40)$$

$$\sigma_E = \frac{\pi^2 \cdot E}{12 \cdot (1 - \mu^2)} \cdot \left(\frac{2 \cdot d}{b} \right)^2 \quad (41)$$

$$\overline{\lambda_p} = \sqrt{\frac{R_e}{k_\sigma \cdot \sigma_E}} \quad (42)$$

$$\chi_p = \frac{0,6}{\sqrt{\overline{\lambda_p}^{\,2} - 0,13}} \le 1 \quad (43)$$

where:
$c_p = 1$ - non-dimensional coefficient, according to [14]

C. The criterion of local stability of the web plate of I-profile

This criterion is satisfied if the condition from equation (44) is fulfilled, according to [13]:

$$\left(\frac{\sigma_I}{\sigma_{kr}} + \frac{\sigma_M}{\sigma_{Mkr}} \right)^2 + \left(\frac{\tau_{sr}}{\tau_{kr}} \right)^2 \le 0.81 \quad (44)$$

$$\sigma_I = \nu_1 \cdot \sigma_2 \quad (45)$$

$$\sigma_M = \nu_1 \cdot \sigma_y \quad (46)$$

$$\sigma_{kr} = K_2 \cdot \left(\frac{d}{h} \right)^2 \cdot 100000, \ \frac{\sigma_M}{\sigma_I} \ge 3,939 \quad (47)$$

$$\sigma_{kr} = 6,3 \cdot \left(\frac{s}{h} \right)^2 \cdot 100000, \ \frac{\sigma_M}{\sigma_I} < 3,939 \quad (48)$$

$$\sigma_{Mkr} = K_{11} \cdot \left(\frac{s}{a} \right) \cdot 100000, \ \frac{\sigma_M}{\sigma_I} \ge 3,939 \quad (49)$$

$$\sigma_{Mkr} = K_{12} \cdot \left(\frac{2 \cdot s}{a} \right) \cdot 100000, \ \frac{\sigma_M}{\sigma_I} < 3,939 \quad (50)$$

$$\tau_{sr} = \frac{\nu_1 \cdot F_T}{s \cdot h} \quad (51)$$

$$\tau_{kr} = \left[125 + 95 \cdot \left(\frac{h}{a} \right)^2 \right] \cdot \left(\frac{s}{h} \right)^2 \cdot 1000 \quad (52)$$

where:
K_2, K_{11}, K_{12} - non-dimensional coefficients, according to [13]

D. The criterion of global stability of the girder

The global stability (buckling) of the girder is checking in compliance with [15]. The following condition must be fulfilled:

$$\frac{h}{s} \le 3 \cdot \sqrt{\frac{E}{R_e}} \quad (53)$$

This criterion is satisfied if the condition from equation (54) applies:

$$\sigma_b = \nu_1 \cdot \frac{M_V}{W_{xb}} \le \min\left(\sigma_{b,d}, R_e \right) \quad (54)$$

$$I_D = \frac{1}{3} \cdot \left(2 \cdot d^3 \cdot b + s^3 \cdot h \right) \quad (55)$$

$$K = 1 + 0,156 \cdot \left(\frac{L}{H} \right)^2 \cdot \frac{I_D}{I_{yb}} \quad (56)$$

$$\phi = \frac{\sqrt{K + \rho^2} - \rho}{\sqrt{K + \rho^2}} \quad (57)$$

$$I_{p1} = \frac{b^3 \cdot d}{12} + \frac{s^3 \cdot h}{72} \quad (58)$$

$$A_{p1} = b \cdot d + \frac{h \cdot s}{6} \quad (59)$$

$$i_p = \sqrt{\frac{I_{p1}}{A_{p1}}} \quad (60)$$

$$\lambda_y = \frac{L}{i_p \cdot \sqrt{\eta}} \quad (61)$$

$$\sigma_{wd} = \frac{\pi^2 \cdot E}{\lambda_y^{\,2}} \quad (62)$$

$$\sigma_{vd} = \frac{\eta \cdot \pi}{L \cdot W_{xb}} \cdot \sqrt{G \cdot E \cdot I_D \cdot I_{yb}} \quad (63)$$

$$G = \frac{E}{2\cdot(1+\nu)} \tag{64}$$

$$\sigma_{crd} = \phi \cdot \sqrt{\sigma_{wd}^{\ 2} + \sigma_{vd}^{\ 2}} \tag{65}$$

$$\overline{\lambda_D} = \sqrt{\frac{2\cdot S_{x2b}}{W_{xb}} \cdot \frac{R_e}{\sigma_{crd}}} \tag{66}$$

$$\chi_M = \left(\frac{1}{1+\overline{\lambda_D}^{2\cdot n}} \right)^{1/n}, \ \overline{\lambda_D} \geq 0,4 \tag{67}$$

$$\chi_M = 1, \ \overline{\lambda_D} < 0,4 \tag{68}$$

$$\sigma_{b,d} = \alpha_b \cdot \chi_M \cdot R_e \tag{69}$$

where:

$\eta = 1,35, \ \rho = 0,55$ - coefficients, according to [15]

$n = 1,5$ - non-dimensional coefficient, according to [15]

E. *The criterion of stresses in the welded connection*

The value of stress σ_s in the welded connection (Fig. 2) must be less than the value of permissible stress $\sigma_{s,d}$.

$$\sigma_s \leq \sigma_{s,d} = 0,75 \cdot \sigma_d \tag{70}$$

$$\sigma_s = \sqrt{V_n^{\ 2} + V_p^{\ 2}} \tag{71}$$

$$V_n = \frac{F_C}{2\cdot a_s \cdot z_1} \tag{72}$$

$$V_p = \frac{F_T \cdot S_{x2}}{I_x \cdot 2 \cdot a_s} \tag{73}$$

$$a_s \leq 0,7 \cdot \min(s,d) \tag{74}$$

where:

V_n, V_p - stresses in the welded connection

F. *The criterion of deflection of the girder*

To satisfy this criterion, the total deflection f_u in the vertical plane must have the value smaller or equal to the permissible value f_d:

$$f_u = f_F + f_q \leq f_d = K_f \cdot L \tag{75}$$

$$f_F = \frac{F_C \cdot L^3}{48 \cdot E \cdot I_x} \cdot \left\{ 1 + \frac{F_D}{F_C} \cdot \left[1 - 6 \cdot \left(\frac{L_t}{L} \right)^2 \right] \right\} \tag{76}$$

$$f_q = \frac{5 \cdot q \cdot L^4}{384 \cdot E \cdot I_x} \tag{77}$$

V. THE OBTAINED RESULTS OF OPTIMIZATION

The optimization process was done in MATLAB software using CPA code [12], without any modifications.

Algorithm parameters taken in all examples for this optimization process are: $N_a = 60$ - population size (number of aphids), $N_c = 4$ - number of colonies, $F_r = 0,4$ - parameter to determine the ratio of aphids of each colony to be considered as female, $\alpha_1 = 1, \alpha_2 = 2$ - search step size parameters, $\max N = 3000$ - maximum number of objective function evaluations.

Bound values of variables for all example are:

$100 \leq x_1 \leq 300$, $300 \leq x_2 \leq 800$, $6 \leq x_3 \leq 40$, $5 \leq x_4 \leq 20$, $3 \leq x_5 \leq 7$

TABLE I THE VALUES OF INPUT PARAMETERS

	F_W (kN)	L (m)	L_t (m)	M_p (kg)
1	32,5	12	2	1871
2	28,5	5	2,5	290
3	54	7	2,5	1085

Input parameters are taken from project documentations of three existing solutions of crane runway beams (Table I). In all examples, dimensions for the rail are b_s *x* h_s = 30 *x* 50 *mm*; the material of crane runway beams is S235. For this material, mechanical properties are: R_e = 23,5 *kN/cm*^{2}, σ_d = 15,67 *kN/cm*^{2}, and $\sigma_{s,d}$ = 11,75 *kN/cm*^{2}.

For the problem of the crane runway beam analysis defined in this way, coefficients for the criterion of local stability of the web plate are: K_2 = 17,79, K_{11} = 17,57, and K_{12} = 4,81, [13].

Table II shows the results of the optimization (optimal values of the geometric parameters and convergence characteristics) for all examples of the girders of the crane runway beams. Table III shows the rounded values of optimal geometrical parameters, optimal mass, and savings in material. Table IV shows the values of all constraint functions, for the rounded optimal values.

where:

M_p - the value of the mass of I-girder (Table I)

M_o - the value of the optimal mass of the welded I-girder (Table III)

TABLE II THE VALUES OF OPTIMAL GEOMETRIC PARAMETERS AND CONVERGENCE CHARACTERISTICS OF THE CPA METHOD

	b (mm)	h (mm)	d (mm)	s (mm)	a_s (mm)	n_v	Best (kg)	Worst (kg)	Mean (kg)	Std	time (s)
1	142,89	459,55	40,0	5,12	3,00	13	1397,5	1898,7	1413,3	59,82	4,38
2	227,45	351,07	6,00	5,00	3,39	8	207,4	283,9	208,0	4,52	4,13
3	299,99	494,95	10,71	5,52	3,58	7	570,3	741,7	573,5	15,35	4,15

TABLE III THE ROUNDED VALUES OF OPTIMAL GEOMETRIC PARAMETERS, OPTIMAL MASS AND SAVINGS IN MATERIAL

	b (mm)	h (mm)	d (mm)	s (mm)	a_s (mm)	M_o (kg)	Saving (%)
1	143	460	40	6	3	1438,3	23,13
2	228	351	6	5	4	210,9	27,28
3	300	495	11	6	4	594,1	45,24

TABLE IV THE VALUES OF CONSTRAINT FUNCTIONS

	σ_1	σ_2	σ_y	τ_2	$\sigma_{2,u}$	σ_3	σ_p	$\sigma_{p,d}$	$\leq 0,81$	σ_b	$\sigma_{b,d}$	σ_s	f_u	f_d
1	6,10	5,10	2,86	1,40	5,05	7,47	9,16	23,50	0,014	11,96	11,96	3,18	1,59	1,60
2	3,83	3,65	5,33	1,47	5,36	6,67	5,74	14,79	0,008	13,30	13,35	3,45	0,13	0,67
3	5,97	5,67	7,55	1,79	7,48	7,96	8,95	22,14	0,027	13,20	13,61	5,82	0,48	0,93

VI. CONCLUSIONS

In this study, the mass of the welded girder of the crane runway beam was optimized. The mass of the girder was optimized using Cyclical Parthenogenesis Algorithm (CPA) in MATLAB software. The results were compared with the existing solutions of the crane runway beams. The results show that the method used is reliable, convenient, and rapid (Table II).

Justification of the application of the proposed procedure and method resulted in significant savings in material, within the range of 23,13 ÷ 45,24% (Table III), with none of the constraint functions is not exceeded. (Table IV). The adopted optimization algorithm was used for the reason that it has proven to give good results in different types of engineering problems, [11].

Table IV shows the criterion of global stability is the most critical, which was to be expected, as it is a girder with the I-cross section. In the first example, the deflection criterion is also critical, since it is a large value of the girder span. Also, the criterion of local stability of the web plate could be ignored for the observed examples.

The presented procedure is very useful for designers and researchers and can be applying for similar optimization problems. In further analysis should include the FEM, to verify the results of optimization.

The procedure should be further improved, which includes in the analysis of other important criteria, such as the position of stiffeners (vertical and horizontal), the fatigue of materials, types of materials, manufacturability, etc.

ACKNOWLEDGMENT

This work has been supported by the Ministry of Education, Science and Technological Development of the Republic of Serbia.

REFERENCES

[1] M. Maali, A.C. Aydin, and M. Sagiroglu, “Investigation of innovative steel runway beam in industrial building”, *Sadhana*, Vol. 40, pp. 2239–2251, 2015.

[2] F. Pelayo, C. Rodríguez and A.F. Canteli, “Failure and repair analysis of a runway beam: Influence of the standard applied to lifetime prediction”, *Engineering Failure Analysis*, Vol. 56, pp. 89–97, 2015.

[3] D. Beg, U. Kuhlmann, L. Davaine and B. Braun, *Design of Plated Structures - Eurocode 3: Design of Steel Structures Part 1-5 – Design of Plated Structures*, ECCS – European Convention for Constructional Steelwork, Belgium, 2010.

[4] P. Bieranowski, “The Modernisation of Steel Construction Beam Gantry for the Work of Transport Suspended – Using the Example of Track Length Expansion by a Short Bracket”, *Czasopismo Techniczne*, Vol. 2-B, pp. 3-16, 2016.

[5] M. Gašić, M. Savković, N. Zdravković, G. Marković and H. Hot, “Stress determination in reinforced I-section bottom flange of single girder crane”, *The Fifth International Conference On Transport And Logistics til 2014*, Serbia, pp. 123-128, 5–6 June, 2014.

[6] G. Pavlović, M. Savković, N. Zdravković, G. Marković and M. Gašić, “Optimization of the Welded I-Girder of the Double-Girder Bridge Crane”, *MTC AJ*, Vol. 16, Issue 3/3, article No. 1667, 2018.

[7] G. Pavlović, M. Savković, N. Zdravković, R. Bulatović and G. Marković, “Analysis and Optimization Design of Welded I-Girder of the Single-Beam Bridge Crane”, *IV International Conference "Mechanical Engineering in the 21st Century – MASING 2018"*, Serbia, pp. 145-150, 19–20 April, 2018.

[8] W.T. Hsu, D.M. Lue and Y.F. Chen, “Design Aid for Moment Strength of Built-up Crane Runway Girders”, *International Journal of Steel Structures*, Vol. 12(3), pp. 403-417, 2012.

[9] D.S. Ellifritt and D. Lue, “Design of Crane Runway Beam with Channel Cap”, *Engineering Journal*, Second Quarter, pp. 41-49, 1998.

[10] N.S. Trahair, “Lateral buckling of monorail beams”, *Engineering Structures*, Vol. 30, pp. 3213-3218, 2008.

[11] A. Kaveh and A. Zolghadr, “Cyclical Parthenogenesis Algorithm: A New Meta-Heuristic Algorithm”, *Asian Journal of Civil Engineering (Building and Housing)*, Vol. 18(5), pp. 673-701, 2017.

[12] A. Kaveh and T. Bakhshpoori, *Metaheuristics: Outlines, MATLAB Codes and Examples*, Springer Nature Switzerland AG, Switzerland, 2019

[13] Z. Petković and D. Ostrić, *Metalne konstrukcije u masinogradnji 1*, Institute for Mechanization of the Faculty of Mechanical Engineering of the University in Belgrade, Serbia, 1996.

[14] SRPS U.E7.121:1986, *Provera stabilnosti nosećih čeličnih konstrukcija - Proračun izbočavanja limova*, Jugoslovenski zavod za standardizaciju, Beograd, 1986

[15] SRPS U.E7.101:1991, *Provera stabilnosti nosećih čeličnih konstrukcija - Bočno izvijanje nosača*, Jugoslovenski zavod za standardizaciju, Beograd, 1991.

THE 5th INTERNATIONAL CONFERENCE
MECHANICAL ENGINEERING IN XXI CENTURY

December 9-10, 2020
Faculty of Mechanical Engineering in Niš, Serbia

Sanation of the Synchronous Valve Casing of Hydroelectric Generating Set on Hydro Power Plant Pirot

Miodrag ARSIĆ[1], Srđan BOŠNJAK[2], Vencislav GRABULOV[1], Mladen MLADENOVIĆ[1], Zoran SAVIĆ[1]

[1] Institute for Materials Testing, Bulevar vojvode Mišića 43, Belgrade, Serbia
[2] Faculty of Mechanical Engineering, Kraljice Marije 16, Belgrade, Serbia
miodrag.arsic@institutims.rs, sbosnjak@mas.bg.ac.rs, venciclav.grabulov@institutims.rs, mladen.mladenovic@institutims.rs, zoran.savic@institutims.rs

***Abstract* – Corrosion, erosion and cavitation have a significant influence on parts of turbine and hydromechanical equipment in exploitation. The same can be said when it comes to damaging of surfaces of the synchronous valve which is a part of the vertical Francis turbine runner of the hydroelectric generating set A1 at HPP ''Pirot'', with nominal power of 40 MW. Erosion of surfaces of hydraulic machine components exposed to the effect of cavitation can become a large scale problem in a short while, while depths of cavities can reach up to 100 mm. This paper contains the technology of sanation of damages through repair welding, tests performed after sanation, as well as suggestions for execution of optimal anticorrosion protection that refer to the synchronous valve of the hydroelectric generating set A1 at HPP 'Pirot'.**

***Keywords* – synchronous valve, damage, reparation, surface welding**

I. Introduction

Components of turbine and hydromechanical equipment of hydro power plants in exploitation are subjected to stationary and dynamic loads and effects of corrosion, erosion, cavitation etc. Damages which occur on surfaces could cause the failure of components, as well as standstill of the hydroelectric generating set as a whole. Therefore it's necessary to repair damages through the use of appropriate techniques.

Managements of hydro power plants are interested in developing means of protection of components and structures against undesirable occurrences of degradation of base material and / or welded joints caused by corrosion, erosion, cavitation or their combined effect, which is the case with the casing of the synchronous valve. Therefore, on one hand, the researches regarding the development of new structural materials resistant to those effects are being carried out, and on the other researches which deal with development of new technological procedures and materials needed for reparation and preventive protection of equipment in exploitation.

Casing of the synchronous valve has been made of structural steel 422.712.5, while stiffening ribs have been made of Cr-Ni steel 17246. Both types of steel have been produced in Czech Republic. Conical valve seat has been surface welded with bronze

There are several procedures for the reparation of damaged surfaces. For that purpose metals, ceramic materials and metal carbides are most commonly being used. For the application of above mentioned materials, in order to perform repairs, the methods which predict the use of gas combustion, electric arc or plasma are being employed. When hydraulic turbine components are concerned, it is necessary for the procedure to meet the requirements which refer to structural properties or means needed for repair performing, in other words:

it should not predict heat input which could cause the change in the structure of the material, occurrence of cracks and /or internal stresses,

it should not predict complex preparation and finish machining on damaged locations,

it should predict surfacing in all positions (horizontal, overhead, etc.), as well as in hardly accessible locations,

it should not predict production of special scaffolds or disassembling of parts of equipment,

it should enable fast execution of works,

it should require special means of protection at work,

it should enable easy handling of coating equipment.

For this paper the welding/surfacing procedure as a method of reparation of damages on the casing of the synchronous valve was analyzed. Damages are approximately 10 mm deep, fig. 1. Role of the synchronous valve is to protect the runner and blades from the hydraulic impact of water when the turbine stops, or in other words to release water from the turbine when it ceases to operate, because at that moment the water posseses the kinetic energy of such a level that it could cause the breakdown of the hydroelectric generating set as a whole.

a) Casing of the synchronous valve b) Stiffening ribs

Fig. 1 Damages on the synchronous valve

II. Experimental Procedure

A. *Effect of Corrosion*

Erosion of metal occurs as a result of chemical and electrochemical action of aggressive corrosion. Effect of corrosion on structural steels the casing of the synchronous valve was made of in high humidity conditions, due to the presence of freshwater, causes the damaging of metal due to the occurrence of initial cracks and their propagation, as well as variable loading. In such a case, inspections and maintenance are of highest importance. A large number of loading cycles and high amplitudes can lead to failure in a very brief period of time. Quantity of eroded metal is closely linked with properties of operational environment, pressure and temperature. Product of corrosion is the material with entirely different physical and mechanical properties in comparison with the initial material.

B. *Effect of Erosion*

Presence of solid particles in the fluid, which can not be avoided, is the basic cause of erosion of the casing of synchronous valve. Those are, mainly, products of the corrosion of metal the casing was made of, but there is also a possibility that they ended up in the operational environment due to wearing of other components. Erosion rate of the metal, at room temperature, depends on many influential factors: particle dimensions, velocities of particles, particle concentration, physical and mechanical properties of particles, material that wears out etc. In order to reduce severe influence of erosion on the casing, certain technical measures had to be taken: use of the erosion resistant material in order to significantly extend the service life, application of the coating with good resistance to wearing and fluid flow control by avoiding severe transitions, bends, broadenings and constrictions.

C. *Effect of Cavitation*

Cavitation refers to the occurrence of cavities on the surface of the metal. Cavitation is one of mechanisms of liquid erosion, which comprises formation and implosion of bubbles within the fluid. Process of removal of material from the surface is called cavitation erosion, and the resulting damage is cavitation damage. Erosion of surfaces of components of hydraulic machines exposed to the effect of cavitation can become a large scale problem in a short while, while depths of cavities can reach up to 100 mm.

Cavitation damages on elements of turbine and hydromechanical equipment occur as a consequence of the erosion of surfaces on which the implosion of cavitation bubbles formed due to exceeding of critical velocity which mostly depends on overall pressure occurs. Process of erosion is in direct connection with conditions of exploitation. Cavitation damages on the casing of synchronous valve are especially visible at locations of sudden change of direction of streamlines and liquid velocity.

Cavitation has not been fully investigated yet, but it is known that one of the causes of its occurrence are high velocities of liquid drops which hit the surface of the metal. Conditions which enable reaching of critical velocities are being restricted by structural solutions. Occurrence of cavitation damages on components of turbine and hydromechanical equipment on hydro power plants during exploitation gets detected due to vibrations and noise. At locations where cavitation occurs local pressures can build up to 200 bar, which causes mechanical erosion of material (formation of cavities and wearing). Therefore the favorable effect of turbine operation gets reduced due to the conversion of energy into heat.

III. REPARATION OF DAMAGES ON THE CASING

Reparation of damages that occur on the casing of synchronous valve comprises the technology for damage reparation by surface welding, post-repair inspections and suggestions that refer to optimal anti-corrosion protection. Chemical composition of materials valve casing and stiffening ribs were made of is presented in Tables 1 and 2.

TABLE 1 CHEMICAL COMPOSITION OF SYNCHRONOUS VALVE CASING MATERIAL

Steel 422.712.5	
Czech Republic	
C	0,17 - 0,25
Si	0,20 - 0,50
Mn	0,90 - 1,40
Ni	max 0,40
P	max 0,04
S	max 0,04
Cr	max 0,30
Cu	max 0,30

TABLE II CHEMICAL COMPOSITION OF STIFFENING RIB MATERIAL

Steel 422.712.5	
Czech Republic	
C	min 0.12
Si	min 1.00
Mn	min 2.00
Ni	8.00 – 11.00
P	max 0,045
S	max 0,030
Cr	max 17.00 – 20.00
Ti	max 0,30

D. *Technology for Damage Reparation by Surface Welding*

This procedure and technology for the reparation of the casing of synchronous valve by surface welding could also be used for reparation of other damaged components of turbine and hydromechanical equipment on hydroenergetic facilities subjected to corrosion, erosion and/or cavitation during exploitation.

Order of actions in the damage reparation process is as follows:

• disassembling of the valve,

• visual and dimensional inspection of all elements of which the valve consists and creation of the list of parts that need to be replaced,

• grinding of internal surfaces of the casing in the zone of cavitation damages by small angle and straight grinders, 600 – 1200 W power,

• removal of corrosion products from external and internal surfaces by sandblasting or mechanically,

• magnetic particle inspection of surfaces of components made of structural steels,

• dye-penetrant inspection of valve components made of stainless materials,

• filling of grinded locations with filling material which increases resistance to cavitation of weld metal,

• machining of repaired locations by grinding, so that the height of weld reinforcement with respect to base material is 0,5 mm,

• dye-penetrant inspection of surfaced areas,

• strengthening of surface welded areas (pneumatic hammer with a rounded tip of 5-8 mm radius),

• hardness testing of strengthened surface welded areas,

• machining of the valve seat until damages that affect tightness are removed,

• machining of the valve seat by polishing paste, assembled with the blocking element, until value of surface roughness Ra=0,8 μm is reached,

• machining quality inspection on all vital valve surfaces,

• quality class of machining defined by technical documentation,

• replacement of components that can not be repaired, but could jeopardize the functionality of the valve,

• optimum anti-corrosion protection of all areas covered by technical documentation depending on the type of fluid they are in contact with,

• application of coatings resistant to cavitation on internal surfaces of the valve,

• valve assembling,

• valve functionality check,

• valve check by water pressure, pi = 3,9 MPa.

Surface welding has been performed by electric arc process 111, through the use of Castolin Eutectic electrodes. For cavities with t < 5 mm Cavitec SMA ø 3,.2 and ø 4 mm (welding technology specification No 89 - 1/09) electrodes were used, figure 2. For cavities with t ≥ 5 mm CP 33700 ø 3,2 or ø 4 mm electrodes were used for the intermediate layer, and for remaining 2 layers 4-5 mm were left to be filled with ø 3,2 or ø 4 mm electrodes, with the weld reinforcement 1 – 2 mm high (welding technology specification No 89 - 2/09), figure 3. During surface welding short arc has been sustained. After the application of every layer slag has been removed.

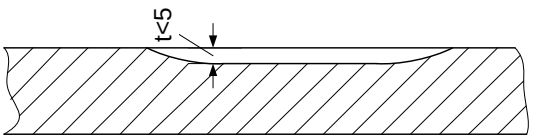

a) Cavities t < 5mm

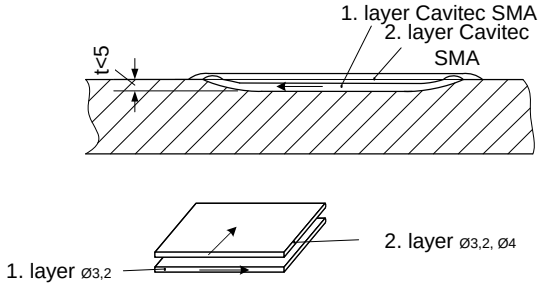

b) Order of activities

Fig. 2 Preparation and surface welding with t < 5 mm

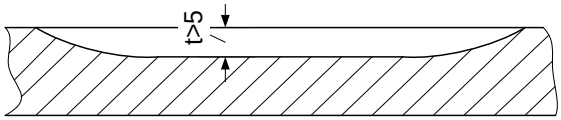

a) Cavities t ≥ 5mm

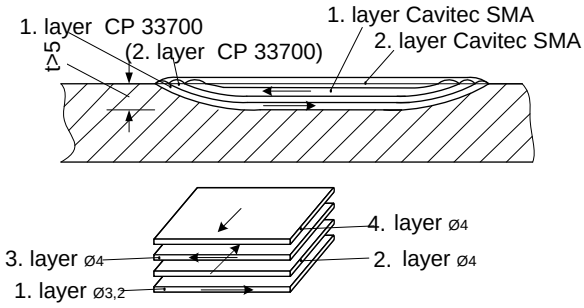

b) Order of activities

Fig. 3 Preparation and surface welding with t ≥ 5 mm

IV. Results and Discussion

After the reparation and strengthening by pneumatic hammer blows hardness testing on locations where surface welding was performed has been carried out. Surfaces on which hardness testing was performed were prepared in accordance with requirements of manufacturers of measurement equipment. Testing has been performed on 3 locations, with 3 measured values for each. The mean value of measurements performed on 3 locations has been adopted as an overall value of hardness. Hardness value has been, in accordance with recommendations of the manufacturer of filler material, increased from 230 – 250 HV to more than 400 HV after strengthening. Dye-penetrant testing has been performed in order to detect eventual defects which occur after surface welding.

A. Anti-corrosion Protection of Internal Surfaces of the Valve Exposed to the Water Stream

Internal surfaces of the synchronous valve are exposed to high velocity water flows which cause cavitation damage. Anti-corrosion protection process consists of adequate, strictly controlled, preparation of surfaces and application of 3 layers of protective material Belzona 1341 (Supermetalglide). Prepared surfaces have to meet the following conditions: minimum profile depth 75 μm, purity SA 2,5, sharp angle profile of surface roughness, no presence of contaminants: grease, salt, etc. Time schedule for coating application has to be followed strictly in order not to contaminate the metal surface. Previously applied layers have to possess characteristics

necessary for the application of the next layer. Works can not be carried out unless the ambient air temperature is higher than 10°C. The other condition is that humidity must not be higher than 90%.

B. *Anti-corrosion Protection of External Surfaces of Valve Body Exposed to the Water Stream*

External surfaces of valve body, exposed to the water stream, after the surface preparation by use of sand-blasting should be protected with the water-resistant system Nº1. The process comprises the application of basic coatings (feropks based on epoxy resin, 1 x 40 μm thick), intermediate coatings (tankplast based on epoxy resin, 1 x 100 μm thick) and finishing coatings (plastolak based on epoxy resin, 2 x 30 μm thick).

C. *C. Anti-corrosion Protection of Internal Surfaces of Valve Body Not Exposed to the Water Stream*

Internal surfaces of valve body not exposed to the water stream, after the surface preparation, should be protected with the water-resistant system Nº2. The process comprises the application of basic coatings (feropks based on epoxy resin, 2 x 40 μm thick) and finishing coatings (balastin based on epoxy resin, 2 x 200 μm thick).

V. Conclusions

Methodological approach to state analysis and determination of causes of degradation of base material and welded joints, as well as reparation technology for the casing of synchronous valve by surface welding can be used for reparation of other damaged components and structures of turbine and hydromechanical equipment subjected to corrosion, erosion and/or cavitation damaging during exploitation.

Fast and reliable solution of the problem that concerns vital components and elements of structure on hydro power plants can be established exclusively through creation of databases. Backup software packages increase the efficiency regarding the use of databases, analysis of some influential factors, improvement techniques, possibilities for damage/erosion prevention and browsing in order to find alternative solutions.

Acknowledgment

This work was supported by the Ministry of Education, Science and Technological Development of the Republic of Serbia (Contracts No. 451-03- 68/2020-14/200012 and 451-03-68/2020-14/200105).

References

[1] B. Sirok., M. Hocevar, I. Kern, M. Novak, “Turboinst, Monitoring of the cavitation in the Kaplan turbine“, *Industrial Electronics*, 1999. ISIE '99, Vol. 3, pp. 1224-1228, Slovenia, 2002.

[2] B. Međo, M. Rakin, M. Arsić, Ž. Šarkoćević, M. Zrilić, S. Putić, “Determination of the Load Carrying Capacity of Damaged Pipes Using Local Approach to Fracture”, *Materials Transactions. JIM*, 2012, Vol. 53, No.1, pp. 185-190.

[3] M. K. Sharma, G. S. Grewal, A. K. Singh, “Silt Erosion in Indian Hydroelectric Projects - Laboratory Studies of Thermal Spray Coatings over Hydro Turbine Components”, *Hydro Vision 2008*, Conference Papers CD-Rom, HCI Publications, Kansas City, Mo., USA, 2008.

[4] K. P Mamata., R. P .Saini, “A review on silt erosion in hydro turbines“, *Renewable and Sustainable Energy Reviews*, Vol. 12, No. 7, 2008, pp. 1974-1987.

[5] K. Pardeep, R.P. Saini, “Study of cavitation in hydro turbines - A review“, *Renewable and Sustainable Energy Reviews*, Volume 14, No. 1, 2010, pp. 374-383.

[6] S. Raghuvir, S. K.Tiwari, K. M. Suman, “Cavitation Erosion in Hydraulic Turbine Components and Mitigation by Coatings: Current Status and Future Needs“, *Materials Engineering and Performance*, doi.10.1007/s11665-011-0051-9.

[7] S. I. Monica, D. C. Gabriel, A. François, “Analysis of the Cavitating Draft Tube Vortex in a Francis Turbine Using Particle Image Velocimetry Measurements in Two - Phase Flow“, *J. Fluids Eng.*, 2008, Vol. 130, Issue 2, 021105 (10 pages), .doi.org/10.1115/1.2813052

THE 5th INTERNATIONAL CONFERENCE
MECHANICAL ENGINEERING IN XXI CENTURY

December 9-10, 2020
Faculty of Mechanical Engineering in Niš, Serbia

Transient Finite Element Analysis (FEA) in Material Selection Process: Introduction

Dušan ĆIRIĆ[1], Jelena MIHAJLOVIĆ[1] and Miroslav MIJAJLOVIĆ[2]

[1] PhD Student: University of Niš, Faculty of Mechanical Engineering, Aleksandra Medvedeva 14, Niš, Serbia
[2] Associate Professor: University of Niš, Faculty of Mechanical Engineering, Aleksandra Medvedeva 14, Niš, Serbia

dusan.ciric@hotmail.com, jelena.mihajlovic@masfak.ni.ac.rs, miroslav.mijajlovic@masfak.ni.ac.rs

***Abstract*— The suitable material selection for a particular mechanical part or assembly is one of the most important tasks in the product development process. Due to the presence of a vast number of materials with diverse characteristics, the material selection process is a complicated and time-consuming task. There is a need for a systematic and efficient approach to choose the most suitable material type to fulfill the part's requirements and proper use inside the process in which it obtains. Given the function that sub-assembly has inside the production process, the heat distribution will be the most crucial factor in the material selection process. To minimize the risks such as component failure, modeling, and analysis tools such as finite element analysis (FEA) are essential for evaluating material performances non-destructively at the operating temperatures and work conditions. FEA can determine the heat distribution and other relevant mechanical properties necessary for the material selection process. Specifically, this paper introduces the material selection for the tool ("cleaner") responsible for the preparation of the valve application area on the inner tube profile, by transient FEA analysis obtained in Ansys Workbench.**

***Keywords*— Material selection process, finite element analysis (FEA), transient analysis, inner tube profile, valve.**

I. Introduction

Engineering includes designing, manufacturing, and maintaining products, systems, services, and structures [1]. Early design decisions can have a very significant impact on the product's sustainability and application. One of these decisions regards the material selection process.

Material selection plays a vital role in process of mechanical and structural design [2]. The material selection process is often a complicated task due to the fact that nowadays the vast numbers of material types are present. Also, the diversity between the same material categories is substantial. Some properties could be good and in compliance with the set requirements, but some of them are not applicable [3]. Those important characteristics of materials are strength, durability, flexibility, weight, resistance to heat and corrosion, ability to cast, weld or harden their machinability, electrical conductivity, etc.

As a result, the understanding of material properties and their behaviour under working conditions is preferable. Given to this and the knowledge of the product's final characteristics and its use, the material selection process needs a systematic and thorough approach.

In order to make a proper decision and shorten the time necessary to obtain the material selection process, some convenient methods could be applied. The complexity of those methods will depend on the number of confronted criteria. Those methods could be [3]: Ashby plots; multi-criteria decision-making (MCDM) approaches and related techniques; fuzzy logic and soft computing-based approaches, etc.

Opposite from the analytical process, the experimental process could also be applied to the material selection process. The experimental process could be obtained virtually or for real.

Nowadays, as a part of the design process, virtual product modelling and manufacturing presented as proper simulations are mandatory. Advantages are numerous and widely spread through all product development phases.

One of the tools used for virtual experiments is Ansys Workbench. This tool represents the finite element method (FEM) which is a numerical procedure used for the analysis of continua and structures. In most cases, the problem which is being analysed is too complicated to be acceptably solved through classical analytical methods [4]. The problem may concern heat conduction, stress analysis, or many others. The finite element (FE) procedures create many simultaneous algebraic equations, which are generated and solved using a digital computer.

Finite element analysis (FEA) was quickly recognized and accepted as a general method of numerical approximation for all physical problems that can be used for solving structural mechanical problems [4]. At present, FEA is used for problems such as fluid flow, electric and magnetic fields, heat transfer, lubrication, etc.

This paper introduces the applicability of FEA transient thermal analysis via virtual experiment obtained in Ansys Workbench for tracking a heat distribution through the structure of the tool ("cleaner") responsible for the preparation of the area for valve placement on the inner tube profile regarding the material selection problem.

For the proper valve application on the inner tube profile in the assembly stage of its production, the valve area must be correctly prepared. This means that by applying the heated tool ("cleaner") on the surface of the inner tube the outer isolation is being melted, thus the surface becomes clean and preheated. There must be no marks of isolation left as well as the valve area has the proper temperature so that in the next step the valve could be correctly applied.

Preheating the valve area helps in making an adhesive bond between the valve and inner tube profile. As a result, locally and for a moment the vulcanisation process begins.

Otherwise, improper cleaning and insufficient preheating could lead to valve detachment from the inner tube, as well as the occurrence of the air gaps after the vulcanisation process. This means that the inner tube is most luckily going to cause critical failure during exploitation.

Apart from the perfect working surface of the "cleaner" and parallel position between the tool and inner tube profile, the tool must be heated evenly.

In order to see how material, distribute heat from the heater through the "cleaner" transient analysis must be introduced.

Transient analysis can be thermal or structural. A transient analysis, by definition, involves loads that are in a function of time. A transient thermal analysis follows basically the same procedures as a steady-state thermal analysis. The main difference is that most applied loads in a transient analysis are functions of time. That means that transient analysis can show how the heat is distributed through the "cleaner's" body and working surface, and how the heat transcends to the inner tube profile.

II. Literature Review

Material selection is an important problem attracting the theoretical and practical interest of researchers.

Since the material selection process is a crucial step in the design process [5], but also a time-consuming process, methods have been developed to help the designers. Generally, for material selection methods it is essential to have a unique bond between theoretical knowledge and practical experience [3].

Most of the material selection processes include a couple of stages: initial screening, development and comparison of alternatives, and determining the best solution [3, 6, 7]. Furthermore, the systematic study of material selection falls within the classical – analytical optimization techniques (i.e. property limits, geometric restrictions, material indexes, cost, cost-performance relation, etc.) [3, 8].

MCDM methods include multi-objective optimization and multi-attribute decision-making, thus the MCDM methods are used in the material selection process. Many researchers have applied this methodology in various material selection problems (i.e. mechanical or electrical products, medicine, biology, civil engineering, etc).

Opposite from MCDM methods, researchers have also used fuzzy logic approaches. The methods based on fuzzy logic have the capability to deal with the complexity and uncertainty of real-world problems in material selection [3].

Irrelevant to the material selection method or approach, the main goal is to make the right materials choice meeting product requirements, such as weight savings, higher product performance, and cost reduction [9].

Finite element analysis can be used to determine the behaviour of materials chosen for the selected product. Depending on the product's requirements or some of its characteristics the type of analysis will vary.

Ansys Workbench as one of the FEA programs offers numerous possible analyses such as static or dynamic analysis, transient (both thermal and static), thermal, electric, thermal-electric, etc.

Giving the specificity and complexity of the problem (heat distribution), there are plenty of researches done regarding the transient thermal finite element analysis. Heat transfer problems are complex in terms of material characteristics which may be time/temperature-dependent [10]. Consequently, heat transfer behaviours, heat convection, and radiation lead to nonlinear characteristics of transient heat distribution problems [10, 11, 12, 13], thus the traditional FEM-based solution method is computationally expensive. In this case, proper approximations methods are advised.

III. Case Study – Material Selection Process for the "Cleaner"

The process of building inner tubes consists of a couple of phases: preparation of the rubber mixture and creating an inner tube profile, assembly of the inner tube profile by performing a butt weld from both sides of the tube, and proper placement of the valve on top of the inner tube profile; properly prepared inner tube profile continues on the curing where the inner tube gets its final process obtained.

Every phase is crucial for the products' proper and safe usage. Every inner tube with flaws, imperfections, and defects is being declared as scrap and immediately discarded.

Since a couple of phases in the inner tube building process occurs separately, they could also be observed divided. The phase which regards this paper's research is the second phase, the assembly phase.

As previously mentioned, this phase has two sub-phases, butt weld joint, and valve placement. Both processes are obtained on the same machine, simultaneously, but with different tools.

The so-called "upper operations" are responsible for the proper valve placement on the inner tube profile (Figure 1).

The process of placing a valve has three steps. Each of these steps must be performed perfectly to avoid the possibility of flaws occurrences. The first step presents the creation of a hole on the upper side of the profile so the compressed air can flow through the valve into the tube. After making a hole, the whole place around it must be cleaned. A clean surface enables the best conditions for the inner tube and valve cohesion. The surface around the hole is being cleaned by the tool which is called the "cleaner".

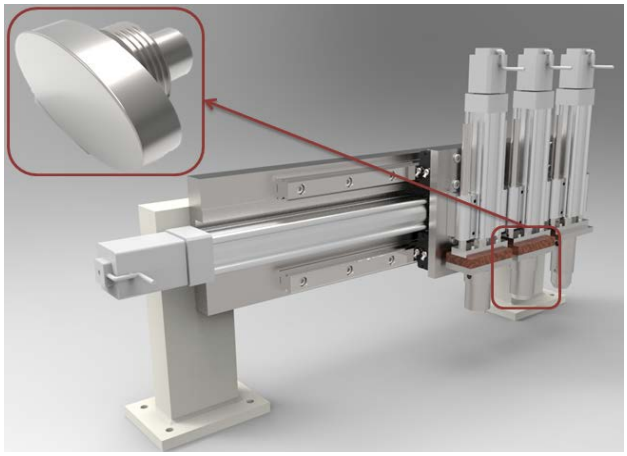

Fig. 1 The assembly responsible for the valve placement on the inner tube profile

The "cleaner" has the exact bottom geometry of the valve and it cleans only the area in which the valve is being applied. Since the cleaner is pre-heated, the outer isolation on the inner tube profile melts, the inner tube profile generates enough heat and it more easily makes a connection with the valve. The final step is to properly place the valve above the hole and over the prepared surface.

"Cleaner" is made of steel and it is screwed into its carrying construction. This construction has two functions: to carry the cleaner and to heat it. The proper heater is also attached around the carrying construction and it conducts a defined amount of heat that passes through it to the working surface (bottom surface) of the "cleaner".

In case that the "cleaner" is not properly mounted into its carrier or that the surface of the cleaner is polluted or imperfect (scratched, bent, etc.) the uniform heat distribution will not be present. Apart from this, the quality of the material from which the cleaner is manufactured has an important role as well. Inadequate material can cause the same effects even on the perfect surface of the cleaner.

The occurrence of the serial flaws (plats and air bubbles, detachment of the valves) indicated that the process is not stable and that there is a problem in the assembly phase.

A thermal inspection of the "cleaner" was performed using the "FLIR C3" compact industrial thermal camera to track the heat distribution during the machine preparation, as well as during the working process. The results of the thermal inspection are presented in Figure 2.

Figure 3 represents the illustration of the working surface of the tool ("cleaner") in the position during the thermal inspection process. This illustration also shows the working surface demands in its need of surface purity and geometrical correctness.

By observing Figure 2, it is clear, that the heat distribution on the working surface of the tool ("cleaner") is not evenly distributed. The centre of the tool is almost at the maximal – set temperature of the heater with a value of 173.8°C (red circle on the centre of the working surface presented on the Figure 2), but the rim area of the surface is approximately evenly distributed with a value of 74.8°C (circle indicator of thermal camera on the Figure 2).

This occurrence could be explained with the process working characteristics in which the "cleaner" is getting colder by transferring the temperature on the inner tube profile, as well as the heat emission in the surroundings.

On the other hand, the consistency of the tool structure and thermal characteristics of the material could also be observed.

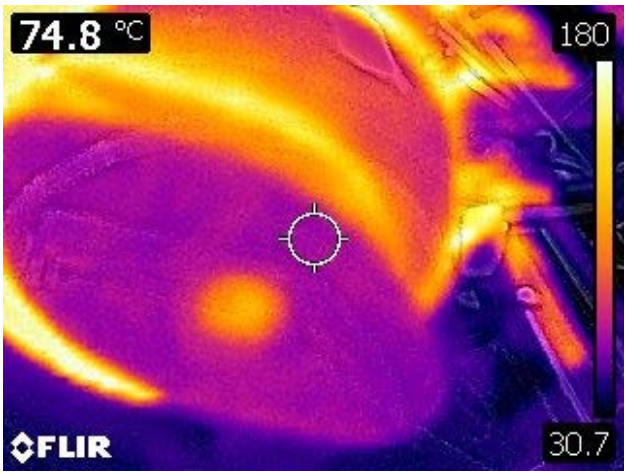

Fig. 1 Thermal camera inspection of the "cleaner" under working conditions

The main idea is to check which type of steel was used for the "cleaner" manufacturing and to try some other types of steel. Since the production process is "unstoppable," a quick and reliable solution must be applied.

Fig. 3 The working surface of the "cleaner"

In order not to raise the cost and the time required for solving this problem. Tests with new "cleaners" manufactured from new types of materials were not possible. Having that in mind, the decision was made to do a transient thermal finite element analysis and see how different types of material react in the same production conditions.

But first, what we wanted to see is how the present material from which the tool was manufactured acts under the production conditions inside the virtual experiment, transient thermal finite element analysis, in the Ansys Workbench. This way we could have a clearer picture of the thermal processes inside the tool structure; observe the heat distribution from the heater, through the tool, to its working surface responsible for the cleaning

process, and make comparison with the results gathered by the real thermal inspection obtained on the assembly machine in the production shop.

The expected results are to see whether the type or structure of material needs to be modified; the construction of the tool ("cleaner") must be redesigned or the type and construction of the heater could also be modified.

A. The Material Selection Process

For this paper's research, the chosen material is by JUS standard Č.1530 which matches the current SRPS EN 10083-2/3 with material reference C45E, steel for annealing, quenching, tempering, and normalizing.

The main reason for selecting this type of material for the FEA analysis is the current material selection of the manufactured tools which are embedded in the production process, as well as the previous experience with the specific material.

Also, the reason for this material selection is to see how tools ("cleaners") with present material behave under working conditions virtually, inside transient thermal finite element analysis.

B. Transient Thermal Finite Element Analysis

As previously mentioned, transient thermal analysis is basically thermal analysis with the addition of time reference. Every FEA analysis regardless of the software has the same principles which must be obtained to gather the desired results.

Those principles involve respectively: material selection (engineering data), the geometrical definition of a solid model, mesh generation, element properties, boundaries, and loads the application and desired outputs (specifically for transient thermal analysis: temperature, total heat flux, directional heat flux, etc.).

After all steps are fulfilled a set of simultaneous linear algebraic equations are being solved in the software background. Output interpretation programs, also referred to as post-processors, will assist the analyst to sort outputs and display them in graphical form.

Respectively to the material selection (steel C45E), the proper inputs are performed regarding the material density, isotropic thermal conductivity, and specific heat capacity [14]. All mentioned values can be found as material properties in textbooks and practicums.

After the material is defined and engineering data imported, the geometry model needs to be built or imported in the design modeller (Figure 1 and 3). Then the model (continuum or structure) must be divided into finite elements. This means that a proper mesh must be generated (Figure 4). This way appropriate type, size, and quantity of elements, as well as their quality, are determined.

Choosing the appropriate type of the element will be determined by the expected response of the model and therefore the accomplishment of the objectives of the analysis [4, 15]. A wide variety of different types is offered by FEA and they can be categorized by family, order and topology.

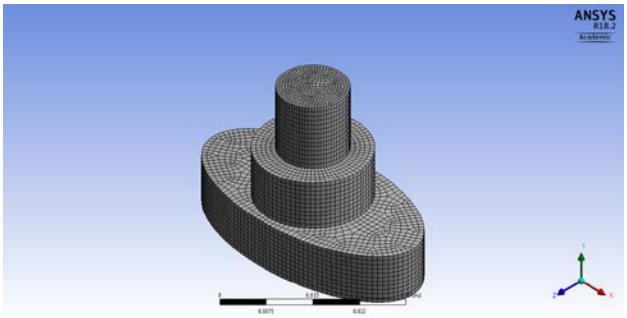

Fig. 4 Mesh generation of the tool structure

One of the crucial steps is to apply loads and define boundaries that represent real working product's conditions (Figure 5).

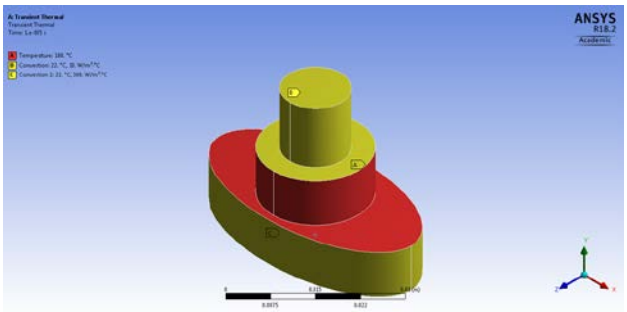

Fig. 5 Loads and boundaries definition

The red area in Figure 5 represents the heating of the "cleaner". The working temperature of the "cleaner" is 180°C which is applied to the model by temperature feature.

The surface above the heated area is placed inside the carrier construction of the tool and it is not in direct contact with the heater, so convection is applied.

The same principle is applied for the surface bellow the heated area, due to the presence of the environment and the contact with the inner tube profile while obtaining the cleaning process.

Finally, the desired output is selected, the heat distribution – temperature analysis.

The mathematical model is created and solved by software and results are shown graphically (Figure 6 and 7).

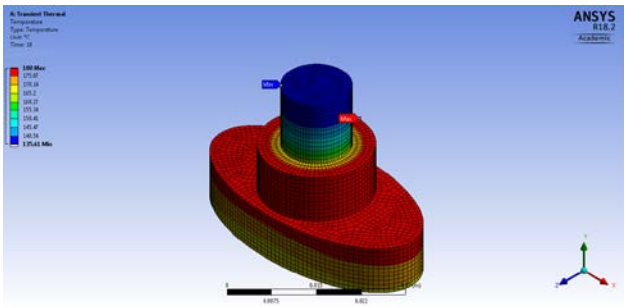

Fig. 6 Results of the analysis

With this research, we wanted to determine the flow of the heat distribution through the tool ("cleaner"). Because of the all mentioned problems regarding the concrete part of the production process (uneven heat distribution on the working surface of the tool) which could lead to unwanted appearances (flaws and imperfections of the inner tube profiles).

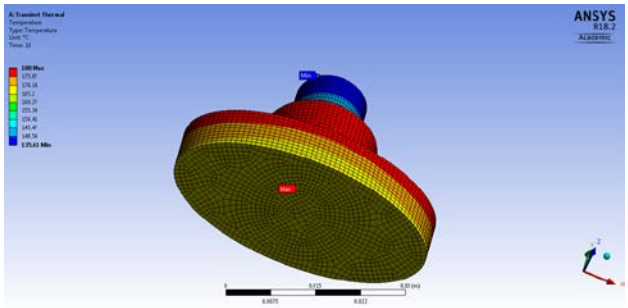

Fig. 7 Results of the analysis focusing the working surface of the tool (“cleaner”)

This way, through the set virtual experiment, we wanted to better understand what is happening inside the tool structure and the results that we managed by the transient thermal FEA analysis were satisfying.

The working surface of the tool (“cleaner”) is getting heated to the production process demanded temperature with the remark that the working surface is getting colder by transferring heat to the inner tube profile during the cleaning process.

Heat distribution through the tool structure during the preheating stage is rather even (Figure 7). At the end of the preheating process working surface of the tool (“cleaner”) is properly heated (Figure 8).

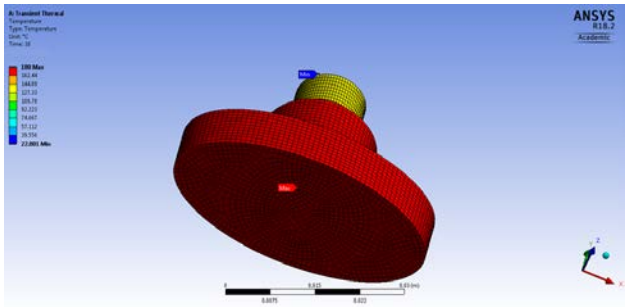

Fig. 8 Results of the analysis focusing the working surface of the tool (“cleaner”) at the end of the heating process

However, the heater has a frequent regulation and it is set in an on-off position, depending on the temperature value. Also, while maintaining the cleaning process, the heat is being transferred to the inner tube profile (isolation melting and profile preheating). Thus, in time, the tool loses some amount of heat and needs to recover it by applying it from the heater.

The results of the analysis have shown a good possibility of the applicability of the experiment and the conclusion is that the heat distribution could be tracked this way. Consequently, transient thermal FEA analysis could be applied in order to compare how different materials distribute the heat during the preheating process as well as under the working conditions. This analysis could be applied in the verification of the material selection process.

In order to solve the problem of the thermal inspection, it is proposed to check the heating source (heater), as well as the connections of the heater-carrying construction and carrying construction-tool (“cleaner”).

IV. Conclusions

The most present main goal of material selection is to minimize the cost while meeting product designed performances. Reality often presents limitations, and the utilitarian factor must be taken into consideration. The cost of the ideal material, depending on the shape, size, and composition, may be prohibitive, and the demands, the commonality of frequently utilized and know items, its characteristics, and even the region of the market dictate its availability.

Apart from cost reduction and time reduction in the product development process, the power of finite element analysis (FEA) resides in its versatility. This versatility is contained within a single computer program.

FEA can be applied to a number of physical problems and the models analysed can have arbitrary shapes, loads, and boundaries. Input data controls the selection of problems, type, geometry, boundary conditions, etc. Another advantage of FEA is the close physical resemblance between the finite element method (FEM) model and the actual structure [4]. This means that the model is not simply an abstraction.

However, the FEA has disadvantages, too. More complex analysis demand high computer performances and therefore processing time increase dramatically. This could be caused by formation of the model at the beginning of the FEA process [4]. In order to maximize the accuracy and to minimize the geometric approximation of the model, the mesh volume of the model is subdivided into a large number of very small elements. Thus the mathematical model becomes bigger as well.

The main focus of this paper was to set a virtual experiment that realistically reproduces the preparation of the subassembly of the “upper operations” responsible for the valve placement.

The observed process refers to the preparation of the machine, specifically on the process of reaching the set temperature of the tool. This way we were observing the heat distribution through the structure of the tool (“cleaner”), from the heat source (heater) to the tool’s working surface. Besides, this experiment also includes heat losses which enhance the quality of the analysis.

For this experiment’s purposes only one material has been used, the C45E steel. This material is used for manufacturing the tool (“cleaner”) which operates on the machine. This way, we got a vivid picture of how the heat is being distributed through the structure of the tool.

For future endeavours, we are planning to obtain a more profound analysis based on the multi-criteria decision-making (MCDM) methodology. This kind of approach would be appropriate to select the most suitable material for the tool (“cleaner”).

The MCDM provides an easy way to observe a wide range of possible alternative solutions (different types of materials) in comparison with multiple confronting criteria (material properties, cost, etc.).

The results of such a kind of analysis would not only be the one best possible alternative solution but also the ranking of all included materials on which further analysis could be applied.

As previously mentioned, the applicability of transient thermal FEA analysis as the verification of the selected materials, from which the tool is being manufactured and the heat distribution criterion is crucial.

The simultaneous analysis of the behaviour of the couple of different materials chosen by a MCDM methodology could show which material is best in

transferring heat from the source to the desired surface. That means that we need to overdo the same virtual experiment (as described in this paper) and maintain the comparative analysis on how those proposed materials react under the same working conditions.

The result of the comparative analysis of the transient thermal FEA analysis would be which chosen material best suits the described problem.

The material selected would be proposed for the tool manufacturing and subjected to real experiments inside the production process and real working conditions.

Only when all those described steps are done, the material selection process verified by FEA analysis could be completed and confirmed.

If the results are insufficient, partial changes (the working surface of the tool cannot be changed because of the structure of the valve) as geometrical optimisation and modification of the tool ("cleaner") could be performed in term of improvement of the tool's heat characteristics and maximal exploitation of the heater.

REFERENCES

[1] B. Vijaya, C. Elanchezhian, J. Jeykrishan, R. Ragavendar, P. K. Rakesh, J. Sujay Dhamodar, A. Danasekar, "Implementation of Reverse Engineering for Crankshaft Manufacturing Industry," Materials Today: Proceedings 5 (2018), pp. 994-999.

[2] A. K. Singh, S. Avikal, N. Kumar K. C., M. Kumar, P. Thakura, "A fuzzy-AHP and M-TOPSIS based approach for selection of composite materials used in structural applications," Materials Today: Proceedings 26 (2020), pp. 3119-3123.

[3] M. B. Babanli, F. Prima, P. Vermaut, L. D. Demchenko, A. N. Titenko, S. S. Huseynov, R. J. Hajiyev, and V. M. Huseynov, "Material Selection Methods: A Review," Springer Nature Switzerland AG 2019, ICAFS-2018, AISC 896, pp. 929-936, 2019.

[4] A. H. Choi, G. Heness, and B. Ben-Nissan, "Using finite element analysis (FEA) to understand the mechanical properties of ceramic matrix composites," Advances in ceramic matrix composites, pp.286-311, 2014.

[5] Q. Zhang, J. Hu, J. Feng, A. Liu, "A novel multiple criteria decision making method for material selection based on GGPFWA operator," Materials and Design, 195, August 2020.

[6] M. Frang, "Quantitative Methods of Material Selection," Handbook of Material Selection, 2002.

[7] M. Ashby, "Materials Selection in Mechanical Design," Butterworth-Heinemann, Oxford, 2010.

[8] D. Cebon, and M. Ashby, "Data systems for optimal material selection," Adv. Mat. Process, 161 (6), pp. 51-54, 2003.

[9] X. Y. Xue, X. J. You, D. X. Lai, and C. H. Lai, "An interval-valued intuitionistic fuzzy MABAC approach for material selection with incomplete weight information," Appl. Soft Comput., 38, pp. 703-713, 2016.

[10] J. Zhang, and S. Chauhan, "Fast explicit dynamic finite element algorithm for transient heat transfer," International Journal of Thermal Science, 139, pp. 160-175, 2019.

[11] K. Yang, G. H. Jiang, H. Y. Li, Z. B. Zhang, and X. W. Gao, "Element differential method for solving transient heat conduction problems," International Journal of Heat Mass Transfer, 127, pp. 1189-1197, 2018.

[12] Y. Islamoglu, "Finite element model for thermal analysis of ceramic heat exchanger tube under axial non-uniform convective heat transfer coefficient," Materials and Design 25 (2004) 479-482.

[13] C. E. Zhou, and F. J. Vecchio, "Nonlinear finite element analysis of reinforced concrete structures subjected to transient thermal loads, "Computers an Concrete, Vol. 2, No.6 (2005) 455-479.

[14] A. Miltenović, M. Tica, M. Banić, and Đ. Miltenović, „Predition of Temperature Distribution in the Worm Gear Meshing," Facta Universitatis, Series: Mechanical Engineering, vol 18-2, pp. 329-339, 2020.

[15] A. Ferla, A. Lavrov, and E. Fjær, "Finite-element analysis of thermal-induced stresses around a cased injection well," 7th International Conference on Modern Practice in Stress and Vibration Analysis, IOP Publishing - Journal of Physics: Conference Series 181 (2009) 012051, doi: 10.1088/1742-6596/181/1/012051.

THE 5th INTERNATIONAL CONFERENCE
MECHANICAL ENGINEERING IN XXI CENTURY

December 9-10, 2020
Faculty of Mechanical Engineering in Niš, Serbia

Experimental Estimation of Footwear Slip Resistance

Dušan STAMENKOVIĆ[a], Milan BANIĆ[a], Milan NIKOLIĆ[b], Aleksandar MILTENOVIĆ[a], Uroš STANKOVIĆ[a]

[a]Faculty of Mechanical Engineering Niš, Aleksandra Medvedeva 14, Serbia,
[b]College of Applied Technical Sciences Niš, Aleksandra Medvedeva 20, Serbia,
dusan.stamenkovic@masfak.ni.ac.rs, milan.banic@masfak.ni.ac.rs, milan.nikolic.nis@gmail.com, aleksandar.miltenovic@masfak.ni.ac.rs, urosstankovic16@gmail.com

***Abstract*— Estimation of anti-slip characteristics of footwear and floor is the most important for the prevention of slipping accidents. Worldwide different countries have adopted various test methods to estimate the slip resistance of footwear and floor. Estimating the slip resistance is often conducted by measuring the coefficient of friction. Coefficient of friction can be determined by measuring of pulling force, friction angle (Ramp test) or energy loss (Pendulum test). Experimental research performed at Faculty of mechanical engineering in Nis is based on pulling force measurement. Measuring of friction force was performed on a test stand specially designed for that purpose. This test stand, test method and obtained measuring data are described in this paper.**

***Keywords*— Slip resistance, footwear, friction, coefficient of friction, experimental estimation**

I. Introduction

A huge number of human injuries are due to slipping at streets, factory halls, open and close public areas, in home etc. In fact, slips, trips, and falls are a serious public health problem and, in most cases, depend on lack of friction. One of the ways to reduce slips and falls is understanding the friction requirements of shoes and pedestrian walkways or floors.

Many institutes and researches were analysing the methods of assessing the slip resistance of footwears and floors. There is a lot of differences in different methods and each of them has some advantages and disadvantages [1,2,3]. There are different European standards that have adopted various test methods and assessing systems [4,5,6,7,8]. These standards include test methods that are based on different principles and are performed under different conditions. Authors consider current potential developments in the international standardization of slip resistance in the papers [9, 10].

In recent years, research has been conducted at the Faculty of mechanical engineering in Niš to determine the appropriate conditions and procedures for reliable measurement of footwear and floors slip resistance [11,12,13]. New experimental research is described and measuring data are commented in this paper.

II. Standards for Slip Resistance Measuring

Some EU standards related with measuring of slip resistance of footwear and floor coverings are adopted in Serbia. Standard for slip resistance estimation of protective footwear is SRPS EN ISO 13287:2014 - Personal protective equipment - Footwear - Test method for slip resistance. Manufacturers and distributors of protective footwear in Serbia are usually required to test their products according to this standard.

Standard for slip resistance estimation of road surface is SRPS EN 13036-4:2012 - Road and airfield surface characteristics - Test methods - Part 4: Method for measurement of slip/skid resistance of a surface: The pendulum test.

Standard for slip resistance estimation of floor (outdoor or indoor) is: SRPS EN 13893:2011 Resilient, laminate and textile floor coverings - Measurement of dynamic coefficient of friction on dry floor surfaces.

The most often used standard tests for floor coverings are Ramp test according to the German norms DIN 51130 and DIN 51097, Pendulum test according to the British and EU norm BS EN 13036-4, and tribometer test according to the norms DIN 51131 and BS EN 13893. The principle of ramp test is measuring the friction angle; the principle of pendulum test is measuring the energy loses owing to the friction and the tribometer test is based on measuring the pulling force which is actually the friction force.

In the ramp test (DIN 51130 Testing of floor coverings – Determination of the anti-slip property – Workrooms and fields of activities with slip danger, walking method – Ramp test), a test person (operator) is wearing standard footwear and walks backwards and forwards over a sample of a flooring material that has been evenly coated with oil (Figure 1). The angle of the ramp is increased until the operator slips [14]. The acceptance angle obtained is used to express the degree of slip resistance. In the ramp test according to the standard DIN 51097 operator walks barefoot.

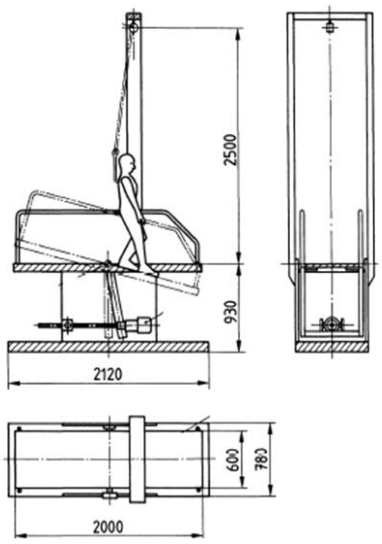

Fig. 1. Ramp test [4]

According the angle of ramp there are five class of slip resistance that is shown in Table 1.

TABLE 1. SLIP RESISTANCE CLASSES OF FLOORINGS ACCORDING TO THE NORM DIN 51130

Classification	R 9	R 10	R 11	R 12	R 13
Slip angle [o]	6÷10	10÷19	19÷27	27÷35	>35

The pendulum test is performed by measuring the loss of energy due to friction as the standard rubber-coated slider assembly slides across the test surface [5]. Pendulum friction tester is presented in Figure 2. It provides a standardized value of slip resistance. This is the pendulum test value (PTV).

The pendulum is the preferred test method in the United Kingdom. Relative risk of slipping is determined with PTVs (Table 2).

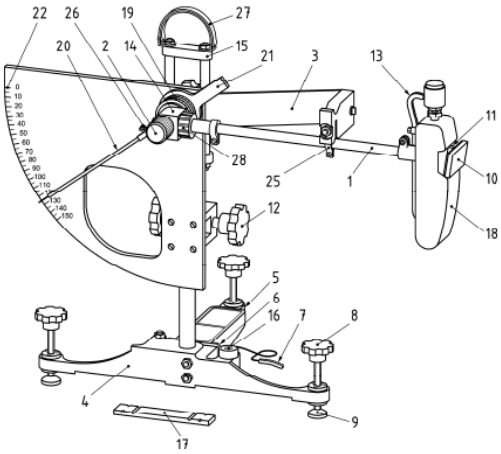

Key

1 pendulum arm
2 mark (in the centre of rotation)
3 release mechanism (knob)
4 frame
5 rear support foot
6 screw for rear support foot
7 spacer of rough adjustment of the sliding length (optional)
8 levelling screw
9 bottom plate (hinged, optional)
10 slider assembly
11 slider support rod
12 vertical screw (for vertical adjustment)
13 slider lifting handle
14 pendulum head
15 clamp for vertical adjustment
16 spirit level
17 gauge (see Figure 2)
18 pendulum foot
19 friction ring (including locking ring)
20 pointer
21 pointer counterbalance
22 unit scale
23 unit scale F
24 unit scale C
25 release catch
26 pointer cam (calibration purpose: pointer adjustment screw)
27 handle
28 lock nut

Fig. 2. Pendulum friction tester [5]

TABLE 2. SLIP POTENTIAL DUE TO PTV

Slip potential	PTV
HIGH	0÷24
MODERATE	25÷35
LOW	>36

Tribometer test method is based upon a friction force measurement. A body equipped with sliders is pulled at a constant speed over the flooring surface. The force required to pull the body is determined over the length of the measuring distance [7]. To determine the sliding friction coefficient, measured pulling force is divided by the vertically acting force (weight). This test can be carried out in wet and in dry conditions both in a laboratory and on-site. This device is predominantly used in Germany, Poland and Austria.

The method for measurement of the slip resistance of shoes is described in EN 13287 [8]. The footwear to be tested is placed on the base of ceramic tile or steel floor, subjected to a given normal force (Figure 3). The base is moved horizontally and sliding of footwear occurs.

Fig. 3. Test equipment for measurement the slip resistance of footwear [15]

Dynamic coefficient of friction is calculated according the measured frictional force. Glycerine or sodium lauryl sulphate solution acts as contaminant on the surface.

III. EXPERIMENTAL RESEARCH AT FACULTY OF MECHANICAL ENGINEERING IN NIŠ

The aim of the experimental research performed at Faculty of Mechanical Engineering in Nis is estimation of the slip resistance of different types of footwear and floor. Principle of determining the friction coefficient in performed experiment is measuring the pulling force. Applied measuring method is based on settings in standards EN 13893 and DIN 51131. Measuring set up in this experimental research is presented in figure 4. The test facility is equipped with sliders which present footwear sole samples and they are pulled parallel to the surface of the floor covering sample. Three sliders with dimensions 10x40 mm are placed on the underside of the body (Fig. 5).

The asynchronous motor drives the screw shaft which rotation moves the ball screw nut along the shaft, together with plate which carries the force transducer. The plate is supported on the opposite end by a linear ball bearing which moves along the linear guide.

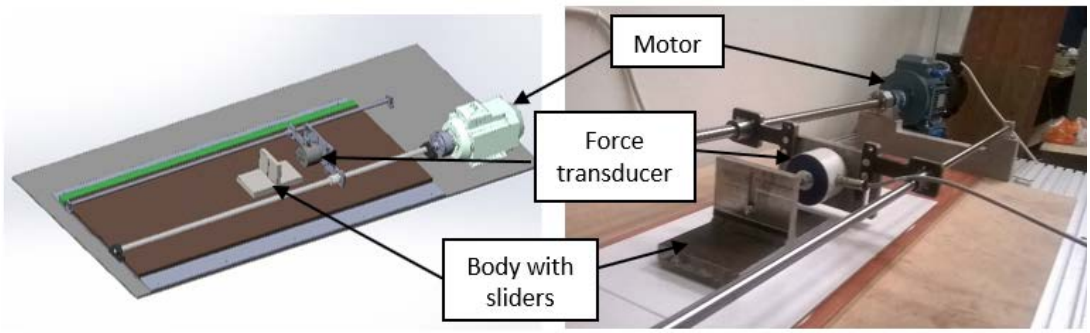

Fig. 4. Measuring set up

The force transducer (HBM S2) pulls the load which carries the footwear sole samples and moves across the floor covering sample. Friction force is measured in that way, and coefficient of friction is determined by dividing the measured friction force and normal force (weight of body).

Materials of sliders were rubber samples for shoe sole 80 Sh hardness, tensile strength 5.6 MPa. Rubber sliders are placed on the underside of the experimental body (Fig. 5)

Fig. 5. Sliders on the underside of the experimental body

Floor samples were plates of granite, parquet, ceramic tiles and vinyl. The masses of body with sliders were 9.18 kg and 17.14 kg. Sliding distance was about 500 mm and velocities 5 and 50 mm/s. Samples was prepared with sandpaper and cleaned. The measurement was carried out on dry and wet surfaces.

Before the main testing, the trial measurement was performed. The sliders used in trial measurement is made of steel, and they slide on the steel plate (Fig. 6).

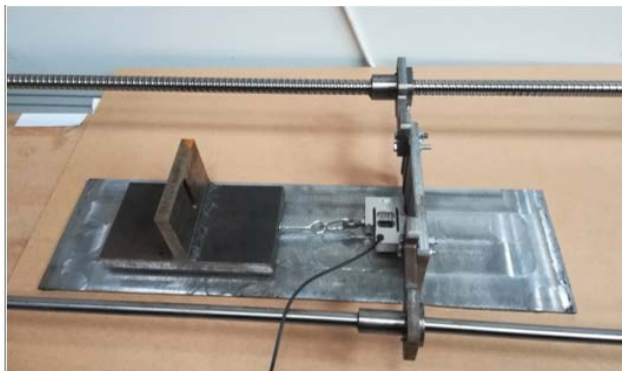

Fig. 6. Measuring set up with sliding samples made of steel

Measured data in trial test are presented in Table 3.

TABLE 3. MEAN VALUES OF STATIC AND DYNAMIC FRICTION COEFFICIENT IN TRIAL TEST

Material of tribopair (sliders/floor)	Contact condition	Friction coefficient	
		Static	Dynamic
Steel/Steel	Contact surfaces dry	0.318793	0.239935
	Contact surfaces wet	0.295018	0.217694
	Contact surfaces lubricated with oil	0.253541	0.204317

Within the main experiment, 68 tests are performed. Minimum value of measured coefficient of friction was 0.453 in sliding of rubber sliders on ceramic tile in wet condition under 50 mm/s sliding speed and maximum value was 1.049 in contact of rubber and parquet in dry condition under 50 mm/s sliding speed.

Mean values of measured dynamic friction coefficient achieved on different floor coverings in each contact conditions and both sliding speeds are presented in Fig. 7. The smallest dynamic friction coefficient mean value was 0.608 in contact rubber-ceramic tile and the biggest one is 0.871 in contact rubber-parquet.

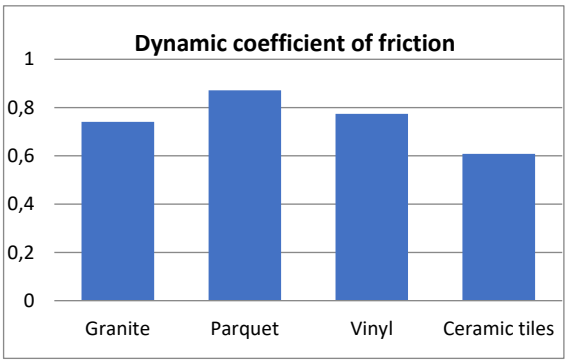

Fig. 7. Mean values of dynamic friction coefficient achieved on different floor coverings

If we compare values of dynamic friction coefficient in dry and wet contact condition, it can be concluded that friction coefficient is smaller in wet than in dry conditions, except the sliding on granite floor coverings where it is inversely. The significant difference in values of friction coefficient in dry and wet contact conditions is in contact rubber-vinyl and rubber-ceramic tiles (Fig. 8).

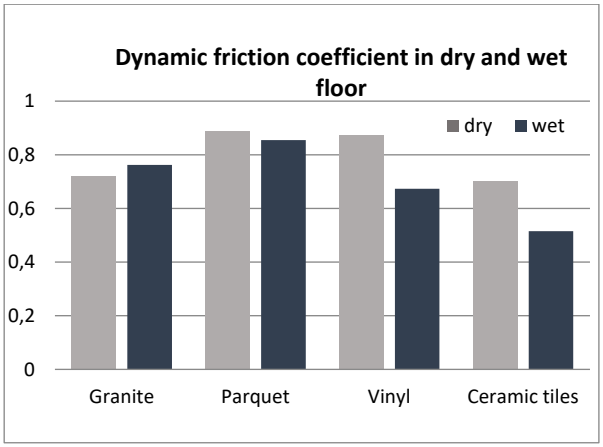

Fig. 8. Mean values of dynamic friction coefficient achieved in dry and wet contact conditions

Sliding speed was also varied in experimental (Fig. 9).

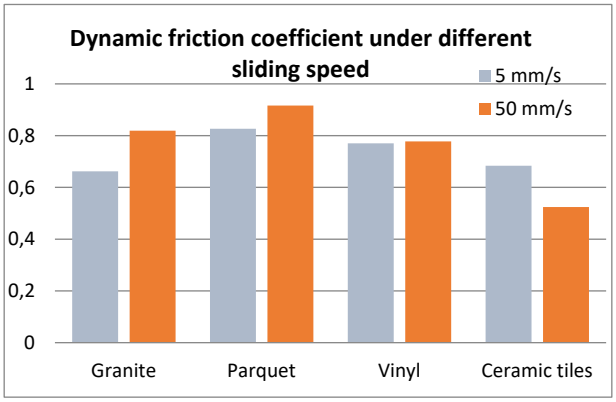

Fig. 9. Mean values of dynamic friction coefficient achieved under different sliding speed

Mean value of dynamic friction coefficient under 50 mm/s sliding speed in contact rubber-granite is 24% higher than under 5 mm/s sliding speed, but in contact rubber-parquet it is 11% higher. In contact rubber-ceramic tiles under 50 mm/s sliding speed, coefficient of friction is 24% less than under 5 mm/s sliding speed.

IV. Conclusions

Estimation of anti-slip characteristics of footwear and floor is the most important for the prevention of slipping accidents and human injures.

In performed experimental research, measuring data show that for the same shoe sole sample there are a wide range of friction coefficients values for different floor coverings and different conditions. Maximum value of friction coefficient is two times bigger than minimum value for same sole material sliding on different floor materials, like ceramic tiles and parquet.

Some type of shoe sole material cannot be the best on all different types of floor coverings and contact conditions, and because of that it is necessary to test different combinations of materials and friction conditions.

Assessment of the shoe slip resistance should be based on the recognition of the basic tribological parameters for specific friction contact and their testing with different floor coverings and in application conditions.

References

[1] HSE: Assessing the slip resistance of flooring, A technical information sheet published by the Health and Safety Executive, 2012.

[2] D. Mewes: Measuring the slip resistance of floorings and footwear, Institute for Occupational Safety and Health of the German Social Accident Insurance, Germany, 2016.

[3] P. Marchal, M. Jacques, A. Sigari: Comparison of measurement methods of the friction coefficient of floor coverings, INRS/CSTB joint publication, 2015.

[4] DIN 51130 Testing of floor coverings – Determination of the anti-slip property – Workrooms and fields of activities of slip danger, walking method - Ramp test, 2010.

[5] BS EN 13036-4 Road and airfield surface characteristics – Test methods; Part 4: Method for measurement of slip/skid resistance of a surface – The pendulum test, 2003.

[6] BS EN 13893 Resilient, laminate and textile floor coverings – Measurement of dynamic coefficient of friction on dry floor surfaces, 2007.

[7] DIN 51131 Testing of floor coverings - Determination of the anti-slip property - Method for measurement of the sliding friction coefficient, 2014.

[8] ISO 13287 Personal protective equipment - Footwear - Test method for slip resistance, 2012.

[9] I.J. Kim, H. Nagata: Research on Slip Resistance Measurement – A New Challenge, Industrial Health, No. 46, pp. 66-76, 2008.

[10] R. Bowman, Slip resistance testing - Zones of uncertainty, Bol. Soc. Esp. Ceram. V. 49, 4, 227-238, 2010.

[11] Nikolić, M., Stamenković, D., Banić, M., Miltenović, A., Biomechanic and Tribology in Human Walking, Proceedings of 15th International Conference on Tribology SERIATRIB '17, ISBN 978-86- 6335-041-0, Kragujevac, 2017, pp. 631-636.

[12] Stamenković, D., Banić, M., Nikolić, M., Mijajlović, M., Milošević, M., Methods and Principles of Determining the Footwear and Floor Tribological Characteristics, Tribology in Industry, Vol. 39, No. 3 pp. 340-348, 2017.

[13] Stamenković, D., Banić, M., Nikolić, M., Miltenović, A., Đekić, P., Influential parameters of footwear slip resistance, 16th International Conference on Tribology, pp 601-606, Kragujevac, 2019.

[14] D.Stamenković, M. Banić, M. Nikolić, "Tribology", Faculty of Mechanical Engineering Nis, 2020.

[15] http://satratechnology.com/files/Slip_Resistance_Guide_2010.pdf

THE 5th INTERNATIONAL CONFERENCE
MECHANICAL ENGINEERING IN XXI CENTURY

December 9-10, 2020
Faculty of Mechanical Engineering in Niš, Serbia

Basic Kinematic Characterstics of Two-Speed Planetary Gear Trains with Brakes on Single Shafts

Sanjin TROHA[a], Jelena STEFANOVIĆ-MARINOVIĆ[b], Željko VRCAN[a]

[a] University of Rijeka, Faculty of Engineering, Vukovarska 58, Rijeka, Croatia
[b] University of Niš, Faculty of Mechanical Engineering, Aleksandra Medvedeva 14, Niš, Serbia
stroha@riteh.hr, jelenas@masfak.ni.ac.rs, zeljko.vrcan@riteh.hr, milovancevic@masfak.ni.ac.rs

***Abstract*— This paper deals with compound two-carrier planetary gear trains (PGTs) with two coupled and four external shafts. Primarly, all possible structural schemes and systematization of these transmissions are pointed. Further research has been made into gear trains using coupling shafts for power input and output, with the controlling brakes acting on single external shafts. The transmission ratio of the PGT is changed by alternating activation of each brake. The kinematic schemes of all analysed PGT variants have been created, and the available transmission ratio ranges have been calculated for both speeds. Also, in some applications it can be necessary to achieve a predefined step between the two transmission ratios, with the actual transmission ratios being irrelevant. Since that, transmission ratio step is indicated too.**

***Keywords*— Two-Speed Planetary Gear Trains, Brakes on single shafts, Transmission ratio, Ideal Torque Ratio, Transmission Ratio step**

I. INTRODUCTION (USE STYLE MASING HEADING 1)

Some engineering applications require mechanical two-speed transmissions. The possibility to change the transmission ratio even under load presents a significant advantage, and in some cases, it is even a necessity.

Planetary gear trains with two coupled and four external shafts due to their characteristics can satisfy that requirements. This paper delas with these transmissions.

First of all, possible structural schemes and systematization of these transmissions are pointed. Next research has been made into gear trains using coupling shafts for power input and output, with the controlling brakes acting on single external shafts. The transmission ratio of the PGT is changed by alternating activation of each brake, enabling their use as transmissions with two mechanical speeds. The relations of ideal torque ratios to the required transmission ratios for both speeds have been given. These relations enable the selection of PGTs designs which will achieve the required pair of transmission ratios. Extreme transmission ratio changes have been determined for each analysed PGT design solution. Also, in some applications it can be necessary to achieve a predefined step between the two transmission ratios, with the actual transmission ratios being irrelevant. Since that, transmission ratio step is indicated too.

II. STRUCTURES OF PLANETARY GEAR TRAINS

A convenient solution is presented in the form of a complex two-carrier planetary gear train (PGT) with two coupled and two single shafts, and two controlling brakes. The direction of the power flow through the PGT, and therefore the transmission ratio, may be controlled by placing the brakes on the two external shafts. Those PGTs are made up by combining two basic planetary gearsets, each consisting of a sun gear 1, planet gear 2, ring gear 3 and planet carrier C (Fig. 1). The possible variants of power flow and brake placement are discussed in [1,2].

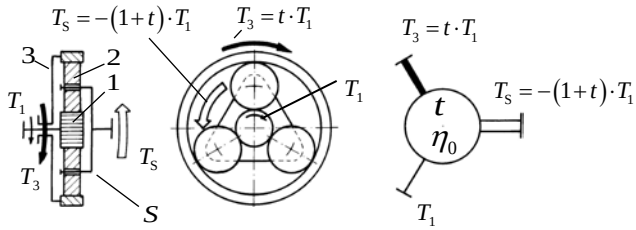

Prerequisite:

$$\eta_0 = \eta_{13(S)} = \eta_{31(S)} = 1$$

Ideal torque ratio:

$$t = \frac{T_3}{T_1} = \frac{|z_3|}{z_1} > +1$$

Torques: $T_1 : T_3 : T_S = +1 : +t : -(1+t)$

Fig. 1 The most often used single-carrier planetary gear train and its torques [3]

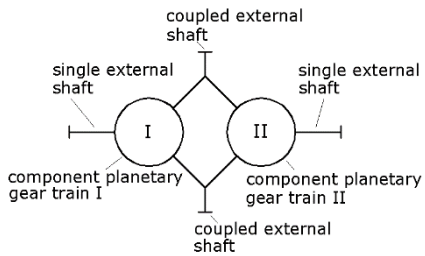

Fig. 2 Planetary gear train with four external shafts (compound train)

Two component trains can be joined in a total of 12 different ways, creating a planetary gear train with four external shafts [4]. An alphanumerical label (S11…S56)

is attached to each of 12 structural schemes, indicating the way in which the shafts of the main elements of both component trains are connected. (Fig. 3). It is possible to place the brakes and connect the driving and driven machine in every presented scheme on external shafts in 12 different ways (V1…V12), which will be referred to as layout variants (Fig. 4).

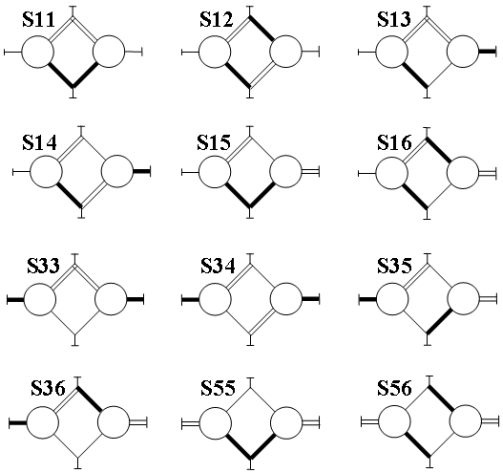

A – input shaft; B – output shaft

Fig. 3 Systematization of all schemes of two-carrier planetary gear train with four external shafts

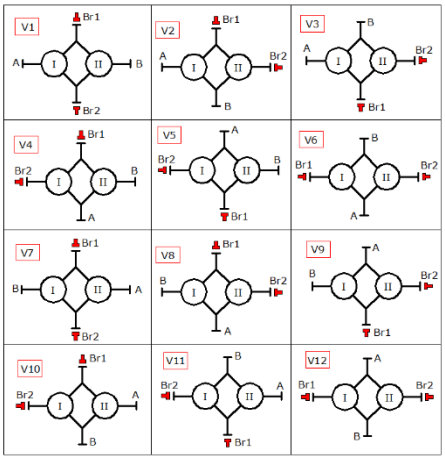

A – input shaft; B – output shaft; Br1, Br2 – brakes; V1-V12 – layout variants

Fig. 4 Systematization of all layout variants of two-carrier planetary gear train with four external shafts

III. Analysis of Operation Process of Compound Gear Trains

By placing the brakes on two shafts a braking system is obtained in which the alternating activation of the brakes shifts the direction of the power flow through the planetary gear train, resulting in a change of the transmission ratio.

The compound trains discussed in this paper can be divided into three different groups depending on the layout of brakes on the shafts. Compound trains with brakes on the coupled shafts are considered to be the first group, compound trains with brakes on the single shafts make the second group, while the third group is made up of compound trains with brakes on the coupled and the single shaft. All compound trains within their separate groups have some specific common characteristics which are described in [4,5].

The PGT with brakes on the single shafts (layout variants V6 and V12) is symbolically shown in Fig 5. When the left brake is turned on, power is transmitted through the left component train (component train I), and when the right brake is turned on, power is transmitted through the right component train (component train II). The power input and output are on the coupled shafts. In this case, regardless of which brake is turned on, power is actively transmitted by only one component train, while the other remains idle. Therefore, the transmission ratios of the compound train are equal to the transmission ratios of the component gear trains.

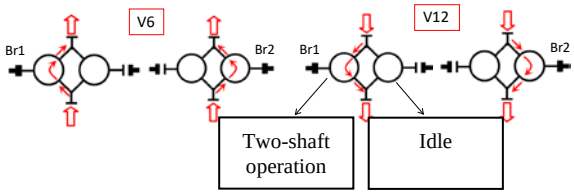

Fig 5 Possible power flows through the train with brakes on the single shafts

Every variant in each group has specific properties which determine its transmission ratio range. It can be said that some variants will enable reduction or multiplication in both ratios, while others will offer reduction in one ratio, and multiplication in the other ratio. Some PGTs will have different directions of rotation of the output shaft, while others will keep the same direction.

All design variants of PGTs with brakes on single shafts including transmissions ratio intervals are presented in [4].

IV. Kinematic Characteristics of PGTs with Brakes on Single Shafts

These variants can achieve transmission ratios limited by the kinematic capabilities of their respective planetary gearsets. It is possible to achieve either two reduction, two multiplication, or one multiplication and one reduction ratio, with both negative and positive values. The transmission ratio of each gearset depends only on the ideal torque ratio of the active gearset.

Such PGTs can provide an adequate solution if the required transmission ratios i_1 and i_2 can be achieved with a single gearset.

Some of these variants have rather interesting kinematic characteristics, which is important for their possible field of application.

For example, layout S36 changes the direction of rotation of the output member when changing the transmission ratio. Therefore, this PGT is suitable for a machine tool which has a high load, low speed working motion, and a fast, low resistance return motion to increase productivity. This layout also gives equal and opposite output shaft speeds with $t_{\mathrm{I}} = 1 + t_{\mathrm{II}}$.

A transmission with inverse ratios can be realised with layouts S34 and S56 with the ideal torque ratios $t_{\mathrm{I}} = t_{\mathrm{II}}$ being equal.

PGTs with brakes on single shafts have some design limitations. For example, a layout using three planets per

gearset can achieve transmission ratios between 0,0769 and 13. PGTs with brakes on connected shafts or with brakes on connected and single shafts should be considered for transmission ratios lower than 0,0769 and greater than 13. Function of ideal torque ratios and transmission ratios of planetary gear trains with brakes on single shafts is shown ih the Table 2

V. TRANSMISSION RATIO STEPS

TABLE I FUNCTION OF IDEAL TORQUE RATIOS AND TRANSMISSION RATIOS FOR LAYOUT VARIANT V6

Layout	Set pair of ideal torque ratios $(t_{\mathrm{I}}, t_{\mathrm{II}})$	Transmission ratio i_{Br1} (Brake Br1 On)	Transmission ratio i_{Br2} (Brake Br2 On)
S11V6	$\left(\frac{1}{i_{\mathrm{Br1}}-1}, \frac{1}{i_{\mathrm{Br2}}-1}\right)$	$\frac{t_{\mathrm{I}}+1}{t_{\mathrm{I}}}$	$\frac{t_{\mathrm{II}}+1}{t_{\mathrm{II}}}$
S12V6	$\left(\frac{1}{i_{\mathrm{Br1}}-1}, \frac{i_{\mathrm{Br2}}}{1-i_{\mathrm{Br2}}}\right)$	$\frac{t_{\mathrm{I}}+1}{t_{\mathrm{I}}}$	$\frac{t_{\mathrm{II}}}{t_{\mathrm{II}}+1}$
S13V6	$\left(\frac{1}{i_{\mathrm{Br1}}-1}, i_{\mathrm{Br2}}-1\right)$	$\frac{t_{\mathrm{I}}+1}{t_{\mathrm{I}}}$	$t_{\mathrm{II}}+1$
S14V6	$\left(\frac{1}{1-i_{\mathrm{Br1}}}, \frac{1-i_{\mathrm{Br2}}}{i_{\mathrm{Br2}}}\right)$	$\frac{t_{\mathrm{I}}+1}{t_{\mathrm{I}}}$	$\frac{1}{t_{\mathrm{II}}+1}$
S15V6	$\left(\frac{1}{i_{\mathrm{Br1}}-1}, -\frac{1}{i_{\mathrm{Br2}}}\right)$	$\frac{t_{\mathrm{I}}+1}{t_{\mathrm{I}}}$	$-\frac{1}{t_{\mathrm{II}}}$
S16V6	$\left(\frac{1}{i_{\mathrm{Br1}}-1}, -i_{\mathrm{Br1}}\right)$	$\frac{t_{\mathrm{I}}+1}{t_{\mathrm{I}}}$	$-t_{\mathrm{II}}$
S33V6	$(i_{\mathrm{Br1}}-1, i_{\mathrm{Br2}}-1)$	$t_{\mathrm{I}}+1$	$t_{\mathrm{II}}+1$
S34V6	$\left(i_{\mathrm{Br1}}-1, \frac{1-i_{\mathrm{Br2}}}{i_{\mathrm{Br2}}}\right)$	$t_{\mathrm{I}}+1$	$\frac{1}{t_{\mathrm{II}}+1}$
S35V6	$\left(i_{\mathrm{Br1}}-1, -\frac{1}{i_{\mathrm{Br2}}}\right)$	$t_{\mathrm{I}}+1$	$-\frac{1}{t_{\mathrm{II}}}$
S36V6	$(i_{\mathrm{Br1}}-1, -i_{\mathrm{Br2}})$	$t_{\mathrm{I}}+1$	$-t_{\mathrm{II}}$
S55V6	$\left(-\frac{1}{i_{\mathrm{Br1}}}, -\frac{1}{i_{\mathrm{Br2}}}\right)$	$-\frac{1}{t_{\mathrm{I}}}$	$-\frac{1}{t_{\mathrm{II}}}$
S56V6	$\left(-\frac{1}{i_{\mathrm{Br1}}}, -i_{\mathrm{Br2}}\right)$	$-\frac{1}{t_{\mathrm{I}}}$	$-t_{\mathrm{II}}$

In some applications it can be necessary to achieve a predefined step between the two transmission ratios, with the actual transmission ratios being irrelevant. The overall transmission ratios of some layouts can be modified at will by adding an extra gearset to their input or output shafts.

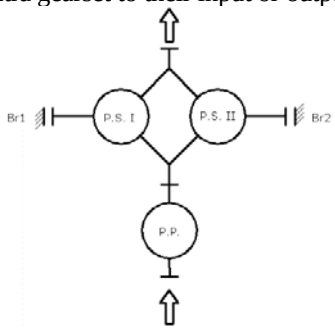

$S_{\mathrm{p}} = const.$

Fig. 5 Application of extra input gearset to adjust the overall transmission ratio

The schematic of a V6 variant layout with an extra input stage is shown in Figure 5. This is used to achieve the required transmission ratios while retaining the predefined step.

It is useful to know the ratio steps of the previously mentioned layouts. The ratio step may be mathematically defined as:

$$\text{if } |i_{\mathrm{Br1}}| > |i_{\mathrm{Br2}}| \text{ then: } S_{\mathrm{p}} = \frac{i_{\mathrm{Br1}}}{i_{\mathrm{Br2}}} \tag{1}$$

$$\text{if } |i_{\mathrm{Br2}}| > |i_{\mathrm{Br1}}| \text{ then: } S_{\mathrm{p}} = \frac{i_{\mathrm{Br2}}}{i_{\mathrm{Br1}}}$$

The minimal and maximal ratio step has been determined for layout V6 for all 12 schemes using expressions from Table 1. The appropriate combination of ideal torque ratios and transmission ratios has been determined for every extreme ratio step.

The data has been presented in Tab. 2. for feasible ideal torque ratios (t_{I} i t_{II} within 2… 12).

It is shown in Tab. 2 that some layouts can achieve large transmission steps, e.g. S34V6, S35V6 and S56V6 (shaded grey). Furthermore, it should be mentioned that layout S36V6 (also shaded grey) can be reversible assuming that condition $t_{\mathrm{II}} = t_{\mathrm{I}} + 1$ is fulfilled. It should be noted that variant V12

has the same extreme transmission ratios as variant V6, as variant V12 is the inverse of variant V6. This is due to the definition of ratio step as laid out in (1) and (2).

Some transmission layouts (e.g. S34V6, S35V6, S56V6) can achieve large transmission steps, and it should be mentioned that layout S36V6 (also shaded grey) can be reversible, providing equal and opposite output shaft speeds, on the condition that $t_{\mathrm{II}} = t_{\mathrm{I}} + 1$.

TAB.II. EXTREME TRANSMISSION STEP VALUES

Layout	$\frac{i_{Br\,max}}{i_{Br\,min}}$	t_I	t_{II}	i_{Br1}	i_{Br2}
	max min	max min	max min	max min	max min
S11V6	1,38461 1	12 (2) t_{II}	2 (12) t_I	1,5 (1,0833) i_{Br2}	1,0833 (1,5) i_{Br1}
S12V6	2,25 1,17361	2 12	2 12	1,5 1,0833	0,6667 0,9231
S13V6	12 2	12 2	12 2	1,0833 1,5	13 3
S14V6	19,5 3,25	2 12	12 12	1,5 1,0833	0,0769 0,3333
S15V6	-18 -2,16667	2 12	12 2	1,5 1,0833	-0,0833 -0,5
S16V6	-11,0769 -1,13333	12 2	12 2	1,0833 1,5	-12 -2
S33V6	4,33333 1	2 (12) t_{II}	12 (2) t_I	3 (13) i_{Br2}	13 (3) i_{Br1}
S34V6	169 9	12 2	12 2	13 3	0,0769 0,3333
S35V6	-156 -6	12 2	12 2	13 3	-0,0833 -0,5
S36V6	-6,5 -1	12 t_I	2 t_I+1	13 $-i_{Br2}$	-2 $-i_{Br1}$
S55V6	6 1	12 (2) t_{II}	2 (12) t_I	-0,5(-0,083) i_{Br2}	-0,0833(-0,5) i_{Br1}
S56V6	144 4	12 2	12 2	-0,0833 -0,5	-12 -2

VI. CONCLUSION

The research in this paper covers all the possible structural schemes of complex two-carrier planetary gear trains (PGTs) with two coupled and two single shafts, focusing on gear trains using coupling shafts for power input and output, with the controlling brakes acting on single external shafts. The transmission ratio of the PGT is changed by alternating the activation of each brake.

PGTs with brakes on the single shafts have a particular power transmission path. As the brakes are acting on the single external shafts, and the power input and output are on the coupled shafts, the power will be transmitted only by the component train whose brake is turned on, while the other component train will rotate idly. Therefore, the transmission ratios that a compound train can achieve will

be equal to the transmission ratios of its component gear trains. A compound PGT will then have either two reduction/multiplication ratios, or one multiplication and one reduction ratio, both of which may be either negative or positive.

The transmission ratio of each stage is defined only by the ideal torque ratio of the active gearset. PGTs with brakes on single shafts have some design limitations. For example, a layout with three planets per gearset is limited to transmission ratios between 0,0769 and 13. PGTs with brakes on connected shafts or with brakes on connected and single shafts should be considered for cases beyond this range.

In some applications it is necessary to achieve a predefined step between two transmission ratios, with the actual transmission ratios being irrelevant, and some layouts can be modified by adding an extra gearset to their input or output shafts.

To sum up, the properties of PGTs with brakes on the single shafts make them interesting for applications in transport and in engineering, especially with the capabilities of some configurations to provide equal transmission ratios, but with different directions of rotation of the output shaft. As they are able to change the transmission ratio under load, they may be applied either as two-speed mechanical transmissions or reverse gearboxes in transportation technology and other engineering applications.

ACKNOWLEDGMENT

This research was financially supported by the Ministry of Education, Science and Technological Development ofthe Republic of Serbia"

REFERENCES

[1] J. Stefanović-Marinović, S. Troha, M. Milovančević, “An Application of Multicriteria Optimization to the Two-Carrier Two-Speed Planetary Gear Trains“, FACTA UNIVERSITATIS Series: Mechanical Engineering, 15(1), 2017, pp 85-95

[2] S. Troha, J. Stefanović-Marinović, Ž. Vrcan, M. Milovančević: **“**Selection of the optimal two-speed planetary gear train for fishing boat propulsion”, FME Transactions 48 (2), 2020, pp. 397-403

[3] K. Arnaudov, D. Karaivanov, “The torque method used for studying coupled two-carrier planetary gear trains”, *Transactions of FAMENA* **37**(1), 2013, pp 49-61

[4] S. Troha, “Analysis of a planetary change gear train's variants”, (in Croatian), PhD Thesis, Faculty of Engineering – University of Rijeka, Croatia, 2011

[5] .S. Troha, Ž. Vrcan, D. Karaivanov, M. Isametova. The Selection of Optimal Reversible Two-speed Planetary Gear Trains for Machine Tool Gearboxes, FACTA UNIVERSITATIS Series: Mechanical Engineering Vol. 18, No 1, pp. 121 – 134, 2020.

THE 5th INTERNATIONAL CONFERENCE
MECHANICAL ENGINEERING IN XXI CENTURY

December 9-10, 2020
Faculty of Mechanical Engineering in Niš, Serbia

Optimization of the Speed Reducer Design Problem using Nature-inspired Algorithms

Mića ĐURĐEV, Eleonora DESNICA, Jasmina PEKEZ, Vladimir ŠINIK

First Author affiliation: Department for Mechanical Engineering, Technical faculty "Mihajlo Pupin", Đure Đakovića bb, Zrenjanin
Second Author affiliation: Department for Mechanical Engineering, Technical faculty "Mihajlo Pupin", Đure Đakovića bb, Zrenjanin
Third Author affiliation: Department for Mechanical Engineering, Technical faculty "Mihajlo Pupin", Đure Đakovića bb, Zrenjanin
Fourth Author affiliation: Department for Mechanical Engineering, Technical faculty "Mihajlo Pupin", Đure Đakovića bb, Zrenjanin
mica.djurdjev@tfzr.rs, desnica@tfzr.uns.ac.rs, pekezjasmina@gmail.com, sinik.vladimir@gmail.com

***Abstract*— Nature-inspired metaheuristic algorithms have recently grown very popular due to their simple implementation and flexibility. They are able to find quality solutions to optimization problems such as constrained engineering design problems. The attempt to solve the speed reducer design problem that belongs to this group has been emphasized in this study. The objective of this problem is to minimize the weight of speed reducer with seven design variables and eleven inequality constraints that speed reducer design should satisfy. Several modern nature-inspired metaheuristic algorithms are employed to optimize the speed reducer design. Comparative optimization results are obtained including minimal, mean, maximal and standard deviation values. The results prove nature-inspired algorithms are efficient techniques. However, additional improvements should be included in order to avoid local optima and achieve faster convergence.**

***Keywords*— Natural inspiration, Metaheuristics, Algorithms, Speed reducer design, Optimization**

I. Introduction

Nature is enriched with various creatures who express certain intelligent behaviour mechanisms, individually or as a part of larger community. Therefore, mutual interaction among living organisms such as fish, fireflies, birds, wolves, bees or ants who live in community are directed towards acquiring local information which is valuable for the entire community. Their social intelligence most often reflects on foraging or hunting behaviour [1]. Also, intelligent behaviour of individual organisms can be noticed in creatures such as dolphins, crows or frogs. Special group of biologically-based solutions is inspired by evolution, genes, biogeography, flower pollination etc. Collective or individual intelligent mechanisms have inspired many authors to develop optimization techniques which are today popularly known as metaheuristic algorithms.

Metaheuristics are search algorithms used in optimization to find the most suitable alternatives in a search space of possible solutions in a reasonable time manner [2]. Metaheuristics are primarily characterized with simplicity, universality and stochasticity while the most important condition each metaheuristic need to fulfil is to achieve an appropriate balance between local and global search, i.e. exploitation and exploration [3]. According to a predefined optimization criterion/criteria and subject to different constraints, metaheuristics have shown promising results in solving different optimization challenges.

Since there are many distinct behaviours of natural organisms and creatures on our planet, many classifications of metaheuristic algorithms can be made. In this paper, the emphasis will be placed on the group of nature-inspired algorithms [4]. The illustrative inspiration of these metaheuristics is given in Fig. 1 [1].

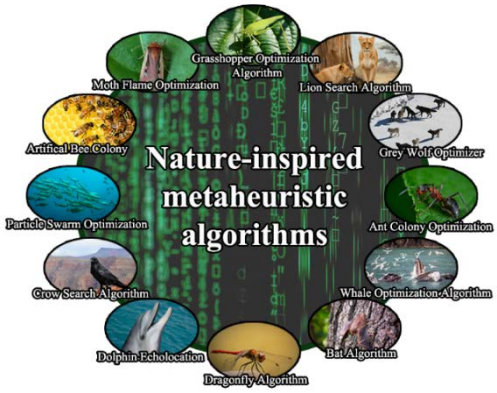

Fig. 1. Inspiration behind metaheuristics

The search procedure of nature-inspired metaheuristic algorithms is based on randomly generated population of individuals which are updated according to the predefined fitness function. Nature-inspired metaheuristic algorithms are population-based search techniques characterized by social as well as individual intelligence. One example of social behaviour can be found in the grasshopper optimization algorithm, the particle swarm optimization or the grey wolf optimizer. On the other hand, individual

intelligence is an intrinsic feature of crows in the crow search algorithm.

The steps of each metaheuristic are determined by equations that characterize or emulate the observed natural behaviour on the basis of which the population evolves. In other words, these individuals are being evaluated using a predefined optimization criterion or criteria and the process is repeated for a predefined number of iterations [1].

In that manner, several nature-inspired metaheuristic algorithms are implemented in order to solve the popular engineering design optimization problem known as the speed reducer design. Eleven different algorithms are employed and comparative results are obtained. The results have shown that some of the algorithms showed their efficiency in finding good or optimal solutions for the weight of the speed reducer. However, improvements are to be made to achieve better convergence and avoid local optima.

II. THE SPEED REDUCER DESIGN OPTIMIZATION PROBLEM

Objective function of the speed reducer design optimization task is to minimize the weight of the speed reducer which is shown in Fig. 2 and Fig. 3. The optimal design of the speed reducer must satisfy constraints on stresses in the shafts, transverse deflection of the shafts, surface stress and bending stress of the gear teeth [5], [6], [7]. Six continuous and one integer decision variable are taken into account: the face width (b or x_1), the module of the teeth (m or x_2), the number of teeth in the pinion (z or x_3), the length of the first shaft between bearings (l_1 or x_4), the length of the second shaft between bearings(l_2 or x_5), the diameter of the first shaft (d_1 or x_6) and the diameter of the second shaft (d_2 or x_7). Mathematical formulation of the speed reducer design problem is given as follows [5], [7]:

Decision variables:

$$\vec{x} = [x_1, x_2, x_3, x_4, x_5, x_6, x_7] \tag{1}$$

Minimize:

$$f(\vec{x}) = 0{,}7854x_1x_2^2 \times (3{,}3333x_3^2 + 14{,}9334x_3 - 43{,}0934) - 1{,}508x_1(x_6^2 + x_7^2) + 7{,}4777(x_6^3 + x_7^3) + 0{,}7854(x_4x_6^2 + x_5x_7^2) \tag{2}$$

Subject to inequality constraints:

$$g_1(\vec{x}) = \frac{27}{x_1\, x_2^2\, x_3} - 1 \leq 0 \tag{3}$$

$$g_2(\vec{x}) = \frac{397{,}5}{x_1x_2^2x_3^2} - 1 \leq 0 \tag{4}$$

$$g_3(\vec{x}) = \frac{1{,}93\, x_4^3}{x_2x_3x_6^4} - 1 \leq 0 \tag{5}$$

$$g_4(\vec{x}) = \frac{1{,}93\, x_5^3}{x_2x_3x_7^4} - 1 \leq 0 \tag{6}$$

$$g_5(\vec{x}) = \frac{1}{110x_6^4}\sqrt{\left(\frac{745x_4}{x_2x_3}\right)^2 + 16{,}9 \times 10^6} - 1 \leq 0 \tag{7}$$

$$g_6(\vec{x}) = \frac{1}{85x_7^3}\sqrt{\left(\frac{745x_5}{x_2x_3}\right)^2 + 157{,}5 \times 10^6} - 1 \leq 0 \tag{8}$$

$$g_7(\vec{x}) = \frac{x_2x_3}{40} - 1 \leq 0 \tag{9}$$

$$g_8(\vec{x}) = \frac{5x_2}{x_1} - 1 \leq 0 \tag{10}$$

$$g_9(\vec{x}) = \frac{x_1}{12x_2} - 1 \leq 0 \tag{11}$$

$$g_{10}(\vec{x}) = \frac{1{,}5x_6 + 1{,}9}{x_4} - 1 \leq 0 \tag{12}$$

$$g_{11}(\vec{x}) = \frac{1{,}1x_7 + 1{,}9}{x_5} - 1 \leq 0 \tag{13}$$

Bound range:

$$2{,}6 \leq x_1 \leq 3{,}6 \tag{14}$$

$$0{,}7 \leq x_2 \leq 0{,}8 \tag{15}$$

$$17 \leq x_3 \leq 28 \tag{16}$$

$$7{,}3 \leq x_4 \leq 8{,}3 \tag{17}$$

$$7{,}3 \leq x_5 \leq 8{,}3 \tag{18}$$

$$2{,}9 \leq x_6 \leq 3{,}9 \tag{19}$$

$$5 \leq x_7 \leq 5{,}5 \tag{20}$$

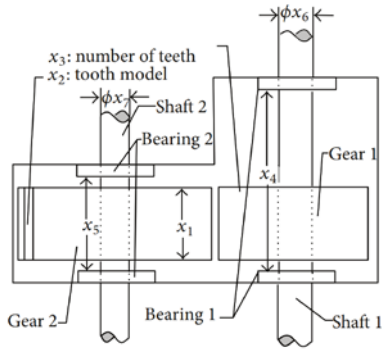

Fig 2. Speed reducer design schematic 2D representation [8]

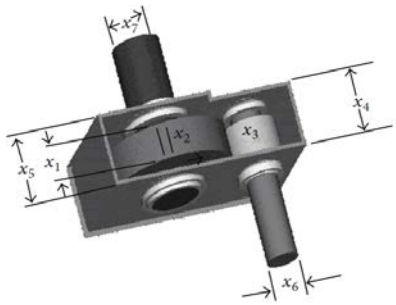

Fig 3. Speed reducer design 3D graphical representation [5]

III. RESULTS AND DISCUSSION

In order to obtain satisfactory results, the speed reducer design problem has been tested using several modern nature-inspired metaheuristic algorithms. Comparative results have been obtained and traditional metaheuristic algorithms have shown their performances. In this study we considered the following nature-inspired metaheuristics: Crow Search Algorithm (CSA) [9], Grey Wolf Optimizer (GWO) [10], Particle Swarm Optimization (PSO) [11], Whale Optimization Algorithm (WOA) [12], Bat Algorithm (BA) [13], Firefly Algorithm (FA) [14], Artificial Bee Colony (ABS) [15], Seagull Optimization Algorithm (SOA) [16], Tunicate Swarm Algorithm (TSA) [17], Harris Hawk Optimization (HHO) [18], and Moth Flame Optimization (MFO) [19]. Almost all the aforementioned metaheuristics are relatively novel optimization techniques. Comparison of the statistical results obtained by these algorithms for the speed reducer design problem are given in Table 1. All of the

metaheuristics have been run 50 times with the standard set of parameters. Number of iterations (12000) and number of search agents/individuals (50) are the only two parameters that were adopted for all metaheuristics. The other parameters are set according to the author's suggestions for traditional approaches.

Table 2 and Table 3 show the best solutions, i.e. best values for the face width, module of the teeth, number of teeth in the pinion, length of the first shaft between bearings, length of the second shaft between bearings, the diameter of the first shaft and the diameter of the second shaft obtained by the GWO and the PSO metaheuristics respectively.

TABLE 1. COMPARISON OF STATISTICAL RESULTS OBTAINED BY NATURE-INSPIRED METAHEURISTICS

Alg.	**Worst value**	**Best value**	**Avg. value**	**St. dev.**
CSA	3297.721	3062.7384	3179.8467	51.581
GWO	3003.5702	2994.8629	2997.4887	2.0099
PSO	3209.2974	2994.4711	3025.7102	50.2623
WOA	3116.174	3000.1165	3041.3686	34.572
BA	4611.4898	2995.0973	3455.0734	502.0624
FA	3013,2808	2997,0494	3004,5919	0,004115
ABC	3068.8812	3009.6362	3042.3021	14.6952
SOA	3017.6562	2996.5916	3005.5293	5.6171
TSA	3026.2981	3002.2431	3015.6283	5.1392
HHO	3066.6655	2995.7371	3013.7134	13.309
MFO	4440.4258	2994.4711	3101.2295	268.7037

Fig. 4 represents the convergence curves for four nature-inspired metaheuristics selected from the study. According to the convergence results, it can be noticed that local optima entrapment is one of the main issues for the traditional and modern nature-inspired metaheuristic algorithms implemented in this study. The GWO has proved to be the most consistent metaheuristic even though the convergence towards global optimum was relatively slow. The optimal results were obtained by the PSO and the MFO metaheuristics but their results were far less consistent compared to the GWO. The GWO as well as HHO, SOA, BA and FA managed to find relatively good results when it comes to the best value for the weight of the speed reducer.

As a conclusion, the additional tuning of parameters and improvements in balance between exploitation and exploration phases in order to avoid local optima entrapments should be considered as the part of the future research. The modern nature-inspired metaheuristic algorithms have proved to be very simple for implementation and managed to find quick and good solutions for constrained optimization problems such as the speed reducer design.

TABLE 2. ONE OF THE BEST SOLUTIONS OBTAINED BY THE GWO ALGORITHM FOR THE SPEED REDUCER DESIGN

Param.	x_1 (b)	x_2 (m)	x_3 (z)	x_4 (l_1)
Value	3,5003	0,7	17	7,3439
Param.	x_5 (l_2)	x_6 (d_1)	x_7 (d_2)	$f(\vec{x})$
Value	7,7437	3,3504	5,2867	2995.721

TABLE 3. ONE OF THE BEST SOLUTIONS OBTAINED BY THE PSO ALGORITHM FOR THE SPEED REDUCER DESIGN

Param.	x_1 (b)	x_2 (m)	x_3 (z)	x_4 (l_1)
Value	3,5	0,7	17	7,3
Param.	x_5 (l_2)	x_6 (d_1)	x_7 (d_2)	$f(\vec{x})$
Value	7,7153	3,3502	5,2867	2994.471

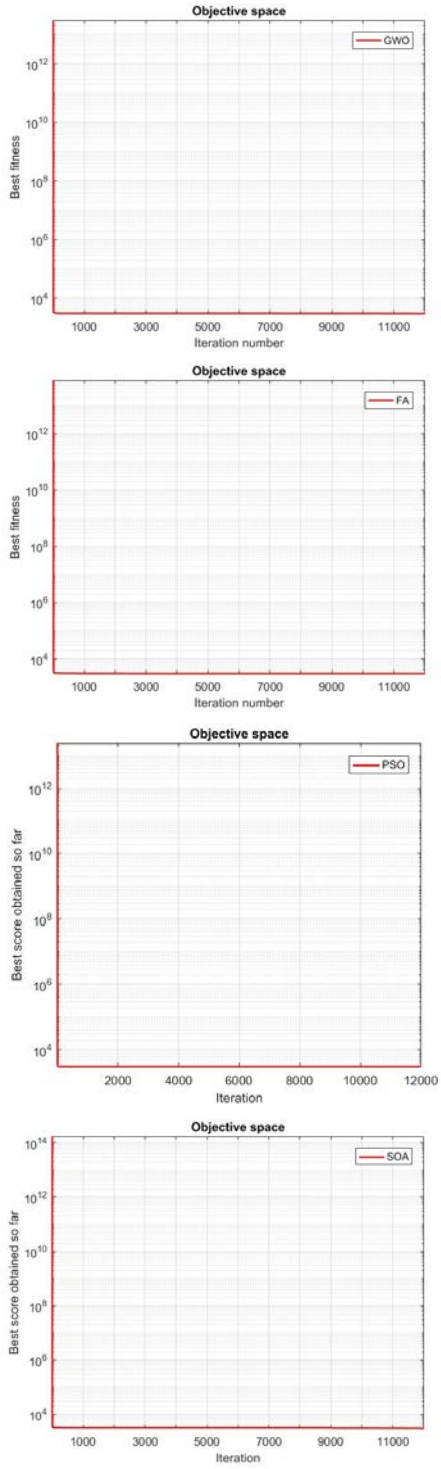

Fig 4. Convergence rates of GWO, FA, PSO and SOA algorithms respectively for finding the best possible fitness of speed reducer design problem

IV. CONCLUSION

A research study presented in this paper was focused on the implementation of several nature-inspired metaheuristic algorithms to solve the constrained engineering optimization problem known as the speed reducer design problem. Inspiration behind nature-inspired metaheuristics taken from the social and individual behaviour in our natural environment was emphasized in the introduction. Also, main aspects of algorithms are considered. Later, several nature-inspired algorithms were implemented and comparative results were obtained. Main statistical parameters were included in this comparative analysis and two solutions from two different algorithms were pointed out. Convergence curves represented the convergence toward best values for four different algorithms. At the end, the most important notions were made on parameter tuning and the improvements in convergence rates as well as avoidance of local optima entrapments.

REFERENCES

[1] M. Milošević, M. Đurđev, D. Lukić, A. Antić, N. Ungureanu, "Intelligent Process Planning for Smart Factory and Smart Manufacturing," Proc. of the 5th Int. Conf. on the Industry 4.0 Model for Adv. Manuf., AMP 2020, pp. 205-214, May 1th, 2020, Lecture Notes in Mechanical Engineering, Springer, Cham.

[2] X.-S. Yang, Engineering Optimization: An Introduction with Metaheuristics Applications. John Wiley & Sons, USA, 2010.

[3] E.G. Talbi, Metaheuristics: From Design to Implementation. John Wiley & Sons, USA, 2009.

[4] M. Đurđev, E. Desnica, J. Pekez, M. Milošević, D. Lukić, B. Novaković, L. Đorđević, Modern Swarm-based Algorithms for the Tension/compression String Design Optimization Problem, X Int. Conf. Industrial Engineering and Environmental Protection 2020, IIZS 2020, Technical Faculty "Mihajlo Pupin", Zrenjanin, pp. 49-53, October, 2020.

[5] M.-H. Lin, J.-F. Tsai, N.-Z. Hu, S.-C. Chang, "Design Optimization of a Speed Reducer using Deterministic Techniques, " Mathematical Problems in Engineering, Vol. 2013, Hindawi Publishing Corporation, 2013, pp. 1-7.

[6] S.E.A. Stephen, D.D.N. Christu, "Weight minimization of Speed Reducer design problem using PSO, SA, PS, GODLIKE, CUCKOO, FF, FP, ALO, GSA and MVO" International Journal Of Scientific & Engineering Research, Vol. 7, No. 7, pp. 1356-1365.

[7] G.R. Miodragović, R.R. Bulatović, "Loop bat family algorithm (Loop BFA) for constrained optimization" Journal of Mechanical Science and Technology, Vol. 29, Springer, 2015, pp. 3329-3341.

[8] S. Lu, H.M. Kim, "A regularized inexact penalty decomposition algorithm for multidisciplinary design optimization problems with complementarity constraints," Journal of Mechanical Design, Vol. 132, No. 4, 2010,12 pages.

[9] A. Askarzadeh, "A novel metaheuristic method for solving constrained engineering optimization problems: Crow search algorithm," Computers and Structures, Vol. 169, Elsevier, 2016, pp. 1-12.

[10] S. Mirjalili, "Grey Wolf Optimizer," Advances in Engineering Software, Vol. 69, Elsevier, 2014, pp. 46-61.

[11] J. Kennedy, R. Eberhart, Particle swarm optimization, Proceedings of ICNN'95 – Int. Conf. on Neural Networks, pp. 1942-1948, Perth, WA, Australia, 1995.

[12] S. Mirjalili, "The Whale Optimization Algorithm," Advances in Engineering Sofware, Vol. 95, Elsevier, 2016, pp. 51-67.

[13] X.-S. Yang, A.H. Gandomi, "Bat Algorithm: A Novel Approach for Global Engineering Optimization," Engineering Computations, Vol. 29, No. 5, Emerald Groupp, 2012, pp. 464-483.

[14] X.-S. Yang, Firefly algorithms for multimodal optimization, International symposium on stochastic algorithms, pp. 169-178, Springer, Berlin, 2009.

[15] B. Basturk, An artificial bee colony (ABC) algorithm for numeric function optimization, IEEE Swarm Intelligence Symposium, Indianapolis, IN, USA, 2006.

[16] G. Dhiman, V. Kumar, "Seagull optimization algorithm: Theory and its applications for large-scale industrial engineering problems," Knowledge-Based Systems, Vol. 165, Elsevier, 2019, pp. 169-196.

[17] S. Kaur, L.K. Awasthi, A.L. Sangal, G. Dhiman, "Tunicate Swarm Algorithm: A new bio-inspired based metaheuristic paradigm for global optimization" Engineering Applications of Artificial Intelligence, Vol. 90, Elsevier, 2020, pp. 1-29.

[18] A.A. Heidari, S. Mirjalili, H. Farris, I. Aljarah, M. Mafarja, H. Chen, "Harris hawks optimization: Algorithm and applications" Future Generation Computer Systems, Vol. 97, Elsevier, 2019, pp. 849-872.

[19] S. Mirjalili, "Moth-flame optimization algorithm: A novel nature-inspired heuristic paradigm" Knowledge-Based Systems, Vol. 89, Elsevier, 2015, pp. 228-249.

THE 5th INTERNATIONAL CONFERENCE
MECHANICAL ENGINEERING IN XXI CENTURY

December 9-10, 2020
Faculty of Mechanical Engineering in Niš, Serbia

Comparison of Interpolation and Approximation Curves and Their Application in Computer Graphics

Aleksandar PETROVIĆ, Milan BANIĆ, Gavrilo ADAMOVIĆ

Department of Mechanical Design, Product Development and Engineering, Faculty of Mechanical Engineering, University of Niš, A. Medvedeva 14, Niš, Serbia
Department of Mathematics, Faculty of Mechanical Engineering, University of Niš, A. Medvedeva 14, Niš, Serbia
Department of Mechanical Design, Product Development and Engineering, Faculty of Mechanical Engineering, University of Niš, A. Medvedeva 14, Niš, Serbia
Department of Computer Science, Faculty of Sciences and Mathematics, University of Niš, Višegradska 33, Niš, Serbia
aleksandar.petrovic@masfak.ni.ac.rs, pedja.rajk@masfak.ni.ac.rs, milan.banic@outlook.com, gavrilo.adamovic@pmf.edu.rs

***Abstract*— This paper deals with the application of interpolation and approximation curves in computer graphics. A graphical representation of Lagrange polynomials, Bezier curves, and cubic splines is considered. The paper presents software created for plotting the mentioned curves, programmed in the Python programming language. Special attention is paid to the comparison of these curves obtained for the same common points that the user can set by clicking the mouse button in the software windows.**

***Keywords*— Cubic spline, Bezier curve, Lagrange interpolation polynomial, Computer graphics, Interpolation, Approximation**

I. Introduction

Polylines can be defined as a sequence of vertices connected by straight line segments. They are useful, but not for smooth curves. Also, it happens that polynomial interpolation often does not give satisfactory results. It has already been established that there are examples where increasing the number of nodes not only does not achieve greater accuracy, but the interpolation polynomial can also lose its approximate properties. In interpolation tasks, a reliable algorithm should be found that will guarantee better approximations of the function with increasing number of nodes. The way to solve this problem is to divide the interval $[a,\ b]$, on which the approximation is performed, into subintervals $[x_i, x_{i+1}]$ $(i = 0,1, \dots, n-1)$, and then to approximate on each subinterval the function by a polynomial of lower degree. When polynomials of degree one are taken as approximation polynomials on each segment, then we get the simplest case. A polygonal function obtained in this way is called a spline of degree one. In fact, polynomials (line segments) are connected so that the obtained function is continuous, while the points $(x_0, x_1, \dots, x_n)$ are points where the function changes its shape and are called nodes. The term spline as a mathematical term in the field of spline interpolation was first introduced I. J. Schoenberg [1] in his works in 1946, and its application in the field of design it began to develop only in 1960. Early research in the field of computer aided projections appeared in the late fifties of the last century and began simultaneously in Europe and the United States. During this period, there is a sudden development of computer-aided design - CAD, primarily driven by interests of large companies in the field of aeronautical engineering, shipbuilding and naval engineering as well as the automotive industry. Research in the United States has been largely focused on the development of interpolation techniques geometry. The papers of Coons [2], and Birkhoff [3] can be singled out here. Coons developed rectangular surface patches between the given smooth ones surface curves. These patches were a standard tool in the sixties but their main one the disadvantage was when merging multiple patches into one more complex surface. Birkhoff also dealt with rectangular surface patches. Today, the prevailing view is that the development of modern CAD software has basically begun with the work of French automotive engineers Pierre Bézier (Renault) and Paul de Casteljau (Citroën). Bézier used Berstein's polynomials (Berstein, 1912) as a basis for modeling curves and surfaces [4]. Casteljau made similar discoveries but did not publish his work scientifically. Citroen did not allow it and all research was kept secret. It was only after many years that he was able to publish his work. The spline development continued thanks to scientists Cox and de Boor [5]. In separate research in 1972, they developed a simple recursive formula for determining B-spline basic functions. The first application of B-spline in the field of computer-aided design (CAD) is related to the doctoral dissertation of Riesenfeld [6] (University of Syracuse) in 1973. In another doctoral dissertation Versprille [7] (University of Syracuse) presented non-uniform rational B-splines which are known today under the acronym NURBS. Since NURBS has certain shortcomings, especially when it comes to a mesh that is not local but refers to the whole row or column of control polygon points, several types of splines based on control points (PB - point based) have been developed. One of them is the T-spline. This type of

geometry was first introduced by Sederberg [8] in 2003. T-joints enable local mesh change.

II. Spline basics

The physical device used by the designers to draw smooth curves (especially in the shipbuilding and naval, aerospace, etc.) is called a spline. This device is actually a longer elastic wooden slat that can be bent so that it passes through several required points of knots. Mathematically speaking the curve can be defined as a continuous 1D set of points in 2D (or 3D) space. Working with splines can also be defined as a way of mapping from the interval S onto the plane. $P(t)$ is the point of the curve at parameter t.

$$P: R \ni S \to R^2, P(t) = \begin{pmatrix} x(t) \\ y(t) \end{pmatrix}$$

Unlike first-order splines of the linear type (Fig. 1), higher-order splines are smooth curves. The user specifies the control points, where the curve is completely determined by the control points. The spline is formed by interpolating the control points with a smooth curve.

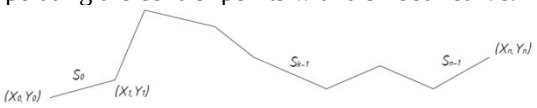

Fig. 1 First-order linear spline

Therefore, it can be written that the spline of degree one is a function S which is defined as:

$$S(x) = \begin{cases} S_0(x), & x \in [x_0, x_1] \\ S_1(x), & x \in [x_1, x_2] \\ & . \\ & . \\ & . \\ S_{n-1}(x), & x \in [x_{n-1}, x_n] \end{cases},$$

$$\textit{while: } S_i(x) = a_i x + b_i.$$

The function S defined in this way is linear by parts (linear on each subinterval) and has the following properties:

1) The domain of definition of the function S is on the interval [a, b];

2) S is continuous on [a, b];

3) There is a division that: $a = x_0 < x_1 < \ldots < x_n = b$ *so that S is a linear polynomial on each subinterval* $[x_i, x_{i+1}]$.

The equation of each segment can be given in the form:

$$S_i(x) = y_i + m_i(x - x_i).$$

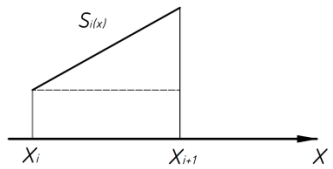

Fig. 2 Spline function on one segment

Symbol m_i is the slope (direction coefficient) of the line given by:

$$m_i = \frac{y_{i+1} - y_i}{x_{i+1} - x_i}.$$

Although the spline of degree one has a certain applications, it can be said that it has certain shortcomings, and is therefore unsuitable for a wider application. Viewed from the point of view of practice, in the field of technical drawing and computer graphics, it is usually necessary to approximate a given data table with a smooth polynomial curve. The goal is to obtain an approximation function that will not only be continuous, but that its derivatives will also be continuous functions. The continuity of the first derivative means that the curve graph is not "broken" in the nodes. However, the continuity of the second derivative is not so obvious, and means that the radius of curvature is defined at each point. So, the approximate function is required to be smooth and to pass through all nodes without sudden changes.

The definition of a spline of arbitrary degree follows. Let the interval $[a, b]$ be divided by points $(x_0, x_1, \ldots, x_n)$ so that $a = x_0 < x_1 < \ldots < x_n = b$, in which case the function S is called spline of degree k if:

1) The domain of definition of the function S is the interval [a, b];

2) The functions $S(x), S'(x), \ldots, S^{(k-1)}$ *are continuous on [a, b];*

3) S is a polynomial of degree k on $[x_i, x_{i+1}]$.

A spline of degree k is a continuous function together with its derivatives $S, S', \ldots, S^{(k-1)}$. If it is desired that the approximation spline has a continuous m-th derivative, it is necessary that the spline be at least of degree $m + 1$. It can be assumed that $x_0 < x_1 < \ldots < x_n$, is still valid, and that a polynomial of degree m is defined on each segment, and that these polynomials are connected in nodes, and also the obtained spline S has m continuous derivatives.

III. Curves plotting in 2D CAD software

In this section, 2D CAD software created with the intention to provide the possibility of plotting curves will be presented based on the Lagrange interpolation polynomials, Bezier curves and cubic splines. The software is programmed in the *Python* programming language, with libraries such as *pygame*, *numpy* and *math* being imported. The software was created so that it can be classified into a group of software in the field of computer graphics, has its own graphical user interface (GUI) and part of the code is programmed with object-oriented programming technology. The first few lines of code imported the previously mentioned libraries, each with its own function: *pygame* to provide the ability to create the appropriate dynamic graphical user interface represented in computer games, *numpy* provides support for large, multidimensional arrays and matrices, and *math* that provides access some common mathematical functions and constants in *Python*, which we can use in the whole code for more complex mathematical calculations.

Programming code 1.

```
import pygame
from sys import exit
import numpy as np
import math
```

After importing the libraries, the parameters that define the software window are created. Namely, the length and width of the window, the margins are set and adjusted so that the window has the ability to maximize and return to the initial length and width. Also, the name of the program is defined, in this case "*Approximation using splines*".

Programming code 2.

```
pygame.init() #Initialize.  () -> f-ja bez parametara
pygame.display.set_mode()
screen = pygame.display.set_mode((width, height), pyga
me.RESIZABLE)
#screen = pygame.display.set_mode((width, height), 0,
32) #Ovde moze da se ukljuci OpenGL za render grafike
#screen = pygame.display.set_mode((width, height),
pygame.FULLSCREEN)
pygame.display.set_caption("Aproksimacija uz pomoc spl
ajnova") #Ime prozora
```

Nodes and segments are initialized as empty sets below the code. The home screen of the software is filled with white and a clock variable is added to which a time domain has been added. In the next step, it is defined the function which "rotates" the function for drawing lines between points, as well as drawing rectangles that define the points that the user enters with the left mouse button. It is achieved by using a “for loop” in the program. Clicking on the defined buttons determines whether the Lagrange interpolation polynomials, Bezier curves or cubic splines will be drawn.

Programming code 3.

```
    def clearAndRedraw():
        screen.fill(WHITE)
        for i in range(count - 1):
            pygame.draw.line(screen, BLUE, pts[i], pts[i+1],
3)
        for i in range(count):
            pygame.draw.rect(screen, BLACK, (pts[i][0] -
 margin, pts[i][1] - margin, 2 * margin, 2 * margin), 5)
```

Figure 3 shows the entry of the first and the second point respectively, and the drawing of such a determined line segment.

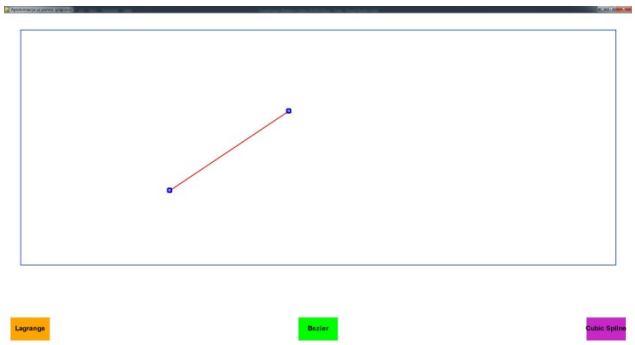

Fig. 3 Entering starting points

By adding the third point outside of this line segment we obtain a curve which passes through the first and the third point which is controlled by the second point. This procedure is shown in Fig. 4.

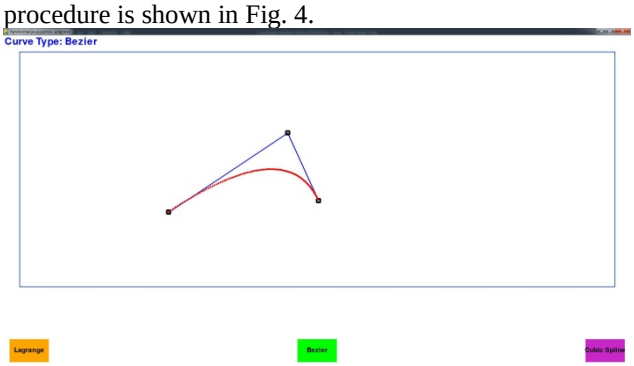

Fig. 4 Drawing the Bezier curve

By including new points, we get the curve which passes through the first and the last point, until all others are control points. Such curve is shown in Figures 5.

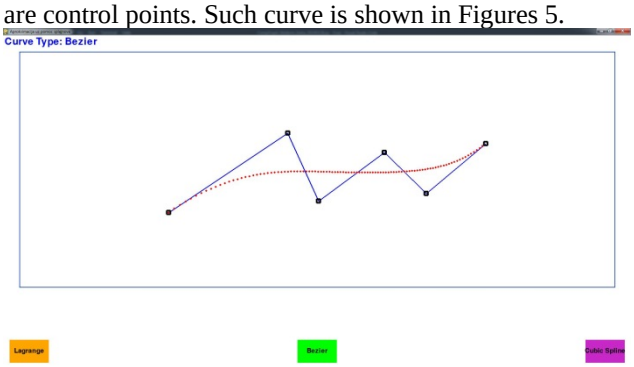

Fig. 5 Bezier curve with 2 external and 4 inner control points

The software is programmed so that it is possible to move the control points, which is in line with Bezier's original idea, that the curve can be manipulated by moving the positions of its control points.

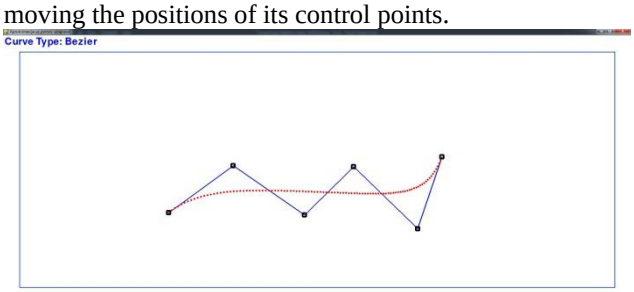

Fig. 6 Displacement of Bezier curve control points

Figure 7 shows the curve obtained by including Lagrange interpolation polynomials for the same control points. Curve transformation is obtained by simply clicking on the Lagrange button.

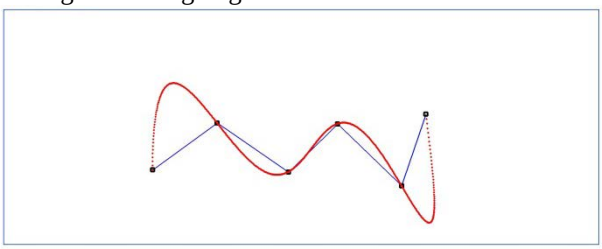

Fig. 7 Drawing of Lagrange interpolation polynomials

In the same way, by clicking on the Cubic Spline button, the curve is transformed into a cubic spline, which is shown in Fig. 8.

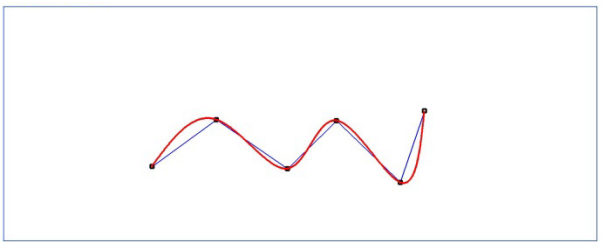

Fig. 8 Drawing of cubic splines

The next functions deal with drawing lines on the screen and the general visual experience. This can include the appropriate scaling of the window, i.e. maintaining the same distance in pixels, e.g. margin buttons when designing, defining local and global variables. A clearly framed space in which lines can be drawn is also defined.

Programming code 4.

```
    def onVideoResizeEvent(localWidth, localHeight):
        pygame.display.set_mode((localWidth, localHeight)
, pygame.RESIZABLE)
        screen.fill(WHITE)
        global width
        width = localWidth
        global height
        height = localHeight
        drawFrameAroundDrawingArea()
    def drawFrameAroundDrawingArea():
        pygame.draw.rect(pygame.display.get_surface(), (0,
50,200),
        (drawingAreaMargins, drawingAreaMargins, width
- 2 * drawingAreaMargins,
        height - drawingAreaMargins -
 drawingAreaBottomMargin), 2)
```

Upgrading this software would reach into the realm of 3D space and drawing three-dimensional splines that can be used to generate free forms and surfaces. Figure 9 shows a 3D model of the vertebrae with discs. The 3D model was generated from the CT scanner data. The scan was processed in SolidWorks with the help of splines and NURBS surfaces in order to become 3D model.

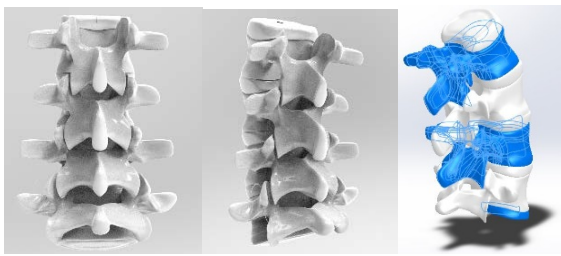

Fig. 9 Vertebrae and discs based on 3D splines and NURBS

The following figure shows the 3D model of injection moulded part based on splines drawn in the CREO PTC software package.

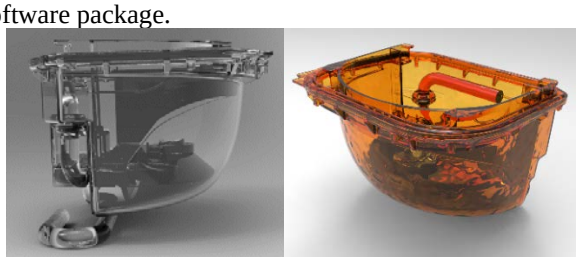

Fig. 10 Preview of 3D splines that make a smooth surface

IV. Conclusions

From technically complex to artistically sublime shapes, the spline outlines contemporary aesthetics because the lingua franca of the design, engineering and manufacturing industries. However, its history seems to be insufficiently researched, and their mathematical and technical basics are mostly not dealt with, even by users of modern 3D software, who often take spline and other computer curves "for granted" and want to solve current problems in a few clicks. For this reason, this paper aims to bring closer the topic of curves that find their applications in engineering and computer graphics. Spline as a curve the most attention is paid in this paper, is an extremely important tool for today's engineers and finds its purpose in 2D illustration (e.g. Adobe Illustrator), fonts (e.g. PostScript, TrueType), 3D modeling (sketches, free form surfaces) and trajectory animation. The significance of this paper is reflected in the fact that the sequential development of the computer curve over the years is exposed, as well as the application of the Python programming language and its libraries in the field of mathematics and computer graphics. Researchers have so far mostly used Wolfram Mathematica and MatLab, as well as OpenGL. This paper presents 2D CAD software, created to provide the possibility of plotting smooth curves, namely cubic splines, Bezier curves and Lagrange interpolation polynomials, which makes it possible to compare the appearance of curves for common entered points. Further aspects of this research from the math-programming side could be setting control points by entering a table with values. The idea of this software is to provide the ability to plot curves according to the current state of the art with respect to said curves. At the moment when plotting curves is completely analogous to modern CAD software, which is largely done, further aspects would be attempts to optimize curves for a certain set of points in order to obtain an even better approximation and thus perhaps modify and improve the existing apparatus.

References

[1] I. J. Schoenberg, “Contributions to the problem of approximation of equidistant data by analytic functions,” Parts A and B, Quarterly of Applied Mathematics. Providence, vol. 4, pp. 45-99 and 112-141, April 1946.

[2] S. A. Coons, “Surfaces for computer-aided design,” Project MAC, MIT, 1967.

[3] G. Birkhoff, “Fluid dynamics, reactor computations, and surface representation,” A history of scientific computing. New York, pp. 63-87, June 1990.

[4] P. Bézier, “Definition numerique des courbes et surfˆaces I,” Automatisme, vol. XI, pp. 625-632, 1966.

[5] C. D. Boor, “On Calculating with B-splines,” Journal of approximation theory. SAD, vol. 6, pp. 50-62, 1972.

[6] R.F. Riesenfeld, “Applications of B-Spline Approximation to Geometric Problems of Computer-Aided Design,” Doctoral dissertation, Syracuse University, NY, 1973.

[7] K.J. Versprille, “Computer-Aided Design Applications of the Rational B-Spline Approximation Form,” Doctoral dissertation, Syracuse University, New York, 1975.

[8] T. W. Sederberg, J. Zheng, A. Bakenov, “T-splines and T-NURCCs,” ACM Transactions on Graphics (TOG) - Proceedings of ACM SIGGRAPH 2003, Vol 22, pp. 477-484, New York, July 2003.

THE 5th INTERNATIONAL CONFERENCE
MECHANICAL ENGINEERING IN XXI CENTURY

December 9-10, 2020
Faculty of Mechanical Engineering in Niš, Serbia

On-line Monitoring of MAG-CMT Welding Process

DejanMARIĆ[a], MijatSAMARDŽIĆ[b], TihomirMARSENIĆ[b], Tomislav ŠOLIĆ[a], Josip PAVIĆ[c], Ivan SAMARDŽIĆ[a]and BožoDESPOTOVIĆ[g]

[a]Mechanical engineering faculty in Slavonski Brod, University in Slavonski Brod, Slavonski Brod 35000, Croatia
[b]Đuro Đaković Power Station - ĐĐTEP, Dr. Mile Budaka 1, SlavonskiBrod, Croatia
[c]ĐĐ Kompenzatori d.o.o., Dr. Mile Budaka 1, SlavonskiBrod, Croatia
[g]DTZSB, SlavonskiBrod, Trg I. B. Mažuranić 2, SlavonskiBrod, Croatia
dmaric@sfsb.hr, tihomir.marsenic@ddtep.power-m.hr, tsolic@sfsb.hr, josip.pavic@kompenzatori.com, ivan.samardzic@sfsb.hr, despotovic.bozo@gmail.com

***Abstract*—By applying the MAG-CMT welding process, it is possible to protect the boiler elements with Ni-alloys in order to prevent the harmful effects of corrosion. The researches gained insight into the influence of certain parameters of MAG-CMT process on the observed properties (content of delta ferrite less than 5% on the surface of the clad Ni-alloy, slight mixing of the base and filler material while retaining the adequate bonding of the substrate (base material) and the cladding layer (filler material), achieving the uniform thickness of the cladding layer, and reducing the rough transitions between the passages). Main welding parameters of the MAG-CMT process (current, voltage, filler wire feed rate, gas flow) are monitored and analyzed. Based on the observed parameters, the area of stable electric arc of MAG-CMT process is defined**

***Keywords*—Overlay cladding, MAG-CMT welding process, Welding parameters, On-line monitoring**

I. INTRODUCTION

There are a number of techniques for applying corrosion-resistant material and some of them are: hot rolling, cold rolling, explosive, centrifugal gluing, soldering, spraying, cladding [1]. As these are positions that, due to their constructional performance, are demanding for the implementation of the process of applying protective layers, the welding technique has proven to be one of the most acceptable techniques [2-4]. The most commonly used material for protection against high temperature corrosion is Inconel. Inconel is a trade name that comes from the nickel alloy manufacturer "International Nickel Co.", the application of Inconel began in 1959 - 1964. Nickel-based alloy (IN625) is most often used as protection of 16Mo3 steel at high temperatures in certain parts of the plant or in waste incineration plants, also by increasing the content of Ni, Cr and Mo generally increases the corrosion resistance of materials [2, 5, 6, 7, 8]. MAG-CMT (Metal Active Gas - Cold Metal Transfer) which enables the reduction of heat input during the welding process by applying certain changes in the welding parameters but also by controlling the flow of wire into the bath. The selected MAG-CMT welding process has the same technological aspects as the conventional MAG welding process with a new feature that allows the wire to go forward into the bath but also to go back out, this process allows exceptional process stability and constant arc length [9-12]. The MAG-CMT welding process has great advantages over some other Ni-alloy welding or deposition processes [13-18]:

- greater stability of the arc,
- abyss reduction,
- use of low power sources,
- reduction of the welded joint / heat affected zone ratio,
- improved microstructure properties,
- reduces residual stresses and strains in the welded joint,
- reduction of the content of delta ferrite on the surface of Ni-alloy,
- reduces the cooling time of the welded joint,
- 30% lower temperature compared to the conventional MIG / MAG process.

Usually, welding processes with MAG-CMT technology take place in automated and robotic systems in order to increase the productivity of the welding process [19, 20]. The required characteristics of welded layers made of Ni-alloys are achieving a delta ferrite content of less than 5% on the surface of the welded Ni-alloy layer, minimal mixing of base and additional material while maintaining adequate bonding to prevent sticking, achieving uniform thickness along the entire surface to be welded , and reducing rough transitions between passes [21]. The type of gas used in arc protection has shown a large impact on obtaining different welding results of Inconel 625 alloy [10, 21, 22].

Satisfactory results of Ni-alloy surfacing are achieved by applying a mixture of Ar+ He + CO_2 + H_2 gas, where He and H_2 enable an increase in thermal conductivity and improve melt spills. A small percentage of CO_2 provides good arc stability [22].

II. GENERAL ABOUT MAG-CMT WELDING PROCESS

The MAG-CMT process is characterized by low heat input, and prevention of the occurrence of cracks by controlling the transfer of a drop of material in the weld pool during short-circuit transfer [23, 24]. The CMT process was patented by the company "Fronius" in 2004, it is a high-speed digitized inverter and processor that controls all welding processes. The process consists of two main phases, the Arcing phase and the Short circuit phase.

An overview of welding parameters that have a great influence on the welding process of Ni-alloy MAG-CMT welding process are:
- welding current, I / A
- welding voltage, U / V
- welding wire speed, v_{wire} / m/min
- welding speed, $v_{wel.}$ / m/min
- gas flow rate, f_g / l/min
- droplet separation frequency, $f_{drop.}$ / Hz
- arc length correction, ALC / %
- dynamic control, DC / %
- distance of the contact wire from the base material, l_t / mm

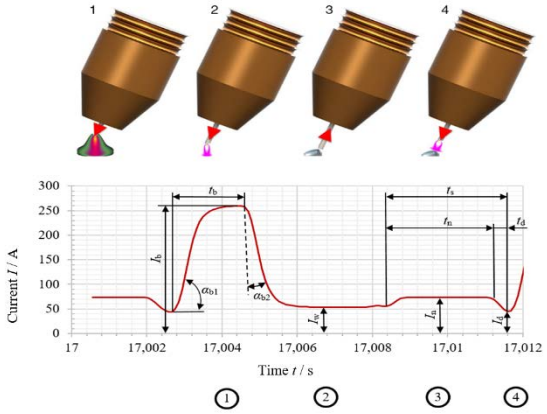

Fig. 1. MAG-CMT process cycle - 1. during arc burning the additional material moves towards the weld bath, 2. when the additional material reaches the arc bath the arc is extinguished - the current decreases, 3. the backward movement of the wire separates the droplet during a short circuit - the short-circuit current remains small, 4. there is an additional wire displacement and the process is repeated continuously [27-29]

New welding sources provide the possibility of more precise control of the transfer of metal droplets in the bath with the application of various systems to maintain the stability of the electric arc. "Synergic" controls of the MAG welding process have also been developed, which means that the strength of the welding current is controlled by adjusting the wire feed rate parameter. Such processes enable synchronization of power supply and wire feeder via microprocessor in order to maintain the stability of the arc and with all welding sources depending on the wire flow rate and current strength are almost the same [25, 26]. Figure 1 shows a schematic representation of the welding cycle of the welding current strength, and the method of droplet separation during the CMT welding process.The basic current curve for the MAG-CMT process consists of peak welding currents (I_b) lasting in the time interval of (t_b), short-circuit waiting current (I_w) and short-circuit cycle time ($t_s = t_n + t_d$). The short-circuit cycle consists of an elevated value of the short-circuit current (I_n) that takes place in the time period (t_n) and the separation current strength (I_d) that takes place in the time interval of (t_d). The rate of increase of current strength to peak values is equal to the angle α_{b1}, while the rate of decrease from the value of peak current depends on the angle α_{b2}. A change in the values of all the above parameters can affect the quality of the welded joint [18, 29]. The ALC and DC parameters adjust the characteristics of the current and voltage waveforms, as a rule, to external variations, such as the distance of the contact wire from the material, or changes in the composition of the shielding gas. In general, the ALC parameter is used as an arc length control parameter, whereby increasing the ALC value achieves a stronger droplet transfer to the arc and the arc stability is higher. When the ALC parameter changes, there are significant changes in the stability of the welding process due to changes in the droplet transmission in the bath. Given all the above, the ALC was chosen as a parameter to be controlled and observed in order to detect changes in droplet transfer in the bath and changes in (U, I) characteristics, in relation to external changes, shielding gas mixture, changes between contact distances conductors of base material). A negative ALC value increases the forward acceleration of the wire decreases the heat input and the average voltage, the length of the return time increases and the process frequency decreases, this all affects the smaller occurrence of larger droplets in the bath. Another characteristic is DC - dynamic correction also affects the transfer of the droplet in the bath, with positive DC indicates lower arc stability with lower values of short-circuit current, while negative DC values represent higher current during short-circuit and the appearance of more cracks during welding [25].

III. EXPERIMENTAL RESEARCH

The welding process was performed on a Fronius VR 7 000 CMT welding source with a CNC controlled interface, shown in Figure 2. The steels most commonly used in boiler construction are 0.5CrMoV, 2.25Cr1Mo, 1CrMoV, X12, 304, 316, P91, P92, 304 H, P22, 13CrMo4-5 and 16Mo3. For the purposes of the experiment, the basic material 16Mo3 was used. While a wire with a diameter of 1.2 mm Thermanit 625 (S Ni 6625 (NiCr22Mo9Nb); ERNiCrMo-3; Mat. No. 2.4831) was chosen as an additional material. The material is highly resistant to corrosion, to the appearance of cracks due to corrosion at high temperatures that can range up to 1100 ° C. The amount of oxygen that occurs on the base material, which can cause porosity in the weld alloy, is controlled by deoxidants, namely silicon and magnesium.

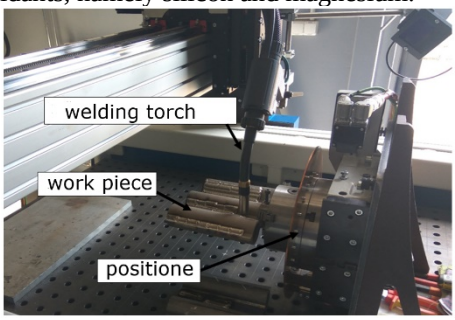

Fig. 2. Equipment for performing the experimental part display of the compressed sample in the positioner

In order to measure the main welding parameters, the WeldAnalyst-S3 system was used with the corresponding sensors. The application of various on-line monitoring enables the detection of defects in the welded joint, and the definition of the area of stability of the welding process.

The characteristics of the data acquisition device and the sensor are shown in Table 1, the data recording capability is 1MHz. The system allows a complete analysis of the dynamic characteristics of the main parameters of all welding processes. The device has 12

analogue channels for connecting different sensors, 4 of which are very fast.

TAB. 1. TECHNICAL CHARACTERISTICS OF ON-LINE MONITORING DATA COLLECTION DEVICES

	Device for measuring of welding data / WeldAnalyst-S3	Process sensors / P1000-S3	Wire feed sensors / DV 25 M	Gas sensor / GM30L10B-S3
Measurement rang	-	+/– 1 500 A, +/– 100 V	from 25 m/min (wire ø 0.8-2 mm)	0 … 30 l/min
Accuracy	-	+/– 1 %	+/– 1 %	+/– 3%
Max. input pressure	-	-	-	10 bar
Supply voltage	90 - 240 V AC / (4 A)	9 … 36 V DC, (10W)	10 … 30 V, (50 mA)	10 … 24 V DC (70mA)
Frequency	1 MHz	100 kHz for current, 20 kHz for voltage	3 660 Hz	3 644,8 Hz
Output voltage	+/– 10 V	0 … +/– 10 V	-	0 … 5 V
Dimensions / mm	260 x 150 x 90	120 x 120 x 105	85 x 60 x 35	98 x 65 x 28

IV. ANALYSIS OF THE RESULTS OF THE DYNAMIC CHARACTERISTICS OF THE MAIN PARAMETERS OF NI-ALLOY WELDING BY MAG-CMT PROCEDURE

Assessing the stability of the welding process of Ni-alloy layers, and possible estimates in the occurrence of errors in the process itself based on the measured surfacing parameters (surfacing current and surfacing voltage) would involve comparing the measured values with the reference values.

On-line monitoring and recording of all surfacing parameters (surfacing current strength, surfacing voltage, wire speed, gas flow) were recorded with the equipment shown in Figure 3 by a WeldAnalyst device during the entire surfacing process. The frequency at which the parameters are recorded is 10870 Hz. Figure 3 shows the appearance of the recorded characteristic for all parameters (surfacing current, surfacing voltage, wire speed, gas flow).

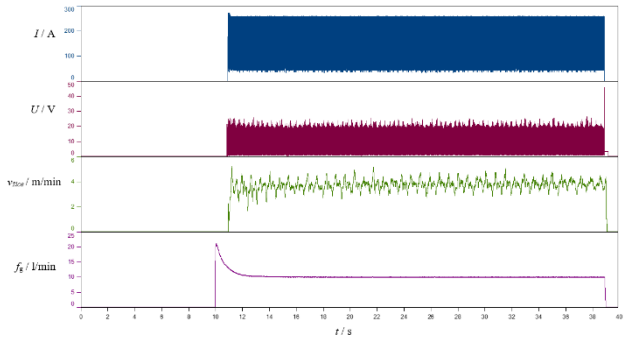

Fig. 3. Recording of weld parameters by WeldAnalyst device

Figure 4 shows the appearance of the dynamic characteristic for a time period of 17 to 17.05 seconds with indications of pulse and short circuit duration. Figure 4 a) shows the dependence of the welding current strength while Figure 4 b) shows the voltage dependences of the welding arc. For segment analysis and clearer display of results, only segments in the period from 17 to 17.05 seconds were displayed. After the recordings, the results of measuring the surfacing current and voltage were displayed, where Table 2 shows all the values of the main parameters characteristic of the applied MAG-CMT surfacing process, and shown in the diagram in Figure 1.

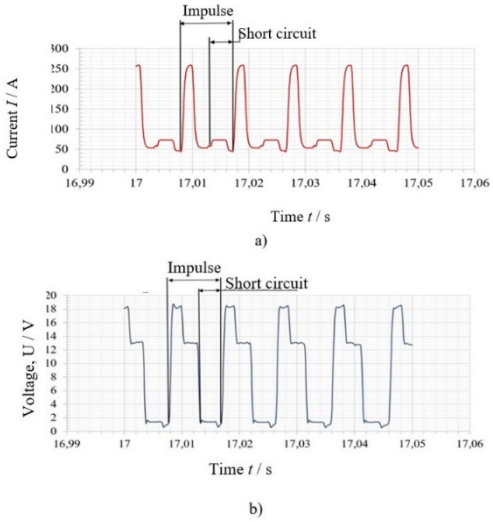

Fig. 4. Dynamic characteristics of main parameters with impulse and short-circuit duration: a) as a function of current, b) as a function of arc voltage

Table 2 shows the characteristic values for the welding parameters at a helium content in the gas mixture of 30%, which is common for practical application.

TAB. 2. CHARACTERISTIC VALUES FOR PARAMETERS AT A HELIUM CONTENT OF 30% IN THE GAS MIXTURE.

Sample	Peak welding currents I_k / A	Duration of peak currents t_k / ms	Duration of waiting Short-circuit current I_w / A	Short circuit currents I_s / A	Separation current I_d / A	Duration of short circuit current t_s / ms	Short circuit cycle time t_c / ms	Mean value - pulse duration t / ms	Peak welding voltage U_k / V	Short circuit waiting voltage U_w / V	Short circuit voltage U_s / V
7	260,00	1,84	53,93	73,44	44,10	2,30	3,86	9,20	17,95	12,90	1,24
8	259,70	1,84	53,57	73,14	42,70	2,30	4,05	13,89	18,89	13,07	1,34
9	260,00	1,84	54,02	73,46	44,30	2,30	3,86	9,48	18,29	12,58	1,58
10	259,90	1,84	54,01	73,47	43,80	2,12	5,15	13,25	17,95	11,87	1,66
11	260,10	1,84	53,91	73,61	44,70	1,47	2,76	8,37	18,55	12,94	1,55
12	259,80	1,93	53,72	73,20	44,10	2,48	4,51	10,86	18,62	12,55	1,47
13	260,20	1,84	54,09	73,72	44,70	1,47	2,85	9,20	18,28	13,16	1,66
14	259,6	1,84	53,55	73,20	44,00	2,12	3,86	10,86	18,41	13,24	1,56
15	259,6	1,84	53,69	73,18	44,50	2,21	3,96	9,57	18,78	11,60	1,74
16	260,00	1,93	53,85	73,49	43,80	1,66	4,60	12,51	18,01	12,87	1,57

Figure 5 shows the dependence of current and voltage during welding with a helium content of 30% with a change in gas flow of (10, 20, 30 l/min), and a correction of the arc length of (0%, 30%).

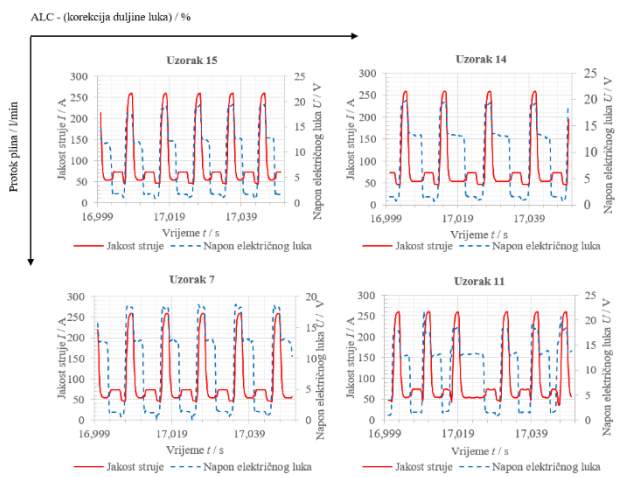

Fig. 5. Voltage change and current strength of Ni-alloy surfacing during a time period of 17 - 17.05 seconds during experimental surfacing with a gas mixture with a content of 30% helium

V. CONCLUSION

On-line monitoring (welding current strength) of the MAG-CMT welding process makes it possible to assess the stability of the process, and classify welded joints into two groups (good, bad) according to the visual assessment of welded Ni-alloy using one of the available machine languages. On-line monitoring enables us new knowledge in the field of current-voltage characteristics and certain changes in the welding process.

REFERENCES

[1] J. R. Davis i Davis and Associates, „Stainless Steel Cladding and Weld Overlays" u ASM Specialty Handbook: Stainless Steels, United States of America, ASM International, 1994, pp. 107-119.

[2] G. Eason, B. Noble, and I.N. Sneddon, "On certain integrals of Lipschitz-Hankel type involving products of Bessel functions," Phil. Trans. Roy. Soc. London, vol. A247, pp. 529-551, April 1955.

[3] S. Soltysiak, M. Selent, S. Roth, M. Abendroth, M. Hoffmann and H. Biermann, "High-temperature small punch test for mechanical characterization of a nickel-base super alloy" Materials Science & Engineering A, pp. 259-263, September 2014.

[4] E. Sadeghimeresht, L. Reddy, T. Hussain, N. Markocsani S. Joshi, "Chlorine-induced high temperature corrosion of HVAF-sprayed Ni-based alumina and chromia forming coatings" Corrosion Science, pp. 170-184, March 2018.

[5] M. Kwiecien, J. Majta and D. Dziedzic, "Shear deformation and failure of explosive welded Inconel-microalloyed steels bimetals" Archives of Civil and Mechanical Engineering, pp. 32-39, January 2014.

[6] M. Morales, J. Chimenos, A. Fernandez and M. Segarra, "Materials Selection for Superheater Tubes in Municipal Solid Waste Incineration Plants" Journal of Materials Engineering and Performance, pp. 3207-3214, September 2014.

[7] C. C. Silva, H. C. d. Miranda, M. F. Motta, J. P. Farias, C. R. M. Afonso and A. J. Ramirez, "New insight on the solidification path of an alloy 625 weld overlay", Journal of Materials Research and Technology, pp. 228-237, September 2013.

[8] "Welding Parameters for Inconel 625 Overlay on Carbon Steel using GMAW", Indian Journal of Science and Technology, pp. 1-5, November 2015.

[9] D. Kulawnski, M. Hoffmann, T. Lippmann, G. Lamprecht, A. Weidner , S. Henkel and H. Biermann, "Isothermal and thermo-mechanical fatigue behavior of 16Mo3 steel coated with high-velocity oxy-fuel sprayed nickel-base alloy under uniaxial as well as biaxial-planar loading", Journal of Materials Research, pp. 4411-4423, december 2017.

[10] A. Benoit, S. Jobez, P. Paillard, V. Kloseki and T. Baudin, "Study of Inconel 718 weldability using MIG CMT process", Science and Technology of Welding and Joining, pp. 477-482, August 2011.

[11] J. C. Dutra, R. H. G. e. Silva, C. Marques and A. B. Vivian, "A new approach for MIG/MAG cladding with Inconel 625", Welding in the World, pp. 1201-1209, November 2016.

[12] J. Frei, A. T. Boian and M. Rethmeier, "Low heat input gas metal arc welding for dissimilar metal weld overlays part I: the heat-affected zone", Welding in the World, pp. 459-473, May 2016.

[13] C. H., B. D., B. L. and D. M., "Overview of modern arc processes and their metal transfer methods in the case of GMA welding", u The 6th International Conference – Innovative technologies for joining advanced materials, Timisoara, 2012.

[14] J. Frostevarg, A. F. Kaplan and J. Lamas, "Comparison of CMT with other arc modes for laser-arc hybrid welding of steel", Welding in the World, pp. 649-660, September 2014.

[15] M. Solecka, P. Petrzak and A. Radziszewska, "The microstructure of weld overlay Ni-base alloy deposited on carbon steel by CMT method", Solid State Phenomena , pp. 119-124, Lipanj 2015.

[16] P. Colegrove, C. Ikeage, A. Thistlethwaite, S. Williams, T. Nagy, W. Suder, A. Steuwer and T. Pirling, "Welding process impact on residual stress and distortion", Science and Technology of Welding and Joining, pp. 717-725, December 2013.

[17] C. Fink and M. Zinke, "Welding of nickel-based alloy 617 using modified dip arc processes", Welding in the World, pp. 323-333, May 2013.

[18] M. Popescu, R. A. Rosu, C. Locovei and I. A. Perianu, "Joining of metallic composite materials by CMT- pulse", u Metal, Brno, 2013.

[19] S. Selvi, A. Vishvaksenani and E. Rajasekar, "Cold metal transfer (CMT) technology - An overview",Defence Technology, pp. 28-44, February 2018.

[20] V. Rajković, B. Despotović, T. Marsenić and V. Magdalenić, "Robots application for membrane panels cladding and collector", u 5. Međunarodno znanstveno-stručno savjetovanje SBZ 2009 Robotizacija i automatizacija u zavarivanju i ostalim tehnikama, Slavonski Brod, 2009.

[21] V. Rajković, B. Despotović and D. Žubrinić, "Application of "CMT" process for membrane walls cladding" u 6. Međunarodno znanstveno-stručno savjetovanje SBZ 2011 Suvremene tehnologije i postupci pri izradi tlačne opreme, zavarenih metalnih konstrukcija i proizvoda, Slavonski Brod, 2011.

[22] B. Despotović, D. Žubrinić and I. Samardžić, "Comparison of the results of Alloy 625 cladding with two shielding gases in boiler production", Zavarivanje i zavarene konstrukcije, pp. 101-111, 2014.

[23] S. Egerland, "Status and Perspectives in Overlaying under Particular Consideration of Sophisticated Welding Processes", Quarterly journal of the Japan Welding Society, pp. 50-54, January 2009.

[24] T. Kursuni and S. Turkiye, "Cold metal transfer (CMT) welding technology", The Online Journal of Science and Technology, pp. 35-39, January 2018.

[25] K. Wu, Z. He, Z. Dong and Y. Lan, "Numerical simulation of the temperature field of cold metal transfer welding pool",Mechanika, pp. 285-290, September 2016.

[26] Nuno Vasco da Costa Pepe, Advances in Gas Metal Arc Welding and Application to Corrosion Resistant Alloy Pipes, Shrivenham, Swindon: Cranfield University, 2010.

[27] C. Zhou, H. Wang, T. A. Perry and J. G. Schroth, "On The Analysis Of Metal Droplets During Cold Metal Transfer", Procedia Manufacturing, pp. 694-707, 2017.

[28] A. S. Azar, "A heat source model for cold metal transfer (CMT) welding", Journal of Thermal Analysis and Calorimetry, pp. 741-746, November 2015.

[29] T. Tucman, "CMT proces - nova revolucija u digitalnom zavarivanju", u 5. SEMINAR – Aluminij i aluminijske legure – rukovanje, priprema, zavarivanje, Pula, 2008.

THE 5th INTERNATIONAL CONFERENCE
MECHANICAL ENGINEERING IN XXI CENTURY

December 9-10, 2020
Faculty of Mechanical Engineering in Niš, Serbia

Surface Roughness of Parts Made by FDM 3D Printing

Marko PERIĆ, Aleksandar MILTENOVIĆ, Dušan STAMENKOVIĆ, Milica BARAĆ

Faculty of Mechanical Engineering, University of Niš, A. Medvedeva Niš 18000
marko.peric@masfak.ni.ac.rs, aleksandar.miltenovic@masfak.ni.ac.rs, dusan.stamenkovic@masfak.ni.ac.rs, milicabarac18@gmail.com

***Abstract*— In this paper, the roughness of surfaces on samples made by 3D printing was examined. A total of nine printed samples with different 3D printing parameters were measured. In the laboratory, a 3D printer with FDM technology and PLA material for sample printing, a device for measuring surface roughness and a hand-held microscope were used. The change in surface roughness of samples with different 3D printing parameters was registered by measuring the parameter Ra and Rz which is defined as the average roughness. The 3D printing parameters considered are Print Speed, Flow material and Layer Height.**

***Keywords*— 3D printing, Fused deposition modelling (FDM), Ra, PLA material**

I. Introduction

Technology 3D printing is a technology that is used in rapid prototyping for the production of functional prototypes, molds, spare parts and tools. 3D printing technology, we can obtain parts with complex geometry, which are more difficult or impossible to obtain by any conventional method. In order to get printed parts with the most accurate geometry, it is necessary to experimentally determine the deviation of the geometry of the printed part in relation to the CAD model from the aspect of surface roughness.

In the continuation of the paper, examples are given of how others measured the surface roughness of certain printed parts.

Mohammed S. Alsoufi et al. [1] experimentally investigated how surface roughness performance of printed parts manufactured by desktop FDM 3D printer with PLA+ is influenced by measuring direction. Among other things stated, concluded that the value of the parameter Ra is highest when the measurement is perpendicular to the direction of the applied layers.

Fuat Kartal [2] investigated examination of the effect of surface roughness of parts produced in the different nozzle temperatures on 3D printers. Concluded that the lowest surface roughness value for PLA filament material with a melting point of 190 degree celsius.

The aim of this paper is to experimentally show the influence of different values 3D printing parameters (print speed, material flow and layer height) on the surface roughness of the obtained samples by measuring the surface roughness with a profilometer [3]. Surface roughness measurement is performed at the micrometer level of unevenness. Based on the obtained results, it will be shown which of 3D printing parameters significantly affect the surface roughness, the arithmetic mean height of the roughness profile Ra will be considered.

II. Experimental Methodology

A. 3D Printer and Material

Table I and II shows the features of 3D printing technology and basic characteristics of the input material.

TABLE I Technology 3D Printing

Technology	FDM (Fused Deposition Modeling)
Name of 3D Printer	FELIX PRO 2
Filament size	1.75 mm
Nozzle Size	0.35 mm
Nozzle Max Temperature	275 $°C$
Heated Bed Max	100 $°C$
Large Build Volume	X=237 mm Y=244 mm Z=235 mm

TABLE III Filament characteristics

Material	100% Poly-lactic acid, PLA
Colour	White
Base temperature	$45 - 55\ °C$
Printing temperature range	$190 - 220\ °C$
Density	$1.25\ g/cm^3$
Room Temperature	$25 \pm 2\ °C$

Fig. 1 shows samples in the form of tiles dimensions $40x80x2\ mm$ obtained by Fused Deposition Modeling printing technology from PLA material. For all samples, the Infill Pattern is Lines where the directions of the applied layers intersect at 45 ° in every another layers.

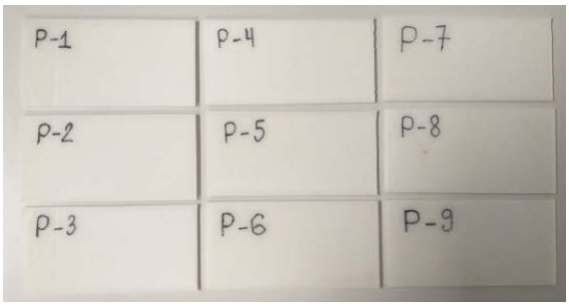

Fig. 1 Samples of obtained FDM technologies

B. Measurement

The device used to measure surface roughness is the Mitutoyo SJ-301 Surftest. The device uses a stylus with a diamond tip with a radius of 2 μm. The interface of the Mitutoyo measuring software is shown in Figure 2. Measurement conditions are defined on the JIS 1994 standard, cut-off is 0.8 mm in 5 segments, which gives a reference measurement length of 4 mm, linear speed is 0.5 mm/s and with a normal distribution of Gaussian type coordinates.

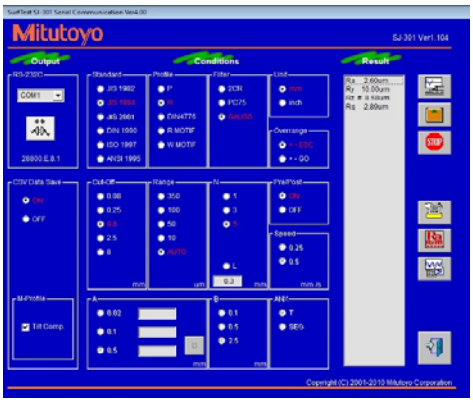

Fig. 2 Display the interface of the Mitutoyo SJ-301 Surftest

Surface roughness measurement was performed so that the sample occupies a total of three positions during measurement, the first position is at an angle of 0 degrees, the second position is at an angle of 45 degrees and the third position is at an angle of 90 degrees relative to the applied layer. The building direction are shown by the white lines and all three positions sample in Figure 3. In all three positions, the same area is measured that is parallel to the surface of the sample that was on the substrate during printing. Surface roughness measurement will be 2D, ie line roughness parameters will be used.

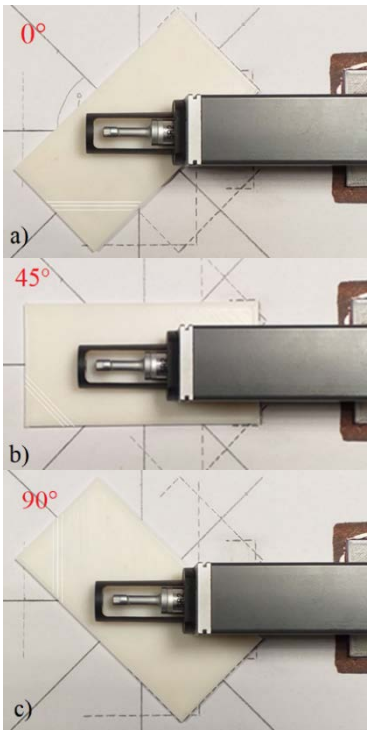

Fig. 3 Measuring directions: a) Parallel to building direction (0°); b) Diagonally across building direction (45°); c) Perpendicular to building direction (90°).

C. 3D Printing Parameters

In order to investigate the influence of 3D printing parameters on the surface roughness of samples obtained by 3D printing technology, it is necessary to consider the conditions or individual parameters that can significantly affect the process of applying layers or making finished parts with 3D printing technology. Parameters that can significantly affect the 3D printing process are mainly print speed, Flow material and layer height. Table III contains nine samples that are divided into three groups depending on the value of the 3D printing parameters.

The first group of samples P-1, P-2 and P-3 differ in the value of the print speed parameter, ie we have that the sample P-1 was printed at a speed of 20 mm/s, then the sample P-2 at a print speed of 40 mm/s and sample P-3 at a print speed of 60 mm/s.

The second group of samples P-4, P-5 and P-6 differ in the values of Flow material, sample P-4 was printed at Flow of 80%, then sample P-5 at 100% Flow and sample P-6 at Flow of 120%.

The third group of samples differs in the values of the layer height parameter during printing, so that sample P-7 is printed with a layer height of 0.1 mm, sample P-8 is printed at a layer height of 0.2 mm and also the back sample in column P-9 is printed at a layer height of 0.3 mm. Other parameters such as Wall Thickness, Top/Bottom Thickness, Horizontal Expansion, Infill Density, Infill Pattern, Printing Temperature, Bulid Plate Temperature and Fan Speed contain constant values that are the same in each sample.

TABLE IIIII Basic parameters of 3D printing

Sample Name	Layer Height [mm]	Wall Thickness [mm]	Top/Bottom Thickness [mm]	Horizontal Expansion [mm]	Infill Density [%]	Infill Pattern	Printing Temperature [C°]	Flow [%]	Bulid Plate Temperature [C°]	Print Speed [mm/s]	Enable Retraction	Enable Print Cooling	Fan speed [%]
P-1	0.1	1	1	0	90	Lines	220	100	70	20	Yes	Yes	100
P-2	0.1	1	1	0	90	Lines	220	100	70	40	Yes	Yes	100
P-3	0.1	1	1	0	90	Lines	220	100	70	60	Yes	Yes	100
P-4	0.1	1	1	0	90	Lines	220	80	70	40	Yes	Yes	100
P-5	0.1	1	1	0	90	Lines	220	100	70	40	Yes	Yes	100
P-6	0.1	1	1	0	90	Lines	220	120	70	40	Yes	Yes	100
P-7	0.1	1	1	0	90	Lines	220	100	70	40	Yes	Yes	100
P-8	0.2	1	1	0	90	Lines	220	100	70	40	Yes	Yes	100
P-9	0.3	1	1	0	90	Lines	220	100	70	40	Yes	Yes	100

III. Experimental Results and Discussion

The results of roughness measurements are shown by linear roughness parameters, ie arithmetical mean height (Ra) and average peak to valley height (Rz) according the standard ISO 4287 in Table IV.

TABLE IVV Obtained Roughness Value

	Ra [µm]			Rz [µm]		
Sample Name	**0°**	**45°**	**90°**	**0°**	**45°**	**90°**
P-1	0,99	3,07	2,86	3,08	17,68	11,86
P-2	0,67	2,56	2,81	2,48	8,67	8,70
P-3	0,54	2,89	3,50	1,64	8,91	10,60
P-4	1,93	7,94	7,86	10,88	29,85	33,05
P-5	0,50	2,95	2,92	1,88	9,03	8,84
P-6	0,41	7,11	7,98	2,66	25,92	29,28
P-7	0,39	3,00	3,92	1,25	13,01	21,88
P-8	0,90	6,34	6,61	3,20	21,43	23,65
P-9	0,39	3,26	4,38	1,45	13,72	18,53

Fig. 4 shows a diagram with the roughness parameter on the ordinate and Print speed parameter on the abscissa expressed in mm/s for each sample. In the conditions of measurement when building direction is parallel to the direction of roughness measurement, ie the angle is 0 degrees, we have that with increasing value of the Print speed parameter get less roughness Ra, ie have roughness decreasing from $Ra = 0.99\ \mu m$ to $Ra = 0.54\ \mu m$ when increasing the Print Speed from 20 mm/s to 60 mm/s.

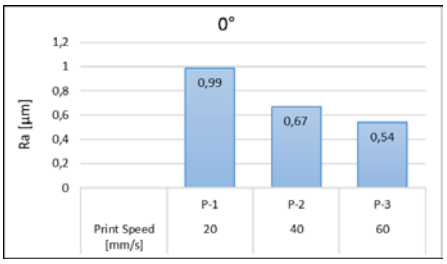

Fig. 4 Obtained roughness value Ra due to the influence of the Print speed parameter for an angle of 0°

Fig. 5 shows a diagram in the measurement conditions when building direction is diagonal to the direction of measurement, ie when the angle is 45 degrees, the highest surface roughness is at the value of the Print Speed parameter of 20 mm/s and it is $Ra = 3.07\ \mu m$ a the smallest surface roughness at Print Speed of 40 mm/s is then $Ra = 2.56\ \mu m$.

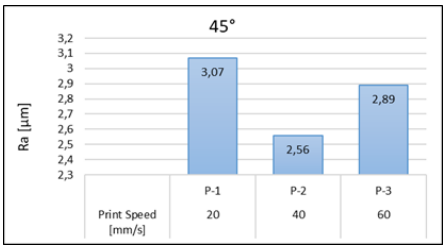

Fig. 5 Obtained roughness value Ra due to the influence of the Print speed parameter for an angle of 45°

Fig. 6 shows a diagram with the approximate value of roughness Ra and Rz at different speeds in the measurement conditions when building direction is perpendicular to the direction of measurement, ie when the angle is 90 degrees. Roughness is $Ra = 2.86\ \mu m$ for Print speed of 20 mm/s, then roughness is $Ra = 2.81\ \mu m$ for Print speed of 40 mm/s and roughness $Ra = 3.5\ \mu m$ at 60 mm/s.

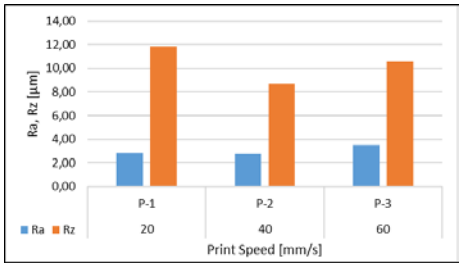

Fig. 6 Obtained roughness value Ra and Rz due to the influence of the Print speed parameter for an angle of 90°

Fig. 7 shows a diagram with the roughness parameter on the ordinate and on the abscissa the Flow parameter expressed as a percentage for each sample. The highest roughness $Ra = 1.93\ \mu m$ occurs at Flow of 80%. And the smallest roughness $Ra = 0.41\ \mu m$ at an increased Flow of 120%.

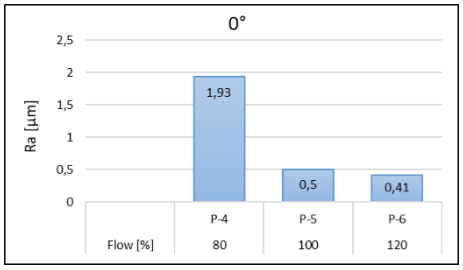

Fig. 7 Obtained roughness value Ra due to the influence of the Flow material parameter for an angle of 0°

Fig. 8 and 9 show diagrams with the lowest roughness $Ra = 2.95\ \mu m$ and $Ra = 2.92\ \mu m$, which is achieved when Flow is 100% under measuring conditions of 45 and 90 degrees in relation to building direction and direction of measurement.

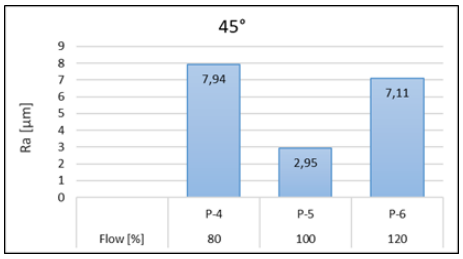

Fig. 8 Obtained roughness value Ra due to the influence of the Flow material parameter for an angle of 45°

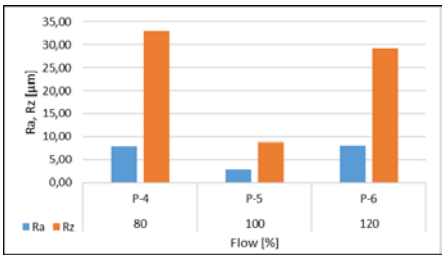

Fig. 9 Obtained roughness value Ra and Rz due to the influence of the Flow material parameter for an angle of 90°

Fig. 10, 11 and 12 show the surface roughness is higher when the value of the Layer Height parameter is 0.2 mm. In the first diagram (Figure 10) the roughness is Ra = 0.39 µm for Layer Height of 0.1 mm, then the roughness Ra = 0.9 µm for Layer Height of 0.2 mm. While for Layer Height of 0.3 mm roughness the surface area is Ra = 0.9 µm. In the second and third diagrams we have an approximate distribution of values.

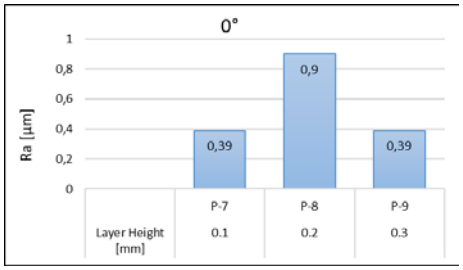

Fig. 10 Obtained roughness value Ra due to the influence of the Layer Height parameter for an angle of 0°

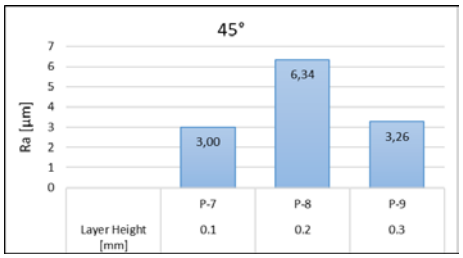

Fig. 11 Obtained roughness value Ra due to the influence of the Layer Height parameter for an angle of 45°

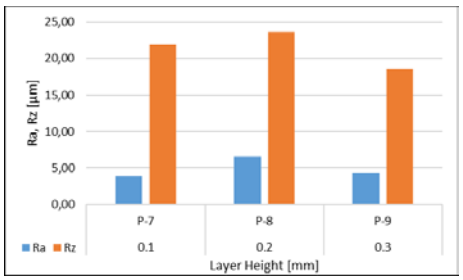

Fig. 12 Obtained roughness value Ra and Rz due to the influence of the Layer Height parameter for an angle of 90°

Fig. 13 shows a microscopic view of the surface measured on the P-2 sample. The last row of the applied layer has the greatest influence on the surface roughness.

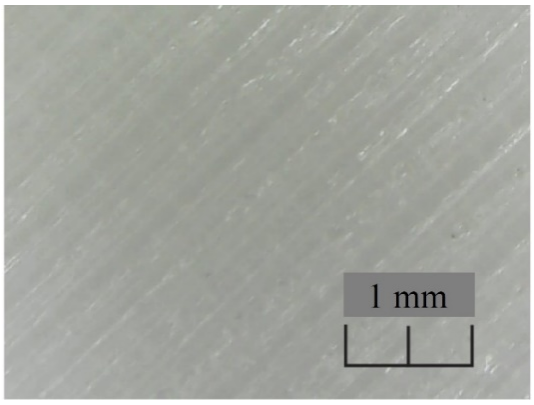

Fig. 13 Microscopic representation of the applied layers on the sample

Fig. 14 shows the appearance of the surface profile lines of the P-2 sample at different measurement directions in relation to the building direction. The length of the roughness measurement (needle path) is given on the apse, and the change in the roughness parameters Ra is given on the ordinate. Roughness was measured at a length of 4 mm. The recorded surface profile lines confirm the values of Ra shown in Table IV.

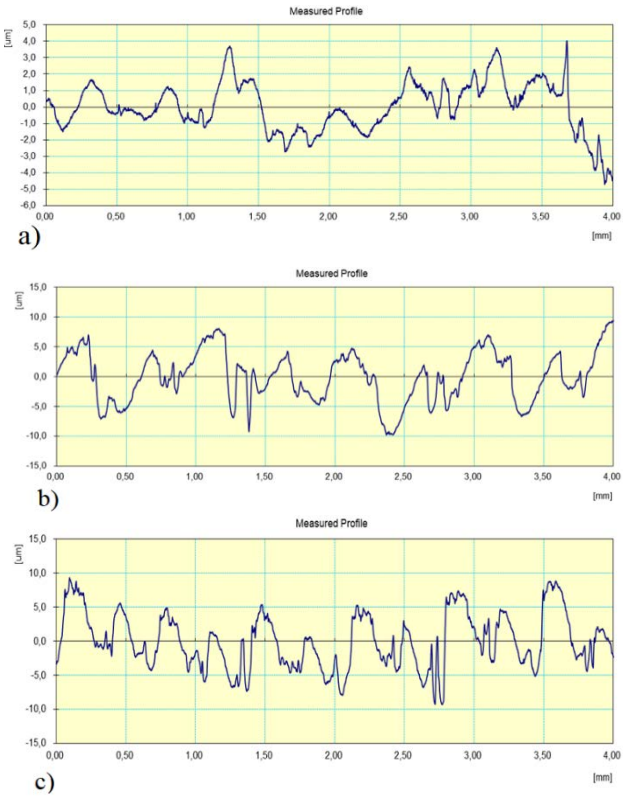

Fig. 14 The profile lines for sample P-2 measuring directions: a) Parallel to building direction (0°); b) Diagonally across building direction (45°); c) Perpendicular to building direction (90°).

IV. Conclusions

Based on measuring the surface roughness of samples obtained from PLA materials and considering the influence of 3D printing parameters. The conclusion is:

- The optimal parameter value for Printing speed is 40 mm/s, then the minimum surface roughness is achieved.
- The optimal value of the Flow material parameter is 100%, increasing or decreasing the value of the Flow parameter does not affect the printing time.
- Minimal surface roughness is achieved with a Layer Height parameter value of 0.1 mm, but the printing time also increases.
- The highest surface roughness is obtained by measuring at 90 ° in relation to the building direction.

References

[1] M. Alsoufi, and A. Elsayed, "How surface roughness performance of printed parts manufactured by desktop FDM 3D printer with PLA+ is influenced by measuring direction" American Journal of Mechanical Engineering, vol. 5, No. 5, pp. 211-222, 2017.

[2] Fuat K., Examination of the Effect of Surface Roughness of Parts Produced in the Different Nozzle Temperatures on 3D Printers, Crimson Publishers, vol. 2 – Issue 4, 2019.

[3] D. Stamenković, M. Banić, M. Nikolić, Tribology, textbook, Faculty of mechanical Engineering Niš, 2020.

THE 5th INTERNATIONAL CONFERENCE
MECHANICAL ENGINEERING IN XXI CENTURY

December 9-10, 2020
Faculty of Mechanical Engineering in Niš, Serbia

Joining Lightweight Components by Resistance Element Welding - REW

Aleksija ĐURIĆ[a], Dragan MILČIĆ[b], Damjan KLOBČAR[c]

[a]University of East Sarajevo, Faculty of Mechanical Engineering, Bosnia and Herzegovina
[b]Faculty of Mechanical Engineering, University of Nis, Niš, Serbia
[c]Faculty of Mechanical Engineering, University of Ljubljana, Ljubljana, Slovenia
aleksijadjuric@gmail.com, dragan.milcic@masfak.ni.ac.rs, damjan.klobcar@fs.uni-lj.si

***Abstract*— Resistance welding is a very cost- and energy-efficient welding process for thin sheets with wide distribution in the automotive manufacturing. With the challenges of lightweight construction in this area, new high-strength steel grades, light metals, and fiber-reinforced plastics are increasingly used. Hence, to that, adjustments of the welding processes are required. New process variants such as the resistance element welding (REW) are used to join mixed compounds of lightweight components and steel. Similar to the welding of functional elements, a low energy input in the base material is targeted, so only a small thermal influence of the materials occurs. The paper presents the mechanical properties, microstructure and macrostructure of the REW joint depending on the welding parameters.**

Keywords— Resistance element welding-REW, Aluminum alloy AW 5754 H22, Dual-phase steel DP500, Microhardness, Macrostructure

I. Introduction

Multi-material design has been developed as a modern design concept for lightweight structures that aims to integrate different types of materials into one structure. This involves using different materials in the same part to reduce its weight and keep its performance the same. Car body weight can be reduced by using different types of materials. Different types of lightweight bodies have been developed with the applying of AHSS steel, aluminum alloy and composite materials. A prerequisite for achieving mullite-material structures is the application of efficient and inexpensive technologies for joining different materials. Steel and aluminum construction has a good perspective for application in the automotive and aviation industries considering the material properties, however, the quality joint of two different materials is the bottleneck in using and popularizing steel and aluminum structures [1]. Joining technologies of different materials can basically be divided into three basic groups: welding, mechanical joining and bonding [2,3].

Resistance spot welding (RSW) is the most commonly used method for joining technology in the automotive industry, so one car has over 5000 RSW points [2]. The joining of aluminum and steel with RSW technology is a very difficult which will be analysed in this paper as well, so today's research focuses on finding alternative technologies that will not require a complete change of equipment in automotive factories. One such technology is Resistance element welding (REW). Resistance element welding is a process that begins with the insertion of steel, called an element, into aluminum, magnesium, or other lightweight material. After the element is inserted into the lightweight material, the procedure of classic resistance spot welding is followed. The complete REW process is shown in Fig. 1.

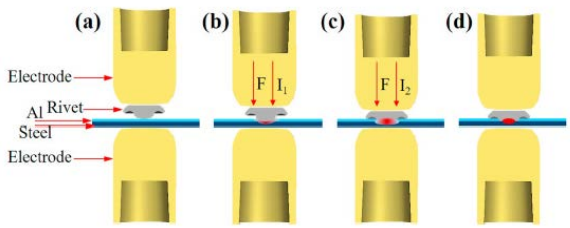

Fig.1 Sketch of the integrated REW process: (a) prepressing stage, (b) thermal piercing stage, (c) welding stage and (d) retreating stage.

The published studies about this promising technology mainly focused on the REW [6–9] or REW bonding process [4,5,10,11] comparison with other technologies.

II. Experiment

AW 5754 H22 Al alloy (1.0-mm-thick) and DP500 steel (1.5-mm-thick) were used as the base materials. Q235 steel rivet developed by Flexweld was used as the auxiliary element. Mechanical properties of the Al alloy, DP 500 steel, and rivet are shown in Table 1 and chemical compositions in Table 2.

TABLE I MECHANICAL PROPERTIES

Brand	Mechanical propertis		
	$R_{p0,2}$(MPa)	R_m(MPa)	A(min %)
DP 500	330	550	20
A 5754	185	245	15
Q235	250	475	20

$R_{p0,2}$ - Yield strength; R_m- Tensile strength; A – Elongation

TABLE II CHEMICAL COMPOSITION

Brand	Chemical composition									
	C	Cr	Si	Mn	P	Fe	S	Mg	Al	Cu
DP 500	0.1	/	0.5	1	0.02	Bal.	0.01	/	0.01	/
A 5754	/	0.3	0.4	0.4	/	0.3	/	3.6	Bal.	0.1
Q235	0.29	/	0.28	1.03	0.04	Bal.	0.05	/	/	0.2

The element was insert into aluminum with force pressure of 300 N as shown in Fig. 2.

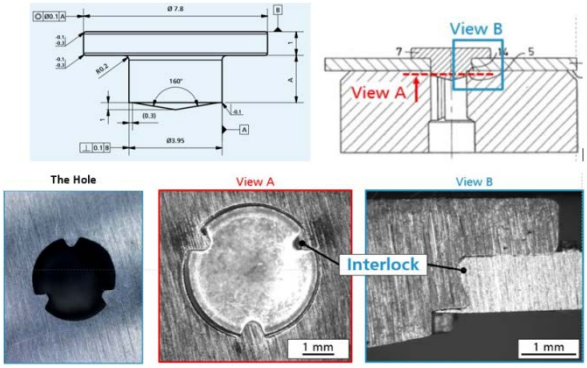

Fig. 2 Flexweld resistance element welding

After inserting the steel element into aluminum, classic RSW welding was done using RSW machine manufactured by Kocevar&sinovi which is managed using the BOSH 6000 software. Welding was carried out using electrode type F1 with parameters showed in Table 3.

TABLE III WELDING PARAMETERS

Mark	Weld current *I* kA	Electrode force *F* kN	Welding time *T* ms
REW-1	6	3.68	60
REW-2	8	3.68	60
REW-3	10	3.68	60
REW-4	8	2.45	60
REW-5	8	4.91	60
REW-6	8	3.68	120
REW-7	8	3.68	180

For the sake of comparison, classic RSW welding of aluminum alloy 5754 and DP500 steel was performed with the parameters showed also in Table 3. Other welding parameters such as squeeze time (SQZ=300 ms), hold time (HLD=300 ms), pre-heating time (Pre-Weld=0 ms), Cool Time (CT=0 ms), Up Slope Time (UST=0 ms) and Down Slope Time (DST=0 ms) were constant during the experiment. All tests were done with three replicates.

The welding specimens were 30 × 100 mm for REW joining. Before welding, alcohol was used to clean the specimens. The specimens were assembled, as shown in Fig. 3, with an overlap distance of 35 mm.

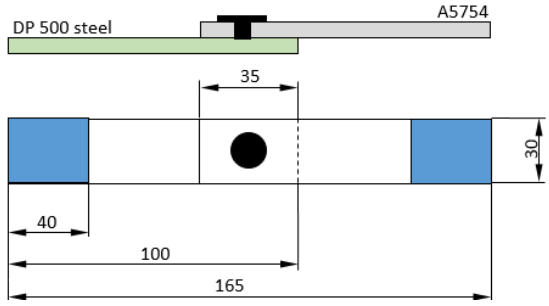

Fig. 3 Lap shear specimen geometry for tensil testing

The tensile-shear tests were performed according to standard ISO 14273:2016 at a cross-head speed of 2 mm/min with a Beta 50-7 / 6x14 testing machine. Metallographic samples were cut from the center of the joints. The samples were ground and polished based on standard metallography procedures. The Q235 and DP500 steel side were etched using 4% nital solution (7 seconds) and the Al side was etched using H_2O and HF solution (25 seconds). Microstructures of joints were observed with an VHX-6000 microscope. Vickers micro-hardness tester Zwick/Roell ZHU 2.5 was used to measure the hardness variations cross the joint under the load of 5 N for 12 s.

III. RESULTS AND DISCUSSION

Fig. 4 compares the typical load-displacement curves of REW joints that failed in IF (interfacial fracture) and PF (pull-out fracture) modes. The PF is accompanied by higher peak load and energy absorption (Fig. 5). All REW specimens fail in PF mode, except specimens marked as REW-5 which fail in IF mode.

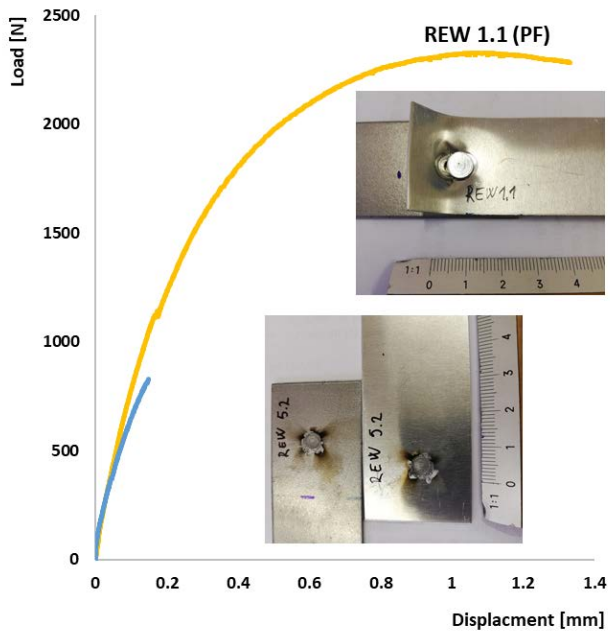

Fig. 4 The variation of lap shear performance with the welding parameters - the typical lap shear curves

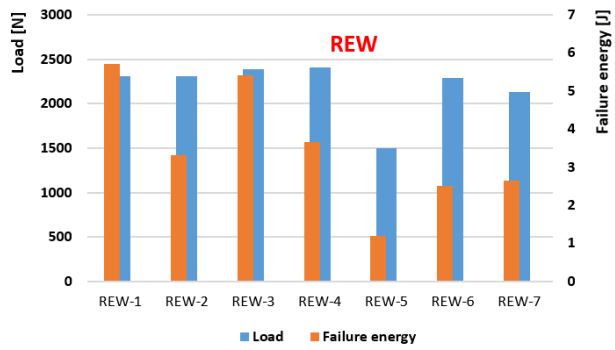

Fig. 5 Peak load and energy absorption of REW joint for different the welding parameters

The typical macrostructure of the REW joint depending on welding parameters for all specimens are shown in Figure 5. As it is clear from the figure, welding parameters have a significant effect on the nugget appearance and dimensions in the REW process. Particularly noticeable is the dimension difference of nugget in the first three specimens where the welding current varies from 6 to 10 kA, because of the remarkable difference in heat input. The larger part of the nugget are in the Q235 steel rivet for all combination. This formation of the asymmetrical nuggets can be attributed to the differences in electrical resistivity and thermal conductivity. By REW-3 (10 kA) and REW-7 (180 ms) specimens, it was observed pore formation in the nugget canter and also the rivet hole widened, as is shown in figure 6 also. This phenomenon can be attributed to the excessive melting of the aluminum alloy due to the high heat input.

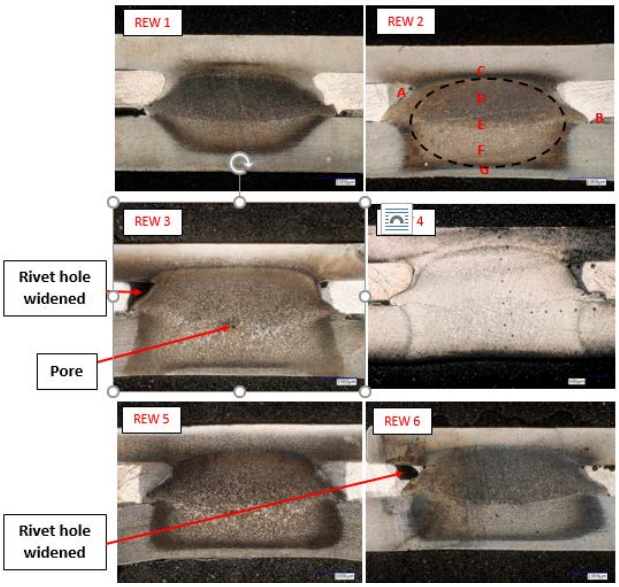

Fig. 6 Macrostructure of REW joint

The welded joint can be divided into three parts: fusion zone (FZ), heat affected zone (HAZ) and base metal (BM). The microstructures of regions A–F denoted in Figure 6 are shown in Figure 7.

Due to the fusion of the rivet during welding, because resistance spot welding was implemented first on the rivet and then on the aluminum alloy near the rivet/Al interface, was led to the diffusion of molten aluminum alloy and steel, and the diffused material subsequently solidified generating FeAl from a-Fe (Region A) (R. Qiu et al 2015). Region B also shows the appearance of an intermetallic compound (IMC) but now between DP steel and aluminum alloy.

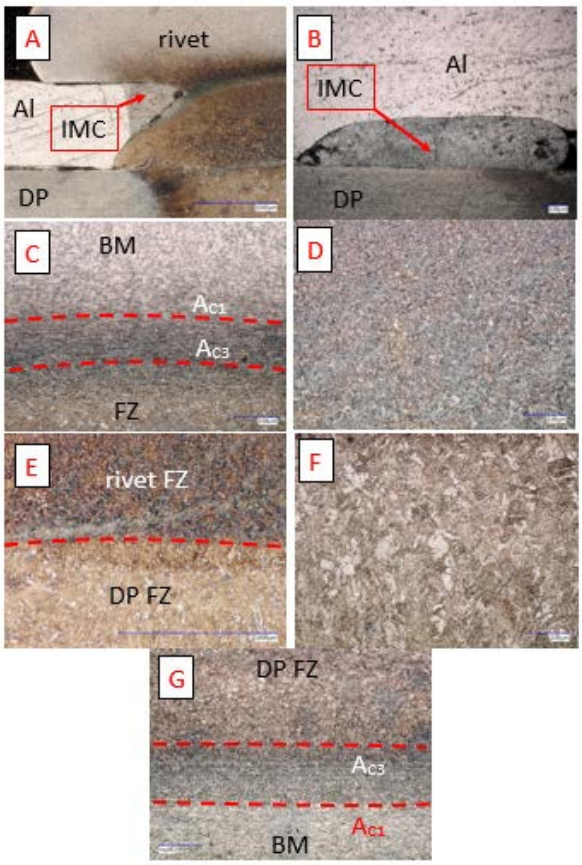

Fig. 7 Microstructure of REW joint

Region C shows the microstructures in the heat-affected zone (HAZ) of rivet Q235. This HAZ can be divided into two different zones: inter-critical HAZ and upper-critical HAZ. The maximum temperature that is attained in this zone is above AC3 (upper-critical HAZ), and the BM completely transforms into austenite. As a result of the fast cooling, the austenite transforms into martensite. The peak temperature reached in this zone is between AC1 and AC3 (inter-critical HAZ), and the BM microstructure transformed into a mixture of ferrite and austenite. After cooling, the austenite transformed in to pearlite while the ferrite is retained. The BM microstructure also consisted of ferrite and pearlite, but the volume fraction of the pearlite is less than that of the inter-critical HAZ. The D show fusion zone (FZ) region at the rivet site and region E show the interface between the DP steel and the rivet.

The vertical hardness profiles of specimen REW-2 across the joint is shown in Fig. 8.

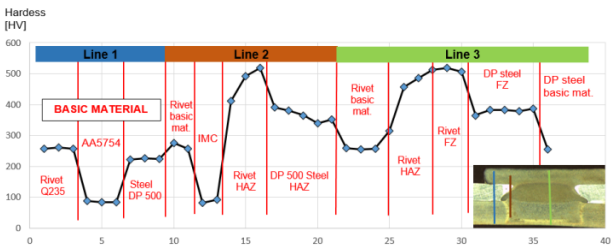

Fig. 8 The vertical hardness profile

As shown in the figure of the hardness of the fusion zone in DP steel is on average 379 HV. The average hardness of the DP steel base material is 223 HV. The formation of bainite and martensite in the FZ explains the higher hardness of the FZ compared to the BM hardness. The HAZ in Q235 steel rivet exhibited the highest hardness (more than 500 HV), which is due to the martensitic microstructure. It is also noted that the hardness of the rivet fusion zone is very high, about 500 HV. The hardness od IMC is similar to the hardness of Al alloy basic material, approximately 85 HV.

IV. Conclusions

In this paper was analysed the macrostructure, microstructure and tensile-shear strength and failure mode of the resistance element welding (REW) of AW 5754 H22 Al alloy (1.0-mm-thick) and DP500 steel (1.5-mm-thick). REW joint is made with different welding parameters (weld current *I*=6-10 kA, electrode force *F*=2,45-4,91 kN, welding time *T*=60-180 ms), which resulted in different heat input.

The larger part of the nugget are in the Q235 steel rivet for all combination. This formation of the asymmetrical nuggets can be attributed to the differences in electrical resistivity and thermal conductivity.

During the lap shear process, both the steel nugget and Al sheet bear the same load simultaneously, thus the competition relationship between mechanical performance of the steel nugget and Al sheet determines the failure modes. The characteristics of macro/microstructure ultimately need to be reflected by the mechanical performance. REW joints failed in IF (interfacial fracture) and PF (pull-out fracture) modes. The PF is accompanied by higher peak load and energy absorption. All REW specimens fail in PF mode, except specimens marked as REW-5 which fail in IF mode. The lap shear strength of integrated REW joints reached the peak point at 8–60-2,45 (*I*-*T*-*F*).

Vertical hardness profile indicates that HAZ in Q235 steel rivet exhibited the highest hardness (more than 500 HV), which is due to the martensitic microstructure.

Acknowledgment

This paper presents the results of the research conducted within the project “Research and development of new generation machine systems in the function of the technological development of Serbia” funded by the Faculty of Mechanical Engineering, University of Niš, Serbia.

References

[1] K. Xu, Q. Cui, G. Li, S. Zhang, „Research Status of Steel - Aluminum Joining Technology for Automobile Parts,“ Advances in Engineering Research, t. 86, pp. 216-218, 2017.

[2] L. Bertin, Tensile Strength of Automotive Aluminum Joints Using Resistance Spot Welding, Self-Piercing Riveting and Adhesive Hybrid Joining -Electronic Theses and Dissertations, University of Windsor, 2014.

[3] P. Kah, R. Suoranta, J. Martikainen, C.l Magnus, „TECHNIQUES FOR JOINING DISSIMILAR MATERIALS: METALS AND POLYMERS,“ Rec. Adv. Mater. Sci., t. 36, pp. 152-164, 2014.

[4] G. Meschut, V. Janzen, T. Olfermann, Innovative and highly productive joining technologies for multi-material lightweight car body structures, J. Mater. Eng. Perform. 23 (5) (2014) 1515–1523.

[5] G. Meschut, O. Hahn, V. Janzen, T. Olfermann, Innovative joining technologies for multi-material structures, Weld, World 58 (1) (2013) 65–75.

[6] N. Holtschke, S. Jüttner, Joining lightweight components by short-time resistance spot welding, Weld. World 61 (2) (2016) 413–421.

[7] Z. Ling, Y. Li, Z. Luo, S. Ao, Z. Yin, Y. Gu, Q. Chen, Microstructure and fatigue behavior of resistance element welded dissimilar joints of DP780 dual-phase steel to 6061-T6 aluminum alloy, Int. J. Adv. Manuf. Technol. 92 (5–8) (2017) 1923–1931.

[8] Z. Ling, Y. Li, Z. Luo, Y. Feng, Z. Wang, Resistance element welding of 6061 aluminum alloy to uncoated 22MnMoB boron steel, Mater. Manuf. Process. 31 (16) (2016) 2174–2180.

[9] S.M. Manladan, F. Yusof, S. Ramesh, Y. Zhang, Z. Luo, Z. Ling, Microstructure and mechanical properties of resistance spot welded in welding-brazing mode and resistance element welded magnesium alloy/austenitic stainless steel joints, J. Mater. Process. Technol. 250 (2017) 45–54.

[10] S.M. Manladan, Y. Zhang, S. Ramesh, Y. Cai, Z. Luo, S. Ao, A. Arslan, Resistance element weld-bonding and resistance spot weld-bonding of Mg alloy/austenitic stainless steel, J. Manuf. Process. 48 (2019) 12–30.

[11] G. Meschut, C. Schmal, T. Olfermann, Process characteristics and load-bearing capacities of joints welded with elements for the application in multi-material design, Weld. World 61 (3) (2017) 435–442.

Mechatronics and control

THE 5th INTERNATIONAL CONFERENCE
MECHANICAL ENGINEERING IN XXI CENTURY

December 9-10, 2020
Faculty of Mechanical Engineering in Niš, Serbia

Trends in Artificial Intelligence for Automated Industrial Systems

Stevan STANKOVSKI[1], Dragan KUKOLJ[1], Gordana OSTOJIĆ[1], Igor BARANOVSKI[1], Sandra NEMET[2]

[1] Faculty of Technical Sciences, University of Novi Sad, Novi Sad, 21000, Serbia
[2] RT-RK Institute for Computer Based Systems, Novi Sad, Serbia
stevan@uns.ac.rs, dragan.kukolj@rt-rk.com, goca@uns.ac.rs, baranovski@uns.ac.rs, sandra.nemet@rt-rk.com

***Abstract*— The influence of Artificial Intelligence (AI) is spreading up rapidly in many areas of automated industrial systems. As automated industrial systems are becoming more complex, the demand for production without faults is growing and it starts to be a huge issue to solve complex problems with limited human resources and knowledge and within a limited time. The right solution is adopting AI in the process of making decisions in these problems. The potential of AI is growing in different aspects of manufacturing management and control of automated industrial systems. Edge computing on PLC gives the opportunity to put in practice the potential of AI, especially in fault prediction. In this paper are given recent trends in artificial intelligence for automated industrial systems.**

***Keywords*— Artificial Intelligence, Industrial Systems, Edge computing, PLC, Prediction**

I. Introduction

From the First industrial revolution, we try to understand how industrial automation has an impact on the labour market and productivity. Usually, we can hear arguments that the oncoming advances in automation will the end of work by humans in automated systems. On the other hand, many researchers claim that is no reason to be concerned because technological breakthroughs in the past have eventually increased the demand for labour and wages [1]. In the first three revolutions, jobs that were realized by human muscles are replaced by machines, while in the fourth revolution decision making jobs have to be replaced by Artificial Intelligence (AI). This is a significant difference between the ongoing revolution (4th revolution) and previous revolutions (see Fig. 1 [2]). Industrial automation typically involves the substitution of machines for hard physical work. From the perspective of workers, it has two sides: good and bad. The good side is that workers will be released from jobs which have a big influence on their health, but on the other side, they can lose their jobs or it can lead to the displacement of workers from the tasks that are being automated, to the tasks for which they are not qualified enough (displacement effect - as capital takes over tasks previously performed by labour). The displacement effect implies that automation reduces the labor share of value-added. The history of industrial automation shows that new technologies came with new tasks in which labour has a comparative advantage [3]. Now, industrial automation coming with AI, which means that we have a situation in which machines are not only the substitution for hard physical jobs, but also for decision making jobs.

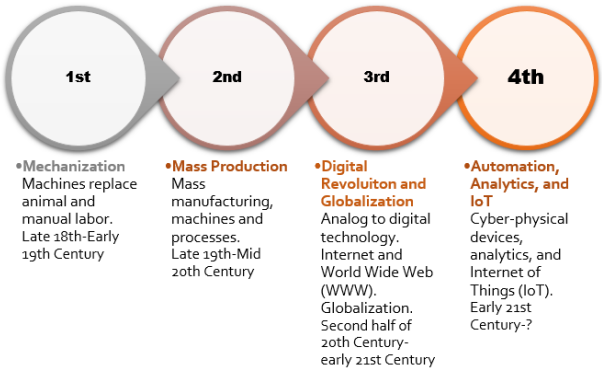

Fig. 1 Difference between industrial revolutions [2]

According to the report from the World Economic Forum (WEF), we are into the Fourth industrial revolution and we must be aware of this fact. WEF named several topics which have a significant influence on the ongoing revolution, including artificial intelligence, robotics, 3D printing, nanotechnology, genetics, biotechnology, etc. All these drivers of changes have additional synergy effect [4].

The key prerequisite for the ongoing revolution is to have quality networks that will enable quality data transfer from all segments of our lives' (business and/or private). Actually, networks are the basic elements of the infrastructure of any complex digital system's infrastructure. Without fast and reliable data transfer, digital drivers of changes will lose percent of their effects.

Many of the major drivers of changes have a global effect on jobs, ranging from significant job creation to job displacement, and from heightened labour productivity to widening skills gaps. Changes in jobs caused by technological progress are always followed by changes in their economic, social, geopolitical and demographic environments. Fig. 2 shows the interaction between these changes [2].

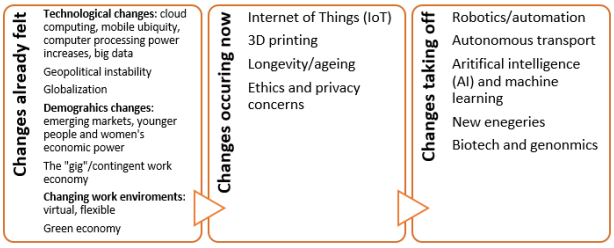

Fig. 2 Technical, socio-economic, geopolitical, and demographic drivers of change [2]

Primarily, thanks to technological changes, automated industrial systems are becoming more complex. Also, the demand for production without faults is growing and it starts to be a huge issue to solve complex problems with limited human resources and knowledge and within a limited time. The right solution is adopting artificial intelligence (AI) in the process of making decisions in these problems. The potential of AI is growing in different aspects of manufacturing management and control of automated industrial systems. Edge computing on a programmable logic controller (PLC) opens new paradigms for the potential use of AI, especially in fault prediction [5-7].

The rest of the paper is organized as follows: the next chapter presents an outline of trends in AI, with an emphasis on the use of AI in manufacturing; chapter three describes an outline of trends in automated industrial systems, and chapter four provides a conclusion based on trends in AI for automated industrial systems.

II. Outline of Trends in AI

Term Artificial Intelligence (AI) was introduced as an academic discipline in the middle of the fifties of the 20th century [8]. From that period to these days, AI has transformed from the pure academic discipline to the desirable industrial discipline. There is no one generally accepted definition of AI. In many definitions of AI, the following definitions are sufficiently representative:

- AI is an umbrella concept that influences and is influenced by many disciplines, such as computer science, engineering, biology, psychology, mathematics, statistics, logic, philosophy, business, and linguistics [9].
- AI is a cognitive science with rich research activities in the areas of image processing, natural language processing, robotics, machine learning, etc. [10].
- AI is the science that enables computers and machines to learn, judge and use their own reasons. As the technologies are becoming more complex, the demand for Artificial Intelligence is growing because of its ability to solve complex problems with limited human resources and expertise and within a limited time [11].

The above definitions show that different kinds of knowledge are necessary to know if we want to apply AI. Usually, AI includes many areas, such as [8, 12]:

- Search and Planning
- Knowledge representation and reasoning
- Expert systems
- Machine learning
- Deep Learning
- Data mining
- Neural networks
- Natural language processing
- Genetic algorithms
- Fuzzy logic, etc.

In the practice, in order to solve a problem, usually, it is necessary to apply more than one area of AI. Like in nature, sometimes we can apply different approaches (areas of AI) to solve some problem, based on our experience and knowledge.

As already mentioned at the beginning of the paper, AI is a discipline that has been in use for several decades. In the past, people were associated to AI with a special entity, such as: General Problem Solver (a program designed to imitate human problem-solving) developed by Allen Newell, Herbert Simon and J.C. Shaw, Deep Blue chess-playing computer developed by IBM or Dexter robot arm developed by Haddington Dynamics. These examples show only how wide the use of AI can be. Nowadays, AI can be found in applications inside cars, machines, sensors, motors, finance, medicine, agriculture, education, etc. Actually, AI can be applied in almost all areas of human activity. So, if we want to know what the current trends in AI, we will see many trends common for different applications all over the Internet. In the outline of these searches, we can find the following trends in [12-16]:

- AI Customer Support and Assistance
- Data Access Enabling Ubiquity
- Predictive Analytics
- Enhanced Customization
- Real-Time Marketing Activities
- AI-Powered Chatbots
- Emerging AI User Interface
- Intelligent Automation
- High-Risk Reputation
- More Data Sharing
- Partnering AI Workforce
- AI will increasingly be monitoring and refining business processes
- More and more personalization will take place in real-time
- AI becomes increasingly useful as data becomes more accurate and available
- More devices will run AI-powered technology
- Human and AI cooperation increases
- AI increasingly at the “edge”
- AI increasingly used to create films, music, and games
- AI will become ever more present in cybersecurity
- More of us will interact with AI, maybe without even knowing it
- AI will recognize us, even if we don’t recognize it
- Increased Overall Automation
- Integration of AI to Aid (Not Replace) Workers
- A shift toward cybersecurity
- Increased focus on personalized services
- Automated ai development
- Auto car manufacturers will launch driverless cars
- Application of facial recognition will increase
- Augmented reality apps are on the rise
- Logistics will become more efficient
- Peer-to-peer networks will enhance transparency
- Content will be designed using artificial intelligence

The wide range of trends in AI shows how AI is present in different industrial and non-industrial applications.

AI will definitely mark many years ahead and it has been confirmed that AI will be one of the main pillars in the implementation of the concept of Industry 4.0.

III. Outline of Trends in Automated Industrial Systems

As mentioned before, automated industrial systems are becoming more complex in many ways. In previous years, the complexity of the system was reflected primarily in the applied technologies, while in the present days, the complexity is reflected not only in the applied technologies but also in the complexity of data processing.

The automated industrial system generates a vast quantity of quantity of valuable data in a single second. Depending on the type of an automated industrial system, data include values from sensors, logs from the production line, orders, payments, etc [17-23]. These data can be structured or unstructured, it can be of different types, with different requirements for memory capacity, etc. The majority of these data must be processed in real-time, which means that we need more computational power.

More computational power involved new approaches in data processing. One approach is to apply Edge computing in the situation where a continual need to monitor the performance of systems and processes to identify or predict faults is needed [5-7, 18]. Typical architecture with Edge computing is shown in Fig. 3 [24].

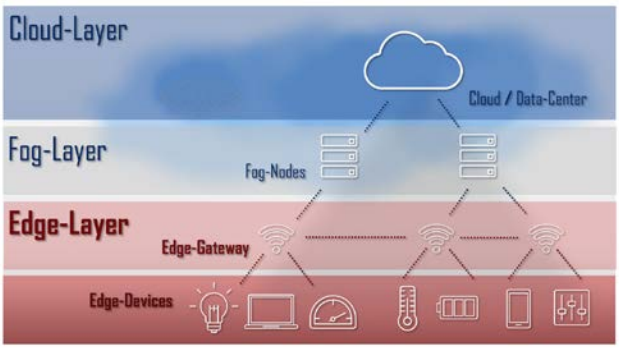

Fig. 3 Typical architecture with Edge computing [24]

Edge computing has several advantages. Some of the advantages are as follows [24]:

- Real-time data processing: Edge computing architectures bring processing units closer to the data source, enabling real-time communication. The latency problem common with classic cloud solutions is avoided.
- Reduced data throughput: Edge computing primarily provides for local data processing in edge gateways. Only data that cannot be evaluated locally or should be available online is loaded into the cloud.
- Data security: Edge computing leaves much of the data on the local network. This makes it much easier for companies to meet compliance requirements.

The main disadvantages of Edge computing are complex network structure, costs of Edge hardware and higher maintenance costs of the system with Edge computing.

Due to the complexity of the automated industrial systems, the approach that uses the system's oversimplification and reduction starts to be useless. Therefore, the approach that tapping the potential of AI, are more likely to benefit from in the long term. AI's impact on automated industrial systems can be viewed in different areas. In the case of the manufacturing systems, AI's impact can be organized into 5 main areas [25]:

- Predictive quality and yield
- Predictive maintenance
- Human-robot collaboration
- Generative design
- Market adaption/supply-chain

Also, these impacts are present in other automated industrial systems. But, the key question in the implementation of AI in automated industrial systems is how to select the right AI solution to address specific challenges and goals. In [26] is presented formula to selecting the right industrial AI solution based on the so-called "The Industrial AI Quadrant" which is shown in Fig. 4.

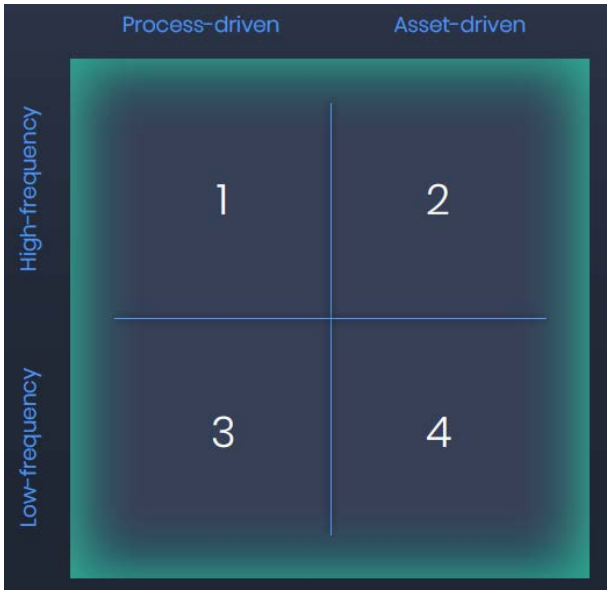

Fig. 4 Typical architecture with Edge computing [24]

This simple and effective methodology involves asking three basic questions:

1. What are your most pressing problems concerning manufacturing production losses?
2. Are these problems rooted in asset performance, or the production process itself?
3. Do these problems occur frequently, or infrequently?

Depending on the answers, it can be determined what kind of AI solution we need for a particular problem. As mentioned before, AI is all about data, so the quality of data that are needed is very important in ensuring trustworthy results.

In [27] we can find the following conclusion: "AI without data is nothing, and AI without computational power is impossible". Aware of this fact, every further step in applying AI must be considered on how valuable data we have.

IV. Conclusions

This paper gives a brief overview of the trends in AI and how these trends affect automated industrial systems. Trends in AI are diverse, and it is difficult to find the main trend. In the case of automated industrial systems, one of the main trends is applying AI for improving manufacturing processes based on prediction.

Many manufacturers of equipment, as an additional value of their equipment, now offer AI modules for predicting the operation lives of their equipment with great reliability. The technological complexity of automated industrial systems has brought great dependence on data processing. The main approach to solve this problem is to apply the approach based on Edge computing and AI.

Acknowledgment

This research has been supported by the Ministry of Education, Science and Technological Development, Government of the Republic of Serbia, through the projects: Grant 401-00-00589/2018-09., and "Innovative scientific and artistic research from the FTN activity domain".

References

[1] D. Acemoglu, P. Restrepo, "Artificial Intelligence, Automation and Work", NBER Working Paper No. 24196, Cambridge, MA, 2019.

[2] https://www.td.org/insights/2025-how-will-we-work-how-will-your-job-change, Accessed: 24.10.2020.

[3] D. Acemoglu, P. Restrepo, "Automation and New Tasks: How Technology Displaces and Reinstates Labor", IZA DP No. 12293, Bonn, 2019.

[4] Report from World Economic Forum 2016. The Future of Jobs: Employment, Skills and Workforce Strategy for the Fourth Industrial Revolution, World Economic Forum, REF 010116, 2016.

[5] S. Stankovski, G. Ostojić, I. Baranovski, M. Babić and M. Stanojević, "The Impact of Edge Computing on Industrial Automation", 2020 19th International Symposium INFOTEH-JAHORINA (INFOTEH), East Sarajevo, Bosnia and Herzegovina, 2020, pp. 1-4, doi: 10.1109/INFOTEH48170.2020.9066341.

[6] S. Stankovski, G. Ostojić, M. Nićin, I. Baranovski, L. Tarjan, "Edge Computing for Fault Detection in Smart Systems", In: Zdravković, M., Konjović, Z., Trajanović, M. (Eds.) ICIST 2020 Proceedings Vol.1, pp.22-26, 2020

[7] S. Stankovski, G. Ostojić, M. Šaponjić, M. Stanojević and M. Babić, "Using micro/mini PLC/PAC in the Edge Computing Architecture", 2020 19th International Symposium INFOTEH-JAHORINA (INFOTEH), East Sarajevo, Bosnia and Herzegovina, 2020, pp. 1-4, doi: 10.1109/INFOTEH48170.2020.9066309.

[8] M. Jocković, Z. Ognjanović, S. Stankovski, Veštačka inteligencija: inteligentne mašine i sistemi, Krug, Beograd, 1988.

[9] W. Wang, K. Siau, "Artificial Intelligence, Machine Learning, Automation, Robotics, Future of Work and Future of Humanity: A Review and Research Agenda", Journal of Database Management, Vol. 30, No. 1, pp. 61-79, 2019.

[10] J. Lee, H. Davari, J. Singh, V. Pandhare, "Industrial Artificial Intelligence for Industry 4.0-based manufacturing systems", Manufacturing Letters, Vol. 18, pp. 20–23, 2018.

[11] S.Shekhar, "Artificial Intelligence in Automation", RESEARCH REVIEW International Journal of Multidisciplinary, Vo. 4. No. 6, pp. 14-17, 2019.

[12] S.Russell, P. Norvig, Artificial Intelligence: A Modern Approach, Prentice Hall, 2010.

[13] https://www.analyticsinsight.net/artificial-intelligence-trends-in-2020/, Accessed: 24.10.2020.

[14] https://minddata.org/ai-trends-Brian-Ka-Chan-AI, Accessed: 24.10.2020.

[15] https://www.forbes.com/sites/bernardmarr/2020/01/06/the-top-10-artificial-intelligence-trends-everyone-should-be-watching-in-2020/?sh=16d00327390b, Accessed: 24.10.2020.

[16] https://www.ecrion.com/11-ai-trends/, Accessed: 24.10.2020.

[17] M. Muro, R. Maxim, J. Whiton, Automation and Artificial Intelligence (How machines are affecting people and places), Metropolitan Policy Program at Brookings, 2019.

[18] L. Miller, Edge Computing For Dummies, John Wiley & Sons, Inc., Hoboken, New Jersey, 2020.

[19] S. Nemet, G. Ostojić, D. Kukolj, S. Stankovski, and D. Jovanovic, "Feature Selection Using Combined Particle Swarm Optimization and Artificial Neural Network Approach," Journal of Mechatronics, Automation and Identification Technology, vol. 4, no. 1, pp. 7–11, 2019.

[20] L. Tarjan, I. Šenk, J. E. Obućina, S Stankovski, G. Ostojić, "Extending Legacy Industrial Machines by a Low-Cost Easy-to-Use IoT Module for Data Acquisition", Symmetry 12(9), 1486; https://doi.org/10.3390/sym12091486, 2020.

[21] G. Ostojić, S Stankovski, Z. Ratković, L Miladinović, R.Maksimović, "Development of hydro potential in Republic Srpska", Renewable and Sustainable Energy Reviews, vol. 28, pp. 196-203, 2013.

[22] S. Stankovski, G. Ostojic, L. Tarjan, D. Skrinjar, M. Lazarevic, "IML robot grasping process improvement", Iranian Journal Of Science And Technology Transaction B-Engineering, Vol. 35, No. 1, pp. 67-71, 2011.

[23] D. Kukolj, G. Ostojić, S. Stankovski, S. Nemet, "Technology Status Visualisation using Patent Analytics: Multi-Compartment Refrigerators Case", Journal of Mechatronics, Automation and Identification Technology, vol. 3, no.3. pp. 6-11, 2018.

[24] https://www.ionos.com/digitalguide/server/know-how/edge-computing/, Accessed: 24.10.2020.

[25] https://www.seebo.com/industrial-ai/, Accessed: 24.10.2020.

[26] The Manufacturer's Guide to Selecting the Right Industrial AI Solution, seebo.com., Accessed: 24.10.2020.

[27] https://www.lanner-america.com/blog/7-ways-ai-will-impact-industrial-automation-in-2020/, Accessed: 24.10.2020.

THE 5th INTERNATIONAL CONFERENCE
MECHANICAL ENGINEERING IN XXI CENTURY

December 9-10, 2020
Faculty of Mechanical Engineering in Niš, Serbia

Classification of COVID-CT Images Utilizing Four Types of Deep Convolutional Neural Networks

Lara LABAN, Mitra VESOVIĆ

Control Engineering, Faculty of Mechanical Engineering, Kraljice Marije 16, Belgrade, Serbia
laralaban@mas.bg.ac.rs, mvesovic@mas.bg.ac.rs

***Abstract*— In this paper a method is presented for the classification of COVID-CT (CT_COVID, CT_NonCOVID) image data set. Four different types of deep convolutional neural networks are proposed, two with the architecture resembling the VGGNet, one resembling the LeNet-5 and one using transfer learning. In addition, neural networks utilized the following techniques: decay, dropout and batch normalization. Since we needed to combat a significantly small dataset, we used data augmentation in order to transform and expand our dataset. Moreover, juxtapositions were made when observing the results given by these four neural networks, as well as the affect made by two different optimizers. The training of the neural networks was done using small batches with a binary cross entropy loss function, in order to achieve an up to scratch classification accuracy.**

***Keywords*— deep learning; convolutional neural networks; image classification; data augmentation; batch normalization; COVID-CT dataset; dropout; transfer learning.**

I. INTRODUCTION

Convolutional neural networks (CNNs) are a subset of deep neural networks, which are used for classifying images. The main idea is to take a set of images correctly labeled as the input data and used them to train our neural network so as to achieve an output with an appropriate categorization [1]. The inspiration for CNNs comes from the observation of the animal visual cortex. Conversely, the flourishing of these networks only came recently due to the increase of computational power and the development of many possible libraries that could be used to battle complex mathematically based problems, such as back propagation. The first paper [2] that introduced the convolutional neural networks as we have come to know them today has demonstrated that a model which consists of a multilayered network can be successfully used for recognition of stimulus patterns according to the differences in their shapes. However, there is some debate that the true begging was when a paper in 1990 [3] demonstrated that a CNN model which aggregates simpler features into progressively more complicated features can be successfully used for handwritten character recognition. In 2012 the ImageNet Large Scale Visual Recognition Challenge [4], at that moment consisting of he 1000 categories and 1.2 million images received a submission that would propel the CNNs development once again. AlexNet [5] achieved a top-5 error of 15.3% , which at the moment surpassed by an astonishing 10% all of the other submissions, and had a much faster training time as it was implemented on a GPU. The following year, the same challenge, now with a larger dataset was won by ZFNet [6]. It had the top-5 error of 14.8%, however even more so important is that it was able to reduce the first layer filter size from to and had a stride of 2, rather than 4 in the pooling layer.

VGG16 is a convolutional neural network model proposed in the paper [7]. This model achieved 92.7% top-5 test accuracy. The main contribution of this model was that it used kernel sized filters, instead of the . It was trained for weeks using GPUs, and had a huge computational cost. However, it introduced a new idea using the same kernels throughout the entire architecture, this aided in generalization for classification problems outside of what they were originally trained on. If for a second we go back to LeNet [8] that was the foundation for all of these previously mentioned CNNs we can observe the main sequence of three layers convolution, pooling and non-linearity still play the key part, and sometimes it is beneficial not to import to many layers when training a smaller dataset [9]. Finally, in recent years transfer learning [10], which addresses cross domain learning problems by extracting useful information from data in a related domain and transferring them for being used in target tasks, has been demonstrating a significant impact.

Coronavirus disease 2019 (Covid19) is an infectious disease caused by severe acute respiratory syndrome coronavirus 2 (SARS-CoV-2) [11]. It was first identified in December 2019 in Wuhan, Hubei, China, and has resulted in widespread pandemic. At the moment Covid19 has caused over one million deaths all around the world and counting. There are several methods that include quick testing, however in order to grasp the full scope of the problem some of the most important ways to battle this disease is to examine the computed tomography (CT) scan images. Chest CT scanning in patients with Covid19 has shown ground-glass opacification, possibly with consolidation, as well as cases of pleural effusion, pleural thickening and lymphadenopathy. Data is collected daily and it is still scarce, howbeit one of the first datasets was proposed and constructed for a marvellous paper [12], that is still

pending publication at the moment, in order to try and aid the ongoing battle against the pandemic. In it multi-task learning and contrastive self-supervising learning were used and achieved an accuracy of 89% in distinguishing between CT_COVID and CT_NonCOVID images. In addition to all that was stated beforehand the pivotal goal of this paper is to try and implement various CNNs to combat this classification problem and if possible obtain a slightly better classification accuracy.

This paper is organised in the following manner: section 2 represents a description of the dataset. In section 3 the main methods which are used are explained in detail, as well as the architecture of the CNN. As a result, in section 4 we discuss the results and compare the methods, based on accuracy and loss functions. In section 5, following a short summary a conclusion is made and future work and possible directions are stated.

II. DATASET AND ITS IMPLEMENTATION

The dataset which is used in this paper consists of 672 CT scan images from patients [13], including 349 CT_COVID and 323 CT_NonCOVID. We took the approach of data augmentation, where we increase the diversity of data by altering the original samples using translation, rotation, shearing, flips and adding them to the training set. Data augmentation covers a wide range of techniques used to generate new training samples using the original input images, by applying random jitters and perturbations in such a manner as to not change the class labels. The main idea here is to decrease the generalization error of the testing (sometimes at the expense of the training error) so as to achieve an increase of generalizability of the model. The neural network is then using slightly modified versions of the input data and it is able to learn more robust features.

However, we introduced scaling of the data, as well, by computing a weight for each class during the training and as an outcome amplifying the loss by a larger weight when we approach the smaller dataset. Even though the difference is small in this example, this benefited the training process. During the preprocessing of images we resized all the images to a fixed size $32x23$, and in doing so we also maintained the aspect ratio. The reasoning behind this being that all the images in a dataset need to have a fixed feature vector size. This means all the images will have identical widths and heights, making it easier to quickly load and preprocess a dataset and briskly move through our convolutional neural network. The aspect ratio will enable us to resize the images along the shorter dimension, be it width or height, and in cropping it, will maintain the ratio. It is important to note that this step is not necessary if you are not working with a difficult dataset. Notwithstanding its benefits, it was implemented in this particular dataset.

A. *ImageNet dataset*

ImageNet is a dataset consisting of over 14 million images, which belong to one thousand classes. It was used as the dataset in the highly respected convolutional neural network model VGG16 which was proposed by Oxford scientists. In this paper the VGG16 network was used as a pre-trained convolutional neural network, in order to incorporate transfer learning.

III. METHODS DESCRIPTION

In order to try and reduce overfitting and increase our classification accuracy on the CT_COVID dataset we endeavour in performing three types of neural network training techniques:

- dropout and decay
- batch normalization
- transfer learning (neural networks as feature extractors)

The first technique that is used in order to improve the generalization error in the convolutional neural network is dropout [14]. Dropout is nothing more than a form of regularization, which succours us in controlling the model capacity. The dropout layers are arranged in the network in such a manner that we have randomly disconnected nodes by a probability of 0.3 in the first few layers; and 0.6 probability in the last layer. The reason for this is that if the first layers are dropped by a higher probability, then that will later affect the training. The dropout is implemented after the pooling layer, and before the next convolutional layer (or last flatten and dense layers). This was used for the neural networks resembling the VGG with data augmentation (DA). The network resembling the VGG without DA used a dropout with a probability 0.25 in the first few layers and double the increase in the last layer, while the LeNet network did not utilize this method. Decay that is used in this neural network is a standard decay that can be obtained using the Keras library in Python. Since the learning rate controls the step that is made along the gradient, larger steps are usually used in the beginning to make sure that we do not stagnate in the local optima, while smaller steps are used deeper in the network and near the end of the convolution in order to converge to a global minimum. We have initialized the learning rate to be 0.01 (for the networks with DA) and 0.05 (for the network without DA), and applied the following formula to adjust it after each epoch,

$$\alpha_{i+1} = \frac{\alpha_i}{1+k\cdot i} \tag{1}$$

where α is the current learning rate, i is the epoch and k is the decay calculated as the division between the learning rate and the number of epochs. This type of adjustment of the learning rate each epoch, can increase accuracy, as well as reduce the loss function and the time necessary to train a network. Batch normalization [15] is used to normalize the activations of a given layer's inputs by applying mean and standard deviation before passing it onto the next layer. In addition, the covariate shift refers to a change in the distribution of the input variables which are present in the training and validation data. Since it has been proven that the training of the neural network is the most coherent when the inputs to each layer are alike, the main intention is that even when the explicit values of inputs layers to hidden layers change, their mean and standard deviation will still remain relatively the same, thus reducing the covariate shift. Batch normalization has demonstrated an immensely effective approach to reducing the number of epochs necessary for training by allowing each layer to learn independently. Here the idea that differs from the original paper and is first proposed in [16] states that the batch

normalization should be implemented after the activation layer. The main reasoning behind this is that we want to avoid setting the negative values coming out of the convolution layer to zero. Instead we pass them through the batch normalization layer, right after the activation (ReLU) layer, and assure that some of the features that otherwise would not have made it do. This yields a higher accuracy and lower loss, and is to this day a debate amongst the creators of Keras.

Finally, the second technique is transfer learning [17], a machine learning technique where networks can behave as feature extractors. Transfer learning is nothing more than the ability to use a pre-trained model to learn patterns from data, on which the original network was not trained on. As previously stated deep neural networks trained on a large scale dataset ImageNet have demonstrated to be superb at this task.

When treating networks as feature extractors we choose a point, in this case before the fully connected layer and remove it. Subsequently, in this particular example while using the VGGNet pre-trained on the ImageNet we removed the fully connected layer and stopped at the last pooling layer where the output shape is $7 \times 7 \times 512$, 512 filters with the size 7×7. Now, our feature vector has $7 \times 7 \times 512 = 25088$ values and it will be used to quantify the contents of the images, which were not included in the original training process. The format which allows us to extract these features is the hierarchical data format version 5 (hdf5), which is used to store and organize large amount of data.

Transfer learning is an optimization, which has been proven to yield a better performance and drastically save time. This is precisely why we used it in this paper, to see if we could obtain a higher classification, and perform faster. Transfer learning relaxes the hypothesis that the training data must be independent and identically distributed with the test data, which we clearly stated as a must in the beginning of this chapter. Moreover, transfer learning is able to solve the problem of insufficient training data. Furthermore, there is the option to remove the fully connected layers of the existing network in order to add a new fully connected layer to the CNN and fine tune the weights to recognize object classes. However, here it was not implemented since treating networks as arbitrary feature extractors was enough.

A. *Convolutional Neural Network*

Into the bargain all that was explained, we picked the following CNN architecture shown in Fig. 1. It is consisted of multiple convolutional and pooling layers, as well as the fully connected layers. The first two convolutional layers learn 32 filter each with a size 3×3.

Sequentially, the fourth and the fifth layers learn 64 filters with the size 3×3 and the last two learn 128 filters with the size 3×3. The pool layer is used to reduce the computational load and the number of parameters, thus reducing the risk of overfitting. We used a max pooling layer with a pool size 2×2 and a stride 2. Finally, we have the fully connected layer which consists of 2048 parameters, input values which learn 512 nodes. The activation layers which were used are Rectified Linear Unit (ReLU) defined as,

$$f(x) = \max(0, x) \tag{2}$$

where x is the input into the neuron. Softmax or the normalized exponential function assigns normalized class probabilities for each prediction, and is represented by,

$$S(y_i) = \frac{e^{y_i}}{\sum_{j=1}^{k} e^{y_j}} \tag{3}$$

for $i = 1, \dots, k$ and $\mathbf{z} = (z_1, \dots, z_k) \in \mathbb{R}^k$.
Softmax takes an input vector and normalizes it into a probability distribution between $[0,1]$. Therefore the sum of all output values is equal to 1, which in turn makes the training converge more quickly. In order to achieve this, before training we must include one hot encoding in order to convert the labels from integers to vectors.

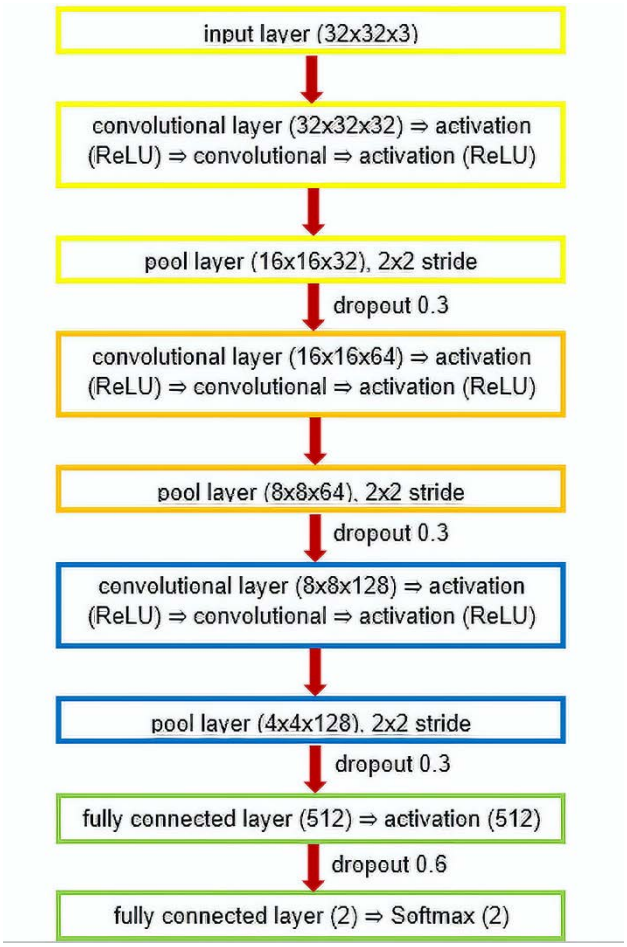

Fig. 1 A schematic of the convolutional neural network without batch normalization, that resembles the VGGNet. All of the convolutional layers that precede the fully connected layers have filters 32, 64, 128 that are the same size . The probability distribution is applied in the last layer using Softmax and the output yields two class labels CT_Covid and CT_NonCovid.

In addition, later when we want to add the batch normalization layer, we can apply it after each activation layer, as discussed previously.

B. *Implementation and training of a simpler version of the LeNet*

Taking into the bargain all that was explained before, the implementation of this CNN was done by using the Python programming language. We used Keras [18] which is mainly used for implementing of activation

functions, optimizers, convolutional and pooling layers, and is actually able to do backpropagation automatically.

Right after we load and preprocess our images dataset it is necessary to use one hot encoding. This is done by using a part of the Sklearn library LabelBinarizer. However beforehand we must split the training data and the validation data, here we opted to split it 75% and 25%, sequentially. The next step is the implementation of an optimizer, here we used the Adam optimizer. The Adam optimizer is short for Adaptive Moment Estimation optimization algorithm [19]. Its main purpose is to attempt to rectify the negative effects of a globally accumulated cache by converting the cache into an exponentially weighted moving average, just like the Root Mean Square Propagation (RMSProp). The Adam optimizer is essentially a combination of momentum and RMSProp. Momentum is implemented into the neural network, by adding a temporal element to the update vector of the past time step to the current update vector,

$$\Delta \boldsymbol{w}(k) = -\alpha \nabla E(k) + \gamma \Delta \boldsymbol{w}(k-1) \tag{4}$$

where γ is usually set between 0.8 and 0.9 and function E is the index of performance.

This network resembles the architecture of the LeNet in such a way that we have 5×5 filters with a stride of 20 in the first convolution layer, and 50 in the second convolutional layer. The mini batch method were the neural network selects a part of the training data and updates the weights, but trains the network with the average weight update. Usually the smallest standard batch size which is used is 32, however we opted to use 24, as it complemented our data. The reasoning behind this is that present research confirms that using small batch sizes achieves the best training stability and generalization performance, for a given computational cost, across a wide range of experiments. The loss function which was used is the binary_crossentropy function. This was done because we only had two classes, if there were more we would have had to use categorical_cross_entropy, but have in mind we could have used categorical as well, but studies show that binary is much more efficient in this case. The training of the CNN was done in 30 epochs.

C. *Implementation and training of a simpler version of the VGGNet*

We constructed two different neural networks resembling the VGG, the first one had a dropout of 0.25 in the first few layers and no data augmentation or batch normalization layers. The training data and the validation data were split 75% and 25%, sequentially. Here we utilized the SGD optimizer, which was set to a learning rate of 0.05, with a decay in order to slowly reduce the learning rate over time and converge to the global solution more efficiently. Decaying the learning rate is beneficial in reducing overfitting and obtaining a higher classification accuracy. The smaller the learning rates are, the smaller the weight update will be enabling us to converge. The gradient descent method is an iterative optimization algorithm that operates over an optimization surface. It is a simple modification to the standard algorithm of gradient descent. The main purpose of SGD is to calculate the gradient and adjust the weights of the training data (but not on the whole dataset, but rather on a mini batch). All the images were resized to 32×32 aspect ration, the batch size we used was again 24 and the loss fucntion was the binary_crossentropy function. The training of the CNN was done in 30 epochs.

The second neural network resembling the VGG had a similar architecture as depicted in Fig. 1, with the addition of batch normalization layers. Here our training data and the validation data were split 80% and 20%. Here we trained our network once with the SGD optimizer and once more with the Adam optimizer. The learning rate was set to 0.01, with decay and adjustment after each epoch. Both times data scaling, as well as data augmentation was used. All the images were resized to 32×32 aspect ration, the batch size we used was 32 and the loss function was the binary_crossentropy function. The training of the CNN was done in 30 epochs (utilizing the Adam optimizer) and in 100 epochs (using the SGD optimizer).

After the training we implemented a method that takes the weights and the state of the optimizer and serializes them to the disc in a hdf5 format, in order to load them and test the labeling.

D. *Implementation using transfer learning*

The first step in this process is to extract features from VGG16, in doing so we are forward propagating the images until a given layer, and then taking those activations and treating them as feature vectors. Here the main two differences are that we used the standard a batch size of 32 and the training and test split is done at the same time as training, we again split it into 75% training data and 25% test data. Once the extraction of the features was done, we trained the classifier on those features. We also implement the GridSearchCV class to assists us to turn the parameters to the LogisticRegression classifier.

The final results are presented in the following chapter, comparisons are made and a visual representation of the graphs is shown using Matplotlib in order to estimate if there is overfitting.

IV. Results and Comparisons

The results of the CNN resembling LeNet are presented in Table 1. We clearly see that our neural network has classification accuracy of 68%.

Fig. 2 A graph depicting a convolutional neural network that resembles the LeNet – training and validation loss and accuracy curves

In the following table we use the term precision which represents true positive divided by a sum of true positive

and false positive, recall which represents true positive divided by a sum of true positive and false negative. Therefore, precision is good to determine when the cost of false positives is high, on the other hand recall tells us the number of correctly labeled data. Ultimately, we have the f1-score used to find the weighted average of recall and precision. In analyzing the curves shown in Fig. 2 we see that our network learned until the 30 epoch, beyond that overfitting would occur, as we can clearly see a generalization gap forming in both loss and accuracy curves. Fig. 3 depicts the results when using the network resembling the VGG without data augmentation, here we can observe that the training and validation curves show a wide generalization gap at the 30 epoch resulting in overfitting. The classification accuracy is 76% (Table 1.), this is no good if we have overfitting, that is why the next approach uses data augmentation in order to combat this problem.

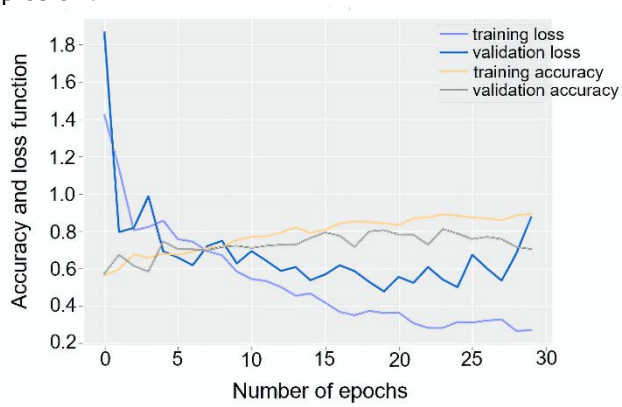

Fig. 3 A graph depicting a convolutional neural network without data augmentation and with batch normalization, that resembles the VGGNet – training and validation loss and accuracy curves

Fig. 4 represents the neural network resembling the VGG, with data augmentation and the SGD optimizer. The classification accuracy obtained after 30 epochs is 72%, and the training and loss curves show slight deviations.

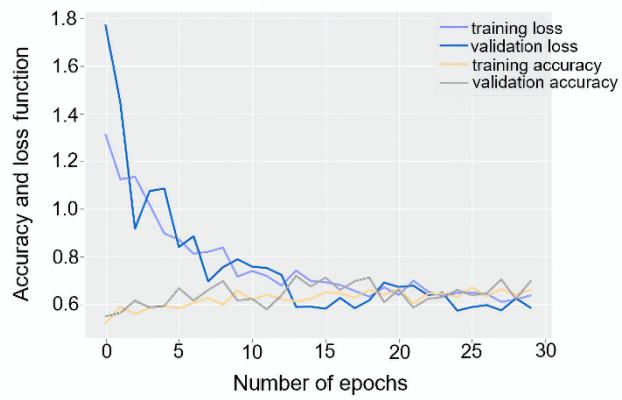

Fig. 4 A graph depicting a convolutional neural network with data augmentation and batch normalization (optimizer SGD), that resembles the VGGNet – training and validation loss and accuracy curves – 30 epochs

The same classification accuracy is acquired when utilizing the Adam optimizer, only then we need 100 epochs to achieve so. Fig. 6 depicts the same neural network explained beforehand when using the SGD optimizer over the course of 100 epochs resulting in a classification accuracy of 75%. We can conclude that data augmentation does indeed help in reducing the generalization gap, however this particular dataset was quite faulty to begin with.

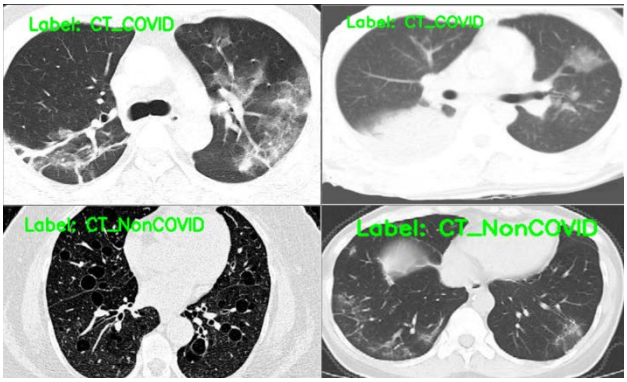

Fig. 5 The pre-trained CNN weights are loaded from the disk and make predictions for 30 randomly selected images. In the upper left and right corner we have an example of CT_COVID scans, and in the lower left and right corner an example of CT Non_COVID scans.

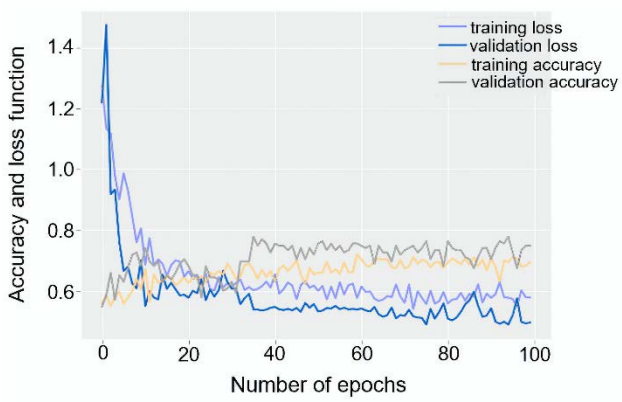

Fig. 6 A graph depicting a convolutional neural network with data augmentation and batch normalization (optimizer SGD), that resembles the VGGNet – training and validation loss and accuracy curves – 100 epochs

TABLE I
EXPERIMENTAL RESULTS

	precision	recall	f1-score
CNN resembling LeNet (Adam optimizer, with data augmentation)			
macro avg	0.68	0.68	0.67
CNN resembling VGG (SGD optimizer, without data augmentation, without batch normalization)			
macro avg	0.76	0.71	0.69
CNN resembling VGG (Adam optimizer, with data augmentation, 100 epochs, with batch normalization)			
macro avg	0.72	0.72	0.72
CNN resembling VGG (SGD optimizer, with data augmentation, 30 epochs, with batch normalization)			
macro avg	0.72	0.70	0.69
CNN resembling VGG (SGD optimizer, with data augmentation, 100 epochs, with batch normalization)			
macro avg	0.75	0.75	0.75
Transfer learning using VGG16			
macro avg	0.90	0.91	0.90

In Table 1 we can see the results obtained by using transfer learning have a classification accuracy of 90%,

which is by far the best. Furthermore, we observe that the CNN in Fig. 4 is the best one if we opted to use a method that does not include transfer learning. Nevertheless, it is clear then when taking into account all four approaches we shall choose transfer learning, because not only does it yield a higher classification accuracy, but it also wasted less computational time. Compared with the original paper that combated this classification problem [12] we were able to achieve only slightly better classification accuracy, with an increase being 1%.

V. Conclusions

In this paper we described four different approaches of using convolutional neural networks to classify a dataset consisting of CT_COVID and CT_NonCOVID images. We used CNNs that we constructed based on the VGGNet and LeNet5 and implemented them with and without data augmentation. Furthermore, we used a transfer learning technique by extracting features of the neural network VGG16 trained on the ImageNet dataset. The main idea of this paper was to see if a different approach can have better results on this particular dataset, as well as see if a smaller neural network could have almost as good classification as transfer learning. The final results, when compared showed a clear advantage when using transfer learning, however it also showed us the importance of data augmentation when approaching a rather small dataset.

Further research will focus on implementing different types of optimizers, including metaheuristic algorithms as optimizers. Also, we will focus on battling larger datasets consisting of Covid19 CT scans, once they become available, as well as obtaining a higher classification accuracy utilizing different methods.

Acknowledgment

This research was supported by the Science Fund of the Republic of Serbia, grant No. 6523109, AI-MISSION4.0, 2020-2022.

This paper was conceived within the research on the project: "*Integrated research in the field of macro, micro and nano mechanical engineering - Deep machine learning of intelligent technological systems in production engineering*", The Ministry of Education, Science and Technological Development of the Republic of Serbia (contract no. 451-03 -68 / 2020-14 / 200105), 2020.

This work was financially supported by the Ministry of Education, Science and Technological Development of the Serbian Government, Grant TR-35029 (2018-2020).

References

[1] L. Laban, R. Jovanović, M. Vesović, V. Zarić, "Classification of Chest X-Ray Images Using Deep Convolutional Neural Networks", International Conference on Electrical, Electronic, and Computing Engineering, Belgrade, Serbia, September 28-30, 2020, to be published.

[2] K. Fukushima, S. Miyake, "Neocognitron: A new algorithm for pattern recognition tolerant of deformations and shifts in position," Pattern Recognition, vol. 15, no. 6, pp. 455-469, 1982.

[3] Y. LeCun, B. E. Boser, J. S. Denker, D. Henderson, R. E. Howard, W. E. Hubbard, L. D. Jackel, "Handwritten digit recognition with a back-propagation network," Advances in Neural Information Processing Systems 2, pp. 396-404, June, 1990.

[4] O. Russakovsky, J. Deng, H. Su, J. Krause, S. Satheesh, S. Ma, Z. Haung, A. Karpathy, A. Khosla, M. Bernstein, A. C. Berg, L. Fei-Fei, "ImageNet large scale visual recognition challenge," International Journal of Computer Vision, vol. 115, no. 3, pp. 211-252, April, 2015.

[5] A. Krizhevsky, I. Sutskever, G. E. Hinton, "ImageNet classification with deep convolutional neural networks," Advances in Neural Information Processing Systems, vol. 25, no. 2, pp. 1097-1105, 2012.

[6] M. D. Zeiler, R. Fergus, "Visualizing and understanding convolutional networks," 13th European Conference, Zurich, Switzerland, pp. 818-833, September 6-12, 2014.

[7] K. Simonyan, A. Zisserman, "Very deep convolutional networks for large-scale image recognition," arXiv preprint arXiv:1409.1556, 2014.

[8] Y. LeCun, L. Bottou, Y. Bengio, P. Haffner, "Gradient-based learning applied to document recognition," Proceedings of the IEEE, vol. 86, n. 11, pp. 2278-2324, November, 1998.

[9] Z. Li, W. Yang, S. Peng, F. Liu, "A survey of convolutional neural networks: Analysis, applications and prospects," arXiv preprint arXiv:2004.02806, 2020.

[10] L. Shao, F. Zhu, X. Li, "Transfer learning for visual Categorization: A survey," IEEE Transactions on Neural Networks and Learning Systems, vol. 26, no. 5, pp. 1019-1034, May, 2015.

[11] https://www.mayoclinic.org/diseases-conditions/coronavirus/symptoms-causes/syc-20479963, (last accessed 13/10/2020).

[12] X. Yang, X. He, J. Zhao, Y. Zhang, S. Zhang, P. Xie, "COVID-CT-Dataset: A CT Scan Dataset about COVID-19", https://arxiv.org/abs/2003.13865, 2020, to be published.

[13] Dataset provided on GitHub, https://github.com/UCSD-AI4H/COVID-CT, (last accessed 23/07/2020).

[14] G. E. Hinton, N. Srivastava, A. Krizhevsky, I. Sutskever, R. R. Salakhutdinov, "Improving neural networks by preventing co-adaptation of feature detectors", arXiv preprint arXiv:1207.0580, July, 2012.

[15] S. Ioffe, C.Szegedy, "Batch normalization: Accelerating deep network training by reducing internal covariate shift", Proceedings of the 32nd International Conference on Machine Learning, vol. 37, pp. 448-456, July, 2015.

[16] A. Rosebrock, Deep Learning for computer vision with Pyhton: Starter Bundle, 1st ed. PyImageSearch, 2017.

[17] C. Tan, F. Sun, T. Kong, W. Zhang, C. Yang, C. Liu, "A survey on deep transfer learning," 27th International Conference on Artificial Neural Networks, Rhodes, Greece, October 4-7, 2018.

[18] Keras; Python Deep Learning Library https://keras.io, (last accessed 09/03/2020).

[19] D. P. Kingma, J. Ba, "Adam: A Method for Stochastic Optimization", 3rd International Conference for Learning Representations, San Diego, 2015.

THE 5th INTERNATIONAL CONFERENCE
MECHANICAL ENGINEERING IN XXI CENTURY

December 9-10, 2020
Faculty of Mechanical Engineering in Niš, Serbia

Modelling and Speed Control in a Series Direct Current (DC) Machines Using Feedback Linearization Approach

Mitra VESOVIĆ, Radiša JOVANOVIĆ, Vladmir ZARIĆ

Faculty of Mechanical Engineering, University of Belgrade, Kraljice Marije 16, 11120 Belgrade, Serbia
mvesovic@mas.bg.ac.rs, rjovanovic@mas.bg.ac.rs, vzaric@mas.bg.ac.rs, llaban@mas.bg.ac.rs

***Abstract*— In this paper the nonlinear feedback control system is presented for the speed control in direct current - DC motor. Nonlinear functions of dead zone, Coulomb and viscous friction were investigated and used for obtaining the mathematical model. The effectiveness and the comparison between linear and nonlinear control signal have been confirmed using Matlab/Simulink software. From the conclusions, based on the experimental results, it is easy to see that nonlinear control system is more acceptable and has a better performance for speed control. The validity of using feedback linearization in DC motors has been proven.**

***Keywords*— feedback linearization; nonlinear systems; nonlinear control; identification**

I. INTRODUCTION

Speed control in a direct current motor (DC) has been challenging, widely studied task. Many researches have been done to model electrical machines. For example, serial DC motor has often been modelled as linear object. On the other hand, models in which motor current or flux are found as essential parameters are considered to be nonlinear [1]. This paper presents the design and implementation concerning both, linear and nonlinear models for the system and it represents a continuation of the research done by the authors on the similar topic [2]. Disparate controllers have been proposed to lead the speed of DC machines into the desired value. For example Proportional-Integral-Derivative (PID) controller is a popular controller in industries due to simple structure, low cost and easy to implementation. It provides reliable performance for the system if PID parameter is identified properly. But it suffers due to lack of robustness [1]. The linear approximation, of the nonlinear state space representation of the series DC motor, around the equilibrium point and PI controller design the tracking performance is deteriorated in the periods in which the speed is reduced. This is due to the fact that the input signal is limited to a minimum of 0 [V]. That is, in this condition the motor is actually operating in open loop [3].

Besides linear, there are plenty of nonlinear controllers: the fuzzy logic and genetic – based new fuzzy models [4], artificial neural networks [5], adaptive control technique [6], and others.

It is important to make this comparison to find out under what conditions a technique presents a superior performance over the other one and thus have the certainty when it is useful to implement nonlinear controllers, which have greater complexity [7].

The aim of this study is the development and later implementation of a nonlinear control system, by the feedback linearization method, for a laboratory installed DC motor, SRV02 Rotary Servo Base Unit, which has been considered as a single-input-single-output (SISO) system.

Feedback linearization is an approach to nonlinear control design which has attracted a great deal of research interest in recent years. By a combination of a nonlinear transformation and state feedback (feedback linearization), the nonlinear control design is reduced to designing a linear control law [8]. The central idea of the approach is to algebraically transform a nonlinear system dynamics into a (fully or partly) linear one, so that linear control techniques can be applied. This differs entirely from conventional linearization in that feedback linearization is achieved by exact state transformations and feedback, rather than by linear approximations of the dynamics [9]. This technique has been successfully implemented in many applications of control, such as industrial robots, high performance aircraft, helicopters and biomedical dispositifs, more tasks used the methodology are being now well advanced in industry [10].

II. LINEAR MODEL OF SYSTEM DYNAMICS

One of the first steps in the synthesis of a control system is constructing an accurate model, because it saves time and it brings the cost-effectiveness. An appropriately developed system model is essential for reliability of the designed control. A DC series motor is an example of a simple, controlled process that can serve as a vehicle for the evaluation of the performance of the various controllers [4].

A schematic diagram of the DC motor is given in Fig. 1.

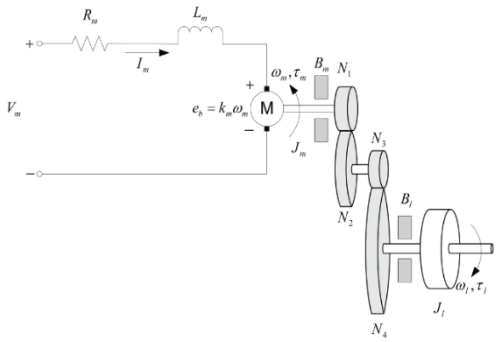

Fig. 1 SRV02 DC motor armature circuit and gain train [11]

The equations that describe the motor electrical components are as follows:

$$V_m(t) = R_m I_m(t) + L_m \frac{dI_m(t)}{dt} + e_b(t) \tag{1}$$

$$e_b(t) = k_m \omega_m(t) \tag{2}$$

where V_m , e_b , k_m and ω_m are motor voltage back electromotive voltage, back electromotive voltage constant and speed of the motor shaft, respectively. Since the motor inductance L_m is much less than its resistance R_m , it can be ignored [11]. Solving the system of equations for motor current I_m , we get an electrical equation of DC motor:

$$I_m(t) = \frac{V_m(t) - k_m \omega_m(t)}{R_m}.$$

The linear model can be obtained using the Second Newton's Law of Motion and connection between moment of inertia of the load J_l and of the motor shaft J_m, speed of the load shaft ω_l, viscous friction acting on the motor shaft B_m and on the load shaft B_l, total torque applied on the load τ_l and on the motor τ_m, with resulting torque acting on the motor shaft from the load torque denoted as τ_{ml}:

The linear model can be obtained using the Second Newton's Law of Motion and connection between moment of inertia, viscous friction constants, and torque of load and motor:

$$J_l \frac{d\omega_l(t)}{dt} + B_l \omega_l(t) = \tau_l(t) \tag{4}$$

$$J_m \frac{d\omega_m(t)}{dt} + B_m \omega_m(t) + \tau_{ml}(t) = \tau_m(t) \tag{5}$$

so the mechanical equation is:

$$J_{eq} \frac{d\omega_l(t)}{dt} + B_{eq} \omega_l(t) = \eta_g K_g \tau_m(t) \tag{6}$$

where J_{eq} and B_{eq} are total moment of inertia and damping term. η_g and K_g are, respectively, the gearbox efficiency and the total gear ratio. Combining electrical and mechanical equations, assuming that motor torque is proportional to the voltage, the final equation becomes:

$$\left(\frac{d}{dt}\omega_l(t)\right) J_{eq} + B_{eq,v} \omega_l(t) = A_m V_m(t) \tag{7}$$

where the equivalent damping term is given by:

$$B_{eq,v} = \frac{\eta_g K_g^2 \eta_m k_t k_m + B_{eq} R_m}{R_m} \tag{8}$$

and the actuator gain equals:

$$A_m = \frac{\eta_g K_g \eta_m k_t}{R_m} \tag{9}$$

Linear mathematical model is:

$$J_{eq} \dot{\omega}_l(t) + B_{eq,v} \omega_l(t) = A_m V_m(t). \tag{10}$$

Choosing $y = \omega_l$ as output variable and $u = V_m$ as input signal, state equation of the system is obtained as follows:

$$J_{eq} \dot{y}(t) + B_{eq,v} y(t) = A_m u(t). \tag{11}$$

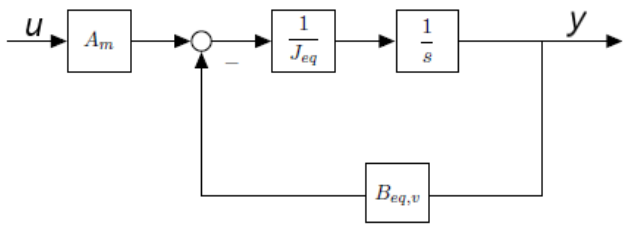

Fig. 2. Block diagram of a linear system

III. EXPERIMENTAL VERIFICATION OF THE OBTAINED LINEAR MATHEMATICAL MODEL

Responses of the system represented with the block diagram in the Fig. 2 are shown in the Fig. 3 and Fig. 4. After recording the responses of the object, comparisons were made with the responses obtained by simulations of the linear model, for step and sinusoidal inputs [2].

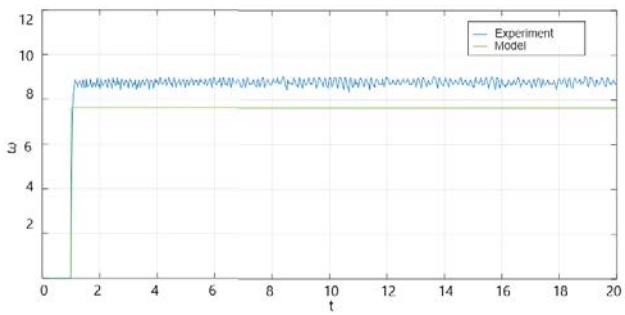

Fig. 3 Experimental results: comparison between real and model data for step input

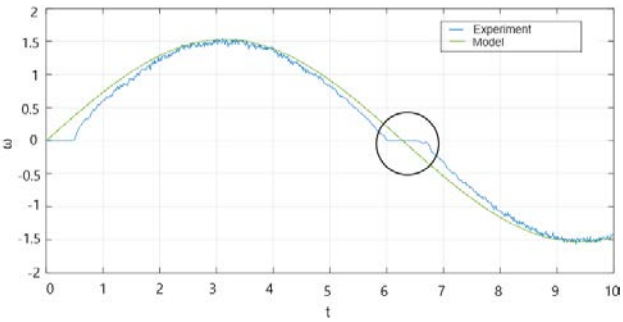

Fig. 4 Experimental results: comparison between real and model data for sinusoidal input

IV. FEEDBACK LINEARIZATION

Feedback linearization approach differs from the classical linearization (about the desired equilibrium point) in that no approximation is used; it is exact. Exactness, however, assumes perfect knowledge of the state equation and uses that knowledge to cancel the nonlinearities of the system. Since perfect knowledge of the state equation and exact mathematical cancellation of terms are almost impossible, the implementation of this approach will almost always result in a close-loop system, which is a perturbation of a nominal system whose origin is exponential stable. The validity of the method draws upon Lyapunov theory for perturbed systems [12] (that can be further studied in Chapter 9 of literature [12]).

Consider the single – input – single – output nonlinear SISO system [12]:

$$\dot{\boldsymbol{x}} = \boldsymbol{f}(\boldsymbol{x}) + g(\boldsymbol{x})u \qquad y = h(\boldsymbol{x}) \tag{12}$$

where $\boldsymbol{f}(\boldsymbol{x})$, $g(\boldsymbol{x})$ and $h(\boldsymbol{x})$ are sufficiently smooth in a domain $D \subset R^n$ (the mapping $f : D \longrightarrow R^n$, $g : D \longrightarrow R^n$ are vector fields on D) and $\dot{\boldsymbol{x}} = [x_1\ x_2 \dots x_n]^T$ is a state vector. It is necessary to find a state feedback control u, that transforms the nonlinear system into an equivalent linear system. Clearly, generalization of this idea is not possible in every nonlinear system: there must be a certain structural property that allows performing in such a manner of cancellation.

Using feedback to cancel nonlinearities requires the nonlinear state equation to have a structure:

Definition [12]:

$$\dot{\boldsymbol{x}} = \boldsymbol{A}\boldsymbol{x} + B\gamma(\boldsymbol{x})[u - \alpha(\boldsymbol{x})] \tag{13}$$

where $\boldsymbol{A}$ is $n \times n$ and B is $n \times p$ matrix, the functions $\alpha : R^n \longrightarrow R^p$, $\gamma : R^n \longrightarrow R^{p \times p}$ are defined on domain $D \subset R^n$ that contains the origin. Furthermore, two conditions must be satisfied. The first one is that the pair (A, B) must be controllable. The second one is that γ(x) must be nonsingular for all $x \in D$. This is consequence of the control law form: $u = \alpha(x) + \frac{1}{\gamma(x)} v$ that provides a new control signal v. Even if the state equation does not have the structure (13), sometimes it is possible to execute feedback linearization for another choice of variables. Therefore, a more comprehensive definition is given [12].

A nonlinear system:

$$\dot{x} = f(x) + G(x)\,u \tag{14}$$

where $f : D \longrightarrow R^n$ and $G : D \longrightarrow R^{n \times p}$ are sufficiently smooth on a domain $D \subset R^n$, is said to be feedback linearizable (or input – state linearizable) if there exist a diffeomorphism $T : D \longrightarrow R^n$ such that $D_z = T(D)$ contains the origin and the change of variables $z = T(x)$ transforms the system (12) into the form:

$$\dot{z} = Az + B\gamma(x)[u - \alpha(x)] \tag{15}$$

with (A,B) controllable and $\gamma(x)$ nonsingular for all $x \in D$.

V. DETERMINATION OF THE RELATIVE DEGREE

The relative degree of a linear system is defined as the difference between the poles (degree of the transfer function's denominator polynomial number) and zeros (degree of its numerator polynomial). To extend this concept to nonlinear systems more mathematical treatment will be needed. The following definition is given and repeated here for completeness: Definition [13]: The system, outlined in (12), is said to have relative degree r at a point x_0 if:

i) $L_g\, L_f^k\, h(x) = 0$ for all x in a neighborhood of x_0 and all $k < r - 1$

ii) $L_g\, L_f^{r-1}\, h(x) \neq 0$

The terms L_g and L_f^k represent the Lie derivative of $h(x)$ taken along $g(x)$ and $k - times$ along (x), respectively.

NONLINEAR MATHEMATICAL MODEL

The nonlinear mathematical model of the DC motor was obtained considering the speed dependent friction nonlinearity. Reference [14] shows that in this case the nonlinear mathematical model of DC motor can be adopted as follows:

$$J_{eq}\dot{\omega}_l + T_{st}(\omega_l) + B_{eq,n}\,\omega_l = A_m V_m \tag{16}$$

The part of the obtained friction curve $T_{st}(\omega_l)$, for low angular velocity values, where the Stribeck effect is dominant, is shown in Fig. 5. It is assumed that friction characteristics are symmetrical, for negative and positive values of angular velocity.

(13)

TABLE I THE NUMERICAL VALUES OF THE PLANT PARAMETERS

Parameters	Values and units
Jeq	0.0021 kgm^2
Rm	2.6 Ω
kt	0.0077 Nm/A
ηm	0.69
ηg	0.9
Kg	70

It is assumed that friction characteristics are symmetrical, for negative and positive values of angular

velocity. Applying standard optimization techniques with Matlab, the friction parameters were obtained (16).

In order to overcome the jump discontinuity of the proposed friction model, at $\omega_l = 0$, that jump is replaced by a line of finite slope, up to a very small threshold ε, whose boundaries are given with red dash line, as is shown in Fig. 5 [14].

$$T_{st} = 0.0174 sgn(\omega_l) + 0.0087 e^{-\frac{\omega_l}{0.064}} sgn(\omega_l), \quad B_{eq,v} = 0.0721 \tag{17}$$

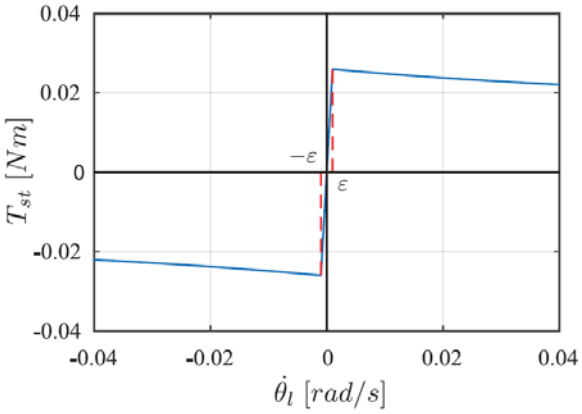

Fig. 5. Friction characteristics of DC motor [14]

This the line of finite slope will be used only for comparison with the hyperbolic tangent function (Fig. 6), because method of feedback linearization requires differentiable functions (as can be seen from the given definitions in the previous section). In this way only Coulomb and viscous friction is modelled and static friction is neglected [2].

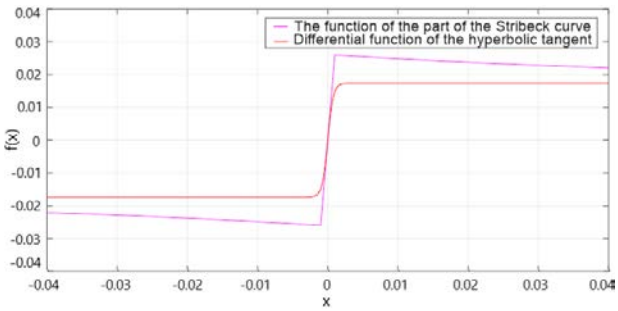

Fig. 6. Differential function of the hyperbolic tangent

Choosing $x = \omega_l$ as state variable, $y = \omega_l$ as measured variable and $u = V_m$ as control variable and denoting nonlinearity by $f(x)$, state equation of the system was obtained as follows:

$$\dot{x} = -\frac{B_{eq,n}}{J_{eq}} x - f(x) + \frac{A_m}{J_{eq}} u \tag{18}$$

$$y = x \tag{19}$$

To ensure that this model is an equivalent representation of the original system, an experiment was performed, with the results shown below on Fig. 7 for step and Fig. 8 for sinusoidal response.

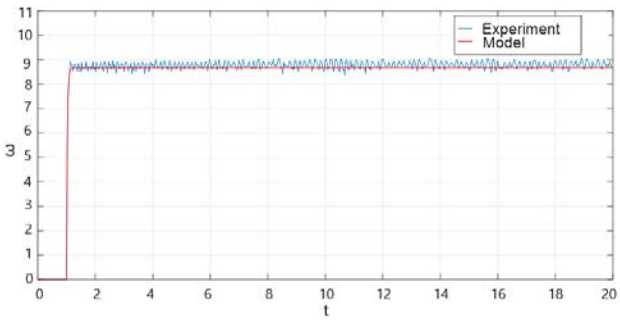

Fig. 7. Experimental results: comparison between real and model data for step input

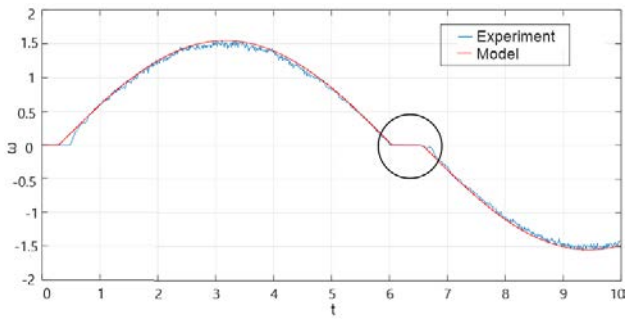

Fig. 8. Experimental results: comparison between real and model data for sinusoidal input

VI. EXPERIMENTAL RESULTS

Applying Definition [12] to the system (18) – (19) yields:

$$A = -\frac{B_{eq,n}}{J_{eq}} \tag{20}$$

$$B = \frac{A_m}{J_{eq}} \tag{21}$$

$$\alpha(x) = \frac{J_{eq}}{A_m} f(x) \tag{22}$$

$$\gamma(x) = 1. \tag{23}$$

First condition is met:

$$U = B. \tag{24}$$

Order of system is n = 1 and, because rank U =n, the pair (A, B) is controllable:

$$U = B = \frac{A_m}{J_{eq}}. \tag{25}$$

System transformation is not required and all functions are smooth and differentiable. γ(x) is not equal to zero, so the second condition is also met. With both conditions met feedback linearization is permitted.

The first derivative of the system (18) – (19) output depends on the control signal, which means that the relative degree of the system is 1:

$$y = x. \tag{26}$$

$$\dot{y} = \dot{x} = L_f\, h(x) + L_g h(x)\, u \tag{27}$$

$$\dot{x} = -\frac{B_{eq,n}}{J_{eq}}x - f(x) + \frac{A_m}{J_{eq}}u \tag{28}$$

$$L_f\, h(x) = -\frac{B_{eq,n}}{J_{eq}}x - f(x) \tag{29}$$

$$L_g h(x) = \frac{A_m}{J_{eq}} \tag{30}$$

Conclusion is that relative degree of this system is equal to the system order $r = 1$. The desired time – domain specifications for controlling the position of the load shaft are overshoot: $PO < 5\%$ and peak time: $t_p \leqslant 0.05\ s$. Choosing the control signal in the following form:

$$u = \frac{J_{eq}}{A_m}[f(\boldsymbol{x}) + v] \tag{31}$$

with $v = K_p\varepsilon + K_i\int_0^t \varepsilon d\tau$, where $K_p = 1.34$, $K_i = 124.9$, are obtained by calculating the minimum damping ratio and natural frequency and x_{ref} is desired output or reference, system is linearized. Linear control is obtained in the same way, with the same coefficients, but without canceling the nonlinearity:

$$u_l = K_p\varepsilon + K_p\int_0^t \varepsilon d\tau \tag{32}$$

The experiments were performed with Quanser rotary servo motor, SRV02. This model is equipped with the optical encoder and tachometer, for motor position and speed measuring, respectively [14].

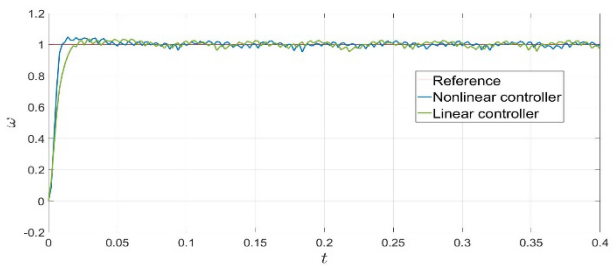

Fig. 9. Experimental results: speed tracking of step signal for the linear and nonlinear controller

The advantages of a nonlinear controller, for a step input, are seen in the shorter peak time and a little bit faster system response, although the output controlled with linear controller has a slightly smaller overshoot. Greater superiority of the nonlinear controller can be observed from the sinusoidal inputs (or any other inputs that consist change of the direction in the rotation of the load shaft in the motor because of the friction effect, which is the most noticeable in those cases).

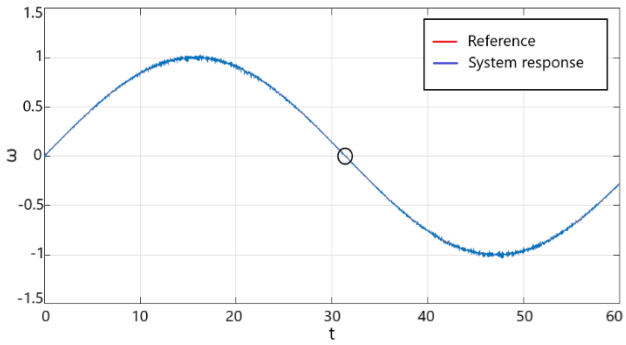

Fig. 10. Experimental results: speed tracking of sine signal for the nonlinear and nonlinear controller

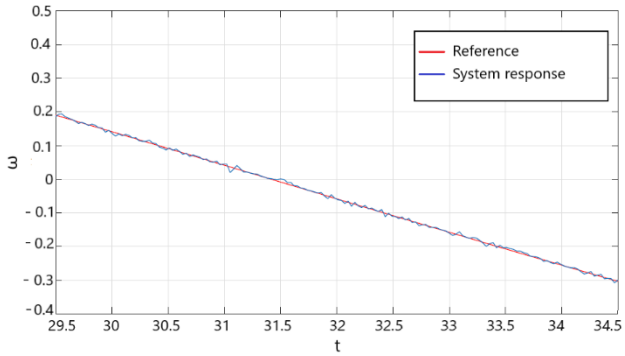

Fig. 11. Detail from Fig. 10.

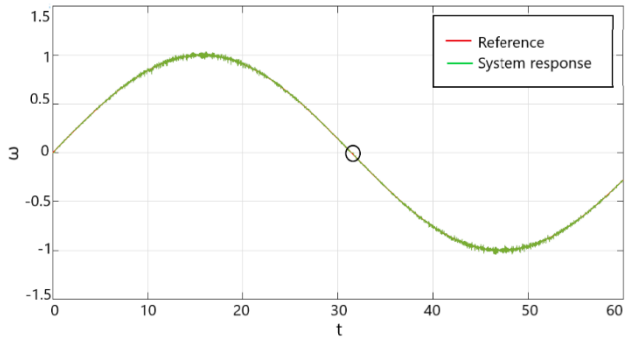

Fig. 12. Experimental results: position tracking of sine signal for the linear and nonlinear controller

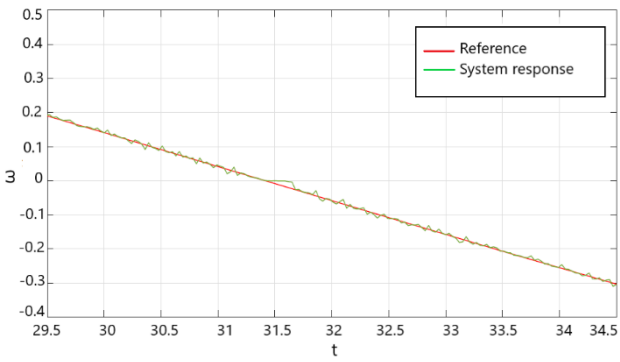

Fig. 13. Detail from Fig. 12.

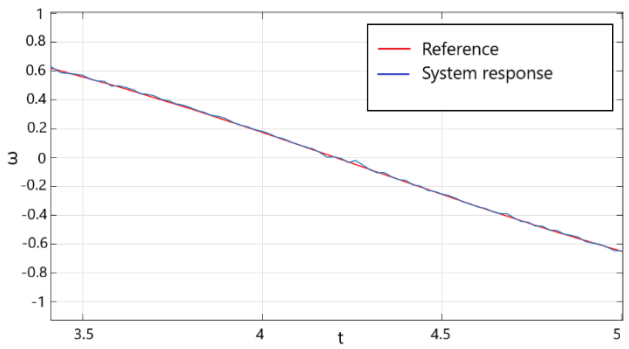

Fig. 14. Detail from experimental results: position tracking of chirp signal for the nonlinear controller

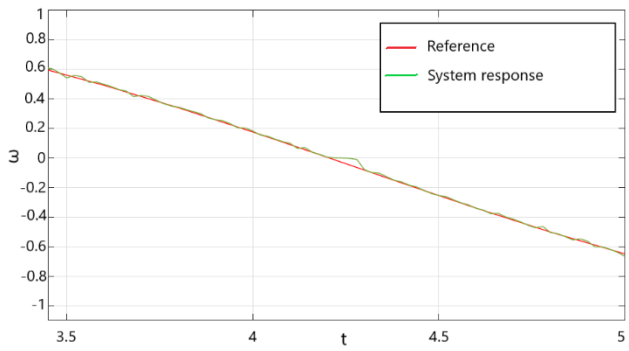

Fig. 15. Detail from experimental results: position tracking of chirp signal for the linear controller.

It can be observed, from the Fig. 9 - 15, that the specific requirements are met. The overshoot and the peak time are in the domain of desired values. Furthermore, it is observed that the nonlinear controller is more convenient and has better achievements for speed management.

VII. CONCLUSION

The feedback linearization method was proposed for controlling the DC motor. The goal was to confirm this method for controlling speed of the load shaft. After it has been shown that linear equations do not track the behavior of the object well enough, the nonlinear model was proposed by including Stribeck model of the friction. The conditions for fulfilling feedback linearization approach were studied. In order to satisfy those conditions an approximation of the function, which represent nonlinearity, was found as hyperbolic tangent.

It could be noted, through the experiment and analysis results, that the desired response was followed by the plant response. The comparison of the linear and nonlinear controller is given. The results show that both of the controllers are able to satisfy requirements, but that nonlinear controller gives better results.

ACKNOWLEDGMENT

This research was supported by the Science Fund of the Republic of Serbia, grant No. 6523109, AI-MISSION4.0, 2020-2022. This paper was conceived within the research on the project: “Integrated research in the field of macro, micro and nano mechanical engineering - Deep machine learning of intelligent technological systems in production engineering”, The Ministry of Education, Science and Technological Development of the Republic of Serbia (contract no. 451-03 -68 / 2020-14 / 200105), 2020.

This work was financially supported by the Ministry of Education, Science and Technological Development of the Serbian Government, Grant TR-35029 (2018-2020).

REFERENCES
(USE STYLE MASING HEADING 4)

[1] Design for AC and DC Machines: Partial Feedback Linearization Approach”, International Journal of Dynamics and Control, vol. 6, pp. 679 – 693, May, 2017.

[2] M.Vesović, R. Jovanović, L. Laban, V. Zarić “Modelling and Control of a Series Direct Current (DC) Machines Using Feedback Linearization Approach”, IcEtran Conference, Belgrade, Serbia, 2020, unpublished

[3] J. U. Liceaga-Castro, I. I. Siller-Alcalá, J. Jaimes-Ponce, R. A. Alcántara-Ramírez, E. A. Zamudio, “Identification and Real Time Speed Control of a Series DC Motor,” Mathematical Problems in Engineering, vol. 2017, March 2017.

[4] D. Park, A. Kandel, G. Langholz Author, “Genetic-Based New Fuzzy Reasoning Models with Application to Fuzzy Control,” IEEE Transactions on Systems, Man, and Cybernetics, vol. 24, no. 1. January 1994.

[5] S. Valluru, N. Singh, M. Kumar, “Implementation of NARMA-L2 neuro controller for speed regulation of series connected DC motor,” IEEE 5th India International Conference on Power Electronics (IICPE), Delhi, India, pp. 1 – 7, 2012.

[6] T. Furuhashi, S. Sangwongwanich, S. Okuma, “A Position and Velocity Sensorless Control for Brushless DC Motors Using an Adaptive Sliding Mode Observer,” IEEE Transactions on Industrial electronics, vol. 39, no. 2, pp. 89 – 95, 1992.

[7] C. Rengifo, N. Casas, D. Bravo, “A performance comparison of nonlinear and linear control for a DC series motor,” Revista Ciencia en Desarrollo, vol. 8, May 2017.

[8] S. Metha, J. Chiasson, “Nonlinear Control of a Series DC Motor: Theory and Experiment,” Proceedings of the American Control Conference, Albuquerque, New Mexico, June, 1997.

[9] J. E. Slotine, W. Li, “Feedback linearization,” in Applied Nonlinear Control, Englewood Cliffs, New Jersey, United States: P.H, 1991, ch. 6, sec. x, p. 207.

[10] W. Ghozlane, J. Knani, “Nonlinear Control via Input-Output Feedback Linearization of a Robot Manipulator,” Advances in Science, Technology and Engineering Systems Journal, vol. 3, October, 2018.

[11] J. Apkarian, M. Levis, H. Gurocak, Student Workbook, SRV02 Base Unit Experiment For Matlab/Simulink Users

[12] H. K. Khalil, Nonlinear Systems; 3rd ed. New Jersey, United States: Prentience Hall, 2002

[13] A. Isidori, Nonlinear Control Systems, 3rd ed. London, United Kingdom: Springer, 2002

[14] L. T. Gruyitch, Z. M. Bučevac, R. Ž. Jovanović & Z. B. Ribar (2019): Structurally variable control of Lurie systems, International Journal of Control

THE 5th INTERNATIONAL CONFERENCE
MECHANICAL ENGINEERING IN XXI CENTURY

December 9-10, 2020
Faculty of Mechanical Engineering in Niš, Serbia

Identification of a Coupled-Tank Plant and Takagi-Sugeno Model Optimization Using a Whale Optimizer

Vladimir ZARIĆ, Radiša JOVANOVIĆ, Lara LABAN

Affiliation of all Authors: Control Engineering, Faculty of Mechanical Engineering, Kraljice Marije 16, Belgrade,Serbia
vzaric@mas.bg.ac.rs, rjovanovic@mas.bg.ac.rs, llaban@mas.bg.ac.rs, mvesovic@mas.bg.ac.rs

***Abstract*— The process industries have continually combated the problem concerning liquid level control. Effective control of a system depends largely on the accuracy of the mathematical model that predicts its dynamic behavior. In this paper the Takagi-Sugeno fuzzy model for the coupled-tank system was acquired based on empirical technique. Furthermore, a metaheuristic algorithm was used as an optimizer on the coupled-tank model. Then, a juxtaposition was made when comparing models which were identified and optimized, leading to satisfactory results. Experimental results obtained on the coupled-tank system are provided.**

***Keywords*—coupled-tank system; Takagi-Sugeno; metaheuristic optimization algorithm; identification; discrete-time systems.**

I. Introduction

The liquid level control is used in the process industries such as petro-chemical, biochemical, spray coating, waste water treatment and purification, beverages and pharmaceutical industries, and within the scope of them presents with an extensive number of applications.

In [1] authors have expressed and emphasized the issue of performance analysis of three control schemes for couple tank system, PI (based on pole placement, Ziegler Nichols and Ciancone correlation tuning methods), PI-plus-feedforward and model predictive control. Moreover, this paper is mostly based of off the research in our previous paper [2], where we dabbled on the similar complexities considering only one tank. In addition, the article [3] combats the problem of the fuzzy-PID controller applied to the nonlinear dynamic model of the liquid level of the coupled tank system, not neglecting the effects of noise. Described by fuzzy IF-THEN rules, the fuzzy model proposed by Takagi and Sugeno [4] depicts local linear input-output relations of a nonlinear system. Furthermore, when it comes to control purposes fuzzy logic has many forms that can be implemented. A procedure used to make two-variable fuzzy logic controllers (FLCs) set for the levels in a laboratory coupled-tank system is submitted in the paper [5].

The fuzzy design can be considered as an optimization problem, where the structure, antecedent, and consequent parameters of fuzzy rules are prerequisites that need to be identified. Metaheuristic methods can deal with non-convex, nonlinear, and multimodal problems subjected to linear or nonlinear constraints with continuous or discrete decision variables as global optimization algorithms. In the literature [6] appealing points of view on this grouping are discussed. In recent years, a dozen metaheuristic methods have been proposed. Some of them include the genetic algorithm (GA) [7], particle swarm optimization (PSO) [8], gray wolf optimization (GWO) [9], whale optimization algorithm (WOA) [10] and ant colony optimization algorithm (ACO) [11]. The WOA has proven to be outstanding at resolving a variety of models, multimodal and problems that are not linear. The foremost supremacies of this algorithm, and all of the metaheuristic algorithms in general, are that it avoids getting stuck in the local minimum because of random distributions.

In this paper, the structure and consequent parameters are known (number of rules, shapes of input membership functions and linear models in the consequent part of the rules), while the antecedent parameters are concluded using the whale optimizing algorithm.

II. Mathematical Modeling

The Coupled Tanks plant is a “Two-Tank” module made up of a pump with a water basin and two tanks as is shown on Fig. 1.

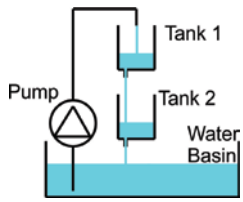

Fig. 1 The Coupled Tanks plant

A. Analytical model

The input into the process is the voltage to the pump V_p and its output is the water level in tank, H_2. The volumetric inflow rate to tank 1, Q_{i1}, is intended to be directly proportional to the applied pump voltage, $Q_{i1} = KV_p$. When applying Bernoulli’s equation for small orifices, the outflow velocity from tank 1, V_{o1}, can be expressed by a succeeding relationship,

$$V_{o1} = \sqrt{2gH_1}, \quad Q_{o1} = A_o V_{o1}, \tag{1}$$

where A_o is an area of the outlet orifice of tank 1 and tank 2, while Q_{o1} is the outflow rate from tank 1. In attaining the tank’s equation of motion the mass balance principle can be applied to the water level in tank, i.e.

$$A_t\dot{H}_1 = Q_{i1} - Q_{o1} = K\,V_p - A_oV_{o1} =$$
$$= K\,V_p - A_o\sqrt{2gH_1}\,, \quad (2)$$

where A_t is the area of tank 1 and tank 2. The nonlinear differential equation that describes the change in level in tank 1 is

$$\dot{H}_1 = \frac{K}{A_t}V_p - \frac{A_o}{A_t}\sqrt{2gH_1}. \quad (3)$$

The water level equation of motion in tank 2 still needs to be obtained. The input to the tank 2 process is the water level, H_1, in tank 1 (generating the outflow feeding tank 2) and its output variable is the water level, H_2, in tank 2 (i.e. bottom tank). The obtained equation of motion should be a function of the system's input and output, as defined beforehand,

$$A_t\dot{H}_2 = Q_{i2} - Q_{o2}\,, \quad (4)$$

$$Q_{i2} = Q_{o1}\,, \quad V_{o2} = \sqrt{2gH_2}. \quad (5)$$

The nonlinear differential equation that describes the change in level in tank 2 is described as

$$A_t\dot{H}_2 = A_o\sqrt{2gH_1} - A_o\sqrt{2gH_2}\,. \quad (6)$$

B. Takagi-Sugeno fuzzy model and identification

The main idea of the TS fuzzy modeling method is to partition the nonlinear system dynamics into several locally linearized subsystems, so that the overall nonlinear behavior of the system could be captured by fuzzy blending of such subsystems. Thus, a fuzzy model and identification of a liquid level system will be implemented in accordance with the TS model containing three rules. The fuzzy rule associated with the i-th linear subsystem, can then be defined as i-th rule:

IF $x_2(k)$ is M_i THEN

$$\boldsymbol{x}(k+1) = A_i\boldsymbol{x}(k) + B_iu(k), \quad i = 1,2,3, \quad (7)$$
$$y(t) = C_i\boldsymbol{x}(t), \quad i = 1,2,3.$$

Here M_i is the fuzzy set, $\boldsymbol{x}(k) \in \mathbb{R}^n$ is the state vector, $u(k) \in \mathbb{R}$ is the input, $y(k) \in \mathbb{R}$ is the output variable, $A_i \in \mathbb{R}^{2x2}$, $B_i \in \mathbb{R}^{2x1}$, $C_i \in \mathbb{R}^{1x2}$. In our case, the selected state space variable is equal to the output variable $x_2(k) = y(k) = H_2(k)$.

The overall output, using the fuzzy blend of the linear subsystems, will then be as follows:

$$\boldsymbol{x}(k+1) = \frac{\sum_{i=1}^{3} w_i(x_2(k))\{A_i\,\boldsymbol{x}(k) + B_i\,u(k)\}}{\sum_{i=1}^{3} w_i(x_2(k))}, \quad (8)$$

$$h_i(x_2(k)) = \frac{w_i(x_2(k))}{\sum_{i=1}^{3} w_i(x_2(k))}\,, \quad (9)$$

$$\boldsymbol{x}(k+1) = \sum_{i=1}^{3} h_i(x_2(k))\{A_i\,\boldsymbol{x}(k) + B_i\,u(t)\}, \quad (10)$$

$$y(k) = \frac{\sum_{i=1}^{3} w_i(x_2(k))C_i\,\boldsymbol{x}(k)}{\sum_{i=1}^{3} w_i(x_2(k))} = \sum_{i=1}^{3} h_i(x_2(k))C_i\,\boldsymbol{x}(k)\,, \quad (11)$$

where $w_i(x_2(k)) = M_i(x_2(k))$ is the grade of membership of $x_2(k)$ in M_i and $h_i(x_2(k))$ is normalized weight. The linear models in the consequent rules (7) can be obtained by utilizing an analytical linearization of a non-linear equation. Besides that, another approach is to apply the methods of identification in accordance with the measured input output data. The identification methods were used based on the step response. Since models obtained by identification experimentally turned out to be more of an adequate approximation, in comparison with the analytically obtained linearized models, they were used. Linear models can be represented by transfer functions as the relationships of outputs and inputs,

$$G_{1i}(z) = \frac{H_{1i}(z)}{V_{pi}(z)}, G_{2i}(z) = \frac{H_{2i}(z)}{H_{1i}(z)}, i = 1,2,3. \quad (12)$$

Nominal levels in the tanks H_{1Ni}, H_{2Ni}, nominal voltages V_{pNi} and corresponding identified Z-transfer functions, for the sampling time $T = 0.01$ second, are given in Table 1. Matrices for the state space plant model A_i and B_i are given in Table 2.

TABLE I
NOMINAL VALUES AND LINEAR MODELS

i	1	2	3
$V_{pNi}\ [V]$	4.4	6	7.1
$H_{1Ni}\ [m]$	0.077	0.1665	0.2415
$H_{2Ni}\ [m]$	0.075	0.1645	0.233
$G_{1i}(z)$	$\frac{2.3124 \cdot 10^{-5}}{z - 0.99952}$	$\frac{2.626 \cdot 10^{-5}}{z - 0.9996}$	$\frac{2.642 \cdot 10^{-5}}{z - 0.9997}$
$G_{2i}\ (z)$	$\frac{6.6976 \cdot 10^{-4}}{z - 0.99928}$	$\frac{5.269 \cdot 10^{-4}}{z - 0.9994}$	$\frac{4.216 \cdot 10^{-4}}{z - 0.9995}$

TABLE II
MATRICES FOR THE STATE SPACE SYSTEM MODEL

i	A_i	B_i
1	$\begin{bmatrix} 0.99952 & 0 \\ 6.6976 \cdot 10^{-4} & 0.99928 \end{bmatrix}$	$\begin{bmatrix} 2.3124 \cdot 10^{-5} \\ 0 \end{bmatrix}$
2	$\begin{bmatrix} 0.99958 & 0 \\ 5.2685 \cdot 10^{-4} & 0.99944 \end{bmatrix}$	$\begin{bmatrix} 2.6264 \cdot 10^{-5} \\ 0 \end{bmatrix}$
3	$\begin{bmatrix} 0.99965 & 0 \\ 4.216 \cdot 10^{-4} & 0.99954 \end{bmatrix}$	$\begin{bmatrix} 2.6415 \cdot 10^{-5} \\ 0 \end{bmatrix}$

In this article a nonlinear TS fuzzy model is obtained by combining three linear models around 0.08 m, 0.16 m and 0.24 m. The membership functions are depicted in Fig. 2.

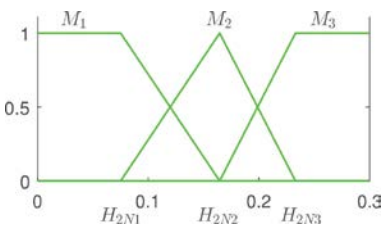

Fig. 2 Membership functions.

III. THE WHALE OPTIMIZER

Whale Optimization Algorithm has demonstrated to be remarkable at solving a variety of nonlinear and multimodal problems. The advantages of this method, and all metaheuristic algorithms in the main, are the random distribution. This distribution allows avoiding getting stuck in the local minimum. WOA has been first proposed by Seyedali Mirjalili and Andrew Lewis in [10]. The paper was inspired by the idea of the attack of dozen whales. The flock consists of a number of whales that

hunt, on the principle of surrounding prey, immersion whales to a greater depth, then gradually spiraling to the surface with the release of bubbles which form a "wall" and thus prevent prey from leaving the formed area. The hunt contains three phases. The leader whale has a job to find the fish. The rest follow information. Each takes exactly the same position in every lunch. The first phase is encircling the prey by defining the best search agent and updating the position of others. The mathematical model of this phase is proposed using the distance vector $\boldsymbol{D}$ and vector $\boldsymbol{X}$ which is used to update the position:

$$\boldsymbol{D} = |\boldsymbol{C}\boldsymbol{X}'(t) - \boldsymbol{X}(t)|\,, \tag{13}$$

$$\boldsymbol{X}(t+1) = \boldsymbol{X}'(t) - \boldsymbol{A}\boldsymbol{D}\,, \tag{14}$$

$$\boldsymbol{A} = 2\boldsymbol{a}\boldsymbol{r} - \boldsymbol{a}, \quad \boldsymbol{C} = 2\boldsymbol{r}, \tag{15}$$

where t is the current iteration, $\boldsymbol{A}$ and $\boldsymbol{C}$ are coefficient vectors. Coefficient $\boldsymbol{a}$ is linearly decreased from 2 to 0 and $\boldsymbol{r}$ is a random vector in [0,1]. $\boldsymbol{X'}$ is the position vector of the best solution obtained so far and $\boldsymbol{X}$ is the position vector. The shrinking encircling mechanism (defining the new position of the searching agent using $\boldsymbol{A}$) and the spiral-shaped path (first calculation distance between whale and prey using helix-based movement) are the basic mathematical models that mimic the hunt of the second phase. The new position of the agent is located between the current best agent and the original position. The function for this approach is:

$$\boldsymbol{X}(t+1) = \begin{cases} \boldsymbol{X}'(t) - \boldsymbol{A}\boldsymbol{D} \text{ if } p < 0.5 \\ \boldsymbol{D}' - e^{bl} \cdot cos(2\pi l) + \boldsymbol{X}'(t) \text{ if } p \geq 0.5 \end{cases} \tag{16}$$

where p is a random number in [0,1], b is a constant for defining the shape of the logarithmic spiral, l is a random number in [-1,1] and $\boldsymbol{D'}$ indicates the distance of the i-th whale from the prey [10]. The third phase is based on adoptive variation that depends of the value search vector $\boldsymbol{A}$, which provides good correspondence between first two phases.

IV. Takagi-Sugeno Model Optimization

In the Fig. 2 we observe the beforehand mentioned TS model which was obtained based on the symmetric shape of the membership functions. The configuration of the functions is triangular and the centers of the membership functions are located in the selected nominal points in which the linear models are identified. However, in order to achieve a better approximation of the non-linear characteristics and overall behavior of the plant, a more adequate approximation of the non-linear model is presented by adjusting the parameters of the membership functions. We can view the parameters as the width of the membership functions. So in conclusion, in this case we only optimized the parameters that were located in the rule premise. Moreover, the mentioned TS parameters are all coded into one whale, per say one agent, that is presented with a vector which contains the premise parameters, in our case it has four parameters. In the proposed WOA algorithm the population is set to 40, while the total number of iterations is set to 20. The population size and the number of iterations, viewed as a criteria of stopping, are determined based on a series of experiments with different values, all the while taking in account the specificity of our problem which is that the dimensionality of the problem is small (only 4 unknown parameters). Furthermore, in this optimization method, one agent represents one potential optimal fuzzy model. The mean square error (MSE) is taken as an objective function and it can be calculated as

$$MSE = \frac{1}{n}\sum_{i=1}^{n}(y(i) - y_m(i))^2, \tag{17}$$

where n is the number of data points, $y(i)$ is the measured output of the plant, $y_m(i)$ is the output of the model.

A dataset for the learning process of the WOA algorithm, in other words for the optimization of the TS model, is obtained from the plant operation in 1600 seconds. All of the parameter values that were used in the implementation of the WOA were taken from the original paper [10]. In the aim of identification we bring the input voltage which has a shape as depicted in Fig. 3.

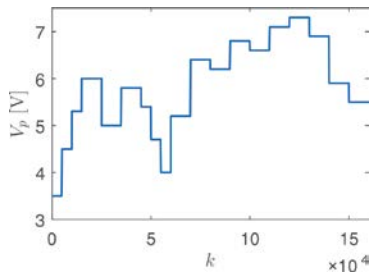

Fig. 3 Voltages used for model optimization

There it should be observed that the values are between the nominal voltages, this is done in order to cover the range of interest. Optimized membership functions are shown on Fig. 4.

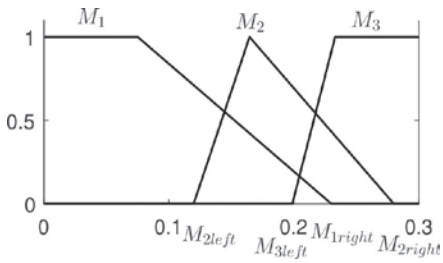

Fig. 4 Optimized membership functions

where $M_{2left} = 0.11975$, $M_{3left} = 0.19875$, $M_{1right} = 0.23$, $M_{2right} = 0.28$.

The same input output data is utilized, with 160001 points that where used for the previous identification, based on the Fig. 3. On the other hand, we now have the second way of identification. This means that we will also acquire unspecified parameters in the rule premise. This approach gives smaller dimensionality of unknown parameters. Fuzzy rules of this system have the same shape as in the eq. (7), with the difference being the selection of the Gaussian membership functions. Three Gaussian membership functions, each with one parameter - slope s_i, for $i = 1,2,3$, were used. Utilizing the WOA for the estimation of the unknown parameters we can conclude that each agent consists of three parameters. Their optimized numerical values are $s_1 = 0.05, s_2 = 0.0134, s_3 = 0.05$. Moreover, the membership functions are shown on Fig. 5.

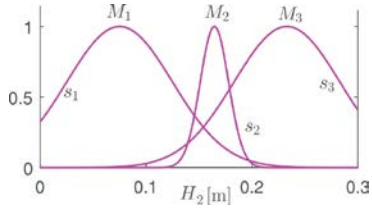

Fig. 5 Optimized Gaussian membership functions

V. Simulation and Experimental Results

Comparison of the nonlinear analytical model (analytical, red color), TS model based on initial membership functions (TS identified, green color), TS model based on optimized membership functions (TS optimized widths and TS optimized slopes, black and magenta colors) with experimentally obtained results (experiment, blue color) is showed on Fig. 6.

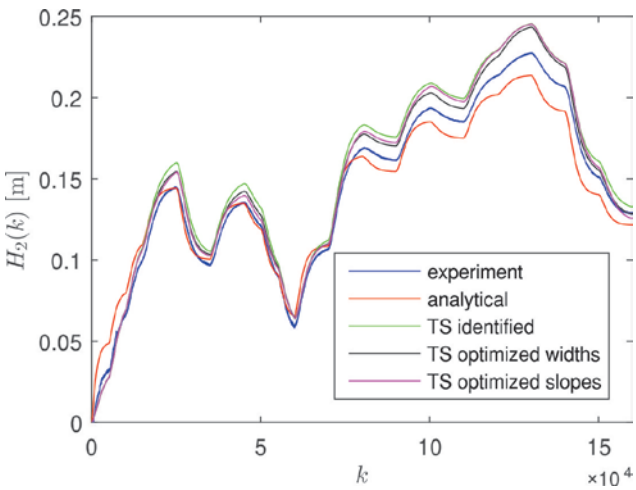

Fig. 6 Comparison of different models with experiment

To explicitly see the improvement caused by the optimization, the numerical values of the MSE, calculated using eq. (17), are given. Mentioned values for four different models (analytical, TS identified, TS optimized widths, TS optimized slopes) are respectively: $1.0054 \cdot 10^{-4}$, $1.4614 \cdot 10^{-4}$, $7.122 \cdot 10^{-5}$, $9.6 \cdot 10^{-5}$. These results show us that the analytical nonlinear model is the least accurate. The initial TS model is better than analytical nonlinear and with optimization we get an even greater improvement in the accuracy of the TS models.

VI. Conclusions

At first, mathematical model of the liquid level system was analytically and experimentally acquired. Further, TS fuzzy model was obtained built on three identified local linear models. In order to improve the model, an optimization, using WOA metaheuristic, was performed using triangular and Gaussian membership functions. Numerical values of MSE are given in order to show the achieved better approximation using optimized membership functions in relation to the analytical and identified model. The initial TS model is better than analytical nonlinear model while optimization further increases the accuracy of the TS fuzzy models. In addition, it is simple and consists only of three fuzzy rules. Future research will focus on other metaheuristic algorithms, using more fuzzy rules and bringing neuro-fuzzy controller in to the set.

Acknowledgment

This research was supported by the Science Fund of the Republic of Serbia, grant No. 6523109, AI-MISSION4.0, 2020-2022. This paper was conceived within the research on the project: "*Integrated research in the field of macro, micro and nano mechanical engineering - Deep machine learning of intelligent technological systems in production engineering*", The Ministry of Education, Science and Technological Development of the Republic of Serbia (contract no. 451-03 -68 / 2020-14 / 200105), 2020. This work was financially supported by the Ministry of Education, Science and Technological Development of the Serbian Government, Grant TR-35029 (2018-2020).

References

[1] A. S. Tijjani, M. A. Shehu, A. Alsabari, Y. A. Sambo, N. L. Tanko, "Performance analysis for coupled-tank system liquid level control using MPC, PI and PI-plus-feedforward control scheme," Journal of Robotics and Automation, vol. 1, no. 1, pp. 42-53, June, 2017.

[2] R. Jovanović, V. Zarić, M. Vesović, L. Laban "Modeling and Control of a Liquid Level System Based on the Takagi-Sugeno Fuzzy Model Using the Whale Optimization Algorithm" , IcEtran, Belgrade, Serbia, 2020, unpublished.

[3] T. L. Mien, "Liquid level control of coupled-tank system using fuzzy-PID controller," International Journal of Engineering Research & Technology, vol. 6, no. 11, pp. 459-464, November, 2017.

[4] T. Takagi, M. Sugeno, "Fuzzy identification of systems and its applications to modeling and control," IEEE Transactions on Systems, Man, Cybernetics, New York, New York, vol. 15, pp. 116-132, 1985.

[5] S. Yordanova, "Fuzzy logic approach to coupled level control," Systems Science & Control Engineering, vol. 4, no. 1, pp. 2015-222, September, 2016.

[6] F. S. Gharehchopogh, H. Gholizadeh, "A comprehensive survey: Whale optimization algorithm and its applications," Swarm and Evolutionary Computation, vol. 48, pp. 1-24, August, 2019.

[7] O. Cordón, F. Herrera, "A two-stage evolutionary process for designing TSK fuzzy rule-based systems," IEEE Transactions on Systems, Man, and Cybernetics - Part B: Cybernetics, vol. 29, no. 6, pp. 703–715, December, 1999.

[8] S. H. Tsai, Y. W. Chen, "A novel identification method for Takagi-Sugeno fuzzy model," Fuzzy Sets and Systems, vol. 338, pp. 117-135, May, 2018.

[9] M. Ghanamijaber, "A hybrid fuzzy-PID controller based on gray wolf optimization algorithm in power system," Evolving Systems, vol. 10, pp. 273-284, 2018.

[10] S. Mirjalili, A. Lewis, "The whale optimization algorithm," Advances in Engineering Software, vol. 95, pp. 51-67, May, 2016.

[11] M. Z. Kamali, K. Nallasamy, K. Ratnavelu, "Takagi–Sugeno fuzzy modelling of some nonlinear problems using ant colony programming," Applied Mathematical Modelling, vol. 48, pp. 635-654, August, 2017.

[12] M. Sugeno, G.T. Kang, "Structure identification of fuzzy model," Fuzzy sets and systems, vol. 28, pp. 15-33, 1988.

THE 5th INTERNATIONAL CONFERENCE
MECHANICAL ENGINEERING IN XXI CENTURY

December 9-10, 2020
Faculty of Mechanical Engineering in Niš, Serbia

Influence of Flexure Hinges Design on Guiding Accuracy of Roberts-Чебышев Compliant Mechanism

Dušan STOJILJKOVIĆ, Nenad T. PAVLOVIĆ

Department of Mechatronics and Control, Faculty of Mechanical Engineering, University of Niš, Aleksandra Medvedeva 14, Niš, Serbia
dusan.stojiljkovic@masfak.ni.ac.rs, nenad.t.pavlovic@masfak.ni.ac.rs

***Abstract*— Compliant mechanisms gain some or all of their mobility from the compliance of their joints rather than from rigid-body joints only. They can be built in one piece and represent material coherent structure being able to transfer the forces and transform the motion due to energy stored in compliant joints - flexure hinges. The investigations in the paper present the potential of improving the accuracy of the coupler point rectilinear path of the Roberts-Чебышев four-bar linkage. This is done by developing the Roberts-Чебышев compliant mechanism and by applying the new specific design of the flexure hinge. Hence, it will be described that the position of this flexure hinges and their geometry are of a vital issue for performing approximately rectilinear path. Therefore, several designs are investigated by means of finite elements method (FEM) simulation.**

***Keywords*— Compliant Mechanism, Flexure Hinges, Roberts-Чебышев Mechanism, Rectilinear Path, FEM Analysis**

I INTRODUCTION

There are many rigid-body four-bar linkages used as compliant counterparts for rectilinear guiding (Hoecken, Watt etc.). This is because there are many advantages and benefits of using flexure hinges rather than classic joints. Hence, defects like friction, clearance, wearing, noise are eliminated with implementing flexure hinges. The shape of the flexure hinges determines how efficiently the compliant mechanism can perform a given, in this case, rectilinear path. As this is an important factor and the main disadvantage of flexure hinges, many papers deal with the study of the influence of different forms of flexure hinges on the operation of the compliant mechanism.

The basic nomenclature of the flexure hinges has been established in the papers [1], [2], [3]. Paper [4] provide the new-designed compliant mechanism for realizing guiding accuracy of link translation. Paper [5] aims to analyze the guiding accuracy of the "coupler" point on the path segment for each of three new-designed compliant mechanisms, as well as to analyze the influence of the input force acting point location on the guiding accuracy. In the papers [6] and [7] the influence of the geometry, as well as the material type of the compliant joints on a mobility of the single compliant joints and entire compliant mechanisms is described. Papers [8] and [9] exhibits, with the help of the finite elements method (FEM), compliant straight-line mechanisms and compliant grippers analysis.

Compliant four-bar linkages for rectilinear guiding used in this paper is based on Roberts-Чебышев four-bar linkage. This paper aims to ameliorate rectilinear guiding of Roberts-Чебышев compliant mechanism by use of the new specific design of the flexure hinge. On two of four flexure hinges, the new design was applied (on joints A and B, joints of fixed supports A_0 and B_0 are not changed). The position of this flexure hinges and their geometry is of a vital issue for performing approximately rectilinear path. Hence, a new parameter H_p was introduced. It represents the position of the neutral axis of newly designed flexure hinges relative to joints of Roberts-Чебышев four-bar linkage. Hence, the influence of this parameter will be described in this paper through a FEM simulation of various model designs.

II ROBERTS-ЧЕБЫШЕВ FOUR-BAR LINKAGE

Roberts-Чебышев four-bar linkages represent a mechanism for approximate rectilinear guiding of the coupler point C (Fig. 1). This coupler point C is located in the corner of the coupler as a ternary link and with the angular displacement of just 5° of the input crank (crank labeled A_0A) realize approximate horizontal displacement of $\Delta x_C = 5$ mm.

As the dimensions and the length of the link members of this mechanism and their relationship have already been given through previous paper ([2],[5]), these values will be used in this paper as well.

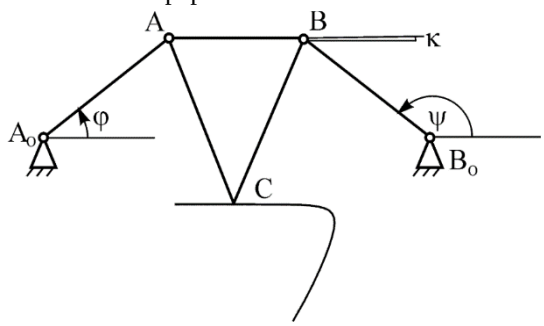

Fig. 1 Roberts-Чебышев four-bar linkage

Described rectilinear displacement is not pure horizontal. Displacement of coupler point C, caused by the rotation of the input crank, also contains a small parasitic displacement in the vertical direction (Δy_C = 0.8 µm). This inaccuracy in rectilinear guidance is the essence of the tendency for Roberts-Чебышев four-bar linkages to be designed as a compliant mechanism in order to improve guidance accuracy.

III The New Design of Flexure Hinges

In order to be able to compare the values obtained by FEM analysis with the values from the other mentioned papers ([2], [5]), some of the already given parameters of flexure hinges will be used in the paper (Fig. 2). This was done in order to avoid the influence of these parameters on the change in the accuracy of the mechanism and to emphasise how much the design of the new flexure hinge and its position favourably affect the more precise guidance.

Width of flexure hinge W_e is a parameter that is constant in all designed models (W_e = 1 mm). Also, the thickness of the flexure hinges is δ = 4 mm [6]. Thus the influence of these parameters is neutralized.

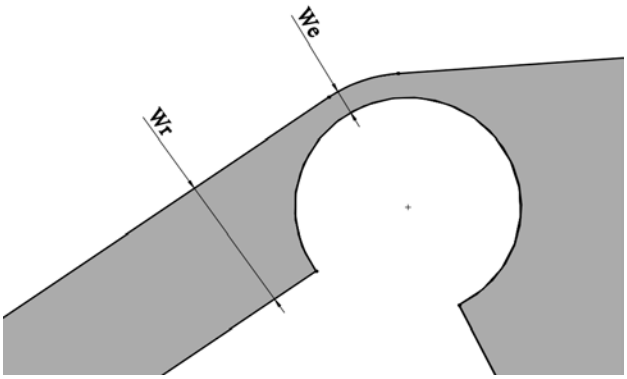

Fig. 2 A new-designed flexure hinges

Subsequently, in this paper, the change in the width of the rigid segment W_r will be given in an adequate explanation, but it can already be established that the value of this parameter does not change significantly and thus does not influence the rectilinear guidance.

IV Roberts-Чебышев Compliant Mechanism

Design of Roberts-Чебышев compliant mechanism is given on Fig. 3. With the blue colored dash-dot type of line, the Roberts-Чебышев four-bar linkage can be seen. With a new design, flexure hinges are positioned on top of the classical joints A and B of the four-bar linkage. Designs of notch flexure hinge A_0 and B_0 is completely taken from the previously cited papers.

Two types of loads can be applied to provide the desired rectilinear guidance. In the first case, the input force (F_a) is set to act in the middle of crank A_0A, and in second, input force (F_b) is set in the middle of crank B_0B. The direction of these forces can be seen in Fig. 3.

V FEM Analysis of Roberts-Чебышев Compliant Mechanism

Nonlinear FEM simulation of the Roberts-Чебышев basic compliant mechanism given in Fig. 3 is performed (Fig. 4).

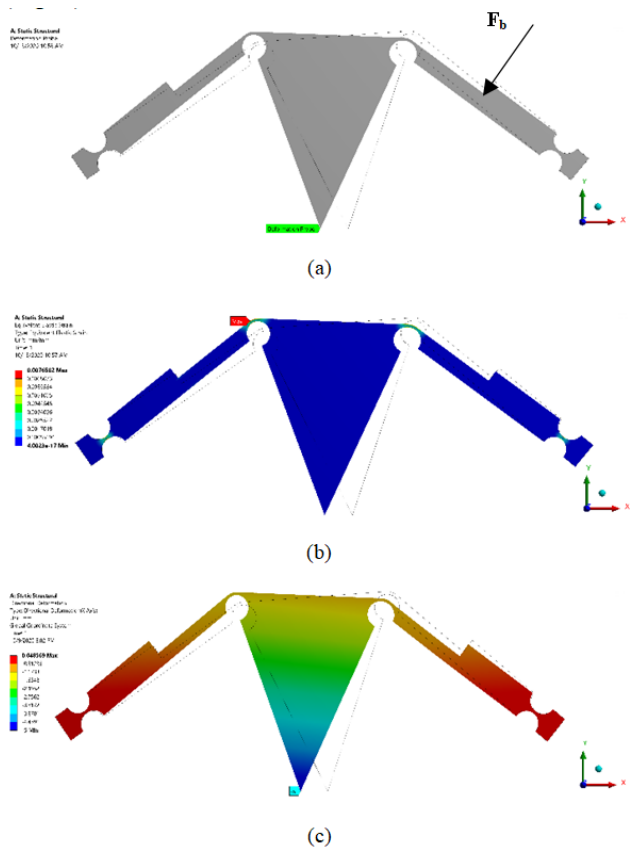

Fig. 4 FEM analysis of the Roberts-Чебышев basic compliant mechanism: (a) Deformation probe of coupler point C, (b) The equivalent von-Mises elastic strain, (c) The directional deformation (X axis deformation)

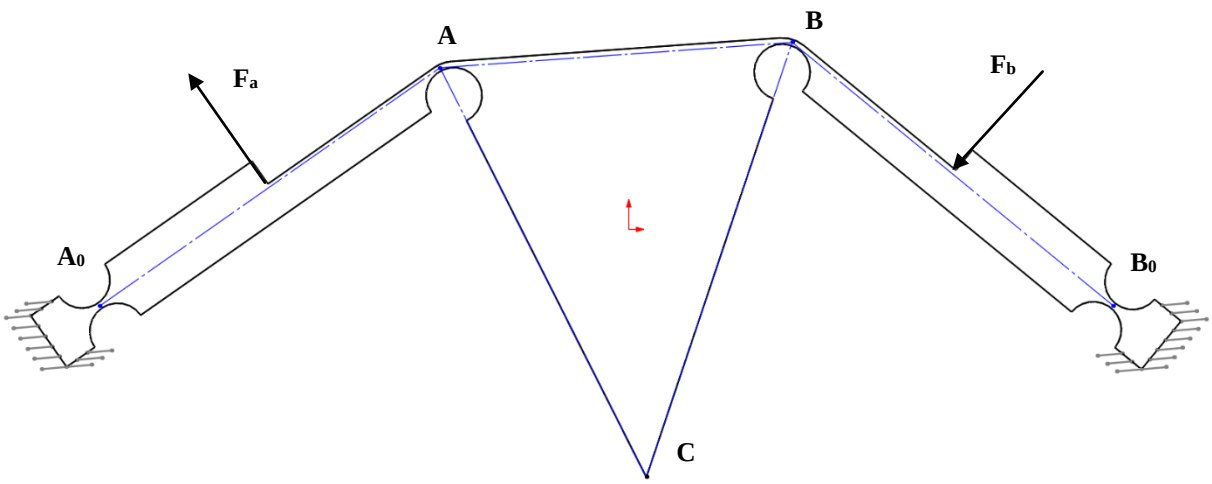

Fig. 3 Roberts-Чебышев compliant mechanism

Desired horizontal displacement of Δx_C = 5 mm is a constant parameter in relation to which all subsequent model analyzes will be performed (Fig. 4c). The mechanism analyzed in this way gave poorer results, especially in terms of the input displacement by the force F_a on crank A_0A (Table 1).

Therefore, the Roberts-Чебышев basic compliant mechanism must be modified. It can be observed that by moving flexure hinges A and B in the negative direction, the results of the guiding accuracy are improved. Hence, a new parameter H_p was introduced. It represents the position of the neutral axis of newly designed flexure hinges relative to joints of Roberts-Чебышев four-bar linkage (Fig. 5). This can be noticed even with a small displacement of 0.6 mm (Table 1).

TABLE 1 GUIDING INACCURACY OF THE ROBERTS- ЧЕБЫШЕВ COMPLIANT MECHANISMS

Roberts-Чебышев compliant mechanism	Input Force	Input Force F [N]	Straight-line deviation Δy_c [μm]	Maximum Strain ε_{max} [%]
Basic	Case F_a	3.008	14.726	0.76582
	Case F_b	3.963	2.2605	0.82273
H_p = 0.6 mm	Case F_a	3.031	21.521	0.76206
	Case F_b	4.011	0.90305	0.82805

VI DIFFERENT VARIATION AND FEM ANALYSIS OF ROBERTS-ЧЕБЫШЕВ COMPLIANT MECHANISMS

The main parameter that varies in the design of all compliant mechanisms is the position of the neutral axis, and thus the middle of the flexure hinges (H_p). Hence, a different variation of a given Roberts-Чебышев compliant mechanism was analyzed. Among other parameters that change during this design change, the width of the rigid segment W_r is also changing. Table 2 shows that this change is negligible.

TABLE 2 WIDTH OF THE RIGID SEGMENT WR WHIT DIFFERENT COMPLIANT MECHANISM VARIATION

Roberts-Чебышев compliant mechanism	Width of the rigid segment Wr [mm]
Basic	5.5
H_p=1,00mm	4.56
H_p=1,05mm	4.51
H_p=1,10mm	4.46
H_p=1,15mm	4.41
H_p=1,20mm	4.36

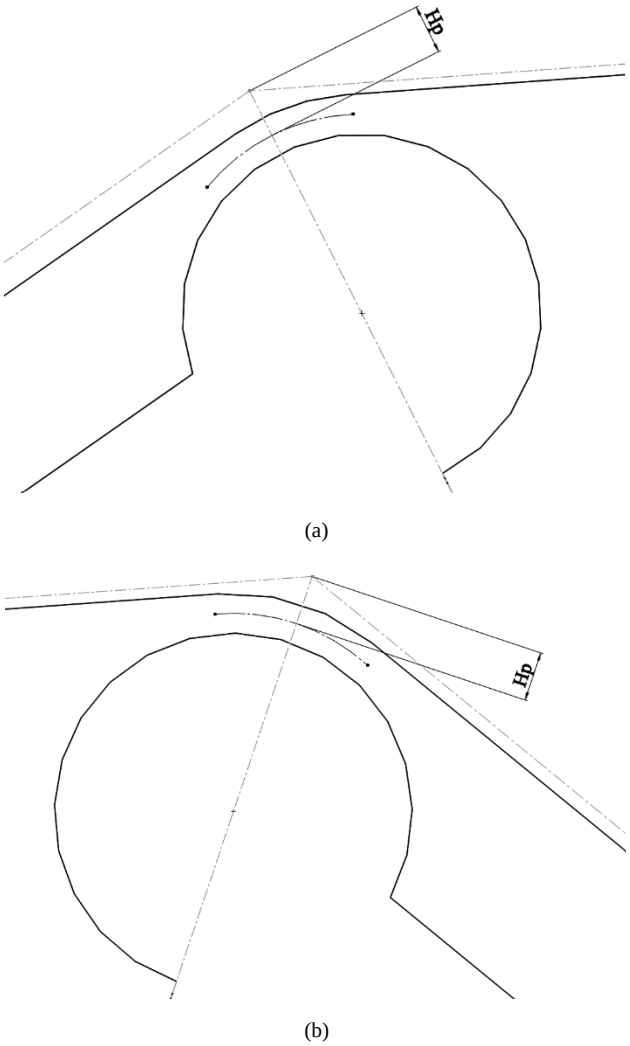

Fig. 5 Position variation: (a) Flexure hinge A, (b) Flexure hinge B

The same quasi-static structural 3D FEM simulation performed in the ANSYS software package, on the Roberts-Чебышев basic compliant mechanism, is used for variants of mechanisms, thus providing information on the deformation at the output (coupler point C). Material that was used is Polylactide/polylactic acid (PLA) with modulus of elasticity E = 3450 N/mm^2, bending strength σ_{bs} = 54.1 N/mm^2.

In case of input force F_a on the crank A_0A, Roberts-Чебышев compliant mechanism gave poorly results. With a displacement of 5 mm at the endpoint of the ternary link (coupler point C), straight-line deviation Δy_c is in average 28,36 μm (Table 3).

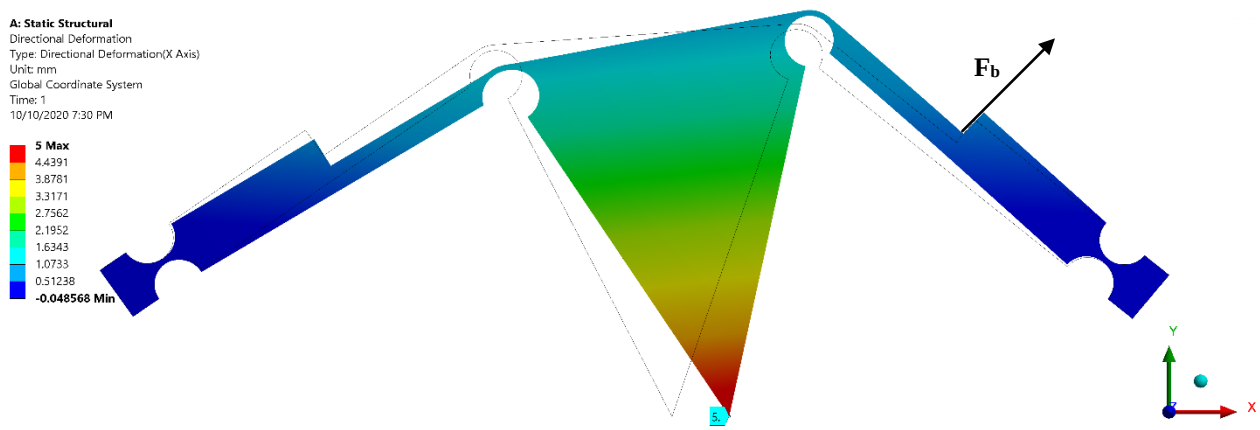

Fig. 6 FEM results of directional deformation (X axis deformation)

TABLE 3 GUIDING INACCURACY OF THE ROBERTS- ЧЕБЫШЕВ COMPLIANT MECHANISM VARIATIONS

Position of flexure hinges Hp	Input Force	Input Force F [N]	Straight-line deviation Δyc [μm]	Maximum Strain εmax [%]
1,00mm	Case Fa	3.043	26.862	0.75822
	Case Fb	4.039	0.50302	0.83225
1,05mm	Case Fa	3.044	27.612	0.7513
	Case Fb	4.042	0.47838	0.83255
1,10mm	Case Fa	3.045	28.346	0.74996
	Case Fb	4.045	0.4725	0.83332
1,15mm	Case Fa	3.046	29.109	0.75415
	Case Fb	4.048	0.47673	0.83304
1,20mm	Case Fa	3.047	29.88	0.75873
	Case Fb	4.051	0.49654	0.83347

In Table 3 it can be seen that with implementing input force F_b on the crank B_0B, Roberts-Чебышев compliant mechanism variation Hp = 1,10 mm has produced so far the greatest guidance accuracy with a straight-line deviation of Δyc = 0.4725 μm.

If the force is given in this way (input force F_b on the crank B_0B) changes direction (Fig. 6), the similar satisfactory results are obtained. The results of such loaded Roberts-Чебышев compliant mechanism can be seen in Table 4. In this case, too, the Roberts-Чебышев compliant mechanism variation Hp = 1,10 mm produces the least deviation from guidance accuracy (Δyc = 0.47652 μm).

TABLE 4 GUIDING INACCURACY OF THE ROBERTS- ЧЕБЫШЕВ COMPLIANT MECHANISMS VARIATIONS IN CASE OF INVERTED FORCE F_B

Position of flexure hinges Hp	Input Force F [N]	Straight-line deviation Δy_c [μm]	Maximum Strain ε_{max} [%]
1,00mm	4.039	0.50319	0.83225
1,05mm	4.042	0.48148	0.83255
1,10mm	4.045	0.47652	0.83332
1,15mm	4.048	0.47937	0.83304
1,20mm	4.051	0.5014	0.83347

VII CONCLUSIONS

There are many rigid-body four-bar linkages used as compliant counterparts for rectilinear guiding (Hoecken, Watt etc.). Compliant four-bar linkages for rectilinear guiding used in this paper is Roberts-Чебышев four-bar linkage. This paper aims to ameliorate the rectilinear guiding of the Roberts-Чебышев compliant mechanism. This is done by developing the Roberts-Чебышев compliant mechanism with the new specific design of the flexure hinge. A vital issue for performing approximately rectilinear path the position of this flexure hinges and their geometry. Based on this knowledge different variations of compliant mechanisms are presented throughout the paper. Hence, the nonlinear FEM analysis was applied in order to obtain valid results of such Roberts-Чебышев compliant mechanism models.

The best-guiding accuracy has been provided by the Roberts-Чебышев compliant mechanism whit remote position of the neutral axis H_p = 1,10 mm from the basic Roberts-Чебышев compliant mechanism (straight-line deviation is Δyc = 0.4725 μm).

ACKNOWLEDGMENT

This research was financially supported by the Ministry of Education, Science and Technological Development of the Republic of Serbia.

REFERENCES

1 N.T. Pavlović, N.D. Pavlović, "Compliant mechanisms" (in Serbian), Faculty of Mechanical Engineering, University of Niš, Serbia, 2013

2 S. Linß, S. Henning, and L. Zentner, “Modeling and Design of Flexure Hinge-Based Compliant Mechanisms,” in *Kinematics-Analysis and Applications*, IntechOpen, 2019.

3 Howell LL, Magleby SP, Olsen BM. Handbook of Compliant Mechanisms. Chichester: Wiley; 2013. 324 p

4 N.T. Pavlović, N.D. Pavlović, "Compliant mechanism design for realizing of axial link translation. Mechanism and Machine Theory. 2009; 44(5):1082-1091. DOI: 10.1016/j. mechmachtheory.2008.05.005

5 N.T. Pavlović, N.D. Pavlović, "Design of Compliant Cognate Mechanisms", Proceedings in the 4th international conference mechanical engineering in XXI century, Niš, 2018, pp. 253-258.

6 N.T. Pavlović, N.D. Pavlović, "Improving of Mechanical Efficiency of Compliant Mechanisms",50th Internationales Wissenschaftliches Kolloquium Technische Universität Ilmenau, 2005

7 N.T. Pavlović, N.D. Pavlović, "Rectilinear guiding accuracy of Roberts-Чебышев compliant four-bar linkage with silicone joints", Механика на машините, vol. 12 (4), 2004, pp. 53-56.

8 Sebastian Linss and Andrija P. Milojević, Lena Zentner, “Considering the design of the flexure hinge contour for the synthesis of compliant linkage mechanisms”, 58th Ilmenau scientific colloquium, Ilmenau, 2014

9 Sebastian Linss, Andrija P. Milojević, “Flexure Hinges for Rectilinear Guiding with Compliant Mechanisms in Precision Systems for rectilinear guiding with compliant”, 58th Ilmenau scientific colloquium, Ilmenau, 2014

THE 5th INTERNATIONAL CONFERENCE
MECHANICAL ENGINEERING IN XXI CENTURY

December 9-10, 2020
Faculty of Mechanical Engineering in Niš, Serbia

Design of a New Micro-robotic Appendages Comprised of Active Thin-film Piezoelectric Material

Andrija MILOJEVIĆ[1], Kenn OLDHAM
[1] Laboratory of Intelligent Machines, Department of Mechanical Engineering, School of Energy Systems, Lappeenranta University of Technology, Yliopistonkatu 34, 53850 Lappeenranta, Finland
[2] Vibration and Acoustics Laboratory: Microsystems, Department of Mechanical Engineering, University of Michigan Ann Arbor, 2380C GGB (George G. Brown Laboratory), 2350 Hayward, Ann Arbor, MI 48109-2125, MI USA
Andrija.Milojevic@lut.fi, oldham@umich.edu

***Abstract*— This paper introduces, a novel MEMS terrestrial micro-robot structure, i.e. micro-robotic appendages, realized by utilizing recently developed thin-film piezoelectric actuators (PZT). Thin-film PZT's offer many benefits for the micro-robots, including large out-of-plane motions and fast actuation speeds. A synthesis methodology for micro-robotic appendages comprised fully of the thin-film PZT is presented. The developed method is inspired by structural topology optimization. Different obtained solutions of the robotic appendage designs are shown, and their performance is investigated. The deformation behaviour of the micro-robotic appendages is further verified via finite element method simulations. It is shown how such robotic appendages can realize a different range of output motions when all thin-films PZT is activated. The presented design method could lead to the realization of different MEMS micro-robots.**

***Keywords*— thin-film PZT, micro-robots, appendages, synthesis, optimization**

I. Introduction

In recent years micro-robotics has become a relevant and important research topic [1]-[3]. Traditional large-scale robots cannot be applied in all places where they are needed to solve various engineering problems. Micro-robots offer several benefits over classical ones: access to small places to perform inspection, exploration, monitoring without disturbance, and/or rescue missions, ability to realize targeted drug delivery or other biomedical interactions, a high degree portability and disposability, minimal power requirements to operate, and ability to work in teams thus exploiting swarm intelligence [3]. But often the actuation of robots at the micro-scale represents a challenge [4]. Different materials and actuation techniques have been proposed in the past, like electrothermal stick-slip actuation, electrostatic linear motors, electrothermal polymer actuators, and shape-memory alloy actuators [4], [5]. But these actuators [4], [5] have several drawbacks including limited forces, small payloads, limited range of motion, and slow actuation time i.e. reduced speeds. Recently developed thin-film lead-zirconate-titanate (PZT) piezoelectric actuators [3], [6] offer one promising solution for the micro-robot actuation due to high working density per unit area and fast actuation speeds. Thus, in this paper, the thin-film PZT is further utilized for the realization of MEMS terrestrial micro-robots, more specifically micro-robotic appendages.

Fig. 1 shows the conceptual design of one micro-robotic appendage proposed here. The appendage is comprised of multiple discrete thin-film PZT's (Fig. 1a and 1b). But when having multiple PZT actuators at one's disposal there is a question of how to realize the optimal design of such micro-robots. Previously, the design of MEMS terrestrial micro-robots included trial and error approach [6] or seeking inspiration from nature [3], where the synthesis process has been mostly left to the designer choice. Thus. the general synthesis framework is lacking.

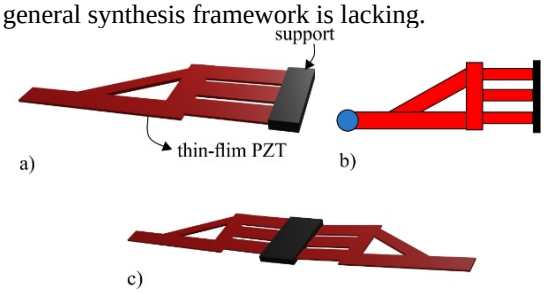

Fig. 1 Conceptual design of the thin-film PZT based micro-robot: a) design of one robotic appendage; b) corresponding beam like representation; c) full design of the micro-robot with two appendages

In this paper, the synthesis methodology for the automated optimal design of the micro-robots/micro-robotic appendages comprised of thin-film PZT is developed. The introduced method is inspired by topology optimization [7], [8], and includes several synthesis steps-problem setup, parameterization, and optimization. Different obtained solutions for the robotic appendage designs are presented, realized for various initial problem setups, where their performance is investigated. The deformation behaviour of the micro-robotic appendages is further verified via nonlinear finite element method simulations. It will be shown how such optimized robotic appendages can realize a different range of output motions when all the thin-film PZT's are activated.

In our previous paper [9], the synthesis method for the micro-robotic appendages comprised of passive soft (parylene-C), passive rigid (Si), and active (thin-film PZT) elements is introduced. In this paper, the synthesis method is realized for the appendages that are comprised fully of active thin-film PZT elements.

II. Synthesis Method for the Thin-Film PZT Micro-Robotic Appendages

The goal of the synthesis is to realize the optimal design of a micro-robotic appendage that can achieve relatively large output displacement of its end-effector when all thin-film PZT's are activated. In other words, the goal is to find optimal distribution of discrete thin-film PZT's net, forming the robotic leg topology that can achieve the set task (maximal output displacement in the desired direction of motion). From a synthesis perspective the robotic appendage is comprised of only active beam-like elements:

- thin-film PZT actuators, with three layers: top- Au, middle- PZT material, and bottom- SiO_2 (Fig. 2),

where thin-film PZT contracts and bends when the input voltage is applied. Here PZT's represent an inherent part of the appendage structure, and they deformed with the whole micro-robot. Further, the actuators serve as both force generators and structural elements of the appendage design.

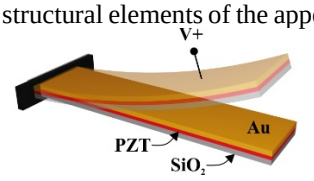

Fig. 2 Thin-film PZT actuator model

To develop the synthesis, a structural topology optimization approach is adopted [7] and evolutionary optimization algorithms are utilized [8], [9]. Past work in structural optimization in the MEMS domain includes mainly topology synthesis of structures comprised of only passive elements [10], a combination of different passive materials [7], both passive and active materials [8], [9], or only active materials [11]. But all these approaches [7] - [11] are limited to planar 2D problems. To realize the optimal design of micro-robotic appendages that can achieve motion in different directions in space, the spatial 3D structural optimization approach is developed here, considering only active materials (not reported before).

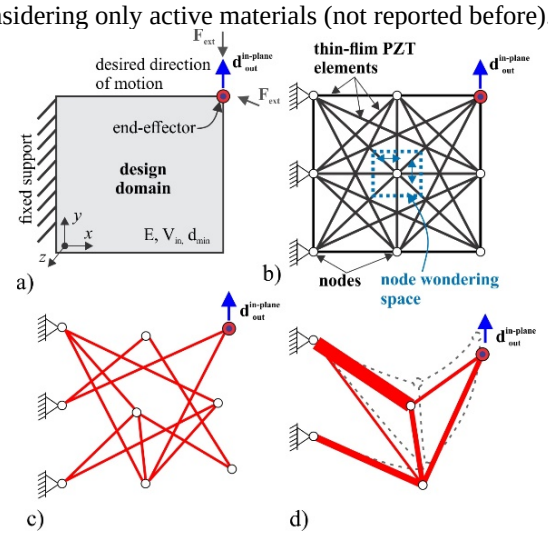

Fig. 3 Synthesis of the thin-film PZT micro-robotic appendage: a) problem definition; b) parameterization; c) optimization; d) illustration of obtained optimal appendage design solution (deformation position shown with dash lines)

The proposed synthesis framework includes the following steps:

- problem definition – setting the initial design problem, parameters, and desired performances (Fig. 3a),
- parameterization – translation of the problem definition into a set of variables that can be optimized (Fig. 3b),
- optimization – application of search algorithm to find the optimal solution of the given problem (Fig. 3c and 3d).

The synthesis steps are described in detail in the next subsections.

A. Problem Definition

As a first step in the synthesis process, a problem needs to be defined (Fig. 3a). This includes defining the design domain shape and size (space where the micro-robotic appendage solutions should fit) – here the rectilinear design domain is defined, end-effector output point – the upper right edge point is selected, the desired direction of output motion – the Y direction is set, location of the supports – left edge part of the design domain is selected, desired input voltage for the thin-film PZT's, external forces that act on the appendage – here placed at the end-effector point in directions opposite of the desired direction of motion, material characteristic for the PZT (Young modulus), and other constraints (volume of the structure, desired minimal displacement). Although a planar-appearing problem is defined (due to MEMS fabrication requirements), the spatial analysis is realized in 3D (appendage can realize motion in the out-of-plane direction as well). The rest of the design parameters are given in Table 1.

Table 1 Design Parameters for the Synthesis of Micro-Robotic Appendages

Parameters	**case 1**	**case 2**
design domain size	1000 x 1000 μm	
net size	3 x 3	
end-effector	node 3	
supports	nodes 1, 4, 7	
total number of thin-film PZT elements	28	
input voltage	V_{in} = 15 V	
element modulus	E_{base} = 80 GPa, E_{PZT} = 56 GPa, E_{top} = 60 GPa	
element out-of-plane thickness	t_{base}=0.5 μm, t_{PZT}= 1 μm; t_{top}=1 μm	
range of element width	w_{PZT} = 50:10:150 μm	
node wandering region	50 x 50 μm	100 x 100 μm
external loads	F_y = 1 μN, F_z= 1 μN	
minimal desired end-effector displacement	d_{out}^{des} = 1 μm	

B. Parameterization

The next step in the synthesis is parameterization. The given design problem needs to be somehow translated into a set of variables that can be optimized. Here for the parameterization, the ground structure approach (GSA) is used [8]. The design domain is discretized by a net of nodes and beam elements connecting these nodes (Fig. 3b). The initial ground structure represents a design space among which the optimal solution is search (i.e. initial guess), where all the elements represent active thin-film PZT. The optimal design is reached by simultaneous turning on/off the individual elements from the ground structure (Fig. 3c). Thus here, the design variable t_{el}^{i} is set, which can take values 0 and 1; 0 meaning that the selected element will be eliminated from the structure. For each of the elements, one

such variable exists, meaning that number of variables i is equal to the total number of elements. Additionally, the width of thin-film PZT elements is optimized as well. Thus for each element variable t_{wel}^{i} that defines the possible width of elements is set, ranging from 50 μm to 150 μm, dictate by fabrication possibilities. The out of the plane thickness of the PZT is predefined rather than optimized due to manufacturing limits. To realize shape optimization of the appendages, a node wandering approach is applied [10]. The length and position of the individual thin-film PZT are optimized by allowing individual nodes of the structure to wander within predefined design space. Thus, for each node, two variables n_x^j, n_y^j exist that defines the node wandering range in two directions in in-plane.

Initially, all the nodes in the ground structure are interconnected (Fig. 3b), leading to a fully connected ground structure. But such an initial structure can lead to solutions with overlapping elements (one thin-film PZT on top of other), which are difficult to produce in the micro-domain. Thus, a certain filter is applied that eliminates these overlapping elements before the optimization. Further, such reduced ground structure can lead to appendages solutions that contain intersecting overlaying elements (one above the other, where elements cross each other forming imaginary intersecting point). The potential appendage structure with overlaying crossing elements is also changeling to realized. To eliminate this, a filter in form of a computer algorithm is developed that searches the intersecting points between elements, where the total number of such intersections is minimized.

The structure net size, number of nodes and elements, number and range of variables, and other discretization parameters are given in Table 1.

C. *Optimization of the Thin-Film PZT Micro-Robotic Appendages*

In the end, the optimization is realized (Fig. 3c). A search algorithm needs to be applied to find the optimal solution of the set problem i.e. to find the optimal design of the robotic appendage among the initial set structure (Fig. 3d). Here is a search method, the optimization is applied. The goal of the optimization is to obtain a micro-robotic appendage solution that can achieve large output displacement of its end-effector when thin-film PZT is activated. In other words, the goal is to maximize the end-effector output displacement.

For optimization to reach the desired goal, an objective function is needed, based on which the performances of the appendages will be evaluated as well. Several function formulations are investigated for the design of the micro-robotic appendages, via a trial-and-error approach. The final form of the objective function that is used for the appendages synthesis is given in:

$$\max\left[d_{out} - w_1 \cdot d_{out}^{\perp} - w_2 \cdot d_{ext} - w_3 \cdot \left(d_{out}^{des} - d_{out}\right) - w_4 \cdot n_{int}\right] \quad (1)$$

where:

- d_{out} represent the realized output displacement of the end-effector- here set to be maximized,
- $d_{out}^{\perp}$ is end-effector displacement in the direction perpendicular to the desired direction of motion – here formulated to be minimized,
- d_{ext} is the end-effector displacement when external forces are acting – minimized so that relatively large appendage payload capacity can be achieved,
- d_{out}^{des} represent the desired minimum value of the output displacement that needs to be realized – formulated so that this condition is achieved,
- n_{int} is the total number of intersections in the structure – here set to be minimized.

It is important to mention that the synthesis of the micro-robotic appendages represents the multiobjective optimization problem that is reduced to a single-objective problem by using weighting constants. The terms in the Eq. (1) are calculated by using linear analysis, implemented in the optimization.

Among many different existing optimization algorithms, here the Genetic Algorithms (GA) are applied [8]. The design of the micro-robotic appendages represents a complex problem with a design domain that contains a large number of variables with many possible solutions. GA's are especially suitable for finding a global optimum over a space with a large number of variables. Further, GA's represent a discrete optimization method that is suitable for solving discrete problems (the micro-robotic appendages represent a discrete like structures where elements are either on or off). Moreover, the GA's have been efficiently applied before in the structural optimization problems [8], [10]. The Genetic Algorithm parameters that are used for the synthesis of the micro-robotic appendages are the initial population of 200 designs, a total of 1000 generations, selection function type roulette, crossover probability of 95%, elite count of 2 members, and mutation probability of 9%.

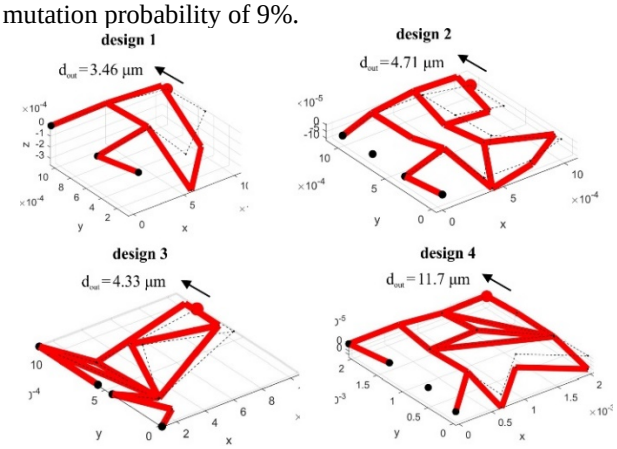

Fig. 4 Obtained optimal solutions of the thin-film PZT micro-robotic appendages designs realized for different synthesis parameters and weighting constants (deformed position is shown with dash lines)

D. *Results*

Multiple GA's are run for the set synthesis problem (Fig. 3a). During the optimization, thin-film PZT's are simultaneously turned on and off from the initial ground structure, and the width of the elements is varied (Fig. 3b and 3c). The remaining PZT's in the structure will form the potential optimal design of the micro-robotic appendage (Fig. 3d). This process is repeated where for each generation, the resulting appendage design performance is evaluated via the Eq. (1). The solution that best satisfies the objective function, in the last generation, is selected as the optimal appendage design.

Different solutions of the appendages are obtained for the various initial synthesis parameters and different values

of weighting constants. Fig. 4 show some of the realized optimal designs of the micro-robotic appendages. Based on the results it could be concluded that all the appendages solutions realize end-effector displacement in the desired direction when all thin-film PZT's are activated.

III. Finite Element Analysis of the Micro-Robotic Appendages Solutions

To verify the obtained results (Fig. 4) and investigate the appendages deformation behaviour when thin-film PZT's are active a nonlinear Finite Element Method- FEM simulations are performed. The FEM simulations are exemplarily realized for the two appendages designs.

Based on the obtained solutions (Fig. 4) a solid 3D models of the micro-robotic appendages are designed (Fig. 5a). The designs reflect the characteristics and components of the porotypes that would be produced. The FEM simulations are realized by using commercially available software *Comsol Multiphysics*. The structural mechanics coupled with the piezoelectric module is used from the *Comsol* available problem setup. The FEM problem definition includes applying the Au material to the upper layer, the PZT-5H to the middle layer, and SiO_2 to the bottom layer of the whole appendage structure (Fig. 5a). The fixtures are applied at the surfaces that correspond to the location of the supports in optimized designs (Fig. 4), while the input voltage (15 V) is applied at the upper surface and the ground is applied at the bottom surface of the PZT layer (Fig. 5a). The realized output displacement of the end-effector (the point at the same location as in Fig. 4), is read out from the FEM analysis.

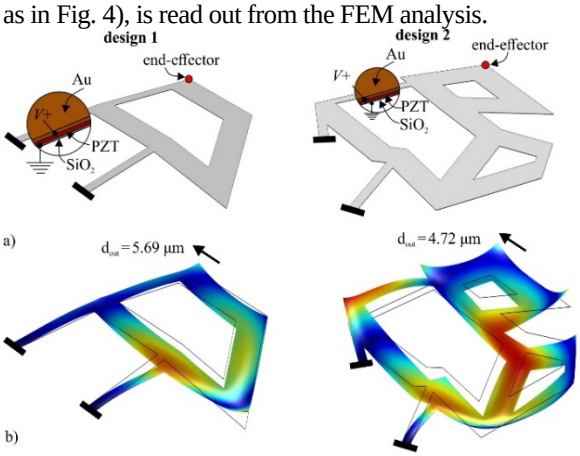

Fig. 5 a) 3D solid model of the micro-robotic appendages designs and FEM setup; b) deformation behaviour of the appendages when the input voltage is applied (results of FEM simulations)

Fig. 5b shows the deformation behaviour of the micro-robotic appendages when thin-film PZT's are activated. In both cases, the appendages realize displacement in the desired direction of motion. A similar range of motion is realized like in the case of optimized design (Fig. 4), with notably higher out-of-plane deformations due to the curly of the PZT's, large deformations, and nonlinear effects that could not be captured with linear analysis from the optimization. But nonetheless, the initial results show that the developed synthesis approach can lead to micro-robot solutions that realize the motion of the end-effector in the desired direction of motion.

IV. Conclusions

The proposed topology-based synthesis demonstrates a first implementation of design synthesis for multi-element, fully-active structural design, applied to the problem of appendage design in micro-robots. Results provide candidate designs for micro-robot legs with comparatively large vertical displacement relative to compliance under an external load, dependent on weighting for specific criteria in the objective function.

The approach for the micro-robotic appendage designs does have some limitations due to implemented linear analysis. Still, nonlinear FEM simulation confirm that obtained solutions of the appendages can realize desired output motions under assumed material properties and thin-film thicknesses. The presented method can be utilized further for the development of different micro-robotic appendages that are fully comprised of thin-film PZT actuators.

Acknowledgment

This work was supported by the Academy of Finland Research Council for Natural Sciences and Engineering [grant number. 318390].

References

[1] S. Palagi, and P. Fischer, "Bioinspired microrobots. Nat. Rev. Mater., vol 3, pp. 113–124, 2018.

[2] M. Sitti, and D.S. Wiersma, "Pros and Cons: Magnetic versus Optical Microrobots," Adv. Mater. 2020, p. 1906766, 2020.

[3] K. Oldham, J. Pulskamp, R. Polcawich, P. Ranade, and M. Dubey, "Thin-film piezoelectric actuators for bio-inspired micro-robotic applications," Integrated Ferroelectrics, vol. 1, pp. 54–65, 2007.

[4] J.E. Huber, N.A. Fleck, and M.F. Ashby, "The selection of mechanical actuators based on performance indices," Proc. Mathematical, Physical and Engineering Sciences, vol. 453, pp. 2185–2205, 1997.

[5] Sugita K., Tanaka D., Ono S., Chiba S., Iwata K., Han Y., et al., "SMA actuator and pulse-type hardware neural networks IC for fast walking motion of insect-type MEMS microrobot," in Advanced Intelligent Mechatronics (AIM), 2016 IEEE International Conference on, 2016, pp. 431-435.

[6] J. Qu, J. Choi, and K.R. Oldham, "Dynamics structural and contact modeling for a silicon hexapod microrobot," Journal of Mechanisms and Robotics, vol. 9, pp. 061006, 2017.

[7] A. Saxena, "Topology design of large displacement compliant mechanisms with multiple materials and multiple output ports," Structural and Multidisciplinary Optimization, vol. 30, pp. 477–490, 2005.

[8] A. Milojević, and N.D. Pavlović, "Development of a new adaptive shape morphing compliant structure with embedded actuators," Journal of Intelligent Material Systems and Structures, vol. 27, pp. 1306-1328, 2016.

[9] A. Milojević, V. Krokhmal, B. Wu, and K. Oldham, "Topology Optimization of Micro-robotic Appendages Combining Piezoelectric, Polymer, and Silicon Beams," In: 2019 International Conference on Manipulation, Automation and Robotics at Small Scales (MARSS), pp. 1-6. Helsinki, Finland, 2019.

[10] L.L. Howell, S.P. Magleby, and B.M. Olsen, Handbook of Compliant Mechanisms. Chichester: John Wiley & Sons, 2013.

[11] R.E.K. Moussa, M. Grossard, M. Boukallel, N. Chaillet, and A. Hubert, "Observation-oriented design of a monolithic piezoelectric microactuator with optimally integrated sensor," 41st International Symposium on Robotics and ROTOTIK 2010., Jun 2010, Munich, Germany. Verlag, 1, pp. 954-961, 2010.

THE 5th INTERNATIONAL CONFERENCE
MECHANICAL ENGINEERING IN XXI CENTURY

December 9-10, 2020
Faculty of Mechanical Engineering in Niš, Serbia

Design Optimization of Terrestrial-Walking Soft Robots

Andrija MILOJEVIĆ[1], Kyrre GLETTE[2]

[1] Laboratory of Intelligent Machines, Department of Mechanical Engineering, School of Energy Systems, Lappeenranta University of Technology, Yliopistonkatu 34, 53850 Lappeenranta, Finland
[2] RITMO Centre for Interdisciplinary Studies in Rhythm, Time and Motion, Department for Informatics, University of Oslo, P.O box 1080 Blindern 0316 OSLO, Norway
Andrija.Milojevic@lut.fi, kyrrehg@ifi.uio.no

***Abstract*—Unlike classical rigid body-based robots, soft robots are built from soft materials and they utilize elastic deformation (of its body) to achieve motion and different tasks. This paper introduces a new type of soft terrestrial walking robots realized by using compliant mechanisms. The synthesis approach for the optimal design of terrestrial robots is presented i.e. for one soft robotic leg. The design method is based on a structural optimization approach and using evolutionary algorithms, here expanded to spatial problems and topologies. Two different obtained solutions of the robotic legs are shown, and their performance is investigated. Based on this a concept of full two-leg robots is realized. The deformation behaviour of the designs is further analysed using the nonlinear finite element method. The prototype of one terrestrial two-leg soft robot is shown as well. The presented synthesis method and robot designs can lead to the realization of different types of walking soft robots with advanced locomotion capabilities.**

***Keywords*— Soft robotics, synthesis, evolutionary algorithms, compliant mechanisms, terrestrial robots**

I. Introduction

In recent years soft robotics became a very relevant and expanding research field [1]-[9]. Unlike classical rigid body-based robots, soft robots are usually built from soft/elastic materials and they utilize elastic deformation (of its body) to realize motion and different tasks [1]. Due to their continuously deformable-body soft robots offer several advantages over traditional ones: simple to realize, a low-cost solution, can move through small and confined spaces, safe interaction with humans, theoretically can reach every point in space with infinity number of configurations and overcome limited degrees of freedom of rigid systems, can realize fast shape changing, and achieve various locomotion gaits [1]. Different solutions of soft robots are introduced in the past like continuous robots [2], soft grippers [3], terrestrial robots- crawling [1], walking [4], and running/galloping [5], or swimming/underwater [6], [7], and untethered robots [1]. In this paper, terrestrial soft robots are of special focus [1], [4], [5]. These robots utilize elastic deformation of its body and can realize motion over different terrains without the need for complicated control algorithms, making them advantageous over classical robots. Most of the previously developed concepts of terrestrial soft robots are based on fluid-mechanically driven soft elastomer actuators i.e. pneumatically driven structures [8]. Rarely other concepts are explored like hybrid soft robots (tendon driven) [4] or smart material actuators [9]. Such robotic concepts have different disadvantages: limited range of motion, slow locomotion speeds, and small payload. Moreover, the synthesis of terrestrial soft robots is mostly based on designer experience, using a trial and error approach, or seeking inspiration from nature (insect, animal-like) [4], [7]. A unified synthesis method for the design of rigid body based terrestrial robots has been done in [10], [11] but it is rarely introduced for soft robots and mostly is focused on pneumatically driven structures [12]. Thus, this paper proposes a synthesis framework for the optimal design of a new type of terrestrial soft walking robot developed by utilizing compliant mechanisms [13].

Unlike classical rigid-body mechanisms, compliant mechanisms represent monolith structures that achieve motion/force transmission via elastic deformation of its segments. Compliant mechanisms offer many advantages over conventional ones like reduce complexity, monolithic concept, easy to manufacture, no assembly, wear or friction, zero backlashes, no lubrication, can be scale down easily, high precision, build-in restoring force, and low-cost. Thus, compliant mechanisms are very suitable for the realization of soft robots and are used here for the development of the terrestrial walking robots that can overcome most of the disadvantages of existing solutions [1], [4].

The synthesis method for the optimal design of these robots is presented for one robotic leg (as based on these multiple leg robots can be realized). Here the designer only needs to define the desired input parameters and thought algorithmic (computer-based) approach the optimal solution of the robotic leg is automatically obtained. The design method is developed based on the structural optimization approach [13] and evolutionary optimization algorithms [14], but here expended to spatial problems. Two different solutions of the robotic leg are obtained for different problem setups, and their performances is investigated (realized range of motion as one of the important parameters). Based on these solutions, a concept of a full two-leg walking robot is realized. The deformation behaviour of the soft terrestrial robots is further investigated via nonlinear finite element method analysis. Exemplarily, the prototype of one two-legged soft robot is produced via 3D printing. We show how such a concept of walking soft robots can realize a relatively large range of output motions when only small input displacement is needed.

The proposed terrestrial robots can be used in different applications for inspection, monitoring, sample collection, transport, and in future planetary explorations.

II. Synthesis Method

The main goal of the synthesis is to obtain the optimal design of one soft robotic leg that can realize relatively large output displacement of its end-effector (tip of the robotic leg that comes in contact with the ground) when small input displacement is applied. In other words, the goal is to obtain a robotic leg solution that can achieve a high motion transmission ratio (geometric advantage- GA of the leg mechanism), as then actuators that realize small input strokes can be used (e.g. smart material based actuators [9]). The optimal solution of one robotic leg is synthesized first, as based on these walking robots with multiple legs can be realized.

To develop a synthesis framework, a structural topology optimization approach is adopted [13], [14], but here expended and realized for spatial problems. The outline of the developed methodology for the optimal design of terrestrial walking soft robotic leg is illustrated in Fig. 1. The synthesis steps include:

- problem setup – definition of desired input parameters (Fig. 1a),
- parameterization – translation of defined problem into a set of variables that can be optimized (Fig. 1b),
- optimization – application of search algorithm to find the optimal solution of the given problem (Fig. 1c, 1d, 1e).

The steps are described in detail in the following subsections.

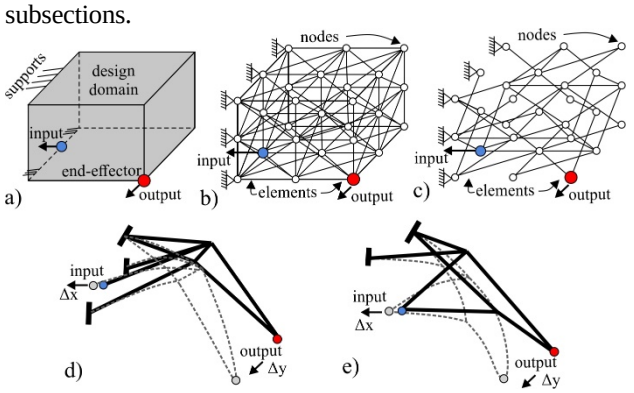

Fig. 1 Synthesis of terrestrial walking soft robots (realized for one robotic leg): a) problem setup; b) parameterization; c) optimization process; d) optimal solution of soft robotic leg design 1 (deformed position shown with dash lines); e) optimal solution of soft robotic leg design 2 (deformed position shown with dash lines)

A. Problem Setup

As a first step in the synthesis, the problem needs to be defined (Fig. 1a). Problem setup includes defining the design domain (space in which the robotic leg solution needs to fit) were here the rectilinear shape is defined, the location of the input actuation port (here defined at the mid-bottom edge part of the design domain left side), the direction of input displacement (*X* direction is selected), location of the robotic leg end-effector point (right-bottom edge point is selected as output point), the desired direction of leg output motion (here defined in the Y direction), supports (placed at the left side of the design domain), external loads that act on the robotic leg (here applied in all three directions at leg end-effector), material properties for the soft robotic leg (Young modulus), and other constraints (e.g. the desired volume of the leg mechanisms solution and minimal value of the output displacement that needs to be achieved). The rest of the design parameters are given in Table 1. Two synthesis cases are realized for different values of design domain dimensions (Table 1).

B. Parameterization

The next step in the synthesis process is the parameterization of the set problem (Fig. 1b). The design domain needs to be somehow represented by a set of variables that can be optimized. Here the parameterization is realized by using the Ground Structure Approach (GSA) [13] but developed for the spatial-3D topologies. Thus, the design domain is divided by the net of nodes and beam elements connecting these nodes. The ground structure (Fig. 1b) serves as an initial guess, among which the optimal robotic leg design is searched. Elements are simultaneously turned on and off from the initial ground structure to yield the optimal solution. Here the variable that turns on/off the individual elements is defined- t_{el}^{i}. The variable can take values of 0 and 1; 0 meaning that the selected element will be removed from the initial structure. For each of the elements, one such variable exists t_{el}^{i} (i is equal to the total number of elements). The thickness of elements is predefined rather than optimized, to simplify the synthesis process. The initial net size, total number of elements, and rest of the parameters used for the soft robotic leg optimization are given in Table 1.

Table 1 Design parameters for the soft robotic legs synthesis

Design parameters	**case 1**	**case 2**
design domain (mm)	50 x 30 x 20	50 x 50 x 25
grid size	3 x 3 x 2	
number of elements	89	
input port	13	
output port	18	
supports	1, 4, 7, 10, 15	
element thickness (mm)	1	
element modulus (MPa)	800	
input displacement - d_{in}	5	
external loads (N)	2	
minimal desired output displacement (mm)	1	
desired volume - L_{des}^{el} (mm)	185	220

C. Optimization

As a final step in the synthesis process, the optimization is realized. A search algorithm needs to be defined to find the optimal solution of the set problem (Fig. 1c).

The main goal of the optimization is to realize a soft robotic leg design that can achieve a relatively large output displacement of its end-effector (output point) when small input displacement is applied (so that most of the available smart material actuators can be used [9]). This means that the large motion transmission ratio of the robotic leg mechanism will be realized. Here the transmission ratio is also defined as a geometric advantage- GA of the mechanism, and it is calculated as:

$$GA = \frac{d_{out}}{d_{in}} \tag{1}$$

where d_{out} represents achieved output displacement of the robotic leg end-effector and d_{in} is applied input displacement. Thus, GA represents a term that needs to be maximized.

The objective function is needed to drive the optimization algorithm towards a set goal. The resulting formulation of the objective function that will lead to desired robotic leg solutions is given as:

$$\max\left[\frac{d_{out}}{d_{in}} - w_1 \cdot d_{ext} - w_2 \cdot d_{out}^{\perp} - w_3 \cdot \left|L_{des}^{el} - L_{real}^{el}\right| - w_4 \cdot n_{\text{int}}\right] \quad (2)$$

where d_{ext} represents the displacement of end-effector when external loads are applied (here minimized to realize robot with larger payload capacity), $d_{out}^{\perp}$ is the displacement of the end-effector in a direction perpendicular to the desired direction of motion (here set to be minimized to achieve linear motion), L_{des}^{el} is the desired volume of a robotic leg design (expressed as the total sum of all elements length), L_{real}^{el} is the realized volume of robotic leg structure, and n_{int} represents the total number of interesting points (crossing points between overlapping elements) in the structure that needs to be minimized (this is set to yield a robotic leg designs that could be easily manufactured). It is important to mention that the synthesis of a soft robotic leg represents a multiobjective optimization problem, reduced to a single-objective problem by using weighting constants w_j. All the terms in the objective function Eq. (2) are calculated by using linear analysis, implemented in the optimization algorithm.

Among many different Evolutionary algorithms (EA) here the Genetic Algorithms [13], [14] are applied as the optimization search method. Due to a complex design domain with a large number of variables, the design space contains many possible optimal solutions. EAs are very efficient in finding global optimum over a large design space. The synthesis of soft robotics legs represents a discrete problem (discrete like structures, Fig. 1) where the variables are discrete as well (elements are either on or off). EAs are also suitable for solving discrete optimization problems. Moreover, EAs have been efficiently used in structural optimization problems [13], [14], thus they are utilized here as well. The Genetic Algorithm parameters that are used for the synthesis of the soft robotic leg are given in Table 2.

TABLE 2 GENETIC ALGORITHM PARAMETERS FOR THE SOFT ROBOTIC LEG SYNTHESIS

Parameters	Values
Initial population	200
Generations	200
Selection function type	roulette
Crossover probability	95%
Elite count	2
Mutation probability	9%

D. Results

Multiple EAs runs (5) are conducted for both investigated synthesis cases (Table 1) to reach the optimal solution of the soft robotic legs. During optimization elements are simultaneously turned on/off i.e. some elements are kept and some elements are eliminated from the initial ground structure (Fig. 1b and 1c). The process is repeated and the remaining elements in the structure will form the robotic leg solution. The performance of the leg designs is evaluated based on the objective function values, and the solution that best satisfies the Eq. (2) in the last generation is taken as the optimal.

Fig. 1d and 1e show two obtained solutions of the soft robotic leg realized for the set problem cases (Table 1). Both robotic leg designs realize output displacement of the end-effector in the desired direction of motion when input displacement is applied. Table 3 shows the characteristics of the obtained soft robotic leg solutions. High values of the geometric advantage (GA) are realized in both cases. Notably, solution 1 achieves much higher GA but have higher stiffness as well, where lower values of GA are realized with solution 2 having lower stiffness of the robotic leg structure.

TABLE 3 PERFORMANCE PARAMETERS OF SOFT ROBOTIC LEG DESIGNS

Design	GA	d_{outY} (mm)	F_{in} (N)	stiffness (N/m)	d_{ext} (mm)
1	8.61	43	0.71	142	21.43
2	2.73	13.66	0.13	26	2.39

III. NONLINEAR FINITE ELEMENT METHOD CHARACTERIZATION AND PROTOTYPE

Based on the obtained solutions (Fig. 1d and 1e) a 3D solid models of a full two-leg robot are designed (Fig. 2). To verify the optimization results and investigate the deformation behaviour of the terrestrial soft robots, nonlinear Finite Element Method (FEM) simulations are performed using software ABAQUS. For the FEM analysis setup, the input displacement of 5 mm at the input port of both robotic legs (Fig. 2a) is applied, to simulate the action of the contracting actuator. The fixed support is applied at the bottom surface part of the robot body to investigate only the leg mechanism motion characteristics. The realized output displacement of the robot end-effector and required input force are read out from the analysis. Fig. 2b shows the obtained FEM results for both solutions of the two-leg soft walking robots.

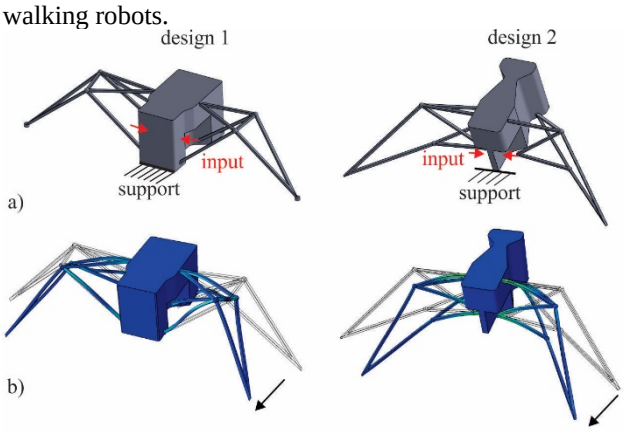

Fig. 2 Two leg terrestrial walking soft robots: a) 3D solid design and FEM setup; b) FEM simulation results- deformation behaviour when input displacement of 5 mm is applied at each leg

It could be seen that in both cases robotic legs realize output motion in the desired direction when input displacement is applied, like the optimization predicted (Fig. 1d, 1e). Fig. 3 shows the results of the realized GA and required input force to drive the motion of one robotic leg with respect to the applied input displacement.

In the case of robotic design 1, high GA values are achieved for smaller input displacement. The GA drops as input motion increase, due to the large deformations of the leg structure and nonlinear effects that could not be captured in the optimization with linear analyses. But still, high values of GA are realized. For design 2, mostly constant GA is achieved through the motion, as nonlinear effects are notably less expressed.

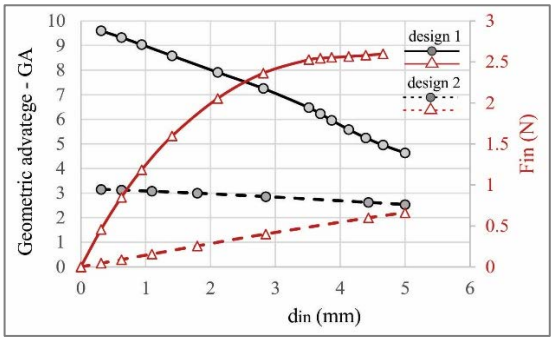

Fig. 3 Realized geometric advantage – GA and required input force for the two-leg terrestrial walking soft robots (Fig. 2) concerning the applied input displacement

Table 4 shows the results for maximal and average values of realized GA and required input force. Compare to results from optimization (Table 3), a similar range of values are realized, especially in the case of soft robotic design 2.

TABLE 4 FEM RESULTS FOR TWO-LEG SOFT ROBOTIC DESIGNS

Design	GA max	GA average	F_{in} max (N)	F_{in} average (N)
1	9.6	6.98	2.62	1.89
2	3.15	2.9	0.66	0.27

Exemplary the prototype of one terrestrial soft robot is realized via 3D printing (Fig. 4). The initial test shows that a similar output motion of the leg end-effector is realized when input displacement is applied at the input port.

Fig. 4 Prototype of the terrestrial walking soft robot design 1 realized with 3D printing

IV. CONCLUSIONS

This paper introduces a new synthesis method for the optimal design of a novel terrestrial walking soft robots, realized by using compliant mechanisms. It is shown how with the developed method, the optimal solution of one soft robotic leg can be realized, based on which walking robots with multiple legs can be developed. Two different solutions of the robotic legs are obtained for different initial design parameters. Based on these the two-leg terrestrial soft robots are realized, and their deformation behaviour is verified via nonlinear FEM simulations. An initial porotype of one soft robot is presented as well. In general, the results show that the proposed synthesis method can lead to optimal solutions of walking soft robots that realize desired output motions, with even better performance than predicted by optimization (for a certain range of input displacement). Future work will include developing the soft robot with real smart material-based actuators and testing the robot locomotion over different terrains.

ACKNOWLEDGMENT

This work was supported by the Academy of Finland Research Council for Natural Sciences and Engineering [grant number. 318390]. This work was partially supported by the Research Council of Norway through its Centres of Excellence scheme, project number 262762.

REFERENCES

[1] S.I. Rich, R.J. Wood, and C. Majidi, “Untethered soft robotics,” Nature electronics, vol. 1, pp. 102-112, 2018.

[2] W. Felt, M.J. Telleria, T.F. Allen, G. Hein, J. Pompa, K. Albert, and D. Remy, “An inductance-based sensing system for bellows-driven continuum joints in soft robots,” Autonomous Robots, vol. 43, pp. 435–448, 2019.

[3] J. Shintake, V. Cacucciolo, D. Floreano, and H. Shea, “Soft Robotic Grippers,” Advanced materials, vol. 30, p. 1707035, 2018.

[4] M. Jiang, Z. Zhou, and N. Gravish, “Flexoskeleton Printing Enables Versatile Fabrication of Hybrid Soft and Rigid Robots,” Soft robotics, ahead of print, 2020.

[5] Y. Tang, Y. Chi, J. Sun, T-H. Huang, O.H. Maghsoudi, A. Spence, J. Zhao, H. Su, and J. Yin, “Leveraging elastic instabilities for amplified performance: Spine-inspired high-speed and high-force soft robots,” Science Advances, vol. 6, p. eaaz6912, 2020.

[6] T. Chen, O.R. Bilal, K. Shea, and C. Daraio, “Harnessing bistability for directional propulsion of soft, untethered robots,” Proceedings of the National Academy of Sciences, vol. 115, pp. 5698-5702, 2018.

[7] C.A. Aubin, S.J. Choudhury, A. Rhiannon, A. Lynden, J.H. Pikul, R.F. Shepherd, “Electrolytic vascular systems for energy-dense robots,” Nature, vol. 571, pp. 51 – 57, 2019.

[8] H-C. Fu, J.D.L .Ho, K-H. Lee, Y.C. Hu, S.K.W. Au, K-J. Cho, K.Y. Sze, and K-W. Kwok, “Interfacing Soft and Hard: A Spring Reinforced Actuator,” Soft robotics, vol. 7, pp. 44–58, 2020.

[9] P. Boyraz, G. Runge, A. Raatz, “An Overview of Novel Actuators for Soft Robotics,” Actuators, vol. 7, p. 48, 2018.

[10] H. Lipson, and J.B. Pollack, “Automatic design and manufacture of robotic lifeforms,” Nature, vol. 406, pp. 974–978, 2000.

[11] E. Samuelsen, K. Glette, and J. Torresen, “A hox gene inspired generative approach to evolving robot morphology”. In GECCO 2013 - Proceedings of the 2013 Genetic and Evolutionary Computation Conference, pp. 751–758, 2013.

[12] F. Corucci, N. Cheney, F. Giorgio-Serchi, J. Bongard, C. Laschi, “Evolving Soft Locomotion in Aquatic and Terrestrial Environments: Effects of Material Properties and Environmental Transitions,” Soft robotics, vol. 5, pp. 475–495, 2018.

[13] A. Milojević, and N.D. Pavlović, “Development of a new adaptive shape morphing compliant structure with embedded actuators,” Journal of Intelligent Material Systems and Structures, vol. 27, pp. 1306–1328, 2016.

[14] R. Parsons, and S, Canfield, “Developing genetic programming techniques for the design of compliant mechanisms,” Structural and Multidisciplinary Optimization, vol. 24, pp. 78–86, 2002.

THE 5th INTERNATIONAL CONFERENCE
MECHANICAL ENGINEERING IN XXI CENTURY

December 9-10, 2020
Faculty of Mechanical Engineering in Niš, Serbia

Smart Mitkovic External Fixation System for Bones

Sava RAMANOVIĆ, Nenad PAVLOVIĆ, Miloš STOJKOVIĆ, Žarko ĆOJBAŠIĆ

Faculty of Mechanical Engineering, University of Niš, Ul. Aleksandra Medvedeva 14, 18000 Niš, Srbija
savaramanovic@gmail.com, zcojba@gmail.com

***Abstract* — The use of external fixators has gained great popularity due to simple application, as well as the successful and fast treatment of bone fractures. In addition to the treatment of fractures, its use has found a place in bone correction surgery, such as in lengthening, angular correction, or reconstruction of long bones. These corrections were made manually until the advent of the computer assistance, which enables monitoring of the parameters of sensor use and positioning of the fracture fragments by means of actuators integrated into the fixator itself. This method of fracture treatment and bone correction led to flexibility of operational procedures, but the problem remained that the control and engagement of surgeons remained frequent. The aim of this research is to introduce the smart features in the external fixation system of Mitkovic type that would move actuators through the data obtained from the sensors and thus make a decision on postoperative treatment of the patient and reduce the engagement of the surgeon.**

***Keywords*— Mitkovic external fixator, smart system, bone lengthening, sensors, stepper motor**

I. Introduction

External fixation is a surgical treatment used to stabilize fracture of bone. They provide unobstructed access to the relevant skeletal structures for their primary healing and also for secondary interventions needed to restore bone continuity. External fixation contains two main components, the frame with its sub-components (bar, clamps, clamps carrier, and others optional elements) and the implants (Schanz pins, Kirschner wire or/and Stainnman pins). The frames are set outside a patient's body, where are with the help of clamps connected to implants which are into patient body, respectively shall screwed into fractured bone. External fixation is an alternative to internal fixation, where the components used to provide stability are positioned entirely within the patient's body.

Further the external fixation is used in bone correction surgery too, where it is used for angular correction, reconstruction and lengthening of bones. External fixators for angular correction are used when is important to correct “X”, “Y” or “O” form of lower extremities [1] and also this method is used when there is need to correct bed union of a bone, after fracture healing, and for other similar usages. Reconstructive external fixation is used for bone union when is there is one segment of long bone which is damaged or has to be removed [2], such as a gunshot wound, insidious infection, bone tumour or similar. External fixator for bones lengthening is used when it is necessary to increase length of bone [3], as is a case with shortened extremities in dwarf growth, asymmetrical length of extremities, or similar deformities.

For all mentioned cases different methods of the fixation are used with different mechanical designs for their aim [4]. Most of external fixation devices are pure mechanical medical devices without electrical or electronic components. In last decade of past century, designers are searching for solution about fixators which will be flexible to position a fracture segment. Results of these efforts are the Hexapod and Octopod frames, which are based on the Ilizarov’s circular external fixator, but those devices are very cumbersome to use manually and because of that the need to start developing of the computer aid software (CAS) emerged. In addition to the mentioned application, CAS is now starting to be developed for other types of applications. One of example is presented in the work [5] where the authors have developed CAS for simulation of reposition of the long bone fracture, in that case tibia and femur. It is provided that the surgeon can visualize the applied different treatment scenarios a priori per patient. In another paper [6] authors have presented advantage of CAS where it is to avoid the frequent use of fluoroscopy throughout operation process, when it used early in preoperative steps to measure parameters of fracture and choose a size of drill and pin and then locate applicable places for their placement.

Besides for circular frames, the computer aid software is applied for the unilateral (planar) eternal fixation frames, and also for the hybrid external fixation, which is combination of the previous two. In the study [7] authors used CAS for repositioning of the long bones with unilateral external fixation devices, which in this research are called the bone reposition devices. In study [8] CAS is applied on hybrid external fixation frame where CAS is used for reconstruction of fracture model from some type of source clinical images, then computer assisted reduction, and finally to prepare parameters data for the robot assisted reduction and for the control of actuators.

In paper [9] authors searched for possible solution to solve problems in the use of fixation frames, where complications and difficulties in promptly identifying problem occurrence and sensitivity to the specific co-morbidities (e.g. osteoporosis) with sometimes unreliable tracking of healing process, especially in cases of massive injuries and homecare of discharged patients, are considered. In order to face these challenges, authors in this research suggest using of self- and patient-aware,

sensing, smart and active external fixation devices. This development has been motivated by the need to identify the major requirements for the development of Internet of Things (IoT) platform for orthopaedics surgery. Authors presented several studies regarding aware, sensing, smart and active external fixation devices. In study regarding aware external fixation device a tag is embedded within fixation device, storing the detailed manufacturers (material, component-specific, type and dimensions), internal logistics (e.g. storage location, handling history), patient-specific (anonymized) general data, and others. In this sense, the fixation device is self and patient aware. In the second study regarding sensing external fixation device, device is equipped with sensing sensors, capable to observe, collect and store physiological and environmental data, continuously or in regular intervals. Device in this study contains several types of sensors for list of observations: injured bone electrical impedance is being measured non-invasively at discrete intervals, by using external fixation device's pins as electrodes; bone temperature is measured by the contact temperature sensor embedded in pins; force and torque values in clamps are being measured at discrete intervals; inertial sensor is embedded in the device and continuously collects data, based on which a sudden movement or an impact of the body/device can be inferred. In the third study regarding smart external fixation device, besides sensing capability, the fixation device also stores knowledge, relevant for making the meaningful conclusions by using the collected data. It also embeds the processing unit for making these conclusions. Following types of conclusions would become possible: the data, collected by the conductivity sensor is used in inferring the current healing stage of fracture; Contact temperature sensor observes critical temperatures likely to cause thermal necrosis, during the pin application; Force/torque sensors are capable to identify the suboptimal stress and deformation values, based on which the likely occurrences of the specific complications (namely, pin loosening and malunion) can be explicitly inferred; Variations in stress measurements can be combined with the data collected by the inertial sensor in order to infer the nature of these variations (sudden movement, possible impact). In final study in mentioned research regarding active external fixation device, active device is a realization of closed-loop control system with a feedback. In addition to the above listed capabilities, active device is capable: a) to report on the complication or the inferred healing stage transition (low risk research scenario), or in a long-term b) to trigger the corrective action, for example, to react on the incidental variation of the stress values by pin screw tightening.

In connection with the mentioned researches the study [10] could be mentioned, where the authors propose the improvement of a fixation device design, which implements paradigms of aware, sensing, smart and active devices and thus, enables real-time monitoring of bone fracture healing. The design is based on the discussion of possible complications and efficiency savings and it is implemented in the example of classifying patient's compliance to the prescribed behaviour in the postoperative treatment, namely to risk monitoring in a homecare. The authors state that the main prerequisite for effective, efficient, customized healthcare is to achieve access to vast data about the patient's pre-conditions, current health status, as well as patient's environment. Such access, combined with advanced data interpretation algorithms, facilitates accurate diagnoses and real-time decisions in treatment fine tuning and customization. It is presented how the device makes possible to make real-time observations regarding behaviour of the patient with fractured tibia in a homecare. Those observations can be easily used to alert or advise the patient in a real-time on adjusting the prescribed behaviour. Also, those observations scan can determine the cause of the mechanical issues in fixation device after their occurrences.

Devices application, healing and tracking complication occurrences highly depend on the experience of the surgeon. In addition, this does not fully consider the patient-specific circumstances and its relative compatibility with MRI procedures, which further introduces some difficulties in observing the healing stages and possible complications. Therefore, this case studies can be step to solve mentioned problems and many others, such as frequent x-ray exposure of a surgeon through operative and postoperative activities.

In this paper we are oriented solely towards bone lengthening fixation method. This is one of the familiar problems in orthopaedic long bone correction surgery, and its consequence is usually malunion fractures or congenital defects. In design of external fixation for mentioned purposes, we propose implementation of CAS to change a traditional manual actuation on compression-distraction (CD) device, replacing it with the mechatronic system. This mechatronic system mainly consists of a stepper motor, stress sensor and position sensor. This whole system is monitored by an intelligent controller. Also, this mechatronic system is IoT enabled [9][10] with aim to improve its functionality and efficiency of a patient postoperative treatment, and to reduce the frequency of medical examinations. For our research we used classic model of the Mitkovic external fixation for lengthening of lower limbs, product of Ortokon ltd., Niš, Serbia, which is upgraded to become the smart system for external fixation.

II. Material and methods

Mitkovic external fixator for lengthening of lower limbs, which is considered here, consists of one bar, telescope devices, compression-distraction devices (CD devices) and appropriate number of Clamps and Pins (Figure 1).

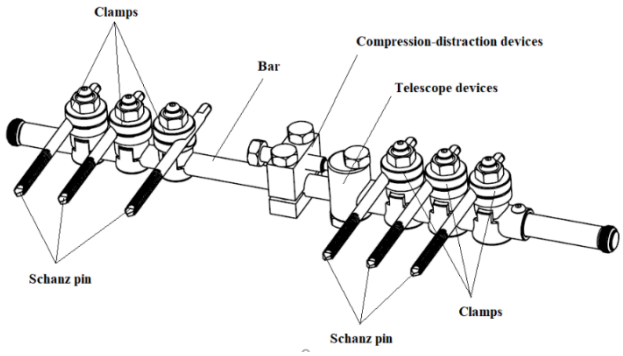

Fig. 1 Mitkovic external fixator for lengthening of lower limbs

Half of appropriate number of clamps are positioned on the telescope device's tube, where CD devices push telescope device along the bar. Telescope device carries appropriate number of clamps with them, those creating

the fragment bone transport in the direction of the desired lengthening.

In our proposed design CD device is changed with stepper motor with the pair of strain gauge sensors, that send feedback signal for actuation of stepper motor. The brain of this action should be an intelligent controller that would process the feedback from the strain gauge sensor and decides about the next step of the actuation or deactivation of stepper motor. Blok diagram of intelligent compression-distraction system is present in Figure 2.

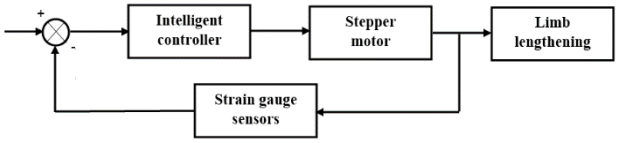

Fig. 2 Block diagram of actuation bone lengthening system with feedback information from strain gauge sensors

Model of the Mitkovic external fixator for lengthening of lower limbs with proposed installed stepper motor instead of the CD devices is presented in Figure 3.

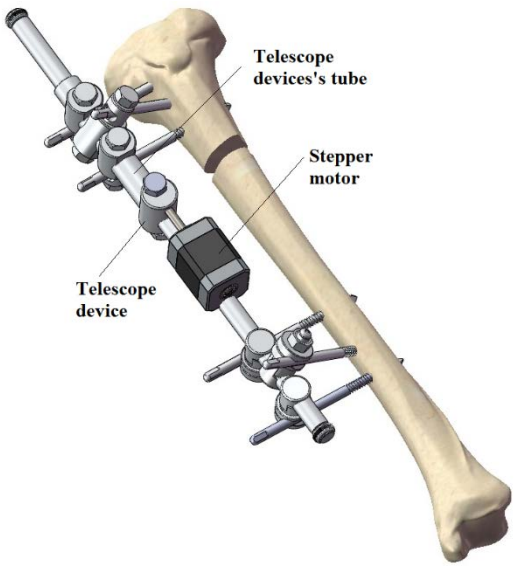

Fig. 3 Mitkovic external fixator for lengthening of lower limbs with installed stepper motor

One pair of the strain gauge sensors have been set on location of stepper motor's shaft, where they perform the necessary measurements (Figure 4).

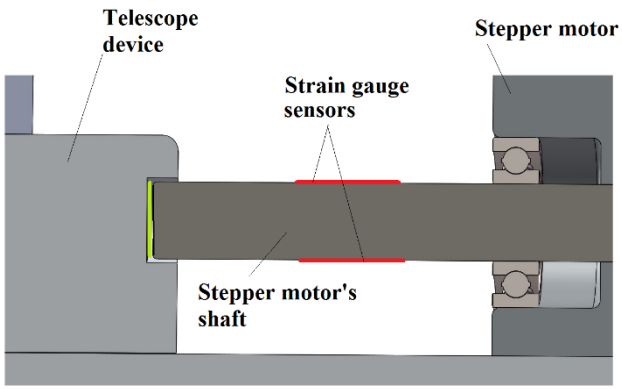

Fig. 4 Location of strain gauge sensors on the stepper motor shaft

Measurement of start and current position of the telescope devices can be helpful to measure a current bone lengthening status. This is very important for collecting necessary information for the objective of the surgical operation, and to stop the system actuation, when the satisfactory bone length is obtained.

The first implementation idea was for the measurement of current bone length to be carried out by the intelligent controller, which would convert the number of revolutions into a linear movement of the shaft. But it has been found that this method would bring a lot of risks in terms of information accuracy. Therefore the second approach was to position the IC distance sensor on the telescope devices. Such design makes the classic Mitkovic external fixation system for bone lengthening to be fully automated robotic system with the closed loop control. Such updated system block diagram is presented in Figure 5:

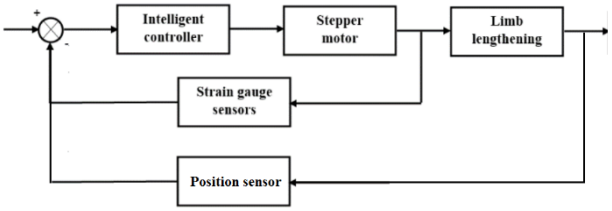

Fig. 5 Mitkovic external fixator for lengthening of lower limbs with installed full closed loop robotic system

Finally, to provide this system with smart capabilities, we add sensors mentioned in [9] [10]. These sensors collect information on the status of postoperative treatment, i.e. of bone lengthening. That is, to predict the occurrence of possible complications during treatment and send information to the surgeon, so that he can react timely.

III. Discussion

One of the problems in development proposed system is to determinate correct limit value of the resistance force when the bone is in the process of lengthening, and that information from sensor is sent to the controller for assessment and decision regarding next step in actuation of the system. Main parameter to determine this information is to find the threshold of pain. This can be individual for each patient, which depends on the constitution of the body, but also on the age of the patient. A lower limit must be set for each constitution and age of the patient, in order for the system to be safe and reliable for clinical use. Data of the threshold of pain may be collected before operation. This is the most important parameter regarding muscle stretching during bone lengthening and flexible postoperative treatment.

We have also carefully collected some information from other studies regarding bone lengthening and considered forces, in order to provide directions for further development of our smart Mitkovic fixator. The time of removal of the fixator is deduced from clinical and radiological information, independent of the stiffness result [11]. In a series of 30 leg lengthenings there were no refractures when the tibial stiffness had reached 15 Nm/° or the femoral stiffness reached 20 Nm/°. Applied measurement technique of stiffness included the temporary removal of the fixator. Clamps were applied separately for each set of pins to attach a goniometer for the measurement of angular displacement. The use of spirit levels in each clamp ensures consistency in the plane for both the goniometer and the displacement force. This measurement may have more to do with angular bone correction, but the results were certainly helpful.

Axial distraction force was found to vary according to the underlying pathology [12]. For post-traumatic shortening in adults both the peak and the resting forces rose steadily during lengthening reaching maximum forces of the order of 300 N. Patients with congenitally short limbs developed very high peak forces (in some cases over 1000 N) and also showed large amounts of force relaxation (typically 400 to 500 N). For these measurements authors used a pre-calibrated compression load cell that was incorporated within the lengthening mechanism of the fixator at the time of initial application.

Forces generated during limb lengthening in the distraction and consolidation phases have been measured on 19 patients between 6 and 22 years of age with 10 femoral and 11 tibial lengthenings of 1 mm/day by means of a monotube external fixator, fitted diaphysially and modified to measure tension and weight-bearing forces [13]. Peak force measured during the lengthening period amounted to about 14 N/kg of body mass. Generally, distraction forces levelled off at between 8 and 10 N/kg of body mass. During the consolidation period, the average force carried by the fixator dropped from 55% initially to about 10% of the force transmitted to the ground, consistent with increased load carrying capacity of the bone as healing progressed. The maximal length discrepancy was 72 mm on the femur and 70 on the tibia. For measurements the resistive strain gauge type with a full-bridge measuring has been used.

IV. Conclusions

In discussion section we have presented several data for parameters that are planned to be further included in our research. Regarding the step motor, it is expected to have the following specifications: to be light and not bulky; maximum elongation must be greater than 72 mm and to be able to overcome a force of 1000N. There are many models on the market that would meet the required specifications of the step motor. Problem remains the muscular resistance force during lengthening. We failed to gather enough relevant data to determine limit of resistance force when the bone is in process of lengthening and to determine reliable limit for broad groups of patients. And finally, the decision remains to be made regarding what is best to be used as an intelligent controller in proposed smart Mitkovic fixation device. In further research we will explore fuzzy, neuro and neuro-fuzzy controller alternatives, in order to provide for efficient use of expert knowledge and measured data alike.

This research is a first step in developing smart Mitkovic external fixator for bones lengthening of lower limbs. Besides controller development and other important remaining goals, future research must include In Vivo measurements involving patients. Many factors must be monitored that are discussed in previous sections. Still, we believe that there is a great potential in the presented research directions that could lead to significant results.

Acknowledgment

This research is part of the project “Artificial intelligence and Advanced FEM Based Biomedical Engineering - Next Level BME” from bilateral Serbia-Germany scientific co-operation programme and project “Research and Development of mechanical engineering systems of the new generation for the sake of technological development”, funded by the Faculty of Mechanical Engineering of the University of Niš. Support from Ortokon ltd. Niš, Serbia, is also greatly acknowledged.

References

[1] Hoon Park, Hyun Woo Kim, Hui-Wan Park, and Ki Seok Lee, "Limb Angular Deformity Correction Using Dyna-ATC: Surgical Technique, Calculation Method, and Clinical Outcome," Yonsei Med J, pp. 818-830, 2011.

[2] Yevgeniy Palatnik and S. Robert Rozbruch, "Femoral Reconstruction Using External Fixation," Advances in Orthopedics, pp. 1-10, Mart, 2011.

[3] Kyung Rae Ko, Jong Sup Shim, Chae Hoon Chung, Joo Hwan Kim, "Surgical Results of Limb Lengthening at the Femur, Tibia, and Humerus in Patients with Achondroplasia," Clinics in Orthopedic Surgery, pp. 226-232, 2019.

[4] Predrag Grubor, Milan Grubor, "Results of Application of External Fixation with Different Types of Fixators," Predrag Grubor1, Milan Grubor2, pp. 332-338, Maj-Jun 2012.

[5] Ercan Avşar, Kerem Ün, "Automatic 3D modeling and simulation of bone-fixator system in a novel graphical user interface," Elsevier - Informatics in Medicine Unlocked, pp. 78-91, 2016/2.

[6] Adnan Kara, Haluk Celik, Ali Seker, Ozgur Karakoyun, Raffi Armagan, Ersin Kuyucu and Mehmet Erdil, "Treatment of open fractures with a computer-assisted external fixator system without the use of fluoroscopy," Journal of Orthopaedic Surgery and Research, pp. 11-51, 2016.

[7] Terry K.K. Koo & M. Owen Papuga, "A computer aided method for closed reduction of diaphyseal tibial fracture using projection images: A feasibility study," Computer Aided Surgery, pp. 45-57, December 2009.

[8] Irwansyah, N P Sinh, J Y Lai, T Essomba, R Asbar, P Y Lee, "Integration of computer-assisted fracture reduction system and a hybrid 3-DOF-RPS mechanism for assisting the orthopedic surgery," in 10th International Conference Numerical Analysis in Engineering, 2018.

[9] Zdravković M., Korunović N., Vitković N., Trajanović M., Milovanović J., Jardim-G. R., Sarraipa J., "Towards the Internet-of-Things platform for orthopaedics surgery – the smart external fixation device case studies," in Conference: 8th International Conference - Interoperability for Enterprise Systems and Applications (I-ESA 2016). Workshop B4: Sensing Enterprise: Opportunities and Barriers, Guimarães, Portugal, 2016.

[10] Mišić Dragan, Zdravković Milan, Mitković Milorad, Vitković Nikola, Mitković Milan, "Real-time monitoring of bone fracture recovery by using aware, sensing, smart and active orthopedic devices," IEEE Internet of Things Journal, pp. 1-8, March 2018.

[11] J. S. M. Dwyer, P. J. Owen, G. A. Evans, J. H. Kuiper, "Stiffness measurements to assess healing during leg lengthening," J Bone Joint Surg, pp. 286-289, June 1995.

[12] A. H. R. W. SIMPSON, J. L. Cunningham, J. Kenwright, "The forces which develop in the tissues during leg lengthening," J Bone Joint Surg, pp. 979-983, 16 May 1996.

[13] Martin Th. Lauterburg, G. Ulrich Exner, Hilaire A.C. Jacob, "Forces Involved in Lower Limb Lengthening: An In Vivo Biomechanical Study," Journal of orthopaedic research september, pp. 1815-1822, 2006

Production and information technologies

THE 5th INTERNATIONAL CONFERENCE
MECHANICAL ENGINEERING IN XXI CENTURY

December 9-10, 2020
Faculty of Mechanical Engineering in Niš, Serbia

Overview of Grain Size Determination in Metallography

David POTOČNIK, Lucijano BERUS, Mirko FICKO

Faculty of Mechanical Engineering, University of Maribor, Slovenia
d.potocnik@um.si, lucijano.berus@um.si, mirko.ficko@um.si

***Abstract*— This paper represents an overview of methods for grain size determination in metallography, developed in recent years. Microstructures play an important role in the mechanical properties of alloy products, thus it is essential to precisely detect details such as shape, size and orientation of grains and other smaller defects. The most known and commonly used method for grain boundary detection is a microscopic examination, where experienced examiner interprets results. These results can be highly susceptible to the subjective assessment of the examiner. However, in recent years commonly known microstructure tasks in microstructure data science has begun to change by exploring the utilisation of machine vision and image processing. One of the approaches is machine vision based method for edge detection based on optical microscopy images set with different grain size values where evaluated performance based on intercept method is compared with the results, obtained by manual grain size determination method. Research has shown that a novel approach has the potential to automate the manual grain size determination process and thereby lower processing times.**

***Keywords*— Optical microscopy, Metallography, Grain boundary detection, Machine vision**

I. Introduction

The characterisation and measurement of grain structures are of great importance to materials scientists because not only does grain size strongly affect the mechanical properties, but it also influences physical properties, surface properties and phase transformations [1]. The ability to locate the grain boundaries in materials is critical for a wide number of applications, e.g. process control and property optimisation. The mechanical and physical properties of metallic materials are frequently related to grain size, e.g. via the Hall-Petch relationship where strength is inversely dependent on the square root of grain size [2].

Researchers often need to observe and measure microstructures manually. For example, to obtain the grain size, they need to draw the observed and hidden grain boundaries manually. Then, they need to measure grain sizes several times to get a statistically valid result based on the drawn boundaries. In fact, the slices from different sections (longitudinal and cross-section) and different positions of the alloy products can provide various and valuable information, which is conducive to analysis microstructures comprehensively.

An example is shown in Fig. 1. Such a task, for experts, is quite time-consuming. Besides, different metallographic workers, due to their preferences and understanding, may get different marking results [3].

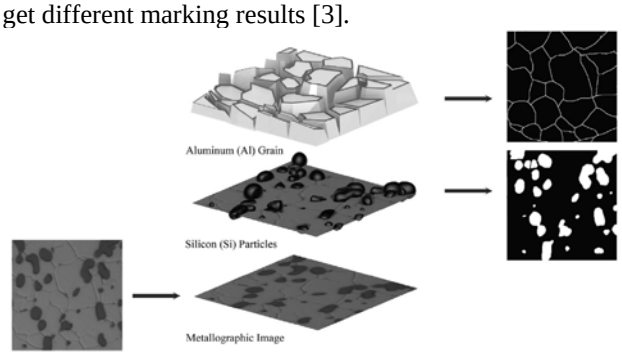

Fig. 1 The microstructures in Al-Mg-Si alloys. Bottom: the observable metallographic image. Middle: embedded silicon particles and corresponding binary ground truth. Top: aluminium grain and binary ground truth of grain boundaries [3]

Various methods have been developed recently to eliminate the mentioned problem as much as possible. In order to extract pictures of microstructures, which are then the input for machine vision-based algorithms, different techniques can be used. Traditionally, a small piece of a specimen is taken from material and polished for microstructure imaging using either optical microscope or electron backscattering diffraction (EBSD) method [4]. The two mentioned methods are briefly described below.

A. Optical microscopy

Among the various techniques used to characterise steel and cast-iron microstructure, the most common is optical microscopy where the sample is adequately illuminated with visible light, and the reflected light reaches the observer, as schematically shown in Fig. 2.

Different observation techniques may be used in optical microscopy (oblique lighting, polarised light, dark field imaging, etc.). Oblique (or inclined) illumination may be used to highlight some aspects of the microstructure or to change the way contrast is perceived. The most common form of illumination, however, is parallel to the optical axis of the microscope. In general, this type of illumination produces lighter images of flat or nonetched regions of the sample and darker images of the nonflat regions such as cracks, pores, and etched regions. In some special cases, objectives that can illuminate the specimen surface in an oblique way with a conical light beam can be used - this is called dark field illumination. Light beams that reach the flat regions of the sample are not reflected into the observation path of the microscope. These areas appear dark. Etched regions and the edges of pores, cracks, and

other irregularities can reflect the oblique beam into the optical path and appear bright in the image [5].

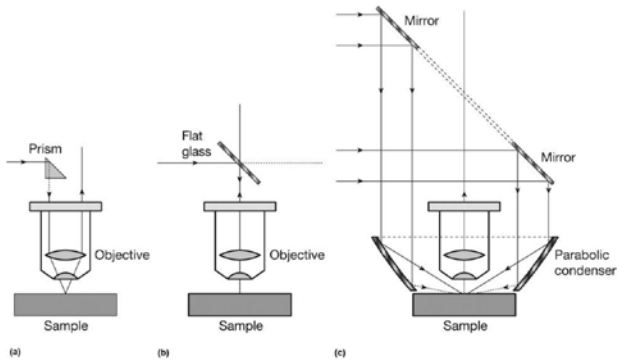

Fig. 2 Schematic illustration of lighting methods in metallographic optical microscopes: (a) oblique or inclined illumination; (b) normal illumination or illumination parallel to the optical axis—the most common method; (c) dark field illumination [5]

B. Electron backscattering diffraction (EBSD)

Electron backscattered diffraction (EBSD) is a technique that provides crystallographic information by analysing crystalline samples in the scanning electron microscope (SEM) [6].

The basic requirement is a scanning electron microscope and an EBSD system. The EBSD acquisition hardware generally comprises a sensitive CCD camera, and an image processing system for pattern averaging and background subtraction. Fig. 3 shows a schematic diagram of the main components of an EBSD system. The EBSD acquisition software controls the data acquisition, solve the diffraction patterns, and store the data. Additional software is required to analyses, manipulate, and display the data [1].

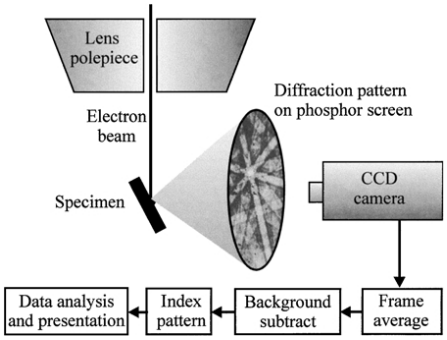

Fig. 3 Schematic diagram of a typical EBSD installation [1]

EBSD is carried out on a specimen which is tilted between 60° and 70° from the horizontal. This is achieved by mounting the specimen so that the surface is normal to the electron beam, which is the optimum position for examining the microstructure using backscattered electrons. If a backscattered image is required from the tilted sample, additional backscattered electron detectors must be used and these are typically positioned close to the transmission phosphor screen [7], [8].

Many comparisons have been made over the years between optical microscopy and EBSD method. For example Gao, Wang, Ubhi and Starink [2] made a comparison between optical and the EBSD image from the low carbon steel, shown in Fig. 4. From the comparison of low magnification photos with a step size of 2 μm for the EBSD image, it seems that both methods provide almost similar information. However, a careful comparison of the details in higher magnification photos with a step size of 1 μm indicates that the EBSD image reveals more grains than the optical image.

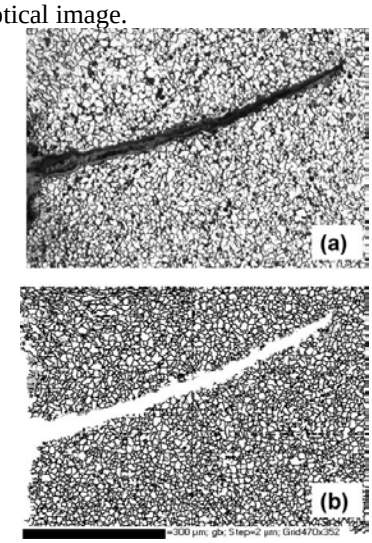

Fig. 4 Low magnification micrograph of optical observation (a) and EBSD analysis (b) of low carbon steel [2]

C. Machine vision-based methods

Image processing in the field of material science is a relatively new research area gaining importance nowadays. Image processing technique improves the visual appearance of the microstructural images to compute the features and structures present, thereby improving reproducibility and repeatability [9]. In fact, the main interest of automatic methods based on computer vision is because they enable precise measurements and make possible the analysis in a relatively short time [10].

Various researchers employed automatic methods and mathematical morphologies to determine the features present during the processing of metals. For example, Dutta et al. [11] adopted automatic texture and fractal analysis to analyses the fracture surface of Cu-strengthened high-strength low alloy (HSLA) steel. In reference [12] the automatic image analysis is applied using the top-hat transformation in the morphological characterisation of the microstructure during the sintering of Ceria. On the other hand, an intelligent system for the prediction of mechanical properties of material has been developed [13], where metallographic images were used to carry out the prediction. In the same way, microstructure characterisation, an image processing system to classify the microstructure of copper alloys has been proposed in Abouelatta [14]. Dengiz, Smith and Nettleship [15] developed a neural network and fuzzy logic algorithms to find the grain boundary of steel alloys. Other works have been focused on the size of the grain in a material. Heilbronner [16] developed a methodology that automatically prepares grain boundary maps in a reduced time.

In contrast, Lu, Lin and Wang [17] proposed a grain identification by processing two input polarising images which permit one to obtain the edges. In reference [18] an image processing method for determining the grain sizes of the metallographic images was proposed. Derivation of the grain sizes of the digital metallographic images is made by digital image processing and extraction of grain boundary by proposing a new edge detection algorithm based on fuzzy logic. On the other hand, an image

processing algorithm is proposed to determine the average grain size in a metallic microstructure by counting the number of grains using support vector regression [9]. Finally, in reference [19], the authors propose an image processing-based technique for refinement of raw plain carbon steel microstructure images, into a digital form, usable in experiments related to heat treatment processes of steel in diverse applications. Reference [20] shows that size distribution and porosity of anodic alumina structures have been determined based on the mathematical morphology analysis. In [21], the authors proposed a methodology to characterise the graphite nodules in cast iron materials based on morphological image processing as well as the notion of compacity is introduced instead of the nodules density. The last work was carried out by Peregrina-Barreto et al. [22] in which a novel image processing methodology was introduced to segment images in steels for automatic size determination.

Frequently, grain size determination is carried out by manual or semiautomatic methods. In this case, the analyst visually selects the grain boundaries. The observation criterion is affected by different factors, such as tiredness, distraction, perception differences. It involves a slow process and higher variability of the results. This is the reason for the development of systems for automatic analysis.

One of such developed method is described in this paper, where a new grain boundary detection procedure is presented. Proposed sequence of image processing tasks enables the grain boundary detection, and edge concatenation by connecting the edges procedure. The developed method is used for grain size measurements and is compared to other conventional and edge retrieval procedures.

II. Materials and methods

A. Samples preparation

The material used for samples was Al 99.5% (ENAW1050A). The chemical composition of material is as follows: 0.02% Cu, 0.003% Mn, 0.016% Mg, 0.13% Si, 0.28% Fe, 0.05% Zn, 0.018% Ti, 0.006% Pb, 0.005% Sn, and balance Al. To achieve the identical initial microstructure of specimens, they all had equal treatment. That procedure consisted of homogenisation, uniaxial upsetting (Rastegaev test) to achieve logarithmic strain of $\varphi = 0.25$, and then again, heat treatment to initiate grain growth. The uniform grain size and chemical homogenisation of specimens were obtained in this way.

B. Image preparation and preprocessing

To use the RGB pictures obtained with optical microscopy, a few steps are necessary before starting with proposed image processing method for grain boundary detection.

Image preprocessing was done with local Laplacian pyramid. Local Laplacian filters produce a variety of different effects using the standard Laplacian pyramids. The discussed method was introduced by Paris et al. [23], where edges are be preserved and the details enhanced simultaneously. The algorithm offers a robust method and enables a wide range of effects manipulation. The algorithm's performance can be altered by setting up the three parameters (σ_L, α and β). Sigma σ_L defines a difference between small variation (that is considered as a texture) and a larger-one (such as edge), α parameter for altering the level of detail, and β parameter for dynamic range compression.

Because most images are affected by unexplained variation in data or noise, the proper smoothing filter must be used. The Gaussian, beside the moving average, is one of the most widely used smoothing filters. The Gaussian filters have weights specified by the probability density function of a normal distribution with variance ${\sigma_G}^2$. The Gaussian can also be used to simultaneously smooth and interpolate between image pixels. At location (x, y), where y is the row index and x column index, the estimated output intensity is an average of local pixel values, weighted by the Gaussian density function.

The preprocessed images were then transformed to a digitised binary image, which is represented as a matrix $IT(i, j)$. Each point is either 0 (white point) or 1 (dark point). For the thinning process, the Zhang thinning algorithm was used. It is used to iteratively transform the pattern into a thin line drawing, with deleting the specific dark points.

The last process of picture preparation is connecting the edges procedure. The first step in the so-called concatenation process is finding and indexing the continuously connected edges with connected components labelling (CCL) method [24]. Connectivity is determined as 8- or 4-connected neighbourhood. The number of different sets representing connected edges m is computed. The procedure starts with two sets of labels $PL = \{\boldsymbol{E}_1\}$ and $TL = \{\boldsymbol{E}_2, \ldots, \boldsymbol{E}_m\}$, where $\boldsymbol{E}_j$ is comprised of two vectors representing $\boldsymbol{x}$ and $\boldsymbol{y}$ coordinates of connected edge belonging to j-th connected component of binary edge image (BE). Next step is repeated throughout the procedure $m - 1$ iterations, where m is defined as the number of all connected regions in BE. In every iteration, the two closest points, based on Euclidean distance, from sets PL and TL are found . In the next step, closest points are graphically connected with a straight line, representing the newly formed edge, previously not detected by edge retrieval process.

C. The conventional method for grain size determination

A quantitative analysis of the apparent grain size according to procedure EN ISO 643:2012 was done. A circular intercept method was used to obtain the apparent grain size, which, according to standard EN ISO 643:2012 averages out variations in the shape of equiaxed grains and avoids the problem of lines ending within grains. The recognition of grains boundaries was performed manually, by optical (eye) recognition of grains boundaries on obtained microstructure images. For the measurement, the 3 concentric circles were used.

D. The proposed method for grain size determination

In this study used optical microscopy RGB images consisted of 724×724 and 1536×1536 pixels. The procedure consists of two parts, in the first one binary edge image (BE) is retrieved with the implementation of the local Laplacian, Gaussian smoothing, Gradient and Zhang's thinning algorithm. To further improve the detection of grain boundaries, a special edge connecting procedure is presented (BE+). However, it must be stressed that the produced algorithm enables the manual adding of edges (preliminary missed by filters), to increase

the accuracy of the second part further discussed below. In the second part, grain size measurements are performed with linear intercept method [25], multiplied with 1.106 (according to standard EN ISO 643:2012) to obtain a mean diameter of grains (d_{mean}) [26]. Based on recommendation of ASTM E1382 [27], four equally spaced directions of 0°, 45°, 90° and 135° were used (Fig. 5).

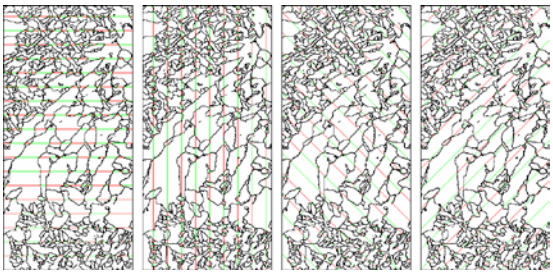

Fig. 5 Measurement of ASTM E1382 linear intercept method [28]

III. Results and Discussion

The implementation of practical image processing using newly proposed approach and discussion of implementation details is given in the subsequent text.

Firstly, the edge retrieval process is explained, which is used to extract the binary image (representing the edges) that serves as a basis for grain size calculations. On Fig. 6a the original (unaltered) specimen's microstructure image is shown. The Laplacian and Gaussian filters are used for further preprocessing. The Local Laplacian filter is an edge-aware processing filter, meaning the large discontinuities (such as edges) remain in place. It is defined with local contrast manipulation parameter α controlling the image detail smoothing, the edge amplitude parameter σ_L and large-scale variations parameter β. With Laplacian (Fig. 6b) the detail enhancement and the balance between global and local contrast are controlled. Increase in contrast with Laplacian filter enables better distinction between different grains. After the Laplacian filter use stage, the image is further processed with the use of Gaussian filter (Fig. 6c).

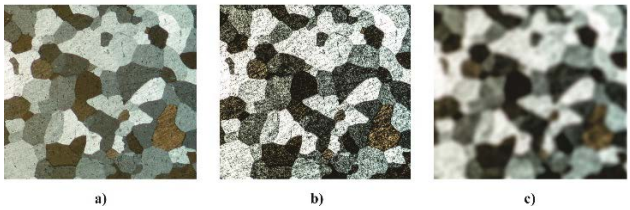

Fig. 6 The original microstructure image (a). Contrast manipulation (b) based on local Laplacian filter with $\alpha = 0.1$, $\sigma_L = 0.5$ and $\beta = 0$. Gaussian filtering (c) to blur the image with 47 by 47 Convolution Kernel and standard deviation $\sigma_L = 8$ [29]

The Gaussian filter blurs the processed image to eliminate small image imperfections (such as inclusions or etching artefacts, seen as little black spots at an image of microstructure), which have been additionally enhanced with Laplacian, and could disturb the later-on edge extraction. The Gaussian also ensures homogenous colour along with certain grain structure. Choice of standard deviation and convolution kernel values is application dependent; in this case the most suitable vales are adopted as given in Fig. 6, and further on.

Binary image with enlarged edges is retrieved in with gradient filter based on Sobel operator, where a certain threshold is used on the preprocessed image, shown in Fig. 6c. The Sobel based gradient filter with different threshold values for edge detection is used and shown in Fig. 7. If the threshold value is too low, too many edges are recognised (Fig. 7a), but on the other hand, there are too little edges with a too big threshold (Fig. 7c). It turned out that the best-suited edges representation is achieved with a moderate threshold value set to 30 [29], where only the representative edges are recognised (Fig. 7b).

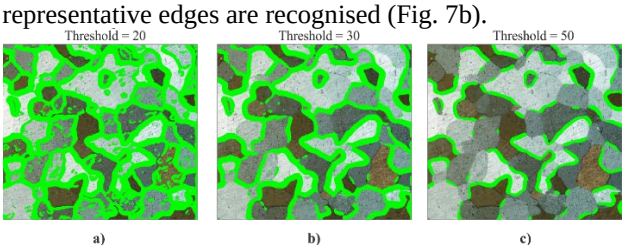

Fig. 7 Different threshold values of Sobel gradient filter: $threshold1 = 20\ (a)$, $threshold2 = 30\ (b)$, $threshold3 = 50\ (c)$ [29]

The first part of the proposed method is completed in the next step, with the enlarged edges being morphologically altered by Zhang's thinning algorithm. The algorithm calculated a thinned image of the binary edge (BE also serves as the basis for the BE+ process), where the edges are only one pixel wide after 20 iterations. Besides, the edges can be manually inserted by the tester (before or after the dilution phase) for further improving of grain size detection rate.

The image of binary thinned edges (BE) is processed by connected components labelling method to find and index the continuously connected edges. Connectivity is defined as an 8-connected neighbourhood. With each iteration, the two closest points (belonging to different continuously connected edge areas) are found and graphically connected with a straight line representing the newly formed edge that was previously missed by the edge search process. When all the edge areas are connected in one area, the so-called connected edge binary image (BE+) is computed [29]. The operation of the proposed edge joining process (BE+) is shown in Fig. 8, where the newly formed edges are shown as red lines. At the same time, the green regions represent BE (without connecting the edges procedure results).

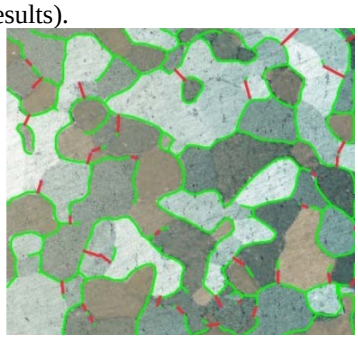

Fig. 8 Connecting the edges procedure, green regions represent BE, combined green and red regions represent BE+ [29]

The precision rates of the edge detection procedures presented; BE (without connecting the edges) and BE+ (with connecting the edges procedure), are compared with conventional method (EN ISO 643:2012) and the Canny based edge detection procedures. All test images (TI) are enhanced with the local Laplace filter with parameters $\alpha = 0.1$, $\sigma_L = 0.5$ and $\beta = 0$. The value of the Gaussian blur standard deviation and convolution kernel values is set to $\sigma_G = 8$ for smaller resolution TI, and $\sigma_G = 16$ for the

larger resolution TI. The threshold of the Sobel gradient filter for smaller resolution TI set is equal to 30 and for larger resolution TI is set to 15. The thinned binary edge image in case of BE and BE+ is retrieved within 20 iterations for all TI.

The vertical and horizontal intercept line spacings parameters of linear intercept method are set to 10 pixels, while 45° and 135° are set to 14 pixels since $10/sin45° \approx 14$ ensuring equal line spacings compared to horizontal and vertical directions.

The results of grain size measurements with conventional Canny, BE, and BE+ methods for all TIs are shown in Fig. 9. On TI6, the best accuracy achieved with BE was 5.33% higher compared to the conventional method. On the other hand, on TI3 BE achieved the worst accuracy, 24.76% higher compared to the conventional method. The BE+ method achieved the best accuracy of 2.67% for TI2 processing and the worst accuracy of 15.94% for TI3 processing (compared to the conventional method). Using the Canny edge detection technique test images with higher resolution such as TI4, TI5 and TI6 achieved lower levels of grain size accuracy compared to test images of lower resolution TI1, TI2 and TI3. BE and BE+ precision rates indicate the robustness of the proposed method. In concordance with logic, the grain size measurement of BE is always greater compared to BE+, since BE is a subset of BE+ (BE⊆BE+).

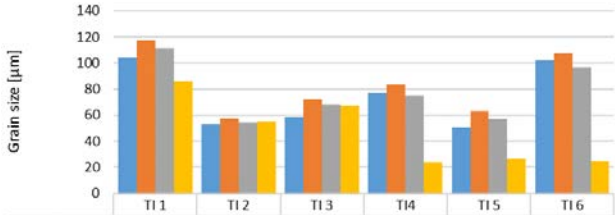

	TI 1	TI 2	TI 3	TI4	TI 5	TI 6
Conventional	104,2	53,1	58,6	77	50,6	102,3
BE	117,89	57,59	72,15	83,19	63,13	107,76
BE+	111,62	54,52	67,94	74,87	56,9	96,49
canny	85,97	55,23	67,54	24,18	26,44	24,73

Fig. 9 Results of average grain size predictions of tested images (TI1 to TI6), based on conventional method, BE, BE+ and Canny edge detection filter [29]

IV. Conclusion

In the presented study, the grain size characteristics of the samples are detected based on microstructural images and innovative image processing procedure [29]. The conventional grain size measurement methods involve the use of a planimetric method for image analysis, where the recognition of grains boundaries is performed manually, with optical (eye) recognition on obtained microstructure images performed via examiner. The procedure in question was found to be rather time consuming and required a great deal of concentration, experience, and observational skills on the part of the examiner.

Newly suggested image processing workflows (BE and BE+) offer a faster alternative and are for the most part performed automatically. Only a few parameters need to be set manually by the examiner. These parameters are the preprocessing settings of local Laplace filter, Gaussian blur, threshold value for edge detection based on gradient filter and number of thinning iterations of Zhang's algorithm. If the missed edges occur after automatic edge retrieval procedure, the edges can be manually added by the examiner or further processed with connecting the edges procedure to achieve higher degree accuracy.

Discussed methods are compared among each other based on the obtained mean grain size diameter values. Grain size diameter values of the proposed methods (BE and BE+) are comparable to conventional methods and have outperformed classical edge detection techniques. The BS+ procedure gives the most comparable results with conventionally (manually) determined grain size results with negligible disappearances in practical use.

Acknowledgment

The authors acknowledge the financial support from the Slovenian Research Agency (research core funding No. P2-0157).

References

[1] F. J. Humphreys, "Review - Grain and subgrain characterisation by electron backscatter diffraction," (in English), J Mater Sci, vol. 36, no. 16, pp. 3833-3854, August 2001, doi: 10.1023/A:1017973432592.

[2] N. Gao, S. C. Wang, H. S. Ubhi, and M. J. Starink, "A comparison of grain size determination by light microscopy and EBSD analysis," vol. 40, ed, 2005, p. 4971.

[3] M. Li, D. Chen, S. Liu, and F. Liu, "Grain boundary detection and second phase segmentation based on multi-task learning and generative adversarial network," Measurement, Article vol. 162, October 2020, doi: 10.1016/j.measurement.2020.107857.

[4] J. Zhang, Y. Song, X. Li, and C. Zhong, "Comparison of Experimental Measurements of Material Grain Size Using Ultrasound," Journal of Nondestructive Evaluation, vol. 39, no. 2, p. 1, June 2020. [Online]. Available: https://login.ezproxy.lib.ukm.si/login?url=http://search.ebscohost.com/login.aspx?direct=true&db=edb&AN=143018881&lang=sl&site=eds-live.

[5] H. Colpaert, Metallography of Steels. Materials Park: ASM (in English), 2018.

[6] S. Nafisi, A. Roccisano, R. Ghomashchi, and G. Vander Voort, "A Comparison between Anodizing and EBSD Techniques for Primary Particle Size Measurement," Metals (2075-4701), vol. 9, no. 5, p. 488, May 2019. [Online]. Available: https://login.ezproxy.lib.ukm.si/login?url=http://search.ebscohost.com/login.aspx?direct=true&db=edb&AN=136755455&lang=sl&site=eds-live.

[7] D. J. Prior, P. W. Trimby, U. D. Weber, and D. J. Dingley, "Orientation contrast imaging of microstructures in rocks using forescatter detectors in the scanning electron microscope," Mineralogical Magazine, vol. 60, no. 403, pp. 859-869, 1996, doi: 10.1180/minmag.1996.060.403.01.

[8] A. P. DAY and T. E. QUESTED, "A comparison of grain imaging and measurement using horizontal orientation and colour orientation contrast imaging, electron backscatter pattern and optical methods," Journal of Microscopy, vol. 195, no. 3, pp. 186-196, 1999, doi: 10.1046/j.1365-2818.1999.00571.x.

[9] K. Gajalakshmi, S. Palanivel, N. J. Nalini, S. Saravanan, and K. Raghukandan, "Grain size measurement in optical microstructure using support vector regression," (in English), Optik, vol. 138, pp. 320-327, 2017, doi: 10.1016/j.ijleo.2017.03.052.

[10] C. A. Paredes-Orta, J. D. Mendiola-Santibanez, F. Manriquez-Guerrero, and I. R. Terol-Villalobos, "Method for grain size determination in carbon steels based on the ultimate opening," (in English), Measurement, vol. 133, pp.

193-207, Februar 2019, doi: 10.1016/j.measurement.2018.09.068.

[11] S. Dutta, K. Barat, A. Das, S. K. Das, A. K. Shukla, and H. Roy, "Characterization of micrographs and fractographs of Cu-strengthened HSLA steel using image texture analysis," Measurement, vol. 47, pp. 130-144, 2014, doi: https://doi.org/10.1016/j.measurement.2013.08.030.

[12] M. Coster, X. Arnould, J. L. Chermant, L. Chermant, and T. Chartier, "The use of image analysis for sintering investigations: The example of CeO2 doped with TiO2," Journal of the European Ceramic Society, vol. 25, no. 15, pp. 3427-3435, 2005, doi: https://doi.org/10.1016/j.jeurceramsoc.2004.09.003.

[13] M. Paulic, D. Mocnik, M. Ficko, J. Balic, T. Irgolic, and S. Klancnik, "Intelligent system for prediction of mechanical properties of material based on metallographic images," Tehnicki Vjesnik, Article vol. 22, no. 6, pp. 1419-1424, 2015, doi: 10.17559/TV-20130718090927.

[14] O. B. Abouelatta, "Classification of copper alloys microstructure using image processing and neural network," J. Am. Sci., vol. 9, no. 6, pp. 213-223, 2013.

[15] O. Dengiz, A. E. Smith, and I. Nettleship, "Grain boundary detection in microstructure images using computational intelligence," Computers in Industry, vol. 56, no. 8, pp. 854-866, 2005, doi: https://doi.org/10.1016/j.compind.2005.05.012.

[16] R. Heilbronner, "Automatic grain boundary detection and grain size analysis using polarization micrographs or orientation images," Journal of Structural Geology, vol. 22, no. 7, pp. 969-981, 2000, doi: https://doi.org/10.1016/S0191-8141(00)00014-6.

[17] B. Lu, C. G. Lin, and H. Wang, "Grain identification of polarising images with level set method," in 2011 IEEE 3rd International Conference on Communication Software and Networks, May 2011, pp. 192-195, doi: 10.1109/ICCSN.2011.6013807. [Online]. Available: https://ieeexplore.ieee.org/document/6013807/

[18] L. X. Zhang, Z. G. Xu, S. L. Wei, X. C. Ren, and M. L. Wang, "Grain Size Automatic Determination for 7050 Al Alloy Based on a Fuzzy Logic Method," (in English), Rare Metal Mat Eng, vol. 45, no. 3, pp. 548-554, Mar 2016. [Online]. Available: <Go to ISI>://WOS:000373754600003.

[19] S. Gupta, A. Panda, R. Naskar, D. K. Mishra, and S. Pal, "Processing and refinement of steel microstructure images for assisting in computerized heat treatment of plain carbon steel," Journal of Electronic Imaging, vol. 26, no. 6, p. 063010, 2017. [Online]. Available: https://doi.org/10.1117/1.JEI.26.6.063010.

[20] D. S. Raimundo, P. B. Calíope, D. R. Huanca, and W. J. Salcedo, "Anodic porous alumina structural characteristics study based on SEM image processing and analysis," Microelectronics Journal, vol. 40, no. 4, pp. 844-847, 2009, doi: https://doi.org/10.1016/j.mejo.2008.11.024.

[21] L. A. Morales-Hernández, I. R. Terol-Villalobos, A. Domínguez-González, F. Manríquez-Guerrero, and G. Herrera-Ruiz, "Spatial distribution and spheroidicity characterization of graphite nodules based on morphological tools," Journal of Materials Processing Technology, vol. 210, no. 2, pp. 335-342, 2010, doi: https://doi.org/10.1016/j.jmatprotec.2009.09.020.

[22] H. Peregrina-Barreto, I. R. Terol-Villalobos, J. J. Rangel-Magdaleno, A. M. Herrera-Navarro, L. A. Morales-Hernández, and F. Manríquez-Guerrero, "Automatic grain size determination in microstructures using image processing," Measurement, vol. 46, no. 1, pp. 249-258, 2013, doi: https://doi.org/10.1016/j.measurement.2012.06.012.

[23] S. Paris, S. W. Hasinoff, and J. Kautz, "Local Laplacian Filters: Edge-Aware Image Processing with a Laplacian Pyramid," Communications of the ACM, Article vol. 58, no. 3, pp. 81-91, 2015, doi: 10.1145/2723694.

[24] L. He, X. Ren, Q. Gao, X. Zhao, B. Yao, and Y. Chao, "The connected-component labeling problem: A review of state-of-the-art algorithms," Pattern Recognition, vol. 70, pp. 25-43, 2017, doi: https://doi.org/10.1016/j.patcog.2017.04.018.

[25] P. Lehto, H. Remes, T. Saukkonen, H. Hänninen, and J. Romanoff, "Influence of grain size distribution on the Hall-Petch relationship of welded structural steel," 2014, doi: 10.1016/j.msea.2013.10.094.

[26] S. Plavka et al., "Metallographic Determination of Strain Distribution in Cold Extruded Aluminum Gear-Like Element," Metals, article vol. 10, no. 589, pp. 589-589, 04/01/ 2020, doi: 10.3390/met10050589.

[27] K. J. Kurzydlowski, "A Model for the Flow-Stress Dependence on the Distribution of Grain-Size in Polycrystals," (in English), Scripta Metall Mater, vol. 24, no. 5, pp. 879-883, May 1990, doi: 10.1016/0956-716x(90)90129-5.

[28] P. Lehto. "Characterization of average grain size and grain size distribution." https://wiki.aalto.fi/display/GSMUM/Characterization+of+average+grain+size+and+grain+size+distribution (accessed 15. 9. 2020).

[29] L. Berus, P. Skakun, D. Rajnovic, P. Janjatovic, L. Sidjanin, and M. Ficko, "Determination of the Grain Size in Single-Phase Materials by Edge Detection and Concatenation," Metals, vol. 10, no. 10, p. 1381, 2020. [Online]. Available: https://www.mdpi.com/2075-4701/10/10/1381.

THE 5th INTERNATIONAL CONFERENCE
MECHANICAL ENGINEERING IN XXI CENTURY

December 9-10, 2020
Faculty of Mechanical Engineering in Niš, Serbia

ANFIS Prediction of Mean Surface Roughness and Material Removal Rate in Plasma Arc Cutting

Milos MILOVANČEVIĆ[1], Dragan MILČIĆ[1], Dalibor PETKOVIĆ[2]

[1] University of Niš, Faculty of mechanical engineering, A. Medvedeva 14, Nis, Serbia
[2] University of Niš, Pedagogical Faculty in Vranje, Partizanska 14, 17500 Vranje, Serbia
milos.milovancevic@masfak.ni.ac.rs, dragan.milcic@masfak.ni.ac.rs

***Abstract*— Plasma arc cutting process is very sensitive process which has to be optimized before application. There are different input factors which need adjustment in order to find the optimal combinations for the best final product. Therefore the main aim of the study was to establish predictive models for the plasma arc cutting in order to determine the cutting quality before real application of the plasma arc cutting. As cutting material Quard-400 was used. Input factors cutting speed and gas pressure were used during experimental procedure and for the predictive models crating. As the output quality parameters, mean surface roughness – Ra and material removal rate – MRR were used. Higher material rate means more profit for industry and vice versa. In the same time higher removal rate could increase surface roughness which is not desirable. Surface roughness needs to be minimized as much as possible which depends on the product application purpose. Predictive models were created based on adaptive neuro fuzzy inference system – ANFIS, which is suitable for nonlinear and redundant dataset. Results shown high predictive accuracy for the both output parameters.**

***Keywords* — Plasma arc cutting; prediction; surface roughness; ANFIS.**

I. INTRODUCTION

Plasma state is the fourth state of material after solid, liquid and gaseous states. Plasma state occurs after very high heating of the material. In other words the first state is solid state which converts in the liquid state after heating. The liquid state converts further in gaseous state after more heating. And finally the gaseous state converts into plasma state after more heating. Plasma represent in ionized gas which is electro conductive and operated on temperatures between 10000ºC and 14000ºC. Plasma arc cutting is based on the ionized gas and it represents one type of thermal cutting process which uses a jet of the plasma gas in order to melt and cut material. The plasma arc cutting is very attractive process for material removal or cutting because of high quality of the final product. However the plasma arc cutting process is very expensive process in comparison to laser cutting or cutting by oxygen fuel.

Plasma arc cutting (PAC) is well recognized non-conventional machining processes widely used to fabricate intricate part profiles for diverse electrically conductive materials including superalloys and composites [1]. Plasma arc cutting process is frequently used to cut stainless steel, alloy steel, aluminum and other materials [2]. The application of teaching learning based optimization (TLBO) algorithm in order to analyze the effect of process parameters on surface roughness in plasma arc cutting of AISI D2 steel has been performed in article [3]. The optimum selection of process parameters is essential for smoother and faster cutting and in research work [4], experimental investigation of plasma arc cutting has been carried out where Taguchi based desirability analysis (TDA) was observed to find the optimal cutting conditions for improving the quality characteristics of the plasma arc cutting process. The quality of the cut of the plasma arc cutting procces has been monitored by measuring the kerf taper angle (conicity), the edge roughness and the size of the heat-affected zone (HAZ) [5]. Results in paper [6] have been shown that this fuzzy control and PID neural network improves the precision, ripples, finish and other comprehensive indexes of the workpiece compared with conventional PI control, and the plasma arc cutting power supply based on the fuzzy-neural network has excellent control performance. Plasma arc cutting (PAC) is a thermal cutting process that makes use of a constricted jet of high-temperature plasma gas to melt and separate (cut) metal [7]. In work [8], the microstructural modifications of the Hf insert in plasma arc cutting (PAC) electrodes operating at 250 A were experimentally investigated during first cycles, in order to understand those phenomena occurring on and under the Hf emissive surface and involved in the electrode erosion process where macrocracking was observed in the oxide layer, while microcracking and grain growth were detected in the remelted Hf. The paper [9] pointed out that high quality parts of the plasma arc cutting can be obtained as a result of an experimental investigation aimed at selecting the proper values of process parameters. There is need to develop and optimize novel plasma arc heat source such as cross arc and coupling arc [10]. In study [11] has been studied the influences of plasma arc remelting on the microstructure and properties of thermal sprayed Cr3C2-NiCr/NiCrAl composite coating. To reduce the kerf width and to improve the kerf quality, the hydro-magnetically confined plasma arc was used to cut engineering ceramic plates [12]. The quality of cuts performed on titanium sheets using high tolerance plasma

arc cutting (HTPAC) process was investigated under different process conditions and a comparison between predicted thermal cycles, experimental measurements and microstructural observations confirmed the reliability of the estimation in terms of extension of microstructural modifications [13].

In order to decrease price of the plasma arc cutting process there is need to establish predictive models of the process. In other words the models could suggest future quality of the plasma arc process for the given combination of the input parameters. In order to do the predictive models there is need for an advanced computational models like soft computing or computational intelligence. Therefore in this article is used adaptive neuro fuzzy inference system or ANFIS [14-18] in order to predict laser arc cutting output parameters based on the input processing factors like cutting speed and plasma gas pressure. The output factors are mean surface roughness and material removal rate.

II. Methodology

A. Experimental procedure

Figure 1 shows the total experimental procedure of the plasma arc cutting. As can be seen there are nine main steps of the procedure. The torch body contains cathode which is non-melting. Working material represent anode or positive electrode where high temperature plasma gas or primary gas will be impinged. Kerf represent width of material removal during cutting process where molten metal is removed. For the cooling purpose secondary gas is used.

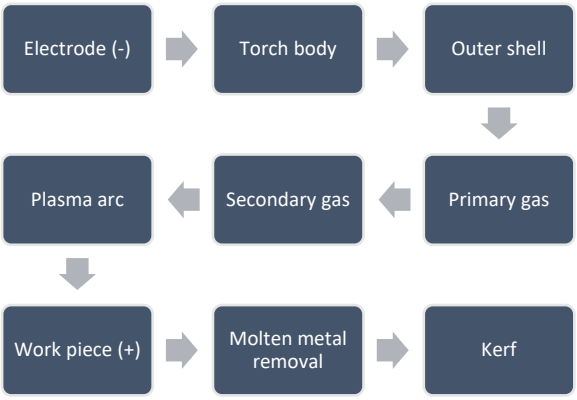

Figure 1: Experimental procedure of the plasma arc cutting process

As working material Quard-400 is used which is abrasion resistant steel. This material has optimal combination of hardness, ductility and strength and it is very suitable for cutting process. Chemical composition of the material has following elements: C, Mn, P, Si, Al, Cu, Nb, Ni, Cr, V, Ti, N_2, B and Fe.

For the experimental procedure CNCN plasma arc cutting machine is used. Cutting specimens are dimension of 20x20x10mm. As cutting gas oxygen is used. Table 1 shows the numerical values (minimum and maximum) of the input and output factors which are used and obtained during cutting process.

Material removal rate or MRR is calculated based on the weight of the final product after cutting process. Surface roughness is measured by surface roughness tester and Ra value is measured based on three positions of the work piece. Based on the three measurements mean surface roughness is calculated.

TABLE 1: INPUT AND OUTPUT FACTORS OF THE PLASMA ARC CUTTING PROCESS

Input factors		Output factors	
Cutting speed (mm/min)	Pressure (psi)	Mean surface roughness, Ra (μm)	Material removal rate (gm/sec)
1000-4000	65-90	1.17-2.47	1.02-2.49

B. ANFIS methodology

ANFIS network has five layers as it shown in Figure 2. The main core of the ANFIS network is fuzzy inference system. Layer 1 receives the inputs and convert them in the fuzzy value by membership functions. In this study bell shaped membership function is used since the function has the highest capability for the regression of the nonlinear data.

Figure 2: ANFIS layers

Bell-shaped membership functios is defined as follows:

$$\mu(x) = bell(x; a_i, b_i, c_i) = \frac{1}{1+\left[\left(\frac{x-c_i}{a_i}\right)^2\right]^{b_i}} \quad (1)$$

where $\{a_i, b_i, c_i\}$ is the parameters set and x is input.

Second layer multiplies the fuzzy signals from the first layer and provides the firing strength of as rule. The third layer is the rule layers where all signals from the second layer are normalized. The fourht layer provides the inference of rules and all signals are converted in crisp values. The final layers sumarized the all signals and provied the output crisp value.

III. Results

C. Accuracy indices

Performances of the proposed models are presented as root means square error (RMSE), Coefficient of determination (R^2) and Pearson coefficient (r) as follows:

1) RMSE

$$RMSE = \sqrt{\frac{\sum_{i=1}^{n}(P_i - O_i)^2}{n}}, \quad (2)$$

Pearson correlation coefficient (r)

$$r = \frac{n\left(\sum_{i=1}^{n} O_i \cdot P_i\right) - \left(\sum_{i=1}^{n} O_i\right)\cdot\left(\sum_{i=1}^{n} P_i\right)}{\sqrt{\left(n\sum_{i=1}^{n} O_i^2 - \left(\sum_{i=1}^{n} O_i\right)^2\right)\cdot\left(n\sum_{i=1}^{n} P_i^2 - \left(\sum_{i=1}^{n} P_i\right)^2\right)}} \quad (3)$$

2) Coefficient of determination (R^2)

$$R^2 = \frac{\left[\sum_{i=1}^{n}\left(O_i - \overline{O_i}\right)\cdot\left(P_i - \overline{P_i}\right)\right]^2}{\sum_{i=1}^{n}\left(O_i - \overline{O_i}\right)\cdot\sum_{i=1}^{n}\left(P_i - \overline{P_i}\right)} \quad (4)$$

where P_i and O_i are known as the experimental and forecast values, respectively, and n is the total number of dataset.

D. ANFIS prediction

Figure 3 shows ANFIS prediction of mean surface roughness (Ra) based on cutting speed and for three different values of pressure, 65, 80 and 90 (psi). Figure 4 shows ANFIS prediction of Ra based on pressure and for six different values of cutting speed, 1000, 1500, 2500, 3000, 3500 and 4000 (mm/min). Figure 5 shows ANFIS-Ra prediction based on the both inputs simultaneously.

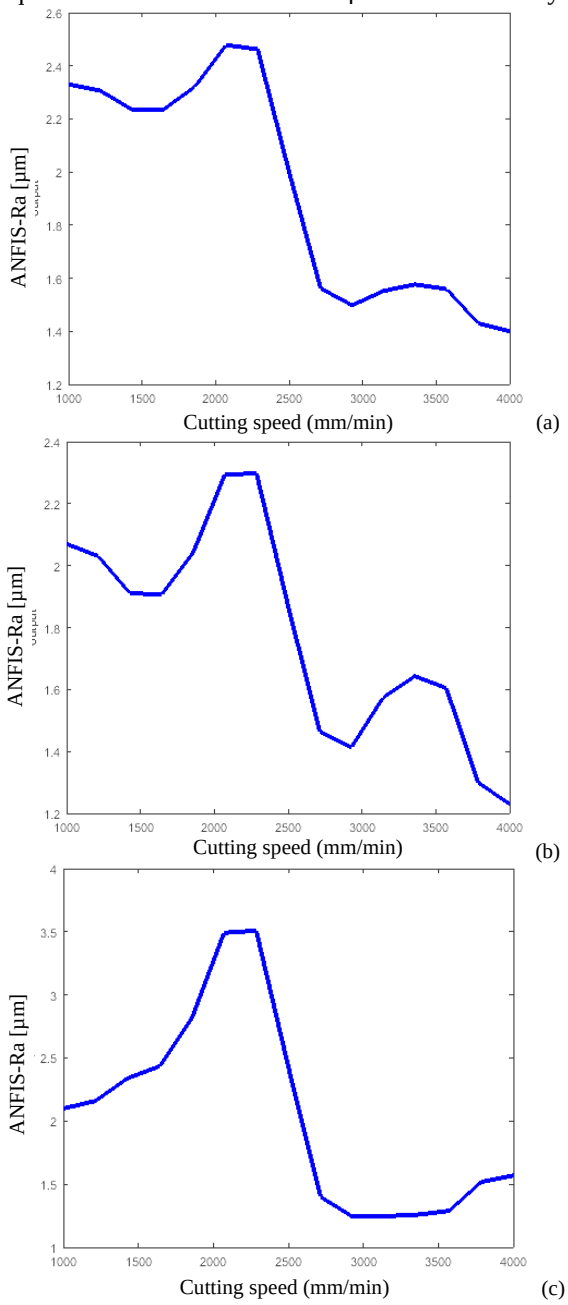

Figure 3: ANFIS-Ra prediction based on cutting speed and for pressure of: (a) 65, (b) 80 and (c) 90 (psi)

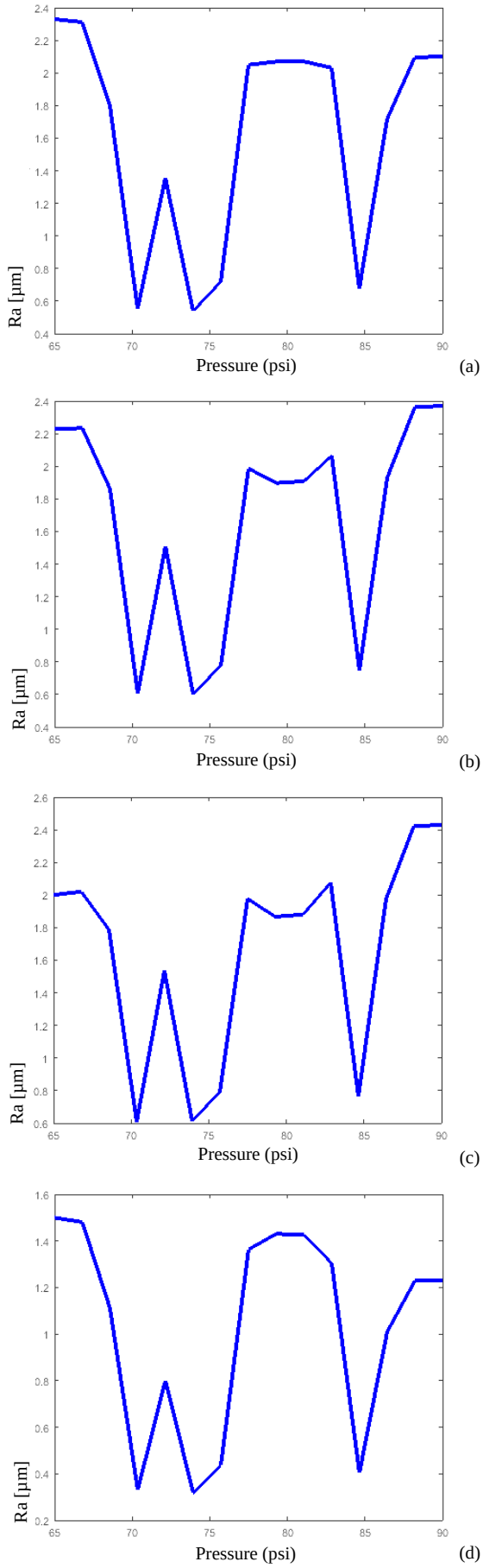

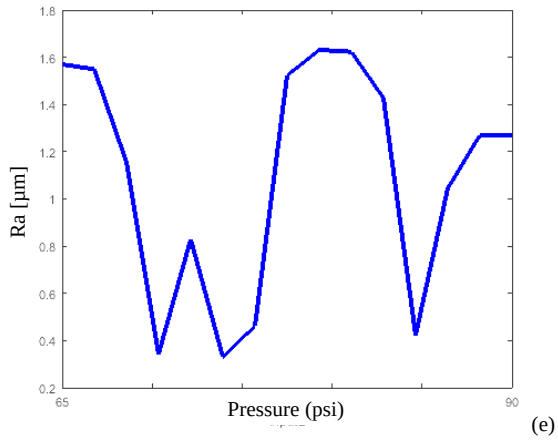

(e)

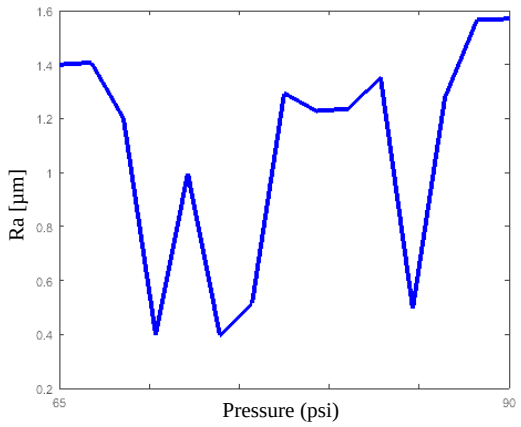

(f)

Figure 4: ANFIS-Ra prediction based on pressure and for cutting speed of: (a) 1000, (b) 1500, (c) 2500, (d) 3000, (e) 3500 and (f) 4000

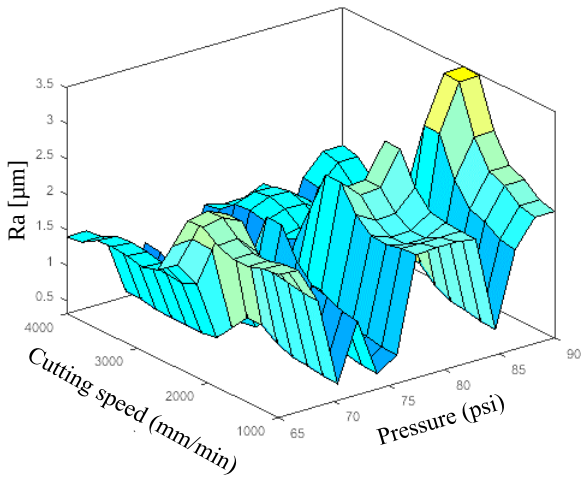

Figure 5: ANFIS-Ra prediction based on pressure and for cutting speed

Figure 6 shows ANFIS prediction of material removal rate (MRR) based on cutting speed and for three different values of pressure, 65, 80 and 90 (psi). Figure 7 shows ANFIS prediction of MRR based on pressure and for six different values of cutting speed, 1000, 1500, 2500, 3000, 3500 and 4000 (mm/min). Figure 8 shows ANFIS-MRR prediction based on the both inputs simultaneously.

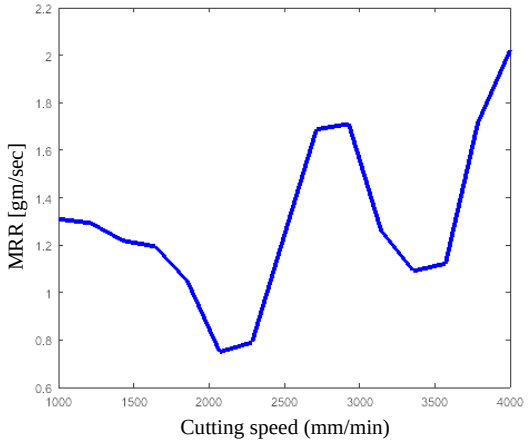

(a)

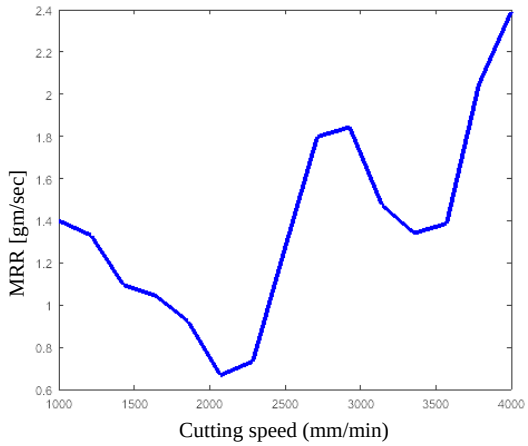

(b)

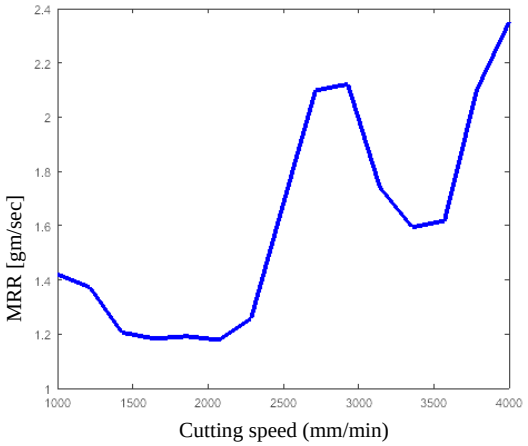

(c)

Figure 6: ANFIS-MRR prediction based on cutting speed and for pressure of: (a) 65, (b) 80 and (c) 90 (psi)

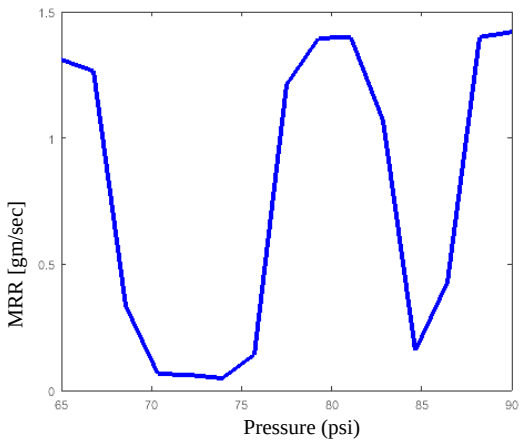

(a)

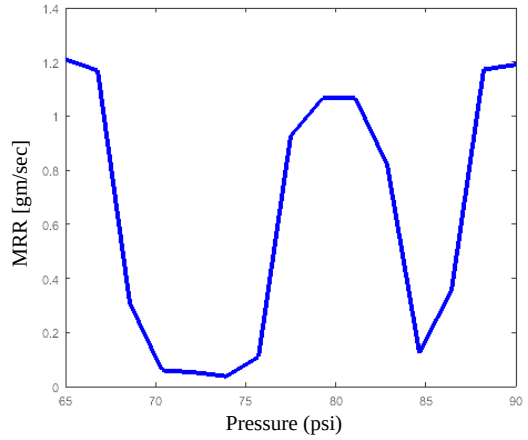

(b)

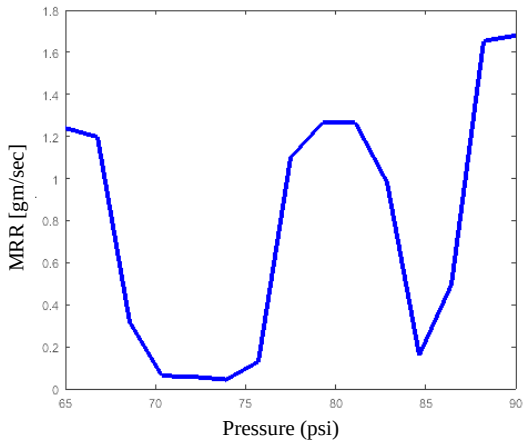

(c)

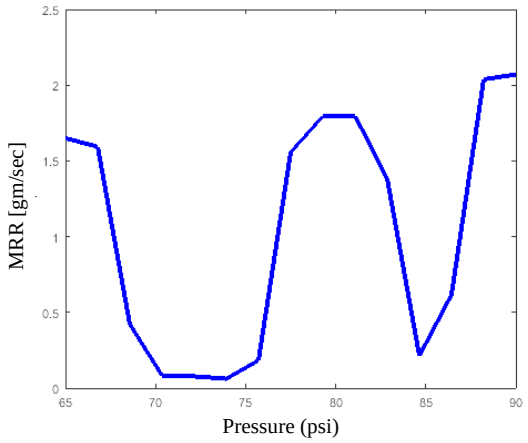

(d)

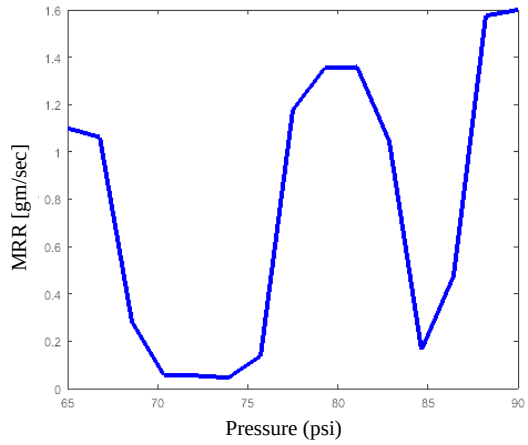

(e)

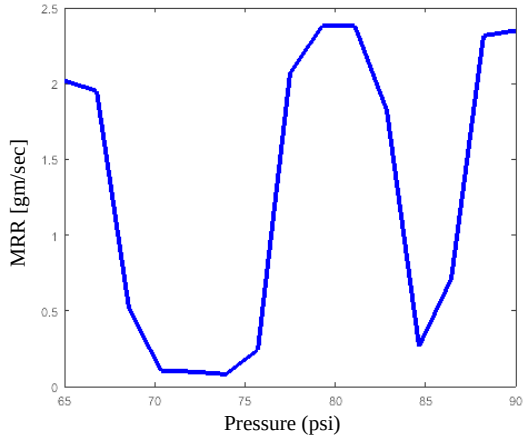

(f)

Figure 7: ANFIS-MRR prediction based on pressure and for cutting speed of: (a) 1000, (b) 1500, (c) 2500, (d) 3000, (e) 3500 and (f) 4000

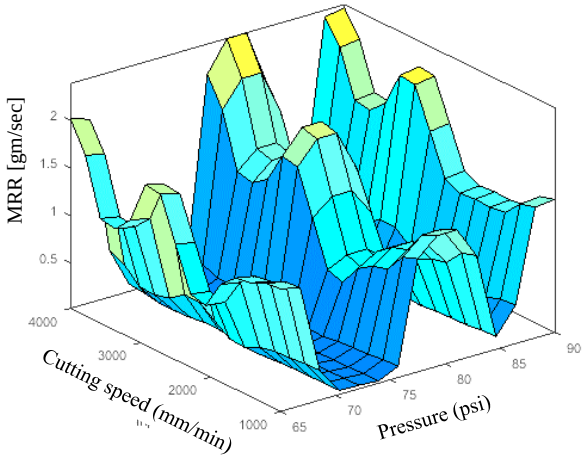

Figure 8: ANFIS-MRR prediction based on pressure and for cutting speed

Figure 9 shows scatter plots of the ANFIS prediction of Ra based on the experimental measured data. It can be noted high predictive accuracy based on R^2 coefficient. Also, Pearson coefficient (r) is 0.873243 and root mean square error (RMSE) is 0.873243 for the Ra prediction.

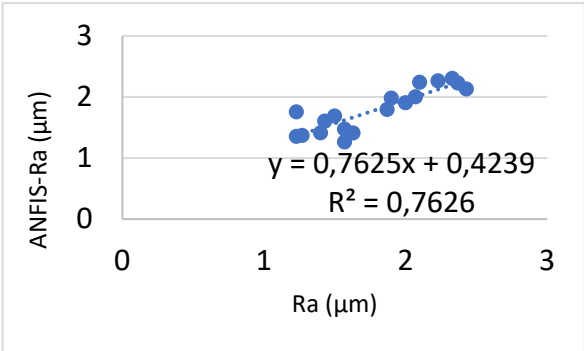

Figure 9: Scatter plot of ANFIS-Ra prediction

Figure 10 shows scatter plots of the ANFIS prediction of MRR based on the experimental measured data. It can be noted high predictive accuracy based on R^2 coefficient. Also, Pearson coefficient (r) is 0.804839 and root mean square error (RMSE) is 0.173676 for the Ra prediction.

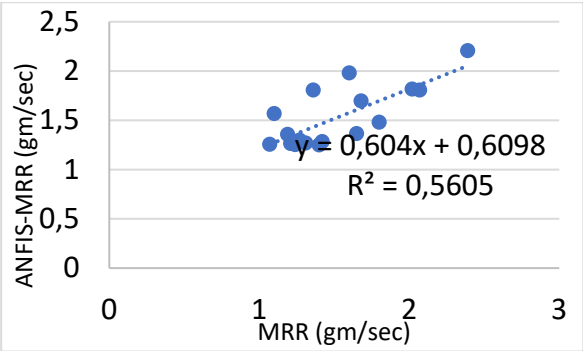

Figure 10: Scatter plot of ANFIS-MRR prediction

IV. Conclusion

In this paper was investigated predictive performance of adaptive neuro fuzzy inference system or ANFIS for prediction of output factors of plasma art cutting process. The output factors are mean surface roughness and material removal rate. The main purpose of the ANFIS predictive models was to determine which cutting quality will be obtained for different set of input parameters. ANFIS can eliminate the vagueness in the process in order to produce the best prediction conditions. In other words ANFIS network was used to convert the multiple performance characteristics into the single performance index.

References

[1] Ananthakumar, K., Rajamani, D., Balasubramanian, E., & Davim, J. P. (2019). Measurement and optimization of multi-response characteristics in plasma arc cutting of Monel 400™ using RSM and TOPSIS. *Measurement*, *135*, 725-737.

[2] Bhowmick, S., Basu, J., Majumdar, G., & Bandyopadhyay, A. (2018). Experimental study of plasma arc cutting of AISI 304 stainless steel. *Materials Today: Proceedings*, *5*(2), 4541-4550.

[3] Patel, P., Nakum, B., Abhishek, K., Kumar, V. R., & Kumar, A. (2018). Optimization of Surface Roughness in Plasma Arc Cutting of AISID2 Steel Using TLBO. *Materials Today: Proceedings*, *5*(9), 18927-18932.

[4] Kumar Naik, D., & Maity, K. P. (2017). An optimization and experimental analysis of plasma arc cutting of Hardox-400 using Taguchi based desirability analysis.

[5] Salonitis, K., & Vatousianos, S. (2012). Experimental investigation of the plasma arc cutting process. *Procedia CIRP*, *3*, 287-292.

[6] [6] Deli, J., & Bo, Y. (2011). An intelligent control strategy for plasma arc cutting technology. *Journal of Manufacturing Processes*, *13*(1), 1-7.

[7] Chamarthi, S., Reddy, N. S., Elipey, M. K., & Reddy, D. R. (2013). Investigation Analysis of Plasma arc cutting Parameters on the Unevenness surface of Hardox-400 material. *Procedia Engineering*, *64*, 854-861.

[8] Rotundo, F., Martini, C., Chiavari, C., Ceschini, L., Concetti, A., Ghedini, E., ... & Dallavalle, S. (2012). Plasma arc cutting: Microstructural modifications of hafnium cathodes during first cycles. *Materials* Chemistry and Physics, 134(2-3), 858-866.

[9] Bini, R., Colosimo, B. M., Kutlu, A. E., & Monno, M. (2008). Experimental study of the features of the kerf generated by a 200 A high tolerance plasma arc cutting system. *Journal of materials processing technology*, *196*(1-3), 345-355.

[10] Chen, S., Zhang, R., Jiang, F., & Dong, S. (2018). Experimental study on electrical property of arc column in plasma arc welding. *Journal of Manufacturing Processes*, *31*, 823-832.

[11] Ji-yu, D., Fang-yi, L., Yan-le, L., Li-ming, W., Hai-yang, L., Xue-ju, R., & Xing-yi, Z. (2019). Influences of plasma arc remelting on microstructure and service performance of Cr3C2-NiCr/NiCrAl composite coating. *Surface and Coatings Technology*.

[12] Xu, W. J., Fang, J. C., & Lu, Y. S. (2002). Study on ceramic cutting by plasma arc. *Journal of Materials Processing Technology*, *129*(1-3), 152-156.

[13] Gariboldi, E., & Previtali, B. (2005). High tolerance plasma arc cutting of commercially pure titanium. *Journal of Materials Processing Technology*, *160*(1), 77-89.

[14] Jang, J.-S.R, ANFIS: Adaptive-Network-based Fuzzy Inference Systems, IEEE Trans. On Systems, Man, and Cybernetics (1993), Vol.23, 665-685.

[15] Petković, D., Issa, M., Pavlović, N.D., Pavlović, N.T., Zentner, L., Adaptive neuro-fuzzy estimation of conductive silicone rubber mechanical properties, Expert Systems with Applications, ISSN 0957-4174, 39 (2012), 9477-9482.

[16] Petković D, Ćojbašić Ž (2012) Adaptive neuro-fuzzy estimation of automatic nervous system parameters effect on heart rate variability, Neural Computing & Application, *21(8):2065-2070* (*2012*)

[17] Kurnaz S, Cetin O, Kaynak O, Adaptive neuro-fuzzy inference system based autonomous flight control of unmanned air vehicles, Expert Systems with Applications (2010), 37, 1229-1234.

[18] Petković, D., Issa, M., Pavlović, N.D., Zentner, L., Ćojbašić, Ž., Adaptive neuro fuzzy controller for adaptive compliant robotic gripper, Expert Systems with Applications, ISSN 0957-4174, 39, (2012), 13295-13304.

THE 5th INTERNATIONAL CONFERENCE
MECHANICAL ENGINEERING IN XXI CENTURY

December 9-10, 2020
Faculty of Mechanical Engineering in Niš, Serbia

Application of Fuzzy Logic for Modeling and Predicting the Electrical Discharge Machining Accuracy

Dragan RODIĆ, Marin GOSTIMIROVIĆ, Milenko SEKULIĆ and Anđelko ALEKSIĆ

University of Novi Sad, Faculty of Technical Sciences, Novi Sad, Serbia,
rodicdr@uns.ac.rs, maring@uns.ac.rs, milenkos@uns.ac.rs, andjelkoa94@uns.ac.rs

***Abstract*— The dimensional accuracy of EDM is directly influenced by the gap distance created between the electrodes in the working zone. However, determining the gap distance between the tool (anode) and the workpiece (cathode) is a difficult point in this type of machining process. In this study a fuzzy logic theory is presented so that the EDM process can be modeled from the point of view of accuracy. The purpose is to develop a fuzzy logic model to analyze and predict the gap distance of the EDM process. The effect of the discharge current and the pulse duration was observed as developed input parameters. The fuzzy model offers a very advantageous option of the EDM input parameters to achieve the best machining accuracy. Moreover, the obtained model can be used in the generalization phase, where the gap distance information is needed and where direct measurement is not possible.**

***Keywords*— EDM, Discharge Current, Pulse Duration, Gap distance, Fuzzy model**

I. Introduction

The modern manufacturing industry follows the trends of high-precision machining. Industries such as aerospace, automotive, electronics, production of micro parts, plastic molds etc. increasingly demand this type of machining. Electrical discharge machining (EDM) has recently taken an important place in production areas, as it can machine both difficult to machine materials and complex contours and shapes. As with other machining processes, one of the most important technological features of EDM is machining accuracy [1].

The dimensional accuracy of the EDM machine depends primarily on general factors related to the EDM machine itself (machine accuracy, rigidity of the machining system, positioning accuracy of tool and workpiece), accuracy of tool manufacture, thermal expansion of the electrode, changes in the working gap, tool wear, etc. [2]. Most of the factors mentioned above can be influenced before processing. However, it was necessary to investigate and conclude what the dimensional stability during machining [3]. This problem is being considered by many researchers. Deris et al. investigate the diameter overcut in EDM and concluded that dimensional accuracy could be influenced by the input parameters of the processing such as discharge current, pulse duration, voltage and servo speed [4]. A similar study was carried out by Sahu and Mandal, who found that the discharge current and pulse duration have the greatest influence on dimensional accuracy [5]. The influence of individual input processing parameters and optimal values are determined mainly by classical statistical methods.

A new trend in EDM modeling with an artificially intelligent approach has clearly developed. Singh et al. used various soft computing techniques to predict technological properties of EDM [6]. They compared intelligent and classical techniques, and it turned out that the fuzzy logic approach gave the best results. Shivakoti et al. investigated the influence of input parameters on the performance of micro-EDM [7]. They also carried out a comparative analysis of experimental, fuzzy and regression predictions and confirmed that the fuzzy model gives better results than the regression model. Mathai et al. conducted experimental studies on EDM and developed a fuzzy-based model for predicting tool wear, which is directly related to dimensional accuracy. The development of fuzzy models is mainly based on experimental data [8].

In the present study the experiments are performed with Taguchi's orthogonal L18 array. The discharge current, pulse duration and different tool materials are considered for the EDM process. In order to obtain an intelligent model, a fuzzy logic approach was used to generate and test data to predict and analyze the overcut. The gap distance generated between tool and workpiece is used as overcut in different machining regimes. The most important parameter that influences AISI O2 during EDM of cold work tool steel is analyzed by ANOVA. Finally, the recommended machining regime is given to obtain the minimum overcut. The results of this study suggest that the fuzzy logic approach can be effectively used for the prediction and analysis of the overcut during EDM.

II. Experimental setup

The machining process was carried out with a CNC die-sinking EDM machine. Experiments were carried out with hydrocarbon oil as dielectric fluid by natural flushing. Cold work tool steel AISI O2 with a hardness of 62 HRC is used as the workpiece. Two types of tools were used for the present work. One of the tools was electrolytic copper with a purity of 99.9%. The other tool was the nodular graphite with an average grain size of 12 μm. The processing conditions included variable discharge current and pulse duration. The range of the discharge current was 5 to 13 A, while the pulse duration was selected from the interval of 2 to 7 μs to accommodate the selected current.

The other parameters of the electric pulse were kept constant according to the manufacturer's recommendations (voltage 100 V, duty cycle 0.8 and positive polarity of the tool electrode).

The dimensional accuracy of EDM (overcut) was monitored by changing the side gap distance a between the workpiece and the electrode. The gap distance was calculated as half the difference between the dimensions of the tool and the workpiece contour. The measurements were made with electronic callipers (accuracy: 0.001 mm).

The experiments were performed according to the Design of Experiments (DOE) using the Taguchi approach. In this study three parameters were selected, one of the parameters is on two levels (tool material) and the rest of the parameters are on three levels (discharge current and pulse duration), the design becomes a mixed level design. For this experiment the orthogonal arrangement L18 was chosen. The experimental conditions are shown in Table 1.

TABLE 1. EXPERIMENTAL RESULTS

No.	Tool	Discharge current [A]	Pulse duration [µs]	Overcut [mm]	
				Exp.	Fuzzy logic
1.	Copper	13	7	0.200	0.191
2.	Copper	5	7	0.105	0.113
3.	Copper	5	2	0.095	0.098
4.	Copper	13	5	0.180	0.174
5.	Copper	9	2	0.130	0.136
6.	Copper	13	2	0.165	0.156
7.	Copper	9	5	0.140	0.137
8.	Copper	9	7	0.155	0.156
9.	Copper	5	5	0.100	0.113
10.	Graphite	9	5	0.130	0.137
11.	Graphite	5	7	0.095	0.098
12.	Graphite	9	2	0.110	0.114
13.	Graphite	13	5	0.170	0.174
14.	Graphite	13	2	0.140	0.136
15.	Graphite	5	5	0.095	0.099
16.	Graphite	13	7	0.190	0.191
17.	Graphite	9	7	0.150	0.137
18.	Graphite	5	2	0.090	0.098

III. FUZZY LOGIC MODELING

The design of the model based on fuzzy logic takes place in three phases. In the first phase fuzzy variables are defined. Then unclear sets are determined with corresponding membership functions. Finally, fuzzy rules are defined and adapted. The complete modeling process is explained below.

The considered input variables of the fuzzy model are tool material, discharge current and pulse duration. While the output variable is overridden The basic step in fuzzy modeling is to select suitable forms of the membership function for the development of the algorithm to select the input parameters of the EDM. These functions are a graphical representation of the magnitude of the intervention of each input parameter. Fuzzy expressions for input parameters were divided into two (for tool material) and three (for discharge current and pulse duration) membership functions, Table 2.

The fuzzy logic uses membership functions that are an arbitrary curve. Although there are many different membership functions, such as triangular, trapezoidal, bell-shaped, gaussian, etc. The modeling of the overcut in this paper is done with the bell type (bell). This function is very convenient due to its simple setup.

TABLE 2. FUZZY EXPRESSION OF INPUT PARAMETERS

	Fuzzy expression	Tool material	Discharge current [A]	Pulse duration [µs]
1.	Small	-	5	2
2.	Medium	-	9	5
3.	High	-	13	7
4.	Copper	1	-	-
5.	Graphite	2	-	-

For example, the membership functions considered for tool material are "copper" and "graphite", as shown in Figure 2. Similarly, for other parameters, the membership functions "Small" "Medium" and "High" have been considered, as shown in Figures 2 and 3.

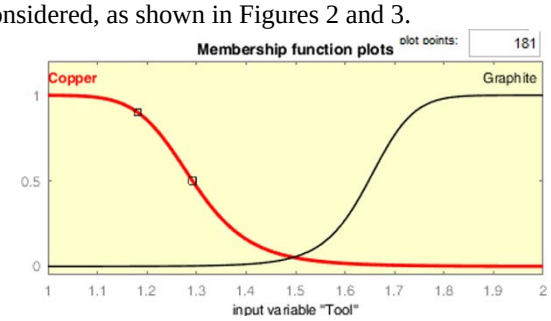

Fig. 1. Membership functions for tool material

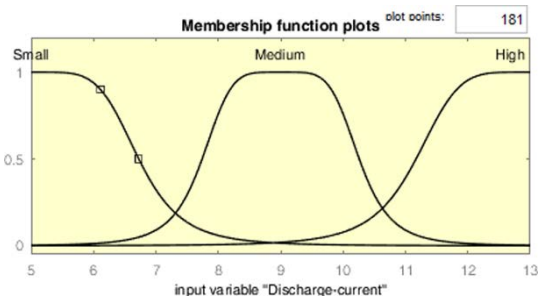

Fig. 2. Membership functions for discharge current

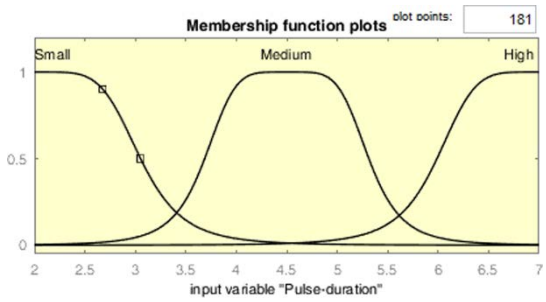

Fig. 3. Membership functions for pulse duration

The number of membership functions used for the output response (overflow) is six, such as "Smallest", "Smaller" "Small", "High", "Higher" and "Highest", Figure 4.

These sets of output variables are defined based on the experience of the model builder. In practice, a larger number of functions at the output of the model has been shown to produce more accurate results. However, this number has its limitations, as it can lead to over-adaptation of the model, i.e. the inability to predict the output variable with data that was not involved in creating the rules.

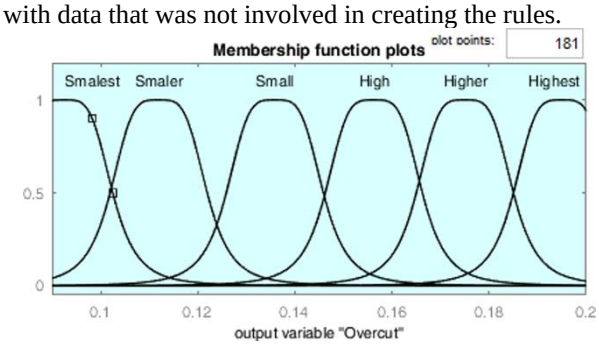

Fig. 4. Membership functions for overcut

The concept of fuzzy reasoning for a fuzzy logic unit with three inputs and one output implies the following. The fuzzy rule base consists of a set of IF - THEN rules with three inputs, x_1 (tool material), x_2 (discharge current) and x_3 (pulse duration) and one output y (overcut). Overhead form of the rule base with several inputs and one output:

$$\begin{array}{l} \textit{Input}: \quad x_1 \text{ is } A_i \text{ and } x_2 \text{ is } B_i \text{ and } x_3 \text{ is } C_i \\ \hline R_1: \quad x_1 \text{ is } A_1 \text{ and } x_2 \text{ is } B_1 \text{ and } x_3 \text{ is } C_1 \text{ THEN } y \text{ is } D_1 \\ R_2: \quad x_1 \text{ is } A_2 \text{ and } x_2 \text{ is } B_2 \text{ and } x_3 \text{ is } C_2 \text{ THEN } y \text{ is } D_2 \\ \vdots \\ R_i: \quad x_1 \text{ is } A_i \text{ and } x_2 \text{ is } B_i \text{ and } x_3 \text{ is } C_i \text{ THEN } y \text{ is } D_i \\ \hline \qquad\qquad \textit{Output}: \quad y \text{ is } D' \end{array}$$

Where x_1, x_2 and x_3 are input parameters that describe the state of the system and represent the input variable of a fuzzy system, while y is the output of a fuzzy model. For A (tool material), B (discharge current), C (pulse duration) and D (overcut) are linguistic values defined by fuzzy sets in the areas x_1, x_2, x_3 and y respectively.

This is followed by the implication function, which modifies this fuzzy set to the degree specified by the predecessor. Each rule can be regarded as a fuzzy implication, so the rule is defined accordingly:

$$\begin{aligned} \mu_{Ri} &= \mu_{(Ai \wedge Bi \wedge Ci \Rightarrow Di)}(x_1, x_2, x_3, y) = \\ &= [\mu_{Ai}(x_1) \wedge \mu_{Bi}(x_2) \wedge \mu_{Ci}(x_3)] \Rightarrow \mu_{Di}(y) \end{aligned}$$

In this model the implication operator Mamdani MIN is used. Where antecedent is named $[\mu_{Ai}(x_1) \wedge \mu_{Bi}(x_2) \wedge \mu_{Ci}(x_3)]$ antecedent while consequent is $\mu_{Di}(y)$. Each rule has a weighting (number between 0 and 1) that is applied to the number specified by the antecedent.

Finally, a defuzzification method is used to transform the fuzzy output into a non-fuzzy value y0. The defuzzification is performed with the center of gravity defuzzification method. The non-fuzzy value specifies the output intersection value in numerical form. For example, the overlap value is obtained as 0.136 mm for the input parameters, tool material is copper, discharge current of 9 A and pulse duration of 2 μs.

IV. Results and Analysis

In Table 1, the comparison values obtained by experiment and fuzzy logic are preset. The average deviation of the fuzzy model is 4.62%. This error showed that the fuzzy logic model provides an accurate prediction in case of overcut. The results obtained with the fuzzy logic model based on the Mamdani argumentation and rules defined by experimental data show agreement with the experiment.

The one-to-one diagram of the test and model values of the overcut is shown in Figure 5. Where the linear fit, equation and coefficient of determination R^2 are also shown in the same figure. The R^2 or index of agreement is used to measure the degree of linearity of trial and fuzzy values. The range of this coefficient is between 0 and 1, with or without perfect correlation.

The model can be considered appropriate if the errors are less than 10 percent, which is confirmed in several investigations. From this it can be concluded that the fuzzy model is appropriate for the prediction of overcut in EDM.

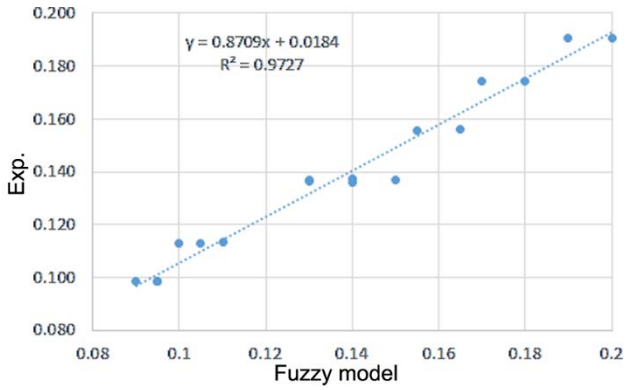

Fig. 5. One-to-one diagram actual and predicted values of overcut

The model verification was carried out with another 4 experiments, which were not involved in the development of the rule base. The average error or discrepancy between the fuzzy model and the experimental results is 8.39 % for the test data. This shows that the selected parameters of the fuzzy model are a good choice.

From the analysis of ANOVA and the F-test (Table 4) it can be concluded that the most influential parameter is the discharge current, followed by the pulse duration and the tool material. This statement is also shown in the main effect plot in Figure 6.

Table 3. Test fuzzy model

	Tool material	Discharge current [A]	Pulse duration [μs]	Overcut [mm]	
				Exp.	Fuzzy
1.	Copper	9	10	0.155	0.156
2.	Copper	13	10	0.210	0.190
3.	Graphite	9	10	0.170	0.192
4.	Graphite	13	10	0.200	0.137
Average error: 8.39 %					

TABLE 4. ANALYSIS OF VARIANCE

Parameter	DF	Adj SS	Adj MS	F-value	P-Value
Tool material	1	0.000556	0.000556	7.84	0.16
Discharge current	2	0.018019	0.009010	127.2	0
Pulse duration	2	0.002269	0.001135	16.02	0
Error	12	0.000850	0.000071	-	-
Total	17	0.021694	-	-	-

The main effect diagram shows the influence of the individual input parameters. If the line is not horizontal, there is a main effect. It can be seen that each parameter influences the overcut, but the slope is greatest for the discharge current.

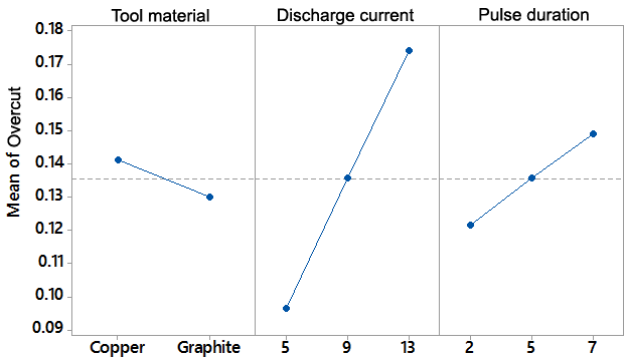

Fig. 6. Main effect plot for overcut

After the analysis from ANOVA it can be concluded that the graphite tool has received a smaller overcut. Therefore, the 3D spatial diagrams for graphite tool material are shown in Figure 7. These figures show the surface viewer for the overcut of the graphite tool as a function of the combined machining parameters (discharge current - pulse duration). The minimum overcut is achieved at a discharge current of 5 A and a pulse duration of 7 µs.

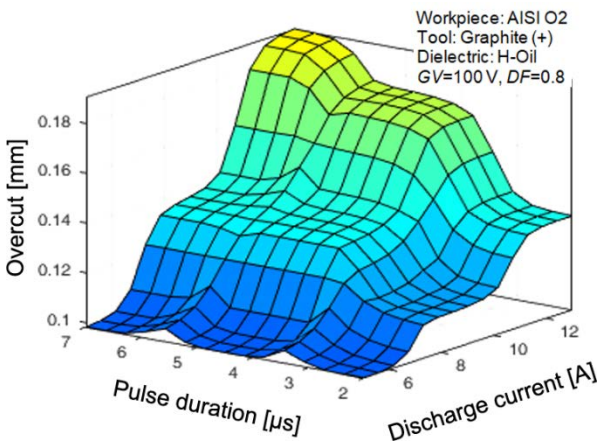

Fig. 7. Fuzzy 3D diagrams for the overcut for graphite tool

From the diagram shown, a minimal overcut can be obtained with a pulse of 2 µs. However, it is known that the rate of material removal decreases with decreasing pulse duration [9]. Therefore a pulse duration of 7 µs is the better choice.

V. CONCLUSION

In the present study, the modeling and analysis of EDM of the cold work steel AISI O2 is shown. The main contribution of the research is therefore the proposal of a fuzzy logic to design an intelligent model for the prediction of the overcut. On the basis of 18 tests, 4 test points of experiments and statistical analysis, it has been concluded that the obtained model can predict and that the fuzzy logic has been successfully applied. The results of the fuzzy model are in good agreement with the test experiment. The average error of the test data represents an acceptable error, which is 8.39%. The ANOVA for overcut shows that the discharge current is the most influential parameter. The fuzzy model is only applicable within the limits of experimental research. A minimum overcut can be achieved with a discharge current of 5 A and a pulse duration of 7 µs.

ACKNOWLEDGMENT

The paper is the result of the research within the project financed by the Ministry of Science and Technological Development of the Republic of Serbia.

REFERENCES

[1] Gostimirovic, M., et al., Evolutionary optimization of jet lag in the abrasive water jet machining. The International Journal of Advanced Manufacturing Technology, 2019. 101(9-12): p. 3131-3141.

[2] Singh, N.K., et al., Intelligent hybrid approaches for ensuring better prediction of gas-assisted EDM responses. SN Applied Sciences, 2020. 2: p. 1-15.

[3] Gostimirovic, M., et al., Inverse electro-thermal analysis of the material removal mechanism in electrical discharge machining. The International Journal of Advanced Manufacturing Technology, 2018. 97(5): p. 1861-1871.

[4] Deris, A., et al. Harmony search optimization in dimensional accuracy of die sinking EDM process using SS316L stainless steel. in Journal of Physics: Conference Series. 2017.

[5] Sahu, D.R. and A. Mandal, Critical analysis of surface integrity parameters and dimensional accuracy in powder-mixed EDM. Materials and Manufacturing Processes, 2020. 35(4): p. 430-441.

[6] Singh, N.K., et al., Comparative study of statistical and soft computing-based predictive models for material removal rate and surface roughness during helium-assisted EDM of D3 die steel. SN Applied Sciences, 2019. 1(6): p. 529.

[7] Shivakoti, I., et al., Experimental Investigation and Fuzzy-Based Modeling of Micro-EDM Process Parameters, in Advances in Greener Energy Technologies. 2020, Springer. p. 665-683.

[8] Zindani, D., et al., Fuzzy logic for machining applications, in Advanced Fuzzy Logic Approaches in Engineering Science. 2019, IGI Global. p. 341-361.

[9] Rodic, D., et al., Fuzzy model-based optimal energy control during the electrical discharge machining. Neural Computing and Applications, 2020: p. 1-16.

THE 5th INTERNATIONAL CONFERENCE
MECHANICAL ENGINEERING IN XXI CENTURY

December 9-10, 2020
Faculty of Mechanical Engineering in Niš, Serbia

Empirical model to predict surface roughness for drilling GFRP

Pawan KUMAR

Department of Mechanical Engineering, National Institute of Technology Kurukshetra, Kurukshetra - 136119, India
pawank76@gmail.com

***Abstract*— The GFRP (glass fibre reinforced plastics) composites are finding up numerous application in many engineering and domestic fields due to their excellent mechanical properties and corrosion resistance. Maintain of proper surface roughness in drilling hole is very important and is to be controlled. In this work an attempt is made to predict surface roughness using empirical model. The experiment study is planed using Taguchi approach to know the influence of machining parameters on surface roughness. The experimental results are studied using analysis of variance and it is found the feed (36.84%) and drill diameter (27.33%) is the most affect parameter affecting the surface roughness. A machining parameter based model has been developed to predict the response parameter in drilling of glass fibre reinforced composite.**

***Keywords*—Drilling, GFRP, Taguchi method, Surface roughness, Regression.**

I. Introduction

Composite materials consist of at least two separate anticipated materials that mutually enhance product performance and lower production costs []. Glass fibre reinforced composites (GFRP) material gaining more attention these days due to their better performance over convention engineering materials, such as excellent mechanical strength, lightweight, and low cost [2]. Composites materials are commonly used in various fields such as aerospace, automotive, civil engineering, and consumer goods. Among different machining practices for joining structures, drilling is widely used for polymer composite laminates [3]. During the drilling process, a previous study with commercial composites has established that several parameters can affect the drilling operation and may damage the material [4].

Surface roughness is an indicator of surface quality, and is one of the most specified customer requirements in a machining process. But it can be controlled by proper selection of machining parameters. Therefore proper selection of machining parameter becomes essential to obtain better performance of drilling operation. Modelling of machining parameters is one of the most critical elements in machining processes [5]. GFRP composite materials have specific characteristics that impel their machining behaviour. Therefore, when drilling composite materials, the process occupied complexity in comparison to drilling homogeneous materials like metals [6].

In this study, drilling is performed of GFRP with an high-speed steel (HSS) twist drill, and an empirical model is purposed using the cutting parameters. The input process parameters which may show a major impact on surface roughness such as speed, feed, drill diameter, and point angle are considered in the drilling process for investigation.

II. Material and Method

The workpiece taken for the experiment is GFRP. A 10 mm thick sheet is taken, which later cut down into small pieces of 11×11 cm^2 dimension. Matrix for the composite was epoxy resin in which glass fibre was reinforced. Another technical specification of GFRP material is shown in Table 1. The tool used for GRFP drilling in this work were of HSS. These drill bits are extensive usage in industry due to ease of availability and economic concerns [7,8]. These drill bits of three different point angle and diameter are taken. So in total, nine drill bits were used as per the requirement of L_{18} orthogonal array (OA).

TABLE I Properties of GFRP Material

Properties	Unit	Value
Density	g/cm^3	1.70 – 1.90
Bending strength	kgf/cm^2	4000 - Longitudinal 3000 - Horizontal
Tensile strength	kgf/cm^2	3500 - Longitudinal 2500 - Horizontal
Impact strength (Charpy)	kj/m^2	33
Flexural strength	MPa	340

Taguchi methodology is simple and widely used for optimization, experimental design, sensitivity analysis, parameter estimation, model prediction, etc.. Taguchi's L_{18} OA is used to perform the experimentation as it saves the resources and helps to draw meaningful conclusions from experimental outcomes [9,10]. The factor and their level of interest, which may influence the drilling system, are shown in Table 2.

TABLE II Factors and their levels

Factors	Units	Levels		
		1	2	3
Feed (f)	mm/rev	0.1	0.15	-
Speed (s)	rpm	290	580	890

Drill diameter (d)	mm	6.0	7.1	9.1
Point angle (θ)	degree	78	98	118

III. Result and Discussion

L_{18} OA was found perfect for this study. The experimentation was performed using randomisation concept. The surface roughness of the drilled holes was obtained by using surface roughness tester MITUTOYO, SJ-400. A sampling length of 0.08 mm and a trace length of 3 mm were taken for measurement. The experimental outcome is shown in Table 3.

TABLE III Results for Surface Roughness

Trial Runs	f	s	d	θ	Surface Roughness (microns)	
					Experimental	Regression
1	0.1	290	6.0	78	0.29	0.31656
2	0.1	290	7.1	98	0.43	0.43192
3	0.1	290	9.1	118	0.37	0.63152
4	0.1	580	6.0	78	0.30	0.27016
5	0.1	580	7.1	98	0.51	0.38552
6	0.1	580	9.1	118	0.80	0.58512
7	0.1	890	6.0	98	0.38	0.23296
8	0.1	890	7.1	118	0.25	0.34832
9	0.1	890	9.1	78	0.39	0.51072
10	0.15	290	6.0	118	0.60	0.62036
11	0.15	290	7.1	78	0.74	0.69852
12	0.15	290	9.1	98	1.10	0.89812
13	0.15	580	6.0	98	0.60	0.56156
14	0.15	580	7.1	118	0.50	0.67692
15	0.15	580	9.1	78	0.75	0.83932
16	0.15	890	6.0	118	0.54	0.52436
17	0.15	890	7.1	78	0.44	0.60252
18	0.15	890	9.1	98	0.96	0.80212

A. *Statistical study*

The statistical study is also performed to draw meaning full conclusions from the experimental outcomes. The analysis is conducted at a 95% significance level. Table 4 is representing the model summary statistics.

TABLE IV Model Summary Statistics

Source	Std. Dev.	R-squared	Adj. R-squared	Pred. R-squared	PRESS
Linear	0.16	0.6714	0.5703	0.3281	0.64
2FI	0.18	0.7695	0.4402	-1.7527	2.62
Quadratic	0.16	0.8949	0.5532	-8.5543	9.09

The model selection which correlates the influential factors and response parameters depends upon complexity of phenomenon, research objective, experimental plan as well as quantity and quality of available information [11]. As we aim for higher, adjusted and predicted R-squared values. Therefore the linear model is selected among the three models suggested in this study for prediction purposes.

B. *Analysis of variance (ANOVA)*

ANOVA is also performed on surface roughness results. It is found that the feed (f) followed by drill diameter (d) is the main factor affecting the surface quality of the drilled hole. The percentage contribution of each factor can also be noticed from Table 5.

TABLE V Analysis of Variance Results for Surface Roughness

Source	SS	df	MS	F Value	p-value Prob > F	% C
Model	0.64	4	0.16	6.64	0.0039	Significant
f	0.35	1	0.35	14.55	0.0021	36.84
s	0.028	1	0.028	1.14	0.3043	2.896
d	0.26	1	0.26	10.79	0.0059	27.33
θ	1.875×10^{-3}	1	1.875×10^{-3}	0.078	0.7845	0.197
Residual	0.31	13	0.024			
Cor Total	0.95	17				
SS - Sum of Squares, MS – Mean Square, df – degree of freedom, C – Contribution						

IV. Empirical Modelling

An empirical relation also developed using the input cutting parameter to predict the surface roughness within the parametric range, which as follows:

$$SR\ (\mu m) = -0.83701 + 5.58 \times f + 0.0936 \times d$$

It is a multiple linear regression model with two independent variables. As resulted from ANOVA analysis, the speed (s) and point angle (θ) are having a small contribution to surface roughness. Moreover, to keep the model as simple as possible, these two independent variables are omitted from the regression equation. The resulted regression model was also tested for the lack of fit. Fig. 1 is showing the plot between measured and predicted surface roughness values depicting the goodness of fit.

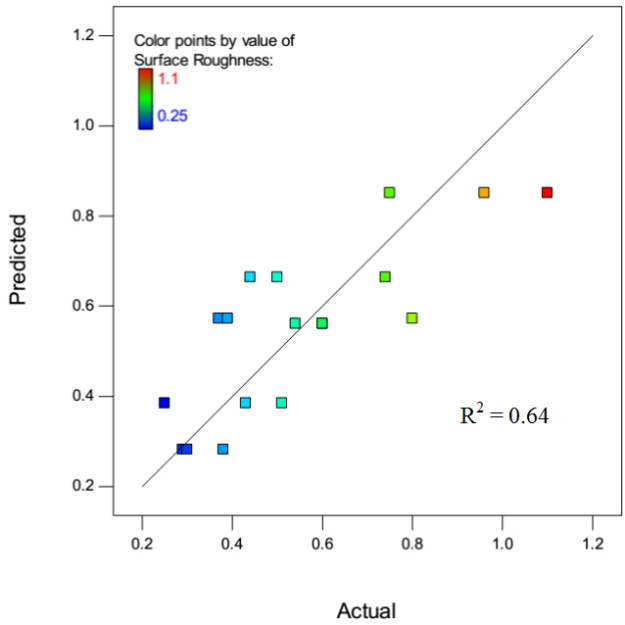

Fig. 1 Correlation plot between actual and predicted values of surface roughness

To get a visualization of the regression model performance, experimental and predicted values are also plotted against experiment runs. Fig. 2 is depicting model performance while predicting surface roughness. It can be

observed the model lacks at some point to capture the variability present in the drilling process.

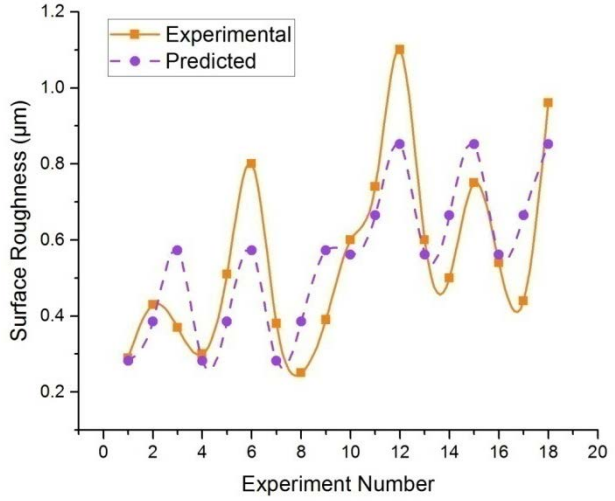

Fig. 2 Experimental and predicted values against experimental run

Furthermore, the model was also subjected to an adequacy test to check its prediction capability. Fig. 3 is depicting the normal probability plot of the residuals. As it is visible that residuals are approximately along diagonal line, therefore it satisfies the normality assumption.

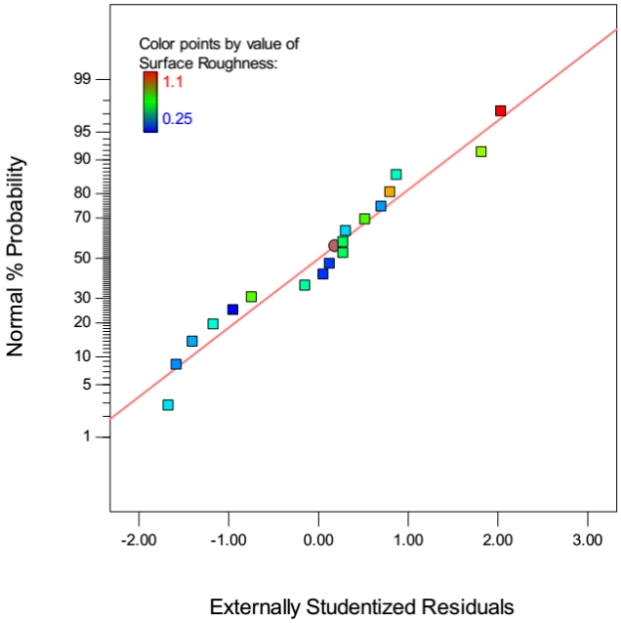

Fig. 3 Normal probability plot of residuals

Fig. 4 presents a plot of residuals versus the predicted response values. As it is observable from this plot that residuals are scattered randomly, and there is no pattern between data points. This suggests that the variance is constant for all measured surface roughness values. Therefore the developed regression model is adequate for prediction purposes.

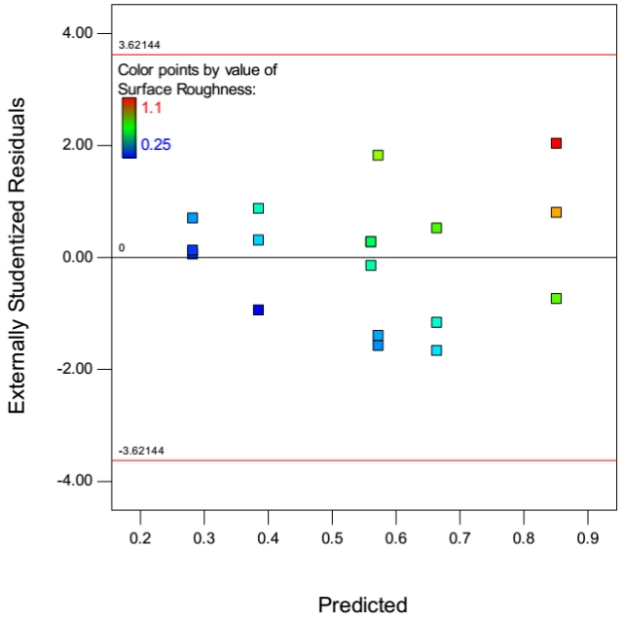

Fig. 4 Scatter plot of residuals

Confirmation runs were performed to verify the study. Table 6 is showing the results of the confirmation test. Thus prediction capability of developed model is evaluated.

TABLE VI CONFIRMATION RUN RESULTS

Sr. No.	Input Parameters				Surface Roughness, Ra (µm)		% Error
	f	s	d	θ	Exp.	Predicted	
1.	0.1	445	9.1	118	0.76	0.57275	24.63
2.	0.15	445	6	118	0.48	0.56169	-17.01
MAPE							20.82

V. CONCLUSIONS

In this experimental study, an attempt has been made to develop a predictive model for the surface roughness during drilling of GFRP using HSS driil bits. The experimentation was performed using Taguchi's method and L_{18} OA found suitable for the study. The feed and drill diameter is found significant cutting parameter in this study affecting the surface roughness of the drilled hole. Later on, an empirical model is developed using regression analysis with 64.05% prediction efficiency. Although adding a variable to the model will always increase R^2, the model was kept simple for its easy adaptability by researchers and machinist.

REFERENCES

[1] W. D. Callister, Materials Science and Engineering an Introduction, John Wiley, 2007.

[2] A. Mortensen, Concise Encyclopedia of Composite Materials, Elsevier, 2006.

[3] B.V. Kavad, A.B. Pandey, M.V. Tadavi, and H.C. Jakharia, 'A review paper on effects of drilling on glass fiber reinforced plastic', Procedia Tech., vol. 14 (2014), pp. 457-64, 2014.

[4] C. Santiuste, X. Soldani, and M. H. Miguélez, 'Machining FEM model of long fiber composites for aeronautical components', Compos. Struct., vol. 92,pp. 691-98, 2010.

[5] R. Teti, 'Machining of Composite Materials', *CIRP Annals*, vol. 51 ,pp. 611-34, 2002.

[6] J. P. Davim, P. Reis, and C. C. Antonio, 'Experimental Study of drilling glass fiber reinforced plastics (GFRP) manufactured by Hand Lay-Up', Compos. Sci. Technol., vol. 64, pp. 289-97, 2004.

[7] S. O. Ismail, H. N. Dhakal, I. Popov, and J. Beaugrand, 'Comprehensive study on machinability of sustainable and conventional fibre reinforced polymer composites', Eng. Sci. Technol. an Int. J., vol. 19, pp. 2043-52, 2016.

[8] V. K. Vankanti, and V. Ganta, 'Optimization of process parameters in drilling of GFRP composite using Taguchi Method', J. Mater. Res. Technol., vol. 3 ,pp. 35-41, 2014.

[9] M. S. Phadke, Quality Engineering Using Robust Design, Prentice Hall PTR, 1995.

[10] D. Lazarević, M. Madić, P. Janković, and A. Lazarević, 'Cutting parameters optimization for surface roughness in turning operation of Polyethylene (PE) using Taguchi Method', Tribol. Ind., vol. 34, pp. 68-73, 2012.

[11] A. Lazarević, and D. Lazarević, 'Non-Linear mathematical models in the theory of experimental design: Application in the manufacturing processes', FU Mech. Eng., vol. 13, pp. 181-91, 2015.

THE 5th INTERNATIONAL CONFERENCE
MECHANICAL ENGINEERING IN XXI CENTURY

December 9-10, 2020
Faculty of Mechanical Engineering in Niš, Serbia

Optimization of Cutting Parameters for Minimizing Part Production Costs in Multi-Pass Rough Turning of EN-GJL-250 Grey Cast Iron

Milan TRIFUNOVIĆ, Predrag JANKOVIĆ, Nikola VITKOVIĆ

Faculty of Mechanical Engineering in Niš, University of Niš, Aleksandra Medvedeva 14, 18106 Niš, Serbia
milan.trifunovic@masfak.ni.ac.rs, madic@masfak.ni.ac.rs, jape@masfak.ni.ac.rs, nikola.vitkovic@masfak.ni.ac.rs

***Abstract*— The best way to reduce part production costs in turning is by increasing productivity, which is achieved by optimization of cutting parameters. Therefore, an optimization model for the multi-pass rough turning of grey cast iron, with part production costs considered as objective function, incorporating several practical constraints, was developed. The optimization problem was solved using a deterministic approach, i.e. brute force optimization algorithm, which guarantees the optimality of the optimization solutions in the given discrete space of input variables values. Results confirm that part production costs can be noticeably reduced by optimizing the main cutting parameters, compared to the part production costs for the cutting parameters recommended by the insert manufacturer. For the production of one part, part production costs can be reduced by 13,7 %, while unit production time can be reduced by 10,98 %. For the batch of 100 parts, total production costs can be reduced by 27,11 %, while total production time can be reduced by 25,18 %, leading to total savings of 44,44 EUR in production costs and 57,84 min in production time. In situations when the cutting parameters are adopted based on the insert manufacturer's recommendations, it is important to pay attention to certain constraints, such as the relationship between depth of cut and feed rate.**

***Keywords*— multi-pass turning, optimization model, part production costs, practical constraints, grey cast iron**

I. Introduction

Turning is a machining method in which the material is removed from the surface of a rotating workpiece by using a single-point tool. Resulting geometry is determined by the feed trajectory of the cutting tool. For a given workpiece material and available machine tool, it is necessary to select the appropriate cutting tool (material and geometry) and cutting parameters for each of the machining operations required to manufacture the finished part. Cutting parameters are directly related to turning process performances such as quality, machining economy, and productivity [1]. One of the key quantities of interest in machining economy is part production costs. In turning, as well as in all industrial operations, the cost of running the operation is increasing at a faster rate than the price of the goods that are sold. The best way to reduce part production costs in turning is by increasing productivity, which is achieved by optimization of cutting parameters.

There are several recent multi-pass turning optimization studies based on analytical modelling and formulation of a mathematical optimization problem, that consider part production costs as objective function [2], [3], [4]. All these studies considered already developed mathematical optimization models. Optimization problems in these studies were solved using meta-heuristic algorithms: firefly algorithm [2], cuckoo search algorithm [3], and particle swarm optimization [4].

The present study considers newly developed optimization model for multi-pass rough turning [5]. Since meta-heuristic optimization algorithms cannot guarantee optimal solutions [6], single-objective optimization problem for multi-pass rough turning developed in this study was solved using a deterministic approach, i.e. a brute force optimization algorithm, which guarantees the optimality of the optimization solutions.

II. Case Study

The longitudinal turning operation (multi-pass roughing) of grey cast iron using a carbide tool is considered to verify the proposed optimization problem and applied optimization approach (Fig. 1).

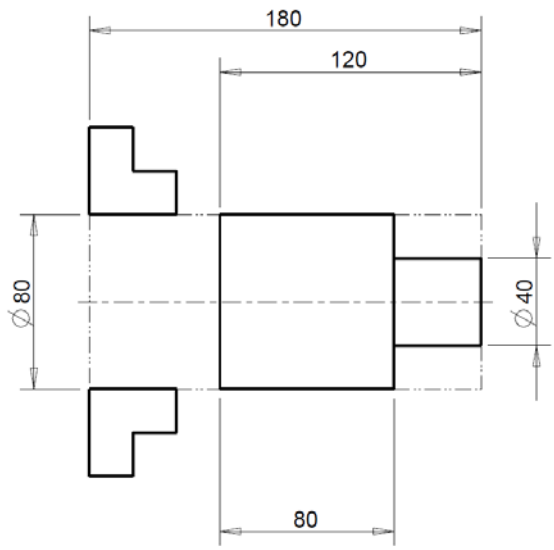

Fig. 1 Technical drawing of the finished part and stock

Stock is a bar with the diameter of 80 mm and the length of 180 mm made of EN-GJL-250 grey cast iron with a specific cutting force for the unit cutting cross-section $k_{c1.1}$ = 1225 N/mm^2 and m_c = 0,25. Grey cast iron is commonly used in the automotive industry, primarily due to the possibility of obtaining parts of complex shapes. It is relatively soft, but also very abrasive [7].

The multi-pass roughing starts at the diameter of 80 mm, and finishes at the diameter of 40 mm. The mean cutting diameter for multi-pass roughing is D_m = 60 mm. The cutting length is $L = l + l_1 = 40 + 2 = 42$ mm, where l is the length and l_1 is the cutting tool approach distance.

To define the part production costs, one needs to analytically express the unit production time. The unit production time [8] for multi-pass roughing is defined as:

$$t_1 = t_{mp} + t_c + t_r + t_p + t_{rm} + t_m + t_{tc} \tag{1}$$

where:

$$t_{rm} = \frac{L}{v_{fmax}} \cdot i \tag{2}$$

$$t_m = \frac{L}{n \cdot f} \cdot i = \frac{\pi \cdot D_m \cdot L}{1000 \cdot v_c \cdot f} \cdot i \tag{3}$$

$$t_{tc} = t_m \cdot \frac{t_{tc1}}{T} \tag{4}$$

The unit production time for multi-pass roughing in the final form is:

$$t_1 = t_{mp} + t_c + t_r + t_p + \frac{L}{v_{fmax}} \cdot i + \frac{\pi \cdot D_m \cdot L}{1000 \cdot v_c \cdot f} \cdot i \cdot \left(1 + \frac{t_{tc1}}{T}\right) \tag{5}$$

where t_1 (min) is the unit production time, t_{mp} (min) is the total machine tool preparation time (t_{mp} = 3 min), t_c (min) is the stock clamping time (t_c = 0,25 min), t_r (min) is the workpiece release time (t_r = 0,25 min), t_p (min) is the positioning time (t_p = 0,047 min), t_{rm} (min) is the return motion time, t_m (min) is the machining time, t_{tc} (min) is the tool changing time reduced to one workpiece, L (mm) is the cutting length, v_{fmax} (mm/min) is the maximal feed velocity, i is the number of passes, n (rpm) is the spindle speed, f (mm/rev) is the feed rate, D_m (mm) is the mean cutting diameter, v_c (m/min) is the cutting speed, t_{tc1} (min) is the tool changing time (t_{tc1} = 1 min), T (min) is the tool life.

The machine tool is the CNC lathe Gildemeister NEF 520 with the motor power of P_m = 12 kW and the efficiency of η = 0,8. The spindle speed range is n = 10 – 3000 rpm and the maximal feed velocity is v_{fmax} = 5000 mm/min. The maximum force is F_{max} = 5000 N.

The cutting tool is a toolholder PCLNR 2020K-12 (cutting edge angle of κ = 95° and rake angle of γ_{0h} = -6°) with a CNMA 120408 insert for roughing, rake angle of γ_{0i} = 0°, nose radius r_ε = 0,8 mm, and grade of IC8150 (coated carbide). Recommended cutting conditions are the depth of cut of a_p = 1,0 – 4,0 mm, the feed rate of f = 0,05 – 0,43 mm/rev, and the cutting speed of v_c = 115 – 229 m/min. Recommended cutting conditions are valid for the tool life of T_c = 15 min without a coolant [9].

III. Formulation of optimization problem

The initial part production cost model for multi-pass rough turning is:

$$C_1 = C_{ml} \cdot t_1 + C_t \cdot \frac{t_m}{T} \tag{6}$$

where C_1 (EUR) is the part production cost, C_{ml} (EUR/h) is the sum of machine (C_m = 30 EUR/h) and labour (C_l = 2,5 EUR/h) costs ($C_{ml} = C_m + C_l$), t_1 (min) is the unit production time, C_t (EUR) is the tool cost, t_m (min) is the machining time, T (min) is the tool life.

The machining time (t_m) is given as:

$$t_m = \frac{L}{f \cdot n} \cdot i = \frac{L \cdot \pi \cdot D_m}{1000 \cdot f \cdot v_c} \cdot i \tag{7}$$

where: L (mm) is the cutting length, f (mm/rev) is the feed rate, n (rpm) is the spindle speed, D_m (mm) is the mean cutting diameter, v_c (m/min) is the cutting speed and i is the number of needed passes.

From the well-known Taylor's tool life equation, the tool life (T (min)) can be expressed as:

$$T = C_0 \cdot a_p^x \cdot f^y \cdot v_c^z \tag{8}$$

where: C_0, x, y and z are the empirical constants (based on the data in [10], $C_0 = 8{,}89 \cdot 10^6$, x = -0,399, y = -0,759, and z = -2,75 for turning EN-GJL-250 grey cast iron with a K10 grade carbide tool), a_p (mm) is the depth of cut, f (mm/rev) is the feed rate, v_c (m/min) is the cutting speed.

The cost of the tool with indexable inserts (C_t) can be approximated as [11]:

$$C_t = \frac{C_i}{n_{ie}} \tag{9}$$

where: C_i (EUR) is the cost of the insert (C_i = 14 EUR), n_{ie} is the number of the insert cutting edges (n_{ie} = 4).

Considering the previous equations, the final form of the part production cost for multi-pass turning can be expressed as:

$$C_1 = C_{ml} \cdot t_1 + \frac{C_i}{n_{ie}} \cdot \frac{\frac{L \cdot \pi \cdot D_m}{1000 \cdot f \cdot v_c} \cdot i}{C_0 \cdot a_p^x \cdot f^y \cdot v_c^z} \tag{10}$$

Cutting parameters selection with respect to the given objective function via an optimization approach would be an easy task if there were no additional constraints. These constraints are related to the part quality, machine tool and cutting tool limitations.

The goal in roughing is to attain as high as possible material removal rate while considering that cutting power (P_c) does not exceed the maximum available power of the machine tool (P_m):

$$\frac{P_c}{\eta} = \frac{F_c \cdot v_c}{60000 \cdot \eta} = \frac{k_{c1.1} \cdot a_p \cdot f \cdot v_c \cdot \left(\frac{1}{f \cdot \sin\kappa}\right)^{m_c} \cdot \left(1 - \frac{\gamma_0}{100}\right)}{60000 \cdot \eta} \leq P_m \tag{11}$$

where: η is the efficiency, F_c (N) is the cutting force, $k_{c1.1}$ (N/mm^2) is the specific cutting force for the unit cutting cross-section of 1 mm^2, κ (°) is the cutting edge angle, m_c is the material dependent constant and γ_0 (°) is the rake angle.

The chip form is of great importance for undisturbed machining, part quality and the protection of the machine tool operator [11]. The chip morphology in turning depends on the ratio of the depth of cut and feed rate, known as chip slenderness ratio [12]. To avoid unfavourable chip forms (long smooth, wrinkled, coiled), this ratio has to be kept at a certain range. With respect to favourable chip slenderness the following constraint may be added:

$$4 \leq \frac{a_p}{f} \leq \xi_{max} \tag{12}$$

where ξ_{max} is the maximal chip slenderness ratio which depends on the workpiece material [13] (ξ_{max} = 6 for grey cast iron).

The following set of constraints can be formulated based on the suggested value ranges of cutting parameters provided by the cutting insert manufacturer (Iscar):

$$\begin{gathered} v_{cmin} \leq v_c \leq v_{cmax} \\ a_{pmin} \leq a_p \leq a_{pmax} \\ f_{min} \leq f \leq f_{max} \end{gathered} \tag{13}$$

Additionally, considering the available spindle speed range on the machine tool used, as well as the change in the workpiece diameter during machining, the following cutting speed constraint is valid:

$$\frac{\pi \cdot D \cdot n_{min}}{1000} \leq v_c \leq \frac{\pi \cdot D \cdot n_{max}}{1000} \tag{14}$$

In order to avoid unmachined areas on the workpiece surface [11], the following inequality constraint was also considered:

$$f \leq r_\varepsilon \tag{15}$$

where r_ε (mm) is the tool nose radius.

The proposed mathematical model of the multi-pass rough turning optimization problem aims at determining the set of cutting parameter values in order to minimize part production cost, while considering several constraints. It considers one objective function, four parameters (feed rate, depth of cut, cutting speed and number of passes), four machining constraints and three machining parameter bounds, and can be defined as follows:

$$Minimize: C_1 = C_{ml} \cdot t_1 + \frac{C_i}{n_{ie}} \cdot \frac{\frac{L \cdot \pi \cdot D_m}{1000 \cdot f \cdot v_c} \cdot i}{C_0 \cdot a_p^x \cdot f^y \cdot v_c^z}$$

Subject to:

$$\frac{k_{c1.1} \cdot a_p \cdot f \cdot v_c \cdot \left(\frac{1}{f \cdot \sin\kappa}\right)^{m_c} \cdot \left(1 - \frac{\gamma_0}{100}\right)}{60000 \cdot \eta} \leq P_m$$

$$4 \leq \frac{a_p}{f} \leq \xi_{max}$$

$$v_{cmin} \leq v_c \leq v_{cmax}$$

$$a_{pmin} \leq a_p \leq a_{pmax}$$

$$f_{min} \leq f \leq f_{max}$$

$$\frac{\pi \cdot D \cdot n_{min}}{1000} \leq v_{cr} \leq \frac{\pi \cdot D \cdot n_{max}}{1000}$$

$$f \leq r_\varepsilon$$

IV. Results and discussion

The optimization problem for multi-pass roughing was coded and solved in the Brutomizer software tool [14], using the brute force algorithm. Values of all turning parameters are discretized by defining appropriate step sizes, in order to obtain practically feasible solutions that could be easily set on machine tool. In this way all possible candidates for the solution are enumerated. By checking whether each candidate satisfies the problem's statement, brute-force algorithm guarantees the optimality of the solution for the given discrete search space.

The optimization solutions were determined in 9 s, which represents a reasonable optimization time.

The cutting regimes which were realized with the depth of cut of 2,5 mm (eight passes), feed rate of 0,43 mm/rev, and cutting speed of 148 m/min, ensured minimal part production costs and represented the optimization solutions. The values of constraints for these cutting regimes are cutting power (P_c/η) of 5,32 kW and chip slenderness ratio of 5,81. The resulting tool life is 12,59 min.

Recommended cutting regimes (starting values at the middle of the range) for the insert used for roughing are: depth of cut a_p = 2,5 mm (eight passes), feed rate f = 0,24 mm/rev, and cutting speed v_c = 172 m/min. Resulting chip slenderness in this case is 10,42, which is higher than the maximal chip slenderness for grey cast iron. Part production costs for the cutting regimes representing the optimization solutions (2,8 EUR) are lower compared to the part production costs of 3,25 EUR for the recommended cutting regimes. Unit production time for the cutting regimes representing the optimization solutions (4,69 min) is lower compared to the unit production time of 5,27 min for the recommended cutting regimes.

V. Conclusions

The analysis of the obtained solutions, leads to the following conclusions:

- Part production costs can be noticeably reduced by optimizing the main cutting parameters starting from the initial parameter hyper-space as recommended by tool manufacturers. Part production costs can be reduced by 13,7 % (0,45 EUR).
- Unit production time is reduced by 10,98 % (0,58 min) for the cutting regimes representing the optimization solutions.
- For the batch of 100 parts, total production costs can be reduced by 27,11 %, while total production time can be reduced by 25,18 %, leading to total savings of 44,44 EUR in production costs and 57,84 min in production time.
- The cutting regimes recommended by tool manufacturer do not necessarily meet certain constraints, such as the relationship between depth of cut and feed rate. On the other hand, the cutting regimes determined with the help of the optimization model presented in this study meet all the constraints.

Acknowledgment

This research was financially supported by the Ministry of Education, Science and Technological Development of the Republic of Serbia.

References

[1] Q. Yi, C. Li, Y. Tang, and X. Chen, "Multi-objective parameter optimization of CNC machining for low carbon manufacturing," J. Clean. Prod., vol. 95, pp. 256-264, 2015.

[2] G.R. Miodragović, V. Đorđević, R.R. Bulatović, and A. Petrović, "Optimization of multi-pass turning and multi-pass face milling using subpopulation firefly algorithm," Proc. Inst. Mech. Eng. Part C J. Mech. Eng. Sci., vol. 233, pp. 1520-1540, 2019.

[3] M.A. Mellal, and E.J. Williams, "Cuckoo optimization algorithm for unit production cost in multi-pass turning operations," Int. J. Adv. Manuf. Technol., vol. 76, pp. 647-656, 2015.

[4] P. Chauhan, M. Pant, and K. Deep, "Parameter optimization of multi-pass turning using chaotic PSO," Int. J. Mach. Learn. Cybern., vol. 6, pp. 319-337, 2015.

[5] M. Trifunović, M. Madić, and M. Radovanović, "Pareto optimization of multi-pass turning of grey cast iron with practical constraints using a deterministic approach," Int. J. Adv. Manuf. Technol., vol. 110, pp. 1893-1909, 2020.

[6] S. Diyaley, and S. Chakraborty, "Optimization of multi-pass face milling parameters using metaheuristic algorithms," Facta Universitatis, Series Mechanical Engineering, vol. 17, pp. 365-383, 2019.

[7] L. Čerče, and F. Pušavec, "Increasing machinability of grey cast iron using cubic boron nitride tools: Evaluation of wear mechanisms," Indian J. Eng. Mater. Sci., vol. 23, pp. 65-78, 2016.

[8] G. Cukor, Proračuni u obradi skidanjem strugotine. Rijeka, Republika Hrvatska: Sveučilište u Rijeci, Tehnički fakultet, 2006.

[9] Iscar Ltd., Non-Rotating Tool Lines (Metric Version Catalog). 2017.

[10] H. Tschatsch, Applied Machining Technology. Berlin Heidelberg, Germany: Springer-Verlag, 2009.

[11] F. Klocke, Manufacturing Processes 1: Cutting. Berlin Heidelberg, Germany: Springer-Verlag, 2011.

[12] Z. Demir and O. Adiyaman, "Investigation of influence of approach angle and chip slenderness ratio on vibration, chip formation and surface quality in turning of AISI 1050 steel," J. Braz. Soc. Mech. Sci. Eng., vol. 41, article number: 467, 15 pages, 2019.

[13] J. Kopač, Odrezavanje. Ljubljana, Slovenija: Fakulteta za strojništvo, 1991.

[14] Brutomizer, 2019. http://www.virtuode.com/index.php/products/brutomizer/

THE 5th INTERNATIONAL CONFERENCE
MECHANICAL ENGINEERING IN XXI CENTURY

December 9-10, 2020
Faculty of Mechanical Engineering in Niš, Serbia

Optimization of Variable Costs Considering Process Constraints in CO2 Laser Cutting of P265GH Steel

Miloš MADIĆ, Marko VELIČKOVIĆ, Nikola JOVANOVIĆ, Dimitrije PETROVIĆ

Department of Production and Information Technologies, Faculty of Mechanical Engineering in Niš, A. Medvedeva 14, 18000 Niš, Serbia
madic@masfak.ni.ac.rs, markomasfak@gmail.com, nikolamasfak96@gmail.com, dimitrijepetrovic17@gmail.com

***Abstract*— In laser cutting, selection of cutting parameter values has significant influence on the production cost, material removal rate and different cut quality characteristics. In the present study, in order to find optimal cutting conditions for minimization of variable costs in CO2 laser cutting of P265GH steel, laser cutting optimization model was developed. In order to take into account cut quality characteristics, several process constraints were included in the optimization model. Experimental data, obtained upon realization of central composite design, were used so as to develop empirical models in terms of three process parameters such as cutting speed, assist gas pressure and nozzle diameter. The developed optimization problem was solved using interior-point algorithm and genetic algorithm. It was observed that with respect to currently used cutting conditions savings of around 40% can be made without compromising cut quality.**

***Keywords*— CO_2 laser cutting, Variable costs, Optimization algorithms, P265GH steel**

I. Introduction

As in the case of other production technologies, the laser cutting technology is defined by the parameters which are selected depending on the type of workpiece material, workpiece thickness and applied laser cutting method. In theory and praxis no strict rules are defined, but only general guidelines and recommendations for the selection of main laser cutting parameter values. On the other hand, it is well known that slight deviations from general recommendations may lead to unwanted side effects [1] such as wide kerf, tapered kerf, excessive gas consumption, dross formation, eroded surface, pittings, etc. Also, the complexity of laser cutting technology is reflected also in the fact that for fulfilling different process performances, such as low surface roughness, low costs, low cutting time, high material removal rate, narrow kerf, particular cutting conditions are required, which are mutually contradictory. With this in mind, the optimization of laser cutting parameters for fulfilling required process performances necessities formulation of optimization problems. To this aim mathematical modeling of laser cutting process, empirical using response surface methodology, artificial neural networks, fuzzy logic and/or analytical, is used in line with the application of different optimization algorithms [2-7].

Integration of previous mathematical, statistical and artificial intelligence tools enables an increase in efficiency of laser cutting technology which can result in reduced costs, improved quality, scrap reduction, repeatability improvement of the cutting process, decrease of negative impact on the environment.

The goal of the present study is optimization of laser cutting parameter values so as to minimize variable costs in CO_2 laser cutting of P265GH steel while considering several process constraints so as to take cut quality characteristics into account at the same time. The single-objective laser cutting optimization problem was formulated considering mathematical models that were developed upon realization of central composite design where three cutting parameters (cutting speed, oxygen pressure and nozzle diameter) were varied at three levels.

II. Experimental Details

Pressure vessel steel P265GH in sheet form of 5 mm thickness was used as workpiece material. This steel is carbon non-alloy steel designed for high temperature applications. Because of a good weldability it is widely used for manufacturing pressure vessels, piping elements, boilers, heat exchangers and similar components.

Laser cutting experimental trials were performed by means of Prima Industry laser cutting machine delivering a maximum output power of 4 kW at a wavelength of 10.6 μm, operating in continuous wave mode. A focusing lens with focal length of 127 mm was used to perform the cutting with a Gaussian distribution beam mode (TEM_{00}). Oxygen as assist gas with purity of 99.95 % was supplied coaxially with the laser beam. In experimentation the following conditions were constant: laser power 1.3 kW, lens focal length of 127 mm, focal point position of 0 mm and standoff distance of 1 mm. On the other hand, in accordance with central composite face-centered factorial design, oxygen pressure (p), cutting speed (v) and nozzle diameter (d) were varied at three levels (Table I).

TABLE I Laser Cutting Parameter Levels

Level	p (bar)	v (m/min)	d_n (mm)
-1	0.7	2.6	1.25
0	1.1	2.9	1.5
+1	1.5	3.2	2

Empirical assessment of cut quality involved the measurement of the surface roughness (R_z) and kerf width. The measurements of R_z were made using digital, stylus type measuring instrument MahrSurf-XR1. The averaged value of three measurements taken along the cut at approximately in the middle of the workpiece thickness was recorded for each specimen. A top and bottom kerf widths were measured using Mitutoyo QuickScope vision measuring machine with resolution of the length measuring system of 0.5 μm. The kerf width of each specimen was measured by analyzing pictures of the top (laser beam entry) and bottom surface (laser beam exit) of the specimens using Q-spark image processing software.

On the basis of obtained experimental data, two empirical non-linear mathematical models were developed for the prediction of surface roughness and kerf width.

III. Laser Cutting Optimization Model

The objective of the developed laser cutting optimization model is to determine the optimal laser cutting parameter values, i.e. oxygen pressure, cutting speed and nozzle diameter, in order to minimize variable costs. In addition, such combination of laser cutting parameters should not violate any of the imposed process constraints related to parameter bounds, kerf width, surface roughness, specific cutting energy and oxygen flow inside the kerf.

A. Objective function

Variable costs, for a specific laser cutting application, consists of laser electrical power cost and assist gas cost [8]:

$$C_v = C_e + C_{ag} \tag{1}$$

where C_v (EUR/h) is total variable costs, C_e (EUR/h) is laser electrical power cost and C_{ag} (EUR/h) is assist gas cost.

Laser electrical power cost can be determined as the function of the CO_2 laser cutting machine electrical power, electricity price and maximal and operational laser power in the following form [9]:

$$C_e = 0.8 \cdot c_e \cdot P_E \cdot \frac{P}{P_{\max}} \tag{2}$$

where 0.8 stands for power factor, c_e (EUR/kWh) is electricity price, P_E (kW) is CO_2 laser cutting machine electrical power, P (kW) is laser power and P_{max} (kW) is the maximal laser power.

The assist gas cost can be determined as:

$$C_{ag} = c_{ag} \cdot Q_{ag} \tag{3}$$

where c_{ag} (EUR/m^3) is the price of the assist gas and Q_{ag} (m^3/h) is the consumption of the assist gas.

For estimation of assist gas consumption the following general mathematical model can be used:

$$Q_{ag} = 0.411 \cdot d^2 \cdot (p+1) \tag{4}$$

where d (mm) is the nozzle diameter and p (bar) is the assist gas pressure.

In accordance with Equations 1-4, the total variable costs in CO_2 laser cutting can be represented by the following model:

$$C_v = 0.8 \cdot c_e \cdot P_E \cdot \frac{P}{P_{\max}} + 0.411 \cdot d^2 \cdot (p+1) \tag{5}$$

B. Process constraints

Due to limitations of the validity of mathematical model for the covered experimental space, laser cutting parameters are constrained with the bottom and top allowable bounds:

$$\begin{aligned} p_{\min} &\le p \le p_{\max} \\ v_{\min} &\le v \le v_{\max} \\ d_{\min} &\le d \le d_{\max} \end{aligned} \tag{6}$$

Here it should be noted that oxygen pressure and cutting speed are continious variables, whereas the nozzle diameter is discrete variable.

In order to take into account cut surface quality, surface roughness constraint, related to the ISO 9013 standard which is relevant for thermal cutting, is given as:

$$\begin{aligned} R_z = {} & 57.4512 - 35.9717 \cdot p - 36.4236 \cdot v + 32.0211 \cdot d + \\ & 8.7694 \cdot p^2 + 11.6484 \cdot v^2 + 1.5282 \cdot d^2 + \\ & 0.1807 \cdot p \cdot v + 9.2282 \cdot p \cdot d - 18.0648 \cdot v \cdot d \le R_{z\max} \end{aligned} \tag{7}$$

where R_{zmax} is the maximal allowable surface rougness with respect to sheet thickness and desired cut class.

In order to enahnce CNC path programming, kerf width constraint was considered as:

$$\begin{aligned} K_w = {} & 1.189 + 0.3575 \cdot p - 0.2458 \cdot v - 0.75041 \cdot d - 0.01764 \cdot p^2 + \\ & 0.0339 \cdot v^2 + 0.15976 \cdot d^2 - 0.1057 \cdot p \cdot v - 0.01649 \cdot p \cdot d + \\ & 0.08793 \cdot v \cdot d = K_{ws} \end{aligned} \tag{8}$$

where K_{ws} is the desired kerf width.

In order to ensure cut quality, constraint related to the specific cutting energy was imposed as:

$$E_{s\min} \le E_s = \frac{1000 \cdot P}{16.67 \cdot v \cdot s} \le E_{s\max} \tag{9}$$

where s is the sheet thickness and E_{smin} and E_{smax} are minimal and maximal recommended specific cutting energies for the given laser cutting method, sheet thickness and material.

In order to maintain thermodynamic stability, control gas flow and assure inevitable gas pressure for melt removal in the cut zone, constraint related to the assist gas flow was also included as:

$$Q_{ag\min} \le Q_{ag} \tag{10}$$

where Q_{agmin} is the minimal required assist gas flow in the kerf.

C. Formulation of the laser cutting optimization problem

After setting the values from Table II the final formulation of the laser cutting optimization model can be reduced to:

$$Q_{ag\,\min} \le Q_{ag}$$

$$\text{Minimize: } C_v = 0.8 \cdot c_e \cdot P_E \cdot \frac{P}{P_{\max}} + 0.411 \cdot d^2 \cdot (p+1)$$

$$\begin{aligned} \text{Subject to: } & R_z \le R_{z\max} \\ & K_w = K_{ws} \\ & E_{s\min} \le Es \le E_{s\max} \\ & Q_{ag\,\min} \le Q_{ag} \\ & p_{\min} \le p \le p_{\max} \\ & v_{\min} \le v \le v_{\max} \\ & d_{\min} \le d \le d_{\max} \end{aligned} \tag{11}$$

TABLE II LASER CUTTING OPTIMIZATION MODEL DATA

Parameter	Value	Parameter	Value
d_{min}	1.25 mm	R_{zmax}	12.4 μm
d_{max}	2 mm	K_{ws}	0.4 mm
p_{min}	0.7 bar	E_{smin}	6 J/mm^2
p_{max}	1.5 bar	E_{smax}	10 J/mm^2
v_{min}	2.6 m/min	Q_{agmin}	1.66 m^3/h
v_{max}	3.2 m/min	c_e	0.12 EUR/kWh
P_E	55 kW	P_{max}	4 kW
P	1.3 kW		

Formulation in Equation 11 represents nonlinearly constrained single-objective laser cutting optimization problems with two continuous independent variables and one discrete independent variable.

IV. APPLIED OPTIMIZATION ALGORITHMS

Interior point algorithm is gradient-based method that uses first and second order derivatives, gradients and hessians, to find local minima [10].The idea of the interior point algorithm is to iteratively approach the optimal solution from the interior of the feasible set by solving a sequence of approximate minimization problems. This algorithm was selected for solving the developed laser cutting optimization problem since interior point algorithm is robust and require a small number of iterations and function evaluations to converge [11].

Genetic algorithm (GA) is general purpose stochastic optimization algorithm which apply the rules of natural selection and genetics to explore a given search space [12]. By using the population of individuals, each representing a possible solution for the given optimization problem, GA iteratively generates and evaluates individuals using a fitness function until a stopping criterion is meet. To this aim GA uses three key genetic operators: crossover, mutation, and selection. Although originally GA are intended for solving unconstrained optimization problems, with the use of penalty functions that penalize infeasible solutions, GA can be used for solving constrained optimization problems.

V. RESULTS AND DISCUSSION

In the present study in order to determine the set of optimal laser cutting parameter values interior-point algorithm and genetic algorithm were applied. As a result of the optimization process, the minimal feasible variable costs of 7.93 EUR/h (0.051 EUR/m) was obtained with the following laser cutting parameter values: v=2.6 m/min, p=1.19 bar and d=1.5 mm. The determined optimal solution, along with the values of constraints, is given in Table III.

TABLE IIII LASER CUTTING OPTIMIZATION RESULTS

Optimal laser cutting parameters			Objective function
v (m/min)	p (bar)	d (mm)	C_v (EUR/h)
2.6	1.19	1.5	7.93
Optimization constraints			
R_z (μm)	K_w (mm)	E_s (J/mm^2)	Q_{ag} (m^3/h)
9.15	0.4	7.5	2.02

In the actual production conditions P265GH steel with thickness of 4 mm is cut using the combination of the following laser cutting parameters: v=2.6 m/min, p=1.5 bar and d=2 mm. This set of laser cutting parameter values provides acceptable cut quality without dross formation, but because of wider nozzle diameter and higher oxygen pressure results in variable costs of C_v=13.84 EUR/h, which is equivalent to C_v=0.089 EUR/m. The obtained optimization solution for minimization of variable costs suggests the use of nozzle with smaller diameters which is in accordance with general laser cutting recommendations [13, 14].

It is worth noting that the optimization solution was constantly determined by the interior-point algorithm, whereas genetic algorithm yielded approximate but somewhat worse solutions at each algorithm run. For the present study it can be argued that genetic algorithm has not been found robust in finding the optimum solution.

VI. CONCLUSIONS

In the present study, laser cutting optimization model with process constraints for minimization of variable costs in CO_2 laser cutting of P265GH steel was developed. In order to take into account cut quality characteristics, several process constraints such as surface roughness, kerf width, specific cutting energy and assist gas flow were included in the optimization model. Two optimization approaches based on the use of interior-point algorithm and genetic algorithm were applied to solve the developed laser cutting optimization problem. The main observations can be summarized as follows:

- Both optimization approaches are able to provide feasible set of laser cutting parameter values within reasonable computational time.
- Interior-point algorithm proved to be robust and capable to escape local minima. In the case of genetic algorithm a number of evaluations are to be performed in order to avoid a non-robust solution.
- Optimization of laser cutting parameters through the formulation of an optimization problem stands for higher level of laser cutting process planning enabling the consideration of a number of process performance characteristic by defining different objective functions and process constraints. One may argue that it is especially suitable when it comes to cutting of large quantity of material and ensure acceptable overall quality.
- It was observed that with respect to currently used cutting conditions savings of around 40% can be made without compromising cut quality.

The developed laser cutting optimization problem may be used for assessment of other optimization methods and metaheuristic algorithms.

ACKNOWLEDGMENT

This research was financially supported by the Ministry of Education, Science and Technological Development of the Republic of Serbia.

REFERENCES

[1] A.K. Dubey, V. Yadava, "Multi-objective optimisation of laser beam cutting process", Optics and La-ser Technology, Vol. 40, No. 3, pp. 562-570, 2008.

[2] S. Rao, A. Sethi, A. Kumar Das, N. Mandal, P. Kiran, R. Ghosh, A.R. Dixit, A. Mandal, "Fiber laser cutting of CFRP composites and process optimization through response surface methodology", Materials and Manufacturing Processes, Vol. 32, No. 14, pp. 1612-1621, 2017.

[3] A. Tamilarasan, D. Rajamani, B. Esakki, "Parametric optimisation in Nd-YAG laser cutting of thin Ti-6Al-4V super alloy sheet using evolutionary algorithms", International Journal of Materials and Product Technology, Vol. 57, No. 1-3, pp. 71-91, 2018.

[4] D. Pramanik, A.S. Kuar, S. Sarkar, S. Mitra, "Optimisation of edge quality on stainless steel 316L using low power fibre laser beam machining", Advances in Materials and Processing Technologies, doi.org/10.1080/2374068X.2020.1745734

[5] R.G. Baldovino, I.C. Valenzuela, A.A. Bandala, E.P. Dadios, "Optimization of CO_2 laser cutting parameters using adaptive neuro-fuzzy inference system (ANFIS)", Journal of Telecommunication, Electronic and Computer Engineering, Vol. 10, No. 1-9, pp. 103-107, 2018.

[6] H. Ding, Z. Wang, Y. Guo, "Multi-objective optimization of fiber laser cutting based on generalized regression neural network and non-dominated sorting genetic algorithm", Infrared Physics & Technology, oi.org/10.1016/j.infrared.2020.103337

[7] P. Joshi, A. Sharma, "Simultaneous optimization of kerf taper and heat affected zone in Nd-YAG laser cutting of Al 6061-T6 sheet using hybrid approach of grey relational analysis and fuzzy logic", Precision Engineering, Vol. 54, No. 1, pp. 302-313, 2018.

[8] M. Madić, M. Radovanović, B. Nedić, M. Gostimirović, "CO_2 laser cutting cost estimation: mathematical model and application", International Journal of Laser Science: Fundamental Theory and Analytical Methods, Vol. 1, No. 2, pp. 169-183, 2018.

[9] H.A. Eltawahni, M. Hagino, K.Y. Benyounis, T. Inoue, A.G. Olabi, "Effect of CO_2 laser cutting process parameters on edge quality and operating cost of AISI316L", Optics and Laser Technology, Vol. 44, No. 4, pp. 1068-1082, 2012.

[10] J. Agnarsson, M. Sunde, I. Ermilova, "Parallel optimization in MATLAB". Project in Computational Science Report, 2013.

[11] L. Hei, J. Nocedal, R.A. Waltz, "A numerical study of active-set and interior-point methods for bound constrained optimization", In: Modeling, Simulation and Optimization of Complex Processes, pp. 273-292, Springer, Berlin, Heidelberg, 2008.

[12] A. Homaifar, C.C. Qi, S.H. Lai, "Constrained optimization via genetic algorithms", Simulation, Vol. 62, No. 4, pp. 242-253, 1994.

[13] W. Schulz, C. Hertzler, "Cutting: modeling and data", pp. 187-218, In: Laser Physics and Applications, Subvolume C: Laser Applications/Eds. Poprawe R., Weber H., Herziger G.. Berlin: Springer-Verlag, 2004.

[14] C.J. Berkmanns, U.M. Faerber, "Facts about laser technology". Laser cutting. Linde AG. Linde Gas Division. Hollriegelskreuth. Germany.

THE 5th INTERNATIONAL CONFERENCE
MECHANICAL ENGINEERING IN XXI CENTURY

December 9-10, 2020
Faculty of Mechanical Engineering in Niš, Serbia

The future of Manufacturing Processes with Support I4.0

Saša RANĐELOVIĆ[1], Mladomir MILUTINOVIĆ[2], Vladislav BLAGOJEVIĆ[1], Dejan MOVRIN[2],

[1]Production and Information Technology, Faculty of Mechanical Engineering, A. Medvedeva 14, 18000 Niš, Serbia
[2]Department for production engineering, Faculty of technical science, Trg D. Obradovića 6, Novi Sad, Serbia
sassa@masfak.ni.ac.rs, mladomil@uns.ns.rs, vlada@masfak.ni.ac.rs, movrin@uns.ns.rs .

***Abstract*— The fundamental objective I4.0 is to utilize the progress achieved in information and communications technologies (ICT) and that expected in the near future for the benefit of manufacturing enterprises. Preparation therefore has to be made for the increasing and consistent embedding of those technologies in production systems – and that in ever smaller partial systems and components. Additional communications capability and (partial) autonomy in reactions to external influences and internally stored specifications are transforming mechatronic systems into Cyber-Physical Systems (CPS). The objectives derived from that transformation are developments and adjustments in ICT for manufacturing applications: robustness, resilience, information security and real time capability.**

***Keywords*—production process, information technology, industry 4.0**

I. INTRODUCTION

In 2011, at Hannover Messe, professor Wolfgang Wahlster (director and CEO of the German Research Centre for Artificial Intelligence) gave a keynote speech to the opening session. His key theme was how German manufacturers could be more competitive in global markets through better use of information technology and the Internet. The term he used to describe this future was Industrie 4.0 (I4.0) and so the fourth Industrial Revolution began.

It refers to the introduction of a fourth Industrial Revolution in the manufacturing sector, the fusion of the cyber and physical worlds to drive value and competitiveness in a global marketplace [1].

Utilizing the four design principles of interoperability, information transparency, technical assistance, and decentralized decision-making and building on the nine pillars of big data, augmented reality, simulation/digital twin, Internet of Things, cloud computing, cybersecurity, systems integration, aditive manufacturing, and autonomous systems, factories can be transformed to meet future needs [1].

The journey to I4.0 will not be smooth; there will be many issues to overcome such as security, adoption, connectivity, standardization, and the aging workforce. However, the biggest challenge will perhaps be that of dealing with legacy systems. Systems that have been working successfully for many years.

Standardization is of central importance for the success of the future-oriented project Industry 4.0. Industry 4.0 requires an unprecedented degree of system integration across domain borders, hierarchy borders and life cycle phases. This is only possible if it proceeds from standards and specifications based on consensus [2]. Close cooperation between researchers, industry and the standardization bodies is required to create the necessary conditions for sweeping innovation: methodical soundness and functionality, stability and security of investments, practicability and market relevance.

For that reason, I4.0 should be seen as a multiyear journey. Indeed, some predict that I4.0 will take until 2030. to be fully realized. It is a journey that needs to be carefully planned, funded, and executed to derive the fullest benefits. However, failing to embrace I4.0 could lead to lack of efficiency and competitiveness and, ultimately, failure [3].

Underpinning I4.0 will have to be a secure, reliable, and robust communications infrastructure to ensure that machines, sensors, and people can connect in the most effective way. Since 2011, many countries have adopted, or adapted, I4.0 for their own purposes. Indeed, many countries will give tax relief or credits for I4.0-related projects as a means of stimulating innovation.

II I4.0 DEFINITION AND CONCEPT

The underlying premise of I4.0 is the bringing together of cyber and physical systems, automation, the Internet of Things (IoT), and better vertical and horizontal integration. Hermann, Pentek, and Otto [2,3] have identified four design principles for I4.0 :

Interoperability: The ability of machines, devices, sensors, and people to connect and communicate with each other via the IoT or the Internet of People (IoP).

Information transparency: The transparency afforded by I4.0 technology provides operators with vast amounts of useful information needed to make appropriate decisions. Interconnectivity allows operators to collect immense amounts of data and information from all points in the manufacturing process, thus aiding functionality and identifying key areas that can benefit from innovation and improvement.

Technical assistance: First, the ability of assistance systems to support humans by aggregating and visualizing information comprehensively for making informed decisions and solving urgent problems on short notice. Second, the ability of cyber-physical systems to physically support humans by conducting a range of tasks that are

unpleasant, too exhausting, or unsafe for their human co-workers.

Decentralized decisions: The ability of cyber-physical systems to make decisions on their own and to perform their tasks as autonomously as possible. Only in the case of exceptions, interferences, or conflicting goals are tasks delegated to a higher level.

There are nine accepted pillars involved in building I4.0 these are:

Augmented reality, providing additional visual data to workers to help enable process and product improvements. An example would be the use of connected glasses to help operators fit components correctly. Taking it to the next level, virtual reality allows testing of things like ergonomics without building physical representations.

Systems integration, better connectivity of systems and hardware to be used together to drive increased value.

Cloud computing, the use of, often, third-party hosting services to reduce cost and complexity while offering flexibility and scalability. An example here might be the use of cloud compute services for periodic test workflows rather than building in-house server infrastructure.

Big data, organizations are, or can be, creating huge volumes of data that are not being exploited. This data can be used to unlock value for business improvement and growth.

Internet of Things, the rapidly growing field of internet-connected devices developing new data (for example, deploying sensors for asset condition monitoring or energy usage). The key benefit of IoT is not so much the sensors themselves but in the data that they create. I4.0 can turn that data into actionable value.

3D printing, the use additive manufacturing technology and 3D printers to make element or components faster, lighter, and cheaper. Additive manufacturing could also be of use in maintenance and repair operations, where a replacement part could be made locally rather than shipped from source.

Cybersecurity, all these new interconnected systems must be adequately secured against unwarranted intrusion. This could include enhanced firewalls, malware detection, and segmentation of networks.

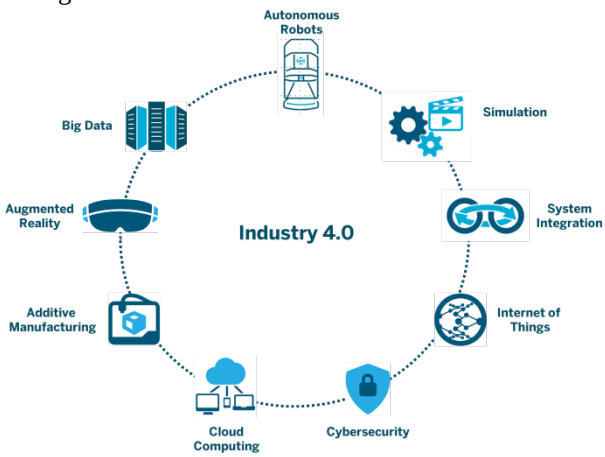

Fig.1. The nine pillars of I4.0

Autonomous robots, technology such as robotics and artificial intelligence have developed to the stage where systems can operate independently on tasks without frequent human interaction. This could be manufacturing machines themselves or delivery platforms within the factory such as autonomous vehicles.

Simulation and digital twin, trialing new ideas in the virtual world can be more cost-effective than building physical prototypes. An example here is mocking up production lines/processes on a CAD system to test before a live deployment.

III MANUFACTURING PROCESS SUPPORT WITH I4.0

Manufacturers process face a number of challenges in global markets, as productivity, innovation, customer service and competitiveness. The first major challenge is productivity, how to do more, faster, using fewer resources (table 1). Factors affecting productivity include:

TABLE I PRODUCTIVITI MANUFACTURING PROCESS

Factor	Impact	Solution	I4.0 pillar/s
Machine reliability	Equipment failure stops production	● Asset condition monitoring ● Proactive maintenance ● Use maintenance windows ● Reduce plant disruption	● Internet of Things ● Big data ● Cloud computing
Machine utilization	Inefficient use of plant and machines	● Product line optimization ● Production planning ● Machine-machine communication	● Systems integration ● Big data ● Augmented reality ● Autonomous systems ● Digital twin
Line reconfiguration	Plant shutdown time during refit	● Computer modeling and planning	● Augmented reality
Defect detection	Rework required at cost	● Automated processes ● Augmented reality to help workforce	● Augmented reality ● Autonomous systems
Energy management	Unnecessary expense	● Energy monitoring and management	● Integrated systems ● Autonomous systems

The reliability and age of machinery and equipment has always been a critical component for a higher level of productivity. This is not a problem in developed countries, but in less developed and underdeveloped countries we always come to the question of which equipment to purchase and which equipment manufacturer to choose. It is logical that the latest equipment cannot be obtained in that way, because it represents the privilege of the most powerful countries and companies that are at the very top of technological development. Existing equipment can affect productivity, from machine layout, quick identification and troubleshooting, to energy efficiency, which is a very interesting and topical issue today. Each of these problems can be solved according to the concept of Industry 4.0 with the application of software tools and methods [4,5].

The second major challenge is driving innovation in manufacturing process, table2. The process of innovation today is perhaps a crucial factor in the global world market. Being the first in technological innovation, implementation of new solutions, time and conditions of launch on the market represent issues and dilemmas that are solved today by teams of experts from different fields of science and technology.

In order for the entire production process to be completed, it is necessary for the user to be involved in each of its segments. It is the user who generates feedback from the market to which the process owner adapts [6].

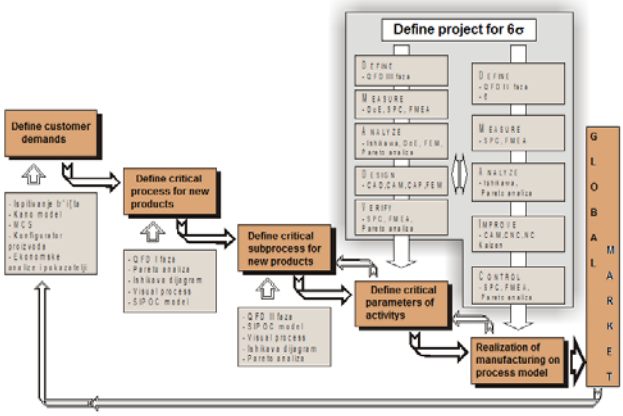

Fig.2. New product generate for customer on global market [6]

The level of development of user awareness will determine the behavior of the process owner. The product itself with its characteristics reflects the customer in that part of the global market. Today, the segmentation of the global market is very pronounced because the final products, although with similar characteristics, still have technological differences that greatly change the purpose and its possibilities.

We need to keep in mind that methods and techniques for idea evaluation are just tools; and should be used as such. Tools don't solve competitiveness issues automatically. They should be used in accordance with the overall company strategy and the ideas selected in the evaluation process must be implemented.

TABLE III INOVATION IN MANUFACTURING PROCESS

Factor	Impact	Solution	I4.0 pillar/s
Faster time to market	Lost market share	● Computer simulation ● 3D manufacturing	● Augmented reality ● Digital twin ● Additive manufacturing
Identify and implement innovation	Being left behind by competitors	● Learning organization	● Big data
Supply chain visibility / traceability	Increased stockholding or stockouts	● Supply chain integration	● Big data ● Systems integration

To show the complexity of improving competitiveness of SMEs we can exploit some of the idea expressed in the literature [7]. European Commission established IMProve project with the aim to improve the innovation performance of SMEs in Europe3. The model approach of the project is holistic (it covers all areas of Innovation Management) and modular (company can select in which area it needs the improvement and still keep the »big picture« in mind.

The IMProve approach draws our attention that not only generating better ideas but also minimizing development time and effective commercializing of new products has to be taken care of. As we can see from the above picture the idea management (or even more specifically the idea evaluation phase with the tools and techniques needed) is a very tiny part of the whole process from the stage of perceiving the need to the final result of satisfying the need.

It should therefore be kept in mind, that the creation of ideas and their evaluation is a part of a broader picture that includes goal setting, target definition, evaluation of capabilities company has on its disposal, etc, as it can be seen from the figure 2.

Every idea management process starts with idea generation. In the framework project the »responsibility« for idea generation goes to other modules, where as many ideas as possible should be generated. As we have focused on the companies the main concern is not only the selection of ideas but also whether the selected ideas could contribute to sustained competitiveness and creating sufficient level of profit [7].

New components, new suppliers or an improved deal with the existing suppliers could improve products and profits significantly. A number of companies have integrated the suppliers into the manufacturing processes to ensure online visibility on inventory at various stages and quality control.

E-auctions and reverse auctions_to manage material costs are other examples of increasing efficiency in procurement.

Companies can innovate in the way products are developed or manufactured, either within the firm or across the supply chain. Such innovations are termed as 'Process Innovation'. It is typically aimed at garnering competitive advantage through improved quality, reduced costs or reduced time-to-market [8].

For example, one of the greatest innovations to impact manufacturing in the 20th century was the assembly line model for manufacturing cars, developed by Henry Ford. The concept, however, did not change the product, but it significantly and permanently changed the process for manufacturing and delivering the product.

Several automotive companies, today, use the collaborative product development to shorten their new product development cycles, in collaboration with Tier I suppliers. For example, Mahindra & Mahindra (M&M) adopted an innovative production process called the Integrated Design and Manufacturing (IDAM) for the development of its multi-utility vehicle (MUV), Scorpio. The IDAM team consisted of cross-functional teams including suppliers, who catered to every aspect of product development, from design and testing to vendor development and marketing.

Management innovation refers to innovation in management principles and processes that will eventually change the practice of what managers do, and how they do it. Typically, such innovations have long lasting impact on the organization. Innovation in business model falls under this category. Toyota's lean manufacturing model is a good example of such a practice. It not only addressed key processes; but moved beyond the definition of Process Innovation, by involving a fundamental shift in management philosophy. Toyota's model has transformed the way the manufacturing industry works

Technology has been a tremendous driving force for innovation in businesses; especially in the recent times. Many breakthrough concepts and development in businesses have been primarily driven by the development of new generation technology. New materials could improve products or their packaging and presentation.

Over the past few decades, there has been a growing concern globally about the fast depletion of global resources and the need to conserve them for the future. These include both natural and human resources. Another key concern is the need to control pollution and to safeguard the environment. These have also been the key drivers for innovation in developing greener technologies and manufacturing practices; for example: development of electric / hybrid vehicles.

Such innovations typically take time to gain acceptance and become commercially successful; as the long-term advantages offered by the technology are not immediately evident to consumers. Hence, companies that innovate in these areas need to have a long-term view.

TABLE IIIII CUSTOMER SERVICE

Factor	Impact	Solution	I4.0 pillar/s
Improved customer response time	Improved customer satisfaction	● Remote asset condition monitoring	● Internet of Things ● Autonomous systems ● Big data
Improved Mean Time To Repair (MTTR)	Improved customer satisfaction	● Remote expert	● Big data ● Internet of Things ● Additive manufacturing ● Systems integration
Customization	Improved customer satisfaction	● Use customer data to tailor offering to needs	● Big data ● Systems integration

IV CONCLUSION

Key strategy of Industrie 4.0 is the creation of new innovation for smart systems such as smart products, smart production systems, smart logistics or smart grids based on the integration of internet based communication and embedded control software to ensure sustainablity and environmental soundness. New advanced engineering methods are required to support the developemnt of smart products able to self - control their functionality and to communicate with other smart systems as well as with humans.

REFERENCES

[1] Drath, R. Horch, A., "Industrie 4.0 Hit or Hype? IEEE Industrial Electronics Magazine." pp.56–58, June 2014.

[2] Hermann, M. Pentek, T. Otto, B., "Design Principles for Industrie 4.0 Scenarios." Presented at the 49th Hawaii International Conference on System Sciences. 2016.

[3] Kagermann H., Wahlster W., Helbig J., "Recommendations for Implementing the Strategic Initiative Industrie 4.0." 2013.

[4] Kagermann, H. Anderl, R. Gausemeier, J. Schuch, G. Wahlster, W., "Industrie 4.0 in a Global Context." ACATECH 2016.

[5] Diedrrich, E., Engel, K., Wagner, K., European Innovation Management Landscape, European Commission, Brussels, pp. 6. 2006.

[6] Ranđelović S, Modeliranje procesa istosmernog istiskivanja šupljih elemenata koji obezbeđuje visoku sposobnost procesa, Doktorska disertacija, pp.149, Niš, Oktobar 2006.

[7] European Commission, Information note from the Commission services: Progress report on the Broad-based innovation strategy, 2008.

[8] European Commission: Putting knowledge into practice: A broad-based innovation strategy for the EU, 2006.

THE 5th INTERNATIONAL CONFERENCE
MECHANICAL ENGINEERING IN XXI CENTURY

December 9-10, 2020
Faculty of Mechanical Engineering in Niš, Serbia

The Expert System for Investigation of Hydraulic and Pneumatic Combinatory Automata - CAR-ex

Vladislav BLAGOJEVIĆ[1], Saša RANĐELOVIĆ[1], and Saša MILANOVIĆ[2]

Department of Production Information Technologies, Faculty of Mechanical Engineering, Niš, Serbia
Department of Hydroenergetics, Faculty of Mechanical Engineering, Niš, Serbia
vladislav.blagojevic@masfak.ni.ac.rs, sasa.randjelovic@masfak.ni.ac.rs, sasa.milanovic@masfak.ni.ac.rs

***Abstract*— To examine the hydraulic or pneumatic combinatory automata realization, direct connection and control by the combinatory diagram are most frequently applied. This way of investigation is very slow, and if any errors occur re-connecting is usually required. The automated investigation of the hydraulic and pneumatic combinatory automats realization, no matter of the number of inputs and outputs, with the aid of the personal computer and by using purposely developed Expert system is presented in the paper. This enables to eliminate possible errors in connections and forbidden states before the realization itself takes place. In this paper, Clips (C Language Integrated Production System) is used as a tool for developing expert systems. The properties of the proposed expert system for investigation of combinatory automata realization (CAR-ex) are demonstrated by computer simulation.**

***Keywords*— Pneumatic, Hydraulic, Expert, System, Investigation**

I. Introduction

The combinatory automats are widely applied for automation of technological processes in different industries like automotive, semiconductor industry, food processing, wood processing, textile industry, machine production, etc. Commonly, the pneumatic or hydraulic systems are applied for combinatory automats' realization. The main reason is that those systems offer many benefits in terms of small cost and easy installation and maintenance, etc. It is very important to design those systems appropriately, because any error in connecting elements leads to malfunction and disruption of the system [1], [2], or increasing energy consumption [3]-[5]. The correctness of the system design is possible to check only at the end of the realization. The expert knowledge in the field of pneumatic or hydraulic design of combinatory automats is the most important. Furthermore, it is very important and good to have the information about system correctness even before the realization, just after the designing process. This shortens the time for inspection of the pneumatic or hydraulic scheme of combinatory automata.

An expert system is a computer program conceived to simulate some forms of human reasoning (by the intermediary of an inference engine) and capable of managing an important quantity of specialized knowledge. It can be also said that an expert system is a computer application that solves complicated problems that would otherwise require extensive human expertise.

In this paper, the expert system for the investigation of combinatory automats realization, no matter is it the hydraulic or pneumatic systems. The quality of the work of the proposed expert system is illustrated by computer simulation

II. Combinatory Automats

Combinatory automats fall into the category of finite automata with a fixed number of input and output channels [1], [2], [6]. There are two types of combinatory automata according to the number of output channels. The first is (n,1) type with n input and one output channel, Fig.1a. The second is (n, m) type with n input and m output channels, Fig. 1b. A program of the technological process should be given at the input by using binary signals, and at the output, actuators are activated i.e. the appropriate technological operations are performed.

With this type of automata, the state of the output is determined only by combining the values of input signals, present in the observed moment, regardless of the preceding input combinations. It is as well determined by the logic of the automata. It is, therefore, said that this automate has no memory. The input variables (independent variables – x_i, i=1,2,...n) and the output variables (dependent variables – y_j, j= 1,2,...m) have a binary value (0,1).

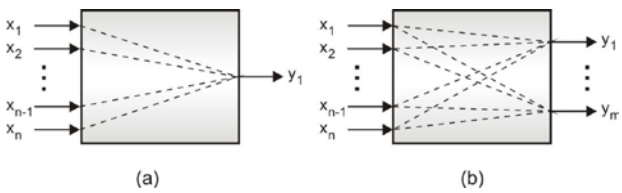

Fig. 1 Combinatory automata: a) (n,1) type, b) (n,m) type

Technical realizations of some combinatory automata logical function can be done by using pneumatic or hydraulic logical elements in appropriate schemes. The logical elements are linked in a way that the output of one or more element is input to another one. So, the pneumatic or hydraulic combinatory realization consists of several levels of linked elements, Fig.2. Outputs from

level 1 are also outputs from combinatory automata logical function.

In the real automatic control of technological processes, the output signals are used either for direct activation of the actuator or as a command to some other control element for indirect control.

In pneumatic or hydraulic systems, different valves are used as logical elements. The most applied valves are: 2/2, 3/2, 4/2, 5/2, 5/3 way, monostable or bistable, normally open or closed, AND valve and OR valve.

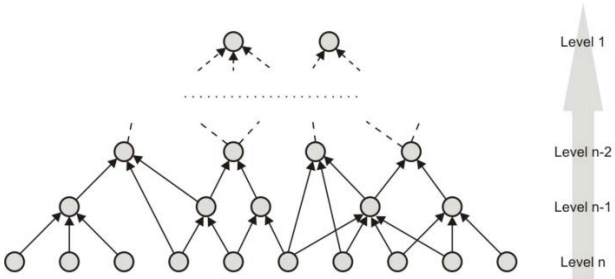

Fig. 2 Schematic diagram of pneumatic or hydraulic combinatory realization

III. Expert Systems

An expert system, Fig. 3, is normally composed of a knowledge base (information, heuristics, etc.), inference engine (analyses the knowledge base), and the end user interface (accepting inputs, generating outputs).

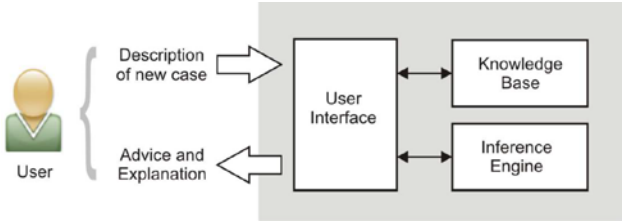

Fig. 3 Major parts of an expert system

The path that leads to the development of expert systems is different from that of conventional programming techniques. The concepts for expert system development come from the subject domain of artificial intelligence (AI), and require a departure from conventional computing practices and programming techniques. A conventional program consists of an algorithmic process to reach a specific result. An AI program is made up of a knowledge base and a procedure to infer an answer.

One of the most powerful attributes of expert systems is the ability to explain reasoning. Since the system remembers its logical chain of reasoning, a user may ask for an explanation of a recommendation, and the system will display the factors it considered in providing a particular recommendation. This attribute enhances user confidence in the recommendation and acceptance of the expert system.

Advantages of the expert system are numerous. Compared to traditional programming techniques, expert-system approaches provide the added flexibility (and hence easier modifiability) with the ability to model rules as data rather than as code. In situations where an organization's IT department is overwhelmed by a software-development backlog, rule-engines, by facilitating turnaround, provide a means that can allow organizations to adapt more readily to changing needs. In practice, modern expert-system technology is employed as an adjunct to traditional programming techniques, and this hybrid approach allows the combination of the strengths of both approaches. Thus, rule engines allow to control through programs (and user interfaces) written in a traditional language, and also incorporate the necessary functionality such as inter-operability with existing database technology.

A shell (or inference engine) is a complete development environment for building and maintaining knowledge-based applications (expert system). It provides a step-by-step methodology, and ideally, a user-friendly interface such as a graphical interface, for a knowledge engineer that allows the domain experts themselves to be directly involved in structuring and encoding the knowledge. There are many different shells, including [7]-[9]: Drools, CLIPS, JESS, d3web, Prolog, Java DON, G2, eGanges, openKBM (initially developed as a replacement for G2), etc

IV. Development of CAR-EX

The expert system for investigation of combinatory automata realization – CAR-EX, is designed by CLIPS and consists of three lists of facts such as:

- base of elements (BASE-OF-ELEMENTS.TXT) containing data about the operation of logical elements,
- diagram (DIAGRAM.TXT) containing data about the connecting the logical elements of the combinatory diagram,
- input (INPUT.TXT) containing the input combinations of the combinatory automata.

These three lists of facts introduce the hole either hydraulic or pneumatic realization of some combinatory automata.

After entering these data files, CAR-ex checks the principal pneumatic diagram based on the list of rules. If the diagram is correct at the input, the value of output is obtained for a certain combination at the input. If the diagram is incorrect, the program indicates the connection error.

The programs written in Clips consist of a sequence of rules; in order to execute these, the left-hand side of the rule should be fulfilled. Namely, it is necessary for the facts which make up the left-hand side of the rule to exist; thus, the rule can be executed and, if the program has been started, the rule itself will be executed, whereby a change in the fact list occurs in the form of reading-in of new facts or deleting the old ones.

The program CAR-ex consists of several rules as well, to be more precise, of twelve rules, which are executed in the aforementioned manner.

In order to enable the execution of the program, after it has been opened, the fact (initial-fact) should be read in by using the directive (reset), and started by directive (run). The rule start (START) can now be executed since on its left-hand side, there is only a fact (initial-fact). The execution of this rule results in reading-in of the base of elements (BASE-OF-ELEMENTS), fact list referring to the diagram itself (FACT-LIST) and list of input facts (INPUT). The content of the base of the elements and fact lists can be altered (edited) by a simple text editor. The rule start is:

```
(defrule START
        (initial-fact)
=>
        (load-facts BASE-OF-ELEMENTS.TXT)
        (load-facts DIAGRAM.TXT)
        (load-facts INPUT.TXT))
```

After that is possible to execute all the other rules.

The rules that contain the "connection-element" in their name are the rules which, based on data about the element to which they are linked, data about the element being linked, data of the connection itself and rule of a manner of operation of the element being linked, enable that the element being linked, changes its state and the executed connection transforms in a used connection. Under the term "element" is supposed the pneumatic, Fig. 4 or hydraulic valves with the corresponding inputs and outputs. For these purposes, the only difference of pneumatic and hydraulic valves is in working medium.

There are several rules in this group differing in whether the input elements (elements to which others are linked) have two, three, four or five inputs and whether their a or b input is connected to the element being linked. These rules are:

- connection-element-2-input-a
- connection-element-3-input-a
- connection-element-4-input-a
- connection-element-4-input-b
- connection-element-5-input-a
- connection-element-5-input-b

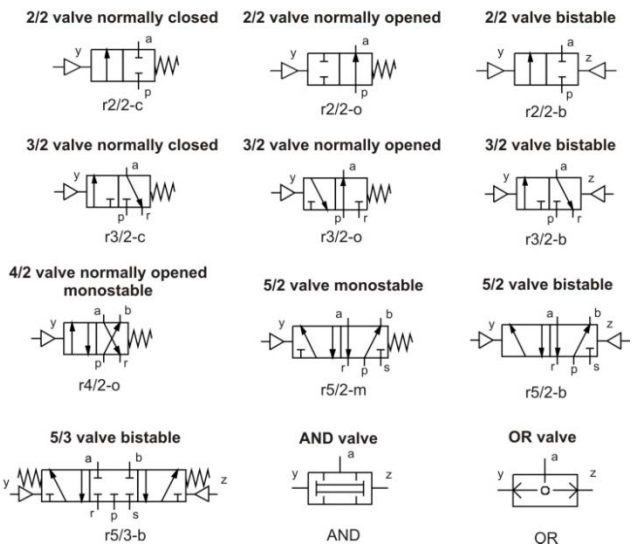

Fig. 4 Pneumatic and Hydraulic valves designations

For a simpler explanation, the rule connection-element-3-input-a is shown:

```
(defrule connection-element-3-input-a
 (level ?bn)
 (element ?r1 ?n1 ?a ?a1 ?a2 ?a3 ?a4 ?a5 ?a6)
 ?delete1 <- (element ?r2 ?n2 ?b $?forward ?u ?u+1
 $?behind)
 ?delete2 <- (connection ?n1 ?a a ?n2 ?b ?u)
 (rule ?r1 ?a1 ?a2 ?a3 ?a4 ?a5 ?a6 a ?i+1 $?behind)
=>
 (retract ?delete1)
 (assert (element ?r2 ?n2 ?b $?forward ?u ?i+1
 $?behind))
 (assert (finis-connection ?n1 ?a a ?n2 ?b ?u))
 (retract ?delete2))
```

Field marks are:

?bn - Number of levels;
?r1, ?r2 - element mark (r2/2, r3/2-z, r3/2-o, r4/2, r5/2, r5/3, AND and OR);
?n1 - the first digit in marking the element to which others are linked;
?a - the second digit in marking the element to which others are linked;
?a1 - mark of the first input of the element to which others are linked;
?a2 - value of the first input of the element to which others are linked;
?a3 - mark of the second input of the element to which others are linked;
?a4 - value of the second input of the element to which others are linked;
?a5 - mark of the third input of the element to which others are linked;
?a6 - value of the third input of the element to which others are linked;
?n2 - the first digit in marking the element being linked;
?b - the second digit in marking the element being linked;
$?forward - fields in front of mark of the input being linked;
?u - mark of the input of the element being linked;
?u+1 - value of the input of the element being linked;
$?behind - fields behind the value of output a of the element to which it is linked;

The operation of CAR-ex starts with rules of the highest level value. Once there are no more connections in the corresponding level, the rule cross is executed and the lower level asserted; therefore, the program can proceed with operating.

The rule cross is:

```
(defrule cross)
        ?delete <- (level ?bn)
        (not (connection ?n1 ?bn ?))
=>
        (bind ?bn (- ?bn 1))
        (if (> ?bn 0)
                then
                (retract ?delete)
                (assert (level ?bn))
```

If, during the execution of the program, a forbidden state occurs on any element, the rule forbidden-state sends a message about the presence of such a state and the manner of testing.

The rule forbidden-state is:

```
(defrule forbidden-state)
        (element ?r1 ?n1 ?a $?forward ?u forbidden-state
   $?behind)
        (finis-connection ?n2 ?b ?i ?n1 ?a ?u )
=>
        (printout t "Forbidden state: Check the input
    signals for y and z channels of element " ?n2 ?b
    crlf))
```

At the end of operation of CAR-ex the rule finish-n is executed. Parameter n means the number of outputs of combinatory automata.

For a simpler explanation, the rule finish-1 is shown:

```
(defrule finish-1
        (level 1)
```

```
        (element ?r ?n1 ?a $?other)
        (rule ?r $?other a ?output)
=>
        (printout t "*************************" crlf)
        (printout t "Element: " ?n ?a crlf)
        (printout t "Output: " ?output crlf)
        (printout t "*************************" crlf)
```

and Field marks:
$?other - all fields behind previous field;
?output - combinatory automata output;

V. Example of CAR-ex Application

A. (n,1) Type Combinatory Automata

The best way for demonstrating all advantages of the operation of CAR-ex is to use the real combinatory automata realized by the pneumatic components.

In this example, the combinatory automata consist of four sensors (x_1, x_2, x_3, x_4) for activating the actuator. This combinatory automata is (n,1) type.

The conditions for combinatory automata activating are:

- When x_1 and x_4 are not activated.
- When x_2 and x_3 are activated.
- When x_1 is not and x_3 is activated.

In these conditions, the states of the other sensors are not important for combinatory automata operation and activation.

After the minimization process, the minimal disjunctive normal form (MDNF) is:

$$y = \overline{x_1}(x_3 + \overline{x_4}) + x_2 x_3$$

Assuming MDNF, a principal pneumatic diagram is showed in Fig. 5, where x_1 is designated with 4.1, x_2 is designated with 4.2, x_3 is designated with 4.3, x_4 is designated with 4.4. The principal diagram, Fig. 5, has four element levels.

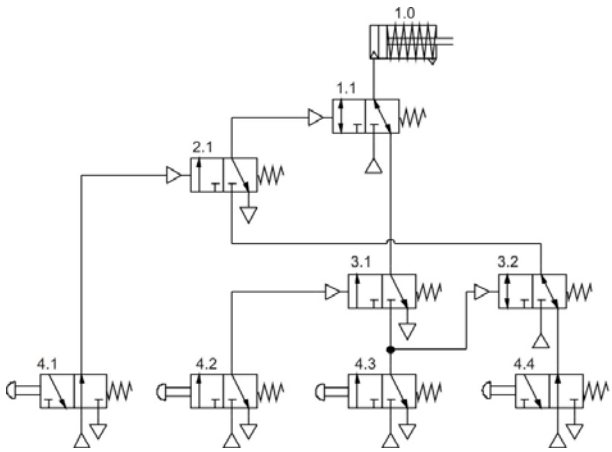

Fig. 5 Pneumatic Scheme of Combinatory Automata (4,1) Type

Based on the principal pneumatic scheme, data are entered into the data file DIAGRAM.TXT.

```
(initial-fact)
(level 4)
(element r3/2-c 1 1 y 0 p 1 r 0)
(element r3/2-c 2 1 y 0 p 0 r 0)
(element r3/2-c 3 1 y 0 p 0 r 0)
(element r3/2-c 3 2 y 0 p 1 r 0)
(connection  4 1 a 2 1 y)
(connection  4 2 a 3 1 y)
(connection  4 3 a 3 1 p)
(connection  4 3 a 3 2 y)
(connection  4 4 a 3 2 r)
(connection  3 1 a 1 1 r)
(connection  3 2 a 2 1 p)
```

When the DIAGRAM.TXT data file has been formed, data are entered into INPUT.TXT data file.

By entering the input values from the combinatory table for decimal equivalent 7:

```
(element r3/2-o 4 1 y 0 p 1 r 0)
(element r3/2-c 4 2 y 1 p 1 r 0)
(element r3/2-c 4 3 y 1 p 1 r 0)
(element r3/2-o 4 4 y 1 p 1 r 0)
```

The output y is obtained as:

```
--------------------------
Element 1.1
Output y: 1
--------------------------
```

By entering the input values from the combinatory table for decimal equivalent 12:

```
(element r3/2-o 4 1 y 1 p 1 r 0)
(element r3/2-c 4 2 y 1 p 1 r 0)
(element r3/2-c 4 3 y 0 p 1 r 0)
(element r3/2-o 4 4 y 0 p 1 r 0)
```

The output y is obtained as:

```
--------------------------
Element 1.1
Output y: 0
--------------------------
```

In this manner, it is possible to check the principal pneumatic diagram for the appropriate automata for each of the input combinations from the combinatory table. Furthermore, if there are some forbidden states in pneumatic realization, CAR-ex can detect that states.

For demonstrating the forbidden states in the realization, the pneumatic diagram with three element levels, shown in Fig. 6, is used.

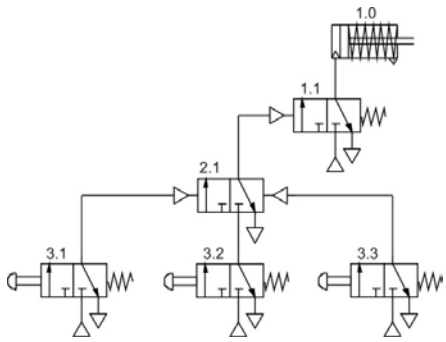

Fig. 6 Pneumatic Scheme of Combinatory Automata

Data referring to the principal diagram itself.

```
(initial-fact)
(element r3/2-z 1 1 y 0 p 1 r 0)
(element r3/2 2 1 y 0 p 0 r 0 z 0)
(connection 2 1 a 1 1 y)
(connection 3 1 a 2 1 y)
(connection 3 2 a 2 1 p)
(connection 3 3 a 2 1 z)
(level 3)
```

When sensors 3.1, 3.2 and 3.3 have the values 1, 1 and 0:

```
(element r3/2-z 3 1 y 1 p 1 r 0)
(element r3/2-z 3 2 y 1 p 1 r 0)
```

(element r3/2-z 3 3 y 0 p 1 r 0)

The output y is:

Element 1.1

Output y: 1

When all sensors 3.1, 3.2 and 3.3 have the values 1:

(element r3/2-z 3 1 y 1 p 1 r 0)

(element r3/2-z 3 2 y 1 p 1 r 0)

(element r3/2-z 3 3 y 1 p 1 r 0)

The output is the following message:

Forbidden state-Check the input

signals for y and z channels of

element 2.1

At this level of development of CAR-ex, it only detects the forbidden states if they exist. At the next, more advanced level, the computer can solve the existing mistakes; however, it is not included in this paper.

B. (n,m) Type Combinatory Automata

In this example, the combinatory automata consists of four sensors (x_1, x_2, x_3, x_4) for activating the three actuators. This combinatory automata is (4,3) type.

Outputs y_1 and y_2 are used for activating the single acting pneumatic cylinders 1.0 and 2.0. Output y_3 is used for activating the double acting pneumatic cylinder 3.0 via its supplying valve 3.1.1.

The conditions for combinatory automata activating are given in a perfect disjunctive normal form (PDNM), as:

$$y_1 = \sum^{4}(0,1,2,3,7,11,15)$$

$$y_2 = \sum^{4}(0,1,2,3,5,7,13,15)$$

$$y_3 = \sum^{4}(3,5,7,11,13,15)$$

After the minimization process, the minimal disjunctive normal form (MDNF) is:

$$y_1 = \overline{x_1}\,\overline{x_2} + x_3x_4$$

$$y_2 = \overline{x_1}\,\overline{x_2} + x_2x_4$$

$$y_3 = x_2x_4 + x_3x_4$$

Based on MDNF, a principal diagram is presented in Fig. 7, where x1 is designated with 4.1, x2 is designated with 4.2, x3 is designated with 4.3, x4 is designated with 4.4. The principal diagram, showed in Fig. 7, has three element levels.

Based on the principal pneumatic scheme, given in Fig.7, data are entered into the data file DIAGRAM.TXT.

(initial-fact)

(level 3)

(element r3/2-c 1 1 y 0 p 1 r 0)

(element r3/2-c 1 2 y 0 p 1 r 0)

(element r3/2-c 1 3 y 0 p 1 r 0)

(element r3/2-c 2 1 y 0 p 0 r 0)

(element r3/2-c 2 2 y 0 p 0 r 0)

(element r3/2-c 2 3 y 0 p 0 r 0)

(connection 3 1 a 2 1 y)

(connection 3 2 a 2 2 y)

(connection 3 2 b 2 1 p)

(connection 3 3 a 2 3 y)

(connection 3 4 a 2 2 p)

(connection 3 4 a 2 3 p)

(connection 2 1 a 1 1 y)

(connection 2 1 a 1 2 r)

(connection 2 2 a 1 2 y)

(connection 2 2 a 1 3 y)

(connection 2 3 a 1 1 r)

(connection 2 3 a 1 3 r)

When the DIAGRAM.TXT data file has been formed, data are entered into the INPUT.TXT data file.

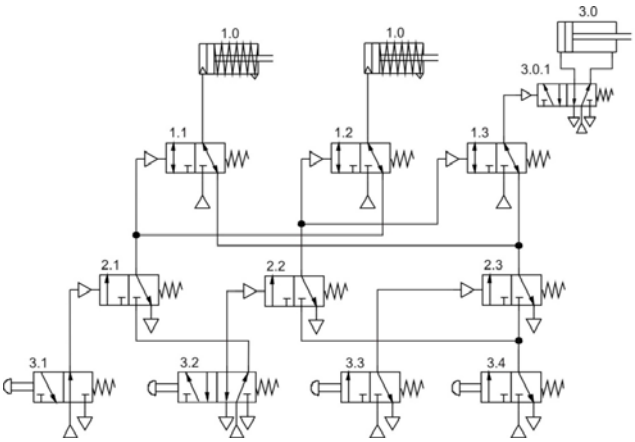

Fig. 7 Pneumatic Scheme of Combinatory Automata

For instance, by entering the input values from PDNF for decimal equivalent 5:

(element r3/2-o 3 1 y 0 p 1 r 0)

(element r5/2-m 5 2 y 1 r 0 p 1 s 0)

(element r3/2-c 3 3 y 0 p 1 r 0)

(element r3/2-c 3 4 y 1 p 1 r 0)

The output y is obtained as:

Element 1.1

Output y: 0

Element 1.2

Output y: 1

Element 1.3

Output y: 1

By entering some other input value from PDNF the CAR-ex will count the values of outputs.

In this manner, it is possible to check the principal pneumatic diagram for the appropriate automata for each of the input combinations from the combinatory table or PDNF. Furthermore, if there are some forbidden states in the pneumatic realization, the CAR-ex can detect that states in a same way as it was explained in previous chapter.

VI. CONCLUSIONS

The paper presents the development and utilization of some of the possibilities of CLIPS tool for development of an expert system for investigation of combinatory automata realization – CAR-ex. It enables a prompt investigation of the pneumatic and hydraulic diagrams of a combinatory automata. The paper presents that CAR-ex can be used on (n,1) type as well as (n, m) type combinatory automata. Furthermore, if there are some forbidden states in the pneumatic or hydraulic realization, the CAR-ex can detect that states and in more advanced level, the computer can solve the existing mistakes. Besides, the program itself offers a solid basis for its further advancement for sequential automats, as well.

REFERENCES

[1] M. Stojiljković, "Logical synthesis of pneumatic control", University of Nis, Faculty of Mechanical Engineering, Serbia, 2009.

[2] W. H. Kautz, "Automatic fault detection in combinational switching networks" IEEE Xplore, 2010.

[3] V. Blagojević, "Contribution to the Development of Efficient Control of Pneumatic Executive Organs", Ph.D. Thesis, Faculty of Technical Sciences, Novi Sad, Serbia, 2010.

[4] V. Blagojević, D. Šešlija, and M. Stojiljković, "Cost Effectiveness of Restoring Energy in Execution Part of Pneumatic System", Journal of Scientific & Industrial Research, Vol. 70, No. 2, pp. 170-176, 2011.

[5] V. Blagojević, S. Ranđelović, V. Nikolić, S. Dudić, "Automatic Generation of the PLC Programs For the Sequential Control of Pneumatic Actuators", Facta Universitatis, Series: Mechanical Engineering, University of Niš, vol. 17, no. 3, pp. 405 - 414, 2019.

[6] D. M. Harris, S. L. Harris,S. "Digital Design and Computer Architecture", Elsevier, Morgan Kaufmann Publishers, San Francisco, USA, 2007.

[7] J.C. Giarratano, "CLIPS User's Guide", NASA Lyndon B. Johnson Space Center, USA, 1997.

[8] J.C. Giarratano, "CLIPS Reference Manual", NASA Lyndon B. Johnson Space Center, USA, 1997.

[9] J.C. Giarratano, "CLIPS User's Guide", Quicksilver Beta, USA, 2007.

THE 5th INTERNATIONAL CONFERENCE
MECHANICAL ENGINEERING IN XXI CENTURY

December 9-10, 2020
Faculty of Mechanical Engineering in Niš, Serbia

Comparison of Optical Measuring Systems and CMM for Smaller Parts

Marko SIMONOVIĆ[1], Bogdan NEDIĆ[1], Milan SIMONOVIĆ[1], Dragan LAZAREVIĆ[2]

[1] Faculty of engineering University of Kragujevac
[2] Faculty of Technical Sciences in Kosovska Mitrovica, University of Pristina
marko.2594.simonovic@gmail.com, nedic@kg.ac.rs, miki2504994@gmail.com, dragan.lazarevic@pr.ac.rs

***Abstract*— This paper aims to compare the accuracy of measurement of modern optical measuring systems and coordinate measuring machines. It is characterized by the theoretical publication of the way of functioning and analysis of experimental tests of two measuring systems and each coordinate measuring machine. Data were compared for measurements. These are modern measuring systems ATOS and TRITOP and the coordinate measuring machine Tesa micro-hite 4-5-4. The measurements were performed on the part that has the role of a stopper in one assembly.**

***Keywords*— modern measuring systems, coordinate measuring machine, metrology, industrial production**

I. INTRODUCTION

From ancient times there is a need to make different types of parts, which are small or large in size, small or large complexity of shape, small or large requirements for the functionality of the system to which they belong. Consequently, there was a need to control the accuracy of their production. A large number of different complex technical systems require precisely made parts, in order to perform their function in accordance with the requirements. In order to ensure that the parts meet the prescribed requirements by the designer, it is necessary to inspect the parts after their manufacture. Control is performed by various measuring instruments and systems, which have been developed and improved with increasing demands in production. It is often necessary, when making a work, to respect the tenth, hundredth, and even the thousandth part of a millimeter. In production, the most commonly used measuring instruments are: movable beak meter with vernier (Fig. 1a), micrometer (Fig. 1b), subitor (Fig. 1c) [1]…

a) b) c)

Fig. 1. The most commonly used measuring instruments

The disadvantage of their application is reflected in the human factor. Measurement accuracy significantly depends on the operator's training, sense of measurement, his concentration, etc. Due to the growing demands for the production of parts of very complex configurations using modern CNC machines, it is not always possible to use simple measuring instruments, but there is a need to use far more complex and modern measuring systems of higher accuracy. With them, it is possible to measure parts of complex shapes much easier. The principle of measurement comes down to the application of a measuring probe, laser scanning or making images of parts and processing the collected data in the form of point clouds using appropriate software. The analysis of the collected data provides information on the accuracy of the work. Control using scanners or optical measuring systems is called non-contact measurement, and the technology of determining the accuracy of parts and structures in this way is called 3D digitization. Contactless measurement is increasingly used in industry. This method of measurement achieves a significant reduction in production costs, because, above all, it reduces the control time of manufactured parts. Measurement achieves a large amount of data, which later provides measurement results at a high level of quality [2]. With this measurement technology, the produced parts are recorded and entered into the software, whereby a 3D model of the part is obtained. Recording of parts is done with devices such as digital cameras, cameras, scanners, laser sensors, etc. Before recording the work, uncoded and coded reference points are glued, the coordinates of which are later collected in the software. These collected points gave a digital form of the work. The set of points obtained in this way, due to its shape in space, is called a point cloud. There is a possibility of digitizing parts from a few millimeters to several tens of meters [3]. Digitization can be done in two ways: in two-dimensional and three-dimensional form, depending on the technical capabilities of the device. One of the optical systems, which works on this principle, is ATOS (Fig. 2.b).

Photogrammetry is based on the production and analysis of photographs. It is applied to optical 3D coordinate measuring systems, and is the basis for measuring parts. The photogrammetric camera does not measure the object directly, but measures the center of the reflective mark. Recording is done with one camera, whose position in space is constantly changing, or with

two fixed cameras. Once the image creation is complete, the software analyzes and processes the photos. The photogrammetric device defines the position of points on the part via photogrammetric markers on its surface [3].

One of the systems, based on the principle of photogrammetry, is the measuring optical system TRITOP (Fig. 2a).

a) b)

Fig. 2. Measuring systems TRITOP [4] and

ATOS [5]

Contact measurement of parts is most often performed on coordinate measuring machines (Fig. 3). Over time, coordinate metrology has become an indispensable branch in the industry. There is information that this system in the UK annually controls products worth 100 million pounds [6].

Fig. 3. Coordinate measuring machine [7]

It is possible to measure simultaneously in all three axes. This machine is formed by three guides, which are normal to each other and which actually represent the axes of the coordinate system. Coordinate measuring machines can be divided into two groups: portable and stationary [3]. The contact between the probe probes and the surface to be tested gives the necessary data for the analysis of the accuracy of construction.

The development of modern measuring systems has made it easier and faster to determine the accuracy of parts. The complex configuration and size of the part is now not the biggest problem to measure, because they can measure almost all manufactured parts. In addition to dimensional testing of parts, these systems can be used to check whether shape requirements have been met during fabrication, such as parallelism, straightness, concentricity, cylindricality, directionality, etc. Modern optical measuring systems are the subject of many researches, published in professional and scientific papers, doctoral dissertations. Many researchers, through many experimental tests and comparative analyzes, have strived to improve their application. The aim was to achieve full automation of parts control. If there is a reference CAD model with control directives and corresponding non-contact measured data of the examined part, then a complete report on the accuracy of the part can be obtained in a fully automated way [8]. It is also important to plan the control process. Planning is an integral part of development and production activities and today it is mostly done in a computerized way. It determines the characteristics of the product, the method of control, when and where, using which measuring equipment, given the great variety of products and parts, narrow tolerances and the required high quality of products [9].

II. EXPERIMENT

In order to compare the measurement accuracy of several measuring systems, an experiment was performed, in which two optical measuring systems, ATOS and TRITOP and the coordinate measuring machine Tesa micro-hit 4-5-4, were used for measurement. As a sample for measurement, a stopper (Fig. 4) from a complex technical system was used.

Fig. 4. Stopper

The stopper was chosen due to its small size and complex configuration. The measurement was performed at a temperature of 21°C, in conditions where there is a possibility of easy change of ambient conditions, temperature, humidity, etc. These changes may affect the measurement accuracy of the ATOS measurement system.

A. Stopper measurement using the ATOS optical measurement system

Scanning with the ATOS system requires prior preparation of the part. First, the surfaces were cleaned and degreased. Then the stopper, due to the gloss on the surfaces, is subjected to matting. The glossy surface achieved by pre-machining is a problem when scanning, due to the appearance of very high contrast. Matting is done with white powder (developer penetrant). The next operation is pasting uncoded reference points. They are used to determine the position of the scanner in space. In addition to the preparation of the work, it is necessary to prepare the measuring system. The scanner (Fig. 5a) is placed on a suitable stand (Fig. 5b) and left on for at least 30 minutes before calibration is performed. Calibration is performed using calibration boards (Fig. 5c) and contains 18 points, which need to be followed in order for this process to be complete and accurate.

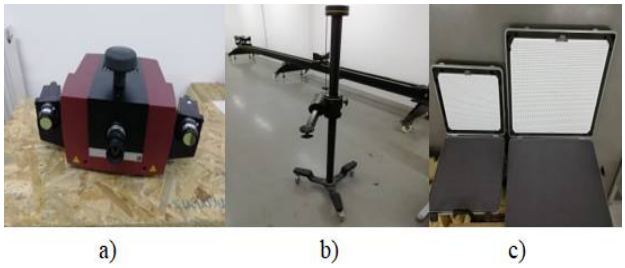

Fig. 5. ATOS optical system

After scanning the stopper, the collected data was processed in the software "GOM Inspect V7.5 SR2". First, two bases were formed, in relation to which the accuracy of construction will be checked. Fig. 6 shows base A, which is actually approximate plane 1 (shown in blue) and base B, which is in the form of approximate cylinder 2. Base B is marked in red.

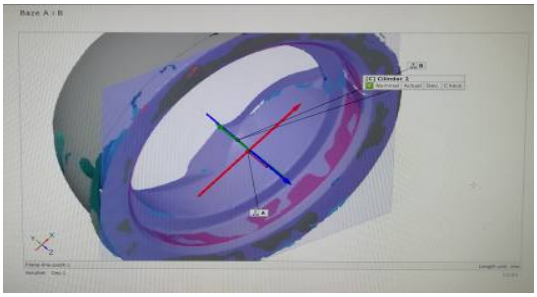

Fig. 6. Bases A and B

An approximate plane 2 was then formed, above base A (Fig. 7), to determine the distance between the two horizontal surfaces.

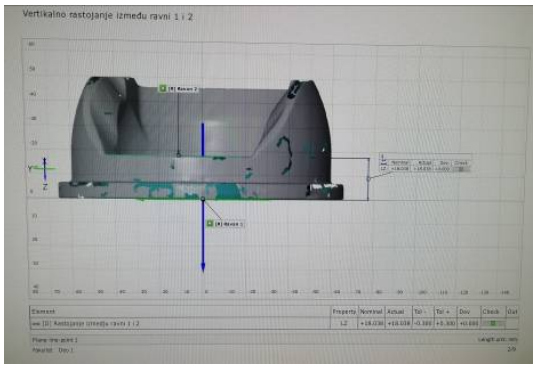

Fig. 7. Forming of the approximate plane 2

For the purpose of determining the accuracy of making the height of the boundary ring in relation to the base A, an approximate plane 3 was formed (Fig. 8).

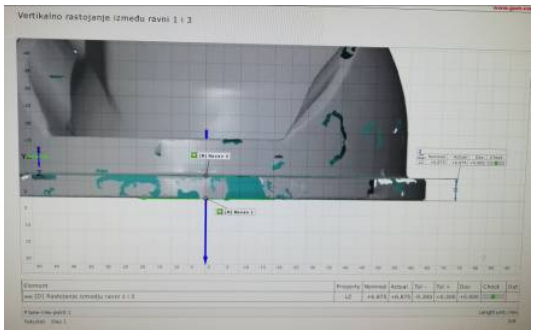

Fig. 8. Forming of an approximate plane 3

Approximate plane 4 was also formed in the software, but it was not necessary for the examination of the work, so it is not shown in the pictures. Fig. 9 shows the formation of an approximate plane 5, with respect to base A. A plane 5 is necessary to determine the realized height of the delimiter.

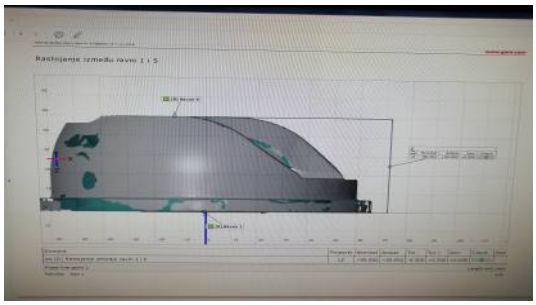

Fig. 9. Forming of an approximate plane 5

Fig. 10 shows the formation of approximate cylinders 1, 2 and 3, in order to determine the realized diameter.

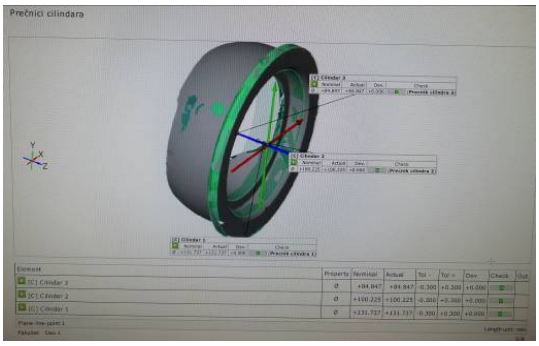

Fig. 10. Forming of approximate cylinders

1, 2 and 3

Since all the necessary bases, planes and cylinders have been formed, the distance (diameter, concentricity, parallelism and normality between them) are determined (measured). The measurement results will be shown in Table 1.

B. Stopper measurement using the TRITOP optical measuring system

The measurement with the TRITOP system was performed under the same conditions as the previous measurement. This measuring system does not require special preparation of the part, but it is enough to clean and degrease its surface. The TRITOP measuring system consists of the following elements: measuring rods, coded and uncoded reference points, camera and measuring cross (Fig. 11).

Measuring rods are used to determine the measuring range. The coded reference points are set so that at least 5 points are visible on each image, so that the image is authoritative for processing. Their role is reflected in determining the position of the camera in space. Before taking a photo, it is necessary to perform a calibration. Calibration is performed by imaging the part (stopper in this case) by rotating the camera 4 times by 90 °. After that, the photographing of the stopper is approached from several angles, in order to obtain the required number of photographs for photogrammetry. Since it is necessary to photograph the lower surface of the stopper, it is done by

rotating it, and forming another group of photographs for photogrammetry. The software, which is the same as ATOS, combines these two photogrammetries. Then the formation of the coordinate origin is performed, which serves for further data processing. Approximate cylinders, points and planes are made, on the basis of which the measured dimensions of the work are measured and controlled.

Fig. 11. TRITOP optical system

First, approximate plane 1 is formed (Fig. 12), then approximate plane 2 (Fig. 13), and then approximate plane 3 (Fig. 14).

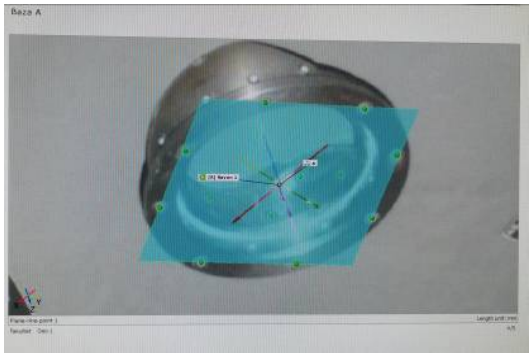

Fig. 12. Forming of the approximate plane 1

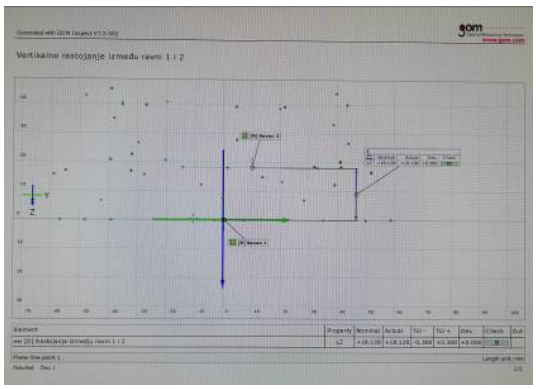

Fig. 13. Forming of the approximate plane 2

Dimensional control, using the software "GOM Inspect V7.5 SR2", the distance between the formed approximate planes, as well as the diameter of the cylinder obtained the results shown in Table 1.

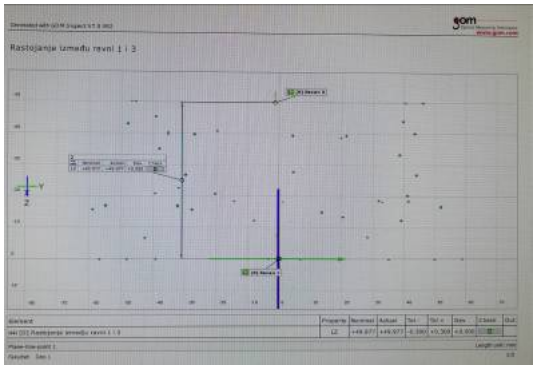

Fig. 14. Forming of an approximate plane 3

TABLE 1. MEASUREMENT RESULTS

	Type of test	Nominal measure	Measured measure	± tolerances		Deviation
ATOS measuring system	Distance between planes 1 and 5	50.002	50.002	-0.3	0.3	0
	Distance between planes 1 and 3	6.875	6.875	-0.3	0.3	0
	Distance between planes 1 and 2	18.038	18.038	-0.3	0.3	0
	Cylinder diameter 3	84.847	84.847	-0.3	0.3	0
	Concentricity of cylinder 3 with respect to base B	0	0.436	0	0.1	0.436
	Cylinder diameter 2	100.225	100.225	0.3	-0.3	0
	Normality of cylinder 2 in relation to base A	0	0	0	0.1	0
	Cylinder diameter 1	131.737	131.737	-0.3	0.3	0
	Cylinder diameter 4	119.545	119.545	-0.3	0.3	0
	Concentricity of cylinder 1 with respect to base B	0	0.067	0	0.1	0.067
	Parallelism of plane 5 with respect to base A	0	0.052	0	0.1	0.052
TRITOP measuring system	Distance between planes 1 and 3	49.977	49.977	-0.3	0.3	0
	Distance between planes 1 and 2	18.128	18.128	-0.3	0.3	0
	Cylinder diameter 4	119.545	119.545	-0.3	0.3	0
	Parallelism of plane 3 with respect to base A	0	0.182	0	0.1	0.182
	Parallelism of plane 2 with respect to base A	0	0.203	0	0.1	0.203
Coordinate measuring machine	Cylinder diameter 2	100.349	100.349	-0.05	0.05	0
	Cylinder diameter 1	131.739	131.739	-0.05	0.05	0
	Cylinder diameter 4	119.549	119.549	-0.3	0.3	0
	Distance between planes 1 and 3	6.918	6.918	-0.3	0.3	0
	Distance between planes 1 and 2	18.041	18.041	-0.3	0.3	0
	Distance between planes 1 and 5	50.04	50.04	-0.3	0.3	0

C. Stopper measurement using a coordinate measuring machine

As the third measuring system for checking the accuracy of the stopper, the coordinate measuring machine "TESA micro-hit 4-5-4" was used (Fig. 15).

Fig. 15. Coordinate measuring machine

As with the TRITOP measuring system, no special preparation of parts or measuring equipment is required here. It is only necessary to clean and degrease well. Fig. 16 shows the measurement of the stopper using a coordinate measuring machine.

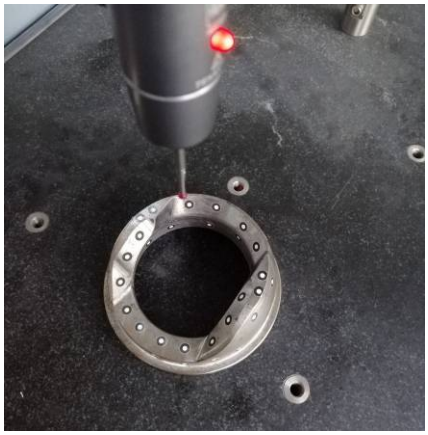

Fig. 16. Measurement with a coordinate measuring machine

The operator proves the measuring probe with the measuring probe manually to the surfaces of the part (in this case manually). Many different types of measuring probes can be mounted on the probe, depending on what needs to be measured and how to approach it most easily. The software "PC-DMIS CAD 2015.1" was used for data processing, Fig. 17.

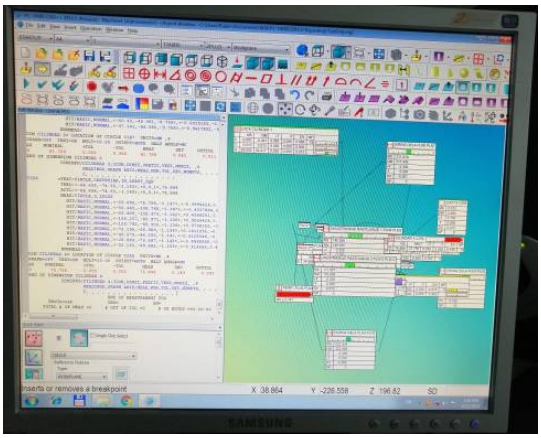

Fig. 17. Data processing software "PC-DMIS 2015.1 CAD"

This procedure measured the diameters within the stopper and the distances between the approximate planes, which represent the heights of the horizontal surfaces in the section. The measurement results are shown in Table 1.

III. TEST ANALYSIS

After measuring with the mentioned measuring systems, the analysis of the measurement results was performed. With the ATOS optical system, it is necessary to thoroughly clean the part beforehand, apply white powder on it in order to neutralize the reflection, and stick uncoded dots. Preparing the ATOS scanner requires special ambient conditions, where there are no vibrations, shocks, sudden changes in temperature, etc. The disadvantage of this measuring system is the need for its calibration, which is not simple. It is carried out through 18 points, where the calibration plate and the scanner are placed in precisely defined positions, with the proviso that the ATOS must be turned on for at least 30 minutes before the start of calibration. With the appearance of any factors that damage the ambient conditions (vibrations, shocks, ...), decalibration easily occurs, and this procedure must be repeated, which is a disadvantage, because it significantly increases the time required to prepare measurements. For these reasons, ATOS is best applied in laboratory conditions, not in industrial ones. The TRITOP optical system does not require special preparation of the part, it is enough to clean and degrease its surfaces. Uncoded reference points are glued on smooth places that do not contain cracks, crevices, dirt products, etc. After gluing the uncoded points, the coded reference points and measuring rods are placed. All this is done in a short period of time, which is an advantage over ATOS. The camera takes 4 images, rotating 4 times by 90°. In this way the measuring system is calibrated. It can be noticed that its calibration is much simpler than the calibration of ATOS. With a coordinate measuring machine, the requirements for part preparation are the same as with TRITOP. This means that, from the aspect of preparation for measurement, ATOS is much more complicated than other measuring systems. The following analysis refers to the method of measuring the work and processing the data. Scanning with the ATOS measuring system gives a 3D scan using the appropriate software. Polygonization is performed, after which the formation of approximate elements begins. ATOS has the ability to scan almost all surfaces of the work, which further results in the ability to measure almost all dimensions of the object. With TRITOP, photographing a work from multiple angles allows you to create photogrammetry in data processing software. The bearing surface of the stopper is also photographed, but it must be rotated first. Rotating the work for photography conditions the creation of another photogrammetry. When processing data, photogrammetries must be linked. Then approximate elements are formed. The disadvantage of TRITOP is that smaller parts cannot be measured so that every detail on it is fully covered. Specifically, when measuring the stopper, it was not possible to cover the inner surfaces, as well as the height of the rim. The measurement with a coordinate measuring machine belongs to the test by the contact method, where the measuring probe with a very sensitive measuring probe is pressed against the surface of the part, after which the contact is registered. Coordinate measuring machines have higher measurement accuracy than optical measuring systems.

Not all 3D stopper measurements used a 3D model, which would serve as a reference model. Table 1 shows the measurement results using these measurement systems.

The table 1 shows that some dimensions are missing in TRITOP. This indicates the impossibility of TRITOP to record internal surfaces of smaller diameters, as well as cylindrical surfaces at lower heights, where there is no place for gluing uncoded reference points. The coordinate measuring machine and the ATOS provided almost identical measurement results.

The ATOS measuring system ensures high

measurement accuracy. Measurements were performed by researchers, using several types of this system, with the intention of determining their efficiency and discovering which type of ATOS provides the best data. The researchers previously performed the measurement on the coordinate measuring machine and took the data obtained by it as a reference, since it gives even more accurate data from ATOS. By processing the data, they came to the conclusion which type of ATOS deviates the least and which deviates the most from the reference values [10].

It is important to establish the area of application of measuring systems, in order to know at the beginning of control planning which system can be used most efficiently. In order to determine the area of application, measurements were performed with a coordinate measuring machine, a scanner, a measuring arm and a digital camera. In addition, the experiment examined the measurement uncertainty, measurement volume, measurement speed, resolution, as well as the possibility of synergy of several measurement systems [11].

IV. CONCLUSION

The need for constant improvement of production technology has conditioned the development of control technologies for parts and assemblies. In production, measuring instruments such as movable beak gauges, subits, micrometers, comparators, etc. are most often used today. They easily check the tolerated measures, given by the technical drawing. However, the application of these measuring devices in the final control is often slow with insufficient accuracy, and in many cases the measurement cannot be performed.

Therefore, it is necessary to design, make and use special measuring devices. This primarily refers to the control of tolerance of shape and position, such as parallelism, normality, concentricity, etc. Experimental testing by measuring the limiters of the mentioned systems enabled a clear view of their possibilities. The table with the measurement results shows that some data were obtained using all three systems, while for some this is not the case. For example, the diameter of cylinder 4 is easily measured using all three systems, and the values obtained are almost identical. On the other hand, the diameter of cylinder 1 could be measured with an ATOS and a coordinate measuring machine, but not with a TRITOP. The obtained values are close to each other. The same applies to the diameter of cylinder 2. The values of the distance between planes 1 and 2 are approximate by measuring with ATOS and a coordinate measuring machine, while TRITOP gave a slightly larger deviation. The same situation applies to the values of the distance between planes 1 and 5. These are just some of the results of this test, which clearly conclude that the ATOS system and the coordinate measuring machine provide very similar results, compared to the TRITOP system.

ACKNOWLEDGEMENTS

This paper is part of project TR35034 The research of modern non-conventional technologies application in manufacturing companies with the aim of increasing efficiency of use, product quality, reducing costs and saving energy and materials, funded by the Ministry of Education, Science and Technological Development of Republic of Serbia.

REFERENCES

[1] https://www.yell.rs/profil/alati-tehnoalat-3/, June, 2019

[2] S.Martinez, E. Cuesta, J. Barreiro, B. Alvarez, „Analysis of laser scanning and strategies for dimensional and geometrical control“, Springer-Verlag London Limited 2009. Int J Adv Manuf Technol (2010)46:621-629, DOI 10.1007/s00170-009-2106-8

[3] D. Lazarević „Regenerisanje NC koda primenom 3D identifikacije i analize geometrijskih odstupanja“, Doktorska disertacija, Fakultet inženjerskih nauka, Univerziteta u Kragujevcu, 2018

[4] http://www.topomatika.rs/ , June, 2019..

[5] http://www.topomatika.rs/ATOS.html, June, 2019.

[6] D. Flack. „CMM measurement strategies“, Measurement Good Practice Guide No.41, ISSN 1368-6550. National Physical Labratory, 2014

[7] https://www.industrija.rs/vesti/clanak/koordinatna-merna-tehnika, June, 2019.

[8] G. Lukacs, J. Lockhart, M. Facello „Non-contact whole-part inspection“, Geomagic, Inc.

[9] F. Zhao, X. Xu, S. Q. Xie „Computer – Aided Inspection Planning – The state of the art“, Computers in Industry 60 (2009) 453-466

[10] D. Lazarević, B. Nedić, Ž. Šarkoćević, I. Čamagić, J. Dedić „Razvoj optičkog sistema za on-machine inspekciju delova dobijenih mašinskom obradom“, Cometa 2018, 4th. International Scientific Conference, 27th-30th november, 2018. Jahorina, Bih Republika Srpska, 203-210

[11] A. Grdić „Moderni trokoordinatni mjerni sustavi“, Fakultet strojarstva i brodogradnje, Sveučilište u Zagrebu, 2019

THE 5th INTERNATIONAL CONFERENCE
MECHANICAL ENGINEERING IN XXI CENTURY

December 9-10, 2020
Faculty of Mechanical Engineering in Niš, Serbia

Engineering Economic Analysis of Abrasive Water Jet Machining Quantitative Characteristics

Mileta JANJIĆ, Ramiz KURBEGOVIĆ, Milan VUKCEVIĆ

University of Montenegro, Faculty of Mechanical Engineering, 81000 Podgorica
mileta@ucg.ac.me, rkurbeg@gmail.com, milanvu@ucg.ac.me

***Abstract*— Abrasive waterjet machining (AWJM) is one of the unconventional manufacturing technologies of recent date. To find a wider application in the industry and to improve its performance, it is necessary to understand the numerous input and output machining parameters and their interaction on the machining. This paper aims to investigate the effect of process parameters such as traverse speed and abrasive flow rate, on the abrasive water jet machining quantitative characteristics – productivity and price. All findings obtained during the investigation indicate that process parameters of the machining influence its quantitative characteristics.**

***Keywords*— Abrasive Water Jet, Engineering economic analysis, Water jet lagging, Quantitative characteristics, Material machining**

I. Introduction

The principles on which the abrasive water jet machining process is based on is erosion. Some authors explain the process of erosion as a kind of abrasive wear, at which abrasive particles and water jet repeatedly impact the surface, resulting in flushing of the material from that surface [1,2].

Several papers are dealing with the formation of cut front geometry and the factors that influence its final appearance. Mostly, the cutting front geometry of the workpiece machined by the abrasive water jet is influenced by machining parameters such as operating pressure, stand-off distance, traverse speed, abrasive flow rate [1,3].

Defining the geometry of the cutting front, is in fact, the determination of the deviation - lagging, Ylag, of the abrasive water jet from the vertical line. The line that defines the lagging of abrasive water jet is described by Zeng, Heines and Kim [4] as a parabola.

The aim of this paper is to analyse the influence of abrasive water jet machining parameters, such as traverse speed, vc, and abrasive mass flow rate, ma, on the quantitative characteristics of the machining – productivity and price. From our previous work [5], we concluded that the variation of operating pressure represents an economically wrong approach.

Analysing and comparing costs represents the basic aspects of engineering practice [6]. Since there are a large number of costs that affect the final price of the abrasive water jet machining, the analysis of the most dominant operating costs like water, electricity, and abrasive material, will be used.

II. Experimental work

To achieve better machining quantitative characteristics, productivity and price, influence of machining parameters such as traverse speed and abrasive flow rate were analysed.

Samples presented by Kurbegovic, Janjic, Vukcevic and Durovic [7], concerning the influence of the water pressure (p), traverse speed (vc), abrasive flow rate (ma) and stand-off distance (x) on the abrasive water jet lagging, were used for creating experimental variants for this work. Samples and its machining parameters are shown in tab. I.

The system used for machining the samples is the product of WJS, model NCX 4020, Sweden. The diameter of the water orifice was 0,254 mm and the abrasive nozzle (focusing tube) diameter was 0,768 mm (ROCTEC 100). The abrasive material was Garnet mesh 80.

The material used for the experiment is high-speed tool steel EN HS6-5-2 (JUS c.7680, AISI M2), produced with the Electro Slag Remelting (ESR) method in a round-shaped ingot, normalized, bandsawed to 42 mm thick discs and lathe cut to 40±0,05 mm. Material is then water jet machined to a 40x40x110±0,05 mm specimens. The side which is water jet machined is milled and flatten to 38±0,05 mm for distinction purposes. The material was cut to a length of 30 mm. Then the flow of abrasives was stopped and then the machine was stopped. After that, the specimens were cut till the end with Wire Electric Discharge Machining. Cutting with Wire Electric Discharge Machining was done to avoid damaging the cut front line and that it could be possible to measure the jet lagging.

Measurements for determining water jet lagging were performed in twenty places (at the same distance) along the sample thickness using an optical microscope.

Measured values of jet lagging for samples shown in table I, are shown in Table II.

TABLE I SAMPLES AND ITS PARAMETERS [7]

Sample 5	
	m_{a1} = 395 g/min p = 413,7 MPa x = 2 mm v_c = 20 mm/min
Sample 11	
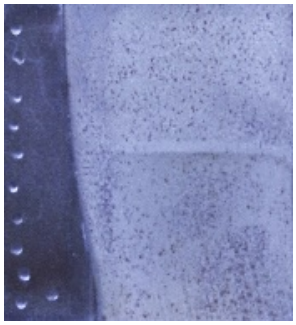	m_a = 395 g/min p = 413,7 MPa x = 2 mm v_{c3} = 30 mm/min
Sample 12	
	m_a = 395 g/min p = 413,7 MPa x = 2 mm v_{c4} = 40 mm/min
Sample 14	
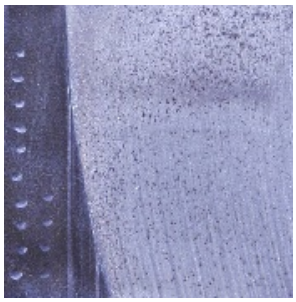	m_{a1} = 166,5 g/min p = 413,7 MPa x = 2 mm v_c = 20 mm/min
Sample 15	
	m_{a2} = 229 g/min p = 413,7 MPa x = 2 mm v_c = 20 mm/min

TABLE III MEASURED VALUES OF JET LAGGING

h	5	11	12	14	Calc.	15
0	0.000	0.000	0.000	0.000	0.000	0.000
2	0.045	0.093	0.093	0.093	0.093	0.093
4	0.091	0.185	0.185	0.185	0.185	0.185
6	0.136	0.278	0.278	0.278	0.278	0.278
8	0.181	0.370	0.370	0.370	0.370	0.370
10	0.226	0.435	0.435	0.472	0.472	0.472
12	0.272	0.523	0.663	0.628	0.628	0.628
14	0.317	0.625	0.893	0.822	0.766	0.746
16	0.362	0.834	1.172	1.083	0.969	0.928
18	0.408	1.044	1.451	1.424	1.175	1.087
20	0.479	1.339	1.841	1.776	1.452	1.336
22	0.533	1.634	2.231	2.129	1.729	1.585
24	0.638	1.963	2.626	2.515	2.016	1.838
26	0.743	2.293	3.021	2.869	2.265	2.049
28	0.849	2.764	3.505	3.248	2.599	2.367
30	0.954	3.234	3.998	3.626	2.933	2.685
32	1.112	3.705	4.472	4.005	3.267	3.003
34	1.270	4.175	4.956	4.384	3.602	3.321
36	1.428	4.618	5.464	4.957	4.118	3.817
38	1.586	5.061	5.971	5.593	4.680	4.353
40	1.745	5.504	6.478	6.107	5.145	4.800

The maximum installed power of the system was Pmax = 49,4 kW. Oil pump is driven by asynchronous motor with a nominal power of 37 kW. Other consumers, with an installed power of POP = 12,4 kW, are: air compressor, water treatment system, abrasive supply system, oil cooling system and CNC (Computer Numerical Control) workstation with automation. The maximum water flow of the system is 3,8 l/min (QA).

Conditions for electricity cost calculation are:

- η_P = 90 % - efficiency of the pump,
- η_{EM} = 93 % - efficiency of the electric motor,
- η_{CM} = 98 % - efficiency of the pipe network,
- η_{MP} = 90 % - efficiency of the intensifier,
- cos φ = 1 - power factor, and
- k = 0,5 - other consumers simultaneity coefficient.

Variant A of this work will be sample 14 from table 1. For getting almost identical values of water jet lagging, as in sample 14, linear interpolation was used on traverse

speeds on samples 11 and 12. The calculated value of traverse speed is vcx = 36,61 mm/min and that will be the Variant B of this work. Both variants and its parameters are presented in Table III.

TABLE IIIII VARIANTS FOR THE ANALYSIS

Variant A	Variant B
m_{a1} = 166,5 g/min p = 413,7 MPa x = 2 mm v_c = 20 mm/min	m_a = 395 g/min p = 413,7 MPa x = 2 mm v_{cx} = 36,61 mm/min

Costs will be analysed for a year of machining, with straight-line machining of 18 m/day, 20 working days/month. Water price will be JCV = 1 € /m3 and the price of abrasive Garnet # 80 will be JCA = 400 € /t. Electricity price will be calculated in accordance with the Price List of Elekroprivreda Crne Gore A.D. Niksic [8] for a basic model consumer with a two tariff meter connected to a 10 kV line, measuring the average 15-minute load, active and reactive power. The usage of electricity is divided evenly for both tariffs.

The needed Power for the pump (and motor) is described with equation (1).

$$P_P = \frac{p \cdot Q_A}{\eta_U} \tag{1}$$

III. RESULTS AND DISCUSSION

According to the given length of machining (lD) and the traverse speeds (vc) we can get daily machining time (tO) for both variants (tO,A and tO,B).

$$t_{O,A} = \frac{l_D}{v_c} = 900\ \frac{min}{day} \tag{2}$$

$$t_{O,B} = \frac{l_D}{v_{cx}} = 491{,}67\ \frac{min}{day} \tag{3}$$

Using the tO, number of working days (NRD), abrasive mass flow rates for variants A (ma1) and B (ma) and unity price of abrasive (JCA), we can calculate abrasive grand total for A (CKAA) i B (CKAB):

$$CK_{AA} = t_{O,A} \cdot N_{RD} \cdot m_{a1} \cdot JC_A \cdot 10^{-6} \cong 14385{,}60\ \frac{€}{year} \tag{4}$$

$$CK_{AB} = t_{O,B} \cdot N_{RD} \cdot m_a \cdot JC_A \cdot 10^{-6} \cong 18644{,}13\ \frac{€}{year} \tag{5}$$

Total price of water consumption for A (CKVA) and B (CKVB) is:

$$CK_{VA} = JC_V \cdot Q_A \cdot t_O \cdot N_{RD} \cdot 10^{-3} \cong 820{,}80\ \frac{€}{god} \tag{6}$$

$$CK_{VB} = JC_V \cdot Q_A \cdot t_O \cdot N_{RD} \cdot 10^{-3} \cong 448{,}40\ \frac{€}{god} \tag{7}$$

From the given conditions for electricity cost calculation, total system efficiency (ηU) is 73,823 %.

The power needed by the abrasive water jet system, for both variants, is:

$$P_U = P_P + k \cdot P_{OP} = 27{,}49\ kW \tag{8}$$

The price of the electricity, for variants A and B, are shown in tabs IV, V and VI.

TABLE IVV MONTHLY PRICE OF THE ELECTRICITY FOR A VARIANT A

Name	Unit	Unity price [€c/kWh]	Consum. [kWh]	Price [€]
Active High	kWh	5.5340	4124	228.22
Active Low	kWh	2.7670	4124	114.11
Engaging	kW	7.3224	27.49	201.29
Losses High	kWh	0.5645	4124	23.28
Losses Low	kWh	0.2822	4124	11.64
Enc.Sus.En.	kWh	0.9439	8248	77.85
			Price w/o VAT (21%)	656.39

TABLE V MONTHLY PRICE OF THE ELECTRICITY FOR A VARIANT B

Name	Unit	Unity price [€c/kWh]	Consum. [kWh]	Price [€]
Active High	kWh	5.5340	2253	124.68
Active Low	kWh	2.7670	2253	62.34
Engaging	kW	7.3224	27.49	201.29
Losses High	kWh	0.5645	2253	12.72
Losses Low	kWh	0.2822	2253	6.36
Enc.Sus.En.	kWh	0.9439	4506	42.53
			Price w/o VAT (21%)	449.92

TABLE V PRICE OF THE ELECTRICITY

Name	Price [€/year]
Price of the electricity for variant A (CK_{EEA})	7876,68
Price of the electricity for variant B (CK_{EEB})	5399,04

The total price of the machining for variants A (CKA) and B (CKB) is:

$$CK_A = CK_{AA} + CK_{EEA} + CK_{VA} = 23083{,}08\ \frac{€}{god} \tag{9}$$

$$CK_B = CK_{AB} + CK_{EEB} + CK_{VB} = 24491{,}57\ \frac{€}{god} \tag{10}$$

The relationship between the total price of the machining for variants A and B is shown in equation 11.

$$\frac{CK_B}{CK_A} = 1{,}061 \tag{11}$$

Calculating the price difference, we can improve the productivity of the variant A for the given difference. Improvement in the abrasive flow of the variant A (ma1') will be:

$$m'_{a1} = \frac{(CK_B - CK_A)}{JC_A \cdot N_{RD} \cdot t_O} \cdot 10^6 + m_{a1} \cong 183 \text{ g/min} \tag{12}$$

For getting almost identical values of water jet lagging for newly abrasive flow rate, linear interpolation was used on samples 14 and 15. Calculated values of Ylag are shown in tab. II.

To get the productivity improvement, linear interpolation was carried on samples 5 and 11 (shown in tab. II) to get traverse speed value. Calculated value of traverse speed is vcy = 28,8 mm/min.

Improvement in productivity of the abrasive water jet system will be:

$$\frac{v_{cy}}{vc} = 1{,}44 \tag{13}$$

IV. Conclusions

The total price of the machining, using parameters from variant B, is 6,1% higher than the total price of the machining using parameters from variant A, with a same jet lagging and quality of the machining.

Machining speed of variant A could be improved to 28,8 mm/min, for the same jet lagging and quality of the machining, and the price as in variant B. Improved productivity of the system will be 44%.

Acknowledgment

This paper presents the results of research conducted on the doctoral research project "Investigation of Abrasive Water Jet Machining Parameters" which is financially supported by the Ministry of Science of Montenegro.

References

[1] A.W. Mombar and R. Kovačević, Principles of abrasive water jet machining, Springer, London, 1998.

[2] D. Arola and M. Ramulu, Mechanism of material removal in abrasive waterjet machining, In: Proceedings of the 7th Water Jet Conference, Washington, pp.46-64, 1993.

[3] M. Hasish, A modeling study of metal cutting with abrasive waterjets, Journal of Engineering Materials and Technology, vol. 106, pp.88-100, 1984.

[4] J. Zeng, R. Heines, and T.J. Kim, Characterization of energy dissipation phenomena in abrasive water jet cutting, In: Proceedings of the 6th American Water Jet Conference, St. Louis, pp.163-177, 1991.

[5] R. Kurbegovic, M. Janjic, and M. Vukcevic, Engineering economic analysis of water, electricity and abrasives costs and their effect on the price of abrasive water jet machining, 1st International Conference on new research and development in technical and natural science, Radenci, Slovenija, pp. 32-36, 2019.

[6] M. Vukčević, Inženjerska ekonomija, Univerzitet Crne Gore - Mašinski fakultet, Podgorica, 2012.

[7] R. Kurbegovic, M. Janjic, M. Vukcevic and D. Durovic, Effect of abrasive water jet machining process parameters on jet lagging, 42. Jupiter conference, Belgrade, Serbia, pp. 3.81-3.87, 2020.

[8] Elektroprivreda Crne Gore A.D. Nikšić. Cijene za snabdijevanje krajnjih kupaca električne energije, from https://www.epcg.com/sites/epcg.com/files/multimedia/main_pages/files/2014/04/cijene_za_snabdijevanje_krajnjih_kupaca_elektricne_energije_01.01.2020-31.12.2020.pdf#overlay-context=media-centar/odluke-o-cijenama-elektricne-energije, visited 01.11.2020.

THE 5th INTERNATIONAL CONFERENCE
MECHANICAL ENGINEERING IN XXI CENTURY

December 9-10, 2020
Faculty of Mechanical Engineering in Niš, Serbia

Decision Support System for Biomaterial Selection

Dušan PETKOVIĆ, Miloš MADIĆ, Goran RADENKOVIĆ

Faculty of Mechanical Engineering, University of Niš, A. Medvedeva 14, Niš, Serbia
dusan.petkovic@masfak.ni.ac.rs, milos.madic@masfak.ni.ac.rs, goran.radenkovic@masfak.ni.ac.rs

***Abstract*— Biomaterials have a great impact on the functionality, durability and especially on the health safety of the implants. Biomaterial selection process is a complex and responsible multi-criteria decision making (MCDM) problem with specific and conflicting objectives. In order to help decision makers in solving this complex task, a decision support system named MCDM Solver is proposed. MCDM Solver is used in decision-making process to rank the biomaterials with respect to several criteria. In this paper, MCDM Solver was used to select hip prosthesis material.**

***Keywords*— Biomaterial selection, multi-criteria decision making (MCDM), MCDM Solver, decision support system, hip prosthesis**

I. Introduction

Selection of the suitable material for an application necessitates the simultaneous consideration of many conflicting and diverse criteria. Knowledge of material properties, cost, design considerations and their influences are mandatory for design and manufacturing of different types of biomechanical components.

Material selection process involves the study of a large number of factors, such as mechanical, chemical, biocompatibility, corrosion, wear and physical properties as well as cost of the materials. Mechanical properties of the materials are given the top priorities, when mechanical design is priority. The most important mechanical properties usually encountered in the material selection process are strength, stiffness, toughness, hardness, density, modulus of elasticity, and creep resistance [1].

The objectives and criteria in the material selection process are often in conflicts which involves certain trade-offs amongst decisive factors. Therefore, only with a systematic and structured mathematical approach the best alternative for a specific engineering product can be selected [2]. The material selection problems with multiple non-commensurable and conflicting criteria can be efficiently solved using multi-criteria decision making (MCDM) methods. The MCDM methods have the capabilities to generate decision rules while considering relative significance of considered criteria upon which the complete ranking of alternatives is determined [3,4].

Biomaterials are commonly characterized as materials used to construct artificial organs, rehabilitation devices, or implants to replace natural body tissues [5]. Selection of an appropriate biomaterial is important from more points of view – medical, technological, and economic.

In last decade, there is a large number of biomedical materials and manufacturing processes, each having its own properties, applications, advantages and limitations. Therefore, many difficult decisions need to be made while selecting a material for a specific biomedical implant [6]. Decision maker should have a complete understanding of the functional requirements of the product and a detailed knowledge of the considered criteria for a specific biomedical application in order to select the most suitable biomedical material. Unsuitable choice of a biomedical material may lead to a premature failure of the product, a need for repeated surgery, a cell death, chronic inflammation or other impairment of tissue functions as well as an extension of healing period and overall increasing of the costs.

Decision support system (DSS) is a special class of information system oriented to the decision-making process and aims to support, mainly business decision-doing processes. DSS is a symbiosis of information systems, application of functional knowledge and ongoing decision-making process [7]. Their main goal, as the goal of other information systems, is to improve the efficiency and effectiveness of an organization.

This paper is focused on the application of developed DSS named MCDM Solver for solving biomaterial selection problem. The most suitable material for femoral component of the hip prosthesis was selected by applying MCDM Solver

II. MCDM Solver

MCDM Solver is an “on-line” DSS which was developed within the doctoral dissertation of Dušan Petković. The developed DSS is located on the “Virtuode” Company web site (https://virtuodeportalapp.azurewebsites.net/WebTools/MCDMSolver) and it is available to everyone who registers by creating an account (Fig 1). This DSS offers the possibility of working with maximization, minimization and target criteria [8].

The input data for *MCDM Solver*:

- Initial matrix of decision-making with target value of criteria (**Step 1**);
- η - Confidence level of decision maker in significance of the selected criteria (where η=1 corresponds to 100% confidence level, while η=0 corresponds to a confidence level of 0);
- Pairwise significance evaluation of the selected criteria.

Fig. 1 MCDM Solver – initial layout

Based on the input data, *MCDM Solver* can determine the values of the criteria weights (**Step 2)** and ranking alternatives (**Step 3)** with the corresponding values by means of Extended TOPSIS [9], Comprehensive VIKOR [10] and Comprehensive WASPAS [8, 11] methods.

Developed DSS architecture is flexible and easy to upgrade, so it enables the inclusion of new models that will come in the future. *MCDM Solver* has a user-friendly interface, which enables a simple and efficient way of entering the necessary data. Its use simplifies the solution of the MCDM problems because it does not require expert knowledge from the decision making theory from the user.

III. Material selection for hip prosthesis

A hip prosthesis comprises three main components, as shown in Fig. 2: (1) femoral component – common called stem or pin, (2) acetabular cup, and (3) acetabular interface – ball with neck [12].

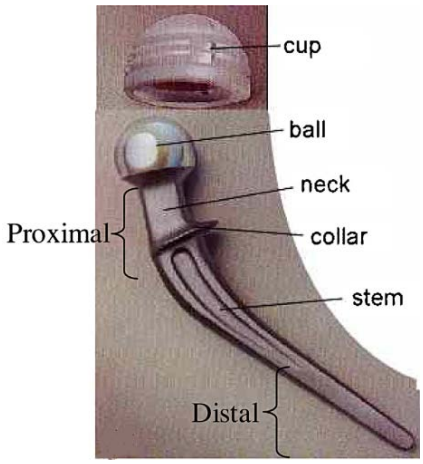

Fig. 2 Hip prosthesis elements

The femoral component is a rigid metal pin which manufactured as a precision machined forging in cobalt chrome or titanium alloy but previously also in stainless steel, with either an integral polished head or separately attached ceramic ball head. This component is implanted into the hollowed out shaft of the femur, replacing the natural femoral head.

The hip socket (acetabulum) is inserted with an acetabular cup; a soft polymer molding (a variety of materials have been used in the past but is now predominantly in polypropylene), which is fixed to the ilium.

The acetabular interface is placed between the femoral component and the acetabular cup and comes in variety of material combinations (metal on polypropylene, ceramic on ceramic, and metal on metal) to reduce wear debris generated by friction [13].

In order to select the most suitable material for femoral component of hip prosthesis, *MCDM Solver* was applied. Before that, it is necessary to create a short list of alternative materials (preselecting) which is given in Table 1. Additionally, determination the most favourable values in all criteria (*Target values* - T_j) should to be done.

The compressive strength of compact bone is about 140 MPa and the elastic modulus is about 14 GPa in the longitudinal direction and about 1/3 of that in the radial direction. These values of strength and modulus for bone are modest compared to most engineering materials. However, live healthy bone is self-healing and has a great resistance to fatigue loading [14].

TABLE I List of potential biomaterials (Alternatives)

Material	Commercial name
M1	SS 316
M2	SS 317
M3	SS 321
M4	SS 347
M5	Co-Cr cast alloy
M6	Co-Cr wrought alloy
M7	Unalloyed Ti
M8	Ti-6Al-4V
M9	Composites Epoxy-70% glass
M10	Composites Epoxy-63% carbon
M11	Composites Epoxy-62% aramid

A. *Alternative materials*

The pin and cup are fixed to the surrounding bone structure by adhesive bone cement and perform different functions. In this example, the material for the pin has been considered whose requirements are tissue tolerance, corrosion resistance, mechanical behaviour, elastic compatibility, weight, and cost. The pin's candidate materials, criteria and objectives (target values of attributes) are listed in Table 2 [15].

B. *Criteria for biomaterial selection*

The considered material property criteria are:

1. Tissue tolerance (C1)
2. Corrosion resistance (C2);
3. Tensile strength (C3);
4. Fatigue strength (C4);
5. Relative toughness (C5);
6. Relative wear resistance (C6);
7. Elastic modulus (C7);
8. Specific gravity (C8);
9. Cost (C9).

Values for C1 and C2 are ordinal data or categorical data where there is a logical ordering to the categories that have been used for description of nonnumeric attributes. C3, C4, C7, and C8 are numeric attributes that represent absolute measure of material properties. Finally, C5, C6, and C9 are ratio values.

TABLE II INITIAL DECISION MATRIX FOR FEMORAL COMPONENT OF HIP PROSTHESIS MATERIAL SELECTION

Material	Criterion								
	C1	**C2**	**C3**	**C4**	**C5**	**C6**	**C7**	**C8**	**C9**
	Tissue tolerance	Corrosion resistance	Tensile strength (MPa)	Fatigue strength (MPa)	Relative toughness	Relative wear resistance	Elastic modulus (GPa)	Specific gravity	Cost
M1	10	7	517	350	8	8	200	8	1
M2	9	7	630	415	10	8.5	200	8	1.1
M3	9	7	610	410	10	8	200	7.9	1.1
M4	9	7	650	430	10	8.4	200	8	1.2
M5	10	9	655	425	2	10	238	8.3	3.7
M6	10	9	896	600	10	10	242	9.1	4
M7	8	10	550	315	7	8	110	4.5	1.7
M8	8	10	985	490	7	8.3	124	4.4	1.9
M9	7	7	680	200	3	7	22	2.1	3
M10	7	7	560	170	3	7.5	56	1.6	10
M11	7	7	430	130	3	7.5	29	1.4	5
T_j	***10***	***10***	***985***	***600***	***10***	***10***	***14***	***2.1***	***1***

IV. RESULTS AND DISCUSSION

Based on the input data, i.e. initial decision matrix, confidence level η=1 and pairwise significance evaluation of the criteria, weights of the criteria are determined (shown in Fig 3).

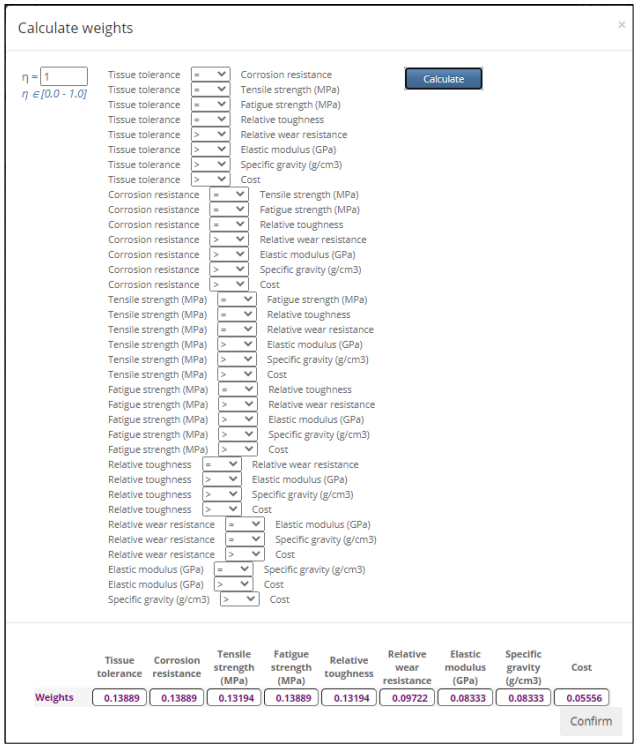

Fig. 3 Pairwise significance evaluation of the criteria

MCDM Solver calculation of the subjective weightings (confidence level η=1) of criteria were carried out based on modified digital logic (MDL) method [16]. This is a pair-wise comparison method, where participants/criteria are presented with a worksheet and asked to compare the importance of two criteria at a time (Fig 3).Thereby tissue tolerance (C1), corrosion resistance (C2), and fatigue strength (C4) are considered as the most influential criteria with weight of 0.1389. Tensile strength (C3) and relative toughness (C5) are the second most influential criteria with weight of 0.1319. The cost is the least influential criterion with weight of 0.0556.

The Step 3 is the ranking of the biomaterials by means of MCDM Solver. Ranking orders of biomaterials for femoral component of the hip prosthesis using different MCDM methods (TOPSIS, WASPAS and VIKOR) are shown in Fig. 4. In order to make ranking results clearer and more readable, they are also shown in Table 3. As could be seen, the first two top ranked biomaterials are M6 and M8 respectively, while the worst ranked materials are M10 and M11.

Moreover, the material M1 (stainless steel 316) is steadily ranked as the eighth one. Ranked results indicate unambiguously that Co-Cr wrought alloy and Ti-6Al-4V alloy are the most preferable materials for the hip stem, while composites epoxy-63% carbon and composites epoxy-62% aramid are the worst ranked biomaterials.

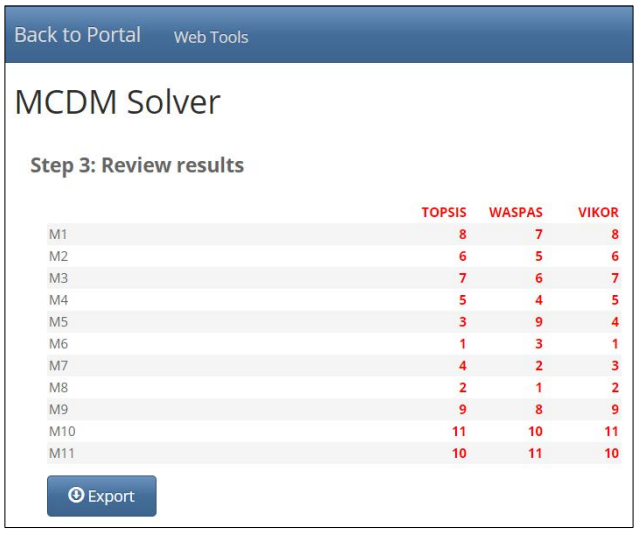

	TOPSIS	WASPAS	VIKOR
M1	8	7	8
M2	6	5	6
M3	7	6	7
M4	5	4	5
M5	3	9	4
M6	1	3	1
M7	4	2	3
M8	2	1	2
M9	9	8	9
M10	11	10	11
M11	10	11	10

Fig. 4 Ranking results

The third ranked materials are M7 (unalloyed Ti) and M5 (Co-Cr cast alloy). M7 has a very good corrosion and biomedical properties, while low fatigue strength is the main its shortcoming. On the other hand, M5 has an excellent corrosion and biomedical properties but a very low relative toughness which is a shortcoming that excludes it from consideration.

TABLE III RANKING RESULTS OBTAINED BY USING MCDM SOLVER

Material	TOPSIS	WASPAS	VIKOR
M1	8	7	8
M2	6	5	6
M3	7	6	7
M4	5	4	5
M5	3	9	4
M6	**1**	**3**	**1**
M7	4	2	3
M8	**2**	**1**	**2**
M9	9	8	9
M10	11	10	11
M11	10	11	10

It is also interesting that there is a total matching of the TOPSIS and VIKOR results for the best (M6 and M8) and worst (M11 and M10) ranked materials.

V. CONCLUSIONS

In this paper, the application of developed DSS named *MCDM Solver* for solving biomaterial selection problem is considered. Thanks to *MCDM Solver*, the material selection process is carried out much faster and easier, because it comes down to selection of potential materials and pairwise significance evaluation of the selected criteria. Hence a complex mathematical apparatus is avoided and ranking process became fast, comfortable to work and reliable.

Ranked results showed that Co-Cr wrought alloy and Ti-6Al-4V alloy are the most preferable biomaterials for the hip stem, while composites epoxy-63% carbon and composites epoxy-62% aramid are the worst ranked biomaterials.

Also, based on the study could be concluded that stainless steels are inferior to both titanium and Co-Cr alloys for this biomedical application.

ACKNOWLEDGMENT

This research was financially supported by the Ministry of Education, Science and Technological Development of the Republic of Serbia.

REFERENCES

[1] P. Chatterjee et al., “Selection of materials using compromise ranking and outranking methods,” Materials and Design, vol. 30, 2009, pp. 4043–4053.

[2] D. Petković et al., “Decision Support System for Selection of the Most Suitable Biomedical Material,” ICIST 2015 Proceedings, pp, 28-31, Kopaonik 2015.

[3] P. Chatterjee and S.Chakraborty; “Material selection using preferential ranking methods”, Materials and Design, Vol. 35, 2012, pp. 384-393.

[4] D. Petković, M. Madić, G. Radenković, “Gear material selection using WASPAS method”, SMAT 2014 Proceedings, pp. 45-48, Craiova, Romania 2014

[5] D. Petković, G. Radenković, M. Mitković, “Fractographic investigation of failure in stainless steel orthopedic plates,” Facta Universitatis: Series Mechanical engineering, Vol. 10, 2012, pp. 7–14.

[6] D. Petković, M. Madić, G. Radenković, “Application of Extended TOPSIS Method for Biomaterial Selection”, MASING 2018 Proceedings, pp. 353-356, Niš 2018.

[7] M. Čupić, R. Tummala, M. Suknović, Odlučivanje - formalni pristup, Fakultet organizacionih nauka, Beograd, 2001.

[8] D. Petković, “Selection of biomaterials - Multi-criteria decision analysis and development of decision support system”, PhD dissertation, University of Niš, Faculty of Mechanical Engineering, Niš 2017.

[9] A. Jahan, M. Bahraminasab, K.L. Edwards, “A target-based normalization technique for materials selection”, Materials and Design, Vol. 35, 2012, pp. 647-654.

[10] A. Jahan, F. Mustapha, M.Y. Ismail, S.M. Sapuan, M. Bahraminasab, “A comprehensive VIKOR method for material selection”, Materials and Design, Vol. 32, 2011, pp. 1215-1221.

[11] D. Petković, M. Madić, G. Radenković, “Ranking of Biomedical Materials by Using Comprehensive WASPAS Method”, MASING 2015 Proceedings, pp. 339-344, Niš, 2015.

[12] Chen Q., Thouas G.A., „Metallic implant biomaterials“, Materials Science and Engineering R, Vol. 87, pp 1–57, 2015.

[13] A. Jahan, et al., “A comprehensive VIKOR method for material selection”, Materials and Design, Vol. 32, 2011, pp. 1215–1221.

[14] G. Radenković, D. Petković, “Metallic Biomaterials”. In: Zivic F., Affatato S., Trajanovic M., Schnabelrauch M., Grujovic N., Choy K. (Eds.) Biomaterials in Clinical Practice. Springer, Cham, 2018.

[15] A. Jahan and K. L. Edwards, Multi-criteria Decision Analysis for Supporting the Selection of Engineering Materials in Product Design, Butterworth-Heinemann, 2013.

[16] B. Dehghan-Manshadi, H. Mahmudi, A. Abedian, R. Mahmudi, “A novel method for materials selection in mechanical design: combination of non-linear normalization and a modified digital logic method.” Materials & Design, vol. 28, 2007, pp. 8-15.

THE 5th INTERNATIONAL CONFERENCE
MECHANICAL ENGINEERING IN XXI CENTURY

December 9-10, 2020
Faculty of Mechanical Engineering in Niš, Serbia

A Review of Cutting Fluids in Manufacturing Engineering and Environmental Impact

Milica BARAĆ, Nikola VITKOVIĆ, Miodrag MANIĆ, Marko PERIĆ

Faculty of Mechanical Engineering, University of Niš, Aleksandra Medvedeva 14, 18106 Niš
milica.barac@masfak.ni.ac.rs, nikola.vitkovic@masfak.ni.ac.rs, miodrag.manic@masfak.ni.ac.rs, marko.peric@masfak.ni.ac.rs

***Abstract*— Metalworking process is a major polluter of the environment due to cutting fluids in no small part. While on one hand cutting fluids have positive effects on tool life, surface quality and productivity, on the other hand they cause harmful effects on the environment and human health. In order to reduce the negative impacts, it is necessary to use more environmentally friendly cutting fluids, as well as reduce the use and losses of cutting fluids. In this paper, attention is focused on a review of cutting fluids and their characteristics as well as a review of the negative impacts of cutting fluids on the environment, human health and the economy.**

***Keywords*— Cutting fluids (CF), Manufacturing engineering, Environmental, Coolants, Lubricants**

I. Introduction

Coolants and lubricants are important components of the cutting process. By focusing on processes, there is a need to achieve optimized technological improvements and process planning in order to reduce energy and resource consumption, as well as reduce toxic emissions and waste and achieve cleaner and sustainable production [1]. Organized and regulated management of cutting fluids (CF) is one of the starting points for the establishment of a quality system and ensuring the humane aspect of quality aimed at protecting the environment. Worrying data is that world consumption is about 2.2 billion liters of CF, of which 54% is used during the cutting processes. The Americas is the leading region in terms of consumption with a total share of 36%, followed by Asia with a share of 30%, as shown in Fig. 1 [2].

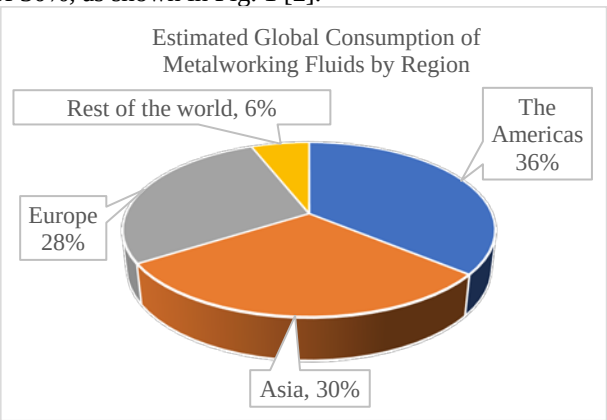

Fig. 1 Global CF consumption by region [2]

Therefore, the machine industry is a serious consumer of energy and an environmental polluter [3]. Due to worrying data such as this, as well as the fact that large quantities of CF are inadequately treated and disposed of, the EU has adopted a regulation covering all types of CF used in production and rules ranging from their application to adequate treatment and disposal [4].

Although coolants and lubricants are known to improve tool life and surface quality, they have detrimental effects on human health as well as the environment, due to the presence of potentially harmful chemicals. Global demand for CF was 39.4 million tons in 2015, and it is expected to reach 43.9 million tons in 2022 [5]. Therefore, it is not enough just to satisfy the regulations and limit values for the use of CF, but to go towards their maximum possible reduction in order to achieve cleaner production. Also, care should be taken with the choice of the type of CF and alternative methods of application, in order to achieve zero (or at least reduced) toxicity and pollution levels [1]. This approach to the use of CF is another trend of sustainability in the metalworking industry and due to high environmental pollution is becoming one of the most important goals of all manufacturers [6].

In order to eliminate the impact on the environment by minimizing the use of CF, without a significant impact on energy consumption, the process must be analyzed and the process parameters must be optimized.

The main tasks of CF are cooling, lubrication and chip removal.

The secondary tasks of CF are corrosion protection, protection of tools through extension of tool life, cleaning of tools and workpieces, increase of productivity, better surface quality. The biggest problems in the application of CF are inappropriate use, excessive quantities, inadequate type in relation to the requirements of the metalworking process and the use of degraded CF. Depending on the machining process and the material being machined, as well as the material from which the tool is made, the appropriate CF is selected depending on the required characteristics.

When choosing coolants and lubricants, the optimal choice should be sought, taking into account all necessary factors such as: types and shape of tools, condition of tools used, conditions of machine tool, specific conditions

of machining mode (cutting speed, depth of cut, chip cross section, treated surface quality).

The choice of type, concentration and type of additive therefore depends on the type of metalworking, tool material and workpiece as shown in Fig. 2.

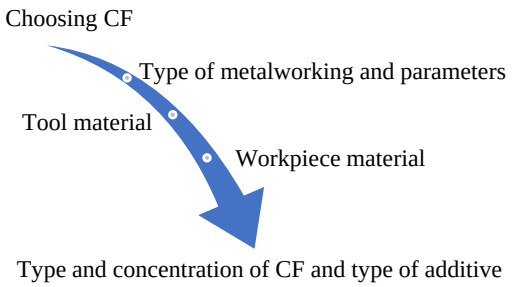

Fig. 2 Choice of CF

II. Division and Characteristics of CF

CF can be roughly divided into:

- Pure cutting oils which are more used in operations that primarily require lubrication (at low speeds where the increase in temperature is not significant, and there are high resistances to cutting). To promote heat dissipation oils of lower viscosity are used.
- Emulsions consisting of oil, water and an emulsifier that keeps the oil in fine droplets in water. They are used in operations that primarily require cooling (at high cutting speeds where lower cutting resistances occur, but there is a significant increase in temperature).

Pure cutting oils can be mineral, vegetable, animal, synthetic or mixtures of these oils. The main physico-chemical characteristics required of pure cutting oils are: viscosity, ignition point in open and closed vessel, saponification number, total sulfur content, corrosion of copper strip, chlorine content, foaming, extreme pressure (EP), anti-wear properties, protection from rust, the appearance of oil mist, compatibility with paints and synthetic materials.

Biodegradable oils as more environmentally friendly oils are a good alternative to mineral oils and find various applications in metalworking operations by cutting various types of metals such as aluminium, titanium and others. This conclusion was reached on the basis of the application of the experimental Taguchi method by testing newly developed plant - based emulsions in the process of scraping AISI 304L material [7].

Pure cutting oils can be inactive and active. Inactive cutting oils do not have a corrosive effect on non-ferrous metals and their alloys, because they contain additives based on sulfur, phosphorus and chlorine in inactive form. Due to their characteristics, as recommended by the machine tool manufacturer, they can be used for lubrication of the machine itself and for filling the hydraulic systems of the machine, which is why they are called three-purpose oils. On the other hand, active cutting oils contain additives in active form that react chemically at lower temperatures and as such adversely affect non-ferrous metals. Therefore, they are used in the metalworking of steels and their alloys, where their pronounced activity gives good results.

The main physico-chemical characteristics required of water-soluble and emulsion fluids for metalworking process are: corrosion protection, foaming, emulsion stability, compatibility with metals and lubricating oils, paints and sealants, pH value of fresh and used mixtures, extreme pressure (EP), anti - wear properties, saponification number.

In order to achieve the required physico-chemical characteristics, if necessary, additives that serve to improve or add the functional properties of the basic substances that are needed can be added to oils and emulsions.

Additives include corrosion inhibitors (nitrites, amines, amides), antifoams (zinc diacyclophosphates, siloxanes), stabilizers (alcohols), extreme pressure additives (EP additives), surfactants and emulsifiers (sulfonates), additives for prolongation of tool life and bactericides (nitrogen compounds, heterocyclic sulfur) [8]. It is not uncommon for CF to contain small amounts of various heavy metals. Some additives are legally forbidden to use, due to their negative properties, such as chloroparaffins, and there are also recommendations not to use chlorine-containing additives.

The presence of water affects the stability of emulsions and the corrosive properties of CF, therefore they are considered more complicated in composition than pure cutting oils. However, the use of these agents is widespread due to the properties they have in processes that primarily require cooling and chip removal.

The basic division has been made according to the content of mineral oil, i.e. synthetic components in the following way:

- Products with more than 60% mineral oil in addition to mineral oil contain emulsifiers, bactericides, and may also contain EP additives. Their properties largely depend on the composition of the water, and they are used in concentrations of 3 to 10%. They are known as drilling oils.
- Semi-synthetic liquids are products with less than 60% mineral oil. They differ from the first group in the lower content of mineral oil (usually 30-60%) and the higher content of emulsifiers. Emulsifiers usually have a synthetic base, which is why they are called semi-synthetic products. As emulsifiers are usually a good substrate and food for the development of microorganisms, biostable synthetic emulsifiers have been developed that prevent the development of microorganisms. In this way, semi-synthetic biostable products stable to microbiological degradation have been developed, which enables long-term use without the need for the addition of bactericides. EP additives can also be added and they can be used for difficult metalworking operations. They are transparent in appearance and are most often used in concentrations of 3 to 5%.
- Products based on synthetic raw materials without mineral oil content are organic and inorganic chemical compounds, with added additives to reduce the surface tension of water, corrosion inhibitors, if necessary, and EP additives. They have a number of advantages in terms of increasing the cooling and lubricating effect, so that the quality of the treated surface is high. They are transparent in appearance and have a very long-lasting use.

- Products based on soluble inorganic and organic salts and alcohols (without mineral oil) are used mainly in grinding processes, where lubrication is not of great importance. These are transparent aqueous solutions that can usually contain polar additives. They meet the requirements of cooling, rinsing and corrosion protection.

Just as there are wet CF such as vegetable oil or mineral dissolved in water, there are also solid CF such as graphite and boric acid [9].

III. Impacts of Cutting Fluids on the Environment, Health and Economy

A. *Environmental Impact*

When using CF, their degradation occurs, which is caused by various causes, such as the development of microorganisms, chemical imbalance, the appearance of metal particles or mixing with some other foreign oil. It is important to prevent and minimize the degradation of CF through proper maintenance, adequate cleaning of machines and the entire plant. Actions to prevent oil degradation contribute to their longer use and reuse, which has a beneficial impact on the environment. It also prevents the occurrence of negative consequences of using degraded oil, such as increased friction, poor and inaccurate metalworking, corrosion, unpleasant odours, tool wear, sticking, seemingly increased concentration, precipitation, clogging and more.

Depending on the metalworking, the choice of CF that is most often used differs. Milling for light working conditions requires semi-synthetic emulsion and synthetic water-soluble agents with a higher content of EP additives, while for more difficult working conditions pure cutting oil with a high content of EP additives is used [10].

Most of the heat generated during turning is dissipated through chip removal, but in order to reduce friction, good lubrication must be provided. Therefore, emulsion and water-soluble agents with improved lubricating properties are most often used in this type of treatment. In CNC lathes, due to the danger of mixing CF with other oils (hydraulic, sliding tracks), pure inactive cutting oils are used, which have a dual use, as CF and for general lubrication of the machine. When high-strength materials are processed on lathes, CF with increased cooling effect are mainly used, due to high temperatures that occur in the cutting zone [11].

A big problem is the loss of CF from the production system. Fig. 3 shows the ways in which CF is lost from the production system, with the indicated average percentages of losses [12].

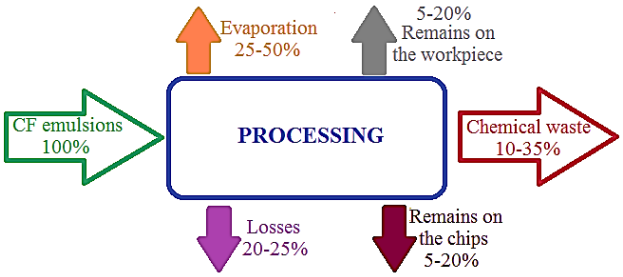

Fig. 3 CF losses [12]

High temperatures in the cutting zone lead to CF evaporation, so it is necessary to carefully choose which one will be used depending on the material being processed and the temperatures that occur in the cutting zone. The property of CF which should be kept in mind in this case is the evaporation point, in order to prevent harmful vapors that negatively affect both the environment and the machine operator.

The problem is also the losses caused by leakage, spraying or spillage in various stages of metalworking, which in addition to the negative impact on the environment is also potentially dangerous for the machine operator and has a negative impact on the hydraulic system. This type of waste should never be discharged into watercourses and sewage system, before the necessary treatment, which mainly includes the separation of mechanical impurities, separation into water and oil phase and destruction of microorganisms in adequate treatment plants. CF decomposition procedures are: incineration, filtration, distillation, flotation, centrifugation and electrolysis [13].

Fig. 4 shows the actions aimed at achieving clean production. From the aspect of cleaner production, it is necessary to minimize the use of CF used in cutting processes. When use in the process is minimized, the second task is to minimize losses as well as the impacts of CF. Finally, it is necessary to adequately collect and treat waste generated by the use of CF.

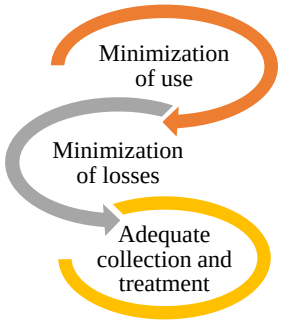

Fig. 4 Actions aimed at achieving clean production

Given that CF is one of the most complex types of waste for containing large amounts of potentially hazardous materials, there are issues with disposal of it, whether it is recycling or treatment before adequate disposal [14].

B. *Impact on Human Health*

In addition to the negative effects on the environment, handling CF also poses a risk to the health of the machine operator. The use of CF can be considered responsible for a large number of occupational diseases. Contact can be made directly through the original liquid, mist, vapor or by-products generated during the metalworking process [15]. Accordingly, it is important to reduce this risk by adequate selection and moderate use of CF, using less harmful additives and more environmentally friendly types of CF. That is, it is necessary to minimize the use and optimize the selection of CF with minimal amount of dangerous characteristics that can cause harmful effects on human health. CF in some cases causes lung cancer, asthma and genetic disorders. Adverse effects that may occur may be, for example, toxicity (formaldehyde, some biocides) and formation of carcinogenic substances (chlorinated paraffins, aromatic amines). Evaporation and inhalation of hazardous substances is very dangerous, as

well as their contact with the skin which can cause various skin diseases [16]-[17].

The ways through which CF can enter the human body are dermally (through the skin), by inhalation (breathing in), orally (through swallowing) or through wounds (cuts, scratches).

In addition to the experimentally confirmed negative effects that CF can cause with its content, there are also those that have been insufficiently investigated and those that occur by degradation. That is why it is important not only to choose carefully, but also not to use degraded CF. In addition to the hazardous properties, toxicity and carcinogenicity, the explosiveness and flammability of CF should be taken into consideration, as well as the oxidizing and irritating properties they may cause. The fact that 1.2 million workers are exposed to the influence of CF annually, is a sufficient data on how important it is to keep in mind all the negative impacts and act to minimize them.

Due to all the negative effects on human health (cancerous and non-cancerous diseases) confirmed so far, caused by the use of CF, there are certain norms, rules and provisions related to business, marginal exposure, handling and use. From a humane point of view, it is not only necessary to follow the rules and norms, but to go further in the direction of preserving health and the environment as much as possible.

C. Economic Consequences

In addition to all the negative effects on health and the environment, a big problem are the costs associated with the use of CF, which take a serious share in the overall cost of production, on average up to 17%, which is not a negligible percentage. It is important to note that of this part, only 6% relates to price, and the remaining 94% are costs related to the use of CF. The conclusion is that minimization, as well as the proper use of CF, can save a significant amount of money allocated for these purposes, which is very important for companies that are hesitant to turn to clean production.

IV. Conclusions

Cutting processes are accompanied by various types of negative effects. Large part of negative effects are due to the use of CF, thus it is necessary to know their characteristics and processes where they are applied, in order to reduce their use.

Modern demand for sustainable production encourages the use of more eco-friendly CF, such as fluids with less harmful additives, biodegradable oils, as well as plant-based oils. In accordance with the need to achieve cleaner production, it is necessary to analyze and optimize process parameters in order to minimize the use of CF. It is important to prevent the degradation and use of degraded CF, as well as losses that occur during the cutting process, which are dangerous to the health of the machine operator. The possible negative effects when CF are used are reflected in the appearance of unpleasant odors and vapors, discoloration and stability, corrosion of elements of the technological system, foaming, infections, allergies and other harmful effects.

The basic way to achieve cleaner production and reduce the harmful effects on the environment arising from the use of CF is in the first place raising the awareness about the issue. Reduction in level of pollution, human health and harmful effects on the environment is achieved by adequate selection of CF (type, concentration, etc.), quality preparation of CF, constant control, minimizing the use of CF and ultimately adequate collection, treatment and disposal.

Finally, an additional incentive for companies to turn to cleaner production, in terms of environmental and humane aspects, is the reduction of material costs associated with the use of CF which amounts to a significant share of total production costs.

Acknowledgment

This research was financially supported by the Ministry of Education, Science and Technological Development of the Republic of Serbia.

References

[1] G. Loglisci, P.C. Priarone, and L. Settineri, "Cutting tool manufacturing: a sustainability perspective", 2013.

[2] T.F. Glenn, "Opportunities and market trends in metalworking fluids", Tribology & Lubrication Technology, vol.54, pp.31, 1998.

[3] S. Dambhare, S. Deshmukh, A. Borade, A. Digalwar, and M. Phate, “Sustainability issues in turning process: A study in Indian machining Industry”, Procedia CIRP, vol.26, pp.379-384, 2015.

[4] European Comission: “EU REACH Directive”, Environment Directorate General, 2006/121/EC, 2006.

[5] E. Benedicto, D. Carou, and E.M. Rubio, "Technical, economic and environmental review of the lubrication/cooling systems used in machining processes", Procedia engineering, vol.184, pp.99-116, 2017.

[6] P. Sheng, M. Srinivasan, and S. Kobayashi, "Multi-objective process planning in environmentally conscious manufacturing: a feature-based approach", CIRP annals, vol.44, pp.433-437, 1995.

[7] M.H. Cetin, B. Ozcelik, E. Kuram, and E. Demirbas, “Evaluation of vegetable based cutting fluids with extreme pressure and cutting parameters in turning of AISI 304L by Taguchi method”, Journal of Cleaner Production, vol.19, pp.2049-2056, 2011.

[8] H. Bergmann, A. Rittel, T. Iourtchouk, K. Schoeps, and K. Bouzek, “Electrochemical treatment of cooling lubricants”, Chemical Engineering and Processing: Process Intensification, vol.42, pp.105-119, 2003.

[9] R. Sharma, V. Bansal, and N. Chhabra, "Effect of Cutting Parameter on Hard Turning by using Different Lubricating Conditions: A Review", International Journal of Engineering Trends and Technology (IJETT), vol.30, pp.75-82, 2015.

[10] S. Kalpakjian, S.R. Schmid, and H. Musa, Manufacturing Engineering and Technology, 7th Edition. Prentice Hall, 2013.

[11] https://www.nisotec.eu/sr-lat/fluidi-za-obradu-metala-shp 20.10.2020.

[12] V.P. Astakhov, Tribology of metal cutting, Elsevier, 2006.

[13] B. Nedić, and M. Lazić, "Proizvodne tehnologije - Obrada metala rezanjem", Mašinski fakultet, Kragujevac, 2007.

[14] P.M. Chazal, "Pollution of modern metalworking fluids containing biocides by pathogenic bacteria in France", European journal of epidemiology, vol.11, pp.1-7, 1995.

[15] M. Monteiro, “Negative aspects of the cutting fluid application in metal-working process for the environment and workers’ health”, 2005.

[16] S. Ueno, Y. Shiomi, and K. Yokota, "Metalworking fluid hand dermatitis", Industrial health, vol.40, pp.291-293, 2002.

[17] P. Kumar, S. Jafri, P. Bharti, and M. Siddiqui, “Study of Hazards Related to Cutting Fluids and Their Remedies”, International Journal of Engineering Research & Technology (IJERT), vol.3, 2014.

THE 5th INTERNATIONAL CONFERENCE
MECHANICAL ENGINEERING IN XXI CENTURY

December 9-10, 2020
Faculty of Mechanical Engineering in Niš, Serbia

Overview of Software for Simulation and Verification of G-code for CNC machine

Rajko TURUDIJA, Miodrag MANIĆ, Miloš STOJKOVIĆ,

University of Niš, Faculty of Mechanical Engineering, A. Medvedeva 14, Niš, Serbia
miodrag.manić@masfak.ni.ac.rs, milos.stojkovic@masfak.ni.ac.rs, turudija.rajko8@gmail.com

***Abstract*— All companies want to be as efficient as possible. Engineers of companies that use CNC machines in their production spend a lot of time programming, and as a result provide G-codes. These codes are rarely checked before insertion into CNC machine, which can lead to collisions that causes financial damages. To avoid such damages it is recommended to use G-code simulation and verification software. These software check G-code before inserting it into the machine. In addition, these software provide features that can speed up the cutting process itself, such as cutting optimization, tool path optimization, tool life maximization etc. This paper presents a brief overview of some G-code simulation and verification software, with the aim of helping companies which production is based on use of CNC machines, mainly milling and lathe machines.**

***Keywords* — G-code; CNC; Simulation; Verification; CAM.**

I. INTRODUCTION

CNC machines have become an indispensable part of every manufacturing company. Quality CNC machines that can satisfy all that production needs cost tens of thousands of euros, so their failures must be avoided in every possible way. In addition, their work is expensive, so it is necessary to use the work of these machines efficiently in order to maximize the possible profits. Traditionally, checking the G-code (instruction list which tells the machine what to do) is done with the process popularly called “cutting air”. This process is based on running the program above the work piece, so the tool doesn’t come in contact with the material, until the programmer is sure that the program is working properly. Problem with this method is that it is very time consuming, and it ties up the CNC machine so it can’t be used for anything else. Also, it is not very accurate. Other way of proofing the G-code is by prior machining on a model made of foam, wood, resin, etc., often with reduced cutting speeds. This is a better way of validating the program, because it provides a real model that was produced by the G-code. This model can’t be used as a selling product because of the material it is made from, but it can be used in purpose of measuring the geometry and checking the tolerances. Even though this method is better than cutting air method, it also consumes lot of time and it ties up the machine so it can’t be used for processes that will bring profit. Also, often it is needed for the operator to oversee the whole cutting process, so that he can stop the improper operation of the machine, before it comes to breakage of the equipment.

The best way for proofing G-code is by using software for simulation and verification of G-code, which are specially designed for this purpose. They check the syntax of G-code, path of the cutting tool during the cutting process, feeds, speeds, tolerances, etc. Programs are being checked block by block, so when error occurs, its location can be found easily. These software have machine and tool simulations that provide visual confirmation that the program works properly. To provide arguments for formally justifying the adoption of software for G-code simulation and verification, we shall take a look at some situations in which the use of this software is recommended to avoid unnecessary costs.

- frequent programming activities – the more times programming new programs or editing old ones is being done, the greater the time and cost savings by using G-code simulation and verification software are;
- breakage – the breakage of equipment or machines generates the cost of repairs, but also is a source of risk for operators that work around the machine. Additionally, the downtime of repairs can be very long, and it can be avoided with G-code simulation and verification software;
- scrap – cost of producing scraps from stock material must be taken into account while assessing if the use of G-code simulation and verification software is justified. In some cases, the part can be repaired, but that repair evokes additional costs;
- reworking – time needed and cost needed to rework the existing part or the scraped stock material;
- disruption of manufacturing process – when a problem occurs during a machine operation, it can disrupt the whole manufacturing process. This disruption caused by things going out of sync in the work schedule can generate significant knock-on costs that are not always easy to identify and assess;
- dismantling and refitting – programs that need long modifications cause users to stop production and move on to some other manufacturing task, until the program has been modified. This evokes additional cost of removing the unfinished part and refitting a new part for machining, which can be

significantly high if complex assemblies are involved.

In addition to all the cost savings, stress experienced by programmers and operators while proofing a new machining program should be mentioned, as it is a significant factor in the quality of their work, as well as factor in their happiness and satisfaction at their work environment. This stress can be significantly reduced with use of these software.

II. G-CODE

Numerical control is a form of automatic control of the machine in which the process is controlled by instruction list (program), formed from numbers and letters. Most widely used type of program for numerical control is the G-code. G-code contains all the information needed so the machine can finish the needed process. Blocks are main elements that the G-code is made from, and blocks are made from words. Words in G-code have their function addresses that are marked using letters, and numerical values [1] (Fig. 1).

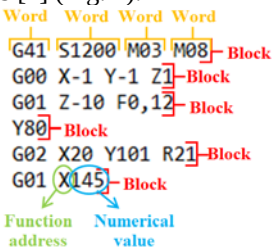

Fig. 1 G-code structure

Commonly, one G-code program is made from many individual blocks, and blocks are made from one or more words. Together they form an instruction list that tells the machine what tool to use, where to move it, at what speed, with what feed, etc. G-code got its name from function address G that is most often used. This function gives information to the machine about how to move tools, but it is not the only function used in G-code. Other commonly used function addresses can be seen in table 1 [1].

TABLE 1 COMMONLY USED FUNCTION ADDRESSES IN G-CODE [1]

Commonly used function addresses	Meaning
N	Ordinal number of blocks
X, Y, Z	Coordinate points on the adopted main axes
I, J, K	Auxiliary parameters for circular interpolation
S	Function address for defining the spindle speed
F	Function address for defining a value of auxiliary motion
T	Function address for defining the ordinal number of the tool
M	Function address that defines auxiliary functions (for example, M06 – tool change, M30 – end of program, etc.)

G-code can be obtained in one of three ways:

1. Manual programming - this is the slowest way of programming. Programmer is required to know all the information related to the machine, tools, materials, parameters, etc., and is required to write all words and blocks of the G-code manually, which greatly complicates the programming process;
2. Programming using machine control unites - faster than the previous way of programming, because programming is being done with help of a keyboard, using specially developed menus that facilitate the work of the programmer. It is not needed from the programmer to manually write all the blocks and words of the G-code;
3. Computer programming – programmer creates a program on the computer software and then inserts it into machine. This way of programming gives much faster program creation, because it does not need the programmer to write all blocks and words, computer software does that for him. Programmer uses specially developed options in computer software and graphic display of the processing part, tools, machine, movements etc., to facilitate his work.

From those three ways of obtaining the G-code, computer programming is the best, and software that allows this are the main part of computer aided manufacturing (CAM) system. Any manufacturing company that wants to be competitive in the market place needs to have CAM as a part of their manufacturing process. Integrated within every CAM software is a postprocessor that translates the information obtained within the CAM software into a language that the machine can interpret, G-code. Machine has to have a control unite that will decrypt the G-code and send the appropriate commands to the output devices. Problem with this system is that the G-code obtained using the postprocessor is not checked anywhere. Most good CAM software contains simulators, but they do not check the G-code that is inserted into the machine, but the errors that occur during the time that programmer is working in the software. Those simulators are very useful because they speed up the programming process, display collisions in virtual environment, provide information about processing times, as well as much other useful information related to the virtual environment, but they do not guarantee that the G-code obtained after the postprocessor will not cause problems in the real environment. To ensure the correct operation of the machine controlled by G-code it is recommended to use G-code simulation and verification software, before inserting the G-code into the machine itself [1].

III. SIMULATION AND VERIFICATION SOFTWARE

As stated in previous chapter, CAM software has simulators integrated within them, but they do not simulate G-code that was obtained after the postprocessor, they just help the programmer with process visualization. To be sure that the G-code which is inserted in the machine is exactly what the programmer wanted, G-code has to be checked with G-code simulation and verification software. There is a difference between the simulation and the verification G-code software. Namely

simulators are simpler versions of software that contain features such as:

- visual representation of tool movement (tool paths shown by lines of different colours);
- graphical representation of tools, machines, cutting process;
- error display signals;
- calculation and display of processing times;
- since each manufacturer of CNC machines uses its own version of the G-code, a good simulator must know a large number of different versions of the G-code;
- each simulator must have options for viewing G-code, possibility to select any word within the G-code, as well as option for editing it;
- well organized interface, etc.

On the other hand, as already mentioned, verification software are more advanced versions of simulation software. In addition to having all the characteristics of a simulator, verification software should also have options such as tolerance check, cutting parameter optimisation, etc. Even though there is a difference between simulation and verification software, it is difficult to make an exact distinction between them, since many manufacturers of G-code verification software call their software simulators, and vice versa. For the sake of simplifying this problem, for the purpose of this paper, G-code simulation, and G-code verification software will be considered the same and will be processed together, since their purpose is the same, to check the G-code and prevent possible failures, machine and tool breaks and other errors during the operation of the CNC machine [1].

The number of G-code verification and simulation software is not too large, but certainly not small enough for all software to be tested in a relatively normal period of time. If we add here the prices of most non-free software, the process of trying out all the software is not cost-effective at all. In order to help companies that use CNC machines in their manufacturing processes, some G-code simulation and verification software will be shown hereinafter, as well as a comparative test between these software in form of a table with some important features that make G-code simulation and verification software competitive in the market place. But first let us divide G-code simulation and verification software in 3 categories [1]:

- web G-code simulation and verification software;
- integrated G-code simulation and verification software;
- standalone G-code simulation and verification software.

Web G-code simulation and verification software are software that are accessed using an internet browser. The biggest advantage of such software is that they are free and that they do not need to be installed on a computer. On the other hand, these software are very simple, and are only used for simple representation of tool paths. Integrated G-code simulation and verification software are a part of some bigger CAM/CAD software, and can't be installed separately. This gives the programmer an easy transition from one program module to another, and thus speeds up and facilitates the work. Standalone G-code simulation and verification software run independently on computers, and are not a part of any other software packages. Usually such software has the largest number of options since the software manufacturer has focused exclusively on producing the best possible software for G-code simulation and verification, but this also entails an increased price of the software [1].

IV. Comparative Test of G-code Simulation and Verification Software

After explaining what G-code is, what G-code simulation and verification software are and what categories of these software exist, we need to select a number of software from each category and compare them. Software that were selected are:

- NCViewer
- G-Cide Q'n'dirty toolpath simulator;
- NX CAM IS&V
- CAMWorks Virtual Machine
- Vericut
- CAMotics
- NCSimul
- CNC Simulator Pro
- Eureka Virtual Machine;
- G-Wizard Editor.

First two are web based software, second two are integrated software, and the last six are standalone software. Comparative test of these software will be performed using selected features and properties, which are considered essential for every good G-code simulation and verification software to possess, and seeing what software has them. If the software has the appropriate feature it will be indicated by a "+" sign, and if it does not, it will be indicated by "–" sing. If additional explanations of certain program features are required, the "+" and "–" sign will be marked in red, and explanations will be given in the text after the table. If information about some feature was not found it will be indicated with "/" sign. Features and properties that were selected are:

- price (it is difficult to know exact price of the software because it depends on many factors);
- does the software support different G-code dialects;
- graphical representation of machines in software;
- graphical representation of tools in software;
- graphical representation of a stock;
- graphical representation of tool change in software;
- graphical representation of tool path in software;
- graphical representation of cutting process in real time;
- collision detection;
- ability to add, modify, create tools;
- library of machines;
- ability to add more machines;
- library of tools;
- options for efficient reviewing of the G-code;
- options for efficient modifying the G-code directly in the program;
- cutting parameters optimisation;
- cross-section view;
- option for verification of tolerance;

TABLE 2 COMPARATIVE TEST OF G-CODE SIMULATION AND VERIFICATION SOFTWARE

	NCViewer [2]	G-Cide Q' n' dirt y toolpath [3] simulator	NX CAM IS&V [4]	CAMWorks Virtual Machine [6]	Vericut [8]	CAMotics [9]	NCSimul [10]	CNC Simulator Pro [11]	Eureka Virtual Machining [13]	G-Wizard Editor [14]
price	free	free	5900$ - 30000$ [5]	>10000 $ [7]	/	free	/	free/99$ per year for Platinum [12]	/	60-300 [15]
does the software support different G-code dialects	+	-	+	+	+	-	+	+	+	+
graphical representation of machines in software	-	-	+	+	+	+	+	+	+	-
graphical representation of tools in software	+	-	+	+	+	+	+	+	+	+
graphical representation of a stock	-	-	+	+	+	+	+	+	+	-
graphical representation of tool change in software	-	-	+	+	+	-	+	-	+	-
graphical representation of tool path in software	+	+	+	+	+	+	+	+	+	+
graphical representation of cutting process in real time	-	-	+	+	+	-	+	+	+	-
collision detection	-	-	+	+	+	-	+	+	+	-
ability to add, modify, create tools	-	-	+	+	+	+	+	+	+	+
library of machines	-	-	+	+	+	-	+	+	+	-
ability to add more machines	-	-	+	+	+	-	+	+	+	+
library of tools	-	-	+	+	+	-	+	+	+	+
options for efficient reviewing of the G-code	+	-	+	+	+	+	+	+	+	+
options for efficient modifying the G-code directly in the program	+	+	-	+	+	+	+	+	+	+
cutting parameters optimisation	-	-	-	+	+	-	+	-	+	+
cross-section view	-	-	+	+	+	-	+	+	+	-
option for verification of tolerance	-	-	+	+	+	-	+	-	+	-

NCViewer is web based software that is essentially a tool path simulator with a clean, easy to understand interface. One should not expect too much from this software since even a cutting visualization and graphic representation of machines does not exist (graphic representation of tools exists, but is very simple and does not contribute to new knowledge related to operation errors), let alone some more advanced options such as optimization of cutting parameters. But for what it is intended for, a quick check of the G-code as well as a visual display of the tool path, this software is very good. There is a benefit for Autodesk Fusion 360 users, because NCViewer can be embedded into its CAM workspace that allows the user to drag and drop NC code live into the NC Viewer palette and watch a simulation of the code within Autodesk Fusion 360.

G-Cide Q'n'dirty toolpath simulator is essentially a worse version of NCViewer, because it does not understand different G-code dialects. Also, many canned cycles and macros are not supported in this software. If we add the not so pleasant appearance of the interface, conclusion is that it is more advisable to use NCViewer as free web based software.

NX CAM IS&V is integrated module in SIEMENSE NX software, and as such it contains various advantages over standalone software. For example, the transition from one module to another within the software is very efficient, which allows great flexibility during programming. NX CAM IS&V software contains all the options needed for quality simulation and verification of G-code. From detailed cutting views, to a large number of analyses, this software is a great solution for all

programmer needs. Although it is integrated within the NX CAM software, the NX CAM IS&V can also work with G-codes obtained from other CAM software. One of the few drawbacks of this software is the price that can range between 6000$ and 30000$ (the price information of this software is not necessarily accurate, because vendors of any of these software won't provide price information, unless they see that you are a serious buyer, but on sites such as Reddit, this information can be found, as is the case with price information shown in this paper). Cutting parameters optimization and modification of the G-code directly in the module NX CAM IS&V is not possible because this is all done in CAM module of this program. Never the less, the transition from one module to another is efficient enough that this does not cause problems during the programming process.

CAMWorks Virtual Machine is a very popular simulation and verification software for G-code because it is integrated in SOLIDWORKS and CAMWorks CAD environment. CAMWorks virtual machine can come in one of three ways:

- standard – can be launched only from CAMWorks, and is not really a G-code simulator because it does not check the G-code. It is more like an advanced version of some CAM software simulation;
- professional – can be lunched only from CAMWorks, and is a proper G-code simulation and verification software;
- premium – can be launched from CAMWorks or as a standalone application, so it is used in cases when a user wants to simulate a G-code obtained from some other CAM software. Only in this package is it possible to create your own machines.

As a simulation and verification software for G-code, professional version of this software satisfies the widest range of users, and is probably the best in terms of price-performance ratio from all three versions.

Vericut is one of the best G-code simulation and verification software on the market. This software contains all possible advanced options needed for quality G-code simulation and verification software, and CGTech company, that produces this software, often leads in introducing new options that eventually become the norm of G-code simulation and verification software. For example, lot of simulation and verification software have options for optimization of tool paths, feeds and speeds of the machine, some have force optimization, but Vericut even has a chip thickness optimization for advanced users. One of the more interesting features of Vericut software that it has a free add-on module called "Vericut reviewer", that can be installed on many different electronic devices (PCs, tablets, etc.), and is used for fast and easy review of G-code simulated programs. This allows much easier communication between workers, operators and engineers within the company, leading to more efficient work.

CAMotics is free open sourced G-code simulator and verificatory software that was released in 2011. It is simple software that does not have lot of advanced features and options. Also, it only supports a subset LinuxCNC G-code, and more so, lot of canned cycles (G73, G76, G83, etc.), tool compensations (G40, G41, G42, etc.) and other G-code functions are not supported. Thankfully, the manufacturers of this software has an easy to understand, and detailed view of all G-code functions that are supported and not supported by this software [16]. Also, things that should be noted are that graphical representations of machines and tools are very simple in this program, and lathe simulation is not supported.

NCSimul, as well as Vericut, is on the forefront in G-code simulation and verification technologies that often sets the standards for other software to achieve in order to be competitive in the market. This software has all the options of a good simulation and verification software, for example parameter optimisation which can on average reduce production times by 15-20 %, all of the graphical representations, tolerance verifications, as well as other advanced options, but one of the greater thing about this software (that Vericut software also has) is that the customer support department helps manufacturing companies that use their software to create exactly those machines that are in companies production facilities, which greatly facilitates the job of the engineer. Vericut and NCSimul often copy advanced options from each other, so deciding which software to use depends mostly on personal preference, as well as the offers in terms of price and payment offered by software vendors.

CNC Simulator Pro is not just a G-code simulation and verification software, it is a CAD/CAM system, CNC programing editor, 3D model milling software, and above all else is a training tool. This program comes in one of two ways. First is a free version that can be downloaded on their site, and second is a Premium version which is paid for (the price can range from 99$ to 1040$, depending on how many sets of licences is being purchased). The software does not support any special brands standard G-codes, but it does follow the ISO standard, as well as common Fenuc codes [17]. The software is ferly easy to understand and use, and there are free online courses from which the users can learn. Not many advanced options exist in this software, and it will not satisfy more advanced users, but it is very recommendable software for schools and learning centres.

Eureka Virtual Machine performs complete 3D simulation cutting process with visually pleasing and easy to understand interface. There are for main modules in Eureka software.

- Eureka G-code is a module that simulates and verifies the G-code that will be inserted into the machine. It has everything you need from a good G-code simulation and verification software;
- Eureka Robot is a module that simulates the working of a robot. It converts APT code generated by CAM software into a program for 6 or more axes robot. During the process of conversion, Eureka software calculates optimal tool paths, and then it simulates the whole process;
- Eureka Chronos is an optimize feature inside Eureka Virtual Machine software. It optimizes G-code by tweaking the feed rate, so that more efficient program can be ensured;
- As well as some other software in this paper, Eureka has the module for additive manufacturing called Eureka Additive. It can simulate the whole process of 5-axis additive manufacturing.

As most other G-code simulation and verification software, Eureka Virtual Machine can be used for

learning purposes, as it can simulate everything that happens in a production process, and can find problems and mistakes created during the programming process.

G-Wizard Editor is easy to use G-code simulation and verification software focused on simplifying the options and facilitating the work. Because the manufacturers of this software have paid the most attention on software simplification, it is a great choice for the purpose of learning CNC programming. This is best shown with the "hint" feature which exists inside the software, and describes in English each code meaning that is entered into the software (e.g. if the block in the G-code looks like this "N85 M06 G43 H0", and the user clicks on this block, in the hint menu the meaning of the codes will be explained as follows: "N05: Block or sequence number; M06: Tool Change; G43: Apply tool length compensation (plus); H is a tool offset #0"). Even though it has a great learning features, this is not the best simulation and verification software. It doesn't have graphical representation of machine, stock, cutting process, it can't check the collisions. But never the less, in regards to the G-codes and checking their errors, editing them, optimizing cutting speeds and feeds (with G-wizards feeds and speeds calculator), it does a great job. It should be mentioned that even though this software does not have machine library, when starting the software user has to put detailed description of the machine that is used (in terms of large number of different parameters that define the machine), so that the software can find errors in the G-code in regards to the machine.

V. Conclusion

In order to increase the efficiency of work in companies engaged in production using CNC machines, reducing the costs of equipment breakage caused by improper G-codes and costs of producing scraps, as well as potential reduction of worker stress when launching new programs, it is recommended to use software for G-code simulation and verification. There are plenty of software that provide a large number of features for these purposes, some of which are free and some very expensive. With the increase in price of software, the quality is also increased, but that does not mean that cheaper/free software don't have their use. For someone that is looking for a quick check of the G-code, web based free software called NCViewer could be a good choice. For someone in need of a more advanced G-code check-up, and for a great learning tool, G-Wizard Editor is a great choice, even more so because of its relatively cheap price. For simulation of the whole cutting process (with graphical representations) CNC Simulator Pro can be used. And for companies that have large sums of money to invest in their software equipment, and that are looking in relatively longer return time on its investments, more expensive software like Vericut or NCSimul are great choices.

Certainly the final decision on which software is best for particular need depends on a number of factors, and is up to the user to make the choice between the different software. This paper presents only an overview of some of possible choices.

Acknowledgment

This research was financially supported by the Ministry of Education, Science and Technological Development of the Republic of Serbia.

References

[1] M. Manić, R. Turudija, Software for Simulation and Verification of Control Code for Numerically Controlled Machines, pp. 14-18; 22-38, 2019.

[2] NCViewer software, https://ncviewer.com/, last accessed November 20, 2020

[3] G-code Q'n'dirty tool path simulator, https://nraynaud.github.io/webgcode/, last accessed November 20, 2020

[4] NX CAM IS&V software, https://www.youtube.com/watch?v=Ph5u_8D3TFA, last accessed November 20, 2020

[5] NX CAM price, https://www.reddit.com/r/cad/comments/23advz/siemens_nx_cost/, last accessed November 20, 2020

[6] CAMWorks Virtual Machine software, https://camworks.com/modules/camworks-virtual-machine/, last accessed November 20, 2020

[7] CAMWorks Virtual Machine price, https://www.cnczone.com/forums/camworks/154014-software.html, last accessed November 20, 2020

[8] Vericut softwar, https://cgtech.com/, last accessed November 20, 2020

[9] CAMotics software, https://camotics.org/, last accessed November 20, 2020

[10] NCSimul software, https://www.ncsimul.com/, last accessed November 20, 2020

[11] CNC Simulator Pro software, https://cncsimulator.info/, last accessed November 20, 2020

[12] CNC Simulator Pro price, https://cncsimulator.info/order, last accessed November 20, 2020

[13] Eureka Virtual Machine software, https://www.roboris.it/en/home-01/, last accessed November 20, 2020

[14] G-Wizard Editor software, https://www.cnccookbook.com/g-code-simulator-viewer-generator-gwizard/, last accessed November 20, 2020

[15] G-Wizard Editor price, https://www.cnccookbook.com/g-wizard-calculator-pricing/, last accessed November 20, 2020

[16] G-code functions that are supported and not supported by CAM, https://camotics.org/gcode.html, last accessed November 20, 2020

[17] G-codes supported by CNC Simulator Pro software, https://cncsimulator.info/OnlineHelp2/g_codes.htm?ms=AAAAAA%3D%3D&st=MA%3D%3D&sct=Njk4&mw=MjQw, last accessed November 20, 2020

Traffic engineering, transport and logistic

THE 5th INTERNATIONAL CONFERENCE
MECHANICAL ENGINEERING IN XXI CENTURY

December 9-10, 2020
Faculty of Mechanical Engineering in Niš, Serbia

The Design of Unconventional Piston Mechanism for 3.0 L IC Engine

Ivan GRUJIĆ[a], Nadica STOJANOVIĆ[a], Jovan DORIĆ[b]

First Author affiliation: University of Kragujevac, Faculty of Engineering, Department for Motor Vehicles and Motors, Kragujevac, Serbia
Second Author affiliation: University of Kragujevac, Faculty of Engineering, Department for Motor Vehicles and Motors, Kragujevac, Serbia
Third Author affiliation: University of Novi Sad, Faculty of technical sciences, Novi Sad, Serbia
ivan.grujic@kg.ac.rs, nadica.stojanovic@kg.ac.rs, jovan_d@uns.ac.rs

***Abstract*— The application of the IC engine as drivetrain represents long tradition, which will probably sustain and in the future. How the usage of IC engines is guaranteed, especially because new oil reserves are found every day, it should think about designing new, maybe better IC engines. In this paper is presented unconventional conception of the piston mechanism, which is more compact than classic, even for IC engine with relatively big displacement. Are shown geometrical differences and are listed advantages and disadvantages in the case of usage of such piston mechanism.**

***Keywords*— Design, IC engines, Unconventional piston mechanism, Geometrical differences, Advantages and Disadvantages**

I. INTRODUCTION

IC engines are tracked with the rich history of technical development. From the beginning of their usage till today, IC engines didn't changed very much by their construction. However, performances of firs engines are drastically different tin respect to today engines. This is the case how for the gasoline, as well as for the diesel engines. In order to improve the performances of the engine, it is necessary in some way to improve the working cycle. As the result of these improvements, almost always we have been increasing in engine speed and/or cylinder pressure.

By increasing the cylinder pressure, the forces in piston mechanism are growing. As the result of increased forces, we have the higher stresses. One of the most dangerous forces, is the normal force. This force directly influence on the wear of the cylinder [1]. This can be a very bad, because this directly influence on the engine life cycle. In the case of working or more accurate agricultural machine, this one very important parameter, because from this kind of machines, reliability is expected. Besides the cylinder pressure, as well the speed can influence on stresses. As the not sure product of piston speed, we have piston acceleration. The piston acceleration is a main component of the inertial force that is a very influential parameter in piston mechanism, which means that kinematic is also important, not only the dynamics [2].

One of the solutions for possible improvement in engines industry, in order to prolonger the life cycle of the IC engines, is the construction of new engine constructions. One such research is performed by Kukuča et al. [3]. They have concluded in their research that the kinematic properties of the engine with FIK unconventional crank mechanism are comparable to the kinematic properties of the classical piston combustion engine with the same value of the piston stroke. This solution has the potential to reduce the wear of the cylinder and the noise caused by the tilting of the piston due to the small deflection of the connecting rod from the vertical axis of the piston.

The efficiency of a new internal combustion engine concept with variable piston motion was investigated by Dorić and Klinar [4]. They have expressed in their research, that represented engine have the variable compression ratio, than with this concept it is possible to avoid the classical approach for partial load operation via variable displacement. Finally presented concept is able to provide heat addition during constant volume. All of these mentioned advantages show that the potential to increase the efficiency of the SI engine conditions is not yet exhausted. As shown in the research results above, variable displacement methods have the best potential to increase the efficiency of the engine at part load conditions. To avoid engine operation below the unthrottled load limit, facilitate smooth mode changes and further improve the vehicle fuel economy. With the constant volume combustion cycle, the piston movement is significantly slower around TDC and BDC, in fact piston actually stops for a while, this have significant impact on volumetric efficiency and engine efficiency.

The aim of this paper is to investigate the forces in the piston mechanism of simple nonconventional engine, as well as the comparison with the conventional engine, in order to determine, which engine is the better from the aspect of mechanical stresses.

II. 3D MODEL AND EXPLANATIONS

The designed piston mechanism is the combination of two existing piston mechanism, flat and Wankel, show on Fig. 1.

By analysis of Fig. 1, it can be seen that the designed piston mechanism don't have the connecting rod, as conventional piston mechanism. This is first advantage of

this piston mechanism. By removing the connecting rod, the Normal force is neutralized, and which is shown on the Fig. 2.

Fig. 1 The designed piston mechanism

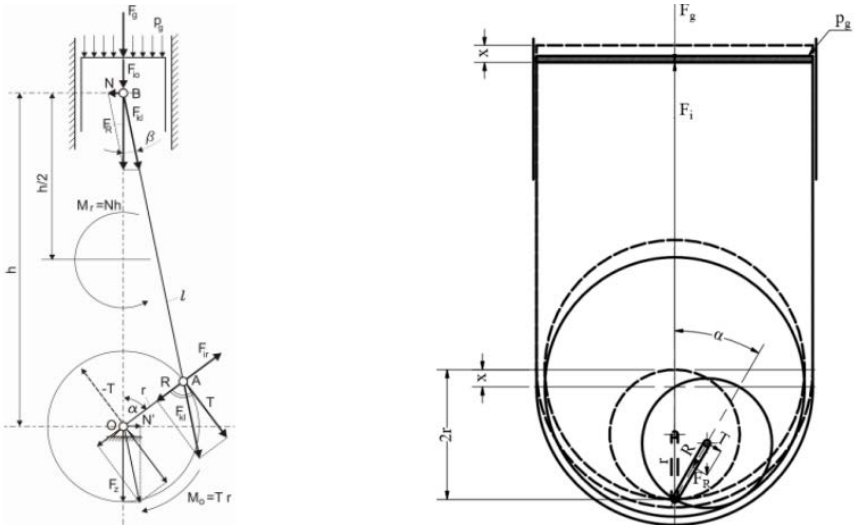

Fig. 2 Dynamic scheme of conventional and designed non-conventional piston mechanism [5]

This is significant result, because the normal force in piston mechanism is the main component that influence on the friction in the cylinder and by this on wear. This means that this piston mechanism can prolong the engine life cycle. Also because the connecting rod is removed from the piston mechanism, the overall dimensions of piston mechanism will be reduced significantly.

Because of specific design of this piston mechanism, during the piston movement, the piston almost stays one moment in the TDC (Top Dead Center). This means that the combustion process occurs almost during the constant volume. By this the working cycle can be approximated to the ideal working cycle. All this information's lead to the conclusion that this piston mechanism can be good replacement for the conventional piston mechanism. However, every machine assembly and part, besides advantages have and disadvantages. The main disadvantage of the designed piston mechanism is the complicated design because of the internal tooth gear, Fig. 3.

From Fig. 3 can be seen that the gear that goes into the piston is not the part of the piston, so the manufacturing of this gear is not to big problem. The only what is added to the classic spur gear with internal teeth is the shaped wedge, on both side of the gear. This wedge is important, so the spur gear can be mounted in the piston in only one side. The little complication which may be a main disadvantage is the spur gear which is the part of the crankshaft. This spur gear cannot be mounted as separate part, so it must be manufactured as the part of the crankshaft.

However, this disadvantage is not so dangerous, because today exist many technologies for gears manufacturing.

How in the title is defined, in this case, the subject is the design for the 3.0 L engine. 3.0 L engines mainly are used in luxury expensive cars, so the disadvantage of complicated design, that maybe can increase the production costs, is not to important factor. The geometrical parameters of the designed piston mechanism are given in Table 1.

TABLE I THE GEOMETRICAL PARAMETERS OF THE DESIGNED PISTON MECHANISM

Name	*Values*	*Units*
Bore	95	mm
Stroke	70	mm
Displacement	2977	cm^3
Compression ratio	9.37	-

By the compression ratio, it can be concluded that this engine corresponds to the gasoline engines, which probably have beater future than diesel engines. However with modifications of combustion chamber shape and size, the compression ratio can be increased or reduced. One more advantage of this piston mechanism are overall dimensions. The logical conclusion is that engines with great displacement are bigger, and by this heavier. In this case the dimensions and weight of the engine can be significantly reduced, which can be concluded by overall dimensions of the designed piston mechanism, shown on Fig. 4.

Fig. 3 Internal gears of piston mechanism

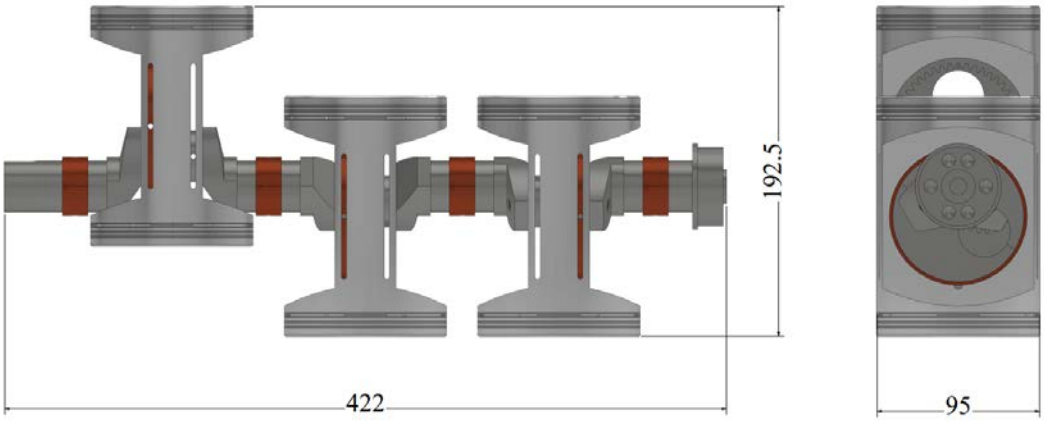

Fig. 4 The overall dimensions of the designed piston mechanism

Besides the overall dimension, it can be seen, that are not too big, the weight of the entire piston mechanism is only 6.92 kg. Of course by addition of the other components which are necessary for the engine work, the mass will increase. However, it can be concluded that the mass of the entire engine will be significantly smaller in comparison with conventional piston mechanism.

The reduction of the engine size can be a very important parameter. Reduction of size and weight automatically means the reduction of fuel consumption. By reduction of fuel consumption which is in direct connection with the exhaust emission, the exhaust emission will be also reduced. This means that the implementation of such piston mechanism can be good for satisfying the strictest norms about exhaust emission. By comparing the advantages and disadvantages of the designed piston mechanism, it can be concluded that such type of IC engine, maybe can have the future for development.

III. Conclusions

The IC engines have long tradition as powertrains for many mobile and stationary systems. For now the adequate replacement is not found. So it is important to work on the possible improvements of the IC engines. In the paper is designed and analyzed the 3.0 L engine with non-conventional piston mechanism. The analyzed piston mechanism is smaller and lighter than conventional piston mechanism in the same category. All this influence on the reduction of the entire vehicle, which further can lead to the decrement of fuel consumption which is fallowed with less exhaust emission. Also, the designed piston mechanism neutralizes the normal force, which can prolong the engine life cycle.

Acknowledgment

This paper was realized within the framework of the project “The research of vehicle safety as part of a cybernetic system: Driver-Vehicle-Environment”, ref. no. TR35041, funded by the Ministry of Education, Science and Technological Development of the Republic of Serbia.

References

[1] I. Grujic N., Stojanovic, J. Doric, J. Glisovic, S. Narayan, and A. Davinic, “Engine load impact on maximum value of normal force in piston mechanism”, Tractors and power machines, Vol. 23, No. 1/2, pp. 10-16, 2018.

[2] I. Grujic, D. Miloradovic, and N. Stojanovic, “Nonlinear kinematics of engine crank-piston mechanism”, The Ninth International Symposium KOD 2016, Machine and Industrial Design in Mechanical Engineering, Balatonfüred, Hungary, 9 - 12 June, pp. 93-98, ISBN 978-86-7892-821-5, 2016.

[3] P. Kukuča, D. Barta, J. Dižo, and J. Caban, “Piston kinematics of a combustion engine with unconventional crank mechanism”, MATEC Web of Conferences, Vol. 244, 2018.

[4] J. Dorić, and I. Klinar, “Efficiency of a new IC engine concept with variable piston motion”, Thermal Science, Vol. 18, No 1, pp. 113-127, 2014.

[5] I. Grujić, N. Stojanović, J. Dorić, S. Vasiljević, and R. Pešić, “The analysis of conventional and non conventional piston mehanism from aspect of mechanical stresses”, tractors and power machines, Vol. 24, No. 1/2, pp. 5-8, 2019.

THE 5th INTERNATIONAL CONFERENCE
MECHANICAL ENGINEERING IN XXI CENTURY

December 9-10, 2020
Faculty of Mechanical Engineering in Niš, Serbia

Influence of Rear Spoiler Inclination on Aerodynamics and Stability of Car

Nadica STOJANOVIĆ[a], Ivan GRUJIĆ[a], Jasna GLIŠOVIĆ[a], Danijela MILORADOVIĆ[a] and Jovan DORIĆ[b]

First Author affiliation: University of Kragujevac, Faculty of Engineering, Department for Motor Vehicles and Motors, Kragujevac, Serbia
Second Author affiliation: University of Kragujevac, Faculty of Engineering, Department for Motor Vehicles and Motors, Kragujevac, Serbia
Third Author affiliation: University of Kragujevac, Faculty of Engineering, Department for Motor Vehicles and Motors, Kragujevac, Serbia
Fourth Author affiliation: University of Kragujevac, Faculty of Engineering, Department for Motor Vehicles and Motors, Kragujevac, Serbia
Fifth Author affiliation: University of Novi Sad, Faculty of technical sciences, Novi Sad, Serbia
nadica.stojanovic@kg.ac.rs, ivan.grujic@kg.ac.rs, jaca@kg.ac.rs, neja@kg.ac.rs, jovan_d@uns.ac.rs

***Abstract*— The design of the vehicle has great influence on the aerodynamics and stability of the car. Today, how technology has achieved high level, traditional experiments performed on the road or in the laboratory can be replaced by virtual experiments. In order to reduce the time and costs for optimization of the rear spoiler setting angle, mainly specialized software for conducting virtual experiments were used. Determination of the optimal installation angle of the rear spoiler was performed by usage of the ANSYS software package, Fluid Flow CFX module. The angle of the spoiler starts from -15° ÷ 15°. Going from negative to positive angle (negative mathematical direction), lift force decreases, while this is not the case with aerodynamic force. However, the difference between the maximum and minimum aerodynamic force is about 12 N, which is negligible. While the difference between the maximum and minimum values of buoyancy force is about 130 N. So it is concluded that it is best to install the rear spoiler at 15° angle.**

***Keywords*— Design, Optimization, Virtual experiments, Lift force, Drag force**

I. Introduction

The vehicle aerodynamic is a very important parameter, which should be taken into the consideration during the development of the cars shape and that from more aspects: greater vehicle dynamics, less fuel consumption, the increased lateral stability of the vehicle, the increased safety during the braking [1]. From early days, the engineers have think about vehicle aerodynamic improvement [2], which shows the shape shown in bottom left corner of Fig. 1. Besides that, on the figure 1 is given the drag coefficient trough vehicles history.

The researches, where was investigated the value of the drag and lift coefficient, if the rear spoiler is applied or not, have shown that by application of the rear spoiler, the lift coefficient can be reduced up to 32%, while the implementation of rear spoiler cause the increment of the drag coefficient, but not too much, only 3.4% [3], if the drag coefficient is compared with the lift coefficient. Besides determination, whether the vehicle is more stable with the rear spoiler, it comes to the idea to investigate how the spoiler angle in respect to the horizontal plane, influence on the vehicle stability. Das and Riyad [4] have investigated one rear spoiler, which has been mounted under 6 different angles in respect to the vehicle horizontal plane, and every angle were investigated under different vehicle speeds. From the research conducted by Das and Riyad, can be concluded that during the vehicle driving, the lift coefficient should be as less possible, in order not to disturb the vehicle stability. Of course by technology progressing in automotive industry, the vehicles can be equipped with adjustable spoilers. By implementation of such spoilers, the safety increases [5], usually are applying on the sport cars. By implementation of different sensors on the vehicle, it is possible to estimate the road conditions, and automatically to change the vehicle aerodynamic characteristics [6, 7].

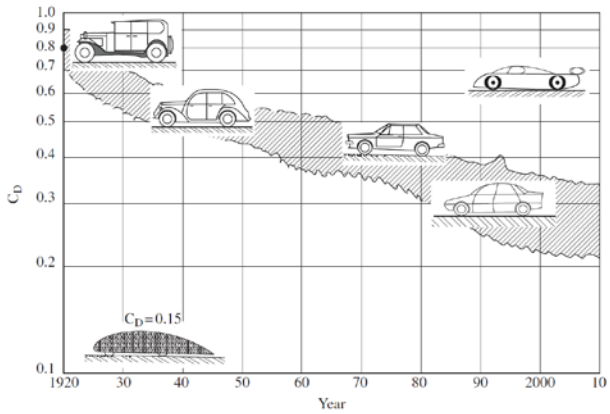

Fig. 1 The reduction of the drag coefficient with the vehicle development [2]

One of the reasons from which users are investing in the rear spoiler implementation is the reduction of costs for fuel consumption. The applied rear spoilers are pushing the air around the vehicle, and on this way are reducing the

resistances, which gives greater vehicle efficiency. By introducing increasingly stringent norms, the car manufacturers are forced to reduce the level of exhaust emission, and this in one part can be achieved by implementation of rear spoilers [8]. The reduction of the exhaust emission is in direct connection with the fuel consumption, as greater is the fuel consumption, the greater is the exhaust emission. The global emission of the CO_2 caused by the passenger vehicles as source in 2018. is 70%, while by observing on the global level, the entire emission from transport is 24% [9]. The only disadvantage of rear spoiler usage is the high costs of mounting and maintaining, as well as the laws which refer to the cars modifications, and to mounting of rear spoilers, which are different from country to country.

This paper looks in the optimization of the mounting angle of the rear spoiler in respect to the vehicle horizontal plane, with purpose of the lift force reduction and stability increment during the vehicle driving. Besides that, the aim of this paper is to show the air speeds, as well as the turbulences that appear for that vehicle where the rear spoiler is mounted as such, to not come to the stability disturbing, that is for that variant where is achieved the smallest value for the lift force.

II. 3D MODEL

The model of the passenger car was created in the SolidWorks software package, Fig. 2. The vehicle was created in the proportion 1:1. In order to determine the influence of the rear spoiler mounting angle, on the drag force and lift force, it was created one type of spoiler, Fig. 3. The mounting angle of the rear spoiler is shown in Table 1, where can be seen that the mounting angle goes from -15º ÷ +15º in respect to the horizontal plane.

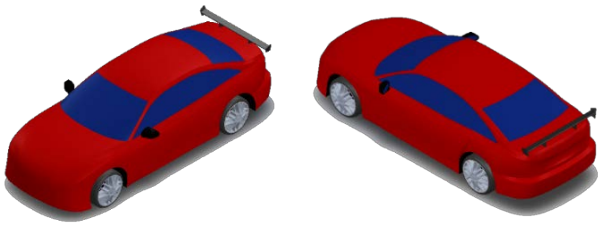

Fig. 2 3D model of the passenger car

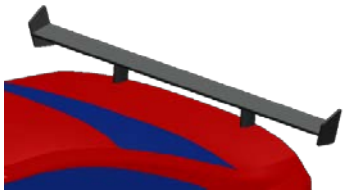

Fig. 3 Spoiler appearance

TABLE I THE SPOILER POSITION IN RESPECT TO THE HORIZONTAL PLANE

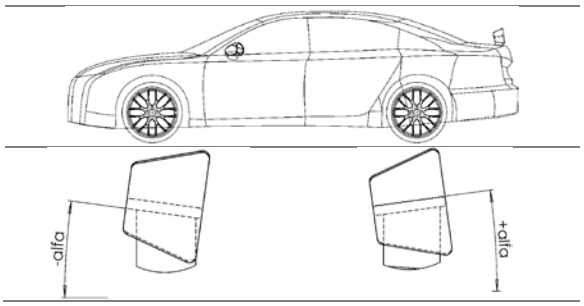

5°
10°
15°
0° (neutral position)

In order to determine the optimal position of the rear spoiler in respect to the horizontal plane, in the paper are conducted seven analyses. As the output parameters of determination of the optimal angle for the rear spoiler mounting, were analyzed the lift and drag forces.

III. RESEARCH METHODOLOGY

In this chapter will be presented the procedure of performing the virtual experiment, which illustratively is shown on the Fig. 4. The analysis will be performed in ANSYS software package, Fluid Flow CFX module. Before defining the boundary conditions, it is necessary to define the mesh. Fig. 5 is shown the look of the applied mesh type. By Table 2 is show the number of elements and nodes in depending from the position of the rear spoiler in respect to the horizontal plane. On the vehicle surface, the mesh refinement was performed, with purpose to increase the results accuracy, while by increasing the distance from the vehicle surface, the size of mesh increases too. The next step in the analysis is the defining of the boundary conditions, which given on the algorithm, under the input data. The input data can be separated into two groups and that:

1. The characteristics of environmental air:
   - Environment pressure $p = 101325$ Pa;
   - Environment temperature $T = 25$ ºC, и
   - Air density $\rho = 1.225$ kg/m^3,
2. The vehicle exploitation characteristics:
   - Vehicle speed $v = 100$ km/h.

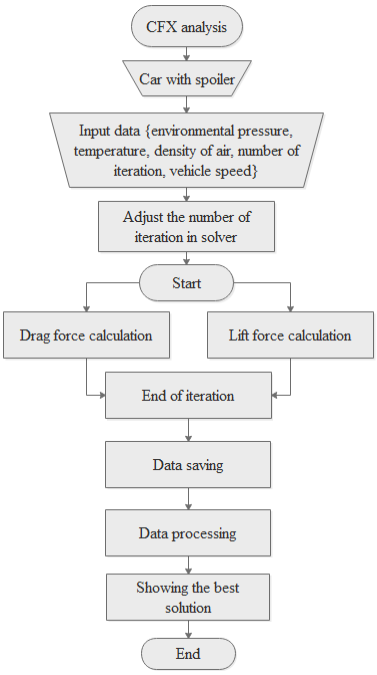

Fig. 4 The algorithm of the CFX analysis

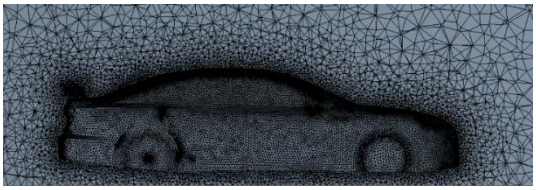

Fig. 5 Mesh visualization

After defining the mesh and boundary conditions, the calculation can be conducted. The outputs of the calculation are lift and drag forces, after that conclusions are making in order to obtain as stable as possible vehicle under defined boundary conditions.

TABLE III THE NUMBER OF ELEMENTS AND NODES IN RESPECT TO THE REAR SPOILER POSITION

Angle, °	Number of elements	Number of nodes
-15	3332311	615954
-10	3276174	606004
-5	3344008	618111
0	3330418	615415
5	3329364	615435
10	3290230	608544
15	3333961	616408

The chosen *k-ε* model during determination of vehicle aerodynamics have shown as very good [10]. The values for *k-ε* are obtaining by application of equations (1) and (2) [11].

$$\frac{\partial(\rho k)}{\partial t}+\frac{\partial}{\partial x_j}\left(\rho U_j k\right)= =\frac{\partial}{\partial x_j}\left[\left(\mu+\frac{\mu_t}{\sigma_k}\right)\frac{\partial k}{\partial x_j}\right]+P_k+\rho\varepsilon+P_{kb} \quad (1)$$

$$\frac{\partial(\rho k)}{\partial t}+\frac{\partial}{\partial x_j}\left(\rho U_j k\right)=\frac{\partial}{\partial x_j}\left[\left(\mu+\frac{\mu_t}{\sigma_\varepsilon}\right)\frac{\partial \varepsilon}{\partial x_j}\right]+ +\frac{\varepsilon}{k}\left(C_{\varepsilon 1}P_k-C_{\varepsilon 2}\rho\varepsilon+C_{\varepsilon 1}P_{\varepsilon b}\right) \quad (2)$$

Where $C_{\varepsilon 1}=1.44$, $C_{\varepsilon 2}=1.92$ and $\sigma_\varepsilon=1.3$ are constants [12]. P_{kb} and $P_{\varepsilon b}$ are representing the influence of buoyancy forces. P_k is the turbulence production due to viscous forces. In addition to the independent variables, the following were also used: density (ρ), the velocity vector (U_j), the dynamic viscosity (μ) and the turbulence viscosity (μ_t).

IV. RESULTS AND DISCUSSION

The numerical approach for resolving problems, such is the influence of the rear spoiler mounting angle, provides the reduction of costs during the development of the new product. The boundary conditions for all seven analyses, which were performed for different rear spoiler positions, are the same.

A. *The drag and lift force*

In the case of the vehicle speed 100 km/h, for different angles of mounting the rear spoiler, the values of the obtained drag and lift forces are differencing. By going from negative to positive rear spoiler mounting angle, the lift force decreases for 40.79%, while the lift force increases for the 3.67%. By observing the lift force from negative to positive rear spoiler mounting angle, it has constant fall. However, from the Figs. 6 and 7, it can be seen, where exist grow of the drag force, between the first and final value the variations are existing.

The size of reduction of the lift force for the vehicle speed 100 km/h is not negligible. Which means that on this way, it can be made positive influence on the increment of the vehicle stability, which will increase the safety how of the driver so of the other traffic participants. While the increase of the drag force is not big, if on the vehicle is mounted rear spoiler under angle $\alpha=15°$.

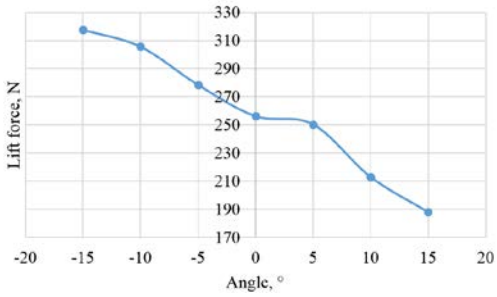

Fig. 6 Lift force in the function of spoiler angle

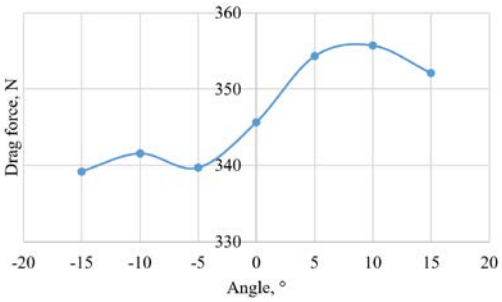

Fig. 7 Drag force in the function of spoiler angle

B. *The stress field on the vehicle surface due to driving*

Due to vehicle driving in the peaceful environment (without the wind), on the vehicle surface appears the stress field, Fig. 8. The highest values are appearing on the surfaces which are vertical in respect to the toad. This is because the air has direct impact on these surfaces that is acting normal on these surfaces. The good known fact is that when force acting normal on the surface, the pressure is highest, while in the case when the force acting under angle, the value of the pressure is falling. The one more reason for high pressure on the frontal surface of the vehicle, is because the vehicle with this surface literally pushes the air in front of itself, which causes additional resistances, Fig. 8. By observing the Fig. 8, which represents the environment, where the vehicle is driven, it can be seen that the value of the pressure behind the vehicle is lower than the pressure that appear in front of the vehicle.

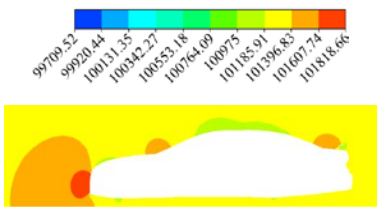

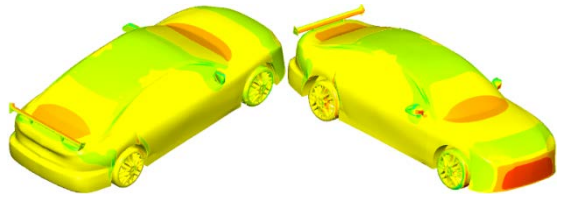

Fig. 8 The stress field on the vehicle surface and around the vehicle when the rear spoiler is under angle 15º in respect to the horizontal plane

C. *The air flow speed around the vehicle, and appearance of turbulences as the cause for vehicle stability disturbing*

The vehicle speed is the 100 km/h, that is 27.78 m/s. from the Fig. 9 it can be noticed that the air flow speed around the vehicle is higher than the vehicle speed. This is the consequence of the vehicle shape, as well as of the pressure difference between the front and rear side of the vehicle. When the vehicle is moving, it pushes the air in front of itself, and this cause greater air density in front of the vehicle, in comparison the rear side.

How the pressure value is not the same by vehicle height (Fig. 8), the air tends to equalize the pressures and because of this comes to the turbulences [13], Fig. 10. The highest values for turbulences appear around mirrors and behind the vehicle.

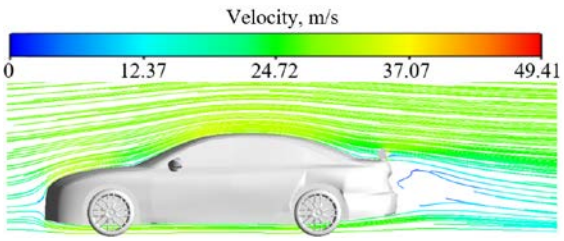

Fig. 9 The air flow speed around the vehicle ($\alpha = 15°$)

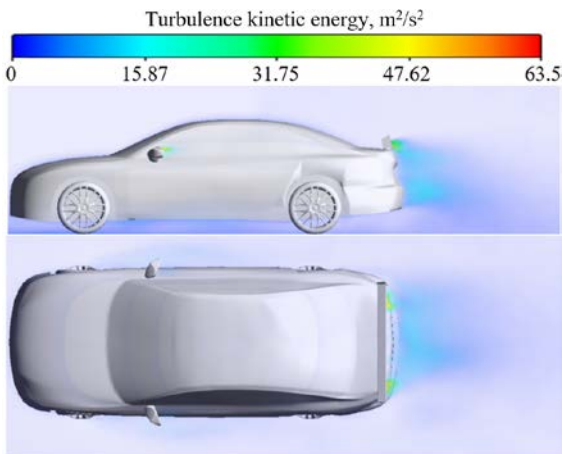

Figure 10 The turbulences around the vehicle due to driving, when $\alpha = 15°$

V. Conclusions

In order of the vehicle stability achievement under higher speeds, on vehicles rear spoilers are implementing, which is the case for the sport cars. In this paper were performed seven investigations on the same vehicle, under the same boundary conditions, the only difference is the mounting angle of the rear spoiler. On the basis of the conducted analysis and represented results, it comes to the conclusion that on the vehicle when is driving with speed of 100 km/h, the best angle for the rear spoiler mounting is $\alpha = 15°$. By the spoiler mounting, the greater safety under higher speed is achieving.

For further researches, should investigate, which values of drag and lift forces will be obtained for different vehicle speeds. Besides that, it should investigate when on the vehicle acts and lateral wind, and when vehicle is driven in a convoy of vehicles, behind truck or other car. Also, should take the influence of distance between the vehicles.

Acknowledgment

This paper was realized within the framework of the project “The research of vehicle safety as part of a cybernetic system: Driver-Vehicle-Environment”, ref. no. TR35041, funded by the Ministry of Education, Science and Technological Development of the Republic of Serbia.

References

[1] A. Janković, “Vehicle Dynamics,” Kragujevac, 2008. (in Serbian)

[2] J. Katz, “Automotive Aerodynamics,” Wiley, USA, 2006.

[3] N. Stojanović, D. Miloradović, O. I. Abdullah, I. Grujić and S. Vasiljević, “Effect of Rear Spoiler Shape on Car Aerodynamics and Stability,” Proceedings of 5th International Conference "New Technologies, Development and Application III” NT-2020, Sarajevo, pp. 340-347, 27-29. June 2020.

[4] R. C. Dasa and M. Riyad, “CFD Analysis of Passenger Vehicle at Various Angle of Rear End Spoiler,” Procedia Eng., vol. 194, pp. 160-165, 2017.

[5] K. Kurec, M. Remer, J. Broniszewski, P. Bibik, S. Tudruj and J. Piechna, “Advanced Modeling and Simulation of Vehicle Active Aerodynamic Safety”, J. Adv. Transp., vol. 2019, Article ID 7308590,

[6] A. Eskandarian, “Handbook of Intelligent Vehicles,” Springer, 2012

[7] W. Jarisa, “Future technology – Road condition classification using information fusion,” in Proceedings of the 7th International Munich Chassis Symposium 2016, Springer Fachmedien, Wiesbaden, Germany, pp. 939–957, 2017.

[8] Grand View Research, https://www.grandviewresearch.com/industry-analysis/rear-spoiler-market, accessed 15.08.2020.

[9] IEA, Transport sector CO2 emissions by mode in the Sustainable Development Scenario, 2000-2030, IEA, Paris, https://www.iea.org/data-and-statistics/charts/transport-sector-co2-emissions-by-mode-in-the-sustainable-development-scenario-2000-2030, accessed 15.08.2020

[10] T.H. Shih, W.W. Liou, A. Shabbir, Z. Yang and J. Zhu, “A new k-e eddy viscosity model for high Reynolds number turbulent flows,” Comput. Fluids, vol. 24, pp. 227-238, 1995.

[11] ANSYS Inc: ANSYS CFX-Solver Theory Guide (2011). http://read.pudn.com/downloads500/ebook/2077964/cfx_thry.pdf, accessed 18.11.2019

[12] Z. Yuan and Y. Wang, Effect of underbody structure on aerodynamic drag and optimization. J. Meas. Eng. vol. 5, 194–204 (2017)

[13] R. Pütz and T. Serné, “Rennwagentechnik - Praxislehrgang Fahrdynamik: Eine praktische Anleitung für Amateure und Profis,” Springer-Vieweg-Verlag, 2017. (in Germany)

THE 5th INTERNATIONAL CONFERENCE
MECHANICAL ENGINEERING IN XXI CENTURY

December 9-10, 2020
Faculty of Mechanical Engineering in Niš, Serbia

Determining the Impacts of Passenger Transport Modes on Air Pollution in the European Union

Nikola PETROVIĆ, Vesna JOVANOVIĆ, Jovan PAVLOVIĆ, Jelena MIHAJLOVIĆ

University of Niš, Faculty of Mechanical Engineering, Department of Transport Engineering and Logistics, 18000 Niš
petrovic.nikola@masfak.ni.ac.rs, vesna.jovanovic@masfak.ni.ac.rs, jovan.pavlovic@masfak.ni.ac.rs, jelena.mihajlovic@masfak.ni.ac.rs

***Abstract*—Transport is one of the largest emitters of harmful substances that affect air quality. Each transport mode has different volume of passenger transport and at the same time has a differentiated negative impact on air quality. That is why in the European Union has been making special efforts for many years to create and implement strategies aimed at improving air quality. The main goal of this paper is to present a methodology that enables quantification and analysis of the impacts of each passenger transport mode on air quality using feed-forward neural networks. The developed model uses parameters for EU member states in the period from 2000 to 2014. In addition to the scientific and practical contribution, the development of model provides a good basic for the universal platform formation in order to create and develop strategies, i.e. measures to improve air quality on global level.**

***Keywords*—Transport, Air quality, Extreme Learning Machine, European Union**

I. Introduction

Air pollution ie reduction of air quality, is one of the types of environmental degradation. Since a negative impact on the environment, climate, flora and fauna, pollutants have the same negative impact on human health. Air pollution from transport is one of the biggest air pollutants with a tendency to increase its share in the period from 1990 to 2014 in relation to other economic activities in the EU, which are valid for member states. In the observed period, for the countries of the European Union, transport increased its share in the total GHG (Green House Gasses) emission from 15% to 23%, while agriculture kept the same share, and other activities recorded a decrease in the share in the total GHG emission [1].

As road transport is the largest source of pollutant emissions (46% of EU emissions), as well as a source of Particulate matter (13% PM_{10} i 15% $PM_{2.5}$) emissions, many EU cities specifically restrict access to the city center by motor vehicle based on their emissions level [2]. About 200 cities in Denmark, Germany, Italy, Netherlands, Sweden and the UK have low-emission zones or environments where only low-emission vehicles and with special permits are allowed. Based on forecasts it is expected that cities could reduce emissions of pollutants that affect air quality by 50% [3].

The railway is the cleanest way to transport passengers. Specific emissions from rail passenger transport remained approximately constant from 1990 to 2004. Emissions from trains depend on the technical level and the method of energy production which is used.

In developed countries, attention is still paid to the development of maritime, but also on inland waterway transport. In the transport system of developed countries, inland waterway transport occupies a significant place due to its negligible impact on environmental degradation in relation to road transport.

Air transport is highly unbalanced due to population division as well as due to different levels of development and concentration of transport in a limited number of transport nodes. Although it does not appear as the largest source of greenhouse gas emissions, of all transport modes, air transport records the highest growth rate of these emissions [4].

According to the White Paper [5] by 2030, the goal for transport will be the reduction of greenhouse gas emissions by 20% below its level in 2008. The plan is to complete the European high-speed rail network by 2050 and triple the length of existing high-speed rail networks. It should also be a greater part of the passengers transport at medium distances is performed by rail.

Transport has become more energy efficient, but in the EU transport is still dependent on oil and their products for 96% of its energy needs [5]. Transport has become cleaner, but the increase in volume means that it is still the main source of local air pollution.

Given the growing conflict between increased mobility requirements and increased pressure on environmental capacity, sustainable development is set as the only possible concept of long-term transport development. When the concept of sustainable development has become one of the most important priorities the interest in evaluating transport performance increases respecting the principles of sustainability [6]. The role of transport in sustainable development is reflected in the ability to provide a greater degree of mobility while respecting social responsibility, economic and environmental efficiency [7]. Therefore, special efforts have been made in the EU for many years to assess possible scenarios for the development of sustainable transport, as well as the formation and

implementation of strategies aimed at reducing the negative impacts of transport on the environment.

Today, due to advances in technology, data is being generated at an incredible rate, leading to data sets of enormous dimensions. That is why it is important to have efficient computational methods and algorithms that can deal with such large data sets, so that they can be analyzed within a reasonable time frame.

Artificial neural networks (ANNs) are a relatively new concept for data analysis and a completely different approach from that used in multivariate methods. Instead of conceptualizing the problem in mathematical form, neural networks use the principles of the human brain and its structure to develop a data processing strategy. The most important property of neural networks is the ability to approximate an arbitrary nonlinear function with the desired accuracy. This makes neural networks suitable for identifying and managing nonlinear processes.

Learning time is an important factor in modeling computational intelligence algorithms for processes of classification, prediction, etc. One of the biggest disadvantages of classical ANN learning is the too long training time which was the main obstacle to the wider use of ANN. There are a number of algorithms for learning ANN, such as Back Propagation (BP) method, Support Vector Machine (SVM), Hidden Markov Model (HMM), etc. One particular approach has become popular with Artificial Neural Networks in recent years, the Extreme Learning Machine (ELM) method [8, 9], which uses randomization in its hidden layer and with the help of which it is possible to effectively train network.

State authorities, regulatory agencies and other institutions adopt and implement measures to improve air quality. Taking into account the dynamic and heterogeneous composition of the air, controlling and monitoring air degradation is a major challenge for scientists, researchers and transport policy makers.

II. Literature Review

Population growth is one of the significant factors of air pollution in developed and developing countries [10, 11, 12]. Using a dynamic approach [13], in the paper examines the relationship between CO_2 emissions and population growth in the period from 1980 to 2009 and the results indicated that population growth in the long run affects the increase in CO_2 emissions.

Adaptation and mitigation of climate change have become a significant problem in many cities. The research conducted by Reckien et al. [14] covered 200 European cities during 2014. It showed that 65% of the surveyed cities had a plan to reduce pollution. The results of the same research indicated that only 25% of the total number of cities surveyed had an adaptation and mitigation plan, and that they set quantitative targets for reducing GHG emissions.

Research by Arvin et al. examines the causal relationship between traffic intensity, economic growth, CO_2 per capita emitted by transport, and urbanization [15]. The results indicated that there is interdependence between the observed variables in the short term, as well as that in the long term economic growth affects changes in traffic intensity, urbanization and CO_2 per capita emitted by transport.

ANN methodology was used in [16] to analyze the impact of population growth in indifferent areas on carbon dioxide emissions. After that, an analysis was conducted to see how transport affects the quality of the environment. The results showed that urban population growth has the greatest impact on carbon dioxide emissions.

The authors in [17] gave an overview the basic principles of machine learning techniques, among which the ELM method was observed. The research adopts 38 relevant studies in the field of environmental science and engineering that have applied machine learning techniques over the last 6 years.

III. Input Data

Modeling the impacts of transport modes on the air quality is required appropriate information base - indicators and statistical data. The quantification of the factors that impact on air pollution and air quality is conditioned by the availability of data on air pollution.

The first step in impacts modeling with ANN methodology is to define the input and output parameters (variables) of the model in order to observe the regularities and connections between them. Data for the analysis were collected from the website of the European Commission for EU countries in the period from 2000 to 2014 [18]. In the process of collecting, the problem of incomplete data arose and an important advantage of artificial neural networks was used, which can use incomplete data in its work.

As input parameters were used (Fig. 1): Passenger kilometers achieved by Passenger cars, Buses and Railways as well as the Number of passengers transported by Air and Waterways. Emissions of Greenhouse gases (GHG), Carbon dioxide (CO_2), Nitrogen oxides (NOx), Particulate matter ($PM_{2.5}$) and Sulfur dioxide (SO_2), respectively, were analyzed as output parameters.

IV. The approach, case study and results discussions: European Union

The developed ANN model represents a three-layer feed-forward neural network, which consists of one input, one hidden and one output layer (Fig. 1). The input layer consists of 5 neurons or 5 different inputs to the neural network. The output layer of the neural network always consists of one neuron, whose output for each combination of input variables is one of the emissions originating from transport, respectively Greenhouse gases (GHG), Carbon dioxide (CO_2), Nitrogen oxides (NOx), Particulate matter ($PM_{2.5}$) and Sulfur dioxide (SO_2). The choice of this network was made on the basis of the ability to approximate any arbitrary continuous function from several real variables.

All data for EU countries are divided into groups of 50% for training and 50% for testing. It is important that these two groups of data are the same for the selecting process of the most influential input parameters. In testing Root Mean Square Error (RMSE) error is used to monitor and control the flow of regression between data sets for training and testing.

In a defined ANN model for training the neural network was used ELM method. The adopted learning algorithm independently adjusts the parameters of the neural network in order to find their right combination with which the neural network approximates the

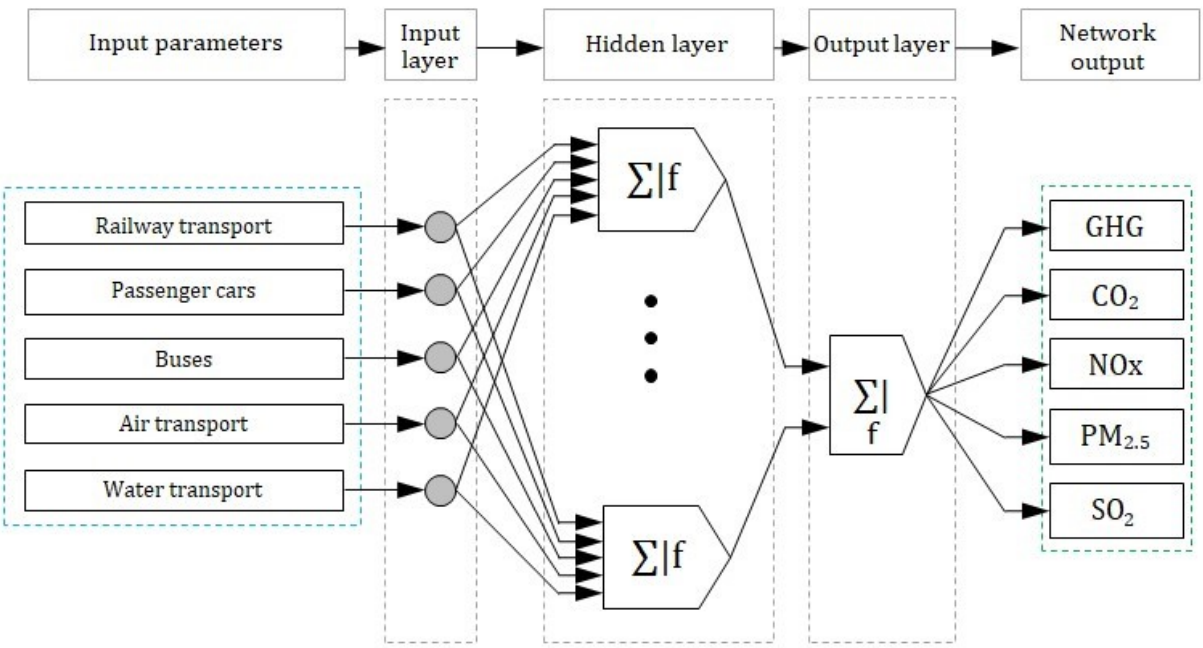

Fig. 1 ANN model for determining the impacts of passenger transport modes on air pollution [19]

TABLE I IMPACTS OF PASSENGER TRANSPORT MODES ON AIR POLLUTION [19]

Input parameters	GHG		CO_2		NOx		$PM_{2.5}$		SO_2	
	RMSE		RMSE		RMSE		RMSE		RMSE	
	training	testing	training	testing	training	testing	training	testing	training	testing
RTp	41,9743	45,4586	*9,5844*	13,8944	14,0359	24,4855	7726,2607	10326,7895	5646.1953	6929.2138
PC	43,4293	47,0690	8,2930	15,1279	11,4384	30,5961	7889,9994	10413,8731	*5702,5856*	5908,2769
BS	42,3833	36,7776	7,5359	13,6804	*16,5756*	21,1666	7986,2748	11052,4919	5550,9830	6766,5937
ATp	*44,0520*	48,787	9,3125	14,0945	16,0271	27,1264	*8207,515*	11396,324	5459,28	6289,49
WTp	42,9851	37,3124	8,9876	14,8765	15,9765	26,5432	7997,9876	10143,7654	5664,9873	5898,4321

nonlinear function with high quality. Networks are trained for input data in a way to determine the specific RMSE error of each input to a specific output. The input variable with the obtained smallest RMSE training error has the greatest influence on the observed output variable and vice versa, ie the input variable with the largest RMSE error has the smallest influence on the adopted output variable. The neural network training process needs to be stopped when the RMSE testing error starts to show its rapid growth in relation to the RMSE training error, ie a deviation occurs between the data sets for training and testing. The sigmoid (logistic) function was used as the activation function for the output layer, while the linear (purelin) function was used for the hidden layer. All input and output variables are modeled within the Matlab software. The obtained values of the smallest RMSE training error are marked with Underline while the highest values are marked with Italic.

Based on the obtained results, it can be seen that the input parameter RTp (Rail passenger traffic) has the smallest RMSE training error and therefore has the greatest impact on Greenhouse gases (GHG) and Particulate matter ($PM_{2.5}$) while on the other hand the same input parameter has the largest RMSE error and therefore has the smallest impact on Carbon dioxide (CO_2) emissions (Table 1).

The input parameter PC (Passenger cars) has the smallest RMSE training error and therefore the greatest impact on Nitrogen oxides (NOx) emissions while they have the smallest impact on Sulfur dioxide (SO_2) emissions based on the largest RMSE error.

BS (Buses) record the smallest RMSE training error, ie the largest impact on Carbon dioxide (CO_2), and the largest RMSE training error, ie the smallest impact on the emission of Nitrogen oxides (NOx) from transport.

Also, ATp (Passenger air transport) has the smallest RMSE training error, ie the largest impact on Sulfur dioxide (SO_2) and the largest RMSE training errors, ie. the smallest impacts on Greenhouse gases (GHG) and Particulate matter ($PM_{2.5}$) emissions.

WTp (Water passenger transport) as an input parameter did not record extreme values of RMSE errors and there are no minimum or maximum impacts on the adopted output variable parameters.

To reduce Greenhouse gases (GHG) and Particulate matter ($PM_{2.5}$) emissions, it is necessary to direct passenger transport from rail to air transport. The use of buses is not suitable due to the greatest impact on Carbon dioxide emissions from transport, and passenger transport by car should be reduced and replaced by other transport modes.

V. CONCLUSION

Transport is an economic activity that records the largest increase in environmental degradation and air quality. The conducted research refers to the analysis of each passenger transport mode on air quality using feed-forward neural

networks. The presented model enables the determination of the impacts of transport modes on air quality.

In order to conduct modeling of the impacts of ANN methodology, the input and output parameters (variables) of the model were defined to determine the impacts of passenger transport mode on air pollution in the period from 2000 to 2014 for the countries of the European Union.

As input parameters were used Passenger kilometers achieved by Passenger cars, Buses and Railways as well as the Number of passengers transported by Air and Waterways. Emissions of Greenhouse gases, Carbon dioxide, Nitrogen oxides, Particulate matter and Sulfur dioxide, respectively, were analyzed as output parameters.

Based on the obtained results, it can be seen that the input parameter RTp (Rail passenger tratransport) has the greatest impact on Greenhouse gases (GHG) and Particulate matter ($PM_{2.5}$) while on the other hand the same input parameter has the least impact on Carbon dioxide (CO_2) emissions. The input parameter PC (Passenger cars) has the greatest impact on Nitrogen oxides (NOx) emissions while has the smallest impact on Sulfur dioxide (SO_2) emissions. BS (Buses) records the largest impact on Carbon dioxide (CO_2) and the smallest impact on the emission of Nitrogen oxides (NOx) from transport. Also, ATp (Passenger air transport) has the largest impact on Sulfur dioxide (SO_2) and the smallest impacts on Greenhouse gases (GHG) and Particulate matter ($PM_{2.5}$) emissions. WTp (Water passenger transport) as an input parameter did not record minimum or maximum impacts on the adopted output variable parameters.

Having in mind the increased demands and needs of the population in the EU, the measures applied by the European Union in order to reduce air pollution are pointed out. Measures to reduce air pollution are being implemented in EU cities. One of the measures is to reduce the use of passenger cars and the use of other transport modes. One of the ways of transporting passengers is public transport. In order to increase the use of public transport to contribute the improvement of air quality in EU cities, it is necessary to replace buses that use conventional fuels with buses that use alternative propulsion technologies.

New technologies for vehicles and transport management will be key to reducing transport emissions in the EU, as in the rest of the world. Delayed action and the shy introduction of new technologies would condemn the EU transport industry to decline irreversibly.

Although in theory the ELM method has proven to be a universal approximator in practice it is significantly important how many samples are available for training; whether there are elements in the data that do not belong to others; and which variables are used as inputs. Therefore, it is necessary to pay attention to get a robust and precise model and prevent too big a mistake.

ACKNOWLEDGMENT

This research was financially supported by the Ministry of Education, Science and Technological Development of the Republic of Serbia.

REFERENCES

[1] http://ec.europa.eu/eurostat/statisticsexplained/index.php/Greenhouse_gas_emission_statistics

[2] European Commission, The State of European Cities: Cities leading the way to a better future, Unhabitat, 2016.

[3] http://www.ecofys.com/en/blog/non-stateactors-account-for-growing-share-ofemission-reductions

[4] S. Kaplanović, “Internalisation of external costs for the purpose of providing sustainable development of road transport“, Doctoral dissertation, University of Belgrade, Faculty of Economics, 2012.

[5] European Commission, White paper on transport: Roadmap to a single European Transport area — towards a competitive and resource-efficient transport system, Publications Office of the European Union, 2011.

[6] I. Kolak, D. Akin, I. Birbil, O. Feyzioglu, N. Noyan, “Multicriteria Sustainability Evaluation of Transport Networks for Selected European Countries”, Proceedings of the World Congress on Engineering 2011, London, U.K., 2011.

[7] N., Bojković, M. Petrović, “Odabrani modeli za politiku transporta i komunikacija”, Saobraćajni fakultet, Beograd, 2015.

[8] H. Guang-Bin, Z. Qin-Yu, S. Chee-Kheong, “Extreme Learning Machine: A New Learning Scheme of Feedforward Neural Networks”, International Joint Conference on Neural Networks, Vol. 2, 2004, pp: 985-990.

[9] W. Dianhui, H. Guang-Bin, “Protein Sequence Classification Using Extreme Learning Machine”, Proceedings of International Joint Conference on Neural Networks, Vol. 3, pp: 1406- 1411, 2005.

[10] R. Engelman, “Stabilizing the atmosphere: population, consumption and greenhouse gases”, Washington DC: Population Action International, 1994.

[11] R. Engelman, “Profiles in carbon: an update on population, consumption and carbon dioxide emissions”, Washington DC: Population Action International, 1998.

[12] O. Neill, C. Brian, F. L. MacKellar, W. Lutz, “Population and Climate Change”. Cambridge University Press, 2001.

[13] M.D. Mamun, K. Sohag, M.A.H. Mia, G.S. Uddin, I. Ozturk, “Regional differences in the dynamic linkage between CO_2 emissions, sectoral output and economic growth”, Renew Sustain Energy Rev, 38, 2014, pp. 1–11.

[14] D. Reckien, J. Flacke, R. J. Dawson, O. Heidrich, M. Olazabal, A. Foley, J. J.-P. Hamann, H. Orru, M. Salvia, S. De Gregorio Hurtado, D. Geneletti, F. Pietrapertosa, Climate change response in Europe: What’s the reality? Analysis of adaptation and mitigation plans from 200 urban areas in 11 countries, Climatic Change, 122 (1-2), 2014, pp. 331–340.

[15] M. B. Arvin, R. P. Pradhan, N. R. Norman, “Transportation intensity, urbanization, economic growth and CO_2 emissions in the G-20 countries”, Utilities Policy, 35, 2015, pp. 50-66.

[16] N. Petrović, N. Bojović, J. Petrović, “Appraisal of urbanization and traffic on environmental quality”, Journal of CO_2 Utilization, Vol. 16, 2016, pp. 428-430.

[17] A. Masih, “Machine learning algorithms in air quality modeling”, Global Journal of Environmental Science and Management, 5(4), 2019, pp. 515-534.

[18] https://ec.europa.eu/transport/facts-fundings/statistics

[19] N. Petrović, “Managing the impacts of urbanization and transport modes on the environment quality”, University of Belgrade, Faculty of transport and traffic engineering, 2018.

THE 5th INTERNATIONAL CONFERENCE
MECHANICAL ENGINEERING IN XXI CENTURY

December 9-10, 2020
Faculty of Mechanical Engineering in Niš, Serbia

Mobility as a Service: Key Topics and Challenges

Tanja ŽIVOJINOVIĆ[a], Nataša BOJKOVIĆ[a], Marijana PETROVIĆ[a], Nikola PETROVIĆ[b]

[a] University of Belgrade, Faculty of Transport and Traffic Engineering, Department for Economy, Management and Organization in Traffic and Transport, 11000 Belgrade
[b] University of Niš, Faculty of Mechanical Engineering, Department of Transport Engineering and Logistics, 18000 Niš
t.zivojinovic@sf.bg.ac.rs, n.bojkovic@sf.bg.ac.rs, marijanap@sf.bg.ac.rs, petrovic.nikola@masfak.ni.ac.rs

***Abstract*— Mobility as a Service (MaaS) represents an innovative concept that enables multi-modal daily travelling. Taking into account user preferences, MaaS combines different transportation options (e.g. public transport, taxi, sharing mobility services, etc.) through a single platform. Starting from the MaaS research findings, this paper summarises the main topics that are enjoying popularity in the scientific discussion. Also, the paper elaborates on key issues and challenges of MaaS running, with special emphasis on operational, social, financial and institutional related issues.**

***Keywords*— digital platform, fully integrated service, MaaS, on-demand transport**

I. INTRODUCTION

Complementarity of different modes of transport catalysed by information and communications technologies have opened up the opportunity for new forms of transport integration. It is about a new approach in the realisation of mobility, so-called Mobility as a Service (MaaS), which is based on the principle that mobility is primarily a user-oriented service. The MaaS concept meets the natural desire of users to have their seamless point-to-point mobility. At the same time, the individual types of transport cease to be in the foreground for the user.

The logic of MaaS is in a way close to the principle of technological neutrality established within the regulation of electronic communications, which essence is not to favour individual transmission technologies [1]. Since the MaaS concept abandons the idea of owning a vehicle and promotes the principle of access, it also strives for service that would be a worthy alternative to free and independent movement by private car.

The added value of MaaS service crucial for its users is based on the concept of the “four Cs” - Costs, Convenience, Choice and Customisation [2]. For customers that means cost savings, accommodation and comfort during the transportation process, a wide range of transportation options, and transportation services tailored to their personal needs.

In this paper, we analyse MaaS concept – its main characteristics, stakeholders and worldwide ventures. The aim is to summarise the main topics regarding MaaS that are enjoying popularity in the scientific discussion. Also, we elaborate on the key issues and challenges of MaaS running, with special emphasis on operational, social, financial and institutional related issues.

The paper proceeds as follow. Section 2 brings elementary of MaaS service: key actors, real-world applications and its main characteristics. In the next section, we have made a systematisation of topics regarding MaaS from the most recent scientific sources. The section after is about critical issues and challenges of MaaS service, following by the concluding remarks.

II. MOBILITY AS A SERVICE CONCEPT

Mobility as a Service (MaaS) represents an emerging concept that enables multi-modal daily travelling. Taking into account user preferences, MaaS combines different transportation options (e.g. public transport, taxi, sharing mobility services, etc.) through a single and specially designed digital platform. MaaS concept enables real-time connectivity and ability of transport supply to meet transport demand promptly – usually right after the user expresses his requirement.

One of the first conceptual explanation of MaaS was given by Sonja Heikkilä in her master thesis. In her opinion Mobility as a Service is *"a system, in which a comprehensive range of mobility services are provided to customers by mobility operators."* [3]. According to the one of the most frequent definition from the literature formed by MaaS Alliance [4], MaaS represents *"the integration of various forms of transport services into a single mobility service accessible on demand."* Detailed overview of 29 actual definitions of MaaS service can be found in the study of Jovic and Baron [5].

MaaS is still in the early stages of the development, and its implementation is currently being realised in the form of pilot projects in most cases, which have been launched in several cities across the globe (Table 1). Pioneer of MaaS implementation in Europe was Gothenburg (Sweden) with its experimental application called UbiGo [6].

TABLE I SELECTED MAAS SERVICE WORLDWIDE*

Launched	MaaS service name	City (country)	Modes
2014	*UbiGo*	Gothenburg (Sweden)	bike-sharing, car-sharing, car rental, urban public transport
2015	*Shift*	Los Angeles (United States)	bike-sharing, car-sharing, car rental, urban public transport
2016	*Whim*	Helsinki (Finland)	bike-sharing, car-sharing, car rental, urban public transport, taxi, e-scooter, ferry
2016	*Optymod*	Lyon (France)	bike-sharing, car-sharing, car rental, rail, urban public transport, taxi + flight, freight transport
2016	*Switchh*	Hamburg (Germany)	bike-sharing, car-sharing, car rental, rail, urban public transport, taxi + ferry
2016	*Moovel*	Hamburg (Germany)	bike-sharing, car-sharing, car rental, rail, urban public transport, taxi
2016	*STIB+Cambio*	Brussels (Belgium)	car-sharing, rail, urban public transport, taxi
2016	*Hannovermobil*	Hannover (Germany)	car-sharing, car rental, rail, urban public transport, taxi
2017	*NaviGoGo*	Dundee (Scotland, United Kingdom)	public transport, taxis, car clubs, bike schemes
2018	*Mobilleo*	Bradford (United Kingdom)	public transport, taxis, ride-hailing
2018	*Qixxit*	Berlin (Germany)	bike-sharing, car-sharing, car rental, rail, urban public transport, taxi + flight, coach
2018	*Bixi/Communauto*	Montreal (Canada)	urban public transport, bike-sharing, car rental
2018	*WienMobil Lab*	Vienna (Austria)	bike-sharing, car-sharing, car rental, rail, urban public transport, taxi
2018	*MobilityMixx*	Almere (Netherlands)	bike-sharing, car-sharing, car rental, rail, urban public transport, taxi
2019	*Zipster*	Singapore (Republic of Singapore)	urban public transport, ride-hailing, bike-sharing
2019	*Jelbi*	Berlin (Germany)	bus, train, motor scooter, electric kick scooter, bike, car and ridesharing
2020	*Yumuv*	Zurich (Switzerland)	urban public transport, car-sharing, e-bike, e-scooter

*Source: compiled by authors, based on different sources

Not long after, this concept was developed in Helsinki (Finland), where was widely recognised as a 'one-click' solution that *"carries the scale of ambition you would more typically expect from a tech start-up and is defining mobility as a service agenda globally"* [7]. Its specialised platform "Whim" started with operation in autumn 2016, and after less than two years recorded one million trips [8].

MaaS operating essentially involves three types of actors: MaaS provider, transport operators (service providers), and customers - MaaS users. There are also additional market actors such as city authorities, IT and data providers, insurance firms, and many others, with no less importance. The major players of the MaaS ecosystem and their mutual relationships are shown in Fig. 1.

Service delivery in MaaS system is done by the MaaS provider that brings together and coordinates the work of various public and private transport operators. The services of different transport providers with multiple modes of transport are integrated through the specialised digital platform.

Using a mobile application or internet platform, the user expresses his preferences and request a ride. As a result, the possible transport options with prices and travel times are displayed. The user can choose whether he wants to pay for one single trip (so-called *pay-as-you-go* or *pay-per-trip*) or to subscribe to a package of services, e.g. on a daily, weekly, monthly or annual basis (partial and full subscription). Accordingly, with a personal user account, the customer is able to do registration, journey planning, booking and payment.

The key elements of the MaaS attractiveness are [10]:

- Personalised principle of service provision, which means that the relationship between the user and the MaaS provider is built in such a way that travel choices can be anticipated and provided concerning individual preferences;
- Simple payment system (cashless, with 'smart' cards or mobile phones) that allows both full and partial subscriptions, as well as *pay-as-you-go/pay-per-trip* option;

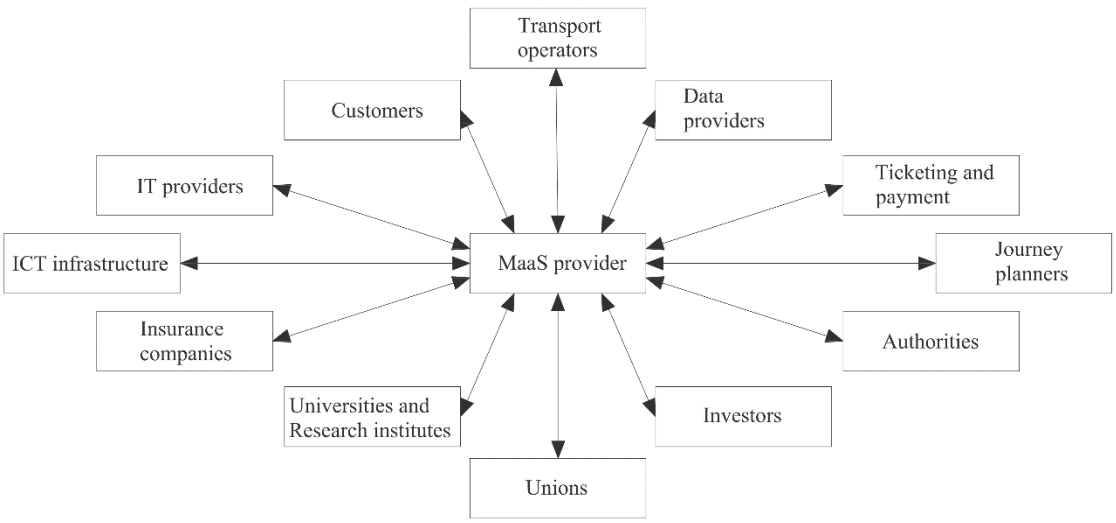

Fig. 1 MaaS ecosystem [9]

- Dynamic travel management - a service that informs users in real-time about the travel plan and possible changes;
- Travel planning that allows the best solutions to be offered while taking into account user' preferences. This function corresponds to Multimodal Journey Planners.

What MaaS conceptually sets apart from similar transport integration initiatives is user care from the beginning to the very end of the journey, including the final stage that is often overlooked – e.g. from the public transport station to the final destination (so-called *last-mile* problem). Another essential component of MaaS is a transfer of travel data, which the MaaS provider distributes to transport operators. Thanks to this joint effort, transport operators can plan their resources to meet individual requirements better and to improve service quality. At the same time, collected data can be useful at higher levels of decision-making, i.e. in the function of infrastructure planning and traffic management.

III. State of the Art – Key Topics on MaaS in the Literature

At this moment, MaaS is very popular in scientific sources. From the appearance of this concept (in 2014), multiple studies have been published in this field so far. After reviewing the literature published, we have made systematisation of main topics that are currently holding attention in the scientific discussions (Table 2). In essence, we distinguish several directions in which the MaaS studies are developing.

TABLE II KEY TOPICS ON MAAS IN THE LITERATURE

Objective(s) of the publication	Source/publication
Conceptualising of MaaS	[11] - [13]
Analysis of stakeholders' perspectives on and expectations for MaaS developments	[14] - [19]
MaaS user preferences and travel behaviour, users' willingness to pay	[20] - [23]
Estimation of the effects of MaaS expansion and MaaS implication on other transportation modes	[24] - [27]
MaaS business models	[28] - [32]
Identification of key issues of MaaS performance	[14], [18], [31], [33]
MaaS review papers	[34] - [37]

Discussion about MaaS terminology and conceptualisation is expounded in the first line of studies. These papers mainly examine the core elements of the MaaS concept, emphasizing the user perspective and sustainability as the most essential parts.

The role and expectation of its various market actors is also a part of MaaS research findings. One of the most important challenges that MaaS facing is how to get that all its actors work together.

Next line of studies focuses on MaaS potential users – their preferences and travel behaviour, as well as their willingness to pay for the new mobility service. Given that MaaS success depends on user acceptability, studies like these are of particular importance. The results of these researches indicate that MaaS primarily can succeed in areas where users are willing to give up a private car.

Another stream in the literature refers to recent papers which give insight about potential implications of MaaS performance on other modes of transport, especially on public transport. The findings of these researches indicate that MaaS can be expanded in different ways with diverse impacts on other transportation modes. What is certain, MaaS development will largely depend on proper regulations and adequate measures.

A part of the reviewed studies is dealing with the analysis of real-life application or potential MaaS business models. This part of literature investigates and evaluates real-world MaaS ventures that are under development or at a pilot phase.

Potential barriers and drivers for MaaS have been discussed in several papers. These studies were also used for overview significant obstacles of MaaS development which are given in the next chapter. Finally, several studies, like this one, provide an overview and analysis of up-to-date scientific papers.

Starting from the research findings, it can be concluded that current literature lacks papers which scrutinise adequate policy support and regulatory framework for MaaS implementation. Also, only few scientific papers relating to the future upgrading of MaaS service (such as electric Mobility as a Service – eMaaS [38], [39]) or its integration with other innovative concepts (like Air Taxi Service [40]) can be found in the literature.

IV. Key Issues and Challenges of MaaS

Since MaaS is a relatively new concept that is still conquering transportation markets, and its ecosystem is very complex, the question is what kind of preconditions have to be met in order for MaaS to experience successful implementation.

The starting point for the MaaS performance in cities is the existence of a wide range of transportation options. This is primarily related to well-developed public transport - the backbone of MaaS, which should allow users to move around easily. Existence of various transportation solutions in the field of sharing mobility is another prerequisite essential for MaaS utilisation [41]. Fulfilment of these conditions led to the fact that Scandinavian cities were the birthplace of the MaaS concept. In [9], authors pointed out some more fundamental requirements of MaaS operation such as physical and schedule integration of modes, spatial and temporal coverage of the service for 24 hours in urban and suburban areas, a strong data privacy policy, etc.

Another precondition for implementation of MaaS is related to relevant and real-time information. A reliable database is a basis for timely informing users, and also for matching supply and demand. For that reason, main participants in the MaaS system must be ready to provide and share information (users about the location, providers about available capacities, prices, etc.). Since the service is provided in the real-time, this condition can be a challenge for service providers, especially for privately-owned ones. According to Shaheen & Cohen [42], these data-sharing partnerships can improve transportation and trip planning, operations, and fare integration.

In the most recent papers ([18], [31]), the authors identified and classified potential barriers to MaaS implementation (Fig. 2). Although these barriers are given for the MaaS schemes in Greater Manchester and Budapest, they can also be seen as general obstacles that any MaaS system can face (before and/or during implementation).

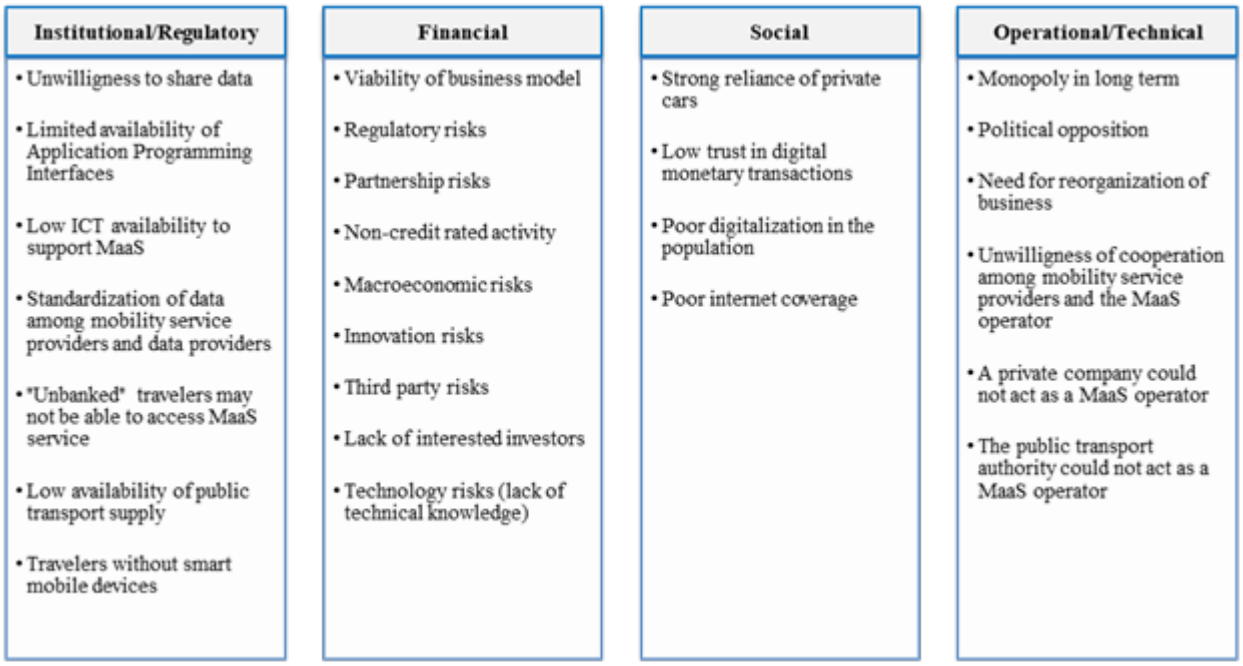

Fig. 1 Barriers of MaaS implementation [18]

The standardisation of data among mobility service providers and data providers and the unpreparedness of transport operators to share data are seen as the most significant operational/technical barriers in MaaS implementation. One of the most critical social barriers of MaaS performance is the strong dependence of people on their private cars. This finding was confirmed by the results of researches [14] and [21], which indicated that high mobility ownership need, as well as low technology adoption, are crucial obstacles to MaaS acceptance.

V. Conclusion

Mobility as a Service is a novel mobility concept which puts customers in the first place, offering them door-to-door mobility solutions that perfectly meet their individual transportation needs. A large number of studies in this area indicate that MaaS is a mobility option that will be increasingly used, especially among the young population since they are familiarised with smart technologies [43].

According to previous knowledge and experiences, MaaS is going to be an influential part of smart mobility. Although more and more countries are starting with MaaS implementation, a large number still have not included this concept in their mobility schemes and planning strategies. Until that happens, this emerging user-oriented approach serves as a mock-up for mobility service design and implementation in the future.

Acknowledgement

This paper is part of the project "Critical infrastructure management for sustainable development in postal, communication and railway sector of the Republic of Serbia", funded by the Ministry of Education and Science of the Republic of Serbia, Project number: TR36022.

References

[1] Bojković, N., Petrović, M. (2018). Uvod u saobraćaj i transport. Beograd: Saobraćajni fakultet. (In Serbian)

[2] Harms, L., Durand, A., Hoogendoorn-Lanser, S., Zijlstra T. (2018). Exploring mobility-as-a-service: insights from literature and focus group meetings. Available on https://maas-alliance.eu/wp-content/uploads/sites/7/2018/11/MaaS-brochure-ENG.pdf (Accessed 01.09.2020.)

[3] Heikkilä, S. (2014). *Mobility as a service-a proposal for action for the public administration, Case Helsinki*. Master's thesis. Aalto University – School of Engineering

[4] MaaS Alliance, White Paper: Guidelines and Recommendations to Create the Foundations for Thriving MaaS Ecosystem, 2017. Available on https://maas-alliance.eu/ (Accessed 03.09.2020)

[5] Jovic, J., & Baron, P. (2019). Implications for improving attitudes and the usage intention of Mobility-as-a-Service–Defining core characteristics and conducting focus group discussions. *Proceedings of International Conference on Mobility as a Service, Tampere, Finland*, 182-197.

[6] Smith, G., Sochor, J., & Sarasini, S. (2018). Mobility as a service: Comparing developments in Sweden and Finland. *Research in Transportation Business & Management*, *27*, 36-45.

[7] Hietanen, S., & Sahala, S. (2014). Mobility as a Service: Can it be even better than owning a car. *ITS Canada*.

[8] https://whimapp.com/history-of-maas-global/ (Accessed 15.09.2020)

[9] Arias-Molinares, D., & García-Palomares, J. C. (2020). The Ws of MaaS: Understanding mobility as a service from a literature review. *IATSS Research*. https://doi.org/10.1016/j.iatssr.2020.02.001

[10] Datson, J. (2016). Mobility as a Service: Exploring the Opportunity for Mobility as a Service in the UK. Transport Systems Catapult, United Kingdom.

[11] Giesecke, R., Surakka, T., & Hakonen, M. (2016). Conceptualising Mobility as a Service: A user centric view on key issues of mobility services. In *International Conference on Ecological Vehicles and Renewable Energies* (p. 7476443). IEEE.

[12] Jittrapirom, P., Caiati, V., Feneri, A. M., Ebrahimigharehbaghi, S., Alonso González, M. J., & Narayan, J. (2017). Mobility as a service: A critical review

of definitions, assessments of schemes, and key challenges. *Urban Planning*, *2* (2), 13-25.

[13] Sochor, J. L., Arby, H., & Karlsson, M. (2017). The topology of Mobility as a Service: A tool for understanding effects on business and society, user behavior, and technical requirements. In *24th World Congress on Intelligent Transportation Systems*, Montreal, October 29-November 2, 2017.

[14] Li, Y., & Voege, T. (2017). Mobility as a service (MaaS): Challenges of implementation and policy required. *Journal of transportation technologies*, *7*(2), 95-106.

[15] Haahtela, T., & Viitamo, E. (2017). Searching for the potential of MaaS in commuting–comparison of survey and focus group methods and results. In *1st International Conference on Mobility-as-a-Service, Tampere, Finland.*

[16] Ho, C., Hensher, D. A., Mulley, C., & Wong, Y. (2017). Prospects for switching out of conventional transport services to mobility as a service subscription plans–A stated choice study. In *International Conference Series on Competition and Ownership in Land Passenger Transport (Thredbo 15). Stockholm, Sweden*, pp.13-17.

[17] Kamargianni, M., Matyas, M., Li, W., & Muscat, J. (2018). Londoners' attitudes towards car-ownership and Mobility-as-a-Service: Impact assessment and opportunities that lie ahead. University College London, London (2018). Retrieved from https://www.ucl.ac.uk/consultants/images/casestudies/maas

[18] Polydoropoulou, A., Pagoni, I., & Tsirimpa, A. (2020). Ready for Mobility as a Service? Insights from stakeholders and end-users. *Travel Behaviour and Society*, 21, 295-306. https://doi.org/10.1016/j.tbs.2018.11.003

[19] König, D., Sochor, J., Eckhardt, J., & Böhm, M. (2016). State-of-the-art survey on stakeholders' expectations for Mobility-as-a-Service (MaaS). In *23rd World Congress on Intelligent Transport Systems, ITS Australia*.

[20] Polydoropoulou, A., Tsouros, I., Pagoni, I., & Tsirimpa, A. (2020). Exploring Individual Preferences and Willingness to Pay for Mobility as a Service. *Transportation Research Record*, 0361198120938054.

[21] Alonso-González, M. J., Hoogendoorn-Lanser, S., van Oort, N., Cats, O., & Hoogendoorn, S. (2020). Drivers and barriers in adopting Mobility as a Service (MaaS)–A latent class cluster analysis of attitudes. *Transportation Research Part A: Policy and Practice*, *132*, 378-401. https://doi.org/10.1016/j.tra.2019.11.022

[22] Hesselgren, M., Sjöman, M., & Pernestål, A. (2020). Understanding user practices in mobility service systems: Results from studying large scale corporate MaaS in practice. *Travel Behaviour and Society*, *21*, 318-327. https://doi.org/10.1016/j.tbs.2018.12.005

[23] Goodall, W., Dovey, T., Bornstein, J., & Bonthron, B. (2017). The rise of mobility as a service: reshaping how urbanites get around. *Deloitte Review*, *20*, 112-129. Available at https://dupress.deloitte.com/content/dam/dup-us-en/articles/3502_Mobility-as-a-service/DR20_The%20rise%20of%20mobility_reprint.pdf (Accessed 30.09.2020)

[24] Rantasila, K. (2015). The impact of Mobility as a Service concept to land use in Finnish context. In *2015 International Conference on Sustainable Mobility Applications, Renewables and Technology (SMART)* (pp. 1-7). IEEE.

[25] Hensher, D. A. (2017). Future bus transport contracts under a mobility as a service (MaaS) regime in the digital age: Are they likely to change? *Transportation Research Part A: Policy and Practice*, *98*, 86-96.

[26] Smith, G., Sochor, J., & Karlsson, I. M. (2018). Mobility as a Service: Development scenarios and implications for public transport. *Research in Transportation Economics*, *69*, 592-599.

[27] Pangbourne, K., Stead, D., Mladenović, M., & Milakis, D. (2018). The case of mobility as a service: A critical reflection on challenges for urban transport and mobility governance. *Governance of the smart mobility transition*, 33-48.

[28] Sarasini, S., Sochor, J., & Arby, H. (2017). What characterises a sustainable MaaS business model. In *1st international conference on Mobility as a Service (ICOMaaS), Tampere* (pp. 28-29).

[29] Eckhardt, J., Aapaoja, A., Nykänen, L., & Sochor, J. (2017). Mobility as a Service business and operator models. In *12th European congress on intelligent transportation systems, Strasbourg* (pp. 19-22).

[30] Aapaoja, A., Eckhardt, J., & Nykänen, L. (2017). Business models for MaaS. In *1st International Conference on Mobility as a Service*. (pp. 8-20).

[31] Polydoropoulou, A., Pagoni, I., Tsirimpa, A., Roumboutsos, A., Kamargianni, M., & Tsouros, I. (2020). Prototype business models for Mobility-as-a-Service. *Transportation Research Part A: Policy and Practice*, *131*, 149-162.

[32] Garcíaa, J. R. R., Havemana, S., Westerhofa, M. W., & Maarten, G. (2020). Business models in the shared electric mobility field: A market overview towards electric Mobility as a Service (eMaaS). In *8th Transport Research Arena, TRA 2020: Rethinking transport-Towards clean and inclusive mobility: Rethinking transport*.

[33] Sochor, J., Eckhardt, J., König, D., & MariAnne, I. C. (2016). Future needs and visions for Mobility as a Service: Insights from European workshops. In *23rd World Congress on Intelligent Transport Systems, ITS Australia*

[34] Kamargianni, M., Li, W., & Matyas, M. (2016). A comprehensive review of "Mobility as a Service" systems. The National Academies of Sciences, Engineering, and Medicine.

[35] Jittrapirom, P., Caiati, V., Feneri, A. M., Ebrahimigharehbaghi, S., Alonso González, M. J., & Narayan, J. (2017). Mobility as a service: A critical review of definitions, assessments of schemes, and key challenges.

[36] Utriainen, R., & Pöllänen, M. (2018). Review on mobility as a service in scientific publications. *Research in Transportation Business & Management*, *27*, 15-23.

[37] Arias-Molinares, D., & García-Palomares, J. C. (2020). The Ws of MaaS: Understanding mobility as a service from a literature review. *IATSS Research*. https://doi.org/10.1016/j.iatssr.2020.02.001

[38] Jnr, B. A., Petersen, S. A., Ahlers, D., & Krogstie, J. (2020). Big data driven multi-tier architecture for electric mobility as a service in smart cities. *International Journal of Energy Sector Management*, *14* (5), 1023-1047, https://doi.org/10.1108/IJESM-08-2019-0001

[39] Reyes García, J. R., Lenz, G., Haveman, S. P., & Bonnema, G. M. (2020). State of the Art of Mobility as a Service (MaaS) Ecosystems and Architectures—An Overview of, and a Definition, Ecosystem and System Architecture for Electric Mobility as a Service (eMaaS). *World Electric Vehicle Journal*, *11*(1), 7. https://doi.org/10.3390/wevj11010007

[40] Rajendran, S., & Srinivas, S. (2020). Air taxi service for urban mobility: A critical review of recent developments, future challenges, and opportunities. *Transportation Research Part E: Logistics and Transportation Review*, *143*, 102090. In Press. https://doi.org/10.1016/j.tre.2020.102090

[41] Arias-Molinares, D., & Palomares-García, J. C. (2020). Shared mobility development as key for prompting Mobility as a Service (MaaS) in urban areas: the case of Madrid. *Case Studies on Transport Policy*. In Press. https://doi.org/10.1016/j.cstp.2020.05.017

[42] Shaheen, S., & Cohen, A. (2020). Similarities and Differences of Mobility on Demand (MOD) and Mobility as a Service (MaaS). *Institute of Transportation Engineers. ITE Journal*, *90*(6), 29-35.

[43] Casadó, R. G., Golightly, D., Laing, K., Palacin, R., & Todd, L. (2020). Children, young people and mobility as a service: opportunities and barriers for future mobility. *Transportation research interdisciplinary perspectives*, *4*, 100107. In Press. https://doi.org/10.1016/j.trip.2020.100107

THE 5th INTERNATIONAL CONFERENCE
MECHANICAL ENGINEERING IN XXI CENTURY

December 9-10, 2020
Faculty of Mechanical Engineering in Niš, Serbia

Smart Technology Application in Spare Parts Management Processes in Company FRITECH

Nikola SIMIĆ, Miladin STEFANOVIĆ, Aleksandar STANKOVIĆ, Goran PETROVIĆ

First Author affiliation: Faculty of Engineering, University of Kragujevac
Second Author affiliation: Faculty of Engineering, University of Kragujevac
Third Author affiliation: Faculty of Mechanical Engineering, University of Niš
Fourth Author affiliation: Faculty of Mechanical Engineering, University of Niš
nikolasimicva@hotmail.com, miladin@kg.ac.rs, aleksandar.stankovic@masfak.ni.ac.rs, pgoran1102@gmail.com

***Abstract*— Information on the status of available resources in company Fritech d.o.o. is invaluable when planning the production process. Media of automatic identification technologies are used as carriers of labels with high data quality and adequate description of assets, in order to ensure a key level of stock visibility. Automatic product identification technologies in the process of work have become an integral part of modern business information systems of a large number of companies, and Fritech must adapt to needs, monitor its performance in order to see its position, advantages and disadvantages. A comparative analysis of the experiences and practices of the application of smart technologies of companies in the environment, provided the information basis for the justification of the application of automatic identification technologies in the storage system of the company Fritech. The material related to decision - making and multicriteria optimization is processed, the problem is set and the concrete application of the TOPSIS method in the selection of the type of automatic identification mark is presented.**

***Keywords*— Automatic identification tehnology, smart, decision making, optimization, TOPSIS.**

I. INTRODUCTION

Changes in society and the economic system also cause changes within the company, primarily due to compatibility and cooperation with the environment. Like companies that have gone through or are in transition, Fritech is implementing radical reforms, within which it should transform the resource monitoring process. This transformation is difficult to perform without adequate use of modern information technologies that provide accurate and timely information on the state of all available resources in the storage function. Given the dynamics of change and continuity of the process as the only solution in the decision-making process in accordance with the basic principles of timeliness and efficiency in the execution of tasks, the use of flexible information systems is imposed. Auto identification technologies in the process of work, they have become an integral part of modern business information systems as a large number of companies. Automatic identification includes the following technologies [3]: BARCODE, OCR (Optical Character Recognition), chip cards, biometric technologies (fingerprints and fingerprints, voice recognition and eye identification) and RFID technology (Radio Frequency Identification). Bearing in mind that BARCODE is the most common [2], and RFID the most advanced technology of automatic identification [4], the emphasis in the paper will be on all aspects of their application.

II. TOPSIS METHOD

The Technique for the Order Preference by Similarity to Ideal Solution (TOPSIS) method was introduced by Hwang and Yoon (1981) according to [1]. The ordinary TOPSIS method is based on the concept that the best alternative should have the shortest Euclidian distance from the ideal solution and at the same time the farthest from the anti-ideal solution. TOPSIS method can be implemented using following steps:

Step 1: Method starts with determination of a *Decision matrix* $X = (x_{ij})_{m \times n}$, in which element x_{ij} indicates the performance of alternative A_i when it is evaluated in terms of decision criterion C_j, (for i = 1, 2, 3,..., m and j = 1, 2, 3,..., n):

$$X = [x_{ij}] = \begin{array}{c} \\ A_1 \\ A_2 \\ \\ A_m \end{array} \begin{array}{c} \begin{array}{cccc} C_1 & C_2 & & C_n \end{array} \\ \begin{bmatrix} x_{11} & x_{12} & \dots & x_{1n} \\ x_{21} & x_{22} & \dots & x_{2n} \\ \vdots & & & \vdots \\ x_{m1} & x_{m2} & \dots & x_{mn} \end{bmatrix} \end{array} ; \quad (1)$$

Step 2: Determine the normalized decision matrix which elements are r_{ij}:

$$r_{ij} = \frac{x_{ij}}{\sqrt{\sum_{i=1}^{m} x^2}} , \quad (2)$$

Step 3: Obtain the weighted normalized decision matrix whose elements are v_{ij} by multiplying each column

j of the normalized decision matrix by its associated weight w_j:

$$v_{ij} = r_{ij} \cdot w_j, \quad (3)$$

Step 4: Determine the positive ideal and the negative ideal solutions:

$$V^+ = (v_1^+, v_2^+, ..., v_n^+) = \{(\max_i \{v_{ij} | j \in B\}), (\min_i \{v_{ij} | j \in C\})\},$$
$$V^- = (v_1^-, v_2^-, ..., v_n^-) = \{(\min_i \{v_{ij} | j \in B\}), (\max_i \{v_{ij} | j \in C\})\} \quad (4)$$

where B and C are associated with the maximization and minimization criteria sets, respectively.

Step 5: Calculate the separation measures (Euclidean metric) from the positive ideal solution and the negative ideal solution. The separation of each alternative from the positive ideal solution is given as:

$$S_i^+ = \sqrt{\sum_{j=1}^{n} (v_{ij} - V_j^+)^2}. \quad (5)$$

The separation of each alternative from the negative ideal solution is given as:

$$S_i^- = \sqrt{\sum_{j=1}^{n} (v_{ij} - V_j^-)^2}. \quad (6)$$

Step 6: Calculate the *relative closeness* of the *i*-th alternative A_i to the positive ideal solution:

$$P_i = \frac{S_i^-}{S_i^+ + S_i^-}. \quad (7)$$

The relative closeness P_i can have values between (0, 1), whereby, $P_i = 0$ represents negative ideal solution, while $P_i = 1$ stands for positive ideal solution. According to P_i values the alternatives can be ranked. The best alternative has the highest value P_i because it is the closest to the positive ideal solution.

III. Case study

Based on all the above, the question arises as to which is more cost-effective for the company, BARCODE or RFID technology. In this chapter, the TOPSIS method will determine the optimal solution of automatic identification for resources in the company Fritech d.o.o.

The following table shows comparative analysis of smart technologies [5].

TABLE I Comparative analysis of technologies

Criteria	1D Barcode	2D Barcode	RFID
Costs	Small	Medium	Very high
Rreading tolerance	High	Medium	Normal
Reading after damage	Not possible	Possible with corrections	Not readable
Reading equipment	Classic equipment	Special scaners	Special tools and equipment
Capacity	Small (15 characters)	Medium amount of data	Huge amount of data
Database access	Not readable	Not readable	Automatic readable
Investments	Relativly cheap	Cheap	Expensive
Standardization	Completely standardized	Completely standardized	Various standards

Based on the table 1, the criteria and alternatives are defined and the initial table 2 of data - alternatives and criteria was formed:

The following criteria are defined:

K1 - STANDARDIZATION
K2 - CAPACITY
K3 - EFFICIENCY
K4 - COSTS
K5 - ADDITIONAL FUNCTIONS.

The following alternatives have been defined also:

A1 - 1D BARCODE
A2 - 2D BARCODE
A3 - RFID

TABLE III Alternatives and criteria

	Criteria				
Alternatives	**K1**	**K2**	**K3**	**K4**	**K5**
A1	complete regulations	small	medium	small	partially exists
A2	complete regulations	medium	high	medium	partially exists
A3	partially regulations	huge	very high	very high	totally exists

After forming the initial table-matrix of initial data, the coefficients are assigned, the values that are minimized and maximized are determined, as well as the weight values are assigned, which is shown in Table 3.

TABLE IIIII Determining the weight of the criteria

	Coefficients				
Alternatives	**K1**	**K2**	**K3**	**K4**	**K5**
	0.1	0.25	0.25	0.3	0.1
A1	5	1	3	1	3
A2	5	3	4	3	3
A3	3	5	5	5	5
Character	max	max	max	min	max

Assignment of coefficients-values of attributes was performed according to the following:

• for K1 STANDARDIZATION - according to existing regulations:
- there are no regulations - 1
- partially there are regulations - 3
- there are complete regulations - 5

• for K2 CAPACITY - represents the amount of data that can be stored in the code:
- small amount - 1
- medium amount - 3
- huge amount - 5

• for K3 EFFICIENCY - according to the performance and efficiency of the device provided in accordance with the technical characteristics prescribed by the manufacturer:

- very small - 1
- small - 2
- medium - 3
- high - 4
- very high –5

• for K4 COSTS - according to the total cost of the device with accompanying consumables:

- small - 1
- relatively small - 2
- medium - 3
- high - 4
- very high - 5

• for K5 ADDITIONAL FUNCTIONS - according to the possibilities provided by the device in accordance with the technical characteristics prescribed by the manufacturer:

- no additional functions- 1
- partially exist - 3
- totally exist - 5.

The allocation of weights for each criterion is determined on the basis of exchange of views with logistics authorities in certain transport companies and amounts to:

• for K1 - 0.1 - considered as the least important because currently regulations are defined and represent a starting point for technology implementation;

• for K2 - 0.25 - presented as an important criterion on the basis of which the choice of technology is examined when managing supplies of spare parts;

• for K3 - 0.25 - presented as an important criterion on the basis of which the choice of technology is examined when managing supplies with spare parts, because it is important to respect the principles of efficient supply;

• for K4 - 0, 3 - presented as the most important criterion on the basis of which the choice of technology is examined when managing supplies of spare parts, because it creates high costs during receipt, storage, issuance, transport and handling;

• for K5 - 0.1 is considered not very important, due to similar solutions that accompany BARCODE devices and RFID technology;.

By forming the initial table-matrix of initial data with the assignment of coefficients, determining the values that we minimize and maximize, as well as assigning weight values, created conditions for applying the method as shown in Figure 1 and according to table 3.

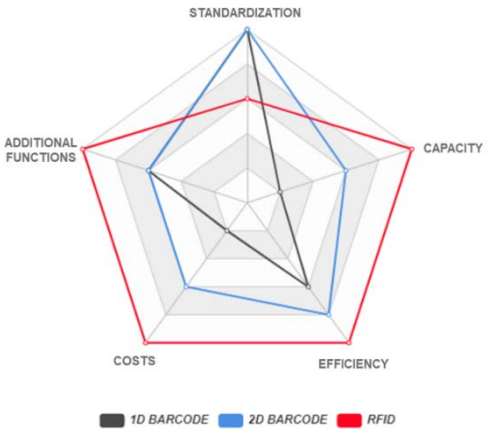

Fig. 1 Display of weight values based on table 3

After that, we determine the values of the criteria, where the values that we maximize-rewrite, and which are minimized-convert to max, and determine the norm, whose values are shown in Table 4:

TABLE IVV NORM VALUES

Coefficients				
K1	**K2**	**K3**	**K4**	**K5**
7.6811457	5.91607	7.07106	4.47213	6.557438

This is followed by the formation of a normalized matrix. This is followed by the determination of weighted values, and the obtained data are shown in Table 5:

TABLE V WEIGHTED VALUES

	Coefficients				
Alternatives	**K1**	**K2**	**K3**	**K4**	**K5**
	0.1	0.25	0.25	0.3	0.1
A1	0.065094	0.04225	0.10606	0.26832	0.04575
A2	0.065094	0.12677	0.14142	0.13416	0.04575
A3	0.039057	0.21128	0.17677	0	0.076249
Best value	0.065094	0.21128	0.17677	0.26832	0.076249
Worst value	0.039057	0.04225	0.10606	0	0.04575

After determining the weighted values, the distance from the ideal and anti-ideal solution is measured, which is shown in Table 6:

TABLE VI DISTANCES FROM IDEAL AND ANTI-IDEAL

	Coefficients				
Distances	**K1**	**K2**	**K3**	**K4**	**K5**
Ideal	0.0650944	0.21128	0.17677	0.26832	0.076249
Anti-ideal	0.0390566	0.04225	0.10606	0	0.04575

Finally, the distance is calculated according to the values shown above and the alternatives are ranked, as shown in Table 7:

TABLE VII FINAL RANKING ALTERNATIVE

Alternatives	S+	S-	proximity to the solution	RANK
A1	0.1857462	0.26958	0.592067	1
A2	0.1652969	0.16453	0.498841	2
A3	0.2695885	0.18574	0.407933	3

The graphical rank of the alternative is shown in Figure 2:

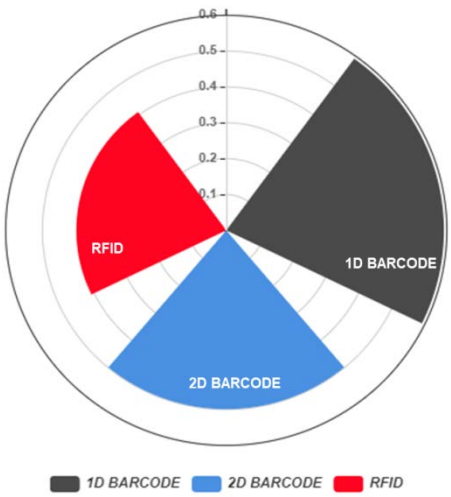

Fig. 2 Graphical representation of the final rank of alternatives by the TOPSIS method

IV. Conclusions

Modern trends in informatics provide many directions in the organization of monitoring, which emphasizes the special importance of quantitative and qualitative monitoring of assets, based on numerous data and reviews that provide management support at all times. The role, significance and place of automatic identification technologies in these processes come to the fore. With the help of BARCODE technology or RFID, provides a handful of data necessary for precise and quality management of processes in the system, which conclude next:

- Real possibility of applying smart technologies on spare parts in Fritech d.o.o.
- Adequate choice of smart technologies with the goal of minimum costs.

Spare parts are a type of asset that can be found relatively easily in the maintenance sector, and tagging them would be considered a job already done in the manufacturer's company. The problem of introducing some of the smart technologies appears at a high cost, which is reflected in marking, storage, tracking and manipulation, and company Fritech is increasingly striving for cheaper technologies. By applying the method of multi-criteria decision-making, the results of selecting the type of labels of automatic identification technologies in accordance with the needs of the company Fritech were obtained. The material related to decision-making and multi-criteria optimization is processed, the problem is set and the concrete application of the TOPSIS method in the selection of the type of label is presented. Based on the obtained research results, the facts were confirmed that due to the minimum cost criterion, the analysis result shows that 1D BARCODE is the optimal solution for introduction into the system of the company Fritech.

The scientific contribution of this project lies in a new theoretical approach, defining the place, role and importance of automatic identification technologies in spare parts management processes, where a comparative analysis of BARCODE and RFID technology is performed in one place and a model of multicriteria optimization is proposed, which offers an optimal solution for the application of automatic identification technology in company Fritech. In addition, the professional contribution of the project is reflected in the practical fields of application of automatic identification technologies in company Fritech, which will increase efficiency and loss reduction, provide solutions to reduce the number of workers and "reduce the volume of logistics resources strain", and will have a special contribution in situations where information availability and accuracy information of inestimable importance for decision making.

References

[1] C.L. Hwang & K. Yoon, “Multiple Attribute Decision Making Methods and Applications”, Berlin: Springer Verlag, 1981.

[2] F. Al-Saedi & A. Al-Bayaty, *“Development of a Barcode Reader System”*, International Journal of Emerging Trends & Technology in Computer Science 30(1), pp.50-58, December 2015, DOI: 10.14445/22312803/IJCTT-V30P109

[3] R.M. Rathod and others “Review on 1D & 2D Barcode with QR Code Basic Structure and Characteristics”, IJSRD, Vol.1, Issue 11, 2014, ISSN: 2321-0613.

[4] R. Want, “An introduction to RFID technology”, IEEE Pervasive Computing 5(1), pp.25 – 33, February 2006, DOI: 10.1109/MPRV.2006.2

[5] S. Sremac and others “Information technologies for automatic identification of goods in transport”, XVIII Telecommunication Forum TELFOR, ISBN 978-86-7466-392-9, pp. 43-46, November 2010.

Theoretical and applied mechanics and mathematics

THE 5th INTERNATIONAL CONFERENCE
MECHANICAL ENGINEERING IN XXI CENTURY

December 9-10, 2020
Faculty of Mechanical Engineering in Niš, Serbia

Mathematical Model of Bone Cells Adaptation on External Signals

Julijana SIMONOVIĆ

Department of Theoretical and Applied Mechanics, Faculty of Mechanical Engineering, University of Nis, A.Medvedeva 14, 18000 Niš, Serbia
julijana.simonovic@masfak.ni.ac.rs

***Abstract*— Based on bone mechanobiology research, this paper develops computational analytical models in order to address and better understand mechanotransduction - the molecular mechanisms by which bone cells sense and respond to mechanical signals. Downstream autocrine and paracrine signalling in response to periodic excitation were modelled by cell population system of ordinary differential equations in order to better represent and predict long-term behaviour and consequences of bone cell loading. The S-system (the generalized Lottka-Volterra system) is in charge and is solved deterministically together with its stochastic analog (Gillespie algorithm) used for cross-correlation analysis of the parameters. This research clearly shows the indispensability and beneficial effects of external excitation on balanced and regular bone cell activities.**

***Keywords*— dynamics of bone cells, external periodic excitation, stochastic and deterministic analysis, generalized forced Lotka-Volterra Model.**

I. Introduction

The architecture and quality of bone tissue in an adult organism predominantly depends on bone cellular organisation and communication processes that are highly driven by external mechanical loading. How physical forces and changes in the mechanical properties of cells and tissues contribute to development, cell differentiation, physiology, and disease, in general, is a major interest of mechanobiology. The bone adaptive mechanobiological processes are governed by the cellular populations: osteoblasts, osteoclasts, and osteocytes working in concert, all capable of transducing mechanical strain signals into biochemical cues for osteogenesis [1, 2]. However, Osteocytes (OcY), in particular, have been shown, in vitro, to be the most mechanosensitive bone cell type, demonstrating a higher intrinsic sensitivity to loading than other osteogenic cells [3]. They have also recently been shown to direct osteogenesis in other bone cell types, reinforcing the theory that osteocytes sense mechanical loading in the bone matrix and then orchestrate the adaptive bone remodeling response [4]. Owing to their presence deep within bone matrix, direct experimental observation of osteocytes in vivo has proven extremely challenging. As such, the precise mechanical stimuli, which they experience in vivo, and the mechanisms whereby they sense and transmit these stimuli, remain unknown. Although it is possible to mechanically stimulate bone and quantify the tissue-level changes that occur, it is still extremely challenging to simultaneously delineate the cellular and molecular mechanisms that give rise to these changes.

This paper outlines how mathematical models can help to improve current understanding of bone cellular mechanobiology. The paper introduces an adapted mathematical model for bone remodeling that maintains those fundamental mechanisms captured in previous models [5-10], while incorporating biological aspects of bone mechanosensitivity that have not previously been mathematically considered. In particular, this model includes osteocytes mechanobiology, which, apart from their biochemical processes and their interactions with other bone remodeling cells, includes external periodic signal transduction and influence that represents a significant advance to the field.

From the mathematical point of view, this paper represents a contribution to the research of application and analysis of the generalized nonhomogeneous Lottka-Volterra system with the periodicity of power low coefficients.

II. Mathematical model

A. Homogeneous model

Bone remodelling is the continuous process of resorption and formation occurring in the skeleton of vertebrates throughout their life. Remodelling is accomplished by highly coordinated groups of bone-forming osteoblasts (OBs) and bone-resorbing osteoclasts (OCs) that work together in the so-called “basic multicellular units” (BMUs). Many bone disorders such as osteoporosis, Paget's disease and cancer-related bone diseases can be ascribed to imbalances between resorption and formation. However, exactly how this balance is achieved during normal bone turnover is still unclear. In the last decade a large number of regulatory factors produced by hormonal glands, tumour cells, immune cells, and mechano-sensing bone cells (osteocytes (OcYs) and bone lining cells) influencing different phases of bone remodelling have been identified. To address the question of how different bone cells interact with each other and the bone microenvironment during remodelling, several cell population models have been proposed in [5]-[10].

These types of models are able to monitor changes in cell numbers and bone volume over time.

The formalism of a cell population model can be generalised to be of the form of a S-System of equations of nth order that corresponds to the number of included cellular lineages:

$$\frac{du_i}{dx} = \alpha_i \prod_{j=1}^{2} u_j^{g_{ij}} - \beta_i u_i, i = 1, 2, \dots, n. \qquad (1)$$

Where $\alpha_i$represents formation rate and β_i degradation rate of cells` lineages per day and $g_{ij}$ effectiveness of cells` autocrine or paracrine signalling which are dimensionless parameters. Characterization of the parameters of an established mathematical model is difficult, given its dependency on the accuracy and availability of experimental in-vivo/vitro data. However, proposed mathematical model can be used for check of parameters ranges that can ensure biological model accuracy. There exist a steady-state solution of the system that can be determined and analyzed [8], mathematically it represents self-sustained oscillation of limit cycle and biologically balanced preservation of bone content. In one cycle of targeted remodeling the number of activator cells, both resorbing and forming, is bounded above by approximately 10 OCs and up to 300 OBs around 100 days. Having in mind this constrictions we can conclude that in the dynamics of system (1) the number of OCs drops below one, which occurs frequently. Of course, since we are dealing with exact numbers of cells, such a measurement is unrealistic. Critically, the problem stems from the direct use of differential equations that assume a modelled population is large enough, for a continuum hypothesis to approximately hold. This hypothesis is obviously invalid at such small population sizes. Thus, for such low numbers of cells it is more correct to produce a discrete interaction model. Specifically, we use a stochastic framework, Fig 1., to simulate the creation and degradation, which encapsulates the noisy features of individual cell division and death [11]-[13].

Fig. 1 Schematic diagram of how the next action in a stochastic simulation is calculated. The probabilities of all actions (creation and degradation of OC and OB, and/or OcY embedding) are calculated using the Law of Mass and Action and subsequently normalized to lie within [0, 1]. A uniformly random variable U is chosen between zero and one. Wherever this lies in the interval, this will choose the next action to occur, namely "Degradation of OC".

Using the proposed formalism from Fig 1. we are able to extract the stochiometric creation and degradation relations for system (1), and present its probabilistic analogue:

$$u_i + u_j \xrightarrow{\alpha_i} 2u_i + u_j, u_i \xrightarrow{\beta_i} \emptyset, i = 1, 2, \dots, n \text{ and } j \neq i. \qquad (2)$$

Using the mentioned constraints of cell number per remodelling cycles and 1000 simulations of stochastic model (2) we obtain the cross-correlation diagrams for parameters range presented on Fig 2.

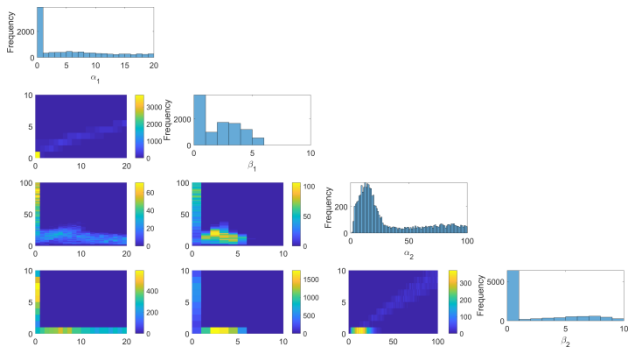

Fig.2 The cross-correlation simulations of the formation/degradation rate parameters. Specifically, a more yellow value suggests that the parameters are more likely to be chosen from this region of the parameters ranges. Four uniformly random variables from intervals: $\alpha_1 \epsilon [0; 20]$, $\beta_1 (\beta_2) \epsilon [0; 10]$ i $\alpha_2 \epsilon [0; 100]$ have been used to simulate the solutions of the Eq. (1). All accepted and presented solutions satisfy conditions: $OC_{max} < 20$, $80 < OB_{max} < 120$; $OB > 1$ after 1 day, and $OB < 5$ and $OC < 1$ for $t > 200$.

The presented cross-correlation of parameters corresponds to the basic system (1) of 3rd order when only OC and OB contribute to the bone turnover as it was analysed by multi-parametric analysis also in the paper [14]. The Fig.3 presents benchmarking of the OC and OB time series obtained deterministically as a result of system (1) and with stochastic simulations form model (2) . In a one cycle of remodelling there is good agreement of results since the average trajectory of stochastic simulation absolutely corresponds to the deterministic solution, bottom diagrams of Fig.3. However, in the next cycle, the population density is insufficient to start a stochastic process. This situation moves us further to the in/vivo/vitro experimental evidence that bone remodelling is not a self-sustained process rather it is strongly forced by an external signal.

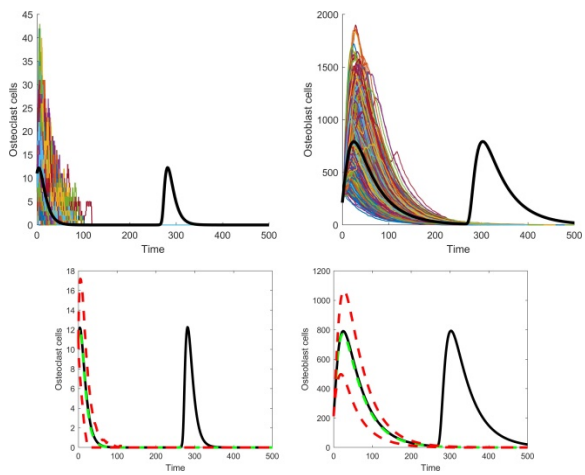

Fig. 3: Top: 1000 stochastic simulations (colored lines, extinct after the first cycle) and 1 deterministic simulation (thick black line, periodically repeated) of the OB-OC model. Initial conditions are constantly (11; 212) in all simulations. Bottom: The black line is the same deterministic line illustrated in the top images. The green dashed line is the average trajectory extracted from the 1000 stochastic simulations. The red dashed lines show one standard deviation about the mean.

In the next chapter we present results of stochastic simulations to investigate whether the model can capture the essential autocrine, paracrine and synergistic characteristics of bone cell communication processes under external excitation.

B. *Non-Homogeneous model*

If we include osteocytes OcY (Ss), OBs (Bs), OCs (Cs) and preosteoblastic (Ps) lineages of cells together with a bone mass equation the system (1) will be system of 5th order ($n = 5$). For this case system (1) of 5th order is a homogeneous system of coupled ordinary nonlinear differential equations that are more specifically described in [9], where the interested reader can find also explanations of all the parameters' biological meaning and experimental values. Although parameter values exist in the literature they are mainly approximate and are proposed to simplify and justify the model. Further, in all of the literature it is assumed that the γ_{ij} parameters are constant. However, in real bone remodelling processes the γ_{ij} parameters may depend on time and other factors. Unfortunately, these parameters cannot be directly measured and have to be estimated. Thus, although initially we consider constant parameters (which simplifies the mathematical treatment and gives a high level of approximation but is useful as a benchmark for model validation), we later adapt the first equation of (1) to include the additional time dependant terms, which are based on the in-vitro experiment of loaded OcYs cell culture. The modification of the model was in editing the power term γ_{31} to time dependent oscillatory function $\gamma_{31}(1 + \sin(\theta t))$, which represents transduced signal of OcY, and inserting the mechanical periodic excitation $A(1 - \cos(\theta t))$ to the responding OcYs into the following form:

$$\frac{dS}{dt} = \underbrace{\alpha_1}_{OB\,embbeding\ rate} B^{\gamma_{31}(1+\sin\theta t)}\left(1-\frac{S}{K_s}\right)_+ + A(1-\cos\theta t) \tag{3}$$

where K_s is the osteocyte carrying capacity.

The frequencies, θ, of the received and transduced signal are same in both functions but with some delay represented as phase shifting of $\pi/2$ or π in the following simulations.

III. Results and Discussion

The simulations eventually stops, when $S = K_s$ because the term $(1 - S/K_s)_+$ evaluates to zero and all dynamics stop, which is highly artificial. However, going forward, we simply consider the production rate of S proportional to $(1 - S/K_s)$, whether positive or negative. This means that the number of OcY (S) is unrestricted and the simulations are observed to have small oscillations around $K_s = 200$ cells per remodeling cycle (blue line on diagrams of Fig.4 a)). Basically, this means that we assume there are a certain number of OcY ready to receive and send external signals and to open cell signaling channels in response to loading.

Many of the published bio/mathematical models represent only free dynamics of the bone cells although the evidence of external loading importance already widely exists. By presenting an experimentally evidenced mathematical model of bone, which includes externally forced turnover, we contribute to the realism of modelling. Critically, we approach the modelling through both deterministic and stochastic methods, which allow us to consider the intrinsic noisiness of the discrete process.

Starting from a set of homogeneous coupled ordinary nonlinear differential equations, and a biologically relevant set of parameter ranges, we are able to derive an analogous stochastic framework. Although the observed dynamics are similar, intrinsic noise produces fluctuations that drive the system toward more realistic descriptions of the process itself. Based on evidence from in-vitro experiments we incorporated both received and transduced signal as periodic rate transitions into the model (3). We find that the model can capture the essential autocrine, paracrine and synergistic characteristics of bone cell communication processes in response to the external incentives.

Specifically, including oscillatory signals with small delays between received and send a signal by OcY provides the closest matches between mathematical data and biology theory. This is straightforward to conclude from Fig 4 c) where, after the period of resorption (the depression of the green line below zero), we observe a significant activation of osteoblasts that results in a formation period (the green line is above zero). Comparing the green line in Fig 4 c) with the green line in Fig 4 a) (which has no over formation) we demonstrate that under the influence of the external periodic signal the local formation of the newly remodelled bone will exceed the amount of resorbed old bone. Furthermore, we investigated the relation between the strength of these two signals and got satisfactory results when the received signal has a smaller value of amplitude. This is our prediction from the model, which has to be addressed experimentally. Namely, we require experiments that explore the magnitudes of information that OcY receives and explores. However, we showed that the steady-state value of total bone content changes depending on the external excitation and also on the interplay of other parameters value that influences the dynamics of the process.

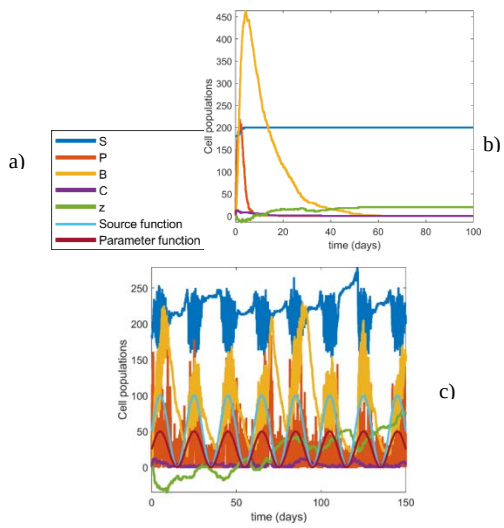

Fig 4. a) Legend for both figures. b) The number of osteocytes (OcY) is restricted to a maximum of 200 cells and diagram correspond to the same system of equations (1) of 5th order without external signaling c) The number of OcY is unrestricted and has small oscillations around a number of 200 and external excitation to both the parameter and the source with a source strength is $A = 10$ and without delay.

IV. Conclusions

Based on bone mechanobiology research, this paper develops computational analytical models in order to address and better understand mechanotransduction - the molecular mechanisms by which bone cells sense and respond to mechanical signals. Downstream autocrine and paracrine signalling in response to periodic excitation were modelled by cell population system of ordinary differential equations in order to better represent and predict long-term behaviour and consequences of bone cell loading. The S-system (the generalized Lottka-Volterra system) is in charge and is solved deterministically together with its stochastic analog (Gillespie algorithm) used for noise check and system behavior dynamics analysis. Population dynamics are illustrated using time series plots, phase portraits, histograms and bifurcation diagrams. In-silico experimenting with a number of responding cells which is up to or around a certain threshold allows us to distinguish and describe different dynamics and relations between involved cells. The external signal can be considered as an additional term affecting the number of responding cells or as the functional periodicity of power low coefficients affecting autocrine signalling of forming cells. This research clearly shows the indispensability and beneficial effects of external excitation on balanced and regular bone cell activities.

Acknowledgment

Some of the results were part of research on project MMoBEER (nov.2017-nov.2019) that has received funding from the European Union's H2020 MGA MSCA-IF-2016 under grant agreement No. 752793.

The part of this research was also financially supported by the Ministry of Education, Science and Technological Development of the Republic of Serbia.

References

[1] Giorgi M, Verbruggen SW, Lacroix D. In silico bone mechanobiology: modeling a multifaceted biological system. Wiley Interdiscip Rev Syst Biol Med. 2016 Nov;8(6), pp.485–505.

[2] Atkins A, Milgram J, Weiner S, Shahar R. The response of anosteocytic bone to controlled loading. J Exp Biol. 2015 Nov; 218(Pt 22), pp. 3559–69.

[3] Yavropoulou MP, Yovos JG. The molecular basis of bone mechanotransduction. J Musculoskelet Neuronal Interact. 2016 Sep;16(3), pp. 221–36.

[4] Bonewald LF. Osteocytes: a proposed multifunctional bone cell. J Musculoskelet Neuronal Interact. 2002 Mar;2(3), pp. 239–41.

[5] Komarova SV, Smith RJ, Dixon SJ, Sims SM, Wahl LM. Mathematical model predicts a critical role for osteoclast autocrine regulation in the control of bone remodeling. Bone. 2003 Aug;33(2), pp. 206–15.

[6] Pivonka P, Komarova SV. Mathematical modeling in bone biology: from intracellular signaling to tissue mechanics. Bone. 2010 Aug;47(2), pp. 181–9.

[7] Pivonka P, Zimak J, Smith DW, Gardiner BS, Dunstan CR, Sims NA, et al. Theoretical investigation of the role of the RANK-RANKL-OPG system in bone remodeling. J Theor Biol. 2010 Jan;262(2), pp. 306–16.

[8] Jerez S, Chen B. Stability analysis of a Komarova type model for the interactions of osteoblast and osteoclast cells during bone remodeling. Math Biosci. 2015 Jun;264, pp. 29–37.

[9] Graham JM, Ayati BP, Holstein SA, Martin JA. The role of osteocytes in targeted bone remodeling: a mathematical model. PLoS One. 2013 May;8(5):e63884.

[10] Buenzli PR. Osteocytes as a record of bone formation dynamics: a mathematical model of osteocyte generation in bone matrix. J Theor Biol. 2015 Jan;364, pp. 418–27.

[11] Kampen V. Nicolaas Godfried. Stochastic processes in physics and chemistry. Volume 1. Elsevier; 1992.

[12] Gillespie DT. Stochastic simulation of chemical kinetics. Annu Rev Phys Chem. 2007;58(1):35–55. https://doi.org/10.1146/annurev.physchem.58.032806.104637 PMID:17037977

[13] Belmonte-Beitia J, Woolley TE, Scott JG, Maini PK, Gaffney EA. Modelling biological invasions: individual to population scales at interfaces. J Theor Biol. 2013 Oct;334:1–12. https://doi.org/10.1016/j.jtbi.2013.05.033 PMID:23770401

[14] Simonovic J., Simultaneous multi-parametric analysis of bone cell population model, New Trends in Nonlinear Dynamics, Proceedings of the International Nonlinear Dynamics Conference (NODYCON 2019), Volume III, Editors: Lacarbonara, W., Balachandran, B., Ma, J., Tenreiro Machado, J.A., Stepan, G. (Eds.), Springer Nature Switzerland AG 2020, pp. 233-241.

THE 5th INTERNATIONAL CONFERENCE
MECHANICAL ENGINEERING IN XXI CENTURY

December 9-10, 2020
Faculty of Mechanical Engineering in Niš, Serbia

Running with Nonlinear Sciences – Nonlinear Mechanics and Nonlinear Dynamics

Katica STEVANOVIĆ HEDRIH

Mathematical Institute of Serbian Academy of Sciences and Arts, Belgrade, Serbia and Faculty of Mechanical Engineering at University of Niš, Serbia
khedrih@sbb.rs

***Abstract*— It's been half a century since I've been running around and with Theoretical and Applied Mechanics, Nonlinear Oscillations, Non-linear Dynamics, as well as in general in Nonlinear Sciences. The impressive symposia and congresses of the International Union of Theoretical and Applied Mechanics (IUTAM), EuroMech Society, as well as the ICNO Conferences of the states of the former Eastern Bloc, or the Conference Series on Nonlinear Mechanics in Shanghai, China, should be noted. Also, must to listed following important Congresses: ICTAM Haifa 1993, Warsaw 2004, Adelaide 2008, Beijing 2012, Montreal 2016, World Congress of Nonlinear Analysits (IFNA WCNA) Orlando 2004 in America, et al. I dedicate this historical paper to School of asymptotic methods of nonlinear mechanics Krilov-Bogolyubov-Mitropolski, a group of the world important scientists, outstanding persons and academicians at the Soviet and Ukrainian Academies of Sciences, and on the occasion of the eleventh decade since birthday of Nikolay Nikolaevich Bogolyubov, great Soviet mathematician and mathematical physicist who has made important contributions in many areas of nonlinear sciences. My start of the running with Nonlinear Sciences in next half a century is foinded in the world known School of asymptotic methods of nonlinear mechanics Krilov-Bogolyubov-Mitropolski, by supervision by Yu.A. Mitropolski and by Professor Danilo P. Rašković. History of development of Mechanics at Faculty of Mechanical Engineering University of Niš should be shortly presented.**

***Keywords*— Nonlinear Sciences, Nonlinear Dynamics, Scientific meetings, History, Scientific legates, Asymptotic methods of nonlinear mechanics Krilov-Bogoqyubov-Mitriopolski.**

I. Introduction

It's been half a century since I've been running around and with Theoretical and Applied Mechanics, Nonlinear Oscillations, Non-linear Dynamics, as well as in general in Nonlinear Sciences. I received my guidance from the wonderful scientists of my professors, Danilo P. Rašković [26, 31] and of academician Yuri Alekseyevich Mitropolski [19-23]. In this commitment to Nonlinear Sciences, I was a “marathon runner”, targeting more than half a century on the course, meeting many scientists with more or less significant scientific legacies in different area of Nonlinear Sciences.

The impressive symposia and congresses of the International Union of Theoretical and Applied Mechanics (IUTAM), EurMeh Sociery, as well as the ICNO Conferences of the states of the former Eastern Bloc, or the Conference Series on Nonlinear Mechanics in Shanghai, China, should be noted. Also, must to listed following important Congresses, I was participated: ICTAM Haifa 1993, Warsaw 2004, Adelaide 2008, Beijing 2012, Montreal 2016, World Congress of Nonlinear Analysts (IFNA WCNA) Orlando 2004 in America, et al. The last of these, of course, is NODYCON 2019 in Rome (400 participants) organized by W. Lacaebinara, and the All-Russian Congress TAM UFA 2019 (1000 participants) in the Russian Federation.

The series of symposiums of Non-linear Mechanics, Non-linear Sciences and Nonlinear Dynamics held in Serbia and Yugoslavia, starting at 1984, certainly lag behind the number of participants, but not by the scientific results presented there.

Running with Nonlinear Sciences, I met and now known many outstanding non-linear science creators, researchers and felt honored, not only to know them, but also because they showed my attention as well as respect for my scientific results to Theoretical and Applied Mechanics and Nonlinear Dynamics as well as in general Nonlinear Sciences, and if I come from Yugoslavia is still today a small state of Serbia, which has long been a villa under groundless aggression, bombing and blockades. I ran to "catch up", the annexes steadily walked and innovated and contributed their scientific results to Nonlinear Science, to which we were all devoted and loving, and our meetings with colleagues inspired us to come up with new results. In this “marathon” course for more than half a century, I would single out the encounters with: Danilo P. Rašković, Tatomir P. Andjelić, Yuri A. Miropolski, Vladimir Matrosov, V. Lashmikantham, Giuseppe Reg, S.T. Ariaratnam, Vitaliy V. Rumyantcev, Chien Wei-Zang, Tomoaki Kawaguchi, Richard Hetnarsky, Hans Trager, Vladimir Beletski, Ilya Blekhman, Ali Nayfeh, Pavel Harlamov, Oleg A. Goroshko, Alexaned Nakonechniy, Jam Awrejcewicz, Tenreiro Machado, and others. Of the younger generation, I am certainly honored to have met the remarkable Walter Lacarbonara, a NODYCON 2019 organizer.ers

II. Short history of Nonlinear sciences

Let us begin this running with elements of the history of the emergence of a special field of general Sciences

named Nonlinear Sciences, whose methods and phenomena have been extended to all fields of science. Thus, the Nonlinear Dynamics as a fundamental part of Nonlinear Sciences has grown into an independent area of science, and today its findings are applied in almost all fields of science, both, natural-mathematical, engineering, bio-medical, and social sciences.

G. Rega writes initially in his article [27] on Nonlinear dynamics in mechanics and engineering:

"Interest toward nonlinear oscillations in mechanics started with Huygens' studies on pendulum dynamics and with the n-body problem in celestial mechanics (which goes back to Kepler, Newton, Lagrange and Poincaré), and continued with the observation of nonlinear phenomena in a number of nineteenth-century industrial applications, for which particular methods fitted to the analytical solution of specific problems were elaborated. In the early twentieth century, there was an important phase of growth, marked by the achievements of two eminent engineers. Georg Düffing [4] is the mechanical engineer who, moved by the interest to solve practical vibration problems, formulated a nonlinear equation later on generalized to represent archetypal oscillators of reference for the analysis of a great variety of dynamical systems. In turn, Balthasar van der Pol [19, 26] is the electrical engineer who obtained important results on self-sustained, and in particular relaxation, oscillations in connection with radio engineering applications, where he also observed "an irregular noise" [49] in certain frequency ranges, likely making the first experimental observation of deterministic chaos. Van der Pol's equation [90] has become another classical equation in nonlinear vibrations. In parallel and more general terms, dynamical system theory originated in the late nineteenth century with Henri Poincaré, who is considered the father of modern nonlinear dynamics, and later on developed mostly within the mathematical community".

Here, we will look at the *a*chievements of scientists from Ukraine and Russia, and in particular The stability theory of Alexander Mikhailovich Lyashunov (June 6 [O.S. May 25] 1857 - November 3, 1918). At the time of his work at Kharkov Polytechnic, in present-day Ukraine, at the Kharkov Polytechnic Museum, we encounter a galaxy of Kharkiv scientists, whose monographs on oscillations of discrete and continuous systems have played a significant role in transferring knowledge of oscillation theory and in general into Nonlinear Sciences.

Among the most magnificent scholars and scientists, whose scientific legates are hidden, in this some important certainly is Alexander Lyashunov with his Theory of Stability, without whose application in studies of all area of the nonlinear sciences as well as in dynamics of the nonlinear system is impossible. Also, scientific legate of the physicist Lav Landau (rus. Lev Davidovich) Landau; Baku, January 22, 1908 - Moscow, April 2, 1968) Nobel Prize winner, who studied the dynamics and properties of super fluidic materials is very important Kharkov and world scientist.

Alexander Michailovich Lyapunov gave the basis of the theory of motion stability which is important in all critical stationary and no stationary states of dynamics in nonlinear systems, passing between different qualitative behaviors. This basis theory of motion stability is in large applications in different area of nonlinear science.

Julius Henry Poincaré give important scientific results into Theory of local and global analysis of nonlinear differential equations, and his earlier 'detection' of chaos in 'simple' mechanical systems are fundamentals of the nonlinear science of nonlinear and complex systems.

Here, we highlight important role of a monograph entitled Theory of Oscillations [1] by three authors Andronov, A.A., Witt, A.A., Khaïkin, S.E., who contributed to the development of science in this field by their scientific results. We emphasize the importance of finding solutions to nonlinear differential equations with solution analysis and stability, as well as numerous graphical and qualitative parameters analyzes of the dynamics of nonlinear systems. For me, in my development as scientist, and in stepping and running with nonlinear sconces the contents of this monograph represented the basis from which, 1967, I set out for Nonlinear Dynamics. To this I add the excellent monograph by Kauderer Nonlinear Mechanics in German and also first monograph Theory of Oscillations [26] written in Serbian language by my Professor of all area of Mechanics Danilo P. Rašković (see Refs [1-3,19-23]).

III. The School of the Asymptotic Methods of Nonlinear Mechanics Krylov – Bogoliubov – Mitropolski

Asymptotic methods of nonlinear mechanics Krylov – Bogoliubov – Mitropolski (see References [2, 3, 19-23]) and the school of the same name in Kiev, to the knowledge of my Professor, Dr. Ing and Mathematics Degree Damilo P. Rašković [42] was evaluated in 1967 as the most promising for the education and guidance of a young and talented researcher and teaching assistant, who should be directed toward Nonlinear Oscillations. So, to me, Professor Rašković suggested that I do graduate work in Mechanical Engineering from nonlinear oscillations, and I suggested the topic: "Nonliear oscillations and applications to nonlinear system with automatic control" [29]. I successfully defended my diploma work and received the award of Electronic Industry for the best diploma thesis done that year at the Technical and Natural-Mathematical Faculties of Yugoslavia.

Today, Professor G. Rega in reference [27] evaluates asymptotic methods of Nonlinear Mechanics of KBM:

"The Krylov–Bogoliubov–Mitropolski school (at Kiev) (see References [2, 3, 19-23] and Figure 1) searched for the solution of equations of nonlinear systems via analytical (i.e., quantitative) methods, mostly dealing with problems in nonlinear mechanics. Around the middle of the twentieth century and mostly in the 1960s and 1970s, novel theoretical ideas and perspectives (e.g., the topological one), and the innovative contributions of computer science, determined an 'explosion' of dynamical system theory, with the strong affirmation of the role of models and the importance of the nonlinear domain, along with intense interactions developed throughout physical and mathematical sciences. Distinct, yet interconnected, theories were developed (of bifurcation, catastrophe, complexity, chaos, fractals, turbulence), with applications to a wide variety of disciplines including not only physics and engineering but also chemistry, biology, neurology, astronomy, geophysics, meteorology and economics".

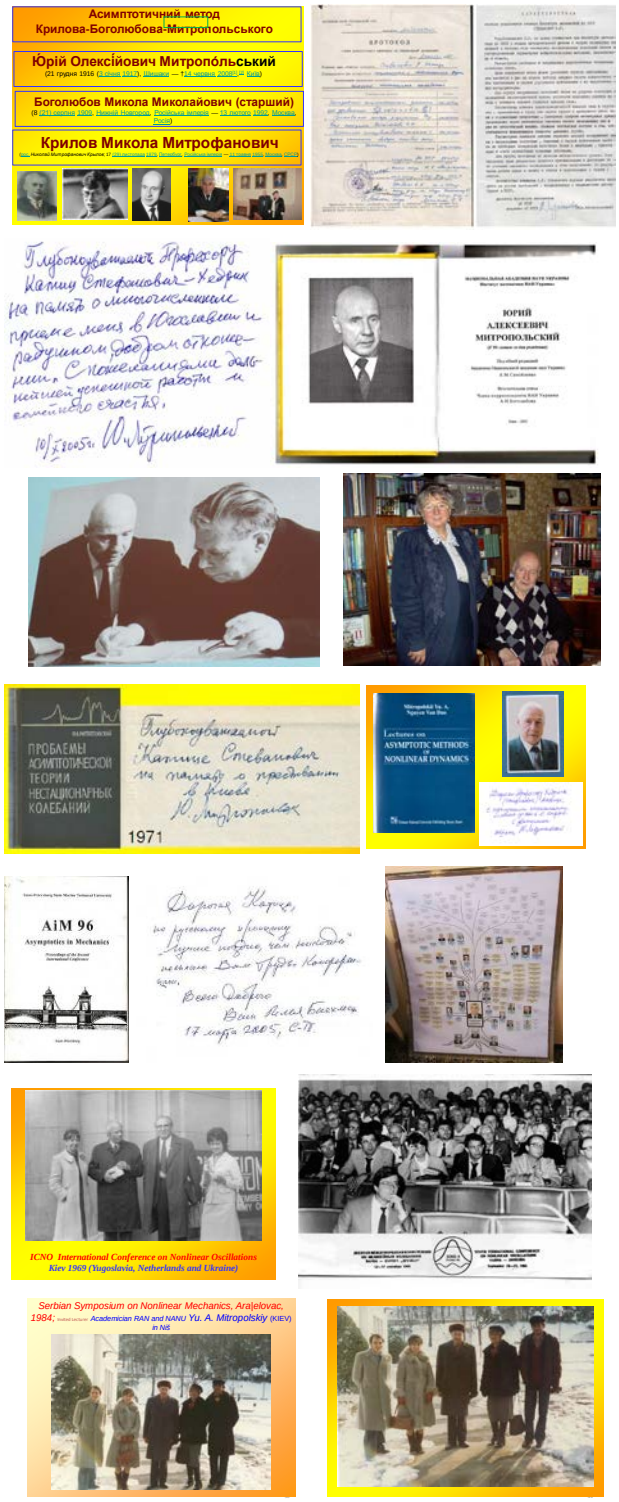

Figure 1. Photo gallery and presentation of the primary influence of the School of Asymptotic Methods of Nonlinear Mechanics Krilov-Bogolyubov- Mitropolski on the development of mechanics and research in the field of nonlinear oscillations and nonlinear dynamics at the University of Niš and in Serbia

I point out here two original monographs by Yuri Alekseevich Mitropolski [20, 22], which are not sufficiently World known between scientists and researchers, in my opinion, and neither is the theory of asymptotic methods of unsteady-non-stationary oscillations known in application, which represents the original contribution of Yu.A. Mitropolski, to this world scientific school. On the occasion of Mitropolski's Life Jubilee 90th birthday anniversary, I was honored to be enrolled as a participant of that famous scientific school of asymptotic methods of nonlinear mechanics, and on the basis of a well-placed Candidate Minimum of the specialty of Theoretical and Mathematical Physics, which is a postgraduate (aspirant) course, which I authorized for 11 months of training under mentorship Yuri Alekseevich Mitropolskii and with the assistance of A. Lapatom at the Institute of Mathematics of the National Academy of Sciences of Ukraine in Kiev, during 1971 (see Figure 1).

IV. International Conference of Nonlinear Oscillations (ICNO) and the European Nonlinear Oscillations Conference (ENOC)

The series of International Conference of Nonlinear Oscillations (ICNO) was held every third year, and continued into the series of European conferences of the International European Nonlinear Oscillations Conferences (ENOC). See details in Figures 2.

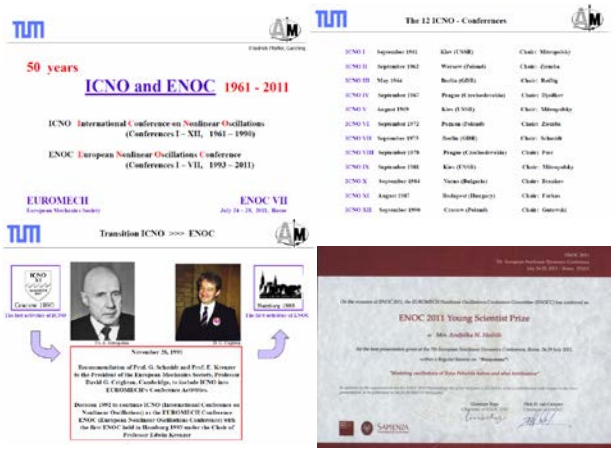

Figure 2. Three slides from Professor Friedrich Pfeiffer's Lecture on the occasion of half a century since the first ICNO Kiev 1961 (International Conference of Nonlinear Oscillations) presented at ENOC Rome in 2011 (the European Nonlinear Oscillations Conference) and Diploma of ENOC 2011 Young Scientist Prize of the European Nonlinear Oscillations Conference Rome 2011, first tine to laureate from Serbian young researcher on Project ON174001 "Sybanics of hybrid systems with complex structures"

The first series of ICNO conferences was founded by my Professor Academician Yu.A. Mittropolski from Kiev. The first of these series of conferences was held in Kiev in 1961, and I first time participated in 1969, as a young assistant, brought with me by Professor Danilo Rašković with the intention of introducing me to Academician Mitropolski and obtaining his consent to accept me for training and to study asymptotic methods of nonlinear mechanics. As a result of the acquired knowledge and further research, references [5-8, 10, 11] and [30, 31] have emerged, among others. Later, in my research, I used a monograph by two authors, Aly Nayfeh, Dean T. Mook, (1976), Nonlinear oscillations, in which my reference [31] was cited, published in the Polish Journal Nonlinear Oscillations, and presented at ICNO Conference in Poznan 1972.

Professor G. Rega in Reference [27] writes:

"*International Conferences on Nonlinear Oscillations (ICNO) was organized in Kiev in 1961 by Yu. A. Mitropolski, the third scientist-founder of the asymptotic methods of nonlinear mechanics referred to in the KBM acronym of the powerful method(s) for the analysis of nonlinear oscillations initiated by N. Krylov and N.*

Bogoliubov [2, 3]; and the series of ICNO events held every 3 years in different cities of those countries lasted for 30 years, until the last one organized in 1990 in Krakow by W. Gutowski".

Based on a recommendation of G. Schmidt and E. Kreuzer to the chairman of the European Mechanics Council D. Crighton to include ICNO into the society's conference activities, with the full support of Yu. Mitropolski, the relevant scientific tradition and the underlying patrimony of knowledge were inherited by EUROMECH, which started the new series of ENOC events at Hamburg, 1993". For details see Figure 3. Series of the Conferences ICNO I attend: Kiev 1969, Poynanj 1972, ICNO Kiev 1981, Varna 1984, Kracow 1990. (see Figures 2).

Numerous times in my hand was the monograph: Aly Nayfeh, Dean T. Mook, (1976), *Nonlinear Oscillations*, John Wiley and Sons, 1976, New York, published first in 1976, but between numerous cited references in this monograph, I haven't read that my paper, published in Poland Journal in 1974, [47], is included in this list of references. I forgot this paper published under my father's family name. In 2016, researcher from my current Project team ON174001 (20011-2019) [31], informed me that my paper titled:

Stevanovich, K. (later merried family name Hedrih) and Raskovich D., (1974), Many frequency vibration in one frequency regime of nonlinear systems with several degrees of freedom, Zagadnienia Drgan Neiliniowych, 15201-220,418., is cited in the list of the references of this important monograph Aly Nayfeh, Dean T. Mook, (1976), Nonlinear oscillations, John Wiley and Sons, 1976, New York.

I have learned about this citation only after four decades late. At the same time in 1976, my other two papers titled:

Katica Stevanovich (later merried family name Hedrih)m (1972), Two-frequency no stationary forced vibrationsof beam, Marhematical Physicsm Kiev, Vol. 12, 1972, pp. 127-140. (in Russian language) and

Katica Stevanovich (later merried family name Hedrih), (1971), Transversal vibrations of a beam loaded by system, moving along beam with chengeable velocity, containing mass particles each excited by corresponding single frequency force, Edition Assymptotic and qualitative methods in theory of nonlineat vibradisons, Editor Yu.A. Mitropolyski, Institute of Mathematics Academy of Sciences of USSR , Kiev, 1971, pages 15. (in Russian language).

published in Ukraine, are cited in the list of the references in the monograph [22, published in 1976, and titled:

Yu.A. Mitropolyski and B.I. Moseenkov: Asymptotic solutions of partial differential equations, Kiev, 1976 (in Russian language).

These three citations through list of the references in two important international monographs of two world important scientists in area of nonlinear mechanics, nonlinear oscillations represent a special honour for me. I was very pleased to learn about scientific relations and warm friendships between these two scientists, Ali Nayfeh (December 21, 1933-March 27, 2017) and Yuri Alekseevich Mitropolyski (January 3, 1917-January 14, 2008), known over the world on the basis of their important scientific legates, life after long time up to numerous next generations of the young scientists.

Researchers of my team of Project ON174001 "Dynamics of hybrid systems with complex Structures" (2011-2019) [12] was participants of the Series of Conferences ENOC: 2011, Rome, G. Rega; 2014, Wien, H. Eckerl; 2017, Budapest, G. Stépan;

V. Scientific meetings in Nonlinear Sciences in Serbia

We will, also, include here some basic information about scientific conferences organized in Serbia in the field of nonlinear mechanics, nonlinear sciences, and nonlinear dynamics.

Series of the Nonlinear Mechanics scientific meetings started with International Symposia on Nonlinear Dynamics in Arandjelovac 1984, organized by Serbian Society of Mechanics under the Yugoslav Society of Mechanics. Invited Plenary Lecturer was academician Yuri Alekseevich Mitropolski, and late was elected as a Honor member of Serbian Society of Mechanics. All the members of the Chair for Mechanics and the Chair for Hydraulic Engineering of the Faculty of Mechanical Engineering University of Niš took part in this and other symposiums; they were co-organizers as well.

Next scientific meeting in nonlinear mechanics held as a International Conference on Nonlinear Mechanics 1991 in Niš, titled "The First Yugoslav Conference on Nonlinear Deterministic and Stochastic Processes in Dynamical Systems with Applications YCNP Niš'91", organized by the Faculty of Mechanical Engineering of University of Niš, and was held in Niš. The Chairman of the Organizing Committee was Prof. Katica (Stevanović) Hedrih. Invited Plenary Lecturer was William Nash from MIT USA and first Editor-in-Chief and founder of International Journal of Non-Linear Mechanics published by Elsevier. Invited Plenary Lecturer was, also, young scientist Kazuyuki Yagasaki from Japan. Proceedings of Abstracts was published; the papers and invited lectures which were approved were publisheed in the first and the following issues of the University Journal – Facta Universitatis, new Series – Mechanics, Automatic Control and Robotics.

The Third Yugoslav Symposium on Nonlinear Mechanics was held in the form of a Minisymposium, as a part of the XXII Yugoslav Congress on Theoretical and Applied Mechanics in Niš in 1995. [1-31].

The Fourth Symposium on Nonlinear Mechanics was held in 1997, again in the form of a Minisymposium, as a part of the XXIII Yugoslav Congress on Theoretical and Applied Mechanics in Vrnjacka Banja.The Chairman of the Scientific Committee was the academician Nikola Hajdin, and the Chairman of the Organizing Committee was Prof. Katica (Stevanović) Hedrih.

The Fifth Symposium on Nonlinear Mechanics – "Nonlinear Sciences at the Threshold of the Third Millenium" was organized in 2000, with the wish for it to become a tradition and to gather the connoisseurs of nonlinear phenomenology from disparate sciences and dynamic systems and for it to become renown all over the world. Academicians N. Hajdin, V.V. Rumyantsev and M. Prvanović and Professors D.S. Sophianopoulos, G.T.Michaltos, Ji Huan He, I. Finogenko, P.S. Krasil'nikov ..... were guests at this symposium. The year

of the Sixth Symposium was the year of the 10 th Jubilant issue of the University Journal – Facta Universitatis Series – Mechanics, Automatic Control and Robotics in Niš 2003. Invited participants were scientists: Giuseppe Rega (member of IUTAM Scientific Committee),

Tomoaki Kawaguchi (President of Tensor Society), V. Lasmikantham (President of International Federation of Nonlinear Analysists IFNA), Ftrantishek Peterka, Jirzi Waerminski, Ulriht Gabert, Professor Leela, Anagaya Vatsala, Liviu Barreyeu and other (see Figure 3, 4 and 5).

Figure 3. Photo Gallery: Participants of two International Synposiums on "Nonlinear Sciences at the Threshold of the Third Millenium" Niš 2000 and 6th ISNM NSA NIŠ '2003 in Niš 2003. (Photo left up: between participants in middle: Academicians N. Hajdin, V.V. Rumyantsev and M. Prvanović and Professors D.S. Sophianopoulos, G.T.Michaltos, Ji Huan He, I. Finogenko, P.S. Krasil'nikov; Photo right up: group of participants from Greece with Organizer; Photo left down: between participants in middle: Tomoaki Kawaguchi (President of Tensor Society), V. Lasmikantham (President of International Federaion of Nonlinear Analysists IFNA), Professor Leela, and Professor Anagaya Vatsala (Luisiana University); Photo righy down: between participants in middle: Giuseppe Rega (member of IUTAM Scientific Committee), Ftrantishek Peterka, Jirzi Waerminski, Ulriht Gabert, Liviu Barreteu and other)

VI. CONCLUDING RENARKS

In conclusion, on a limited surface, for this type of conference article, it remains to refer readers to images 1 to 6, which speak much more than the text itself, because the words often end up in spam, and the images remain in memory.

Figure 4. Incited Lecturer William Nash (MTI, USA) in Niš1991 (Figure left) and Hiroshi Yabuno (Invited Lecturer as Symposium Nonlinear Dynamics Belgrade 2011), Katica (Stevanović) Hedrih and Kazuyuki Yagasaki (Invited Lectirer at Nonlinear Conference Niš 1991) ar random meeting in Maastricht during excursion of ENOC Eindhoven 2005 (Figure Right)

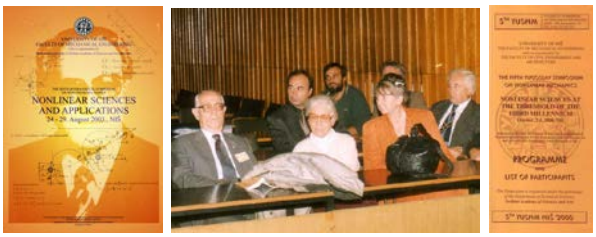

Figure 5. Participants of the Seried of Scientific Seminars named "Theoretical and Applied Mechanics" at Department of Mecjains of Mechanical Engineering University of Niš (1975-2004), late renamed "Nonlinear Dynamics -Milutin Milanković" and supported by Mathematical Institute of Serbian Academy of Science and Arts (2004-). Photo left, between participants of Seminar, in middle, academician Academy of Athens and SASA Antony Kounadis and academician of European Academy of Sciences Jon Katsikadfelis, both "Doctors

Figure 6. Mini-Symposia in the World at International world Congresses: WCNA Orlando 2004, ESMC Lisabon 2009, NODY Shanghai 2007, EFC16-Alexandoupolis 2006, APM S.Petersburg 2007and other.

AKNOWLEDGMENT

Paper is dedicated to the 110th Anniversary since the birth of Nikolay Nikolayevich Bogolyubov (1909-1992).. Let time and the next generations judge objectively about our contributions to the University of Niš and whether running with nonlinear sciences has left a trace for the next generations. .

REFERENCES

[1] Andronov, A.A., Witt, A.A., Khaïkin, S.E.: Theory of Oscillators. Pergamon, London (1966). (Russian edition, Moscow 1937)

[2] Bogoliubov, N. N. Mitropolsky Yu. A. (1961): Asymptotic Methods in the Theory of Non-Linear Oscillations. New York, Gordon and Breach.

[3] Bogoliubov, N. N. Mitropolsky Yu. A. and Samoilenko A. M.. Methods of accelerated convergence in nonlinear mechanics. New York: Springer-Verlag, 1976 (translated from Russian).

[4] Duffing, G.: Erzwungene Schwingungen bei veränderlicher Eigenfrequenz und ihre technische Bedeutung. Vieweg, Braunschweig (1918).

[5] Hedrih (Stevanović) K R., (2013), Linear and nonlinear dynamics of hybrid systems,, Invited Plenary Lecture, Proceedings of Fourth Serbian (29th Yu) Congress on Theoretical and Applied Mechanics, Vrnjačka Banja, Serbia, 4-7 June 2013, pp. 43-58. ISBN 978-86-909973-5-0 , ISBN 978-86-909973-5-0. COBISS.SR-ID 198308876. http://www.ssm.org.rs/Congress2013/authors.

[6] Hedrih (Stevanović) K R., (2013), Linear and nonlinear dynamics of hybrid systems,, Journal of Mechanical Engineering Science, Part C, (2020, in publishing process).

[7] Hedrih (Stevanović) K R., Two-Frequencies Forced Nonstationary Vibrations of the beam, Matematieskaya fizika, Vol. 12, Kiev, 1972, pp. 127-140 (in Russian).

[8] Hedrih (Stevanović) K R., Two-Frequencies Regime of the Nonlinear Transversal Free Vibrations of the Beam, Ed. Analiticheskie i kaestvenie metodi v teorii differencialnih uravneniy, Redaktor Yu. A. Mitropolskiy, Institut Matematiki AN USSR, Kiev, 1972, pp. 233-246. (in Russian)

[9] Hedrih (Stevanović) K R., (2008), Dynamics of coupled systems, Nonlinear Analysis: Hybrid Systems, Volume 2, Issue 2, June 2008, Pages 310-334.

[10] Hedrih (Stevanović) K R., (2008), Transversal vibration of a parametrically excited hereditary beam: Influence of rotatory inertia and transverse shear on stochastic stability of deformable forms and processes, International IFNA-ANS Journal "Problems of nonlinear analysis in engineering systems", ISSN 1727-687X, is published (in two languages, in English and in Russian): (No.2(30), v.14, 2008,115-140). Hedrih (Stevanović) K R., (2012), Advances in Classical and Analytical Mechanics: A review of author' results, Special Issue, Theoretical and Applied Mechanics, Vol. 40 (S1), pp. 293- 383. DOI : 10.2298/TAM12S1293H, ISSN 1450-5584.

[11] Hedrih (Stevanović) K R. with Project Research Team, (2011-2019), Project ON174001 "Dynamics of hybrid systems with complex strycures; Mechanics of materials". Supported by Serbian Ministry of Education, Science and Technological Development and coordinated at Mathematical Institute of Serbian Academy of Science and Arts. http://www.mi.sanu.ac.rs/novi_sajt/research/projects/174001a.php

[12] Hedrih (Stevanović), K., Mitić, Sl., Pavlović, R. and Kozić, P., (1986), Mnogochastotnie vinuzhdenie kolebaniya tonkoy uprugoy oboloschki s nachalynimi nepravilynostyami, (Analiticheskiy analiz) (Multi-frequency forced vibrations of thin elastic shell with initial imperfections (Analytical Analysis)), Theoretical and Applied Mechanics, N 12, pp.41-58, 1986, Beograd.

[13] Hedrih (Stevanović KR., Kozić P. Palović R., (1984), O uzajamnom uticaju harmonica u nelinearnim sistemima sa malim parametrom (On the mutual influence of harmonics in nonlinear systems with a small parameter), Recueil des trawaux de L'Institut Mathématique Nouvelle Série, Tom 4 (12), 1984

[14] Hedrih (Stevanović) KR, Kozić P, Pavlović R. Stashionarniy i nestashionarniy R-chastotniy analiz kolebaniy sistem s konechnim chislom stepeni svobodu kolebaniy i vzaimnoe vliyanie garmonikov (Stationary and no stationary R-freqyebxy analysis of oscillatory systems with finite nymber of degrees of freedom oscillations and interactions between harmonics). Theoretical and Applied Mechanics (Beograd). 1985;11:73-84.

[15] Hedrih (Stevanović) K R. and Simonović J., (2012), Multi-frequency analysis of the double circular plate system non-linear dynamics", Nonlinear Dynamics, Springer, Volume 67, Issue 3 (2012), Page 2299-2315. DOI: 10.1007/s11071-011-0147-7 .

[16] Hedrih (Stevanović) K R. Simonović J. D. , (2010), Non-linear dynamics of the sandwich double circular plate system, Int. J. Non-Linear Mech, Volume 45, Issue 9, November 2010, pp. 902-918, ISSN: 0218-1274.

[17] Hedrih (Stevanović) K R, Tenreiro Machado J. M., (2013), Discrete fractional order system vibrations, International Journal Non-Linear Mechanics (January 6, 2014), Volume 73, July 2015, Pages 2–11,

[18] Mitropolyskiy, Yu. A., (1995), Nonlinear Mechanics – Asymptotic Methods, Institut matematiki NAN Ukraini, Kiev, 1995, pp. 397. (in Russian)

[19] Mitropolyskiy, Yu.A, (1964), Problemi asimptoti-cheskoy teorii nestashionarnih kolebaniy (Prob;ems of asymptotic theory of no stationary oscillations), Nauka Moskva, 1964. (in Russian).

[20] Mitropolyskiy, Yu. A. (1955), Nestashionarnie proshesi v nelinyeynih sistemah (Non stationary sprocesses in nonlinear systems) , AN USSR, Kiev, 1955. (in Russian)

[21] Mitropolskiy Yu.A. and Moseenkov B.I. (1976), : Asymptotic solutions of the Partial Differential Equations, Kiev 1976. (in Russian).

[22] Mitropolskiy Yu.A., Some problems in the development in nonlinear mechanics theory and applications, Facta Universitatis, Series Mechanics, Automatic Control and Robotics, Vol. 1, No. 5,1995, pp. 539-560.

[23] Paunovic S., Cajic M. S., Karlicic D., Mijalkovic M. (2019), A novel approach for vibration analysis of fractional viscoelastic beams with attached masses and base excitation. JOURNAL OF SOUND AND VIBRATION, (2019), vol. 463 br. , str.- (Project ONI 174001, MI SASA)

[24] Karlicic D., Jovanovic D., Kozic P., Cajic M.. Thermal and Magnetic Effects on the Vibration of a Cracked Nanobeam Embedded in An Elastic Medium, JOURNAL OF MECHANICS OF MATERIALS AND STRUCTURES, (2015), vol. 10 br. 1, str. 43-62. (Project ONI 174001, MI SASA)

[25] Rašković, D., Theory of Oscillations, Naučna knjiga, Beograd, 1965, p. 503. (in Serbian)

[26] Rega G., Nonlinear dynamics in mechanics and engineering: 40 years of developments and Ali H. Nayfeh's legacy, Nonlinear Dyn (2020) 99:11–34. https://doi.org/10.1007/s11071-019-04833-w

[27] Simonović J., (2011), Dinamika i stabilnost hibridnih dinamičkih sistema (Dynamics and Stability of Dynamics Hybrid Systems), [in Serbian], Doctor's Degree Thesis, Faculty of Mechanical Engineering in Niš, (submitted 2011), Supervisor K. Hedrih (Stevanović).

[28] Stevanović (Hedrih) K., (1967), Nonliear oscillations and applications to nonlinear system with automatic control, Diploma work of Bachilir (Master) degree of mechanical engineer, Faculty of Technical Sciences in Niš, deefnded September 30, 1967, Supervision: Prof. dr. Ing. Math Danilo P. Rašković (Yugoslavia). (Best Thesis of Bachelor's (Master) degree at Yugoslav Faculties of Engineering and Natural mathematical sciences, 1967, by Electronic Industry EI Niš (presented by director Vladimir Jasić)).

[29] Stevanović (Hedrih) K., Rešrnje jednačone transverzalnih oscilacija jednoraspone grede asimptotskim metodama nelinearne mehanike (Solution of the equation of transversal oscillation one span beam by asymptotic method of nonlinear mechanics), [in Serbian], Magistar of Sciences Degree Thesis, Faculty of Technical Sciences in Niš, 1972. Supervision: Prof. dr. Ing. Math Danilo P. Rašković (Yugoslavia) and academician Yuriy Alekseevich Mitropolskiy (Ukraine).

[30] Stevanović (Hedrih) K. and Rašković D.,(1974), Investigation of Multi-frequencies Vibrations in single-frequency regime in Nonlinear Systems with Many Degrees of the Freedom and with Slowchanging Parameters, Journal Nonlinear Vibrations Problems – Zagadnenia dragan neliniowicz" No. 15., 1974. Warsaw, pp. 201-202.

[31] Hedrih (Stevanović), KR., Janevski G., Nonlinear dynamics of a gyro-disc-rotor and structural dependence of a phase portrait on the initial conditions, Proceedings of Dynamics of Machines 2000, Institute of Thermomechanics, Czech Committee of the European Mechanics Society, Prague, 8 - 9 February, 2000., pp. 81-88.

THE 5th INTERNATIONAL CONFERENCE
MECHANICAL ENGINEERING IN XXI CENTURY

December 9-10, 2020
Faculty of Mechanical Engineering in Niš, Serbia

Methodology of Vibro-Impact Dynamics Research on New Theory of Rolling Body Collisions

Katica STEVANOVIĆ HEDRIH

Mathematical Institute of Serbian Academy of Sciences and Arts, Belgrade, Serbia, and Faculty of Mechanical Engineering at University of Niš, Serbia
khedrih@sbb.rs

***Abstract*— In this paper we start with new and general results on the dynamics of the body in rolling along curved lines given in general form, through the equations of curves in a stationary vertical plane or a vertical plane rotating with constant angular velocity about a vertical axis. In both cases, the generalized rolling pendulums, the corresponding nonlinear differential equations of dynamics of rolling body without slipping and their first integrals, ie the equations of phase trajectories, are derived. The complete Hedrih's theory of the impact and collision of heavy rolling balls, through geometry, kinematics and dynamics of rolling balls, is defined. Based on the both new Hedrih's results, theory of collision between rolling bodies and use phase trajectory method, a new methodology of vibro-impact dynamics investigation is founded and presented trough a number of applications in mechanical system dynamics.**

***Keywords*— Theory of collision, billiards, generalized rolling pendulum, phase trajectory portraits, methodology of vibro-impact system investigation**

I. INTRODUCTION

Now, we start with new and general results on the dynamics of the body in rolling along curved lines given in general form (see References [1-11]), through the equations of curves in a stationary vertical plane or a vertical plane rotating with constant angular velocity about a vertical axis. In both cases, the generalized rolling pendulums, the corresponding nonlinear differential equations of dynamics of rolling body without slipping and their first integrals, ie the equations of phase trajectories, are derived. Phase trajectory portraits fo particular examples of dynamics of generalized rolling pendulous are presented.

The elements of geometry, kinematics and dynamics of rolling homogeneous balls along curvilinear lines are defined (see References [3, 7]). The complete Hedrih's theory of the impact and collision of heavy rolling balls, through geometry, kinematics and dynamics of rolling balls, is defined (see ReferenceS [4, 5]).

A new definition of the coefficient of restitution (collision) was introduced, starting from the hypothesis of the conservation of the sum of angular momentum of the balls in rolling, for instant rolling axes, after the collision in relation to the before collision of the bodied. The expressions for the outgoing angular velocities of the ball rolling after the collision have been derived and their rolling paths after the impact or collision have been determined and various possible anchors have been shown.

Based on the both new Hedrih's results (see ReferenceS [1- 10]), theory of collision between rolling bodies and dynamics of generalized rolling pendulums in successive collisions, and use phase trajectory method, a new methodology of vibro-impact dynamics investigation is founded and presented trough a number of applications in mechanical system dynamics.

We must to point, again, that, the elements of geometry, kinematics and dynamics of rolling homogeneous balls along curvilinear lines are defined (see Reference [6] accepted for ICTAM 2020+1 and Reference [5] accepted for EURODYN 2020). The complete theory of the impact and collision of heavy rolling balls, through geometry, kinematics and dynamics of rolling balls, is defined by Hedrih (Stevanović).

II. HEDRIH'S THEORY OF DYNAMICS OF ROLLING BODY COLLISIONS IN NON-SLIP ROLLING

A. *Basic settings for rolling and collision dynamics in non-slip rolling*

The theory of collision dynamics (and in the special case of impact) is based on the following assumptions:

1* The contact time τ of two bodies in a collision is very short;

2* The impact forces $\vec{F}^{ud}$ and the corresponding impact moments $\vec{M}^{ud}$ of the forces are variable and of high intensity, of the order of magnitude $\frac{1}{\tau}$, and of short duration during the contact time τ of two bodies in the collision and during the collision they have attack points at the contact points in the collision;

3* The change of angular momentum of motion of the material two bodies in rolling for the corresponding rolling axes, during the collision is finite.

4* The impulse (linear momentum) and angular momentum of "ordinary forces" compared to the impulse (linear momentum) and angular momentum of instantaneous collision forces, are much much smaller and can be neglected.

B. *Hipothesis of conservation of sum of angular momentum for instantaneous axes of rolling of two*

bodies in rolling before and after collision of two axisymmetric bodies

Since external active forces and moments of forces of finite intensities have impulses of forces equal to zero, and couplings have kinetic moments equal to zero and, at infinitesimal intervals of time, we consider that two material rigid bodies, which roll with the incoming angular velocities and in collision, are considered as one system. Therefore, the hypothesis of the conservation of the sum of angular momentum (kinetic momentum) for the instantaneous axes of rolling of the body - the movement before and after the collision, can be applied to the dynamics of the same to in the form:

$$\mathbf{J}_{P1}\vec{\omega}_{P1}(t_0)+\mathbf{J}_{P2}\vec{\omega}_{P2}(t_0)=\mathbf{J}_{P1}\vec{\omega}_{P1}(t_0+\tau)+\mathbf{J}_{P2}\vec{\omega}_{P2}(t_0+\tau)\ . \quad (1)$$

This hypothesis about the conservation of the sum of the angular momentum of motion by rolling in a collision of two bodies, which is analogous to the hypothesis of the conservation of the sum of the linear momentum of motion of two bodies in a collision and in translational motion (see References [6-8, 12-15]).

C. Coefficient of restitution or collision of two axisymmetric rolling bodies with one central plane of simetry

When the incoming angular velocities $\vec{\omega}_{P1}(t_0)$ and $\vec{\omega}_{P2}(t_0)$ of rolling and the axial moments of inertia of mass $\mathbf{J}_{P1}$ and $\mathbf{J}_{P2}$ for the instantaneous axes of rolling of the body in a collision, are known, the previous hypothesis relation (1) of the sums of the angular momentum of motion for the instantaneous axes of rolling, before and after the collision, is not sufficient to determine two unknown outgoing angular velocities $\vec{\omega}_{P1}(t_0+\tau)$ and $\vec{\omega}_{P2}(t_0+\tau)$, after the collision of two bodies, which roll just before and after the collision. The ratio k of the relative angular velocities of rolling of the axisymmetric bodies after and before the collision is (for details see electronic version of the extended paper):

$$k=\frac{\omega_r(t_0+\tau)}{\omega_r(t_0)}=\frac{\omega_{P2}(t_0+\tau)-\omega_{P1}(t_0+\tau)}{\omega_{P1}(t_0)-\omega_{P2}(t_0)} \quad (2)$$

and is called the collision coefficient, or the coefficient of restitution, or the coefficient of establishment of rolling bodies in a collision.

D. Intensity of outgoing angular velocities of rolling two bodies after a collision

In order to determine the intensities of the outgoing angular velocities of rolling of two bodies after a collision, $\vec{\omega}_{P1}(t_0+\tau)$ and $\vec{\omega}_{P2}(t_0+\tau)$, it is sufficient to eliminate from the previous relations (1) - (2) the unknown angular velocities of both bodies, $\vec{\omega}_{CP}$, in the collision at the end of the compression at the local environment of the point of contact of the body in the collision. Then solve the relations by unknown outgoing angular velocities and, which is not difficult to do, so for the outgoing angular velocities, $\vec{\omega}_{P1}(t_0+\tau)$ and $\vec{\omega}_{P2}(t_0+\tau)$, after the collision of the balls, we get the following expressions:

$$\vec{\omega}_{P1}(t_0+\tau)=\vec{\omega}_{P1}(t_0)-\frac{1+k}{1+\frac{\mathbf{J}_{P1}}{\mathbf{J}_{P2}}}\left(\vec{\omega}_{P1}(t_0)-\omega_{P2}(t_0)\right) \text{ and}$$

$$\vec{\omega}_{P2}(t_0+\tau)=\omega_{\mathbf{P1}}(t_0)+\frac{1+k}{1+\frac{\mathbf{J}_{P2}}{\mathbf{J}_{P1}}}\left(\omega_{\mathbf{P1}}(t_0)-\omega_{\mathbf{P2}}(t_0)\right) \quad (3)$$

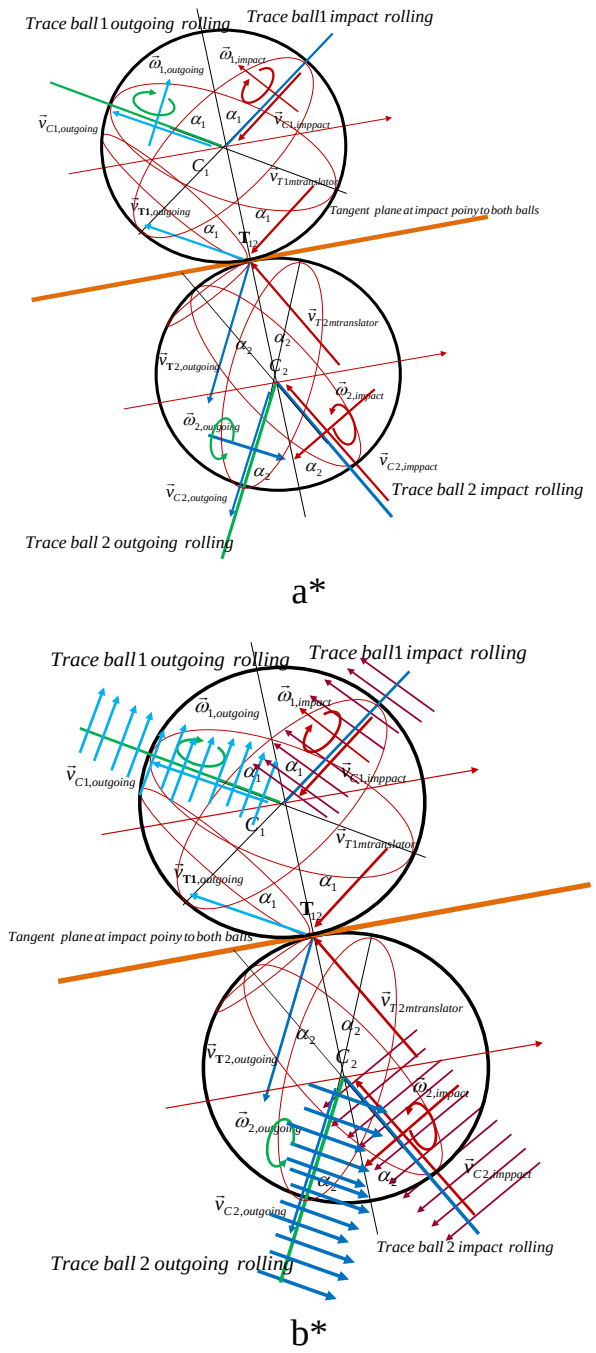

Figure 1. Partial analogies between the central and oblique collisions of two rolling balls: the opening of the traces of ball rolling in oblique(skew) collision (b *) with respect to the central collision of the balls (a *). [8]

In Figure 1 the partial analogies between the central and oblique collisions of two rolling balls are presented. The opening of the traces of ball rolling in oblique (skew) collision (b *) with respect to the central collision of the

balls (a *) are presented. For details see Referemces [6, 7,8].

III. SHORT DESCRIPTION OT THE METHODOLOGY OF VIBRO-IMPACT DYNAMICS INVESTIGATION

Presentation in Figure 2 shown basic idea of the description of the methodology of vibro-impact dynamics investigation based on the Hedrih's theory of collision between rolling bodies along curvilinear lines and phade trajectory method. Figure is from Reference [10].

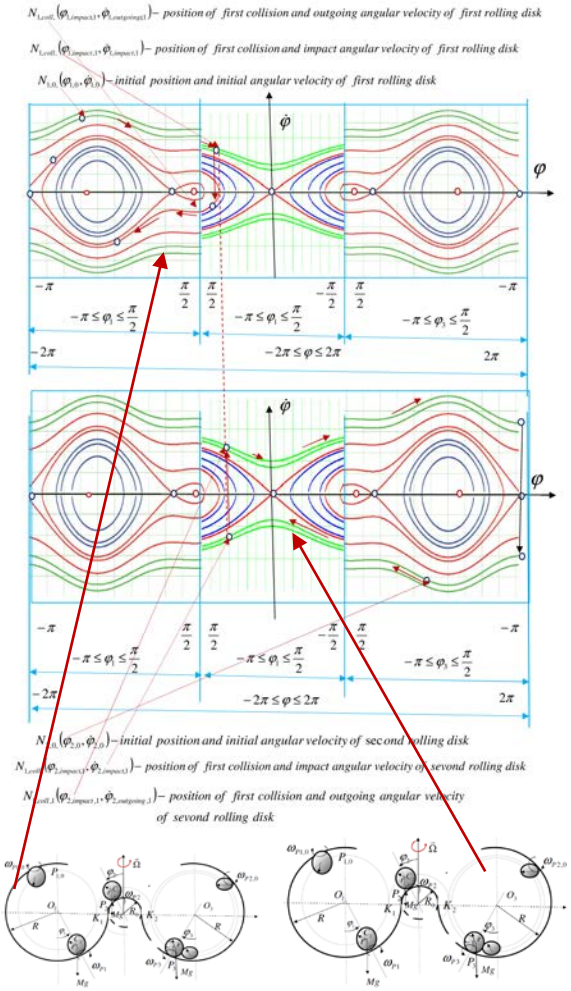

Figure 2 Phase trajectory branches in phase portraits of two rolling heavy thin disks for relative motion in interval between initial condition configuration and configurations of pre-first-collision and post-first-collision between two rolling disks with vibro-impact dynamics on rotating curvilinear trace with constant angular velocity around vertical central axis of its symmetry, and for bifurcation parameters $\lambda_i < 1$, $i = 1,2$. (From Reference [10])

In Figure 3, kinematic plan of the velocities in the collision of two balls in rolling motion along curvilinear line are presented. (Figure from Reference [7])

IV. CONCLUDING CONSIDERATIONS

Using the analysis of the elements of geometry, kinematics and dynamics of impact (see Fig. 1) and collision of bodies, which we have given in the parts of this, as well as in extended paper in electronic version, it is possible to draw some conclusions and generalizations.

Basic idea and results, in methodology of vibro-impact dynamics investigation based on the Hedrih's theory of collision between rolling bodies along curvilinear lines and phase trajectory method, are the constructions of two phase portraits, each of the corresponding nonlinear dynamics of each of two rolling different heavy bodies in successive central collisions along rotate complex curvilinear trace, as well as the determination of the kinetic parameters before and after each successive central collision between rolling bodies. New Hedrih's expressions for outgoing angular velocity after central collision are applied for determination of each of the outgoing angular velocities of the rolling disks after each successive collision. Results include determination of the transformed elliptic integrals for determination of time and position of each of the successive collisions.

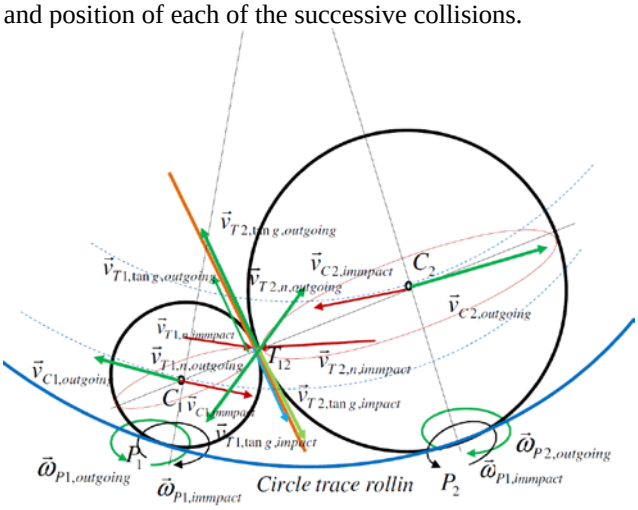

Figure 3. Kinematic plan of the velocities in the collision of two balls in rolling motion along curvilinear line; (Figure from Reference [7])

This presented methodology could be applied for the investigation of numerous engineering vibro-impact system dynamics. The presented methodology for studying the dynamics of vibro-impact systems with rolling elements, based on Hedrih's theory of collisions between rolling bodies, is applicable in the vibro-impact dynamics of railway vehicles. When rolling, the wheels of railway vehicles can collide with accidental obstacles on the railway tracks, so it is important to determine the impact impulses, as well as the effects of outgoing-return impulse angular velocities immediately after the collision, and thus vibro-impact effects on vehicle construction.

In concluding, again, it is possible to point out: In this paper we start with new and general results on the dynamics of the body in rolling along curved lines given in general form, through the equations of curves in a stationary vertical plane or a vertical plane rotating with constant angular velocity about a vertical axis. In both cases, the generalized rolling pendulums, the corresponding nonlinear differential equations of dynamics of rolling body without slipping and their first integrals, ie the equations of phase trajectories, are derived. Phase trajectory portraits fo particular examples of dynamics of generalized rolling pendulous are presented.

The elements of geometry, kinematics and dynamics of rolling homogeneous balls along curvilinear lines are defined. The complete Hedrih's theory of the impact and collision of heavy rolling balls, through geometry, kinematics and dynamics of rolling balls, is defined. A new definition of the coefficient of restitution (collision) was introduced, starting from the hypothesis of the conservation of the sum of angular momentum of the balls in rolling, for instant rolling axes, after the collision in

relation to the before collision of the bodied. The expressions for the outgoing angular velocities of the ball rolling after the collision have been derived and their rolling paths after the impact or collision have been determined and various possible anchors have been shown.

The difference between the content of the term billiards used in mathematical works of many mathematicians, as well as the research that remains in the field of geometry is pointed out. Our theory of ball rolling and collision is based on the examples of the abstraction of real rolling systems of heavy homogeneous billiards to a mechanical model.

Based on the both new Hedrih's results, theory of collision between rolling bodies and dynamics of generalized rolling pendulums in successive collisions, and use phase trajectory method, a new methodology of vibro-impact dynamics investigation is founded and presented trough a number of applications in mechanical system dynamics.

ACKNOWLEDGMENT

Paper is dedicated to Memory and honour of my Professor Dr Ing. Dipl. Math. Danilo P. Rašković (1910-1985), with 120.00 exemplars of university books on mechanics published only in "Naučna knjiga". This work is short review of earlier presented author authentic research original scientific results in establishing new theory of geometry, kinematics and dynamics of collision between rolling bodies or published in different world prestigious scientific journals of Springer and Elsevier listed in the list of the References in cited in this paper.

REFERENCES

[1] Hedrih (Stevanović) KR.: Generalized rolling pendulum along curvilinear trace: Phase portrait, singular points and total mechanical energy surface. Journal Computer Algebra Systems in Teaching and Research, Edited by Alexander Prokopenya and Agnieszka Gil-Swiderska, Publisher Siedlce University of Natural Sciences and Humanities (Siedlce, Poland), 2017, Vol. VI, pp. 204-216. ISSN 2300-7397. http://www.castr.uph.edu.pl.

[2] Hedrih (Stevanovic) KR., *Rolling heavy disk along rotating circle with constant angular velocity*, Computer Algebra Systems, in Teaching and Research, Chapter 2. Problems of Classical Mechanics, Edited by Alexander N. Prokopenya , Mirosław Jakubiak (Eds.), Volume V, pp. 293-304. Siedlce University of Natural Sciences and Humanities, Siedlce 2015, © Copyright Uniwersytet, Przyrodniczo-Humanistyczny w Siedlcach, Siedlce 2015, ISSN 2300-7397; ISBN 978-83-7051-779-3.

[3] Hedrih (Stevanović) KR.: Central collision of two rolling balls: theory and examples. Journal Advances in Theoretical and Applied Mechanics, Vol. 10, 2017, no. 1, 33-79. https://doi.org/10.12988/atam.2017.765.

[4] Hedrih (Stevanović) KR.: Dynamics of Impacts and Collisions of the Rolling Balls, Dynamical Systems: Theoretical and Experimental Analysis, Springer Proceedings in Mathematics & Statistics, Volume Number: 182, Chapter 13, pp. 157-168. © Springer, Part of Springer Science+Business , ISBN 978-3-319-42407-1. ISSN 2194-1009 ISSN 2194-1017 (electronic)

[5] Hedrih (Stevanović) KR., The theory of body collision in rolling through geometry, kinematics and dynamics of billiards, accepted for EURODYN 2020- XI International Conference on Structural Dynamics, M. Papadrakakis, M. Fragiadakis, C. Papadimitriou (eds.), Athens, Greece, 22–24 June 2020-New data caused by COVID 19: November 2020.

[6] Hedrih (Stevanović) KR., Rolling pendulums along curvilinear traces and surfaces: Collinisin theory and dynamics of vibro-impact systems, accepted for Sectional Lecture, XXV International Cngess of Theoretical and Applied Mechanics (ICTAM), 23-28 August 2020, Milano, Italy in organiyation of Interbational Unopn of Theoretical and Applied Mechanics (IUTAM), new data caused by COVID 19: August 22-27, 2021, Milano, Italy.

[7] Hedrih (Stevanović) K., (2019**),** Vibro-impact dynamics of two rolling heavy thin disks along rotate curvilinear line and energy analysis, **Journal** Nonlinear Dynamics, 98(4), 2551-2579, **DOI** 10.1007/s11071-019-04988-6; Springer; ISSN: 0924-090X (print version) ISSN: 1573-269X (electronic version); http://link.springer.com/article/10.1007/s11071-019-04988-6;

[8] Hedrih (Stevanović) K., (2018**),** Non-linear phenomena in vibro-impact dynamics: Central collision and energy jumps between two rolling bodies, Dedicated to memory of Professor and important scientist Ali Nayfeh (December 21, 1933-March 27, 2017). **Nonlinear Dynamics,** February 2018, Volume 91, Issue 3, pp 1885–1907. https://doi.org/10.1007/s11071-017-3988-x. ISSN: 0924-090X (print version) ISSN: 1573-269X (electronic version) https://link.springer.com/article/10.1007/s11071-017-3988-x http://www.springer.com/engineering/mechanics/journal/11071?detailsPage=pltci_1888917

[9] Hedrih (Stevanović) R. K.,, (2016), *Vibro-impact dynamics in systems with trigger of coupled three singular points: Collision of two rolling bodies*, The 24th International Congress of Theoretical and Applied Mechanics (IUTAM ICTAM 2016), Montreal, Canada, 21 - 26 August, 2016, Book of Papers, pp. 212 -213. IUTAM permanent site. ISBN: NR16-127/2016E-EPUB; Catalogue Number: 978-0-660-05459-9

[10] Hedrih (Stevanović) R. K.,, (2017), Vibro-impact dynamics of two rolling balls along curvilinear trace, Procedia Engineering, X International Conference on Structural Dynamics, EURODYN 2017, Edited by Fabrizio Vestroni, Francesco Romeo and Vincenzo Gattu, Volume 199, Pages pp. 663-668. (2017) , Elsevier, (2017) pp. 663-668; DOI information: 10.1016/j.proeng.2017.09.120 ; ISSN: 1877-7058. https://doi.org/10.1016/j.proeng.2017.09.120

Hedrih (Stevanović) K R., Raičević V. and Jović S., Phase Trajectory Portrait of the Vibro-impact Forced Dynamics of Two Heavy Mass Particles Motions along Rough Circle, Communications in Nonlinear Science and Numerical Simulations, 2011 16 (12):4745-4755, DOI 10.1016/j.cnsns.2011.05.027. ISSN: 1007-5704.

THE 5th INTERNATIONAL CONFERENCE
MECHANICAL ENGINEERING IN XXI CENTURY

December 9-10, 2020
Faculty of Mechanical Engineering in Niš, Serbia

Computer Visualization of Popovski-like Methods for Solving Nonlinear Equations

Ivan PETKOVIĆ, Đorđe HERCEG

Faculty of Electronic Engineering, University of Niš, A. Medvedeva 14, 18000 Niš, Serbia
Faculty of Science, University of Novi Sad, Trg D. Obradovića 4, 21000 Novi Sad, Serbia
ivan.petkovic@elfak.ni.ac.rs, herceg@dmi.uns.ac.rs

***Abstract*— The goal of this paper is computer visualization of Popovski-like methods for solving nonlinear equations of the form $f(z) = 0$ and the construction of a new one-parameter family of simultaneous methods for the determination of all simple zeros of a polynomial. For this purpose, advanced computer tools such as symbolic computation, basins of attraction and multi-precision arithmetic are employed. Choosing different values of the involved parameter, the presented family generates a variety of root-finding methods. Computer visualization of these methods indicates a conjecture on globally convergent properties of simultaneous methods. Numerical examples and dynamic study are presented.**

***Keywords*—Parametric iterative methods; basin of attraction, polynomial zeros; computer visualization; global convergence.**

I. Introduction

The aim of this paper is to present families of iterative methods for solving nonlinear equations of Popovski's type [7] using computer visualization. First, we present a dynamic study of three special cases of Popovski's third order family relied on a new methodology that uses computer graphics, more precisely, basins of attraction. Starting from this family for finding a single zero, by a suitable transformation we construct in the second part of the paper a new one-parameter family of Popovski's type for the simultaneous determination of all simple zeros of a polynomial. The order of convergence of the new family of simultaneous methods is four.

Algebraic polynomials and polynomial zeros are of great importance, both from theoretical and practical point of view so that a considerable attention has been devoted for decades to the design of numerical algorithms for finding polynomial zeros, see, e.g., [1]-[6], [8], which was the main motivation for developing a new algorithm.

Taking some specific values of the involved parameter, Popovski-like family generates simultaneous methods of Halley's, Chebyshev's and Euler's type. Computer algebra system Mathematica is employed to perform convergence analysis and numerical experiments of the proposed family. Finally, using computer visualization of the mentioned methods from Popovski-like family and trajectories of Aberth's type [1], we discuss their globally convergent properties.

II. Popovski's Family of Iterative Root-Finding Methods

Let f be at least two times differentiable function and let us introduce the abbreviations

$$u(x) = \frac{f(x)}{f'(x)}, \quad A_2(x) = \frac{f''(x)}{2f'(x)}.$$

Popovski [7] proposed a one-parameter family of cubically convergent iterative methods for finding a simple zero of at least two-times differentiable function f

$$x^{(k+1)} = x^{(k)} - \frac{1-r}{2A_2(x^{(k)})}\left\{\left[1 - \frac{2r}{r-1}u\left(x^{(k)}\right)A_2\left(x^{(k)}\right)\right]^{\frac{1}{r}} - 1\right\} \quad (1)$$

where $r \neq 1$ is a real parameter. Taking different values of r in (1), various root-solvers are generated. In the limit case when $r = 1$ Popovski's method (1) reduces to Newton's method

$$x^{(k+1)} = x^{(k)} - \frac{f(x^{(k)})}{f'(x^{(k)})}$$

of the second order.

The following choices $r = -1, r = 1/2, r = 2$ are of special interest and produce from (1) Halley's method [9], Chebyshev's method [9] and Euler's method [3], respectively, given by

$$x^{(k+1)} = x^{(k)} - \frac{u\left(x^{(k)}\right)}{1-u\left(x^{(k)}\right)A_2\left(x^{(k)}\right)} \quad (1)_{\mathrm{H}}$$

$$x^{(k+1)} = x^{(k)} - u\left(x^{(k)}\right)\left[1 + u\left(x^{(k)}\right)A_2\left(x^{(k)}\right)\right] \quad (1)_{\mathrm{C}}$$

$$x^{(k+1)} = x^{(k)} - \frac{2u\left(x^{(k)}\right)}{1 + \sqrt{1 - u(x^{(k)})A_2(x^{(k)})}} \quad (1)_{\mathrm{E}}$$

Although Popovski's family produces well-known iterative methods, three of which have been presented above, it was rarely studied in literature. In order to give a proper credibility to this method and point to its good convergence properties, in this part we perform dynamic study of some special cases of the family using a new, modern methodology based on basins of attraction. This approach provides not only visual insight into convergence behavior, but also delivers precise data on the executed CPU time for each basin, average number of iterations needed to reach termination criterion and the

percentage of divergent points from the basin. The last characteristic indicates the quality of the tested method concerning the size of domain of convergence.

The basin of attraction is concerned with iterative zero-finding methods applied to a tested function f. Geometrically, it is presented by the set of zero approximations located in a region (usually rectangle R) in the complex plane. Connected, these approximations make trajectories that converge to the sought zeros of f.

Basins of attraction are plotted over the rectangle R centered at the origin and containing all zeros of the tested function. Initial approximations start from equally spaced points inside the square R (making an equidistant lattice L_R with the resolution $m \times n$). Basin is formed from zero approximations that tend to the target zeros (attraction points). Drawing basins of attraction, the following rules are executed:

– Trajectories of approximations x_i to the zeros α_i are plotted until the stopping criterion $|x_i - \alpha_i| < \tau$ is fulfilled for all zeros (τ is usually 10^{-5} or 10^{-6}).

– Each basin is colored by a different color.

– Each basin is divided into several parts, each of which is shaded darker (lighter) as the number of iterations rises (decreases).

– Starting points that lead to the divergence are colored black.

– We set the maximum of I_{MAX} iterations as a limit for every initial point; in the case that the number of iterations exceeds I_{MAX}, we proclaim the considered initial point as divergent and paint it black.

It is preferable that each basin of attraction (counting all iterations) is as large as possible and unvaried, and possesses as small as possible: CPU execution time, average number of iteration, divergent points and fewer number of blobs and fractals.

The basins of attraction for the methods $(1)_H$, $(1)_C$ and, $(1)_E$ applied to the polynomial $p(z) = x^4 - x$, are displayed on Figures 1-3. We have dealt with I_{MAX} =40 and the precision $\tau = 10^{-5}$.

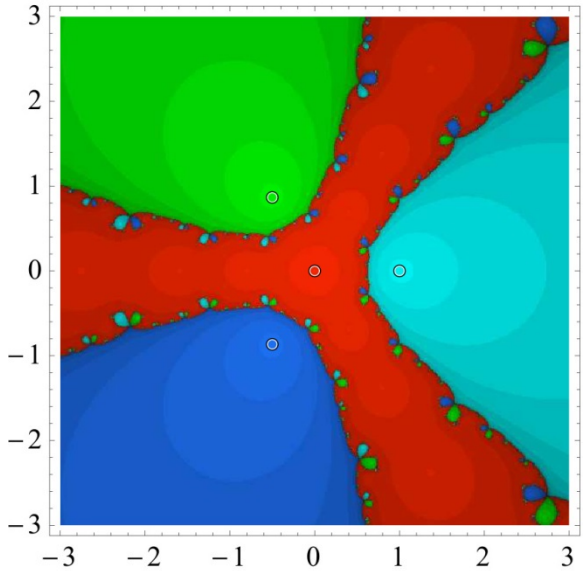

Fig. 1 Basin of attraction for Halley's method $(1)_H$

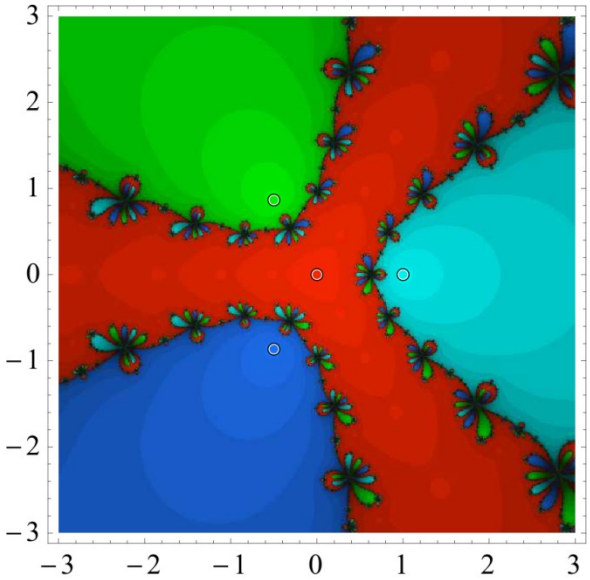

Fig. 2 Basin of attraction for Chebyshev's method $(1)_C$

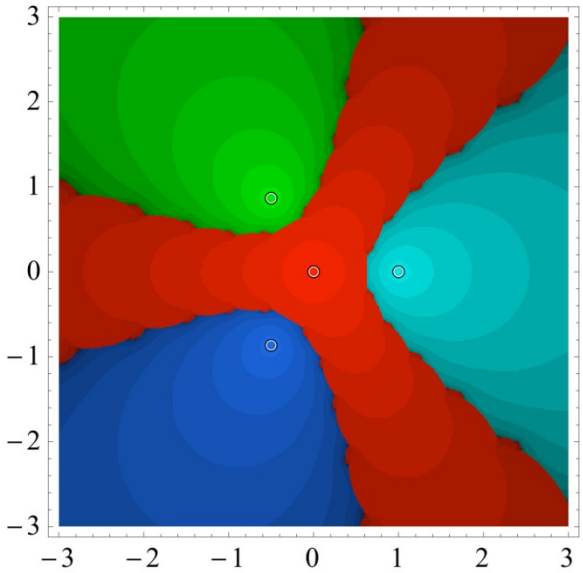

Fig. 3 Basin of attraction for Euler's method $(1)_E$

According to the data obtained during the plotting basins of attractions, see Table I, it turns out that Halley's method is the fastest, it reaches termination criterion in the smallest average iterations and has no divergent points. A number of tested functions (omitted here to save the space) has shown that Halley's methods also demonstrates the best convergence characteristics.

TABLE I DYNAMIC STUDY DATA

Methods	$(1)_H$	$(1)_C$	$(1)_E$
CPU (in sec)	66.09	82.72	91.83
Aver. iterations	5.02	6.22	6.58
Div. points (%)	0	0.0044	0

III. Popovski-like simultaneous methods

In what follows we will apply a suitable transformation to Popovski's family (1) for finding a single zero to derive a new one-parameter family for the simultaneous determination of all simple zeros of a polynomial. We are focused on iterative methods for the simultaneous determination of polynomial zeros since they are often used in applied mathematics but also in solving various problems of a wide variety of scientific disciplines, see, e.g., [3], [4], [8]. The considerably advantage of finding polynomial zeros simultaneously, compared for a method of deflation that finds only one zero at the time, consists of its remarkable self-correcting properties, as presented graphically in Section VI.

For simplicity, in the sequel we will often omit the iteration index k. Let P be a monic polynomial of degree n with simple zeros $\alpha_1, \ldots, \alpha_n$. Then x_i presents the current approximation to the zero α_i and $\hat{x}$ i is a new approximation calculated in the next iteration. Let us introduce

$$\delta_{\lambda,i} = \frac{P^{(\lambda)}(x_i)}{P(x_i)}, \quad S_{\lambda,i} = \sum_{\substack{j=1 \\ j\neq i}}^{n} \frac{1}{(x_i - x_j)^{\lambda}},$$

$$d_i = \delta_{2,i} - (\delta_{1,i})^2 + S_{2,i} \quad (\lambda = 1,2).$$

Let us define the rational function

$$W_i(x) = \frac{P(x)}{\prod_{j\neq i}(x - x_j)} \quad \left(x \neq x_j, i, j \in \{1, \ldots, n\}\right). \qquad (2)$$

Obviously, the function $W_i(x)$ has the same zeros as the polynomial $P(x)$, which is of crucial interest in designing a new family. Setting $x = x_i$ into (2) and applying the logarithmic derivatives to (2) (and then setting $x = x_i$), we find

$$w_{10}(x_i) := \frac{W_i'(x_i)}{W_i(x_i)} = \delta_{1,i} - S_{1,i}\,, \qquad (3)$$

$$w_{21}(x_i) := \frac{W_i''(x_i)}{W_i'(x_i)} = \delta_{1,i} - S_{1,i} + \frac{\delta_{2,i} - (\delta_{1,i})^2 + S_{2,i}}{\delta_{1,i} - S_{1,i}}$$

$$= w_{10}(x_i) + \frac{d_i}{\omega_{10}(x_i)}. \qquad (4)$$

Substitute

$$u(x_i) = \frac{P(x_i)}{P\prime(x_i)} \quad \text{with} \quad \frac{W_i(x_i)}{W_i'(x_i)} = w_{01}(x_i)$$

and

$$A_2(x_i) = \frac{P\prime\prime(x_i)}{2P\prime(x_i)} \quad \text{with} \quad \frac{W_i''(x_i)}{2W_i'(x_i)} = w_{21}(x_i)/2$$

in (1). Using the expressions (3) and (4) we obtain a new one-parameter family of iterative methods for the simultaneous determination of all simple zeros of a polynomial

$$\hat{x}_i = x_i - \frac{1-r}{\omega_{21}(x_i)}\left\{\left[1 - \frac{r}{r-1}\frac{\omega_{21}(x_i)}{\omega_{10}(x_i)}\right]^{\frac{1}{r}} - 1\right\} \quad (i = 1, \ldots, n) \qquad (5)$$

Introducing the iteration index k we present the family (5) in the form

$$x_i^{(k+1)} = x_i^{(k)} - \frac{1-r}{w_{21}(x_i^{(k)})}\left\{\left[1 - \frac{r}{r-1}\frac{w_{21}(x_i^{(k)})}{w_{10}(x_i^{(k)})}\right]^{\frac{1}{r}} - 1\right\}$$

$$(i = 1, \ldots, n, k = 0,1, \ldots, r \neq 1) \qquad (6)$$

where the values ω_{21} and ω_{10} are calculated by (3) and (4) at the points $x_j^{(k)}$ ($j \in \{1, \ldots, n\}$). Taking the values $r = -1, r = 2, r = 1/2$ and $r = 1$ (the limit case) in (6), we obtain Halley-like method $(6)_H$, Euler-like method $(6)_E$, Chebyshev-like method $(6)_C$, and Newton-like method $(6)_N$ (better known as Ehrlich-Aberth's method [1], [2]), respectively.

As example, we present the well-known Ehrlich-Aberth's method of the order three, which is generated from (6) in the limit case $r = 1$:

$$x_i^{(k+1)} = x_i^{(k)} - \frac{1}{\frac{P'(x_i^{(k)})}{P(x_i^{(k)})} - \sum_{j\neq i}\frac{1}{x_i^{(k)} - x_j^{(k)}}}$$

$$(i = 1, \ldots, n, \ k = 0,1, \ldots) \qquad (7)$$

IV. Convergence analysis

In this section we determine the order of convergence of the family of simultaneous methods (6). Introduce the errors

$$\varepsilon_i = x_i - \alpha_i, \ \hat{\varepsilon}_i = \hat{x}_i - \alpha_i.$$

Let $|\varepsilon|$ be the absolute value of the error ε of maximal magnitude, $|\varepsilon| = \max_{1\leq j\leq n}|\varepsilon_j|$. Assume that magnitudes of all errors $\varepsilon_1, \ldots, \varepsilon_n$ are approximately of the same order, then

$$\varepsilon_j = O_M(\varepsilon_i) \text{ and } \varepsilon_j = O_M(\varepsilon). \qquad (8)$$

Starting from the factorization

$$P(x) = \prod_{j=1}^{n}(x - \alpha_j)$$

and using the logarithmic derivative, we find

$$\frac{P\prime(x)}{P(x)} = \sum_{j=1}^{n}\frac{1}{x-\alpha_j}. \qquad (9)$$

Hence

$$\left(\frac{P'(x)}{P(x)}\right)' = \frac{P''(x)}{P'(x)} - \left(\frac{P'(x)}{P(x)}\right)^2 = -\sum_{j=1}^{n}\frac{1}{(x-\alpha_j)^2}. \qquad (10)$$

Let us introduce the abbreviations

$$b_{ij} = \frac{1}{(x_i - \alpha_j)(x_i - x_j)},$$

$$c_{ij} = \frac{x_j + \alpha_j - 2x_i}{(x_i - \alpha_j)^2(x_i - x_j)^2},$$

$$B_i = \sum_{j\neq i} b_{ij}\,\varepsilon_j, \quad C_i = \sum_{j\neq i} c_{ij}\,.$$

Then, setting $x = x_i$ by combining (10) and (11), we find

$$w_{10}(x_i) = \frac{1}{u(x_i)} = \frac{1-\varepsilon_i B_i}{\varepsilon_i}, \quad d_i = -\frac{1+\varepsilon_i^2 C_i}{\varepsilon_i^2} \qquad (11)$$

$$w_{21}(x_i) = w_{10}(x_i) + \frac{d_i}{w_{10}(x_i)} = \frac{-2B_i + \varepsilon_i(B_i)^2}{1-\varepsilon_i B_i}. \qquad (12)$$

Now we get

$$p_i := \frac{w_{21}(x_i)}{w_{10}(x_i)} = \frac{\varepsilon_i(-2B_i - \varepsilon_i C_i + \varepsilon_i(C_i)^2)}{1-\varepsilon_i B_i}.$$

Note that $B_i = \beta_i \varepsilon_i = O_M(\varepsilon_i)$ and $C_i = \gamma_i \varepsilon_i = O_M(\varepsilon_i)$, where $\beta_i = O_M(1)$ and $\gamma_i = O_M(1)$ are some quantities that depend on the polynomial zeros and their approximations.

Let g_1 denote the r-th root in (5). Using symbolic computation in *Mathematica*, by (11) and (12) we find

$$g_1 := \left(1 - \frac{r}{1-r}\, p_i\right)^{1/r} = 1 + \frac{2\varepsilon_i B_i}{r-1} + \frac{\varepsilon_i{}^2 (C_i + (B_i)^2)}{1-\varepsilon_i (C_i)^2} + \frac{2\varepsilon_i{}^3 (r+1)(B_i)^3}{3(r-1)^2} + O_M(\varepsilon \varepsilon_i{}^4),$$

wherefrom

$$g_2 := \left(1 - \frac{r}{1-r}\, p_i\right)^{\frac{1}{r}} - 1 = g_1 - 1$$

$$= \frac{2\varepsilon_i B_i}{r-1} + \frac{\varepsilon_i{}^2 (C_i + (B_i)^2)}{1-\varepsilon_i (C_i)^2} + \frac{2\varepsilon_i{}^3 (r+1)(B_i)^3}{3(r-1)^2} + O_M(\varepsilon^5) \qquad (13)$$

Finally, in view of (13), we obtain from (5)

$$\hat{\varepsilon}_i = \frac{(\varepsilon_i)^3 \varepsilon \left[(\gamma_i)^2 (r-5) + 3\beta_i (r-1)\right]}{6(r-1)} + O_M(\varepsilon^5) \qquad (14)$$

Since $\varepsilon_i = O_M(\varepsilon)$, from (14) we can state the following theorem.

Theorem 1. *Assume that the initial approximations $x_1{}^{(0)}, \dots, x_n{}^{(0)}$ are sufficiently close to the respective zeros $\alpha_1, \dots, \alpha_n$ of a given polynomial P. Then*

$$\varepsilon_i^{(k+1)} = \frac{\left(\varepsilon_i^{(k)}\right)^3 \varepsilon^{(k)} \left[\left(\gamma_i^{(k)}\right)^2 (r-5) + 3\beta_i^{(k)} (r-1)\right]}{6(r-1)} + O_M\left(\left(\varepsilon^{(k)}\right)^5\right),$$

where $\beta_i^{(k)} = O_M(1)$ and $\gamma_i^{(k)} = O_M(1)$ are some quantities that depend on the polynomial zeros and their approximations producedin the k-th iteration. Therefore, the order of convergence of the family of simultaneous methods (5) is equal to four.

V. Numerical experiments

In our numerical experiments, we have applied the simultaneous methods from the family (5) to several algebraic polynomials of relatively high degree. For illustration, we present two examples. As a measure of accuracy of the obtained approximations, we have calculated Euclid's norm

$$e^{(k)} = \left(\sum_{i=1}^{n} |x_i^{(k)} - \alpha_i|^2\right)^{1/2} \quad (k = 0,1,\dots).$$

Example 1. We have applied three methods $(6)_H$, $(6)_C$, $(6)_E$ to the polynomial

$$P_1(x) = (x-4)(x+1)(x^4-16)(x^4+4)(x^2+9)(x^2+2x+5) \times (x^2-4x+5)(x^2-2x+10)(x^2+16)$$

of degree 20. The zeros of $P_1(x)$ can be easily faced from the above factorization. The error norms $e^{(k)}$ of approximations in the first three iterations are given in Table II, where $A(-h)$ means $A \times 10^{-h}$.

TABLE II Norms of approximation errors to the zeros of the polynomial $P_1(x)$

Errors	$(1)_H$	$(1)_C$	$(1)_E$
$e^{(1)}$	1.12(−2)	1.48(−2)	1.49(−2)
$e^{(2)}$	3.63(−10)	1.94(−9)	7.85(−10)
$e^{(3)}$	1.00(−39)	1.31(−36)	3.24(−38)

Example 2. The same methods from Example 1 have been applied to the polynomial of Wilkinson's type

$$P_2(x) = \prod_{j=1}^{15} (x - j)$$

of degree $n = 15$. In spite of the fact that polynomials of this kind are ill-conditioned (small changes of coefficients cause great variations of values of the polynomial zeros) the applied methods have demonstrated good behaviour, which is evident from Table III.

TABLE III Norms of approximation errors to the zeros of the polynomial $P_2(x)$

Errors	$(1)_H$	$(1)_C$	$(1)_E$
$e^{(1)}$	1.39(−2)	1.31(−2)	1.72(−2)
$e^{(2)}$	1.21(−9)	6.64(−10)	5.23(−9)
$e^{(3)}$	3.68(−37)	1.34(−38)	1.28(−34)

The entries displayed in Tables II and III show that all tested methods from the family (5) produce approximations of very high accuracy. From Tables II and III, and many tested polynomials not presented in the paper due to the limit of pages, we are not able to get dominance on some particular method from the family (5).

VI. On global convergence of simultaneous methods

The research of the most intriguing and challenging problem referred to global or almost global convergence of simultaneous methods has become possible only with the great advance of development of computer graphics and computer algebra systems at the beginning of the 21-th century. The crucial idea is the use of so-called Aberth's distribution of initial approximations [1], equidistantly spaced on a circle in the complex plane: starting from Aberth's initial approximations, the complete flow of the implemented iterative process is tracked until the stopping criterion is satisfied.

The described type of computer visualization in the form of trajectories, assigned to each polynomial zero, is of particular interest since it delivers a quite new insight into the possible global convergence characteristics of simultaneous methods and reveals to the extent of their stability and robustness. For more details see the paper [6].

$$\begin{aligned} p(x) = {} & x^{14} - (2.6761309 - 0.26081334\, i)\, x^{13} + (3.227117 - 0.2691845\, i)\, x^{12} - (1.5329053 + 0.9320745\, i)\, x^{11} \\ & - (4.044812 - 2.2129954\, i)\, x^{10} + (12.272863 - 2.040898\, i) x^9 \\ & + (22.97764 + 0.1230355 i)\, x^8 + 31.147546 + 3.3809999\, i) x^7 \\ & - (34.2570503 + 7.0105129\, i)\, x^6 + (31.36610635 + 9.7421391\, i)\, x^5 \\ & - (24.706450 + 10.041725\, i)\, x^4 + (15.899472 + 7.561425811\, i)\, x^3 \\ & - (8.586289 + 4.461636\, i) x^2 + (3.2104514 + 1.8514972\, i)\, x \\ & - (1.1330965 + 0.5266331\, i) \end{aligned}$$

This polynomial has 10 zeros very close to the unit circle. Note that polynomials with zeros on/very close the unit circle (not necessarily all of them) appear in some scientific brunches, for example, in signal processing. The positions of approximations in the course of iterative process are marked by blue points in the complex plane, making trajectories, while the polynomial zeros are coloured red.

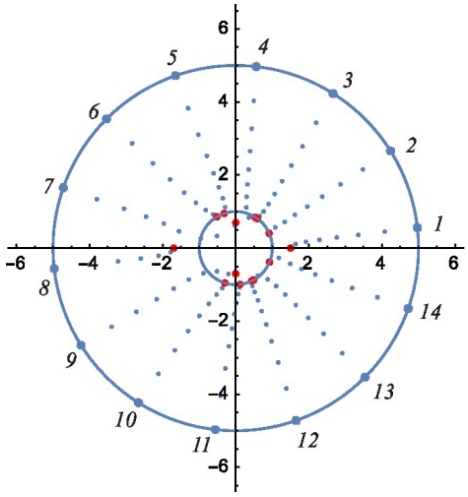

Fig. 4 Trajectories of Halley-like method $(6)_H$

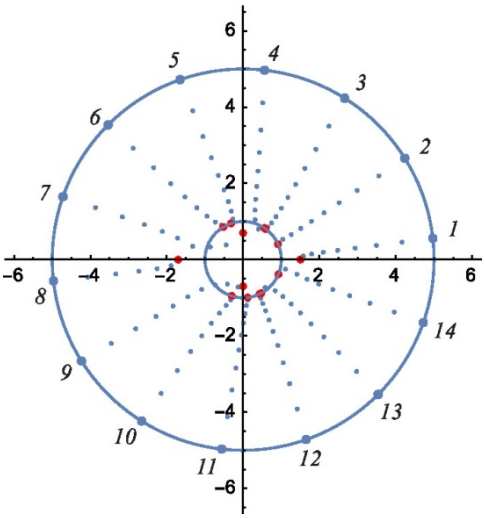

Fig. 5 Trajectories of Chebyshev-like method $(6)_C$

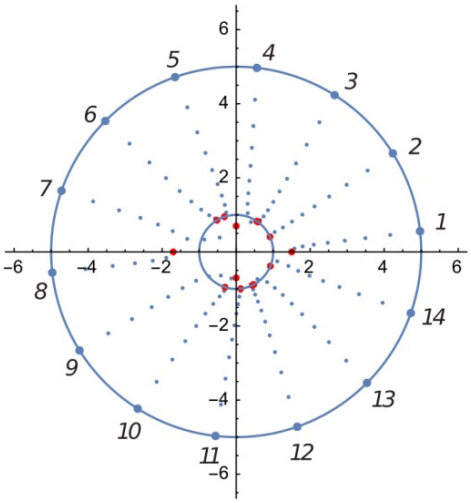

Fig. 6 Trajectories of Euler-like method $(6)_E$

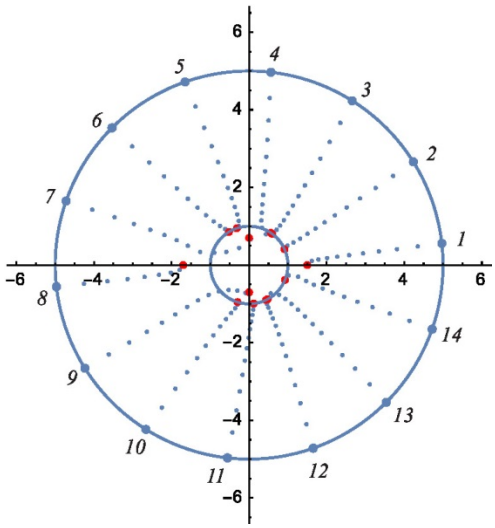

Fig. 7 Trajectories of Erlich-Aberth's method $(6)_N$

From Figures 4, 5, 6 and 7 one can notice that all four tested methods have trajectories of very similar form for the considered polynomial $p(x)$. The methods $(6)_H$, $(6)_C$ and $(6)_E$ have satisfied the stopping criterion in $e^{(k)} < 10^{-5}$ in 12 iterations, while Erlich-Aberth's method $(6)_N$ needed 16 iterations. All trajectories have fairly regular paths; besides, they are almost radially distributed tending straightforwardly to the zeros in the course of iterating. Flows of iterative processes, presented by these trajectories, demonstrate the stability and robustness of the proposed Popovski-like family and point to possible globally convergent properties.

Let us note that the analytical proof of global convergence has not proved yet for any simultaneous methods although a huge number of numerical results indicates a positive answer. However, from a mathematical point of view, this challenging task still remains an open problem.

VII. Conclusions

We have focused our research on almost forgotten one-parameter Popovski's family from 1980. for solving nonlinear equations of the form $f(z) = 0$, iteratively. Using computer graphics relied on basins of attraction, we have performed dynamic study of Popovski's family in the case of a simple zero. This approach, beside computer visualization of iterative process, delivers additional useful information on the tested method such as CPU time, average number of iteration, percentage of divergent points, and so on. Using Popovski's family we have constructed a new one-parameter family of simultaneous methods for the determination of all simple zeros of a polynomial. Choosing different values of the involved parameter, the presented family generates a variety of simultaneous methods for finding polynomial zeros. Aside from numerical experiments, we have paid special attention to the flow of iterative processes using targeting trajectories for each of polynomial zeros. To investigate the mentioned two families of Popovski's type, advanced computer tools such as symbolic computation, basins of attraction and multi-precision arithmetic, have been employed.

REFERENCES

[1] O. Aberth, “Iteration methods for finding all zeros of a polynomial simultaneously,” Math. Comp. vol. 27, pp. 339-344, 1973.

[2] L.W. Ehrlich, “A modified Newton method for polynomials”, Comm. ACM vol. 10, pp. 107-108, 1967.

[3] J.M. McNamee, Numerical Methods for Roots of Polynomials, Part I, Elsevier, Amsterdam, 2007.

[4] J.M. McNamee, V. Pan, Numerical Methods for Roots of Polynomials, Part II, Elsevier, Amsterdam, 2013.

[5] I. Petković, Đ. Herceg, “Symbolic computation and computer graphics as tools for developing and studying new root-finding methods,” Appl. Math. Comput., vol. 295, pp. 95-113, 2017.

[6] I. Petković, Đ. Herceg, “Computer methodologies for comparison of computational efficiency of simultaneous methods for finding polynomial zeros,” J. Comput. Appl. Math., vol. 368, pp. 1-19, ID 112513, 2020.

[7] D.B. Popovski, “A family of one point iteration formulae for finding roots”, Int. J. Comput. Math., vol. 8, pp. 85-88, 1980.

[8] Bl. Sendov, A. Andreev, N. Kjurkchiev, Numerical Solution of Polynomial Equations, Handbook of Numerical Analysis (eds P. Ciarlet, J. Lions), Vol.III, Amsterdam, Elsevier, 1994, pp. 625-778.

[9] J.F. Traub, Iterative Methods for the Solution of Equations, Prentice Hall, New York, 1964.

THE 5th INTERNATIONAL CONFERENCE
MECHANICAL ENGINEERING IN XXI CENTURY

December 9-10, 2020
Faculty of Mechanical Engineering in Niš, Serbia

Functions Defined by Infinite Products and the Corresponding Equations

Predrag RAJKOVIĆ, Slađana MARINKOVIĆ, Miomir STANKOVIĆ

Department of Mathematics, Faculty of Mechanical Engineering, University of Niš, A. Medvedeva 14, Niš, Serbia,
Department of Mathematics, Faculty of Occupational Safety, University of Niš, Čarnojevićeva 10a, Niš, Serbia,
Department of Mathematics, Faculty of Electronic Engineering, University of Niš, A. Medvedeva 14, Niš, Serbia,
pedja.rajk@masfak.ni.ac.rs, miomir.stankovic@gmail.com, sladjana.marinikovic@elfak.ni.ac.rs

***Abstract*— In this paper, we deal with infinite products and functions defined by them. We examine the problems of numerical computing their values. Also, we consider a few modifications of the well-known methods for numerical solving of a equation or a system of equations. Especially, we included Newton's and the Newton-Kantorovich. The purpose was to adapt them to cases when the functions are given in the form of infinite products. The examples comprehend the infinite q-power products and prove that the methods are pretty suitable for them.**

***Keywords*— infinite products, functions, equations, iterative methods, q-calculus**

I. Introduction

A lot of papers were written about the iterative methods for solving of a nonlinear equation of the type $f(x) = 0$, where $f(x)$ is a continuous operator defined on a nonempty subset of a Banach space.

In a few papers were considered some unusual functions such as continuous but non-differentiable functions (Hernandez & Rubio [6]) or non-continuous functions.

Another perspective branch of mathematics is q-calculus. It appears as a connection between mathematics and physics (see Andrews et al. [2], Gasper & Rahman [4], Koekoek & Swarttouw [8]). It has a lot of applications in different mathematical areas, such as: number theory, combinatorics, orthogonal polynomials, basic hypergeometric functions and other sciences: quantum theory, mechanics and theory of relativity.

II. Basics of q-calculus

Let q be a complex number such that $|q| < 1$. A q-complex number $[a]_q$ is defined by

$$[a]_q = \frac{1-q^a}{1-q} \ (|q| < 1;\ a \in C) \tag{1}$$

The factorial of a positive integer number $[n]_q$ and q-binomial coefficient, we define by

$$[0]_q! = 1, \qquad [n]_q! = \prod_{k=1}^{n} [k]_q \quad (n \in N) \tag{2}$$

$$\begin{bmatrix} n \\ k \end{bmatrix}_q = \frac{[n]_q!}{[k]_q![n-k]_q!} \quad (k, n \in N). \tag{3}$$

Hence follows the notion of q-Pochammer symbol

$$(a;q)_n = \prod_{k=0}^{n-1}(1 - aq^k) \ \ (n \in N \cup \{\infty\}). \tag{4}$$

Especially, $(a;q)_0 = 1$.

The fractional order q-Pochammer symbol is defined by

$$(a;q)_\lambda = \frac{(a;q)_\infty}{(aq^\lambda;q)_\infty} \qquad (\lambda \in R). \tag{5}$$

Remark 1. In the software Wolfram Mathematica there is command $\mathrm{QPochhammer}[a, q, n]$ which gives $(a;q)_n$ for $\in N$ and $\mathrm{QPochhammer}[a, q]$ which gives $(a;q)_\infty$.

Even more, $N\big[\mathrm{QPochhammer}[a, q]\big]$ will give the appro-ximated value of $(a;q)_\infty$.

The q-derivative of a function $f(x)$ is

$$D_q f(x) = \frac{f(x) - f(qx)}{(1-q)x} \quad (x \neq 0), \tag{5}$$

$$D_q f(0) = \lim_{x \to 0} D_q f(x). \tag{6}$$

and high q-derivatives

$$D_q^0 f(x) = f(x), \ \ D_q^n f(x) = D_q\left(D_q^{n-1} f(x)\right) \ \ (n \in N). \tag{7}$$

From the above definition, it is obvious that a continuous function on an interval, which does not include zero, is continuously q-differentiable function.

In q-analysis, the q-integral is defined by

$$I_q f(x) = \int_0^a f(t) d_q t = a(1-q) \sum_{k=0}^{\infty} f\,(aq^k)\, q^k, \tag{8}$$

$$\int_a^b f(t) d_q t = \int_0^b f(t) d_q t - \int_0^a f(t) d_q t. \tag{9}$$

When $q \to 1$, we get well-known mathematical notions

$$\lim_{q \to 1} [a]_q = a, \qquad \lim_{q \to 1} \begin{bmatrix} n \\ k \end{bmatrix}_q = \binom{n}{k}, \tag{10}$$

$$\lim_{q \to 1} D_q f(x) = f'(x), \tag{11}$$

$$\lim_{q \to 1} \int_a^b f(t) d_q t = \int_a^b f(t) dt. \tag{12}$$

III. Numerical computing of infinite products

We are not able to compute the exact value of the infinite product in the most cases. That is why a few numerical methods are developed for its approximating.

The simplest way is to omit factors from an index and to compute truncated product

$$P = \prod_{k=1}^{\infty} a_k \approx \prod_{k=1}^{n} a_k = P_n \quad (n \in N). \tag{13}$$

But, it is not an effective method, neither to exactness nor to number of operations. Slater [12] mentioned some computing difficulties for $0.89 < q < 1$, which can be avoided by using the logarithmic form.

The *Euler identity*

$$\prod_{k=1}^{\infty}(1 - aq^k) = \sum_{k=0}^{\infty}(-1)^k a^k \frac{q^{k(k+1)/2}}{(q;q)_k}, \tag{14}$$

enable us to compute an infinite sum instead of product

$$\prod_{k=1}^{\infty}(1 - aq^k) \approx \sum_{k=0}^{n}(-1)^k a^k \frac{q^{k(k+1)/2}}{(q;q)_k}. \tag{15}$$

Sokal [13] proved that the truncated method (13) has linear convergence, which is weaker in comparison with the square convergence of the method (14). Computing by the Euler identity is more precise although it has troubles for q nearby 1 because of dividing by $(q;q)_n$.

Example 1. The numerical evaluating of the infinite product

$$P = (xq;q)_\infty, \tag{16}$$

by the formulas (13) and (15) for $x = 1/3$ and $q = 1/2$ are compared on the Table 1. Here, $a(-n) = a \cdot 10^{-n}$.

TABLE 1. THE COMPARISON OF THE NUMERICAL COMPUTING OF THE INFINITE PRODUCT (16) BY THE FORMULAS (13) AND (15)

n	Error by (13)	Error by (15)
5	0.736 (-2)	0.222 (-8)
10	0.229 (-3)	0.264 (-24)
20	0.223 (-6)	0.959 (-79)
30	0.217 (-9)	0.274 (-163)

Gatteschi [5] has introduced the iterative scheme

$$x_{n+1} = x_n \frac{-(1-q)x_n + (3-q)y_n}{2y_n}, \quad y_{n+1} = \frac{x_{n+1}y_n}{qx_n + (1-q)y_n}. \tag{17}$$

with initial values x_0 wand y_0 which have to be related by $(1-q)x_0 = (1+2a-q)y_0$ (see Allasia[1]).

Then

$$\lim_{n\to\infty} x_n = \lim_{n\to\infty} y_n = P = x_0(a;q)_\infty. \tag{18}$$

But, the rate of convergence is similar as by (13).

Remark 2. The expansions of

$$\prod_{k=1}^{\infty}(1 - q^{ak})(1 - q^{bk}) \tag{19}$$

were studied by Sun [14].

IV. On q-Newton method

Suppose that an equation $f(x) = 0$, has the unique isolated solution ξ: $f(\xi) = 0$. If x_n is an approximation to the exact solution ξ, by using Jackson's q-Taylor formula, we have (see Jackson [7] and Rajković and alt. [10])

$$0 = f(\xi) \approx f(x_n) + D_q f(x_n)(\xi - x_n),$$

wherefrom

$$\xi \approx x_n - \frac{f(x_n)}{D_q f(x_n)}.$$

So, we can *construct q-Newton method*

$$x_{n+1} = x_n - \frac{f(x_n)}{D_q f(x_n)}. \tag{20}$$

This method written in the form

$$x_{n+1} = x_n - \frac{x_n - qx_n}{f(x_n) - f(qx_n)} f(x_n). \tag{21}$$

resembles the method of chords (secants).

Theorem 1 (Rajković et al. [11]). *Let the function $f(x)$ be defined on $(x_0 - R, x_0 + R)$ and the conditions*

$$\left|D_q f(x) - D_q f(y)\right| \le L|x - y|, \tag{22}$$

$$\left|f(x) - f(y) - D_q f(y)(x - y)\right| \le \frac{L}{2}|x - y|^2, \tag{23}$$

are satisfied for all $x, y \in (x_0 - R, x_0 + R)$ and a constant $L > 0$. If here are fulfilled the inequalities

$$\left|D_q f(x_0)\right| \ge \frac{1}{b} > 0, \ \left|\frac{f(x_0)}{D_q f(x_0)}\right| \le a, \ \ h = abL \le \frac{1}{2}, \tag{24}$$

and

$$R > r = a\frac{1 - \sqrt{1 - 2h}}{h}. \tag{25}$$

Then the sequence $\{x_n\}$ converges to the solution $\xi \in (x_0 - r, x_0 + r)$ and it is valid

$$|\xi - x_n| \le \frac{a}{2^{n-1}}(2h)^{2^n - 1}. \tag{26}$$

Theorem 2 (Marinković et al. [9]). *Let a function $f(x)$ be defined on (a, b) and satisfies the conditions*

$$\left|D_q f(x_n)\right| \ge M^{p-1} > 0 \quad (1 \le p \le 2), \tag{27}$$

$$\left|f(x) - f(y) - D_q f(y)(x - y)\right| \le L^{p-1}|x - y|^p, \tag{28}$$

where M and L are positive constants.

If the equation $f(x) = 0$ has the unique isolated solution $\xi \in (a, b)$, then, for all initial values $x_0 \in (\xi - h, \xi + h)$, where $h = min\{a, M/L\}$, the q-Newton method converges to the exact solution ξ and it is valid

$$|\xi - x_n| \le \left(\frac{L}{M}\right)^{p^n - 1} |\xi - x_0|^{p^n - 1}. \tag{29}$$

Example 2. For fixed real numbers b and $q \in (-1,1)$, we consider the equation

$$f(x) \equiv (x;q)_\infty - b = 0, \tag{30}$$

with unknown value x. Fine thing in q-Newton method is appearance of $f(qx) = (xq;q)_\infty - b$. It is the function of the same type as $f(x)$ what makes easier the required computations. In the special case:

$$b = \sqrt[24]{\frac{64}{e^\pi}}, \ q = \frac{1}{e^{2\pi}}, \tag{31}$$

starting with initial value $x_0 = 0.5$, after two iterations by q-Newton method we get the approximation $x_2 = -0.0432139$, what gives the approximation with six exact digits of the exact solution $x = -e^{-\pi}$. It is quite in coincidence with the known product

$$\prod_{n=0}^{\infty}\left(1+e^{-(2k+1)\pi}\right)=\sqrt[24]{\frac{64}{e^{\pi}}}. \tag{32}$$

Remark 3. Let us remind that the small and big q-exponential functions are defined by

$$e_q(z)=\frac{1}{(z;q)_\infty}, \quad E_q(z)=(-z;q)_\infty. \tag{33}$$

Hence, for a chosen q and b, by this method, we can find the unknown value z such that $b=e_q(z)$ or $b=E_q(z)$.

Example 3. For fixed real numbers $a\in(-1,1)$ and $b\in R$, we consider the equation

$$f(x)\equiv(a;x)_\infty-b=0, \tag{34}$$

with unknown value x. Let us consider the special case $b=0.0895642804$ and $a=0.75$. Starting with $x_0=0.5$, and applying q-Newton method with $q=0.75$, after three iterations, we find $x_3=0.538463$. It is very close to $x=7/13$.

Example 4. For fixed real numbers $q\in(-1,1)$ and $b\in R$, we consider the equation

$$f(x)\equiv\frac{(xq;q)_\infty}{(x;q)_\infty}-b=0, \tag{35}$$

with unknown x. Let us consider the special case $b=2.5$ and $q=0.75$. Starting with $x_0=q$, and applying q-Newton method with $q=0.7$, after six iterations, we find $x_6=0.60011$. It is very close to the exact solution $x=0.6$. Namely, the following identity is valid

$$\frac{(xq;q)_\infty}{(x;q)_\infty}=\frac{1}{1-x}. \tag{36}$$

Example 5. For fixed real numbers $a\in(-1,1)$, we consider the equation

$$f(x)\equiv(-a;x)_\infty^8-(a;x)_\infty^8-16a(-a^2;x)_\infty^8=0, \tag{37}$$

with unknown value x. Applying q-Newton method, we get very close approximation of the exact solution $x=a^2$. It comes from known identity

$$(-q;q^2)_\infty^8=(q;q^2)_\infty^8+16q(-q^2;q^2)_\infty^8. \tag{38}$$

Example 6. For fixed real numbers $a,q\in(-1,1)$ and $b\in R$, we consider the equation

$$f(x)\equiv(a;q)_x-b=0, \tag{39}$$

with unknown value x. For the special values

$$a=\frac{1}{2},\ \ q=\frac{3}{4},\ \ b=\frac{(1/2;3/4)_\infty}{(1/\sqrt{3};3/4)_\infty}, \tag{40}$$

applying q-Newton method with initial value $x_0=1$, in the six iterations, we get $x=-0.5$, what is the exact solution.

Example 7. For fixed real numbers $q\in(-1,1)$, we consider the equation

$$f(x)\equiv\prod_{k=1}^{\infty}(1-q^{8k})(1-xq^{16k})-1=0, \tag{41}$$

with unknown value x. Applying q-Newton method with initial value $x_0=1/2$, in a few iterations, we get $x=q^{-8}$, what is the exact solution. It is based on the Euler's identity (see Chen [3]):

$$\prod_{k=1}^{\infty}(1-q^{8k})(1-q^{16k-8})=1. \tag{42}$$

Example 8. Finding zeros of the continuous nowhere differentiable functions is a hard problem because the methods based on the differentiation can't be used. The first known function of this type is Weierstrass function given by the series:

$$f(x)\equiv\sum_{n=1}^{\infty}a^n\cos(b^n\pi x), \tag{43}$$

where b is an odd integer and $0<a<1, ab>1+\frac{3\pi}{2}$.

Wen [15] introduced the function with the same property as an infinite product. Let $0<a_n<1$ for every n and $\sum_{n=1}^{\infty}a_n$ is converging. Let $\{p_k\}$ be a sequence of even integers and $b_n=\prod_{k=1}^{n}p_k$. If $\lim_{n\to\infty}\frac{2^n}{a_np_n}=0$, then

$$f(x)\equiv\prod_{n=1}^{\infty}(1+a_n\sin(b_n\pi x)), \tag{44}$$

is a continuous nowhere differentiable function.

In special, let us take $a_n=\frac{1}{n^2}$, $p_n=4^n$. Applying q-Newton method with initial value $x_0=0.25$, and $q=0.99$ we get very close approximation of the exact solution $x=0.375$ ....

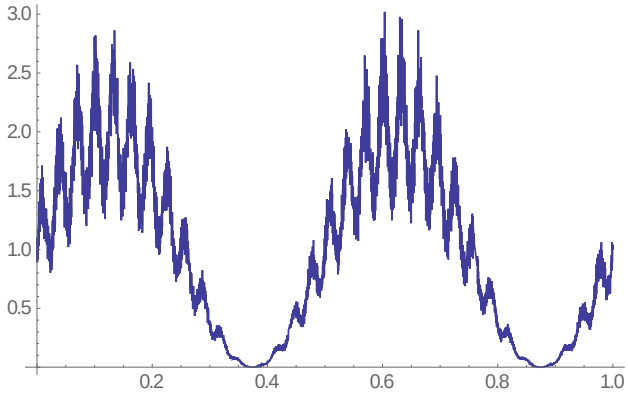

Fig. 1 The Wen's continuous nowhere differentiable function

V. On q-Newton-Kanotrovič method

Let $f_1(x,y)$ and $f_2(x,y)$ be two-variable real continuous functions. The partial q-derivatives of $f_i(x,y)$ $(i=1,2)$ are defined by

$$D_{q,x}f_i(x,y)=\frac{f_i(x,y)-f_i(qx,y)}{(1-q)x}\quad(x\neq0), \tag{45}$$

and

$$D_{q,y}f_i(x,y)=\frac{f_i(x,y)-f_i(x,qy)}{(1-q)y}\quad(y\neq0). \tag{46}$$

Suppose that (ξ,η) is an isolated real solution of the system of the equations

$$f_1(x,y)=0,\ f_2(x,y)=0. \tag{47}$$

If (x_n,y_n) is an approximation to the exact solution (ξ,η), by using Jackson's q-Taylor formula, we have

$$0=f_i(\xi,\eta)\approx f_i(x_n,y_n)+D_{q,x}f_i(x_n,y_n)(\xi-x_n)+D_{q,y}f_i(x_n,y_n)(\eta-y_n). \tag{48}$$

It can be written in the matrix form

$$0\approx\begin{bmatrix}f_1(x_n,y_n)\\f_2(x_n,y_n)\end{bmatrix}+W_n(x_n,y_n)\begin{bmatrix}\xi-x_n\\\eta-y_n\end{bmatrix}, \tag{49}$$

where

$$W_{q,n}(x_n, y_n) = \begin{bmatrix} D_{q,x} f_1(x_n, y_n) & D_{q,y} f_1(x_n, y_n) \\ D_{q,x} f_2(x_n, y_n) & D_{q,y} f_2(x_n, y_n) \end{bmatrix}. \quad (50)$$

If $W_{q,n}(x_n, y_n)$ is regular, there exists the inverse matrix $W_{q,n}^{-1}(x_n, y_n)$ so that we can formulate q–Newton–Kantorovich method in the form

$$\begin{bmatrix} x_{n+1} \\ y_{n+1} \end{bmatrix} = \begin{bmatrix} x_n \\ y_n \end{bmatrix} - W_{q,n}^{-1}(x_n, y_n) \begin{bmatrix} f_1(x_n, y_n) \\ f_2(x_n, y_n) \end{bmatrix}. \quad (51)$$

Its convergence is analysed in the paper Marinković at al. [9].

Example 9. For the fixed real number $q \in (-1,1)$, we consider system of the equations

$$f_1(x,y) \equiv 2(xq;q)_\infty - (y^3 q;q)_\infty = 0, \quad (52)$$

$$f_2(x,y) \equiv (x^2 q;q)_\infty + e^{(yq;q)_\infty} - 2 = 0, \quad (53)$$

with unknown value x and y. Especially, for $q = 0.75$, starting with initial values $x_0 = y_0 = q$, after $n = 8$ iterations provided by q–Newton–Kantorovich method, we find solution with six exact decimal digits $x = 0.3031358$, $y = 0.4522925$.

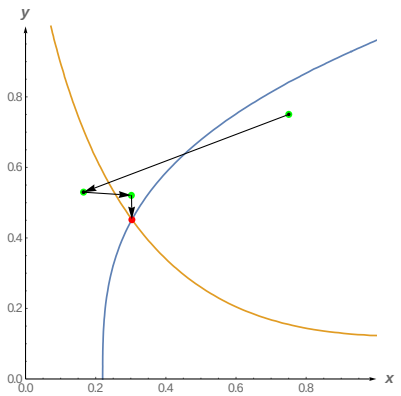

Fig. 2 The convergence of q-Newton-Kanotorovch method to the system solution

Example 10. For the fixed real number $q \in (-1,1)$, we consider system of the equations

$$f_1(x,y) \equiv 2(xq;q)_\infty - (yq;q)_\infty = 0, \quad (54)$$

$$f_2(x,y) \equiv (x^2 yq;q)_\infty - (q;q)_\infty = 0, \quad (55)$$

with unknown values x and y.
Especially, for $q = 3/4$, starting with initial values $x_0 = y_0 = 1/2$, after $n = 10$ iterations provided by q–Newton–Kantorovich method, we find solution with only three exact decimal digits $x = 1.02232$, $y = 0.95596$.

VI. Conclusions

Usage of the infinite products in different areas of mathematics and other sciences motivated us to examine the problems of their numerical computing. We modified the Newton's and the Newton-Kantorovich's method for the cases when the functions are given in the form of infinite products. The examples confirmed that the methods are pretty suitable for the infinite q-power products.

Acknowledgment

This research was financially supported by the Ministry of Education, Science and Technological Development of the Republic of Serbia.

References

[1] G. Allasia, F. Bonardo, On the Numerical Evaluation of Two Infinite Products, Mathematics of Computation 35, No. 151 (1980), pp. 917-931.

[2] G.E. Andrews, R. Askey, R. Roy, "Special Functions", Encyclopedia of Mathematics and its Aplications, Cambridge University Press, Cambridge, 1999.

[3] H-C. Chen, Another Simple Proof of the Quintuple Product Identity, International Journal of Mathematics and Mathematical Sciences 15 (2005), pp. 2511–2515

[4] G. Gasper, M. Rahman, Basic Hypergeometric Series, Encyclopedia of Mathematics and its Applications 96, Cambridge University Press, Cambridge, 2004.

[5] L. Gatteschi, Procedimenti iterativi per il calcolo numerico di due prodotti infiniti, Rend. Sem. Mat. Univ. Politec. Torino 29 (1969/70), pp. 187-201.

[6] M.A. Hernandez, M.J. Rubio, A modification of Newton's method for nondifferentiable equations, Journal of Computational and Applied Mathematics 164 (2004) pp. 409-417.

[7] F.H. Jackson, A q-form of Taylor's theorem, Mess. Math. Math. 38, (1909), pp. 62-64.

[8] R. Koekoek and R. F. Swarttouw, "Askey-scheme of hypergeometric orthogonal polynomials and its q-analogue", Report No 98-17, Delft University of Technology, 1998.

[9] S.D. Marinković, P.M. Rajković, M.S. Stanković, The q-iterative methods in numerical solving of some equations with infinite products, Facta Universitatis (Nis), Ser. Math. Inform. Vol. 28, No 4 (2013), pp. 379–392.

[10] P.M. Rajković, M.S. Stanković, S.D. Marinković, Mean value theorems in q-calculus. Matematički vesnik 54 (2002), pp. 171-178

[11] P.M. Rajković, S.D. Marinković, M.S. Stanković, On q-Newton-Kantorovich method for solving systems of equations, Applied Mathematics and Computation 168, No 2 (2005), pp. 1432-1448.

[12] L.J. Slater, Some new results on equivalent products, Proc. Cambridge Philos. Soc. 50 (1954), pp. 394-403.

[13] A.D. Sokal, Numerical computation $\prod_{n=1}^{\infty}(1 - tq^n)$, arXiv: mathNA /0212035, Dec., 2002.

[14] Z. H. Sun, The expansion of $\prod_{k=1}^{\infty}(1 - q^{ak})(1 - q^{bk})$, Acta Arithmetica 134.1 (2008), pp. 11-29.

[15] L. Wen, A nowhere differentiable continuous function, Amer. Math. Monthly 107 (2000), pp. 450–453.

THE 5th INTERNATIONAL CONFERENCE
MECHANICAL ENGINEERING IN XXI CENTURY

December 9-10, 2020
Faculty of Mechanical Engineering in Niš, Serbia

Parametric Modelling in Architecture

Dragana DIMITRIJEVIĆ JOVANOVIĆ[1], Ljiljana RADOVIĆ[2]

[1] Faculty of Civil Engineering and Architecture, University of Niš, A. Medvedeva 14, Niš, Serbia
[2] Faculty of Mechanical Engineering, University of Niš, A. Medvedeva 14, Niš, Serbia
dragana.dimitrijevic@masfak.ni.ac.rs, ljiljana.radovic@masfak.ni.ac.rs,

***Abstract*— Knowing the right input parameters and understanding geometrical logic, architects could achieve simultaneously a challenging aesthetic shape and an efficient functional design. Parametric modelling is a new approach to architectural design, using algorithms for the generation of virtual entities. The object, or model elements, could be generated automatically by internal logic arguments instead of being manually manipulated. Within this design process, architects could resolve visual, perceptive, material and structural issues while accomplishing significant time and precision improvements. This research paper aims to explore the position of parametric design in architectural practices and present the possibilities of algorithms in modelling architectural forms. Grasshopper will be considered as one of the graphical algorithm editors for a spiral staircase design.**

***Keywords*— parametric, design, geometry, architecture, algorithm**

I. Introduction

According to the Oxford Dictionary, the adjective *parametric* refers to the *parameter*, which originates from the Greek *para*, meaning a subsidiary or assistant, and the word *metron*, which means *measure.* There are two ways of interpreting – first one, predominantly mathematical, a quantity whose value is selected for the particular circumstances and in relation to which other variable quantities may be expressed, and second, a general one, describing the boundary and the scope of a specific process or activity. If we defined parametric as something precise, design is its opposite, unconstrained and impulsive activity. While its origin comes from the Latin word *designare*, which means *to designate*, it often implies an unpredictable or uncertain activity dealing with quite ill-defined problems. Based on the literature, parametric design can be synthesized into a design process based on algorithmic thinking that uses parameters and rules to constrain them [1]. The principle of parametric design can be defined as the mathematical design, where the relationships between the design elements are shown as parameters which could be reformulated to generate complex geometries, these geometries are based on the elements' parameters, by changing these parameters; new shapes are created simultaneously. Many researchers [2] assume the digital as a paradigm that considerably affects domains such as architecture and engineering not only in terms of design thinking and the process of creation but also in production and manufacture.

The first parametric computer-aided design system was programmed by Ivan Sutherland [3] for his Ph.D. thesis on Sketchpad in 1963. Professor Samuel Geisberg was a mathematician who founded the PTC (Parametric Technology Corporation) in 1988 [4] and created the first parametric modelling software called Pro/ENGINEER, which is an integrated CAD/CAM/CAE solution, and was the first rule-based constraint applied software used nowadays in mechanical design in many companies. While many argue that architects have spent decades gradually adopting parametric modelling, some have claimed that architects have always produced parametric models since all design, by definition, derives from parameters. Today architects craft parametric models in a range of software environments: from physical modelling to history-based modellers (CATIA, SolidWorks, Pro/Engineer), and visual scripts (Grasshopper, GenerativeComponents, Houdini).

A. Grasshopper

Grasshopper is a visual programming editor developed by David Rutten. As a plug-in for Rhino3D, Grasshopper is integrated with the robust and versatile modelling environment used by creative professionals across a diverse range of fields, including architecture, urban planning, structural study, environmental analysis, mechanical engineering, and more. Grasshopper and Rhino offer designers the opportunity to define precise parametric control over models, the capability to explore generative design workflows, and a platform to develop higher-level programming logic – all within an intuitive, graphical interface [5].

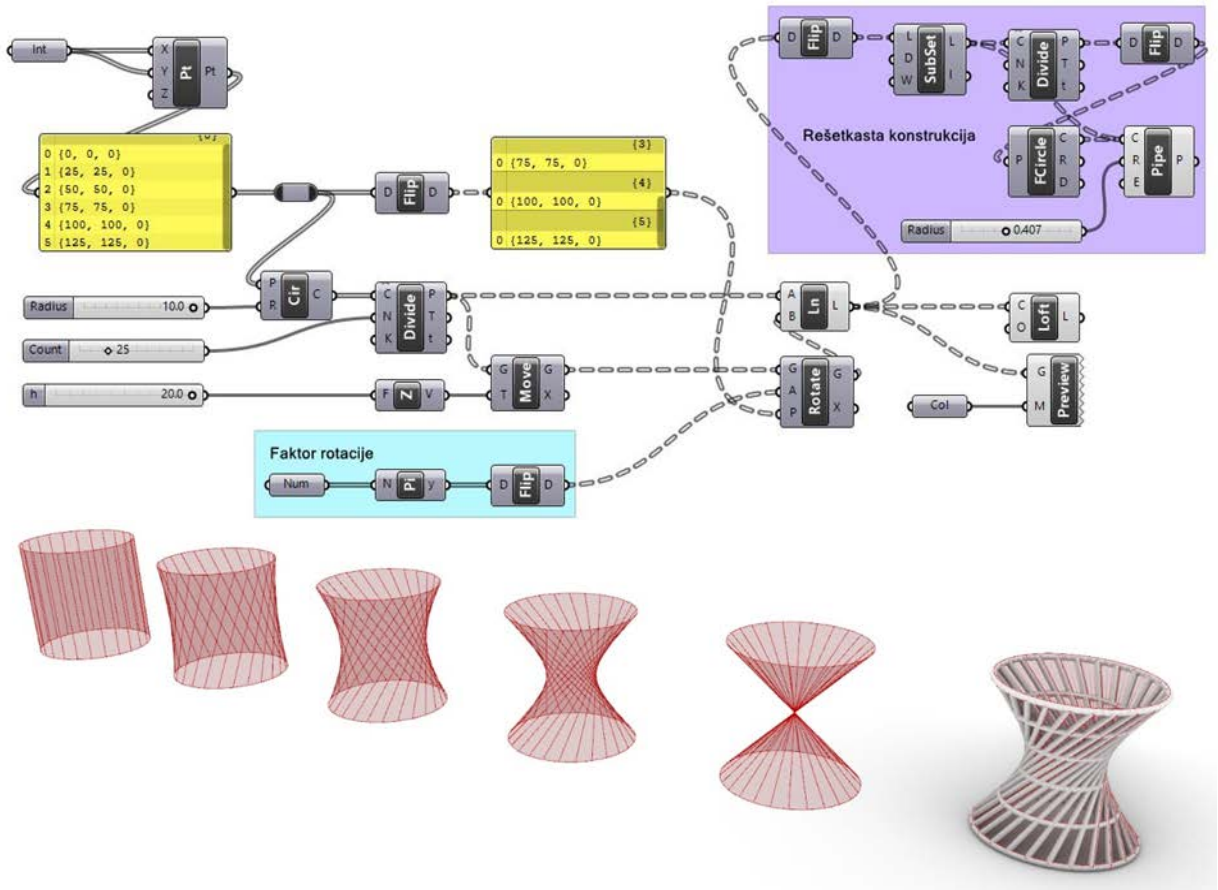

Fig. 1 One-Sheet Hyperboloid definition in Grasshopper (up) and geometrical representation in Rhino3D (down)

Grasshopper provides full control and accurate manipulation of the model's elements by defining form generating components, which can be optimized through the use of sliders, mathematical expressions or simple scripting. The interface consists of objects or nodes connected by wires on canvas in order to build the definition of Grasshopper, and these definitions are visual programs. Grasshopper consists of two primary types of user objects: parameters and components. Parameters store data, whereas components perform actions that result in data. Changing these parameters causes changes to the whole definitions and geometries simultaneously, which could be observed in the Rhinoceros window.

II. From The Second Order Surfaces to Functional Structure

The second-order surfaces, also called quadratic surfaces or quadrics, are defined by algebraic equations of the second-order relative to the Cartesian coordinates [6]. A general equation of the second-order has the following form:

$$Ax^2 + By^2 + Cz^2 + 2Dxy + 2Eyz + 2Fxz + 2Mx + 2Ny + 2Pz + G = 0 \quad (1)$$

where A, B, C, D, E, F, M, N, P, and G are arbitrary real numbers and at least one of them is nonzero.

A. One-Sheet Hyperboloid

A one-sheet hyperboloid is an unclosed central twice ruled surface of the second order of negative Gaussian curvature. Its implicit equation is:

$$\frac{x^2}{a^2} + \frac{y^2}{b^2} - \frac{z^2}{c^2} = 1 \quad (2)$$

where *a*, *b*, *c* are the semi-axes of a one-sheet hyperboloid.

Parameterization of the isoperimetric line:

$$x = a\cos u + av(\cos(u+t) - \cos u)$$

$$y = a\sin u + av(\sin(u+t) - \sin u)$$

$$z = -c + 2cv$$

$$0 \le u \le 2\pi,\ v \in R,\ 0 \le t \le 2\pi, \quad (3)$$

where for $t \neq 0 \wedge t \neq \pi$ we have hyperboloid, and for $t = 0,\ t = \pi$ we have special cases: for $t = 0$ a cylindrical surface and for $t = \pi$ a conical surface. Depending on t, examples are given in Figure 1, from left to right $t = 0, t = \frac{\pi}{4}, t = \frac{\pi}{2}, t = \frac{3\pi}{4}, t = \pi$, and truss structure for $0 < t < 2\pi$.

The Warsaw Spire is a complex of Neomodern office buildings in Warsaw, Poland constructed by the Belgian real estate developer Ghelamco. It consists of a 220-meter main tower with a hyperboloid glass façade.

Fig. 2 The Warsaw Spire buildings complex

An elliptical paraboloid was constructed by a parallel movement of one parabola whose pick slide along the other parabola, while the axes of these two parabolas remain constantly parallel and equally oriented. Paraboloid of the revolution was created revolving the parabola around the z-axis, and the parabolic cylinder was created by the translational motion of a straight line parallel to the y-axis along a given parabola. The Reichstag dome in Figure 4 is a paraboloid glass dome, constructed on top of the rebuilt Reichstag building in Berlin.

The Reichstag dome in Figure 4 is a paraboloid glass dome, constructed on top of the rebuilt Reichstag building in Berlin. It was designed by architect Norman Foster and built by Waagner-Biro in 1999 to symbolize the reunification of Germany. The distinctive appearance of the dome has made it a prominent landmark in Berlin.

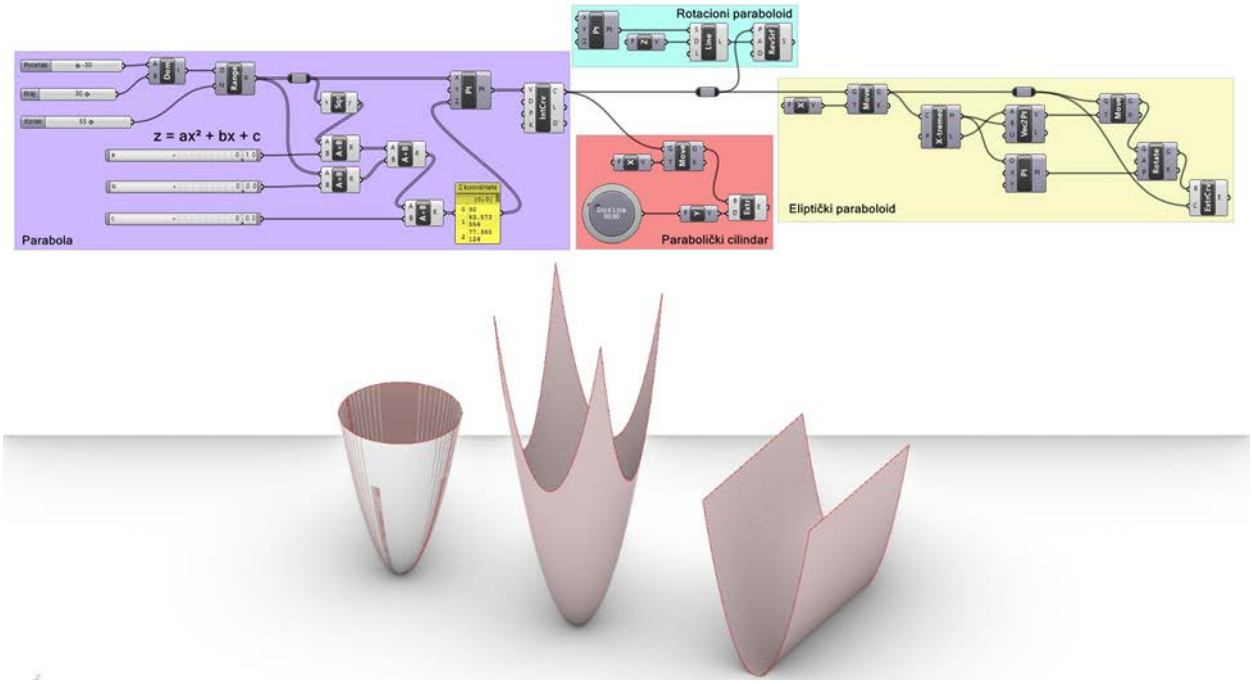

Fig. 3 Paraboloid definition in Grasshopper (up) and geometrical representation in Rhino3D (down)

B. *Elliptic Paraboloid*

The elliptic paraboloid is an unclosed noncentral surface of the second order. On the surface of an elliptical paraboloid, an innumerable set of translational nets exist.

Explicit equation:

$$\frac{x^2}{p} + \frac{y^2}{q} = 2z \tag{4}$$

where $p, q > 0$. When $p = q$, an elliptical paraboloid degenerates into a paraboloid of revolution.

Parameterization of the isoperimetric line:

$$x = \sqrt{2pu}\cos\varphi$$

$$y = \sqrt{2qu}\sin\varphi$$

$$z = u$$

$$u \geq 0, 0 \leq \varphi \leq 2\pi \tag{5}$$

Fig. 4 Reichstag dome

C. *Hyperbolic Paraboloid (Hypar)*

A hyperbolic paraboloid is a twice ruled surface with negative Gaussian curvature and is presented as a geometric locus belonging to the straight lines intersecting three fixed skew lines that are parallel to one plane.

A hyperbolic paraboloid is formed correspondingly to an elliptical paraboloid, except that the two parabolas have oppositely oriented axes. A hyperbolic paraboloid is a saddle surface of the second order with parabolas as the intersections of planes parallel to the axis of the paraboloid, and hyperbolas with the planes perpendicular to that axis of the paraboloid. The Grasshopper definition for this case is given separately and can be seen in Figure 6, while in Figure 5 is the modern structure, CrossRoads School completed in 2015. The artwork consists of a folded square frame that rises up from the roof of the new science building and warps a cable net into the shape of a hyperbolic paraboloid.

Fig. 5 CrossRoads School, Santa Monica, CA

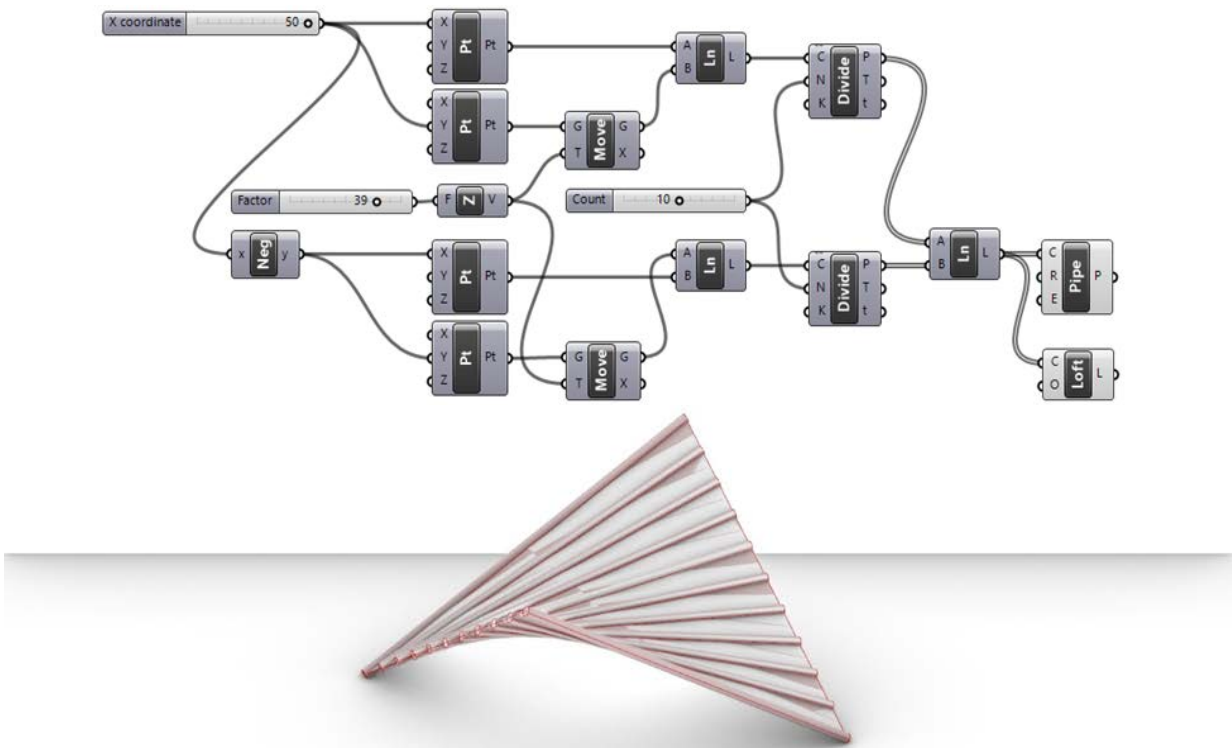

Fig. 6 Hyperbolic paraboloid definition in Grasshopper (up) and geometrical representation in Rhino3D (down)

III. Spiral Staircase Dimensions and Design

Previous examples of geometry have provided insight into the possibility of constructing using Grasshopper. Good knowledge of the software package is vital for any designer when modelling complex 3D models. Spiral stairs take up less space than classic stairs and are a common design challenge.

The goal is to design functional, comfortable stairs that do not pose an obstacle (or danger) for climbing or descending, and at the same time give the space more attractiveness. With daring shapes and diverse configurations, they could be iconic objects in projects.

It's always important to understand the restrictions and underlying concepts. Spiral staircases can adopt different structural configurations. The most common ones have a circular format with a central mast from which the steps are fixed. For the design, three main factors must be taken into account:

1. Distance between floors
2. Angle of rotation
3. Diameter

It's important to declare where the staircase will begin and where it will end at the upper level, according to the flows that have been resolved in the plan. Also, the angle of rotation must be resolved, which is determined by the stair's diameter. To measure the number of steps, it's essential to know the diameter and the length of the staircase.

Bearing in mind that the steps have irregular shapes as they approach the central mast, it's important to define the point at which the calculation of the steps of the staircase will be applied. It's considered that the walking line is located 2/3 from the center.

The minimum radius to be considered in a helical staircase is 70 centimeters, nevertheless, preference for stairs with at least 80 centimeters radius was given while due to the load capacity, the width of the flight did not go above 240 cm. A minimum height of 2 meters between the steps and the roof, or the upper steps was taken into

account. Furthermore, the floor height for a staircase without a landing, ie a resort, was set not to exceed a height of 6 m.

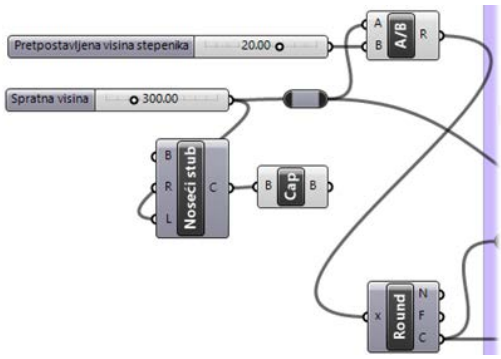

Fig. 7 Grasshopper definition of basic spiral staircase parameters

Fig. 9 The spiral staircase geometrical representation in Rhino3D

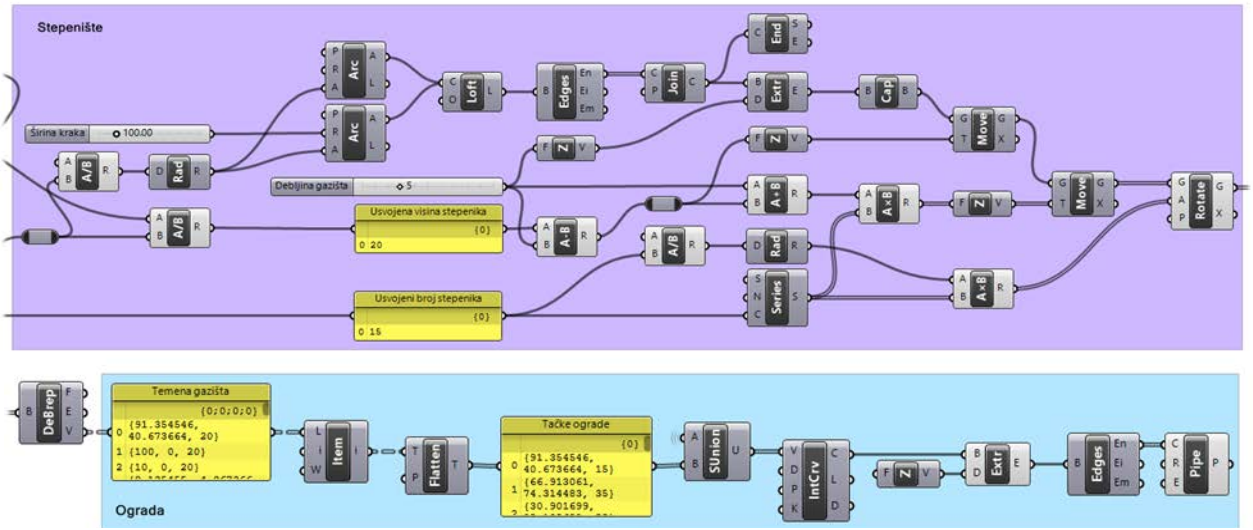

Fig. 8 The spiral staircase treads definition in Grasshopper (up) and the spiral staircase fence definition in Grasshopper (down)

The assumed height of the steps was set in the range of 12 to 24 cm, which is the optimum for pleasant movement, with as little fatigue as possible, of the space occupants in public buildings. We also assumed the position in the space of the staircase, that it would start at the same place where it would end, that is, that the angle of rotation would be 360 degrees. Based on the assumed height of the steps and the floor height, we adopt the number of steps and further adopt the height of the steps. As it is a light construction, the thickness of the tread was expected to be 3-10 cm.

Based on the adopted number of steps and the width of the tread, a tread profile was formed. Following the number of steps, the angle of rotation and the number of multiplications was determined, while based on the adopted height of the steps, the movement of each copy of the tread in the z-direction will be determined until the set floor height is accomplished.

Based on the end vertices of the tread, a curve was formed as the basis for the fence, so the fence would follow all the changes that would occur in the optimization of the tread. The optimal height of the fence was set to 100 cm. The fence is designed as a steel structure of circular cross-section with glass filling.

Following the recommendations, as a restriction in Grasshopper, we had greater autonomy when proposing a spiral staircase design. Within this design process, we were able to resolve visual, perceptive, and structural issues while accomplishing significant time and precision improvements.

IV. Implementations of Parametric Design

Nowadays, parametric design is used in many fields, especially when is not easy to control operations using conventional tools or visualize only using mind, disciplines which consist of complex algorithmic relations, interdisciplinary work, creative forms, and multiprocessing treatments. Due to implementation and advancement in digital design, we can find many applications of parametric design, not only for the design phase in architecture but for urban planning, structural analysis, environmental studies and further.

A. Urban Planning

Parametric design can provide several alternatives in a wide range of designs, while it gives distinctive results in the iterative design process, which couldn't be simply obtained using conventional methods. The discrete method of problem-solving can deal with multiple layers

in urban design cases by saving time in writing formulas and coordinating between these layers.

The pedestrian pathway in one study [7] was chosen to determine the connections between the project's area, concerning the smaller buildings which block the visual connection on streets. The sliced landscape was used to divide the pedestrian circulation into patterns. The formula created in this study was conducted by Grasshopper aiming to determine the shortest pedestrian pathway.

B. Structural Design

Parametric design can calculate algorithmic formulas and manipulate complex connections, and create relations with many kinds of materials.

In a previously mentioned research [7], an example of a spiral building was investigated to study the structural system design. Due to the advantages of the Diagrid system, this shape was chosen for the building. The parametric method was applied to specify deflections and material behavior. By studying the algorithm analysis, the conclusion was that spiral columns were no longer needed. Furthermore, beam profiles could be smaller than standard ones, and additionally, they could be replaced by a spring beam system. That could lead to significant economical savings.

C. Environmental Study

We could anticipate and solve many design issues in the early stages of design by studying and analyzing climatic and environmental changes, as it was done in some researches [8,9]. Sun movement, location, humidity, illumination, radiation, wind speed, heat gain or loss, shadows, could be controlled parametrically in the study. Besides, we could make simulation in the 4th dimension using the time aspect which could further influence building in real time, and observe how the time can change the performance of the building parametrically.

V. Conclusions

The basis of everything is knowing the parameters that determine the object we want to create and restrictions within the object. At all times, it must be borne in mind that by manipulating one parameter, we affect the entire assembly. Parametric modeling in architecture allows rapid optimization of the structure. Also, it enables the creation of countless variations of geometric shapes that meet certain criteria defined by the project task. By applying parametric modeling, complex geometric shapes and structures can be created, which cannot be created in any previously known way applied in architecture. It is possible to achieve automation in the design process, which leads to time savings. By applying a new way of thinking and building, innovative, efficient, and elegant architectural solutions can be achieved by using parametric modeling.

References

[1] W. Jabi, Parametric Design for Architecture. Laurence King Publishing Ltd, London, UK, 2013

[2] M. Carpo, The Alphabet and the Algorithm, Cambridge, Mass., London: MIT Press, 2011.

[3] R. Woodbury, Elements of Parametric Design, London: Routledge, 2010.

[4] EJ. Reddy, C. Sridhar, VP. Rangadu, “Knowledge based engineering: notion, approaches and future trends”, Am J Intell Syst 5(1), 2015, pp. 1–17.

[5] A. Payne, The Grasshopper Primer V3.3, Lift Architects, 2013

[6] S. N. Krivoshapko, V. N. Ivanov, “The Second Order Surfaces”, Encyclopedia of Analytical Surfaces, 2015, pp. 613–626.

[7] IIH Hanan, et al. “Parametric approach as a tool for decision-making in planning and design process. case study: Office tower in Kebayoran Lama,” in Procedia – Soc Behav Sci 184, 2015, pp. 328–37

[8] A. Wagdy, F. Fathy “A parametric approach for achieving optimum daylighting performance through solar screens in desert climates,” in J Build Eng 3, 2015, pp.155–170.

[9] S. Banihashemi, et al. “Climatic, parametric and non-parametric analysis of energy performance of double-glazed windows in different climates,” in Int J Sustain Built Environ 4(2), 2015, pp. 307–22.

THE 5th INTERNATIONAL CONFERENCE
MECHANICAL ENGINEERING IN XXI CENTURY

December 9-10, 2020
Faculty of Mechanical Engineering in Niš, Serbia

Linearity of Multiline Path

Ljiljana RADOVIĆ, Predrag RAJKOVIĆ

Department of Mathematics, Faculty of Mechanical Engineering, University of Niš, A. Medvedeva 14, Niš, Serbia, ljiljana.radovic@masfak.ni.ac.rs, predrag.rajkovic@masfak.ni.ac.rs

***Abstract*—Knowledge about the lines in an image is useful in many applications. There are requests for efficient image verification, identification and recognition. The mathematical tools for defining the shape descriptors are founded on: geometry, fractals, algebraic invariants, combinatorial methods, Fourier analysis, integral transformations, etc. Since every curve can be approximated by a multiline taking enough points, the multiline trajectories are very useful in analysing the linearity of a curve. Multiline itself can be easily represented by arc-length parameterization what gives us opportunity to examine its linearity by a few well-known methods or an integral transform. The whole theory can be extended to the other shapes and multidimensional problems. This procedure is also interesting from the point of view of comparing curves that can be used to determine the class to which a curve belongs, to analyse signatures, to check a batch of products, etc.**

***Keywords*—path, shape, measuring, linearity, integral transform.**

I. Introduction

Someone can extract a lot of useful data by studying an image via examining edges of the objects on it. For their identification and differentiation from the others, measuring their linearity can be used (see, for example Stojmenović [7], Žunić-Martinez [9], Žunić-Pantović [10].

It can be used in recognizing a road or a car in a column by a photo.

An object becomes more easily recognizable if it is split into an ordered collection of curves.

We can find the second application in the linear theory of hydrologic systems Dooge [3].

The whole hydrologic cycle is a closed system in the sense that the water circulating always remains within the system.

Here, we can notice some lines of water transport which express: precipitation, evaporation, transpiration, and runoff.

The third application can be found in the chemistry. A large number of analytical methods require the calibration of the instruments Loco [6].

Instrument calibration is a set of operations that establish the relationship between the output of the measurement system and the accepted values of the calibration standards. From the other hand, the doubled integral transforms were researched from a few authors, such as in Castro[1], Debnath[2] and Eltayeb[4].

Considering importance of the previous applications and their diversity, we conclude that it will be useful to define a new double integral based linear integral transform and examine its properties.

II. A double integral transform

For a function $f(s,s_1)$ integrable on a domain $D \subseteq R^2$, let the *double integral transform* be

$$T[f(u,v)] = \frac{6}{w^2z^2}\int_0^w\int_0^z f(u,v)\,du\,dv = F[w,z]. \qquad (1)$$

It is a linear transform, because of

$$T[Cf(u,v)] = C\,T[f(u,v)] \qquad (C \in R), \qquad (2)$$

$$T[f(u,v)+g(u,v)] = T[f(u,v)] + T[g(u,v)]. \qquad (3)$$

If the first and the second mixed partial derivatives of the function $F[w,z]$ exist, then its *inverse double integral transform* is

$$T^{-1}F[w,z] = \partial_{w,z}\left(\frac{w^2z^2}{6}F[w,z]\right)_{w\to u, z\to v} = f(u,v). \qquad (4)$$

Example 1. It is valid

$$T[u^m v^n] = \frac{6w^{m-1}z^{n-1}}{(m+1)(n+1)} \qquad (m \neq -1,\ n \neq -1\,). \qquad (5)$$

$$T^{-1}[w^m z^n] = \frac{(m+2)(n+2)}{6}\ u^{m+1}v^{n+1}\,. \qquad (6)$$

For any continuous arc-length parameterized path

$$C = \begin{pmatrix} x(s) \\ y(s) \end{pmatrix} : \textbf{Length}\left[\begin{pmatrix} x(0) \\ y(0) \end{pmatrix}, \begin{pmatrix} x(s) \\ y(s) \end{pmatrix}\right] = s\ (\forall s > 0), \qquad (7)$$

the *measure of linearity of the oriented path* C^+ is the special nonlinear case of (1) defined by

$$\textbf{Lin}\left[\begin{pmatrix} x(s) \\ y(s) \end{pmatrix}|z\right] =$$

$$T[(x(s)-x(s_1))^2 + (y(s)-y(s_1))^2][z,z]. \qquad (8)$$

If we denote the moments by

$$\mu_{pq}(z) = \int_0^z (x(s))^p (y(s))^q\,ds, \qquad (9)$$

applying integration via s and s_1, we get the formula

$$\textbf{Lin}\left[\begin{pmatrix} x(s) \\ y(s) \end{pmatrix}|z\right] = \frac{12}{z^4}\cdot$$

$$(z\mu_{20}(z) + z\mu_{02}(z) - (\mu_{10}(z))^2 - (\mu_{01}(z))^2). \qquad (10)$$

Theorem 1. *For any planar curve, it is true*

$$\textbf{Lin}\left[\begin{pmatrix} x(s) \\ y(s) \end{pmatrix}|z\right] \leq 1. \qquad (11)$$

The equality is reached if and only if the curve is straight path.

Example 2. Consider a line segment $P(b,d)Q(b+a,d+c)$ with arc-length parametrization:

$$x(s) = b + \frac{as}{\sqrt{a^2+c^2}}, \qquad y(s) = d + \frac{cs}{\sqrt{a^2+c^2}},$$
$$s \in \left[0, \sqrt{a^2+c^2}\right]. \tag{12}$$

Then

$$\mathbf{Lin}\left[\begin{pmatrix} x(s) \\ y(s) \end{pmatrix} |z\right] = \frac{6}{z^4}\int_0^z \int_0^z (u-v)^2\, du\, dv \equiv 1. \tag{13}$$

Theorem 2. The measure of linearity is invariant under translation, symmetry and rotation, i.e. if

$$X(s) = a + x(s)\cos\alpha + y(s)\sin\alpha,$$
$$Y(s) = b - x(s)\sin\alpha + y(s)\cos\alpha, \tag{14}$$

where $a, b, \alpha \in R$, then

$$\mathbf{Lin}\left[\begin{pmatrix} X(s) \\ Y(s) \end{pmatrix} |z\right] = \mathbf{Lin}\left[\begin{pmatrix} x(s) \\ y(s) \end{pmatrix} |z\right]. \tag{15}$$

For any arc-length parameterized curve, we have its direct orientation when s increases from 0 to $\sigma > 0$. If we consider the reverse orientation

$$x_{\text{rev}}(s) = x(\sigma - s), \qquad y_{\text{rev}}(s) = y(\sigma - s),$$
$$s \in [0, \sigma], \tag{16}$$

the graphics holds on. But, the linearity measure of the reverse oriented curve can be expressed by

$$\mathbf{Lin}\left[\begin{pmatrix} x_{\text{rev}}(s) \\ y_{\text{rev}}(s) \end{pmatrix} |z\right] = \frac{12}{z^4} \cdot$$
$$(zM_{r20}(z) + zM_{r02}(z) - (M_{r10}(z))^2 - (M_{r01}(z))^2), \tag{17}$$

Where

$$M_{rij}(z) = \mu_{ij}(\sigma) - \mu_{ij}(\sigma - z). \tag{18}$$

Example 3. Let us consider the oriented multi-line path with the unit length: $A(0,0)\ B(2/3,0)\ C(2/3,1/3)$ which is shown on Fig 1a. The direct orientation gives

$$x_1(s) = s, \qquad y_1(s) = 0, \qquad s \in [0,2/3], \tag{19}$$
$$x_2(s) = \frac{2}{3}, \qquad y_2(s) = s - 2/3, \qquad s \in [2/3,1]. \tag{20}$$

Its linearity is

$$\mathbf{Lin}[C|z] = \begin{cases} 1, & 0 \le z < 2/3, \\ 1 - \frac{72z^2 - 96z + 32}{27z^4}, & \frac{2}{3} < z \le 1. \end{cases} \tag{21}$$

The reverse orientation gives

$$x_{\text{rev},1}(s) = \frac{2}{3}, \qquad y_{\text{rev},1}(s) = \frac{1}{3} - s, \qquad s \in [0,1/3], \tag{22}$$
$$x_{\text{rev},2}(s) = 1 - s, \qquad y_{\text{rev},2}(s) = 0, \qquad s \in [1/3,1]. \tag{23}$$

The linearity of the reverse oriented curve is

$$\mathbf{Lin}[C_{\text{rev}}|z] = \begin{cases} 1, & 0 \le z < 1/3, \\ 1 - \frac{18z^2 - 12z + 2}{27z^4}, & \frac{1}{3} < z \le 1. \end{cases} \tag{24}$$

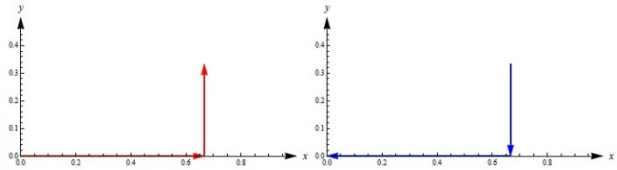

Fig. 1 The oriented multi-line: a) direct (red); b) reverse (blue)

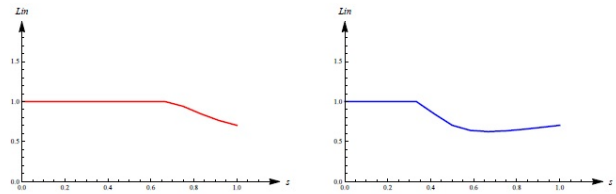

Fig. 2 The linearity of oriented multi-line: a) direct (red); b) reverse (blue)

III. Linearity of the multi-line

Suppose that n points $M_i(x_i, y_i)$ are connected in a multi-line $M_1M_2 \cdots M_n$. It consists of the segments which have the lengths

$$\sigma_i = \sqrt{(x_{i+1} - x_i)^2 + (y_{i+1} - y_i)^2} \quad (1 \le i \le n-1) \tag{25}$$

Also, empty and whole line have lengths

$$\sigma_0 = 0, \qquad \sigma = \sum_{i=1}^{n-1} \sigma_i\,. \tag{26}$$

The arc-length parametrization of the multi-line is

$$x(s) = x_i + \frac{x_{i+1} - x_i}{\sigma_i}\left(s - \sum_{j=1}^{i-1}\sigma_j\right), \tag{27}$$

$$y(s) = y_i + \frac{y_{i+1} - y_i}{\sigma_i}\left(s - \sum_{j=1}^{i-1}\sigma_j\right), \tag{28}$$

$$s \in \left(\sum_{j=1}^{i-1}\sigma_j, \sum_{j=1}^{i}\sigma_j\right) \qquad (1 \le i \le n-1). \tag{29}$$

It able us to compute the linearity measure.

Example 4. Here is an example which emphasizes continuously moving along the curve. Let us consider a multi - line through the points

$$O(0,0)\ A(1,0)\ B\left(1 + \frac{a}{\sqrt{a^2+b^2}}, \frac{b}{\sqrt{a^2+b^2}}\right). \tag{30}$$

The arc-length parametrization of OAB is

$$x(s) = \begin{cases} s, & 0 \le s < 1, \\ 1 + \frac{a(s-1)}{\sqrt{a^2+b^2}}, & 1 \le s \le 2, \end{cases} \tag{31}$$

and

$$y(s) = \begin{cases} 0, & 0 \le s < 1, \\ \frac{b(s-1)}{\sqrt{a^2+b^2}}, & 1 \le s \le 2. \end{cases} \tag{32}$$

Different cases are shown shown on the Figure 3.

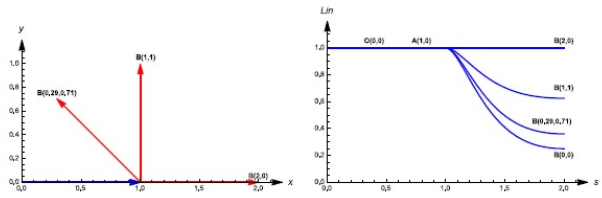

Fig. 3 Path O (0, 0) A (1, 0) B (a, b) and its linearity.

The most interesting case is the path $O(0,0) \rightarrow A(1,0) \rightarrow B(0,0)$. The moving in the opposite direction in the point A(1, 0), influenced on linearity measure of the path.

IV. Application on Approximating Curves

In exact computation of the linearity of an ordinary curve path, we can have two problems. One problem can appear in the very beginning when we do not have the arc-length parametrization of the path. In that case we can choose points on the path, consider multi-line which connects them and solving this problem we will get the numerical solution for linearity of initial problem.

TABLE I Arc length parametrization

$\binom{x_1(t)}{y_1(t)}$	$\mathcal{S}\binom{x_1(t)}{y_1(t)}$
$\binom{t}{1}$	t
$\binom{t}{t}$	$t\sqrt{2}$
$\binom{t}{t^2}$	$\frac{t}{2}\sqrt{1+4t^2}+\frac{1}{4}\sinh^{-1}(2t)$
$\binom{t}{t^a}$	$\frac{t\sqrt{1+a^2t^{2a-2}}}{(a-2)a^3}\left((a-2)a^2+\frac{a-1}{t^{2a-2}}\ {}_2F_1\left(\begin{matrix}1,1-\frac{1}{2(a-1)}\\ \frac{3a-4}{2(a-1)}\end{matrix}\middle\vert z\right)\right)$
$\binom{t}{\cosh t}$	$\sinh t$
$\binom{t}{\sqrt{1-t^2}}$	$\arcsin t$
$\binom{t\cos t}{t\sin t}$	$\frac{1}{2}\left(t\sqrt{1+t^2}+\sinh^{-1}(t)\right)$
$\binom{t}{e^t}$	$\frac{1}{2}\ln\left(2+e^{2t}-2\sqrt{1+e^{2t}}\right)+\sqrt{1+e^{2t}}-t+\frac{1}{2}\cosh^{-1}(3)-\sqrt{2}$
$\binom{t}{\ln(1+t)}$	$\sqrt{1+(1+t)^2}+\ln\frac{1+t}{1+\sqrt{1+(1+t)^2}}+\sinh^{-1}(1)-\sqrt{2}$
$\binom{t-\sin t}{1-\cos t}$	$4\left(1-\cos\frac{t}{2}\right)$
$\binom{t}{\cos t}$	$E(t\vert-1)$
$\binom{t}{\sin t}$	$\sqrt{2}\,E(t\vert 1/2)$
$\binom{t}{\sinh t}$	$-iE(it\vert 1/2)$
$\binom{\cos t(a\cos t+b)}{\sin t(a\cos t+b)}$	$2(a+b)E\left(\frac{t}{2}\middle\vert\frac{4ab}{(a+b)^2}\right)$

In another case, even we have the arc-length parametrization of the path as it is shown on the Table I, but we are not able to express the linearity in the closed form. Here, we will use the numerical integration.

If the arc-length parametrization can not be done exactly, we can apply numerical approach.

Let us consider a curve

$$C = \begin{pmatrix} x_0(t) \\ y_0(t) \end{pmatrix} : \ [a,b] \rightarrow R^2, \tag{33}$$

which has length σ.

Firstly, for a chosen $n \in N$, we take n points on the curve and form the multi-line which we use to approximate the curve and her linearity.

Example 5. Consider the Archimedean spiral:

$$x(t) = t\cos t, \quad y(t) = t\sin t, \quad t \in [0, 3\pi], \tag{34}$$

Although we know the connection to arc-length parametrization

$$s = \frac{1}{2}\left(t\sqrt{1+t^2} + \operatorname{arcsinh} t\right), \tag{35}$$

we must work numerically, for example to use the multi-line approximation. The path and linearity are shown on the Figure 4. For example, the linearity of whole spiral is Lin(C) = 0.222477.

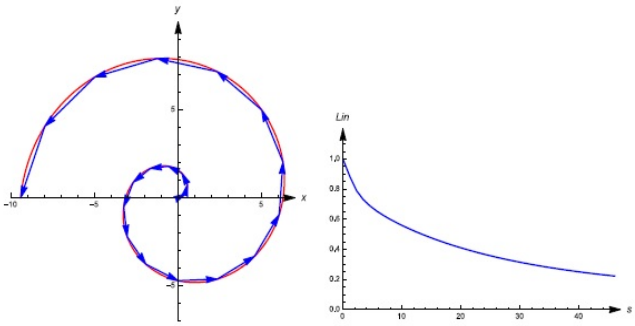

Fig. 4 The Archimedean spiral and its linearity.

Example 6. Two persons wrote the letter N. We approximated it with multiline with n = 80 points. The paths and linearity are shown on the Figure 5.

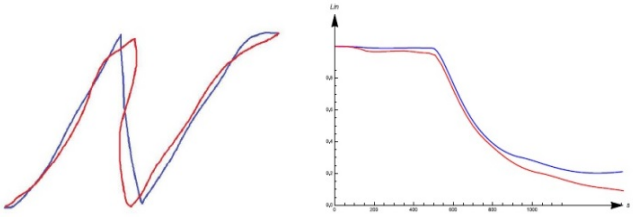

Fig. 5 Two writings of N and their linearity.

If the arc-length parametrization can not be done exactly, we can apply numerical approach. We are interesting in linearity of a curve

Example 7. Suppose that are given *m* points inside the unit circle and *n* points on its border. Starting from the center O of the circle, choose *k* points inside and a point on the border so that this multi-line has the maximal linearity.

Especially, let *S* be a set of the random points inside the unit circle is given. Suppose that we want to connect the origin *O*(0, 0) with the point *X*(1, 0) using path through a point from *S*. Is the most linear path the shortest at the same time? On the on the Table 2 and Figure 6 are shown the cases when the path with the maximal linearity and the shortest path are not the same.

TABLE I The shortest and most linear path

Path	Linea.	Length
$OA(0.8, 0.095)X$	0.9736	1.0270
$OB(0.5, -0.1)X$	0.9712	1.0198

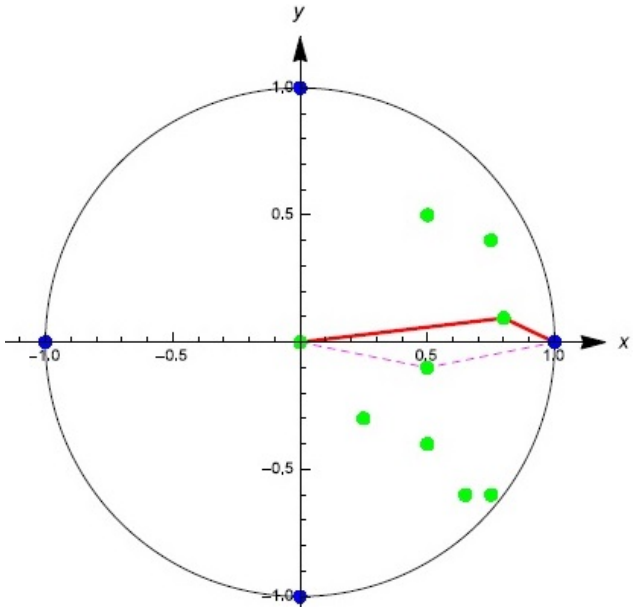

Fig. 6 The shortest path and the path with the maximal linearity.

V. Conclusions

In this paper, an integral transform is used identification and recognition straight lines and estimating of the linearity of any curve. The whole theory can be extended to the other shapes and multidimensional problems. This procedure able comparison of the curves that can be used to determine the class to which a curve belongs, to analyze signatures, to check a batch of products, etc.

Acknowledgment

This research was financially supported by the Ministry of Education, Science and Technological Development of the Republic of Serbia.

References

[1] L.P. Castro, M.R. Haque, M.M. Murshed, S. Saitoh, N.M. Tuan, Quadratic Fourier transforms, Annals of Functional Analysis 5, No. 1 (2014) 10-23.

[2] L. Debnath, The Double Laplace Transforms and Their Properties with Applications to Functional, Integral and Partial Differential Equations, International Journal of Applied and Computational Math. 2 (2016) 223-241.

[3] J.C.I. Dooge, Linear Theory Of Hydrologic Systems, Technical Bulletin 1468, Hydrologic systems, 1973.

[4] H. Eltayeb, A. Kilicman, A Note on Double Laplace Transform and Telegraphic Equations, Hindawi P. C., Abstract and Applied Analysis, Article ID 932578 (2013), 6 pages.

[5] Y.C. Kim, S. Ponnusamy, T. Sugawa, Geometric Properties of Nonlinear Integral Transforms of certain analytic functions, Proceedings of the Japan Academy, Series A, Mathematical Sciences 80, Ser. A (2004), 57-60.

[6] Van J. Loco, M. Elskens, C. Croux, H. Beernaert, Linearity of calibration curves: use and misuse of the correlation coefficient, Accreditation and Quality Assurance 7 (2002) 281-285.

[7] M. Stojmenović, A. Nayak, J. Žunić, Measuring Linearity of a Finite Set of Points, IEEE International Conference on Cybernetics and Intelligent Systems (CIS) Bangkok, Thailand (2006) 222-227.

[8] J. Žunić, P.L. Rosin, Measuring linearity of open planar curve segments, Image and Vision Computing 29 (2011) 873-879.

[9] J. Žunić, C. Martinez-Ortiz, Linearity measure for curve segments, Applied Mathematics and Computation 215 (2008) 3098-3105.

[10] J. Žunić, J. Pantović, P.L. Rosin, Measuring Linearity of Planar Curves, A. Fred and M. De Marsico (eds.), Pattern Recognition Applications and Methods, Advances in Intelligent Systems and Computing 318, Springer, (2015) 257-271.

THE 5th INTERNATIONAL CONFERENCE
MECHANICAL ENGINEERING IN XXI CENTURY

December 9-10, 2020
Faculty of Mechanical Engineering in Niš, Serbia

Reconstruction of Strain Energy Surfaces at The Crack Tip Vicinity

Dragan JOVANOVIĆ

Faculty of Mechanical Engineering, University of Niš, A. Medvedeva 14, 18000, Niš, Serbia,
dragan.bsj@gmail.com

***Abstract*— Results of applying the idea of reconstructing the spatial surface, that describes the potential strain energy distribution at the region of crack, and basic procedures of the reconstruction method, are presented. Relevant limitations and specificity of the method are pointed out in the evaluation of the the best fitting curves, and the best fitting three-dimensional surfaces of stress components, and potential strain energy. Based on the reconstructed potential strain energy surfaces, the isoenergy lines in front of the crack tip, are presented. It is observed that distribution of potential strain energy are very similar in both analysed cases, which indicates a significant influence of geometric shape of contour surfaces of the crack. For comparison, stress state and potential strain energy state, which are obtained by using relations from literature, are shown.**

***Keywords*— potential strain energy surfaces, crack, stress components, reconstruction.**

I. Introduction

Experimental research in which was initially created this idea was realized in 1992, 1995, 1996 and 1997 in the Laboratory for Experimental Mechanics of the University of Waterloo in Canada. During 1997, 1998, 1999, due to the impossibility to realize an experiment in a real physical condition, I decided to carry out a numerical experiment using the method of finite elements and ALGOR software package that was at that time available on Faculty of Mechanical Engineering Niš, and based on the results of numerical experiments provide an assessment of the stress and strain state in the vicinity of the crack in the plate, and that some of the assumptions that I made during the experimental research in Canada confirm or refute. The first results of this research on the basis of numerical experiments have been published in the papers [4], [5], and before that in [3]. During the review of the work [5], which was published in 2002, I learned about the work of Parsons, Hall, and Rosakis [6], dealing with three-dimensional stress state and the state of deformation around the crack tip, in which was applied the finite element method. In this paper, was not analyzed or reconstructed energy distribution of deformation around the crack tip, but only stress and strain state. Authors used multigridd method in paper [6], but it was not the same as the method that I used. All of that indicated that there are thoughts that go in a similar direction.

II. Reconstruction Procedure Of The Strain Energy Surface

The reconstruction procedure of the potential energy surface has previous steps in which at first is modeling for crack in the plate. That means a choice between different forms of an initial crack (Figs. 1, 2), definition of boundary conditions on the contour of the crack.

The second step in the work was calculation of the distribution of stress components in the plate, for the assumed global stress state and the assumed shape of the crack. For this software packages was used. Data obtained in this way were used to graphically display the obtained stress distribution (Figs. 3, 4, 5, 6, 7, 8) as the basis for determining the value of stress components and component displacements in selected directions and in selected sections. The third step in the work is editing of data in units that are needed for further work. The fourth step is a graphical representation of curves that describe the distribution of stress components σ_x, σ_y, σ_z, τ_{xy}, τ_{yz}, τ_{zx} on selected directions. The fifth step is the calculation of the potential strain energy, where Equation (1) was used.

$$\mathbf{A}'_{def} = \frac{1}{2E}\left[\begin{array}{l}\left(\sigma_x^2+\sigma_y^2+\sigma_z^2\right)-2\nu\left(\sigma_x\sigma_y+\sigma_x\sigma_z+\sigma_y\sigma_z\right)+\\ +2\left(1+\nu\right)\left(\tau_{xy}^2+\tau_{xz}^2+\tau_{yz}^2\right)\end{array}\right] \quad (1)$$

The sixth step is to edit the data of the potential strain energy and graphical representation of its distribution for selected directions and intersections. The seventh step is the reconstruction of the potential strain energy surface by process of networking (gridding) of points obtained in the previous procedure. It was also used polynomial regression procedure. The procedure was repeated iteratively to obtain the spatial surface, in which the influence of selected parameters for networking is eliminated or imperceptible. Figs. (11 and 12) show a step in the process of reconstruction, where the density of points with predetermined values of the potential strain energy, affects the result of the reconstruction. Periodic changes in the strain energy, which you can see in these figures, starting at a distance the size of a double thickness of middle plate, or 1.5 thickness of the crack tip, are consequence of the insufficient density of points, which determined the value of the potential deformation energy, interacting with the reconstruction method.

Consequently, increase in the number of data points resulted in the ironing of surface in this part. The appearance of the surface waves or curves in the reconstruction as a result of uneven density of data points, was observed previously [7], [8]. Experience from experimental research, have been used to successfully overcome and resolve the problem with the uneven density of measurement points.

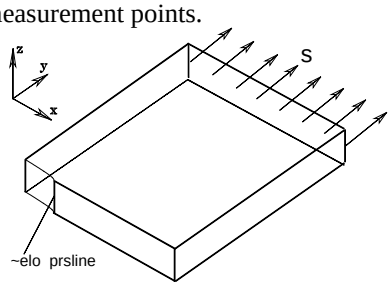

Fig. 1 Elliptical crack in plate, loaded by normal stress σ to tension in the direction perpendicular to the crack plane, which is processed in the file PR-Z-16.

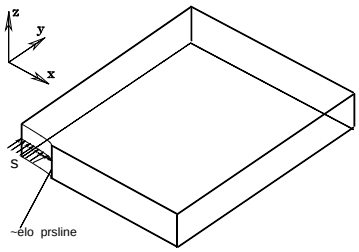

Fig. 2 Elliptical crack in plate loaded by normal stress σ to pressure in the direction perpendicular to the crack plane, which is processed in the file PR-P-22.

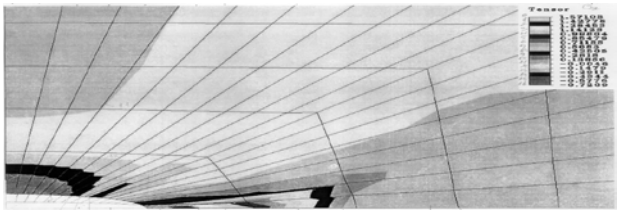

Fig. 3 PR16 normal stress distribution σ_x , for a flat cross-section z = 0, detail.

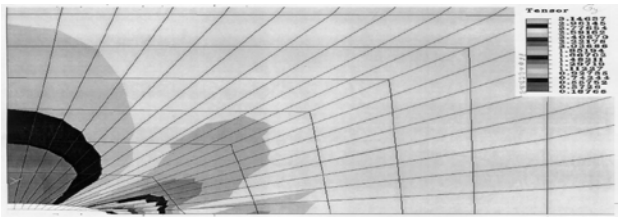

Fig. 4 PR16 normal stress distribution σ_y , for a flat cross-section z = 0, detail.

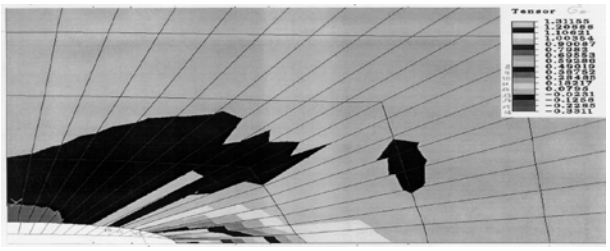

Fig. 5 PR16 normal stress distribution σ_z , for a flat cross-section z = 0, detail.

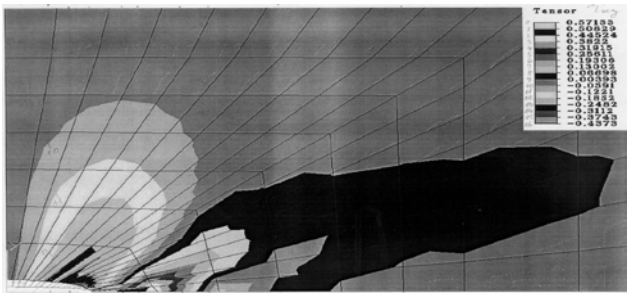

Fig. 6 PR16 shear stress distribution τ_{xy} , for a flat cross-section z = 0, detail.

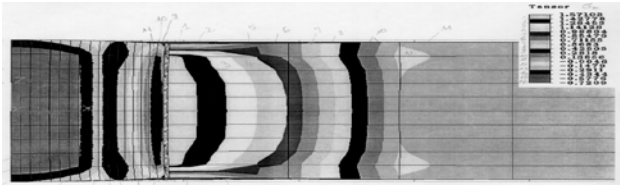

Fig. 7 PR16 normal stress distribution σ_x , for a flat cross-section y = 0, detail.

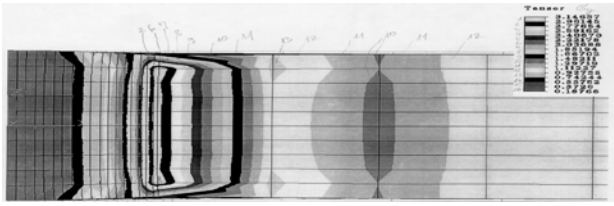

Fig. 8 PR16 normal stress distribution σ_y ,for a flat cross-section y = 0, detail.

In Fig. 9, and Fig. 10 are shown distribution of the potential strain energy for selected directions z = 0 mm, z = 1 mm of the intersection y = 0 mm. Then, data files are merged into a single file with data on potential strain energy of the flat section defined by y = 0 mm. Then, a series of iterative steps were done, in which was reconstructed surface describing the potential energy distribution in the plane y = 0 mm, as shown in Fig. 11. and Fig. 12.

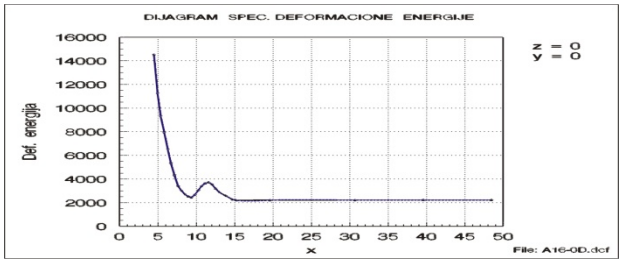

Fig. 9 Diagram of the specific strain energy in the direction determined by the coordinates z = 0 mm and y = 0 mm.

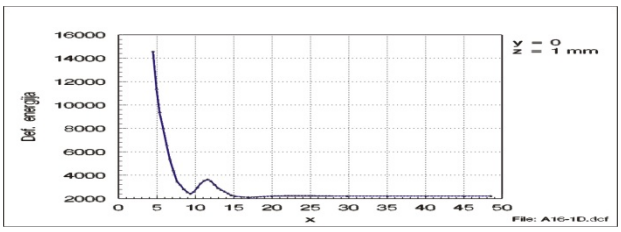

Fig. 10 Diagram of the specific strain energy in the direction determined by the coordinates z = 1 mm and y = 0 mm.

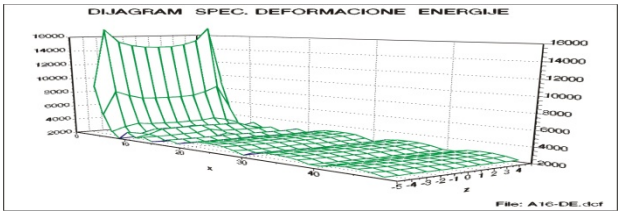

Fig. 11 Diagram of surface of the specific strain energy of the flat section for coordinate y = 0 mm, in front of the crack's front line (one of previous steps of reconstruction).

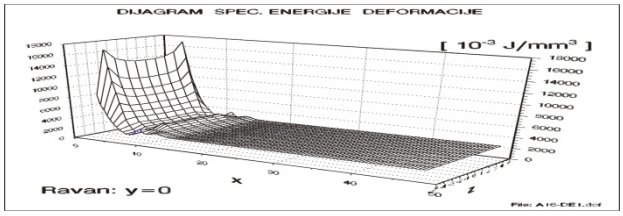

Fig. 12 Diagram of surface of the specific strain energy of the flat section for coordinate y = 0 mm, in front of the crack's front line (the final form of reconstruction).

Fig. 13 shows diagram of the potential strain energy in the direction x = 4.5 mm, and plane cross-section y = 0 mm. This diagram shows that minimum of potential strain energy ahead of the crack in the middle of the plate cross-section, and maximums near the outer surfaces of the plate. This fact suggests that the points on front line of crack, which are located near the outer surface of plate will get crack propagation, before than middle of the cross section of the plate.

Fig. 14. shows the isoenergy lines in the cross section at the z direction. These lines show the constant value of the potential energy of deformation, illustrating the distribution and concentration of potential strain energy, and hence point to places where it can be expected crack propagation. Fig. 15. shows a step in iterative procedure.

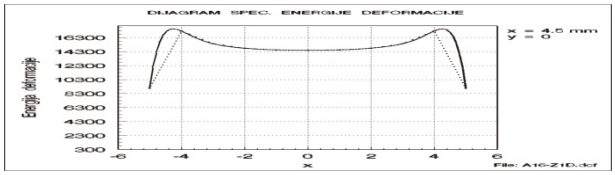

Fig. 23 Diagram of specific strain energy in direction determined by the coordinates x = 4.5 mm and y = 0 mm.

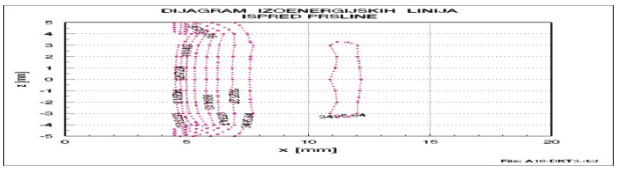

Fig. 14 Diagram of isoenergy lines in front of crack in plane section of plate, coorindate y = 0 mm.

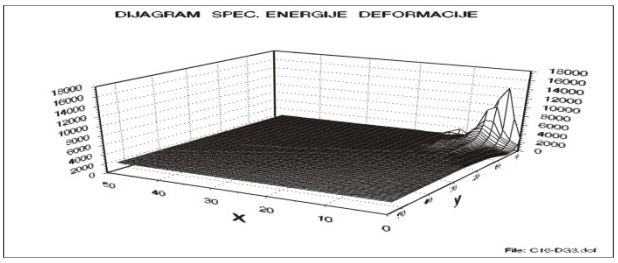

Fig. 15 Diagram of the specific strain energy for flat section of plate, coordinate z = 0 mm (one of previous steps of reconstruction).

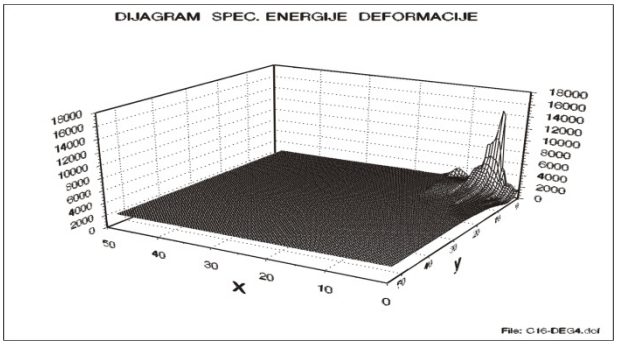

Fig. 16 Diagram of the specific strain energy for flat section of plate, coordinate z = 0 mm (final step of reconstruction).

In Fig. 16, which represents the distribution of the potential strain energy in the middle plane, is seen peak energy $A'_{def} = 14517 \cdot 10^{-3}\ J/mm^3$ in front of the front line of crack, which is, like in the diagram in Fig. 12.

In Figs. 17 and 18 shows the isoenergy lines for middle plane of plates, where can be seened the concentration of strain energy ahead of the crack tip and depression of energy field above the crack in the case PR16.

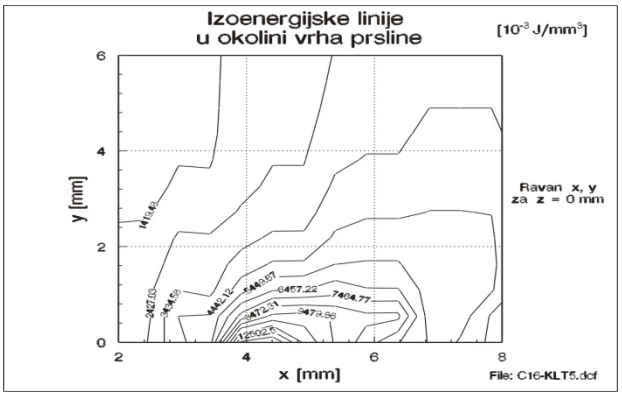

Fig. 17 PR16 Isoenergy lines in the vicinity of the crack tip, plane of section (x-y) for z = 0 mm (shown in enlarged detail).

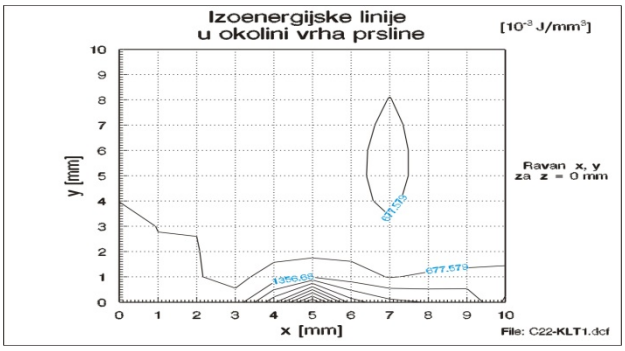

Fig. 18 PR22 Isoenergy lines in the vicinity of the crack tip, plane of section (x-y) for z = 0 mm (shown in enlarged detail).

III. Stresses And Strain Energy In Front Of The Crack Tip According To The Literature

We can compare the results of stress and deformation potential energy obtained from the relation from references [1] and [2]. D. Broek on page 95 ref. [1] gives relations for stresses, in the polar system of coordinates.

All these solutions are based on the assumption that for crack propagation is critical stress state in front of the crack, not the status of the potential strain energy or state of energy density distribution in the vicinity of the crack.

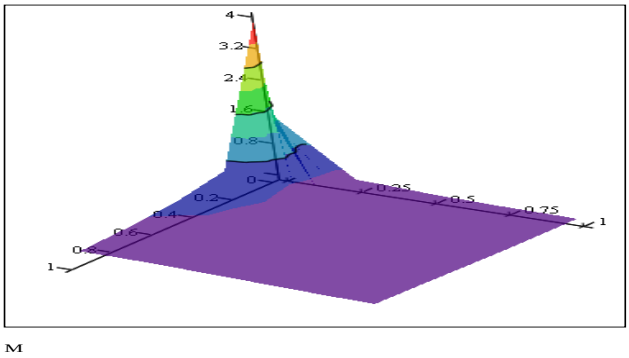

Fig. 19 Distribution of normal stress σ_x, in the coordinate system (x, y).

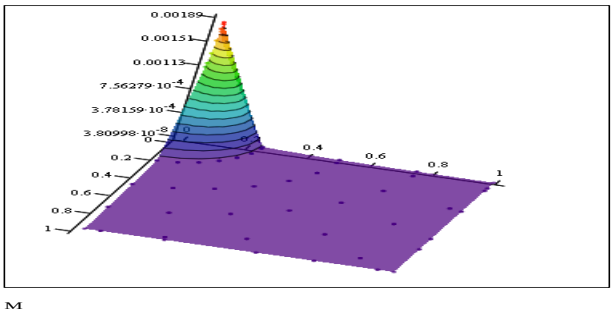

Fig. 20 Distribution of the potential strain energy A_{def} ahead of the crack tip in the coordinate system (x, y).

Based on the stress values obtained from equations in reference [1] and by using the expression for the potential strain energy (1) is obtained a diagram of the potential strain energy, shown in Figs. 19 and 20. Pronounced linearity of this graph does not correspond to real physical conditions, because distribution of potential strain energy around the crack tip as well as distribution of stresses is non-linear. Nonlinearity of stresses has been demonstrated in experimental studies [7], [8], and analytical studies.

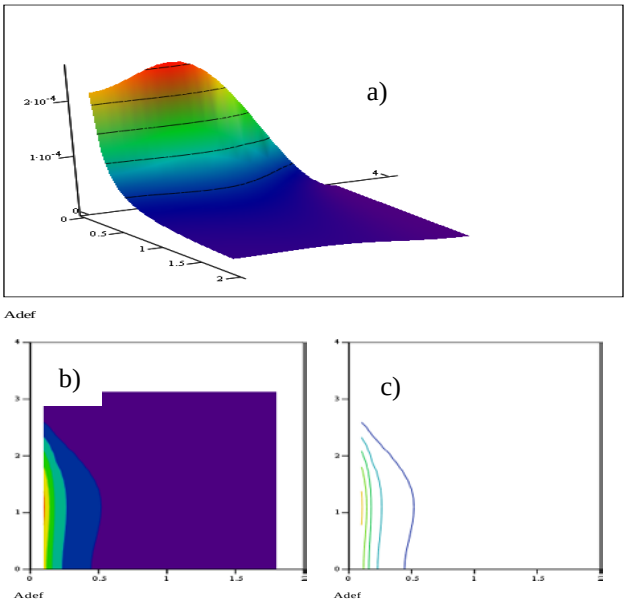

Fig. 21 a) Surface of potential strain energy (type I), b) The projection of the potential strain energy surface at the x-y plane, c) Isoenergy lines in front of the crack tip

We can compare the results of reconstruction with the graphical presentation of potential strain energy obtained from the relations (6) based on literature [1], [2]. Gdoutos on page 34 of ref. [2], gives relations for stresses, in the polar system of coordinates of the form of crack propagation **type I** (opening).

By applying relations from [2] we get distribution of potential strain energy ahead of the crack tip shown in Fig. 21. (a, b, c).

IV. Conclusions

Results of applying the idea of reconstructing the spatial surface, that describes the potential strain energy distribution in the vicinity of the crack, are presented. Based on the reconstructed potential strain energy surface we got the isoenergy lines in front of the crack tip, for both analyzed examples. It is observed that the distribution of stresses, and distribution of the potential strain energy is very similar in both cases, indicating the main role of geometric shape of contour surface of the crack. Finally, for comparison of stress and potential strain energy surfaces, which are based on the relations from literature were shown.

Acknowledgment

This work was supported by Ministry of Education and Science, Republic of Serbia, through the project ON174011, and Faculty of Mechanical Engineering, University of Niš.

References

[1] Broek D., (1982) Elementary Engineering Fracture Mechanics, Martinus Nijhoff Publishers, The Hague.

[2] Gdoutos E. E., (1993) *Fracture Mechanics*, Kluwer Academic Publishers, Dordrecht.

[3] Jovanović D. B., Jovanović M., (2000) Local stress and strain state in the region of crack for different global stress states in a plate, *YUSNM, Niš 2000, Facta Universitates, Series Mechanical Engineering,Vol. 1, No. 7*, pp. 925-934.

[4] Jovanović D. B., Jovanović M., (2001) Stress state and strain energy distribution at the vicinity of elliptical crack with compression forces acting on it's contour, *Facta Universitates, Series Mechanics, Automatic Cont. and Rob.*, Vol. 3, No.11, pp. 223-230.

[5] Jovanović D. B., (2002) Stress state and deformation (strain) energy distribution ahead crack tip in a plate subjected to tension, *Facta Universitatis., Series Mechanics, Automatic Control and Robotics*, Vol. 3, No. 12, pp. 443-455.

[6] Parsons I. D., Hall J. F., Rosakis A. J., (1986) A Finite Element Investigation of the Elastostatic State Near a Three Dimensional Edge Crack , *SM Report* 86-29, Division of Engineering and Applied Science, California Institute of Technology, Pasadena, California.

[7] Pindera J. T., Josepson J., Jovanović D.B., (1997) Electronic Techniques in Isodyne Stress Analysis: Part 1. Basic Relations, *Experimental Mechanics*, Vol. 37, No. 1, pp. 33-38.

[8] Pindera J. T., Josepson J., Jovanović D.B., (1997) Electronic Techniques in Isodyne Stress Analysis: Part 2. Illustrating Studies and Discussion, *Experimental Mechanics*, Vol. 37, No. 2, pp. 106-110.

Challenges of the engineering profession in modern industry

THE 5th INTERNATIONAL CONFERENCE
MECHANICAL ENGINEERING IN XXI CENTURY

December 9-10, 2020
Faculty of Mechanical Engineering in Niš, Serbia

ICT Study Programs in Higher Education in Serbia: Analysis of Main Trends

Dušan MOJIĆ[1], Branka MATIJEVIĆ[2]

[1] Faculty of Philosophy, University of Belgrade, Čika Ljubina 18-20, Belgrade, Serbia
[2] Institute of Social Sciences, Kraljice Natalije 45, Belgrade, Serbia
dmojic@f.bg.ac.rs, bmatijevic@idn.org.rs

***Abstract* — The paper analyzes main trends in development of ICT study programs at higher education institutions (HEIs) in Serbia. Significant increase in number and scope of these programs has been one of the most important characteristics of Serbian higher education sector in the last two decades. Such development has been the result of a complex interplay of global, national and sectorial factors. What all of these factors have in common is the market principle, which has also become one of the corner-stones of the HEIs' development strategies. Such strong environmental pressures has forced HEIs to undergo transformations that will maintain and improve their market positions. The market principle has prompted the proactive behavior of HEIs towards customers/future students. These transformation strategies to a large extent depend on the labor market trends, represented on the level of individual actors/customers by the perception of employment possibilities enabled by a specific degree. The goal of the paper is to provide general insight into the diversity of ICT study programs at HEIs in Serbia, which represents one of the key strategic responses to said market pressures.**

***Keywords*— ICT Study Programs, Higher Education Institutions, Serbia**

I. Introduction

Higher education institutions (HEIs) in Serbia has underwent radical transformations in the recent decades. These transformations has coincided with overall transformations of Serbian society from socialism to (semi-peripheral) capitalism, to a large extent caused by global economic, political, cultural and social trends. Capitalism as a world system [1] "reintegrated" former socialist societies, although at a different pace and to an unequal degree. Serbia has shared some similar characteristics in that respect, being however a rather unsuccessful example regarding the overall transition processes [2].

"Paradoxically, being rather unsuccessful in economic transition, Serbia has established a fairly free market in higher education. Institutional transformation in higher education in Serbia has been carried out through the accreditation process in the overall Bologna process implementation, followed by the full implementation of a three-cycle system (bachelor studies, MSc studies and PhD studies) and ECTS system in all study programs" [3, p. 3510].

The market principle has prompted the proactive behavior of HEIs towards customers/future students. As the main outcome of changed competitive landscape, the relationship between students and HEIs has developed into a customer–service supplier relationship. Generally, on the global level, the student–university relationship has become more marketised [4]. Students are perceived as customers, while universities' mission becomes delivering added value compared to competitors and finding effective ways of market positioning.

Students, as customers, have been mostly interested in employability when deciding which HEI to enroll. Therefore, wider labor market trends and transformations are the key determinants of these customer orientations. These transformations have been mostly influenced by the rapid development of information and communication technologies (ICT) in the last decades.

According to famous sociologist Manuel Castells these technologies include the converging set of technologies in micro-electronics, computing (machines and software), telecommunications/broadcasting, and opto-electronics. Castells adds to this list the application of information technologies in genetic engineering [5, p. 29].

This influential author emphasizes the terms "informational economy" and "informational society" to denote a specific form of economic and social organization in which "information generation, processing, and transmission become the fundamental sources of productivity and power because of new technological conditions emerging in this historical period" [5, p. 21].

How do HEI in Serbia respond to these trends and transformations? The main goal of this paper is to present main trends in development of ICT study programs in Serbian higher education.

II. Theoretical Considerations

Various theoretical approaches have been applied in explanations of the role and organization of higher education institutions [6]. Universities and faculties belong to a common category or entity – organizations. Scientific studies of organizations have experienced radical paradigm shift in the 1960s, offering theoretical frameworks for understanding relationships between organizations and their environment. This paradigm shift refers to a transition from the notion of organization as a closed system to a

comprehension of organization as an open system (influenced by various aspects of its environment).

Modern theories of organization have been main embodiments of this radical paradigm shift. The most prominent representatives of this theoretical stream are the system theories and the contingent (situational) theories of organization. The system approach had proposed that organizations are open systems, constantly interacting with their environment. The basis of this approach had been found in the Ludwig von Bertalanffy's general system theory, while its application in understanding the nature and the functioning of organizations refer to the ideas of social psychologists Katz and Kahn [7, p. 5]. According to this approach, elements of organization interact with each other, simultaneously interacting with the environment of the organization.

Contingent or situational theoretical approaches have been viewed as the most developed and the most influential in the field of organization studies in general [8, p. 133]. According to these theories, every organization adapts to each situation (defined through various factors) [9, p. 157]. There is no "one best way" of organizing and different types of organizations respond to different kinds of situations. The degree in which particular organization ensures "best match" between the characteristics of the situation and its own structural characteristics determines the success of the organization as a whole. Most important aspects of organizational environment can be broadly categorized as social, cultural, economic, technological, political, and legal [9].

III. Serbian Higher Education landscape

Last decades has brought radical and dramatic changes in all aspects of the organizations' environment. Economic globalization and the rise of the multinational companies (MNC) had influenced all the aforesaid aspects of the environment. These changes (among others) have also influenced the role, organization and strategies of higher education institutions. Different environmental challenges led some authors [10, p. 11] to a conclusion that modern universities have been "under pressure". These pressures operate on global, national, regional and local levels.

Higher education institutions in Eastern Europe have been under additional pressure in the recent decades. Transition in former socialist countries brought political, economic and overall social transformation toward the "western capitalist model" of society and its institutions. These transformations refer to formal (constitutions, laws, statutes) and informal (beliefs, values, norms) institutional changes [11, p. 231].

Universities have experienced organizational changes under these institutional circumstances or environmental pressures. Higher education institutions in Serbia have been additionally "pressured" by political conflicts (including armed conflicts), the UN sanctions, hyperinflation and overall economic and social crisis in the 1990s. Although political changes in 2000 brought some political and economic stability, environmental changes "surrounding" universities have been even more turbulent. For example, the Bologna process imposed radical institutional transformation through the accreditation process. The accreditation process is *par excellence* a process of putting institutional pressure on universities as basic units in the higher education sector [12, p. 1554].

These institutional pressures have been strengthened by inadequate state financial support for public universities and dramatically increased share of private sector in higher education. Furthermore, competition for university attendees between privately-owned and state founded universities has been taking place in a very unfavorable demographic situation primarily characterized by severe depopulation and youth emigration.

Different strategic responses have been noted among higher education institutions in Serbia [12]. These transformation strategies have been mainly based on the perception of the prospective demands of the labor market. The main strategic tool available to universities and faculties have been curricular transformations. Responding to this needs, HEI also have to adapt their organizational structures, systems and processes to various aspects of environmental changes in last decades. Our focus will be on the analysis of ICT study programs.

IV. ICT Study Programs in Serbian Higher Education institutions

Higher education in Serbia has got rich and prominent tradition in the field of informatics since 1980s within the Faculty of Electrical Engineering, Faculty of Mathematics, and Faculty of Organizational Sciences (University of Belgrade), Electronic Faculty (University of Niš), Faculty of Technical Sciences, and Faculty of Sciences (University of Novi Sad) [13, p. 183]. However, the period of blocked postsocialist transformation in the 1990s had dramatic negative impact on higher education, particularly in highly advanced technological sectors such as ICT. One of the important consequences of such situation had been the prevailing interest of prospective students for study programs in social sciences.

Nevertheless, this trend has reversed in the last years – the number of students associated with technical skills in general is rising year by year recently. As for ICT study programs, in 2018/2019 school year, 22,339 out of 249,771 students have been in this field of study (Table I). Further 45,960 students are in the technical areas (engineering, manufacturing, and construction). The share of ICT students in overall student population in Serbia is slowly but constantly increasing. Negative demographic trends in Serbia (depopulation and emigration) led to decrease in number of students from 2015 to 2018 (from 251162 to 249771). However, all categories of HEI in Serbia (state and private universities, state and private higher schools) recorded growth of number of ICT students.

TABLE I Proportion of Students Enrolled in ICT Programs in Overall Number of Students in HEI in Serbia [14], [15]

	2015/2016	**2018/2019**
Overall number of students	251,162	249,771
Number of students enrolled in ICT programs	19,285 (7.68%)	22,339 (8.94%)
State universities	10,660 (55.26%)	11,978 (53.62%)
Private universities	2,266 (11.75%)	3,369 (15.08%)
State higher schools	5,578 (28.92%)	6,026 (26.98%)
Private higher schools	781 (4.05%)	966 (4.32%)

The proportion of ICT students in state and private HEIs has slightly changed from 2015 to 2018 in favor of private universities and higher schools. In 2015 the percentage of ICT students in private HEIs in overall number of ICT students in Serbia was 15.8%, raising to 19.41% in 2018. This could be explained by the stronger orientation of private HEIs to labor market needs, unlike state universities and higher schools, which have been more inclined to development of traditional study programs (although state HEIs also had more ICT students in 2018 than in 2015).

More than 16% of all Serbian newly-enrolled students in 2018 were ICT enrollees (9,747), which is a clear indicator of interest of Serbian young people in studies related to informatics [13, p. 182]. In the period 2012-2018, an impressive growth of new students was registered in Serbian HEIs – from 5,523 in 2012 up for 76.5% in 2018, with average growth rate in the six-year period of 9.9%. Demand for experts in ICT has been so high that only 60% of enrolled students graduate, while a certain number of students get employment during studies (which is the main reason why majority of those never graduates). With or without a diploma in ICT in Serbia, significant number of ICT students find job very easily [13, p. 185].

TABLE III REGIONAL DISTRIBUTION OF ICT STUDENTS IN STATE UNIVERSITIES [14], [15]

	2015/2016	2018/2019
Overall number of students	177352	181310
Number of students enrolled in ICT programs	10660 (6.01%)	11978 (6.61%)
Belgrade Region	3800 (35.65%)	4119 (34.39%)
Vojvodina	5064 (47.50%)	5304 (44.28%)
Šumadija and Western Serbia	1258 (11.8%)	1231 (10.28%)
Southern and Eastern Serbia	990 (8.27%)	1324 (11.05%)

Regional distribution of ICT students has been (as expected) to a large degree determined by an existing distribution of (predominantly state) HEIs in Serbia (Table II). Nevertheless, although the University of Belgrade is by far the biggest university in Serbia, in relative terms, University of Novi Sad has got the largest proportion of ICT students (47.50% in 2015 and 44.28% in 2018, with Faculty of Technical Sciences and Faculty of Sciences (both located in Novi Sad) as the strongest institutional stands of ICT study programs.

TABLE IIIII REGIONAL DISTRIBUTION OF ICT STUDENTS IN PRIVATE UNIVERSITIES [14], [15]

	2015/2016	2018/2019
Overall number of students	28,203	29,174
Number of students enrolled in ICT programs	2,266 (8.34%)	3,369 (11.55%)
Belgrade Region	2,007 (88.57%)	3018 (89.58%)
Vojvodina	141 (6.22%)	232 (6.89%)
Šumadija and Western Serbia	118 (5.21%)	119 (3.53%)
Southern and Eastern Serbia	-	-

As for regional distribution of ICT students enrolled in private universities (Table III), centralization in the main university center is enormous (almost 9/10 of all ICT students in this type of HEIs attend their study programs in Belgrade). On the other hand, this is expected, since great majority of private universities have been founded (and majority of their faculties located) in the capital of Serbia.

TABLE IVV REGIONAL DISTRIBUTION OF ICT STUDENTS IN STATE HIGHER SCHOOLS [14], [15]

	2015/2016	2018/2019
Overall number of students	41,467	34,567
Number of students enrolled in ICT programs	5,578 (13.45%)	6,026 (17.43%)
Belgrade Region	2,820 (50.56%)	3,383 (56.14%)
Vojvodina	724 (12.98%)	796 (13.21%)
Šumadija and Western Serbia	1,288 (23.1%)	1,241 (20.59%)
Southern and Eastern Serbia	746 (13.37%)	606 (10.06%)

State higher schools also have got an important tradition in offering study programs in ICT. Decrease in overall number of students is here more dramatic than in state universities – 20% in just three years, but in spite of that fact, the absolute number of ICT students in fact increased 8% in this period. Belgrade located state higher schools account for majority of ICT students – 50.56% in 2015, and 56.14% in 2018. As for other Serbian regions, Šumadija and Western Serbia has relative majority of students enrolled in ICT study programs (23.1% in 2015 and 20.59% in 2018) compared to Vojvodina and Southern and Eastern Serbia (Table IV).

As for private higher schools, the relative share of ICT students is 20.47% in overall student population of this type of HEI. Vast majority of them attend study programs in Belgrade (936 of 966, or 96.89%).

Finally, an interesting topic related to ICT studies is gender distribution of students. ICT studies are still male dominated, as well as the ICT profession in general. For example, the average share of female students in ICT programs in HEI in Europe is 19%. In Serbia, to a large extent still traditional and patriarchal society [16], this share is 7% higher – 26% [13]. How can this be explained?

TABLE V GENDER DISTRIBUTION OF ICT STUDENTS IN SERBIAN HEIS [14], [15]

	2015/2016		2018/2019	
	All	Women	All	Women
Number of students enrolled in ICT programs	19,285	4,959 (25.71%)	22,339	6,283 (28.13%)
State universities	10,660	3,375 (31.66%)	11,978	4,377 (36.54%)
Private universities	2,266	377 (16.64%)	3,369	735 (21.82%)
State higher schools	5,578	1058 (18.97%)	6,026	1,101 (18.27%)
Private higher schools	781	149 (19.08)	966	170 (17.60%)

The legacy of socialism has certainly significant impact in that respect. Namely, women from Eastern Europe enrolled engineering studies significantly more often than

women in the Western Europe. The similar pattern can be identified in Serbia today regarding engineering studies, as well as ICT studies. The proportion of female students in ICT study programs in Serbian HEIs increased from 25.71% in 2015 to 28.13% in 2018 (Table V). There are considerable differences between four main types of HEIs in Serbia in that respect. State universities have more than 1/3 of female students in ICT programs (36.54% in 2018), while private universities, state higher schools and private higher schools have 21.82%, 18.27%, and 17.60%, respectively.

V. Conclusions

The impact of technology on society has been an important topic of social studies, especially during dramatic changes brought about by the early stages of modernization and industrialization. The standpoint of technological determinism was very common in these considerations [17]. Recently, the variant of social constructivism called social construction of technology (SCOT) [18] has been the dominant paradigm in studying the interrelationship of technology and society. The fundamental proposition of this theoretical approach is understanding of technology as a product of dynamic interaction of relevant social actors.

Very important social actors in this process are higher education institutions. HEIs represent key institutional actors in the process of professionalization of occupations related to ICT sector, providing theoretical knowledge and formal educational credentials for work of ICT experts [19]. HEIs in Serbia have responded to threats and opportunities from the changing environment by developing existing and introducing new study programs in ICT. Challenges posed by transformations in social, cultural, economic, technological, political, and legal aspects of the environment exist on different but interconnected levels – global, national, regional and local.

As for social aspect of the environment, Serbia can be regarded as a society of semi-peripheral capitalism [20]. In cultural terms, norms and values in Serbia have shown to be rather inconsistent and mixture of traditional, modern and postmodern elements [16]. Being a part of capitalism as a world system [1], Serbia have benefited in the recent decades from economic globalization through foreign direct investments (FDI). Multinational companies (MNCs) brought advanced ICT and increased the technological level of Serbian economy. Nevertheless, on a global scale Serbian economy has been rather uncompetitive in terms of ICT [13, p. 28]. The main reasons for that can be found predominantly in two remaining aspects of the environment – political and legal.

"Serbia is an economic growth laggard due to deficient institutions, specifically lacking rule of law and control of corruption, and due to low investment, which itself is curbed by corruption and poor rule of law" [21, p. 17]. According to these Serbian economists, Serbia has been growing 2 percentage points below its potential in recent years. Their estimate is that roughly one half of the growth gap could be explained by underperforming institutions (1 p.p.), and the other half by low investment (0.7 p.p.) and education (0.2 p.p.).

Having in mind these analysis, it is clear that HEIs function in a rather unfavorable institutional environment, but still bear a part of the responsibility for Serbian economic and overall social underdevelopment. Our analysis of the official statistical data on ICT programs in higher education in Serbia have strongly confirmed both – external threats and internal weaknesses of HEIs. Further development of quality ICT study programs would definitely be a very successful strategy to turn these weaknesses into strengths of Serbian higher education. Such transformations could also represent strong impetus for institutional transformation of Serbian economy and society.

References

[1] I. Volerstin, *Uvod u analizu svjetskog sistema*. OKF, Cetinje, 2005.

[2] M. Lazić and S. Cvejić, "Stratificational Changes in Serbian Society: A Case of Blocked Post-socialist Transformation". Faculty of Philosophy, Institute for Sociological Research, 2005.

[3] S. Mitić and D. Mojić, "Student Choice of Higher Education Institutions in a Post-transitional Country: Evidence from Serbia", *Economic Research-Ekonomska Istraživanja*, Vol. 33, No. 1, pp. 3509-3527, 2020.

[4] F.Maringe and P.Gibbs, *Marketing Higher Education: Theory and Practice*. Open University Press, Buckingham.

[5] M. Castells, *The Information Age: Economy, Society, and Culture. Volume I: The Rise of the Network Society*. Second edition, Wiley-Blackwell, Malden, MA; Oxford, 2010.

[6] A. Altmann and B. Ebersberger, "Universities in Change: As a Brief Introduction", Universities in Change: Managing Higher Education Institutions in the Age of Globalization (pp.1-6) Springer, 2013.

[7] R. W. Scott, "Reflections on a Half-Century of Organizational Sociology". *Annual Review of Sociology*, Vol. 30, pp. 1-21, 2004.

[8] K. Grinth, *The Sociology of Work: Introduction*. Third Edition. Polity Press, Cambridge, 2005.

[9] P. Sikavica, *Organizacija*. Školska knjiga, Zagreb, 2011.

[10] E. P. Berman and C. Paradeise, "Introduction: The University under Pressure". in Berman, E. P. and Paradeise, C. (eds). *The University under Pressure* (pp. 11-19). Emerald Group Publishing Limited, Bingley, UK, 2016.

[11] S. Pejovich, "The Uneven Results of Institutional Changes in Central and Eastern Europe: The Role of Culture". *Social Philosophy and Policy*, Vol. 23, No. 1, pp. 231-254, 2006.

[12] N. Janićijević, "The Reactions of Universities to Imposing a New Institutional Pattern: The Case of Higher Education in Serbia". No. 174, pp. 1550-1559, 2015.

[13] M. Matijević and M. Šolaja, *ICT in Serbia: At a Glance*. Vojvođanski IKT klaster, Novi Sad, 2020.

[14] *Highed Education (2015/2016)*, Statistical Office of the Republic of Serbia, Belgrade, 2017,

[15] *Highed Education (2018/2019)*, Statistical Office of the Republic of Serbia, Belgrade 2019,

[16] J.Pešić, *Promena vrednosnih orijentacija u postsocijalističkim društvima Srbije i Hrvatske: politički i ekonomski liberalizam.* Filozofski fakultet, Univerzitet u Beogradu, Beograd, 2017.

[17] D. Petrović, *Društvenost u doba interneta: studija komunikacione upotrebe interneta u Srbiji.* Akademska knjiga, Novi Sad, 2013.

[18] T. Pinch and W. E. Bijker. "The Social Construction of Facts and Artefacts: Or How the Sociology of Science and the Sociology of Technology Might Benefit Each Other." *Social Studies of Science*, Vol. 14, No. 3, pp. 399-441, 1984.

[19] C. Turner and M. N. Hodge, "Occupations and Professions". in Jackson, J. A. (ed). *Profession and Professionalization* (pp. 17-50). Cambridge, University Press Cambridge, 1970.

[20] M. Lazić and J. Pešić, *Making and Unmaking State Centered Capitalism in Serbia*. Faculty of Philosophy, Institute for Sociological Research, Belgrade, 2012.

[21] P. Petrović, D. Brčarević and M. Gligorić, "Why is Serbia an Economic Growth Underachiever?" *Ekonomika preduzeća*, Vol. 67, No. 1-2, pp. 17-33, 2019.

THE 5th INTERNATIONAL CONFERENCE
MECHANICAL ENGINEERING IN XXI CENTURY

December 9-10, 2020
Faculty of Mechanical Engineering in Niš, Serbia

Instrumentalization of Knowledge in Neoliberalism

Vesna STANKOVIĆ PEJNOVIĆ

Institute for Political Science, Svetozara Markovića 36, Belgrade
vesna.stankovic.pejnovic@gmail.com

***Abstract*— Education has been powerfully affected by the rise of a neoliberal political, economic and cultural agenda. Education is social process of nurturing capacities for practice. Recent changes in education can be understood in the general context of transition, where, despite appearances to the contrary, capitalism is in decline and competing with the burgeoning movements of the potential future society.The commodification of services and the privatization of public sector agencies demands institutional and cultural change. The profit-seeking corporation is promoted as the admired model for the public sector, and for much of civil society too. Schemes of organization and control are imported from business to public institutions. But the policy changes all move in the same direction – increasing the grip of market logic on schools, universities and technical education.**

***Keywords*— education systems, markets, education, neoliberalism, society**

I. Introduction

What is the true purpose of education at a time when machines are getting smarter and smarter?

Education systems all over the world have been impacted by the rise of neoliberal ideology and practices of government. Education is not alone: business-friendly governments and market-driven agendas have re-shaped all areas of public life. [1]. [2]

Global educational system is facing with a profound change. Politicians and corporate leaders are replacing our public school system with a private, for-profit, competitive, market- based system that increases inequality and undermines democracy. To continue to ignore and not resist the changes may result in the demise of public schooling. The lack of interest in higher education research by policymakers and administrators may be secondary to more fundamental questions about the purpose of research about higher education. Is the primary purpose to inform organizational and managerial elites about the social dynamics of the higher learning, or is it to contribute to society's knowledge of itself and its processes of self-organization? [3].

II. Neoliberalism as base of reformed society

Neoliberalism has a definite view of education, understanding it as human capital formation. It is the business of forming the skills and attitudes needed by a productive workforce – productive in the precise sense of producing an ever-growing mass of profits for the market economy. „Human capital „is a metaphor, and in itself too narrow. But this economistic idea does catch an important feature of education, that it is a creative process oriented to the future. In this respect, the neoliberal model is superior to the view widespread in other areas of social science, including the sociology of education, that education is a process of social reproduction. The neoliberal policy claim that public schools are being freed from stifling bureaucracy and heavy-handed state control. Schools are being tied more tightly into a system of remote control, operated by funding mechanisms, testing systems, certification, audit and surveillance mechanisms.

Effect of neoliberalism on the knowledge is based on an increasing technicization of knowledge and knowledge production. What can be most readily marketed is patentable knowledge. There is a stark irony that universities set up for the advancement of knowledge now is striving to restrict knowledge to extract a commercial benefit from it.

The instrumentalization of knowledge in universities has led to a decline of critical disciplines because do not seem to have the art of attracting million-dollar research grants. Corporate interests globally have mounted a fierce and well-funded attack on science when scientific findings challenge profit-making teacher-effectiveness policy agenda being pushed by the rich countries' neoliberal economic think-tank, the OECD (Organization for Economic Co-operation and Development). In this way, the neoliberal policy regime produces its own knowledge base, in a closed loop that does not allow other kinds of knowledge to enter policy debate. As it happens, there is a considerable amount of other research on the powerfully divisive social consequences of the market agenda in education, tracing which groups are advantaged by it and which are disadvantaged. Indeed, we have had this information for years, from different countries and continents [4]. Neoliberal educational reform policies reflect a number of the key features of capitalism in its stage of "globalization," or "capitalism with the gloves off and on a world scale." [5]. The aim of neoliberalism is to put into question all collective structures capable of obstructing the logic of the pure market. [6]. Neoliberal educational reform policies focus on creation of curriculum standards (where the state defines the knowledge to be taught) and "accountability." The specification of curriculum standards is nearly always accompanied by accountability strategies. it does no good to establish expectations if one does not ensure they are met and, if they are not met that there is a planned remedy.

Central to the neoliberal project is the information society. According to this paradigm, the management, quality, and speed of information become essential for economic competitiveness. [7]. Schools that are not run by businesses may become public shells—public schools with many educational services privatized (e.g., teaching, curriculum, special services), union contracts nullified, the real danger of policies that privatize education and throw it into the corporate market is that they "will erode the public forums in which decisions with social consequence can be democratically resolved" [8].

III. GROWTH OF MANAGERIALISM

We are facing today with driving the growth of managerialism in universities. The growth of managerialism in turn has undermined academic democracy (power of central managers and deans rising, departmental decision-making declining, students redefined simply as customers).

A sustained attempt to create competitive markets in modularized training services meant that both public and private institutions became simply 'providers', competing with each other for fees and subsidies. [9]. The universities are controlled by a neoliberal managerial regime. Education is displaced by competitive training, competition for privilege, social conformity, fear and corruption, while protest and rational alternatives are marginalized. It is easy to despair about the current scene. But education itself has a resilience, has a grounding in social needs, that cannot be suppressed – and that will be heard.

Knowledge has been packaged in textbook-type formats, so that students become customers for products. Moreover, higher education has become more synonymous with training for employability, for example, skills to solve problems, which are set by one's superiors. [10].

Recent tendencies have been called academic capitalism. Although university staff are still largely state funded, they are increasingly driven into entrepreneurial competition for external funds. Under such pressure, staff devise "institutional and professorial market or market-like efforts to secure external monies" [11].

The market model currently threatens education at its core. The opposition between education's logic of value and that of the corporate market is contradictory because clearly the aims and processes of education and the market are distinct 12].

IV. ROLE OF CAPITAL IN EDUCATION

Today schools are pushed to produce efficient workers who can compete within the global workforce by adapting and developing new skills, but who do not question the hierarchical work structure. On the one hand capital requires educated and flexible labourers, but on the other hand it refuses the idea that labourers should think for themselves. While education of the labourer appears important it cannot be the kind of education that permits free thinking" [13].

Education is transformed into a market in which schools compete with one another not only for test grades, but also for the students and teachers to fill the school, students and teachers become commodities, with some students and teachers valued over others. Moreover, because the control over schooling has shifted from the local school and district to the state directed by capital, teachers have less control of their own work and become, like other workers, alienated from their own creative capacities. [14].

The educational reforms have been a means for the state and corporations (who also often fund commissions and organizations that support such reforms) to take an active role in reforming society by introducing a competitive market system in which some students and schools succeed and some fail. The reforms are couched within a discourse in which the previously neglected will now be helped through a system of high standards, objective testing, and equal opportunity. The system of testing and account- ability permits the state to determine the goals and output without directly intervening in the process itself, thereby reducing resistance. Education privatization is one result of the hollowed- out neoliberal state and the marketization of the public sphere.

"Higher education has special stakes for capitalist rule. Universities define the skills of professional workers for labour markets, reinforce ruling ideologies, and represent the needs of the state and industry as those of society. Despite that prevalent role, students and staff often succeed in creating spaces for critical citizenship, even for overt challenges to capitalist agendas."

Economic restructuring has created a highly segmented workforce and polarized social structure along lines of class, race, national origin, and gender. Contrary to claims about the need to prepare all students to be postindustrial knowledge workers the bulk of jobs do not require sophisticated new knowledge but basic literacies, ability to follow directions, and certain (accommodating) dispositions toward work. [15].

A national system of standardized tests with strict penalties for failure helps to ensure a workforce that has the basic literacies and compliant dispositions needed by the low-wage labour force. [16]. There is philosophical incompatibility between the demands of capital and the demands of education, inter alia, with respect to critical thought. [17].

Governments throughout the world are resolving this incompatibility more and more on terms favorable to capital. The university's role as an independent institution is increasingly threatened by the interests of corporations in both subtle and obvious ways. [18].

The capitalist State will seek to destroy any forms of pedagogy that attempt to educate students regarding their real predicament—to create an awareness of themselves as future labor powers and to underpin this awareness with critical insight that seeks to undermine the smooth running of the social production of labor power. This fear entails strict control of teacher education and training, of the curriculum, of educational research. [19].

Within universities the language of education has been very widely replaced by the language of the market, where lecturers "deliver the product," "operationalize delivery," and "facilitate clients' learning," within a regime of "quality management and enhancement," where students have become "customers" selecting "modules" where "skill development" at universities has surged in importance to the derogation of the development of critical thought. [20].

Education businesses produce a range of "knowledge products" that can be sold and traded internationally because we live in capital's social universe [21]. All aspects of our lives are potentially open to invasion by capital—for this is one way in which the social universe of capital expands. [22].

Specifically in the context of school life, capital produces new human productive and intellectual capacities in alienated form. [23]. Education "links the chains that bind our souls to capital. It is one of the ropes comprising the ring for combat between labor and capital, a clash that powers contemporary history: 'the class struggle'" Schools therefore act as vital supports for, and developers of, the class relation, "the violent capital–labor relation that is at the core of capitalist society and development" [24].

Education and training are processes of labor-power production. They are subspecies of relative surplus-value production (the raising of worker productivity so that necessary labor is reduced) that leads to a relative increase in surplus labor time and hence surplus value. Human capital development is necessary for capitalist societies to reproduce themselves and to create more surplus value. The core of capitalism can thus be undressed by exploring the contradictory nature of the use value and exchange value of labor power.

V. V.CONCLUSIONS

The world now moves for the first time in history to a global struggle between knowledge and misrepresentation as the finally contending forces. [25].

According to many authors higher education has become too technocratic, too narrow, too specialized, too self-serving, too inwardly focused, and irrelevant to public policy and social practice. [26]. [27]. [28].

Education involves nurture and involves encounter between persons, and that encounter involves care. Learning from a computer is not education; the machine does not care. Learning from a person behaving like a machine is not education; that person's capacity for care is being suppressed.Encounter implies respect and reciprocity, a degree of mutual engagement by learner and teacher. And despite the distinction between learners and teachers, that mutual engagement requires a strong kind of equality, an equal citizenship in the educational situation.

In academia, as elsewhere, labor power is never completely controllable. To the degree that capital uses the university to harness general intellect, insisting its work force engage in lifelong learning as the price of employability, it runs the risk that people will teach and learn something other than what it intends" [29].

Critical educators push this "something other" to the extreme in their pedagogical praxis centered on a social justice, anti-capitalist agenda. The key to resistance is to develop a critical pedagogy that will enable the working class to discover how the use value of their labor power is being exploited by capital but also how working-class initiative and power can destroy this type of determination and force a recomposition of class relations by directly confronting capital in all of its hydra-headed dimensions.

Scholars now talk of a "post-academic science", or "mode-2 science", contrasting it with the "mode-1 science" that arose in the post-war period, and some commentators have even identified a "second scientific revolution" comparable to the one that generated modern science in the sixteenth and seventeenth centuries [30].

Education needs invention, and there are certainly enough lively minds in the teaching workforce to be confident that invention will come. Education needs coalitions of social groups able to create the spaces in which educational invention will work. Those requirements are clear enough. How they can be turned into practice, we still have to discover.

REFERENCES

[1] R. Connell, Understanding neoliberalism. In S. Braedley & M. Luxton (Eds.), Neoliberalism and everyday life Montreal & Kingston: McGill-Queen's University Press. 2010, pp.22-36.

[2] D. Harvey, Spaces of hope. Berkeley: University of California Press, 2000.

[3] J. Welsh, The Unchained Dialectic, Critique and Renewal of Higher Education Research, in Neoliberalism And Education Reform E. Wayne Ross and Rich Gibson (eds.), New Jersey: Hampton Press, Inc.Cresskill, 2006, 217- 235.

[4] S. J. Ball, Class strategies and the education market: The middle classes and social advantage. London: Routledge Falmer, 2003.

[5] Ollman, B. (2001). How 2 take an exam… and remake the world. Montreal: Black Rose Books..p.. 7.

[6] W. Tabb. *Unequal Partners: A Primer on Globalization*, New York: The New Press, 2002., p.9

[7] S. Mathison, S. (2004). Educational assessment and standards-based educational reform. In S. Mathison & E. W. Ross (Eds.), Defending public schools: The nature and limits of standards-based reform and assessment Westport, CT: Praeger., 2004, vol. 4, pp. 3–14.

[8] C. Ascher, C., Fruchter, N., & Berne, R. Hard lessons: Public schools and privatization. New York: Twentieth Century Fund., 1996, p.9

[9] R Connell, The neoliberal cascade and education: an essay on the market agenda and its consequences, Critical Studies in Education, 54:2, 2013, 99-112,

[10] L. Levidow, Marketizing Higher Education Neoliberal Strategies and Counterstrategies 237-257, in Neoliberalism And Education Reform E. Wayne Ross and Rich Gibson (eds.), Hampton Press, Inc.Cresskill, New Jersey, 2006, p. 238.

[11] S.Slaughter, L.Leslie, Academic capitalism: Politics, policies and the entrepreneurial university. Baltimore, MD: Johns Hopkins University Press, 1997,

[12] J. McMurtry, . Education and the market model. Paideusis. 5(1), 1991, pp. 36-44.

[13] D.Harvey, D. Spaces of hope. Berkeley: University of California Press, 2000.

[14] D. Hursh, Marketing Education,The Rise of Standardized Testing, Accountability, Competition, and Markets, 15-34, in: Public Education in Neoliberalism And Education Reform E. Wayne Ross and Rich Gibson (eds.), Hampton Press, Inc.Cresskill, New Jersey, 2006

[15] P. Lipman, "No Child Left Behind", Globalization, Privatization, and the Politics of Inequality, 35-59, in: Neoliberalism And Education Reform E. Wayne Ross and Rich Gibson (eds.), Hampton Press, Inc.Cresskill, New Jersey, 2006, p.37.

[16] C.A. Ray, & Mickelson, R. A. (1993). Restructuring students for restructured work: The economy, school

reform, and non-college-bound youths. Sociology of Education, 66, pp.1–20.

[17] J. McMurtry, Unequal freedoms: The corporate market as an ethical system. Toronto: Garamond Press, 1998.

[18] S. Mathison, & E. W. Ross, The hegemony of accountability in schools and universities. Workplace: a Journal for Academic Labor, 5(1)., 2002, Retrieved from http://www.louisville.edu/journal/workplace/issue5p1/mathison.html

[19] G. Rikowski, After the manuscript broke off: Thoughts on Marx, social class and education, Paper presented at the British Sociological Association Education Study Group, 2001, London: King's College, London.

[20] D.Hill, Educational Perversion and Global Neoliberalism, 107-140, in Neoliberalism And Education Reform E. Wayne Ross and Rich Gibson (eds.), Hampton Press, Inc.Cresskill, New Jersey, 2006, 131.

[21] Rikowski, G. (2001a). The battle in Seattle. London: Tufnell Press.

[22] G. Rikowski,. The Great GATS buyout, Red Pepper, 101,2002, 25–27.

[23] P. McLaren, Critical Pedagogy and Class Struggle in the Age of Neoliberal Globalization, Notes From History's Underside, 257-289, in: Neoliberalism And Education Reform E. Wayne Ross and Rich Gibson (eds.), Hampton Press, Inc.Cresskill, New Jersey, Hampton Press, Inc, 2006., p.264.

[24] G. Rikowski, After the manuscript broke off: Thoughts on Marx, social class and education, Paper presented at the British Sociological Association Education Study Group, King's College, London, 2001, .2-19.

[25] McMurtry, J. (1998). Unequal freedoms: The corporate market as an ethical system. Toronto: Garamond Press, 1998, 395

[26] Leslie, D. (2002). Thinking big: The state of scholarship on higher education. In W. Tierney & L. Hagedorn (Eds.), From research to policy to practice to research (pp. 1-7). Los Angeles: Center for Higher Education Policy Analysis, University of Southern California.

[27] Peterson, M. (2000). Emerging developments in postsecondary organization theory and research: Fragmentation or integration. In C. Brown (Ed.), Organization and governance in higher education (pp. 71–82). Boston: Pearson Custom Publishing.

[28] Kezar, A., & Eckel, E. (Eds.). (2000). Making higher education research useful. New Directions for Higher Education. San Francisco: Jossey-Bass.

[29] Dyer-Witheford, N. (1999). Cyber-Marx: Cycles and circuits of struggle in high-technology Capitalism. Urbana: University of Illinois Press.

[30] M. Gibbons, M. Trow, P. Scott, S. Schwartzman, The New Production of Knowledge: The Dynamics of Science and Research in Contemporary Societies, *Contemporary Sociology* 24(6) · November 1995

THE 5th INTERNATIONAL CONFERENCE
MECHANICAL ENGINEERING IN XXI CENTURY

December 9-10, 2020
Faculty of Mechanical Engineering in Niš, Serbia

Engineers, Ethics and Professionalism

Ivana ILIĆ-KRSTIĆ, Vesna MILTOJEVIĆ

University of Niš, Faculty of Occupational Safety, Niš, Serbia
ivana.ilic@znrfak.ni.ac.rs, vesna.miltojevic@znrfak.ni.ac.rs

***Abstract*— Sustainable development, a topic exhaustively discussed ever since the Brundtland Report in 1987, provides a broad framework for pro-environmental activities of industrial engineers. This paper is based on the previous findings concerning the negative pressure of engineering activities on the environment and it highlights the necessity of reinterpreting the engineers' roles and activities under the current ecological conditions. The concept of sustainable development provides engineers with a key role in designing and managing "clean technology", i.e. technological systems that are less harmful, more efficient, and socially and environmentally more acceptable. The paper examines to what extent engineers can work and contribute to sustainable development within their professional roles and specifies their roles and responsibilities. Special emphasis is placed upon creativity, ethics, and professionalism in view of the new role of engineers, as well as upon the investigation of the identified ethical and professional dilemmas facing the 21st century engineers. The paper also highlights the changes in industrial systems and the changed roles of engineers in order to determine the new educational needs of the engineers who represent the driving force behind industrial activities for the future.**

***Keywords*— Engineering, Ethics, Professionalism, 21st century**

I. Introduction

Owing to engineers' ability and inventiveness in applying scientific knowledge and technological achievements, it would be reasonable to claim that they created the world we know today. By first creating various tools and then using them to build buildings, means of transport, energy production facilities, and artificial intelligence, they recognized the needs of humankind and society and shaped the world in which we live [1]. Engineers have been and still are scattered among a plethora of different jobs and professions, working as researchers, designers, constructors, technologists, analysts, controllers, managers, agricultural engineers, bioengineers, architects, and builders of roads, bridges, railways, machines, tools, and buildings, and facilities for various purposes. They create new value by diving into the unknown and added value through high quality, productive, and effectively led work processes [2]. In their work, engineers have been meeting the current needs of people, thus aiding societal progress, but they have also contributed to new forms of risk.

Since modern society is also known as the society of risk and the society of knowledge, the engineers are faced with a new task – to help society adapt technology to its needs in keeping with the principles of sustainable development. Accordingly, "considering the ten-year time horizon, the question is raised about the role of engineers within society and the problems and challenges they will be and are facing" [1].

This paper discusses the changes occurring in modern civilization and affecting the engineering profession, the importance of teaching social sciences and humanities to engineers, and the development of their professional ethics, which nowadays must be attuned to the principles of sustainable development.

II. Social Changes Shaping the Engineering Profession

Globalization processes, networking, global population increase, and the need to conserve the environment and ensure further development according to sustainability principles are shaping our society, politics, economy, environment, technology, and the market, thus influencing the tasks and ethics of engineers [3].

Globalization is an important social change facing the engineering profession. It involves the creation of a unified economic, political, and cultural space on the planet, where people, ides, goods, and capital circulate freely.

The ongoing globalization is a new, dynamic, complex, multidimensional, and globally ubiquitous phenomenon, which is interpreted differently by different scholars. Globalization itself is a centuries-old process, as old as the first caravans and transoceanic vessels. It was accelerated by the construction of railways and roads and the emergence of air travel, until it reached a period of unprecedented expansion with the rapid development of telecommunications followed by the rise of the Internet. Globalization is the logical result of technological progress, with fast information flow and highly-developed information and communication technologies serving as its connective tissue [4]. Globalization has two faces [5] as it undoubtedly has both a positive and a negative impact on the society and the environment. It was the negative impact of globalization that incited Ulrich Beck to call modern society the society of risk, suggesting that risks are present in the technosphere, the sociosphere, and the ecosphere [6]. According to him, the risks from technological development are unpredictable, which is why the present authors believe that the responsibility for risk prevention also lies with engineers, who convert new knowledge to new technologies.

The interconnectedness among people, and consequently their power, has never been greater. This does not merely refer to friends and acquaintances but to the

possibility of easily finding and reaching a large number of like-minded persons, wherever they may be. People are connecting ever more easily but are paradoxically less familiar with each other. The Internet is the key factor for such connections, while the phenomenon of social networks is its paradigm [7]. Owing to the Internet, scientists and engineers of various profiles are not only able to use databases to find information about new findings, but are also able to interconnect with their colleagues worldwide and to exchange their experiences.

Scientific progress over the last two centuries, primarily medical and pharmaceutical but also engineering, and the relatively calm period in the development of human civilization over the previous 65 years (no world wars and systematic annihilation of the population) have led to a more rapid population rise on the planet. There are predictions that the world population will increase to 1.5 times its current size of 6.8 billion in only 40 years and that it will exceed 9 billion as early as 2050 [8]. This means that the global population rise is exponential. There is a significant issue with the understanding and management of the changes that occur according to this model. Namely, the extent of such phenomena is difficult to follow, as the effects of changes remain unobserved for a long time until they suddenly emerge, almost out of nowhere, carrying new challenges. Population rise burdens many professionals, including different engineers, with a number of tasks, such as how to provide sufficient space for living, working, and leisure and how to provide sufficient food, drinking water, and other necessities.

The most significant change pertains to the need for maintaining the harmony between people and the environment. A series of devastating natural disasters during the past decade, global warming, climate change, and the rapid extinction of plant and animal species throughout the world have emphasized the necessity for sustainable development, which needs to assume a primary role in shaping our future. Sustainability has become an imperative as a basis of economic, technological, social, and cultural development in order to meet the needs of the present without preventing future generations to meet their own needs [9]. The crossing of the four megatrends has resulted in a dramatic increase of the population's mobility and migration, individualized lifestyle, easier access to knowledge, lower limits for doing new business, increased competition, and a search for talented people in every part of the world.

III. Challenges of the Engineering Profession

The engineering profession encompasses theoretical knowledge and practical skills and involves long and comprehensive education that includes the acquisition of knowledge from technical and technological sciences, natural sciences, social sciences, philosophy, ethics, and art. It presupposes continuing education and self-education. "They will need this not only because technology will change quickly but also because the career trajectories of engineers will take on many more directions—directions that include different parts of the world and different types of challenges and that engage different types of people and objectives. Hence, to be individually/personally successful, the engineer of 2020 [and the 21st century in general (authors' remark)] will learn continuously throughout his or her career, not just about engineering but also about history, politics, business, and so forth" [11].

It is a profession of advanced skills, enlightenment, and commitment to the common good (both its mission and its vision). The engineering profession includes its own professional associations as self-regulatory organizations that: set professional standards and high ethical standards (to reach a higher goal of personal commitment to the engineering profession); establish ethical codes; establish codes of conduct within and beyond the profession; and determine how the profession is represented before the public, the government, and the 'face of justice'. A good example of such an association is the American Society of Mechanical Engineering (ASME). In addition to an institutionally sanctioned code, like the one in Serbia, the development of professional ethics of engineers, which nowadays needs to contain the eco- prefix, also benefits from higher education that adds content from social sciences and humanities to its curricula and from "control of engineers' conduct by a professional association" [10]. In terms of the common good, the engineering profession has a social duty to find adequate technical and technological solutions for increased public benefit, individual and social wellbeing, human safety, and environmental protection and conservation, which means "that engineers so educated must embrace continuing education as a career development strategy" [11].

Modern global trends produced numerous challenges for engineers. Some of them include the following: optimization of fast-rising urban infrastructures; use of clean energy sources; provision of drinking water for all people; expansion of ICT infrastructure; adaptation of technology to the needs of the aging population; environmental conservation; management of complex interdisciplinary issues and growing global socio-political tensions; assurance of safety in physical and virtual environments; and handling of growing consumer demands in terms of quality, flexibility, and personalization of products [1].

The fact remains that we live in a consumer society in which the majority of the population on the planet attempts to copy the lifestyle of the developed parts of the world. Unfortunately, such a lifestyle is unsustainable, due to the limited natural resources and capacities of the planet. Factors such as population rise, profit-oriented technologies targeting the consumer mentality, and the attitude that humans and technology can compensate for everything that has been destroyed in nature disrupt the balance between humans, society, and nature. It is therefore to be expected that in the upcoming years engineers will be the ones to solve the numerous issues pertaining to the environment and energy shortage, bioengineering and medicine, microengineering, population growth and social issues, management of globalization trends, and the existing technologies [12]. Simultaneously, they will have to deal with the models of leading the global societal development.

In order to adequately solve the existing and potential issues, engineers require knowledge from different fields. "Strong analytical skills, […] practical ingenuity, […] creativity (invention, innovation, thinking outside the box, art), […] communication, […] leadership, […] high ethical standards […] and a strong sense of professionalism" [11] are traits, skills, and competences that all engineers will

need for the current century of rapid technological innovation and globalization, and they can be acquired through multidisciplinary education. In addition to the required multidisciplinary formal education, continuing education is another requirement for the engineers of today.

IV. Engineering Ethics and Professionalism

Studies [13] have shown that engineers are nowadays mostly improving known technologies and existing innovations. Yet, the biggest challenge lies in the creation of completely new products and services, rather than in the extension of the existing ones. In modern society, engineers will be required to use numerous known elements and combine them into previously unknown mosaics, to tap into their emotions, and to try to harmonize the relationship between science, technology, and the environment.

The phenomenon of engineering ethics is too complex to receive a fixed, definitive, and concise definition. "The two main components of engineering ethics are (1) the problems specific to engineering and the responsibility of engineers contained within the principles of knowledge application and professional experience and (2) the specific establishment of general ethical norms and virtues as they are used in the context of engineering" [14]. That is why it is applied and preventive, as it refers to the prevention of what is morally wrong and the avoidance of ethical dilemmas. It also represents a practical morality (moral values and actions of engineers). Engineering ethics includes personal strivings and goals of engineers towards commitment to ethical engineering. It is a corpus of social dimensions of engineering: beliefs, public opinion, and documents of professional engineering associations. It encompasses both policies and laws, and the rights and responsibilities of engineers. It is a process and a practice of creating humane interpersonal relationships during work and for the purpose of work. It contributes to human integrity in specific historical conditions through the norms, actions, and practices, striving towards the essence of morality – humanity (in the sense of humaneness, benevolence). In his "The Sociology of Morals", renowned Serbian academician Radomir Lukić considered the Serbian word čovečnost (Engl. humaneness) to be the most appropriate Serbian term for morals. Even though it is an important 'compass' for the philosophy of work, engineering ethics is the dynamic structure of every action and every work process. It describes the morality, but also always (theoretically) uncovers and indicates the possibility of the (a)morality of (normative) ethics. Engineering ethics helps maintain the existing and create new social and work relations on the individual, micro, meso, and macro social levels. The possibilities of engineering ethics increase with the development of productive forces. However, this does not mean that the possibilities will necessarily materialize, because the technological progress and ethical progress are not necessarily proportional and are sometimes inversely proportional [15].

Engineering ethics denotes a set of values to which engineers adhere when faced with moral issues while performing different technical tasks. Those values are then combined with the cultural norms, life experience, and practice to create an awareness of what constitutes responsible actions. It is such actions that become the chief characteristic of engineering professionalism.

Generally, engineering professionalism refers to the acceptance of values such as safety and health of all people and the wellbeing of the entire planet. Professional behaviour of engineers involves their adherence to the following rules: to do only those jobs that are within their professional domain and to act professionally in any type of contact with an employer or a client.

Engineering ethics is an open and mobile system as well as a process. Humaneness and good life are some of the highest goals of engineering ethics, with humaneness being the ultimate goal. Nevertheless, humaneness is also a 'moving target' [16].

In the age of extensive environmental degradation, increased consumption, and global networks of companies, the engineering profession is facing a new primary task – to be able to use the existing elements and new ideas to produce or create unique combinations that have not previously existed and that contribute to environmental conservation. Accordingly, creativity becomes the key competence of engineers in the society of knowledge.

Yet, creativity requires vast knowledge, ideally of several different fields. In order to connect different pieces of knowledge into new ideas, one first needs to possess the knowledge of the field in which one wishes to express their creativity. However, a creative solution must fall within the scope of professional engineering ethics, as this is the only way for it to have a socially accepted and justified role.

V. Conclusions

Modern society is a society of knowledge and risk. It is not only a society founded on the use of ICT in which knowledge is the most expensive product, but also a society that imposes new challenges, seeks new methods of organization, and assigns new roles to the engineering profession. Rapid environmental changes and convergence of knowledge from many different fields will move the modern engineers beyond the strictly technical patterns. In order to assume the leading role in responding to global and local technological, economic, and social challenges and risks of the 21st century, engineers have to understand and acknowledge nature, ethics, the economy, the society, and the culture. Only if this requirement is met will they be able to identify needs and to create and implement sustainable and efficient solutions in a rapidly changing environment. For the engineering profession to benefit from this and to be considered the most desirable in the constant race for new talents, it is necessary to constantly and ubiquitously emphasize the importance of results accomplished by engineers to make our lives easier and more comfortable. Furthermore, it is necessary to mould easily recognizable role models from the engineering profession, so that young people would be able to identify with them more easily. The multidimensionality of the world we live in and, consequently, of the problems we face warrants new knowledge and skills. The current age is characterized by the use and misuse of intelligence to gain profit and benefit in the shortest time possible while ignoring the long-term effects of such behaviour. Global application of this model has resulted in instability and crises throughout the world. Such one-dimensional behaviour requires evolutive corrections. Human activities must be returned to the centre of balance between intelligence on the one hand and ethics and wisdom on the other hand. This is the only way to overcome the turbulent process of globalization and to steer

the world into the age of post-globalization. Education in the 21st century will have to provide a set of knowledge, skills, and competences that will allow engineers to handle the environmental degradation and to help adapt the entire humankind to the new circumstances. The rate of technological progress has surpassed the needs of the society; thus, if the society is to maximally benefit form the existing technologies, it needs to learn how to adapt the technologies to its own needs without disrupting nature. This is an essential new task for engineers [17].

Therefore, engineers also need to acquire knowledge from social sciences and humanities during their education. It would appear that the Serbian educational system and its curricula encourage the culture of disengagement, which, according to Erin A. Cech, considers public welfare and benefit as irrelevant for the engineering practice [18]. She believes that the culture of disengagement is based on three ideological pillars: (1) public welfare is irrelevant to engineering work; (2) technical/social dualism diminishes the importance of social competences; and (3) meritocratic ideology, in which those who are the most capable are the ones who lead, which is why the status quo is fair and just. "However, the culture of disengagement may prevent students from developing a reflexive and nuanced understanding of their professional responsibilities to public welfare, and may actually undermine the public welfare leanings they held on entering college" [18] and, in our opinion, also their actions in practice. Previous studies on the presence of content from social sciences and humanities that help engineers accept ecological-humanistic values and develop their professional ethics in the curricula of Serbian engineering faculties after the introduction of the Bologna Declaration have shown that such content is generally lacking [19, 20]. Unfortunately, it is reasonable to assume that such a trend will continue even in the upcoming new accreditation cycle.

Acknowledgment

The research is funded by Ministry of Education, Science and Technological Development of the Republic of Serbia (Contract No. 451-03-68/2020-14/200148).

References

[1] B. Katalinić, I. Ćosić, V. Katić, and Ž. Tekić, "Inženjeri za inovativno društvo" [Engineers for an Innovative Society], u Zbornik radova VII Skup Trendovi razvoja: "EVROPA 2020: društvo zasnovano na znanju" Kopaonik, 07-10.03.2011. Available from http://www.trend.uns.ac.rs/stskup/trend_2011/radovi/uvodni/UP1-1.pdfwww.trend.uns.ac.rs (28.09.2020)

[2] D. Zelenović, Inteligentno privređivanje i efektivni menadžment [Intelligent Entrepreneurship and Effective Management]. Novi Sad: FTN, 2003.

[3] I. Ćosić, and Ž. Tekić, "Promenama ka društvu znanja" [Changes towards the Society of Knowledge], u Zbornik radova XXXII savetovanje proizvodnog mašinstva. Novi Sad: Fakultet tehničkih nauka, 2008, pp. 21-25.

[4] A. Giddens, The Consequences of Modernity. Cambridge: Polity Press, 1990, p. 64.

[5] M. Pečujlić, Globalizacija: dva lika sveta [Globalization: Two Faces of the World]. Beograd: Gutenbergova Galaksija, 2002.

[6] U. Bek, Rizično društvo [Risk Society]. Beograd: Filip Višnjić, 2001.

[7] M. Castells, Informacijsko doba: Ekonomija, društvo i kultura (svezak 1) – Uspon umreženog društva [The Information Age: Economy, Society and Culture, Volume 1: The Rise of the Network Society]. Zagreb: Golden marketing, 2000.

[8] T. P. Soubbotina, Beyond Economic Growth: Meeting the Challenges of Global Development. Washington: The World Bank, 2000. Available from: www.worldbank.org/depweb/beyond/global/chapter3.html#fig3_1 (10.02.2011)

[9] Our Common Future. Oxford: World Commission on Environment and Development, 1987.

[10] D. B. Đorđrvić, "Profesija inženjer: stanje i perspective" [Engineering Profession: Current State and Future Prospects], u Profesija inženjer, D. B. Đorđević & B. Đurović, Eds. Niš: Univerzitet u Nišu, Mašinski fakultet, 2013, p. 5.

[11] The Engineer of 2020: Visions of Engineering in the New Century. Washington, DC: The National Academies Press. National Academy of Engineering, 2004, p. 25, 55-77. Available from: https://www.nap.edu/read/10999/chapter/3#24 (1.10.2020)

[12] Educating the Engineer of 2020: Adapting Engineering Education to the New Century. Washington, DC: The National Academies Press, 2005. Available from: www.nap.edu/catalog.php?record_id=11338#toc (1.10.2020)

[13] D. E. Goldberg, Creative Modeling for Tech Visionaries. Available from: www.slideshare.net/deg511/creative-modeling-for-tech-visionaries (28.10.2020)

[14] J. Babić, "Etika inženjera" [The Ethics of Engineers], u Profesionalna etika inženjera, D. B. Đorđević & B. Đurović, Eds. Niš: Univerzitet u Nišu, Mašinski fakultet, 2011, p. 10.

[15] S. Trifunović, "Inženjerska etika – sinteza čovečnosti inženjera" [Engineering Ethics – Synthesis of Engineering Humaneness]. IMK-14 – Istraživanje i razvoj u teškoj mašinogradnji, vol. 23 no. 1, pp. 21-24, 2017. Available from https://scindeks-clanci.ceon.rs/data/pdf/0354-6829/2017/0354-68291701021T.pdf

[16] M. V. Martin and R. Šincinger, Etika u inženjerstvu [Engineering Ethics], Beograd: Službeni glasnik, 2011.

[17] D. E. Goldberg, The Missing Basics: What Engineers Don't Learn and Why They Need to Learn It. Available from www.slideshare.net/deg511/the-missing-basics-what-engineers-dontlearn-and-why-they-need-to-learn-it (10.09.2020)

[18] E. A. Cech, "Culture of Disengagement in Engineering Education?", Science, Technology and Human Values, vol. 39, no. 1, pp. 42-72, 2014.

[19] T. Inđić, "Social Studies of Technology and Serbian University Curricula,", Zbornik Matice srpske za društvene nauke, 2016, vol. 159-160, no. 4, pp. 709-720, 2016. https://doi.org/10.2298/ZMSDN160709I

[20] V. Miltojević, "Higher education in Serbia and environmental ethics for engineers", Didactica Slovenica – Pedagoška obzorja, 2012, vol. 27, no. 3-4, pp. 184-194, 2011.

THE 5th INTERNATIONAL CONFERENCE
MECHANICAL ENGINEERING IN XXI CENTURY

December 9-10, 2020
Faculty of Mechanical Engineering in Niš, Serbia

Bounded Rationality and Engineering Ethics

Alpar LOŠONC, Andrea IVANIŠEVIĆ

Faculty of Technical Sciences, University of Novi Sad, Trg Dositeja Obradovića 6, 21000 Novi Sad, Serbia
Faculty of Technical Sciences, University of Novi Sad, Trg Dositeja Obradovića 6, 21000 Novi Sad, Serbia
alpar@uns.ac.rs, andreai@uns.ac.rs

***Abstract*— Bounded rationality and engineering ethics are related since the concept of bounded rationality shapes the conditions for making decisions, which includes the conditions for ethical decisions too. Consequently, this raises the question of nature of the said connection. This paper presents a thesis on indirect connections, in contrast to some thinkers who view bounded rationality as a direct constitutive element of moral reasoning. Engineering ethics is a normative discipline, and the concept of bounded rationality is not normative in its character. Thus, in the light of some interpretations, bounded rationality can be considered as highly valuable for engineering ethics.**

***Keywords*— Bounded Rationality, Engineering, Ethics, Company, Organization.**

I. Introduction

Bounded rationality has a long and vast tradition in the theory of science and decision-making [1], but a proper in-depth study would take us in different directions and we are simply unable to do that on this occasion. The mentioned form of rationality can be generally treated as a form of expression for the "limitation" (Simon) of our cognitive abilities in terms of achieving certain goals. Setting and interpreting the set goals and finding resources depend on the way we process objective "constraints" that we face. Yet, the logic of bounded rationality implies that our rationality in the decision-making process is inherently ″deficient".

We primarily refer to the orientation that was paradigmatically formulated a few decades ago by Herbert Simon, the Nobel Prize winner ([2], [3]). Although Simon was originally focused on the economic discourse, his reflections spread to many domains, so we can say that it is a transdisciplinary phenomenon as the traces of "bounded rationality" can be found in different segments of different disciplines today.

II. The contours of bounded rationality

Bounded rationality can be best understood as the opposition to earlier decision-making criteria. This can be simply expressed as a critique of "unbounded rationality" which starts from the maximally employed cognitive capacities of a person who is, at the same time, aware of himself/herself as such. Namely, earlier orientations presented the search for the "optimum" as the ultimate goal, and accordingly, rationality in the context of means and goals ("instrumental rationality") was weighed against the search for optimization. Achieving the optimum (in economic discourse, for example, it is the optimal level of profit) conditioned the "optimal level of rationality".

Unlike his predecessor, Simon offered a broad perspective of the constitutive role of widely understood "suboptimality" [4] in relation to decision-making processes. In short, bounded rationality shows a different picture of the decision-maker who confronts the "complex environment" compared to earlier ideas. It is logical to assume that all subjects simultaneously face a large number of possibilities, that is, they enter a multidimensional field where contradictions are also possible. Human subjects cannot be the "eyes of God" and comprehensively "compute" the information and data to make an intact optimal decision. The cognitive "limitations" that determine human performance do not allow subjects to develop "problem-solving" capacities in order to achieve optimality. Although some earlier theories emphasized the capacities of subjects in the light of optimality ("optimal benefit", "optimal profit", "optimal power", "maximizing happiness" depending on the field of subject), we point to the "limits" that arise in the context of a "complex environment". Our cognitive determinations are the reason why we should give up on the "hunt for the optimum" which is both "epistemologically" and "ontologically" unattainable for us. Instead of "optimum", Simon proposes another motivational category, "satisficing": subjects should not be focused on achieving "optimum" but "satisficing". The category of optimality, which can be added to certain mathematical procedures, does not explain human procedures in organizations, institutions, the market, but the same subjects are either "rule-following" and extensively use "heuristics", "bias-based", "rules of thumb" in the decision-making process, or they simply mimetically follow other subjects in the decision-making processes. The omniscient subject focused on "utility-maximization" has been replaced by another mode of subjectivity that is "limited" in terms of "computational abilities" (Simon): different subjects faced with a multitude of references are forced to invent other procedures regarding the optimality [5]. The same subjects are neither temporally nor spatially comprehensive; the loop between knowledge and information-circulation does not allow subjects to be described as "optimizing agency".

Simon's "behavioristic" argument is often rightly described as such. Indeed, a certain form of *behavior* has been placed at the center of attention. This assessment is

based on the fact that the center of argumentation is no longer the predetermined, apriori placed subject ("agency") who has mastered the situation and achieved balance between all the preferences, and implemented a decision that manifests the precisely harmonized preferences. It describes behavioral patterns positioned between "mind" (Simon) and "environment". It is no longer a strong "agency" that has dominated the tradition and that can resolve the relationship between goals and means with "unbounded rationality". The same patterns are open for contextual-empirical decision-making moments. Namely, the same moments influence the formation of conditions in terms of choice, or as some other theorists would say, the same moments determine the "framing" [6] of the perceived problem.

Of course, this, otherwise briefly described program of bounded rationality has experienced and still is experiencing numerous interpretations. Some commentators and critics have tried to blunt the edge of "bounded rationality" by limiting it to the "costs-account" [7] of the economizing agency, which particularizes the problem, that is, they tried to limit its scope and the challenging aspect. Bounded-rationality is, as we have said, a transdisciplinary problem, and if it is really relevant for our world then it must be of universal significance. Other commentators aimed at expanding the scope of bounded rationality with the principle of "radical uncertainty" ([7], p. 917) which (along with the category of complexity) already occupies an extremely important place in today's considerations [8]. "Radical uncertainty" synthesized with the phenomenon of complexity and the theory of probability really adds important dimensions to the theory of decision making. After all, bounded rationality and "satisficing" have experienced a remarkable boom in the last two or three decades: in addition to intensive theoretical pursuits, we must note the fact that research in the European Union is based on (neo) behavioral research [9] and that even numerous political decisions at European level should be considered from behavioristic viewpoint. In other words, today, public policies are influenced by behaviorism which is a confirmation of its importance and the fact that it did not remain at the level of theoretical articulations.

III. Bounded rationality and ethical dimensions in engineering: elements of critique

Still, what is the relationship between engineering ethics and bounded rationality?

Ethics involves certain decision-making processes, although it is clear that the degrees and intensities of decision-making change in ethical practice. Thus, ethical orientations that we are familiar with (consequentialist, deontological, or ethics based on goods) should not ignore the phenomenon of bounded rationality and "satisficing" as a measure of human actions. This implies that the agency of engineering and its confrontation with complex problems must be described in the perspective of limited cognitive capacities instead of "maximization of utility". Of course, engineering practice can be identified in different fields: we can talk about the ethical aspects of mechanical or genetic engineering, accordingly, as long as it is in accordance with today's technologies, we can also list here engineering of "human nature".

However, it is possible to discuss about engineering ethics as a whole, as implied by various representative authors [10]. Moreover, our attitude may be supported by the claim that in terms of "logic" there is no difference between business ethics and engineering ethics: "the distinction between a profession and other jobs is a distinction of power and prestige rather than a distinction based on service/profit or expert knowledge/common knowledge" [11]. In other words, from an ethical perspective, engineering is a "set of attitudes" that faces the same epistemological and ontological problems as the subjects in "business ethics". That is, if we recognize bounded rationality in the sphere of business ethics, then "logically", the same problem exists in "engineering ethics".

Some authors have recognized the importance of "bounded rationality" for morality. They claim that there is a pattern of "behavior" in the moral sphere, that is, we can talk about "moral behavior" ([12], [13]) which is subject to the logic of bounded rationality. Furthermore, we can talk about "moral behavior as bounded rationality", that is, the scheme of bounded rationality with "social heuristics" can be a model for ethics in general.

Could we use this logic to conclude that we have found the engineering ethics principle for the mentioned "set of attitudes" in bounded rationality? Some define engineering as a "social experiment" [10] and we define it as a social practice in which the loop between technology and technique plays a crucial role.

We believe that bounded rationality is of crucial importance for understanding the different situations that contemporary engineers are facing. We can take technology as an example. The often-mentioned claim that there is a contradiction between the intensified human power based on the expansion of technology and the inability to control the consequences with products of technology especially deeply affects engineers. It is impossible to discuss serious ethics without considering technology [14], and the same claim applies even more to the engineering domain - the articulation of engineering ethics depends on understanding the long-term consequences of technology. This means that: "the ambivalence of technology is bound up with its "bigness", the supersize of technological effects in space and time. What is big and what is small is determined by the finitude of our terrestrial environment, which must never be absent from our mind" ([14], p. 897). Engineers, too, face the problem of predicting indirect consequences of technology in the long run. Yet, the mentioned contradiction clearly points to the existence of bounded rationality; engineers are in a decision-making position that reflects the logic of bounded rationality. There is an impossibility of comprehensive consideration of all consequences, existing possibilities are in a conflicting position, there is a contrast between short and long term, etc. In terms of finding different examples of bounded rationality, the field of engineering involved in technology can be a very useful and valuable field.

However, the fact that we can recognize bounded rationality in engineering decision-making, it still does not mean that we can equalize this type of "limited" rationality with engineering ethics. We have emphasized that the concept of bounded rationality is the articulation of a certain form of behavior based on "rule-following" versus

the „logic of optimality". Undoubtedly, there are certain normative elements in "social heuristics" too, the way decisions are made involves certain normative and even ethical dimensions. Still, engineering ethics as a form of ethics that thematizes the ethical problem regarding engineering is much more normative than any form of "social heuristics". The concept of bounded rationality can only be normative to a small extent.

Ethics, as well as engineering ethics, depend on the scope of normative reflexivity: it raises and tackles the questions of specific "needs" and responsibilities. Ethics, which implies rethinking of the conditions for "respecting" the other and others, as well as dignity [15] cannot be encompassed by the logic of bounded rationality. In other words, engineering ethics cannot be exhausted with the logic of bounded rationality; this type of rationality can exist as an indispensable admixture, but not to be exhausted.

Then, what is bounded rationality for engineering ethics? The critics who deal with technological processes and wish to articulate appropriate ethical horizons often narrow the field of ethics. This way, ethics becomes even with "risk management" and "prudence" which is related to "risk management".[1] This coincides with our recently stated opinion regarding certain (neoclassical) theorists who have tried to reduce the significance of bounded rationality by treating it from a "cost-account" perspective. Here, it happens again: the engineering ethics that confronts various risks and global forms of uncertainty is equated with "prudence" in terms of "processing" and "computing of costs". Indeed, "prudence" was very important in the history of ethics, especially in the Aristotelian ethics of virtue. However, by reducing it to "cost-processing" for some insightful balance, little of those challenges related to engineering ethics are dealt with. Bounded rationality is indispensable for ethical decision-making, but its scope is determined by the fact that the concept behind it is determined by "empiricism" and "inductivism", which significantly takes into account those empirical conditions that contextually determine all decision-making processes. Engineers appear in different situations, that is, in different, institutionally determined situations: they can be individual entrepreneurs in the market, they can be corporate managers, they can be partners in certain business ventures, and so on. If we insist on "rule-following" as the basis of bounded rationality, then we need to know the institutional context where bounded rationality is situated.

This concept already faces certain problem and "from the start, it does not inquire as part of the logic of the program into where the rules come from. This is precisely why the rhetoric of behaviorism insists on the importance of observation, almost to the point of inductivism: the program has no underlying theory of rule-following" [18].

IV. Conclusion

Bounded rationality is a constitutive part of our idea about rationality today in various fields. Therefore, engineering ethics cannot ignore its existence. We paid particular attention to the moment of operationalization of technology which induces numerous ethical problems. Still, normative structure of engineering ethics prevents bounded rationality to be affirmed as the absolute basis of ethical reasoning. Inadequate expansion of bounded rationality has overlooked some crucial moments that are important for engineering ethics, namely, the multidimensional positioning of engineers in different contexts. Although bounded rationality also contains certain normative elements, it is insufficient for the reasoning in engineering ethics.

References

[1] M. Klaes and E.-M. Sent, "A Conceptual History of the Emergence of Bounded Rationality," Hist. Polit. Econ., vol. 37, no. 1, pp. 27-59, 2005.

[2] H. Simon, Models of Bounded Rationality, vols. 1–2. Cambridge: MIT Press, 1982.

[3] H. Simon, "Bounded Rationality," in The New Palgrave Dictionary of Economics, J. Eatwell, M. Milgate, and P. Newman, Eds. London: Macmillan, 1987, pp. 221-225.

[4] J. Conlisk, "Why Bounded Rationality?", J. Econ. Lit., vol. 34, no. 2, pp. 669-700, 1996.

[5] N. Luhmann, Zweckbegriff und Systemrationalität. Tübingen: J. C. B. Mohr, 1968, p. 45.

[6] D. Kahneman and A. Tversky, "The Framing of Decisions and the Psychology of Choice," Science, vol. 211, pp. 453-458, 1981.

[7] D. Dequech, "Bounded Rationality, Institutions, and Uncertainty," J. Econ. Issues, vol. 35, no. 4 pp. 911-929, Dec. 2001.

[8] M. Cooper, "Complexity Theory After the Financial Crisis," J. Cult. Econ., vol. 4, no. 4, pp. 371-385, 2011.

[9] P.W. Zuidhof, "Behavioralizing Europe: How Behavioral Economics Entered EU Policymaking", https://ecpr.eu/Events/Event/PaperDetails/27723, accessed, 10/3/2020.

[10] M.W. Martin and R. Schinzinger, Ethics in Engineering. New York: McGraw-Hill, 1996.

[11] N.E. Bowie, "Are Business Ethics and Engineering Ethics Members of the Same Family?," J. Bus. Ethics, vol. 4, no. 1. p. 44, Feb. 1985.

[12] G. Gigerenzer, "Moral Satisficing: Rethinking Moral Behavior as Bounded Rationality," Top. Cogn. Sci., vol. 2, pp. 528–554, 2010.

[13] R. Tietz, "Semi-normative theories based on bounded rationality," J. Econ. Psychol., vol. 13, iss. 2, pp. 297-314, June 1992.

[14] H. Jonas, "Technology as a Subject for Ethics," Social Research, vol. 49, no. 4, p. 891, Winter 1982.

[15] C. Taylor, Source of the Self: The Making of the Modern Identity. Cambridge, Mass.: Harvard University Press, 1989, p. 34.

[16] J.-P. Dupuy, "Some Pitfalls in the Philosophical Foundations of Nanoethics," The Journal of Medicine and Philosophy: A Forum for Bioethics and Philosophy of Medicine, vol. 32, iss. 3, pp. 237–261, 2007.

[17] J.-P. Dupuy, "Alexei Grinbaum, Living with Uncertainty: Toward the Ongoing Normative Assessment of

[1] We support this claim which can be found in [16], [17].

Nanotechnology," Techné, vol. 8, no. 2, pp. 5-25, Winter 2004.

[18] R. Langlois, "Bounded Rationality and Behavioralism: A Clarification and Critique," J. Inst. Theor. Econ., vol. 146, no. 4, p. 694.

THE 5th INTERNATIONAL CONFERENCE
MECHANICAL ENGINEERING IN XXI CENTURY

December 9-10, 2020
Faculty of Mechanical Engineering in Niš, Serbia

The World of Machines and Engineers in Kurt Vonnegut's Negative Utopia

Gordana STOJIĆ

Department of Sociology, Faculty of Philosophy, University of Niš, Serbia
gordana.stojic@filfak.ni.ac.rs

***Abstract*— The subject of the paper is Vonnegut's negative utopia Player Piano, which describes a society in which machines replace the physical and mental work of people, from production to the deployment of people to jobs. The society is divided into the elite (engineers and directors) and unclassified, pushed out of the sphere of work. People's needs are met, but they are deprived of the feeling that they are useful and needed, which is the basis of self-esteem.**

By depicting a world in which machines rule people by doing exactly what people created them for, Vonnegut raises issues that are relevant today: the consequences of automation, organization and pursuit of efficiency on labor, freedom, social inequalities, leisure and identity. He points out the responsibilities of engineers regarding the creation of such "better world"

***Keywords*—Vonnegut, technology, automation, work, engineers, professional ethics.**

I. Introduction

Kurt Vonnegut's novel *Player Piano* like other utopias and dystopias discloses what future society might be like if some of the contemporary tendencies develop to their extreme capacities. Describing the world in which machines rule people while doing, after all, what people have designed them for, Vonnegut poses the questions of relevance for the modern society such as consequences of automation, organization and tendencies to efficiency on labor, freedom, social inequalities, spare time, identity.

What is specific for this dystopia is its focus upon labor and this in two ways: firstly, the need people have for paid work as a source of their identity and social status, and, secondly, the attitude they take towards their work through that of engineer towards his profession. The novel shows a seemingly perfect world, the world in which machines do almost all the work while the majority of people are provided with a comfortable life without doing any work at all. Machines have replaced people's physical and intellectual work, from production to allotting people to working tasks. The plant premises are devoid of people; the machines supervise other machines while only a few engineers manage the whole automated system. The society is divided into elite (engineers and managers) and the majority of unqualified others, expelled from the sphere of labor. People's material needs are fulfilled while they are deprived of the feeling that they are useful and that the society needs them.

The main protagonists of the novel are engineers, doctors of science holding executive leadership positions. The role of engineers in the novel is double: they are the creators of the system of automated production and contribute to maintenance of the existing order while at the same time they (or rather, some of them) call into question the system and articulate rebellion. The novel closely follows the transformation of engineer Paul Proteus, the manager of the Ilium Works, and the most important person in the City of Ilium, a man of a bright career facing the prospect of a glorious future in managing bodies. The uneasiness he feels because people are deprived of jobs or pangs of conscience because of the role he himself plays in all this lead to his questioning the system and joining the protest movement. Another important protagonist is Finnerty, likewise an engineer, Paul's friend and non-conformist who has given up his brilliant career and become one of the revolution leaders.

The central place in Vonnegut's novel is taken by the responsibility of engineers for creating such a „better world." In a short foreword, Vonnegut stresses that our freedom and our lives depend on the skills, imagination and courage of managers and engineers. The action of the novel takes place in the future; yet Vonnegut points to the responsibility of engineers and managers at the moment of his writing the book (in 1952); the consequences of their activities will come out in the future and this is exactly why their responsibility is even greater – to be aware of the fact that their solving technical issues today will shape the freedom and lives of people in the future.

Vonnegut explains why responsibility is upon engineers, not upon scientists. Scientists "simply add to knowledge. It isn't knowledge that's making trouble, but the uses it's put to." (Vonnegut, 1985: 109). It is exactly the engineers who apply scientific discoveries to technical problem-solving; they are mediators between science and practice and should observe not only short-term but also long-term aftermaths of their activities. Though their work is directed towards the goals of the organizations in which they work, they should be aware of the consequences of their activities for other people, social community and mankind.

Vonnegut's novel does not speak only about technological changes but, most of all, about organization (of production, plant, economy, society). Though the action takes place in the future, the book actually presents

the contemporary profession of engineers and, with a dose of humor and irony, contemporary organizational culture. These representations are based on Vonnegut's working experience in a big company.

Starting from the sociological understanding of profession, the paper will analyze, using the example of Vonnegut's novel, engineering professional ethics.

II. Engineers' Attitude towards Their Profession

Professions are characterized, besides other elements, by professional ethics and specific professional subculture that are taken in through the process of education and professional socialization. They equip the experts with a normative-value framework of their activities. Though there are differences among professions, the common characteristics of professional activities are autonomy, authority and altruism (Šporer 1990: 38). Engineers belong to a developed profession although engineering profession has a lower degree of organization and development of professional ethics with respect to, for instance, medical profession (Đorđević, Tasić 2020: 90). The principles that should be regarded as the guiding ones for engineers in doing their professional activity are: responsibility and correctness at work, constant advancement of professional knowledge, commitment to truth as well as scientific and professional norms, advancement of business activities for the benefits of others, environment protection and professional organization (Đorđević, Tasić 2020: 91). Vonnegut's novel offers the possibilities to perceive the problems that may emerge in the realization of these principles.

Engineers' activity is characterized by rationality and efficiency in solving practical problems. Their solutions should be in the function of realization of the goals of the organization in which they work. Vonnegut shows an engineer who does his job admirably even when he himself suffers negative consequences for this. Bud is an engineer who has just invented a machine which has abolished his own job. A few minutes after he, in desperation, speaks about losing his job, he almost automatically reacts to the situation he recognizes as a professional challenge, namely, the procedure of visitors' entrance to the plant. Not only has he, with his invention, abolished his own job (and all such jobs in the whole state) but he endangers the job of his beloved. This episode reveals a deeply rooted logic of the profession which overcomes personal interest besides pointing to the lack of responsibilities for social consequences of it.

Engineers' work also implies innovation and joy of discovery. Three young engineers are assigned the task to automate machine work. "Remember the excitement of recording Rudy Hertz's movements, then trying to run automatic controls from the tape?" (Vonnegut 1985: 378). The engineering is shown as a calling which implies commitment, excitement due to the challenges that the problems pose to them, and problem-solving as a game.

Through professional socialization (within the professional education, and in a company), the individual is identified with his profession – with professional title and profession ideology, with the kind of labor characteristic for this profession, with organizational or institutional position that the given profession usually carries in itself and with the social position of the profession (Šporer 1990: 59). The novel is permeated with a sense of strong identification of engineers with their profession. Proteus has preserved, within his plant, the building of Edison's original machine shop set up in 1886. This reveals a sentimental return to the past which, in his imagination, revives the pioneering setting up of the first machines and then delight in the rhythm of machine operations, sounds and movements – Proteus is proud of his profession and the advancement it has made (what would Edison say if he could see this multitude of machines which work harmoniously with no direct human feeding and controlling them?). Engineering profession is identified to what has always been regarded as American way of thinking, "the restless, erratic insight and imagination of a gadgeteer" (Vonnegut 1985: 11). Engineers are proud of the contribution their profession makes to the society. They have decisively contributed to the victory in war and building of the society which is the biggest manufacturer of industrial goods in the world. On the other hand, the episode with Checker Charley (a contrivance for checker game) shows engineers' idolatrous attitude towards their own creations – machines. When the machine burns out, most of the engineers are horrified and saddened by the destruction of such an invention: "Tragedy was in every face. Something beautiful had died." (Vonnegut 1985: 73). On the other hand, rebellious Finnerty shows man's superiority over machines: "If Checker Charley was out to make chumps out of men, he could damn well fix his own connections. Paul looks after his own circuits; let Charley do the same. Those who live by electronics, die by electronics." (Vonnegut 1985: 74). This ambivalent attitude towards engineering and technology is manifested throughout the novel. The satisfaction with the achieved efficiency, an aesthetic attitude towards the harmony of machine movements and sounds, a feeling of superiority over nature, past generations and other nations as well as an unstoppable progress that knows no unsolvable problem – all these feelings are caused by the technology which is created and controlled by engineers. On the other hand, it also induces other kinds of feelings and thoughts – impersonal technology decides upon people's fates (who is to enroll university, who can apply for what kind of job, who cannot ever get employed at any job whatsoever); technology cannot solve all the problems (care about a little girl who has got on the train without the company of her elders) and, most importantly, technology destroys people's lives by depriving them of the possibility to work. However, most engineers do not manifest any care about social consequences of their work – their utter commitment to the principle of efficiency, their desire to advance in career and their fitting into the system have all suppressed autonomy and altruism as values of the professional ethics.

Vonnegut also shows the relationships within the engineer community. The sense of professional togetherness springs from the processes which are in action during recruitment into profession, identical educational processes that experts have gone through as well as position, status and power of professions in the society (Šporer 1990: 33). The friendships established at the university last throughout their entire careers such as the case with the relationship between Proteus and Finnerty. The novel also offers examples of support and solidarity to fellow colleagues: Proteus cherishes a

benevolent attitude towards his colleague Bud despite the weaknesses and disorientation he shows in some life situations because he appreciates his talent and good-heartedness. A young engineer who approaches Proteus immediately after he has been expelled from the community as a saboteur exhibits honesty which might lead to the destruction of his career. On the other hand, the novel reveals competition, careerism and hostility. With a dose of humor Vonnegut exhibits non-collegial behavior of managers – the desire to advance in the career is not only evident in the attempts to show oneself in the best light but also in imputation and mockery of one's competitors. When the news is spread that Proteus is a saboteur, all his fellow colleagues are boycotting him, even the ones he has worked with for years.

III. Ideology of Engineer Calling

In Vonnegut's imaginary world engineers are not only profession; they are also the ruling class, elite which makes all important decisions in the society (the role of politics is of second rate). This is achieved by merging of professional and managerial roles – all plant and company managers are engineers. Knowing that competition and market are suspended, the role of managers is different from the one in the contemporary capitalism. They are exempt from care about conquering markets, product placement, marketing or organization of employees. Due to this nothing changes in terms of the profession once the managerial positions are undertaken (Šporer 1990: 45): engineers still remain primarily engineers who care about functioning of the automated system and production efficiency. However, the merging of the professional authority and managers' capacities increase engineers' responsibility and creates preconditions for a possible conflict of the roles.

The ideology supporting the existing order justifies the leading role of engineers in the society. It is not called into question. Their job is not simply to make mechanical gadgets: "Our job is to open new doors at the head of the procession of civilization. That's what the engineer, the manager does. There is no higher calling" (Vonnegut, 1985: 148). Engineers' profession brings progress to the society by its innovations. Engineer's job is management and engineering; they should not be asking the question, "if we weren't doing something bad in the name of progress" (Vonnegut, 1985: 132). The instrumental rationality of engineers who do not take into consideration social consequences of their activities is manifest in the example of young engineers (Proteus among them) whose task is to prepare mechanizations of the lathe operations. The foreman in the plant has led them to his best mechanic whose movements they record on the tape; hence the tape would control the machines instead of the mechanics. The mechanic, an old worker who is about to retire, has shown submissiveness before "smart young men" as well as pride for being the one chosen to make his movements perpetuated on the tape. Young engineers will talk the foreman into firing that worker and then they would take him for a drink, as Vonnegut ironically puts it, "in a boisterous, whimsical spirit of industrial democracy" (Vonnegut, 1985: 18). Ecstatic with the triumph of their knowledge and talent, their professional success, they miss to see, before them, the other person who was also proud of his work.

Engineers are identified with their "civilization role" and thus with the existing order. Vonnegut critically shows the actions taken for enhancing cohesion and loyalty of engineers. The metaphor about engineers who open up a new door at the head of the civilization procession is inculcated in schooling and then it is all the time renewed in the minds of engineers through media, clubs and all other forms of the social life of elites. Ideology of the engineer calling expresses the idea "of designing and manufacturing and distributing being sort of a holy war" while technical solutions and production efficiency are the only criterion for success. Gatherings and rituals, customs and tradition confirm and enhance the belief in the righteousness of the system and the engineers' deeds while at the same time emphasize their status and separate them from the rest of the society. A critical attitude towards their own professional activity and the ability of perceiving potential consequences for a wider social community neither develop thorough their schooling nor through their professional socialization at job or through professional community.

IV. Revolution

Engineers are in the centre of the novel in another way, i.e. they question social order and the meaning of life; consequently, they are important actors of the revolution. Through the main protagonist, Proteus, Vonnegut shows the way in which a critical attitude towards the system is gradually developed. Engineer and manager, Proteus enjoys watching the plant filled with harmoniously-working machines, "the machines themselves were entertaining and delightful" (Vonnegut 1985: 16). He is committed to his profession in which he has achieved exceptional results and is rewarded for it. But his attitude towards the system is different from that of his fellow colleagues. He feels that he lacks "something", something that his father had and most of the elite: "the sense of spiritual importance in what they were doing; the ability to be moved emotionally, almost like a lover, by the great omnipresent and omniscient spook, the corporate personality" (Vonnegut 1985: 77). Proteus is a conformist suffocated by his own conformism. Hence he feels the desire to do something that would make him more adaptable, more satisfied with his destiny. However, his job, the system and organizational policy alternately cause in him anxiety, boredom or sickness. Since he cannot adapt, he wishes to do something radical (to rebel, to resign – which is in itself an act of rebellion).

How to change that world? Change it into what? Replace it with who? How can man run away from the system if he does not know anything outside it? The greatest problem is to find something he can believe in: "Somewhere, outside of society, there was a place for a man—a man and wife—to live heartily and blamelessly, *naturally*, by hands and wits" (Vonnegut, 1985: 168). Just like the basic problem being located in the labor sphere, so the solution has to be related to labor. Idleness that he could afford financially would be "as amoral as what he was quitting" (Vonnegut 1985: 169). His first response is farming, but he quickly gives it up since after the first attempt he experiences a discrepancy between what was imagined and what this job, this life truly is.

The circumstances exclude Paul from the society of engineers and managers that he no longer identifies with. He becomes an "unqualified human being" – no longer can he get any job; he is defined as a potential saboteur in the police while the only place where he can be accepted is the Homestead, a settlement on the other side of the river settled by non-classified people, excluded from the sphere of labor. His rebellion develops gradually, first of all due to his sense of responsibility for the loss of jobs of a multitude of people: "If it hadn't been for men like me, he might have a machine in the plant" (Vonnegut 1985: 48) Encounters at the Homestead induce in him a feeling of love for these people and the desire to help them. The relief he feels ("Better to be nothing than a blind doorman at the head of civilization's parade") (Vonnegut 1985: 270) is accompanied with a feeling of uprootedness. At the moment when he admits that he is the leader of the revolution, though he is in prison, he knew "what it was to belong and believe" (Vonnegut 1985: 353).

The revolution is organized with the aim to take over the plants and change their organization. It has Luddite and carnival moments. While the leaders want to rationally make, after the rebellion, such a labor organization in which some of the machines would be removed (in order to make space for people) while other machine would still be kept (in order to realize efficient production), masses non-selectively destroy the machines. The revolution is suppressed. The last scenes in the novel again take us back to engineer profession. Engineer Bud repairs a drink machine on the railroad station. Though he has actively participated in the revolution, his commitment to his profession – making and repairing machines – has not grown less. Though the rebellion has failed, engineers Proteus and Finnerty are still left with a feeling of satisfaction for at least trying to realize their ideas about what engineers should offer to the society.

V. Concluding Remarks

Technological and organizational changes pose challenges to engineering profession. By solving technical problems and introducing innovations, engineers contribute to the changes which influence upon the whole society and everyday lives of people. Their aftermaths are not often immediately visible. By increasing production efficiency engineers contribute to people's welfare. By exempting man from hard physical toil or monotonous routine jobs, they ensure that work of a great many people should be easier and more pleasant. However, production automation creates a sense of insecurity regarding the issue whether there will be enough labor demand in the future and what kind of life would be led by the people who have never worked in their entire lives. In his writing about the utopias which base an ideal society upon technological development, Mumford (2009: 110) stresses that: Subordinate to humanized ends, machinery and organization—yes, complicated machinery and organization—have undoubtedly a useful contribution to make towards a good community; unsubordinated, or subordinated only to the engineer's conceptions of efficient industrial equipment and personnel, the most innocent machine may be as humanly devastating as a Lewis gun.

Dystopias offer to us a comprehensive view of the society thus enabling us to perceive more clearly the entirety of potential changes which are very often beyond the horizon of our personal professional and everyday experience. Vonnegut's novel reflects functional importance that the engineering profession has for contemporary society within the context of the development of computer technologies and automation. Engineering ethics can be regarded in terms of two aspects, namely, the attitude towards profession, and the responsibility to social community and, ultimately, to mankind. Vonnegut shows the engineers who have adamantly adapted the principles of their professional activity and who abide by the professional standards in their practice; their job is creative; they are innovative and open to professional challenges. They are identified with the social status that their profession assigns to them. Since all managers are engineers and since engineers enjoy a privileged position in the sphere of labor, they make up ruling elite of the society which firmly connects them to the system and reduces a critical attitude towards it. Through education and professional socialization in organization their identification with profession is enhanced and so is professional cohesion and, at the same time, loyalty to the system. In this way is their autonomy reduced while the ruling ideology enhances their belief that their work undoubtedly contributes to the social welfare. This is the origin of the refusal to leave the framework of instrumental rationality and critically perceive the consequences of their activities upon other people. They impose their views about people's welfare while totally ignoring the possibility for the people to differently understand what is meant by welfare and to express in their own words what they really want in life. Thus their professional activity loses its altruist character. The engineers who are involved in the revolution show a degree of professional responsibility – this does not mean, however, giving up technology but rather adjustment of technology usage to people's needs. That is why we can, finally, again point to Mumford's attitude (2009: 190) that "an acute practical intelligence such as we find today among the engineers need not be divorced from the practice of the humanities."

Acknowledgment

The paper is prepared within the project *Step Towards Professionalization of Sociology: Analysis of the Need for Profession*, realised at the Department for Sociology, Faculty of Philosophy, Niš.

References

[1] Mumford, L *The Story of Utopias* (*Priča o utopijama*). Čačak, Beograd: Gradac K, Branko Kukić, 2009.

[2] Vonnegut, K, *Player Piano* (*Mehanički pijanino*). Zagreb: „August Cesarec", 1985.

[3] Đorđević, D. B., Tasić, M. Serbian Code of Ethics for Engineers + Oath of American Engineers (Srpski etički kodeks inženjera + Zakletva američkih inženjera). U: D. Đorđević *Pocket sociology for beginners* (*Džepna sociologija za početnike).* Novi Sad, Niš: Prometej, Mašinski fakultet, 2020.

[4] Šporer, Ž. 1990. *Sociology of the profession (Sociologija profesije)*. Zagreb: Sociološko društvo Hrvatske.

THE 5th INTERNATIONAL CONFERENCE
MECHANICAL ENGINEERING IN XXI CENTURY

December 9-10, 2020
Faculty of Mechanical Engineering in Niš, Serbia

Engineers' Perception of the Importance of English in Their Professional and Academic Careers

Miloš TASIĆ, Jelena DINIĆ, Dragoljub B. ĐORĐEVIĆ

First Author affiliation: Department of Social Sciences, Faculty of Mechanical Engineering, University of Niš, Aleksandra Medvedeva 14, 18000 Niš, Serbia
Second Author affiliation: Department of Social Sciences, Faculty of Mechanical Engineering, University of Niš, Aleksandra Medvedeva 14, 18000 Niš, Serbia
Third Author affiliation: Department of Social Sciences, Faculty of Mechanical Engineering, University of Niš, Aleksandra Medvedeva 14, 18000 Niš, Serbia
milos.tasic@masfak.ni.ac.rs, jelena.dinic@masfak.ni.ac.rs, dragoljub.djordjevic@masfak.ni.ac.rs

***Abstract*— As the modern-day lingua franca, English plays a crucial role in all sorts of global communication and correspondence. This is also true of the engineering profession and its current reliance on English as its main vehicle for the exchange of information. Therefore, the adequate knowledge of English poses one of the major challenges in the development of an engineer's professional identity. Bearing this in mind, the paper deals with the engineers' own perception of the importance of English in their professional and academic careers, with a particular emphasis on the potential shortcomings caused by the lack of both oral and written communicative competence and the ways in which such drawbacks could be overcome with the aim of facilitating their further career advancement. The conducted study employs a survey based on a questionnaire used to examine the positive and negative consequences of varying levels of knowledge of English from the viewpoint of engineers. The results obtained through statistical analysis reflect their opinions on the most important aspects of the matter at hand. The paper ends with concluding remarks that contain several recommendations on how the observed issues can be tackled successfully.**

***Keywords*— Engineering Profession, Professional Identity, English as a Lingua Franca, English for Specific Academic Purposes, Communicative Competence**

I. Introduction

There is no doubt that English has become the *lingua franca* of the modern world, and that today it is used worldwide on an unprecedented scale. It is by far the first language of global communication and correspondence, regardless of the area of life in which such exchanges take place. Even though there are six official languages of the UN (Arabic, Chinese, English, French, Russian and Spanish [1]), the role and importance of English in today's globalized world cannot be overstated, which is further reflected in the fact that it is the only language in the world whose number of non-native speakers exceeds the number of native speakers [2], and one can also claim that its status is rapidly changing from that of the foreign language to the one of the second language [3]. All of this is evident in the international engineering community as well, where English has managed to succeed, both globally and locally, even those foreign languages that used to traditionally serve as the means of communication between engineers from different countries (as was the case with German in Serbia, for example). Thanks primarily to the outcome of World War II [4] and the ensuing dominance of the United States "at the cutting edge of technical progress and scientific research" [5], English became the international language of technology and commerce, and has meanwhile grown to the position where it is almost impossible for modern engineers to pursue their careers successfully without possessing a satisfactory level of knowledge of English.

With all this in mind, the main aim of this paper is to direct the attention to the way in which engineers themselves perceive the importance of English in their professional and academic careers, and see whether there is a consensus on the role that this foreign language plays in their lives today. The present study involves a survey based on the questionnaire used to analyse the positive and negative aspects of varying levels of knowledge of English. The questionnaire was distributed online among the teaching staff at the Faculty of Mechanical Engineering, University of Niš, which in this case comprised only the Faculty members who have completed their graduate and postgraduate studies in different engineering disciplines (predominantly mechanical engineering with only a few exceptions). The other non-engineering staff was excluded from the analysis.

The paper is structured as follows. Section 2 will provide a concise theoretical framework, mainly concentrated on the role of English as the new lingua franca and its implications on the international engineering community and engineers' professional identity. Section 3 will present the methodological aspects of the conducted study, while Section 4 will contain the most relevant results of the analysis of the respondents' replies, including a discussion of the most significant findings. Finally, Section 5 ends the paper with concluding remarks that will focus on certain recommendations for the improvement of the current situation, both from the engineers' and the authors' standpoint.

II. English as a lingua franca in the modern engineering profession

It has been well-documented that English has become the new lingua franca (see, for example: [6], [7], [8], [9], [10], [11]), and given that its influence on the globalized world is such that it permeates every aspect of modern life, it is no surprise that it plays a significant role in the engineering community as well. The emphasis in this study is on the academic part of that community and the primary task here is to show what the main areas are in which English dominates the communication. The role of English in the academic engineering community is manifold, yet it can be divided into two major categories, which are oral and written communication [12]. As far as the former is concerned, apart from job interviews and working in multicultural environments, English is also used in oral communication to participate in scientific and professional conferences, workshops and meetings, and this use is not merely limited to foreign countries. The vast majority of these gatherings in one's own country are nowadays, at least partly, organized with English as the official language, and Serbia is no exception to this. Moreover, the level at which the academic engineering community functions requires a substantial knowledge of English among engineers, usually not restricted to the specific purposes of this community but calling for a more comprehensive command of the language in general. Being unable to present one's research results in person, for example, is one of the more serious drawbacks of an insufficient level of knowledge of English. As it will later be shown in the analysis, the respondents agree with this to a high extent.

The other major category of the use of English. i.e. written communication, is perhaps more important for engineers who are not native speakers of English, and even more so for engineers who pursue their careers in academia. It appears that the well-known maxim "publish or perish" has never been more dependent on a single language than it is today in the academic engineering community. Being able to follow state-of-the-art research in scientific literature, on the one hand, and having the capacity to prepare and publish one's own results without the help of translators, on the other, constitute two of the most important uses of written English. This is, indeed, the area in which those who do not possess a proper knowledge of the language encounter the majority of problems in their academic careers related to English, and not only when trying to present their work abroad. All of the Serbian scientific and professional journals that fall under the criteria necessary when being elected to a higher academic rank are exclusively published in English, meaning that even in their own country, Serbian engineers with an insufficient level of knowledge of English need to look elsewhere for help so as to be able to make their research publishable. In addition, all other sorts of correspondence (official letters, contracts, invoices, cooperation with foreign colleagues) rest firmly on the supporting structure provided by English, and it is not hard to imagine what a proper knowledge of English can do for an engineer's career.

Furthermore, English is today one of the main driving forces behind the development of an engineer's professional identity [13]. What this means is that the knowledge of English now occupies such an important part in engineers' academic career, especially when it comes to non-native speakers, that its significance in the creation of the professional identity of engineering students who later become professional engineers cannot really be overemphasized. If professional engineering identity is observed as a relationship between an individual and a specific professional group, which includes both knowledge and skills gained during professional education and attitudes and self-beliefs that an engineer employs in their professional life [14], it becomes clear that without an adequate knowledge of English, one cannot function as a proper member of the international engineering community. In order to improve their professional and academic competence and acumen, engineers simply need to continuously work on their knowledge of English, as one of the major assets for a successful professional and academic career in their field. In what follows, the engineers' own perspective on the above issues reconstructed from their replies to the conducted survey will be presented and analysed in detail.

III. Research methodology

As mentioned above, this quantitative study explores the positive and negative aspects of varying levels of knowledge of English from the viewpoint of engineers employed as the teaching and research staff at the Faculty of Mechanical Engineering, University of Niš. Thus the study represents an attempt to obtain a more comprehensive picture of the engineers' perception of the importance of English in their professional and academic careers, along with their personal attitudes towards the matter at hand. As there are no similar studies, to the best of the authors' knowledge, related to the target population of engineers examined in this paper, it is fair to say that the conducted research is primarily of the descriptive and exploratory type. The study itself is based on the survey carried out online in September 2020, to which the respondents employed at the Faculty of Mechanical Engineering in Niš replied by filling out a questionnaire. The main idea behind this exploratory study was for it to serve as the foundation for identifying basic tendencies that would later be used to expand this research to other members of the Serbian academia.

A. Instrument

A survey questionnaire was developed to investigate the engineers' opinions on the necessity of possessing adequate English language knowledge and skills, their satisfaction with their own knowledge, as well as the main issues they encounter as consequences of the lack thereof. The instrument contained forty questions, some of which branched into several sub-questions asked depending on the discriminative answer. The questions were predominantly of the closed type, including a set of six-level Likert type items, but also two open-type questions. The response rate was over 85%, which is more than desirable in social sciences and humanities.

B. Sample

To reiterate, the target respondents for this study were engineers employed at the Faculty of Mechanical Engineering, University of Niš, and the subsequent analysis will be based on primary data obtained via a predictive, non-experimental research design. The

respondents participated voluntarily by completing an online life survey. Opportunity sampling was used as the method of selecting respondents, whose average age was 44.3 years, with a 10-year deviation. Out of the 53 participants, 40 were male and 13 were female, with 77.4% of them married with 2.2 children on average. The gender distribution is evidently highly uneven, thus the indications obtained in the study apply more to the male than the female population of engineers. Furthermore, most of the participants come from the urban areas (71.1%). Although the place of origin can act as a moderating variable, the size of the sample was too small to analyse the influence this variable might have had in relation to the engineers' satisfaction with their knowledge of English, the frequency of use and the assessment of the importance of the language in their professional and academic careers. Due to these sample constraints, the relations between different areas remained relatively uncorrelated. However, some connections were established using Pearson's *r* and an independent-samples t-test, as will be seen in the next section.

IV. Results and discussion

The vast majority of the respondents are affiliated with the Faculty of Mechanical Engineering in Niš (over 95%), with only two respondents coming from other institutions and teaching part-time at the faculty. Even though the respondents were targeted by affiliation, due to the engineering background of the latter two participants, they were also included in the final analysis. The division by academic rank is as follows: 12 full professors, 13 associate professors, 16 assistant professors, 6 teaching or research assistants and 6 junior teaching or research assistants, comprising a fairly equally distributed sample across this variable.

The first of the six-level Likert type items dealt with the importance of knowing foreign languages in the engineering profession and the response was overwhelmingly in favour of their importance with the mean value of 5.77 (SD=0.42) and no replies below five on the six-level scale ranging from 1 – not important to 6 – extremely important. The result was exactly the same when it came to the importance of English in the engineering profession (M=5.77, SD=0.42), with 75.5% of the respondents claiming that it is by far the most important foreign language in their academic careers, while 79.2% said that it is also important to know another foreign language apart from English. Only 42 respondents answered the following sub-question and 85.7% of them said that German is the second most important foreign language for their profession. All of this shows that the respondents are highly aware of the role that both English and other foreign languages play in the professional engineering community today. As for their satisfaction with the EFL and ESP courses attended in their primary, secondary and tertiary education, the participants' replies amounted to the mean values of 4.19 (SD=1.23) for primary and secondary education, 3.68 (SD=1.52) for tertiary education, and 4.53 (SD=1.11) for private classes, again on a six-level scale, showing a significant drop in the satisfaction with ESP courses compared particularly with private English lessons.

When it came to different uses of English in their careers, 94.3% of the respondents said that it is crucial to both possess general English skills and display adequate mastery of engineering terminology. In their opinion, participating in conferences is the most important area of English use (M=5.32, SD=1.05), followed by academic writing (M=5.23, SD=1.05), and lastly correspondence with foreign colleagues (M=5.23, SD=1.09). However, the results were somewhat skewed when the respondents were asked to report on their personal experiences, saying that they most often use English to write scientific papers (M=4.55, SD=1.10), cooperate with their foreign colleagues (M=4.13, SD=1.43), and participate in conferences (M=4.00, SD=1.33), with other types of communication occupying the second place (M=4.17, SD=1.33). A combined 88.7% of the respondents believe that their knowledge of English has influenced their careers (60.4% positively, 28.3% negatively), with 43.4% claiming that they do not encounter any issues as a consequence of their lack of knowledge (18.9% have problems with publishing their work, the same percentage goes for obstacles in international correspondence, while 13.2% experience difficulties in participating in conferences). About half of the respondents (49.1%) sometimes ask other colleagues or translators for help (with 26.4% doing that often and 24.5% almost never), and this help is most frequently (64.2%) needed for writing scientific papers.

The following three tables will now show the connections established using Pearson's *r* and an independent-samples t-test.

TABLE 1 The relation between age and the perception of different aspects of English (Pearson's *r*)

	Age
Knowledge self-assessment	-0.379**
Knowledge satisfaction	-0.290*
Importance of languages	-0.241
Importance of English	-0.090
Frequency of use	-0.282*

**. Correlation is significant at the 0.01 level (2-tailed).
*. Correlation is significant at the 0.05 level (2-tailed).

As can be seen in Table 1, the age variable showed a significant and negative relation with the self-assessment of the knowledge of English (r=-0.379, p<0.01), the satisfaction with said knowledge (r=-0.290, p<0.05), and the frequency of use of English (r=-0.282, p<0.05). However, the proportion of age that is explained by each of these variables is relatively small, and these factors are responsible for only around 3% each. This is likely a consequence of the sample size and its specificities. These variables were also used in conducting an independent-samples t-test to compare the replies of the respondents who have travelled abroad for academic purposes and those who have not. Due to formatting restrictions, the results of the t-test are presented in two tables:

TABLE 2.1 Descriptives comparing those who have been on academic visits abroad and those who have not

	Yes (33)		**No (20)**	
	M	**SD**	**M**	**SD**
Knowledge self-assessment	4.36	1.32	3.50	1.39
Knowledge satisfaction	4.52	1.03	3.45	1.36
Importance of languages	5.85	0.36	5.65	0.49
Importance of English	5.82	0.39	5.70	0.47
Frequency of use	4.76	1.06	4.35	1.23

TABLE 2.2 *T-TEST* RESULTS COMPARING THOSE WHO HAVE BEEN ON ACADEMIC VISITS ABROAD AND THOSE WHO HAVE NOT

	t	df	p
Knowledge self-assessment	-2.261	51.0	*0.028*
Knowledge satisfaction	-3.227	51.0	*0.002*
Importance of languages	-1.570	31.7	0.126
Importance of English	-0.943	34.6	0.352
Frequency of use	-1.278	51.0	0.207

Significant differences were found in the English knowledge self-assessment, t(51)=-2.261, p=0.028, and the level of satisfaction with that knowledge, t(51)=-3.227, p=0.002. These results indicate that the engineers who have travelled abroad assess their English level knowledge at a higher level and are more satisfied with it than their colleagues who have not been on academic visits to foreign countries before. The other three analysed variables yielded no significant differences.

The last batch of questions dealt with the influence of English in the engineers' everyday life (60.4% confirming that it also affects their personal lives), the need for a satisfactory knowledge of English in the academic world (92.5% saying that this need is only going to increase) and, most importantly, their plans concerning the improvement of their current level of knowledge. Only 15.1% of the respondents believe that they do not need to work further on their English, while 28.3% are planning to start studying as soon as possible and 56.6% are willing to but do not have time for it at the moment. The vast majority of the respondents (96.2%) would like to see some form of English language teaching organized for the members of the teaching and research staff at the faculty, with two thirds claiming that they would attend such classes. Even though the respondents' suggestions concerning the ways in which these classes could be organized vary significantly, a general consensus could still be reached and it shows that they should be conversation-oriented, held in smaller groups comprising learners who are at a similar level, taught preferably online and two or three times a week after work, with a particular focus on specific engineering terminology and business correspondence.

V. CONCLUDING REMARKS

Bearing in mind that a small sample can cause problems in statistical inference, and that its low precision can easily lead to false conclusions, it is important to note that all the above estimates are to be taken carefully and that they are representative only of the affiliation involved. From this study, it can be observed that the English proficiency of the respondents is not generally on the personally desirable level, however, they are also fully aware of the role of English as one of the most important assets in their professional and academic careers. The results of this study clearly indicate the willingness among the engineers employed at the Faculty of Mechanical Engineering in Niš to improve and further develop their general English skills, on the one hand, and to continue addressing the specific academic purposes put forward by their profession, on the other. What is particularly noteworthy here is their perception of the importance of potential English courses that could be organized for the academic personnel at the faculty, with a special emphasis on the respondents' suggestions on the content of such classes and manner in which they could be held. Therefore, the main recommendation of this study follows the opinion expressed by the respondents, believing that properly designed ESP courses for engineers will certainly facilitate their further career advancement, encourage their broader participation in the international engineering community, and eventually lead to a better visibility of their affiliation as a whole. The results presented here, albeit cautiously, provide a solid basis for further research that would include other members of the Serbian academic community.

ACKNOWLEDGMENT

This research was financially supported by the Ministry of Education, Science and Technological Development of the Republic of Serbia.

REFERENCES

[1] United Nations Official Languages. Found at https://www.un.org/en/sections/about-un/official-languages/index.html (accessed on November 3, 2020).

[2] A. Firth, "The discursive accomplishment of normality: On 'lingua franca' English and conversation analysis," *Journal of Pragmatics*, *26*(2), 1996, pp. 237–259.

[3] M.J. Riemer, "English and communication skills for the global engineer," *Global Journal of Engineering Education*, *6*(1), 2002, pp. 91–100.

[4] T. Hutchinson and A. Waters, *English for specific purposes*. Cambridge: Cambridge University Press, 2000.

[5] J. Walters, "Why is English the international lingua franca?" *TranslationDirectory.Com*, 2002. Found at https://www.translationdirectory.com/article171.htm (accessed on November 3, 2020).

[6] D. Crystal, *English as a Global Language*. Cambridge: Cambridge University Press, 1997.

[7] J. Jenkins, "English as a *lingua franca*: interpretations and attitudes." *World Englishes*, *28*(2), 2009, 200–207.

[8] I. MacKenzie, *English as a lingua franca: Theorizing and teaching English*. London: Routledge, 2013.

[9] A. Mauranen, "The corpus of English as *lingua franca* in academic settings." *TESOL Quarterly*, *37*(3), 2003, 513–527.

[10] A. Mauranen and E. Ranta (eds.), *English as a Lingua Franca: Studies and findings*. Newcastle upon Tyne: Cambridge Scholars Publishing, 2009.

[11] B. Seidlhofer, *Understanding English as a Lingua Franca*. Oxford: Oxford University Press, 2011.

[12] M. Tasić and D. Stamenković, "The role of English in the modern engineering profession," *Proceedings of the 2nd International Conference Mechanical Engineering in XXI Century*, pp. 365–368. Niš: Faculty of Mechanical Engineering, 2013.

[13] M. Tasić, "Language and professional identity in an engineering community," in V. Lopičić & B. Mišić Ilić (Eds.), *Identity issues: Literary and linguistic landscapes*, pp. 275–284. Newcastle upon Tyne: Cambridge Scholars Publishing, 2010.

[14] L. Mann, P. Howard, F. Nouwens and F. Martin, "Professional identity: A framework for research in engineering education," *Proceedings of the 2008 AaeE Conference*, pp. 1–6. Yeppoon, 2008.

THE 5th INTERNATIONAL CONFERENCE
MECHANICAL ENGINEERING IN XXI CENTURY

December 9-10, 2020
Faculty of Mechanical Engineering in Niš, Serbia

Mathematics for Human Flourishing in the Time of COVID-19 and Post COVID-19

Mahouton NORBERT HOUNKONNOU[1], Melanija MITROVIĆ[1]

[1] International Chair in Mathematical Physics and Applications (ICMPA-UNESCO chair, University of Abomey-Calavi, Benin,
[2] Department of Mathematics and Informatics, Faculty of Mechanical Engineering Niš, Serbia
norbert.hounkonnou@cipma.uac.bj, melanija.mitrovic@masfak.ni.ac.rs

"So if you asked me: why do mathematics? I would say: mathematics helps people flourish. Mathematics is for human flourishing. Because we are not mathematical machines. We live, we breathe, we feel, we bleed. Why should anyone care about mathematics if it doesn't connect deeply to some human desire: to play, seek truth, pursue beauty, fight for justice? You can be that connection." ([5])

***Abstract*—The International Chair in Mathematical Physics and Applications (ICMPA-UNESCO chair), University of Abomey-Calavi, Benin, and the Center for Applied Mathematics of the Faculty of Mechanical Engineering Niš, CAM-FMEN, organized a webinar on Mathematics for human flourishing in the time of COVID-19 and post COVID-19, 21 October 2020, supported by the City of Niš. The scientific response to COVID-19 is multi-disciplinary, involving health sciences, social sciences, and fundamental sciences such as mathematics. The objectives of the webinar were to give precise information about the work that scientists do to cure the disease, to push forward technology, to understand our society and create new expressions of humanity, and to question the role of mathematics in the responses to this pandemic.**

***Keywords*— COVID-19, Mathematics, Modelling, Pandemic**

I. Introduction

A new coronavirus known under the acronym of SARS-CoV-2 suddenly appeared in a very distant Chinese city, Wuhan, in December 2019, and created a global cataclysm, paralyzing economic and social life in 177 countries and inducing a health catastrophe. More than 4 billion people were confined, or roughly half of the world's population, 5 million were sick at the end of May, and there were nearly 350,000 deaths.

Historically, the bacterial unification of the globe has been taking place since the conquest of the Americas, but COVID-19 is at the origin of a multi-aspect complex mega-crisis, combining political, economic, social, ecological, national, planetary crises with diverse interactions and multiple unknowns and mutually dependent variables, making things strongly linked and unseparable.

The whole world lives in indescribable pain and chaos. Uncertainties have seized our life, time and space, beliefs and thoughts, where only a tiny and virulent monster dictates its law, shaking all the established structures and mentalities.

Science has been shaken in its deepest compartments. The pandemic confirms that science is not a repertoire of absolute truths (unlike religion). Theories are biodegradable under the influence of new discoveries. It is that controversies, far from being anomalies, are necessary for the progress of science. However, the virulence of the controversy and the ad hominem attacks transcend scientific controversy and show that powerful personal or financial interests are at stake.

Scientific progress is generally produced by both competition and cooperation. But the **cooperation** can deteriorate into competition, as in research for treatment or vaccine, to the detriment of cooperation, which would speed up elimination of the virus.

COVID-19 has intensified and exaggerated fault lines in contemporary societies revealing back to us our ways of dealing with inequality, said Julian Sefton-Green in the UNESCO Futures of Education Ideas LAB.

The post-coronavirus is just as worrying as the crisis itself. It could be as apocalyptic as it is hopeful. The world of tomorrow will certainly no longer be that of yesterday. But what will it be? Will COVID-19 and its critical consequences and multifarious crisis lead to the dislocation of our societies? Will we be able to learn the lessons of this pandemic, which has revealed a community of destiny to all humans, in connection with the bio-ecological fate of the planet?

What attitude can we expect from science in general, and from mathematics in particular?

We have entered the era of uncertainties and chaos. We now understand better that the hyper-specialization which leads to the compartmentalization of specialized knowledge is harmful to medicine and to systemic science which brings together the contributions of separate disciplines, in an overall conception, where the spirit is no longer separated from the body, the person is no longer separated from their living environment, enriched by some useful non-academic knowledge, neglected for some abject reasons.

The goals of the webinar were clearly defined. COVID-19 has fundamentally affected our lives. We face this unprecedented challenge. Overcoming COVID-19 and its consequences is impossible without science and scientific work. The scientific response to COVID-19 is multi-disciplinary, involving health sciences, social sciences, and fundamental sciences such as mathematics. The objectives of the webinar were to give precise information about the work that scientists do to cure the disease, to push forward technology, to understand our society and create new expressions of humanity, and to question the role of mathematics in the responses to this pandemic. It is our way to make sciences converse with each other. Without such mutual interactions, we cannot find adequate solutions to the global challenges we face. This is the conviction of prominent experts from four continents (Africa, Asia, Europe, America) who attended this international multidisciplinary webinar.

II. "IS A MATHEMATICS A MODEL, A DESCRIPTION, A METAPHOR FOR REALITY ... OR IS IT REALITY ITSELF? "

Mathematics is "a vast discipline that has been evolving over millennia—there are still vast 'here be dragons' areas on the map", [8]. Even before COVID-19, the external world, with its social problems, technological advances and new scientific areas significantly influences the course of mathematical scientific-research activities.

To paraphrase Mark Turner from the beginning of his book [6]: We, mathematicians, we did not make galaxies. We did not make life. We did not make viruses, the sun, DNA, or the chemical bond. But we do make new ideas—lots and lots of them. But where exactly do new ideas come from? Maybe from our scientific advanced ability to blend ideas to make new ideas, to blend existing knowledge coming from different scientific areas to make new one?

The great German mathematician Carl Friedrich Gauss (1777-1855) pronounced mathematics to be the queen of the sciences. On the other hand, as it is pointed out in [3], "mathematics may well be the queen of the sciences, but she would seem to be an eccentric and obstinate queen". In fact, further following [3], mathematics occupies a unique and privileged position in human inquiry. When we talk about the development of contemporary mathematics, it is generally considered unnatural and counterproductive to draw the line between theory and application.

What is mathematics anyway? We all agree – the origin of the word is Greek, and freely translated it means learning, studying, knowledge. There is no uniqueness about deciding whether mathematics is a science or an art. There is no single definition of mathematics. For some, mathematics is the "language of science", for others it is just "a game of symbols and rules of variables on them", or, simply, mathematics is what mathematicians do.

And mathematicians deal with mathematical structures. A ***mathematical structure*** is a set together with some other sets, relations, functions and operations. Mathematics came to these mathematical structures by abstracting the knowledge derived from counting, measuring and systematically studying the shapes, movements and changes of physical objects. Following [7] "The miracle of the appropriateness of the language of mathematics for the formulation of the laws of physics is a wonderful gift which we neither understand nor deserve".

This webinar was addressed to mathematicians, physicists, biologists, chemists, engineers, medical doctors, social scientists, computer scientists, and anybody interested in explaining the question of how mathematics works and why it works so well in **modeling** (what we perceive as) **the world around us**.

Following definitions taken from [2], ***mathematical models*** mimic reality by using the language of mathematics. What makes a mathematical model useful?

1. Ideas must be formulated precisely;
2. We have a concise "language" which encourages manipulation;
3. We have a large number of potentially useful theorems availble;
4. We have higher speed computers available for carrying our calculation.

The history of mathematical modeling is long and dates back to prehistory. An important example of the effectiveness of mathematics in modeling (and changing) the world around us, taken from the recent history, is Apollo 11 landing on the moon on 20 July 1969. Katherine G. Johnson, a mathematician, one of the first African-American women to work as a NASA scientist, and her calculations connected to the trajectory of this historic space flight, mostly done by hand, were critical to the success of the mission. On the other hand, the seven Serbian scientists, engineers, and management executives – affectionately known as the "Serbo 7" – significantly contributed to the development of the Apollo Space Program. Milojko Vučelić, a member of "Serbo 7", was one of the directors of the US Space Program Apollo in the period from 1966 to 1978. Inspired by this historic example, we came up with the idea to organize this webinar to provide the scientific community with the results of the work by African and Serbian scientists, as well as their eminent guests, related to the problems caused by the appearance of COVID-19 and the ways in which they can be overcome.

As it is pointed out in [4], "mathematical models relating to the spread of an epidemic, management of statistical information on the number of infected people, vaccine research, preventive measures, economic measures... it quite quickly became apparent that we could not separate these different actions if we wanted to effectively combat the pandemic. This has resulted in what we call a *'complex system'*, [...] To understand a crisis like the current COVID-19 pandemic, the approach using the methods and tools of complex systems is an integrated way to tackle questions, which we cannot avoid and which does not bypass disciplines".

The webinar, [1], was unwound in two main sections as follows.

SECTION I – General Introductionary Part of the webinar provides us information about the following topics:

- **Response to the COVID-19 pandemic: Lessons from science academies in Africa** – the lecture given by *Jacqueline Kado*, Network of African Science Academies (NASAC).
- **COVID-19 and intensive medical cares** – on the behalf of the Special Covid-19 crisis group of Benin

National Academy of Sciences, Arts and Letters, Benin, lecture given by academician *Martin Chobli*.

- **Knowledge status and potential impact of socio-economic factors on the spreading of COVID-19 in West African countries** - the lecture given by *Victorien Dougnon* on the behalf of the rest of the authors Esther Deguenon, Jean-Pierre Gnimatin, Mathieu Hounkpatin, Phénix Assogba, Lamine Baba-Moussa, Jacques Dougnon, all coming from the University of Abomey-Calavi, Benin.
- **Digital contact tracing in Belgium** - the lecture given by *Axel Legay*, Université Catholique de Louvain, Belgium.
- **Artificial intelligence and digital technologies in digitally-supported university education** - the lecture given by *Nataša Milosavljević* on the behalf of the rest of the authors Vladimir Pavlović, Vera Pavlović, Branislav Vlahović, Faculty of Agriculture and Faculty of Mechanical Engineering, University of Belgrade, Serbia, and North Carolina Central University, USA.
- **Cross-cultural social influence of Covid-19 pan(info)demi** - the lecture given by *Miloš Milovančević*, Faculty of Mechanical Engineering Niš, Serbia.

We are "convinced that mathematics must be involved, with other disciplines, in systems to study and understand complex phenomena which make up the world today, and in which it is already involved [...] The power of mathematics largely stems from its generic nature, which is necessary to navigate the various concepts. [...] Mathematics is at the heart of the action, as it often structures *simulation models* which will be used en masse to assess the 'efficacy' of an innovation... ", [4]. Besides the language of mathematics and its significance to mathematical practice, the limits of mathematics, the subject matter of mathematics, the relationship between mathematics and the rest of sciences are some of the important topics which are considered during

SECTION II - Mathematics and Responses to COVID-19

Besides the already cited presentation of *Bertrand Jouve*, LISST – CNRS, Université Toulouse Jean Jaurès, Toulouse, France, [4], the list of presented topics and participants follows.

- **Normal science and the hidden lemmas of mathematical epidemiology** - the lecture given by *Hernán G. Solari*,University of Buenos Aires, Argentina.
- **In silico clinical trials for heart disease** - the lecture given by *Nenad Filipović* on behalf of the rest of the authors Igor Saveljić, Miljan Milošević, Vladimir Geroski, Bogdan Milićević, Vladimir Simić, Miloš Kojić, Faculty of Engineering, BioIRC Bioengineering Research and Development Center, University of Kragujevac, Serbia, Methodist Hospital, Houston, USA.
- **Dynamics of COVID-19 pandemic: control problem and equilibrium stability characterization** - the lecture given by *Villévo Adanhounmè*, done jointly with Mahouton Norbert Hounkonnou, University of Abomey-Calavi, Benin.
- **Modeling COVID-19 dynamics in the sixteen West African countries** - the lecture given by *Romain Glèlè Kakaï*, done jointly with Mahouton Norbert Hounkonnou, University of Abomey-Calavi, Benin.
- **The influence of passenger air traffic on the spread of COVID-19 in the world** - the lecture given by *Mintodê Nicodème Atchadé*, done jointly with Yves Morel Sokadjo, University of Abomey-Calavi and National Higher School of Mathematics Genius and Modelization, National University of Sciences, Technologies, Engineering and Mathematics, Abomey, Benin.
- **Rules of thumb for test results** - the lecture given by *Zvonimir Šikić*, University of Zagreb, Croatia.
- **Privacy-preserving contact tracing** - the lecture given by *Silvia Ghilezan*, with co-author Tamara Stefanović, Mathematical Institute of the Serbian Academy of Sciences and Arts, Belgrade, University of Novi Sad, Serbia.
- **On blockchain technology and some applications** - the lecture given by *Miodrag J. Mihaljević*, Mathematical Institute of the Serbian Academy of Sciences and Arts, Belgrade, Serbia.
- **A new class of non-associative algebras with genetic realizations** - the lecture given by *Madad Khan*, Department of Mathematics, COMSATS Institute of Information Technology, Abbottabad, Pakistan.

Presented works give evidence that mathematics is productively applied in engineering, medicine, chemistry, biology, physics, social sciences, communication, computer science, ... On the other hand, "it is the most rigorous and certain of all of the sciences, and it plays a key role in most, if not all, scientific work ", [3].

It is, also, important to note that "only systems which the human is able to understand and therefore control would survive long-term", [4].

According to Paul R. Halmos, "Mathematics is security, certainty, truth, beauty, insight, structure, architecture. I see mathematics, the part of human knowledge that I call mathematics, as one thing-one great, glorious thing."

III. Conclusions

From many points of view, the webinar *Mathematics for human flourishing in the time of COVID-19 and post COVID-19* was successful. Let us mention a few of its results which can be pointed out:

1. Overcoming COVID-19 and its consequences is impossible without science and scientific work. Therefore, it is necessary and compulsory to make the voice of science heard and share it by all stakeholders. The science response to COVID-19 is multi-disciplinary, involving health sciences, social sciences and fundamental sciences like mathematics as well.
2. Mathematics underlies technology and science that we use every day, and there is and will continue to be a need for mathematically able people in lots of professions besides the ones mentioned above.
3. Mathematicians must collaborate across mathematical fields as well as across the borders between sciences; they must build a bridge with physics, biology, chemistry and increasingly also social sciences and humanities.
4. A continuum between theoretical and applied mathematics should be ensured.
5. Mathematicians need training, incitation and incentives, and the creation of interdisciplinary and inter-mathematical teams to stimulate new ways of collaborating.

6. Mathematics should not only focus on today's applications but should leave room for development, even theoretical, that may well be vital tomorrow.

At the very end of this report, let us say something about mathematicians themselves. Who are they? Are they "devices for turning coffee into theorems" as Paul Erdős joked? Or, to be a little bit more serious and follow Paul R. Halmos? "What does it take to be [a mathematician]? I think I know the answer: you have to be born right, you must continually strive to become perfect, you must love mathematics more than anything else, you must work at it hard and without stop, and you must never give up."

REFERENCES
(USE STYLE MASING HEADING 4)

[1] Mathematics for human flourishing in the time of COVID-19 and post COVID-19, Abstract booklet, ISBN: 978-99982-0-614-4, Dépôt légal N°12587 du 12-11-2020 4ème trimestre, Bibliothèque Nationale du Bénin.

[2] E. A. Bender, An Introduction to Mathematical Modeling, Johan Willy, 1978, 2000.

[3] Mark Colyvan, An Introduction to the Philosophy of Mathematics, Cambridge University Press, Cambridge, 2012.

[4] B. Jouve, "Mathematics, the pandemic and complex systems", Webinar Mathematics for Human flourishing in the time of Covid-19 and post Covid-19, 21 of October 2020.

[5] F. Su with reflection by C. Jackson, Mathematics for human flourishing, Yale University Press, New Haven and London, 2020.

[6] M. Turner, The Origin Of Ideas: Blending, Creativity And The Human Spark. Oxford & New York: Oxford University Press, 2014.

[7] E. Wigner, "The Unreasonable Effectiveness of Mathematics in the Natural Sciences", Communications in Pure and Applied Mathematics, Issue 13(I), 1–14, 1960.

[8] J. Woźny, How we understand mathematics - Conceptual Integration in the Language of Mathematical Description, Springer, 2018.

.

Engineering management

THE 5th INTERNATIONAL CONFERENCE
MECHANICAL ENGINEERING IN XXI CENTURY

December 9-10, 2020
Faculty of Mechanical Engineering in Niš, Serbia

Determination of the Optimal Parameters of the Wastewater Systems Based on the Largest Economic Profit

Biljana PETKOVIĆ [1], Dalibor PETKOVIĆ [2] Ivan RADOJKOVIĆ[3] Milos MILOVANCEVIC[4]

[1]Alfa BK University - Faculty of Finance, Banking and Auditing, Belgrade, Serbia
[2] University of Niš, Pedagogical Faculty in Vranje, Partizanska 14, 17500 Vranje, Serbia
[3] Dunav Voluntary Pension Fund, Serbia
[4] University of Niš, Faculty of mechanical engineering, A. Medvedeva 14, Nis, Serbia

***Abstract*— In this article was presented a selection procedure for determination of the most influential parameters of wastewater system for the best economic profit. Optimum wastewater treatment systems require large parameters to be settled in order to achieve optimal solutions. The optimal solutions are often based on the economic profit of the wastewater treatment system. The best economic profit is formulated according the lowest total cost of the wastewater treatment system. By using classical analytical approach for the optimization procedure there is need for time and effort in order to solve the equations since it is very nonlinear system. Therefore in this article the main aim was to determine which parameters of the wastewater treatment system have the largest influence on the economic profit of the system. For the selection purpose adaptive neuro fuzzy inference system (ANFIS) was used since the method is suitable for redundant and nonlinear data. Results revealed that the size of the system has the most influence on the economic profit. Furthermore obtained solutions could be of practical importance since one could select which solutions is the most suitable for particular wastewater treatment system.**

***Keywords*— wastewater; economic profit; optimal solution; ANFIS.**

I. Introduction

Wastewater treatment system is a complex system which has many parameters included in the wastewater process. In order to make large economic profit of the wastewater treatment system in rural areas there is need to determine optimal parameters which has the highest influence on the economic profit. On the other hand the selected parameters have largest impact on the total costs of the wastewater treatment system. The best economic profit could be formulated according the lowest total cost of the wastewater treatment system.

Selection of the optimum solution is the greatest importance to the economic criterion for wastewater treatment system [1]. Studies of sustainable development of wastewater systems require consideration of three sustainability pillars: environmental, social and economic [2]. Two different technological setups have been considered in article [3] for improving the wastewater treatment plant. These are used to construct four alternative wastewater reclamation scenarios. A sequential study for hydrogen and methane production with pollutants reduction from dairy industry wastewater (DIWW) was conducted using bacterial strain of Enterobacter aerogens and methanogenic bacteria of cow dung [4]. Thermo-economic evaluation of hybrid solar-conventional energy supply in a zero liquid discharge plant has been conducted in article [5]. Biogas production through anaerobic digestion of organic waste and manure can potentially reduce greenhouse gas emissions in several sectors such as the waste, transport, energy and agricultural sector greater incentives [6]. A wastewater metabolism input-output model has been developed in article [7] to achieve sustainable development through a novel perspective to depict the industrial wastewater flow among sectors. Nanofiltration membrane (NF) is one of the most important activities employed in wastewater treatment field [8]. Independent hydrogen production from petrochemical waste water containing mono-ethylene glycol (MEG) via anaerobic sequencing batch reactor (ASBR) was extensively assessed under psychrophilic conditions [9]. The high nutrient content of domestic wastewater can be efficiently recovered through specific technologies included in dedicated wastewater treatment plants (WWTPs) [10].

By using classical analytical approach for the optimization of the wastewater treatment system there is need for time and effort to solve the equations since it is very nonlinear system. In this article the main aim is to determine which parameters of the wastewater treatment system have the largest impact on the economic profit of the system. For the selection purpose adaptive neuro fuzzy inference system (ANFIS) [11-15] is used since the method is suitable for redundant and nonlinear data.

II. Methodology

A. Database of wastewater system

In order to apply ANFIS network there is need to prepare database with input/output data samples. Table 1 shows all inputs and output used in the study. The used inputs are size of the system, elongation factor or length

and width ratio of the system settlement, dispersion factor or ration of households' number and sewerage network length, vertical disposition uniformity of terrain, urban centre vicinity or distance between urban centre and settlement, settlements grouping or distance between near settlements and distance between treatment plant and settlement. As the output factor total construction costs of the wastewater system is used.

TABLE 1: INPUT AND OUTPUT PARAMETERS OF THE WASTEWATER SYSTEM

input 1: Size	input 2: Elongation	input 3: Dispersion	input 4: Uniformity	input 5: Vicinity	input 6: Grouping	input 7: Distance	output: Total costs
284.9	3	0.02	4.96	6.01	1.17	0.96	1039705.4

B. ANFIS methodology

ANFIS network has five layers as it shown in Figure 1. The main core of the ANFIS network is fuzzy inference system. Layer 1 receives the inputs and convert them in the fuzzy value by membership functions. In this study bell shaped membership function is used since the function has the highest capability for the regression of the nonlinear data.

Figure 1: ANFIS layers

Bell-shaped membership functios is defined as follows:

$$\mu(x) = bell(x; a_i, b_i, c_i) = \frac{1}{1+\left[\left(\frac{x-c_i}{a_i}\right)^2\right]^{b_i}} \quad (1)$$

where $\{a_i, b_i, c_i\}$ is the parameters set and x is input.

Second layer multiplies the fuzzy signals from the first layer and provides the firing strength of as rule. The third layer is the rule layers where all signals from the second layer are normalized. The fourht layer provides the inference of rules and all signals are converted in crisp values. The final layers sumarized the all signals and provied the output crisp value.

III. RESULTS

C. Accuracy indices

Performances of the proposed models are presented as root means square error (RMSE), Coefficient of determination (R^2) and Pearson coefficient (r) as follows:

1) RMSE

$$RMSE = \sqrt{\frac{\sum_{i=1}^{n}(P_i - O_i)^2}{n}}, \quad (2)$$

2) Pearson correlation coefficient (r)

$$r = \frac{n\left(\sum_{i=1}^{n} O_i \cdot P_i\right) - \left(\sum_{i=1}^{n} O_i\right)\cdot\left(\sum_{i=1}^{n} P_i\right)}{\sqrt{\left(n\sum_{i=1}^{n} O_i^2 - \left(\sum_{i=1}^{n} O_i\right)^2\right)\cdot\left(n\sum_{i=1}^{n} P_i^2 - \left(\sum_{i=1}^{n} P_i\right)^2\right)}} \quad (3)$$

3) Coefficient of determination (R^2)

$$R^2 = \frac{\left[\sum_{i=1}^{n}\left(O_i - \overline{O}_i\right)\cdot\left(P_i - \overline{P}_i\right)\right]^2}{\sum_{i=1}^{n}\left(O_i - \overline{O}_i\right)\cdot\sum_{i=1}^{n}\left(P_i - \overline{P}_i\right)} \quad (4)$$

where P_i and O_i are known as the experimental and forecast values, respectively, and n is the total number of dataset.

D. ANFIS results

Table 3 shows the prediction errors for the total costs or economic profit of the wastewater system for single, two and three input parameters. Training RMSE shows influence of the inputs for the wastewater total costs. Smaller training error more influence on the wastewater total costs. Checking RMSE is used for overfitting tracking between training and checking data. Here one can see there is small overfitting for two and three inputs combinations since checking errors do not track training errors very well. As can be seen for single input parameters influence in Figure 2(a) the input parameters system size has the smallest training error therefore largest influence on the total costs of the wastewater system. Figure 2(b) shows two parameters combinations and their corresponding training and checking errors for the total costs prediction of the wastewater system where combination of vicinity and distance has the smallest training error hence the largest impact on the economic profit of the wastewater system. Finally Figure 2(c) shows three input combinations where one can see that the parameter system size, dispersion and vicinity form the optimal combination of three parameters for the total costs prediction of the wastewater system. Tables 2-4 show the numerical training and checking errors for the all inputs combinations of the total costs prediction of the wastewater system where bolded values represent the optimal combinations.

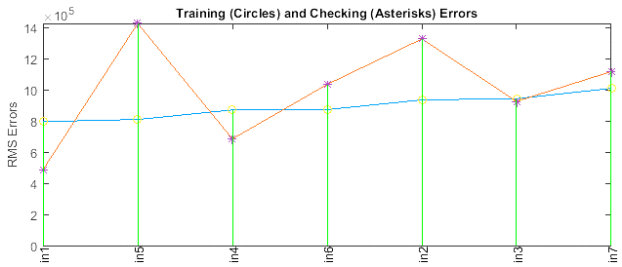

a)

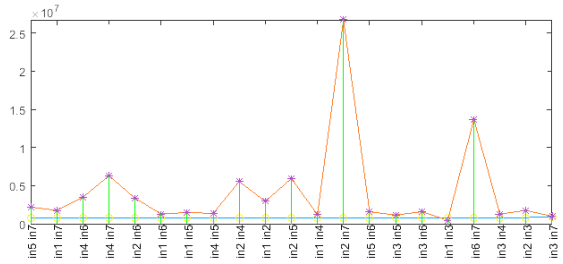

b)

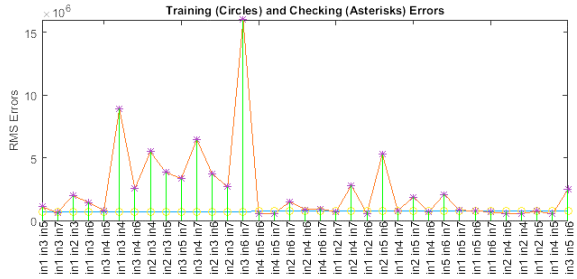

c)

Figure 2: Inputs' influence on the output: (a) single inputs, (b) two inputs, (c) three inputs

TABLE 2: SINGLE INPUT INFLUENCE ON THE OUTPUT

ANFIS model 1: in1 --> trn=795052.3800, chk=486121.6677

ANFIS model 2: in2 --> trn=934493.0105, chk=1325577.0070

ANFIS model 3: in3 --> trn=942358.2941, chk=924852.5804

ANFIS model 4: in4 --> trn=870057.7917, chk=684031.8942

ANFIS model 5: in5 --> trn=809001.7197, chk=1425160.2330

ANFIS model 6: in6 --> trn=872226.5836, chk=1033930.6644

ANFIS model 7: in7 --> trn=1008353.1837, chk=1116116.8827

TABLE 3: TWO INPUTS' INFLUENCE ON THE OUTPUT

ANFIS model 1: in1 in2 --> trn=724825.7907, chk=2931102.1642

ANFIS model 2: in1 in3 --> trn=774927.9722, chk=462781.9739

ANFIS model 3: in1 in4 --> trn=724825.9920, chk=1199555.0113

ANFIS model 4: in1 in5 --> trn=724825.7715, chk=1471737.5135

ANFIS model 5: in1 in6 --> trn=721190.5829, chk=1284921.6765

ANFIS model 6: in1 in7 --> trn=721190.0175, chk=1756868.7562

ANFIS model 7: in2 in3 --> trn=813386.0264, chk=1746867.8528

ANFIS model 8: in2 in4 --> trn=724825.7716, chk=5531286.3668

ANFIS model 9: in2 in5 --> trn=724825.8296, chk=5920287.0186

ANFIS model 10: in2 in6 --> trn=721190.1054, chk=3351655.9556

ANFIS model 11: in2 in7 --> trn=732752.1817, chk=26719811.3762

ANFIS model 12: in3 in4 --> trn=791683.6982, chk=1265159.0159

ANFIS model 13: in3 in5 --> trn=762214.7836, chk=1137596.5035

ANFIS model 14: in3 in6 --> trn=772622.1657, chk=1570964.2008

ANFIS model 15: in3 in7 --> trn=873703.5481, chk=975834.5975

ANFIS model 16: in4 in5 --> trn=724825.7715, chk=1362411.5779

ANFIS model 17: in4 in6 --> trn=721190.0175, chk=3462676.9435

ANFIS model 18: in4 in7 --> trn=721190.1050, chk=6293597.5250

ANFIS model 19: in5 in6 --> trn=756651.3649, chk=1562383.1620

ANFIS model 20: in5 in7 --> trn=721190.0066, chk=2184588.3894

ANFIS model 21: in6 in7 --> trn=788304.2828, chk=13688525.4462

TABLE 4: THREE INPUTS' INFLUENCE ON THE OUTPUT

ANFIS model 1: in1 in2 in3 --> trn=717062.3526, chk=1991830.1402

ANFIS model 2: in1 in2 in4 --> trn=724825.7715, chk=541577.8279

ANFIS model 3: in1 in2 in5 --> trn=724825.7719, chk=727232.1725

ANFIS model 4: in1 in2 in6 --> trn=721190.0012, chk=550695.9397

ANFIS model 5: in1 in2 in7 --> trn=721190.0012, chk=676052.4503

ANFIS model 6: in1 in3 in4 --> trn=717062.3621, chk=8919082.8974

ANFIS model 7: in1 in3 in5 --> trn=717062.3524, chk=1080947.4127

ANFIS model 8: in1 in3 in6 --> trn=717062.3528, chk=1437260.3746

ANFIS model 9: in1 in3 in7 --> trn=717062.3526, chk=642086.9245

ANFIS model 10: in1 in4 in5 --> trn=724825.7729, chk=515033.0225

ANFIS model 11: in1 in4 in6 --> trn=721190.0012, chk=673446.7701

ANFIS model 12: in1 in4 in7 --> trn=721190.0012, chk=774892.2500

ANFIS model 13: in1 in5 in6 --> trn=721190.0068, chk=780201.7730

ANFIS model 14: in1 in5 in7 --> trn=721190.0028, chk=799408.8123

ANFIS model 15: in1 in6 in7 --> trn=721190.0161, chk=667044.1730

ANFIS model 16: in2 in3 in4 --> trn=717062.3679, chk=5470009.1720

ANFIS model 17: in2 in3 in5 --> trn=717062.3735, chk=3823271.6177

ANFIS model 18: in2 in3 in6 --> trn=717062.5549, chk=3718324.6971

ANFIS model 19: in2 in3 in7 --> trn=717063.6139, chk=2667008.2019

ANFIS model 20: in2 in4 in5 --> trn=724825.7714, chk=563687.6772

ANFIS model 21: in2 in4 in6 --> trn=721190.0012, chk=861955.0153

ANFIS model 22: in2 in4 in7 --> trn=721190.0012, chk=2797595.2049

ANFIS model 23: in2 in5 in6 --> trn=721190.0012, chk=5292965.2192

ANFIS model 24: in2 in5 in7 --> trn=721190.0012, chk=1869850.4545

ANFIS model 25: in2 in6 in7 --> trn=721190.0012, chk=1486697.1116

ANFIS model 26: in3 in4 in5 --> trn=717062.3536, chk=779282.7756

ANFIS model 27: in3 in4 in6 --> trn=717062.3626, chk=2528292.0317

ANFIS model 28: in3 in4 in7 --> trn=717062.4691, chk=6453906.4347

ANFIS model 29: in3 in5 in6 --> trn=730327.4828, chk=2471711.0046

ANFIS model 30: in3 in5 in7 --> trn=717062.3805, chk=3332526.6893

ANFIS model 31: in3 in6 in7 --> trn=717679.4983, chk=15975926.5099

ANFIS model 32: in4 in5 in6 --> trn=721190.0012, chk=539168.0373

ANFIS model 33: in4 in5 in7 --> trn=721190.0012, chk=548010.1157

ANFIS model 34: in4 in6 in7 --> trn=721190.0012, chk=925331.3952

ANFIS model 35: in5 in6 in7 --> trn=721190.0023, chk=2079240.9627

Figure 3 shows the ANFIS decision surfaces for the economic profit of wastewater treatment system based on different combinations of inputs. The combinations created based in mean values of the inputs and can be listed as follows:

1. *Input 1 Input 2* 0.02616 4.964 6.015 1.178 0.9673
2. *Input 1* 3.008 *Input 3* 4.964 6.015 1.178 0.9673
3. *Input 1* 3.008 0.02616 *Input 4* 6.015 1.178 0.9673
4. *Input 1* 3.008 0.02616 4.964 *Input 5* 1.178 0.9673
5. *Input 1* 3.008 0.02616 4.964 6.015 *Input 6* 0.9673
6. *Input 1* 3.008 0.02616 4.964 6.015 1.178 *Input 7*
7. 284.9 *Input 2 Input 3* 4.964 6.015 1.178 0.9673
8. 284.9 *Input 2* 0.02616 *Input 4* 6.015 1.178 0.9673
9. 284.9 *Input 2* 0.02616 4.964 *Input 5* 1.178 0.9673
10. 284.9 *Input 2* 0.02616 4.964 6.015 *Input 6* 0.9673

11. 284.9 *Input 2* 0.02616 4.964 6.015 1.178 *Input 7*
12. 284.9 3.008 *Input 3 Input 4* 6.015 1.178 0.9673
13. 284.9 3.008 *Input 3* 4.964 *Input 5* 1.178 0.9673
14. 284.9 3.008 *Input 3* 4.964 6.015 *Input 6* 0.9673
15. 284.9 3.008 *Input 3* 4.964 6.015 1.178 *Input 7*
16. 284.9 3.008 0.02616 *Input 4 Input 5* 1.178 0.9673
17. 284.9 3.008 0.02616 *Input 4* 6.015 *Input 6* 0.9673
18. 284.9 3.008 0.02616 *Input 4* 6.015 1.178 *Input 7*
19. 284.9 3.008 0.02616 4.964 *Input 5 Input 6* 0.9673
20. 284.9 3.008 0.02616 4.964 *Input 5* 1.178 *Input 7*
21. 284.9 3.008 0.02616 4.964 6.015 *Input 6 Input 7*

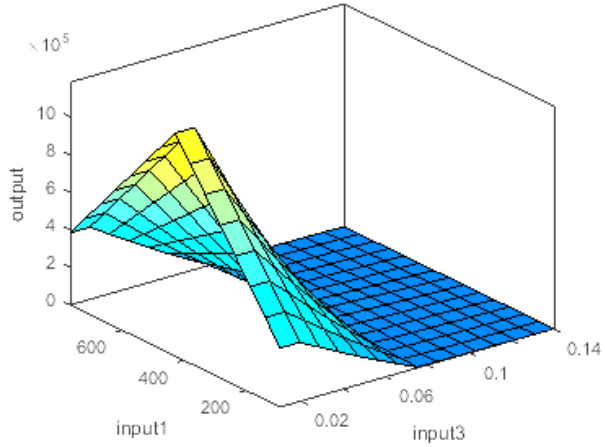

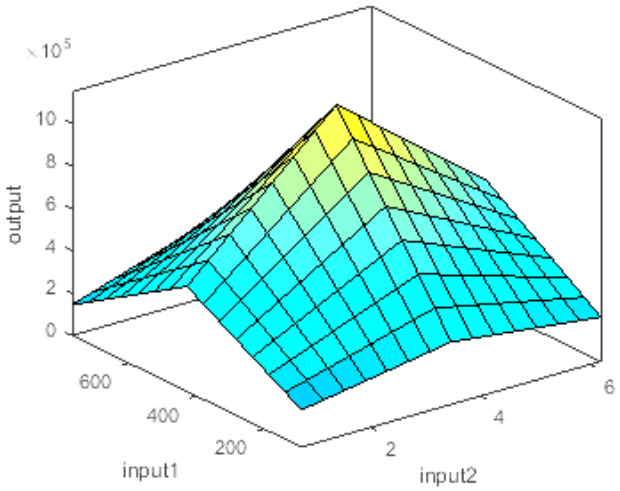

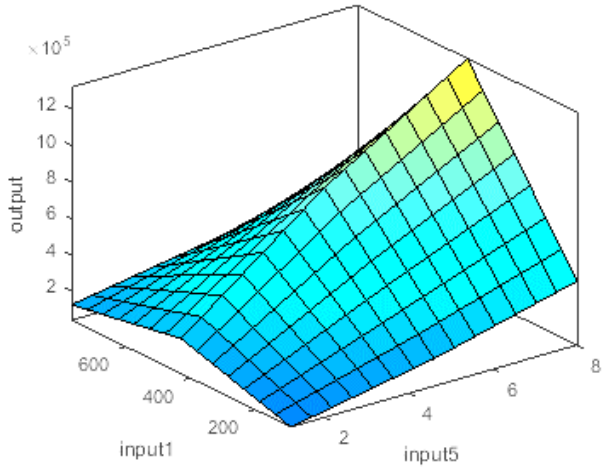

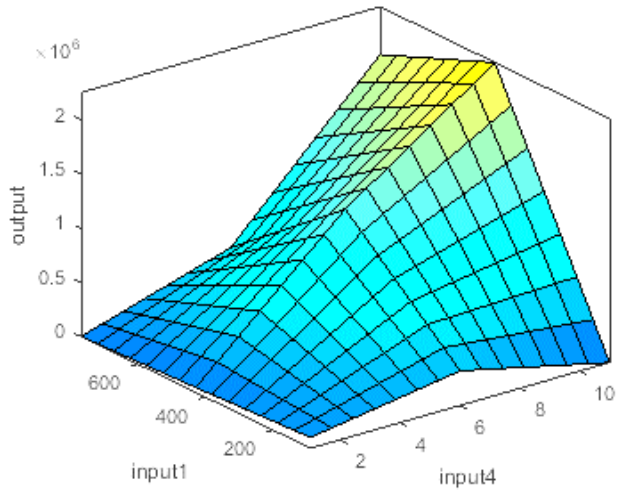

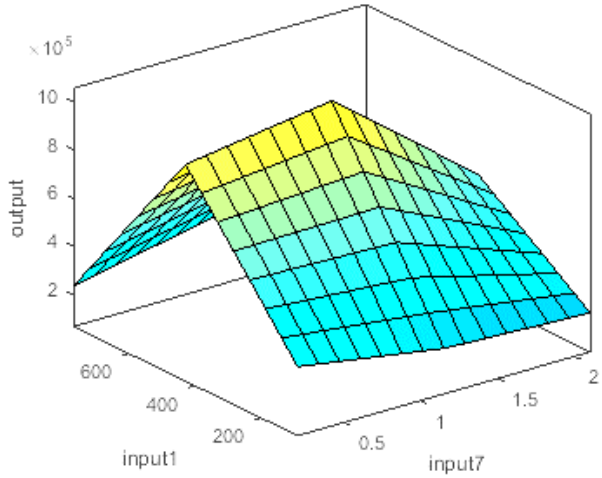

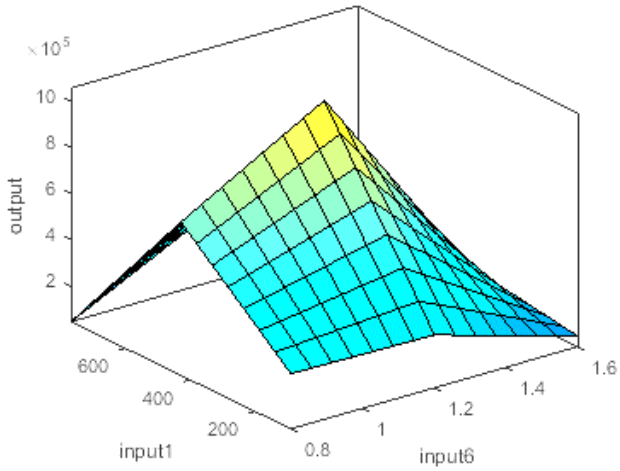

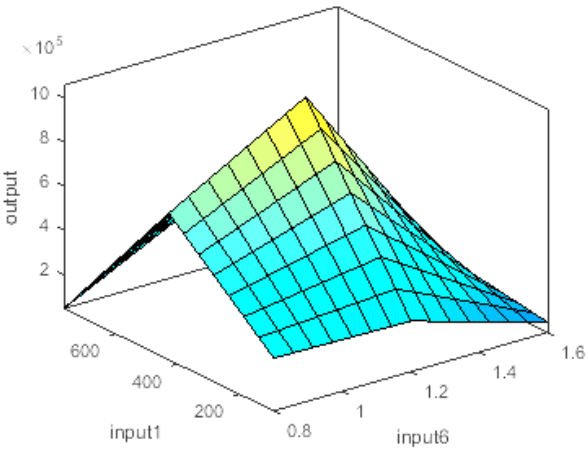

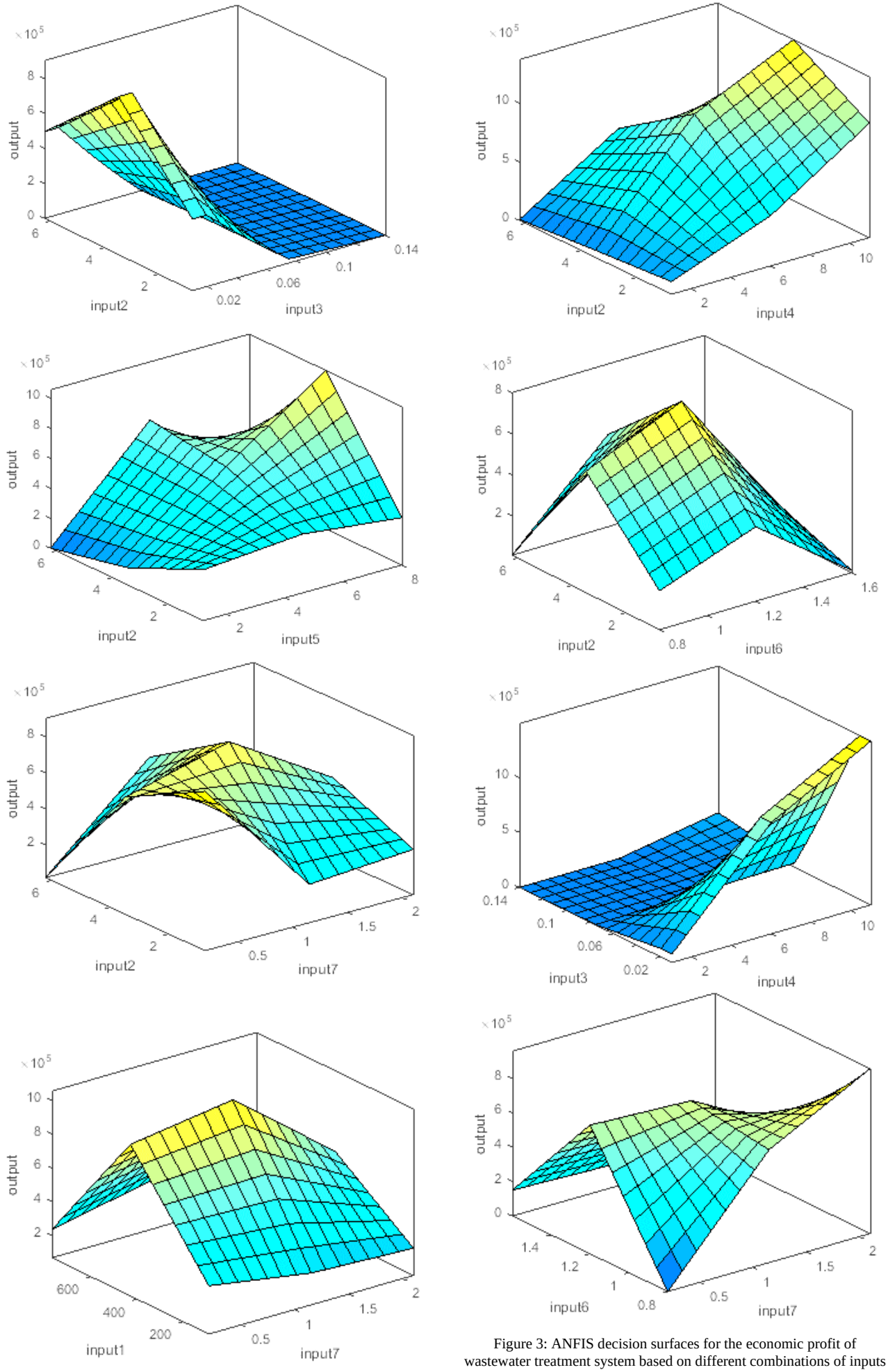

Figure 3: ANFIS decision surfaces for the economic profit of wastewater treatment system based on different combinations of inputs

IV. Conclusion

In this article was used adaptive neuro fuzzy inference system (ANFIS) for selection procedure in order to identify the most influential parameters of wastewater treatment system based on economic profit. Results revealed that the size of the system has the most influence on the economic profit. Furthermore obtained solutions could be of practical importance since one could select which solutions is the most suitable for particular wastewater treatment system.

References

[1] Ansari, F. A., Ravindran, B., Gupta, S. K., Nasr, M., Rawat, I., & Bux, F. (2019). Techno-economic estimation of wastewater phycoremediation and environmental benefits using Scenedesmus obliquus microalgae. *Journal of Environmental Management*, *240*, 293-302.

[2] Padilla-Rivera, A., & Güereca, L. P. (2019). A proposal metric for sustainability evaluations of wastewater treatment systems (SEWATS). *Ecological Indicators*, *103*, 22-33.

[3] Murashko, K., Nikku, M., Sermyagina, E., Vauterin, J. J., Hyppänen, T., Vakkilainen, E., & Pyrhönen, J. (2018). Techno-economic analysis of a decentralized wastewater treatment plant operating in closed-loop. A Finnish case study. *Journal of Water Process Engineering*, *25*, 278-294.

[4] Kothari, R., Kumar, V., Pathak, V. V., & Tyagi, V. V. (2017). Sequential hydrogen and methane production with simultaneous treatment of dairy industry wastewater: bioenergy profit approach. *International Journal of Hydrogen Energy*, *42*(8), 4870-4879.

[5] Najafi, A., Jafarian, A., & Darand, J. (2019). Thermo-economic evaluation of a hybrid solar-conventional energy supply in a zero liquid discharge wastewater treatment plant. *Energy Conversion and Management*, *188*, 276-295.

[6] Lyng, K. A., Stensgård, A. E., Hanssen, O. J., & Modahl, I. S. (2018). Relation between greenhouse gas emissions and economic profit for different configurations of biogas value chains: A case study on different levels of sector integration. *Journal of cleaner production*, *182*, 737-745.

[7] Zheng, B., Huang, G., Liu, L., Zhai, M., & Guan, Y. (2019). Metabolism of urban wastewater: Ecological network analysis for Guangdong Province, China. *Journal of Cleaner Production*, *217*, 510-519.

[8] Abdel-Fatah, M. A. (2018). Nanofiltration systems and applications in wastewater treatment. *Ain Shams Engineering Journal*.

[9] Elreedy, A., Fujii, M., & Tawfik, A. (2019). Psychrophilic hydrogen production from petrochemical wastewater via anaerobic sequencing batch reactor: techno-economic assessment and kinetic modelling. *international journal of hydrogen energy*, *44*(11), 5189-5202.

[10] Boiocchi, R., Matafome, B., Gargalo, C. L., Carvalho, A., & Sin, G. (2017). Techno-economic analysis of resource recovery technologies for wastewater treatment plants. In *Computer Aided Chemical Engineering* (Vol. 40, pp. 1945-1950). Elsevier.

[11] Jang, J.-S.R, ANFIS: Adaptive-Network-based Fuzzy Inference Systems, IEEE Trans. On Systems, Man, and Cybernetics (1993), Vol.23, 665-685.

[12] Petković, D., Issa, M., Pavlović, N.D., Pavlović, N.T., Zentner, L., Adaptive neuro-fuzzy estimation of conductive silicone rubber mechanical properties, Expert Systems with Applications, ISSN 0957-4174, 39 (2012), 9477-9482.

[13] Petković D, Ćojbašić Ž (2012) Adaptive neuro-fuzzy estimation of automatic nervous system parameters effect on heart rate variability, Neural Computing & Application, *21(8):2065-2070* (*2012*)

[14] Kurnaz S, Cetin O, Kaynak O, Adaptive neuro-fuzzy inference system based autonomous flight control of unmanned air vehicles, Expert Systems with Applications (2010), 37, 1229-1234.

[15] Petković, D., Issa, M., Pavlović, N.D., Zentner, L., Ćojbašić, Ž., Adaptive neuro fuzzy controller for adaptive compliant robotic gripper, Expert Systems with Applications, ISSN 0957-4174, 39, (2012), 13295-13304.

THE 5th INTERNATIONAL CONFERENCE
MECHANICAL ENGINEERING IN XXI CENTURY

December 9-10, 2020
Faculty of Mechanical Engineering in Niš, Serbia

Synergy between Industry 4.0 and Lean Methodology

Dragan PAVLOVIĆ, Peđa MILOSAVLJEVIĆ, Srđan MLADENOVIĆ

Faculty of Mechanical Engineering, University of Niš, Aleksandra Medvedeva 14, 18000, Niš, Serbia
dragan.pavlovic@masfak.ni.ac.rs, pedja.milosavljevic@masfak.ni.ac.rs, srdjan.mladenovic@masfak.ni.ac.rs

***Abstract*— Following the ongoing trend of the manufacturing industry digitalization, a new industrial paradigm called Industry 4.0 has emerged as one of the most discussed concept. Industry 4.0 is changing the way the products are manufactured, integrating a smart network of machines and ICT systems and creating an intelligent factory. Lean is widely recognized methodology for improving productivity and decreasing costs in manufacturing organizations. Both of these approaches aim to increase productivity and flexibility. In recent years, there have been few studies and articles showing similarities and differences between Industry 4.0 and Lean methodology, and whether this two approaches are suitable for each other. The goal of this paper is to review the available literature on the relation between Industry 4.0 and Lean, and to show if they can complement each other or are in conflict.**

***Keywords*— Lean, Industry 4.0, Methodology, Manufacturing, Industry**

I. Introduction (use style MASING Heading 1)

Globalization, strong competition, rapid changes of consumers' preferences, as well as the constant evolving trends are pressing businesses to increase their flexibility, in order to be able to instantly respond to those trends and develop the capability to produce highly customized products.

Lean is used for several decades, and it's arguably the most prominent and widely recognized methodology for improving productivity and decreasing costs in manufacturing organisations [1].

This approach supports organisations in their efforts to reduce production cost, improve quality, improve responsiveness by reducing lead times, and increase flexibility through continuous improvement, identification and elimination of waste [2]-[4].

However, in recent years a new paradigm Industry 4.0, so-called fourth industrial revolution, has emerged in the manufacturing sector as one of the most discussed concept, with potential to bring manufacturing capabilities to the next level. It allows creating a smart network of machines, products, components, properties, individuals and ICT systems in the entire value chain to have an intelligent factory [5].

Both of these approaches aim to increase productivity and flexibility and, according to [6], it's possible to integrate Industry 4.0 and Lean into one system.

The connection between Industry 4.0 and Lean has been described in a number of scientific papers published in last few years. The purpose of this paper is to analyse the impacts and opportunities of the integration between Industry 4.0 and Lean. This is achieved through a systematic literature review that is available to the authors.

II. Lean methodology

For decades Lean has been widely known and accepted approach, not only in the manufacturing world where it originates. Lean can be implemented in all types of organizations and processes. It is known as a methodology for maximizing customer value while minimizing waste, i.e. create more output with less input, in order to maintain effectiveness, flexibility, and profitability [7]. Waste is any operation or activity that consumes resources without adding value and customer is not willing to pay. Taiichi Ohno defined 7 Lean wastes within the Toyota Production System as:

- transportation,
- inventory,
- motion,
- waiting,
- overproduction,
- overprocessing,
- defects. [8]

To eliminate waste, Lean is using various tools, techniques and methods. There are over 100 tools, but it's not necessary to know and apply all of them. Some of the most used tools are listed below [9]:

- Single Minute Exchange of Dies (SMED),
- Single Piece Flow,
- Total Productive Maintenance (TPM),
- First-in-first-out (FIFO),
- 5S method,
- Kaizen,
- Just-in-Time (JIT),
- Pull system,
- Kanban;
- Visual management,
- Zero defect,
- SMED;
- Value Stream Mapping (VSM),
- Poka Yoke,
- Cellular manufacturing.

Fundamental principles of Lean, according to [10], are:

- identify value,
- map the value stream,
- create flow,
- establish pull,

- seek perfection.

Fig. 1 Lean principles

III. Industry 4.0

Industry 4.0, originated in 2011 from a German government initiative regarding a high-tech strategy for 2020, changes production processes by using the advancements of Internet of Things (IoT) and information and communication technology (ICT) to integrate digitalization into the production [11]. The main idea behind this term, that supposed to symbolize the fourth industrial revolution, is the digital integration of the physical basic system and software system.

According to [12], Industry 4.0 encounters to a wide range of concepts including increments in mechanization, automation, digitalization, networking and miniaturization. Based on [13], Industry 4.0 focuses on the establishment of intelligent and communicative systems including machine-to-machine communication and human-machine interaction.

The transformation in Industry 4.0, according to [14], is based on eight basic technologies:

- data analytics and artificial intelligence (big data analytics),
- adaptive robotics,
- simulation,
- cyber-physical systems,
- Industrial Internet,
- cloud systems,
- additive manufacturing and virtualization technologies.

Although it can be considered as relatively new research field, the number of publications has grown up in the last few years [15].

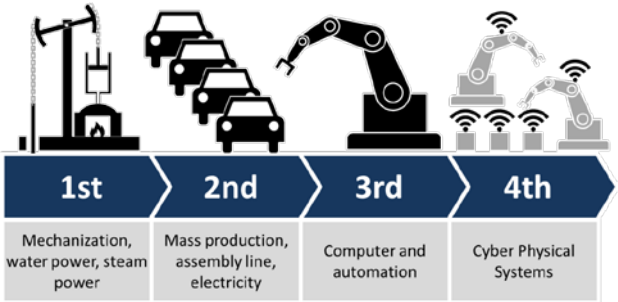

Fig. 2 Industry 4.0 (By Christoph Roser at AllAboutLean.com under the free CC-BY-SA 4.0 license)

IV. Similarities between Industry 4.0 and Lean

Based on their core ideas, Industry 4.0 and Lean have a lot of similarities. Both Industry 4.0 and Lean aim to increase the competitiveness of organizations, but they apply different types of tools to achieve that goal. While Industry 4.0 relies on advances technologies, Lean relies on continuous improvement. Some authors in their publications asked some questions that need to be answered, about differences of these two approaches, and whether they are suitable for each other [16]-[18].

Regardless of that, different studies agree that Industry 4.0 can bring changes to common lean practices and tools. As shown in [19], manufacturers who successfully implement and integrate these two approaches will reduce conversion costs by as much as 40% in five to ten years.

Lean can be defined as “doing more with less”, which is fully valid for the future. Therefore, lean principles for reducing complexity and avoiding anything that does not add value become even more relevant for Industry 4.0 [20].

As in [21], a study of the relationship between advanced communication technologies and Lean was conducted, and the conclusion was that information and communication technologies (ICT) can improve the performance of Lean methodology.

Reference [22] shows that inefficient processes can be automated (digitally supported), but the process itself will remain unstable. Automation of such a process, with no standards or performance indicators, will not improve the operational performance [23]. Therefore, Lean can improve implementation of Industry 4.0 in such processes.

Visual control, which makes it easier to identify problems in the process, is very important in Lean. Based on that, [22] and [24] argues that a Lean implementation must be a prerequisite for a successful transformation of Industry 4.0.

Reference [25] summarizes findings from numerous articles on how Industry 4.0 can enhance Lean, as well as how Lean can support Industry 4.0.

Similar to previous, [26] present a comprehensive table that shows to what degree each one of the principles of Industry 4.0 support each Lean tool.

Based on a survey on 108 European companies that are in process of implementation of Lean and Industry 4.0, [27] found that Lean is easing condition for Industry 4.0 adoption, but they are independent.

The results of the integration of Lean and Industry 4.0 in 110 Brazilian manufacturing companies are shown in [28]. Authors claim that Lean approach is positively associated with Industry 4.0 and that they will lead to improved performance of the companies.

A few articles argues about the fact that implementation of Industry 4.0 does not eliminate Lean, but rather helps to increase the maturity of the Lean effort. Industry 4.0 will be integrated into existing Lean frameworks and will increase the flexibility of Lean processes [16], [29].

Value stream mapping (VSM), as one of the most fundamental Lean tool and principle, is used for mapping the current process and identify improvement areas in the value stream, and [30] claim that Industry 4.0 can improve VSM.

Also, [31] recognizes VSM as one of the most used Lean tool, and [32] gives a survey with collected views of Lean experts regarding of VSM development by means of digitalization.

Another commonly used Lean tool is Jidoka, or automation with human intelligence. As shown in [33], a new term "Lean automation", which uses cyber-physical systems, is presented. Lean automation should expand the application of Jidoka as a way to improve production system flexibility.

Finally, [26] identify VSM, as well as standardization and SMED, as the basic Lean tools that serve as a foundation and support successful implementation of Industry 4.0.

As shown in [34], there are some doubts about smooth integration of Industry 4.0 into Lean, because of the highly cost-intensive implementation process of Industry 4.0 and some risks associated to cyber security.

V. Conclusions (use style MASING Heading 1)

Although Industry 4.0 is a relatively new term, there is a large number of papers describing this approach, as well as a link to a Lean methodology that has been known for decades. The paper shows, through review of literature that benefits from implementation of Industry 4.0 and Lean methodology are undeniable. Vast majority of the published papers confirm benefits and strong correlation between Industry 4.0 and Lean.

Both approaches mentioned above share the same ultimate priorities of waste reduction and efficiency gains. It can be concluded that the Lean methodology will not disappear with the progress of Industry 4.0, moreover it is likely to become more important for successful implementation of Industry 4.0.

Acknowledgment

This research was financially supported by the Ministry of Education, Science and Technological Development of the Republic of Serbia.

References

[1] M. Holweg, "The genealogy of Lean production," Journal of Operations Management, vol. 25, pp. 420-437, March 2007.

[2] J. Bhamu, and K. S. Sangwan, "Lean manufacturing: Literature review and research issues," International Journal of Operations and Production Management, vol. 34, pp. 876-940, July 2014.

[3] G. Chauhan, and T. Singh, "Measuring parameters of Lean manufacturing realization," Measuring Business Excellence, vol. 16, pp. 57-71, August 2012.

[4] S. James-Moore, and A. Gibbons, "Is Lean manufacture universally relevant? An investigative methodology," International Journal of Operations & Production Management, vol. 17, pp. 899-911, September 1997.

[5] B. Mrugalska, and M. Wyrwicka, "Towards Lean production in Industry 4.0," Procedia Engineering, vol. 182, pp. 466-473, 2017.

[6] D. Kolberg, and D. Zühlke, "Lean automation enabled by Industry 4.0 Technologies," IFAC-PapersOnLine, vol. 48, pp. 1870-1875, May 2015.

[7] J. Womack, D. Jones, and D. Roos, The Machine that Changed the World, Rawson Associates, New York, 1990.

[8] T. Ohno, Toyota Production System: Beyond Large Scale Production, Productivity Press, Portland, 1988.

[9] A. Thakur, "A review on Lean Manufacturing implementation techniques: A conceptual model of Lean Manufacturing dimensions," REST Journal on Emerging trends in Modelling and Manufacturing, vol. 2, pp. 62-72, 2016.

[10] J. Womack, and D. Jones, Lean thinking, New York, NY: Simon & Schuster, 2003.

[11] K. Zhou, T. Liu, and L. Zhou, "Industry 4.0: towards future industrial opportunities and challenges," 12th International Conference on Fuzzy Systems and Knowledge Discovery, Changsha, China, pp. 2147-2152, August 2016.

[12] H. Lasi, P. Fettke, T. Feld, and M. Hoffmann, "Industry 4.0," Business & Information Systems Engineering, vol. 6, pp. 239-242, June 2016.

[13] A. Ustundag, and E. Cevikcan, Industry 4.0: Managing the Digital Transformation, 1st ed., Springer, 2018.

[14] S. Wang, J. Wan, D. Zhang, D. Li, and C. Zhang, (2016) "Towards smart factory for Industry 4.0: a self-organized multi-agent system with big data based feedback and coordination," Computer Networks, vol. 101, pp. 158-168, June 2016.

[15] J. Santos, P. Lopez, I. Blanco, and P. Chen, "Assessing the synergies between lean manufacturing and Industry 4.0," Direccion y Organizacion, vol. 71, pp. 71-86, 2020.

[16] B. Ruttimann, and M.T. Stockli, "Lean and Industry 4.0—twins, partners, or contenders? A due clarification regarding the supposed clash of two production systems," Journal of Service Science and Management, vol. 9, pp. 485-500, 2016.

[17] F. Martinez, P. Jirsak, and M. Lorenc, M. "Industry 4.0. The end of lean management?," 10th International Days of Statistics and Economics, Prague, Czech Republic, pp. 1189-1197, September 2016.

[18] T.H. Netland, "Industry 4.0: Where does it leave lean?," Lean Management Journal, vol. 5, pp. 22-23, 2015.

[19] D. Kupper, A. Heidemann, J. Strohle, D. Spindelndreier, and C. Knizek, "When Lean meets Industry 4.0 next level operational excellence," Boston Consulting Group [Web] https://www.bcg.com/ publications/2017/lean-meets-industry-4.0.aspx (Posted December 14, 2017)

[20] L. Cattaneo, M. Rossi, E. Negri, D. Powell, and S. Terzi, "Lean thinking in the digital Era," In Product Lifecycle Management and the Industry of the Future, Cham: Springer, 2017, pp. 371-381.

[21] U. Dombrowski, T. Richter, and P. Krenkel, "Interdependencies of Industrie 4.0 & Lean production systems: A use cases analysis," Procedia Manufacturing, vol. 11, pp. 1061-1068, 2017.

[22] S. Kaspar, and M. Schneider, "Lean and industry 4.0 in the field of intra logistics: Efficienc improvement by combination of the two approaches," Productivity Management, vol. 20, pp. 17-20, 2015.

[23] J. Enke, R. Glass, A. Kreß, J. Hambach, M. Tisch, and J. Metternich, "Industrie 4.0 – Competencies for a modern production system: A curriculum for Learning Factories," Procedia Manufacturing, vol. 23, pp. 267-272, 2018.

[24] Staufen AG., Deutscher Industrie 4.0 Index 2015. Köngen: Staufen AG, 3016.

[25] S. Buer, J. Strandhagen, and F. Chan, "The link between Industry 4.0 and lean manufacturing: Mapping current research and establishing a research agenda,"

International Journal of Production Research, vol. 56, pp. 2924-2940, 2018.

[26] A. Sanders, K. Subramanian, T. Redlich, and J. Wulfsberg, “Industry 4.0 and Lean management – synergy or contradiction?,” IFIP International Conference on Advances in Production Management Systems, Hamburg, Germany, September 3-7, 2017, pp. 341-349.

[27] M. Rossini, F. Costa, G. Luz Tortorella, and A. Portioli-Staudacher, “The interrelation between Industry 4.0 and Lean production: an empirical study on European manufacturers,” The International Journal of Advanced Manufacturing Technology, vol. 102, pp. 3963–3976, 2019.

[28] G. Luz Tortorella, and D. Fettermann, “Implementation of Industry 4.0 and Lean production in Brazilian manufacturing companies,” International Journal of Production Research, vol. 56, pp. 2975-2987, 2018.

[29] D. Roy, P. Mittag, and M. Baumeister, “Industrie 4.0 – Einfluss der digitalisierung auf die fünf Lean-prinzipien schlank vs. intelligent,” Productivity Management, vol. 20, pp. 27-30, 2015.

[30] J. Chen, and K. Chen, “Application of ORFPM system for Lean implementation: An industrial case study,” International Journal of Advanced Manufacturing Technology, vol. 72, pp. 839-852, 2014.

[31] T. Meudt, J. Metternich, and E. Abele, “Value stream mapping 4.0: Holistic examination of value stream and information logistics in production,” CIRP Annals - Manufacturing Technology, vol. 66, pp. 413-416, 2017.

[32] A. Lugert, A. Batz, and H. Winkler, “Empirical assessment of the future adequacy of value stream mapping in manufacturing industries,” Journal of Manufacturing Technology Management, vol. 29, pp. 886-906, 2018.

[33] J. Ma, Q. Wang, and Z. Zhao, (2017). “SLAE–CPS: Smart Lean automation engine enabled by cyber-physical systems technologies,” Sensors, vol. 17, July 2017.

[34] A. Beifert, L. Gerlitz, and G. Prause, (2018). “Industry 4.0-For sustainable development of lean manufacturing companies in the shipbuilding sector,” 17th International Multidisciplinary Conference of Reliability and Statistics in Transportation and Communication, Riga, Latvia, October 2017, pp. 563-573.

THE 5th INTERNATIONAL CONFERENCE
MECHANICAL ENGINEERING IN XXI CENTURY

December 9-10, 2020
Faculty of Mechanical Engineering in Niš, Serbia

Covid-19 Crisis Management in Manufacturing Industry Organizations in the Republic of Serbia

Ivana MARINOVIC MATOVIC[1], Andjela LAZAREVIC[2]

[1]Addiko Bank AD, Belgrade, Serbia
[2]Faculty of Mechanical Engineering, University of Nis, Nis, Serbia
[1]ivana.m.matovic@gmail.com, [2]andjela.lazarevic@masfak.ni.ac.rs

***Abstract*— The crisis caused by coronavirus pandemic has led to major operational changes in manufacturing industry organizations. These organizations have faced the challenges of reducing or suspending the production process, due to restrictions imposed by the state, due to declining demand for their products, as well as due to the fact that their employees cannot do jobs remotely. Focusing on manufacturing industry in the Republic of Serbia, the paper investigates the problems faced by organizations in this sector after the outbreak of Covid-19 pandemic. Secondly, the paper examines the impact of Covid-19 crisis on various segments of their business, and the measures these organizations have taken to meet the major challenges that need to be addressed quickly. Finally, recommendations for successful crisis management in manufacturing industry organizations in the Republic of Serbia are derived. Recommendations include alternative tactics and innovative management concepts for overcoming problems, for survival, and preparing for economically viable operations of manufacturing industry organizations after the Covid-19 crisis**

***Keywords*— Crisis management, Covid-19, manufacturing industry, survival, Republic of Serbia**

I. Introduction

The research is motivated by the importance of manufacturing industry in the Republic of Serbia. The economic growth of the Republic of Serbia today is largely based on the improvement of performances and structural changes in the manufacturing industry. The last 5 years have been marked by the expansion of manufacturing industry. In the period 2015–2019, the number of organizations operating in manufacturing industry increased by 5.1%, the number of employees by 27.2%, income by 17.9%, net result by 35.4%, GVA by 16.8%, capital by 32.7 %, and the accumulated loss decreased by -18.6%, as well as total liabilities by -1.7% [1]. The manufacturing industry is from the position of a net loss in 2015, achieved a positive result in the period 2016-2019 - the net result in 2017 was a record 1.2 billion EUR, while in 2019 the net result was slightly lower and amounted to 940 million EUR, or 28% of net economic performance [1].

Like Europe and the rest of the world, a recession is predicted for the Republic of Serbia in 2020. The scope of recession will depend on the duration of COVID-19 pandemic. IMF forecasts of global GDP for 2020 have been revised downwards due to the economic shock caused by COVID-19 pandemic, estimating a global decline of about 5%, higher in developed economies (of about -8%), smaller in developing countries (-3%) [2]. A global recovery would follow in 2021 (growth of 6%) [2]. The revised forecasts of the European Commission [3] for the most developed EU countries show a double-digit decline in GDP of the most developed EU countries (Italy, Spain and France), and in 2021 there will be growth of 6-7%. Growth projections for 2020 for the countries of the region have been significantly revised, and forecasts show that the smallest decline in 2020 will be in Northern Macedonia (-3.9%) and Republic of Serbia (-4.1%). Economic growth forecasts for the countries of the region in 2021 are optimistic, and Serbia is projected to grow by 6.1% [3].

Current economic challenges caused by COVID-19 pandemic, and the need for strengthening the long-term position and status of manufacturing industry in the Republic of Serbia, are the reason for this research. The research paper analyses the impact of Covid-19 crisis on various segments of manufacturing organizations' business, and the measures these organizations have taken to oppose the Covid-19 pandemic. The study of the most significant problems of manufacturing organizations, as well as the measures they have taken, was carried out in order to determine the recommendations for survival, offensive business strategies and further development of manufacturing organizations, during and after the crisis caused by the Covid-19 pandemic.

II. Literature review

The economic and social consequences of the crisis caused by Covid-19 pandemic have captured the attention of top scientific researchers. The impact of the Covid-19 pandemic crisis on the economy has been summarized in the research done by Gourinchas [4]. Nicola et al. [5] have summarized the socio-economic impact of Covid-19 pandemic, taking into account individual aspects of the world economy.

Kuckertz et al. [6] have confirmed that state role is of great importance as the first aid for small and medium-sized enterprises, at the beginning of crisis, in order to support their liquidity, which is primarily at risk. Following this first aid measures, state should implement

further support measures for the development of SME organizations, and their survival in times of crisis. Baldwin [7] represents the position that government support should be prompt and strong, preventing liquidity problems, and avoiding unnecessary losses. Carlsson-Szlezak et al. [8] explained that policy innovations could have an impact on economic recovery, like “bridge loans” or moratorium on mortgage payments.

Obrenovic et al. [9] concluded that in times of crisis it is very important that organizations have their own contingency plan, which would ensure a smooth workflow during the unforeseen situations, such as Covid-19 pandemic. Based on their research, Alves et al. [10] have proposed crisis resilience model for small and medium-sized enterprises. They have defined five strategies for SME organizations, for their survival and development in crisis conditions. Kraus et al. [11] have found that organizations mostly use three strategies to oppose the crisis. The importance of open access, innovation, and knowledge management for combat and survival in crisis conditions is emphasized in the research of Chesbrough [12].

According to Sodhi [13], losses in the manufacturing industry have led to a decline in economic activity in many countries. Author suggested certain measures that the manufacturing industry should apply in the post-crisis period. In their research, authors Cai & Luo [14] have proposed two-step measures. These measures should be implemented in manufacturing industry, with their help it would be easier to get out of the crisis, and adapt to the new conditions in the post-crisis period. Deshmukh & Haleem [15] have developed measures for adequate positioning of the manufacturing industry in the post-crisis period.

III. Methodology of research

The research was conducted on the territory of the Republic of Serbia during June and July 2020, due to the fact that this was time period when the “first wave” of Covid-19 pandemic has ended, so it could be assumed that research participants will be able to realistically see the first effects of the crisis, and that they have already taken certain measures that would enable them to survive in crisis conditions. The research questionnaire was forwarded directly to the e-mail addresses of business organizations throughout the Republic of Serbia, distributed through the LinkedIn business network, as well as indirectly, using the several business associations as networking links. The survey was responded by 424 business organizations, including 40 from the manufacturing industry. The survey questionnaire was containing 43 questions, methodically arranged within three groups of researched variables: 1. business organization data, 2. problems faced by organizations during the Covid-19 crisis, 3. measures that were applied. All questions were clear and concise; they were listed gradually with appropriate order.

After data collection and database creation, statistical processing started. Data were analysed using IBM SPSS 22.0 statistical software. The following methods of statistical data processing were used: descriptive statistics, normality tests - Kolmogorov-Smirnov and Shapiro-Wilk, and non-parametric Related-samples Sign test.

IV. Results and discussion

The research included 424 business organizations from the territory of the Republic of Serbia, of which 40 were from the manufacturing industry. The results of the research are based on data analysis focused on business organizations from the manufacturing industry only. Demographic and business characteristics of manufacturing organizations are given in Table I.

TABLE I Descriptive Characteristics of the Sample

Variable	Characteristics	Frequency	Percent	Cumulative percent
Size acc. to employee number	Micro	22	55,0%	55,0%
	Small	18	45,0%	100,0%
Size acc. to revenue in 2019	Micro	24	60,0%	60,0%
	Small	16	40,0%	100,0%
How long organization exists	Less than 1	2	5,0%	5,0%
	3-5 years	2	5,0%	10,0%
	6-10 years	8	20,0%	30,0%
	Longer than 10	28	70,0%	100,0%
Owner's gender	Male	28	70,0%	70,0%
	Female	12	30,0%	100,0%
Owner's age	Under 30	0	0,0%	0,0%
	31-40	2	5,0%	5,0%
	41-50	24	60,0%	65,0%
	51-60	10	25,0%	90,0%
	61 and over	4	10,0%	100,0%
Owner's education	Secondary	18	45,0%	45,0%
	Professional	8	20,0%	65,0%
	University	14	35,0%	100,0%
Initial capital	<1000 EUR	12	30,0%	30,0%
	1000-5000	14	35,0%	65,0%
	>5000 EUR	12	30,0%	95,0%
	None of above	2	5,0%	100,0%
International trade	Yes	24	60,0%	60,0%
	No	16	40,0%	100,0%
Online trade	Yes	6	15,0%	15,0%
	No	34	85,0%	100,0%
Revenue generated by online sales	0-25%	4	10,0%	10,0%
	26-50%	0	0,0%	10,0%
	51-75%	2	5,0%	15,0%
	76%-100%	0	0,0%	15,0%
	No online trade	34	85,0%	100,0%
Revenue growth 2019	Yes	30	75,0%	75,0%
	No	10	25,0%	100,0%
Profit growth 2019	Yes	30	75,0%	75,0%
	No	10	25,0%	100,0%

As presented in Table I, observed sample consisted of micro (55%; 60%) and small (45%; 40%) enterprises. The vast majority of organizations that participated in the survey were established more than 10 years ago (70%), most of them participate in international trade (60%), and have achieved revenue and profit growth in 2019 (75%; 75%). Manufacturing organizations mostly do not have online sales (85%). The majority of owners of manufacturing organization are male (70%), and most of them are in the age group 41-50 years (60%). The educational structure is diverse, 45% of respondents have secondary education, and 20% have professional education, while 35% of owners of manufacturing organizations have university education.

Scores' distribution was checked, using the normality tests, and the results are shown in Table II.

TABLE II NORMALITY TESTS

	Kolmogorov-Smirnov[a]			Shapiro-Wilk		
	Statistic	df	Sig.	Statistic	df	Sig.
Employee health issues	,317	40	,000	,743	40	,000
Business interruption	,271	40	,000	,833	40	,000
Organizational difficulties	,201	40	,000	,897	40	,002
Payment delays	,217	40	,000	,807	40	,000
Delivery problems	,227	40	,000	,853	40	,000
Increased costs	,234	40	,000	,870	40	,000
Working hours change	,239	40	,000	,885	40	,001
Business change	,210	40	,000	,894	40	,001
Absence of employees	,259	40	,000	,870	40	,000
Alternative way of doing business	,198	40	,000	,842	40	,000
Difficult access to capital	,169	40	,006	,890	40	,001
Difficult fulfilment of contractual obligations	,183	40	,002	,897	40	,002
Difficult access to business information	,214	40	,000	,900	40	,002
Other	,320	40	,000	,806	40	,000

a. Lilliefors Significance Correction

As shown in Table II, the score distributions deviate significantly from normal.

Using the Related-samples Sign test, we checked the influence of Covid-19 crisis on selected business segments of manufacturing organizations (Table III).

TABLE III IMPACT OF COVID-19 CRISIS ON MANUFACTURING ORGANIZATIONS

	Z	Asymp. Sig. (2-tailed)	Exact Sig. (2-tailed)
Mean - Employee health issues	-3,833	**,000**	/
Mean - Business interruption	-,811	,417	/
Mean - Organizational difficulties	-,530	,596	/
Mean - Payment delays	-,530	,596	/
Mean - Delivery problems	-1,237	,216	/
Mean - Increased costs	/	/	,541[b]
Mean - Working hours change	-1,543	,123	/
Mean - Business change	-,171	,864	/
Mean - Absence of employees	-2,652	**,008**	/
Mean - Alternative way of doing business	-2,373	**,018**	/
Mean - Difficult access to capital	-2,079	**,038**	/
Mean - Difficult fulfilment of contractual obligations	-,530	,596	/
Mean - Difficult access to business information	/	/	,152[b]
Mean – Other	/	/	,454[b]

a. Sign test
b. Binomial distribution used

Using the non-parametric Related-samples Sign test for one sample of a multidimensional variable, we tested the hypothesis that the assessment of average value of Covid-19 crisis impact on the observed business segments of manufacturing industry organizations is greater than 3.

H0 (average value equal to 3)

H1 (average value is greater than 3)

Based on the significance of Related-samples Sign test, we conclude that the average value is significantly higher than 3 for the following business segments: employee health issues (sig. 2-tailed 0,000), absence of employees (sig. 2-tailed 0,008), alternative way of doing business (sig. 2-tailed 0.018), and difficult access to capital (sig. 2-tailed 0.038).

The research results have confirmed that the crisis caused by Covid-19 pandemic had a significant impact on the health of employees, the absence of employees; manufacturing industry organizations had to implement alternative ways of doing business, and there was difficult access to capital to a significant extent.

The results have shown that Covid-19 crisis did not cause significant business interruption in the manufacturing industry (sig. 2-tailed 0.417), that there were no major organizational difficulties (sig. 2-tailed 0.596), no notable large payment delays (sig. 2- tailed 0.596), no big delivery problems (sig. 2-tailed 0.216). The study confirmed that the crisis caused by Covid-19 pandemic did not significantly affect costs (sig. 2-tailed 0.541), working hours (sig. 2-tailed 0.123) or business operations (sig. 2-tailed 0.864). Organizations operating in the manufacturing industry did not face great difficulties in fulfilling contractual obligations (sig. 2-tailed 0.596), nor did they face major problems with access to business information (sig. 2-tailed 0.152).

The research also analysed the application of certain measures, in manufacturing organizations, with the aim of surviving the Covid-19 crisis (Figure 1).

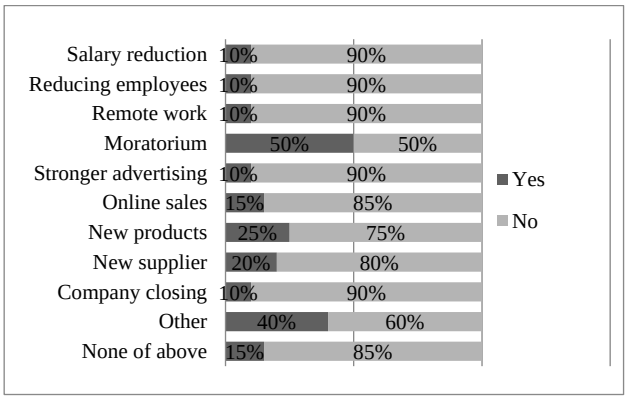

Fig. 1 Measures implemented in manufacturing industry organizations aimed at overcoming the Covid-19 crisis

The results, presented in Figure 1, show that manufacturing industry organizations in the Republic of Serbia mostly used the moratorium for deferral of credit obligations with commercial banks (50% of observed organizations). The introduction of new products in the product range was done in every fourth organization (25%), while 20% of them introduced a new supplier to maintain uninterrupted production flow after the outbreak of Covid-19 crisis. Measures that have been applied to a

small extent are: salary reduction (10%), cutting down the number of employees (10%), introduction of remote work (10%), stronger advertising (10%), and introduction of online sales (15%). Manufacturing organizations, 10% of them, had to suspend their operations due to the Covid-19 crisis. Some other, unmentioned measures were applied in 40% of the observed organizations, while 15% of organizations answered that they did not apply any of the measures covered by the research.

V. Conclusions

This paper investigates the impact of Covid-19 pandemic on the outbreak of global economic crisis, and the provocation of global recession in 2020. The research was conducted with the aim of determining the consequences of Covid-19 crisis on organizations belonging to manufacturing industry. The research was approached with the assumption of the great importance of manufacturing industry for the economic growth of Republic of Serbia.

The analysis demonstrated that Covid-19 crisis has an impact on many business segments of manufacturing organizations, primarily causing negative consequences. The results of the study showed that there is a statistically significant impact of Covid-19 pandemic on employee health issues and absence of employees in manufacturing industry. Respondents particularly emphasized the significant impact of the pandemic on their obligation to find alternative ways of doing business, and difficulties in obtaining liquid funds.

In the short run, we can conclude that the measures taken by manufacturing industry organizations were adequate, and aimed at mitigating the negative consequences of Covid-19 pandemic. The measures primarily included preserving and protecting the health of employees, as well as keeping their salaries at the same level, and maintaining a stable standard of living, which is important in uncertain conditions faced by employees. The manufacturing industry also took advantage of the government support measures offered, represented by a moratorium on credit obligations. They have adapted to the new crisis conditions by introducing new products, new supplies or a new sales channel.

Observed in the medium and long term, and bearing in mind the great importance of manufacturing industry for the economic development of the Republic of Serbia, measures to overcome the crisis must include a strategy at national level, aimed at preserving and strengthening this industry. The manufacturing industry organizations themselves should use this situation for the development of crisis management, which includes plans of preventive measures; and plans of necessary capacities for the smooth production process in conditions of uncertainty caused by unforeseen crisis events. Crisis management in manufacturing organization should include: introduction of new, crisis business models; introduction of modern digital technologies in the production process; development of business continuity plans that would include the permanence of raw materials procurement and finished products sales.

The research results should encourage all stakeholders in the manufacturing industry and competent policy makers to better understand the consequences of the crisis caused by Covid-19 pandemic on this specific industry. This primarily refers to the adoption of certain government support measures that would meet the financial needs in times of crisis, and create an entrepreneurial ecosystem, adaptable to national and global market fluctuations, which is especially important in times of crisis.

References

[1] Republican Bureau of Statistics, Republic of Serbia, TRENDS Business performance of the economy of the Republic of Serbia, 2015-2019, https://publikacije.stat.gov.rs/G2020/Pdf/G20208003.pdf, Belgrade, 2020.

[2] International Monetary Fund, World Economic Outlook A Long and Difficult Ascent, https://www.imf.org/~/media/Files/Publications/WEO/2020/October/English/text.ashx?la=en, October, 2020.

[3] European Commission, European Economic Forecast, Institutional Paper 132, Luxembourg, Publications Office of the European Union, https://ec.europa.eu/info/sites/info/files/economy-finance/ip132_en.pdf, July, 2020.

[4] P.O. Gourinchas, “Flattening the pandemic and recession curves”, in “Mitigating the COVID Economic Crisis: Act Fast and Do Whatever It Takes”, Ed. R. Baldwin and B. Weder di Mauro, CEPR Press VoxEU.org eBook, pp. 31-39, 2020.

[5] M. Nicola, Z. Alsafi, C. Sohrabi, A. Kerwan, A. Al-Jabir, C. Iosifidis, M. Agha and R. Agha, “The socio-economic implications of the coronavirus pandemic (COVID-19): A review”, International Journal of Surgery, Vol. 78, June 2020, pp. 185-193, 2020.

[6] A. Kuckertz, L. Brändle, A. Gaudig, S. Hinderer, C.A.M. Reyes, A. Prochotta and E.S. Berger, “Startups in times of crisis–A rapid response to the COVID-19 pandemic”, Journal of Business Venturing Insights, 2020 June, 13: e00169, 2020.

[7] R. Baldwin, “Keeping the lights on: Economic medicine for a medical shock”, VoxEU.Org, 2020, March 13, https://voxeu.org/article/how-should-we-think-about-containing-covid-19-economic-crisis

[8] P. Carlsson-Szlezak, M. Reeves and P. Swartz, “Understanding the Economic Shock of Coronavirus”, Harvard Business Review, 2020, March 27, https://hbr.org/2020/03/understanding-the-economic-shock-of-coronavirus

[9] B. Obrenovic, J. Du, D. Godinic, D. Tsoy, M.A.S. Khan and I. Jakhongirov, “Sustaining Enterprise Operations and Productivity during the COVID-19 Pandemic: Enterprise Effectiveness and Sustainability Model”, Sustainability, Vol. 12, issue 15, 5981, 2020.

[10] J.C. Alves, T.C. Lok, Y.B. Luo and W. Hao, “Crisis Management for Small Business during the COVID-19 Outbreak: Survival, Resilience and Renewal Strategies of Firms in Macau”, ResearchSquare, June 2020.

[11] S. Kraus, T. Clauss, M. Breier, J. Gast, A. Zardini and V. Tiberius, “The economics of COVID-19: initial empirical evidence on how family firms in five European countries cope with the corona crisis”, International Journal of Entrepreneurial Behaviour & Research, Vol. 26, issue 5, pp. 1067-1092, 2020.

[12] H. Chesbrough, “To recover faster from Covid-19, open up: managerial implications from an open innovation perspective”, Industrial Marketing Management, Vol. 88, Jul, 2020.

[13] H.S. Sodhi, “Effect of Corona Virus on the Manufacturing and Supply Chain Industry across World”, Industrial Engineering Journal, Vol. 13, issue 6, June 2020.

[14] M. Cai and J. Luo, “Influence of COVID-19 on Manufacturing Industry and Corresponding Countermeasures from Supply Chain Perspective”, Journal of Shanghai Jiaotong University (Science), Vol. 25, pp. 409–416, 2020.

[15] S.G. Deshmukh and A. Haleem, “Framework for Manufacturing in Post-COVID-19 World Order: An Indian Perspective”, International Journal of Global Business and Competitiveness, Vol. 15, pp. 49–60, 2020.

THE 5th INTERNATIONAL CONFERENCE
MECHANICAL ENGINEERING IN XXI CENTURY

December 9-10, 2020
Faculty of Mechanical Engineering in Niš, Serbia

The Role and Importance of Standards for the Quality of Services in Educational Institutions in the Field of Mechanical Engineering

Andjela LAZAREVIC[a], Ivana MARINOVIC MATOVIC[b], Srdjan MLADENOVIC[a]

[a] Faculty of Mechanical Engineering, Aleksandra Medvedeva 14, 18.000 Nis, Serbia
[b] Addiko bank a.d., Bulevar Mihajla Pupuna 6, 11.070 Belgrade, Serbia
andjela.lazarevic@masfak.ni.ac.rs, ivana.m.matovic@gmail.com, srdjan.mladenovic@masfak.ni.ac.rs

Abstract- **Besides higher education activities, there is a complex range of services provided by the educational institutions in Serbia in the field of mechanical engineering. In order to provide balance between core activities related to the higher education and additional activities, in accordance with the national Law on higher education, good organization and synchronization of these activities is crucial. There are many tools and techniques that could be used to make this process more effective and easier. This paper considers the role and importance of standards implementation in educational institutions, especially related to the establishment of the quality and laboratory managements systems. The similarities, complementarity and differences of standards SRPS ISO 90001:2015 and SRPS ISO/IEC 17025:2017 are examined, together with challenges for their implementation.**

***Keywords*— ISO Standards, Educational institutions, Quality management system, Laboratory management system**

I. Introduction

Education represents the acquisition and usage of knowledge and is aimed to facilitate learning at various levels of knowledge using different education methods. Although there are various stages of education, the subject of this paper is higher education, which leads to obtaining academic degree. Higher education system is a complex, intentional system, involving huge number of stakeholders. The exact structure of the educational system varies from one country to another, however, it is primary regulated by the national legislation, while the application of international or other guidelines and various directives depends of the country's determination to meet certain criteria or standards, or individual commitment of each educational institution/ faculty.

It is very difficult to provide a definition of quality in higher education, out of many attempts to establish a culture of quality in various education systems. Although the definition of quality in education is not unified, knowing its essence is of key importance to the education quality assurance. Stakeholders in higher education, according to Srikanthan, could be grouped into four categories, each providing its own perspective on quality: funding bodies (state authorities, including tax payers, private parties and all those who ensure the provision of faculty's services), employees of the education sector (professors and other academic and administration staff), students (users of services) and users of output (employers seeking for the well qualified employees) [1]. Quality assurance could be then considered as set of processes, policies and actions performed externally by the accreditation or certification bodies or internally, within the institution [2]. There are several methodologies to measure and guide quality assessment and improvement in various organizations. Some of methodologies that are internationally recognized and validated are ISO standards, mostly ISO 9000, Balanced Scorecard and EFQM Excellence Model [3].This paper mainly concerns the role and importance of ISO standards implementation in faculties of mechanical engineering, especially related to the establishment of the quality and laboratory managements systems.

II. Activities of the Higher Education Institutions in the Field of Mechanical Engineering

Higher education activities, their scope, framework and possibilities of commercialization in Serbia, are regulated by the Law on higher education [4], defining also the institution that are in charge for carrying out those activities in various scientific fields. The subject of this paper are educational institutions in the field of mechanical engineering, whose ranges of activities are wide and provide many opportunities for their commercialization.

In Serbia, the higher education activity in the field of mechanical engineering is covered by five state owned faculties, operating in the group of technical and technological sciences within three Universities: Faculty of Mechanical Engineering University of Belgrade, Technical Faculty in Bor University of Belgrade, Faculty of Technical Science University of Novi Sad, Faculty of Mechanical Engineering University of Nis, Faculty of Engineering University of Kragujevac and Faculty of Mechanical and Civil Engineering in Kraljevo, University of Kragujevac.

Each of these educational institutions has its own foundation acts, statutes and other general acts, prepared in accordance with the statutes of the University of Belgrade, Novi Sad, Nis and Kragujevac, and general

legislation in the field of higher education activities at the republic level and other acts prescribed by the Ministry in charge of higher education affairs.

Higher education in Serbia is aimed to transfer scientific and professional knowledge and skills and to develop science through the activities of scientific research, which support the expert and consultancy activities, publishing activities and other activities that can contribute to the commercializing the outcomes of scientific, artistic and research work. The statutes of each of the abovementioned faculties prescribed the exact scope and range of activities that can be performed in certain institutions. Some of them are related to the education while others are focused on the commercialized use of the obtained knowledge during scientific research activities, grouped in accordance with the national classification of activities [5].

The analysis of the activities showed that the best classification of activities is presented in the Statute of the Faculty of Technical Science University of Novi Sad, where higher education activity is emphasized as core activity (field 85 educational activities in the national classification), while research and development are recognized as separate set of activities (field 72 professional, scientific, innovation and technical activities in national classification). The overall scope of their activities is complemented by classification set of activities named "others". It includes numerous activities that belong to the various fields of the national classification: publishing and multiplication of audio and video recordings, production, repair and installation of various machinery and equipment, retail of different goods, publishing activities, computer programming and related consulting activities, engineering activities and technical consulting, technical testing and analysis, information and internet services, management and related consulting services, market analysis, various legal, financial and business activities and activities of different kinds of associations. Other five faculties in the field of mechanical engineering provide only lists of activities with the corresponding codes from the classification, without grouping them in accordance with any other criteria. However, with minor differences, lists of faculties' activities are very close in their scope and range.

III. Quality of the Higher Education and Other Services in the Educational Institutions

Taking into account large number of faculties' activities, their synchronization and harmonization is necessary to provide required quality of educational activities, which is a priority, together with provision of good quality services other then educational, in order to position faculties as competent institutions at the local, regional or even global market [6].

Quality of education is primary regulated by the Law on higher education [4]. The National Council for Higher Education is in charge of activities that provide the development and enhancement of the quality of the higher education system through the alignment with European and international standards in education, proposal of norms and standards for the works of faculties, as well as measures aimed to improve higher education system. This Council also prescribes standards and procedures for both self-assessments and external appraisal of the quality of higher education system, which is additionally regulated by the Rulebook on standards for self-assessment and Rulebook on standards for external appraisal of the quality of higher education institutions, both published in National Gazette of the Republic of Serbia. The most important standards prescribe that the faculties establish their quality assurance strategy and determine the methods and procedures for ensuring the quality of their education systems. Based on this quality assurance strategy and complementary procedures for quality assurance, the inputs for the external appraisal are provided.

Standards for quality of higher education systems prescribed by the faculties and international standards for quality management systems prescribed by International Standard Organization (ISO) should not be confused. The quality of higher education system is regulated by Serbian legislation, and acting in accordance to these acts is obligatory for every higher education institution in Serbia. In this case, standard means certain level of the quality of services that is agreed to be acceptable by the Serbian regulatory authorities. ISO standards are internationally agreed by the experts in certain fields, and contain their concentrated knowledge formulated as guidelines with respect to well defined, field specific objectives. Acting in accordance with standards created by ISO related to the quality management systems is voluntary and precondition of their adoption is commitment of the top management as well as the overall staff of the educational institution to fulfillment of those standards' requirements. Also, the exact scope of the standard application should be unambiguously defined for each educational institution that implements certain standard, and its requirements are not limited to only higher education activities. To be more precise, their objective is provision of good quality services in relation to the faculties' activities, no matter how many and how complex the institutional processes are.

IV. ISO Standards Applicable in the Educational Institutions in the Field of Mechanical Engineering

The core activity in educational institution – higher education activity, could be significantly improved by the quality management systems implementation. The focus is then shifted from the quality of individual engagement of various professors and lecturers to the overall performance of the faculty. This new approach provides establishment of the quality assurance system and performance-related mechanisms [7]-[9]. However, the overall performance of the educational institution is also influenced by the realization of all other activities of this institution. Taking into account large number of institutions' activities there is a tendency to transfer models from private sector and corporate governance to the educational institutions.

Quality management standards developed and created by ISO could be used by the educational institutions as support to develop and enhance quality of all services that faculties provide in accordance with their core and other activities. As it was mentioned before, these standards are not obligatory, but their implementation can be useful as a tool for easier and more effective synchronization of all faculties' activities especially related to the establishment of the quality managements systems and quality assurance of their services.

The set of standards Quality Management Systems – ISO 9000 was developed to enable organizations to

improve customer satisfaction, continually improve their processes and maintain the efficient quality management system. This set of standards includes the following standards:

- ISO 9000:2015 – Quality Management Systems – Fundamentals and Vocabulary. This standard provides fundamental concepts, principles and vocabulary for quality management systems. It contains the terms and definitions that apply to all quality and quality management system standards.

- ISO 9001:2015 – Quality Management Systems – Requirements. This standard specifies requirements for quality management system when an organization needs to demonstrate its ability to consistently provide services that meet customer requirements and expectations.

- ISO 9004:2009 – Managing for the Sustained Success of an Organization – A Quality Management Approach. This standard is focused on effectiveness and efficiency of quality management system.

- ISO 19011:2011 – Guidelines for Auditing Management Systems. This standard provides principles of auditing, managing an audit program and conducting management system audits, as well as guidance on the evaluation of competence of individuals involved in the audit process [10],[11].

Out of the entire set of quality standards, only ISO 90001:2015 is envisaged for certification purposes and represents one of the generic standards. It distinguishes between the mandatory and non-mandatory elements. Mandatory requirements, include five sections of this standard, where general quality management system requirements are related to the organizational context and its understanding, internal and external issues related to its purposes, leadership or top management responsibilities (commitment) focused on stakeholders, quality management system planning, resource management, including infrastructure, work environment and human resources and continuous measurement, monitoring and improvement of the existing quality management system.

The institutional commitment is also important for standard ISO/IEC 17025:2017 – General requirements for the competence of testing and calibration laboratories, especially in cases when laboratory previously established quality management system [12]. This standard is applicable to all institutions that are in charge of laboratory testing and calibration activities, regardless of the size and number of staff. It is aimed to promote the confidence in the work of laboratories both nationally and around the world. Serbia is one of the countries where it is necessary to obtain accreditation by an independent, internationally recognized authority (Accreditation Body of Serbia) in order to provide proven quality testing and calibration services and to be deemed as technically competent. Usually, holding the accreditation is the only way for test or calibration results of the laboratories to be accepted by other laboratories, suppliers and regulatory authorities. This facilitate cooperation between all stakeholders, while the test and calibration reports can be accepted from one country to another, without the need for additional testing.

There are many challenges of the application of these two ISO standards in the educational institutions. The main difference is their applicability. While ISO 9001 fits to all types of institutions in all sectors, ISO 17025 is limited to the testing and calibration laboratories [13]. The similarity can be observed through the management system requirements of the standard ISO/IEC 17025, where two options to address these requirements were given: within the existing ISO 9001 quality management system, if any or within another quality standard, fulfilling the minimum management requirements.

Another very important issue related to the implementation of ISO 9001:2015 is process approach proposed by this standard. Process approach is recognized as one of the important benefits of its implementation. This is especially true in the case of educational institutions, since their core and other activities are not characterized by well developed and established interconnections. Usually some overlapping among activities appear, since they are more people than process oriented. Implementation of the process oriented approach for the quality improvement in educational institutions can contribute to the integration of various activities in order to meet common objectives, to improve effectiveness of the processes, to use all available knowledge in certain institutions, therefore to improve quality of the services.

V. Conclusions

This paper considers the activities of higher education institutions in the context of quality management system establishment and ways to improve faculty's services provided to all stakeholders. ISO created standards that can be used as tool for establishment of management systems including quality and laboratory management system: standards ISO 90001 and ISO/IEC 17025. Taking into account many advantages of ISO certification, it is very important that educational institutions recognize their significance for all their stakeholders, as well as advantages of their implementation. Both standards ISO 90001 and ISO/IEC 17025 could benefit from the implementation of another one, although sometimes, in the case of testing laboratories in educational institutions, only fulfillment of minimum quality management requirements, besides certification against SRPS ISO/IEC 17025 could be fair enough solution. However, certification against SRPS ISO 90001 provides wider framework for ISO/IEC 17025 implementation through better understanding of risks, organizational context and risk and process based thinking that lead to the long-term benefits for the institution, as well as improvements and advances in many aspects of its activities.

Also, the process approach proposed by standard ISO 9001:2015 can be used for the development, application and effectiveness improvements of the quality management systems. Educational institutions can take many advantages of this approach, which is not customary in this type of institutions. Besides making easier implementation of the quality management system, application of the process based approach can facilitate the implementation of any other management system in the educational institution. This is especially true given the growing need to apply other non-quality standards, for example information system security management system, business continuity management system, energy management system etc. Finally, ISO recently developed a completely new standard ISO 21001:2018 Educational organizations – Management system for educational organizations – Requirements with guidance for use, which represents new challenge for educational

institutions that need to enhance satisfaction of learners, other beneficiaries and staff, improve their educational systems and demonstrate ability to support the acquisition and development of competence through teaching, learning and research.

REFERENCES

[1] G. Srikanthan, and J. Dalrymple, "Developing alternative perspectives for quality in higher education," International Journal of Educational Management, vol. 17 no. 3, pp. 126-136, 2003. DOI: 10.1108/09513540410538859.

[2] L. Schindler, S. Puls-Elvidge, H. Welzant, and L. Crawford, "Definitions of Quality in Higher Education: A Synthesis of the Literature," Higher Learning Research Communications, vol. 5 no. 3, 2015. DOI: 10.18870/hlrc.v5i3.244.

[3] M. J. Rosa, C, S. Sarrico, and A. Amaral, Implementing Quality Management Systems in Higher Education Institutions, UK: IntechOpen, 2012. Doi: 10.5772/intechopen.33922.

[4] Law on higher education, National Gazette No. 88/2017, 73/2018, 27/2018 – other law, 67/2019 and 6/2020 – other law

[5] Regulation on the classification activities, National Gazette No. 54/2010

[6] D. Matorera, Quality Management Systems in Education, Quality Management Systems - a Selective Presentation of Case-studies Showcasing Its Evolution, UK: IntechOpen, 2018. Doi: 10.5772/intechopen.71431.

[7] D. Geun Choi, H. J. de Vries, "Standardization as emerging content in technology education at all levels of education," International Journal of Technology and Design Education 21, pp: 111-135, 2011.

[8] G. Keller, "The Importance Of ISO Certification For Academic Organizations," Monarch Business School Switzerland, July 2019.

[9] SRPS ISO 9001:2015 Quality Management Systems – Requirements, Institute for Standardization of Serbia, 2015.

[10] A. Lazarevic and V. Protic, "Customer satisfaction as ultimate goal of quality management," Insurance Trends, no. 1, pp. 83-94, 2017. Doi: 10.5937/tokosig1903035L.

[11] N. Hampson-Jones, Higher Education and Standardization: Knowledge Management between Generations, UK: BSI Groups, 2011.

[12] SRPS ISO/IEC 17025:2017 – General requirements for the competence of testing and calibration laboratories, 2017.

[13] V. Valdivieso-Gómez and R. Aguilar-Quesada, Quality control in Laboratory, Quality Management Systems for Laboratories and External Quality Assurance Programs, UK: IntechOpen, 2018. Doi: 10.5772/intechopen.69623.

THE 5th INTERNATIONAL CONFERENCE
MECHANICAL ENGINEERING IN XXI CENTURY

December 9-10, 2020
Faculty of Mechanical Engineering in Niš, Serbia

A New Risk Management Model for Auto insurance in Serbia

Ivan RADOJKOVIĆ, Branislav RANĐELOVIĆ

First Author affiliation: Dunav Voluntary Pension Fund, Karadžićeva 8, Niš, Serbia
Second Author affiliation: University of Niš, Faculty of Electrical Engineering, A.Medvedeva 14, Niš, Serbia
ivan.radojkovic@dunavpenzije.com, branislav.randjelovic@elfak.ni.ac.rs

***Abstract* — Importance of automotive industry is significant in every country and economy. It affects the economic development of the country, and in last decade, the number of vehicles has been increasing every day, and hundreds and millions of vehicles are now traveling around the world. As a consequence, motor vehicle insurance is one of the most important branches of insurance. In this paper, we consider a general risk management model of motor vehicle insurance that is actual in Serbia. We propose change of this model and a modification in order to reduce the risk in car insurance, as well as to provide insurance to users with better service, in accordance with characteristics of vehicles. Modification of risk management model is based on mathematical approach and appropriate data analysis.**

***Keywords*— motor vehicles, car insurance, risk management**

I. Introduction

For motor vehicle insurance in Serbia, only the cubic capacity of the vehicle is taken into account. However, as the amount paid by the insured when concluding a vehicle insurance contract should be directly proportional to the probability of collecting the insurance premium, ie to the probability of vehicle damage (ie the probability of an accident), it is desirable to consider whether there are more some factors that significantly affect the possible occurrence of a traffic accident. The following question naturally arises: Can driving style be one of the key factors?

Let's consider two different types of drivers, the first - a driver who drives in accordance with the regulations and the second who drives arrogantly. It happens that second one often exceeds the speed limit, does not respect traffic regulations and / or drives under the influence of alcohol. It is clear that the other driver endangers the traffic with his behavior and thus increases the probability of a traffic accident, while the number one driver is a conscientious participant in traffic.

However, when concluding the insurance contract, the driving history of the insured is not taken into account, ie the number of penalty points in the driving card of the insured. The number of penalty points is currently the only quantitative measure of the behavior of the observed traffic participant. It is logical that drivers without penalty points represent exemplary participants in traffic, while drivers with a large number of penalty points most likely belong to the class of arrogant and reckless drivers. Therefore, it is desirable to make several classes of drivers in relation to the number of penalty points.

Risk management is management approach aimed at preserving the assets and profit power of the company while preventing the risk of loss, especially accidental and unforseen losses.

II. Penalty points as a key factor in the probability of a traffic incident

It is not possible to do a statistical analysis that would confirm that there is a significant difference in the percentage of accidents in persons with a higher number of penalty points, compared to persons who do not have (or have significantly less) penalty points, because data on the number of penalty points of the insured do not exist in the table submitted by AS non/life insurance, joint stock insurance company, for 2011.

However, in order to show that in the general case there is a statistically significant difference in the prevalence of accidents between these two categories, the Nis SUP was asked for data on the number of traffic accidents in 2013, as well as the number of penalty points from the same year. The following data were obtained:

TABLE I Number of Penalty Points

Registered motor vehicles in 2013	Drivers who had a car accident in 2013	Drivers with penalty points in 2013	Drivers with penalty points before the traffic accident in 2013
97248	2348	2084	314

Based on statistical analysis of the data, the following was obtained: there is a statistically highly significant difference in the percentage of accidents between the group of drivers who had previous penalty points and those who did not have it χ ^ 2 = 1441.53; OR = 8.12 (7.13 <OR <9.25) 95% confidence interval.

TABLE IIIII Results of χ^2 test, which compares the prevalence of accidents in the group of drivers who already had penalty points compared to those who did not

	χ^2-test	p
uncorrected	1447.05	<0.001
Mantel – Haenszel	1446.99	<0.001
Yates corrected	1441.53	<0.001

It is concluded that if penalty points were recorded during the conclusion of the contract, there would actualy be multiple benefits. Namely, if the number of penalty points were introduced as an additional coefficient in the proposed logit model (or in an existing one), the price paid by a conscientious traffic participant would be significantly lower than that paid by an arrogant driver. This would not only reward a conscientious driver, but would also motivate other categories of drivers to behave in accordance with the regulations.

III. Model Testing

In this section, we will compare the new model, with existing models that are current in Serbia, Germany, USA and the world. Since we have already presented all the above current models, we immediately start the analysis.

Models for assessing insurance risk in the automotive industry will be studied. As there are currently no developed methods for risk assessment in the domestic car insurance market, ie when insuring vehicles in Serbia, engine power is taken into account as the only risk factor, vehicle insurance in developed countries will be considered here. Germany will be considered as the representative of the largest European economic power. Then, the world economic giant of the United States of America will be considered, and finally the model of Pay-As-You-Drive motor vehicle insurance.

The German car insurance market is characterized by high competitive pressure, and therefore low profitability. In Germany, insurance risks in the automotive industry are traditionally classified on the basis of a large number of risk factors, such as, for example, the occupation of the driver, the type of car and the region. In addition, there are different bonus-malus classes, depending on the previous history of compensation. The bonus-malus system is considered to determine the amount of motor third party liability insurance premium by applying the appropriate premium system, depending on whether the insured had previously reported damage under this insurance for that vehicle, for which he is responsible. The bonus represents a reduction of the basic car liability insurance premium, if there was no damage during the insurance period of at least one year. It is calculated annually, when paying the premium, in a certain percentage. The bonus adjusts the premium to individual risk, because it has been proven that policyholders, who are granted this discount in advance by the insurer, have a significantly lower number of claims than other policyholders. Malus represents an increase in the basic premium if there were reported claims in the previously observed period. So, it is a loss of bonus or a premium supplement paid by the insured, if at least one damage for which the insured is responsible has been reported.

Therefore, risks are determined on the basis of several thousand different tariff classes. The problem that arises within this approach is the difficult fragmentation of data from many classes, which contains only a few risks and often shows little or no data on damage, which makes it difficult to calculate an adequate risk price based on damage history for these tariff classes. So far, several methods have been used to overcome this problem. For example, cluster analysis identifies tariff classes with similar expected claims, in order to achieve a better basis for calculation [1]. Other methods include interpolation [2] or the use of a larger database [3].

On the other hand, the US insurance market uses an approach called “scoring insurance” [4]. Insurers derive one "insurance score" for each potential that is secured by weighting, ie searching for the mean values of certain characteristics of the applicant's credit history, for example, the number of arrears of loan payments [5]. The basic credit record was obtained from a major national credit information provider. The insurance company uses such a score in combination with other factors, in order to assess the risk of insuring the applicant's car. The main reason for using credit history data is to obtain information, which will facilitate the assessment of inconspicuous factors, such as driving caution [5].

Motor vehicle insurance is usually considered a fixed cost in relation to the use of vehicles, ie. drivers do not see insurance savings if they reduce mileage. Distance-based or Pay-As-You-Drive or Per-Mile motor insurance converts the cost of insurance into variable costs, so that the insurance premium is directly related to the annual mileage [26]. Many organizations are exploring ways to implement Pay-As-You-Drive insurance to achieve a variety of planned goals, including increasing accessibility, saving savings, traffic safety, and reducing exhaust emissions [6].

Several insurance companies offer this insurance [7]: Aioi Insurance (*www.ioi-sonpo.co.jp*), Japan; Aryeh (*www.aryeh.co.il*), Israel; Holland PAYD Coverage (*www.payasyoudrive.co.za*), South Africa; MileMeter (*www.milemeter.com*), US; MiDriveStyle (www.miway.co.za/midrivestyle), South Africa; Pago Por Uso (*www.jovenesdesiguales.com*), Spain; *MyRate* (*www.progressive.com/MyRate/myrate-default.aspx*), USA; PAY PER K Coverage (*www.nedbank.co.za*), South Africa, Polis Vor Mij ("Policy for me") (*www.PolisVoorMij.nl*), The Netherlands, Polis Direct Kilometre Policy (*www.kilometerpolis.nl*), The Netherlands, Progressive, Real Insurance PAYD (*www.payasyoudrive.com.au*), Australia.

As a starting point for the theoretical testing of all models, we will take the SWOT analysis and use a matrix of four elements.

TABLE IVVVI German model based on characteristics-tariff classes

Model power A large number of tariff classes	**Weakness of the model** Poor definition of tariff classes
Chances of the Model An analysis of many tariff classes can look at a wide range of insurance	**Model threats** It works if there is a sufficient amount of data across the considered tariff class

TABLE VIIV US model based on credit history

Model power One criterion	**Weakness of the model** Inaccuracy of criteria
Chances of the Model Combination with another criterion	**Model threats** Combination with another criterion

TABLE V Model used in several countries based on milleage

Model power One criterion	**Weakness of the model** Expensive ancillary equipment and maintenance

Chances of the Model	**Model threats**
Combination with another criterion	Non-acceptance of criteria by the insured

TABLE VVIII CURRENT SERBIAN MODEL ON COMPULSORY CAR LIABILITY INSURANCE

Model power	**Weakness of the model**
Two criteria	Inaccuracy of criteria
Chances of the model	**Model threats**
Combination with another criterion	Dissatisfied policyholders

TABLE VIXX NEW PROPOSED MODEL

Model power	**Weakness of the model**
Three criteria	Legal incoherence of criteria
Chances of the model	**Model threats**
It gives a more realistic price of compulsory car insurance	Dissatisfied policyholders

If we compare the elements from the matrix, we conclude that the application of the first, second and third models in Serbia is not possible for several reasons. The first model has the disadvantage that it has many tariff classes and that a large amount of data is needed to be applicable in Serbia. The second model, which is based on the credit indebtedness of the insured, is inapplicable for several reasons, the first to insure insured persons who do not have credit indebtedness, the second, information on credit indebtedness is a personal matter of the individual, the third, 7.3% of the population is late (May 2016, UBS, www.ubs-asb.com), whereby these citizen insured persons are automatically penalized for buying more expensive insurance.

The third model is based on the kilometers traveled, if we assume that the average premium of compulsory car insurance in 2015 was 11,935.00 dinars (Association of Insurers of Serbia, Review of achieved results in motor third party liability insurance in 2015, www.uos.rs), and the price for GPS tracking of kilometers traveled by cars (www.gpspracenje.co.rs) is 85 € plus 20 € fines and monthly subscription for the service of using the vehicle tracking system is 7 €, annual overpayment 84 €, which is a total of 189 € or RSD 23.323,36, it is concluded that the model is economically unprofitable.

The fourth model is the current model of compulsory car insurance - car liability in Serbia, which is based on two criteria of engine power of the insured vehicle and bonus malus system, the current bonus malus system adjusts tariffs according to previous experience, sanctioning compensation with higher premiums compensation by reducing premiums. In other words, if there is compensation, the insured pays it, at least in part, through a higher premium, which should create an incentive to drive more carefully. A simple model that allows careful drivers a lower premium of compulsory car insurance, but does not consider drivers who have or do not have penalty points.

The proposed model is essentially an upgrade of the existing model of compulsory car insurance, which includes the third criterion, which is the criterion of penalty points. By including this criterion, the level of insurance is raised to a higher level, where risky drivers with penalty points are penalized, and drivers without penalty points are rewarded. This model would surely make drivers be even more careful in the driving process itself.

IV. CONCLULSION

Risk is a multifaceted, multidimensional concept that is present in human life on a daily basis. In the broadest sense, risk is uncertainty about the outcome, ie the probability that the outcome will be unfavorable. Wherever there is human activity related to facilities, machines, technologies, and above all traffic, there are also risks. Therefore, risk management has always attracted great attention, both from researchers and scientists, as well as economists and engineers. The main task of this paper was to propose a new model for risk management in auto insurance, which would be more optimal compared to the current model. The proposed model aims, first of all, to directly connect the probability of accidents for a certain category with the price of insurance premiums, which would result in a reduction in the number of casualties in traffic accidents, and thus to reduce the number of paid damages. In order to create such a model, it is necessary to recognize the criteria that affect the occurrence of risk, many of which have not been taken into account so far when concluding contracts on compulsory car insurance.

Risk management is an integral part of the successful business of an insurance company and its market positioning. So far, not many characteristics of drivers or vehicles have been recorded in Serbia, but some basic data are still available. Using currently available data: vehicle age, driver age, driver gender and vehicle cubic capacity, a new insurance premium model was proposed. Namely, using logistic regression, based on the factors listed, the probability of accidents for the appropriate class was calculated. Based on this probability, an insurance premium could be determined, e.g. by multiplying the probability by some fixed value. In this way, the price of insurance would be obtained, which is directly proportional to the probability of an accident, which further results in a suitable model for determining the premium. Unfortunately, due to the small amount of data available to insurance companies, an ideal model cannot be obtained. For example, it has been assumed that the number of driver penalty points is directly related to the probability of an accident, which means that more careful drivers cause far fewer traffic accidents than violent and careless drivers. Until now, this data was not available to insurance companies. Therefore, the main proposal when defining the new model was that the number of penalty points for drivers must be taken into consideration. This new model would not only be more suitable for both insurance companies and insurance users, but would also motivate drivers to behave in accordance with regulations, to adapt their driving to environmental conditions, which would reduce the number of traffic accidents.

The conclusion is that, if penalty points were recorded when concluding the contract, there would actually be multiple benefits. Namely, if the number of penalty points were introduced as an additional coefficient in the proposed logit model (or in an existing one), the price paid by a conscientious traffic participant would be significantly lower than that paid by an arrogant driver. This would not only reward a conscientious driver, but would also motivate other categories of drivers to behave in accordance with the regulations.

The authors are of the opinion that the current system of compulsory motor vehicle insurance in Serbia needs to be modified, the only question is whether this is waiting for better times.

REFERENCES

[1] C. A. Wiliams, R. M. Heins, "Risk Management and Insurance". McGraw-Hill Book Company, New York, 1976.

[2] C. Dugas, Y. Bengio, N. Chapados, P. Vincent, G. Denoncourt, J. Fournier, "Statistical Learning Algorithms Applied to Automobile Insurance. Singapore", World Scientific Publishing Company, 2003.

[3] B. Matijević, "Osiguranje Management-Ekonomija-Pravo", Naklada Zadar, 2010.

[4] R. P. Hartwig, C. Wilkinson, "The Use of Credit Information in Personal", Insurance Issues Series, 2003.

[5] U. Mayer, "Third Party Motor Insurance in Europe", Bamberg, University of Bamberg, 2002.

[6] I. Kovačević, "**Verovatnoća i statistika sa zbirkom zadataka**" Beograd, Univerzitet Singidunum, 2011 (in Serbian)

[7] I. D. Radojković, "**Model upravljanja rizikom u auto osiguranju"**, Doktorska disertacija, Univerzitetu Nišu, Mašinski fakultet, 2016 (in Serbian).

THE 5th INTERNATIONAL CONFERENCE
MECHANICAL ENGINEERING IN XXI CENTURY

December 9-10, 2020
Faculty of Mechanical Engineering in Niš, Serbia

Reengineering of Aluminium Melting and Casting Plants in Aluminum Processing Factory

Dragan TEMELJKOVSKI[1], Marko PAVLOVIC[2], Stojanče NUSEV[3], Dragana TEMELJKOVSKI NOVAKOVIĆ[4]

[1] Faculty of Mechanical Engineering, University of Nis, Aleksandra Medvedeva 14, 18000, Niš, Serbia
[2] Aluminium processing plant "Alu Holding" d.o.o. Niš, Bulevar Sveti Car Konstantina bb, Niš, Serbia
[3] Faculty of Engineering, University St. Kliment Ohridski Bitola, I. L. Ribar bb, Bitola, Macedonia
[4] Research and Development Center "ALFATEC" Bulevar Nikole Tesla 63/5, 18000, Niš, Serbia
temelj@masfak.ni.ac.rs, marko.pavlovic@aluholding.rs, stojance.nusev@uklo.edu.mk, draganatemeljkovskiarh@gmail.com

***Abstract*— This work shows the process of producing melting aluminum and casting of aluminum billets in the foundry of aluminium processing plant Alu Holding d.o.o. Niš by phase, as well as what are the success factors and risks in the development of this semi-product/product. The main causes of production problems that arise through different tools and methods have been analyzed, in order to find adequate solutions to reduce and eliminate them, as well as the ability to invest the company in automating this production process by purchasing a new casting table in the electromagnetic field, which would reduce the biggest production problem – scrap, reduce workplace injuries and ultimately improve overall operations. Finally, proposals for improvement – foundry reengineering, investment in its automation, as well as expectations and goals of implementing them are shown.**

***Keywords* — foundry, reengineering,** SWOT analysis, **Pareto diagram.**

I. INTRODUCTION

In terms of globalisation of markets, great competition and a dynamic environment, it is difficult to single out with its offer and ensure the constant growth and development of businesses. Business success depends on the ability to continuously adapt to such an environment, while continuously improving the production and business processes, and that in accordance with the changes in market needs, ideas about a new product are generated, a wider assortment that would satisfy needs at an acceptable price.

There are several approaches to improving processes in production systems, such as: continuous improvement of business processes, redesigning existing processes, or grouping activities within the process, or overall reengineering. In other words, processes can be improved

gradually, redesigned to the maximum, or fundamentally modified to achieve maximum efficiency. Choosing an approach to overcome individual problems depends on what is wrong and what gains are expected. There are also various methodologies and models used to improve business processes in companies. Implementing such methodologies is unthinkable without the application of various methods and quality tools.

This work will show the reengineering of aluminum bile production processes through different phases in order to improve them, shorten the duration of the process, increase process efficiency and reduce costs, and display a few quality tools. It also shows the possibility of investing the company in automating this production process by purchasing a new casting table in the electromagnetic field and the impact on scrap reduction, and the impact of reengineering on employees and the way their work is managed.

II. THE PROCESS OF ALUMINIUM PRODUCTION

In order to better understand the production process, to analyze and document processes and activities in the organization and facilitate the identification of opportunities for improvement, it is necessary to first show the process of melting aluminium and casting billet in the foundries in stages, shown on Figure 1.

Fig. 1 Aluminum billets

After the delivery of the material, its validity is checked according to the specification, where the type, weight and chemical composition are included, after which the material is sorted according to its chemical composition. It is received in the warehouse and material receipt is made, this is done in an outdated information system. The warehouse men are responsible for this activity. The process of producing aluminum bile consists of the following operations and procedures:

1) *Operation I – Production preparation:* Under production preparation: a range of activities in order to provide production: procurement of materials for production, receipt and sorting of materials, production of recipe by technological craton for the requested alloy, preparation of materials for melting (measuring materials in accordance with the recipe), maintenance of machines and aggregates in the plant. The head of the foundry is responsible for preparing the production, while the responsible executor is the foreman.

2) *Operation II – Preparation of aggregates:* Preparation of aggregates is an action of preparing a technological line to work according to the following instructions: instructions for working on the idling furnace, instructions for working on the foundry machine "Kalamari", instructions for working on the oven for homogenization, instructions for working on the saw "Asimax". The head of the foundry is responsible for preparing the aggregates, while the executors and operational workers are responsible.

3) *Operation III – Melting:* The melting process is done according to the melting instructions. In this process, the smelter performs the following activities: to the melting sting stinger already prepared material for melting, clips handmade aluminum material and legitimate elements in order given in the recipe, during the melting symmetry and compensates for the strength of the furnace according to the amount of melted material, when the melting is achieved it raises the temperature of the foundry, degassed, removes slag from the wall and backward slag, upon completion visually controls the wall of the furnace and cleans the furnace, on all notable irregularities in the work of the furnace informs the shift manager, shown on Figure 2. The manager has been responsible for the melting process, while the responsible executor is the smelter. Upon completion of the meltdown, the foreman enters the melting data into the daily production report, after which the administrative worker enters that data into an outdated information system.

Fig. 2 Melting Aluminium

4) *Operation IV – Casting:* The casting process is done according to the casting work instructions. In this process, the foundry performs the following activities: prepares the casting machine and the casting pathways, controls the correctness of the casting tool (crystallizer), before casting sets the filter in the filter box and heats it with a hand burner, controls the correctness of nozzle in jet clips, pours billets on the work to-do, performs visual control of the surface of the bile during casting, follows and corrects the specified casting parameters, after casting cleans the left, extracts and marks the bile with a dry stamp (alloy label and number of clip), clean jet clip, filter box and left, shown on Figure 3. The foreman and casting leader are responsible for the casting process and the quality of the bill, while the executors of the jobs and the casting are responsible. Upon completion of casting, the jobs enter casting data in the daily production report, after which the administrative worker enters that data into an outdated information system.

Fig. 3 Casting aluminum billets

5) *Operation V – Shortening:* The process of shortening the billets is done according to the briefing instructions. After casting, the billets are delivered to the tester for shorter bile, where the saw shortens the fuselage according to the specified specification from the work to-do. In this process, the tester performs the following activities: performs visual control of the surface of the bile and bile with bad surfaces and cold welds discarded in scrap, the beginning and end of the bile discards 150mm, From each clip, he cuts a single billet by taking a sample (disc) for chemical analysis on which he types the alloy and the number of the clip, the control takes the disk and takes it to the lab for testing, shortens the bile lesser in the basket, re-marks each bill and puts it in the homogenization car, takes care of the validity of the saw leaf and changes it when it deems it necessary, places empty bags for scraping. The foreman was responsible for the short-term process, while the responsible executor was a saw. Upon completion of the briefing, he enters the cut data into the daily production report, after which the administrative worker enters that data into an outdated information system.

6) *Operation VI – Homogenization:* The homogenization process is done according to the instructions for homogenization. In this process, the auxiliary worker in the foundry performs the following activities: after a short eruption, the fuselage is disposed of in the homogenization car, homogenization is performed according to previously specified technological parameters that define the temperature and time of homogenization, as well as the way of cooling the bile after homogenization is completed. For the process of homogenization of bile, it is responsible for the manager who is obliged to write in the daily report on achieved production the date and time of the beginning of homogenization, as well as the date and time of completion of homogenization, the specified temperature of homogenization and the alloy code.

7) *Operation VII – Troop surrender:* After the complete production cycle is completed, the billets are

delayed after ultrasound control. The process of handing over finished billets is financed by order to hand over semi-products after quality control is agreed to. The head of the foundry is responsible for the accuracy of all previously entered bile data, while the responsible executor is an administrative worker who, by checking all previously entered data in the information system, generates all documents and produces a surrender order.

III. REASONS TO APPLY REENGINEERING

Reengineering business processes is a fundamentally change of thinking and understanding of business where first and foremost a decision is made on what, and then how to do, and ultimately what should be the result of this design of a whole new way of executing business, technological and other processes. The primary goal of reengineering is to optimize efficiency and effectiveness, which includes cost reduction, quality improvement, increased production and increased speed of work.

The ability to quickly adopt innovations, market needs, technological development, consumer trends and competition initiatives is a trademark of organizations that use reinventing and reinventing [1].

In order for the company to identify current and future possibilities and threats, but also the advantages and weaknesses in the market game, it must scan the environment [2]. The purpose of such an analysis is to identify strategic factors, external and internal elements that will decide the future of the company and is called the SWOT analysis, which is shown in Table 1.

TABLE I. BOARDS AND SWOT ANALYSIS

Advantages
1) Tradition - in the processing of aluminum and production of 64-year-old Al products Alu Holding Ltd. has acquired the complete production of over 6,000 finished products that include al rod and al-profile production, as well as surface protection and processing of them; **2) Quality** - is an absolute imperative that has been continuously worked on since its inception as evidenced by the following certificates: ISO 9001:2015, ISO 140001:2015, Qualanod, Qualicoat, CE 2787; **3) Aluminum processing** - all products are made of aluminum and there is a constant trend of increased demand for aluminum products at the global level; **4) Market** - expanded distribution network in RS and especially abroad given the status of the predominant exporter we have (Germany, Austria, Italy, Czech Republic, Spain, Bulgaria, Slovenia, etc.).
Weakness
1) Information system - The existing information system does not include all business processes as well as operations tracking processes and as such is not adequate. Implementation of the ERP and DMS is necessary (there are already negotiations and supplier offers for implementation of the new information system); **2) Digital presence** - not developed enough, especially visibility abroad.
Chance
1) Business model innovation - for most industries business models change. Pushing market boundaries and independently developing brand new business models using new technologies is a major challenge for many companies and an important opportunity in the coming years (bringing innovation into business through a new information system, opening new channels of acquisition and sales); **2) Credibility and reputation** - product quality and reliance on forces such as tradition - can be used for "social proof" that is, testimonials; **3) Costumer journey** - mapping the path the client passes in interaction with the Alu Holding brand to work to improve customer experience, increase loyalty, develop a new model of lido generation and win over clients online; **4) Channel - omni channel** - opening new channels of marketing and communication and integrating them creates a favourable environment for a more efficient way of working as well as more opportunities to reach new clients.
Threats
1) Digital presence - following global market trends this trend can be an opportunity for the company and ignoring long-term threats because other companies may be more visible; **2) Training & further training** - it is important to follow the need for continuous improvement of employees and overcome the slow adaptation of a number of employees to the use of new technologies.

Also, using the Pareto diagram, it is possible to identify some sources of problems and detect where production delays are possible. One of the biggest problems in the production of the foundry is the higher quantity of scrap than the allowed level. Some of the important reasons that lead to scraping are: raw material quality, the complexity of the alloy of the billet that is produced, the legitimate errors (human factor), the propulsion failures, and the production planning errors. These are categories that need improvement to make the production process more efficient and effective. The impact of each of these factors on the production process in the foundries is different and for this reason it is important to identify the level of significance of each. The percentage of scrap that occurs in the foundry relative to total production for the previous year is shown on Figure 4.

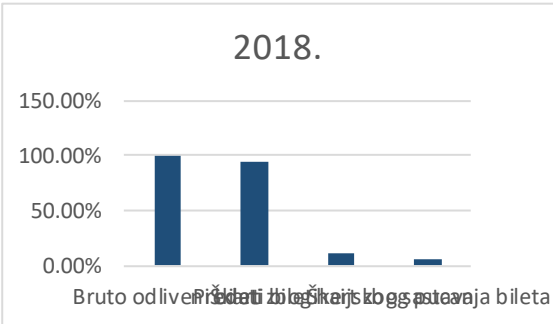

Fig. 4 Percentage of scrap in relation to the total production in the foundry in 2018.

By analysing the impact of these factors on the emergence of scrap in the production of foundry, we come to the conclusion that the biggest impact on the appearance of scraps has two factors – raw material quality and error in alloy (human factor), as shown in Figure 5. These factors take an 80% share in the overall percentage, and it is necessary to conduct a deeper analysis of the factors given in order to eliminate them or reduce their impact on the appearance of scraps.

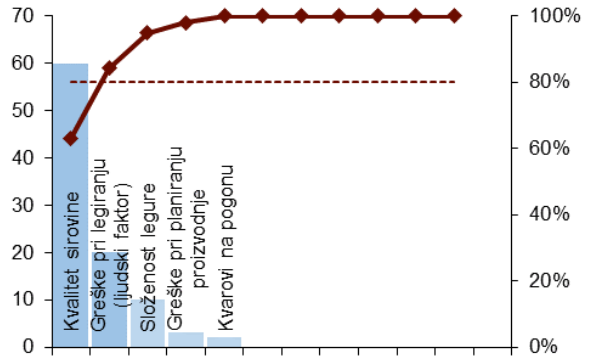

Fig. 5 Pareto display % of scrap-causing participation

A. Improvement measures

In order to increase the efficiency and productivity of the company, it is mandatory to use qualitative methodologies. One of the quality tools used not only in companies, but also in an individual's life, is called '5S'. This tool cleans, edits and organizes the workspace, separates the necessary items from unnecessary items, standardizes all workspace operations, and elaborates on maintaining improvements. The unregulated foundry workspace and the need to apply this quality tool are shown in Figure 6.

As the next measure of improvement would be the introduction of barcode readings that would be printed and pasted on raw material containers. By reading barcode codes through a reader connected via a modem to a computer network, it would automatically show what kind, quantity and chemical composition of the raw material sits in that container. The procedure would make time savings and dry data writing would be eliminated from the procedure.

Fig. 6 Indefinite workspace in foundries

In order for the production process to be continuous, it is necessary to order raw material with a certain percentage of surplus, so that billets in a certain alloy can be produced immediately in sufficient quantity, and not to be additionally ordered, which is currently the case in the foundry. At the same time, tickets for the second alloy are produced due to the production flow, and when the raw material arrives, tickets for the first alloy are made again, due to the delivery deadlines. This requires changing the production program several times, where time is wasted but also disrupts the overall production plan.

To increase production quality, reduce errors and defects would introduce a change in the printing of lists by which a production worker chooses the raw material needed for ongoing production. It is not rare to find larger quantities of visually similar raw materials in the plant at the same time, especially when it comes to legitimate elements. These lists contain codes on the type, quantity and chemical composition of raw materials. It happens that workers make mistakes when taking raw materials (legitimate elements), because visual differences are difficult to notice. However, when this occurs, the chemical composition of the bile is completely adequate for the alloy. Such billets are scrap. To minimize such an error, only the code for a particular raw material would be printed on the lists. By doing so, the worker would not know what the raw material was, but would ask for a code with the correct chemical composition.

Applying reengineering would also introduce barcode readings on the data cards for the production, display on Figure 7. The reading would accurately know each produced billet, which alloy is in question, the exact chemical composition, mechanical properties, the number of the clip in which the billet was produced, and very quickly you can find out which of the workers made the mistake and when. Also, all card content would be archived in the electron database. In order for the whole system to be modem-connected, the control and extraction sectors would be easier to do, because reading the bill would know exactly how much an aluminum billet has arrived in the sector and no extra time would be wasted on controlling them.

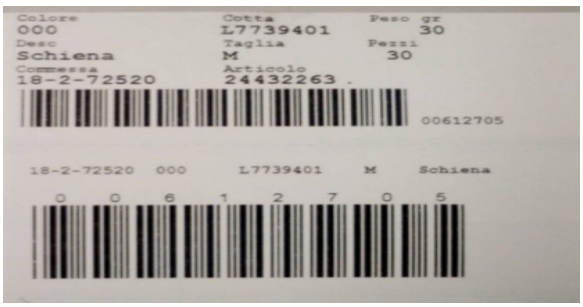

Fig. 7 Barode card

B. Investment activity

In the company's reengineering process, an important activity would be the purchase of a new casting table in the electromagnetic field ECT 8/8-HT that would fully automate the process of casting aluminum biles. The new founding table brings with it a significant step in the production of bile, a view given on Figure 8. Unlike the manual casting of the bile, on this machine the process of casting the bile is fully automated. This system consists of a casting plate in an electromagnetic field, with 8 founding places, a moving platform with commands and a system for distribution of levees. Because of the large number of founding sites, this system is more suitable in terms of maintaining the level and temperature of the founding in all crystallizers, and therefore the stability of the founding process. The very principle of electromagnetic casting improves the homogeneity of the drained structure, prevents the segregation of legitimate elements and the appearance of cracks in the billets. The system is constructed and mane used at the request of the purchaser and is easily adapted to existing induction furnace for melting. Financing of the new founding system would be done through Leasing arrangements, thus

making the company's working capital free to perform the continuous production process. If the company decides to buy a new foundry table, the total value of this investment with installation would be €88,000.

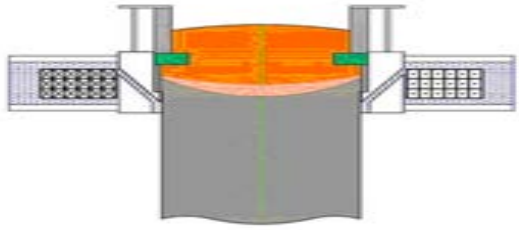

Fig. 8 Casting table in electromagnetic field ECT 8/8 - HT

IV. PRODUCTION REENGINEERING – NEW AUTOMATED PRODUCTION LINE

For all of these improvement measures to be successful, a detailed plan must be in place to implement them. All employees must be included, as it adapts to the new automated bile production system and the entire philosophy of the company needs to be changed. The new production system achieves the following:

Better quality of production – Once installed program does not need to constantly change and waste time for machine styling and time spent manually casting aluminum billets.

Higher production capacity – Automated production of bile requires less time than manual production of them, which ultimately requires more workers.

Fewer defects in production – With the new automated production line, the level of defects would decrease, because casting errors caused by human factor in this way are almost excluded.

Larger assortment of products – New way of automatic casting brings with it the possibility of producing new aluminum alloys and expanding assortment as well as a competitive position in the market.

Advantage for employees – In improved working conditions, adequate and permanent training of workers will be carried out, which in the new working conditions will be better felt and better functioned, because all work subjects will be in a specific and marked place, and as the most important advantage for employees by automating casting would significantly reduce the possibility of injuring employees.

Advantage for the manufacturer – The amount of waste material that requires re-treatment is minimised. Each billet is produced based on digital data programming, thus achieving that this production process is completely standardized.

Advantage for the customer – Shortening the casting time of aluminum bile leads to shortening the total time it takes to produce finished products, which significantly shortens the customer's waiting period for the ordered product. Automation of the process of casting aluminum billets as the greatest advantage for the customer has full standardization of bile production and an identical level of quality of all spilled billets.

Also, reengineering brings certain advantages by increasing the interest of employees in the company itself, improving internal co-operation, communication and team spirit, expanding employees' knowledge of the organization's orientation, its role in the market and its competition, and improving the compliance of employees' skills with their responsibility training and processes [3].

V. CONCLUSION

There is no formal procedure for properly implementing the reengineering process. This means that there are no regulations and phases that guarantee a positive outcome in the implementation of reengineering. In order to achieve the defined goals of reengineering, it is necessary to change the behaviour of employees, structures and how they influence individuals, to develop trust, better motivation, to bring in new values, new content, and this can be achieved, among other things, by changing the mental attitude of employees, the thinking scheme, philosophy and habits. One of the important preoccupations of each manager is the motto "every person in their right place", where organizational solutions enable achieving previously established goals only if each position is occupied by the appropriate person [4].

This paper presents the reengineering of the foundry in the aluminum processing factory Alu Holding d.o.o. Niš, through certain measures of improvement and quality tools, where the transition from manual work to an automated system is corrected and the organization of business is corrected, which reduces the possibility of production errors and the percentage of scrap. Then the work space is cleaned, arranged and organized, which leads to saving time used for unnecessary movement of workers, which leads to increased production efficiency. The advantages of automating this production process by purchasing a new casting table for casting in the electromagnetic field are less time for making aluminum tickets, reduction of scraps and a significant reduction in the possibility of injuring employees, which are quite common in manual casting. This reduces the number of workers needed in this production plant. The introduction of parallel processes strengthens the reengineering process, by increasing security in fulfilling obligations, actions and adopted plans, then shortens the time of completion of planned tasks and eliminates bottlenecks in production and achieves full employment of the engaged workforce. Every improvement of business processes implies the use of new knowledge, experiences and new ideas. To that end, it is necessary to constantly learn and use the available knowledge and available potentials. In the end, it can be said that the success of a company in the future will depend on the speed of human resources response to certain changes, employee competence and continuous learning [5].

REFERENCES

[1] M. Baumbac, “Small Business Management”, Prentice Hall, Inc., Englewood Cliffts, 2000.

[2] P. Milosavljević, “Inženjerski menadžment”, Univerzitet u Nišu, Mašinski fakultet, Niš, 2015.

[3] P. Jovanović, “Reinženjering poslovnih procesa”, Smederevo, 2010.

[4] D. D. Vesić, “Menadžment ljudskih resursa”, Beograd, 2006.

[5] D. Temeljkovski, M. Milovančević, D. Temeljkovski, S. Nusev, “Production Process Reengineering – Human Resource Management”, Faculty of Mechanical Engineering in Niš, The 3rd International Conference, Mechanical Engineering in XXI Century – Proceedings, Niš, 2015.

THE 5th INTERNATIONAL CONFERENCE
MECHANICAL ENGINEERING IN XXI CENTURY

December 9-10, 2020
Faculty of Mechanical Engineering in Niš, Serbia

Economic Challenges and Integration Engineering: The Smart Cities Context

Zorana KOSTIĆ

University of Niš, Faculty of Sciences and Mathematics
zoksinis@gmail.com

***Abstract*—The modern city development policy uses many new concepts including smart cities. In this regard, the implementation of the smart city concept has to be principally reasoned by ensuring higher efficiency and long-term sustainability. Understanding smart cities' importance has a fundamental role in facing new barriers, resolving problems and improving life quality. The aim of this research is to identify economic challenges and explore an engineering and managerial approach to the smart city concept. Smart cities are increasingly under pressure from challenges such as: high implementation costs, high energy consumption, integration of technology, smart management systems, infrastructure, and business changes. The special attention in the paper is devoted to the business process changes and using management tools, techniques, and approaches in the explanation a smart city as a large-scale enterprise.**

***Keywords*—Smart city, Economic challenges, Integration engineering, Business Process Change, Large-scale integrated enterprise**

I. INTRODUCTION

Development of the industry 4.0 has connected cities, improved collaboration among cities, but also created competition among them. The concept of smart city has been gaining popularity and cities have developed strong interest for transformation into smart cities. However, such transformation requires an appropriate approach. Achieving a state of smart can be challenging due to town is a complex system of systems with a dynamic environment.

Smart cities require integration engineering that represents integration of different heterogeneous systems, to optimise the use of technology in the transactions in a way which meets the current and future needs of their citizens. In addition, they require consideration of governance and growth, urban development and infrastructure, the business environment and natural resources, society and community. As urbanisation increases and technologies that offer the opportunity to improve city efficiency and quality of life come on stream at an accelerating rate, so it becomes necessary to ensure flexible and future-proofed city.

Smart cities effectively integrate the influence of physical, digital, and human systems; as well as institutional, technological and human factors. Therefore, they are characterised by having: smart economy, smart citizens, good governance, smart environment, smart mobility, data collection and management excellence, integrated and shared frameworks, efficiency and sustainability.

The real connection between characteristics depends on, how is the perception of their effect in the smart city model in the eyes of the city strategy implementers.

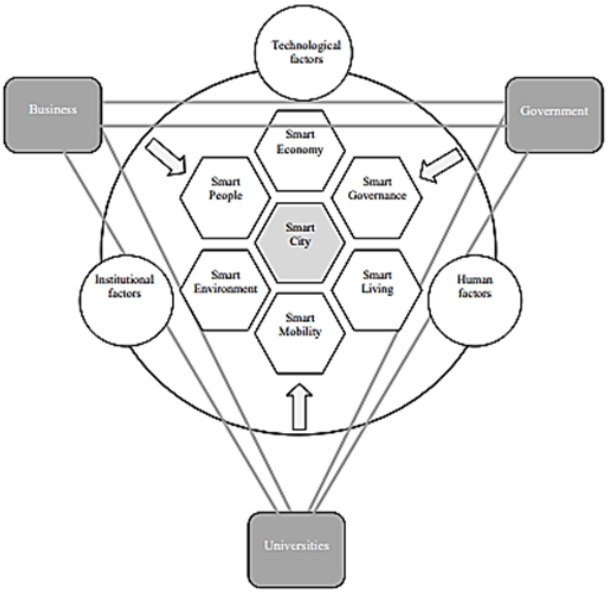

Fig. 1 An integrated approach to the smart city

Source: [1, pp. 782]

The smart city theory should lead to improving the living and business conditions on the basis of smart components involvement, interactions between these components [2] and also the action of each subject has to be considered. That's why it is possible to give the scheme of interactions between academic, business and political dimension (as shown in Fig. 1).

II. AN ENGINEERING APPROACH TO THE SMART CITY CONCEPT

The concept of smart city (SC) has been gaining popularity and cities have developed strong interest for transformation into smart cities. However, given that a city is a complex integrated system, achieving a state of smart city can be challenging. Many studies have covered the design and modelling of a smart city, but their focus has been mostly thematic and lack an integrated view of a

smart city system. Some authors have presented a methodology helped by a Model-Based Systems Engineering (MBSE) approach and Systems Modelling Language (SysML) to develop a model of an integrated smart city system. This model brings all subsystems to operate together in one system and focuses on the information perspective of a city [3].

Smart cities are cities that use integrated processes, and smart engineering to self-regulate its environment and operations. Using smart technologies that are connected through the Internet of Things (IoT), a smart city uses sensors to analyse its environment, and to respond to changes. Ahuja (2016) discussed new trends and paradigms in the smart city sectors and integration of nature and technology for smart cities [4]. Cities are complex, adaptive, social–ecological systems "characterized by a particular human settlement pattern that associates with its functional or administrative region, a critical mass and density of people, man-made structures and activities" [5].

Muvuna et al. (2016) defined engineering approach to design and modelling of smart cities [6]. The need for such integrated platform is driven by numerous factors, such as better monitoring of the city, gathering information from all sources for easy and fast access to information and fast reaction to incidents or any emergencies, dynamically acting on urban population needs, and having reliable information and services to the public for better decision making and efficient use of resources.

Smart city is a larger system that integrates elements of physical, human and technological infrastructures enabling ubiquitous use of mobile and virtual technologies. They use smart technologies to build and integrate critical infrastructures and services to increases in efficiency, effectiveness, transparency, convenience, and sustainability.

TABLE I TYPES OF SMART CITIES BY DIMENSION

Type	Characteristics	
Technological	New technological practice and services	Incremental innovation
Organisational	Internally in the government; project base	Incremental innovation
Collaborative	Public-private networks and partnerships	Radical innovation
Experimental	Innovative urbanism; citizen centric	Radical innovation

Source: [7].

The wave of innovation brings new interactive layers to cities, while it also simplifies and removes barriers from previous models. As shown in Table I, we distinguish: technological, organisational, collaborative, and experimental smart cities. Understanding the challenges and opportunities for smart cities implies the analyse of the most common obstacles to smart city development such as: lack of smart cities on short-term mindsets, lack of political will or lack stakeholder support.

III. ECONOMIC CHALLENGES TO THE DEVELOPMENT OF SMART CITIES

Like any emerging field, smart cities also face several genuine challenges that need to be addressed so they are briefly discussed below [8]:

1. *Implementation cost*: the development of smart cities involves technologies that are incurring huge cost.
2. *High energy consumption*: the sustaining of the technologies needed for running of smart cities requires high energy.
3. *Privacy and security*: privacy and security will play a very vital role due to people in smart cities will use smart city services with smart phones and computers that are connected through networks.
4. *Integration of technologies*: smart cities are fast emerging as a possible solution for brighter future prospects.
5. *Traffic management system*: traffic management systems range from need for a highly reliable and fast access protocol to data forwarding mechanisms for ensuring critical message transmissions that carry information regarding emergency situations on roads.
6. *Infrastructure***:** the key pillars are located in the interconnected sensors, intelligent transportation systems (metro, train, drones), public space with gardens, automatic and efficient lighting, gas system, water, telecommunication and infrastructure for energy sharing [9].
7. *Mobility*: It is very much essential to guarantee uninterrupted service to mobile users while shifting between different access networks.
8. *Scalability*: the limitations with respect to restrictions in storage, bandwidth and computational abilities that act as a hindrance to service providers while handling large number of users should not come in the way of proper functioning of the different services.
9. *Fault-tolerance*: this is a real challenge while designing smart cities as information and communication technologies should be implemented in such a way such that they are highly resilient to system failures.
10. *Upgradation*: This feature is true for the development of any technology and likewise for smart cities too. Upgrading a smart city will incur a huge cost as such a city is very much dependant on communication and technologies.

Some authors discuss how smart city systems could be holistically viewed as a complex system-of-systems, which characterizes: managerial independence of constituent systems, geographical distribution of constituent systems, evolutionary development, and inherent dynamicity [10]. A smart city system-of-systems can integrate both public and private heterogeneous, independent systems across different domains. Integration of different heterogeneous systems should support smart management in different areas. Cavalcante, Cacho, Lopes, & Batista (2017) emphasized some of the main challenges to the development of smart city systems such as:

- scale and inherent complexity,
- multitude of stakeholders,
- multiple disciplines and domains,
- heterogeneity and interoperability,
- unification on information,
- data granularity and data analytics [10].

IV. Business Process Change as one of the Economic Challenges for Smart Cities

Smart city development is a response to the need for flexibility and agility in delivering services to citizens. Thus, similar to systems integration in enterprises, integration of city systems provides access to real-time information and efficient services. In addition, Business Process Change (BPC) is essential for systems integration in smart city development. Similar to business process change in the private enterprises, there are a number of challenging dimensions in smart city development. Javidroozi et al. (2015) consider a city as a large-scale enterprise and attempt to design a business process centric model for city's systems integration. Business Process Change can be defined as analyse, redesign, and improve the existing business processes to achieve a competitive advantage in performance [11].

Four characteristics of systems integration are: interconnectivity, interoperability, semantic consistency, and convergent integration. Three of them are technology-oriented terms, but last one represents systems integration as a convergent of technology, people, process, and knowledge. In addition to functional and inter-organizational aspects, there are four dimensions of people, information and technology, management and structure for BPC. Some researches combine structure and management dimensions into a single managerial category. Moreover, this systems integration can be considered as a radical change in business.

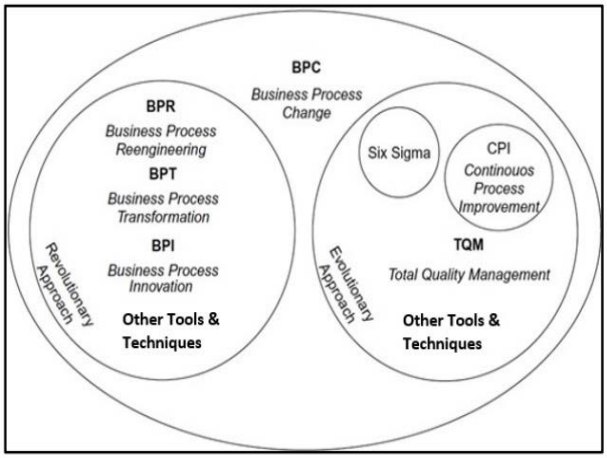

Fig. 2 BPC approaches and management tools

Source: [11] and [12]

Business Process Chance is a complex project, which is affected by enterprise's capabilities such as change management, project management, and IT, and needs to be managed and planned carefully. It is a task for improving business processes and performance. The enterprises and cities are threatened by many economic challenges, risks, and dimensions to go through a comprehensive BPC for systems integration. Therefore, paying attention to all dimensions of BPC especially for cities is essential. Practically, all management tools (Six Sigma, Total Quality Management etc.), techniques, and approaches (Revolutionary approach and Evolutionary approach) have also been developed to facilitate the procedure and address the economic challenges (as shown in Fig. 2). In addition, the success level of business process change depends on capabilities to address those economic challenges.

Smart City, as an integrated enterprise, represents a progressive and repetitive unification of technologies, human performance, operations, and knowledge of the enterprise as a whole. Moreover, any enterprise consists of systems such as finance, human resources, and sales. Likewise, a smart city encompasses a number of sectors/systems such as transport, health care, energy, and education [13].

V. Conclusions

Fast growing urbanization necessitated developing smart cities. This research considered that integrating city's systems is essential for smart cities in order to provide efficient, effective and real-time services for all citizens. The main findings show that smart cities are characterized by having: smart economy, smart citizens, good governance, smart environment, smart mobility, data collection and management excellence, integrated and shared frameworks, and interactions between academic, business and political dimension, as well as numerous institutional, technological and human factors.

The main findings confirm that smart cities integrate processes, and smart engineering to self-regulate its environment and operations. An engineering approach to design and modelling of smart cities can be very useful in modern conditions. Therefore, recent research in this area has showed how smart city systems could be holistically viewed as a complex system-of-systems.

The paper presents the division of smart cities according to key characteristics. It should be distinguished: technological, organisational, collaborative, and experimental smart cities. In addition, we provided and discussed some important economic challenges that might be on focus of further researches such as: high implementation costs, high energy consumption, and complex supporting infrastructure, integration of technologies, mobility, and scalability. More directly, this economic challenges can open opportunities on system design, engineering, and operation in smart cities.

The presented research considers smart city as a large-scale integrated enterprise and attempts to develop a framework for smart management monitoring. The special contribution of the paper is the highlighting Business Process Changes in smart city development, using management tools, techniques and integration engineering. Business Process Chance is a complex project, which is affected by enterprise's capabilities. Given the defined and described methodology, smart city can be understood as integrated system with progressive and repetitive unification of technologies, human performance, operations, and knowledge as a whole.

Acknowledgment

The paper is financed by Ministry of Education, Science and Technological Development of the Republic of Serbia, No. 451-03-68/2020-14/200124.

REFERENCES

[1] S. Rucinska, and J. Knetova, "Development planning optimalization of the Košice city in the context of the smart city and city region conceptions," The 5th Central European Conference in Regional Science, pp. 778-791, 2014.

[2] De Santis, R., Fasano, A., Mignolli, N., and A. Villa, "Smart city: fact and fiction," MPRA Paper No. 54536, 2014, https://mpra.ub.uni-muenchen.de/54536/.

[3] J. Muvuna, T. Boutaleb, K. J. Baker, and S. B. Mickovski, "A methodology to model integrated smart city system from the information perspective. Smart Cities," 2(4), pp. 496-511, 2019, https://doi.org/10.3390/smartcities2040030.

[4] A. Ahuja, and L.B. RCDD, "Integration of nature and technology for smart cities," pp. 200-210. Cham: Springer, 2016, doi: 10.1007/978-3-319-25715-0.

[5] I. Kaltenegger, and H.S. Fink, "Vision of Cities: From the Green City to the Smart City," Integration of Nature and Technology for Smart Cities, pp. 319-332. Cham: Springer, 2016.

[6] J. Muvuna, T. Boutaleb, S. B. Mickovski, J. K. Baker, "Systems engineering approach to design and modelling of smart cities," Proceedings of the International Conference, Newcastle Upon Tyne, UK, pp. 437–440, 2016.

[7] M. Nilssen, "To the smart city and beyond? Developing a typology of smart urban innovation," Technological Forecasting & Social Change 142, p.98–104, 2019. In OECD Smart Cities and Inclusive Growth, pp. 15, 2020.

[8] A. Ghosal, and S. Halder, "Building intelligent systems for smart cities: issues, challenges and approaches," In Smart Cities, pp. 107-125, Cham: Springer, 2018, doi: 10.1007/978-3-319-76669-0_5

[9] O. Thays, M. Oliver, and H. Ramalhinho, "Challenges for Connecting Citizens and Smart Cities: ICT, E-Governance and Blockchain," Sustainability 12(7), 2020, doi: 10.3390/su12072926.

[10] E. Cavalcante, N. Cacho, F. Lopes, and T. Batista, "Challenges to the development of smart city systems: A system-of-systems view," In Proceedings of the 31st Brazilian Symposium on Software Engineering, pp. 244-249, 2017.

[11] V. Javidroozi, H. Shah, A. Cole, and A. Amini, "Towards a City's Systems Integration Model for Smart City Development: A Conceptualization," 2015 International Conference on Computational Science and Computational Intelligence (CSCI), Las Vegas, NV, pp. 312-317, 2015, doi: 10.1109/CSCI.2015.10.

[12] M. C. Jurisch, W. Palka, P. Wolf, and H. Krcmar, H. "Which capabilities matter for successful business process change?" Business process management Journal, vol. 20(1), pp. 47–67, 2014.

[13] V. Javidroozi, H. Shah, A. Amini, and A. Cole, (2014). "Smart city as an integrated enterprise: a business process centric framework addressing challenges in systems integration," The Third International Conference on Smart Systems, Devices and Technologies in Paris, France. pp. 55-59, 2014, doi: 10.13140/RG.2.1.2561.1921.

THE 5th INTERNATIONAL CONFERENCE
MECHANICAL ENGINEERING IN XXI CENTURY

December 9-10, 2020
Faculty of Mechanical Engineering in Niš, Serbia

Energy Management Model for Sustainable Production Process – A Case Study

Milena RAJIĆ, Pedja MILOSAVLJEVIĆ, Rado MAKSIMOVIĆ, Dragan PAVLOVIĆ

First Author affiliation: Department of Management in Mechanical Engineering, University of Nis, Faculty of Mechanical Engineering, Nis, Aleksandra Medvedeva 14, 18000 Nis, Serbia
Second Author affiliation: Department of Management in Mechanical Engineering, University of Nis, Faculty of Mechanical Engineering, Nis, Aleksandra Medvedeva 14, 18000 Nis, Serbia
Third Author affiliation: Department of Industrial Engineering and Management, University of Novi Sad, Faculty of Technical Sciences, Novi Sad, Trg Dositeja Obradovića 6, 21000 Novi Sad, Serbia
Fourth Author affiliation: Department of Management in Mechanical Engineering, University of Nis, Faculty of Mechanical Engineering, Nis, Aleksandra Medvedeva 14, 18000 Nis, Serbia
milena.rajic@masfak.ni.ac.rs, pedja@masfak.ni.ac.rs, rado@uns.ac.rs, dragan.pavlovic@masfak.ni.ac.rs

***Abstract*— Sustainable production processes in industrial organizations require the maximal added value with minimal resource utilization. Rational use of energy and energy resources represents an increasing challenge for companies in Serbia and in the world, all with the aim of preserving the environment. Research on material and energy flows, their correlations and the formation of models that are flexible and applicable to different production and service activities, would provide enough information to design processes with resource savings and negative impact on the environment. This paper presents the energy management model for energy profile identification of industrial organization in food industry sector. The energy flow was identified in order to have full insight in all energy consumption users.**

***Keywords*— energy management, energy performance indicator, food industry, material energy flow analyses**

I. Introduction

Energy flows optimization in the organization requires additional costs, but energy consumption and proper energy management clearly defines the enterprises' energy profile [1,2]. Improved energy performance of the industrial process can provide direct benefits to the organization itself, maximizing the diversity of energy sources, while reducing energy costs and energy consumption [3-6]. It can be said with confidence that energy management is becoming an increasingly critical factor of production. Proper management of energy consumption affects the competitiveness of organizations and their willingness and flexibility to adapt to an increasingly demanding market and ensure their survival [7-11]. Current energy management practices indicate that proper management of energy flows and their optimization have long-term benefits for the enterprises' operations and represent effective indicators of profitability [12-14]. On the other side, there are enterprises that do not see the priority of the energy management application and they solve problems without any systematic approach to the problem [1]. Energy performance includes energy efficiency, energy consumption and/or other indicator. Material flow analysis (MFA) has becoming one of the most important instruments to achieve environmental protection as well as the sustainable development of the organization.

The food industry sector is characterized as a non-energy intensive industry where energy consumption represents small part of the total production costs. It is considered to be approximately 3% [15-17]. But it also represents an important energy consumer due to the size of industry sector and amount of electricity consumed [18-20].

The paper presents a new advanced approach for energy management model application in a production organization in food industry sector, by using the energy performance indicator, as a part of energy management system

II. Energy flow model

The experimental procedure was conducted in selected production company, in order to identify the energy flow model. The experimental energy audit was performed with the aim to identify the critical consumers, monthly consumption and organization's energy demand. The proposed model was used and presented in Fig.1. The data used for energy audit was amount of energy consumed for 2018 on monthly level, as well as the energy demand for end users, types of fuel and production volume.

The model has seven stages including: identification of system boundary for energy audit, identification of energy flow and energy consumption analysis, comparative analysis, determination of energy profile, analyse of detailed energy consumption, identification of possibilities for improvement, estimation of advantages of proposed solutions, as it is shown in Fig. 1.

The first stage is to define the system boundary and to list all included processes and machines. The energy and material flows can be qualitatively sketched by walking

through site. The second stage is to collect different type of data to quantify the flows, such as energy bills, machine specifications, material usage report, data regarding production wastes, production records, etc. Due to the lack of energy metering system, the most challenging task is to break down the energy consumption at the unit process level. However, a rough estimation of load factor can be made based on expert opinions, machine documentation, and published energy profiles of similar processes. In order to validate the estimation, the assumed load factors needs to be reused for calculating different periods and compared with energy bill. The comparison can be further used to adjust the assumptions for load factor. Finally, for analysed period the input as well as output flow can be quantified. For the dynamic process, it is helpful to construct a more detailed process model, which can be further validated with metering results. The generic information obtained from stage 1 can be used to form the base line scenario. The stage 7 begins with screening improvement measures to select potential ones. It is necessary to review the detailed technical specifications and to compare with the limitations of the current process. A technical feasibility report can be generated, which includes all advantages or disadvantages of each option. Another step is revisiting models with different scenarios, in order to compare the total energy consumption and other process parameters directly. The potentials for energy savings can be also predicted relatively accurate. After obtaining the cost information of each option, the financial feasibility study can be reported (Fig.2).

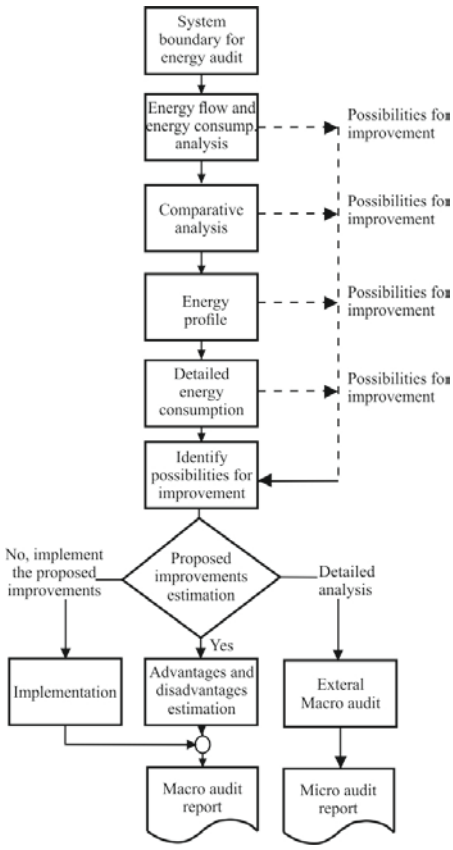

Fig. 1 The proposed model for energy audit in food sector

To identify the energy flow within the production plan, it is necessary to have full insight into the production process. The analysed organization includes processes in a mill and in a bakery. The bakery used electricity and furnace oil as an energy source. Electricity was used for process machines in mill, bakes ovens, cooling system and lightening and furnace oil was used for bake ovens and boilers. The production process is presented in Fig. 2.

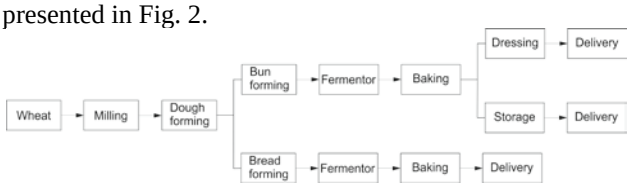

Fig. 2 Production process diagram of the analyzed organization

The mill includes the process of flour milling and its storage in the silos, from where it is transported to the kneading machine by pneumatic system. Flour and other ingredients are mixed in the kneading machine and the dough is made for bread and for bun. Then the dough is formed into the bread and bun or rolled bun. The formed bread is fermented in the unit for fermentation and also baked at 170-330 ºC. The dough bread is baked and then delivered to the customers. The bread moulds and baking trays are washed with hot water approximately 35-40 ºC. On the other side, the bun dough is processed to the unit for fermentation, which is in a form of storage room where the temperature is controlled automatically from -20 to 40 ºC. Then after 12-16h the fermented bun dough is baked at 200-230 ºC. One part of the baked bun is stored in the cold room at temperature -18-25 ºC for postpone delivery. The hot water boilers are used for hot water distribution as well as space heating. The hot water 40 ºC was mainly used for washing the baking plates and dough moulds. The cold room and unit for fermentation are cooled by central absorption chillers.

III. Energy profile and energy indicator

All machines and production lines, as well as units were listed in the production plant, in order to determine the energy profile of the organization. Based on the equipment rated power and the number of operating hours, the total energy consumption was calculated and compared with the previous analysis. The number of operating hours was calculated based on the evidence that is conducted by management. The limitations in identifying the number of effective operating hours were the cases where some equipment was working at different peak demand and time intervals during the operating hours.

To determine the energy profile of the organization, it is important to identify critical consumers and provide a detailed insight into how much energy is spent in the system that is not part of the production process, but represent a support, such as: the system of central heating, cooling and ventilation, lightening, hot water sanitary heating, etc. By using the machine project and also the consumer identification on site, a list of the critical consumers with installed power was made. This data was used to present the consumers and their energy demand (Fig. 3), as well their electricity demand (Fig. 4).

In order to identify the largest consumers, the critical machines and units are identified in the whole production hall. The graphical representation of the consumers is shown in Fig. 5.

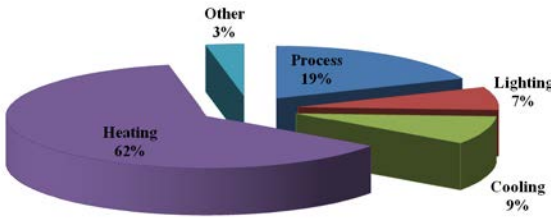

Fig. 3 Energy demand in the production plant: Heating system of the production hall (62% of the total energy demand), Lighting (7%), Cooling System (9%), Production process (19%) and other consumers (about 3%).

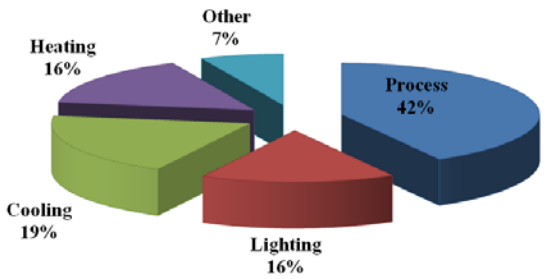

Fig. 4 Electricity demand in the production plant: Heating system of the production hall (16% of the total electricity demand), Lighting (16%), Cooling System (19%), Production process (42%) and other consumers (about 7%).

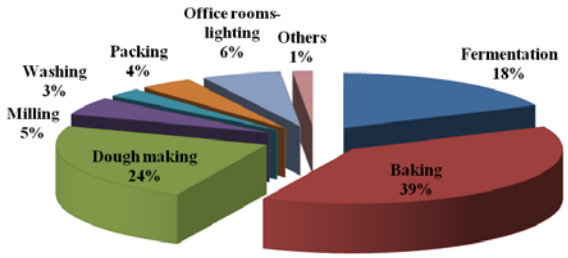

Fig. 5 Consumers overview in the production plant and their electricity demand: Milling (5% electricity demand), Dough making (24%), Baking (39%), Fermentation (18%), Washing line (3%), Packing (4%), Office rooms/lighting (6%), Other consumers (1%).

Presented results are used to analyze the energy performance of the production organization. Energy performance represents the amount of energy consumed in order to meet the different needs of an enterprise. In industrial process it is defined as the realized consumption of energy and energy sources at the organization level in a certain period of time – month or business year. Based on the data on electricity consumption, an overview of the energy performance of the considered processed can be given [21,22]. For analysis is necessary to define the concept of energy performance indicators. Energy performance indicators are defined as specific energy consumption at the organization level in a certain period of time – month and business year. Energy performance indicators are presented as a ratio:

$$IP(t) = \frac{E(t)}{A(t)} \tag{1}$$

Where: $IP(t)$- Energy performance indicator; $E(t)$- Amount of energy consumed; $A(t)$ - Indicator of monitored activity for which energy is used (quantity of products/services, area of heated space and similar); t- Period of time for which the energy performance indicator is calculated.

In the observed process, the production is mainly in bakery, due to the data given in papers [23-25], for monitored activity indicator is mostly used the amount of used/produced flour as a ratio:

$$\mathrm{IP(t)} = \frac{\mathrm{E(t)}}{\mathrm{F(t)}} \tag{2}$$

Where: $F(t)$ - Processed/Used/Produced flour in period of time for which the energy performance indicator is calculated

The data that is used for calculation is for 2018, when the analysed bakery produced and used approximately 281 tons of flour. The specific energy consumption was presented on weekly level for 2018 in Figure 6. Electricity consumption data on a weekly basis are not precisely given, but adopted by using monthly consumption and the number of working hours in each week. Based on the data conducted, the lowest value of indicator can be identified, when electricity is used minimally to reach operational capacity. The critical moments can also be observed when consumption is higher than usual, in order to analyze the causes. This can provide insight into various accident conditions, working failures, break downs in the process and also enable in a preventive way, to avoid such conditions in the future.

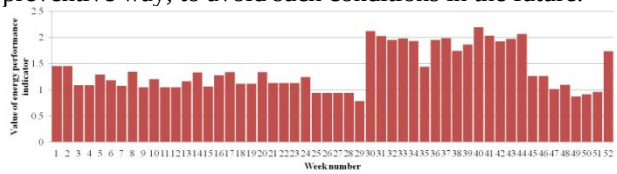

Fig. 6 Energy performance indicator for analysed enterprise in 2018.

According to the calculated data, the minimal energy performance indicator was 0,7996 kWh/kg of flour and maximal 2,1889 kWh/kg of used flour and the average value was 1,3726 kWh/kg of flour. These data can be compared with the one from literature, where the energy performance indicator was 1,37 kWh/kg of flour [23] and the energy performance indicator is in the range of 1,27–1,89 kWh/kg of processed flour depending upon the type of fuel used in the bake ovens [23-26]. With presented data, the analyzed process is in the range of average energy performance indicator. It should be noted the critical weeks (from 30 to 44 in 2018 in Fig. 6), when the indicator was on the maximum level. The phase of monitoring the plant is necessary to be conducted in certain period of time (once a year, two times a year) in order to keep track of the energy consumption and to evaluate the indicators to propose the energy saving measures. This evaluation would enable to predict the energy consumption and to identify the new possibilities of process optimization.

IV. Conclusions

The presented analysis includes a case study of energy management model for identification of energy flows within the production organization in food sector. Proper design of material and energy flows represents the basis of sustainable production processes in order to have minimal resource wastes and loses, but also to provide positive impact on the environment. The aim of the paper was to examine energy flows in the manufacturing sector, to identify the energy demand for such production in order to conduct the comparative analysis with similar

production processes. The production processes in food industry sector is analyzed mostly by using material flow, so the energy flow and energy consumption are usually negligible. Higher energy consumption is related to process itself, but also to the dynamic operations, that should be planned, controlled and monitored. The presented approach of energy management model would be developed in the form to follow the patterns that are established in production processes, as well as to foreseen the consumption peaks and to provide sustain and reliable operation without any unnecessary energy losses

ACKNOWLEDGMENT

This research was financially supported by the Ministry of Education, Science and Technological Development of the Republic of Serbia.

REFERENCES

[1] V. Introna, V. Cesarotti, M. Benedetti, S. Biagiotti, R. Rotunno, "Energy Management Maturity Model: An organizational tool to foster the continuous reduction of energy consumption in companies", Journal of Cleaner Production, 83, 2014, pp. 108–117.

[2] A. Amundsen, "Joint management of energy and environment", Journal of Cleaner Production, 8(6), 2000, pp. 483-494.

[3] J. A. Laitner, "An overview of the energy efficiency potential", Environmental Innovation and Societal Transitions, 9, 2013, pp. 38-42.

[4] V. Dobes, "New tool for promotion of energy management and cleaner production on no cure, no pay basis, Journal of Cleaner Production", 39, 2013, pp. 255-264.

[5] M. Pye, A. McKane, "Making a stronger case for industrial energy efficiency by quantifying non-energy benefits", Resources, Conservation and Recycling, 28(3-4), 2000, pp. 171-183.

[6] K. Bunse, M. Vodicka, P. Schönsleben, M. Brülhart, F.O. Ernst, "Integrating energy efficiency performance in production management – gap analysis between industrial needs and scientific literature", Journal of Cleaner Production, 19(6–7), 2011, pp. 667-679.

[7] S. Thiede, G. Posselt, C. Herrmann, "SME appropriate concept for continuously improving the energy and resource efficiency in manufacturing companies", CIRP Journal of Manufacturing Science and Technology, 6(3), 2013, pp. 204-211.

[8] J. R. Duflou, J. W. Sutherland, D. Dornfeld, C. Herrmann, J. Jeswiet, S. Kara, M. Hauschild, K. Kellens, "Towards energy and resource efficient manufacturing: A processes and systems approach", CIRP Annals-Manufacturing Technology, 61(2), 2012, pp. 587-609.

[9] S. Suh, "Theory of materials and energy flow analysis in ecology and economics", Ecological modelling, 189(3), 2005, pp. 251-269.

[10] S. Doty, W. Turner, Energy Management Handbook. The Fairmont Press, 2009.

[11] J. Beer, Potential for industrial energy-efficiency improvement in the long term, Eco-efficiency in industry and Science, Springer, 2000, Vol. 5.

[12] P. Ghadimi, W. Li, S. Kara, C. Herrmann, "Integrated Material and Energy Flow Analysis towards Energy Efficient Manufacturing", 21st CIRP Conference on Life Cycle Engineering, Procedia CIRP, 15, 2014, pp. 117 – 122.

[13] T. Fleiter, W. Eichhammer, J. Schleich, Energy efficiency in electric motor systems: Technical potentials and policy approaches for developing countries, United Nations Industrial Development Organization, 2011.

[14] R. Y. Yin, Metallurgical Process Engineering, Springer Heidelberg, ISBN 978-3-642-13955-0, 2011, New York, USA.

[15] H. L. F. De Groot, E. T. Verhoef, P. Nijkamp, "Energy savings by firms: decision-making, barriers and policies", Energy economics, 23(6), 2001, pp. 717-740.

[16] P. Sandberg, M. Soderstrom, "Industrial energy efficiency: the need for investment decision support from a manager perspective", Energy policy, 31(15), 2003, pp. 1623-1634.

[17] D. C. A. Muller, F. M. A. Marechal, T. Wolewinski, P. J. Roux, "An energy management method for the food industry", Applied Thermal Engineering, 27(16), 2007, pp. 2677-2686.

[18] D. E. Hathaway, Food Prices and Inflation, Brookings Paperson Economic Activity, 1 (1974), 63–116.

[19] C. Wallgren, M. Hojer, "Eating energy-identifying possibilities for reduced energy use in the future food supply system", Energy Policy 37, 2009, pp. 5803–5813.

[20] C. M. Ma, M. H. Chen, G. B. Hong, "Energy conservation status in Taiwanese food industry", Energy Policy 50, 2012, 458-463.

[21] N. Tasić, Ž. Đurić, D. Malešević, R. Maksimović, N. Radaković, "Automation of Process Performance Management in a Company", Tehnicki vjesnik - Technical Gazette 25(2), 2018, pp. 565-572.

[22] M. Rajić, The Model of the Energy Flow Management in Industrial Systems, PhD Thesis, 2020, University of Novi Sad, Faculty of Technical Sciences, Novi Sad, Serbia.

[23] R. Kannan, W. Boie, "Energy management practices in SME-case study of a bakery in Germany", Energy Conversion and Management 44(6), 2003, pp. 945-959.

[24] Energy Efficiency in a crisp-bread bakery. Centre for the Analysis and Dissemination of Demonstrated Energy Technologies (CADDET). Newsletter, 3, 2000, pp. 4–5.

[25] Heat pipe saves energy in the baking industry. Centre for the Analysis and Dissemination of Demonstrated Energy Technologies (CADDET). Energy Efficiency brochure, Result 277, 1997.

[26] P. Thollander, S. Backlund, A. Trianni, E. Cagno, "Beyond barriers - A case study on driving forces for improved energy efficiency in the foundry industries in Finland, France, Germany, Italy, Poland, Spain, and Sweden", Applied Energy 111, 2013, pp. 636-643.

THE 5th INTERNATIONAL CONFERENCE
MECHANICAL ENGINEERING IN XXI CENTURY

December 9-10, 2020
Faculty of Mechanical Engineering in Niš, Serbia

Personal Income and Aversion to a Sure Loss – Are Money-Makers willing to Risk More to Evade Certain Loss?

Miroslav FERENČAK, Dušan DOBROMIROV, Mladen RADIŠIĆ

Faculty of Technical Sciences, University of Novi Sad, Trg Dositeja Obradovića 6, 21000 Novi Sad, Serbia
ferencak@uns.ac.rs, ddobromirov@uns.ac.rs, mladenr@uns.ac.rs

***Abstract*— In this paper we will present the results of the research done to establish employment status as an influence for aversion to a sure loss under ambiguity. We recognized the need for such research in order to distinguish decision-making process between employed and non-employed persons. Basic behavioral effects that influence investment decision-making process are presented, together with the explanation of different states according to the information available on the market. The methodology is explained in detail, as as it is based on stock simulation rather than on hypotetical cases, and the subject group description is be presented. We utilized Fisher exact test together with descriptive statistics. The results are somewhat inconclusive, giving that there is no difference among two subject groups.**

***Keywords*— Industrial Management, Behavioural Finance, Loss Aversion**

I. Introduction

From simple ones, like what clothes to wear to work today, to more complex ones, like where to invest your life savings, decision – making is daily routine with which people are faced daily. Decision – makers tend to be more cautious when decisions that they should make have certain monetary exposure. To help them in making optimal decision, business decision – makers often employ some decision-making tool, usually at a certain cost for decision-maker. Even the most developed and high-end tools do not guarantee that optimal decision will be made, as decision-makers are open to different influences, both external and internal.

Even with all technological help, human emotions and primal human reactions are hard to avoid. Loss aversion, risk aversion, and heuristics are being extensively researched since publishing of the seminal work of Tversky and Kahneman in 1979 about prospect theory principles. From that day onwards, behavioural approach has become widely accepted part of decision-making theory.

In our previous researches we examined the difference in risk preferences between employed and unemployed subjects. We showed that unemployed subjects exhibit higher risk-aversion under ambiguity than employed subjects. In the continuation of the research, we examined the difference in aversion to a sure loss – are the subjects from different group more prone to make hasty decisions and expose themselves to more risk in order to make a small profit, or are they willing to accept small losses?

II. Literature overview

A. Decision-making

The decision involves choosing from a set of at least two options (alternatives, actions) to which we can achieve the desired goal. If we have only one option, then there are no dilemmas regarding the choice, and therefore there is no problem of decision-making. [1] Options must be defined so that they mutually exclude each other, while the set of options must be final to be able to speak about the correct alternatives.

The goal of decision-making process is to come with the best possible alternative that will maximize the positive aspects and minimize the negative aspects concerning the choice. However, for that to happen, there must be enough information about the alternatives, the probabilities should be known and decision-makers must possess enough knowledge, experience, tools and resources in order to process information in the best possible way. However, decision-makers often do not have adequate information about the core of a problem; they do not have time or means to get information and often are incapable to understand the given information. They are facing the impossibility of memorizing so many information and limited ability of counting. [2] Those situations are called bounded rationality. Investors are often subjected to bounded rationality due to the quickly changing prices and trends, and decisions must be made in the shortest time possible.

1) Programmed and Non - Programmed Decisions: Depending on the previous knowledge and experience with the problem, decision-maker faces two types of decisions: Programmed and non-programmed decisions. Programmed decisions are those decision whose basic characteristics are the routine performance of activities, the predetermined procedures for making the decision and the experience by which decision-making is made. [3] Programmed decisions are characterized by their predictability since they the problems to which decisions are related to tend to occur regularly, regardless of their complexity. Hence the programmed decisions are based on

practices, rules and procedures that are result of past experiences. The decisions are usually decomposed on elements that can be defined, predicted, and analyzed to create best-practice documents, procedures or policies that will help with making programmed decisions.

Non-programmed decisions are those decisions that decision-makers make for the first time and are related to new problems without pre-destined algorithm for its solving, with increased uncertainty compared to the programmed decisions. Behavioural theory is of great significance in making non-programmed decisions because it views decision-making process as a sequential, repeating process of alternative elimination. The rationality is applied on one choice among possible choices that satisfy given criteria of decision-making.

2) *Optimal and satisfactory decisions:* Depending on the clarity and probability of the outcome of the decision, two types of decisions can be identified: optimal and satisfactory decisions.

Optimal decisions are those decisions that maximize the outcome of the action, either being financial outcome or some other type. They are usually made in such cases where there is enough information, and the possible outcomes of actions are clear and the process of decision-making concerning optimal decisions is connected to the classical theory of decision making. Much of the optimal decisions can be made by using decision-making software. Also, mathematics, statistics and algorithms are often used in making optimal decisions.

Satisfactory decisions arose from the cases in which optimal decisions could not be made due to the lack of information or the probability distribution. Given that financial utility cannot be measured, satisfactory decisions present solutions that are "good enough" given the circumstances. The goal of making satisfactory decision is to bring the decision-maker least possible regret concerning the decision. Satisfactory decisions find support in behavioural decision-making theory, which states that psychology, anthropology, philosophy, and other social sciences have influence on decision-making of the individual.

3) *Decision-making process:* Decision-making process is a part of broader process called problem solving, which includes these phases:

- Current situation (initial state) observation and problem identification.
- Precision problem definition.
- Goal definition (of choice criteria),
- Alternative action (option) direction identification.
- Information gathering.
- Alternative evaluation.
- Choosing the alternative,
- Action implementation,
- Results dissemination and analysis. [4]

By valuating efficiency (overseeing the results) it can be concluded if the decision has made expected outcome. In that way decision-making process can be presented as a system with its own subsystems that are interconnected and influence one another. [5]

The process of decision-making is passing though several stages:

- Collection and analysis of needed information.
- Business system goals definition.
- Expected results elaboration.
- Decision concerning resources needed.
- Alternative decisions elaboration.
- Choice of the decision.
- Decision implementation. [6]

The goal of decision-making process is to help the decision-makers choose the best possible alternative among several alternatives given the information that are available.

4) *Experience differences among investors:* The difference among decision-makers with different previous experiences have been thoroughly researched, especially among workers with different entrepreneurship background. Researchers found different risk aversion levels among public and private sector workers, where private sector workers exhibit less risk aversion behaviour [7]. Risk-tolerant individuals can benefit more from the entrepreneurship training than risk-averse individuals [8], supporting the claim that entrepreneurs are generally more risk tolerant than other individuals.

The attitude of decision-makers according to their employment status has been researched; however, the results of different researches are somewhat in contradiction. While Halek and Eisenhauer [9] found that unemployed subjects in their research are much more prone in financially risky behaviour, Pannenberg research showed that unemployed job seekers are risk averse [10].

B. Risk, Uncertainty and Ambiguity

Risk represents the state where numerical probability for occurrence of certain events is known. The decision-making under risk is common practice in programmed decisions, because the frequency of occurrence can provide decision-makers with several instances and better probability calculation.

In case where there is no known probability, but the probability can be calculated from past events by using statistical methods or by expert opinion, decision will be made in uncertainty. Uncertainty represents risk where the numerical probability is set with smaller degree of confidence due to the either lack of necessary information or different use of given information by different decision-makers.

Ambiguity is defined as a decision environment when there are no probabilities that decision-makers can assign to the outcomes of their actions. This situation usually happens when decision-makers are dealing with new problems.

Investors usually work in either uncertainty or ambiguity. In the case of the investments, the future cash flows are usually projected based on current market situation and the results of the similar projects in the past. However, not all investors possess the knowledge or experience needed to interpret data in a way that would help them maximize their wealth. In their case, even with the information that is provided to them, they make decisions under ambiguity.

C. Investment Decision-making

Prospect theory, set by Tversky and Kahneman in 1979 and expanded in 1992, define that decision-makers are influenced by the psychological factors more than it was believed before, and that humans are often unable to make optimal decisions. This is due to the two-phase decision

model, which consists of preliminary analysis of the choices given and their simplification (editing phase) and later evaluation. Because decision-makers during editing phase are susceptible to the certain psychological effects, their decisions are not in line with the expected utility theory. [11]

Effects that, according to the behavioural economist influence decision-making are numerous, and some of better researched are:

- Loss aversion: One of the basic phenomena of choice under both risk and uncertainty is that losses loom larger than gains. The observed asymmetry between gains and losses are to extreme to be explained by income effects or by decreasing risk aversion. [12]
- Heuristics – represent the wide group of psychological tools that help decision makers during their decision-making process under bounded rationality. Heuristics does not necessary help decision-makers make best decisions, but they just speed-up the process of decision making, sometimes leading to the decisions that are neither optimal nor satisfactory. Notable heuristics include anchoring, representativeness, availability, etc.
- Risk aversion – Decision-makers are risk averse in that sense that they prefer sure gains over possibility of larger gains coupled with the possibility of loss.
- Ambiguity aversion – people prefer lotteries with known probabilities over those with unknown probabilities.

Investors decision-making under ambiguity is characterized by the lack of information given to the investors or misunderstanding of the information due to the lack of knowledge. As it is almost impossible to come to the precise probabilities of directions of price movements on the market, it can be argued that investors work either under uncertainty or under ambiguity, with the prior experience, knowledge and access to information making the difference between the two states.

Although there are certain models of decision-making under ambiguity, such as method for measuring loss-aversion under ambiguity by Abdellaoui et al [13], those models are not suitable for the research of investors, due to specific scenarios in which investors operating on the stock exchange might find them. The stock market, in contrast to the most models, is not a lottery, meaning that the maximum gain cannot be measured. Also, the usual volatility of the prices presents a problem because most of the methods take linear approach to the price change, which is usually not the case. However, most of the researchers found that the coefficient for loss aversion is in a region of 2, meaning that people tend to ask for two units in case that one unit can be lost. Although widely accepted, some researchers found that current evidence current evidence does not support that losses, on balance, tend to be any more impactful than gains. [14] Gal also contest that loss aversion is not responsible for some of the effects it produces. [15]

III. Methodology and Sampling

To measure ambiguity aversion under risk, we prepared an on-line questionnaire. The subject group consisted of the current and past students of Industrial engineering and management department of Faculty of technical sciences, University of Novi Sad. Total of 214 invitations were sent, of which 145 were opened and 89 answered the research, of which 50 were women, and 63 were employed at the time. The choice of such subject group was done in order to have a subject group that either has a theoretical or practical knowledge of the stock market principles, as the researches wanted to find out how investors with knowledge and/or experience on the market react in situations under ambiguity. The research was anonymous. The questions were on Serbian language. There were no infractions of the process and not a single result was dropped.

The questionnaire was divided into three parts. The first part consisted of questions concerning date of birth, employment status and gender of the subject, as well as his previous knowledge and experience about stock-market exchange. The first part was used as a check of consistency, as all students who received invitations for research either attended courses connected to the stock-market exchange or were part of the simulation.

Second part of the questionnaire was presented as a hypothetical scenario in which subject took the role of the investor with a certain amount of financial resources. They had a choice of three different stocks that had the same price. The only difference between the stocks were the spread between the potential gains and losses, as the first one had small spread, meaning smaller potential gains and smaller potential losses, second had larger spread between potential gains and losses, and third was presented as a stock with both high potential gains and losses. The only information that subjects had been given is that the market is stable, and it is predicted it will remain stable in the near future. By not giving information needed for the proper assessment of the stocks, the subjects were put under ambiguity for the decision making, as no probabilities were given.

The third part was used to measure aversion to a sure loss. As a continuation of previous part, subjects were presented with the scenario that their chosen stocks lost 0,5$ of their value. They were given the opportunity to either acknowledge the losses and sell their positions, to keep current position or to average-down, buying more of the same stocks, but with the current, lower, price thus giving an opportunity to make a profit if price of the stock returns to the previous level, but exposing itself to larger monetary losses. If the subjects chose to keep the positions, the questions was repeated with another drop in price of 0,5$ for their stock, and continued until they either chose to average down or sell the stocks.

Service used for distribution of questionnaire and collection of answers is sogosurvey.com and excel was used for graphical and statistical presentation of second part of the questionnaire. We used Minitab to calculate descriptive statistics and test hypothesis in the third part, that there is a difference among subjects relative to their employment status. For hypothesis testing we used Fisher's exact test and ANOVA test. Calculation for Fisher's exact test p value is given in an equation (1).

$$p = \frac{(a+b)!(c+d)!(a+c)!(b+d)!}{a!b!c!d!} \quad (1)$$

IV. Results

The result show that unemployed decision-makers exhibit higher risk-aversion under ambiguity than employed decision-makers, which is in contrast to the previous researches. The results of the research can be seen on Figure 1.

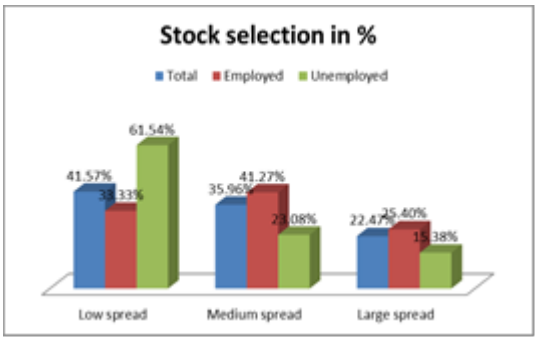

Fig.1 Stock selection depending on gain-loss spread among different groups

Test in aversion to a sure loss showed that there is no correlation between subjects employment status and if they decided to average down their positions, which can be seen on Table 1.

Table I Entry data for Fisher's exact test

	Employed	Unemployed	Total
Average down	56	22	78
No average down	7	4	11
Total	63	26	89

Calculating from the Table 1. We can see that p-value for Fisher's exact test is 0,73, indicating that there is no statistical difference among different subject groups.

Among those who chose to average down their positions, mean price was 8,536$ for employed subjects and 7,864$ for unemployed subjects. Further, we investigated among those that decided to average down if there is a difference among subject groups. We present results of ANOVA test whose results we present in Table 2.

Table II results of ANOVA test

	SS	DF	MS	F	P
Between groups	7.134	1	7.134	3.50	0.065
Inside groups	155.019	76	2.040		
Total	162.154	77			

We can see from Table 2. that there is not enough evidence to discard the hypothesis that there is no difference among subject groups when it comes to the level at which they decided to average-down their positions.

V. Conclusion

The results provided in this paper indicate that our subject group showed the same level of risk aversion as in other researches done before, however employed subjects were more risk-tolerant than unemployed subjects. We failed to prove that there is a difference between subject groups when it comes to difference in aversion to a sure loss, showing that it equally exists among both employed and unemployed subjects.

Among those that chose to average down their position, ANOVA test showed that there is no difference among subject groups at 5% level of confidence, but at 10% level we could say that there is a difference among subject groups, so it seems that unemployed subjects tended to use average-down technique at lower prices, signifying larger appetite for sure loss aversion.

The behavioral aspect of investors decision making is still uncharted territory, with vast potential for further research. Further research should encompass larger number of subjects together with the more sophisticated, software-based simulation tools.

References

[1] D. Pavličić, Decision – making theory, Belgrade, Serbia: Faculty of Economics publishing center, 2010.

[2] H. Simon, Administrative behavior. New York, USA: Free Press, 1976

[3] H. Simon, "Theories of decison-making in economics and behavioral science," The American Economic Review, Vol. 49, pp. 253-283, 1959.

[4] S. Cooke and N. Slack, Making management decisions. New York, USA: Prentice Hall, 1991.

[5] Ž. Radosavljević, Trade management, Belgrade, Serbia: CERK, 2006.

[6] B. Leković, Management principles, Bečej, Serbia: Proleter, 2011.

[7] D. Bellante and A. N. Link, "Are Public Sector Workers More Risk Averse than Private Sector Workers?" Industrial and Labor Relations Review, Vol. 34, No. 3, pp. 408-412, 1981.

[8] R. W. Fairlie and W. Holleran, "Entrepreneurship Training, Risk Aversion and Other Personality Traits: Evidence from a Random Experiment," University of California Santa Cruz Working Paper Series. 2014, accessible at: https://escholarship.org/uc/item/9x83w5k4

[9] M. Halek and J. G. Eisenhauer, "Demography of Risk Aversion," The Journal of Risk and Insurance, Vol. 68, No. 1, pp. 1-24, 2001.

[10] M. Pannenberg, "Risk Attitudes and Reservation Wages of Unemployed Workers: Evidence from Panel Data," Economics Letters, Vol. 106, No. 3, pp. 223-226, 2010.

[11] A. Tverksy and D. Kahneman, "Prospect theory: an analysis of decision under risk," Econometrica, Vol. 47, pp. 263-291, March 1979.

[12] A. Tversky and D. Kahneman, "Advances in prospect theory: cumulative representation of uncertainty," Journal of Risk and Uncertainty, Vol. 5, pp. 297-323, 1992.

[13] M. Abdellaoui, H. Bleichrodt, O. l'Hardion and D. Dolder, "Measuring loss aversion under ambiguity: a method to make prospect theory completely observable," Journal od Risk and Uncertainty, Vol. 52, No. 1, pp. 1-20, March 2017.

[14] D. Gal and D. Rucker, "The loss of loss aversion: will it loom larger than its gain?," Journal of Consumer Psychology, forthcoming.

[15] D. Gal, "The psychological law of inertia and the illusion of loss aversion," Judgment and Decision Making, Vol. 1, No. 1, pp. 23-32, July 2006.